Report No. FHWA-SC-18-04

Characterization of Asphalt Concrete Dynamic Modulus in South Carolina

FINAL REPORT

Sponsoring Agency:

South Carolina Department of Transportation

In Cooperation with:

U.S. Department of Transportation

Federal Highway Administration

Project Investigators:

Serji Amirkhanian, Ph.D.

Feipeng Xiao, P.E., Ph.D.

Mary Corley

Tri County Technical College

P. O. Box 587 | 7900 Hwy 76 | Pendleton SC 29670

March 2018

Technical Report Documentation Page

1. Report No. FHWA-SC-18-04	2. Government Accession No.	3. Recipient's Catalog No.

4. Title and Subtitle Characterization of Asphalt Concrete Dynamic Modulus in South Carolina	5. Report Date March 2018
	6. Performing Organization Code
7. Author(s) Serji Amirkhanian, Ph.D., Feipeng Xiao, P.E., Ph.D. and Mary Corley	8. Performing Organization Report No. TCTC 18-02
9. Performing Organization Name and Address Tri-County Technical College P.O. Box 58, 7900 U.S. Hwy. 76, Pendleton, SC 29670	10. Work Unit No. (TRAIS)
	11. Contract or Grant No. SPR 720
12. Sponsoring Agency Name and Address South Carolina Department of Transportation 1406 Shop Rd., Columbia, SC 29201	13. Type of Report and Period Covered Apr. 2013 – Mar. 2018
	14. Sponsoring Agency Code

15. Supplementary Notes

16. Abstract

Many states around the country still use the 1972, 1986, or 1993 AASHTO Design Guides, which rely on empirical relationships between paving material properties and the structural performance of pavement layers. These empirical relationships were developed based on the 1950's American Association of State Highway Officials (AASHO) Road Test data, which was the most comprehensive and most expensive test conducted to-date to investigate the performance of pavement structures of known thickness under various loading conditions. However, during the implementation of 1986 AASHTO Design Guide, the need for and benefits of a mechanistically-based pavement design procedure were recognized. In 2004, the National Cooperative Highway Research Program (NCHRP) Mechanistic-Empirical Pavement Design Guide (MEPDG) was completed and ultimately released to the public for review and evaluation. For years, SCDOT officials have considered adopting AASHTO's new mechanistic-empirical design guide; however, this would require extensive local calibration. This research project was performed to characterize currently-used South Carolina HMA mixtures and develop a catalog for dynamic modulus value inputs to be used in the MEPDG software in South Carolina.

17. Key Words Asphalt Pavement, Pavement Design, Mechanistic-Empirical, Dynamic Modulus	18. Distribution Statement No restrictions.

19. Security Classif. (of this report) Unclassified	20. Security Classif. (of this page) Unclassified	21. No. Of Pages 586	22. Price

Form DOT F 1700.7 (8–72) Reproduction of completed page authorized

Acknowledgements

The authors wish to extend their appreciation to the South Carolina Department of Transportation (SCDOT) and the Federal Highway Administration (FHWA) for sponsoring this research project. The assistance of Messrs. Thompson, Steagall, Zwanka, Hawkins, Selkinghaus, and Swygert of SCDOT and Mr. Garling of FHWA was instrumental in the completion of this project.

Disclaimer

The contents of this report reflect the views of the authors, who are responsible for the facts and accuracy of the presented data. The contents do not reflect the official views of Tri County Technical College, SCDOT, or FHWA. This report does not constitute a standard, specification, or regulation.

Executive Summary

Overview

Many states around the country still use the 1972, 1986, or 1993 AASHTO Design Guides, which rely on empirical relationships between paving material properties and the structural performance of pavement layers that were developed based on the 1950's AASHO Road test data. However, during the implementation of 1986 Design Guide, the need for and benefits of a mechanistically-based pavement design procedure were recognized. In 2004, the AASHTO Mechanistic-Empirical Pavement Design Guide (MEPDG) was completed and ultimately released to the public for review and evaluation.

For many years, South Carolina Department of Transportation (SCDOT) officials have considered adopting AASHTO's new mechanistic-empirical design guide; however, this would require extensive local calibrations. The major objective of this research was to characterize currently-used South Carolina (SC) asphalt mixtures and to develop a catalog for dynamic modulus value inputs to be used in the MEPDG software.

Literature Review

Dynamic modulus (|E*|) is the ratio of stress to strain under vibratory conditions. The |E*|, commonly used for flexible pavement design, is one of the most important parameters needed for the MEPDG. In addition, |E*| is also one of the key parameters employed to evaluate both rutting and fatigue cracking distress predictions in the MEPDG. Phase angle (δ) is the angle in degrees between a sinusoidal applied peak stress and the resulting peak strain in a controlled stress test and is useful in the prediction of permanent deformation.

The repeated load flow number (FN) test is a dynamic creep test where a haversine type of loading is applied with rest periods between loadings (AASHTO TP79-13). A higher load repetition results in a higher FN, which indicates that the asphalt pavement exhibits a better rutting resistance.

With the |E*| and FN being significant inputs required for flexible pavement design/evaluation in the MEPDG, numerous researchers have explored the various factors affecting these properties, which include aggregate gradation, asphalt binder stiffness, and mixture volumetrics.

Results

In this study, all SCDOT Surface mixture types (A, B, C, D, and E), all SCDOT Intermediate mixture types, (A, B, and C), and two SCDOT Base mixture types (A and B) were evaluated at multiple temperatures and frequencies for dynamic modulus, phase angle, and flow number. Variables included seven aggregate sources in various regions of SC, two asphalt binder sources, two RAP contents (0% RAP and job mix formula % RAP), two warm mix asphalt (WMA) technologies (foaming and a chemical additive), two liquid anti-stripping additives (LASA), and two aging conditions (unaged and long-term aged). Later in the project, a few samples from some newly-approved mixture types were also tested, including Intermediate Type B Special; Surface Type A with updated gradation requirements and corrected optimum asphalt content (COAC); and Surface Type B with COAC. Figures 1 and 2 show that aggregate source affected both |E*| values and FN values of various Surface Type A mixtures containing RAP.

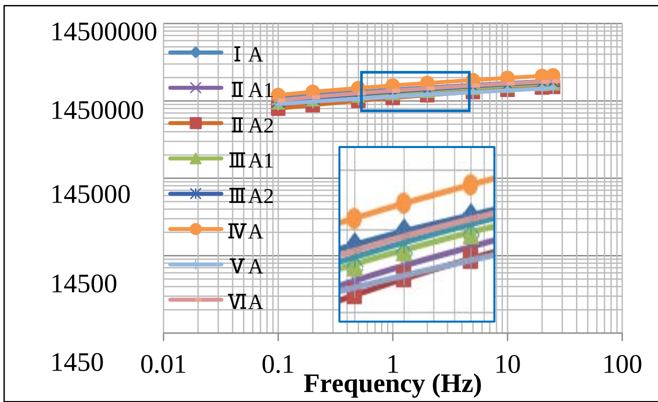

Figure 1. Dynamic Modulus Values of Surface Type A Mixtures with RAP in Terms of Aggregate Source at 4 °C (39.2 °F)

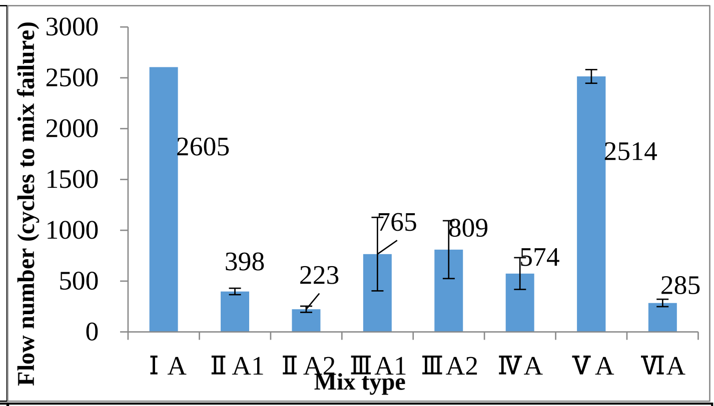

Figure 2. Flow Number Values of Surface Type A Mixtures with RAP in Terms of Aggregate Source at 59 °C (138.2 °F)

Legend for Figures 1 and 2
I, II, III, IV, V, and VI = Aggregate source
A = Surface Type A mix
1* = Mix design used Feb. 2013 SC-M-402 gradation specifications (in effect when study began)
2* = Mix design used July 2017 SC-M-402 gradations specifications + COAC
*Note: Mixtures not labeled "1" or "2" used Feb. 2013 SC-M-402 gradation specifications (in effect when study began).

Conclusions

Mixtures containing the following variables exhibited higher |E*| and lower δ values (which predict greater resistance to rutting) than the corresponding mixtures to which they were compared: aggregate sources I and V, PG 76-22 asphalt binder grade, and RAP. Surface and Intermediate course mixture types designated for higher volume pavements also generally produced higher |E*| and lower δ compared to lower volume mixtures. Base mixture type, asphalt binder source, and WMA type only slightly affected |E*| and δ values, while LASA type and aging had little to no effect.

Mixtures containing the following variables exhibited higher FN values (which predict greater resistance to rutting) than the corresponding mixtures to which they were compared: aggregate sources I and V, PG 76-22 asphalt binder grade, and no WMA. Surface and Intermediate course mixture types designated for higher volume pavements also generally produced higher FN values compared to lower volume mixtures. Several variables had differing results depending upon the aggregate source and/or mixture type. Those variables included asphalt binder source, use of LASA, aging, and use of RAP. Base mixture type only slightly affected FN values, while WMA type and LASA type had little to no effect. Although several mixtures in this study did not meet the minimum flow number values recommended by AASHTO, the scope of this study did not allow for further investigation of the causes of those results. More in-depth studies of some of the individual variables from this study are recommended.

Tables were developed for every material combination tested in this project that contain the necessary input data for pavement design using these materials in the MEPDG software program.

Table of Contents

List of Figures

List of Tables

1 Introduction

1.1 Problem Statement

In the United States, pavement design dates back to 1920s when several road tests were conducted to obtain some information regarding the performance of the pavements and the materials. However, in the late 1950s and early 1960s in Ottawa, Illinois, a Road Test was conducted by the American Association of State Highway Officials (AASHO). This test was the most comprehensive and most expensive test conducted to-date ($27 million, 1960 dollars) to investigate the performance of pavement structures of known thickness under various loading conditions (AASHO, 1961). Some of the specifics of this test section, which eventually became part of I-80, are shown in Figure 1-1 and Figure 1-2 (Pavement Interactive). The Test Road's location represented a typical northern climate. Table 1-1 shows the environmental conditions associated with this project (Pavement Interactive). Many engineering properties were measured including, but not limited to: roughness, deflection, strain, and pavement serviceability index (PSI).

Table 1-1 AASHO Road Test Environmental Condition

Average Mean Temperature (July)	*24.5°C (76°F)*
Average Mean Temperature (January)	*-2.8°C (27°F)*
Annual Average Rainfall	*837 mm (34 inches)*
Average Depth of Frost (for fine-grained soil)	*711 mm (28 inches)*

This Road Test resulted in many new procedures, equations and concepts such as Pavement Serviceability, Equivalent Single Axle Load (ESAL), and Structural Number (SN). In addition, newly-developed design procedures with equations relating these concepts together ultimately became the AASHO-recommended design procedure (Huang, 1993). The Road Test data provided empirical relationships from which equations were developed between many factors (e.g., asphalt concrete slab thickness, load, axle type, and frequency of load).

In 1961, based on the Road Test results, the AASHO Committee on Design published an interim Pavement Design Guide. The American Association of State Highway and Transportation Officials (AASHTO) then published updated interim versions of the Pavement Design Guide in 1972 and 1981. However, no major changes were made to the flexible pavement design procedure in the interim guides (Huang, 1993; AASHTO, 1972 and 1981). The subcommittee of AASHTO on pavement design and other experts revised and expanded the guide during 1984 and 1985 and issued a new interim AASHTO Design Guide in 1986. This work was conducted under National Cooperative Highway Research Program (NCHRP) Project 20-7/24. The 1986 AASHTO Design Guide represented major changes to the original pavement performance model developed from the AASHO Road Test (AASHTO, 1986). During the next several years, many changes and enhancements were made in order to expand the model to be applicable to different climates, materials, and soils found around the country. Another revised version of the AASHTO Design Guide was published in 1993 (AASHTO, 1993).

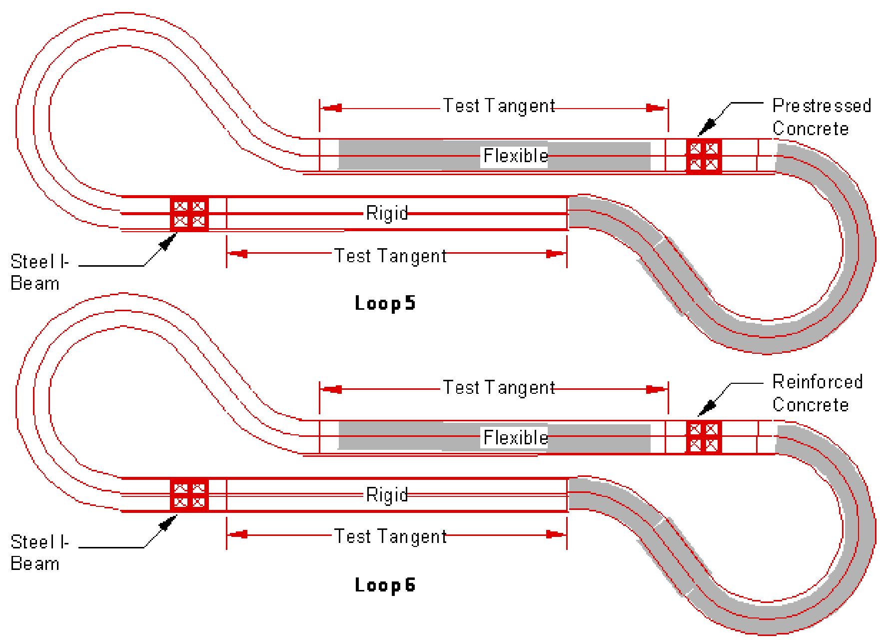

Figure 1-1 Loops 5 and 6 of AASHO Road Test

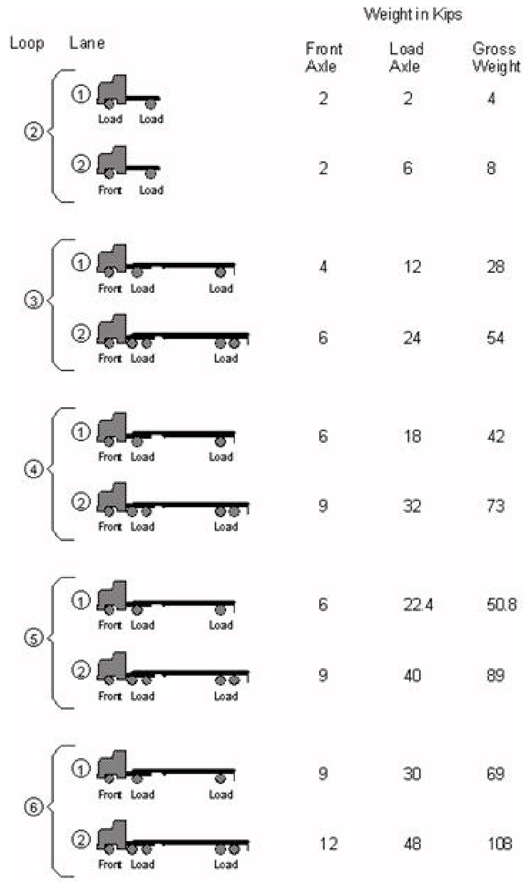

Figure 1-2 Axel Weights and Distributions Used on Various Loops of AASHO Road Test

Many states around the country still use the 1972, 1986, or 1993 AASHTO Design Guides, which rely on empirical relationships between paving material properties and the structural performance of pavement layers that were developed based on the 1950's AASHO Road Test data. However, during the implementation of 1986 Design Guide, the need for and benefits of a mechanistically-based pavement design procedure were recognized. Therefore, the AASHTO Joint Task Force on Pavements (JTFP), the National Cooperative Highway Research Program (NCHRP), and the Federal Highway Association (FHWA) sponsored the development of an AASHTO M-E pavement design procedure. NCHRP Project 1-37A produced a guide that utilized existing mechanistic-based models and databases reflecting current state-of-the-art pavement design procedures. In 2004, the Mechanistic-Empirical Pavement Design Guide (MEPDG) was completed and ultimately released to the public for review and evaluation. Many states across the country, including South Carolina (SC), have begun implementation activities. Figure 1-3 shows a conceptual flow chart of three stages of design, analysis, and process of the MEPDG (Von Quintus and Moulthrop, 2007).

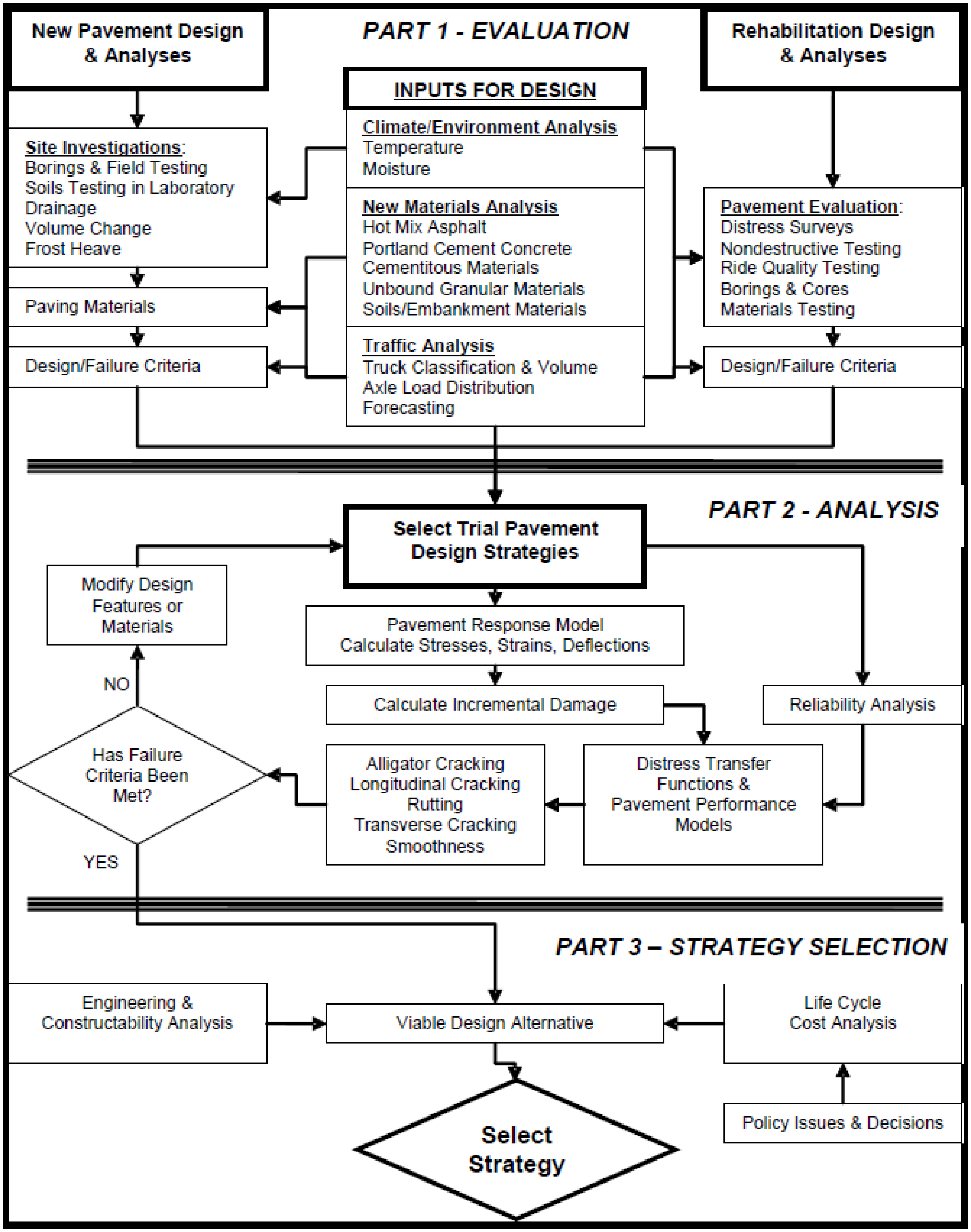

Figure 1-3 Conceptual Flow Chart of 3 Stages of Design, Analysis and Process of the MEPDG

Currently, the South Carolina Department of Transportation (SCDOT) engineers utilize AASHTO regression equation methodology (1972 and later with some modifications) to design flexible and rigid pavements. The SCDOT considered the extensive revisions made in 1986 and 1993; however, many practical problems in these revisions led the Department to continue with the 1972 procedures. For many years, SCDOT officials have considered adopting AASHTO's new mechanistic-empirical design guide; however, this will require extensive local calibration before it can reliably provide better results. SCDOT has estimated that this calibration period will take five to seven years, which is consistent with the calibration of the 1972 procedure. The calibration for the current design was conducted from 1964 to 1972 (SCDOT, 2008).

The input values for the 1972 Design Guide currently used by SCDOT include the following: Soil Support Value (SSV), Equivalent 18,000-lb Single Axle Loads (ESALs), Regional Factor (R), Terminal Serviceability (pt), and Coefficients of Relative Strength for various paving materials (ai). Many of these variables and values were obtained through many years of research and testing. Some of these variables may not be utilized in the new Design Guide.

1.2 Mechanistic Empirical Design Concept

The AASHTO pavement design procedures and concepts have served many highway agencies very well for many years even though many researchers reported on the shortcomings of the existing design procedures. Since the 1960s, many attempts have been made by several researchers around the country to shift from empirical design equations to a more scientific mechanistic-empirical (M-E) design scheme (Figure 1-4). In this concept, information on traffic and climate along with the mechanical properties of the pavement structure are utilized to more accurately analyze the pavement structure and predict its life.

Even though the M-E design somewhat relies on observed performance and empirical relationships, the design process is much more scientific in predicting the life of the pavement. In addition, this new system can incorporate new materials, different traffic distributions, and changing conditions of the pavement. This system also utilizes an analysis procedure that is used in an iterative manner. The design procedure is used to select the proper materials and layer thicknesses to provide the required and desired structural capacity of the pavement. Several considerations should be made, including the main load-related structural distresses: fatigue cracking and structural rutting.

The M-E design and analysis process, as shown in Figure 1-4, integrates several factors (e.g., the environmental conditions and material properties of the HMA) into the pavement structure. The next step is developing models of the structure using a mechanical analysis program. Then, the pavement responses are calculated given the axle load and tire configuration. The pavement responses are then correlated to a cycle to failure (N) for each condition through empirically-derived transfer functions. The next step is calculating a damage factor for each particular condition by using the expected traffic or load cycles for the given design life (n). Using equation 1 (Miner's hypothesis), the damage for each condition is added together, where the failure criteria is reached when the ratio approaches unity:

$$D = \Sigma(\mathrm{ni}/\mathrm{Ni})$$

(Equation 1-1)

Where:

- n_i = Number of load applications at condition, *i*
- N_i = Number of load applications at failure for condition, *i*

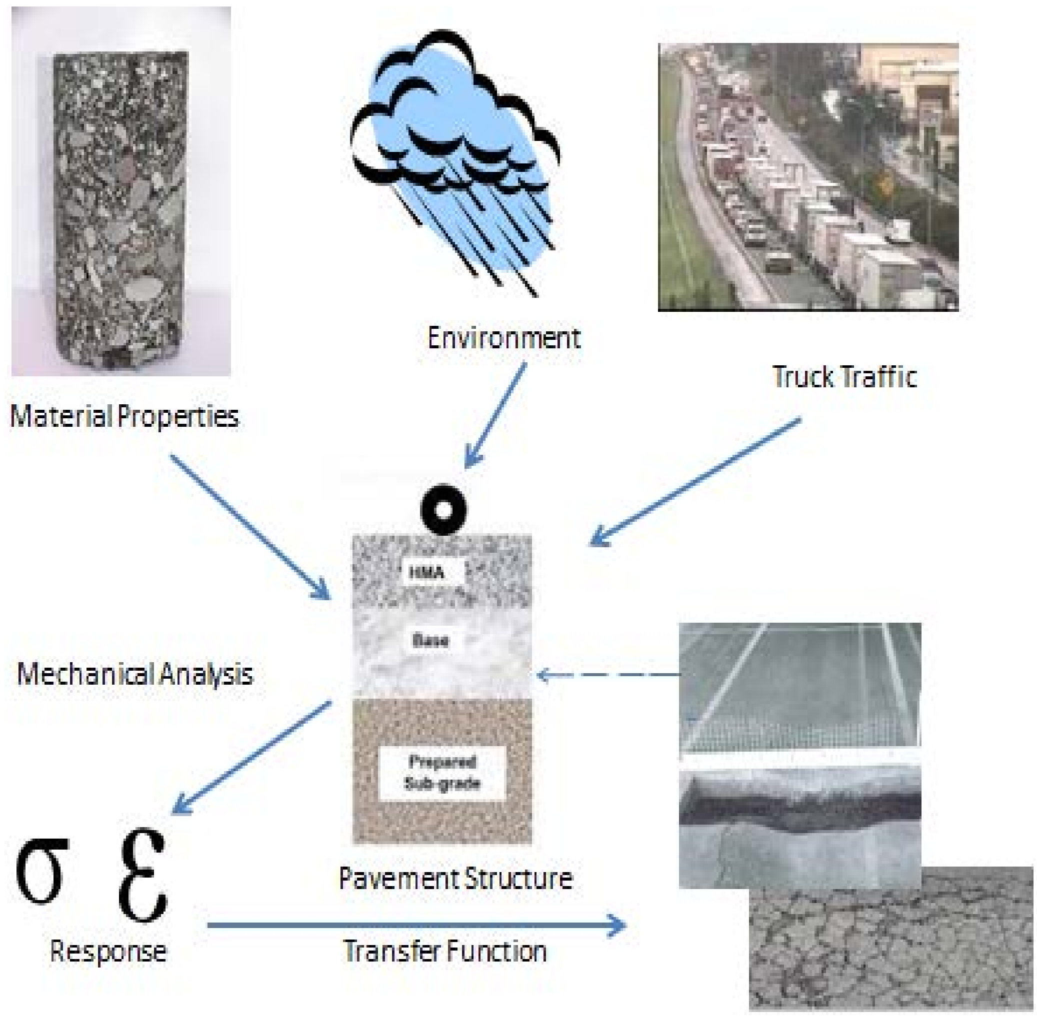

Figure 1-4 Mechanistic-Empirical (M-E) Design Schematic

1.3 Advantages of the System

There are many advantages of a mechanistic-empirical pavement design method compared to the traditional empirical design concept including:

- It can be used for both existing pavement rehabilitation and new pavement construction
- It accommodates changing the types of loads on pavements
- It can better characterize materials since it allows for:
  - Better utilization of available materials
  - Accommodation of new materials
  - A better characterization of existing layer properties

- It uses material properties that relate better to actual pavement performance
- It provides better and more reliable performance predictions
- It considers the environmental and aging effects on materials

2 Scope of the Research Project

2.1 Research Objectives

The objective of this research was to characterize currently-used SC hot mix asphalt (HMA) mixtures and to develop a catalog for dynamic modulus value inputs to be used in the MEPDG software. The specific objectives for this proposed research project included:

- Determining the dynamic modulus (|E*|) and phase angle (δ) at various temperatures and frequencies, in both axial and indirect tension (IDT) modes for many mixtures used by SCDOT;
- Comparing the dynamic modulus test results from the axial and IDT modes;
- Determining the flow number (FN) values;
- Evaluating the performance of mixtures from master curves of |E*|;
- Validating the design models in |E*| prediction for local mixtures;
- Investigating the different parameters sensitive to variations in |E*|, as computed by the MEPDG software;
- Calibrating various prediction models in the MEPDG; and
- Limited evaluation of field cores using AMPT, if possible.

2.2 Significance of Work

For many years, SCDOT has used the AASHTO method of pavement design that was based on empirical data and was established many years ago. This design methodology and guidelines were utilized and are being used by the majority of the states around the country. However, many researchers and the federal government have completed research projects with the final result being a newly-developed pavement design program referred to as MEPDG. The proposed research findings, when implemented, will have a major impact on all aspects of SCDOT's activities. The findings will help all designers and engineers involved with flexible pavements to make the proper decisions based on scientific data obtained from this research work. The results of this research project will be used to establish a systematic method of rehabilitation techniques for pavements in SC. It is anticipated that the future pavement designs conducted by the Agency will be more complicated and comprehensive. However, this will provide longer-lasting pavements, which will save much-needed resources for the state (i.e., limited funding).

Many agencies, including SCDOT, are in the process of establishing a methodology to implement the proposed MEPDG program. Therefore, a thorough understanding of the properties and performance of all materials used in HMA mixtures in SC is necessary in order to implement the proposed system. This concept will consider all factors including the economic factors affecting SC. Since limited research has been conducted in this area in SC, this research project was conducted to answer many of the concerns and to enable the Agency to establish an effective program. As a result, it was necessary to develop technical guidance for the MEPDG to help engineers and administrators understand the benefits and the feasibility of utilizing this program to save money for SCDOT.

2.3 Organization of the Report

The contents of this report have been divided into several sections (chapters). Chapter 3 contains the literature review for many topics studied in this research project. Chapter 4 describes the materials and experimental design used for this work. Chapter 5 describes the concept of various models used in the development of the final system. Chapter 6 contains the results of the research activities. Chapter 7 contains the conclusions and the recommendations for this research study. Chapter 8 includes a partial list of references studied during this investigation. Several appendices contain the laboratory or field testing results.

3 Literature Review

A comprehensive literature review was conducted to investigate the state-of-the-art programs around the country regarding this issue. Several State DOTs' experiences were reviewed and summarized in this report.

3.1 Definitions of Dynamic Modulus and Flow Number

Dynamic modulus (|E*|) is the ratio of stress to strain under vibratory conditions. It is a property of viscoelastic materials, different from complex modulus (E*), which defines the relationship between stress and strain for linear viscoelastic materials. In addition, the normal value of the complex modulus can be calculated by dividing the maximum (peak to peak) stress by the recoverable (peak to peak) axial strain from a material subjected to a sinusoidal loading (AASHTO T 342). Viscoelastic materials display characteristics somewhere in between that of purely viscous and purely elastic materials, exhibiting some phase lag in strain. The phase angle (δ) is the angle in degrees between a sinusoidal applied peak stress and the resulting peak strain in a controlled stress test (AASHTO T 342). The dynamic modulus test is one of the oldest mechanistic tests used to measure the fundamental properties of hot mix asphalt (HMA) mixtures (Witczak et al. 2002).

Dynamic modulus, commonly used for flexible pavement design, is one of the most important parameters needed for the Mechanistic Empirical Pavement Design Guide (MEPDG). In addition, the dynamic modulus is also one of the key parameters employed to evaluate both rutting and fatigue cracking distress predictions in the MEPDG. The dynamic modulus is the basic protocol for characterizing asphalt concrete mixtures used in several publications such as "The Asphalt Institute Airfield Design Procedure" (MS-11), "The Asphalt Institute Highway Design Procedure" (MS-1), and several technical manuals developed for use with designs for U.S. Air Force, Army, and Navy military airfield and highway installations (Harman, D. 2001).

One of the most significant advantages for using |E*| is that many researchers have conducted multiple testing programs and accumulated a wealth of knowledge for the output variables over the last 30 years. This continuously-expanding database was used as the basis for the development of a series of predictive models by Witczak (1996). The most recent versions of the predictive models are based on a database of 2,750 test data points from more than 200 different asphalt concrete mixtures, including a wide range of modified asphalts (Harman D. 2001).

The repeated load flow number (FN) test is a dynamic creep test where a haversine type of loading is applied with rest periods between loadings (AASHTO TP79-13). The typical results between the measured permanent strain and the load cycle can be divided into three major zones, as shown in Figure 3-1. In the primary phase, the strain rate (slope of the permanent strain curve) decreases; in the secondary phase, the permanent strain rate is constant; and in the tertiary phase, the permanent strain rate dramatically increases. At low stress levels, the material may mainly exhibit primary and/or secondary permanent strain. In this case, the permanent strain rate may approach a value equal to zero as the total strain reaches a certain value. This also suggests that at this very low stress level, the tertiary flow region may never appear within a reasonable amount of time. At higher stress levels, the occurrence of the constant secondary permanent strain rate phase will depend on the stress level applied. A higher load repetition results in a higher flow number, and thus the asphalt pavement exhibits a better rutting resistance (Amirkhanian et al. 2014).

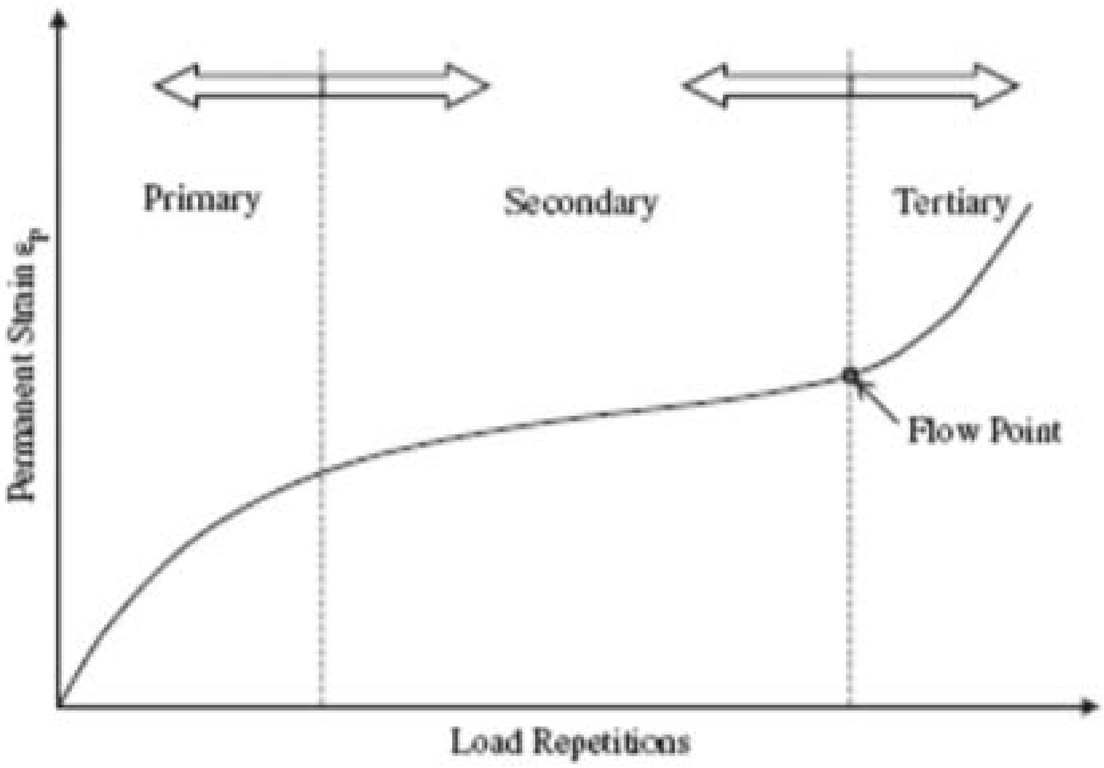

Figure 3-1 Permanent Deformation Responses of Asphalt Pavement Materials under Repeated Loading

3.2 Input of Dynamic Modulus and Flow Number

Before |E*| was adopted by the American Association of State Highway and Transportation Officials (AASHTO) for the AASHTO 2002 Design Guide, at least 15 states evaluated |E*| to make sure that it was practical for use by the states and that it produced reliable and usable results.

The AASHO Committee on Design first published an interim design guide in 1961 based on the results obtained from the AASHO Road Test. The updated AASHO Design Guides were published in 1972 and 1981. The subcommittee on pavement design and a team of consultants revised and expanded the guide based on NCHRP Project 20-7/24 and then issued the AASHTO Design Guide in 1986, which represented a major extension of the original pavement performance model developed from the results of the AASHO Road Test (AASHTO 1981, 1986). Several extensions and enhancements of the 1986 design guide were made in an attempt to expand the applicability of the model to different climates, designs, materials, and soils that exist across the United States. In 1993, a revised version of the AASHTO Design Guide was published (AASHTO 1993, Mohammad et al. 2014).

Although many states in the United States are still using the traditional empirical-based pavement design procedures (AASHTO 1993) for flexible pavement design, some states have realized the advantages of the new MEPDG and are initiating the preparation efforts for the future implementation (Hall 2010 and Flintsch et al. 2008). In the 2002 Guide for Mechanistic-Empirical Design of New and Rehabilitated Pavement Structures, there are significant changes in relating material properties, traffic information, and the climatic impact to pavement distress models and long-term performance. Therefore, a thorough characterization of asphalt materials by each Agency, as well as obtaining appropriate input of fundamental material properties, is critical to the design of new and rehabilitated flexible pavements using the MEPDG.

The MEPDG is a new product resulting from the efforts initiated by the AASHTO Joint Task Force on Pavements and NCHRP to enhance and improve existing design procedures (NCHRP 1-37A). The models were calibrated using data from the long term pavement performance (LTPP) database for conditions representative of the entire U.S. The dynamic modulus is obtained from laboratory testing of asphalt mixtures or prediction equations. The computer software that accompanies the MEPDG provides general default parameters for the dynamic modulus. However, caution has already been issued by the National Cooperative Highway Research Program (NCHRP) researchers as to the appropriateness of these parameters for regional areas, as it was the case with the first Road Test parameters.

With the development and release of the Mechanistic Empirical Pavement Design Guide, MEPDG (NCHRP 1-37A), greater emphasis has been placed on hot mix asphalt (HMA) characterization, and in particular, the modulus or stiffness properties. The MEPDG uses HMA stiffness for various environmental conditions, traffic speeds, and other variables to calculate pavement strains, which are then used to predict pavement distresses.

Currently, AASHTO T 342: Standard Method of Test for Determining Dynamic Modulus of Hot Mix Asphalt is recommended to determine the stiffness properties (Dynamic Modulus or Complex Modulus, |E*|) of HMA.

A master stiffness curve can reflect the dynamic modulus (|E*|) values of one mixture. The |E*| master stiffness curve is a single curve that represents the asphalt material's stiffness relationship to loading frequency and temperature. This procedure is called Level 1 for the MEPDG and provides the most accurate distress predictions during the pavement design (Shen and Yu 2012). The dynamic modulus used in Level 1 is obtained by laboratory testing of asphalt mixtures, while prediction models are used to obtain the dynamic modulus in Level 2.

The measured |E*| values were also compared to that of the Witczak predictive equation and the Hirsch model. The Witczak predictive equation has been selected by the NCHRP researchers for the Level II and III design in the MEPDG. However, many researchers feel that perhaps the Hirsch model provides more accurate results. The Witczak predictive equation is based on the mix gradation, the asphalt binder viscosity properties, and the volumetric properties of the hot mix asphalt, while the Hirsch model is based on the asphalt binder stiffness (G*), the voids in mineral aggregate (VMA), and the voids filled with asphalt (VFA). The accuracy of the predictive equations should be compared to the measured laboratory results (Witczak 1996, 2002). Bhasin et al. (2005) indicated that caution must be exercised in interpreting rut susceptibility of mixtures based on dynamic modulus test parameters, especially when evaluating mixtures containing polymer-modified asphalts.

The parameter inputs of the MEPDG were developed based on a hierarchical approach (Mohammad et al. 2014). This hierarchical approach allows users to enter in project/material-specific information based on actual measured parameters (Level 1) or parameters based on Default and model predictions (Levels 2 and 3). For the most representative pavement distress predictions, it is recommended that state agencies and pavement designers try to utilize the Level 1 inputs. However, due to time constraints and lack of laboratory equipment and personnel as well as requiring a pavement design recommendation almost a year prior to the bidding of a project, many state agencies are relegated to using the Level 2 and/or Level 3 material inputs.

Ideally, the large increase in permanent strain generally occurs at a constant volume within the tertiary zone. The flow number is therefore defined as the postulated cycle when shear deformation under constant volume starts, indicating the start of tertiary flow in the mixture. Practically, the flow number can be determined as the load cycle at which the rate of the change of permanent strain reaches the minimum value. Factors affecting rutting vary since rutting is a complex phenomenon between aggregate, asphalt, and the aggregate-asphalt interface. Additionally, the properties of those components change with the change of time, loading, and temperature (Witczak 2007).

Several testing methods have been proposed by Witczak et al. (2007) for evaluating rutting resistance, including the dynamic modulus (|E*|) test, flow number (Fn) test, and flow time (Ft) test. Particularly, the flow number test was found to correlate with field rut depth as verified by field projects at MNRoad, Westrack, and the FHWA Pavement Testing Facility in the NCHRP Project 9-19 (Witczak 2007). During the NCHRP Project 9-19, the relationship between the reduced flow number and field rut depth at a specific traffic level were studied. Many prediction models were recently developed by some researchers (Kaloush 2001, Witczak, et al. 2002, Kvasnak et al. 2007, Christensen 2009). These models demonstrated the strong correlation between the flow number and the field rutting performance of the pavements. The flow number test is thus recommended to be used for evaluating the rutting potential of asphalt mixtures.

Baus and Stires reported that the SCDOT designed flexible and rigid pavement structures using AASHTO regression equation methodology (1972 and later with some modifications) and that implementation of the MEPDG procedures at the SCDOT would require significant time and resources. Effective use of new MEPDG procedures would require material and traffic databases beyond Level 3 and MEPDG default information currently available at the SCDOT. A better understanding of MEPDG climatic models was also needed. Immediate adoption of the MEPDG using only Level 3 and default inputs with current prediction models calibrated with limited national database information was not advised (Baus and Stires, 2010).

3.3 Tests of Dynamic Modulus and Flow Number

The dynamic modulus can be measured on most servo-hydraulic testing machines capable of producing a controlled, sinusoidal (haversine) compressive load. The testing machine should have the capability of applying a load over a range of frequencies from 0.1 to 25 Hz and a stress level up to 2,800 kPa (400 psi). For sinusoidal loads, the standard error of the applied load shall be less than 5% (AASHTO T342). An environmental chamber is also required to condition the test specimens at different temperatures. The environmental chamber shall be capable of controlling the temperature of the specimen over a temperature range from –10°C to 60°C (14°F to 140°F) with an accuracy of ± 0.5°C (1°F). The system shall be fully computer controlled, capable of measuring and recording the time history of the applied load and the axial deformations, and have a resolution of 0.5 percent. Figure 3-2 shows some of the different types of testing machines utilized for measuring the dynamic modulus of HMA specimens.

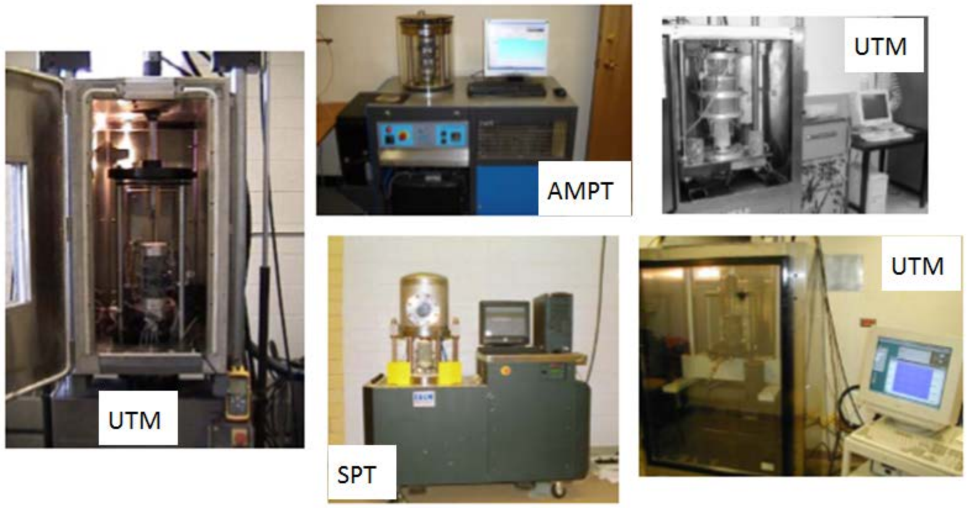

Figure 3-2 Different Testing Machines Used to Measure the Dynamic Modulus of Hot Mix Asphalt (adapted from Bennert 2009)

Dynamic modulus testing is performed on test specimens cored from 150-mm (6 in) gyratory-compacted mixtures. The average diameter of the test specimens must be between 100 and 104 mm (3.94 and 4.1 in) with a standard deviation of 1.0 mm (0.04 in). The average height of the test specimen must be between 147.5 and 152.5 mm (5.81 and 6.00 in). In addition, the laboratory prepared specimens must be conditioned for 4-hour according to AASHTO R 30 (AASHTO T 342). The number of replicates required depends on the number of strain measurements made per specimen and the desired accuracy of the average dynamic modulus.

The specimen can be tested at a temperature setting in accordance with the demand of research. However, the test series for the development of master curves for pavement response and performance analysis is conducted at -10, 4.4, 21.1, 37.8, and 54°C (14, 40, 70, 100, and 130°F) at loading frequencies of 0.1, 0.5, 1.0, 5, 10, and 25 Hz at each temperature. Each specimen is tested for each of the 30 combinations of temperature and frequency of loading, starting with the lowest temperature and then proceeding to the highest temperature and the highest frequency to the lowest. Dynamic modulus testing may be performed in either axial mode or indirect tension (IDT) mode. Research has shown that there is a strong correlation between dynamic modulus values obtained through axial and IDT testing (Mohammad et al. 2014; Kim et al. 2004).

The flow number test (FN) is a repeated-load permanent deformation test that was found to correlate with field rut depths and is recommended by the NCHRP Reports 465 and

580 as a testing method to evaluate the rutting potential of asphalt mixtures (Witczak 2002; Witczak 2007). Tests are performed by applying a uniaxial compressive load to a cored cylindrical specimen which has the same geometry as a dynamic modulus sample. In the flow number test, the compressive load is applied in haversine form with a loading time of 0.1 seconds and a rest duration of 0.9 seconds for a maximum of 10,000 cycles or until a deformation of 50,000 microstrains is reached. A deviatorical stress of 600 kPa is applied to the specimen until the flow point is reached. The flow point represents failure of the specimen, as evidenced by an increasing rate of total permanent strain during the test. Flow number tests are run at the average 7-day maximum pavement temperature 20 mm from the surface at 50 % reliability as determined using LTPPBind version 3.1. Flow number testing is performed at a 0 kPa confining pressure state. Because the dynamic modulus test is considered non-destructive, the samples can be reused in the unconfined flow number evaluation (AASHTO TP79-13; Shen and Yu 2012).

3.4 Impacts on Dynamic Modulus and Flow Number

With the dynamic modulus being one of the prime material inputs required for flexible pavement design/evaluation in the MEPDG, numerous researchers have explored the various factors affecting the dynamic modulus properties, which include aggregate gradation, asphalt binder stiffness, and mixture volumetrics (AASHTO TP62-07; Bonaquist 2008; Bonaquist and Christensen 2005; Christensen et al. 2003; AASHTO T322-07). These studies have also led to different methodologies to predict the dynamic modulus based on these material properties (NCHRP 1-37A; AASHTO T342; King 2004; Shah et al. 2005; Tran and Hall 2006; Birgisson and Roque 2005).

Baus and Stires indicated that the use of MEPDG procedures in SC would require local calibration of each pavement distress prediction. For new flexible pavement structures, this includes: rutting (asphaltic concrete layers; unbound base, subbase, and subgrade layers; and total rut depth), fatigue cracking (surface-down longitudinal cracking and bottom-up alligator cracking), transverse (thermal) cracking, and IRI prediction. The current MEPDG prediction model for surface-down (longitudinal cracking) was known to be unreliable (Baus and Stires, 2010).

Dougan et al. (2003) found that for a single test speed, temperature, and type of aggregate, different |E*| values were produced when the type binder was changed. The variation is, in part, due to the stress levels used. As |E*| is inversely related to strain, the 50 to 150 micron strain range permits a wide range of stress levels and a wide range of |E*| results.

Cross et al. (2007) reported that:

- The presence of 25% RAP in a mixture had a significant effect on measured dynamic modulus.
- The nominal aggregate size did not have a significant effect on measured dynamic modulus.
- PG binder grade, test temperature, and test frequency had a significant effect on measured dynamic modulus.
- Aggregate type did not have a significant effect on measured dynamic modulus.
- The region of the state where the mix was produced and placed did not have a significant effect on measured dynamic modulus.

Yu (2012) indicated that adding shingles to asphalt mixtures requires an increase in δ and b values and a decrease in the α value in the 1999 and 2006 Witczak models for improved prediction of |E*| values. The 2006 Witczak Model tends to overestimate |E*| values for mixes containing RAS. The master curves constructed on that model predicted |E*| values that closely conformed to the master curves constructed on the laboratory tested |E*| values at low temperatures, while the master curves diverged at higher temperatures. Birgisson et al. (2005) indicated in their study that different binder viscosity measuring methods on the 1999 Witczak Model led to underestimating |E*| values.

Shen and Yu (2012) considered that both a modified Hirsch model and a modified flow number prediction model were recommended for future usage to evaluate conventional dense-graded asphalt mixtures for Washington State. Their findings are as follows:

- Air voids had significant impact on both dynamic modulus and flow numbers. The higher the air voids were, the lower the dynamic modulus and flow number values were. The impact of air voids on dynamic modulus was more clear at high |E*| levels (low temperature and high frequency).
- Binder properties, especially the high PG grade, had a significant influence on the dynamic modulus at low |E*| levels (high temperature and low frequency) and flow numbers.
- Aggregate gradation had some impact on the dynamic modulus and flow number of asphalt mixtures. However, the trend of gradation impact was not clear.
- The properties of asphalt mastic had a significant impact on the dynamic modulus of asphalt mixtures. When introducing such a property into the modified Hirsch model, the prediction results of |E*| were greatly improved. Based on this finding, a modified Hirsch model was proposed for predicting the dynamic modulus of Washington mixes.
- A flow number prediction model was locally calibrated for Washington State. It correlates the flow number with the volumetric properties, binder type, and test temperature of the mix. Reasonable prediction results have been achieved for conventional mixes (PG 70-28, PG 64-28 and PG 64-22 binder mixes). However, it has not proven applicable for highly polymer-modified mixes, such as PG76-28.

Mohammad et al. (2014) indicated that dynamic modulus was sensitive to the design traffic level, nominal maximum aggregate size, and the high temperature performance grade of the binder. Mixtures designed for higher traffic levels with larger aggregate and higher grade binder tended to have higher dynamic modulus values at high temperature. The MEPDG simulations carried out using the "nationally-calibrated" default calibration factors overestimated the rut predictions by a significant amount. In addition, both the Witczak and Hirsch models predicted dynamic modulus with reasonable accuracy. Dynamic modulus test results obtained from axial and IDT modes showed no statistical differences for the majority of the mixtures tested.

The research completed by Amirkhanian et al. (2014) indicated that the increased frequency resulted in an increase of |E*| value regardless of polymer type, such as ground tire rubber (GTR), SBS, plastomer, elastomers, etc. The dynamic modulus and flow numbers of various mixtures containing various modified binders, two different aggregate sources, and three ASAs were investigated using the Asphalt Material Performance Tester (AMPT), and the conclusions are shown below:

- With the exception of one case (aggregate II, lime, and lab-blended GTR), all other flow numbers were greater than 50, which is the AASHTO criteria set for a traffic loading of 3 million to less than 10 million ESALs.
- The flow numbers of samples made with aggregate source I, different anti-stripping additives (ASAs), and SBS produced flow numbers that were greater than 190, which is the AASHTO requirement for a traffic loading of 10 million to less than 30 million ESALs.
- The samples made with aggregate source II, different ASAs, and SBS produced only one case of a flow number greater than 190.
- In general, there was no clear trend regarding the flow numbers. For example, samples made with aggregate source I, terminally-blended GTR, and all ASAs produced flow numbers that were all greater than 190; however, none of the flow numbers for aggregate source II for those same mixtures produced any values greater than 110. In most cases, the flow numbers for aggregate source I were greater than those of aggregate source II.
- In the laboratory results from several plant-produced mixtures, flow number results indicated that the mixture containing a liquid ASA might have the weakest resistance to permanent deformation. Additionally, APA rut depth results showed similar trends to the flow number test results in their research.
- The increase of frequency resulted in an increase of dynamic modulus and a reduction of phase angle at the testing temperatures of 4°C (39.2°F) and 20°C (68°F), but it resulted in an increase of phase angle at 45°C (113°F) regardless of mixture type, aggregate source, and ASA type.
- The dynamic modulus values were comparable for the various mixtures. There were some differences in phase angles when tested at a higher temperature.

- Flow numbers were slightly different in general when using different aggregate sources, liquid ASAs or Surface Course mixture types (Amirkhanian et al. 2014).

4 Materials and Experimental Design

4.1 Materials, Sample Fabrication and Test Procedures

4.1.1 Materials

In this study, seven aggregate sources were selected from different quarries in various regions of SC, where aggregate suppliers provided the materials to asphalt contractors to produce the asphalt mixtures. These aggregate sources are all on the SC qualified products list (QPL) and meet the requirements of specifications set by SCDOT. The aggregate sources included quarries in Augusta, Blacksburg, Columbia, Jefferson, Liberty, Rockingham, and Sandy Flats, which were referred to as I, II, III, IV, V, VI, and VII, respectively, in this report. The main mechanical properties of these aggregate sources can be found on SCDOT's website (http://info2.scdot.org/Materials/QualProd/2%20QPL.pdf).

In addition, two asphalt binder sources, Associated Asphalt and Axeon, were selected to yield the asphalt mixtures. The appropriate binder grades (either PG 64-22 or PG 76-22) specified for the particular mix types according to SCDOT specifications were used for each of these sources. PG 76-22 binder is utilized in SC for heavy traffic pavement (Surface Type A), while PG 64-22 binder is used to produce mixtures for Surface Types B, C, D, and E; Intermediate Types A, B, and C; and Base Types A and B.

The utilization of reclaimed asphalt pavement (RAP) was based on currently-approved field Superpave mix designs, or job mix formulas (JMFs). These field mix designs had been designed by contractors with their selected RAP contents (meeting SCDOT specifications) and were approved by SCDOT for use in SC at the time of this project. The RAP materials used to produce the mixtures in the laboratory for this study were collected from the same asphalt plants where the aggregates were obtained. These RAP materials were typically categorized into three types including, +No. 4 RAP, -No. 4 RAP, and non-fractionated RAP. In addition, the aged binder percentage of each RAP source was obtained using an ignition oven at the asphalt plant from which each RAP source was obtained.

In this research, a warm mix asphalt (WMA) chemical additive, Evotherm®, was utilized to yield Surface Type C mixtures made with aggregate sources IV and V at relatively low mixing and compaction temperatures. Meanwhile, WMA foaming technology was also employed to produce Surface Type C mixtures for the same aggregate sources. These two WMA technologies were both on the SCDOT-approved QPL and were selected for this project because they were the most commonly-used WMA technologies in SC at the time of this project.

Two SCDOT-approved liquid anti-stripping additives (ASA), Adhere® and Morlife®, were used to produce mixtures using aggregates IV and V to make samples for Surface Type C mixtures, both with and without RAP. At the time of this study, SCDOT did not allow for the use of liquid ASAs in the highest traffic volume mixes like Surface Types A and B, but these two liquid ASAs were allowed for use in other mix types intended for lower traffic volumes. At the time of this project, Surface Type C (intended for use on high-volume secondary routes) was the highest traffic volume mix that also allowed for the use of liquid ASAs according the SCDOT requirements.

In addition, Surface Types A, B, and C containing aggregate sources IV and V both with and without RAP were used to investigate the aging resistance of asphalt mixtures based on a long-term aging procedure (AASHTO R30). These samples were fabricated in the same way as the samples without the aging process.

The Steering and Implementation Committee requested that an additional mixture type, Intermediate Type B Special, be added for analysis in the project. This mixture type utilizes PG 64-22 binder and the same chemical WMA additive (Evotherm®) that was used in the Surface Type C mixtures in this project. Mix designs were available for two aggregate sources (i.e., II and VII) for the Intermediate Type B Special mix type. It should be noted that the aggregate source VII was solely used in this project for the Intermediate Type B Special mixtures.

To characterize the dynamic modulus value and phase angle as well as flow number of various mixtures in SC, many Superpave mix designs were selected by the Steering Committee to investigate these properties. For this research project, seventy six (76) Superpave mix designs (job mix formulas or JMFs) were utilized involving the following materials: seven aggregate sources; various mix types (e.g., Surface, Intermediate and Base); RAP and non-RAP mixtures; 2 liquid ASAs; and 2 WMA technologies. In this study, most of the mix designs included RAP in order to reflect what was being utilized in actual paving projects in SC at the time of the project. These Superpave mix designs were collected from various contractors and had recently been used in paving many highways around SC. The Superpave mix designs used in this research project are shown in Table 4-1.

4.1.2 Sample Fabrication

In this research, all dynamic modulus samples were fabricated by Superpave gyratory compactor according to the job mix formula. The combined gradation of the aggregate and RAP source for each job mix formula (JMF) met the requirements of the lower and upper gradation specification ranges set by SCDOT. The optimum asphalt binder content of each mixture was in the range of 4.5-6.5% with an air void range of 3.5-4.5%, and all JMFs met SCDOT requirements for optimum binder content and air voids. However, Superpave mix designs of some Surface Course types (i.e., Types D and E) were not available from SCDOT. Thus, based on experience and input from SCDOT officials, an optimum asphalt binder content of 6.0% was selected for these mixtures. However, the stability was tested for these samples at three asphalt binder contents to verify the mixture properties prior to dynamic modulus and flow number testing.

The specimens of all mixtures were compacted (150 mm in diameter and 170 mm in height) in the laboratory according to the JMF. The stored asphalt mixtures were subjected to short-term aging in an oven at compaction temperature for 2 hours before completing the compaction process. These compacted samples were later cored and sawed from the center into the dimensions of 100 mm in diameter and 150 mm in height, as shown in Figure 4-1. The bulk specific gravities and air void contents for each test specimen were measured in accordance with AASHTO T-269.

Table 4-1 Superpave Mix Designs Selected for the Study

RAP	Mix type	Aggregate Source						
		I	II	III	IV	V	VI	VII
With RAP	Surface A	√	√ √	√ √	√	√	√	-
	Surface B	√ √	√	√	√	√	√	-
	Surface C	√	√	√	√	√	√	-
	Surface D	√	√	√	√	√	√	-
	Surface E	√	√	√	√	√	√	-
	Intermediate A	-	-	-	√	√	-	-
	Intermediate B	-	-	-	√	√	-	-
	Intermediate B Special	-	√	-	-	-	-	√
	Intermediate C	-	-	-	√	√	-	-
	Base A	-	-	-	√	√	-	-
	Base B	-	-	-	√	√	-	-
No RAP	Surface A	-	-	-	√	√	√	-
	Surface B	-	-	-	√	√	√	-
	Surface C	-	-	√	√	√	√	-
	Surface D	-	-	√	√	√	√	-
	Surface E	√	-	√	√	√	√	-
	Intermediate A	-	-	-	√	√	-	-
	Intermediate B	-	-	-	√	√	-	-
	Intermediate C	-	-	-	√	√	-	-
	Base A	-	-	-	√	√	-	-
	Base B	-	-	-	√	√	-	-

Notes: I~VII: aggregate source; A~E: mix type; √: Superpave mix design utilized, Two mix designs were referred to as 1 and 2; -: Not utilized or mix design not available

(a) (b)

Figure 4-1 (a) Core Machine; (b) Cored Samples

It should be noted that when the samples from Surface Types D and E were compacted, they were difficult to eject from the mold immediately after compaction without damaging the samples due to their fine gradations. Thus, the samples were left to be cooled in the mold for a short time before they were ejected.

In addition, when liquid ASAs were used to produce samples, these liquid ASAs were first homogeneously blended with the asphalt binder at the dosage recommended by the suppliers. A similar method was used for the WMA mixtures. Additionally, in terms of long-term aging impact, some samples from aggregate sources IV and V were aged in an oven for 5 days at 85°C in accordance with AASHTO R30. Three samples for each mixture in this study were prepared for the dynamic modulus and flow number tests according to the specifications described in AASHTO TP 79. Table 4-2 shows the labels of each mixture used in this research project.

Table 4-2 Labels of Various Mixtures Used in This Study

RAP	Mixture type	Other Variable	Aggregate Source						
			I	II	III	IV	V	VI	VII
With RAP	Surface A		I A	II A1, II A2	III A1, III A2	IV A	V A	VI A	-
	Surface B		I B1, I B2	II B	III B1 III B2	IV B	V B	VI B	-
	Surface C		I C	II C	III C	IV C	V C	VI C	-
	Surface D		I D	II D	III D	IV D	V D	VI D	-
	Surface E		I E	II E	III E	IV E	V E	VI E	-
	Intermediate A		-	-	-	IV IA	V IA	-	-
	Intermediate B		-	-	-	IV IB	V IB	-	-
	Intermediate B Special		-	II IB	-	-	-	-	VII IB
	Intermediate C		-	-	-	IV IC	V IC	-	-
	Base A		-	-	-	IV SA	V SA	-	-
	Base B		-	-	-	IV SB	V SB	-	-
	Surface A	PG 76-22 binder source 2	-	-	-	IV AN	V AN	-	-
	Surface B	PG 64-22 binder source 2	-	-	-	IV BN	V BN	-	-
	Surface C	WMA Chemical Additive	-	-	-	IV CE	V CE	-	-
	Surface C	WMA Foaming	-	-	-	IV CF	V CF	-	-

RAP	Mixture Type	Other Variable	Aggregate Source						
			I	II	III	IV	V	VI	VII
With RAP	Surface C	Liquid ASA1	-	-	-	IV CM	V CM	-	-
	Surface C	Liquid ASA2	-	-	-	IV CA	V CA	-	-
	Surface A - aging	PG 76-22 binder source 1	-	-	-	IV AG	V AG	-	-
	Surface B - aging	PG 64-22 binder source 1	-	-	-	IV BG	V BG	-	-
	Surface C - aging	PG 64-22 binder source 1	-	-	-	IV CG	V CG	-	-
No RAP	Surface A		-	-	-	IV AO	V AO	VI AO	-
	Surface B		-	-	-	IV BO	V BO	VI BO	-
	Surface C		-	-	III CO	IF CO	V CO	VI CO	-
	Surface D		-	-	III DO	IV DO	V DO	VI DO	-
	Surface E		I EO	-	III EO	IV EO	V EO	VI EO	-
	Intermediate A		-	-	-	IV IAO	V IAO	-	-
	Intermediate B		-	-	-	IV IBO	V IBO	-	-
	Intermediate C		-	-	-	IV ICO	V ICO	-	-
	Base A		-	-	-	IV SAO	V SAO	-	-
	Base B		-	-	-	IV SBO	V SBO	-	-

RAP	Mixture Type	Other Variable	Aggregate Source						
			I	II	III	IV	V	VI	VII
No RAP	Surface A	PG 76-22 binder source 2	-	-	-	IV AON	V AON	-	-
	Surface B	PG 64-22 binder source 2	-	-	-	IV BON	V BON	-	-
	Surface C	WMA Chemical Additive	-	-	-	IV COE	V COE	-	-
	Surface C	WMA Foaming	-	-	-	IV COF	V COF	-	-
	Surface C	Liquid ASA1	-	-	-	IV COM	V COM	-	-
	Surface C	Liquid ASA2	-	-	-	IV COA	V COA	-	-
	Surface A - aging	PG 76-22 binder source 1	-	-	-	IV AOG	V AOG	-	-
	Surface B - aging	PG 64-22 binder source 1	-	-	-	IV BOG	V BOG	-	-
	Surface C - aging	PG 64-22 binder source 1	-	-	-	IV COG	V COG	-	-

Notes: All mixtures used binder from source 1 except that those were defined in this Table. In addition, all Surface Type A mixtures used PG 76-22 binder. All other mixtures used PG 64-22 binder.

4.1.3 Dynamic Modulus Test

Each dynamic modulus test specimen was cored to a dimension of 100 mm (4.0 in) in diameter and 150 mm (6.0 in) in height. The procedures for dynamic modulus tests outlined in NCHRP report 614 (Bonaquist, 2008) and AASHTO TP62 were used. The preparation is described below:

- Selected and marked six targets within the surface of the specimen and used epoxy for placing LVDTs, which were used to measure the strains of three sides of samples;
- Conditioned the specimen to the set testing temperature;
- Placed one rubber membrane on each end of the specimen, and placed the spherical stainless steel ball at the center of the top platens after proper conditioning;
- Placed the specimen and the platens inside the environmental chamber on the loading pedestal;
- Placed LVDTs on the specimen, and adjusted them to allow the full range of the LVDTs to be available for the measurement of deformation; and
- Set the chamber temperature to the specific value, and allowed the specimen to be conditioned for the required time in the chamber.

As shown in Table 4-3, each dynamic modulus sample was tested under various frequencies and four temperatures (4°C (39.2°F), 20°C (68°F), and 40°C (104°F) for the PG 64-22 mixtures; 45°C(113°F) for the PG 76-22 mixtures). Based on recommendations from the SCDOT Steering Committee, three replicates were tested for each mixture included in this study.

Table 4-3 Test Frequencies and Tested Temperatures

Frequency (Hz)	Test temperature			
	4C (39.2F)	20C (68F)	40C (104F)	45C (113F)*
25	√	√	-	-
20	√	√	-	-
10	√	√	√	√
5	√	√	√	√
2	√	√	√	√
1	√	√	√	√
0.5	√	√	√	√
0.2	√	√	√	√
0.1	√	√	√	√
0.01	-	-	√	√

*Notes: * Tested temperature for PG 76-22 mixtures only.*

The IPC Asphalt Mixture Performance Tester (AMPT), also called Simple Performance Tester, was utilized to test all specimens to get the dynamic modulus values, flow number values, and flow times. The test equipment and a typical sample testing apparatus are shown in Figure 4-2.

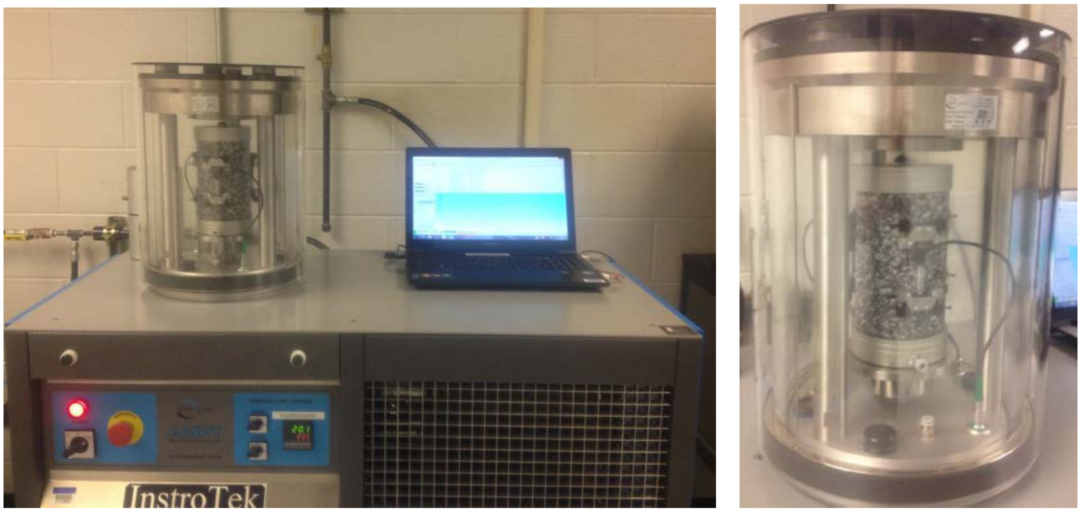

(a) (b)

Figure 4-2 (a) AMPT Test Machine; (b) Tested Sample in Chamber

4.1.4 Flow Test

It is well known that the flow number test (FN) is a repeated-load permanent deformation test, which was found to be able to correlate with the field rut depths and is recommended by the NCHRP Report 465 (Witczak 2002) and NCHRP Report 580 (Witczak 2007) as a testing method to evaluate the rutting potential of the mixtures. This test was performed for all mixtures after the dynamic modulus tests were completed. According to LTPPBind version 3.1, the test temperature for flow number in SC was set at 59°C (138.2°F). Thus, all flow number test results were based on the temperature at 59°C (138.2°F), which is not same as the asphalt pavement analyzer (APA) test or the Hamburg Wheel test.

AASHTO TP 79 indicates that the compressive load of the flow number test is applied in haversine form with a loading time of 0.1 seconds and a rest duration of 0.9 seconds for a maximum of 10,000 cycles or until a deformation of 50,000 microstrains is reached. Typically, a deviator stress of 600 kPa is applied to the specimen until the flow point is reached. Flow number testing was performed at 600 kPa confining pressure state. The recommended flow numbers for various mixtures in AASHO TP 79 are shown in Table 4-4.

Table 4-4 Criteria for Flow Number of Various Mixture Types

Traffic Level, million ESALs	HMA Minimum Average Flow Number	WMA Minimum Average Flow Number
< 3	—	—
3 to < 10	50	30
10 to < 30	190	105
≥ 30	740	415

4.2 Experimental Design

The objectives of this research were achieved through a coordinated series of laboratory experiments to assess the dynamic modulus and flow number (FN) characteristics of mixtures used in SC pavements for the regional calibrations of the MEPDG system. The project work plan was finalized with input from SCDOT officials. The recommended changes to the evaluation procedures for the asphalt mixtures and additives tested are provided to SCDOT in this final report. The experimental design for various phases of this research project included the following items:

- Dynamic modulus (|E*|) and flow number (FN) values of all of the types of asphalt Surface Course mixtures used in SC that are considered to have structural value were evaluated. In this phase, different aggregate sources, RAP percentages (based on the current implementation in the field), and the required binder grades from SCDOT specifications (PG 76-22 and PG 64-22) were used to evaluate the mixes. The optimum asphalt binder contents determined by Superpave mix design procedures were obtained through approved job mix formula (JMF) data provided by the project Steering Committee.
- |E*| and FN values of all types of asphalt Intermediate Course mixtures used in SC were evaluated. In this phase, various aggregate types and RAP percentages were utilized. The optimum binder contents used in this project and any adjustments made to the mixes (e.g., RAP percentages) were either obtained from JMF data provided by the Steering Committee or decided based on input from the Steering Committee.
- |E*| and FN values of two types of asphalt Base Course mixtures used in SC were evaluated. In this phase of the research, various aggregate types and RAP percentages used in the field were evaluated.
- Research on the impact of binder sources (two different grades and sources) on |E*| and FN values of mixtures were conducted.
- Investigations of |E*| and FN values of mixtures using two typical warm mix asphalt technologies (chemical additive and foaming) containing various aggregate types and RAP percentages were completed.

- Assessments of |E*| and FN values of mixtures containing two typical liquid anti-stripping agents (ASAs) (Morlife® and Adhere®) were completed.
- Studies were conducted of |E*| and FN values of mixtures after conditioning through a long-term aging procedure (AASTHO R30).
- Calibration and development of dynamic modulus and flow number predictive models (including Witczak and Hirsch models) from MEPDG based on the data obtained from this study were finalized.

4.2.1 Evaluation of Surface Course Mixtures

This phase of the study included the evaluation of the six Surface Course mixture types used in SC that are considered to have structural value. Six aggregate sources (Liberty, Rock Hill, Jefferson, Columbia, Augusta, and Blacksburg) were selected from varying regions of SC, and two RAP contents were used (0% and the % RAP in each job mix formula provided by SCDOT). Binder source 1 was used for this phase of the project. According to SCDOT specifications, PG 76-22 binder was used for the Surface Type A mixtures, and PG 64-22 binder was used for the Surface Types B through E. The dynamic modulus and flow number tests were performed in accordance with AASHTO TP 62/AASHTO PP 62/AASHTO TP 79. A detailed flowchart of the experimental design for this portion of the research work is shown in Figure 4-3. The number of samples for each test and the entire experimental testing system were discussed and approved by the Steering Committee before initiating the work.

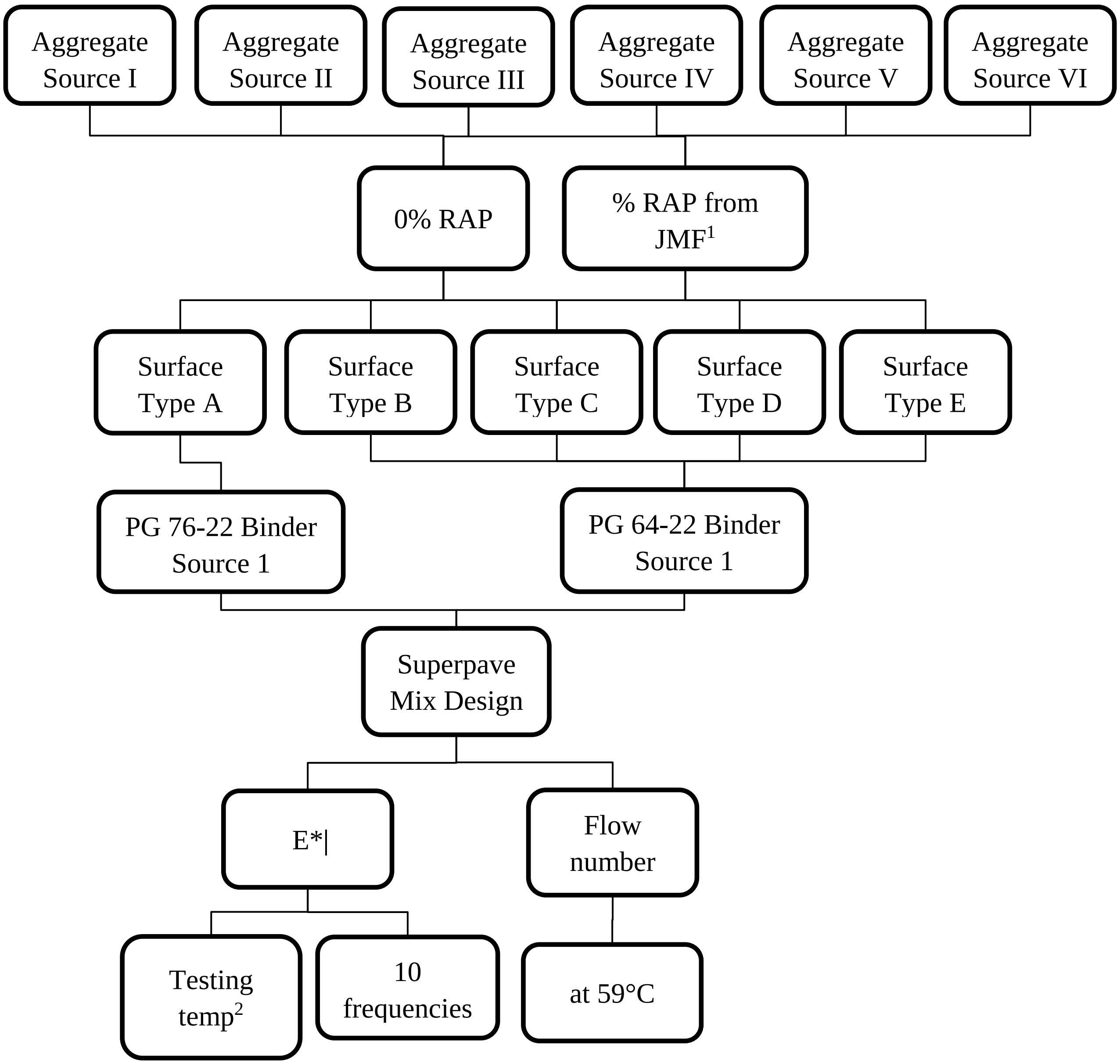

Notes: 1~ RAP Contents Based on RAP in Each Job Mix Formula; 2~ 4°C (39.2°F), 20°C (68°F) and 40°C (104°F) (45°C (113°F) for PG 76-22 mixture)

Figure 4-3 Experimental Flow Chart for Surface Mixtures

4.2.2 Evaluation of Intermediate Course Mixtures

This research also included the evaluation of all Intermediate Course mixture types used in SC. Two aggregate sources (IV and V) were selected from different regions of SC, and two RAP contents were used (0% and the % RAP in each approved job mix formula).

Binder source 1 was also used for this phase of the project, and only PG 64-22 binder was used for the Intermediate Course mixtures per SCDOT specifications. In addition, two additional aggregate sources (II and VII) were used to produce samples for one new mixture type (Intermediate Type B Special) based on recommendations from the Steering Committee. These mixtures contained PG 64-22 binder like the regular Intermediate mixture types; however, they also contained Evotherm® WMA additive. In addition, these Intermediate Type B Special samples all contained the % RAP from their respective mix designs. The dynamic modulus and flow number tests were performed in accordance with AASHTO TP 62/AASHTO PP 62/AASHTO TP 79. A detailed flowchart of the experimental design is shown in Figure 4-4. The number of samples for each test and the entire experimental testing system were discussed and approved by the Steering Committee.

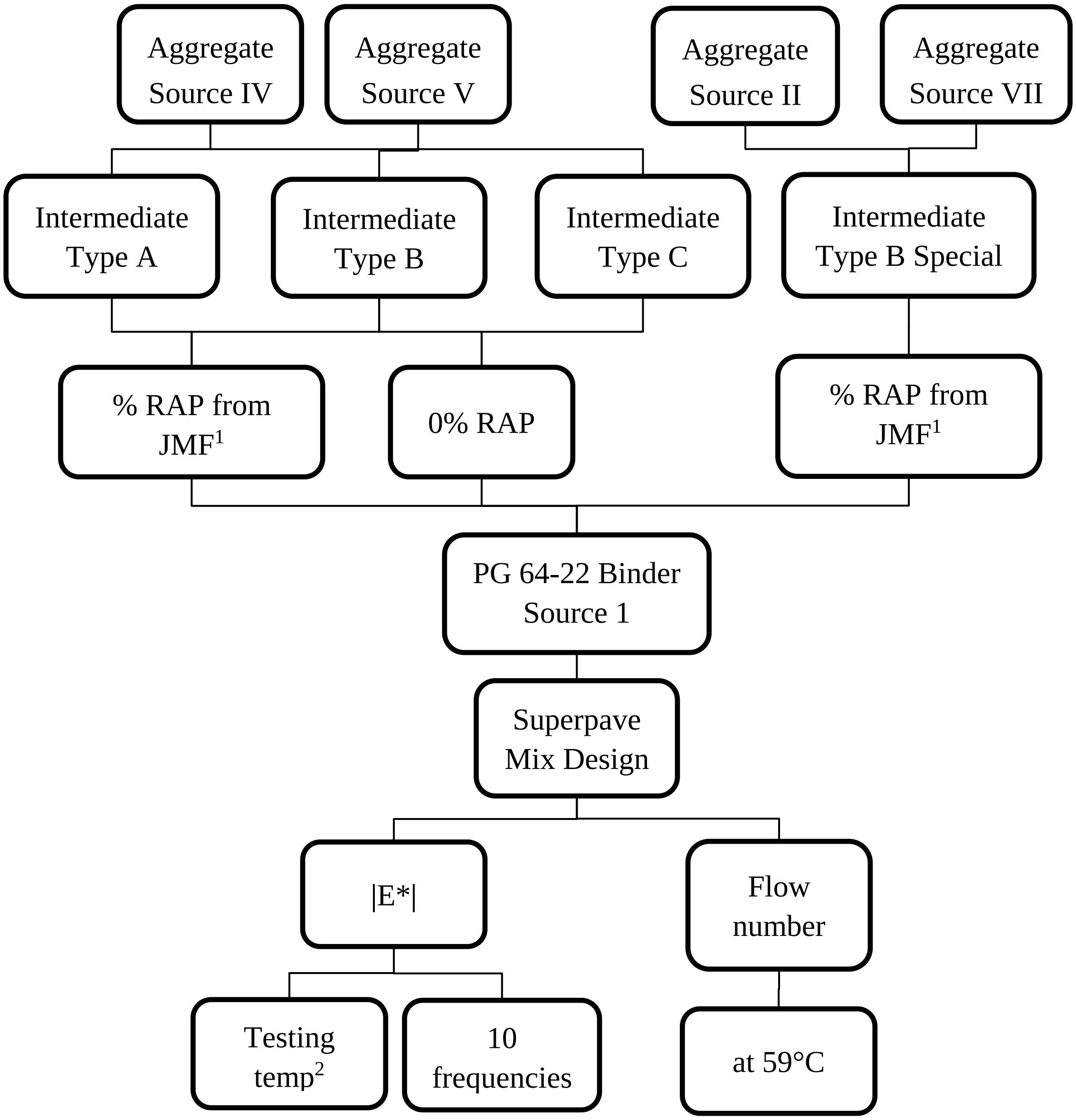

Notes: 1~ RAP Contents Based on RAP in Each Job Mix Formula; 2~ 4°C (39.2°F), 20°C (68°F) and 40°C (104°F) (45°C (113°F) for PG 76-22 mixture)

Figure 4-4 Experimental Flow Chart for Intermediate Mixtures

4.2.3 Evaluation of Base Course Mixtures

This study also included the evaluation of two Base Course mixture types used in SC. The types of mixtures selected (Base Types A and B) are used for interstate, primary, and secondary routes in SC. Two aggregate sources (IV and V) were selected from different regions of SC, and two RAP contents were used (0% and the % RAP in each approved job mix formula). Binder source 1 was also used for this phase of the project, and only PG 64-22 binder was used for the Base Course mixtures per SCDOT specifications. The dynamic modulus and flow number tests were performed in accordance with AASHTO TP 62/AASHTO PP 62/AASHTO TP 79. A detailed flowchart of the full range of testing is shown in Figure 4-5. The number of samples for each test and the entire experimental testing system were discussed and approved by the Steering Committee.

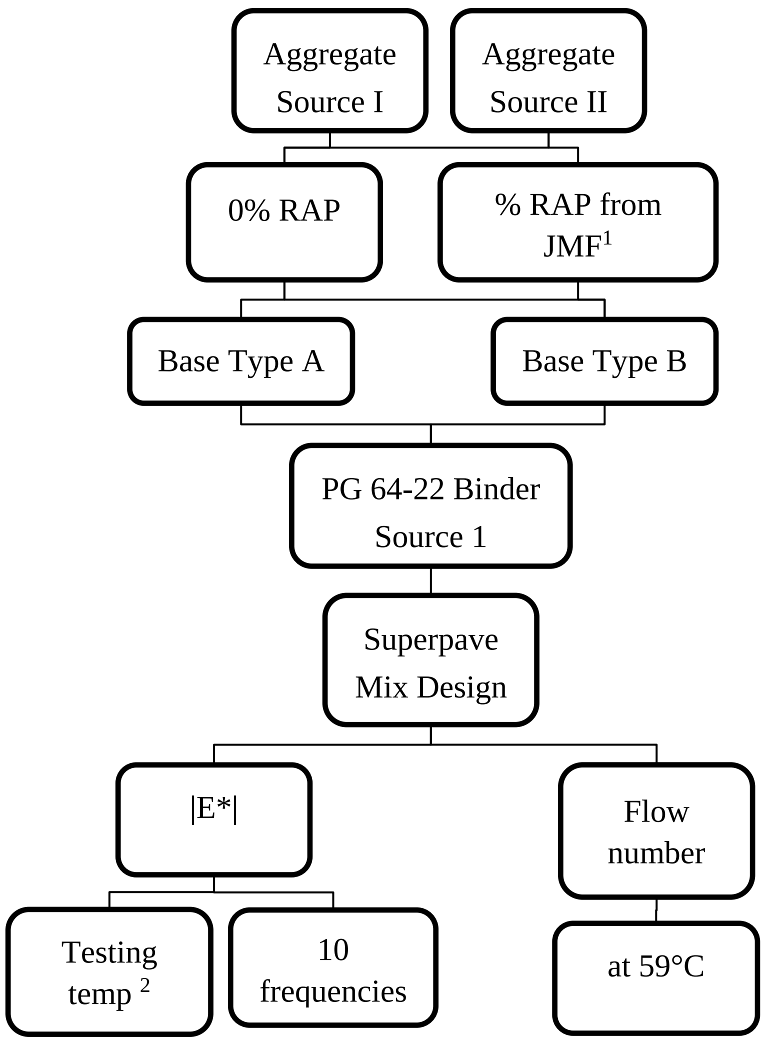

Notes: 1~ RAP Contents Based on RAP in Each Job Mix Formula; 2~ 4°C (39.2°F), 20°C (68°F) and 40°C (104°F) (45°C (113°F) for PG 76-22 mixture)

Figure 4-5 Experimental Flow Chart for Base Mixtures

4.2.4 Evaluation of Binder Source

The research plan also included the evaluation of two binder sources used in SC. For this phase of the project, Surface Types A and B were selected. Both mixture types were made using two aggregate sources (IV and V) from different regions of SC and the % RAP specified in each approved job mix formula. All mixture types, RAP contents, and material sources were selected based on guidance from SCDOT. PG 76-22 binder was used for Surface Type A and PG 64-22 binder was used for Surface Type B according to SCDOT specifications. Both binders in this portion came from binder source 2 (Axeon). The results were then compared to samples made earlier in the project with the same aggregate sources (IV and V) and binder source 1 (Associated Asphalt). The dynamic modulus and flow number tests were performed in accordance with AASHTO TP 62/AASHTO PP 62/AASHTO TP 79. A detailed flowchart of the full potential range of testing is shown in Figure 4-6. The number of samples for each test and the entire experimental testing system were discussed and approved by the Steering Committee.

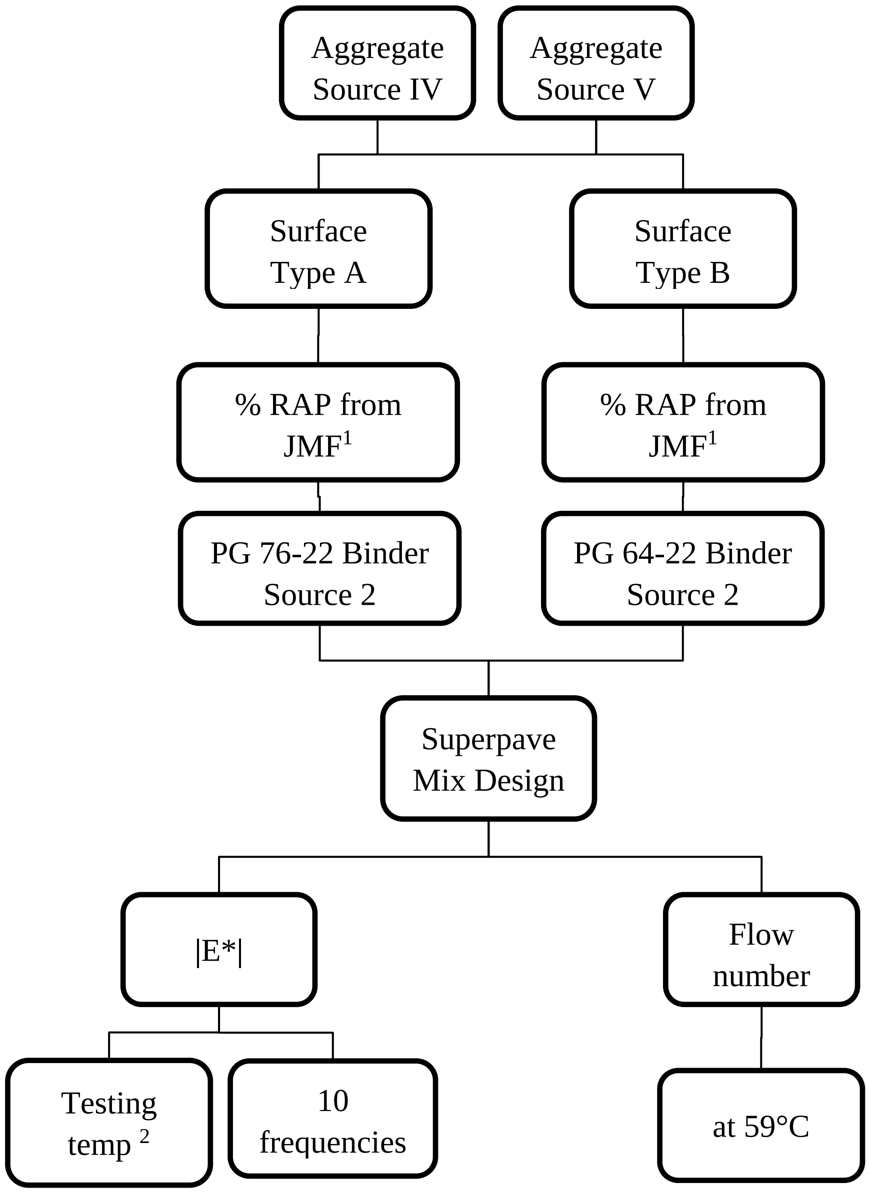

Notes: 1~ RAP Contents Based on RAP in Each Job Mix Formula; 2~ 4°C (39.2°F), 20°C (68°F) and 40°C (104°F) (45°C (113°F) for PG 76-22 mixture)

Figure 4-6 Experimental Flow Chart for Effect of Binder Source

4.2.5 Evaluation of Warm Mix Asphalt (WMA) Types

This study also included the evaluation of two types of warm mix asphalt (WMA) used in SC. One mixture type (Surface Type C), one binder source (source 1) and two aggregate sources (IV and V) were selected for this phase, and the % RAP in each approved job mix formula was utilized. The mixture type, RAP contents, and material sources were selected based on guidance from SCDOT. PG 64-22 binder was used for the Surface

Type C mixtures according to SCDOT's specifications, and two WMA types were used (chemical additive and the foaming process) in the samples. All samples from the foaming WMA process were compacted in the lab following the job mix formula (JMF). The dynamic modulus and flow number tests were performed in accordance with AASHTO TP 62/AASHTO PP 62/AASHTO TP 79. A detailed flowchart of the full range of testing is shown in Figure 4-7. The number of samples for each test and the entire experimental testing system were discussed and approved by the Steering Committee.

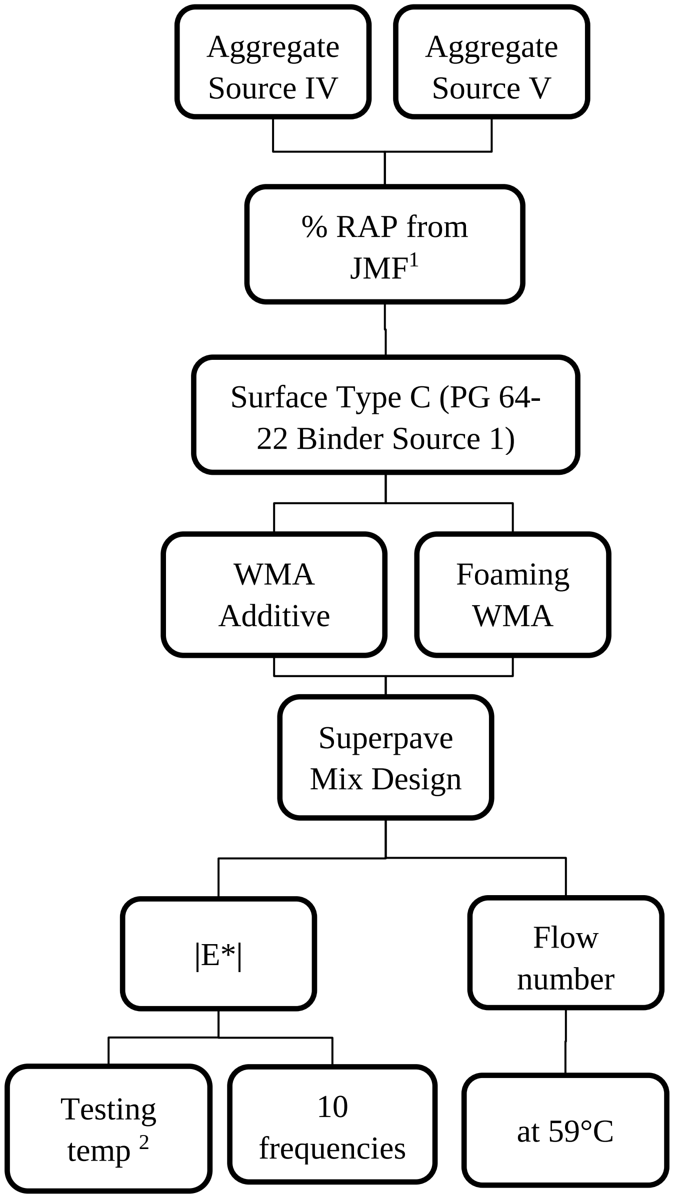

Notes: 1~ RAP Contents Based on RAP in Each Job Mix Formula; 2~ 4°C (39.2°F), 20°C (68°F) and 40°C (104°F) (45°C (113°F) for PG 76-22 mixture)

Figure 4-7 Experimental Flow Chart for Effect of WMA Additives

4.2.6 Evaluation of Liquid Anti-Strip Additives (ASAs)

This experimental design also included evaluation of two types of liquid anti-strip additives (ASAs) used in SC. One mixture type (Surface Type C), one binder source (source 1) and two aggregate sources (IV and V) were selected, and the % RAP in each approved job mix formula was utilized. The mixture type, RAP contents, and material sources were selected based on guidance from SCDOT. PG 64-22 binder was used for the Surface Type C mixtures according to SCDOT's specifications, and two liquid ASAs (Adhere® and Morlife®) were used. The two liquid ASAs were selected based on input from SCDOT officials. The dynamic modulus and flow number tests were performed in accordance with AASHTO TP 62/AASHTO PP 62/AASHTO TP 79. A detailed flowchart of the full range of testing is shown in Figure 4-8. The number of samples for each test and the entire experimental testing system were discussed and approved by the Steering Committee.

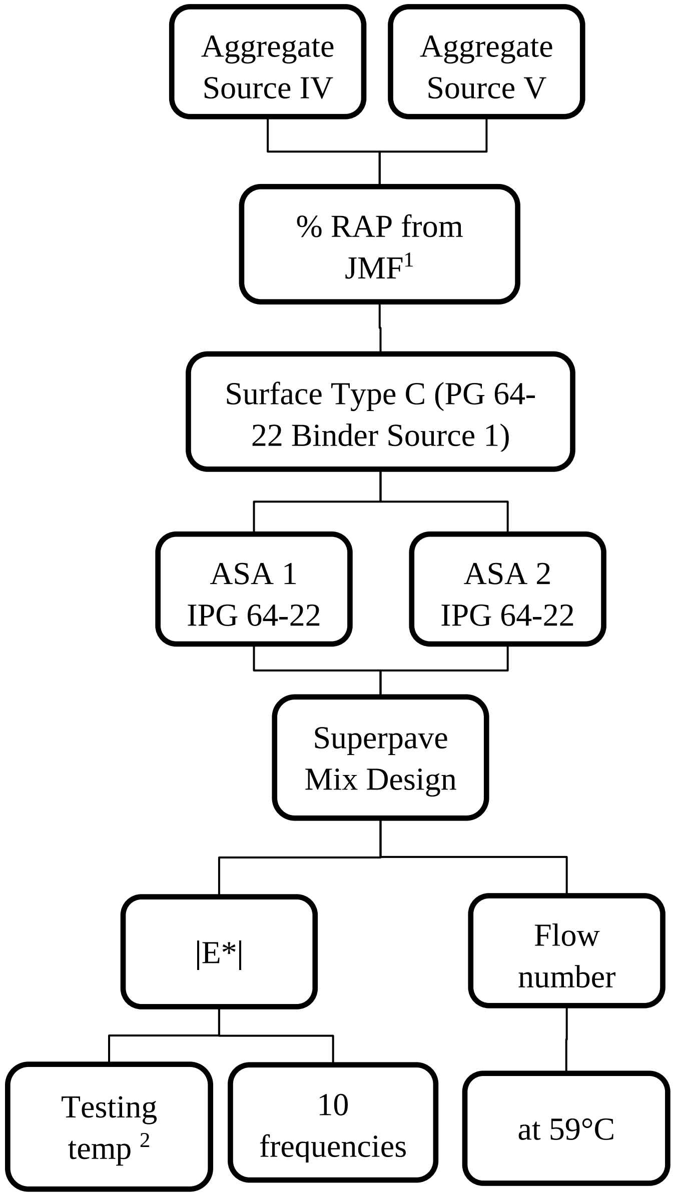

Notes: 1~ RAP Contents Based on RAP in Each Job Mix Formula; 2~ 4°C (39.2°F), 20°C (68°F) and 40°C (104°F) (45°C (113°F) for PG 76-22 mixture)

Figure 4-8 Experimental Flow Chart for Effect of Liquid ASAs

4.2.7 Evaluation of Mixtures after a Long-Term Aging Procedure

Another phase of the research plan included the evaluation of the effect of long-term aging for three types of Surface Course mixes commonly used in SC (Surface Types A, B, and C). One binder source (source 1) and two aggregate sources (IV and V) were selected, and two RAP contents were used (0% and the % RAP from each job mix formula). All mixture types, RAP contents, and material sources were selected based on guidance from SCDOT. PG 76-22 binder was used for the Surface Type A mixtures, and PG 64-22 binder was used for the Surface Types B and C, according to SCDOT requirements. The dynamic modulus and flow number tests were performed in accordance with AASHTO TP 62/AASHTO PP 62/AASHTO TP 79. A detailed flowchart of the full range of testing is shown in Figure 4-9. The number of samples for each test and the entire experimental testing system were discussed and approved by the Steering Committee.

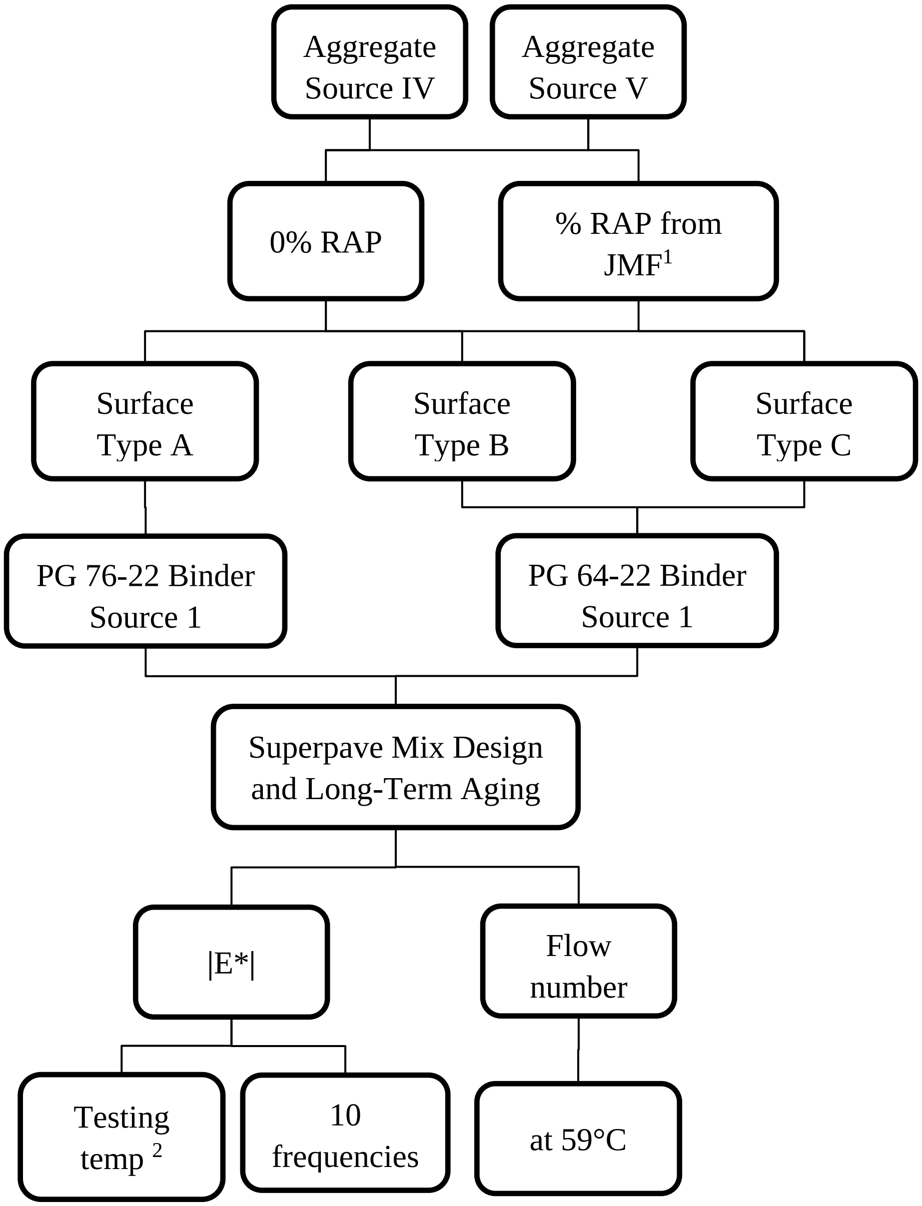

Notes: 1~ RAP Contents Based on RAP in Each Job Mix Formula; 2~ 4°C (39.2°F), 20°C (68°F) and 40°C (104°F) (45°C (113°F) for PG 76-22 mixture)

Figure 4-9 Experimental Flow Chart for Effect of Long-Term Aging

4.2.8 Calibration of Dynamic Modulus and Flow Numbers

This research study also included the calibration of dynamic modulus and flow numbers based on the test results obtained in this study, as shown in Figure 4-10. The modified models from dynamic modulus and flow numbers were employed as the local MEPDG parameter models, which were used for level 2 and level 3 of the pavement design guidelines.

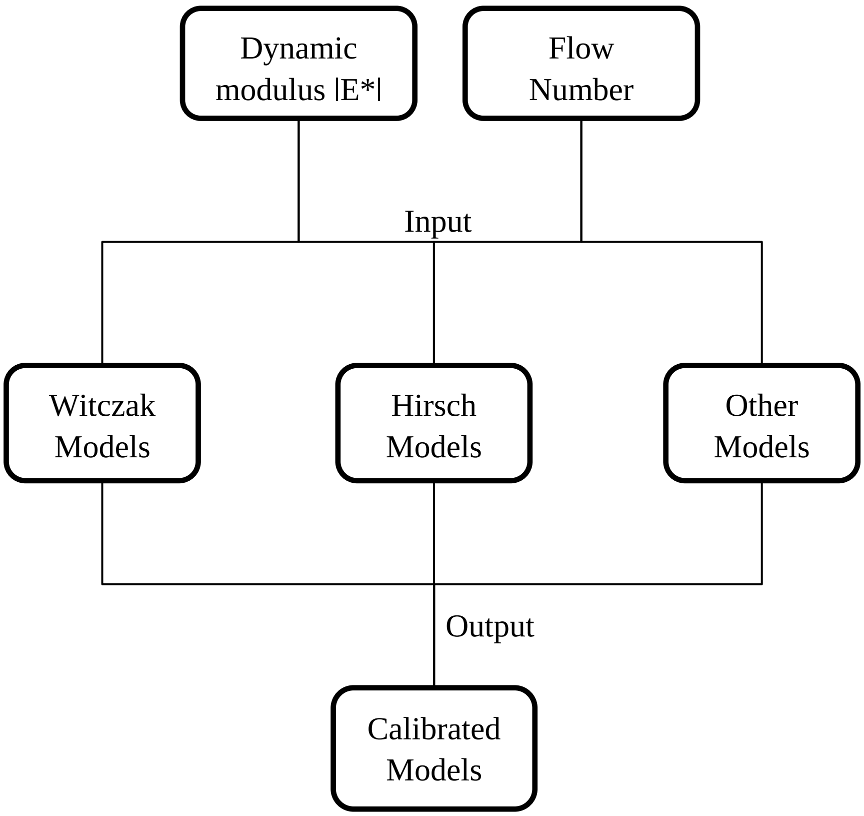

Figure 4-10 Calibrations of Dynamic Modulus and Flow Number Models in Terms of Local Data Sets

5 Methodology for Development of Prediction Models

In general, there are several models that have been developed for predicting the dynamic modulus values and other properties of various asphalt mixtures. The following is a brief description of various methodologies used to develop different models for asphalt mixes. Due to many factors, each state must establish and develop their own models that satisfies the local conditions. Several important factors that must be considered, but not limited to this list, are mentioned below:

- Layer type (e.g., surface)
- Asphalt binder properties (e.g., viscosity)
- Aggregate properties (e.g., gradation)
- Mix properties (e.g., rutting)

5.1 Traditional Witczak model

This Witczak |E*| predictive model was typically utilized to predict the dynamic modulus value of conventional asphalt mixtures as well as the modified asphalt mixtures (Witczak and Fonseca 1996; Witczak, et al, 2002; Shen and Yu 2011). MEPDG is using this model in terms of asphalt mixture properties and also some characteristics of aggregate and binder. The initial Witczak |E*| predictive model was conducted in 1996, which was developed based on a database of 2750 dynamic modulus data points collected from 205 various asphalt mixtures in the last 30 years. The data were obtained from several laboratories, including Asphalt Institute, University of Maryland, and the Federal Highway Administration. This developed predictive model (Witczak |E*|) is shown below:

$$\log|E^*| = 3.750063 + 0.02932\rho_{200} - 0.001767(\rho_{200})^2 - 0.002841\rho_4 - 0.058097V_a - 0.802208\left(\frac{V_{beff}}{V_{beff}+V_a}\right) + \frac{3.871977-0.0021\rho_4+0.003958\rho_{38}-0.000017(\rho_{38})^2+0.00547\rho_{34}}{1+e^{(-0.603313-0.313351\log(f)-0.393532\log(\eta))}}$$

(Equation 5-1)

Where,

- $|E^*|$: dynamic modulus, psi;
- η: bitumen viscosity, 10^6 Poise;
- f : loading frequency, Hz;
- V_a: air void content, %;
- V_{beff}: effective bitumen content, % by volume;
- ρ_{34}: cumulative % retained on the 19-mm (3/4) sieve;

- ρ_{38}: cumulative % retained on the 9.5-mm (3/8) sieve;
- ρ_4: cumulative % retained on the 4.76-mm (No. 4) sieve; and
- ρ_{200}: % passing the 0.075-mm (No. 200) sieve.

The initial Witczak |E*| predictive model used the viscosity of the asphalt binder (η) as a critical input parameter (Shen and Yu 2011). The two main parameters in the equation shown below, A and VTS, are the regression intercept and the regression slope, respectively. These two values can be determined from ASTM D2493-85 "Standard Viscosity-Temperature Chart for Asphalt," as shown in the following equation.

$$\log\log\eta = A + VTS\ \log T_R \qquad \textbf{(Equation 5-2)}$$

Where,

- η: bitumen viscosity, cP;
- T_R: temperature, Rankine;
- A: regression intercept; and
- VTS: regression slope of viscosity temperature susceptibility.

5.2 New Witczak model

A new Witczak model was conducted by Bari and Witczak in 2006, based on a more comprehensive study, and included a larger database with 7400 data points from 346 HMA mixtures (Bari and Witczak 2006). The new model was selected from a number of candidate models based on the tests on rationality, accuracy, precision, bias, trend, sensitivity, and overall performance. In this model, some new parameters were incorporated, such as the binder's dynamic shear modulus (G*) and phase angle (δ), which were used to replace the binder viscosity (η) and loading frequency (f) of initial Witczak model. The new Witczak model is shown in the following equation.

$$\log|E^*| = -0.349 + 0.754\left(|G_b^*|^{-0.0052}\right)\Bigg(6.65 - 0.032\rho_{200} + 0.0027\rho_{200}^2 - 0.011\rho_4 - 0.0001\rho_4^2 + 0.006\rho_{38} - 0.00014\rho_{38}^2 - 0.08V_a - 1.06\left(\frac{V_{beff}}{V_a+V_{beff}}\right)\Bigg) + \frac{2.558+0.032V_a+0.713\left(\frac{V_{beff}}{V_a+V_{beff}}\right)+0.0124\rho_{38}+0.0001\rho_{38}^2-0.0098\rho_{34}}{1+e^{(-0.7814-0.5785\log|G_b^*|+0.8834\log\delta_b)}}$$

(Equation 5-3)

Where,

- $|E^*|$: dynamic modulus, psi;
- ρ_{200}: % (by weight of total aggregate) passing the 0.075-mm (No. 200) sieve;
- ρ_4: cumulative % (by weight) retained on the 4.76-mm (No. 4) sieve;
- ρ_{34}: cumulative % (by weight) retained on the 19-mm (3/4-in.) sieve;
- ρ_{38}: cumulative % (by weight) retained on the 9.5-mm (3/8-in.) sieve;
- V_a: air void content (by volume of the mix), %;
- V_{beff}: effective binder content (by volume of the mix), %;
- $|G_b^*|$: dynamic shear modulus of binder, psi; and
- δ_b: phase angle of binder associated with |Gb*|, degree.

5.3 Hirsch model

It is considered that Hirsch model is a rational, though semi-empirical method for predicting asphalt concrete modulus. The original Hirsch model was developed by T.J. Hirsch to calculate the modulus of elasticity of cement concrete or mortar in terms of one empirical constant, the aggregate modulus and cement mastic modulus, and mix proportions. Hirsch assumed that the response of the constituent materials (cement matrix, aggregate, and the composite concrete) behaved in a linear elastic manner. Christensen et al. (2004) developed a relatively simple version of the Hirsch model to predict the dynamic modulus of hot mix asphalt. Comparing to the Witczak models, Hirsch model is considered relatively simpler which relates the dynamic modulus of the asphalt concrete (|E*|) with binder modulus (G*), percent voids in the mineral aggregate (%VMA), and percent voids filled with asphalt (%VFA). The functional form of the Hirsch model prediction equation is shown below.

$$\boldsymbol{|E^*| = P_c\left[4,200,000\left(1-\frac{VMA}{100}\right)+3|G^*|_{binder}\left(\frac{VFA\times VMA}{10,000}\right)\right] + (1-P_c)\left[\frac{1-\frac{VMA}{100}}{4,200,000}+\frac{VMA}{VFA\times 3|G^*|_{binder}}\right]^{-1}}$$

(Equation 5-4)

Where,

- $|E^*|$: dynamic modulus, psi, (same temperature and loading frequency as G*);
- $|G^*|_{binder}$: binder dynamic modulus, psi;
- VMA: voids in the mineral aggregate, %;
- VFA: voids filled with asphalt, %; and
- P_c: aggregate contact factor.

Where P_c, the aggregate contact factor, is calculated based on the following formula.

$$P_c = \frac{\left(20+\frac{VFA \times 3|G^*|_{binder}}{VMA}\right)^{0.58}}{650+\left(\frac{VFA \times 3|G^*|_{binder}}{VMA}\right)^{0.58}} \qquad \textbf{(Equation 5-5)}$$

5.4 Other |E*| predictive models

Abdo et al. (2009) developed a model to predict |E*| based on the properties of the asphalt mixture constituents. The model parameters were determined by dimensional analysis and new mix design parameters. The developed model is shown below:

$$|E^*| = 1.08\left(\frac{G^* \times GS \times \%G_{mm}}{P_b(1-P_b)}\right)^{0.55} \qquad \textbf{(Equation 5-6)}$$

Where,

- *|E*|:* Dynamic Modulus for Asphalt Mix, MPa;
- *G*:* Dynamic Shear Modulus for RTFO Aged Binder, MPa;
- P_b: Percent Binder Content;
- *GS:* Gyratory Stability, kNm;
- G_{mb}: Bulk Specific Gravity of Mix, Gmb = Gmm (1-AV%);
- G_{mm}: Maximum Specific Gravity of Mix; and
- *%AV:* Percent Air Voids.

In Florida, Yang et al (2011) developed a predicting model to characterize dynamic modulus for 20 selected Superpave asphalt mixtures. This developed model included the variables related to aggregate gradation, mixture volumetrics, and percent weight of asphalt content, loading frequencies, and temperatures. The developed model is shown below.

$$\log|E^*| = 2.312 + 0.01\rho_{200} + 0.01\rho_8 - 0.013\rho_4 - 0.002\rho_{3/8} + 0.024P_b - 0.043VFA + \frac{[-1.34-0.019\rho_8+0.022\rho_4+0.004\rho_{3/8}-0.055P_b+0.052VFA]}{1+e^{(-8.267-0.722\log f+5.397\log T)}}$$

(Equation 5-7)

Where,

- *|E*|*: dynamic modulus, in 10^5 psi;
- *T*: test temperature, in °C;
- *f*: load frequency, in Hz;
- *VFA*: voids filled with asphalt, % by volume;

- P_b: Percent weight of asphalt, % by weight;
- $\rho_{3/8}$: cumulative percent retained on 3/8 in (9.5mm) sieve, % by weight;
- ρ_4: cumulative percent retained on No. 4 (4.75mm) sieve, % by weight;
- ρ_8: cumulative percent retained on No. 8 (2.36mm) sieve, % by weight; and
- ρ_{200}: percent passing on No. 200 (0.075mm) sieve, % by weight.

5.5 Flow number model

Over the past few years, there have been significant efforts in establishing a testing method to evaluate the rutting performance of various asphalt mixtures. Some researchers considered that the flow number was an effective tool as a rutting performance indicator.

The flow number test defined by AASHTO TP 79 provides the three phases of flow (primary, secondary, and tertiary) within an asphalt mix with particular emphasis on tertiary flow of an asphalt mixture. Flow number is obtained from the repeated load permanent deformation test to evaluate the resistance of an asphalt mixture to tertiary flow and it can be obtained based on the AMPT tests. In order to predict the flow number of an asphalt mixture, some researchers have been proposing different prediction models to provide guidance on the understanding of flow characteristics.

Kaloush (2001) developed a model to predict the flow number (FN) of an HMA mixture based on mixtures' volumetric properties, binder type, and test temperature over the last decade. The model used 135 unconfined laboratory FN tests and is presented as follows:

$$\boldsymbol{FN = (432367000)T^{-2.215}Visc^{0.312}V_{beff}^{-2.6604}V_a^{-0.1525}} \qquad \textbf{(Equation 5-8)}$$

Where,

- *FN:* Flow Number;
- *T:* Test Temperature, °F;
- *Visc*: Binder Viscosity at 70°F, 106 poise;
- V_{beff}: Effective Asphalt Content, % volume; and
- V_a: Air Voids, %.

Kvasnak et al (2007) conducted a Flow Number predictive equation, as shown below, based on 17 dense graded mixtures from the State of Wisconsin. In this model, the number of gyrations (Gyr) was found to be the most significant factor. However, it was recommended that the model should only be applied within the data ranges used for the dense graded HMA mixes.

$$\log FN = 2.866 + 0.00613Gyr + 3.86Visc - 0.072VMA + 0.0282\rho_4 - 0.051\rho_{16} + 0.075\rho_{200}$$

(Equation 5-9)

In addition, Rodezno, M. C. and Kaloush, et al (2010) proposed an equation to predict flow number for the mixtures. In this final model, the variables included the viscosity at testing temperature (V_1), the air voids level, the temperature, three variables related with the gradation of the mix (%P_{200}, %R_{04} and %R_{34}), and the shear and normal stresses (p and q) that contribute to the model in the arithmetic and logarithmic terms. The presence of the p and q variables indicates the importance of the combination of stress levels applied to the samples. The equation is shown below.

$$\log FN = 2.174 + 0.649 \,\mathrm{Log}\, V_1 + 0.101P_{200} + 18.465 \,\mathrm{Log}\, p + 0.0140R_{04} - 0.084V_a - 18.901 \log q - 0.872R_{34} + 0.182q - 0.193p - 0.871 \log T$$

(Equation 5-10)

Christensen (2008) applied various statistical techniques to conduct the relationships between the flow number with complex modulus, air void content and applied stress level, and developed a model based on data regression:

$$N_f = 4.96 \times 10^{-8} \beta_i |E^*|^{2.478} \sigma^{-0.089VTM - 0.187|E^*|}$$ **(Equation 5-11)**

Where,

- N_f : flow number;
- β : indicator variable, adjusting regression constant for i[th] projects/sections;
- $|E^*|$: complex modulus (lb/in^2) at 10 Hz and same temperature as flow number test;
- *VTM*: air voids in flow number test specimen, volume %; and
- σ : deviator stress for flow number stress, lb/in^2.

6 Results

Dynamic modulus testing and flow number testing were conducted for each asphalt mixture at three temperatures and at various frequencies as shown in previous chapters. In terms of various types of mixtures, all results were categorized into several sections as described in experimental design section of this report.

Several factors such as aggregate source, binder source, mixture type, warm mix asphalt (WMA) type, and liquid anti-strip additive (LASA) type were used to characterize the dynamic modulus, phase angle, and flow number of the mixtures. These factors were analyzed within several parameters such as temperature and frequency. In addition, some mixtures were produced without RAP, and the results were analyzed against mixes containing RAP. It was found that the general dynamic modulus and phase angles of these mixtures had similar trends to those mixtures with RAP. Therefore, these trends were not analyzed in detail in this chapter, but all figures are presented in Appendices A and B. Table 6-1 shows the abbreviations for all of the mixtures used for this report.

Table 6-1 Labels of Various Mixtures Used in This Study

RAP	Mixture type	Other Variable	Aggregate Source						
			I	II	III	IV	V	VI	VII
With RAP	Surface A		I A	II A1, II A2	III A1, III A2	IV A	V A	VI A	-
	Surface B		I B1, I B2	II B	III B1, III B2	IV B	V B	VI B	-
	Surface C		I C	II C	III C	IV C	V C	VI C	-
	Surface D		I D	II D	III D	IV D	V D	VI D	-
	Surface E		I E	II E	III E	IV E	V E	VI E	-
	Intermediate A		-	-	-	IV IA	V IA	-	-
	Intermediate B		-	-	-	IV IB	V IB	-	-

RAP	Mixture Type	Other Variable	Aggregate Source						
			I	II	III	IV	V	VI	VII
With RAP	Intermediate B Special		-	II IB	-	-	-	-	VII IB
	Intermediate C		-	-	-	IV IC	V IC	-	-
	Base A		-	-	-	IV SA	V SA	-	-
	Base B		-	-	-	IV SB	V SB	-	-
	Surface A	PG 76-22 binder source 2	-	-	-	IV AN	V AN	-	-
	Surface B	PG 64-22 binder source 2	-	-	-	IV BN	V BN	-	-
	Surface C	WMA Chemical Additive	-	-	-	IV CE	V CE	-	-
	Surface C	WMA Foaming	-	-	-	IV CF	V CF	-	-
	Surface C	Liquid ASA1	-	-	-	IV CM	V CM	-	-
	Surface C	Liquid ASA2	-	-	-	IV CA	V CA	-	-
	Surface A - aging	PG 76-22 binder source 1	-	-	-	IV AG	V AG	-	-
	Surface B - aging	PG 64-22 binder source 1	-	-	-	IV BG	V BG	-	-
	Surface C - aging	PG 64-22 binder source 1	-	-	-	IV CG	V CG	-	-

RAP	Mixture Type	Other Variable	Aggregate Source						
			I	II	III	IV	V	VI	VII
No RAP	Surface A		-	-	-	IV AO	V AO	VI AO	-
	Surface B		-	-	-	IV BO	V BO	VI BO	-
	Surface C		-	-	III CO	IF CO	V CO	VI CO	-
	Surface D		-	-	III DO	IV DO	V DO	VI DO	-
	Surface E		I EO	-	III EO	IV EO	V EO	VI EO	-
	Intermediate A		-	-	-	IV IAO	V IAO	-	-
	Intermediate B		-	-	-	IV IBO	V IBO	-	-
	Intermediate C		-	-	-	IV ICO	V ICO	-	-
	Base A		-	-	-	IV SAO	V SAO	-	-
	Base B		-	-	-	IV SBO	V SBO	-	-
	Surface A	PG 76-22 binder source 2	-	-	-	IV AON	V AON	-	-
	Surface B	PG 64-22 binder source 2	-	-	-	IV BON	V BON	-	-
	Surface C	WMA Chemical Additive	-	-	-	IV COE	V COE	-	-
	Surface C	WMA Foaming	-	-	-	IV COF	V COF	-	-
	Surface C	Liquid ASA1	-	-	-	IV COM	V COM	-	-

RAP	Mixture Type	Other Variable	Aggregate Source						
			I	II	III	IV	V	VI	VII
No RAP	Surface C	Liquid ASA2	-	-	-	IV COA	V COA	-	-
	Surface A - aging	PG 76-22 binder source 1	-	-	-	IV AOG	V AOG	-	-
	Surface B - aging	PG 64-22 binder source 1	-	-	-	IV BOG	V BOG	-	-
	Surface C - aging	PG 64-22 binder source 1	-	-	-	IV COG	V COG	-	-

Notes: All mixtures used binder from source 1 except that those were defined in this Table. In addition, all Surface Type A mixtures used PG 76-22 binder. All other mixtures used PG 64-22 binder.

6.1 Dynamic Modulus and Phase Angle

6.1.1 Effect of Aggregate Source on Dynamic Modulus and Phase Angle of Different Types of Surface Mixtures

Figure 6-1 shows the dynamic modulus values of various Surface Type A mixtures containing RAP in terms of six aggregate sources tested at three temperatures. In addition, there were two different Surface Type A mix designs utilized for aggregate sources II and III. The second mix design for each of those aggregate sources (II A2 and III A2) utilized the updated finer SCDOT gradation requirements from SCDOT (SC-M-402, July 2017 version) as well as incorporating the newly-adopted corrected optimum asphalt content (COAC) allowed by SCDOT. It can be seen that the dynamic modulus values increased with the increase of frequency. As shown in Figure 6-1, the order of dynamic modulus values from high to low for Surface Type A mixtures with respect to aggregate source was IV A, I A, I A, III A2, III A1, II A1, and II A2.

The new Surface Type A mix designs containing the finer gradation and the COAC did not appear to affect the dynamic modulus values as much as aggregate source did. However, dynamic modulus values for the new mix design with aggregate source II did appear to be slightly lower than the values for the old mix design with that aggregate source. The scope of this project did not allow further investigation of this effect.

Mixture V A exhibited different trends at different temperatures. Mixture V A generally had a lower dynamic modulus than other mixtures at 4°C (39.2°F), while it had a higher dynamic modulus than other mixtures at 45°C (113°F). It can be concluded that temperature had a larger impact on the dynamic modulus of mixtures using aggregate V than that of other mixtures. In addition, it can be observed in Figure 6-1 that with the increase of temperature, the dynamic modulus values of mixtures decreased. The dynamic modulus values of mixtures ranged from 10,000 to 20,000 MPa at 4°C (39.2°F), but only ranged from 2,000 to 10,000 MPa at 20°C (68°F), and from 100 to 1,000 MPa at 45°C (113°F).

Similar trends of dynamic modulus values were found for the Surface Type B, C, D, and E mixtures in this study. These findings and the corresponding figures are presented in Appendix A.

Figure 6-2 shows the phase angle values of various Surface Type A mixtures containing RAP in terms of six aggregate sources tested at three temperatures. As shown in Figure 6-2, the order of phase angle values from high to low for Surface Type A mixtures was II A2, II A1, III A2, VI A, IV A, III A1, and I A. Similar to the dynamic modulus results, mixture V A exhibited different trends at different temperatures. V A had lower phase angle values than other mixtures both at 4°C (39.2°F) and 20°C (68°F), while it had mid-range phase angle values at 45°C (113°F) and low frequency.

The new Surface Type A mix designs containing the finer gradation and the COAC did not appear to affect the phase angle values as much as aggregate source did. However, phase angle values for the new mix design with aggregate source II did appear to be slightly higher than the values for the old mix design with that aggregate source. The scope of this project did not allow further investigation of this effect.

In Figure 6-2, the phase angle values showed different trends at different temperatures. The phase angle values of mixtures decreased with the increase of frequency at 4°C (39.2°F) and 20°C (68°F). However, with the increase of frequency, the phase angle values of mixtures initially increased and then approximately remained unchanged at 40°C (104°F). The phase angle values of mix V A initially increased and then decreased at 45°C (113°F). Moreover, it can be observed that the phase angle values of mixtures increased with the increase of temperature.

Similar trends of phase angle values were found for the Surface Type B, C, D, and E mixtures in this research. The findings and the corresponding figures have been presented in Appendix A.

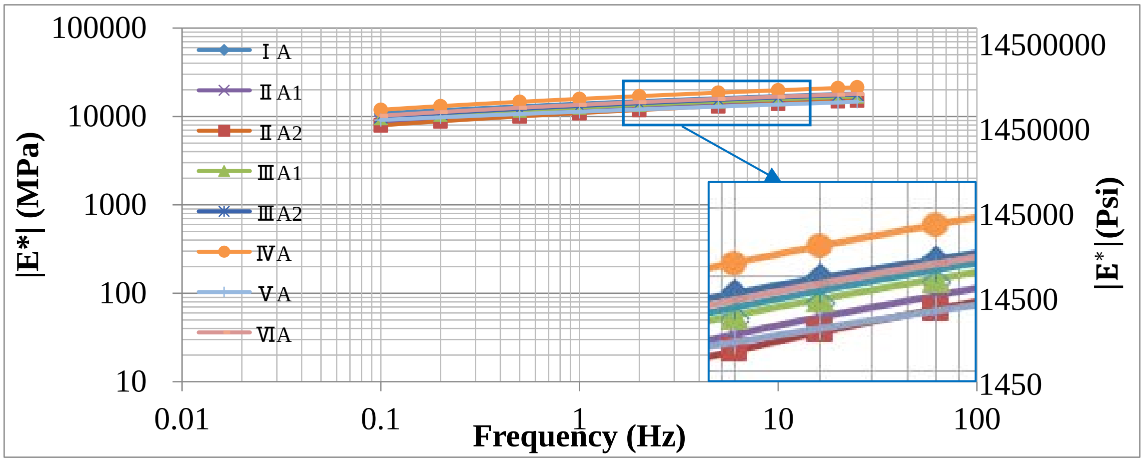

(a)

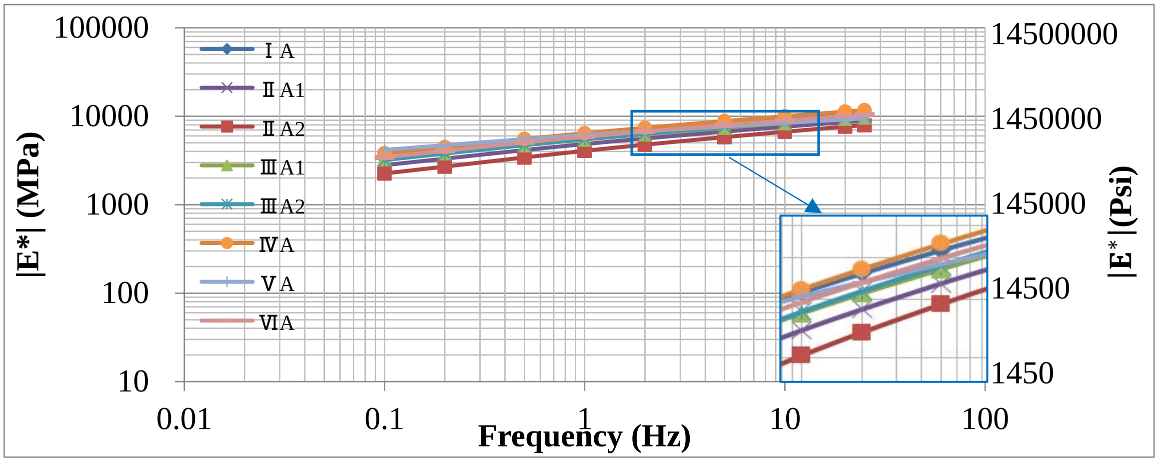

(b)

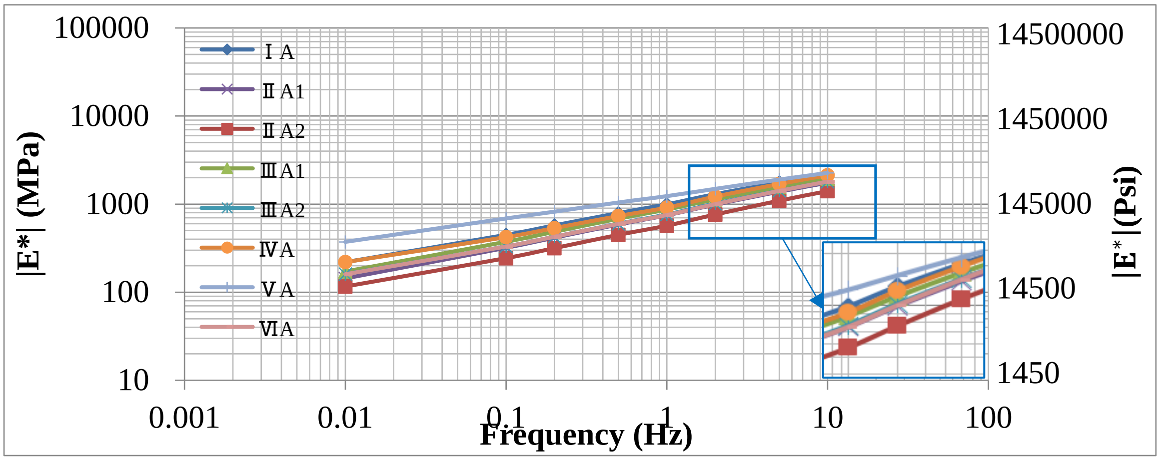

(c)

Figure 6-1 Dynamic Modulus Values of Surface Type A Mixtures with RAP in Terms of Aggregate Source (a) at 4℃ (39.2°F), (b) at 20℃ (68°F), (c) at 45℃ (113°F)

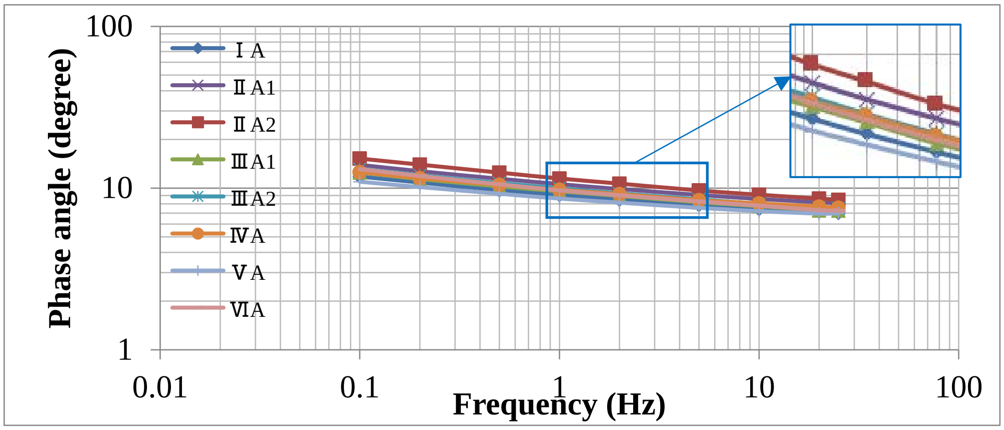

(a)

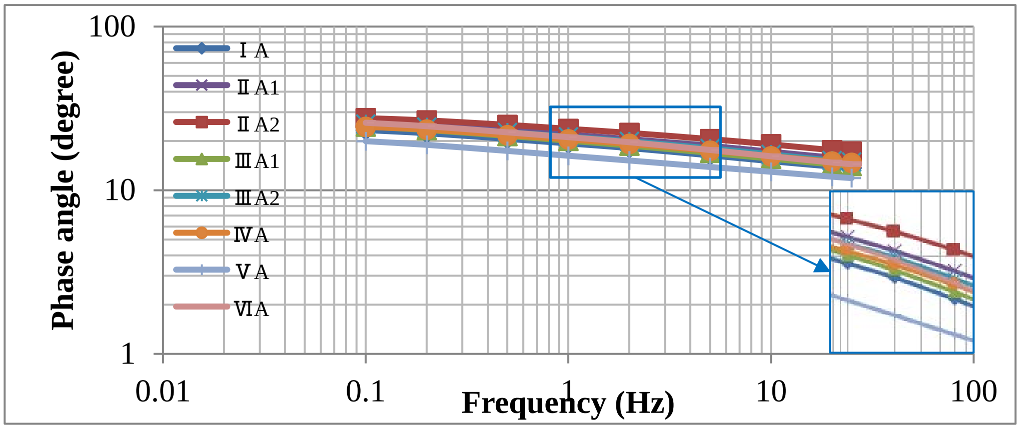

(b)

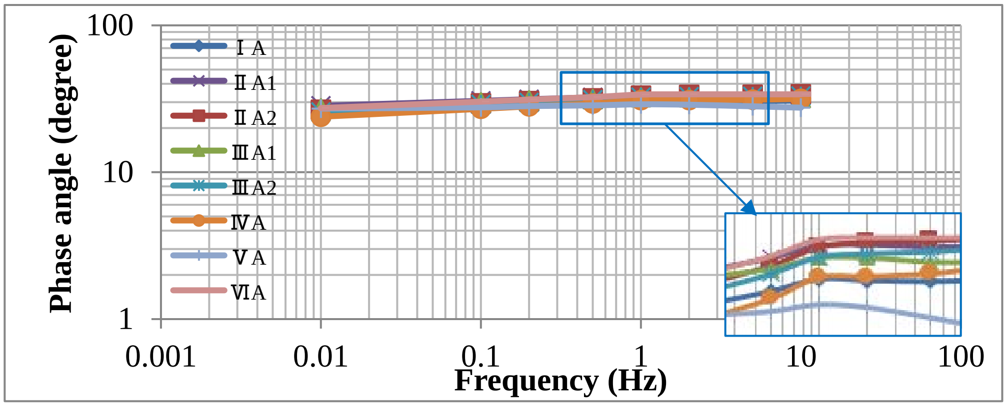

(c)

Figure 6-2 Phase Angle Values of Surface Type A Mixtures with RAP in Terms of Aggregate Source (a) at 4°C (39.2°F), (b) at 20°C (68°F), (c) at 45°C (113°F)

6.1.2 Effect of Aggregate Source on Dynamic Modulus and Phase Angle of Different Types of Intermediate Mixtures

Figure 6-3 shows the dynamic modulus values of various Intermediate Type A mixtures containing RAP in terms of two aggregate sources (IV and V) tested at three temperatures. It can be seen that the dynamic modulus values increased with the increase of frequency. In Figure 6-3, the mixtures containing aggregate IV had slightly higher dynamic modulus values than the mixtures containing aggregate V in most cases. However, mixture V IA had higher dynamic modulus values than mixture IV IA at 40℃ (104°F) at a low frequency. In addition, it can be observed in Figure 6-3 that with the increase of temperature, the dynamic modulus values of mixtures decreased.

Similar trends of dynamic modulus values were found for the Intermediate Type B and C mixtures tested in this study. The findings and the corresponding figures are presented in Appendix A.

In addition to the Intermediate Type A, B, and C mixtures made with aggregate sources IV and V, several Intermediate Type B Special mixtures were made with two additional aggregate sources, II and VII. These mixtures were added towards the end of the project, and aggregate sources were selected by the Steering Committee based on materials used in field pilot projects. The dynamic modulus values of the Intermediate Type B Special mixtures were similar to those of the other Intermediate Type B mixtures, regardless of aggregate source, test temperature, and frequency (Appendix A, Figure 9-23). As with all of the other Intermediate Type B mixtures, increased loading frequency resulted in higher dynamic modulus values, and increased test temperatures resulted in lower dynamic modulus values.

Figure 6-4 shows the phase angle values of various Intermediate Type A mixtures containing RAP in terms of two aggregate sources tested (IV and V) at three different temperatures. Figure 6-4 shows that mixtures IV IA and V IA have similar phase angle values. In Figure 6-4, the phase angle values of mixtures showed different trends at different temperatures. The phase angle values of the mixtures decreased with the increase of frequency at 4℃ (39.2°F) and 20℃ (68°F). However, with the increase of frequency, the phase angle values of mixtures initially increased and then approximately remained unchanged at 40℃ (104°F). The phase angle values of mixture V IA initially increased and then decreased at 40℃ (104°F). Moreover, it can be observed that the phase angle values of mixtures generally increased with the increase of temperature.

Similar trends of phase angle values were found for the Intermediate Type B and C mixtures tested in this study. The findings and the corresponding figures are presented in Appendix A.

In addition to the Intermediate Type A, B, and C mixtures made with aggregate sources IV and V, several Intermediate Type B Special mixtures were made with two additional aggregate sources, II and VII. These mixtures were added towards the end of the project, and aggregate sources were selected by the Steering Committee based on materials used in field pilot projects. The phase angle values of the Intermediate Type B Special mixtures were similar to those of the other Intermediate Type B mixtures, regardless of aggregate source, test temperature, and frequency (Appendix A, Figure 9-24). As with all of the other Intermediate Type B mixtures, phase angle values decreased with the increase of frequency at 4°C (39.2°F) and 20°C (68°F). However, with the increase of frequency, the phase angle values of mixtures initially increased and then approximately remained unchanged at 40℃ (104°F).

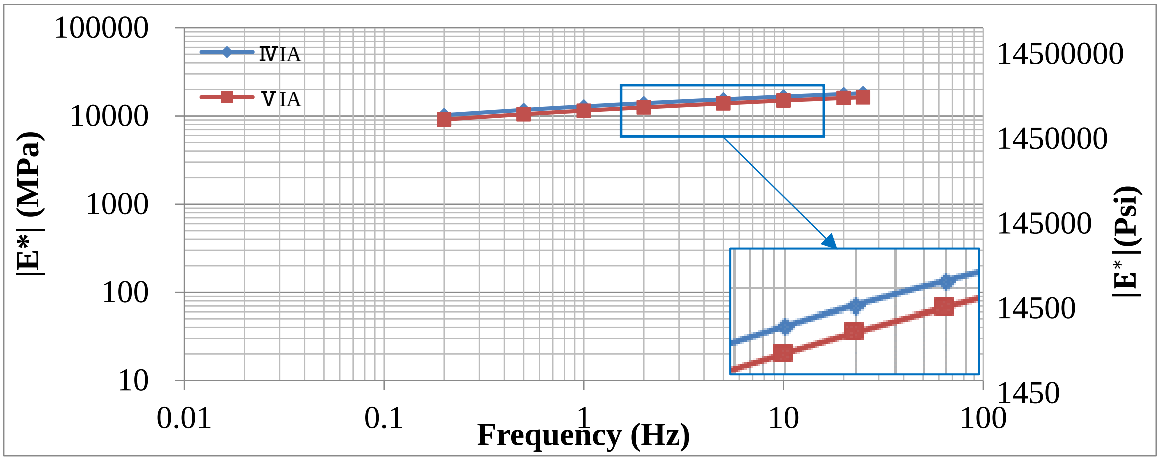

(a)

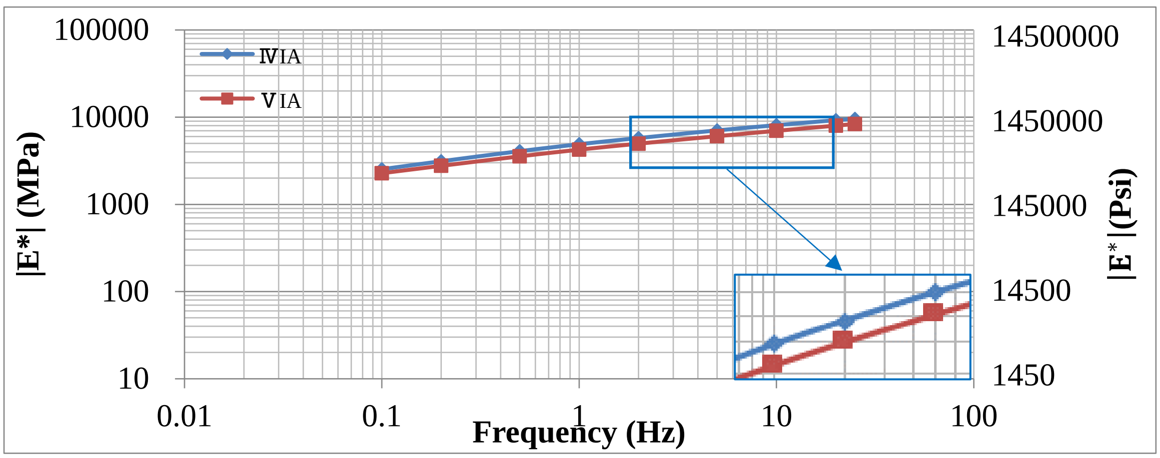

(b)

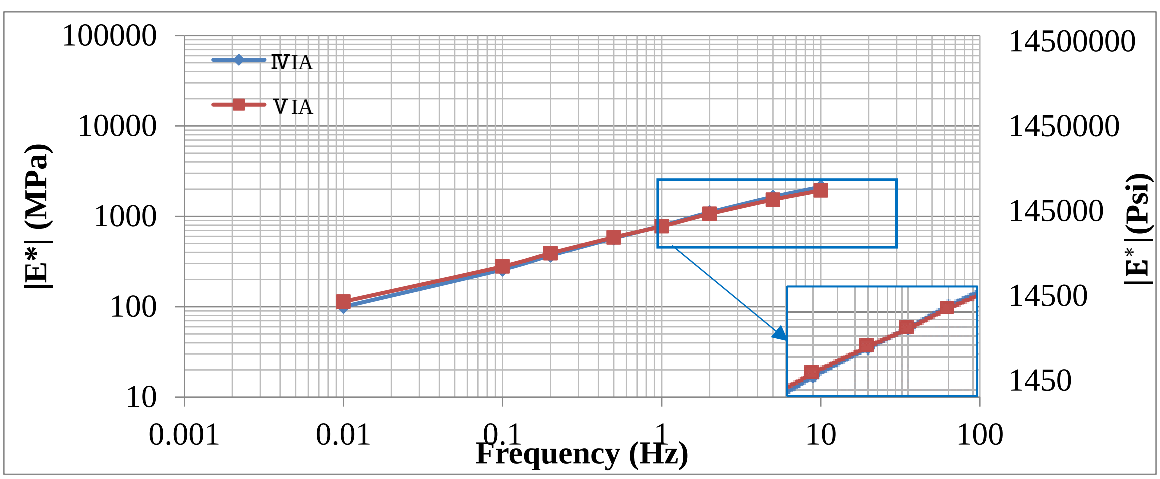

(c)

Figure 6-3 Dynamic Modulus Values of Intermediate Type A Mixtures with RAP in Terms of Aggregate Source (a) at 4°C (39.2°F), (b) at 20°C (68°F), (c) at 40°C (104°F)

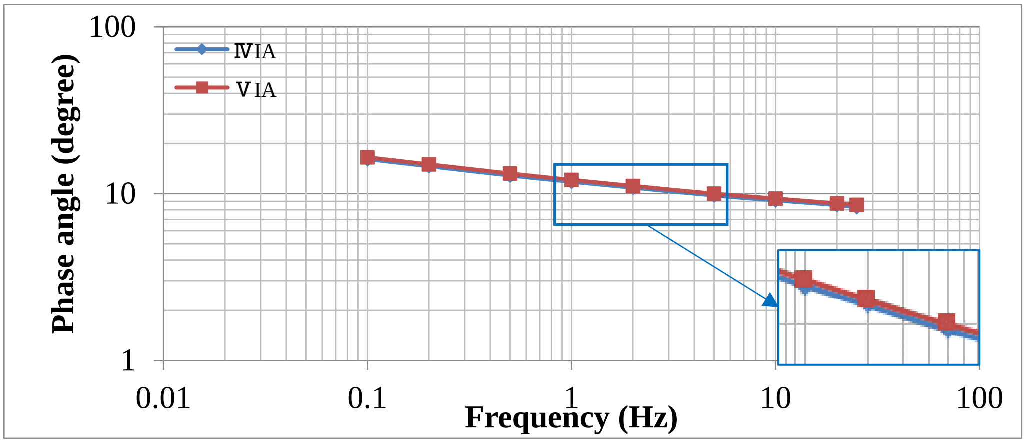

(a)

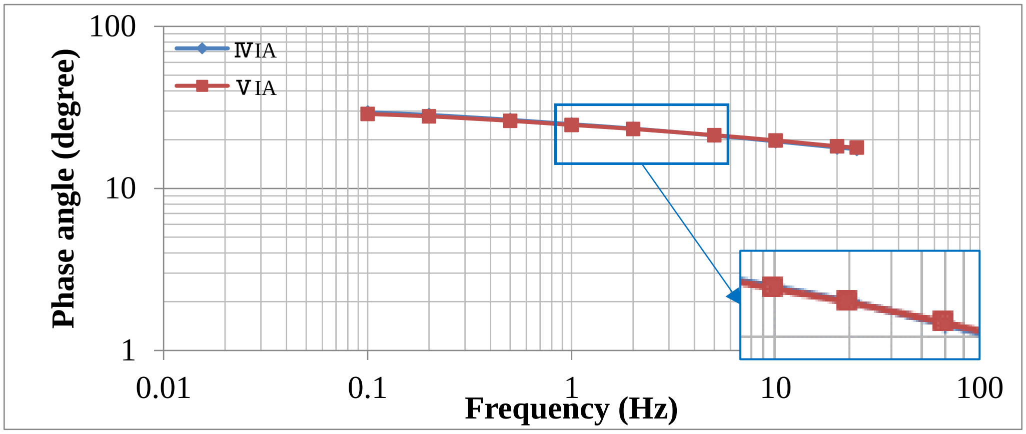

(b)

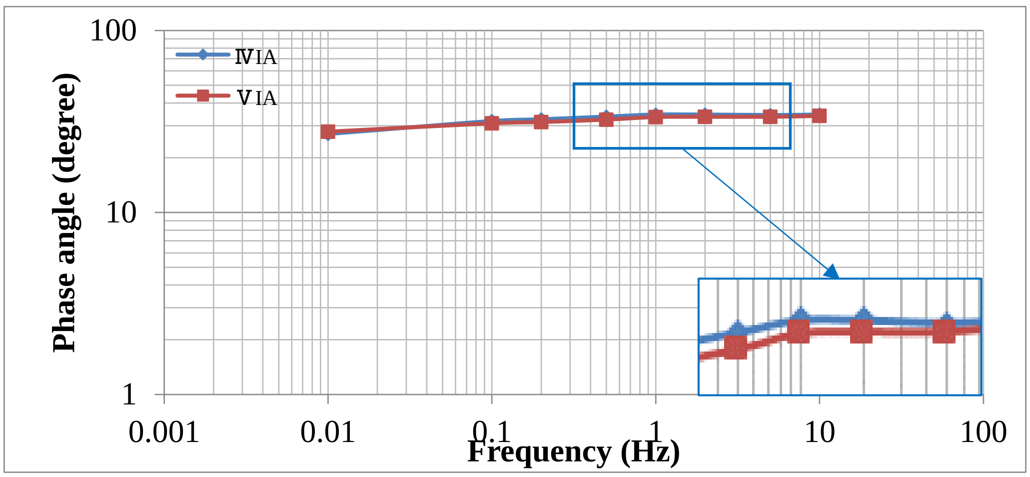

(c)

Figure 6-4 Phase Angle Values of Intermediate Type A Mixtures with RAP in Terms of Aggregate Source (a) at 4°C (39.2°F), (b) at 20°C (68°F), (c) at 40°C (104°F)

6.1.3 Effect of Aggregate Source on Dynamic Modulus and Phase Angle of Different Types of Base Mixtures (Types A and B)

Figure 6-5 shows the dynamic modulus values of various Base Type A mixtures containing RAP in terms of two aggregate sources (IV and V) studied at three temperatures. It can be seen that the dynamic modulus values increased with the increase of frequency. In Figure 6-5, mixtures containing aggregate IV had slightly higher dynamic modulus values than the mixtures made with aggregate V in most cases. However, mixture V SA had higher dynamic modulus values than IV SA at 40°C (104°F) at a low frequency. In addition, it can be observed in Figure 6-5 that with the increase of temperature, the dynamic modulus values of mixtures decreased.

Similar trends of dynamic modulus values were found for the Base Type B mixtures tested in this study. The findings and the corresponding figures are presented in Appendix A.

Figure 6-6 shows the phase angle values of various Base Type A mixtures containing RAP in terms of two aggregate sources (IV and V) tested at three different temperatures. As shown in Figure 6-6, the phase angle values of mixture IV SA were slightly higher than those of mixture V SA in most cases. However, mixture V SA had higher phase angle values than IV SA at 40°C (104°F) at a low frequency. The phase angle values of mixtures decreased with the increase of frequency at 4°C (39.2°F) and 20°C (68°F). However, with the increase of frequency, the phase angle values of mixtures initially increased but then decreased at 40°C (104°F). Moreover, it can be observed that the phase angle values of mixtures increased with the increase in temperature.

Similar trends of phase angle values were found for the Base Type B mixtures tested in this study. The figures and corresponding findings are presented in Appendix A.

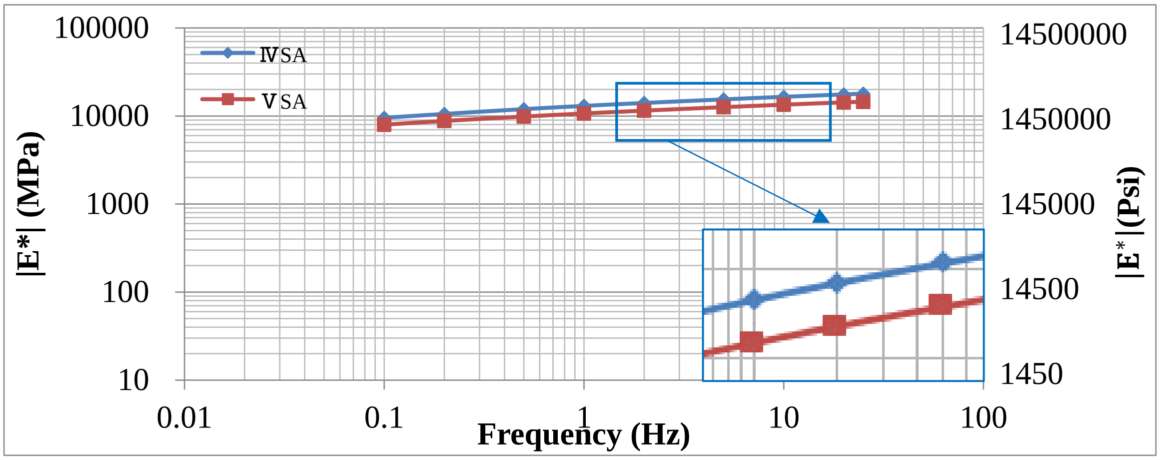

(a)

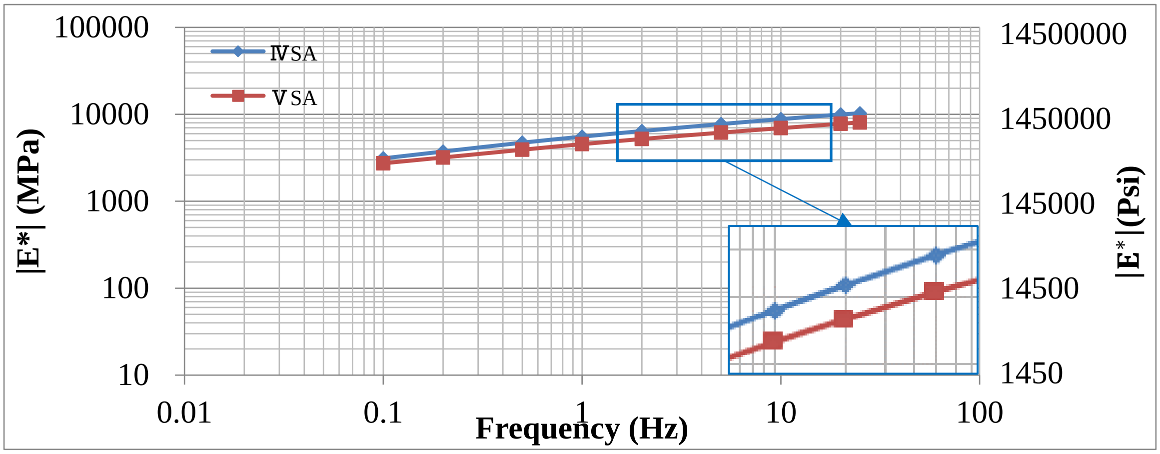

(b)

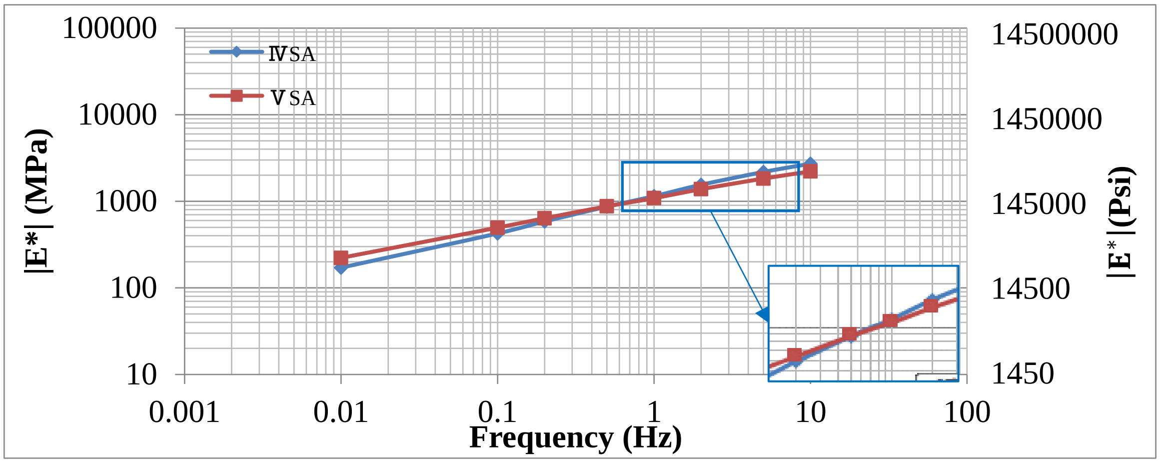

(c)

Figure 6-5 Dynamic Modulus Values of Base Type A Mixtures with RAP in Terms of Aggregate Source (a) at 4°C (39.2°F), (b) at 20°C (68°F), (c) at 40°C (104°F)

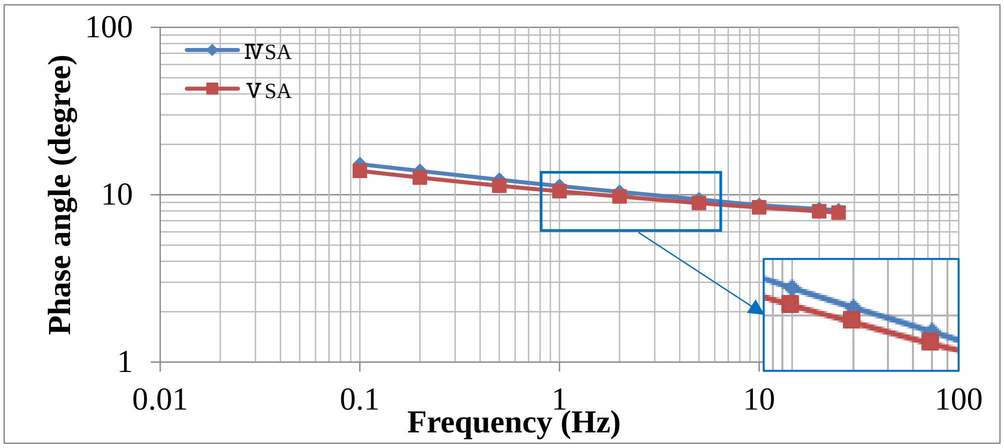

(a)

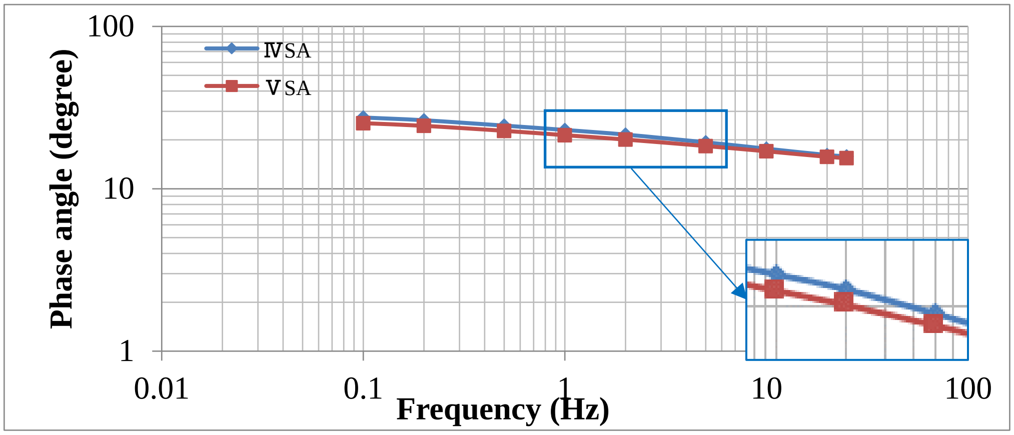

(b)

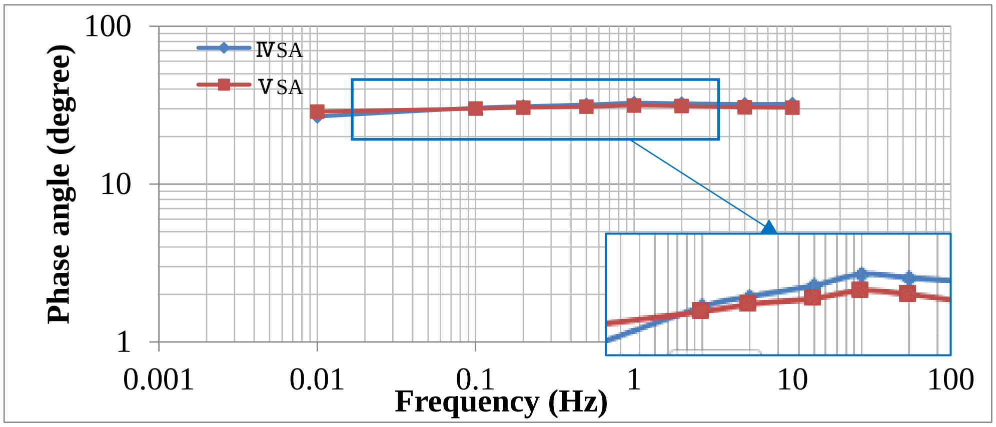

(c)

Figure 6-6 Phase Angle Values of Base Type A Mixtures with RAP in Terms of Aggregate Source (a) at 4°C (39.2°F), (b) at 20°C (68°F), (c) at 40°C (104°F)

6.1.4 Effect of Aggregate Source on Dynamic Modulus and Phase Angle of Surface Mixtures (Types A and B) Made with Different Aggregate Types and Binder Source 2

Figure 6-7 shows the dynamic modulus values of various Surface Type A mixtures containing RAP using PG 76-22 asphalt source 2 (Axeon) in terms of two aggregate sources (IV and V) tested at three temperatures. It can be seen that the dynamic modulus values increased with the increase of frequency. In Figure 6-7 mixtures made with aggregate IV had slightly higher dynamic modulus values in most cases than mixtures containing aggregate V. However, mixture V AN had similar dynamic modulus values compared to mixture IV AN at 40℃ (104°F) at a low frequency. In addition, it can be observed from Figure 6-7 that the dynamic modulus of mixtures decreased with the increase of temperature.

Similar trends of dynamic modulus values were found for the Surface Type B mixtures made with PG 64-22 from asphalt binder source 2 tested in this study. The findings of this portion of the research work are presented in Appendix A.

Figure 6-8 shows the phase angle values of various Surface Type A mixtures containing RAP using PG 76-22 asphalt from source 2 in terms of two aggregate sources (IV and V) tested at three temperatures. In Figure 6-8, the phase angle values of mixture IVAN were slightly higher than that of mixture V AN in most cases. However, mixture V SA had higher phase angle values than mixture IV SA at 40℃ (104°F) at a low frequency. The phase angle values of mixtures decreased with the increase of frequency at 4℃ (39.2°F) and 20℃ (68°F). However, with the increase of frequency, the phase angle values of mixtures increased at 40℃ (104°F). Moreover, it can be observed that the phase angle values of mixtures increased with the increase of temperature.

Similar trends of phase angle values were found for the Surface Type B mixtures containing PG 64-22 from asphalt binder source 2 tested in this study. The findings are shown in figures presented in Appendix A.

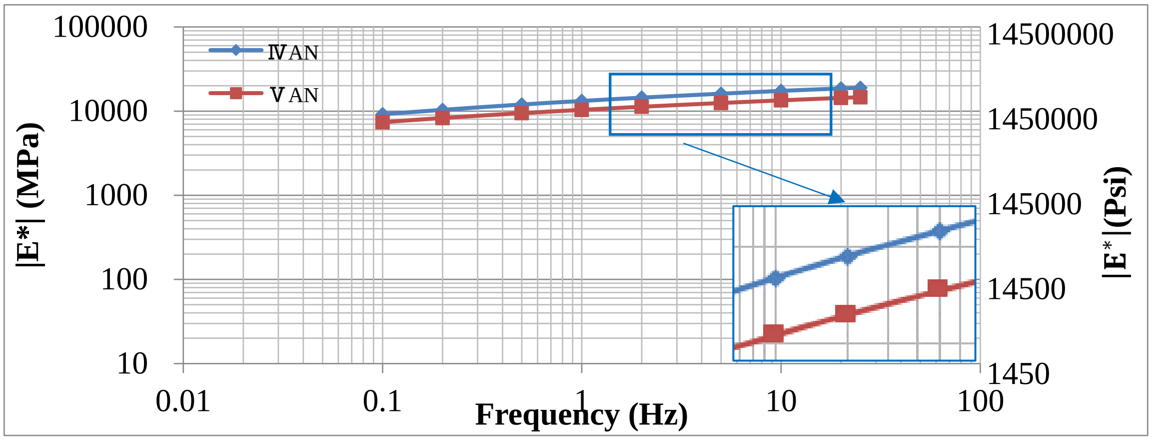

(a)

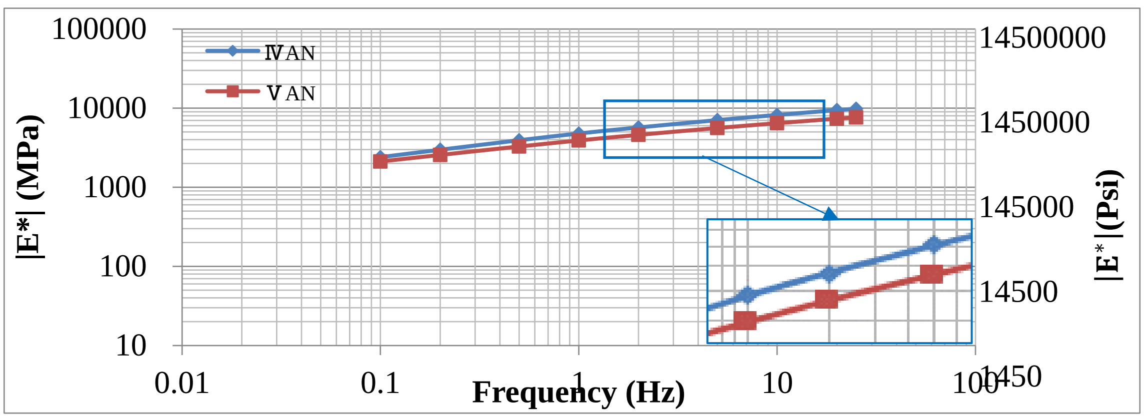

(b)

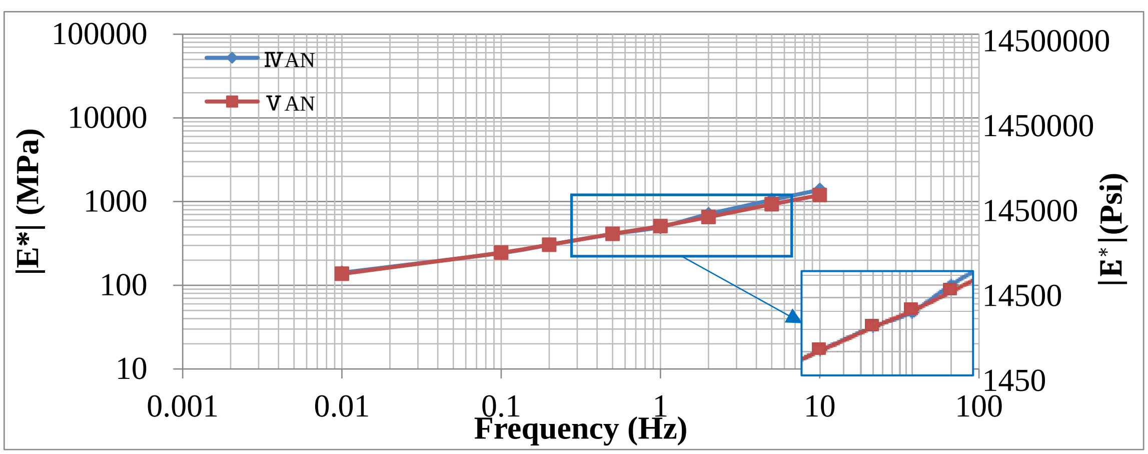

(c)

Figure 6-7 Dynamic Modulus Values of Various Surface Type A Mixtures with RAP and PG 76-22 Asphalt Source 2 in Terms of Aggregate Source (a) at 4°C (39.2°F), (b) at 20°C (68°F), (c) at 45°C (113°F)

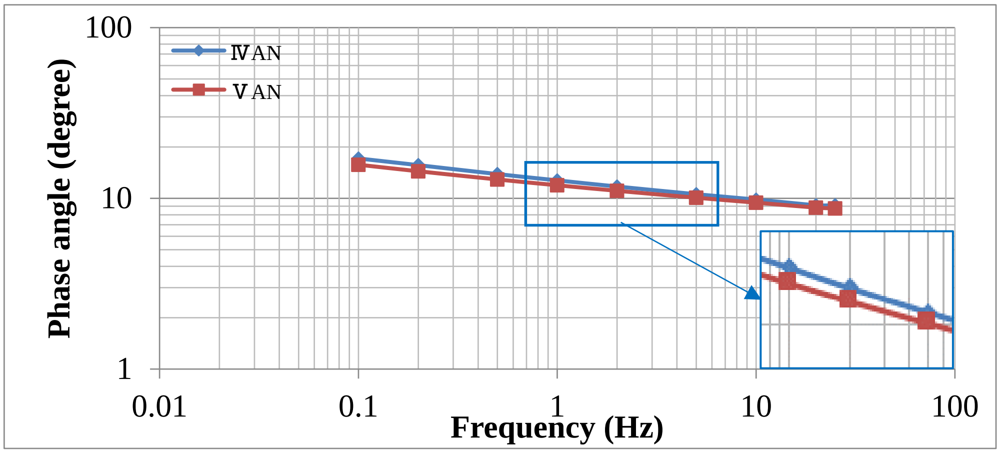

(a)

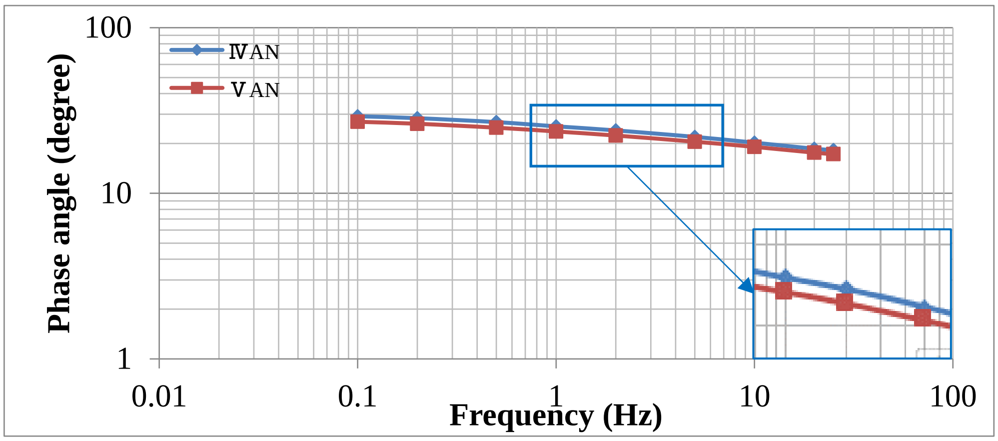

(b)

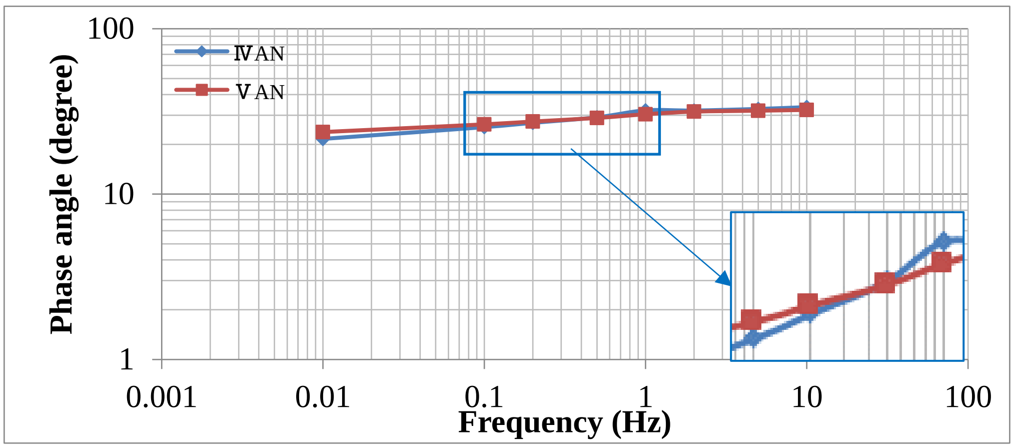

(c)

Figure 6-8 Phase Angle Values of Various Surface Type A Mixtures with RAP and PG 76-22 Asphalt Source 2 in Terms of Aggregate Source (a) at 4°C (39.2°F), (b) at 20°C (68°F), (c) at 45°C (113°F)

6.1.5 Effect of Aggregate Source on Dynamic Modulus and Phase Angle of Surface Type C Mixtures Made with WMA

Figure 6-9 shows the dynamic modulus values of various Surface Type C mixtures containing RAP and a WMA chemical additive in terms of two aggregate sources (IV and V) tested at three temperatures. It can be seen that the dynamic modulus values increased with the increase of frequency. In Figure 6-9, the mixtures made with aggregate Ⅳ had slightly higher dynamic modulus values than the mixtures containing aggregate Ⅴ. In addition, it can be observed in Figure 6-9 that with the increase of the temperature, the dynamic modulus of mixtures decreased.

Similar trends of dynamic modulus values were found for the WMA mixtures made using the foaming technology tested in this study. The figures shown in Appendix A represent the findings.

Figure 6-10 shows the phase angle values of various Surface Type C mixtures containing RAP and a WMA chemical additive in terms of two aggregate sources (IV and V) tested at three temperatures. In Figure 6-10, the phase angle values of mixture IV AN were slightly higher than that of mixture V AN at 40°C (104°F), while the phase angle values of mixture V AN were higher than mixture IV AN at both 4°C (39.2°F) and 20°C (68°F). The phase angle values of mixtures decreased with the increase of frequency at 4°C (39.2°F) and 20°C (68°F). However, with the increase of frequency, the phase angle values of mixtures initially increased and then remained somewhat unchanged at 40°C (104°F). Moreover, it can be observed that the phase angle values of mixtures increased with the increase of temperature.

Similar trends of phase angle values were found for the WMA mixtures made using the foaming technology tested in this study. The figures for the testing for this portion of the research work are presented in Appendix A.

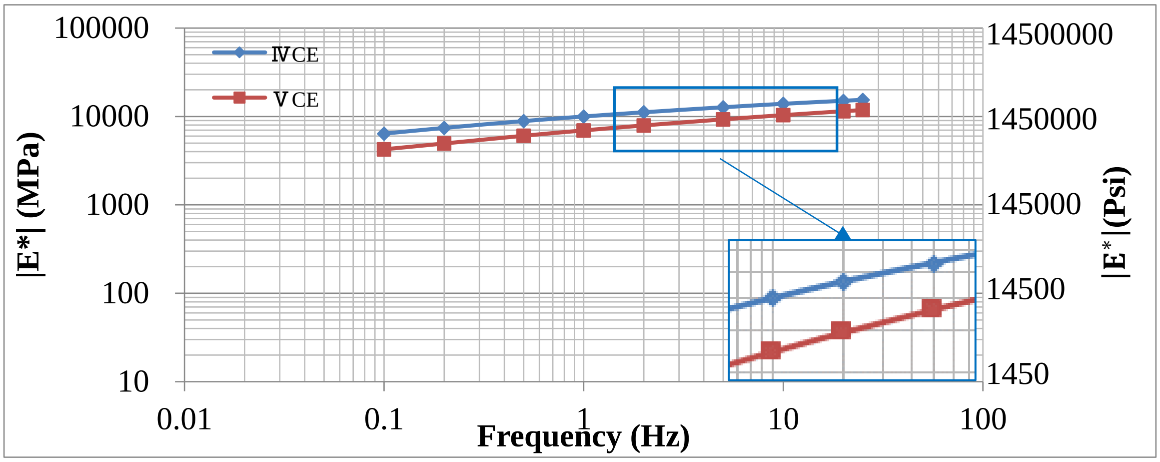

(a)

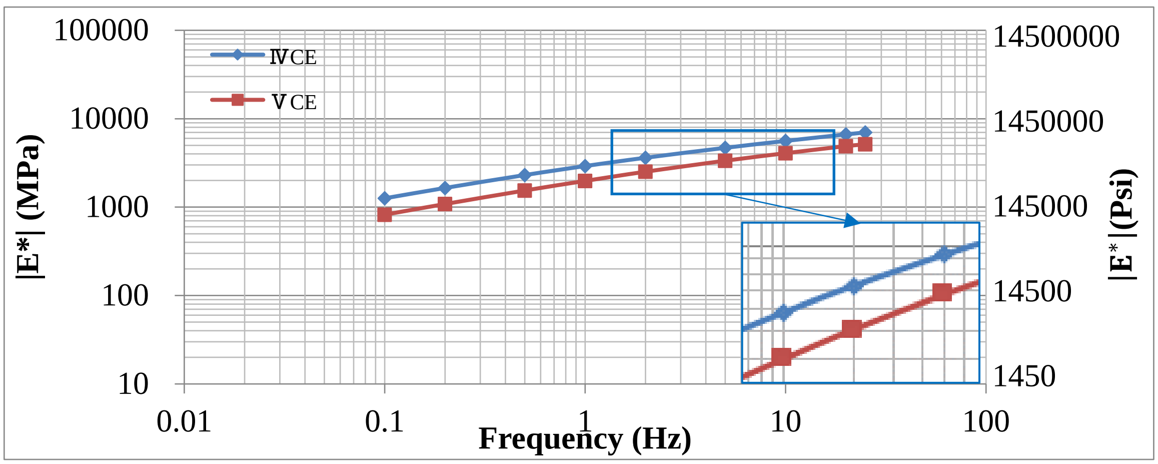

(b)

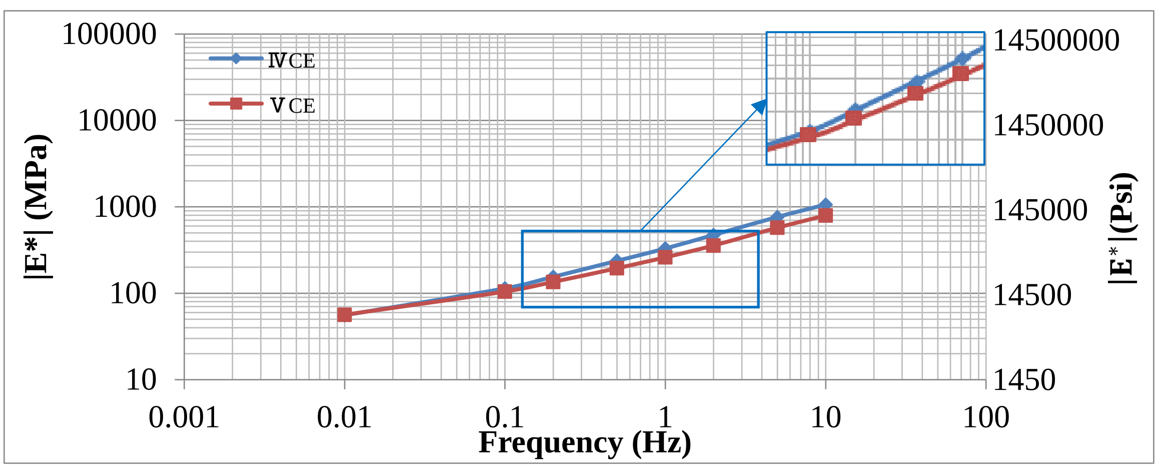

(c)

Figure 6-9 Dynamic Modulus Values of Various Surface Type C Mixtures with RAP andWMA-Chemical Additive in Terms of Aggregate Source (a) at 4°C (39.2°F), (b) at 20°C (68°F), (c) at 40°C (104°F)

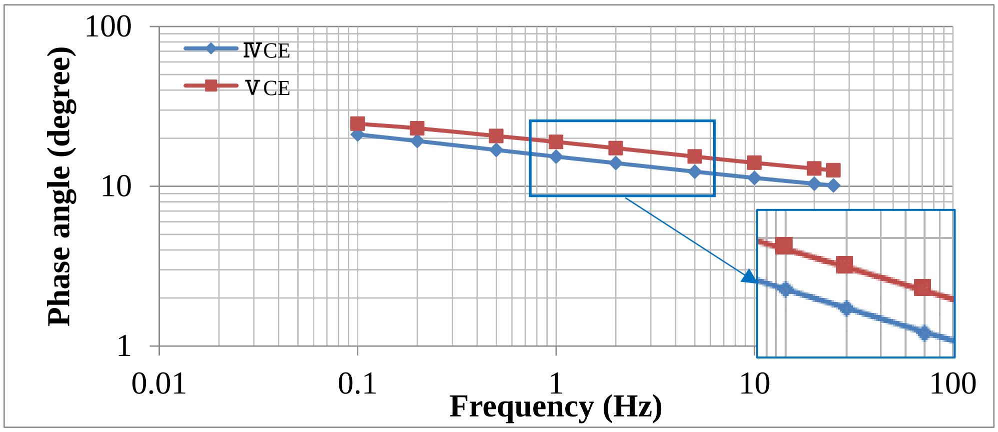

(a)

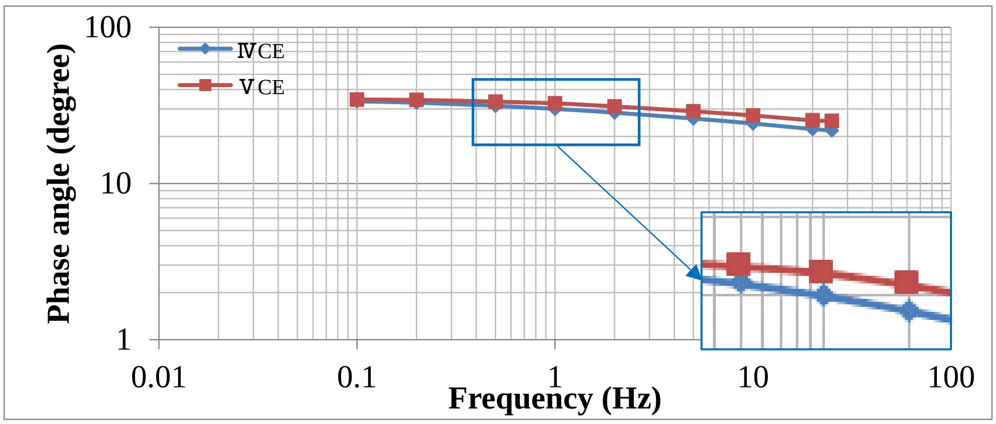

(b)

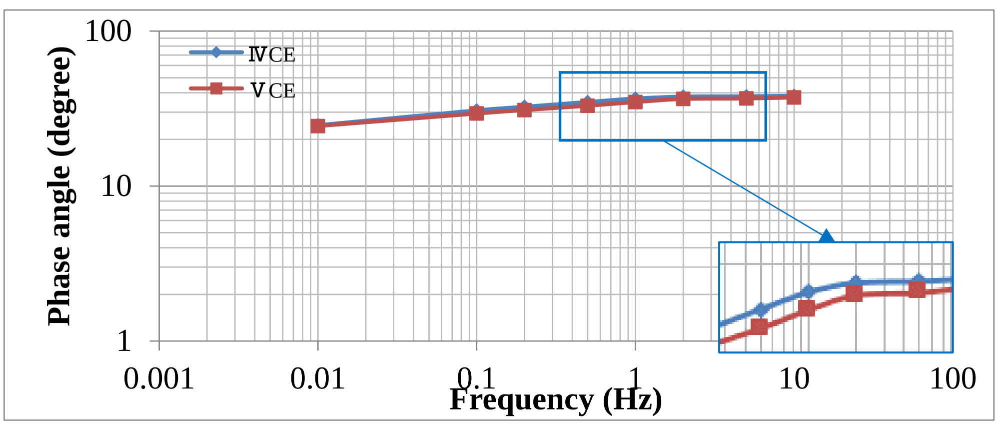

(c)

Figure 6-10 Phase Angle Values of Various Surface Type C Mixtures with RAP and WMA-Chemical Additive in Terms of Aggregate Source (a) at 4°C (39.2°F), (b) at 20°C (68°F), (c) at 40C (104°F)

6.1.6 Effect of Aggregate Source on Dynamic Modulus and Phase Angle of Surface Type C Mixtures Made with Liquid ASA

Figure 6-11 shows the dynamic modulus of various Surface Type C mixtures containing RAP and liquid ASA 1 (Adhere®) in terms of two aggregate sources (IV and V) tested at three different temperatures. It can be seen that the dynamic modulus increased with the increase of frequency. As shown in Figure 6-11, in most cases, mixtures made from aggregate V had slightly higher dynamic modulus values than mixtures containing aggregate IV. However, mix IV CA had higher dynamic modulus values than V CA at 4℃ (39.2°F) and a high frequency. In addition, it can be observed in Figure 6-11 that with the increase of temperature, the dynamic modulus values decreased.

Similar trends of dynamic modulus values were found for the mixtures containing liquid ASA 2 (Morlife®) in this study. The test results are shown in figures presented in Appendix A.

Figure 6-12 shows the phase angle values of various Surface Type C mixtures containing RAP and liquid ASA 1 (Adhere®) in terms of two aggregate sources tested at three temperatures. In Figure 6-12, the phase angle values of mix IV CA were slightly higher than that of mix V CA. The phase angle values of mixtures decreased with the increase of frequency at 4℃ (39.2°F) and 20℃ (68°F). However, with the increase of frequency, the phase angle values of mixtures initially increased and then decreased at 40℃ (104°F). Moreover, it can be observed that the phase angle values of mixtures increased with the increase of temperature.

Similar trends of phase angle values were found for the mixtures made with liquid ASA 2 (Morlife®) in this study. The figures shown in Appendix A correspond to the findings of the testing.

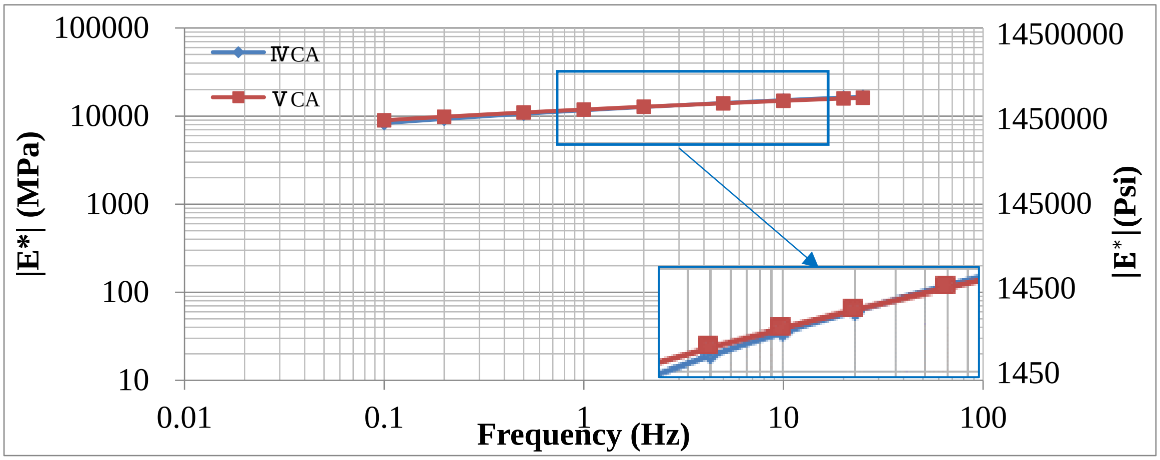

(a)

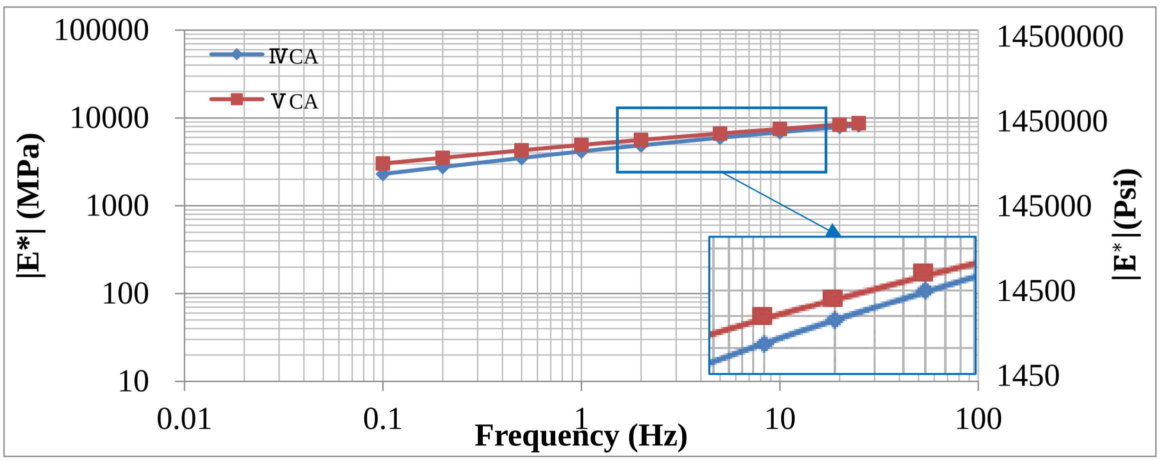

(b)

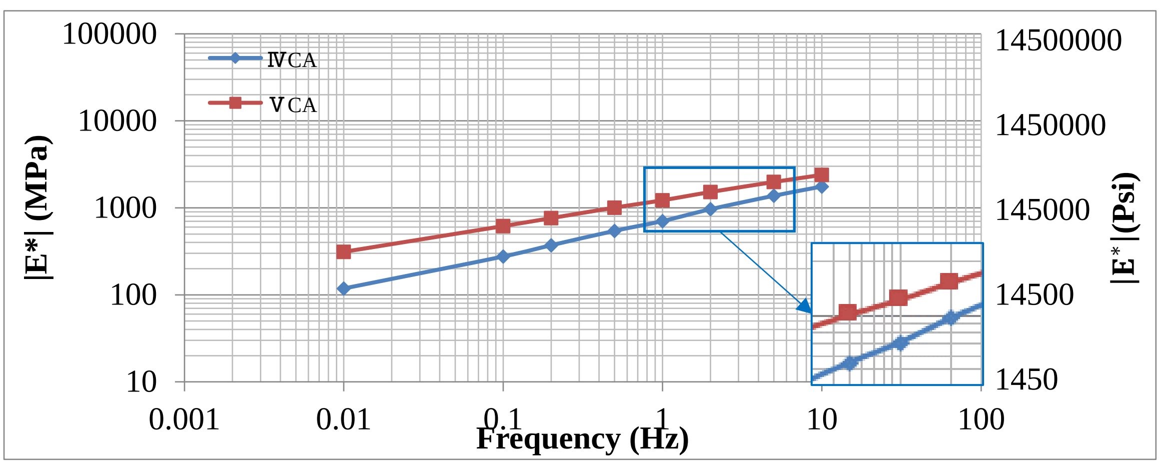

(c)

Figure 6-11 Dynamic Modulus Values of Various Surface Type C Mixtures with RAP and Liquid ASA1 in Terms of Aggregate Source (a) at 4°C (39.2°F), (b) at 20°C (68°F), (c) at 40°C (104°F)

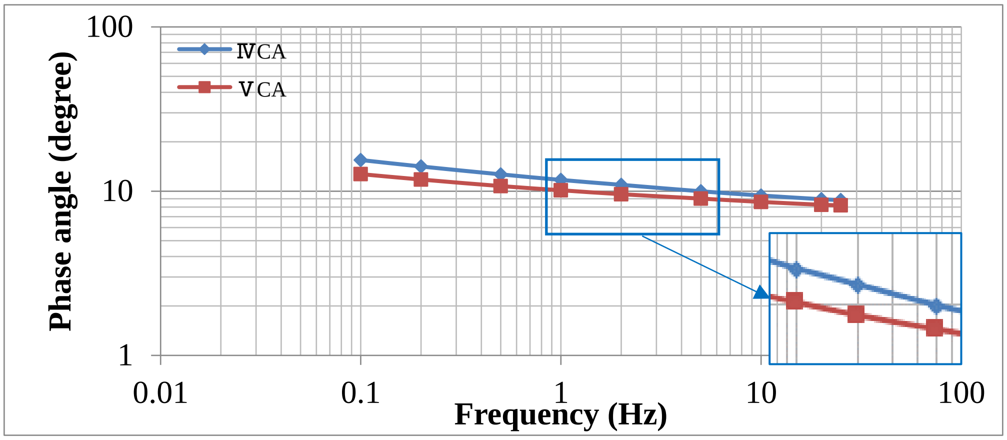

(a)

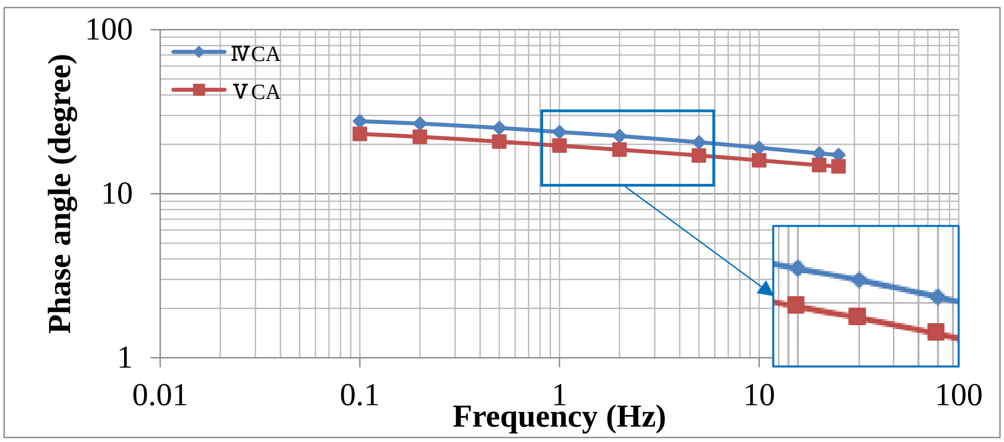

(b)

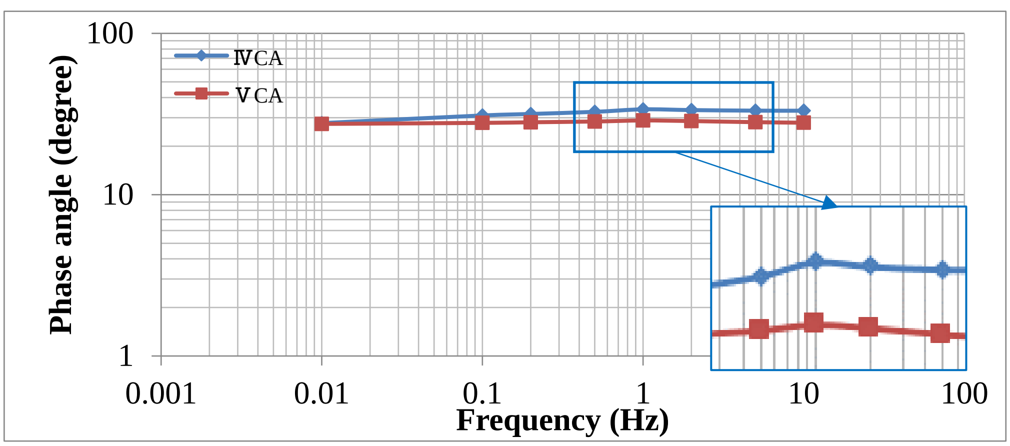

(c)

Figure 6-12 Phase Angle Values of Various Surface Type C Mixtures with RAP and Liquid ASA1 in Terms of Aggregate Source (a) at 4°C (39.2°F), (b) at 20°C (68°F), (c) at 40°C (104°F)

6.1.7 Effect of Aggregate Source on Dynamic Modulus and Phase Angle of Aged Surface Mixtures (Types A, B and C)

Figure 6-13 shows the dynamic modulus of various Surface Type A mixtures containing RAP after long-term aging in terms of two aggregate sources (IV and V) tested at three temperatures. It can be seen that the dynamic modulus increased with the increase of frequency. In Figure 6-13, mixtures made with aggregate IV had slightly higher dynamic modulus values than mixtures containing aggregate V at 4℃ (39.2°F) and 20℃ (68°F). However, mix V CA had higher dynamic modulus values than mix IV CA at 40℃ (104°F). In addition, it can be observed in Figure 6-13 that with the increase of temperature, the dynamic modulus of mixtures decreased.

Similar trends of dynamic modulus values were found for the aged Surface Type B and C mixtures tested in this study. The results of the testing are shown in figures presented in Appendix A.

Figure 6-14 shows the phase angle values of various Surface Type A mixtures containing RAP after long-term aging in terms of two aggregate sources (IV and V) tested at three temperatures. In Figure 6-14, the phase angle values of mix IV AG were slightly higher than that of mix V AG. The phase angle values of mixtures decreased with the increase of frequency at 4℃ (39.2°F) and 20℃ (68°F). However, with the increase of frequency, the phase angle values of mixtures initially increased and then remained approximately unchanged at 40℃ (104°F). Moreover, it can be observed that the phase angle values of mixtures increased with the increase of temperature.

Similar trends of phase angle values were found for the aged Surface Type B and C mixtures tested in this study. The findings are presented using figures shown in Appendix A.

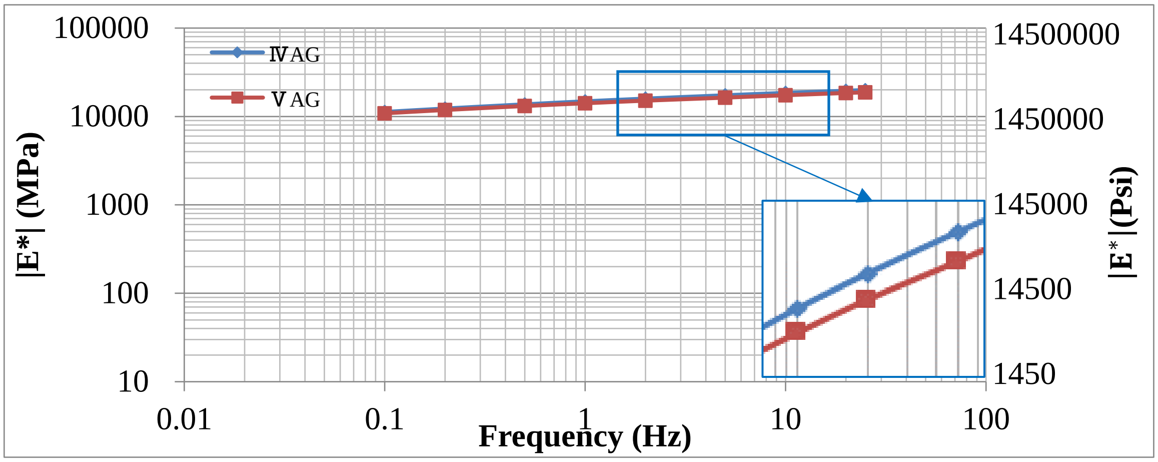

(a)

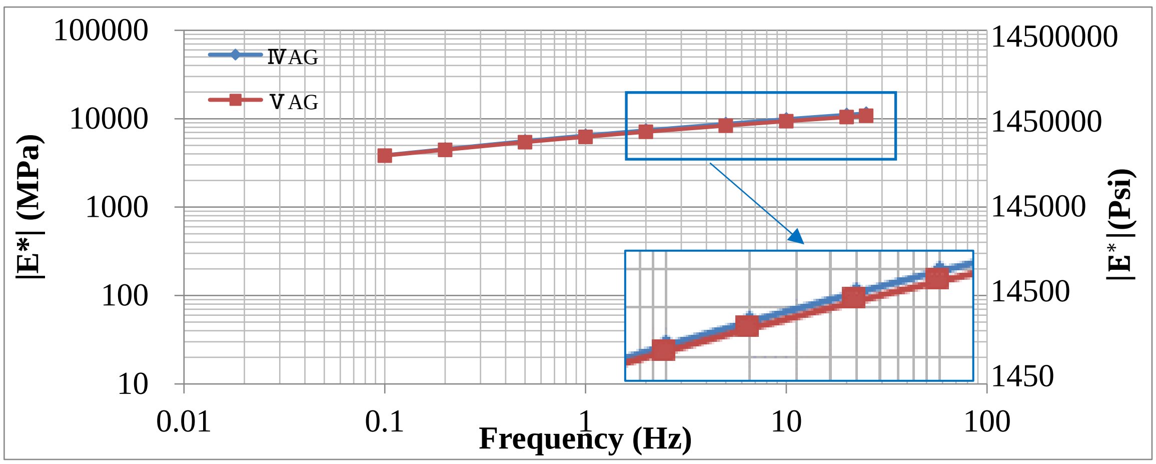

(b)

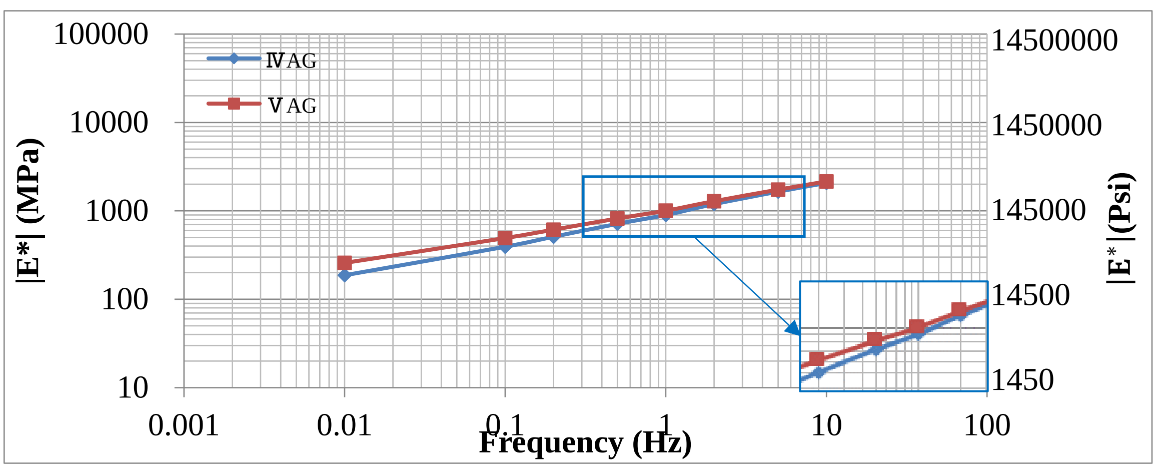

(c)

Figure 6-13 Dynamic Modulus Values of Various Surface Type A Mixtures with RAP after Long-Term Aging in Terms of Aggregate Source (a) at 4°C (39.2°F), (b) at 20°C (68°F), (c) at 45°C (113°F)

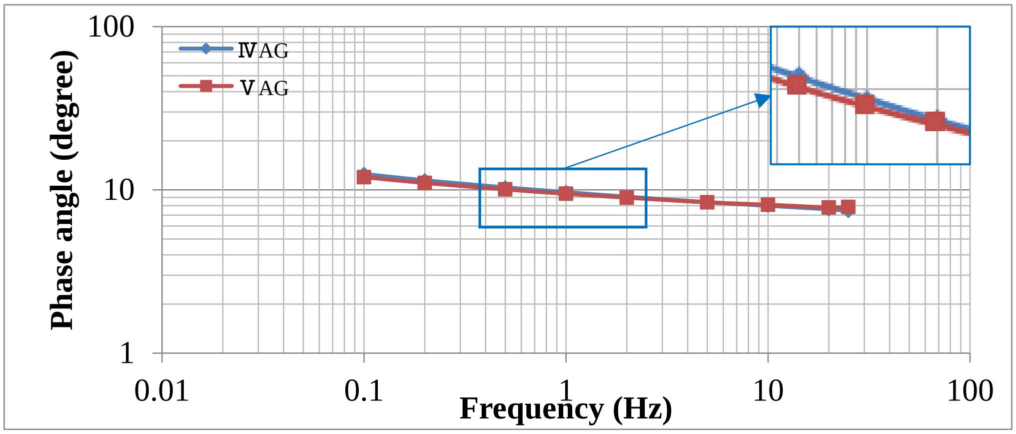

(a)

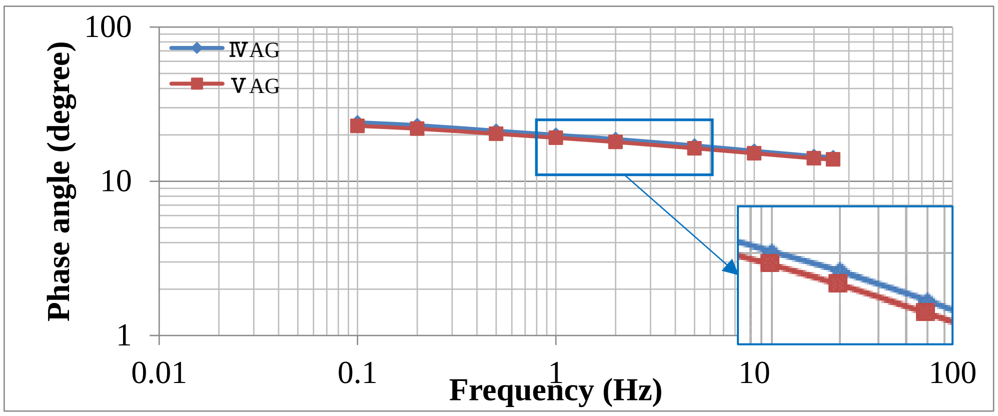

(b)

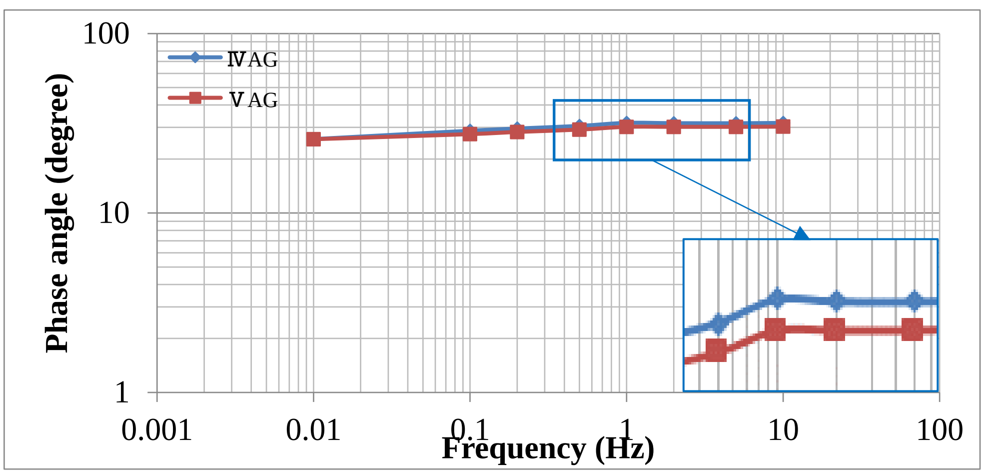

(c)

Figure 6-14 Phase Angle Values of Various Surface Type A Mixtures with RAP after Long-Term Aging in Terms of Aggregate Source (a) at 4°C (39.2°F), (b) at 20°C (68°F), (c) at 45°C (113°F)

6.1.8 Effect of Mixture Type on Dynamic Modulus and Phase Angle of Surface Mixtures Made with Different Aggregate Types

Figure 6-15 shows the dynamic modulus of various mixtures containing aggregate source I and RAP in terms of five Surface Course mixture types (Surface Types A, B, C, D, and E) tested at different temperatures. In addition, there were two different Surface Type B mix designs utilized for aggregate source I. The second mix design for that aggregate source (I B2) incorporated the newly-adopted corrected optimum asphalt content (COAC) allowed by SCDOT. This new mix design was added toward the end of the project. It can be seen that the dynamic modulus increased with the increase of frequency. Figure 6-15 shows that mixture I B1 had the highest dynamic modulus values at all temperatures, while mixture I D had the lowest dynamic modulus values. Mixtures I B2, I C, and I E had mid-range dynamic modulus values that were similar at 4°C (39.2°F) and 20°C (68°F). However, mixes I E and I B2 had higher dynamic modulus values than mix I A at 40°C (104°F). In addition, it can be observed from Figure 6-15 that with the increase of temperature, there was a decrease in the dynamic modulus of the mixtures.

Similar trends of dynamic modulus values were found for the mixtures made with aggregate sources II, III, IV, V, and VI. The findings are shown in Appendix B.

The new Surface Type B mix design containing the COAC appeared to significantly affect the dynamic modulus values. The dynamic modulus values for the new mix design with aggregate source II were lower than the values for the old mix design with that same aggregate source regardless of test temperature and frequency. However, because only one aggregate source for Surface Type B using the new COAC was tested, it is difficult to draw firm conclusions. The scope of this project did not allow further investigation of this effect.

Figure 6-16 shows the phase angle values of various mixtures containing aggregate source I and RAP in terms of five Surface Course mixture types (Surface Types A, B, C, D, and E) tested at different temperatures. In Figure 6-16, mixtures I D and I C generally had higher phase angle values than others at all temperatures, while mixes I A and I E generally had lower phase angle values. However, mixture I A had comparatively-higher phase angle values at 40°C (104°F) and high frequency, and mix I E had comparatively-high phase angle values at 40°C (104°F) and low frequency. It can be observed that the phase angle values of mixtures showed different trends at different temperatures. The phase angle values of mixtures decreased with the increase of frequency at 4°C (39.2F) and 20°C (68°F). However, with increasing frequency, the phase angle values of mixtures initially increased and then remained approximately unchanged at 40°C (104°F). The phase angle values of mixes I B2 and I E initially increased and then decreased at 45°C (113°F). Moreover, it can be observed that the phase angle values of mixtures increased with the increase of temperature.

Similar trends of phase angle values were found for the mixtures made with aggregate sources II, III, IV, V, and VI tested in this study. The figures shown in Appendix B represent the findings.

The new mix design containing the COAC appeared to have varied effect on the phase angle values depending on test temperature. The new Surface Type B mix design with aggregate source II exhibited phase angle values that were lower than the old mix design with that same aggregate source at 4°C (39.2°F), similar to the old mix design at 20°C (68°F), and higher than the old mix design at 45°C (113°F). Because of these varied results combined with the fact that only one aggregate source for Surface Type B using the new COAC was tested, it is difficult to draw any conclusions regarding the effect on phase angle. The scope of this project did not allow further investigation of this effect.

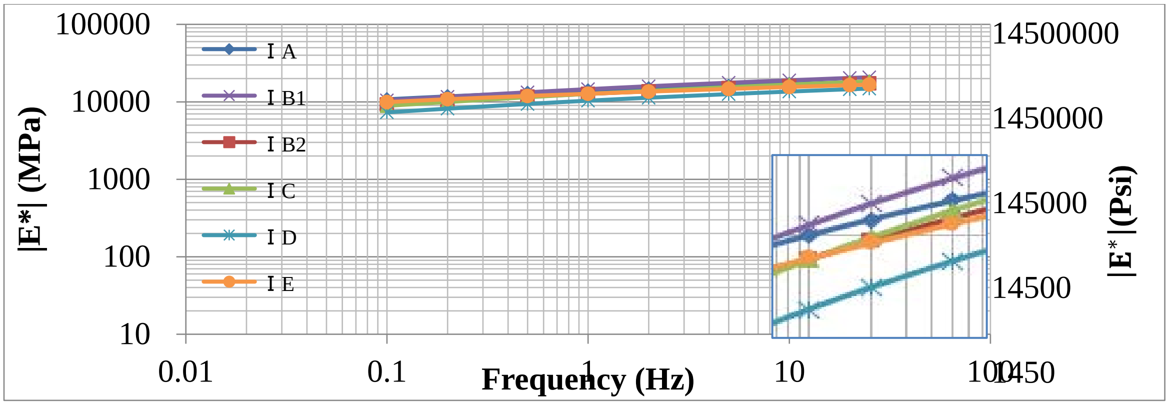

(a)

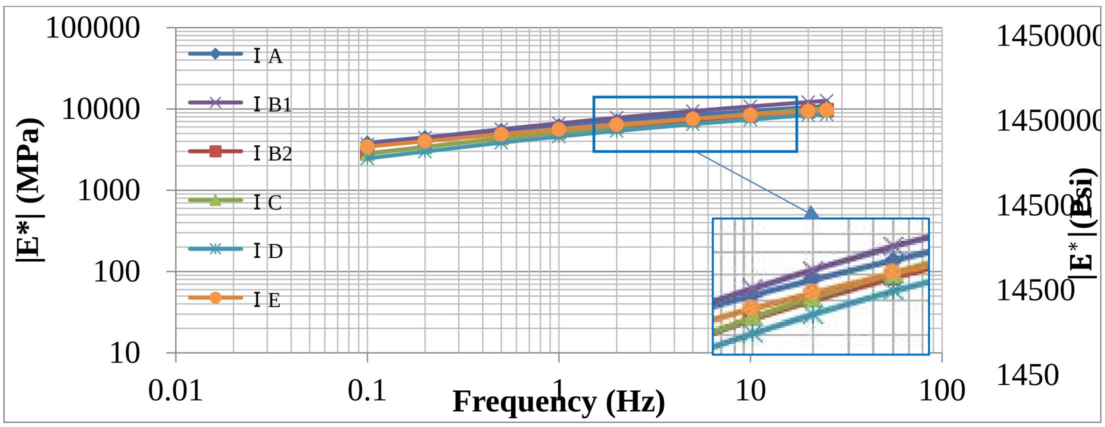

(b)

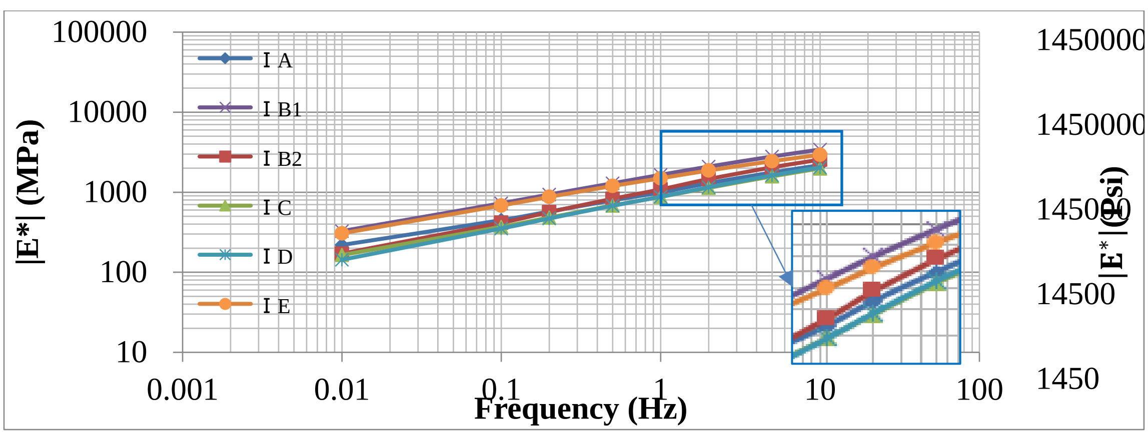

(c)

Figure 6-15 Dynamic Modulus Values of Various Mixtures for Aggregate Source I with RAP in Terms of Surface Mixture Type (a) at 4°C (39.2°F), (b) at 20°C (68°F), (c) at 45°C (113°F) (Surface Type A), 40°C (104°F) (Surface Types B, C, D, and E)

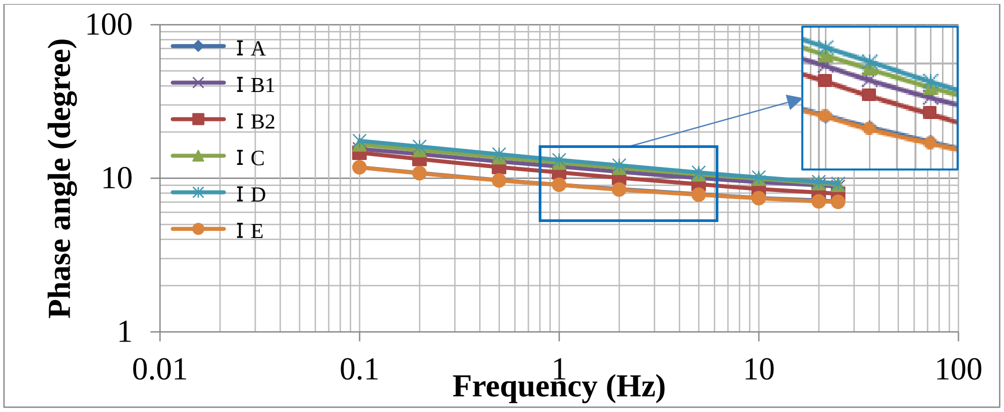

(a)

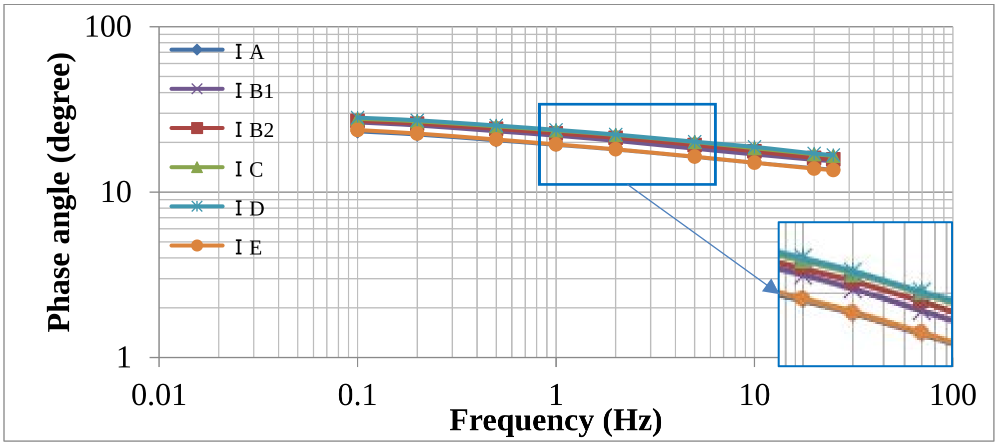

(b)

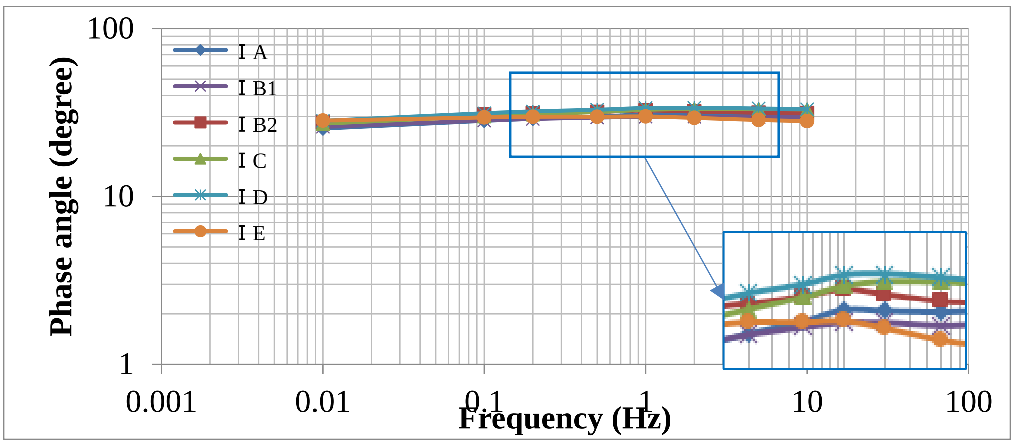

(c)

Figure 6-16 Phase Angle Values of Various Mixtures for Aggregate Source I with RAP in Terms of Surface Mixture Type (a) at 4°C (39.2°F), (b) at 20°C (68°F), (c) at 45°C (113°F) (Surface Type A), 40°C (104°F) (Surface Types B, C, D, and E)

6.1.9 Effect of Mixture Type on Dynamic Modulus and Phase Angle of Intermediate Mixtures Made with Different Aggregate Sources

Figure 6-17 shows the dynamic modulus of various mixtures containing aggregate source IV and RAP in terms of three Intermediate Course mixture types (Intermediate Types A, B, and C) tested at different temperatures. It can be seen that the dynamic modulus increased with the increase of frequency. As shown in Figure 6-17, mixture IV IB had the highest dynamic modulus values at all temperatures, while mixture IV IC had the lowest dynamic modulus values. In addition, it can be observed in Figure 6-17 that with the increase of temperature, the dynamic modulus of mixtures decreased.

Similar trends of dynamic modulus values were found for the mixtures from aggregate source V tested in this study. The findings are presented in Appendix B.

In addition to the Intermediate Type A, B, and C mixtures made with aggregate sources IV and V, several Intermediate Type B Special mixtures were made with two additional aggregate sources, II and VII. These mixtures were added towards the end of the project, and aggregate sources were selected by the Steering Committee based on materials used in field pilot projects. As shown in Appendix B, the dynamic modulus values of the Intermediate Type B Special mixtures were similar to those of the other Intermediate Type A, B, and C mixtures, regardless of test temperature and frequency. As with all of the other Intermediate Course mixtures types, increased loading frequency resulted in higher dynamic modulus values, and increased test temperatures resulted in lower dynamic modulus values.

Figure 6-18 shows the phase angle values of various mixtures from aggregate source IV with RAP in terms of three Intermediate Course mixture types (Intermediate Types A, B, and C) tested at different temperatures. As shown in Figure 6-18, mixture IV IC had the highest phase angle values in most cases, while mixture IV IB had the lowest phase angle values in most cases. However, mixture IV B had the highest phase angle values at 40°C (104°F) and low frequency. It can be observed that the phase angle values of mixtures showed different trends at different temperatures. The phase angle values of mixtures decreased with the increase of frequency at 4°C (39.2°F) and 20°C (68°F). However, with the increase of frequency, the phase angle values of mixtures initially increased and then remained nearly unchanged at 40°C (104°F). The phase angle values of mixture IV B initially increased and then decreased at 40°C (104°F). Moreover, it can be observed that the phase angle values of mixtures increased with the increase of temperature.

Similar trends of phase angle values were found for the mixtures from aggregate source V tested in this study. The figures presented in Appendix B represent the findings of this portion of the research project.

In addition to the Intermediate Type A, B, and C mixtures made with aggregate sources IV and V, several Intermediate Type B Special mixtures were made with two additional aggregate sources, II and VII. These mixtures were added towards the end of the project, and aggregate sources were selected by the Steering Committee based on materials used in field pilot projects. As shown in Appendix B, the phase angle values of the Intermediate Type B Special mixtures were similar to those of the other Intermediate Type A, B, and C mixtures, regardless of test temperature, and frequency. As with all of the other Intermediate Course mixtures, phase angle values decreased with the increase of frequency at 4°C (39.2°F) and 20°C (68°F). However, with the increase of frequency, the phase angle values of mixtures initially increased and then approximately remained unchanged at 40°C (104°F).

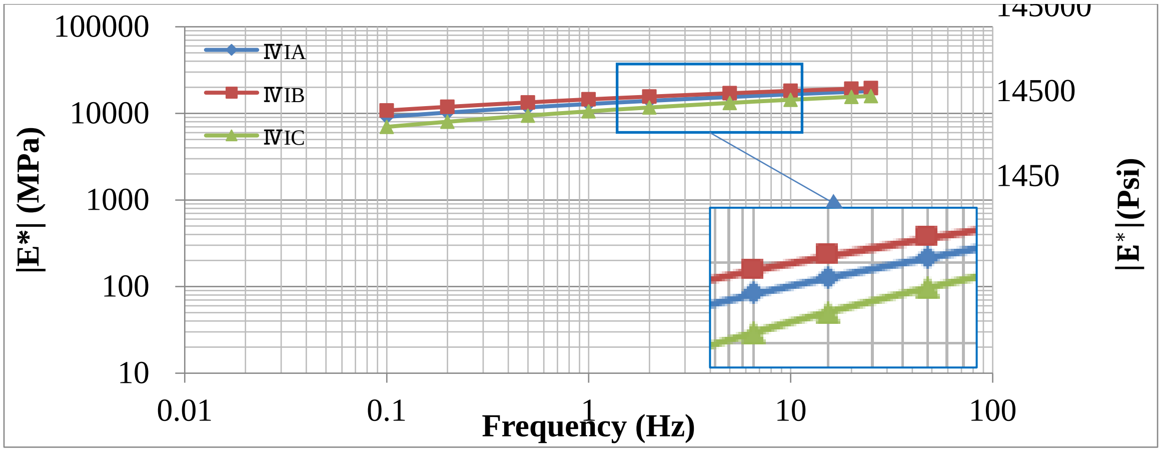

(a)

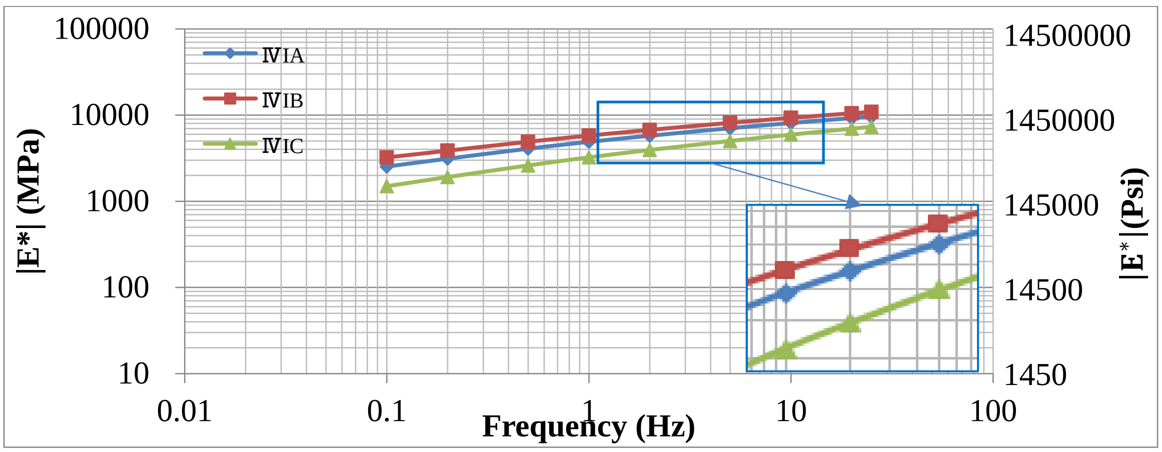

(b)

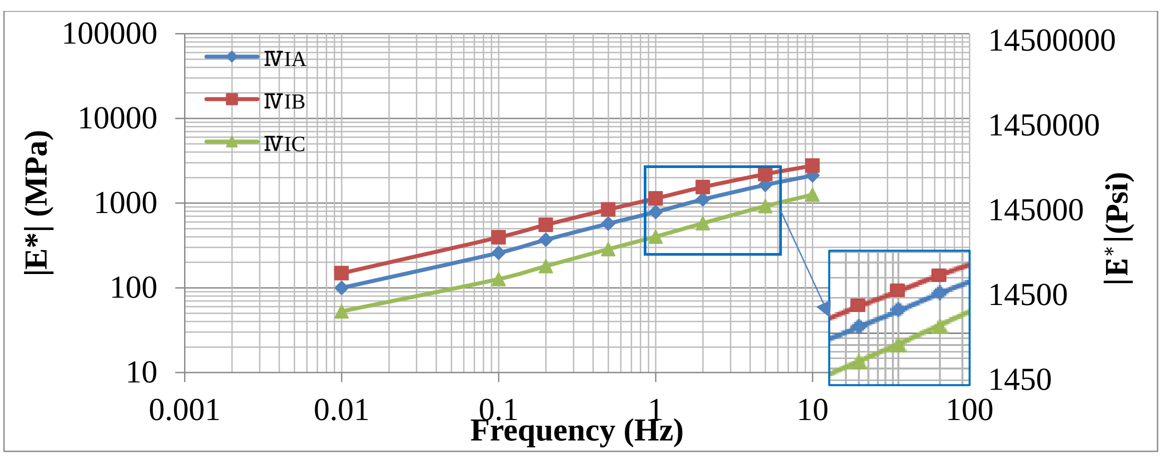

(c)

Figure 6-17 Dynamic Modulus Values of Various Mixtures for Aggregate Source IV with RAP in Terms of Intermediate Mixture Type (a) at 4°C (39.2°F), (b) at 20°C (68°F), (c) at 40°C (104°F)

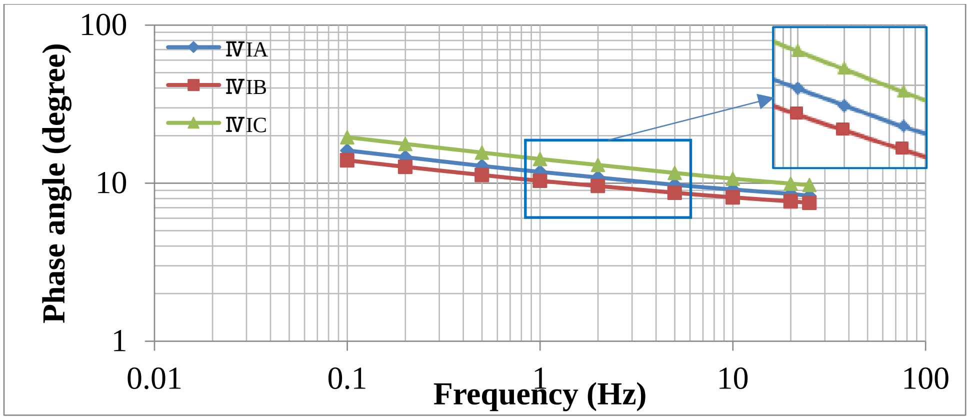

(a)

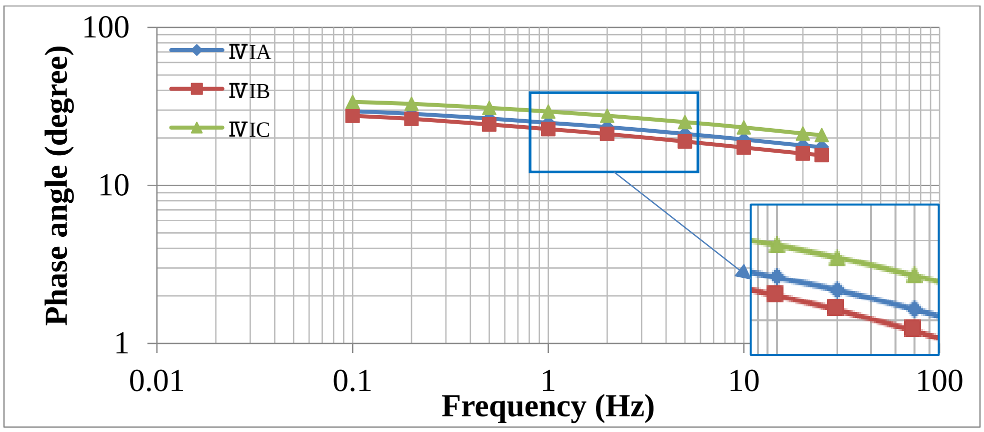

(b)

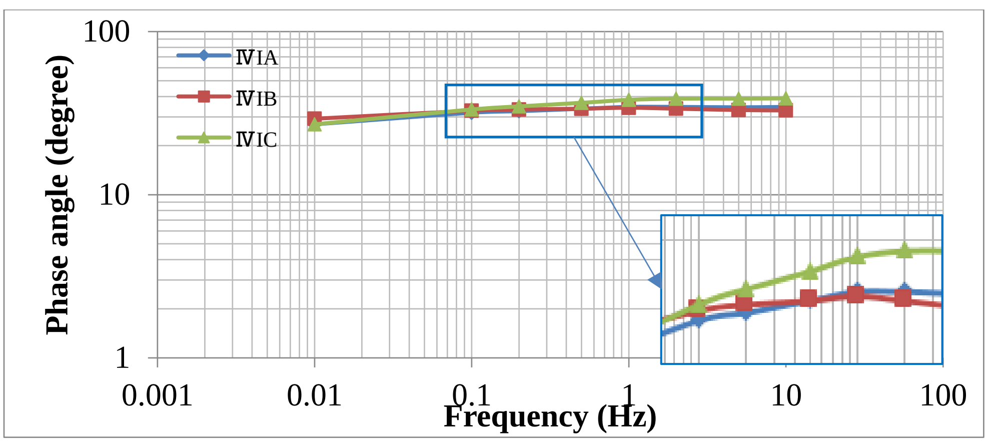

(c)

Figure 6-18 Phase Angle Values of Various Mixtures for Aggregate Source IV with RAP in Terms of Intermediate Mixture Type (a) at 4°C (39.2°F), (b) at 20°C (68°F), (c) at 40°C (104°F)

6.1.10 Effect of Mixture Type on Dynamic Modulus and Phase Angle of Base Mixtures (Types A and B) Made with Different Aggregate Sources

Figure 6-19 shows the dynamic modulus of various mixtures for aggregate source IV containing RAP in terms of two Base Course mixture types (Base Types A and B) tested at different temperatures. It can be seen that the dynamic modulus increased with the increase of frequency. As shown in Figure 6-19, mixture IV SA had slightly higher dynamic modulus values than mixture IV SB. In addition, it can be observed in Figure 6-19 that with the increase of temperature, the dynamic modulus of mixtures decreased.

Similar trends of dynamic modulus values were found for the mixtures made with aggregate source V tested in this study. The figures presented in Appendix B show the findings of this portion of the research project.

Figure 6-20 shows the phase angle values of various mixtures made with aggregate source IV and RAP in terms of two Base Course mixture types (Base Types A and B) tested at different temperatures. As shown in Figure 6-20, mixtures IV SA and IV SB had similar phase angle values. It can be observed that the phase angle values of mixtures showed different trends at different temperatures. The phase angle values of mixtures decreased with the increase of frequency at 4°C (39.2°F) and 20°C (68°F). However, with the increase of frequency, the phase angle values of mixtures initially increased and then remained approximately unchanged at 40°C (104°F). Moreover, it can be observed that the phase angle values of mixtures increased with the increase of temperature.

Similar trends of phase angle values were found for the mixtures made with aggregate source V tested in this study. The research findings for this portion of the research work has been presented in Appendix B.

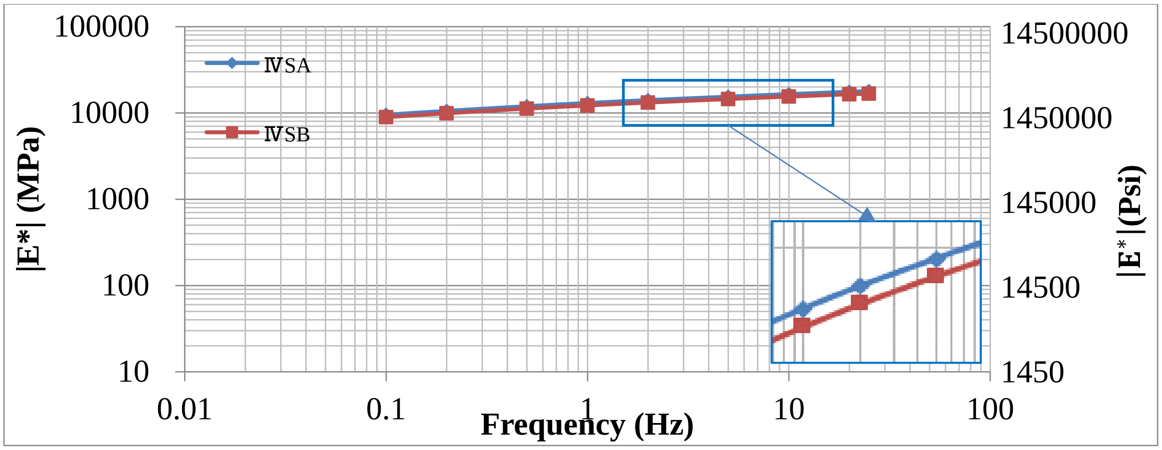

(a)

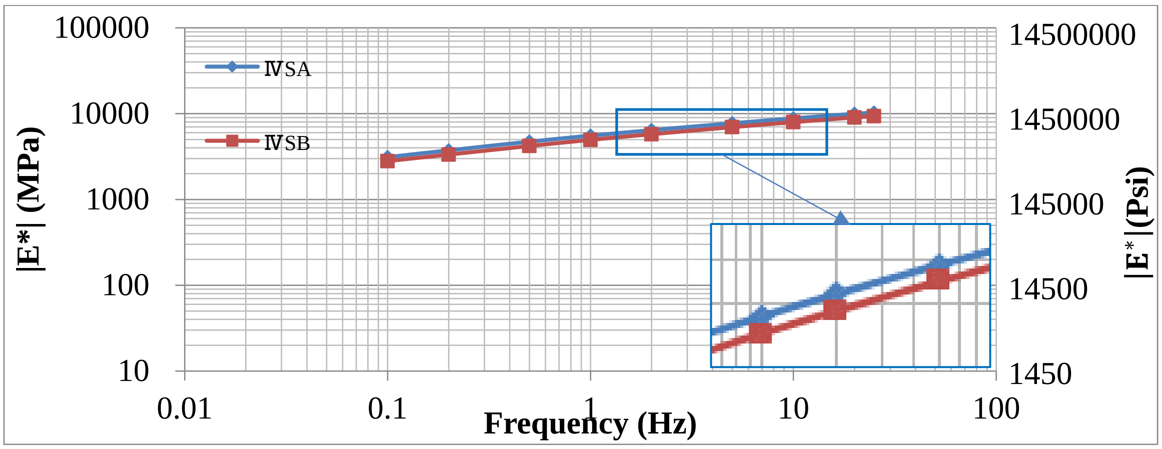

(b)

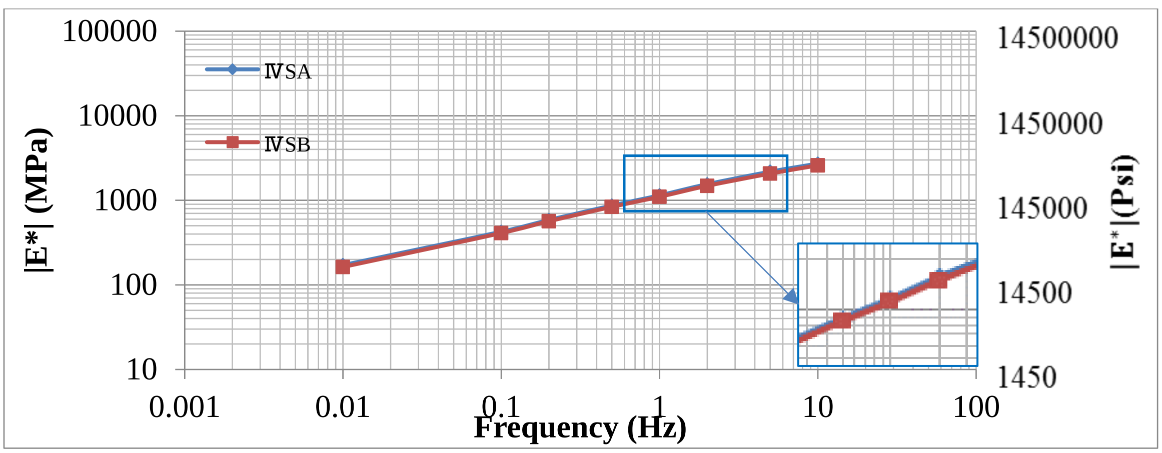

(c)

Figure 6-19 Dynamic Modulus Values of Various Mixtures for Aggregate Source IV with RAP in Terms of Base Mixture Type (a) at 4°C (39.2°F), (b) at 20°C (68°F), (c) at 40°C (104°F)

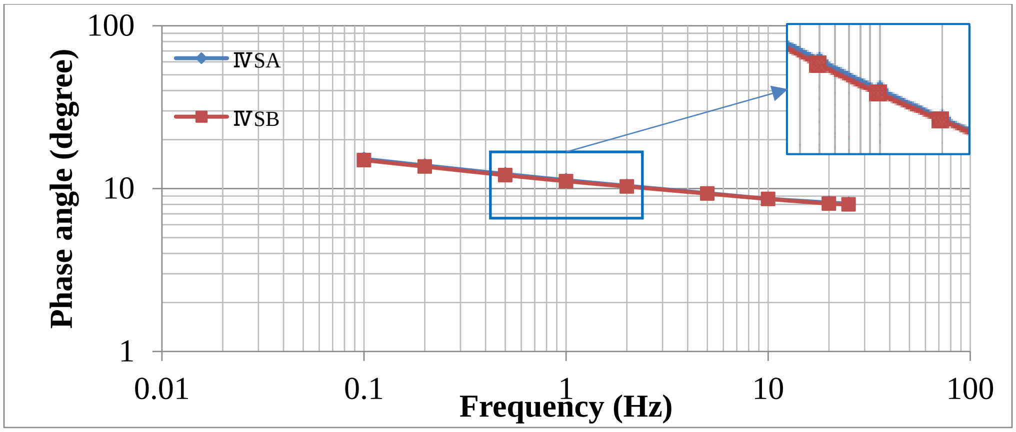

(a)

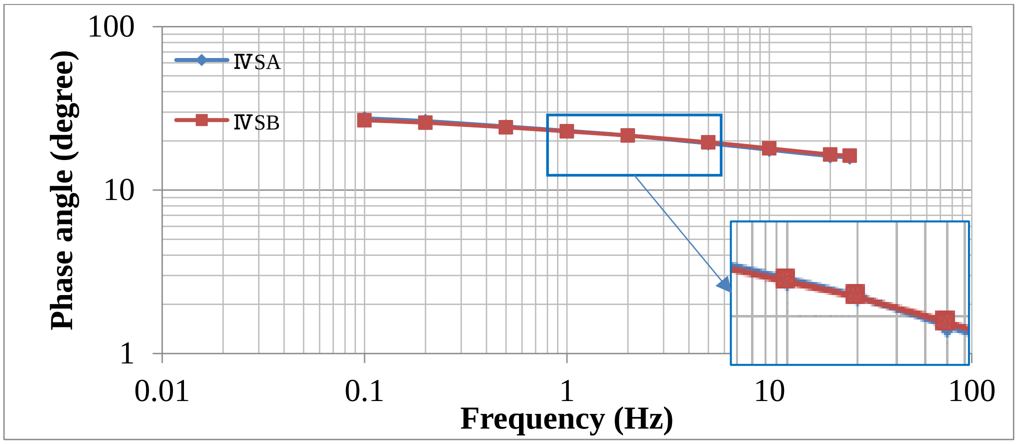

(b)

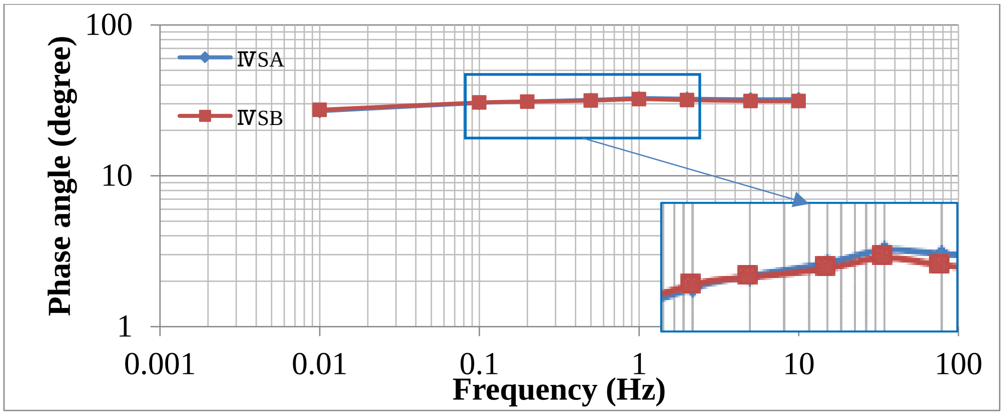

(c)

Figure 6-20 Phase Angle Values of Various Mixtures for Aggregate Source IV with RAP in Terms of Base Mixture Type (a) at 4°C (39.2°F), (b) at 20°C (68°F), (c) at 40°C (104°F)

6.1.11 Effect of Mixture Type on Dynamic Modulus and Phase Angle of Surface Mixtures (Types A and B) Made with Different Aggregate Types and Binder Source 2

Figure 6-21 shows the dynamic modulus of various mixtures for aggregate source IV and containing asphalt source 2 (Axeon) and RAP in terms of two Surface Course mixture types (Surface Types A and B) tested at different temperatures. It can be seen that the dynamic modulus increased with the increase of frequency. As shown in Figure 6-21, mixture IV AN had slightly higher dynamic modulus values than mixture IV BN at 4℃ (39.2°F) and 20℃ (68°F). However, mixture IV BN had higher dynamic modulus values than mix IV AN at 40℃ (104°F) and high frequency. In addition, it can be observed in Figure 6-21 that with the increase of temperature, the dynamic modulus of mixtures decreased.

Similar trends of dynamic modulus values were found for the mixtures made with aggregate source V tested in this study. The figures presented in Appendix B show the findings of this portion of the research work.

Figure 6-22 shows the phase angle values of various mixtures for aggregate source IV and containing asphalt source 2 (Axeon) and RAP in terms of two Surface Course mixture types (Surface Types A and B) tested at different temperatures. As shown in Figure 6-22, mixtures IV AN and IV BN had similar phase angle values at 20℃ (68°F). Mixture IV AN had higher phase angle values at 4℃ (39.2°F), while mixture IV BN had higher phase angle values at 40℃ (104°F). It can be observed that the phase angle values of mixtures showed different trends at different temperatures. The phase angle values of mixtures decreased with the increase of frequency at 4℃ (39.2°F) and 20℃ (68°F). However, with the increase of frequency, the phase angle values of mixtures initially increased and then remained approximately unchanged at 40℃ (104°F). Moreover, it can be observed that the phase angle values of mixtures increased with the increase of temperature.

Similar trends of phase angle values were found for the mixtures made with aggregate source V tested in this study. The figures shown in Appendix B represent the results.

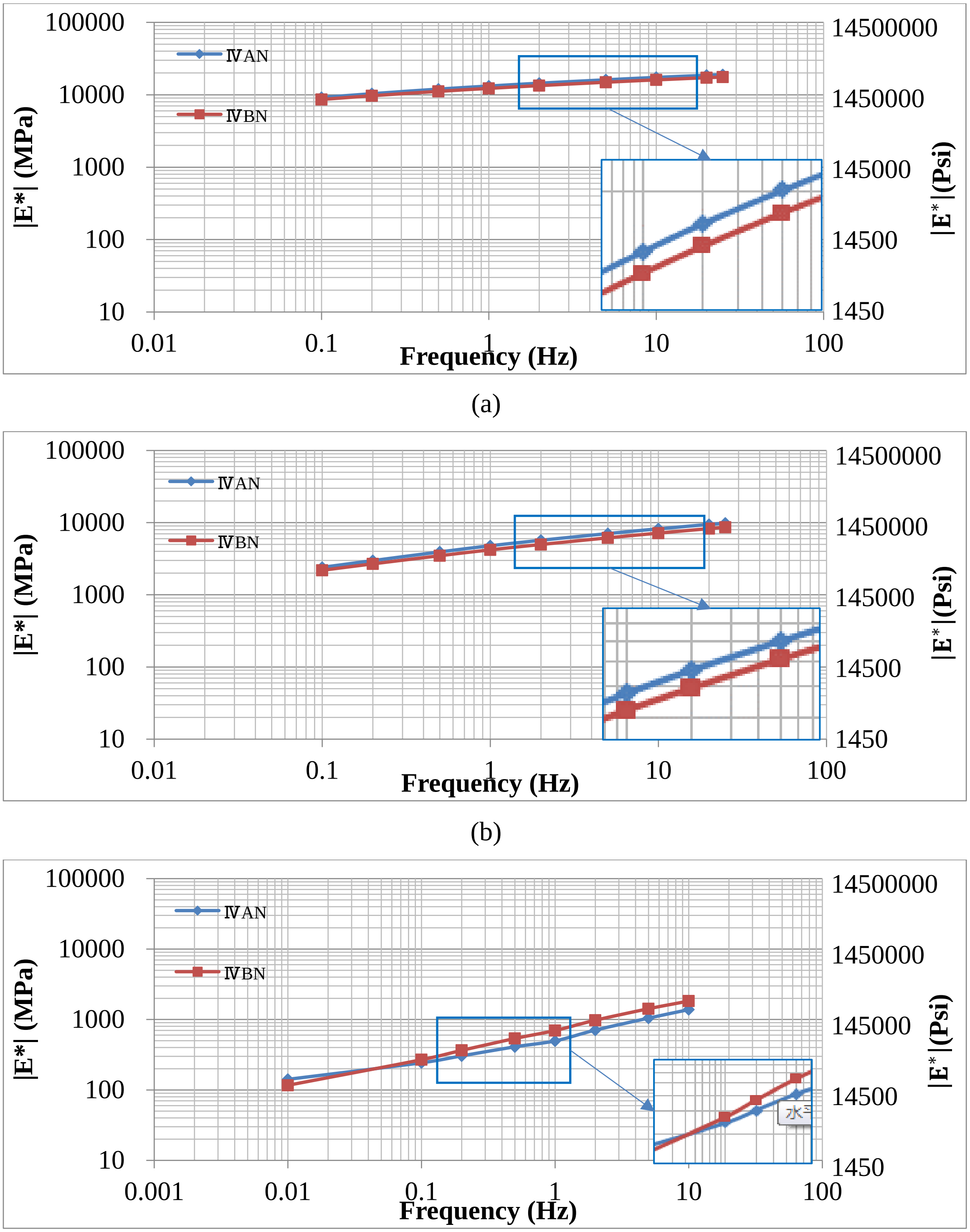

(a)

(b)

(c)

Figure 6-21 Dynamic Modulus Values of Various Mixtures for Aggregate Source IV using Asphalt Source 2 with RAP in Terms of Surface Mixture Type (a) at 4°C (39.2°F), (b) at 20°C (68°F), (c) at 45°C (113°F) (Surface Type A), 40°C (104°F) (Surface Type B)

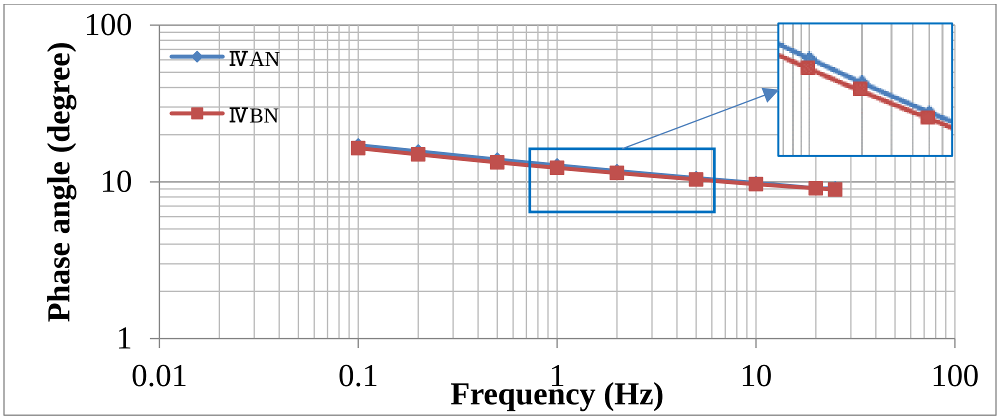

(a)

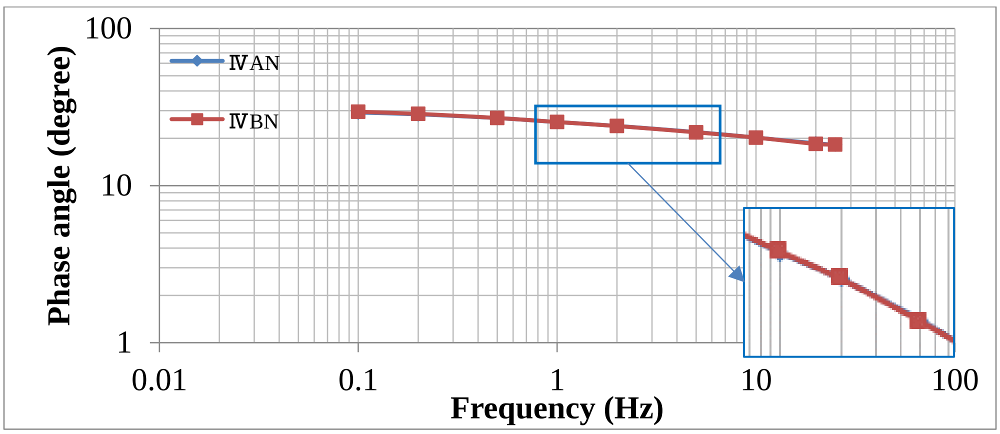

(b)

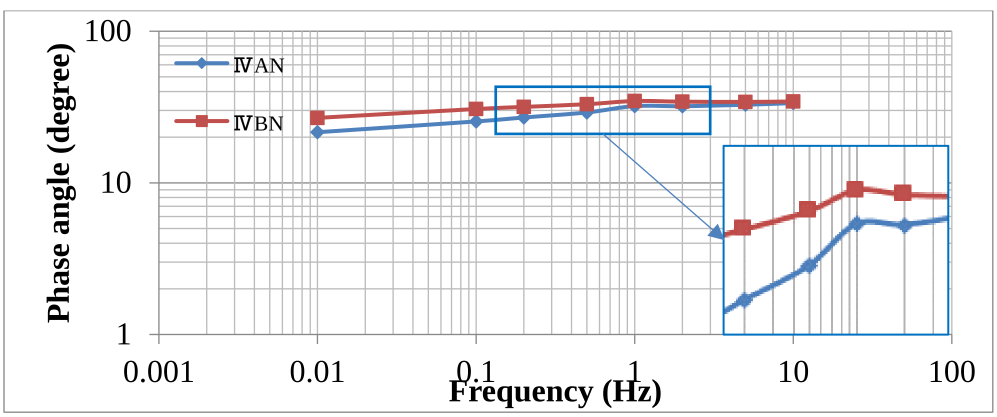

(c)

Figure 6-22 Phase Angle Values of Various Mixtures for Aggregate Source IV using Asphalt Source 2 with RAP in Terms of Surface Mixture Type (a) at 4°C (39.2°F), (b) at 20°C (68°F), (c) at 45°C (113°F) (Surface Type A), 40°C (104°F) (Surface Type B)

6.1.12 Effects of Binder Source on Dynamic Modulus and Phase Angle of Various Surface Mixtures Made with Different Aggregate Types

Figure 6-23 shows the dynamic modulus values of various Surface Type A mixtures containing aggregate source IV and RAP, tested at different temperatures, and compared in terms of binder source. It was found that the dynamic modulus values of mixtures from these two binders were different. The dynamic modulus values of mixtures from binder source 2 were generally lower regardless of loading frequency and test temperature. This effect became more pronounced with the increase of temperature. In addition, it can be observed that with the increase of temperature, the dynamic modulus values of mixtures decreased regardless of binder source.

Figure 6-24 shows the phase angle values of various Surface Type A mixtures containing aggregate source IV and RAP, tested at different temperatures, and compared in terms of binder source. The results indicated that in some cases, the binder source had an influence on the phase angle. For instance, as shown in Figure 6-24, mixture IV A had relatively lower phase angle values compared to mixture IV AN when tested at both 4°C (39.2°F) and 20°C (68°F), while their phase angle values were very similar when tested at 40°C (104°F). In addition, it can be observed that the phase angle values of mixtures showed different trends at various temperatures. The phase angle values of mixtures decreased with increasing frequency at 4°C (39.2°F) and 20°C (68°F). However, at 40°C (104°F), with the increase of frequency, the phase angle values of mixtures initially increased and then remained unchanged. Moreover, it can be observed that the phase angle values increased with an increase in temperature.

Similar trends of dynamic modulus and phase angle values were found for the Surface Type A mixtures made with aggregate source V as well as for the Surface Type B mixtures made with aggregate sources IV and V. The data results are available in other figures in terms of aggregate source and mixture type in Appendices A and B.

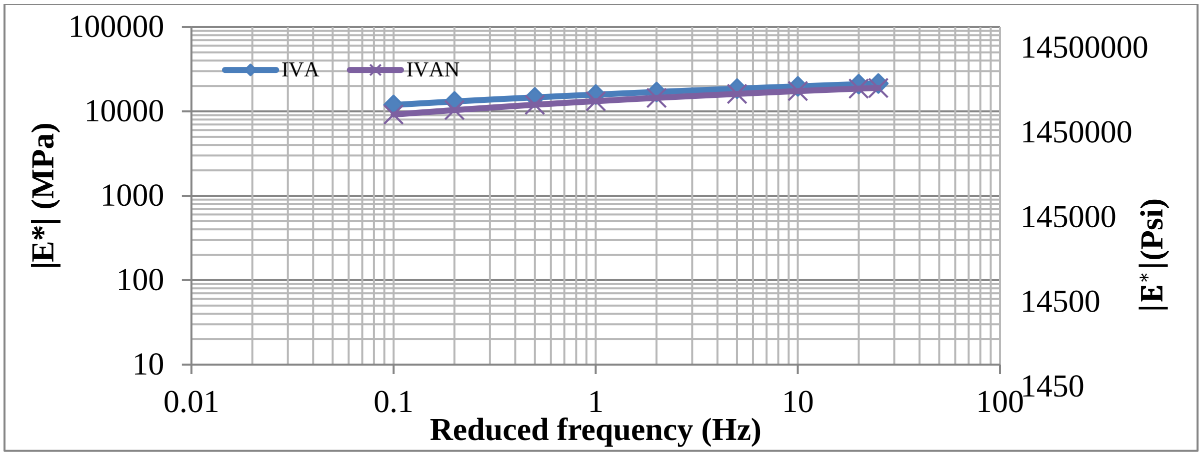

(a)

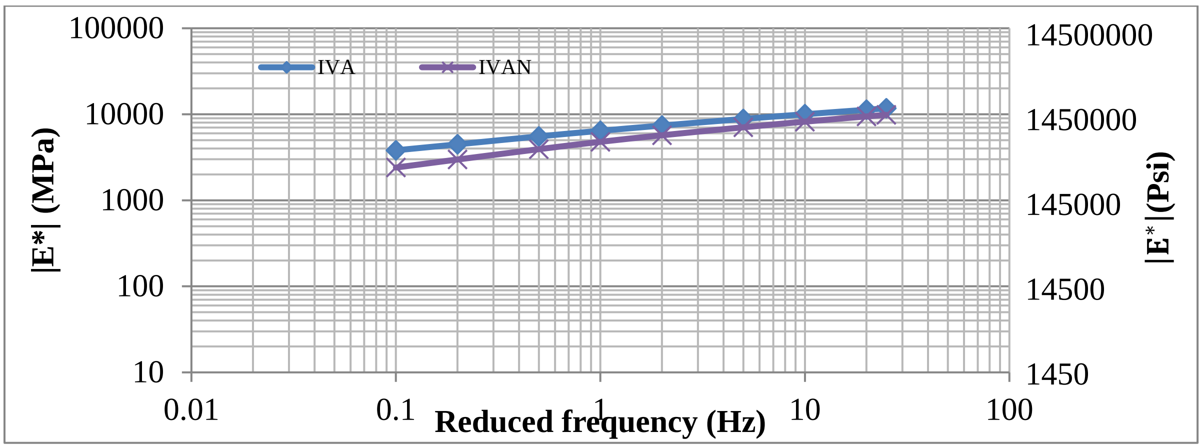

(b)

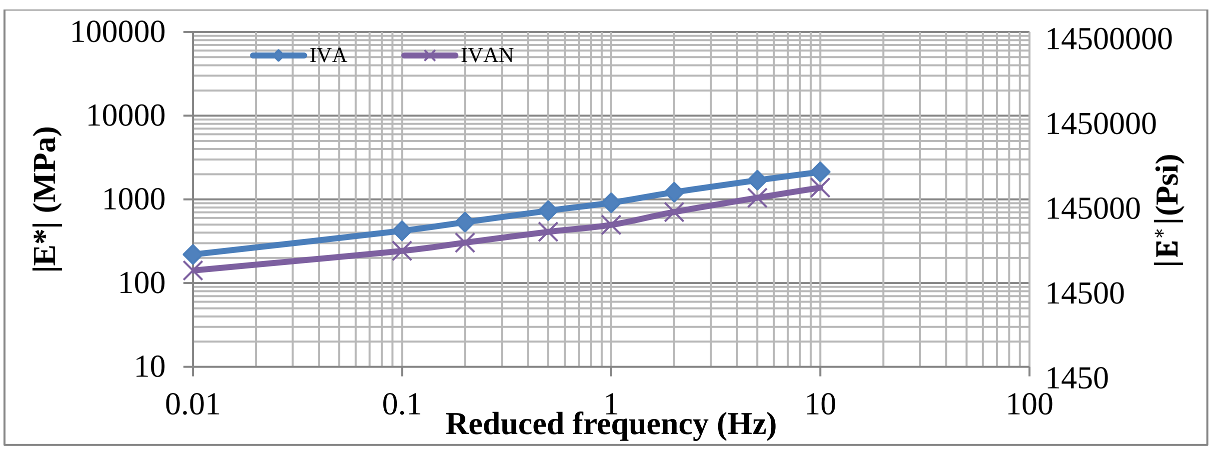

(c)

Figure 6-23 Dynamic Modulus Values of Various Surface Type A Mixtures for Aggregate Source IV Containing RAP in Terms of Binder Source (a) at 4°C (39.2°F), (b) at 20°C (68°F), and (c) at 40°C (104°F)

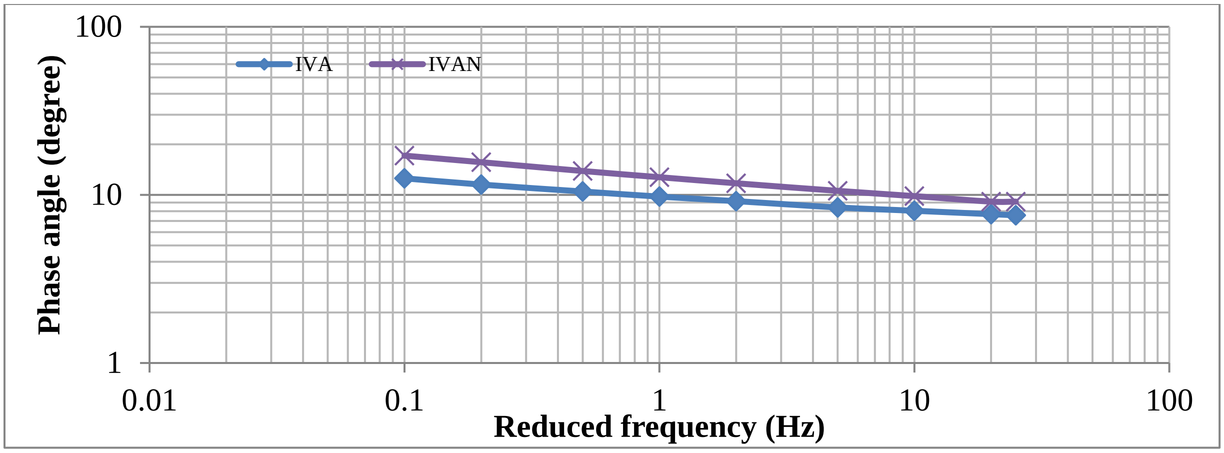

(a)

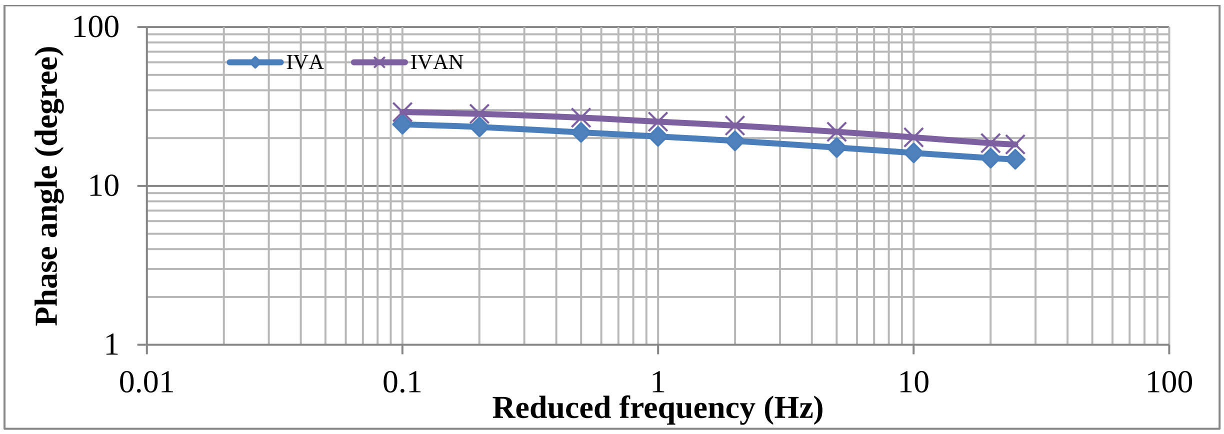

(b)

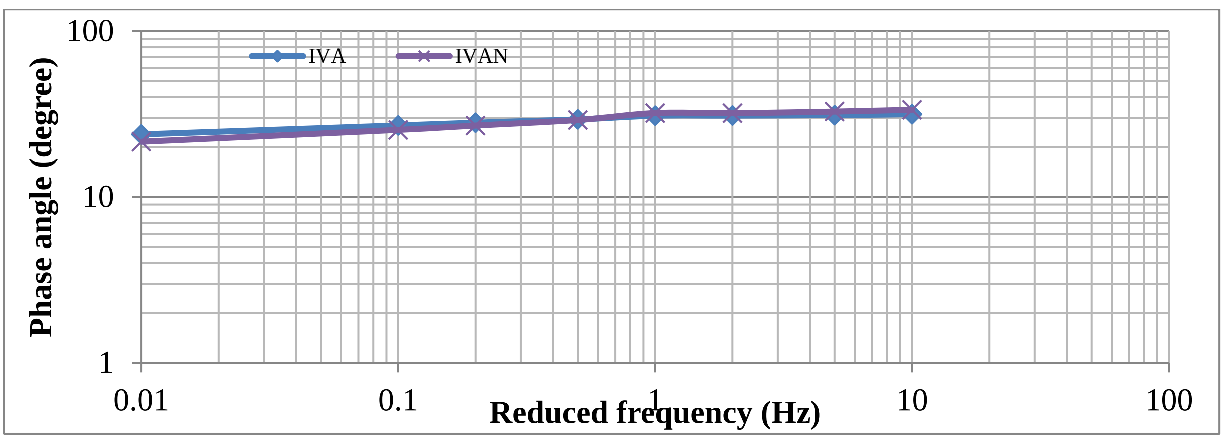

(c)

Figure 6-24 Phase Angle Values of Various Surface Type A Mixtures for Aggregate Source IV Containing RAP in Terms of Binder Source (a) at 4°C (39.2°F), (b) at 20°C (68°F), and (c) at 40°C (104°F)

6.1.13 Effect of WMA on Dynamic Modulus and Phase Angle of Surface Type C Mixtures Made with Different Aggregate Types

Figure 6-25 shows the dynamic modulus of various Surface Type C mixtures for aggregate source IV containing RAP in terms of two WMA technology types (chemical additive and the foaming process) tested at different temperatures. It can be seen that the dynamic modulus increased with the increase of frequency. As shown in Figure 6-25, mixture IV CE had slightly higher dynamic modulus values than mixture IV CF at 4°C (39.2°F) and 20°C (68°F). However, mixture IV CE had similar dynamic modulus values compared to mixture IV CF at 40°C (104°F). In addition, it can be observed in Figure 6-25 that with the increase of temperature the dynamic modulus of mixtures decreased.

Similar trends of dynamic modulus values were found for the mixtures made with aggregate source V and tested in this study. The figures in Appendix B show the findings of the testing for this portion of the research project.

Figure 6-26 shows the phase angle values of various Surface Type C mixtures made with aggregate source IV and RAP in terms of two WMA technology types (a chemical additive and the foaming process) tested at different temperatures. As shown in Figure 6-26, mixtures IV CE and IV CF had similar phase angle values. It can be observed that the phase angle values of mixtures showed different trends at different temperatures. The phase angle values of mixtures decreased with the increase of frequency at 4°C (39.2°F) and 20°C (68°F). However, with the increase of frequency, the phase angle values of mixtures initially increased and then remained approximately unchanged at 40°C (104°F). Moreover, it can be observed that the phase angle values of mixtures increased with the increase of temperature.

Similar trends of phase angle values were found for the mixtures containing aggregate source V tested in this study. The figures presented in Appendix B show the results of the findings.

Figure 6-27 shows the dynamic modulus values of various Surface Type C mixtures containing aggregate source IV and RAP, tested at different temperatures, and compared in terms of with or without WMA chemical additive. The dynamic modulus values of the mixtures made with a WMA chemical additive were lower than the mixtures without WMA regardless of test temperature and loading frequency. Similar trends were found for the mixtures with aggregate source V as well as those with WMA foaming technology and aggregate sources IV and V.

Figure 6-28 shows the phase angle values of various Surface Type C mixtures containing aggregate source IV and RAP, tested at different temperatures, and compared in terms of with or without WMA chemical additive. The phase angle values of the mixtures using a WMA chemical additive were higher than those mixtures made without WMA regardless of test temperature and loading frequency.

Similar trends of phase angle values were found for the mixtures with aggregate source V as well as those with WMA foaming technology and aggregate sources IV and V. The data results are available in other figures in terms of aggregate source and mixture type in Appendices A and B.

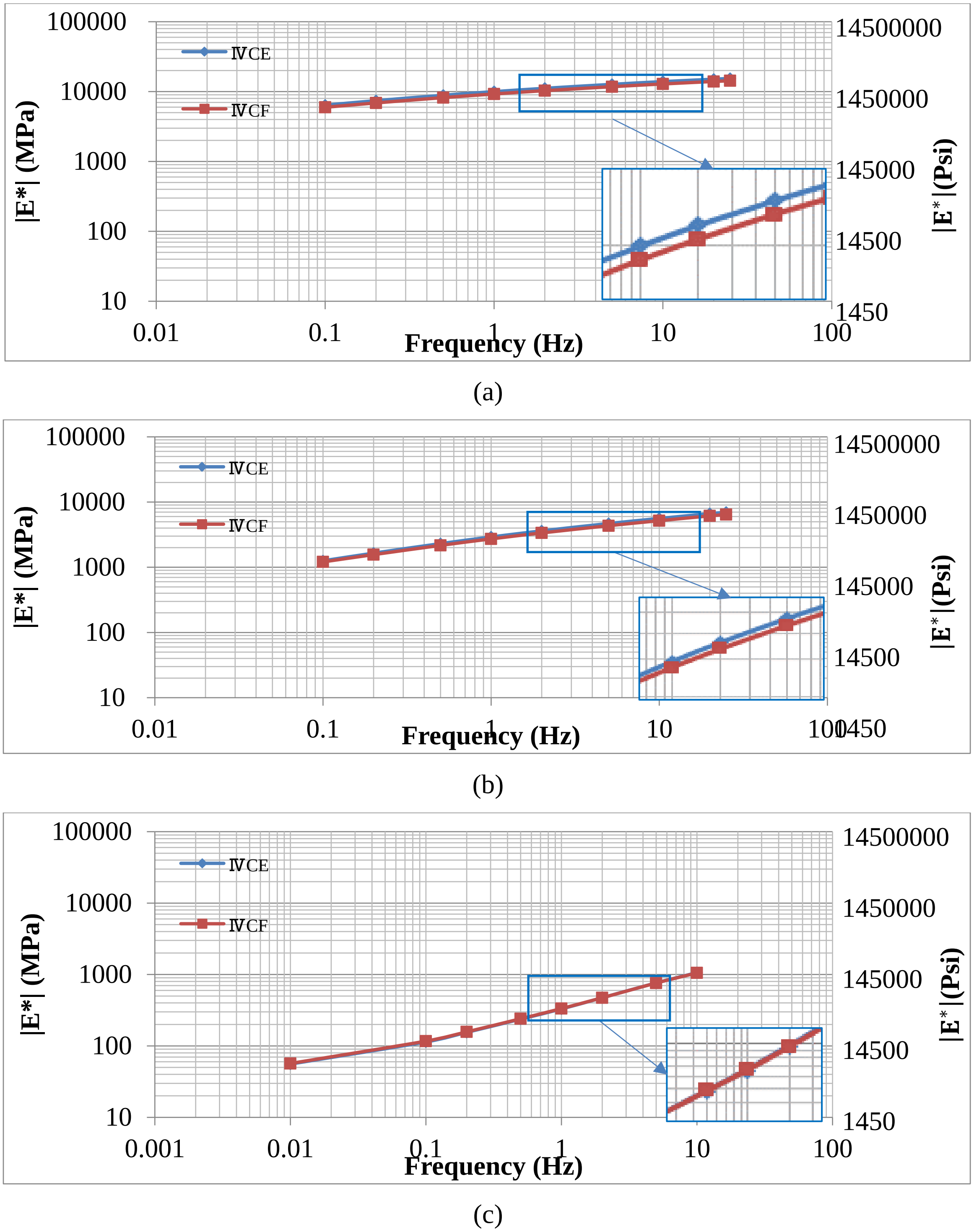

Figure 6-25 Dynamic Modulus Values of Various Surface Type C Mixtures for Aggregate Source IV with RAP in Terms of WMA Technology Type (a) at 4°C (39.2°F), (b) at 20°C (68°F), and (c) at 40°C (104°F)

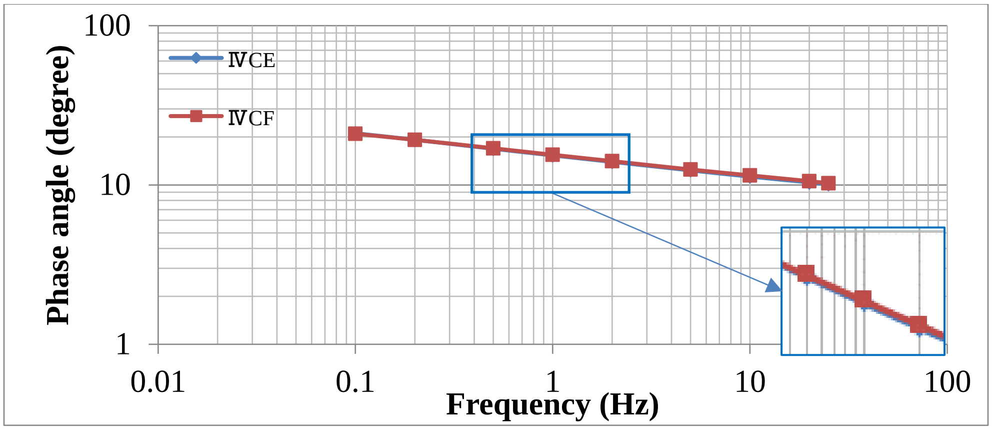

(a)

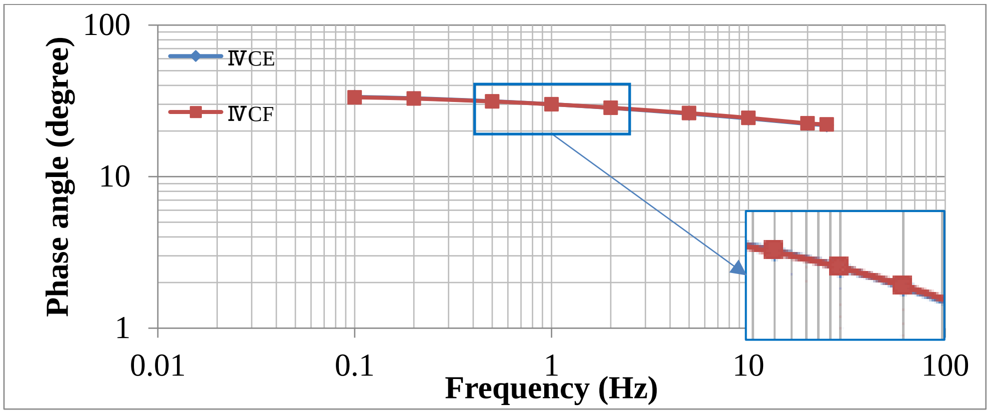

(b)

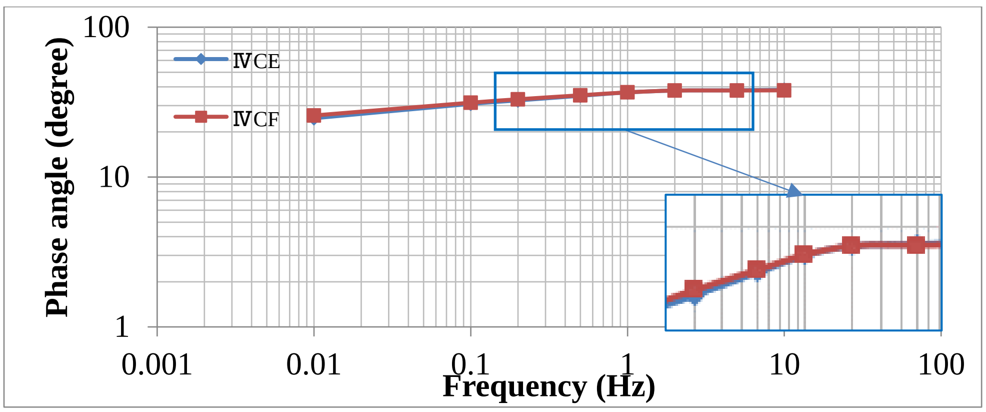

(c)

Figure 6-26 Phase Angle Values of Various Surface Type C Mixtures for Aggregate Source IV with RAP in Terms of WMA Technology Type (a) at 4°C (39.2°F), (b) at 20°C (68°F), and (c) at 40°C (104°F)

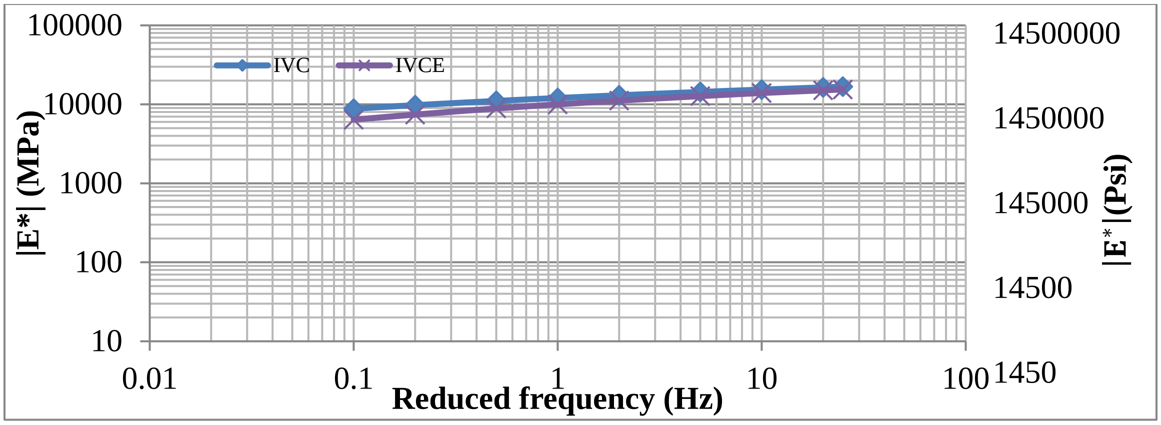

(a)

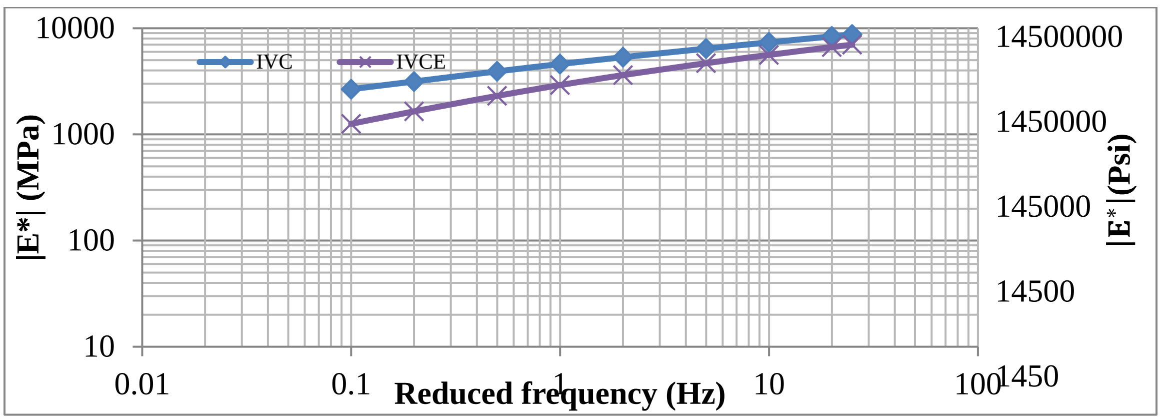

(b)

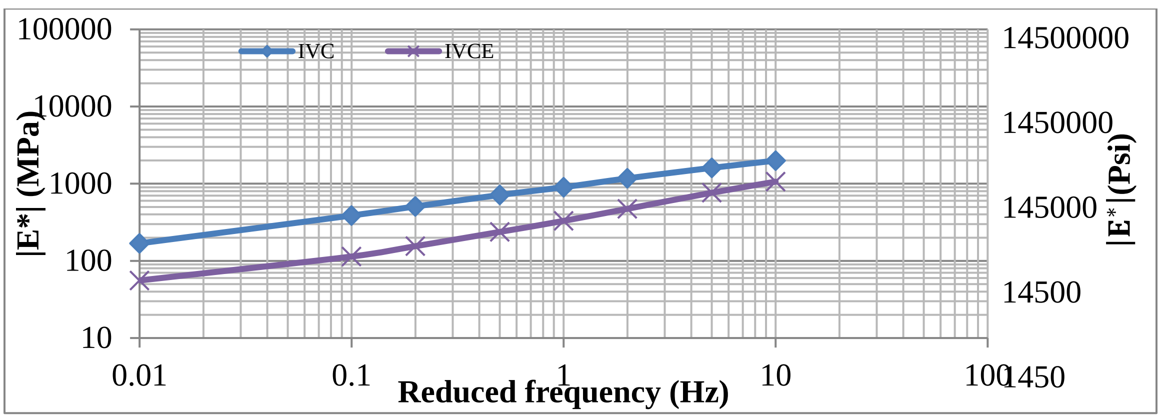

(c)

Figure 6-27 Dynamic Modulus Values of Various Surface Type C Mixtures for Aggregate Source IV with RAP in Terms of with/without WMA Technology (a) at 4°C (39.2°F), (b) at 20°C (68°F), and (c) at 40°C (104°F)

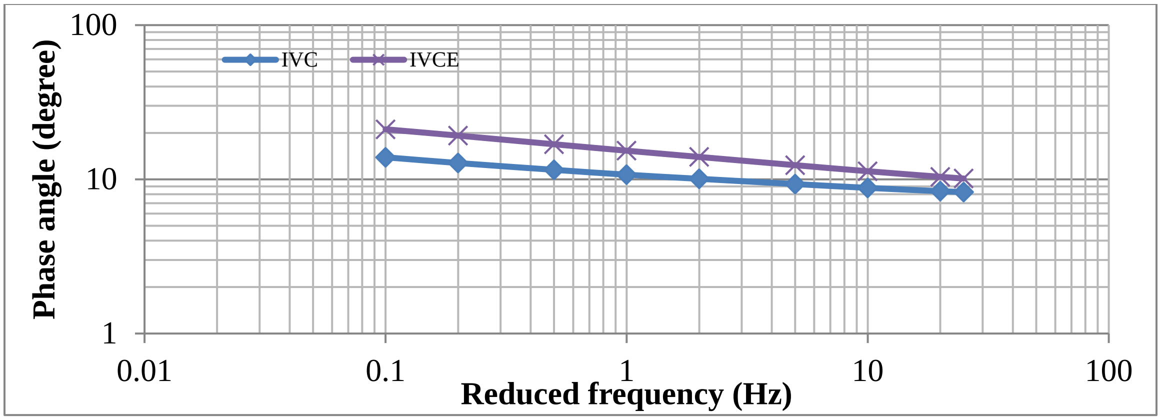

(a)

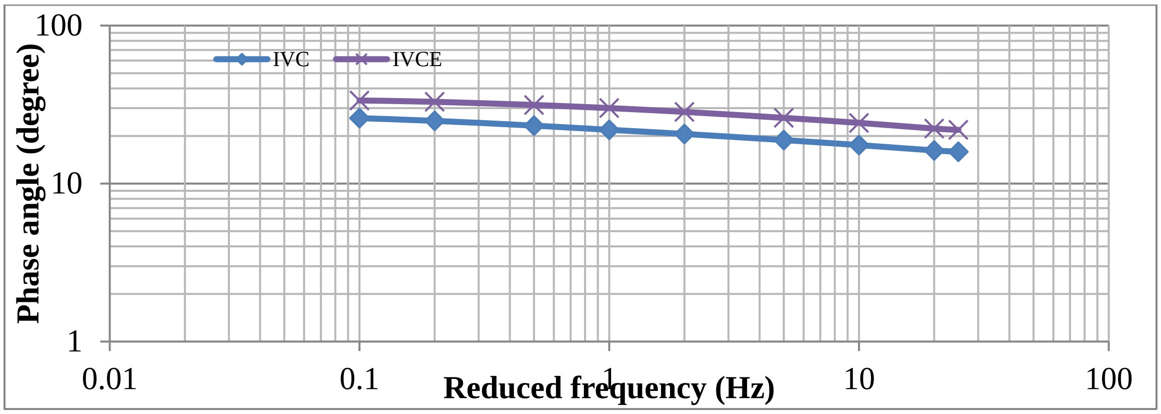

(b)

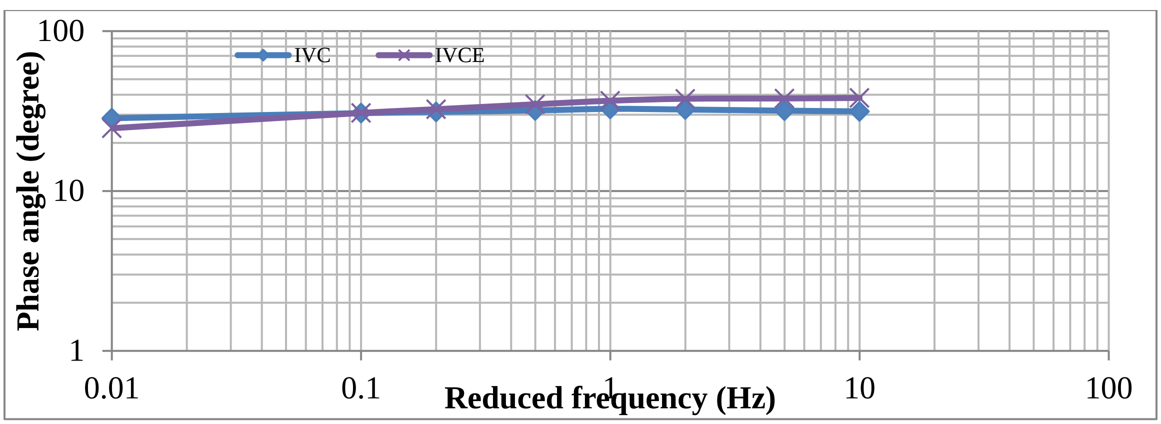

(c)

Figure 6-28 Phase Angle Values of Various Surface Type C Mixtures for Aggregate Source IV with RAP in Terms of with/without WMA Technology (a) at 4°C (39.2°F), (b) at 20°C (68°F), and (c) at 40°C (104°F)

6.1.14 Effect of Liquid ASAs on Dynamic Modulus and Phase Angle of Surface Type C Mixtures Made with Different Aggregate Types

Figure 6-29 shows the dynamic modulus of various Surface Type C mixtures made with aggregate source IV and RAP in terms of two liquid ASA types (Adhere® and Morlife®) tested at different temperatures. It can be seen that the dynamic modulus increased with the increase of frequency. As shown in Figure 6-29, mixture IV CA had similar dynamic modulus values compared to mixture IV CM. In addition, it can be observed in Figure 6-29 that with the increase of temperature, the dynamic modulus of mixtures decreased.

Similar trends of phase angle values were found for the mixtures made with aggregate source V tested in this study. The findings are presented in Appendix B.

Figure 6-30 shows the phase angle values of various Surface Type C mixtures made with aggregate source IV and RAP in terms of two liquid ASA types (Adhere® and Morlife®) tested at different temperatures. As shown in Figure 6-30, mixture IV CA had slightly higher phase angle values than mixture IV CM. It can be observed that the phase angle values of mixtures showed different trends at different temperatures. The phase angle values of mixtures decreased with the increase of frequency at 4℃ (39.2°F) and 20℃ (68°F). However, with the increase of frequency, the phase angle values of mixtures initially increased and then remained approximately unchanged at 40℃ (104°F). Moreover, it can be observed that the phase angle values of mixtures increased with the increase of temperature.

Similar trends of phase angle values were found for the mixtures made with aggregate source V in this study. The results of this portion of the research project are presented in the Appendix B.

Figure 6-31 shows the dynamic modulus values of various Surface Type C mixtures containing aggregate source IV and RAP, tested at different temperatures, and compared in terms of with or without liquid ASA (Morlife®). It can be seen that the dynamic modulus values increased with the increase of frequency. Mixture IV C had similar dynamic modulus values compared to mixture IV CM. Therefore, for the materials tested for this research project, it can be concluded that liquid ASA generally did not have an effect on the dynamic modulus values. Similar trends of dynamic modulus values were found for the mixtures made with aggregate source V as well as the mixtures made with the other liquid ASA (Adhere®) and aggregate sources IV and V.

Figure 6-32 shows the phase angle values of various Surface Type C mixtures containing aggregate source IV and RAP, tested at different temperatures, and compared in terms of with or without liquid ASA (Morlife®). It can be noted that mixture IV C had similar phase angle values compared to mixture IV CM. Therefore, it can be concluded that liquid ASA generally had no effects on the phase angle of Surface Type C mixtures.

Similar trends of phase angle values were found for the mixtures made with aggregate source V and the other liquid ASA (Adhere®) tested in this study. The data results are available in other figures in terms of aggregate source and mixture type in Appendices A and B.

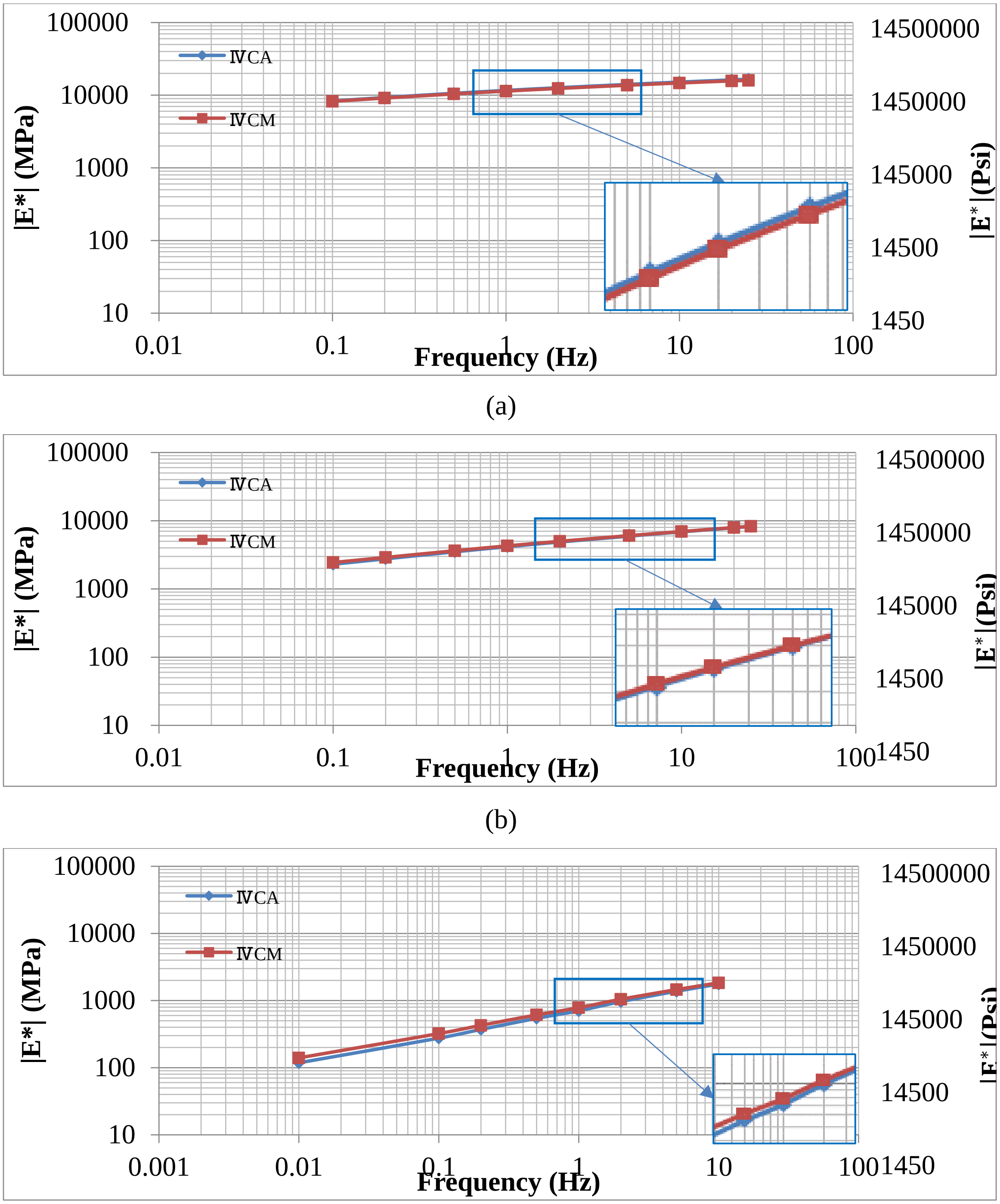

Figure 6-29 Dynamic Modulus Values of Various Surface Type C Mixtures for Aggregate Source IV with RAP in Terms of Liquid ASA Type (a) at 4°C (39.2°F), (b) at 20°C (68°F), and (c) at 40°C (104°F)

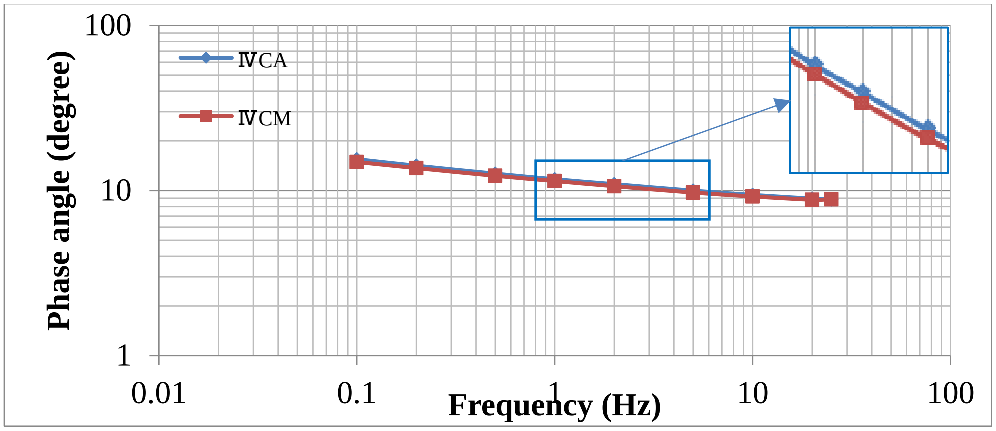

(a)

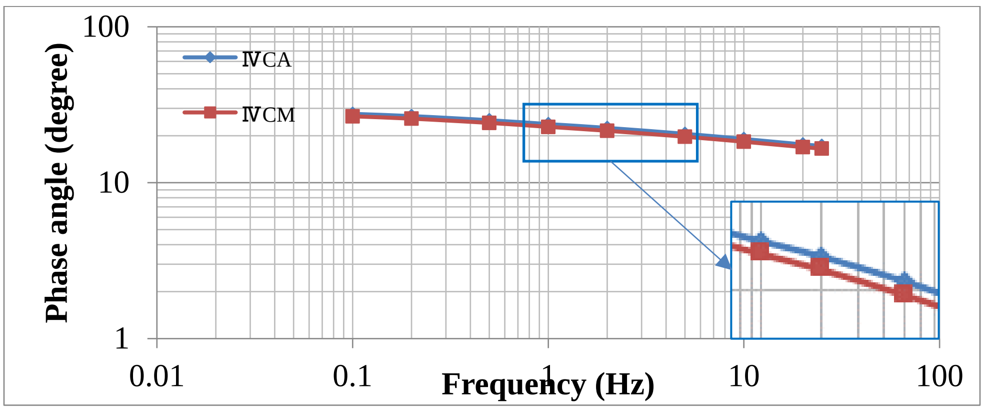

(b)

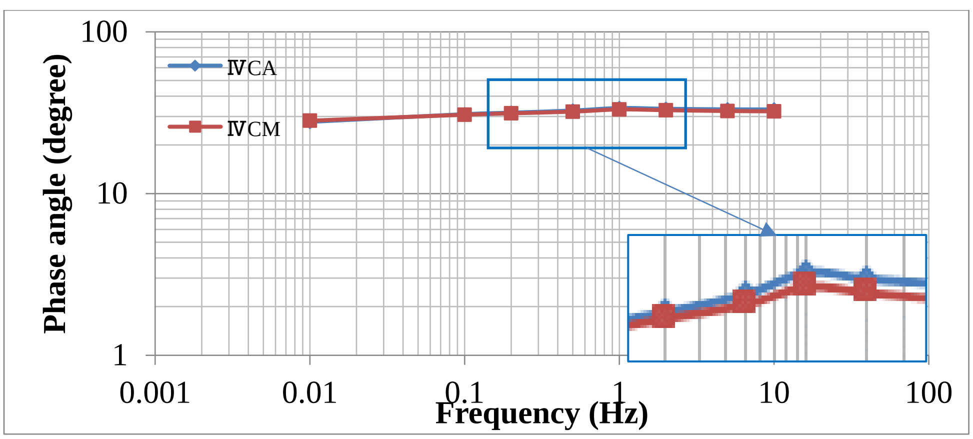

(c)

Figure 6-30 Phase Angle Values of Various Surface Type C Mixtures for Aggregate Source IV with RAP in Terms of Liquid ASA Type (a) at 4°C (39.2°F), (b) at 20°C (68°F), and (c) at 40°C (104°F)

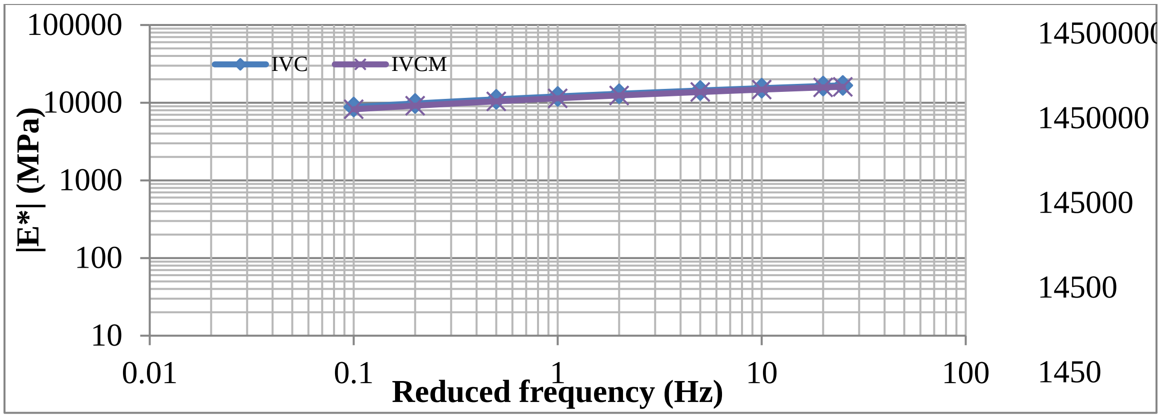

(a)

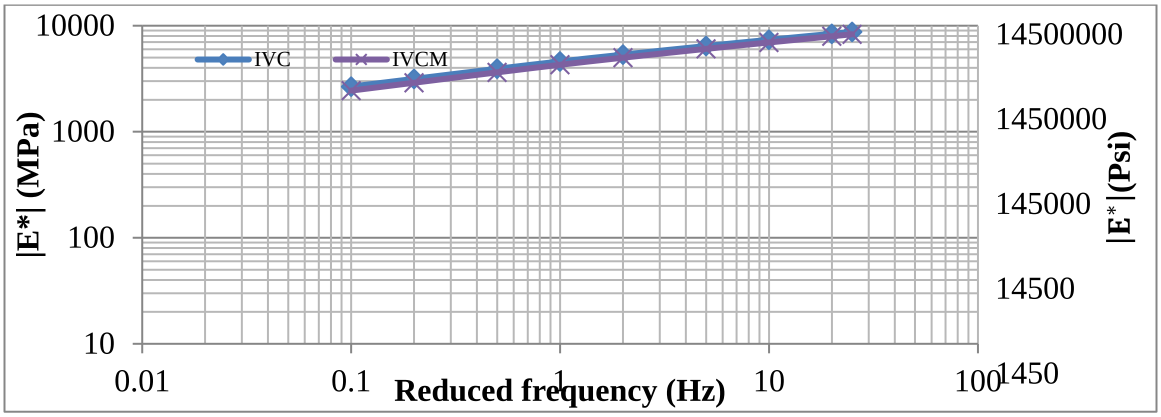

(b)

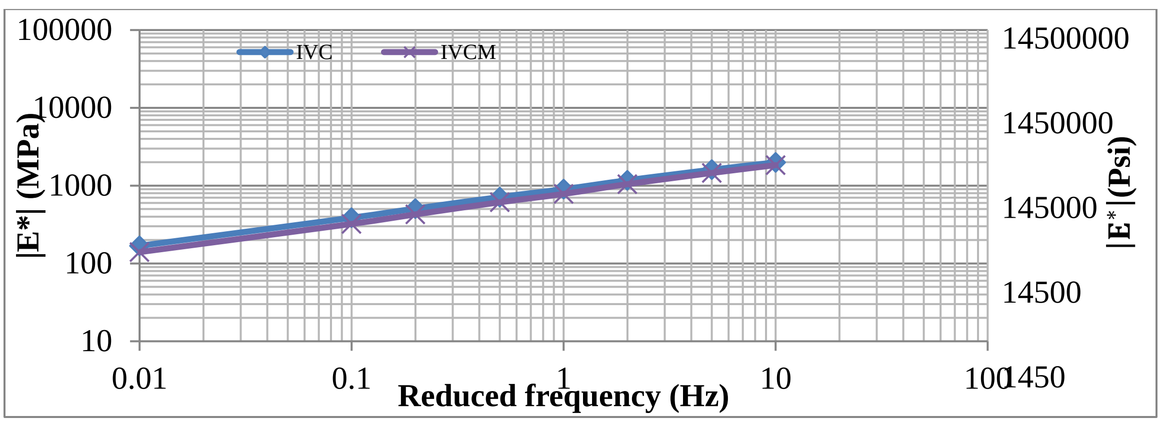

(c)

Figure 6-31 Dynamic Modulus Values of Various Surface Type C Mixtures for Aggregate Source IV with RAP in Terms of with/without Liquid ASA (a) at 4°C (39.2°F), (b) at 20°C (68°F), and (c) at 40°C (104°F)

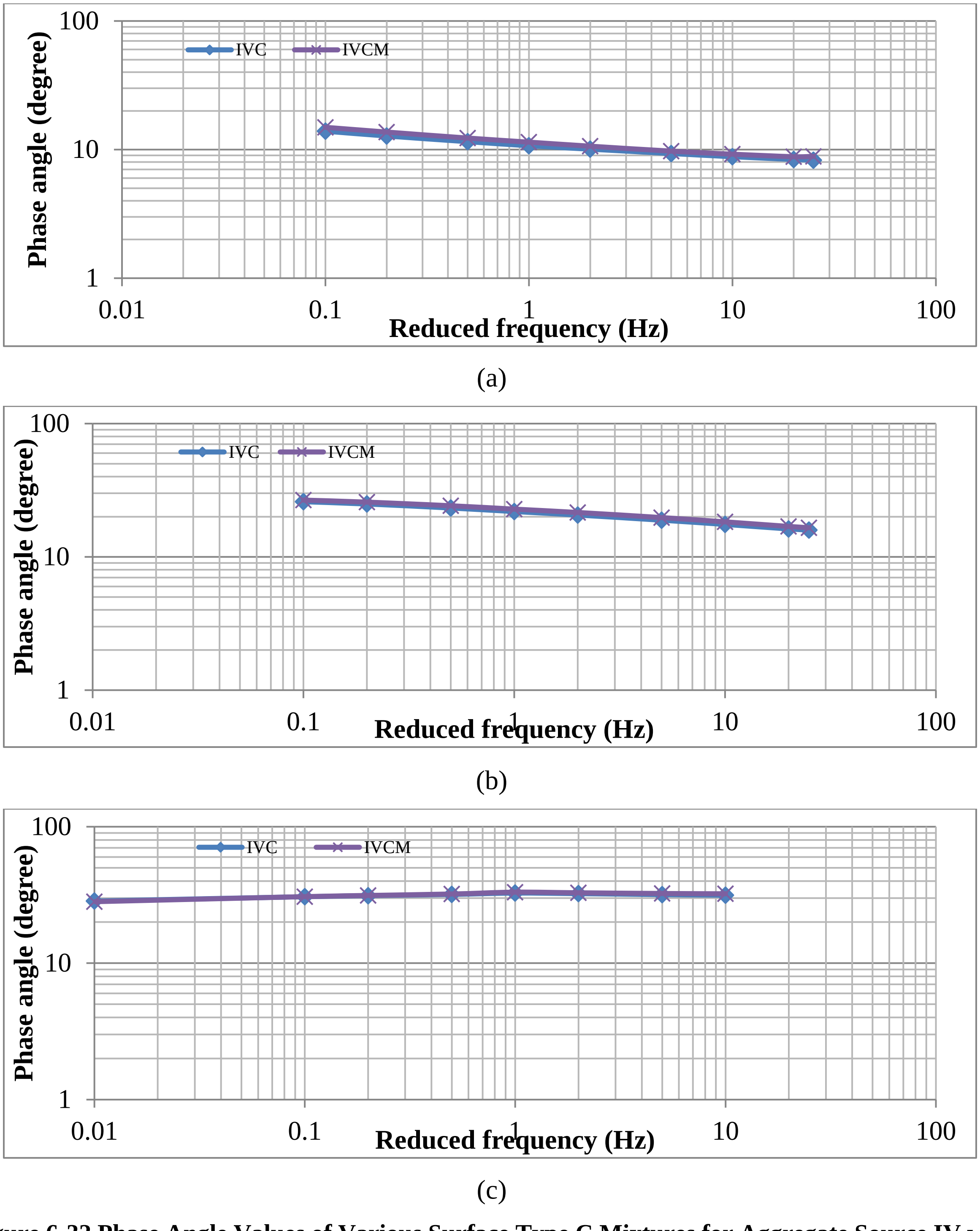

Figure 6-32 Phase Angle Values of Various Surface Type C Mixtures for Aggregate Source IV with RAP in Terms of with/without Liquid ASA (a) at 4°C (39.2°F), (b) at 20°C (68°F), and (c) at 40°C (104°F)

6.1.15 Effect of Aging on Dynamic Modulus and Phase Angle of Surface Mixtures (Types A, B and C) Made with Different Aggregate Types

Figure 6-33 shows the dynamic modulus of various mixtures made with aggregate source IV and RAP after long-term aging in terms of three Surface Course mixture types (Surface Types A, B, and C) tested at different temperatures. It can be seen that the dynamic modulus increased with the increase of frequency. As shown in Figure 6-33, mixture IV BG had the highest dynamic modulus values at 4°C (39.2°F), while mixtures IV AG and IV CG had the highest dynamic modulus at 20°C (68°F) and 40°C (104°F), respectively. It can be concluded that temperature had significant influence on the dynamic modulus of mixtures after long-term aging. In addition, it can be observed in Figure 6-33 that with the increase of temperature the dynamic modulus of mixtures decreased.

Similar trends of dynamic modulus values were found for the mixtures made with aggregate source V tested in this study. The figures shown in the Appendix B show the results of this part of the research work.

Figure 6-34 shows the phase angle values of various mixtures made with aggregate source IV and RAP after long-term aging in terms of Surface Course mixture type (Surface Types A, B, and C) tested at different temperatures. As shown in Figure 6-34, mixture IV BG had the highest phase angle values at 4°C (39.2°F) and 20°C (68°F), while mixture IV AG had the lowest phase angle values. Mixture IV CG had the highest phase angle values at 40°C (104°F) and low frequency, and the lowest values at 40°C (104°F) and high frequency. It can be observed that the phase angle values of mixtures showed different trends at different temperatures. The phase angle values of mixtures decreased with the increase of frequency at 4°C (39.2°F) and 20°C (68°F). However, with the increase of frequency, the phase angle values of mixtures initially increased and then remained approximately unchanged at 40°C (104°F). Moreover, it can be observed that the phase angle values of mixtures increased with the increase of temperature.

Similar trends of phase angle values were found for the mixtures made with aggregate source V tested in this study. The figures presented in the Appendix B show the results of the testing for this portion of the research project.

Figure 6-35 shows the dynamic modulus values of Surface Type A mixtures containing aggregate source IV and RAP, tested at various temperatures, and in terms of aged or unaged condition. It can be seen that the dynamic modulus increased with the increase of frequency. It can be noted that mixture IV A and mixture IV AG had similar dynamic modulus values at the test temperatures. It can be concluded that the long-term aging process generally did not affect the dynamic modulus of mixtures. Similar trends of dynamic modulus values were found for the aged and unaged mixtures made with aggregate source V and Surface Types B and C.

Figure 6-36 shows the phase angle values of Surface Type A mixtures containing aggregate source IV and RAP, tested at various temperatures, and in both aged and unaged conditions. It can be noted that mixtures IV A and IV AG had similar phase angle values at the different test temperatures. It can be concluded that the long-term aging process generally did not affect the phase angle values of mixtures tested for this portion of the research work.

Similar trends of phase angle values were found for the aged and unaged mixtures made with aggregate source V and Surface Types B and C. The data results are available in other figures in terms of aggregate source and mixture type in Appendices A and B.

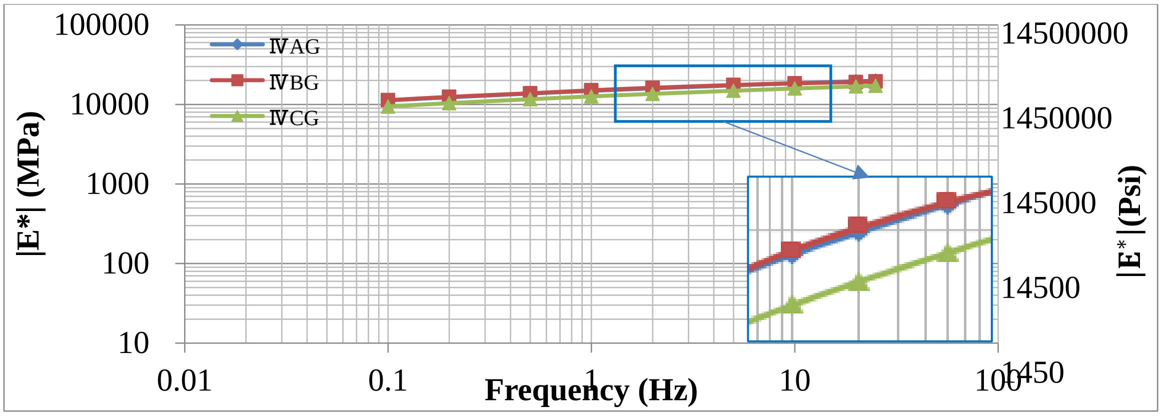

(a)

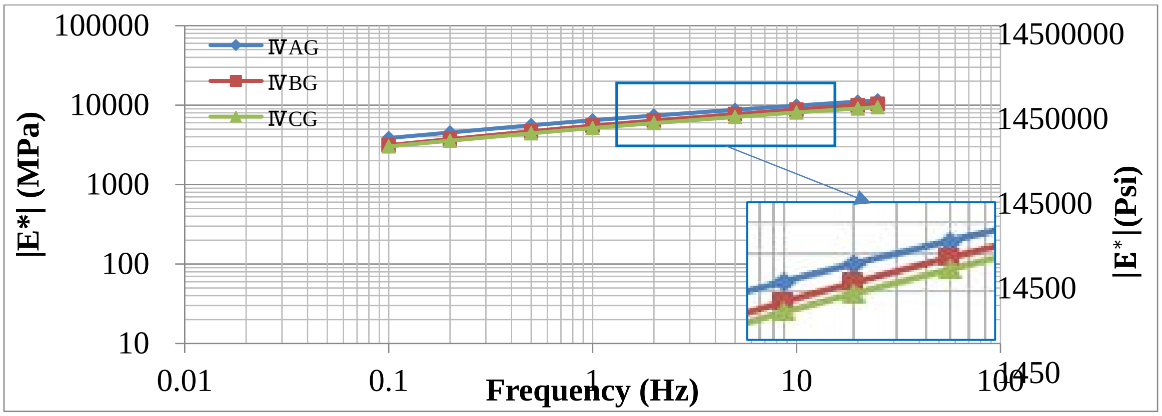

(b)

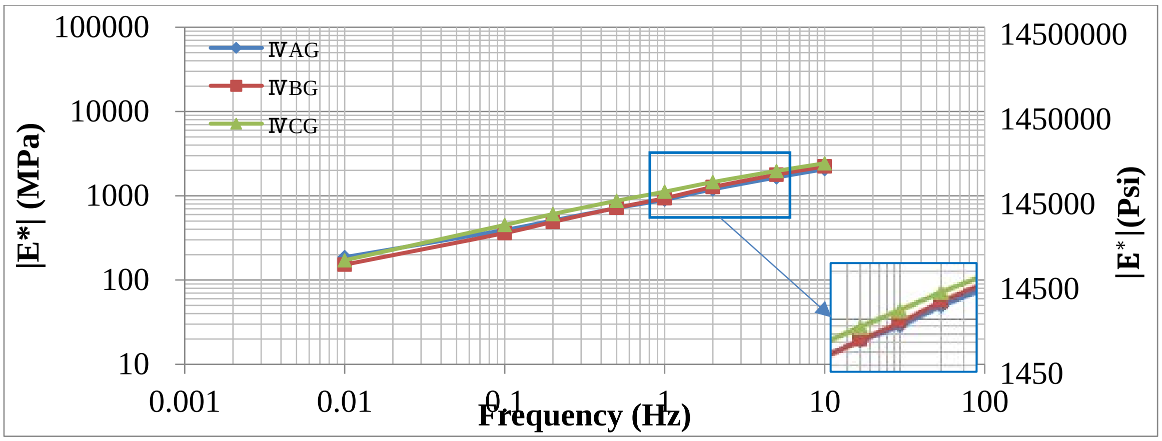

(c)

Figure 6-33 Dynamic Modulus Values of Various Mixtures for Aggregate Source IV with RAP after Long-Term Aging in Terms of Surface Mixture Type (a) at 4°C (39.2°F), (b) at 20°C (68°F), and (c) at 45°C (113°F) (Surface Type A), 40°C (104°F) (Surface Types B and C)

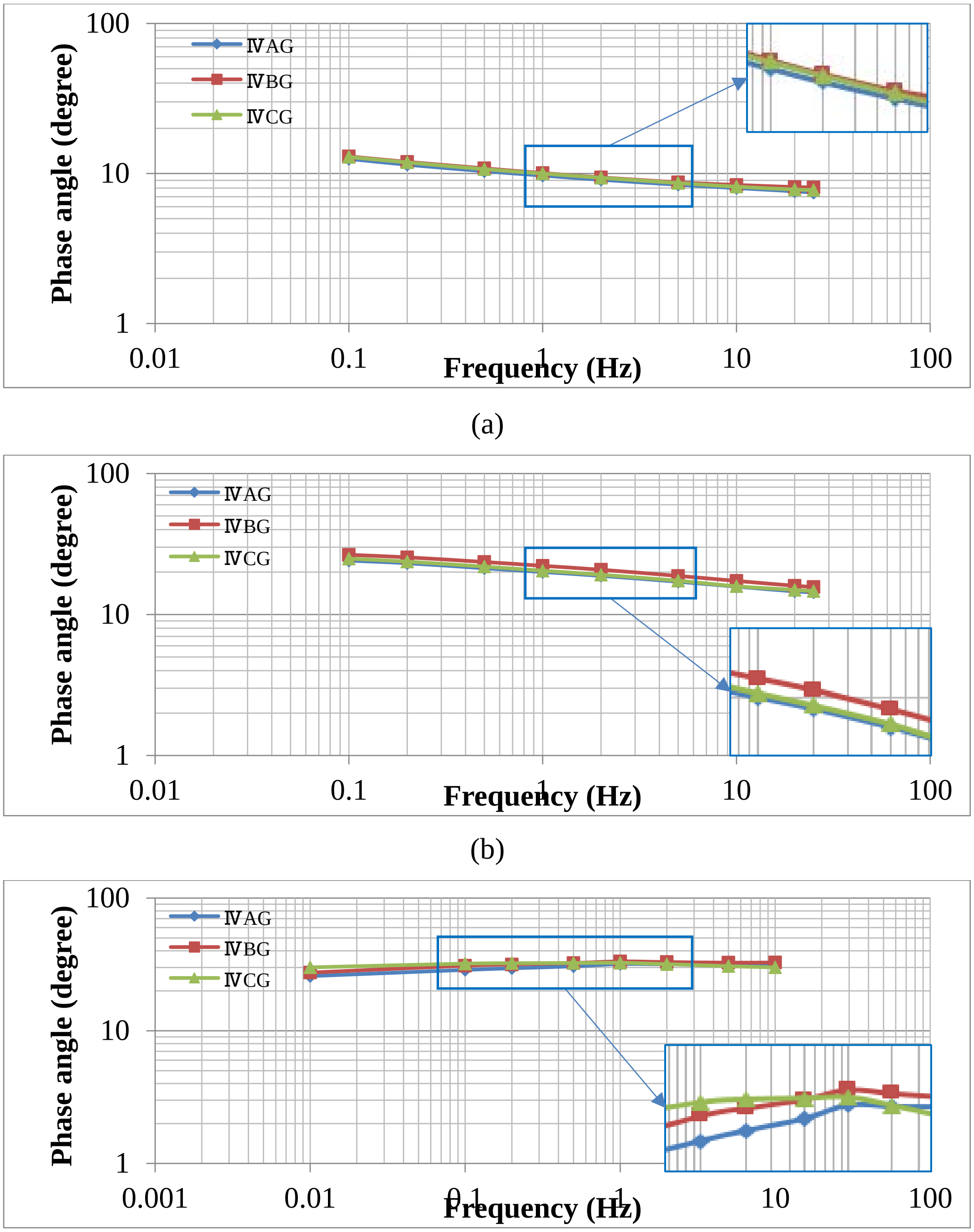

(a)

(b)

(c)

Figure 6-34 Phase Angle Values of Various Mixtures for Aggregate Source IV with RAP after Long-Term Aging in Terms of Surface Mixture Type (a) at 4°C (39.2°F), (b) at 20°C (68°F), and (c) at 45°C (113°F) (Surface Type A), 40°C (104°F) (Surface Types B and C)

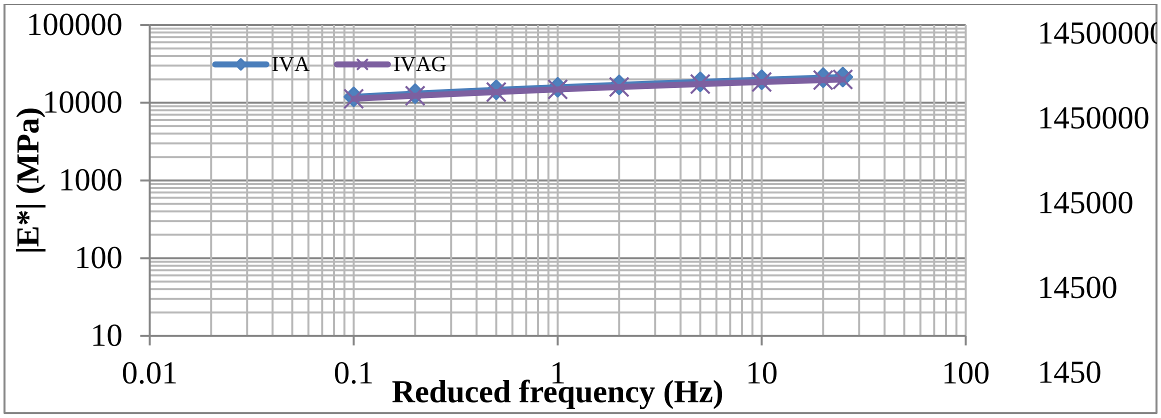

(a)

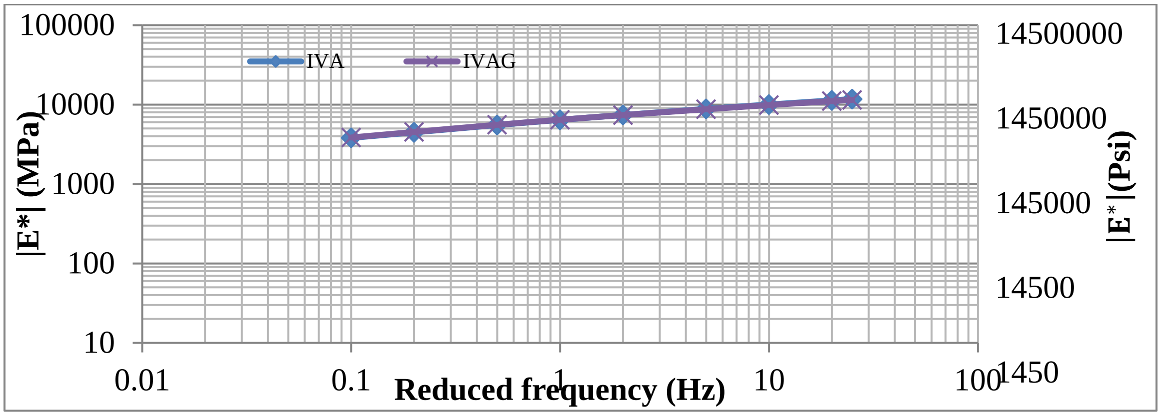

(b)

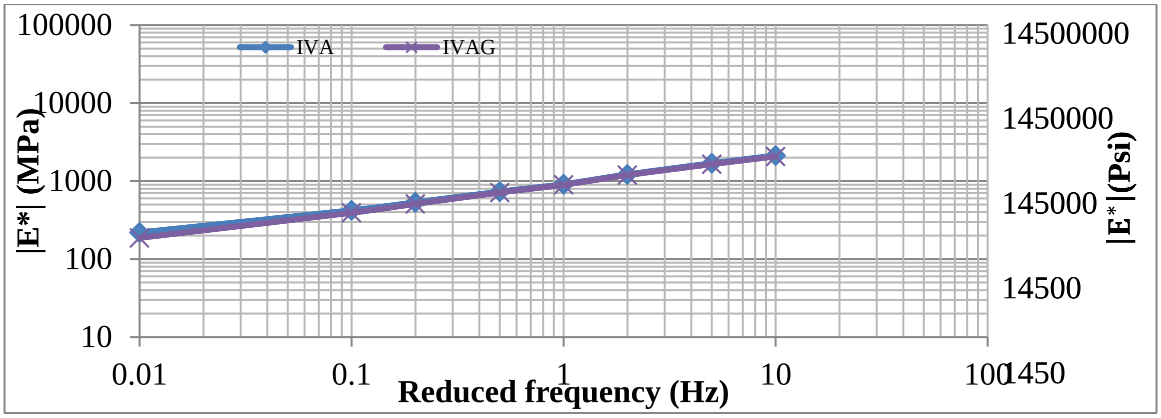

(c)

Figure 6-35 Dynamic Modulus Values of Various Surface A Mixtures for Aggregate Source IV with RAP in Terms of Aged or Unaged status (a) at 4°C (39.2°F), (b) at 20°C (68°F), and (c) at 45°C (113°F)

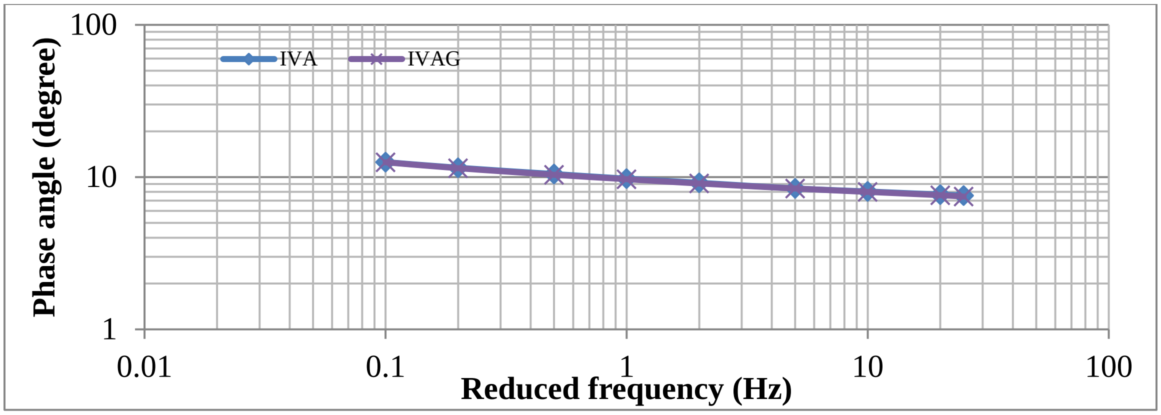

(a)

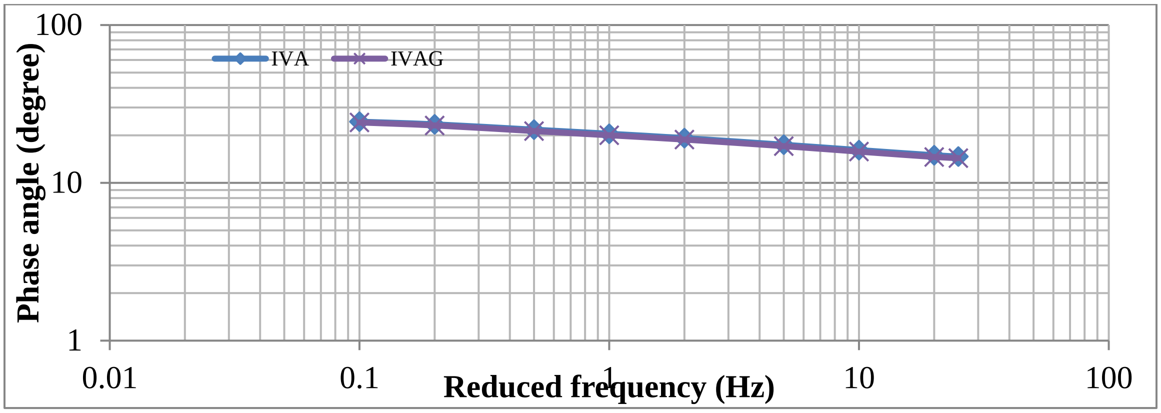

(b)

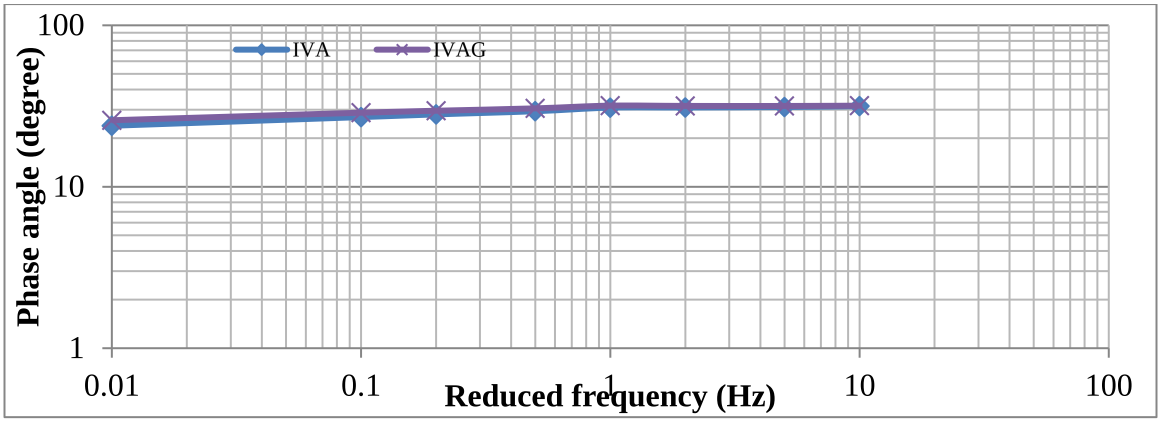

(c)

Figure 6-36 Phase Angle Values of Various Surface A Mixtures for Aggregate Source IV with RAP in Terms of Aged or Unaged status (a) at 4°C (39.2°F), (b) at 20°C (68°F), and (c) at 45°C (113°F)

6.1.16 Effects of RAP on Dynamic Modulus and Phase Angle

6.1.16.1 Effects of RAP on Dynamic Modulus and Phase Angle of Various Surface Mixtures Made with Different Aggregate Types

Figure 6-37 shows the dynamic modulus values of Surface Type A mixtures made with various aggregate sources both with and without RAP and tested at various temperatures. The dynamic modulus values of Surface Type A mixtures containing RAP were higher than the values of Surface Type A Mixtures without RAP regardless of aggregate source, loading frequency and test temperature. It can be seen that the differences in dynamic modulus were more pronounced at a lower frequency.

Similar dynamic modulus results for Surface Types B, C, D, and E are shown in Figure 6-39, Figure 6-41, Figure 6-43, and Figure 6-45, respectively. The only exception was Surface Type C made with aggregate source V, which exhibited lower dynamic modulus values with RAP than without RAP.

Figure 6-38 shows the phase angle values of Surface Type A mixtures made with various aggregate sources both with and without RAP and tested at various temperatures. The phase angle values of Surface Type A mixtures made with RAP were generally lower than the values of Surface Type A mixtures without RAP regardless of aggregate source, loading frequency and test temperature. However, the differences in phase angle values of these mixtures were less pronounced when the test temperature increased to 45°C (113°F).

Similar phase angle results for Surface Types B, C, and E are shown in Figure 6-40, Figure 6-42, and Figure 6-46, respectively. The only exception was Surface Type C made with aggregate source V, which exhibited higher phase angle values with RAP than without.

However, Surface Type D mixtures with and without RAP behaved in a different manner than the other Surface mixture types with respect to phase angle. As shown Figure 6-44, the phase angle values of Surface Type D mixtures made with RAP were generally similar to the values of Surface Type D mixtures without RAP regardless of aggregate source, loading frequency, and test temperature.

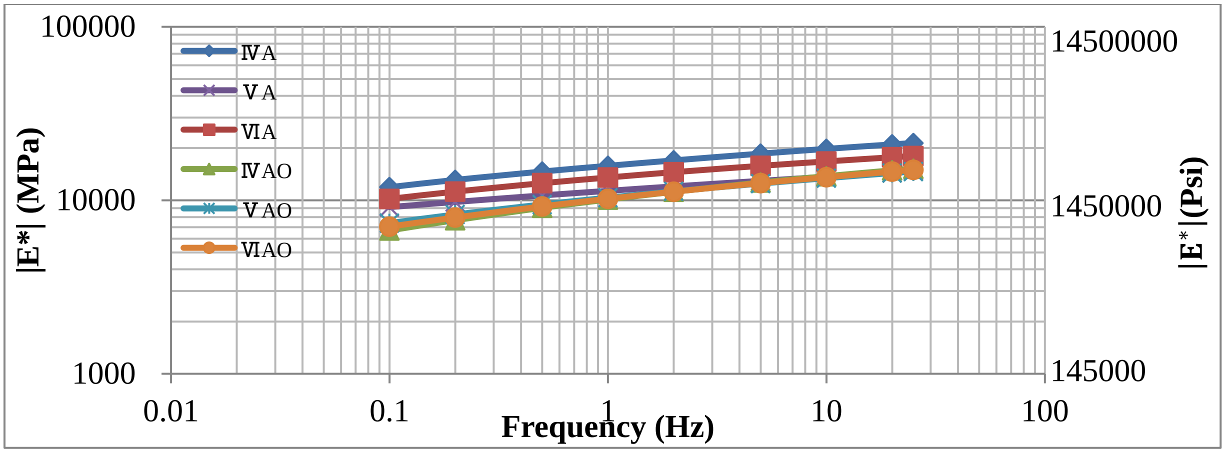

(a)

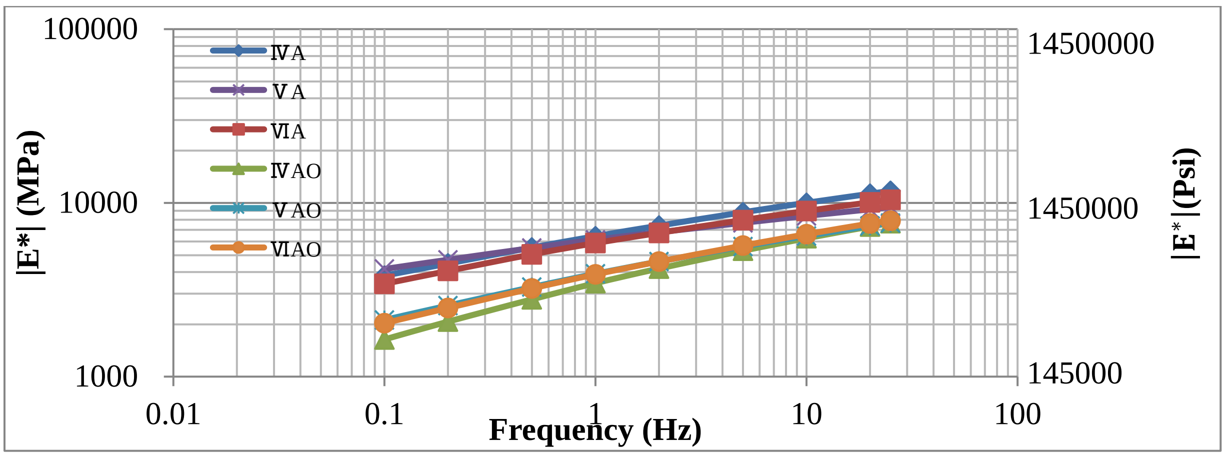

(b)

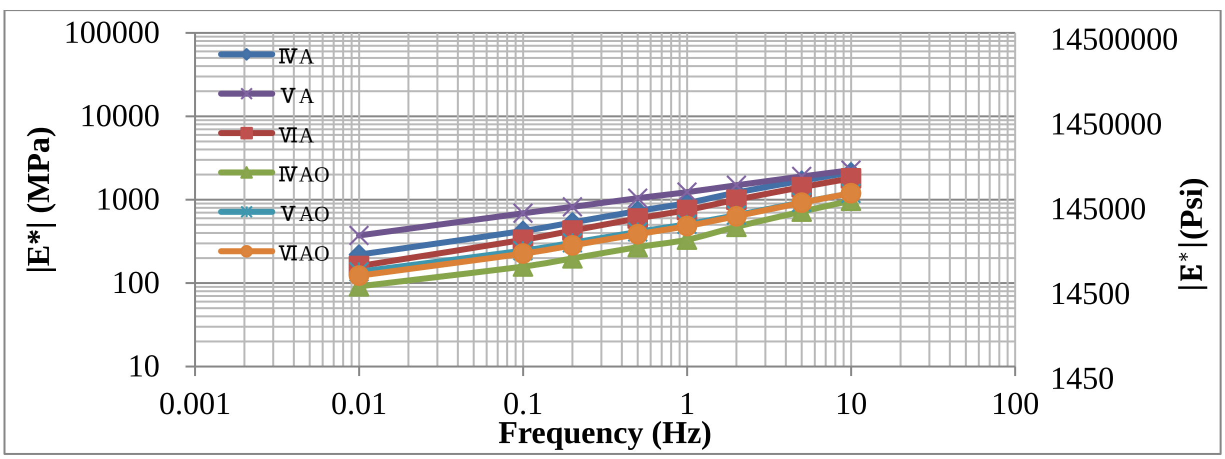

(c)

Figure 6-37 Dynamic Modulus Values of Various Surface A Mixtures with/without RAP in Terms of Different Aggregate Types, (a) at 4°C (39.2°F), (b) at 20°C (68°F), and (c) at 45°C (113°F)

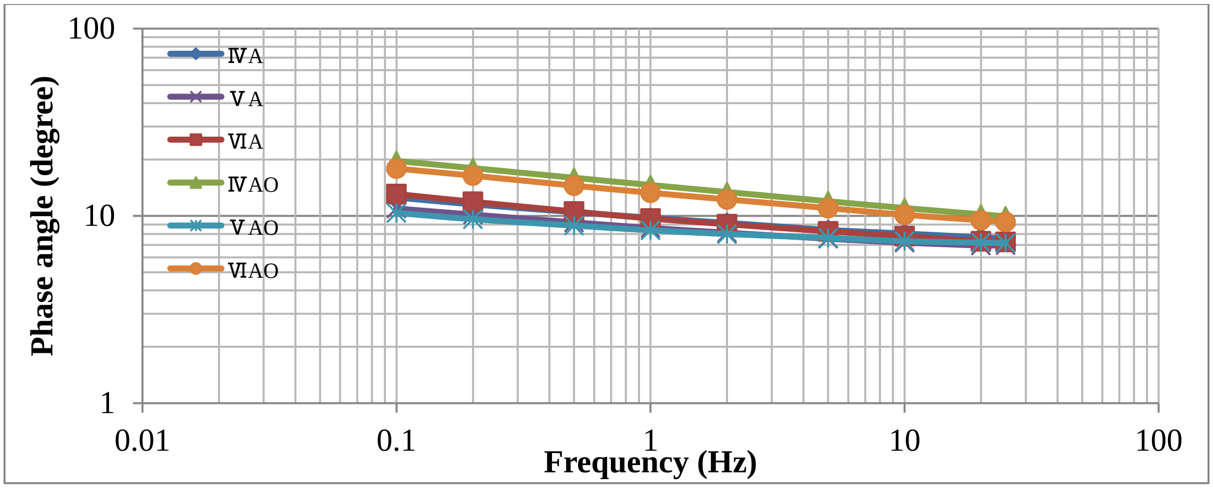

(a)

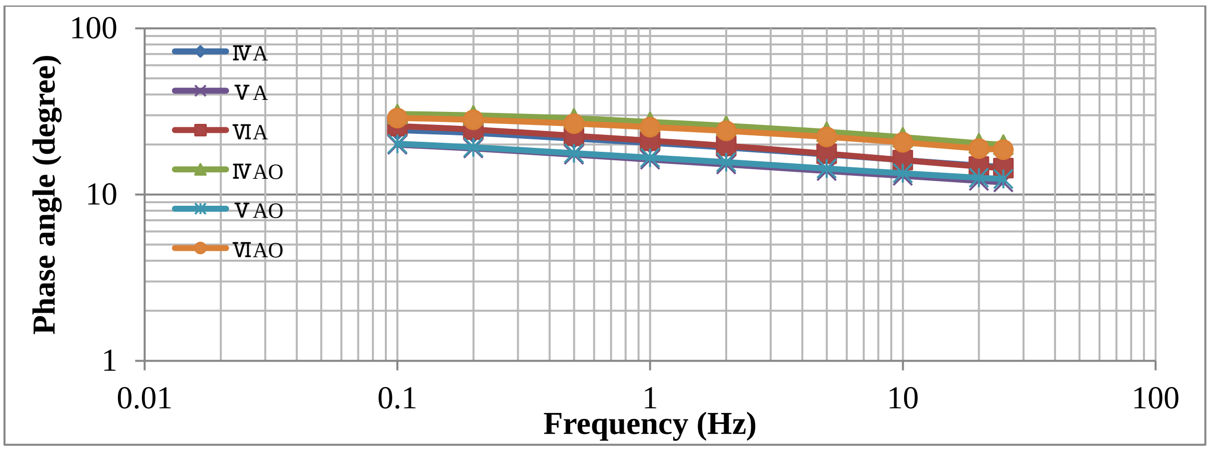

(b)

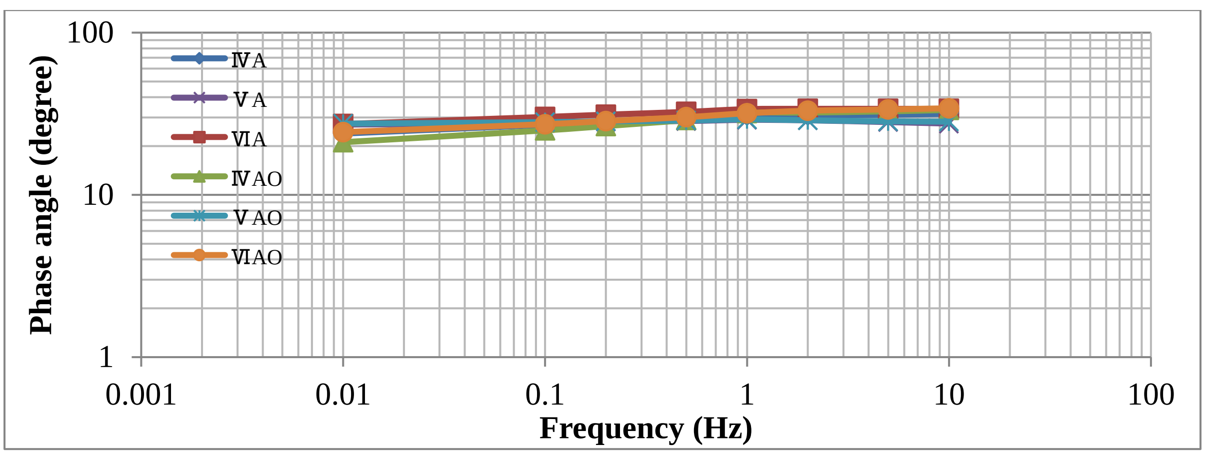

(c)

Figure 6-38 Phase Angle Values of Various Surface A Mixtures with/without RAP in Terms of Different Aggregate Types, (a) at 4°C (39.2°F), (b) at 20°C (68°F), and (c) at 45°C (113°F)

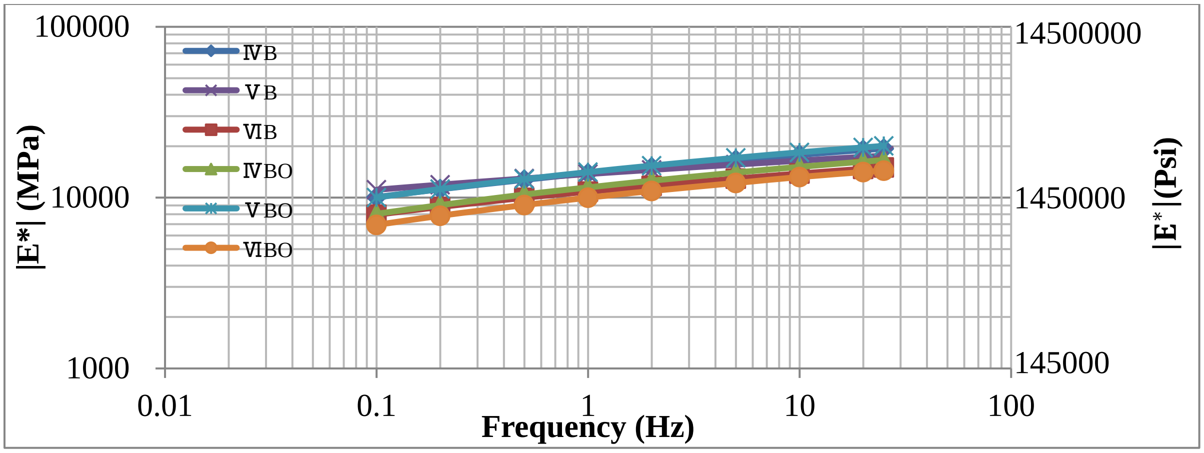

(a)

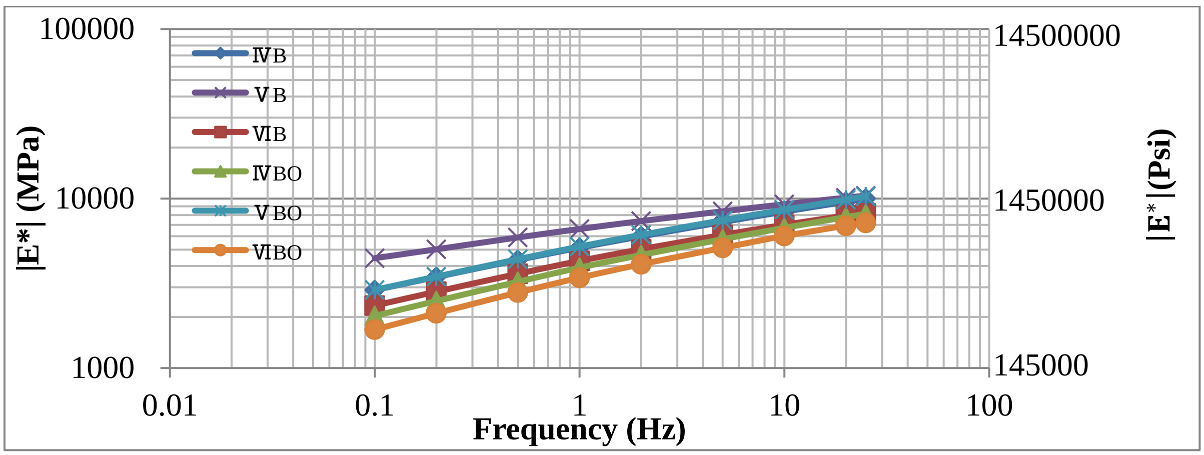

(b)

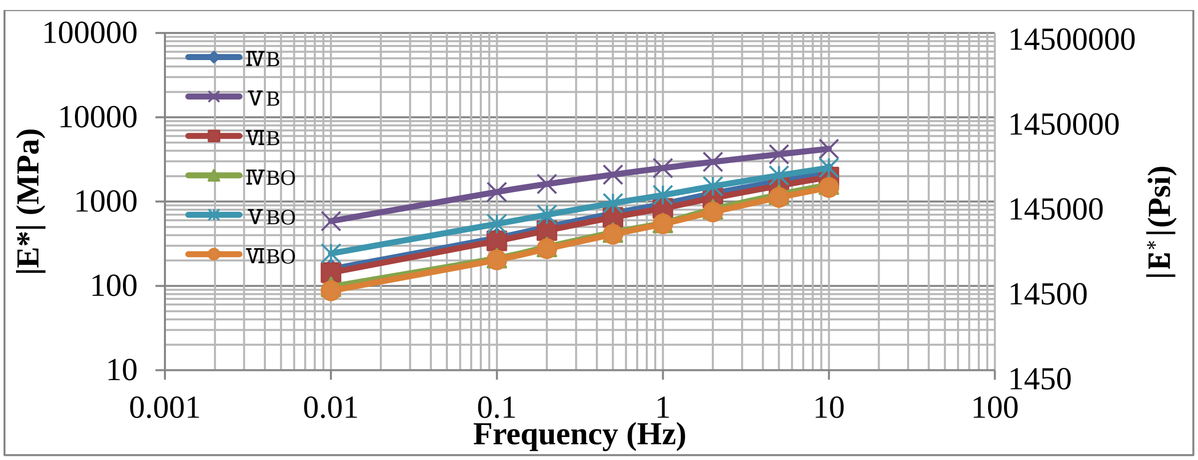

(c)

Figure 6-39 Dynamic Modulus Values of Various Surface B Mixtures with/without RAP in Terms of Different Aggregate Types, (a) at 4°C (39.2°F), (b) at 20°C (68°F), and (c) at 45°C (113°F)

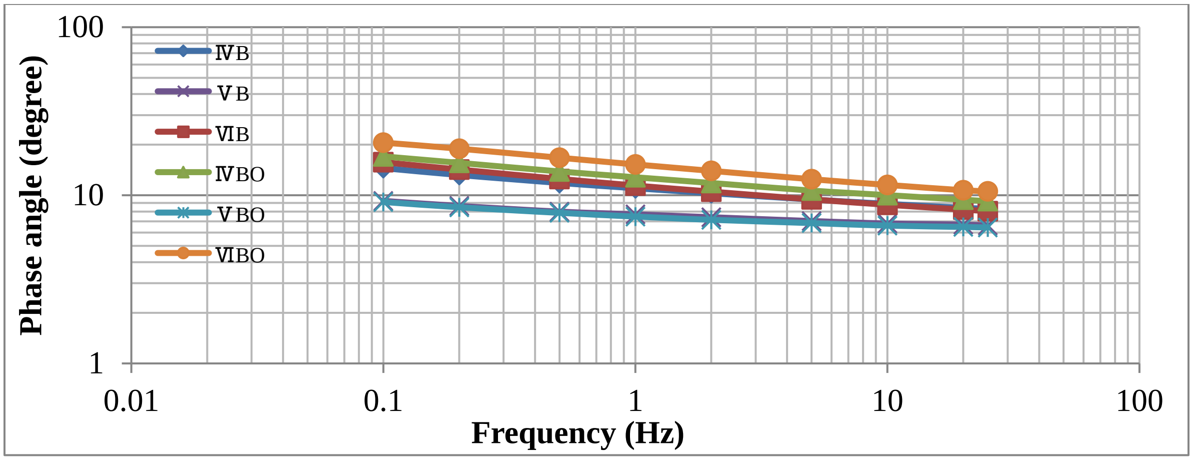

(a)

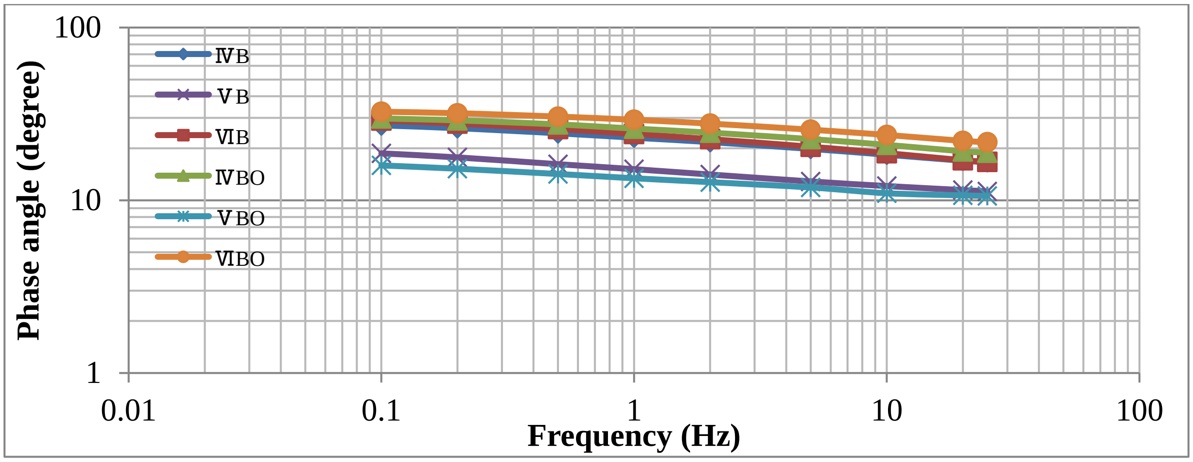

(b)

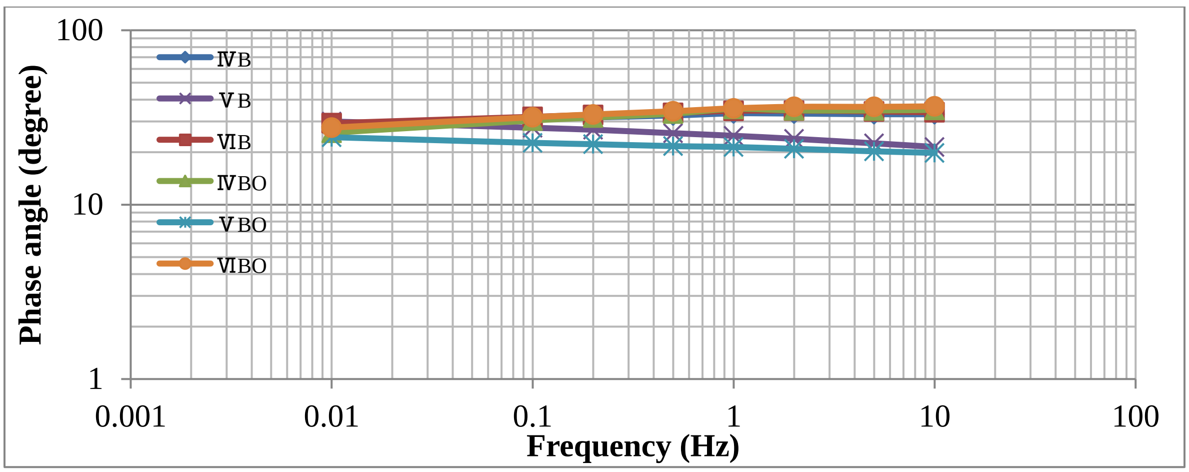

(c)

Figure 6-40 Phase Angle Values of Various Surface B Mixtures with/without RAP in Terms of Different Aggregate Types, (a) at 4°C (39.2°F), (b) at 20°C (68°F), and (c) at 45°C (113°F)

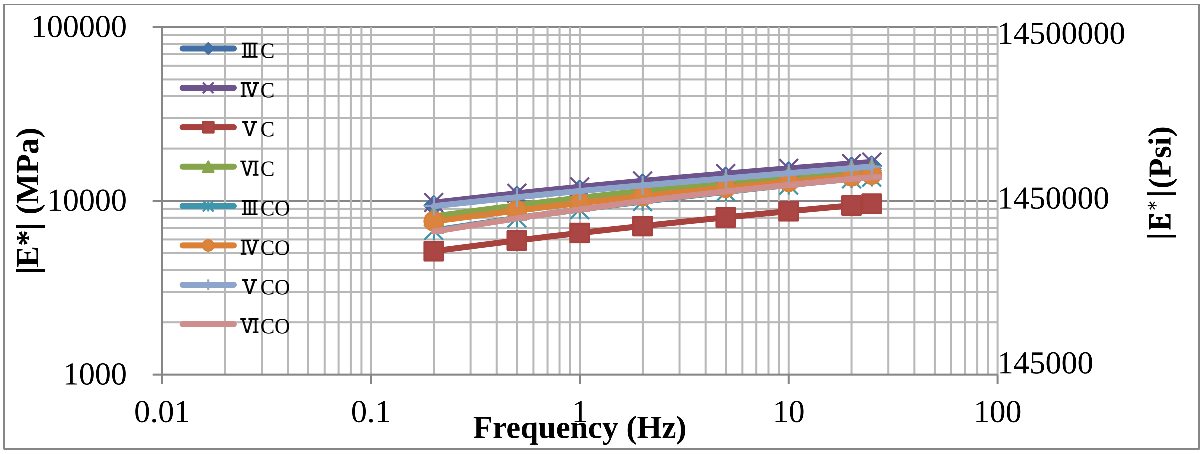

(a)

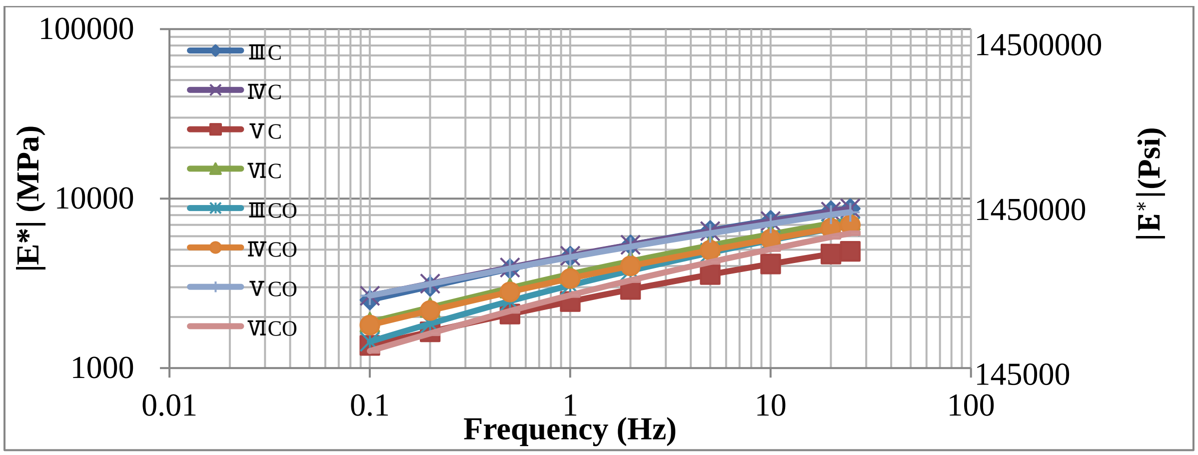

(b)

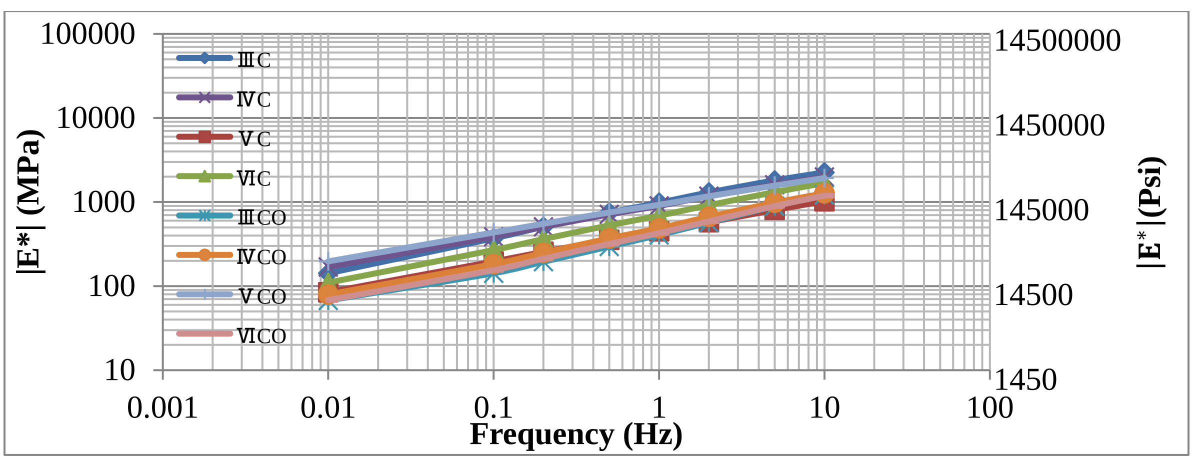

(c)

Figure 6-41 Dynamic Modulus Values of Various Surface C Mixtures with/without RAP in Terms of Different Aggregate Types, (a) at 4°C (39.2°F), (b) at 20°C (68°F), and (c) at 45°C (113°F)

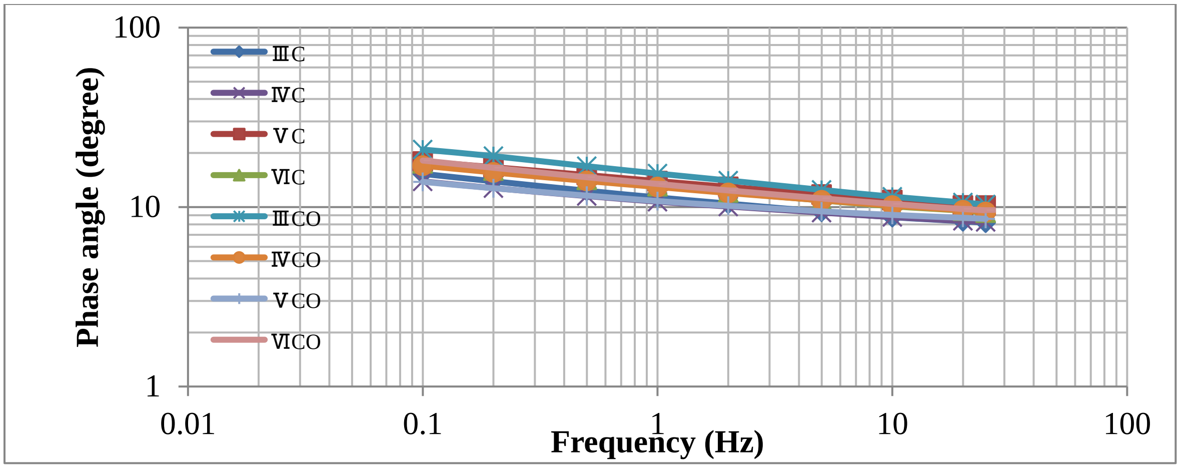

(a)

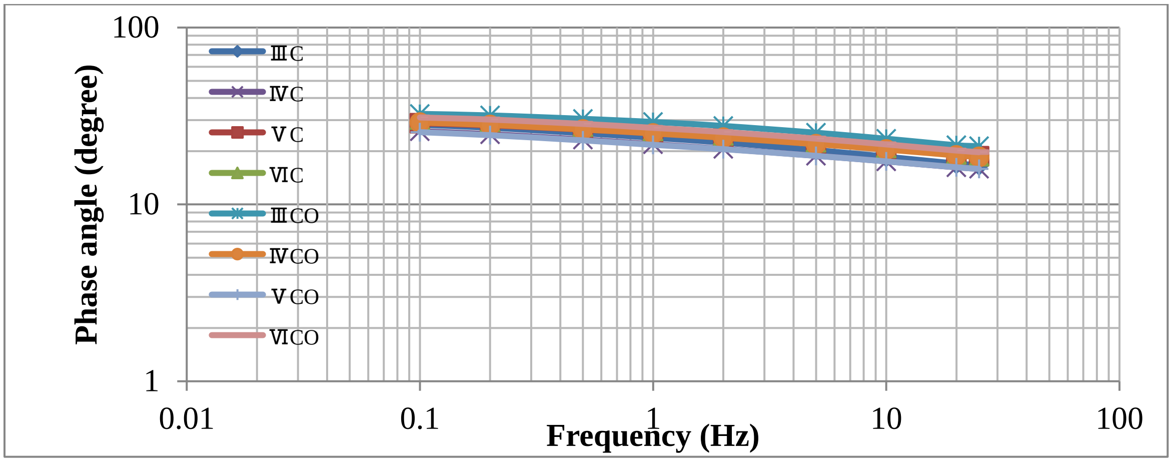

(b)

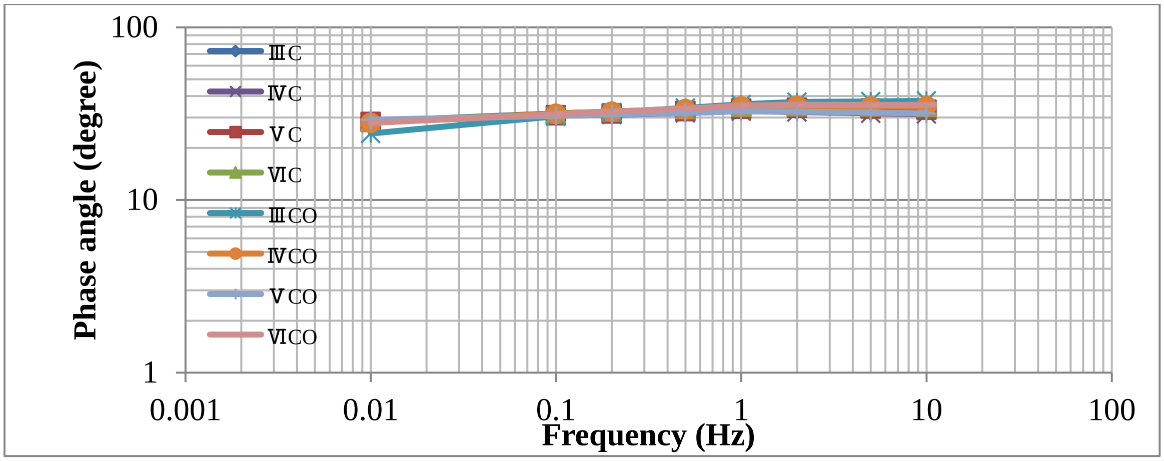

(c)

Figure 6-42 Phase Angle Values of Various Surface C Mixtures with/without RAP in Terms of Different Aggregate Types, (a) at 4°C (39.2°F), (b) at 20°C (68°F), and (c) at 45°C (113°F)

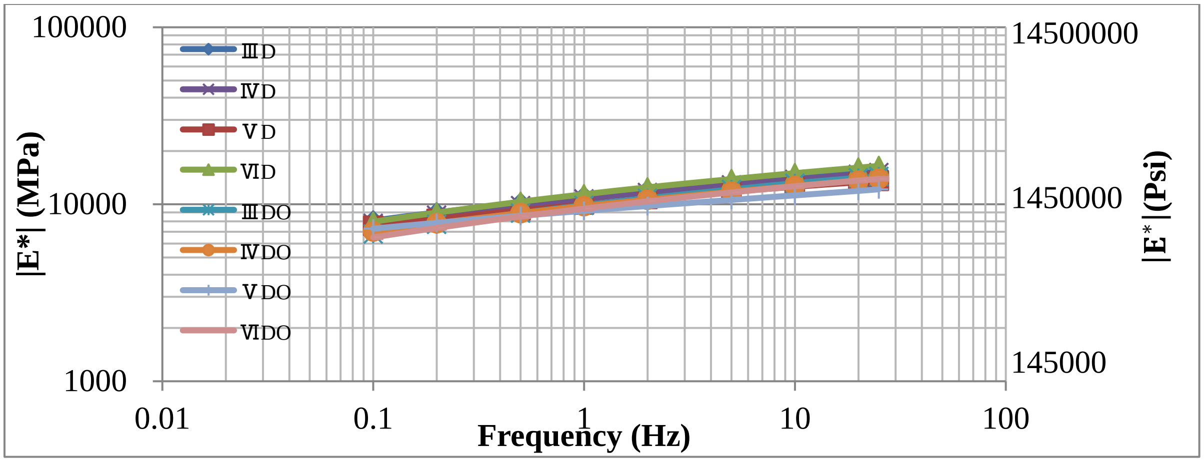

(a)

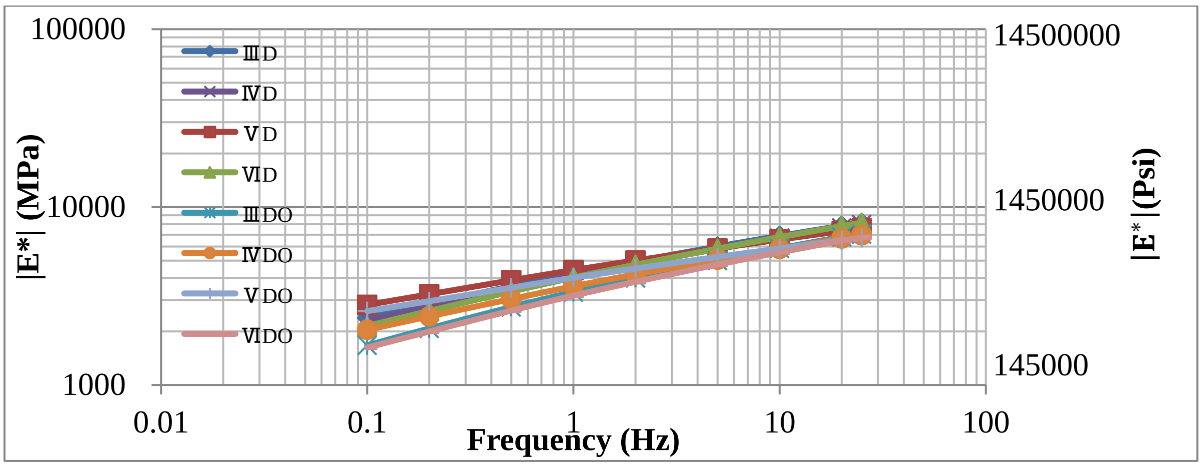

(b)

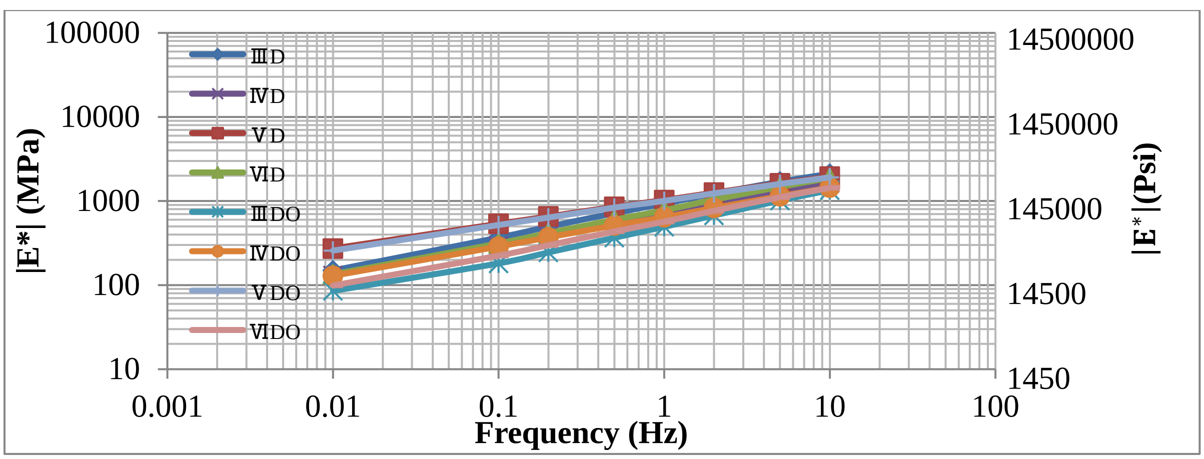

(c)

Figure 6-43 Dynamic Modulus Values of Various Surface D Mixtures with/without RAP in Terms of Different Aggregate Types, (a) at 4°C (39.2°F), (b) at 20°C (68°F), and (c) at 45°C (113°F)

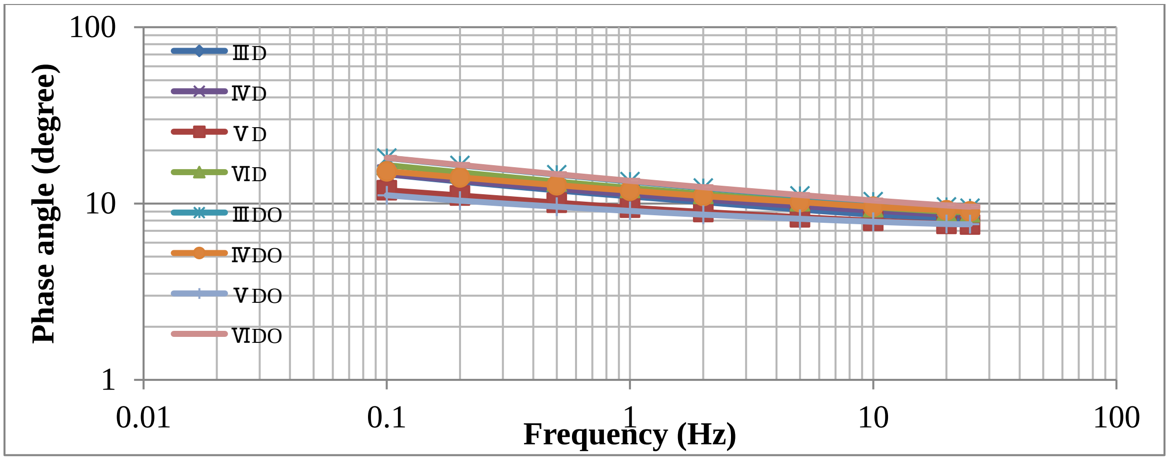

(a)

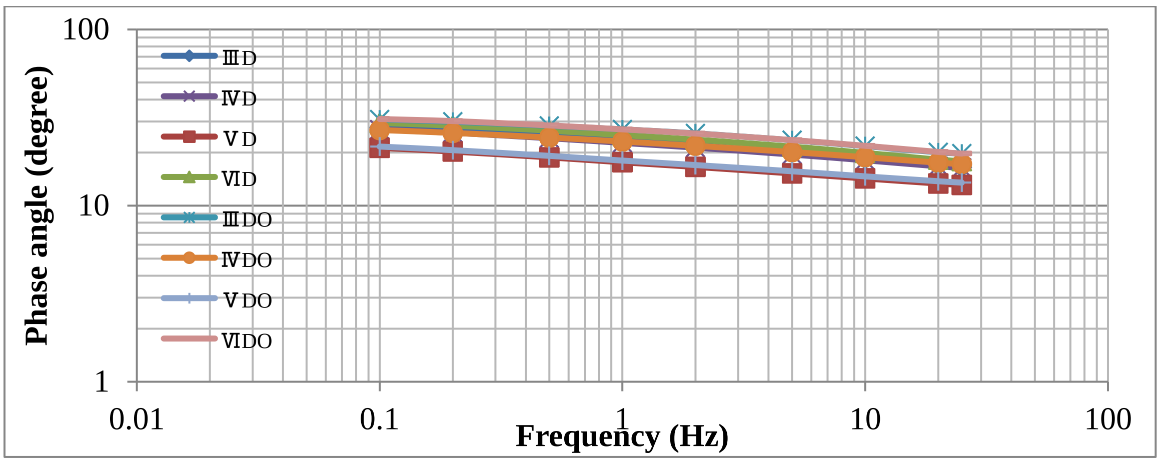

(b)

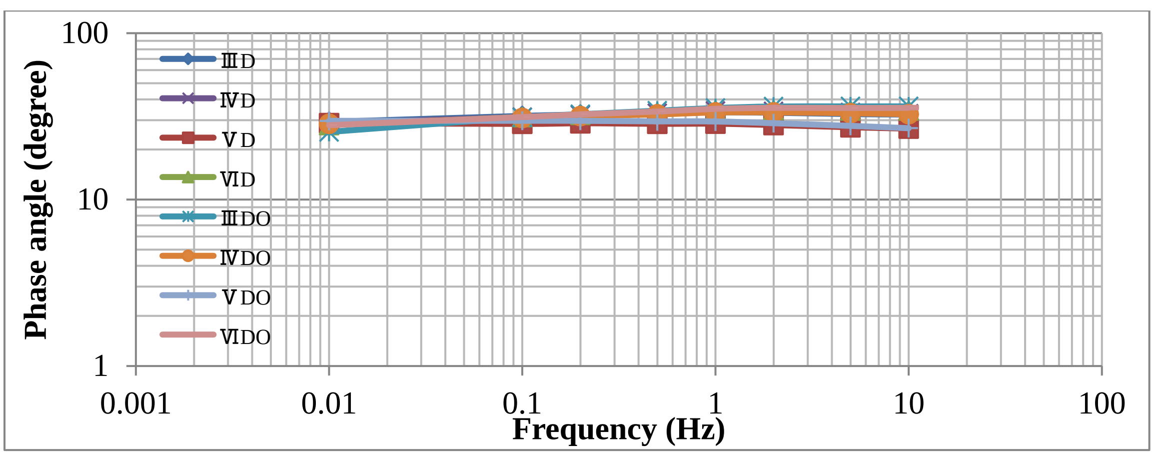

(c)

Figure 6-44 Phase Angle Values of Various Surface D Mixtures with/without RAP in Terms of Different Aggregate Types, (a) at 4°C (39.2°F), (b) at 20°C (68°F), and (c) at 45°C (113°F)

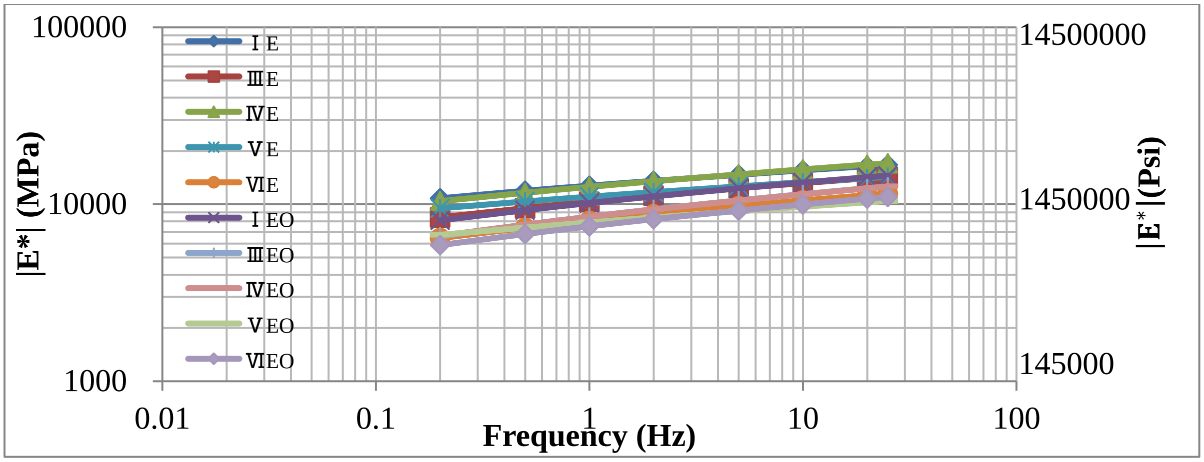

(a)

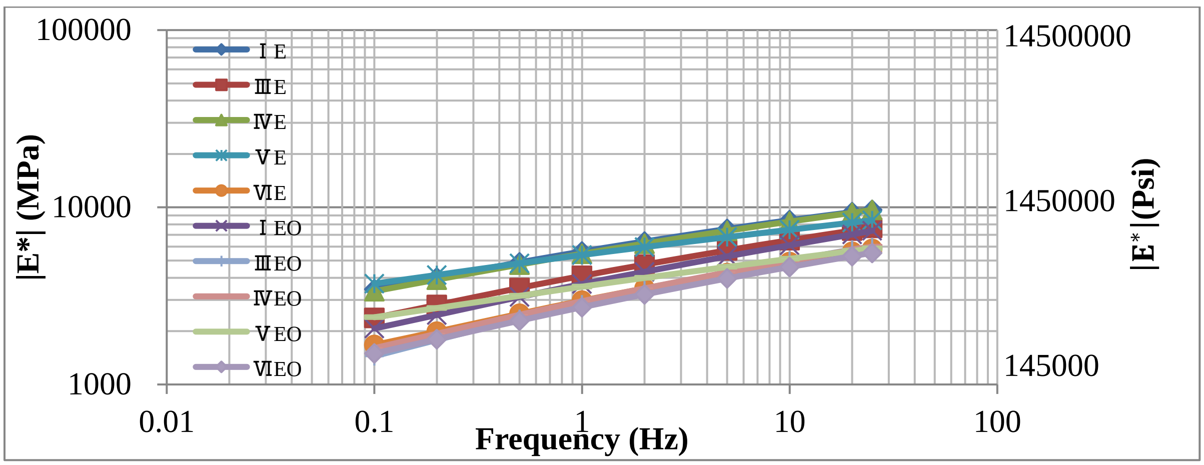

(b)

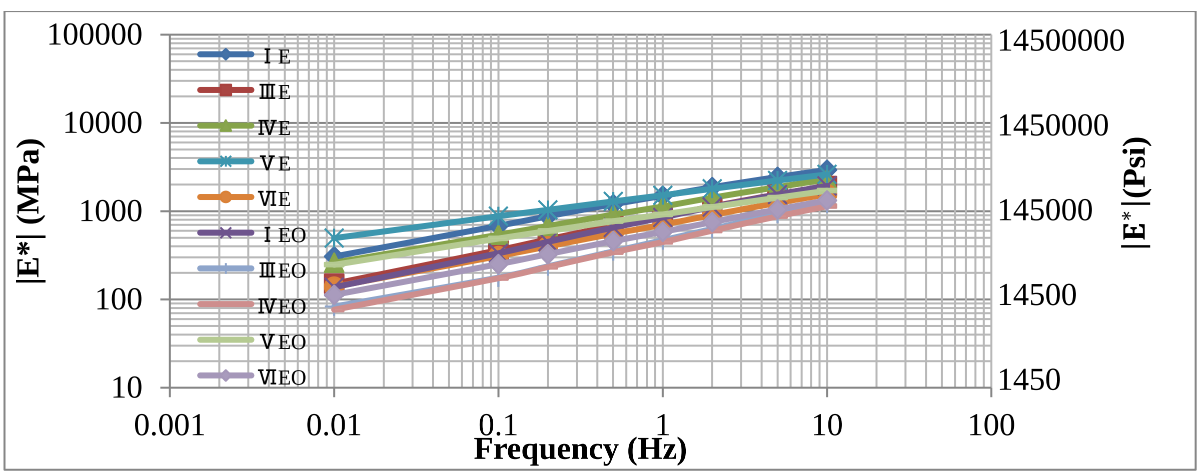

(c)

Figure 6-45 Dynamic Modulus Values of Various Surface E Mixtures with/without RAP in Terms of Different Aggregate Types, (a) at 4°C (39.2°F), (b) at 20°C (68°F), and (c) at 45°C (113°F)

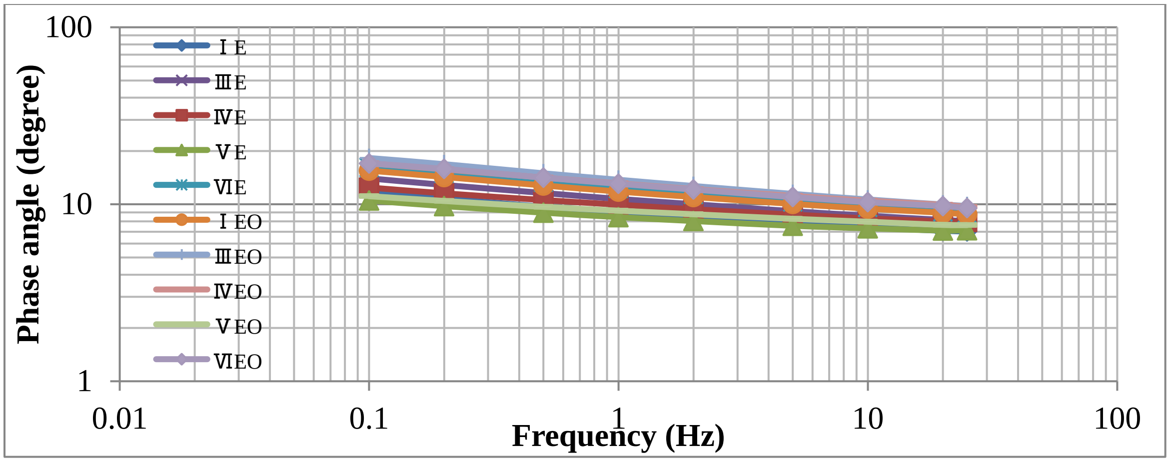

(a)

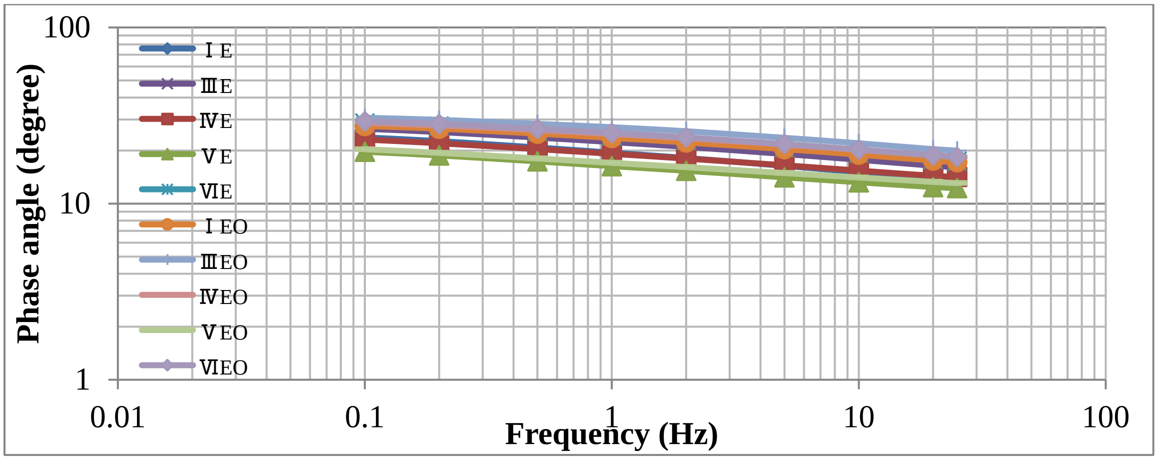

(b)

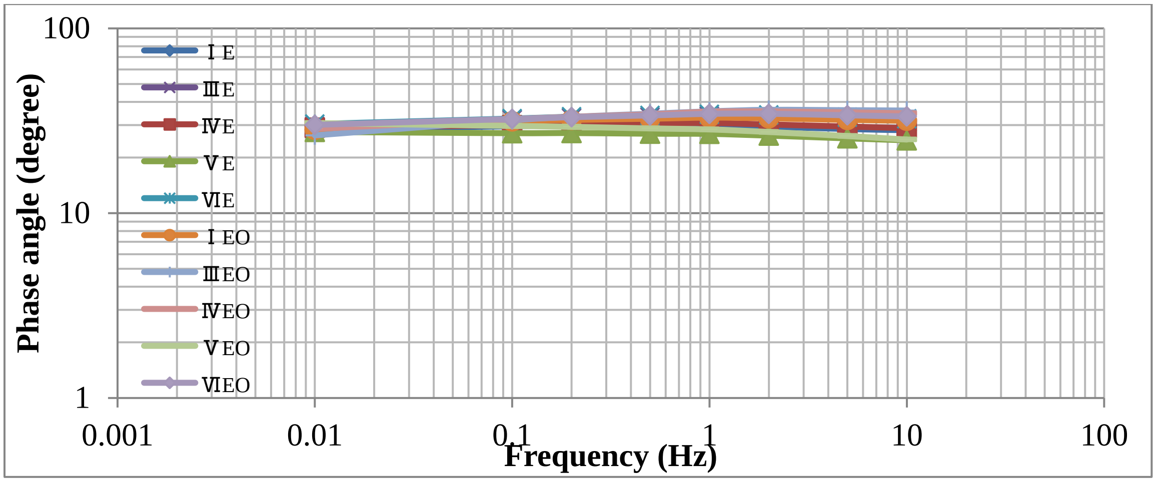

(c)

Figure 6-46 Phase Angle Values of Various Surface E Mixtures with/without RAP in Terms of Different Aggregate Types, (a) at 4°C (39.2°F), (b) at 20°C (68°F), and (c) at 45°C (113°F)

6.1.16.2 Effects of RAP on Dynamic Modulus and Phase Angle of Various Intermediate Mixtures Made with Different Aggregate Types

Figure 6-47 indicates that the dynamic modulus values of Intermediate Type A mixtures containing RAP were generally slightly higher than those values of Intermediate Type A mixtures made without RAP regardless of loading frequency, and test temperature. It can be seen that the differences in dynamic modulus values with and without RAP were more obvious with aggregate source IV.

Similar dynamic modulus results for Intermediate Type B and C mixtures are shown in Figure 6-49 and Figure 6-51, respectively. Similar to Intermediate Type A mixtures, Intermediate Type B mixtures made with aggregate source IV exhibited more obvious differences in dynamic modulus values with and without RAP than aggregate source V. In addition, for both Intermediate Type B and Type C mixtures, the differences in dynamic modulus values with and without RAP were more obvious at a lower frequency.

Figure 6-48 shows that the phase angle values of Intermediate Type A mixtures made with RAP were generally similar to those values of Intermediate Type A mixtures containing no RAP regardless of aggregate source, loading frequency, and test temperature. The phase angle values of these mixtures with and without RAP were closest together when the test temperature was set at 45°C (113°F).

With respect to phase angle, Intermediate Type B and C mixtures with and without RAP exhibited slightly different behavior than the Intermediate Type A mixtures. As shown in Figure 6-50 and Figure 6-52, the phase angle values for Intermediate Type B and C mixtures with RAP were slightly lower than those without RAP regardless of aggregate source and loading frequency at the test temperatures of 4°C (39.2°F) and 20°C (68°F). These differences were more pronounced with aggregate source IV in Intermediate Type B mixtures and with aggregate source V in Intermediate Type C mixtures. However, similar to the Intermediate Type A mixtures, both Intermediate Type B and C mixtures with RAP exhibited similar phase angle values to the corresponding mixtures without RAP when the test temperature was set at 45°C (113°F).

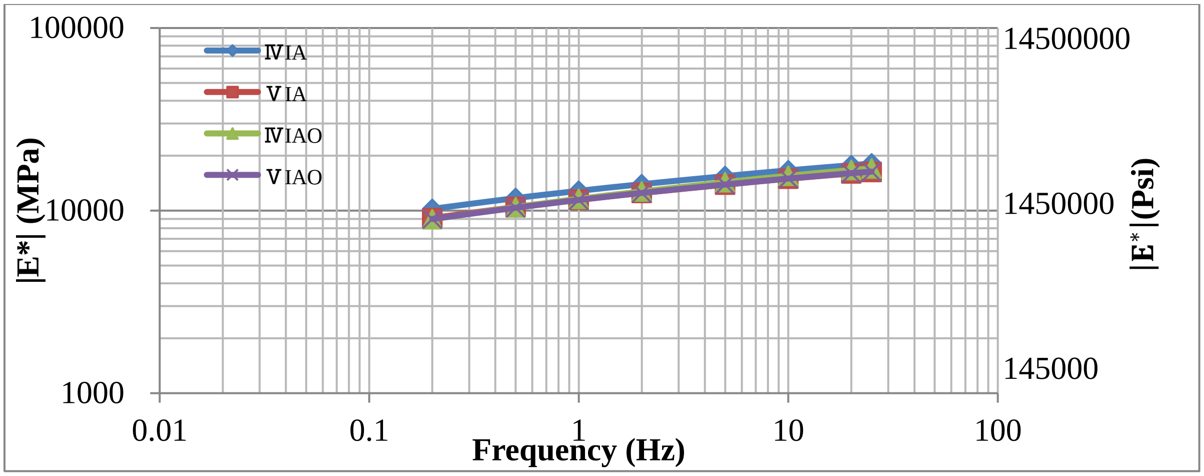

(a)

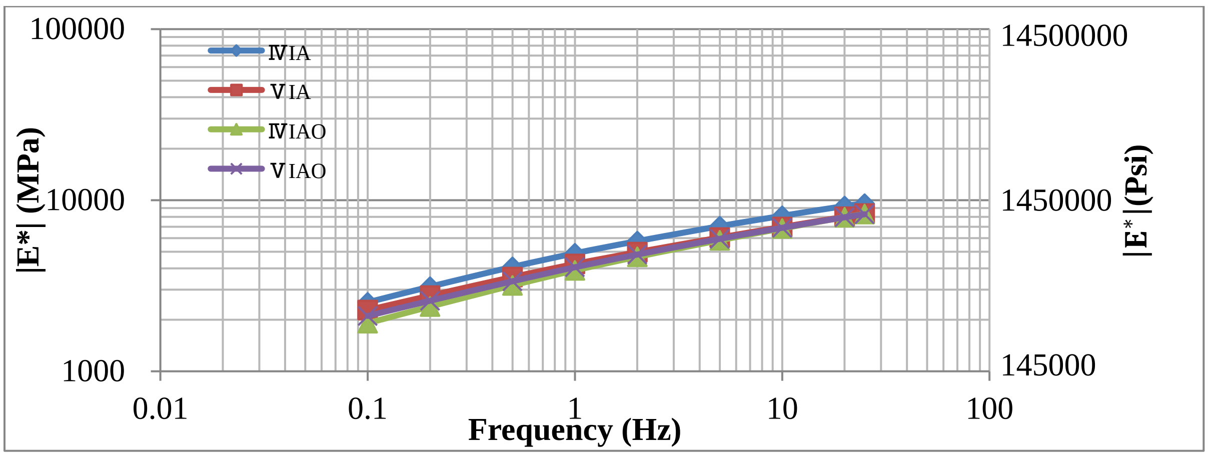

(b)

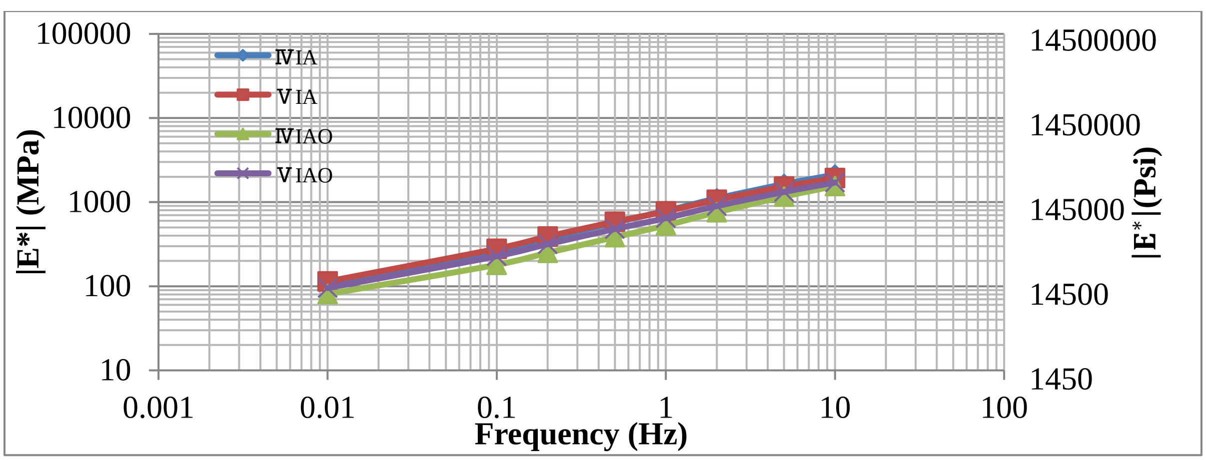

(c)

Figure 6-47 Dynamic Modulus Values of Various Intermediate Type A Mixtures with/without RAP in Terms of Different Aggregate Types, (a) at 4°C (39.2°F), (b) at 20°C (68°F), and (c) at 45°C (113°F)

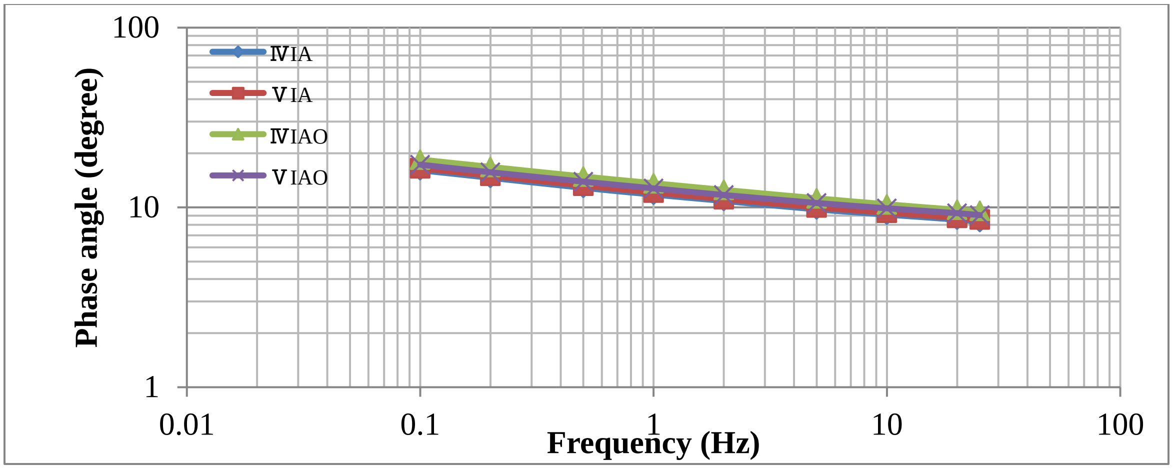

(a)

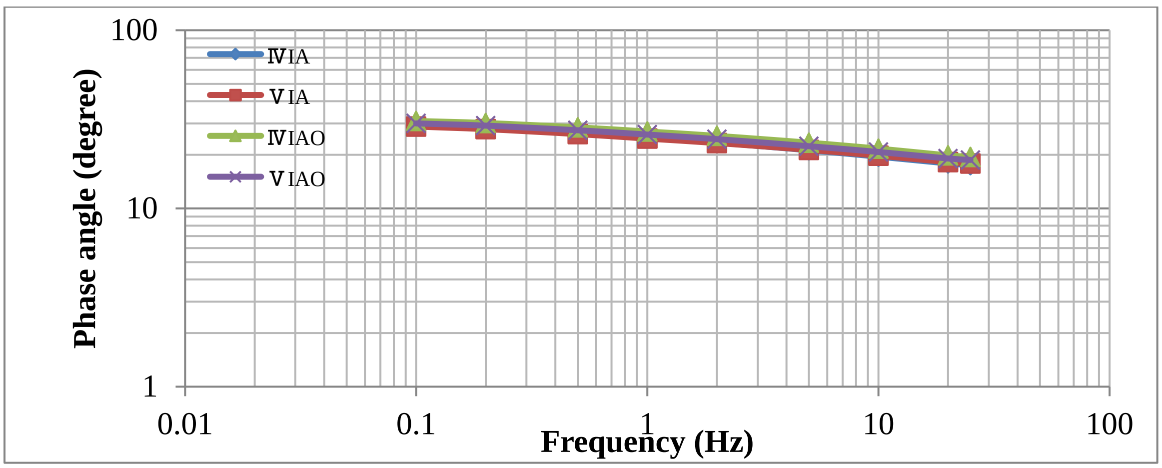

(b)

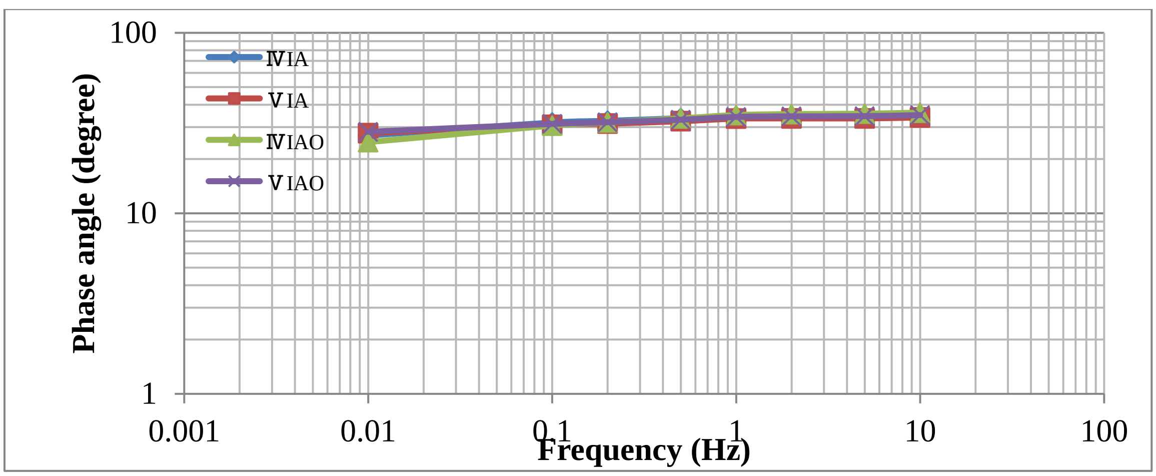

(c)

Figure 6-48 Phase Angle Values of Various Intermediate Type A Mixtures with/without RAP in Terms of Different Aggregate Types, (a) at 4°C (39.2°F), (b) at 20°C (68°F), and (c) at 45°C (113°F)

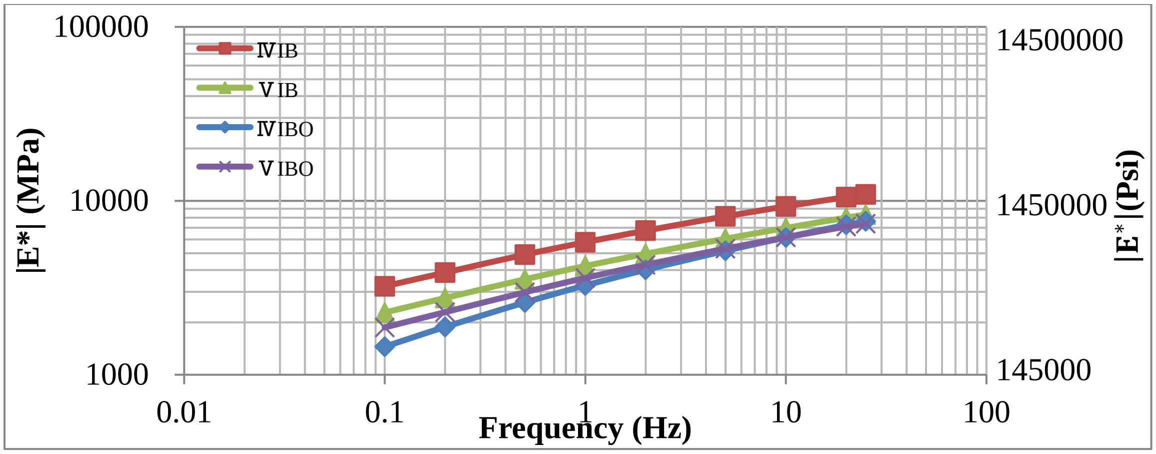

(a)

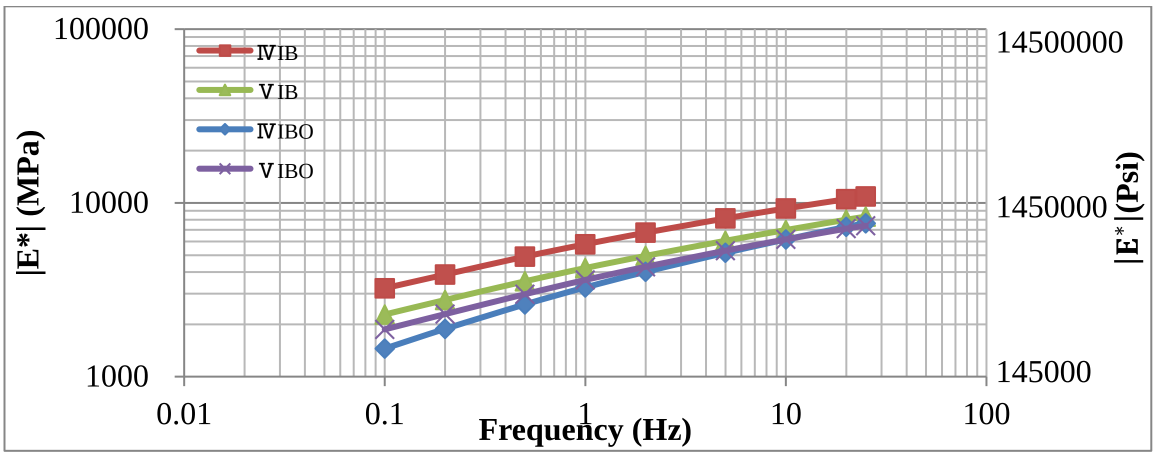

(b)

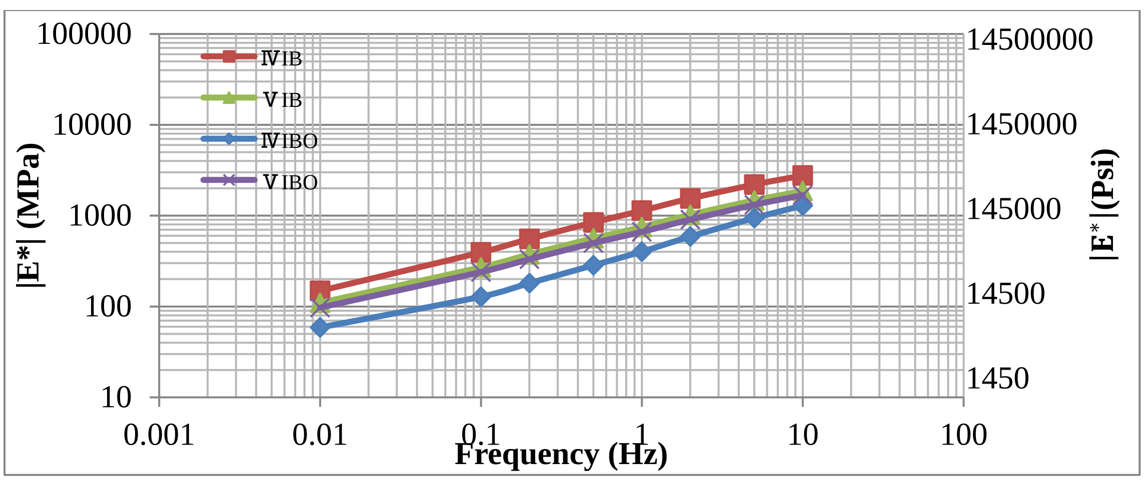

(c)

Figure 6-49 Dynamic Modulus Values of Various Intermediate Type B Mixtures with/without RAP in Terms of Different Aggregate Types, (a) at 4°C (39.2°F), (b) at 20°C (68°F), and (c) at 45°C (113°F)

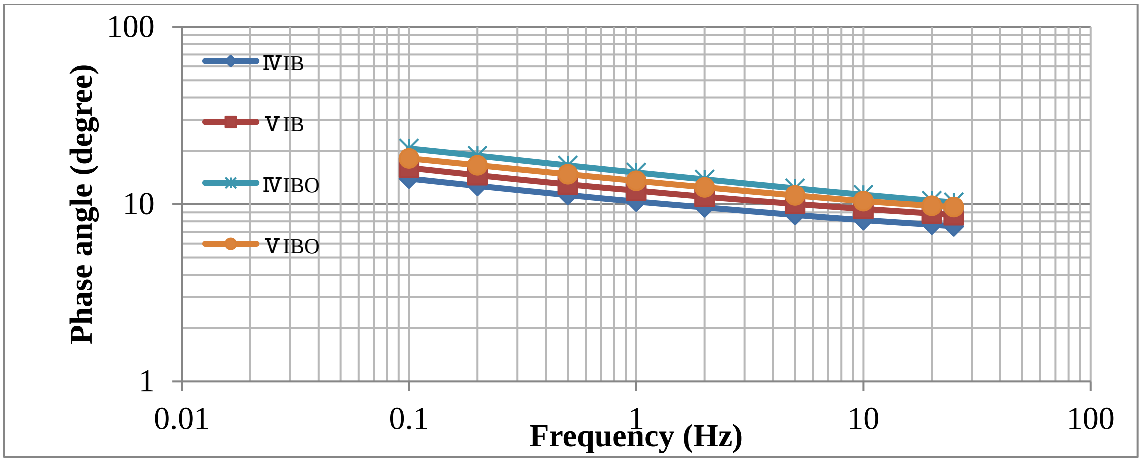

(a)

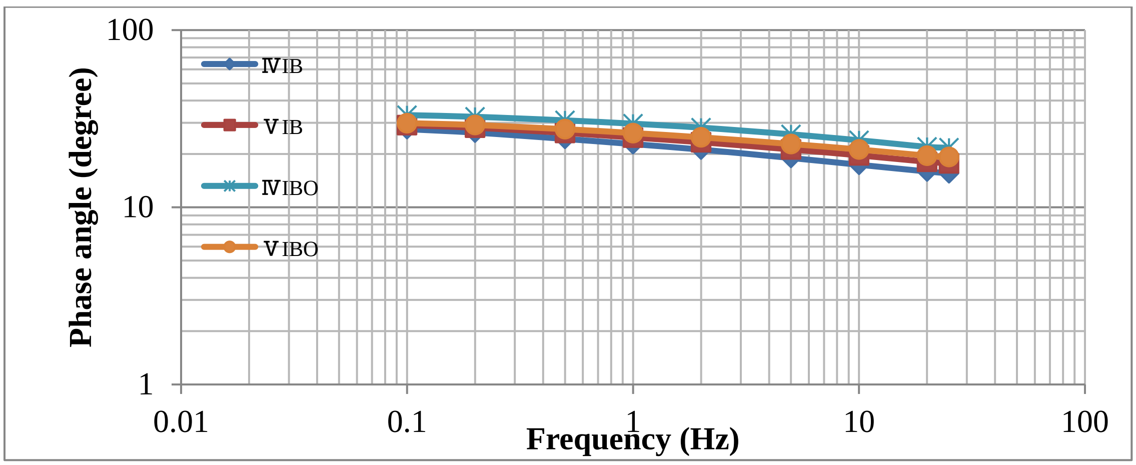

(b)

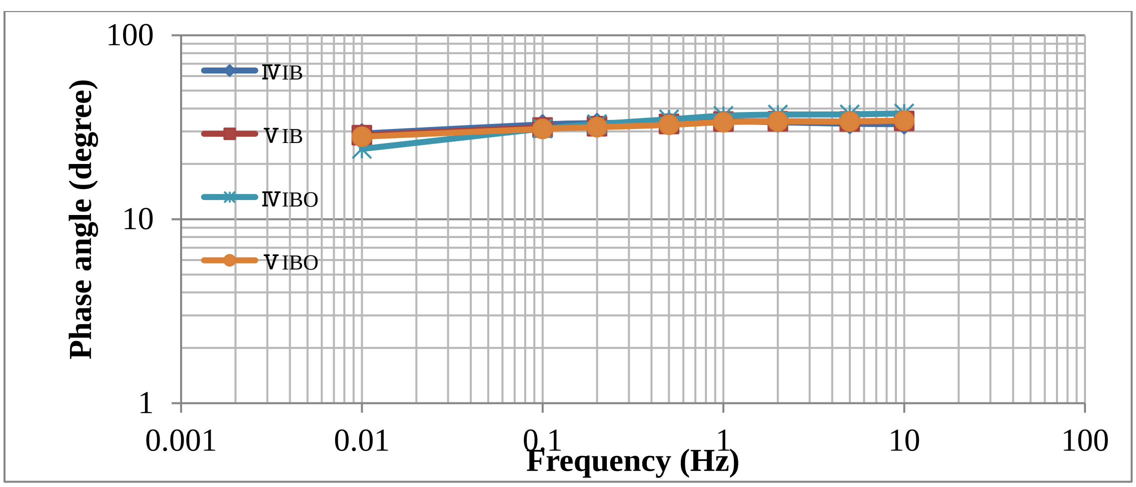

(c)

Figure 6-50 Phase Angle Values of Various Intermediate Type B Mixtures with/without RAP in Terms of Different Aggregate Types, (a) at 4°C (39.2°F), (b) at 20°C (68°F), and (c) at 45°C (113°F)

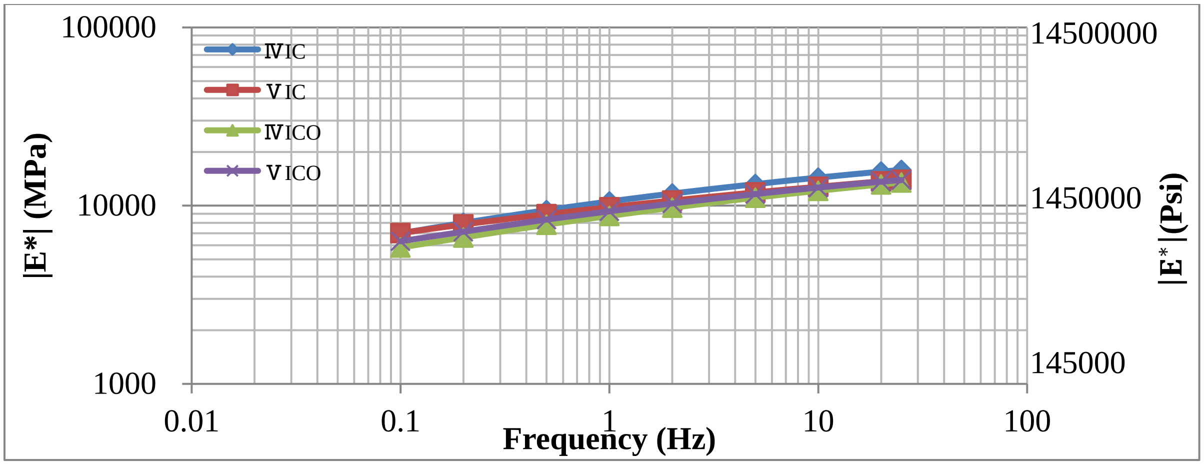

(a)

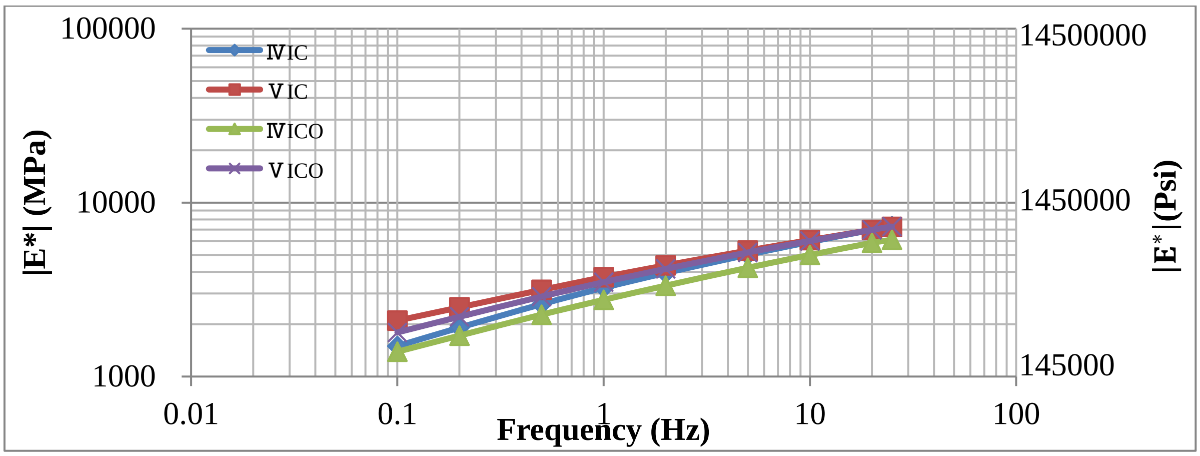

(b)

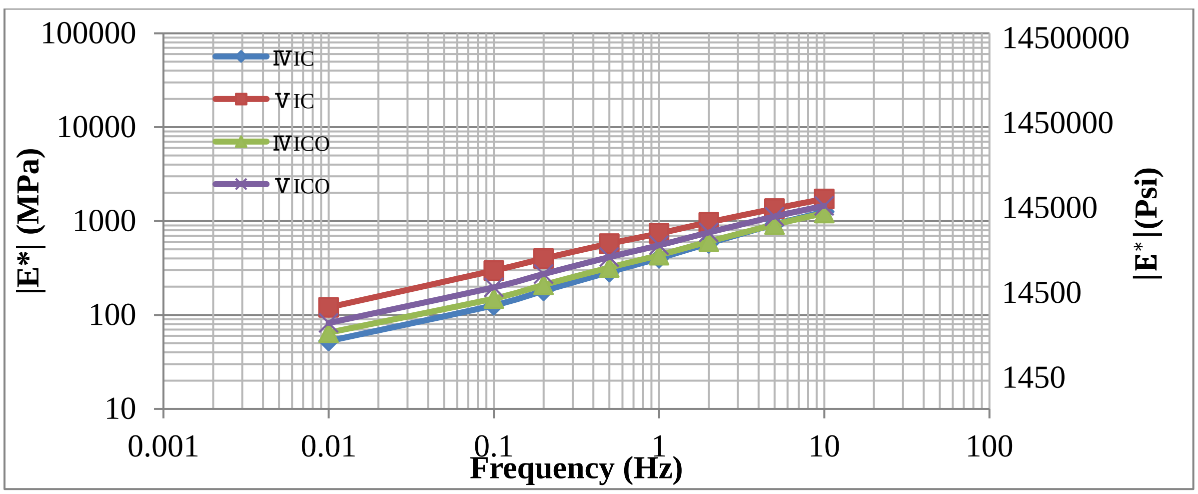

(c)

Figure 6-51 Dynamic Modulus Values of Various Intermediate Type C Mixtures with/without RAP in Terms of Different Aggregate Types, (a) at 4°C (39.2°F), (b) at 20°C (68°F), and (c) at 45°C (113°F)

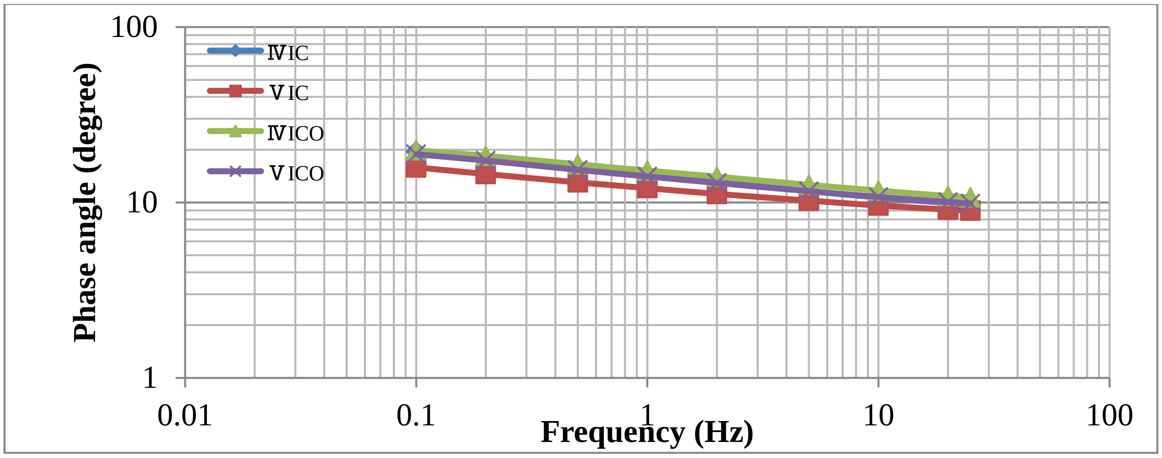

(a)

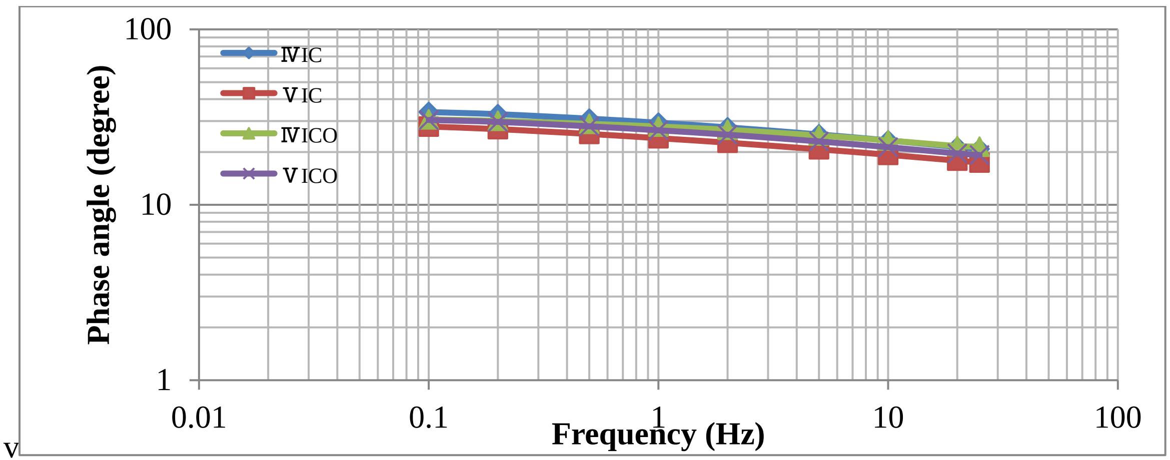

(b)

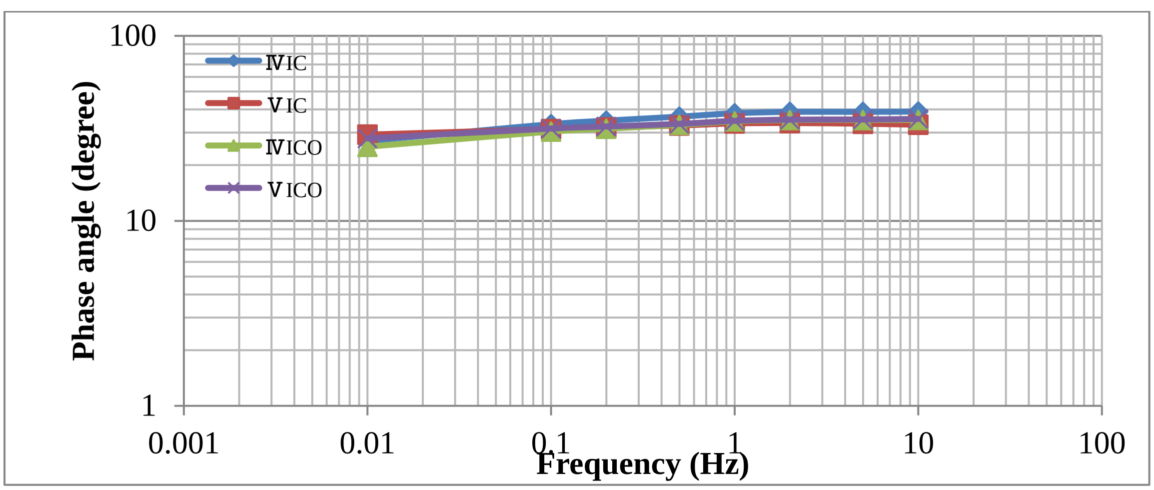

(c)

Figure 6-52 Phase Angle Values of Various Intermediate Type C Mixtures with/without RAP in Terms of Different Aggregate Types, (a) at 4°C (39.2°F), (b) at 20°C (68°F), and (c) at 45°C (113°F)

6.1.16.3 Effects of RAP on Dynamic Modulus and Phase Angle of Various Base Mixtures Made with Different Aggregate Types

Figure 6-53 and Figure 6-55 show the dynamic modulus values of Base Type A and B mixtures, respectively, both with and without RAP. The dynamic modulus values of the mixtures containing RAP were generally higher than those without RAP for both Base Type A and B mixtures regardless of aggregate source, loading frequency, and testing temperature. The only exception was Base Type A when tested at 4° C (39.2° F), which exhibited similar dynamic modulus values both with and without RAP.

Figure 6-54 and Figure 6-56 show that the phase angle values of Base Type A and B mixtures made with RAP were generally lower than those without RAP regardless of aggregate source and test temperature. However, the phase angle values of both Base Type A and B mixtures with and without RAP were similar when the test temperature was increased to 45°C (113°F).

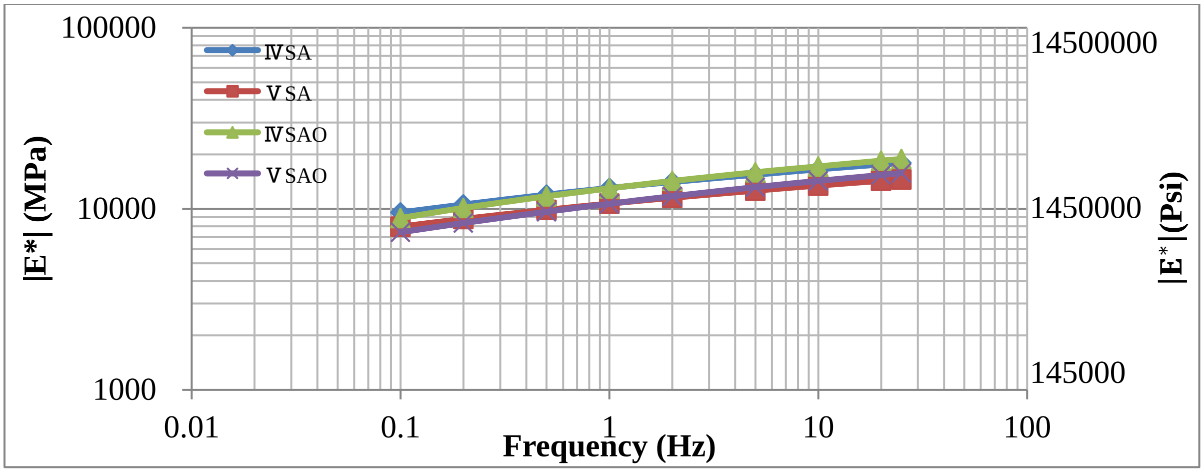

(a)

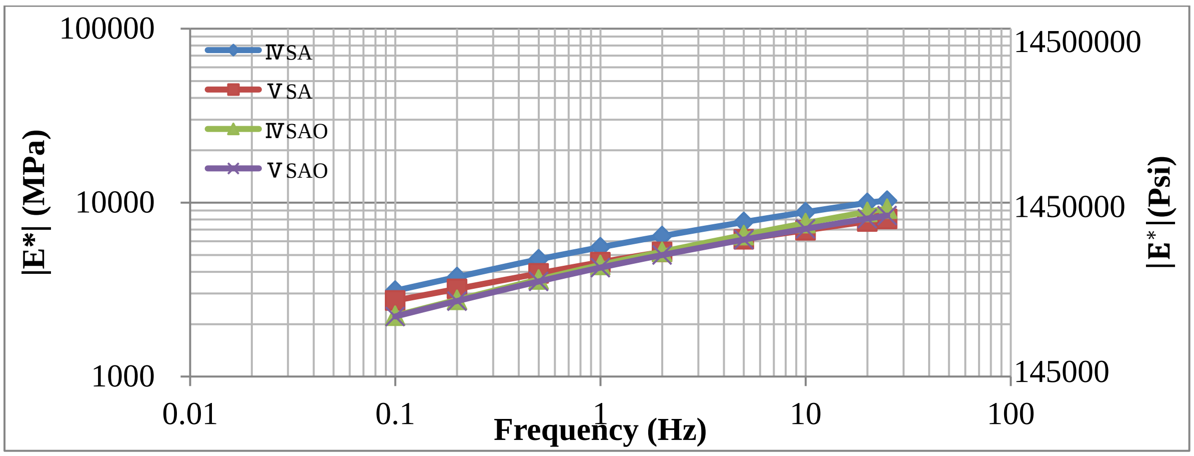

(b)

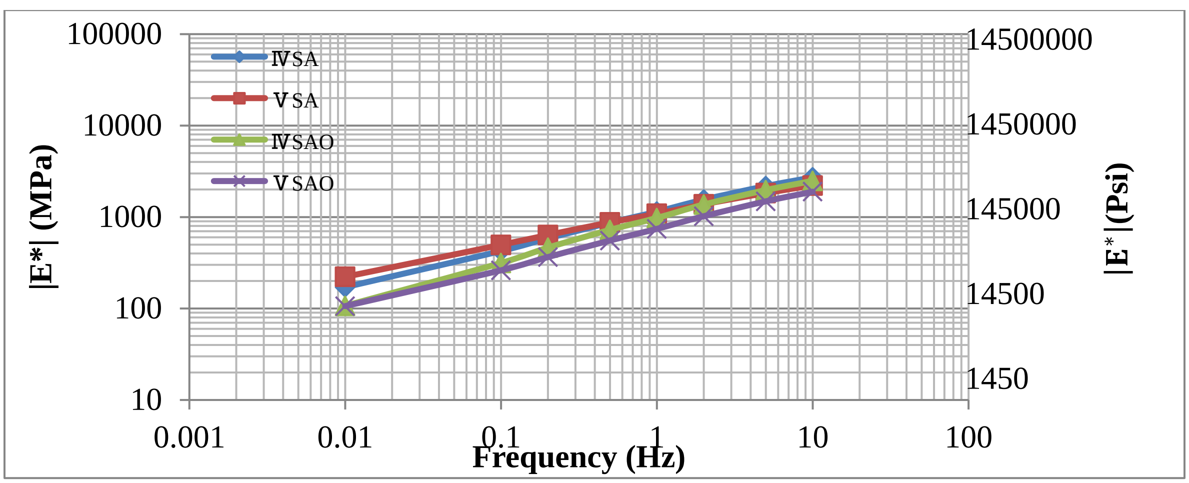

(c)

Figure 6-53 Dynamic Modulus Values of Various Base Type A Mixtures with/without RAP in Terms of Different Aggregate Types, (a) at 4°C (39.2°F), (b) at 20°C (68°F), and (c) at 45°C (113°F)

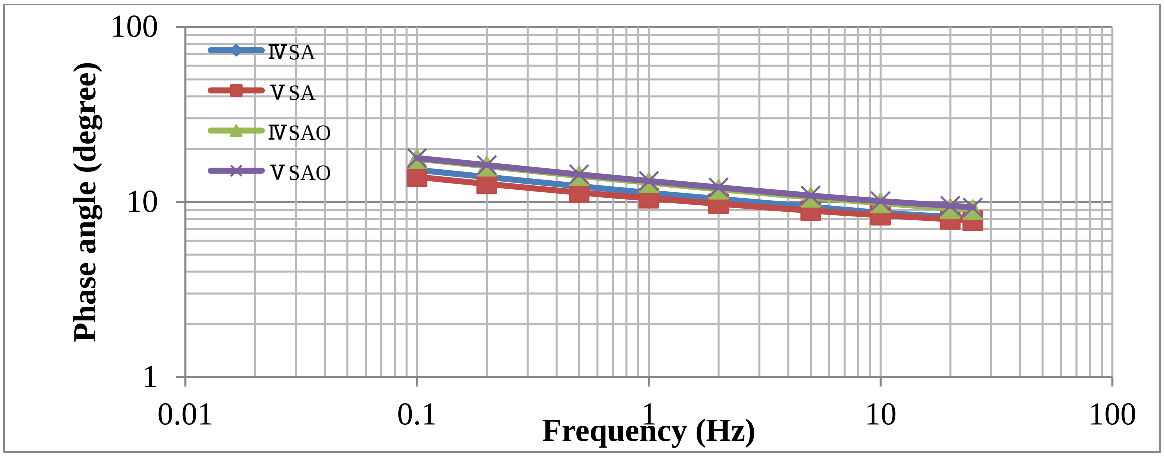

(a)

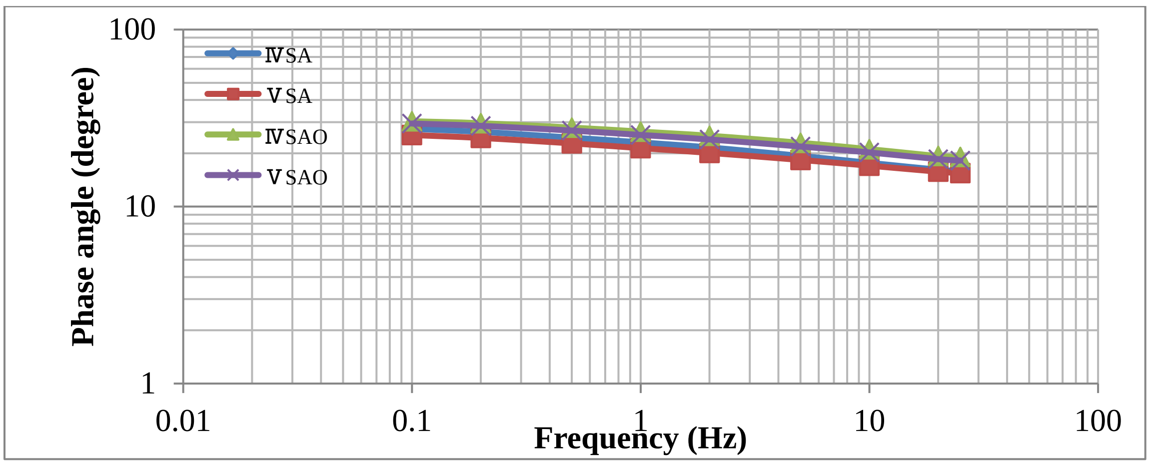

(b)

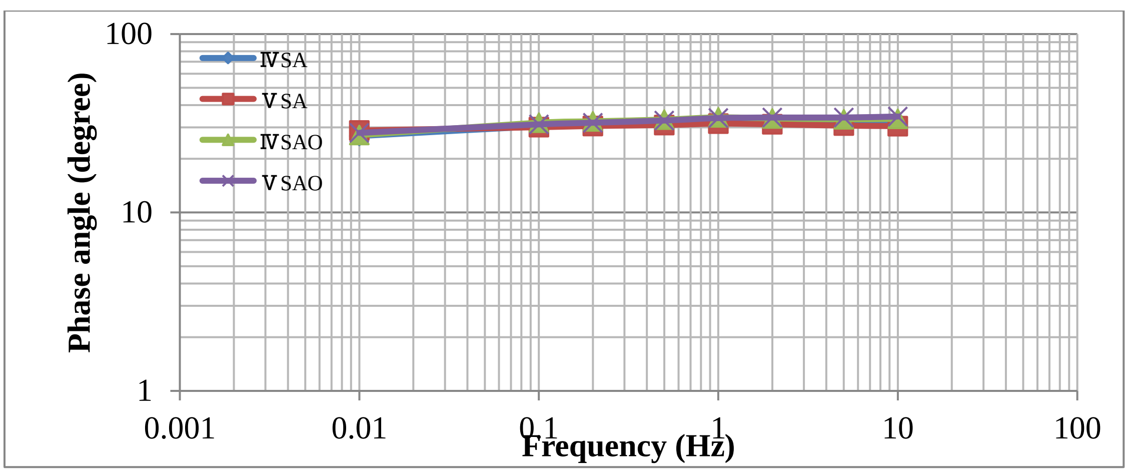

(c)

Figure 6-54 Phase Angle Values of Various Base Type A Mixtures with/without RAP in Terms of Different Aggregate Types, (a) at 4°C (39.2°F), (b) at 20°C (68°F), and (c) at 45°C (113°F)

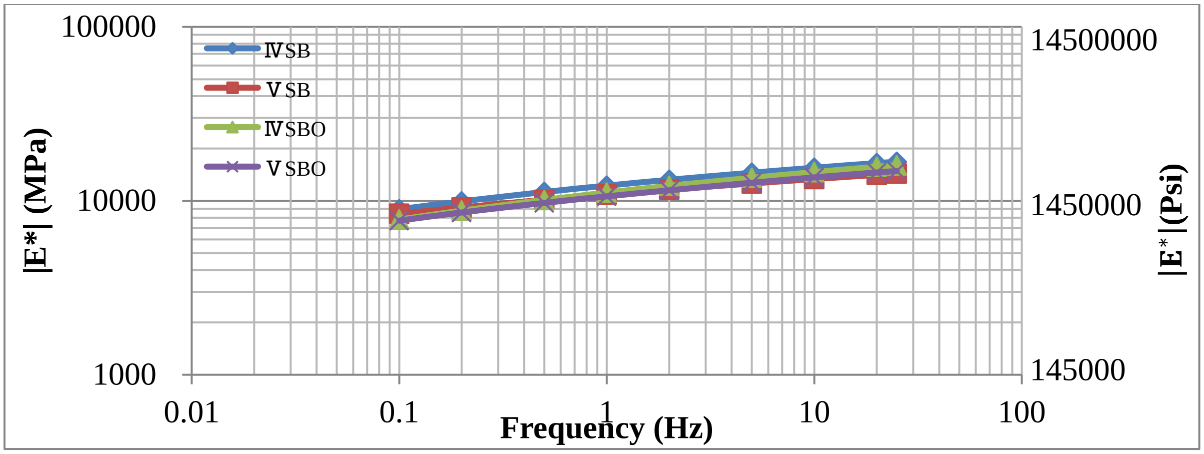

(a)

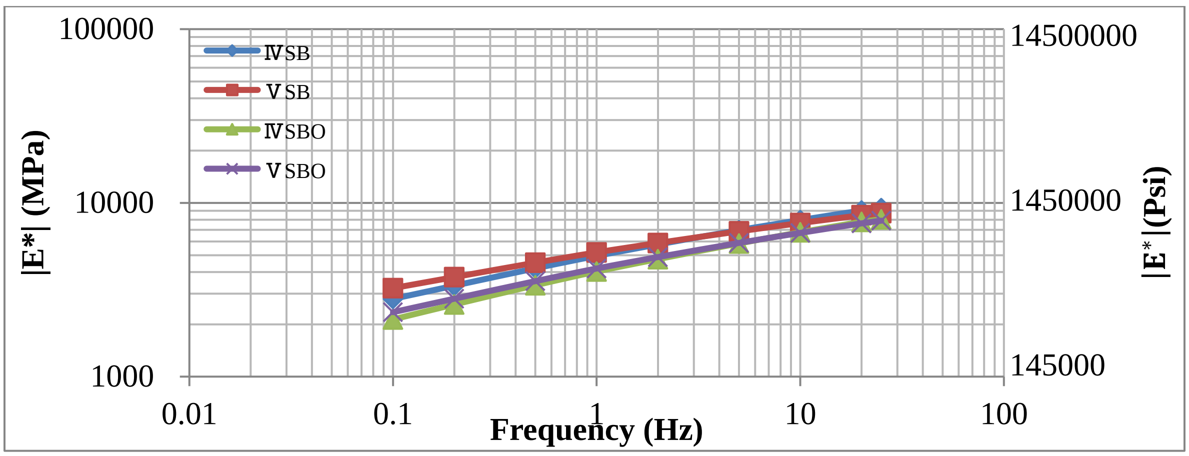

(b)

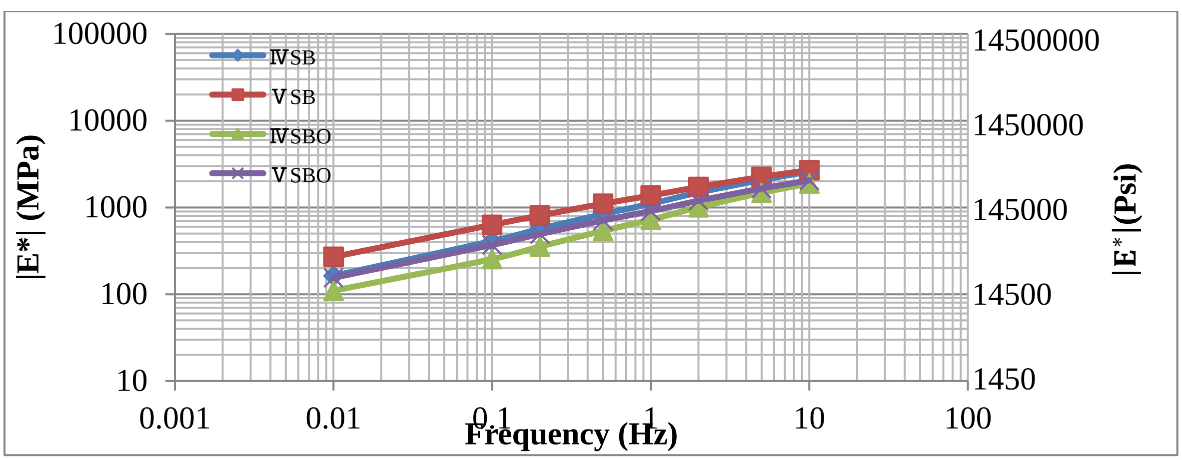

(c)

Figure 6-55 Dynamic Modulus Values of Various Base Type B Mixtures with/without RAP in Terms of Different Aggregate Types, (a) at 4°C (39.2°F), (b) at 20°C (68°F), and (c) at 45°C (113°F)

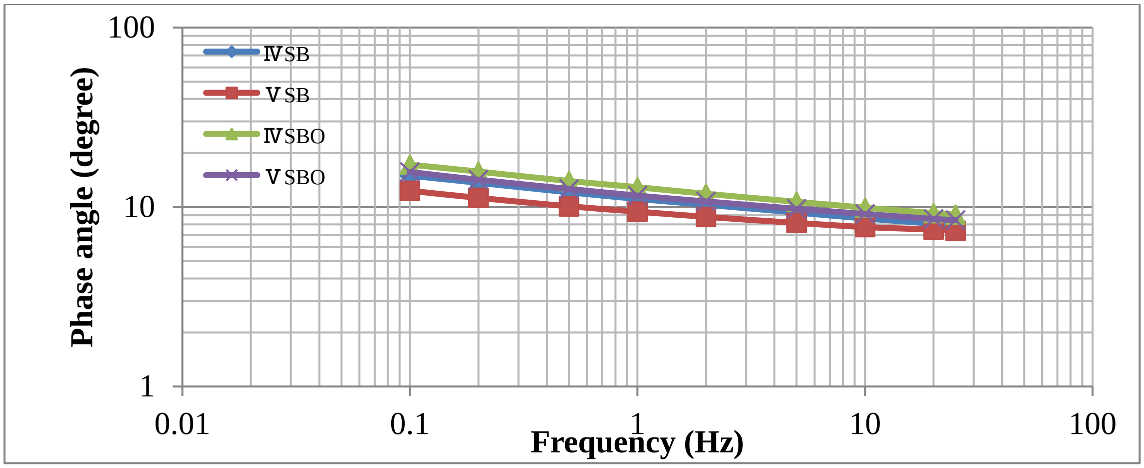

(a)

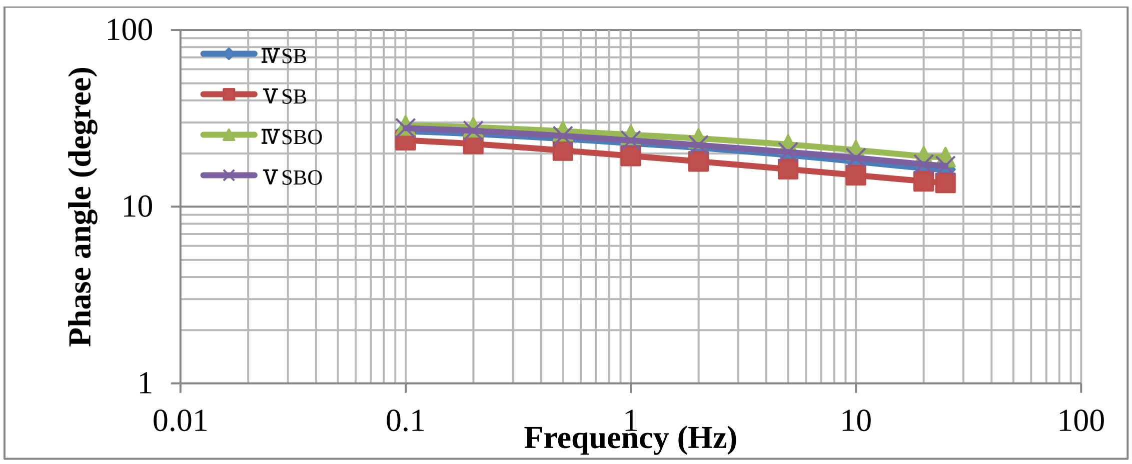

(a)

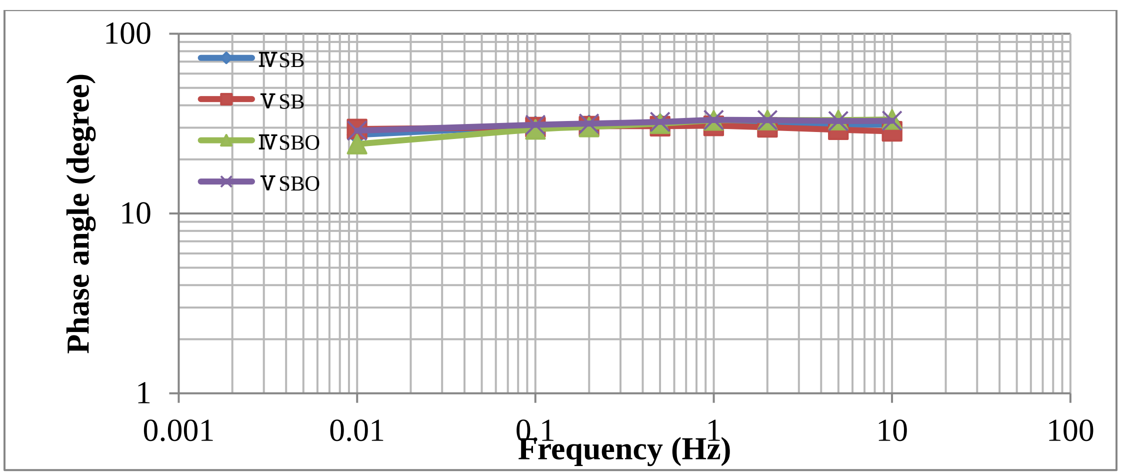

(a)

Figure 6-56 Phase Angle Values of Various Base Type B Mixtures with/without RAP in Terms of Different Aggregate Types, (a) at 4°C (39.2°F), (b) at 20°C (68°F), and (c) at 45°C (113°F)

6.1.16.4 Effects of RAP on Dynamic Modulus and Phase Angle of Surface Mixtures (Types A and B) Made with Binder Source 2 and Different Aggregate Types

Figure 6-57 indicates that the dynamic modulus values of Surface Type A mixtures made with RAP and Binder Source 2 were generally similar to those values of Surface Type A mixtures containing no RAP regardless of aggregate source, loading frequency, and test temperature. Only when tested at 45° C (113°F) did aggregate source V mixtures with RAP exhibit higher dynamic modulus values that the aggregate source V mixtures without RAP.

In addition, Figure 6-58 shows that the phase angle values of Surface Type A mixtures made with binder source 2 with and without RAP varied depending on aggregate source. Aggregate source IV mixtures generally exhibited higher phase angle values with RAP, while aggregate source V mixtures generally exhibited lower phase angle values with RAP. The phase angle values of all Surface Type A mixtures containing binder source 2 both with and without RAP were closer together when the test temperature was at 45°C (113°F), especially as the frequency increased.

Figure 6-59 indicates that the dynamic modulus values of Surface Type B mixtures made with RAP and binder source 2 with and without RAP varied depending on aggregate source. Aggregate source IV mixtures with binder source 2 exhibited similar dynamic modulus values with and without RAP, while aggregate source V mixtures with binder source 2 exhibited higher dynamic modulus values with RAP than without. It can be noted that the differences in dynamic modulus were more obvious at a lower frequency.

In addition, Figure 6-60 shows that the phase angle values of Surface Type B mixtures made with RAP and binder source 2 with and without RAP also varied depending on aggregate source. Aggregate source IV mixtures with binder source 2 exhibited similar phase angle values with and without RAP, while aggregate source V mixtures with binder source 2 exhibited lower phase angle values with RAP than without. The phase angle values of these mixtures with and without RAP were closer together when the test temperature was increased to 45°C (113°F) regardless of aggregate source and frequency.

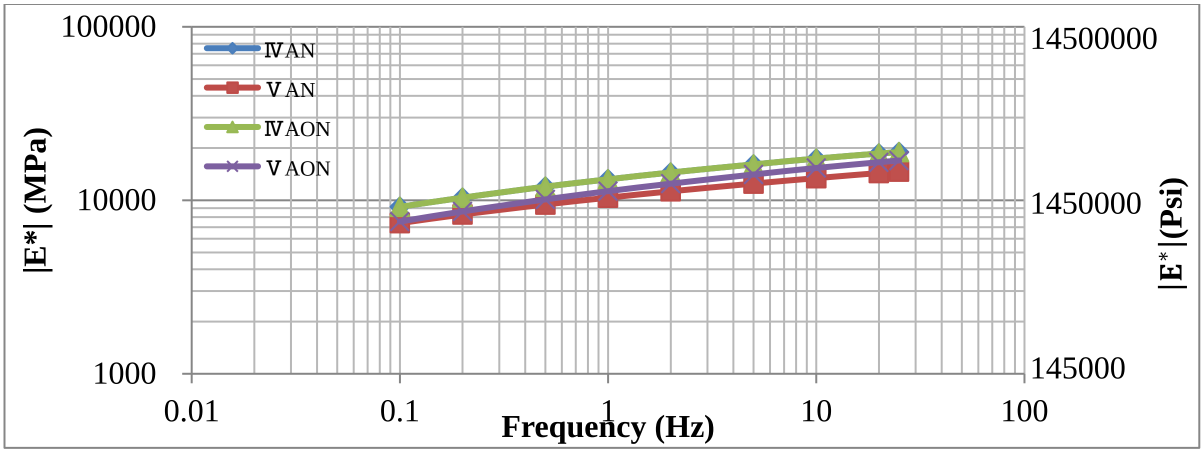

(a)

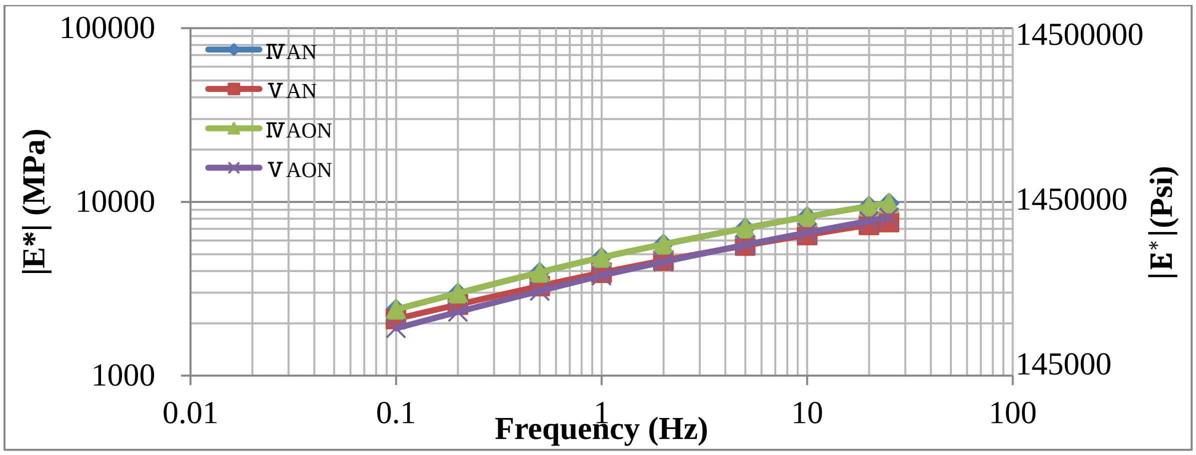

(b)

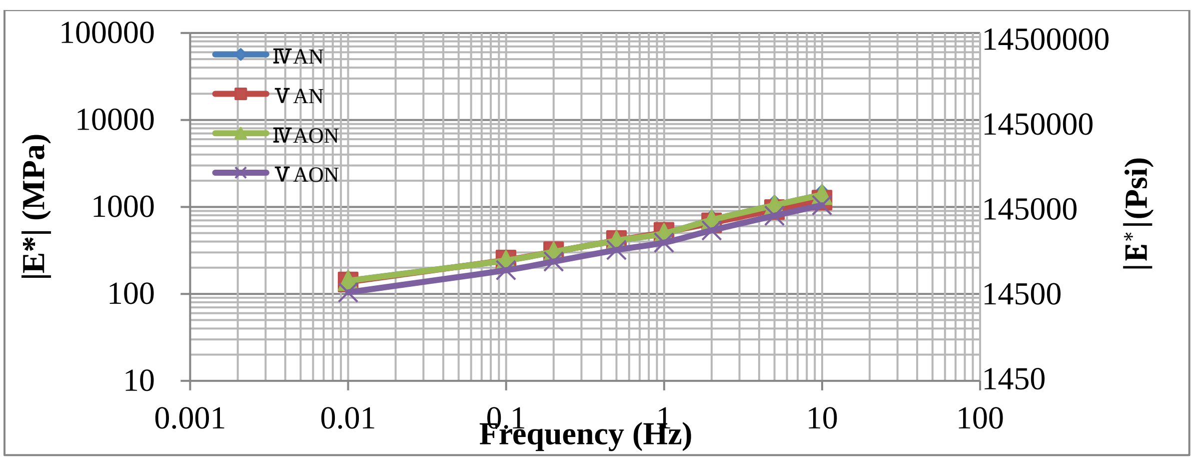

(c)

Figure 6-57 Dynamic Modulus Values of Various Surface Type A Mixtures from Binder Source 2 with/without RAP in Terms of Different Aggregate Types, (a) at 4°C (39.2°F), (b) at 20°C (68°F), and (c) at 45°C (113°F)

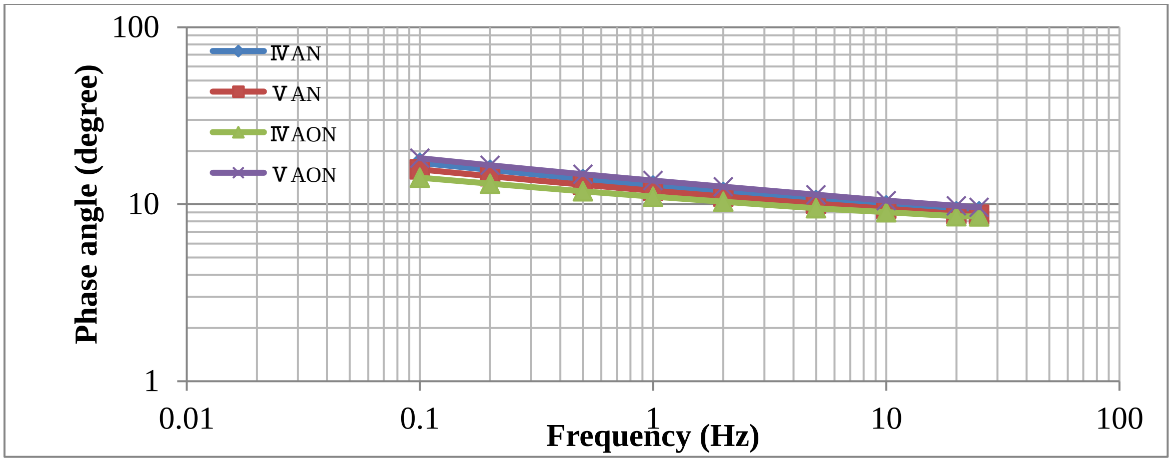

(a)

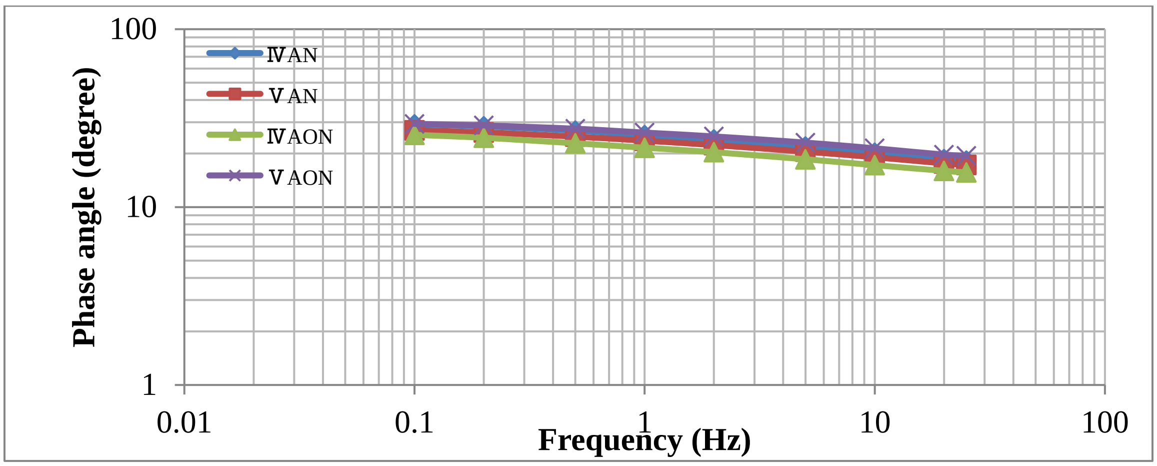

(b)

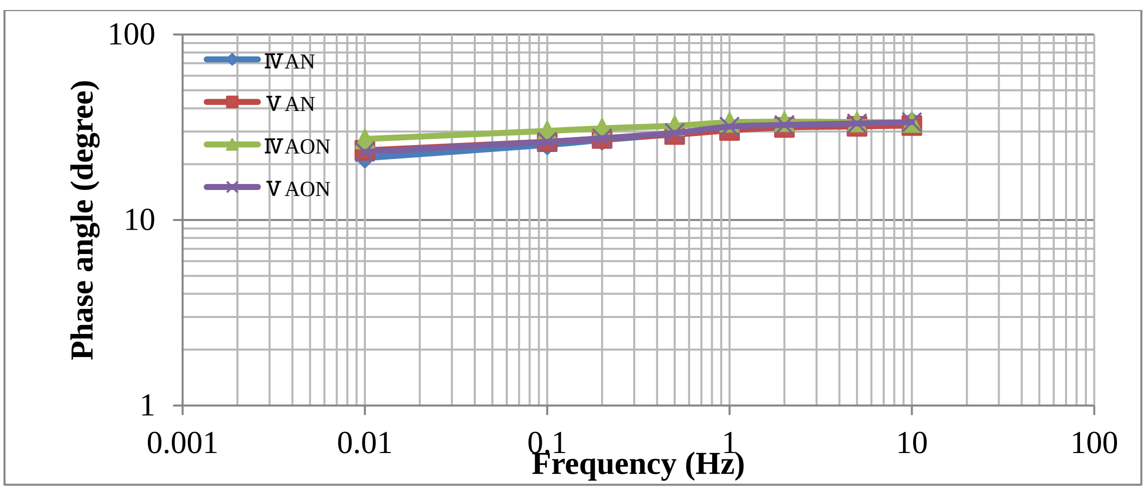

(c)

Figure 6-58 Dynamic Modulus Values of Various Surface Type A Mixtures from Binder Source 2 with/without RAP in Terms of Different Aggregate Types, (a) at 4°C (39.2°F), (b) at 20°C (68°F), and (c) at 45°C (113°F)

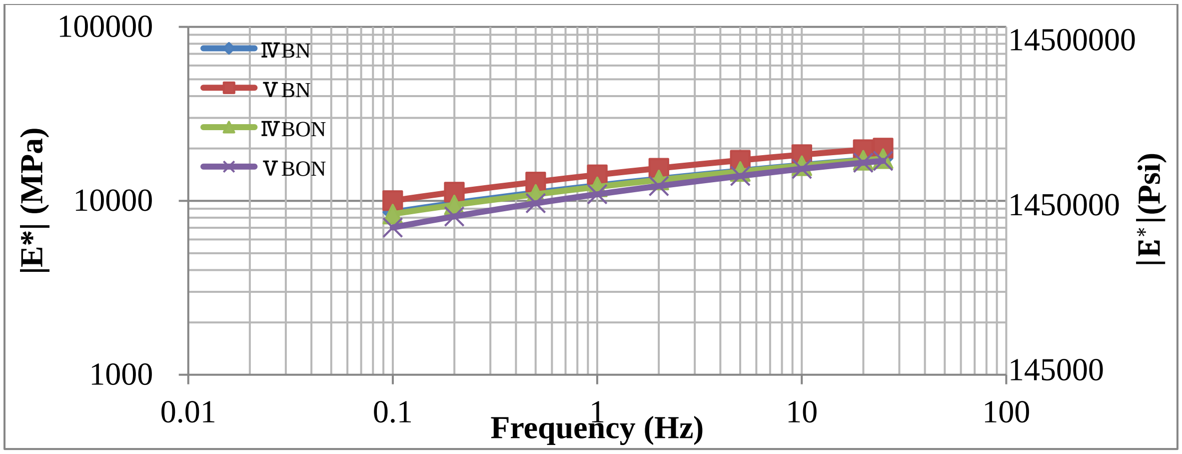

(a)

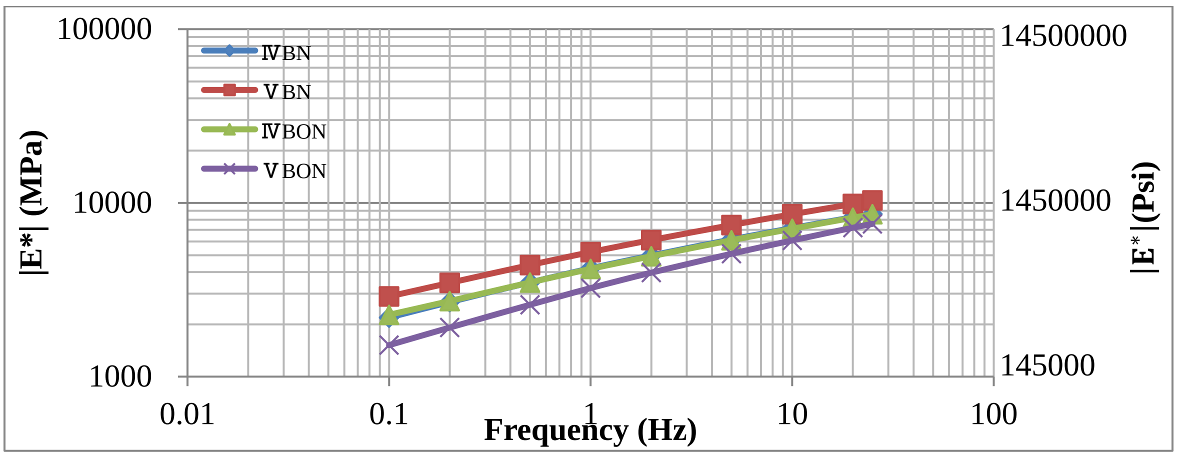

(b)

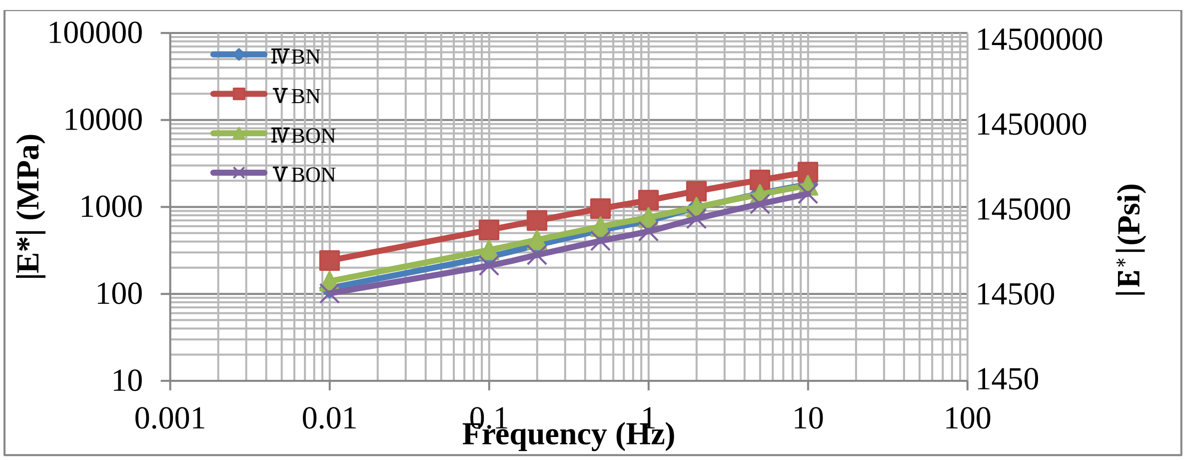

(c)

Figure 6-59 Dynamic Modulus Values of Various Surface Type B Mixtures from Binder Source 2 with/without RAP in Terms of Different Aggregate Types, (a) at 4°C (39.2°F), (b) at 20°C (68°F), and (c) at 45°C (113°F)

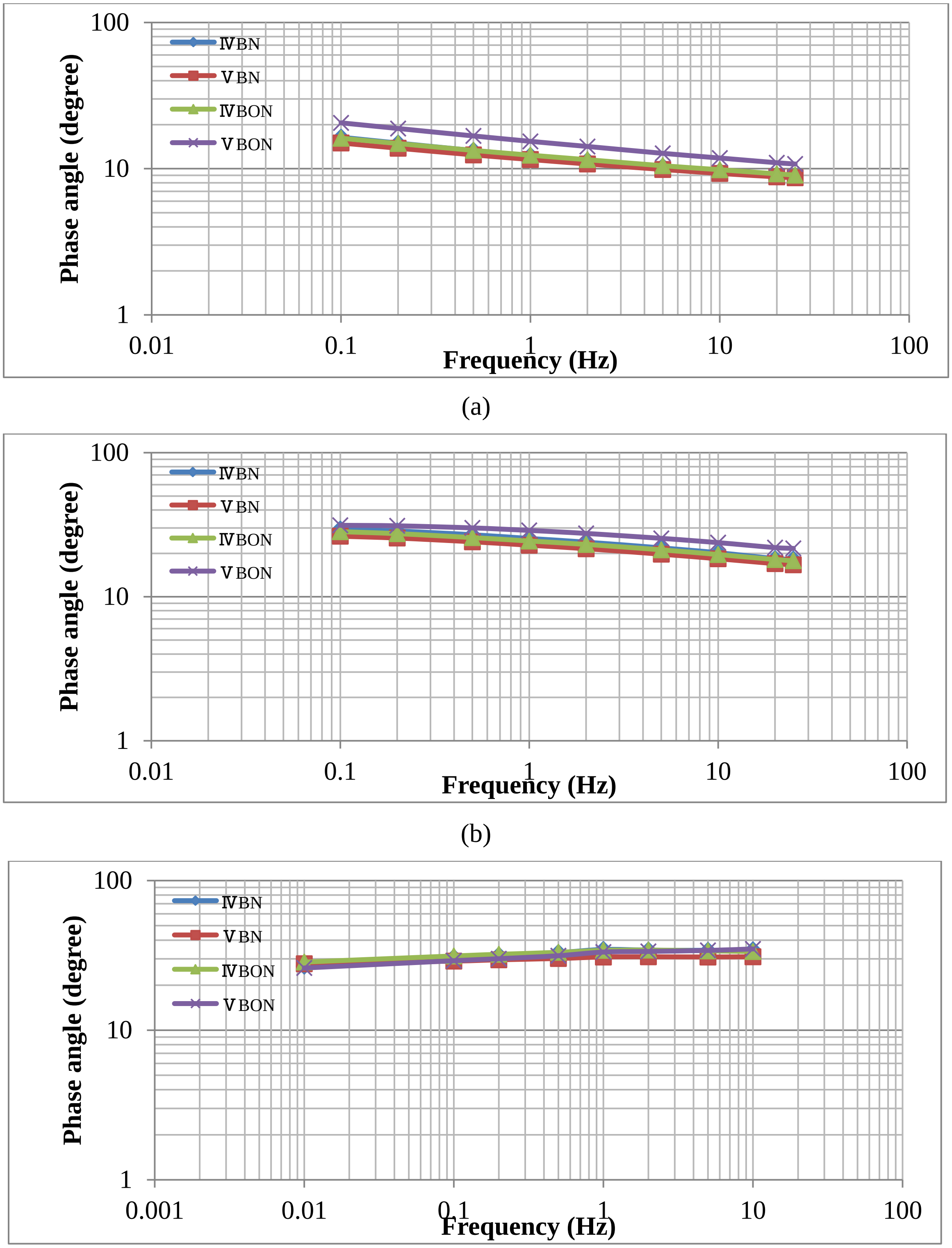

(a)

(b)

(c)

Figure 6-60 Phase Angle Values of Various Surface Type B Mixtures from Binder Source 2 with/without RAP in Terms of Different Aggregate Types, (a) at 4°C (39.2°F), (b) at 20°C (68°F), and (c) at 45°C (113°F)

6.1.16.5 Effects of RAP on Dynamic Modulus and Phase Angle of Surface Type C Mixtures Made with WMA and Different Aggregate Types

Figure 6-61 indicates that the dynamic modulus values of Surface Type C mixtures made with RAP and WMA chemical additive technology varied depending on aggregate source. Mixtures with aggregate source IV generally exhibited higher dynamic modulus values with RAP than without RAP, while mixtures with aggregate source V exhibited lower dynamic modulus values with RAP than without RAP regardless of loading frequency, and test temperature.

In addition, Figure 6-62 shows that the phase angle values of Surface Type C mixtures made with RAP and WMA chemical additive technology varied depending on aggregate source. Mixtures with aggregate source IV generally exhibited lower phase angle values with RAP than without RAP, while mixtures with aggregate source V generally exhibited higher phase angle values with RAP than without RAP. However, phase angle values of these mixtures with and without RAP were similar at higher frequencies when the test temperature was 45°C (113°F).

Figure 6-63 indicates that the dynamic modulus values of Surface Type C mixtures containing RAP and foaming WMA technology were generally higher than those values of Surface Type C Mixtures made without RAP regardless of aggregate source, loading frequency, and test temperature. It can be noted that the differences in dynamic modulus were more obvious at a lower frequency.

In addition, Figure 6-64 shows that the phase angle values of Surface Type C mixtures made with RAP and foaming WMA technology were generally lower than those values of Surface Type C Mixtures made without RAP regardless of aggregate source, loading frequency, and test temperature. The phase angle values of these mixtures with/without RAP were closer together at the test temperature of 45°C (113°F).

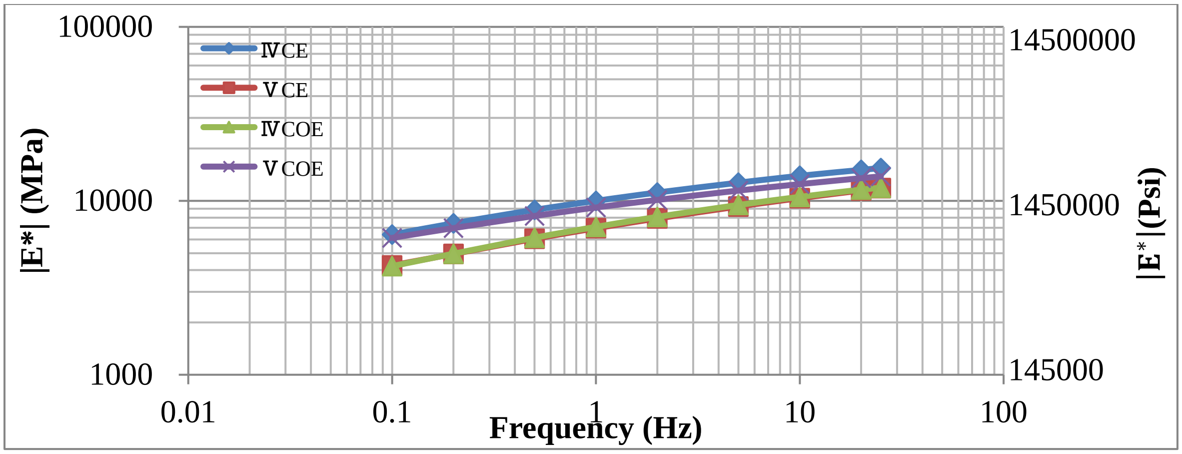

(a)

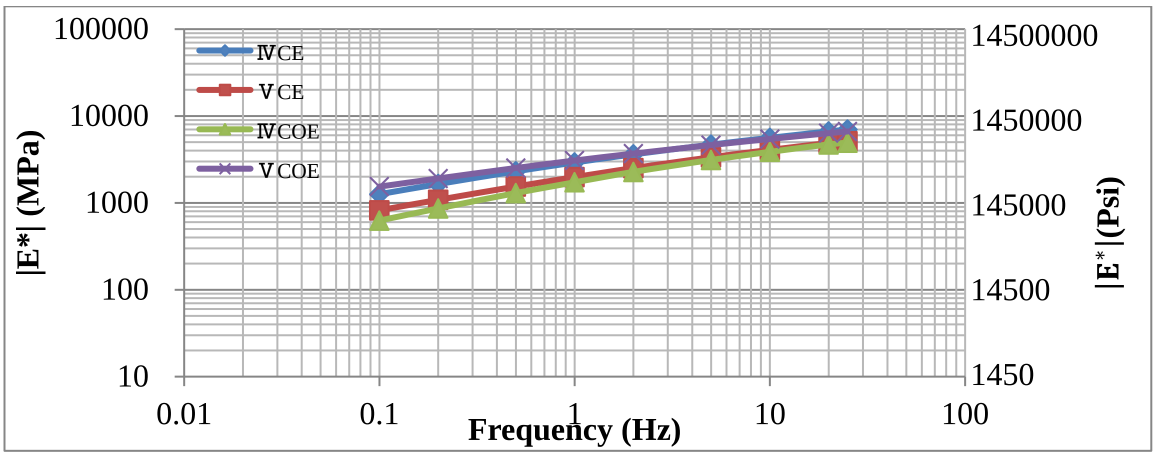

(b)

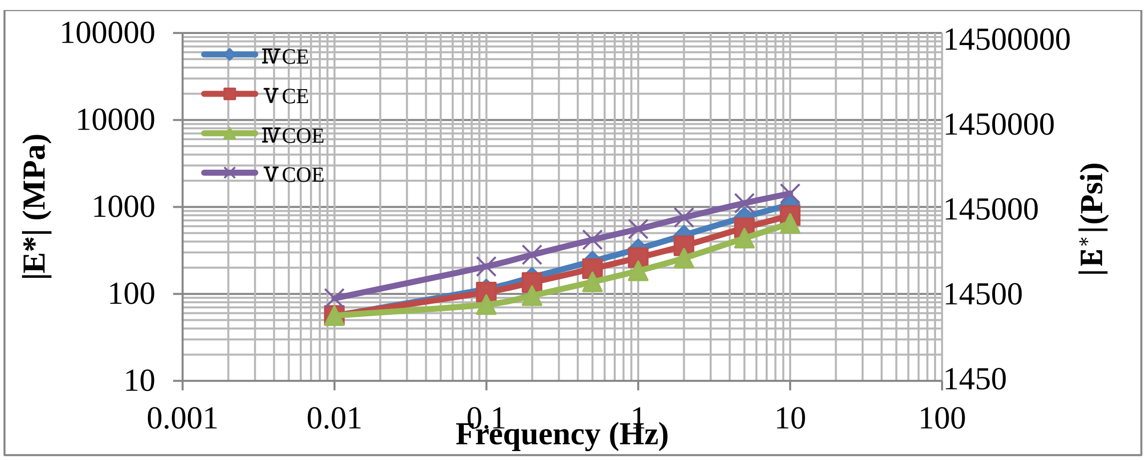

(c)

Figure 6-61 Dynamic Modulus Values of Various Surface Type C Mixtures Used Chemical Additive WMA Technology with/without RAP in Terms of Different Aggregate Types, (a) at 4°C (39.2°F), (b) at 20°C (68°F), and (c) at 45°C (113°F)

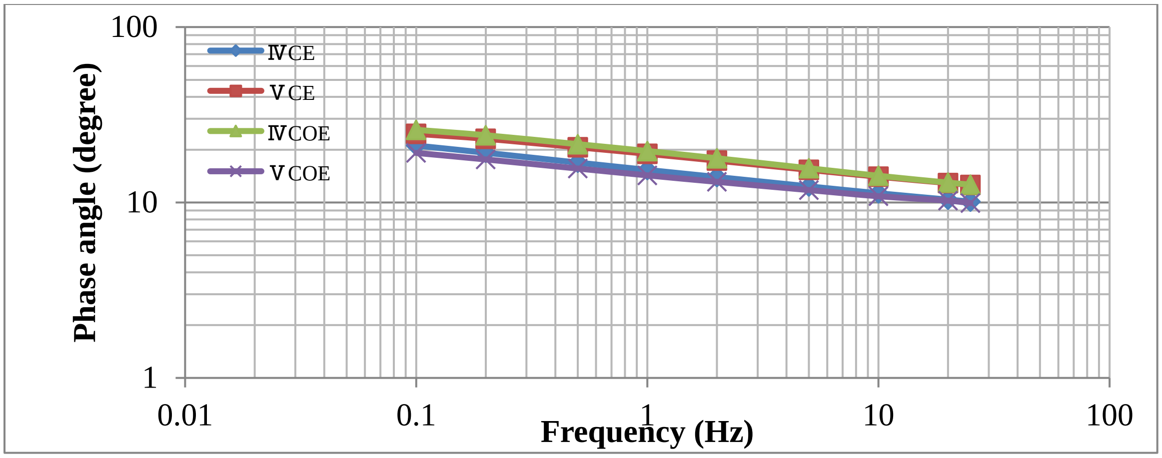

(a)

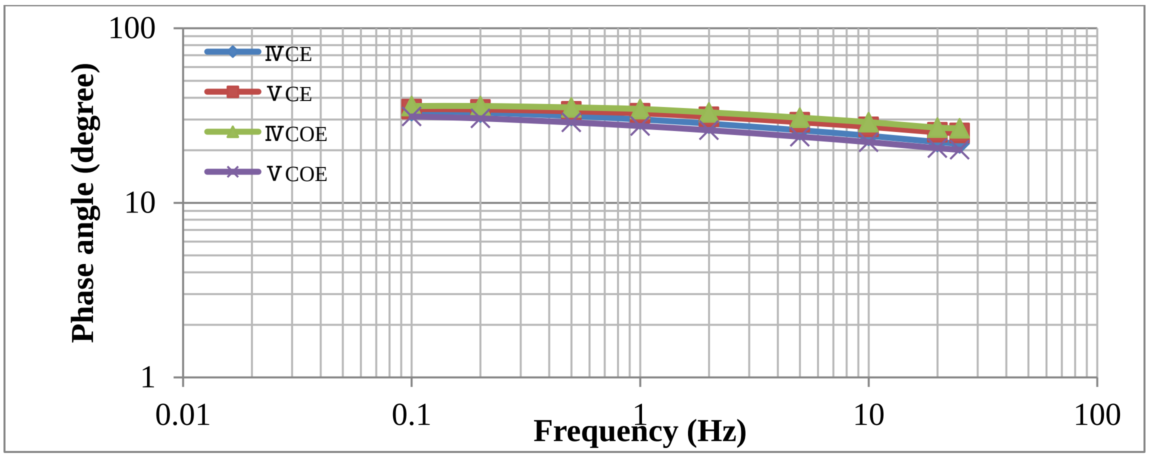

(b)

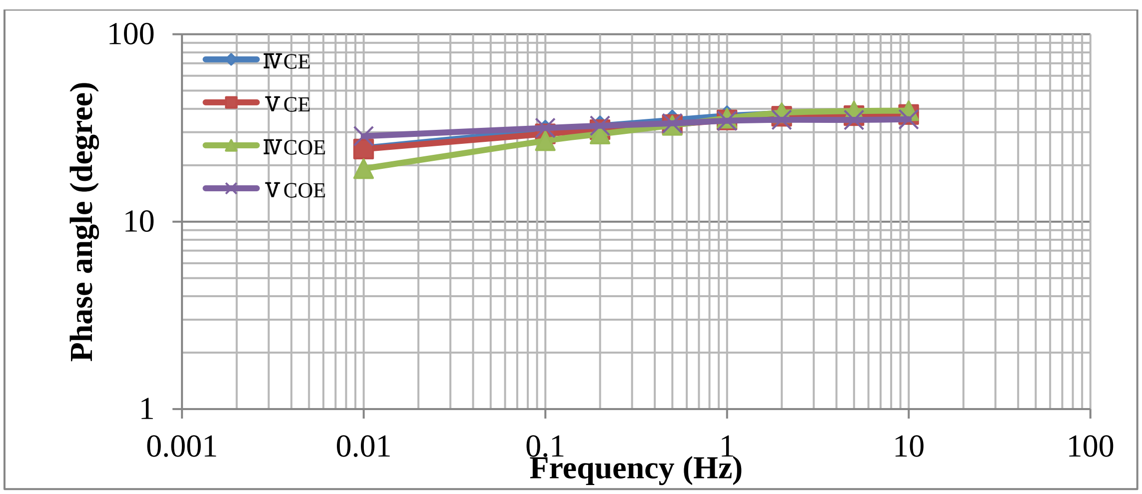

(c)

Figure 6-62 Phase Angle Values of Various Surface Type C Mixtures Used Chemical Additive WMA Technology with/without RAP in Terms of Different Aggregate Types, (a) at 4°C (39.2°F), (b) at 20°C (68°F), and (c) at 45°C (113°F)

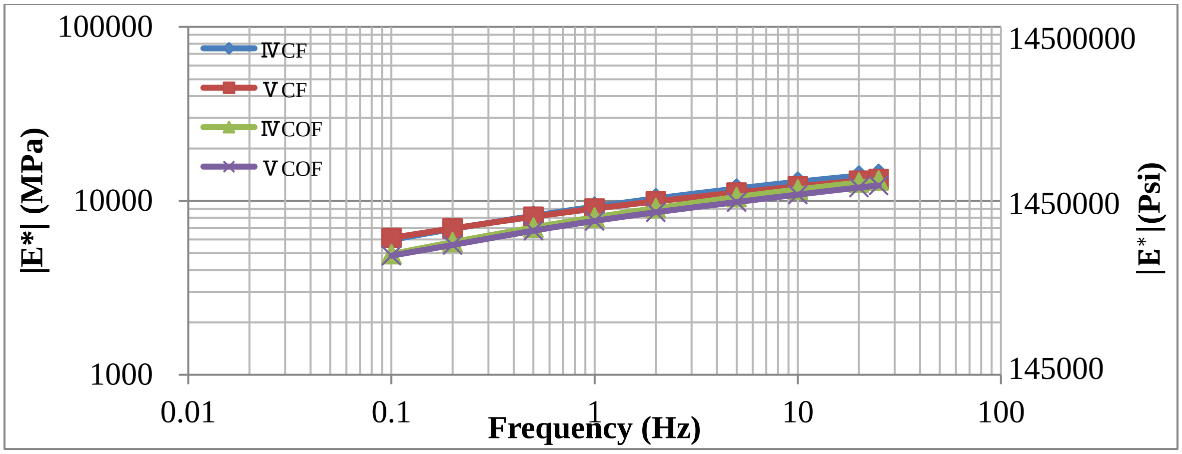

(a)

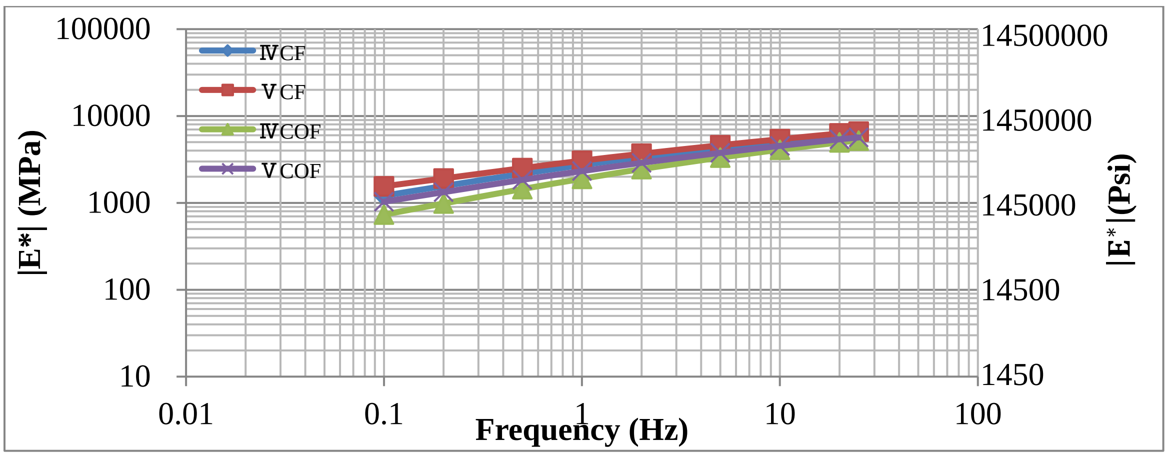

(b)

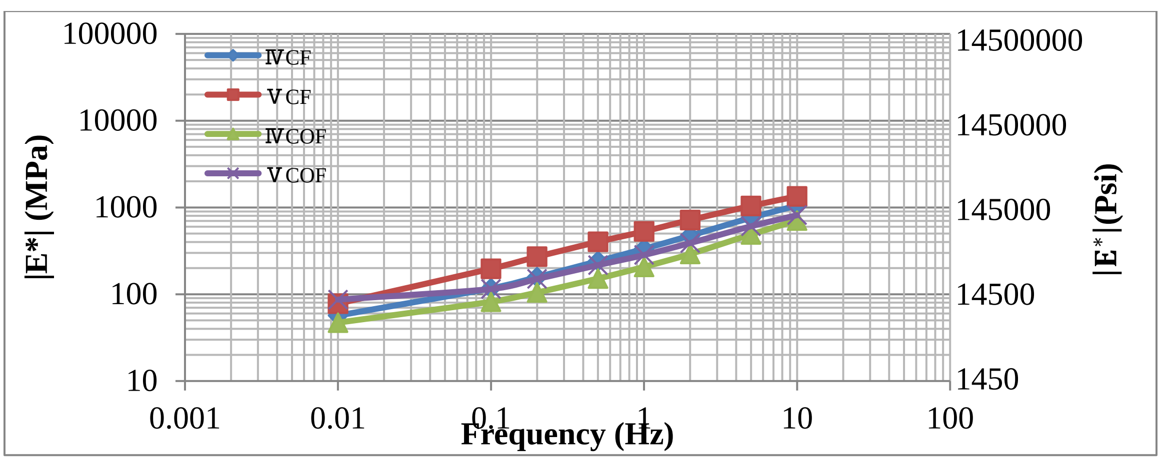

(c)

Figure 6-63 Dynamic Modulus Values of Various Surface Type C Mixtures Used Foaming WMA Technology with/without RAP in Terms of Different Aggregate Types, (a) at 4°C (39.2°F), (b) at 20°C (68°F), and (c) at 45°C (113°F)

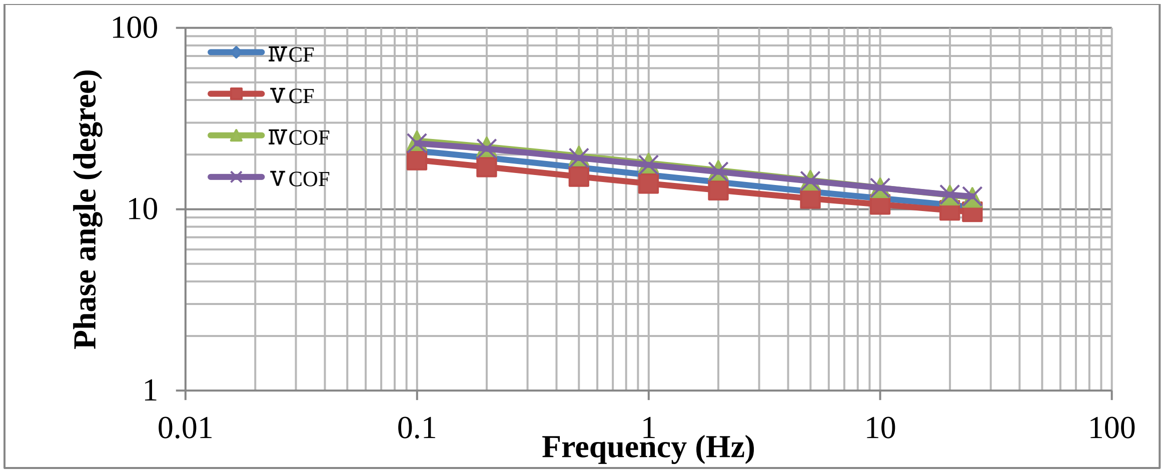

(a)

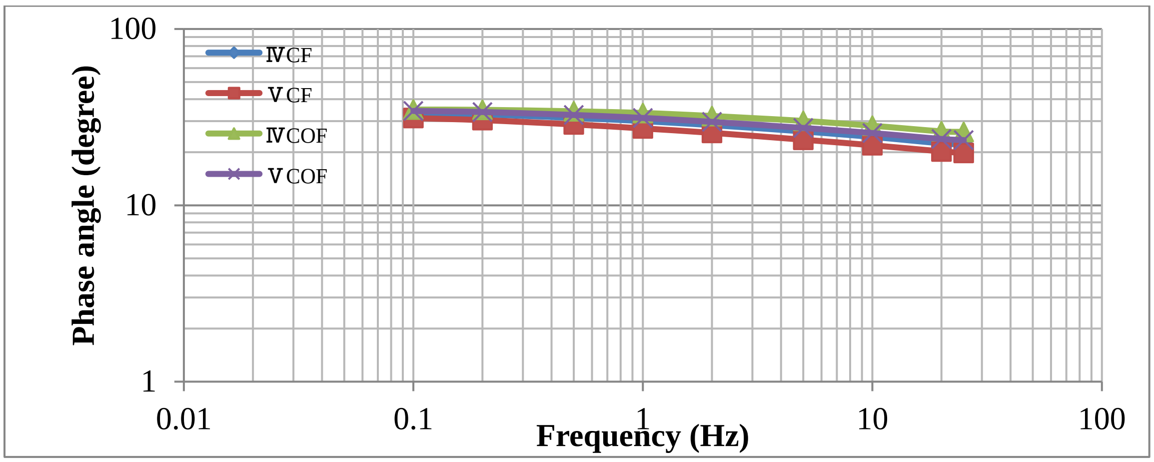

(b)

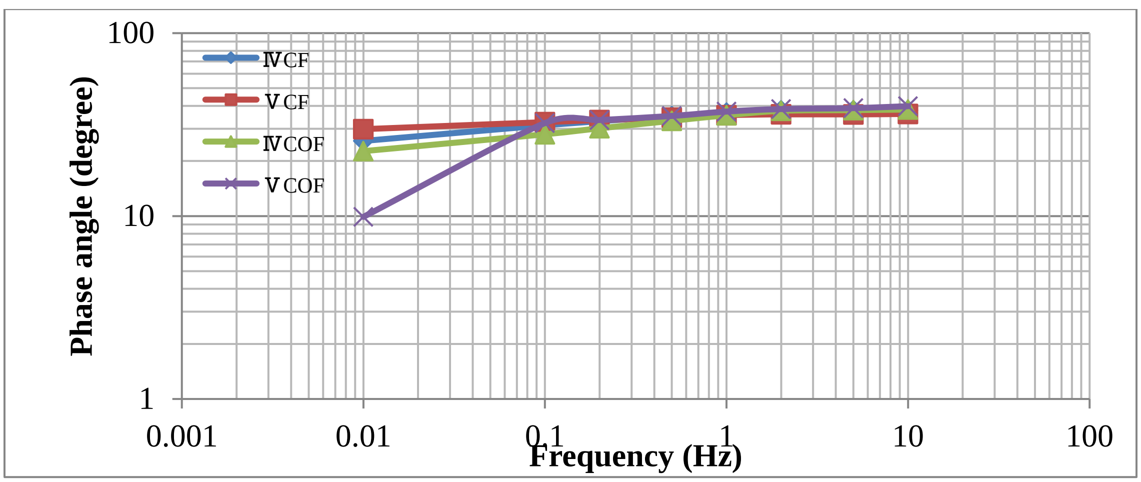

(c)

Figure 6-64 Phase Angle Values of Various Surface Type C Mixtures Used Foaming WMA Technology with/without RAP in Terms of Different Aggregate Types, (a) at 4°C (39.2°F), (b) at 20°C (68°F), and (c) at 45°C (113°F)

6.1.16.6 Effects of RAP on Dynamic Modulus and Phase Angle of Surface Type C Mixtures Made with LASA and Different Aggregate Types

Figure 6-65 indicates that the dynamic modulus values of Surface Type C mixtures made with RAP and liquid ASA1 were generally higher than those without RAP regardless of aggregate source, loading frequency, and test temperature. It can be noted that the differences in dynamic modulus were more obvious at a lower frequency.

In addition, Figure 6-66 shows that the phase angle values of Surface Type C mixtures containing RAP and liquid ASA1 were generally lower than those without RAP regardless of aggregate source, loading frequency, and test temperature. These difference were less obvious when the test temperature was set to 45°C (113°F).

Figure 6-67 indicates that the dynamic modulus values of Surface Type C mixtures made with RAP and liquid ASA2 were generally higher than those without RAP regardless of aggregate source, loading frequency, and test temperature. It can be noted that the differences in dynamic modulus were more obvious at a lower frequency.

In addition, Figure 6-68 shows that the phase angle values of Surface Type C mixtures made with RAP and liquid ASA2 were generally lower than those without RAP regardless of aggregate source, loading frequency, and test temperature. These difference were less obvious when the test temperature was set to 45°C (113°F).

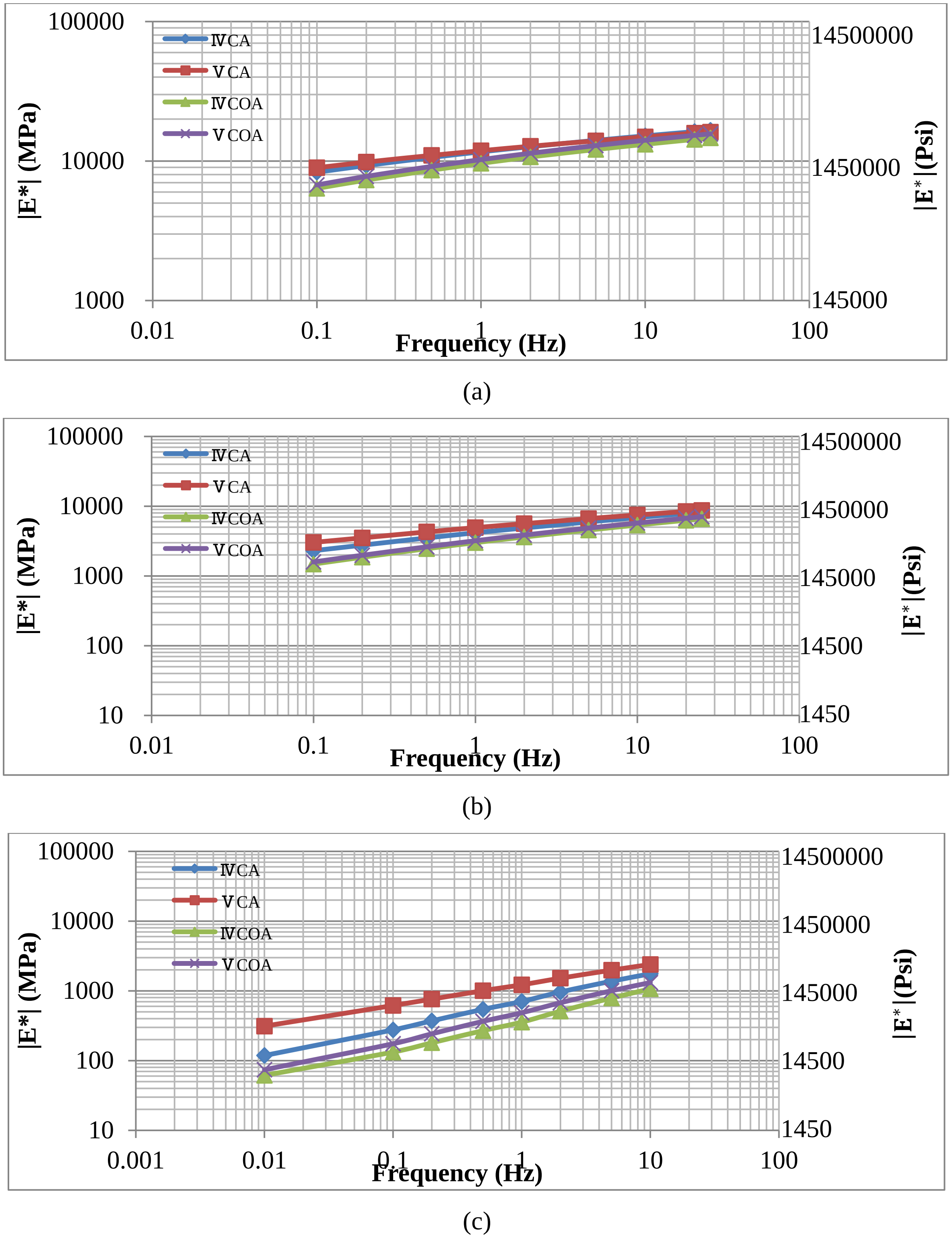

Figure 6-65 Dynamic Modulus Values of Various Surface Type C Mixtures Used Liquid ASA1 with/without RAP in Terms of Different Aggregate Types, (a) at 4°C (39.2°F), (b) at 20°C (68°F), and (c) at 45°C (113°F)

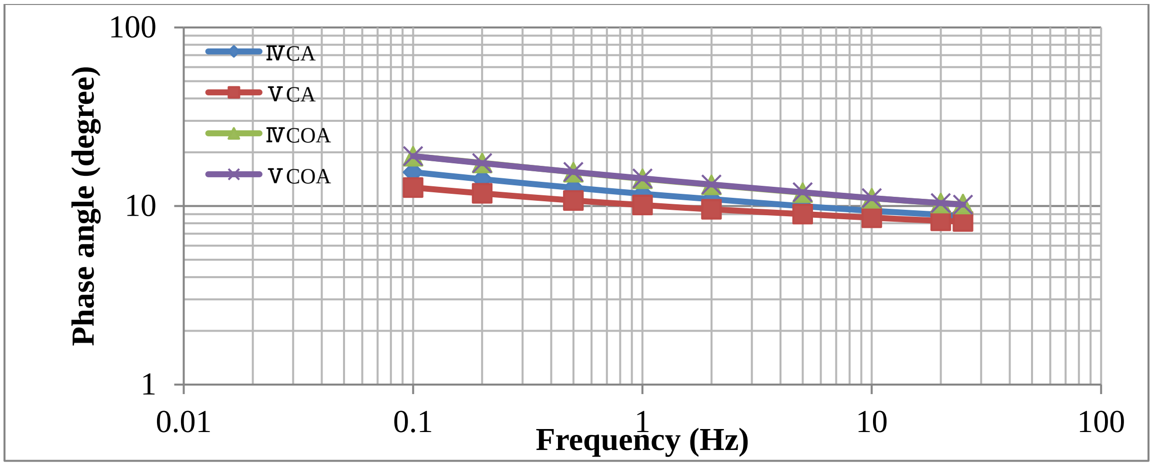

(a)

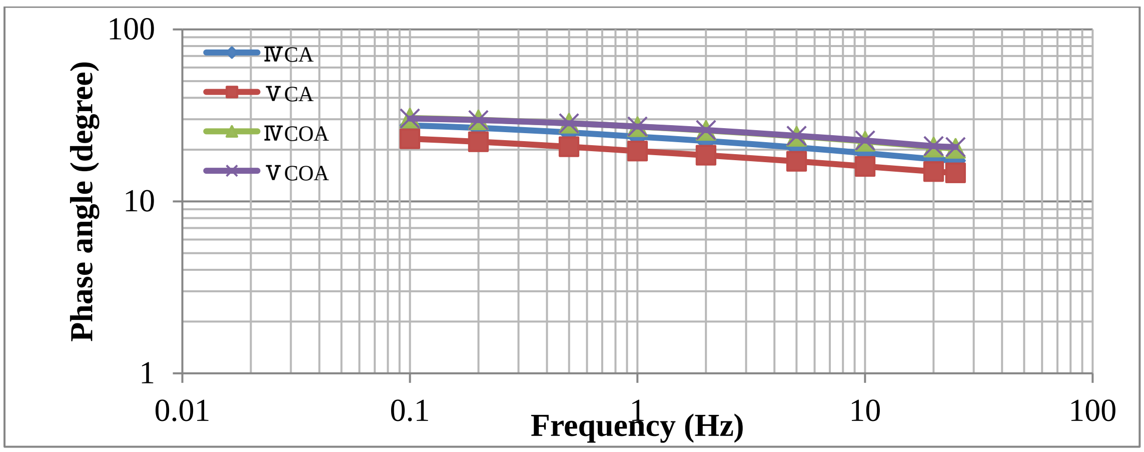

(b)

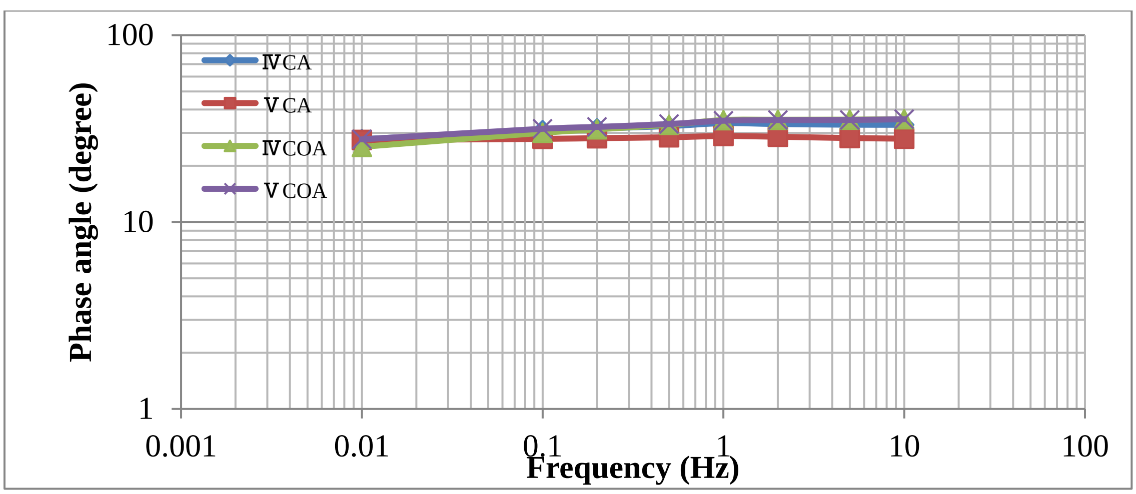

(c)

Figure 6-66 Phase Angle Values of Various Surface Type C Mixtures Used Liquid ASA1 with/without RAP in Terms of Different Aggregate Types, (a) at 4°C (39.2°F), (b) at 20°C (68°F), and (c) at 45°C (113°F)

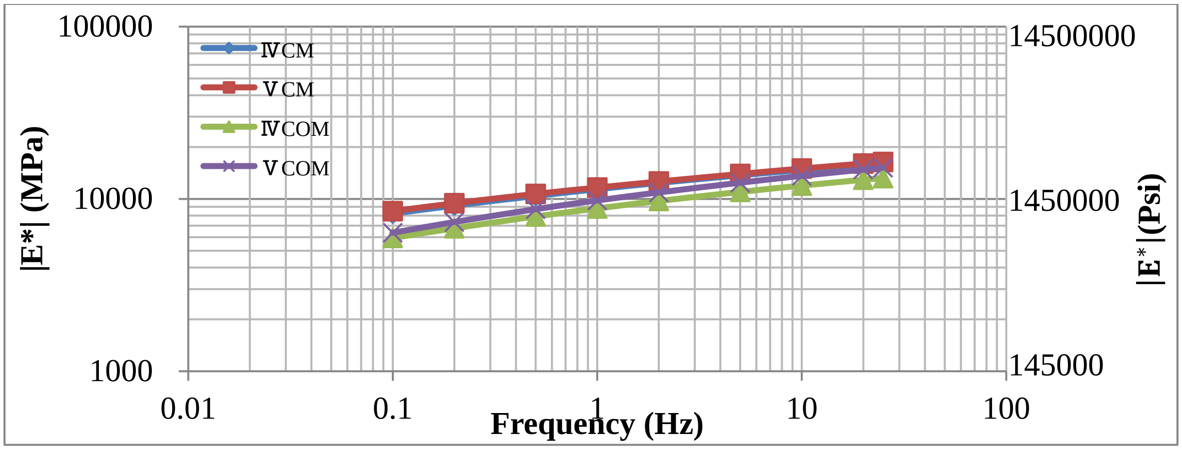

(a)

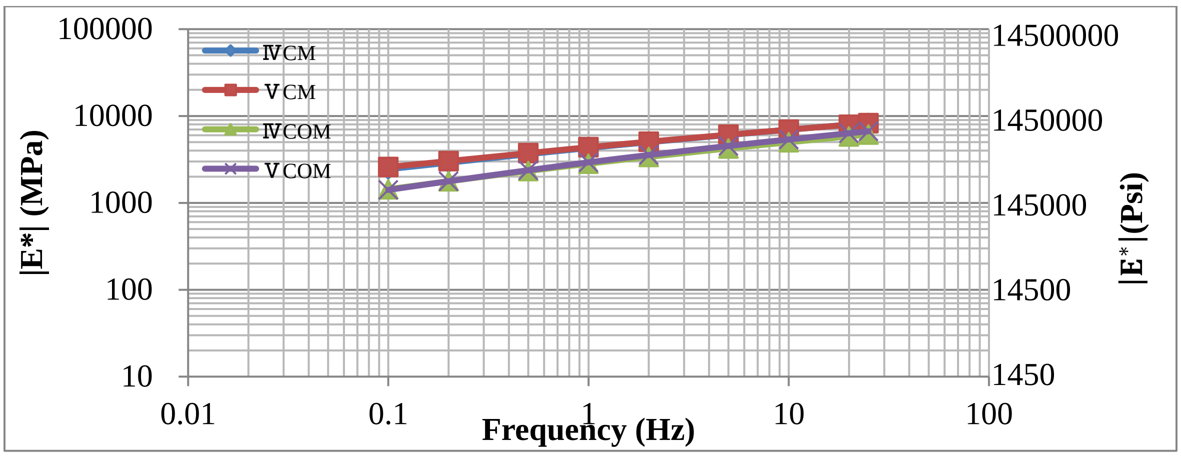

(b)

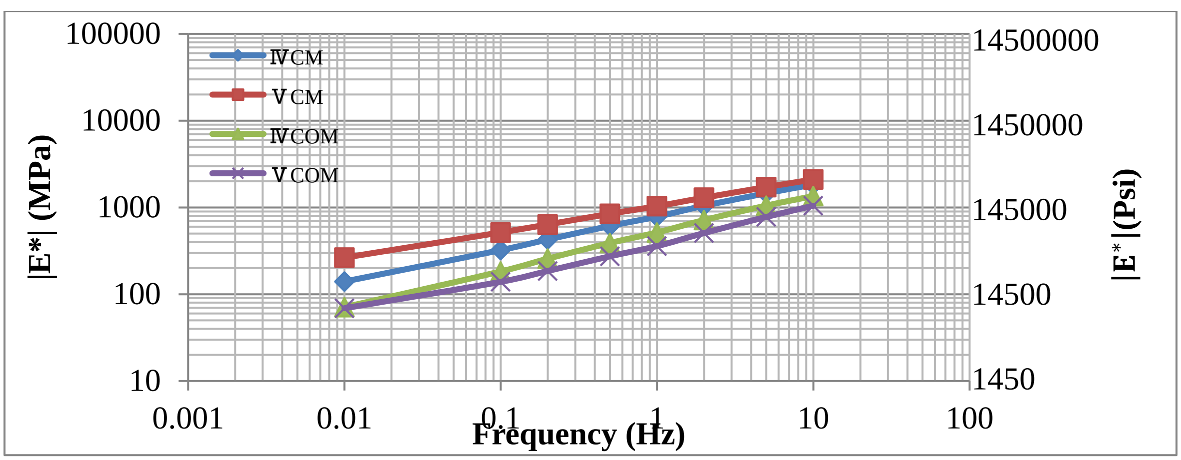

(c)

Figure 6-67 Dynamic Modulus Values of Various Surface Type C Mixtures Used Liquid ASA2 with/without RAP in Terms of Different Aggregate Types, (a) at 4°C (39.2°F), (b) at 20°C (68°F), and (c) at 45°C (113°F)

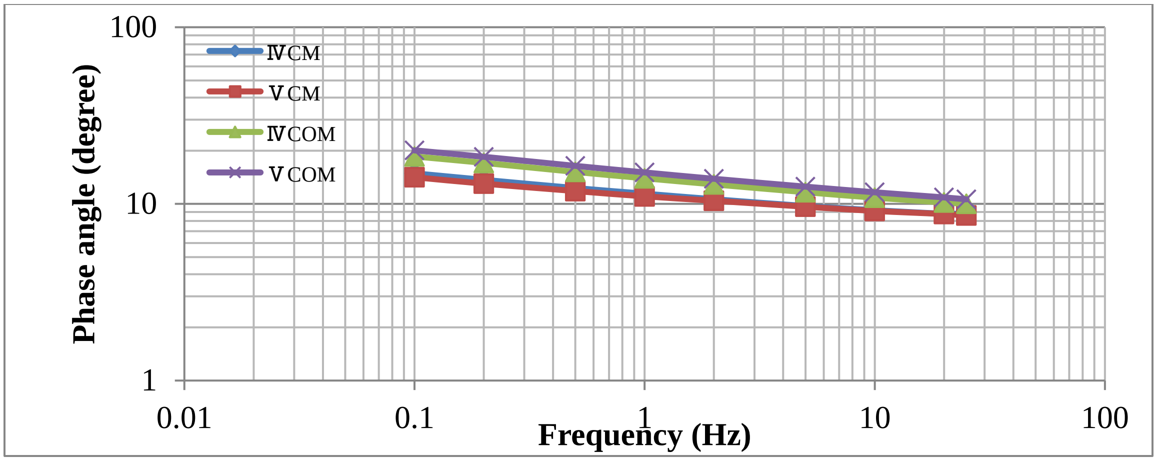

(a)

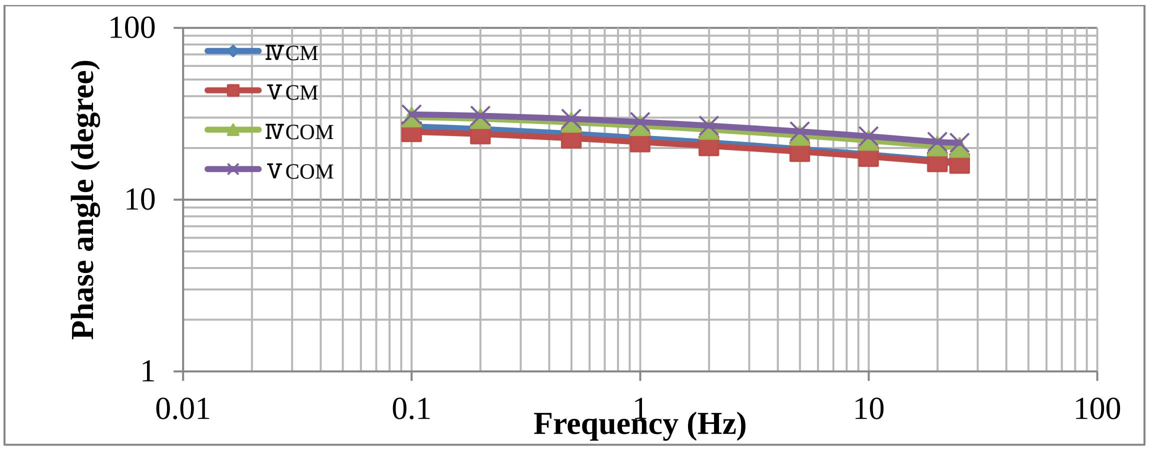

(b)

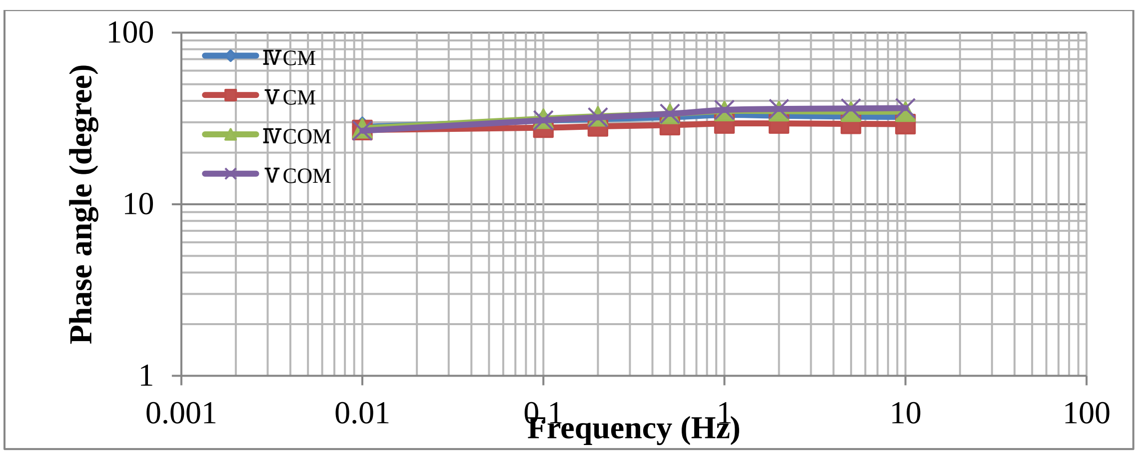

(c)

Figure 6-68 Phase Angle Values of Various Surface Type C Mixtures Used Liquid ASA2 with/without RAP in Terms of Different Aggregate Types, (a) at 4°C (39.2°F), (b) at 20°C (68°F), and (c) at 45°C (113°F)

6.1.16.7 Effects of RAP on Dynamic Modulus and Phase Angle of Aged Surface Mixtures (Types A, B, and C) Made with Different Aggregate Types

Figure 6-69 indicates that the dynamic modulus values of aged Surface Type A mixtures made with RAP varied depending on aggregate source. Aged mixtures from aggregate source IV containing RAP generally exhibited higher dynamic modulus values that those without RAP, while aged mixtures from aggregate source V containing RAP mostly exhibited similar dynamic modulus values compared to the corresponding mixtures without RAP. It can be noted that the differences in dynamic modulus values were more obvious at a lower frequency.

In addition, Figure 6-70 shows that the phase angle values of aged Surface Type A mixtures made with RAP also varied depending on aggregate source. Aged mixtures from aggregate source IV containing RAP generally exhibited lower phase angle values than those without RAP, while aged mixtures from aggregate source V containing RAP mostly exhibited similar phase angle values compared to the corresponding mixtures without RAP. However, the phase angle values of aged mixtures from both aggregate sources with and without RAP were similar when the test temperature was set at 45°C (113°F).

Figure 6-71 indicates that the dynamic modulus values of aged Surface Type B mixtures made with RAP were generally higher than without RAP regardless of aggregate source, loading frequency, and test temperature. Additionally, Figure 6-72 shows that the phase angle values of aged Surface Type B mixtures made with RAP were generally lower than without RAP regardless of aggregate source, loading frequency, and test temperature. However, these differences in phase angle values were much less obvious when the test temperature was set at 45°C (113°F).

Aged Surface Type C mixtures with and without RAP exhibited similar trends to Surface Type B mixtures (Figure 6-73 and Figure 6-74).

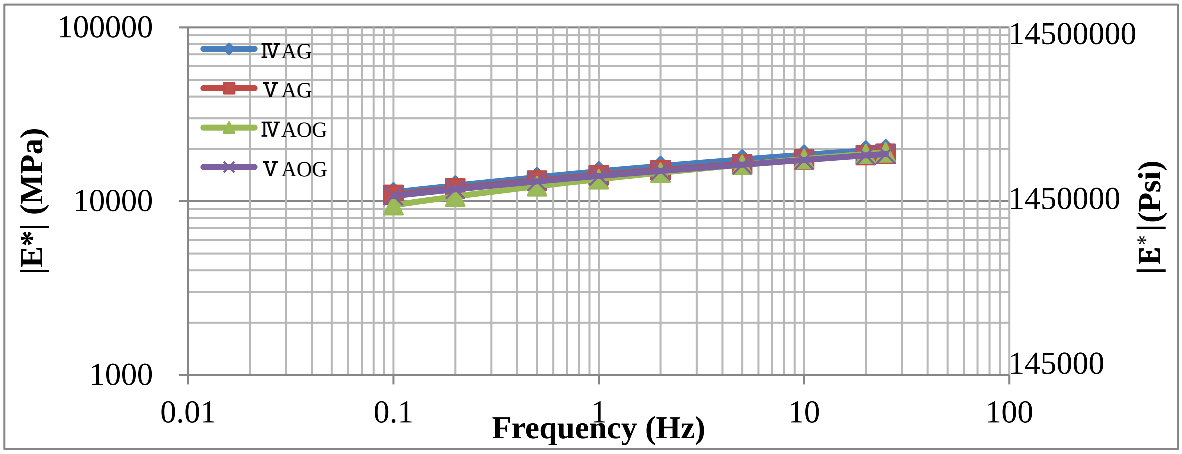

(a)

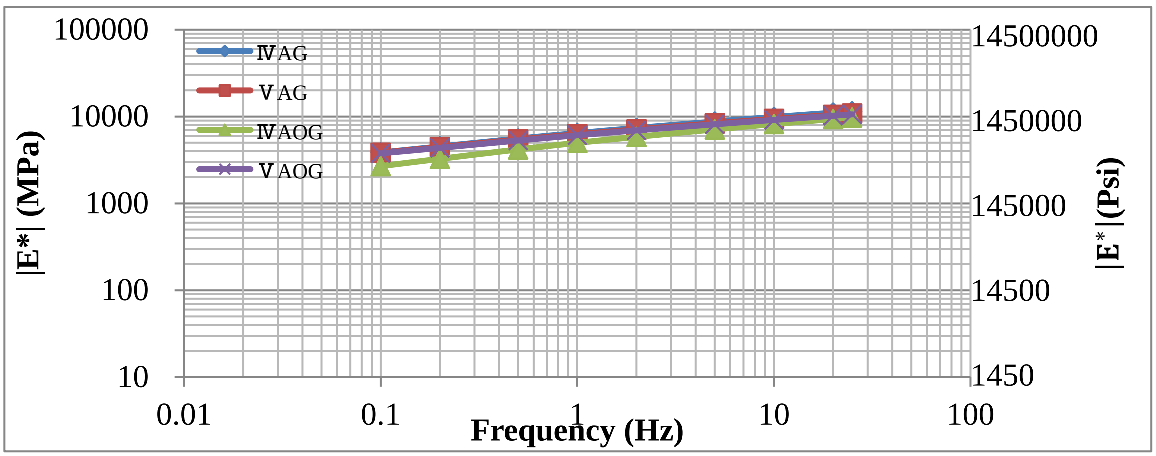

(b)

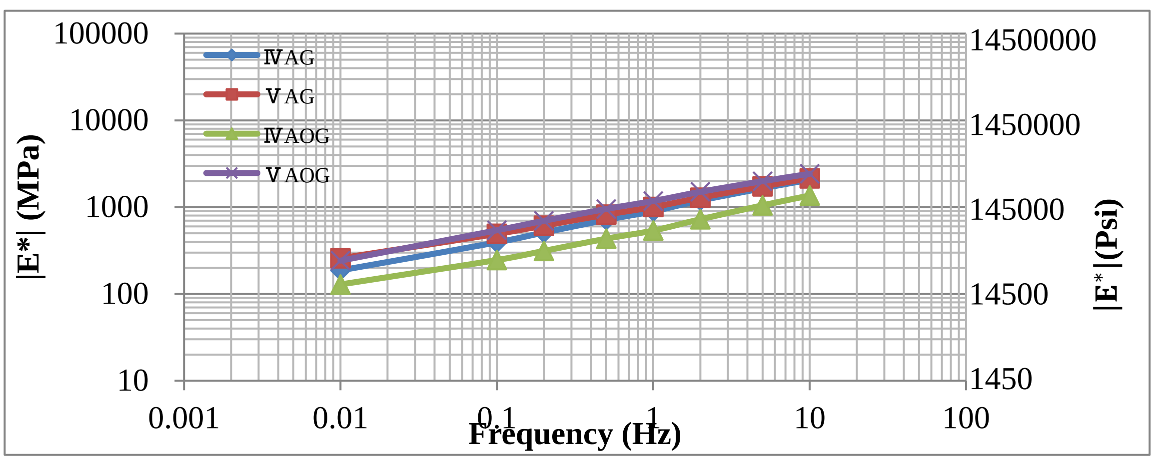

(c)

Figure 6-69 Dynamic Modulus Values of Various Aged Surface Type A Mixtures with/without RAP in Terms of Different Aggregate Types, (a) at 4°C (39.2°F), (b) at 20°C (68°F), and (c) at 45°C (113°F)

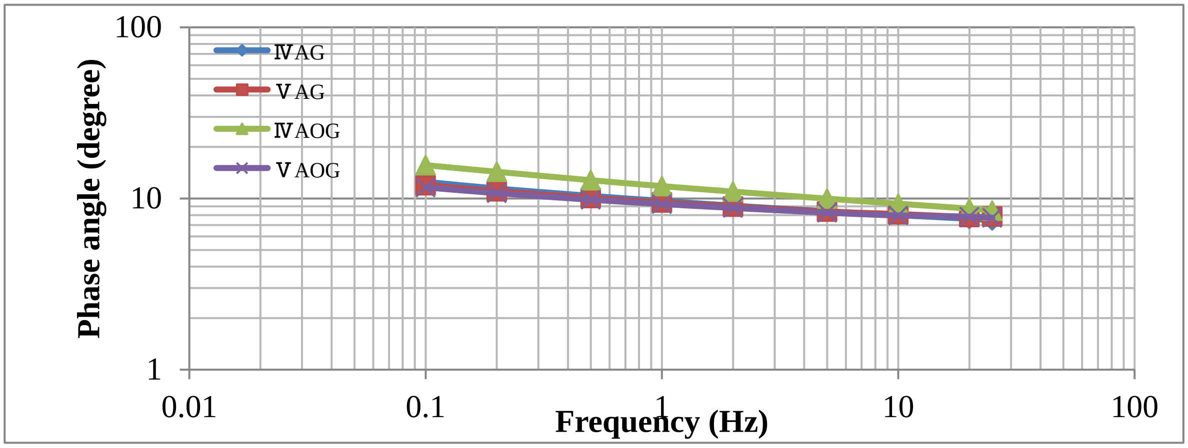

(a)

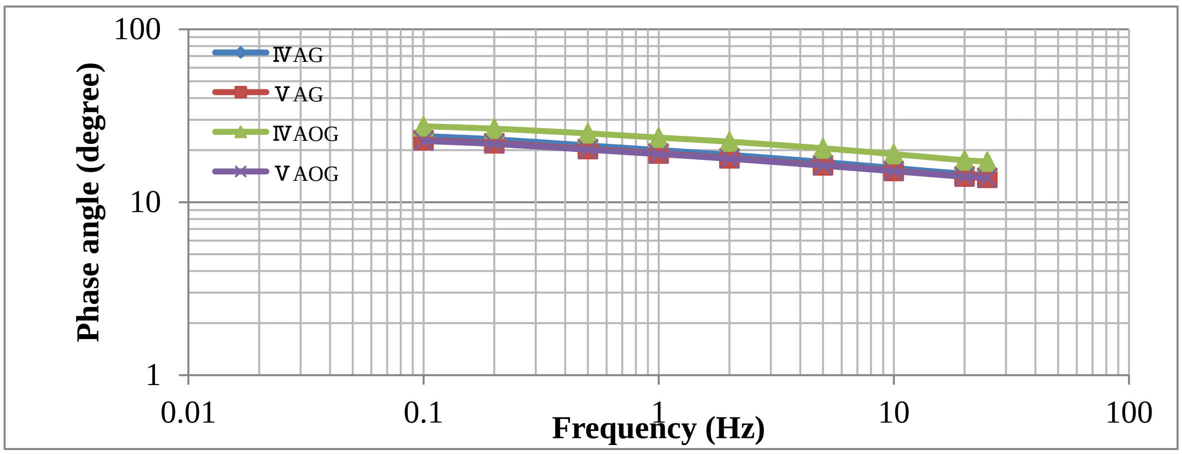

(b)

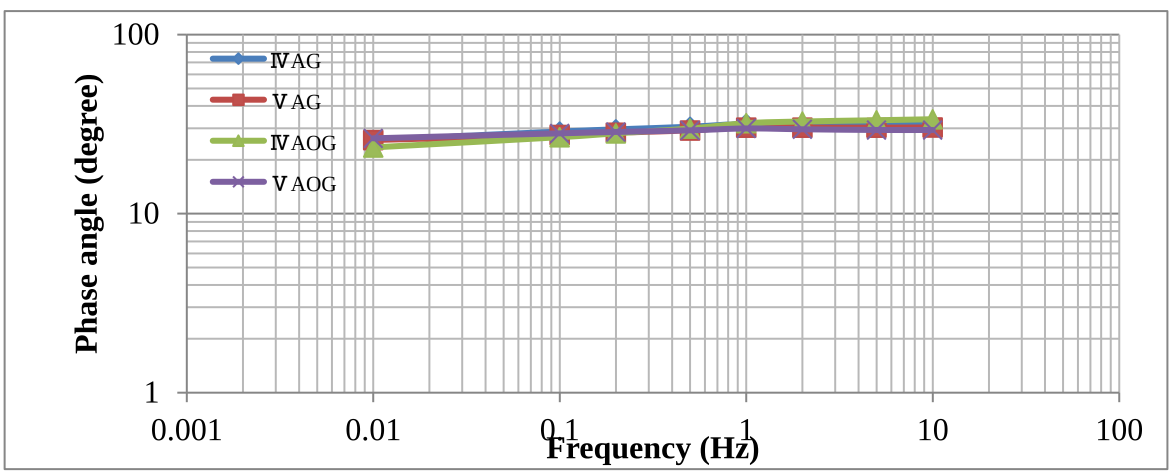

(c)

Figure 6-70 Phase Angle Values of Various Aged Surface Type A Mixtures with/without RAP in Terms of Different Aggregate Types, (a) at 4°C (39.2°F), (b) at 20°C (68°F), and (c) at 45°C (113°F)

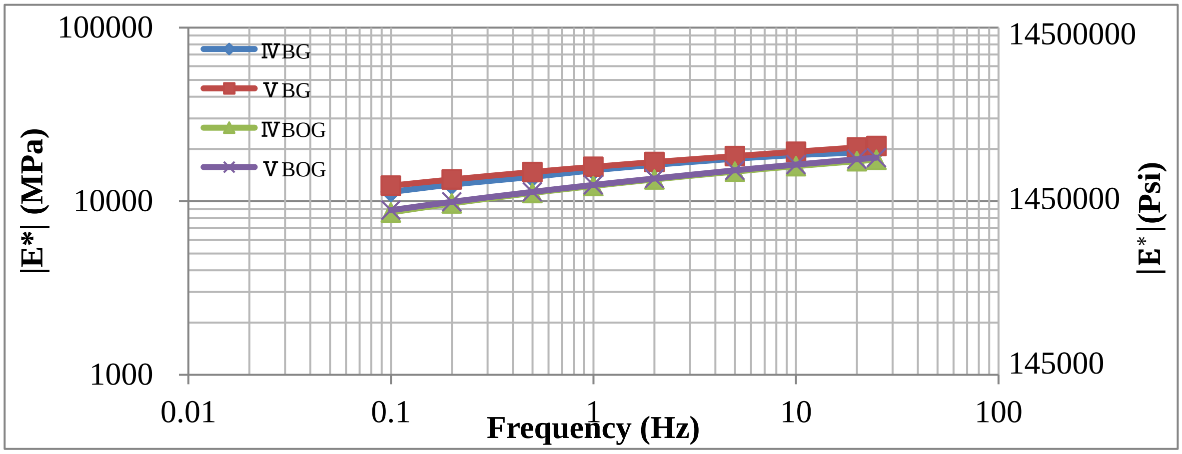

(a)

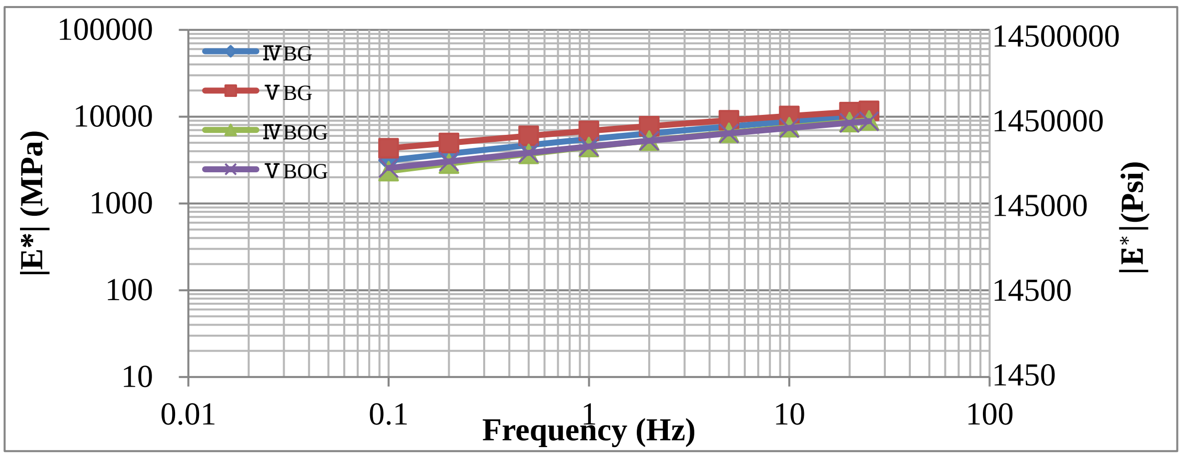

(b)

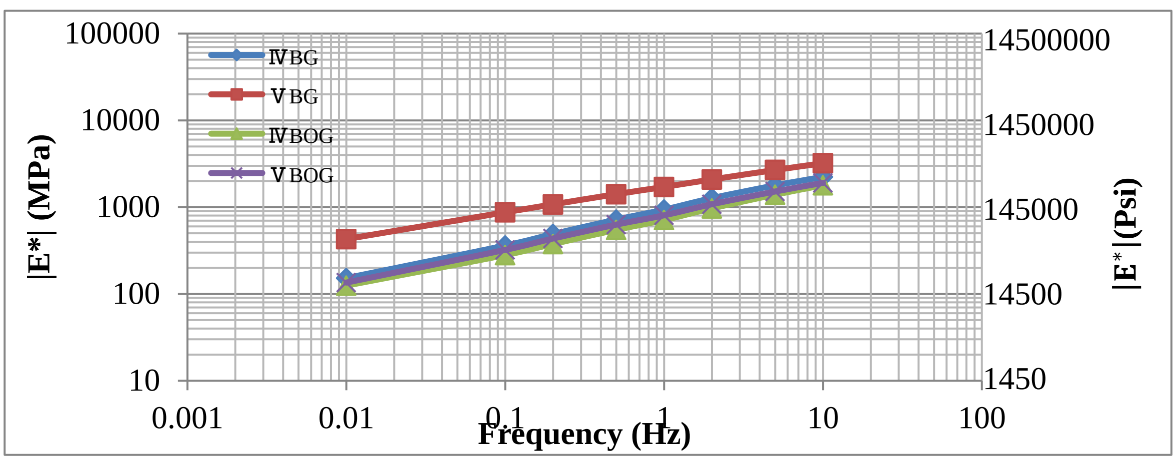

(c)

Figure 6-71 Dynamic Modulus Values of Various Aged Surface Type B Mixtures with/without RAP in Terms of Different Aggregate Types, (a) at 4°C (39.2°F), (b) at 20°C (68°F), and (c) at 45°C (113°F)

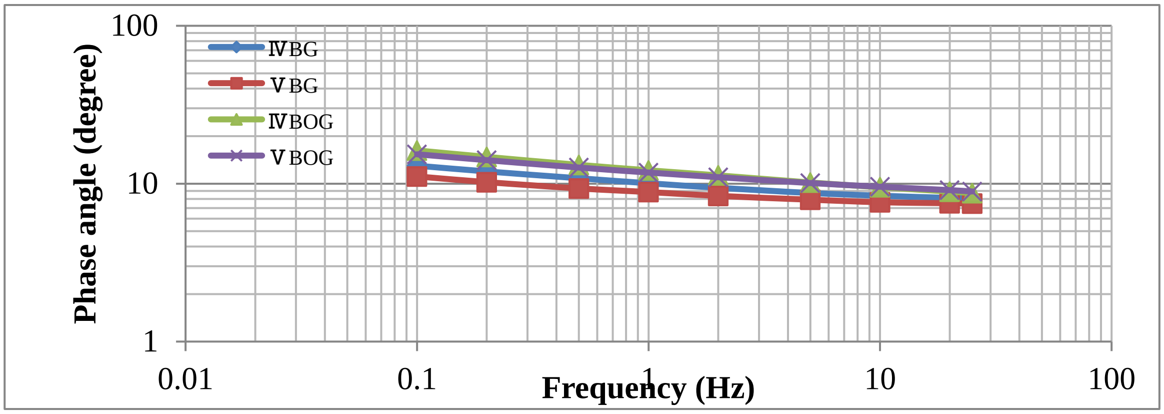

(a)

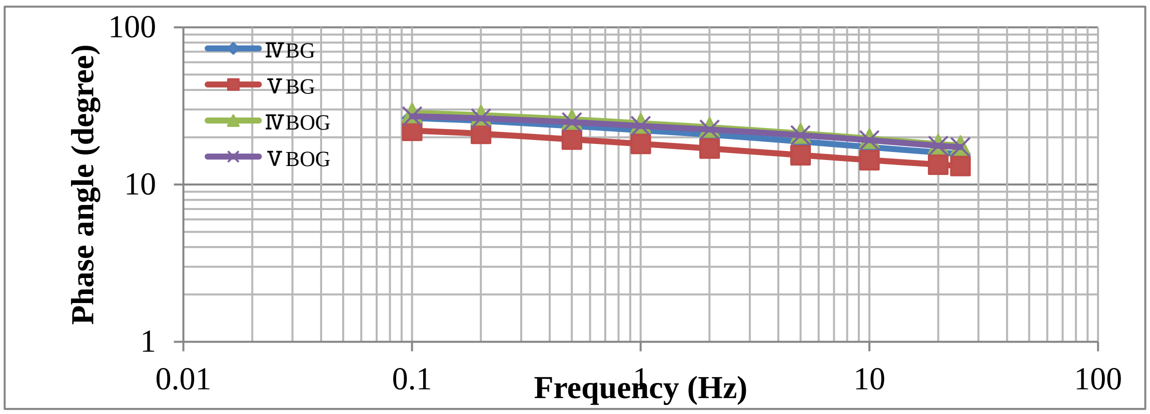

(b)

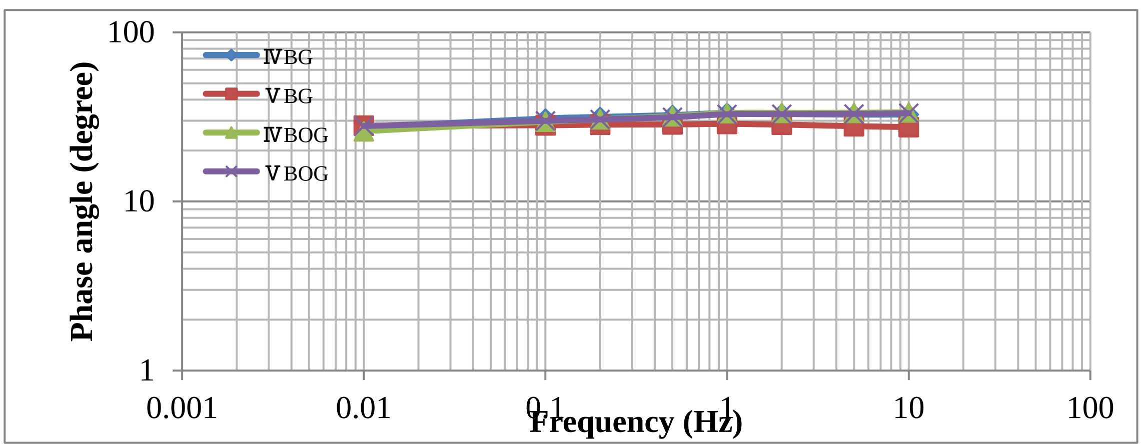

(c)

Figure 6-72 Phase Angle Values of Various Aged Surface Type B Mixtures with/without RAP in Terms of Different Aggregate Types, (a) at 4°C (39.2°F), (b) at 20°C (68°F), and (c) at 45°C (113°F)

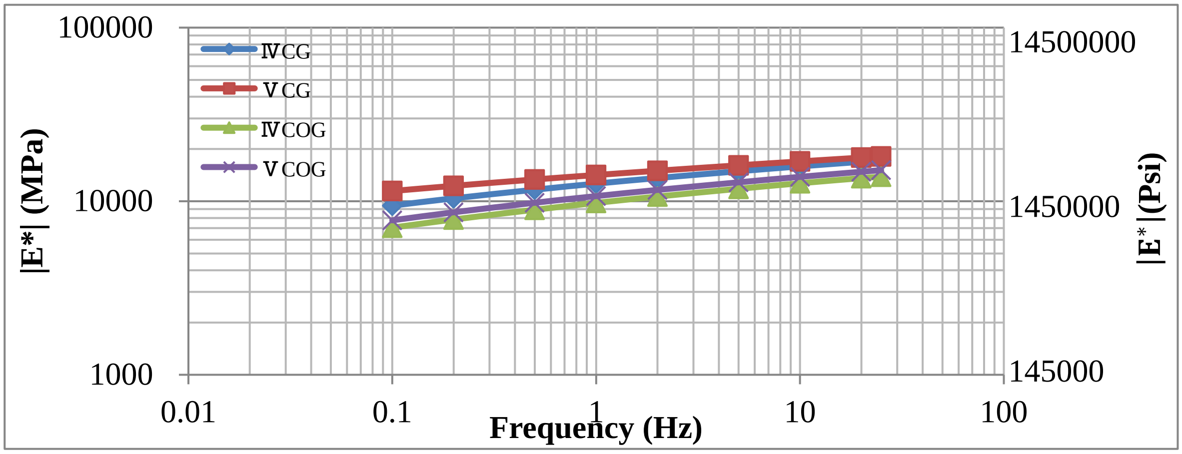

(a)

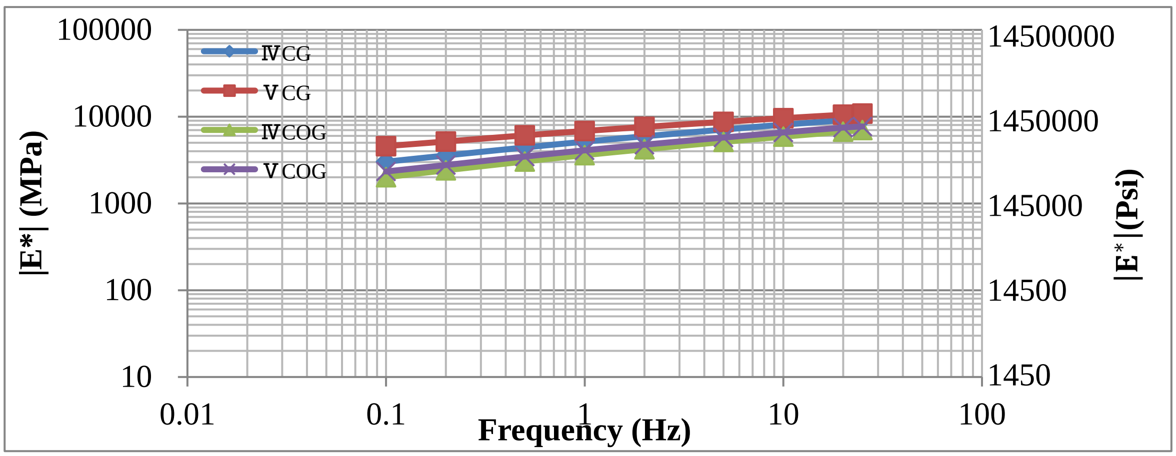

(b)

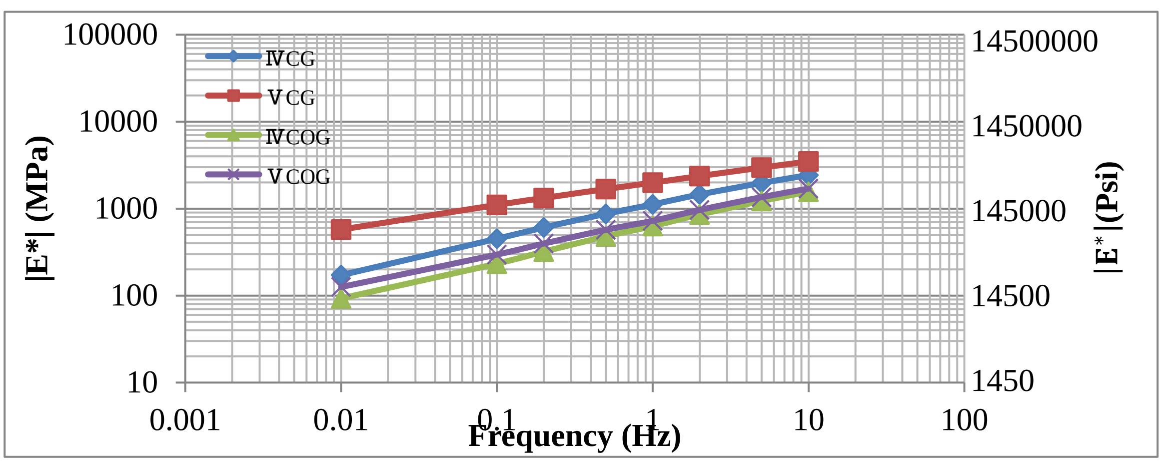

(c)

Figure 6-73 Dynamic Modulus Values of Various Aged Surface Type C Mixtures with/without RAP in Terms of Different Aggregate Types, (a) at 4°C (39.2°F), (b) at 20°C (68°F), and (c) at 45°C (113°F)

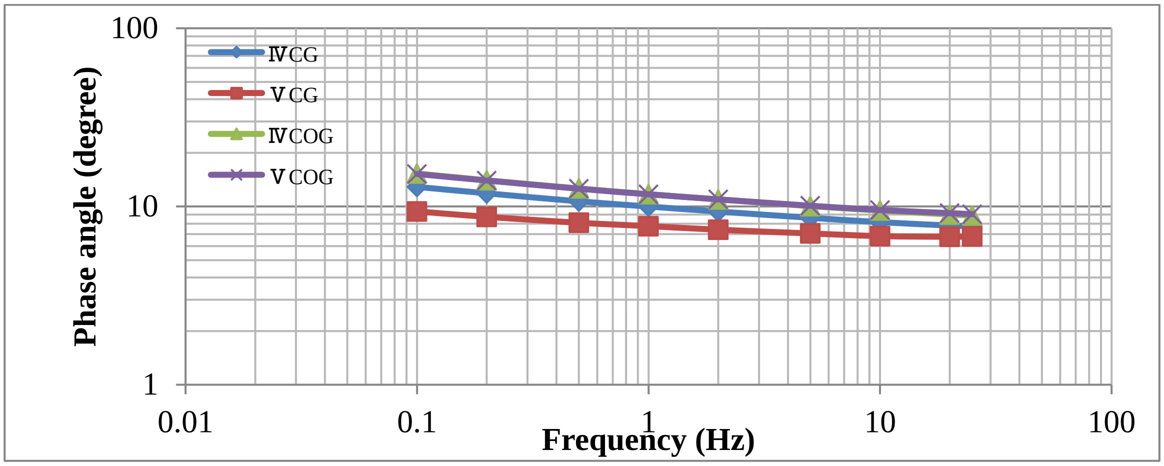

(a)

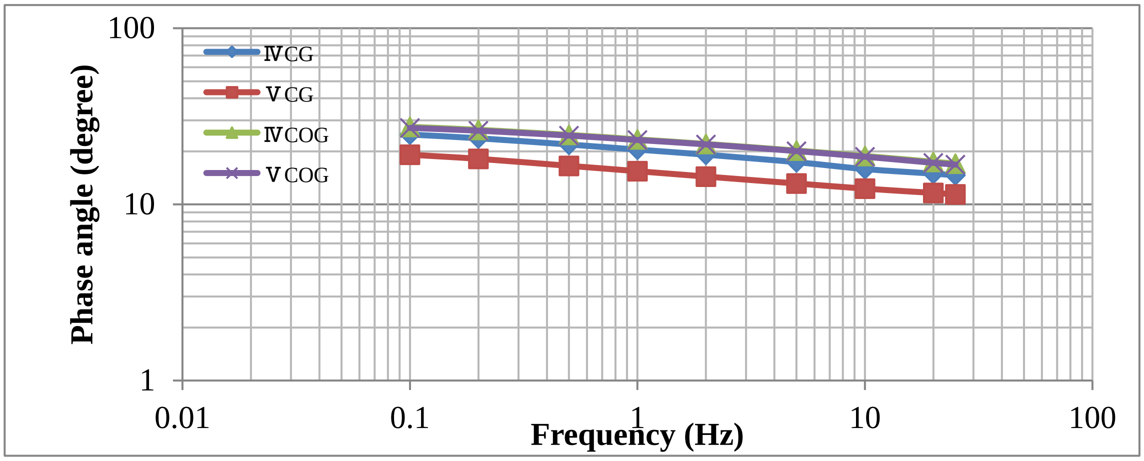

(b)

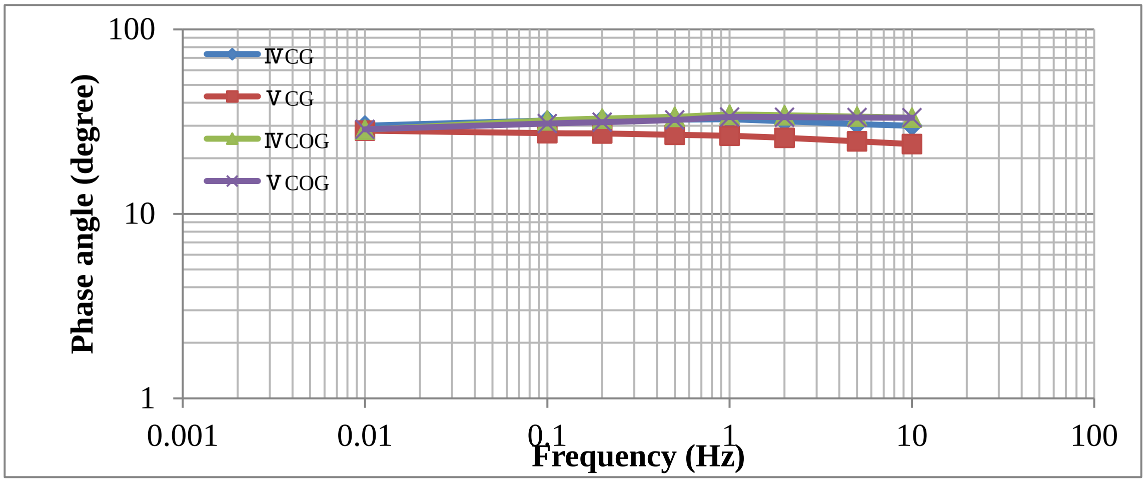

(c)

Figure 6-74 Phase Angle Values of Various Aged Surface Type C Mixtures with/without RAP in Terms of Different Aggregate Types, (a) at 4°C (39.2°F), (b) at 20°C (68°F), and (c) at 45°C (113°F)

6.2 <u>Flow Numbers of Various Mixtures</u>

6.2.1 Effect of Aggregate Source on Flow Number of Different Types of Surface Mixtures

Figure 6-75 shows the flow numbers of various Surface Type A mixtures containing RAP in terms of six various aggregate sources tested at 59°C (138.2°F). In addition, there were two different Surface Type A mix designs utilized for aggregate sources II and III. The second mix design for each of those aggregate sources (II A2 and III A2) utilized the updated finer SCDOT gradation requirements from SCDOT (SC-M-402, July 2017 version) as well as incorporating the newly-adopted corrected optimum asphalt content (COAC). As shown in Figure 6-75, mixtures I A and V A had much higher flow numbers than other mixtures, while mixtures II A2 and VI A had lower flow numbers than other mixtures. Thus, this limited data indicates that the flow number of Surface Course mixtures is generally affected by the aggregate source.

The flow numbers of Surface Type B, C, D, and E mixtures generally had similar trends. These findings and the results are shown in other figures presented in Appendix C.

The effect of the new Surface Type A mix designs containing the finer gradation and the COAC varied with aggregate source. The new mix design with aggregate source II exhibited lower flow numbers than the old mix design with that same aggregate source, while the new mix design with aggregate source III exhibited higher flow numbers than the old mix design with that same aggregate source. The scope of this project did not allow further investigation of this effect.

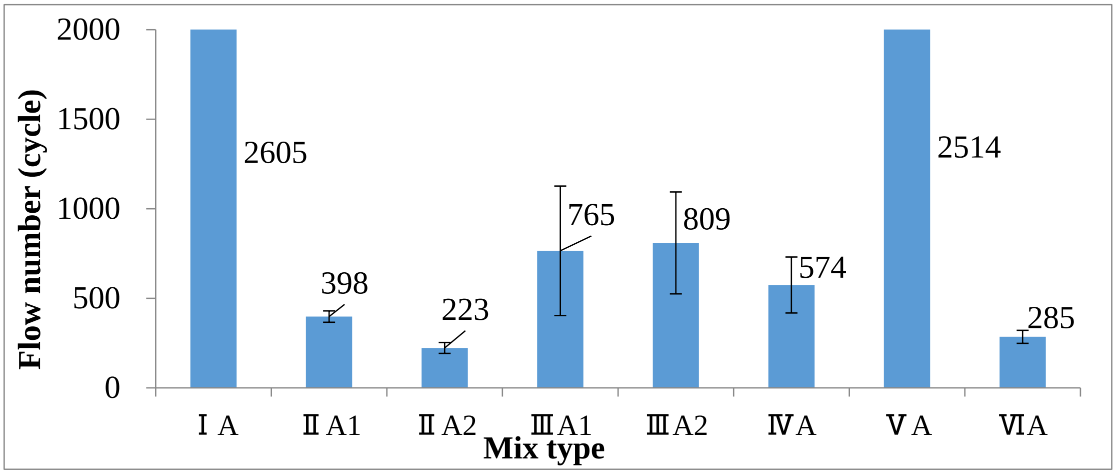

Figure 6-75 Flow Numbers of Various Surface Type A Mixtures with RAP in Terms of Aggregate Source at 59°C (138.2°F)

6.2.2 Effect of Aggregate Source on Flow Number of Different Types of Intermediate Mixtures

Figure 6-76 shows the flow numbers of various Intermediate Type A mixtures containing RAP in terms of various aggregate sources tested at 59°C (138.2°F). As shown in Figure 6-76, mixtures IV IA and V IA had similar flow numbers. Therefore, it could be concluded that with this limited data, the aggregate source generally did not have an influence on the flow numbers of Intermediate Course mixtures. All Intermediate Type A and B mixtures tested in this project exhibited flow number values below AASHTO minimum recommendation of 190 for higher volume pavements. Although the utilization of RAP resulted in somewhat higher flow number values, they still did not reach the minimum recommended value. The scope of this study did not allow for further investigation into the cause of this result.

The flow numbers of other Intermediate Type B and C mixtures generally had similar trends. These results are shown in other figures presented in Appendix C.

In addition to the Intermediate Type A, B, and C mixtures made with aggregate sources IV and V, several Intermediate Type B Special mixtures were made with two additional aggregate sources, II and VII. These mixtures were added towards the end of the project, and aggregate sources were selected by the Steering Committee based on materials used in field pilot projects. The flow number values shown in Figure 11-12 of Appendix C indicate that the Intermediate Type B Special samples containing aggregate source VII generally had only slightly higher values than those containing aggregate source II. Additionally, both Intermediate Type B Special mixtures exhibited higher flow number values than both of the other Intermediate Type B mixtures. However, because the Intermediate Type B Special mixtures contained different aggregate sources (II and VII) than the other Intermediate Type B mixtures (IV and V), it is difficult to conclude whether the differences in flow numbers are due to the effect of aggregate source or mixture type. Intermediate Type B Special mixtures contain a WMA chemical additive and have lower target air void values and higher target asphalt binder content values than Intermediate Type B mixtures.

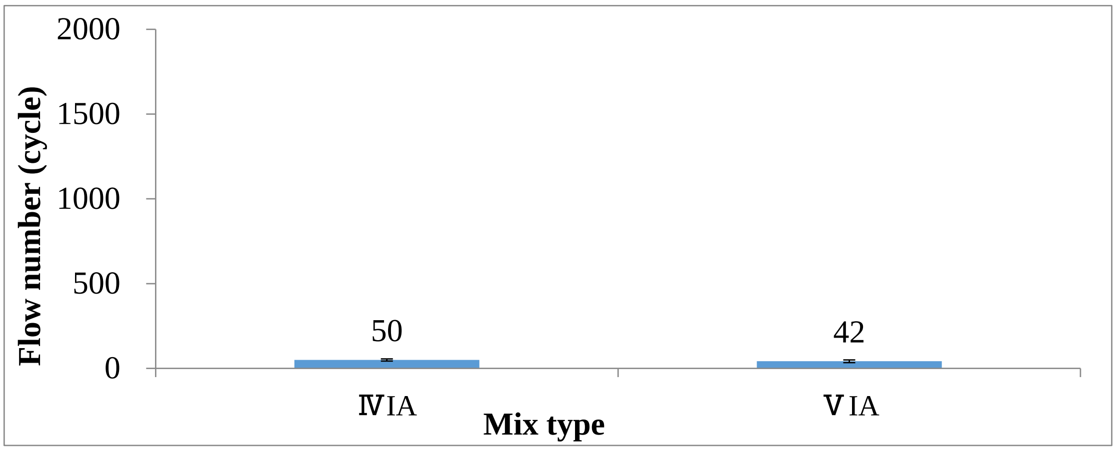

Figure 6-76 Flow Numbers of Various Intermediate Type A Mixtures with RAP in Terms of Aggregate Source at 59°C (138.2°F)

6.2.3 Effect of Aggregate Source on Flow Number of Different Types of Base Mixtures

Figure 6-77 shows the flow numbers of various Base Type A mixtures containing RAP in terms of various aggregate sources tested at 59℃ (138.2°F). As shown in Figure 6-77, mixtures IV SA and V SA had similar flow numbers. Therefore, it could be concluded that for the materials used in this study, the aggregate source generally did not have an influence on the flow numbers of Base Course mixtures.

The flow numbers of other Base Type B mixtures generally had similar trends compared to Base Type A. The results are shown in other figures and are presented in Appendix C.

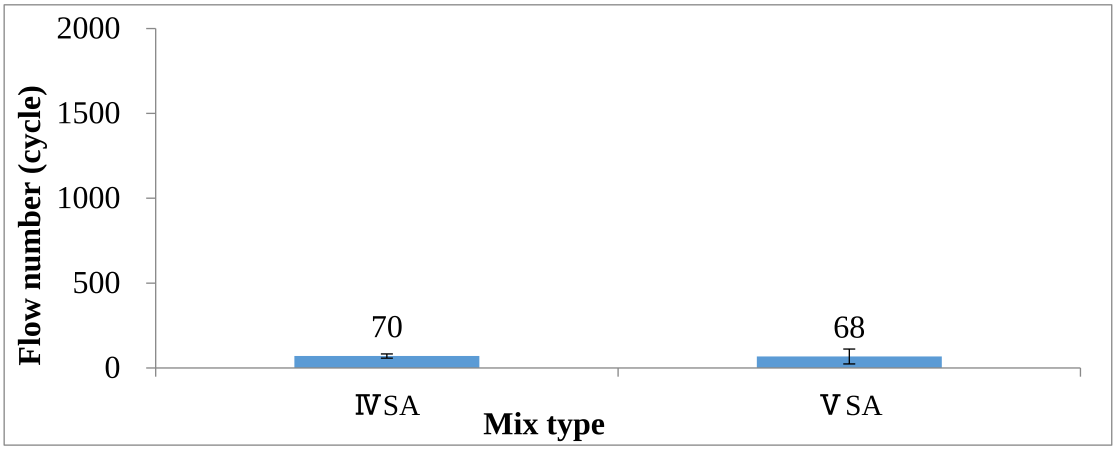

Figure 6-77 Flow Numbers of Various Base Type A Mixtures with RAP in Terms of Aggregate Source at 59°C (138.2°F)

6.2.4 Effect of Aggregate Source on Flow Number of Surface Mixtures (Types A and B) Made with Different Aggregate Types and Binder Source 2

Figure 6-78 shows the flow numbers of various Surface Type A mixtures using PG 76-22 from asphalt source 2 (Axeon) and RAP in terms of two aggregate sources (IV and V) tested at 59°C (138.2°F). As shown in Figure 6-78, mixture IV AN had a higher flow number than mix V AN. Therefore, with the limited data used for this research project, the aggregate source generally did have an influence on the flow numbers.

The flow numbers of the Surface Type B mixtures containing PG 64-22 from asphalt binder source 2 generally had similar trends. The results from those mixtures are shown in figures presented in Appendix C.

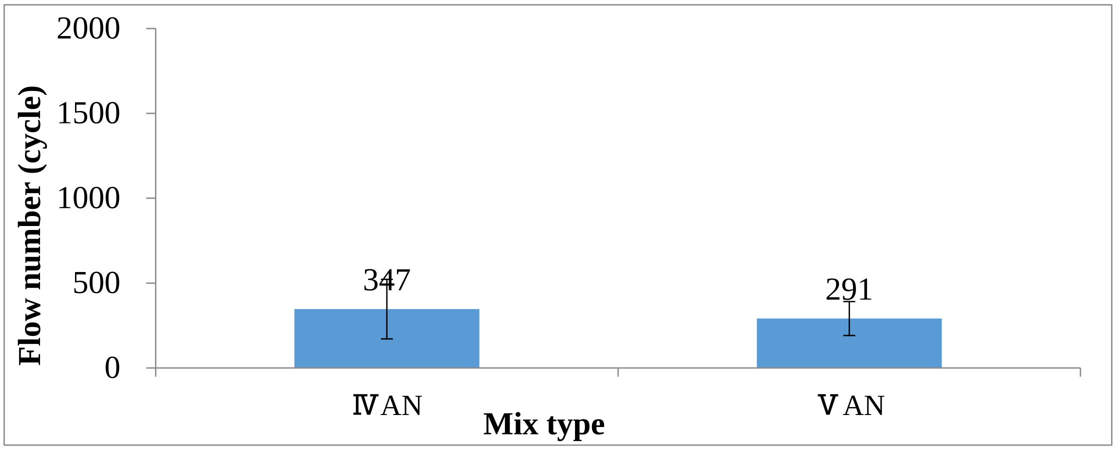

Figure 6-78 Flow Numbers of Various Surface Type A Mixtures with RAP and PG 76-22 Asphalt Source 2 in Terms of Aggregate Source at 59°C (138.2°F)

6.2.5 Effect of Aggregate Source on Flow Number of Surface Type C Mixtures Made with WMA

Figure 6-79 shows the flow numbers of various Surface Type C mixtures made with WMA type 1 (chemical additive) and RAP in terms of two aggregate sources (IV and V) tested at 59°C (138.2°F). As shown in Figure 6-79, mixtures IV CE and V CF both had very low flow numbers. Therefore, the WMA mixtures used in this study generally did not meet the requirements from AASHTO TP 79, similar to the mixtures using the foaming technology selected for this study. These results are shown in other figures presented in Appendix C.

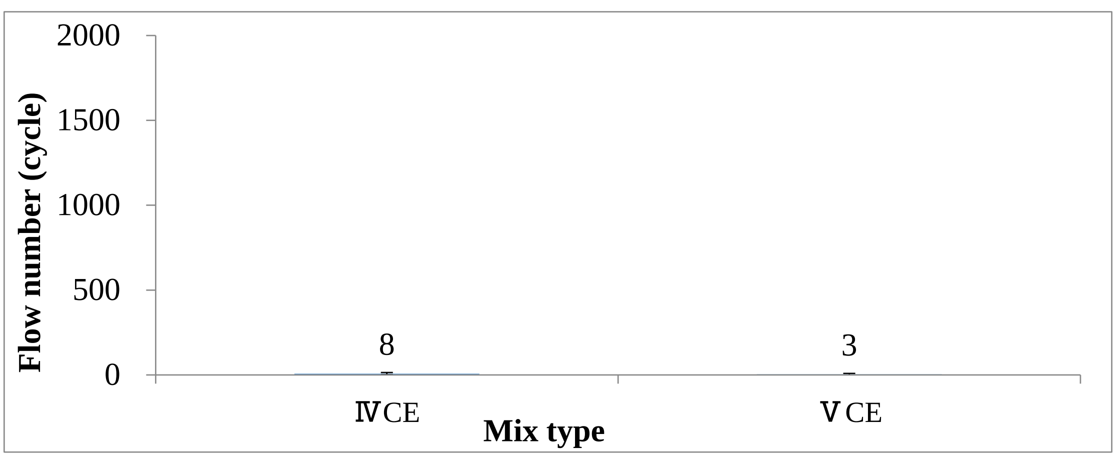

Figure 6-79 Flow Numbers of Various Surface Type C Mixtures with RAP and WMA-Chemical Additive in Terms of Aggregate Source at 59°C (138.2°F)

6.2.6 Effect of Aggregate Source on Flow Number of Surface Type C Mixtures Made with Liquid ASA

Figure 6-80 shows the flow numbers of various Surface Type C mixtures containing liquid ASA 1 (Adhere®) and RAP and made with various aggregate sources tested at 59°C (138.2°F). As shown in Figure 6-80, mix V CA had a much higher flow number than mixture IV CA. Therefore, according to the limited data in this study, the aggregate source generally did have an influence on flow number.

The flow numbers of other mixtures containing liquid ASA 2 (Morlife®) generally had similar trends compared to liquid ASA 1. These results are shown in other figures presented in Appendix C.

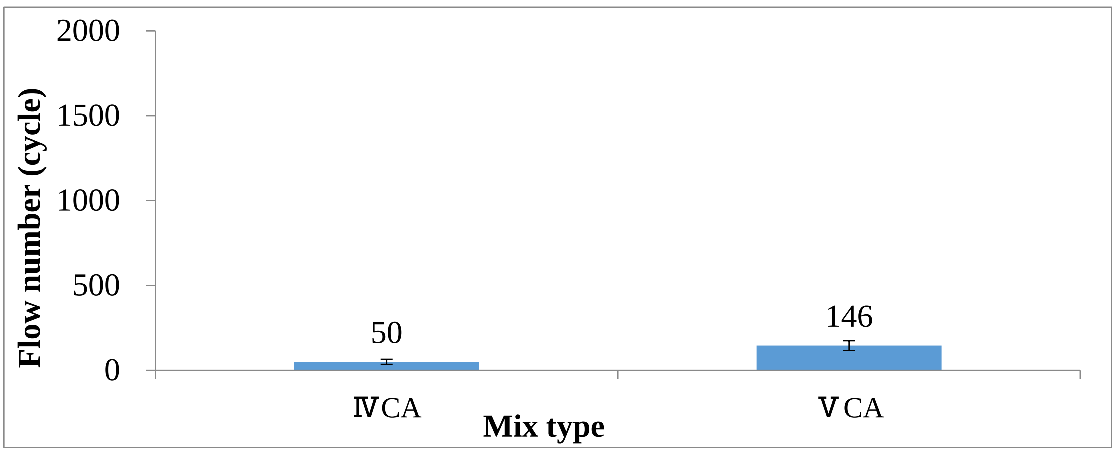

Figure 6-80 Flow Numbers of Various Surface Type C Mixtures with RAP and Liquid ASA 1 in Terms of Aggregate Source at 59°C (138.2°F)

6.2.7 Effect of Aggregate Source on Flow Number of Aged Surface Mixtures (Types A, B and C)

Figure 6-81 shows the flow numbers of various Surface Type A mixtures after long-term aging in terms of two aggregate sources (IV and V) tested at 59°C (138.2°F). As shown in Figure 6-81, mixture V AG had a much higher flow number than mixture IV AG. Therefore, based on this limited data, it can be concluded that the aggregate source generally did have an influence on flow number.

The flow numbers of the Surface Type B and C mixtures after long-term aging generally exhibited similar trends. These results are shown in the figures presented in Appendix C.

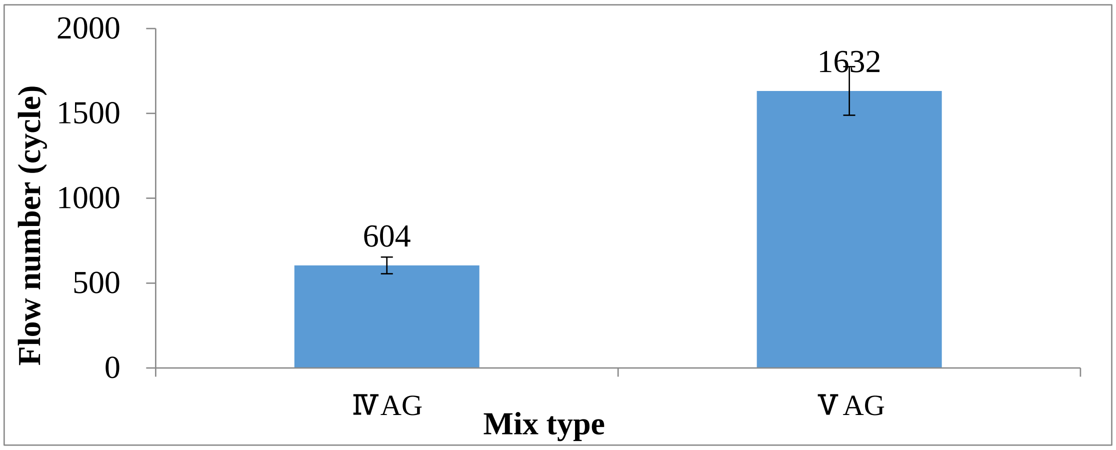

Figure 6-81 Flow Numbers of Various Surface Type A Mixtures with RAP after Long-Term Aging in Terms of Aggregate Source at at 59°C (138.2°F)

6.2.8 Effect of Mixture Type on Flow Number of Surface Mixtures Made with Different Aggregate Types

Figure 6-82 shows the flow numbers of various mixtures containing aggregate source I and RAP in terms of Surface Course mixture type (Surface Types A, B, C, D, and E) tested at 59°C (138.2°F). In addition, there were two different Surface Type B mix designs utilized for aggregate source I. The second mix design for that aggregate source (I B2) incorporated the newly-adopted corrected optimum asphalt content (COAC) allowed by SCDOT. This new mix design was added toward the end of the project. As shown in Figure 6-82, mixtures I A and I B had much higher flow numbers than other mixtures, while I B2 and I D had lower flow numbers than other mixtures. Therefore, considering the materials used for this portion of the research project, one can conclude that the Surface Course mixture type generally did affect the flow number of various mixtures. As expected, the designated layers for heavy traffic generally had higher flow numbers.

In addition, similar trends for flow numbers were found with respect to various aggregate sources. The results are shown in figures presented in Appendix C.

The new Surface Type B mix design containing the COAC appeared to significantly affect the flow number values. The flow number values for the new mix design with aggregate source II were much lower than the values for the old mix design with the same aggregate source. However, because only one aggregate source for Surface Type B using the new COAC was tested, it is difficult to draw firm conclusions. The scope of this project did not allow further investigation of this effect.

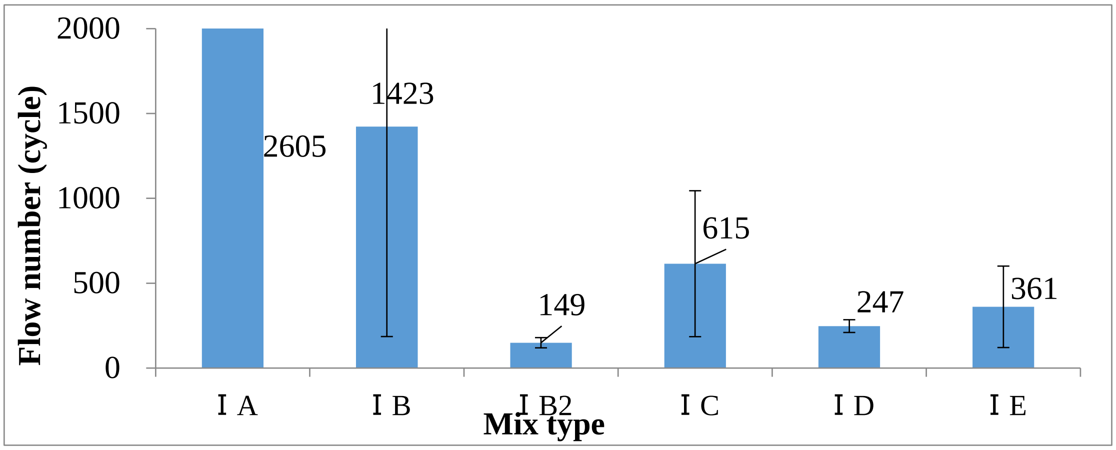

Figure 6-82 Flow Numbers of Various Mixtures for Aggregate Source I with RAP in Terms of Surface Mixture Type at 59°C (138.2°F)

6.2.9 Effect of Mixture Type on Flow Number of Intermediate Mixtures Made with Different Aggregate Sources

Figure 6-83 shows the flow numbers of various mixtures containing aggregate source IV and RAP in terms of Intermediate Course mixture type (Intermediate Types A, B, and C) tested at 59°C (138.2°F). As shown in Figure 6-83, these mixtures had low flow numbers. In addition, mixture IV IB had the highest flow numbers, while mixture IV IC had the lowest flow numbers. However, the figures in Appendix C show that for the other mixtures tested, the Intermediate Type A mixtures generally exhibited the highest flow number values and the Intermediate Type C mixtures exhibited the lowest flow number values. It should also be noted that all Intermediate Type A and B mixtures tested in this project exhibited flow number values below AASHTO minimum recommendation of 190 for higher volume pavements. Although the utilization of RAP resulted in somewhat higher flow number values, they still did not reach the minimum recommended value. The scope of this study did not allow for further investigation into the cause of this result.

In addition to the Intermediate Type A, B, and C mixtures made with aggregate sources IV and V, several Intermediate Type B Special mixtures were made with two additional aggregate sources, II and VII. These mixtures were added towards the end of the project, and aggregate sources were selected by the Steering Committee based on materials used in field pilot projects. The flow number values shown in Appendix C indicate that the Intermediate Type B Special samples containing aggregate source VII generally had only slightly higher values than those containing aggregate source II. Additionally, both Intermediate Type B Special mixtures exhibited higher flow number values than all of the other Intermediate Type A, B, and C mixtures. However, because the Intermediate Type

B Special mixtures contained different aggregate sources (II and VII) than all of the other Intermediate Type A, B, and C mixtures (IV and V), it is difficult to know whether the differences in flow numbers are due to the effect of aggregate source or mixture type. Intermediate Type B Special mixtures contain a WMA chemical additive and have lower target air void values and higher target asphalt binder content values than Intermediate Type B mixtures. The scope of this study did not allow for further investigation of the causes of these differences in flow number values.

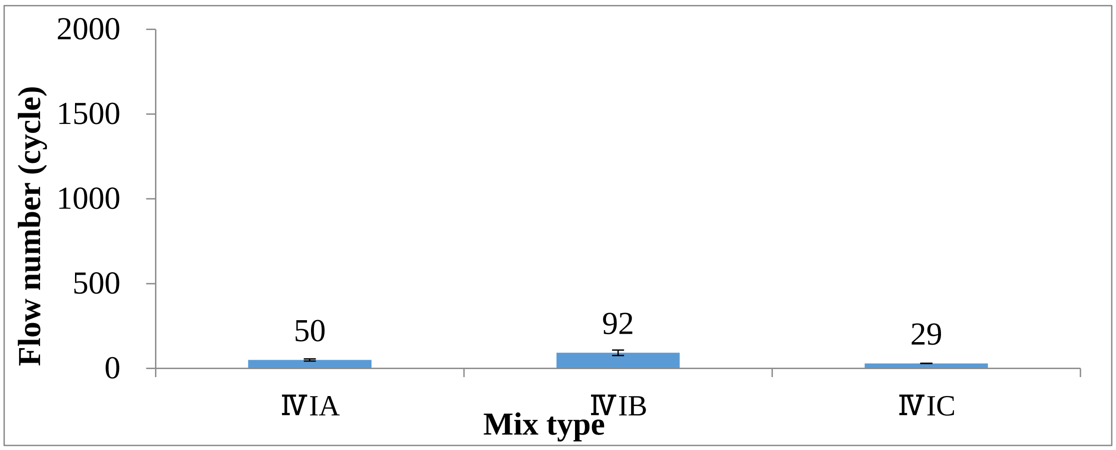

Figure 6-83 Flow Numbers of Various Mixtures for Aggregate Source IV with RAP in Terms of Intermediate Mixture Type at 59°C (138.2°F)

6.2.10 Effect of Mixture Type on Flow Number of Base Mixtures (Types A and B) Made with Different Aggregate Sources

Figure 6-84 shows the flow numbers of various mixtures made with aggregate source IV and RAP in terms of Base Course mixture type (Base Types A and B) tested at 59°C (138.2°F). As shown in Figure 6-84, these mixtures had low flow numbers. In addition, mix IV SA had a higher flow number than mixture IV SB. In general, the mixtures made with aggregate source V had similar trends, as shown in the figures in Appendix C.

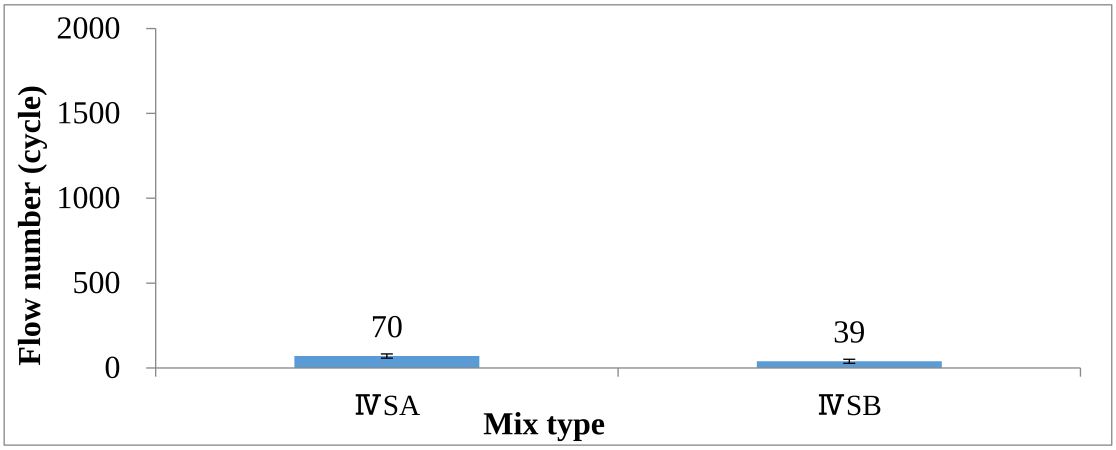

Figure 6-84 Flow Numbers of Various Mixtures for Aggregate Source IV with RAP in Terms of Base Mixture Type at 59°C (138.2°F)

6.2.11 Effect of Mixture Type on Flow Number of Surface Mixtures (Types A and B) Made with Different Aggregate Types and Binder Source 2

Figure 6-85 shows the flow numbers of various mixtures made with aggregate source IV using PG 76-22 from asphalt source 2 (Axeon) and RAP in terms of Surface Course mixture type (Surface Types A and B) tested at 59℃ (138.2°F). As shown in Figure 6-85, mixture IV AN had a much higher flow number than mixture IV BN. In general, the other mixtures tested exhibited similar trends, as shown in the figures in Appendix C. The only exception was aggregate source V with asphalt source 1. In that case the flow number values for Surface Type B (PG 64-22) were slightly higher than Surface Type A (PG 76-22). This seems to validate the utilization of a higher binder grade (PG 76-22 vs. PG 64-22) on higher volume routes.

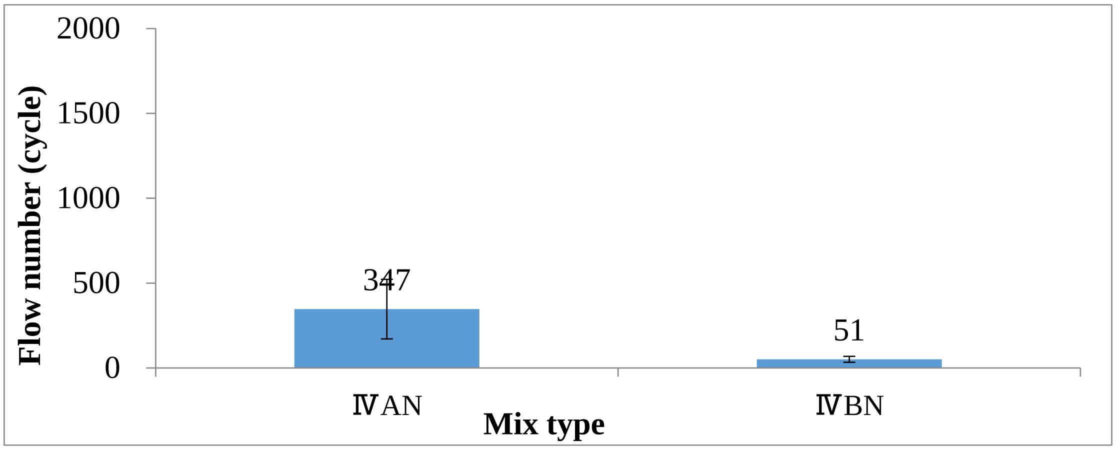

Figure 6-85 Flow Numbers Various Mixtures for Aggregate Source IV with RAP using Asphalt Source 2 in Terms of Surface Mixture Type at 59°C (138.2°F)

6.2.12 Effect of Binder Source on Flow Number of Various Surface Mixtures Made with Different Aggregate Types

Figure 6-86 shows that there were differences in flow number values for Surface Type A and B mixtures containing RAP in terms of binder source. The flow number values of all mixtures using binder source 1 were higher than the corresponding mixtures using binder source 2. In addition, when aggregate source V was utilized, the flow number differences between binder source 1 and 2 were very large. For the binders and materials tested in this research project, it can be concluded that the binder source has a major impact on the flow number. However, binder grade had an even larger impact than binder source. As shown in the figures in Appendix C, the mixtures in this study containing PG 76-22 generally exhibited higher flow number values than the mixtures containing PG 64-22 binders. The only exception was aggregate source V with asphalt source 1. In that case, the flow number values for Surface Type B (PG 64-22) were slightly higher than Surface Type A (PG 76-22). This seems to validate the utilization of a higher binder grade (PG 76-22 vs. PG 64-22) on higher volume routes.

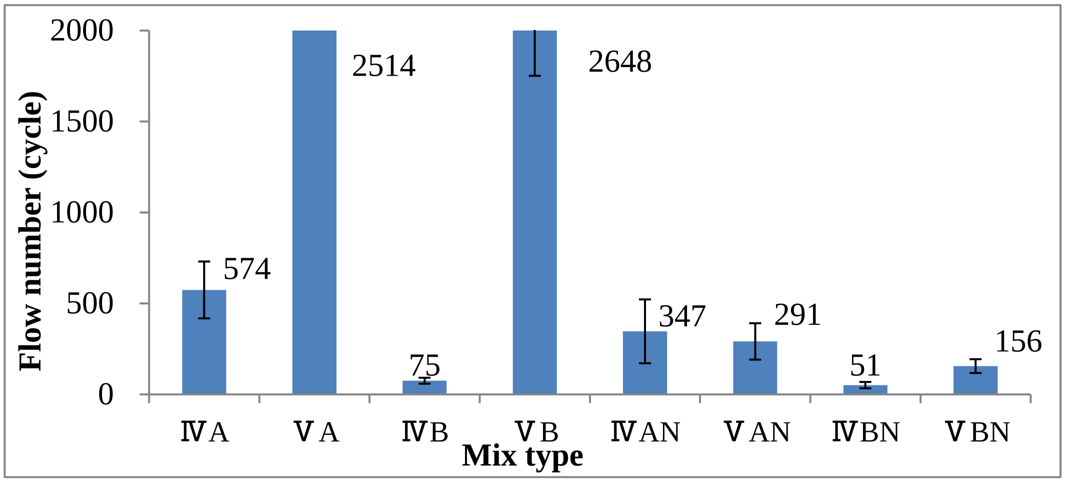

Figure 6-86 Flow Numbers of Various Surface Mixtures for Aggregate Source IV with RAP in Terms of Binder Source at 59°C (138.2°F)

6.2.13 Effect of WMA on Flow Number of Surface Type C Mixtures Made with Different Aggregate Types

Figure 6-87 shows the flow numbers of various Surface Type C mixtures made with aggregate source IV and RAP in terms of WMA technology type tested at 59℃ (138.2°F). As shown in Figure 6-87, these mixtures had similar flow number values that were low and did not meet the recommendations from AASHTO TP 79. In general, the mixtures from aggregate source V had similar trends, as shown in the figures in Appendix C.

In addition, Figure 6-88 indicates that the flow numbers of various Surface Type C mixtures utilizing either WMA technology type (chemical additive or foaming) were generally lower than corresponding mixtures without WMA, although these differences were more pronounced with aggregate source IV than with aggregate source V. It should also be noted that even without WMA, the Surface Type C mixtures from aggregate V produced low flow number values that did not meet recommendations from AASHTO TP 79.

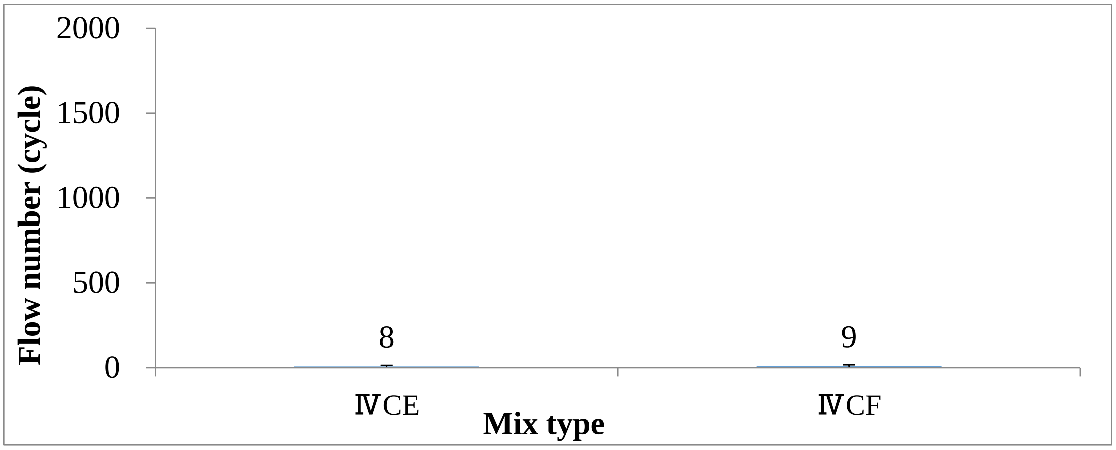

Figure 6-87 Flow Numbers of Various Surface Type C Mixtures for Aggregate Source IV with RAP in Terms of WMA Technology Type at 59°C (138.2°F)

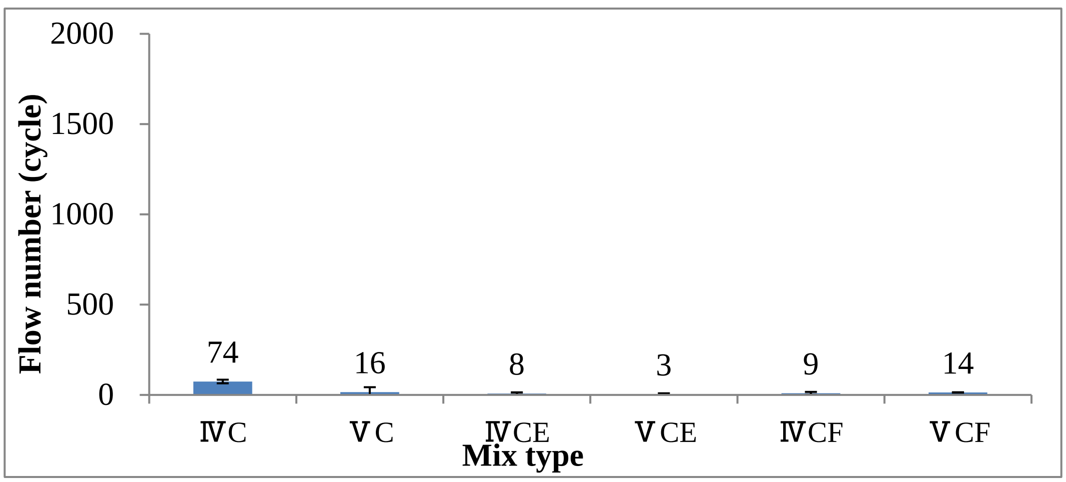

Figure 6-88 Flow Numbers of Various Surface Type C Mixtures for Various Aggregate Sources with RAP in Terms of with/without WMA Technology Type at 59°C (138.2°F)

6.2.14 Effect of Liquid ASAs on Flow Number of Surface Type C Mixtures Made with Different Aggregate Types

Figure 6-89 shows the flow numbers of various Surface Type C mixtures made with aggregate source IV and RAP in terms of liquid ASA type tested at 59℃ (138.2°F). As shown in Figure 6-89, these mixtures had similar flow numbers. Aggregate source V showed a slightly larger difference in flow number values, as shown in the figures in Appendix C.

Figure 6-90 shows the flow numbers of various Surface Type C mixtures made with two aggregate sources (IV and V) and containing RAP in terms of with and without liquid ASA tested at 59℃ (138.2°F). It is important to note that these flow number results varied based on the aggregate type. For aggregate source IV, the flow numbers for mixtures containing either type of liquid ASA were only slightly lower than without liquid ASA. However, the flow numbers for aggregate source V mixtures containing either type of liquid ASA were significantly higher than those without liquid ASA.

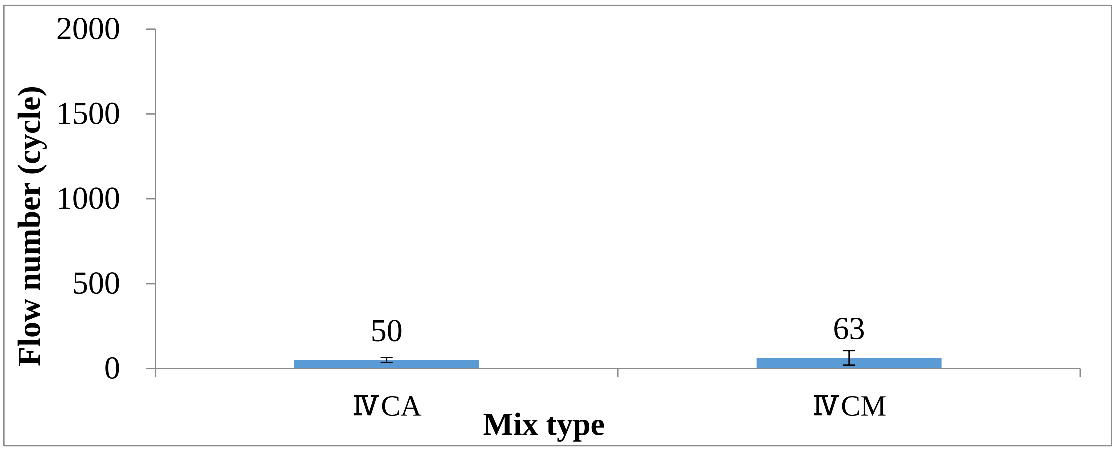

Figure 6-89 Flow Numbers of Various Surface Type C Mixtures for Aggregate Source IV with RAP in Terms of Liquid ASA Type at 59°C (138.2°F)

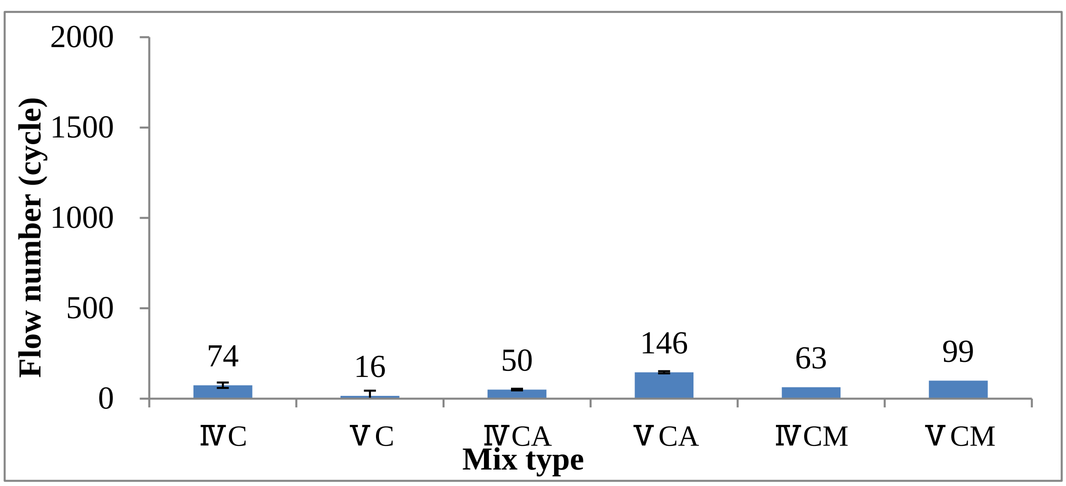

Figure 6-90 Flow Numbers of Various Surface Type C Mixtures for Aggregate Source IV with RAP in Terms of with/without Liquid ASA at 59°C (138.2°F)

6.2.15 Effect of Aging on Flow Number of Surface Mixtures (Types A, B and C) Made with Different Aggregate Types

Figure 6-91 shows the flow numbers of various mixtures made with aggregate source IV and RAP after long-term aging in terms of Surface Course mixture type (Surface Types A, B, and C) tested at 59°C (138.2°F). As shown in Figure 6-91, mix IV AG exhibited much higher flow number values than the other two mixture types. In general, the mixtures made with aggregate source V had similar trends, as shown in the figures in Appendix C.

Figure 6-92 shows the flow numbers of various mixtures, both with and without long-term aging, made with two aggregate sources (IV and V) and RAP in terms of Surface Course mixture type (Surface Types A, B, and C) tested at 59°C (138.2°F). The flow number values varied based on both aggregate type and mixture type. For aggregate source IV, flow number values of all three types of Surface mixtures were either similar or slightly higher after aging. However, for aggregate source V, Surface Type A and B mixtures exhibited significantly lower flow number values after aging, while Surface Type C mixtures exhibited the opposite.

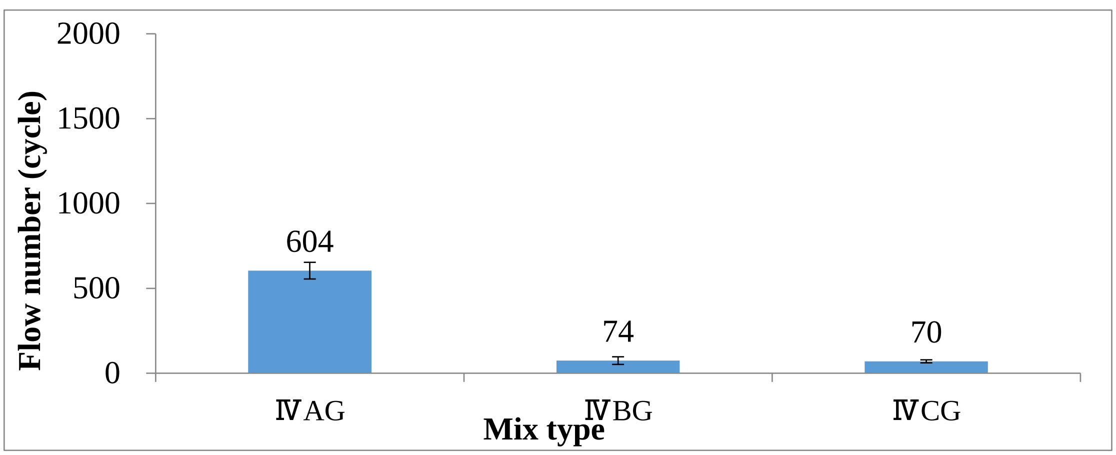

Figure 6-91 Flow Numbers of Various Mixtures for Aggregate Source IV with RAP after Long-Term Aging in Terms of Surface Mixture Type at 59°C (138.2°F)

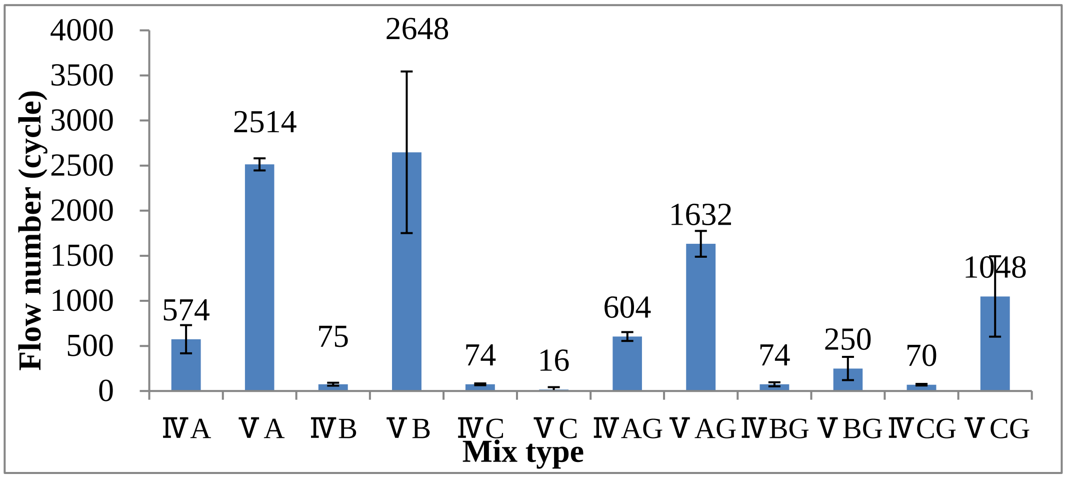

Figure 6-92 Flow Numbers of Various Mixtures for Aggregate Source IV and V with RAP after Long-Term Aging or Not in Terms of Surface Mixture Type at 59°C (138.2°F)

6.2.16 Effects of RAP on Flow Number of Various Mixtures Made with Different Aggregate Types

6.2.16.1 Effects of RAP on Flow Number of Various Surface Mixtures Made with Different Aggregate Types

For the various types of Surface mixtures tested in this study, the effect of RAP varied with Surface mixture type. Figure 6-93 indicates that the flow number values of Surface Type A mixtures made with RAP from three aggregate sources were much higher than the flow number values of the mixtures containing no RAP and made from the same aggregate sources. Figure 6-94 indicates that the flow number values of Surface Type B mixtures made with RAP from three aggregate sources were similar to the flow number values of the mixtures containing no RAP made from the same aggregate sources. Figure 6-95, Figure 6-96, and Figure 6-97 indicate that Surface Type C, D, and E mixtures made with RAP from various aggregate sources generally exhibited higher flow number values than the corresponding mixtures containing no RAP. It should be noted that this was true even when the mixtures had relatively low flow number values. The only exception was Surface Type C made with aggregate source V, which exhibited higher flow number values without RAP when compared to mixtures with RAP.

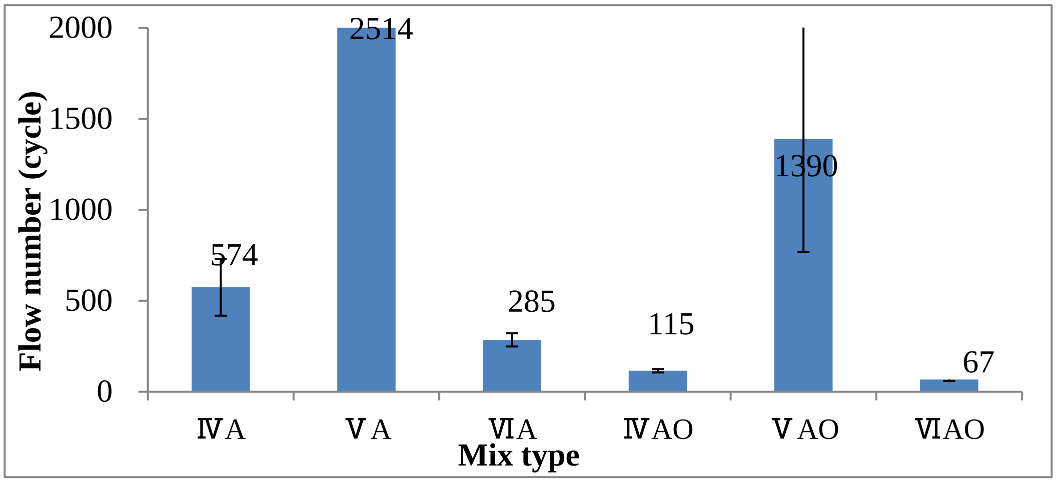

Figure 6-93 Flow Numbers of Various Surface Type A Mixtures with/without RAP at 59°C (138.2°F)

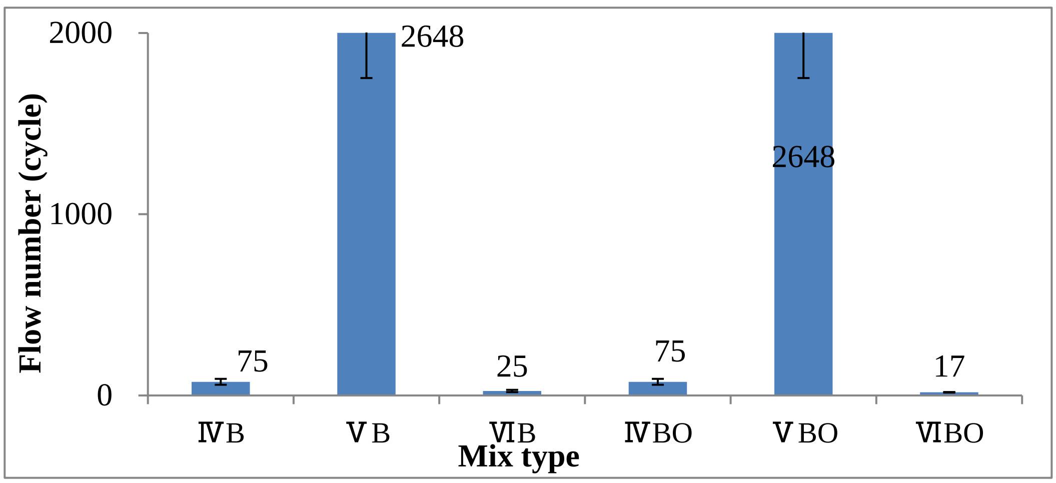

Figure 6-94 Flow Numbers of Various Surface Type B Mixtures with/without RAP at 59°C (138.2°F)

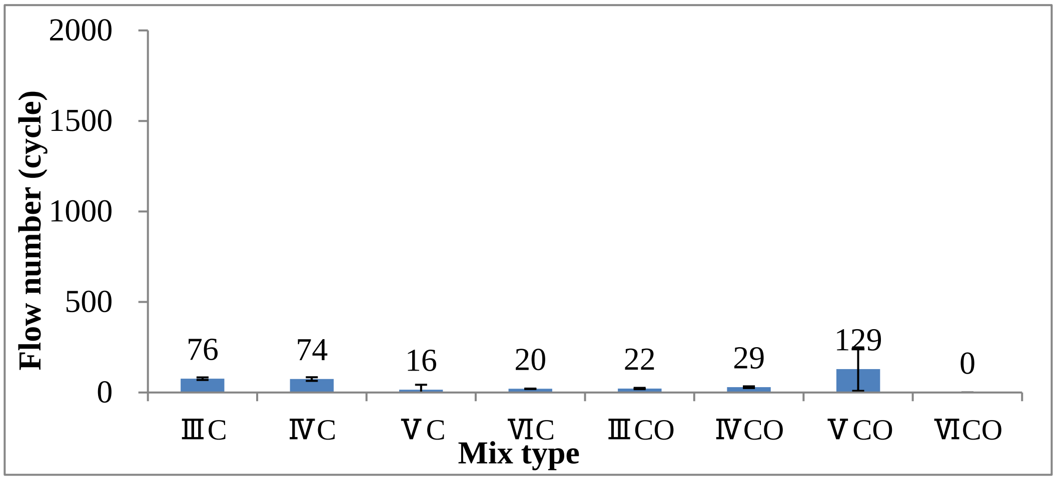

Figure 6-95 Flow Numbers of Various Surface Type C Mixtures with/without RAP at 59°C (138.2°F)

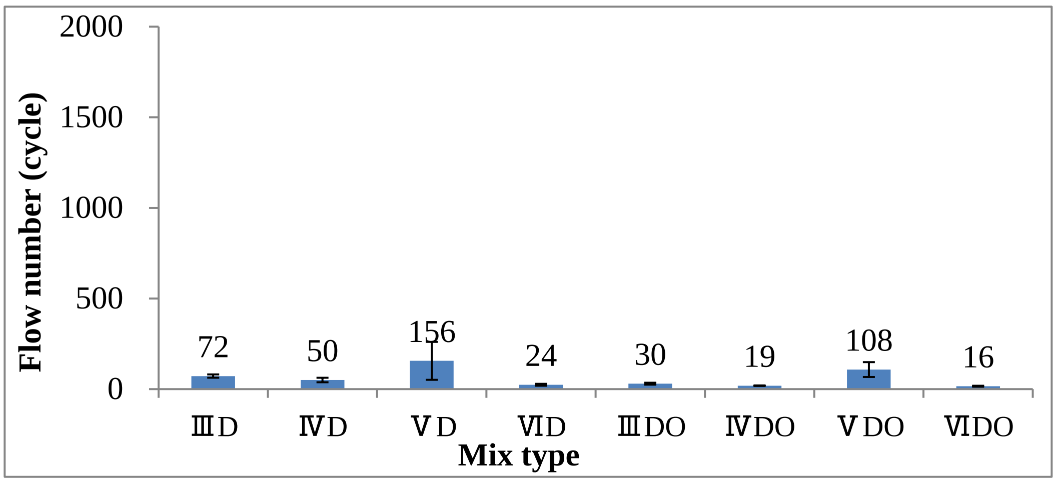

Figure 6-96 Flow Numbers of Various Surface Type D Mixtures with/without RAP at 59°C (138.2°F)

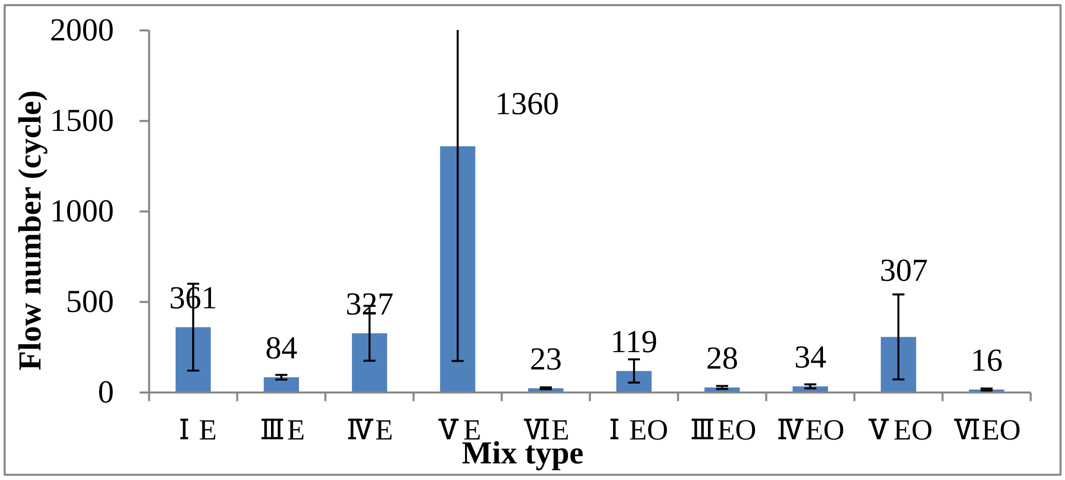

Figure 6-97 Flow Numbers of Various Surface Type E Mixtures with/without RAP at 59°C (138.2°F)

6.2.16.2 Effects of RAP on Flow Number of Various Intermediate Mixtures Made with Different Aggregate Types

Figure 6-98 indicates that flow number values of Intermediate Type A mixtures made with RAP from two aggregate sources were generally higher than the flow number values of the mixtures containing no RAP from the same aggregate sources. This was true even though all of these mixtures had relatively low flow number values. Figure 6-99 and Figure 6-100 indicate similar results for Intermediate Type B and C mixtures made with and without RAP. It should be noted that all Intermediate Type A and B mixtures tested in this project exhibited flow number values below AASHTO minimum recommendation of 190 for higher volume pavements. Although the utilization of RAP resulted in somewhat higher flow number values, they still did not reach the minimum recommended value. The scope of this study did not allow for further investigation into the cause of this result.

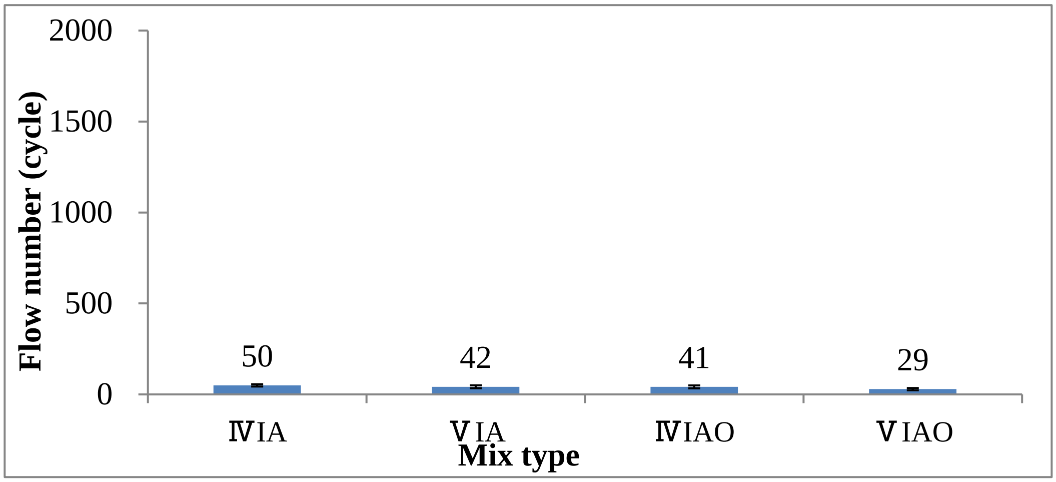

Figure 6-98 Flow Numbers of Various Intermediate Type A mixtures with/without RAP at 59°C (138.2°F)

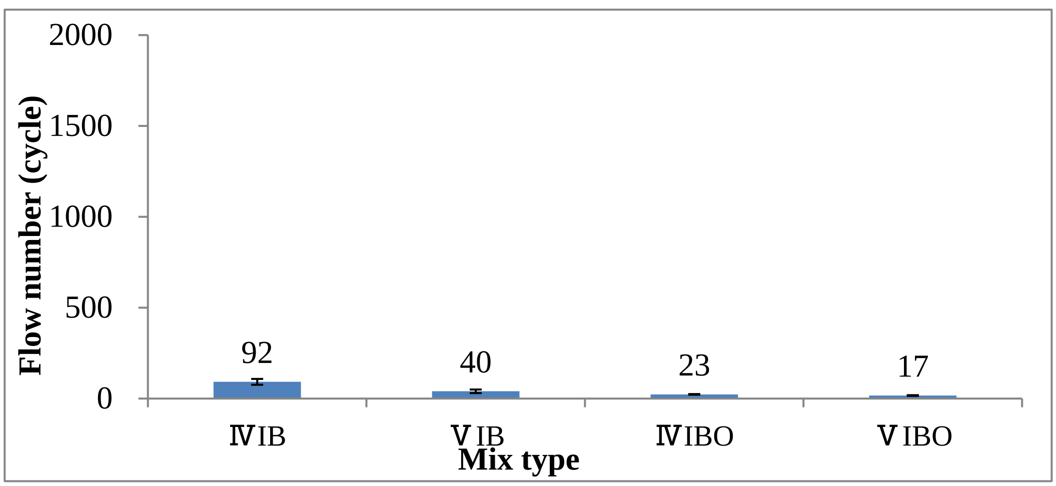

Figure 6-99 Flow Numbers of Various Intermediate Type B mixtures with/without RAP at 59°C (138.2°F)

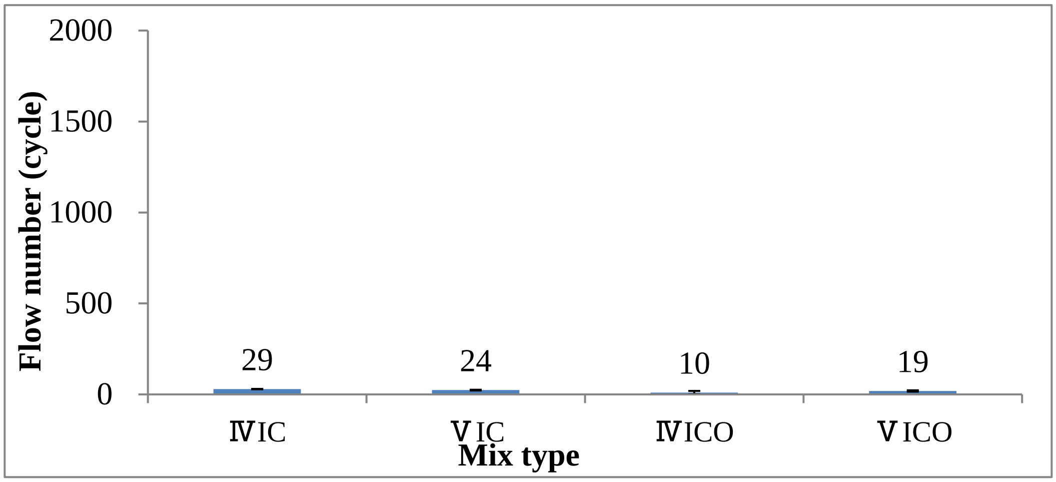

Figure 6-100 Flow Numbers of Various Intermediate Type C mixtures with/without RAP at 59°C (138.2°F)

6.2.16.3 Effects of RAP on Flow Number of Various Base Mixtures Made with Different Aggregate Types

Figure 6-101 shows the flow number values of Base Type A mixtures made with and without RAP and two aggregate sources. The results indicate that the flow number values of mixes containing RAP were generally higher than the flow number values of the mixtures without RAP even though these mixtures had relatively low flow number values. Figure 6-102 shows similar results for Base Type B mixtures.

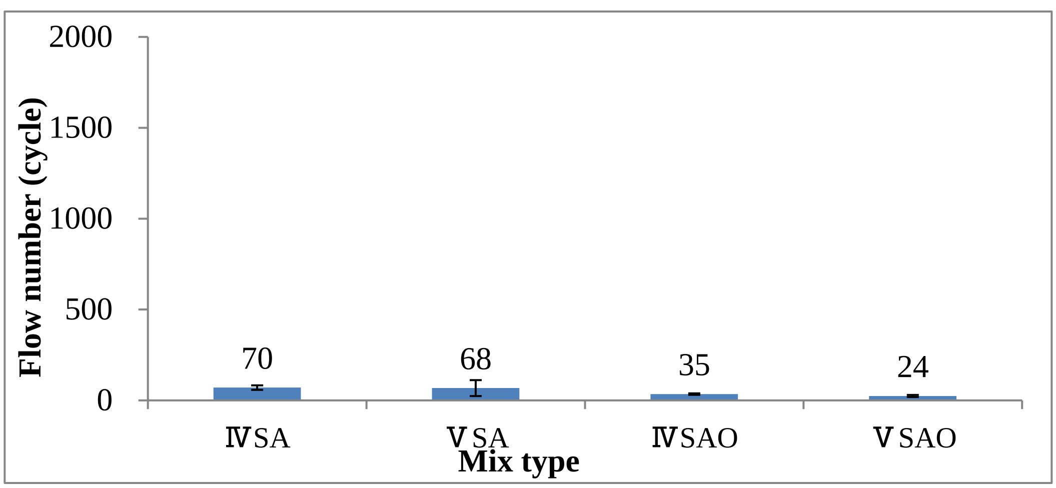

Figure 6-101 Flow Numbers of Various Base Type A mixtures with/without RAP at 59°C (138.2°F)

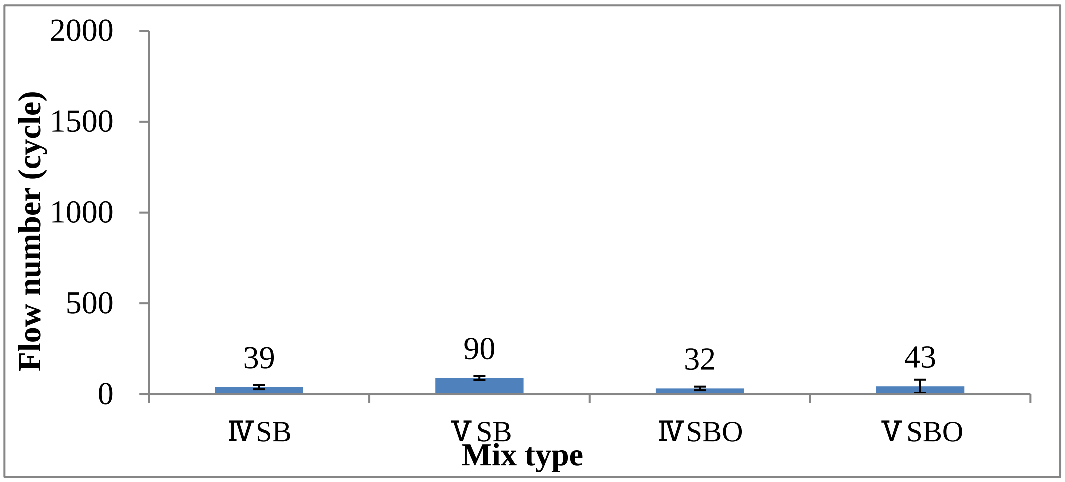

Figure 6-102 Flow Numbers of Various Base Type B mixtures with/without RAP at 59°C (138.2°F)

6.2.16.4 Effects of RAP on Flow Number of Surface Mixtures (Types A and B) Made with Binder Source 2 and Different Aggregate Types

Figure 6-103 and Figure 6-104 indicate that the flow number values of Surface Type A and B mixtures with and without RAP made with binder source 2 were generally affected by the aggregate sources used in this study. In both the Surface Type A and Type B mixtures, the flow number values were higher without RAP for aggregate IV, but they were lower without RAP for aggregate V. These differences were more obvious in the Surface Type A mixtures made with aggregate IV.

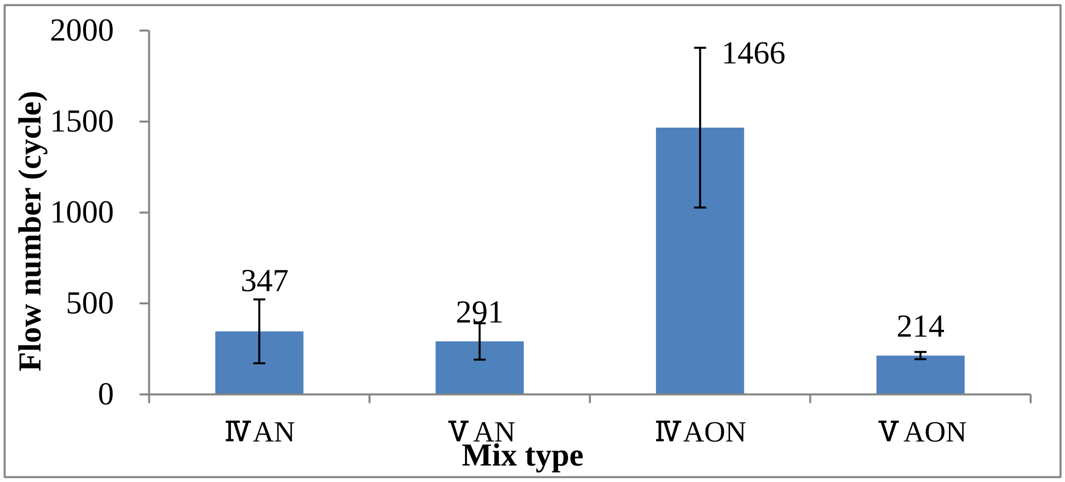

Figure 6-103 Flow Numbers of Various Surface Type A Mixtures from Binder Source 2 with/without RAP at 59°C (138.2°F)

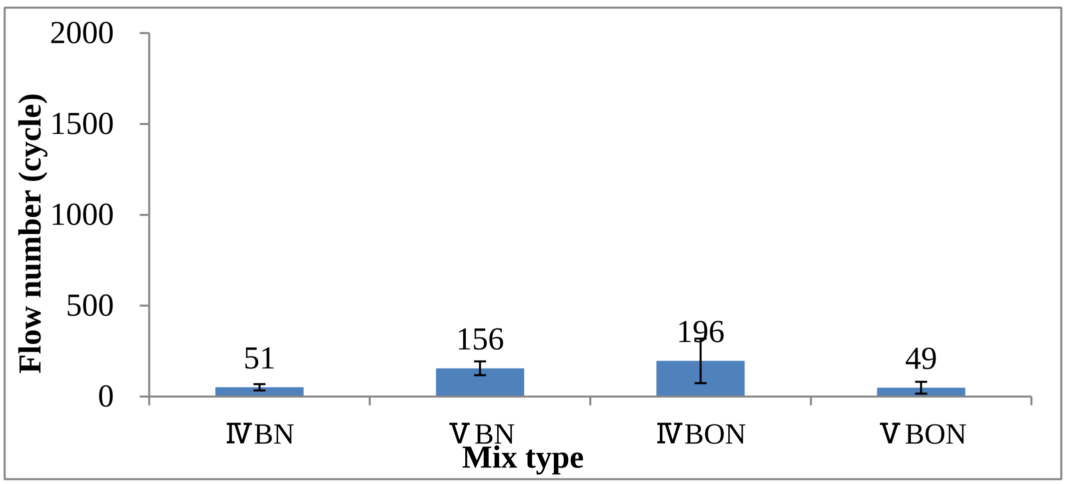

Figure 6-104 Flow Numbers of Various Surface Type B Mixtures from Binder Source 2 with/without RAP at 59°C (138.2°F)

6.2.16.5 Effects of RAP on Flow Number of Surface Type C Mixtures Made with WMA and Different Aggregate Types

Figure 6-105 and Figure 6-106 show the flow number values of Surface Type C mixtures from two aggregate sources utilizing WMA technologies, both with and without RAP The flow number values were all low, and the presence of RAP did not affect the results.

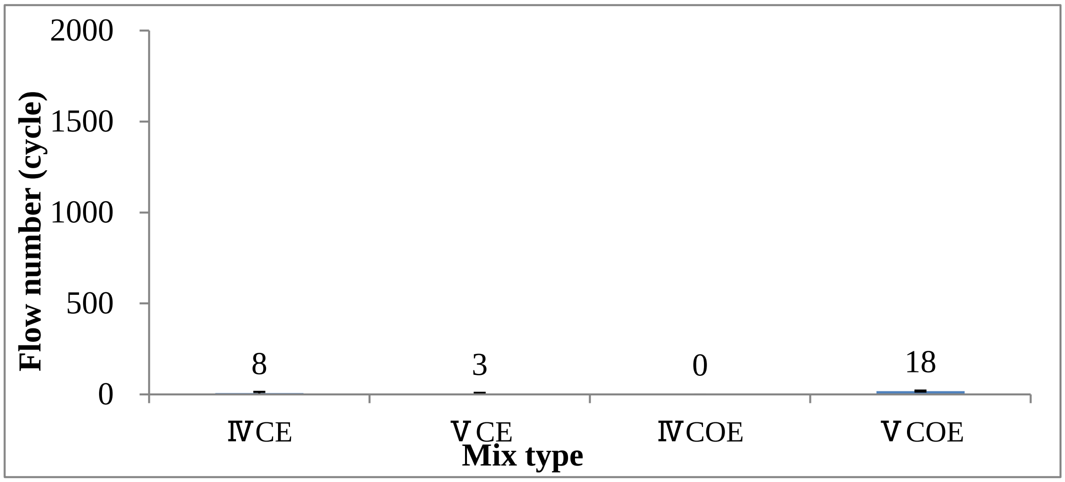

Figure 6-105 Flow Numbers of Various Surface Type C Mixtures from Chemical Additive WMA Technology with/without RAP at 59°C (138.2°F)

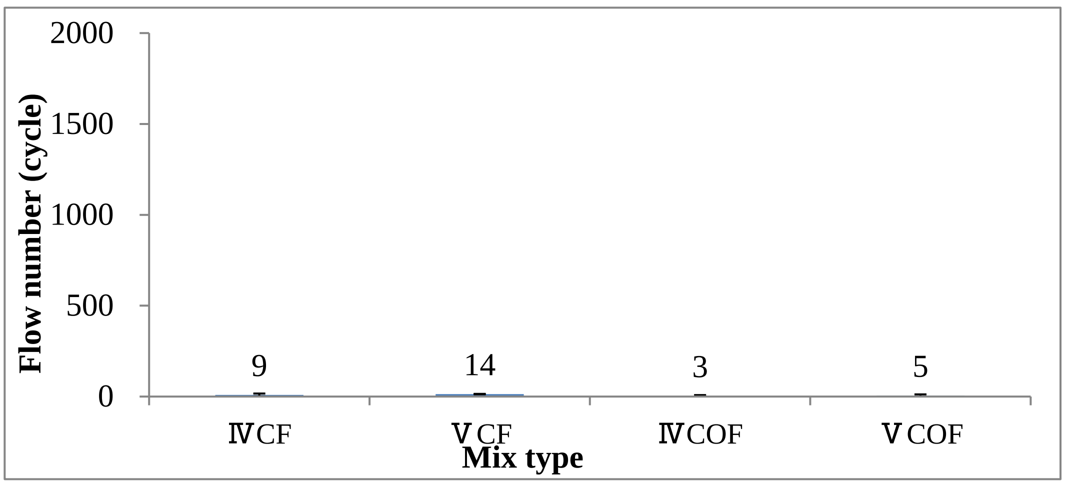

Figure 6-106 Flow Numbers of Various Surface Type C Mixtures from Foaming WMA Technology with/without RAP at 59°C (138.2°F)

6.2.16.6 Effects of RAP on Flow Number of Surface Type C Mixtures Made with Liquid ASA and Different Aggregate Types

Figure 6-107 indicates that the flow number values of Surface Type C mixtures from two aggregate sources containing liquid ASA 1 and RAP were generally higher than the flow number values of the corresponding mixtures without RAP. This was true even though these mixtures exhibited relatively low flow number values. Figure 6-108 shows similar results for liquid ASA 2.

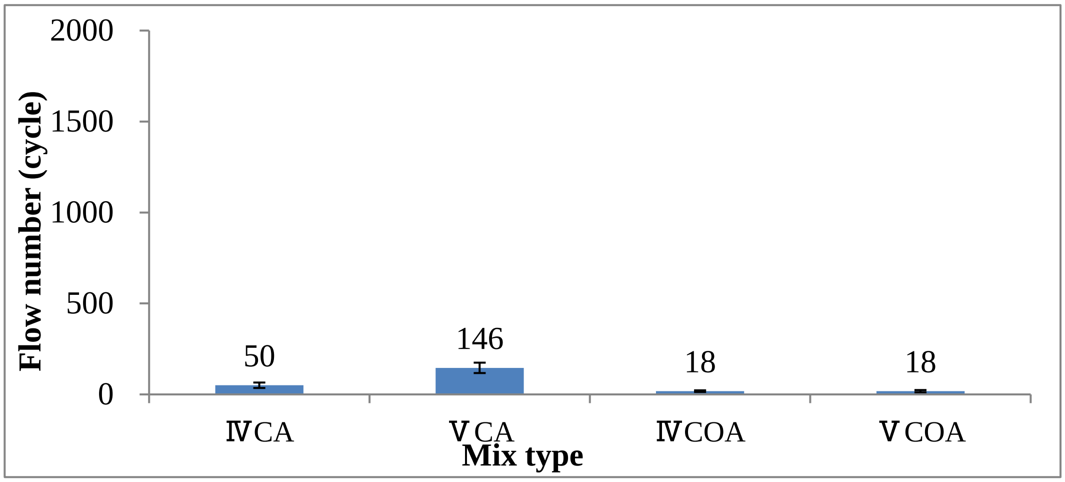

Figure 6-107 Flow Numbers of Various Surface Type C Mixtures with Liquid ASA 1 with/without RAP at 59°C (138.2°F)

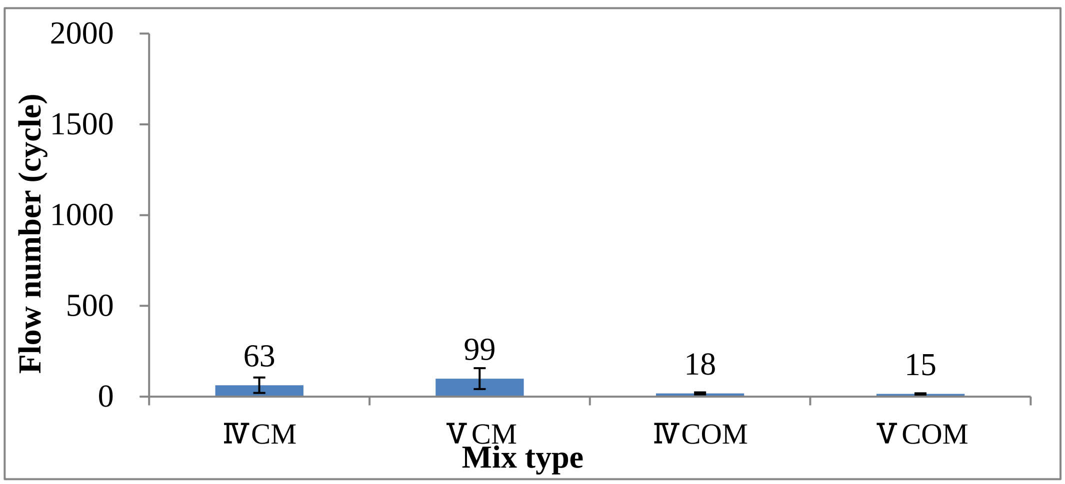

Figure 6-108 Flow Numbers of Various Surface Type C Mixtures with Liquid ASA 2 with/without RAP at 59°C (138.2°F)

6.2.16.7 Effects of RAP on Flow Number of Aged Surface Mixtures (Types A, B, and C) Made with Different Aggregate Types

Figure 6-109, Figure 6-110, and Figure 6-111 shows the flow number values of Surface Type A, Surface Type B, and Surface Type C mixtures made with two aggregate sources, containing RAP, and subjected to a long-term aging procedure. The results indicate that the flow number values of the mixtures containing RAP were generally higher than the flow number values of the corresponding mixtures made without RAP. The only exception was Surface Type B made with aggregate source IV, which exhibited similar flow number values for the aged mixtures, both with and without RAP.

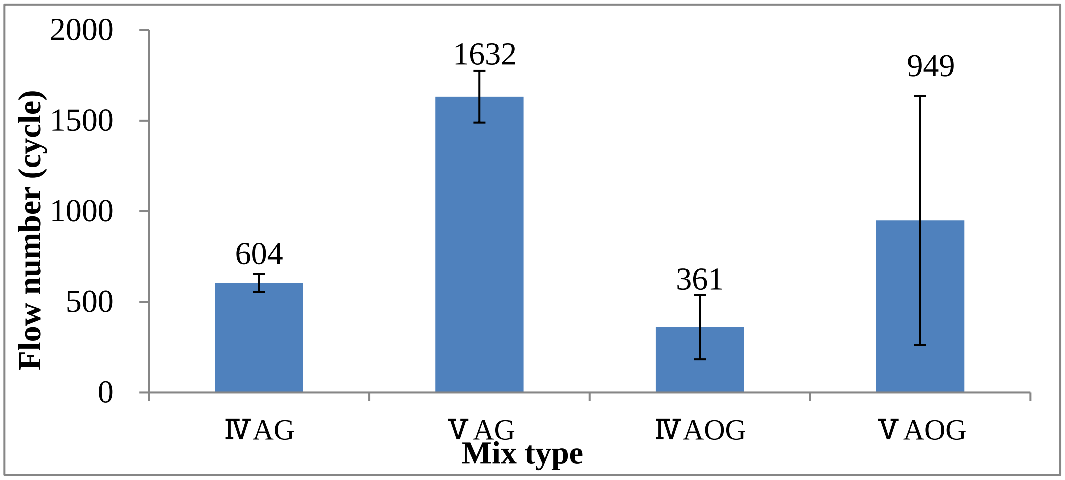

Figure 6-109 Flow Numbers of Various Surface Type A Mixtures after A Long-Term Aging Procedure with/without RAP at 59°C (138.2°F)

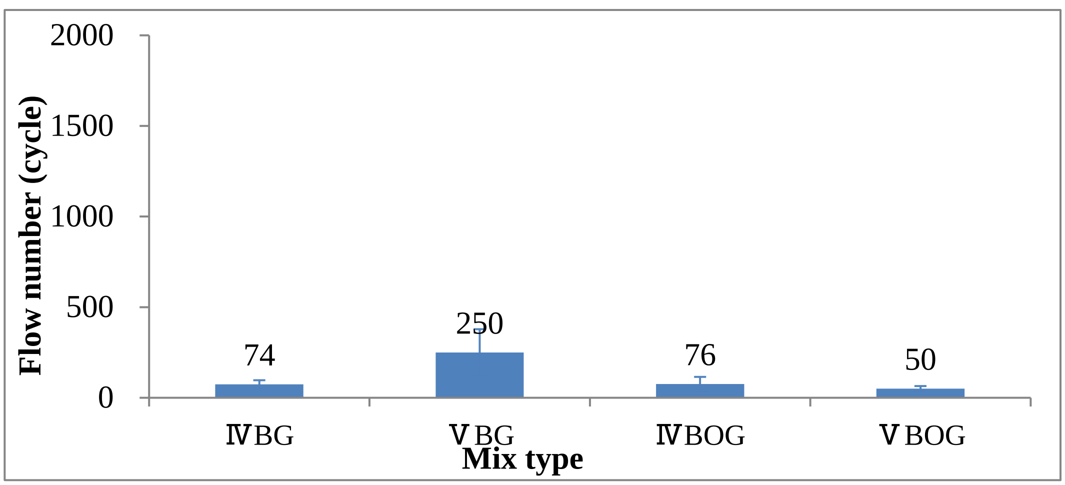

Figure 6-110 Flow Numbers of Various Surface Type B Mixtures after A Long-Term Aging Procedure with/without RAP at 59°C (138.2°F)

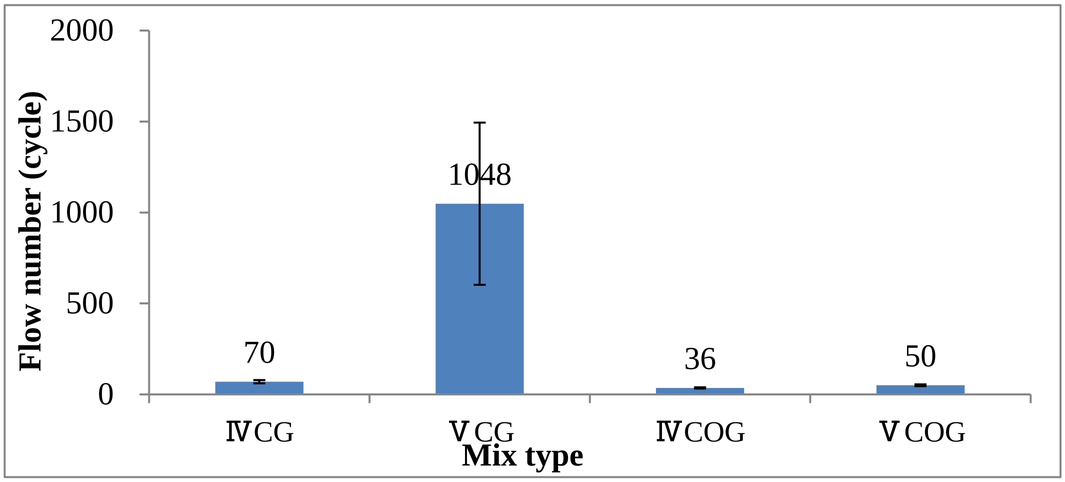

Figure 6-111 Flow Numbers of Various Surface Type C Mixtures after A Long-Term Aging Procedure with/without RAP at 59°C (138.2°F)

6.3 Master Curves of Various Mixtures

6.3.1 Analysis Method

The master curve model adopted in the Mechanistic-Empirical Pavement Design Guide (MEPDG) has the form of a sigmoidal function as shown below:

$$\log|E^*| = \delta + \frac{(|E^*|_{max} - \delta)}{1 + e^{\beta + \gamma\{\log(f_r)\}}} \qquad \textbf{(Equation 6-1)}$$

Where,

- $|E^*|$: The dynamic modulus, MPa;
- f_r: The reduced frequency, Hz;
- $|E^*|_{max}$: Limiting maximum modulus, MPa;
- δ, β, and γ: Fitting parameters.

The maximum limiting modulus is estimated from mixture volumetric properties using the Hirsch model and a limiting binder modulus is 1GPa (145,000 psi) in these equations:

$$|E^*|_{max} = P_c\left[4.2 \times 10^6\left(1 - \frac{VMA}{100}\right) + 4.35 \times 10^5\left(\frac{VFA \times VMA}{10000}\right)\right] + \frac{1 - P_c}{\left[\frac{\left(1 - \frac{VMA}{100}\right)}{4.2 \times 10^6} + \frac{VMA}{4.35 \times 10^5 VFA}\right]}$$

(Equation 6-2)

Where,

$$\boldsymbol{P_c} = \frac{\left(20+\frac{4.35\times10^5 VFA}{VMA}\right)^{0.58}}{650+\left(\frac{4.35\times10^5 VFA}{VMA}\right)^{0.58}} \qquad \textbf{(Equation 6-3)}$$

- VMA: Voids in mineral aggregates, %; and
- VFA: Voids filled with asphalt, %.

The reduced frequency is defined as follows:

$$\boldsymbol{f_r = f \times \alpha_T \text{ or } \log f_r = \log f + \log \alpha_T} \qquad \textbf{(Equation 6-4)}$$

Where,

- f: The loading frequency, Hz; and
- α_T: The time-temperature shift factor;

The Williams-Landel-Ferry (WLF) and Arrhenius equations are the most common used models for α_T of asphalt concrete. In this report the Arrhenius equation was used as shown in the following equation:

$$\boldsymbol{\log \alpha_T = \frac{\Delta E_a}{19.14714}\left(\frac{1}{T} - \frac{1}{T_r}\right)} \qquad \textbf{(Equation 6-5)}$$

Where:

- T: Test temperature,°K;
- T_r: Reference temperature,°K; and
- ΔE_a: Activation energy (treated as a fitting parameter)

The master curves of dynamic modulus and phase angle values can be generated following the steps shown below:

Step 1. Estimate the Limiting Maximum Modulus, $|E^*|_{max}$

Using the average %VMA and %VFA of each specimen to calculate the limiting maximum modulus value as shown in Equation 6-2.

Step 2. Select the Reference Temperature, T_r

In this report, 20°C (68F) (293.15°K) was used as the reference temperature.

Step 3. Perform Numerical Optimization

Substitute $|E^*|_{max}$ and T_r selected into (Equation 6-5. Using numerical optimization to determine the four model coefficients of Equation 6.1 (δ, β, γ, and ΔE_a). The initial estimates recommended are the following: $\delta = 3.0$, $\beta = -1.0$, $\gamma = -0.5$, and $\Delta E_a = 200000$.

Step 4. Compute the Time-Temperature Shift Factor, α_T

Using $\log \alpha_T$ (Equation 6-4 to compute α_T under 4°C (39.2°F) (277.15°K) , 40°C (104°F) (313.15°K), and 45°C (113°F) (318.15°K for Surface Type A). The values of α_T under reference temperature 20°C (68°F) (293.15°K) were 1.0. Table 6-2 summarizes the values of $\log \alpha_T$.

Table 6-2 Shift Factor Values of α_T under Various Testing Temperatures

Mixture type	Shift factors		Mixture type	Shift factors		Mixture type	Shift factors	
	4°C (39.2°F)	45°C (113°F)		4°C (39.2°F)	45°C (113°F)		4°C (39.2°F)	45°C (113°F)
IA	2.10	-2.85	ⅤA	2.41	-3.28	ⅤAN	2.12	-2.89
ⅡA1	2.01	-2.73	ⅥA	2.15	-2.92	ⅣAON	2.06	-2.81
ⅡA2	2.01	-2.73	ⅣAO	1.98	-2.70	ⅤAON	2.02	-2.75
ⅢA1	2.06	-2.80	ⅤAO	2.28	-3.10	ⅣAG	2.09	-2.84
ⅢA2	2.08	-2.84	ⅥAO	2.02	-2.75	ⅤAG	2.13	-2.90
ⅣA	2.05	-2.79	ⅣAN	1.99	-2.71	ⅣAOG	2.10	-2.86
						ⅤAOG	1.98	-2.70
ⅠB1	1.83	-2.03	ⅣCM	2.09	-2.32	ⅤCF	1.94	-2.15
ⅠB2	1.97	-2.18	ⅣCOA	2.17	-2.40	ⅤCG	2.02	-2.23
ⅠC	2.13	-2.35	ⅣCOE	2.19	-2.42	ⅤCM	2.31	-2.55
ⅠD	2.01	-2.22	ⅣCOF	1.97	-2.18	ⅤCOA	2.15	-2.38
ⅠE	2.08	-2.30	ⅣCOG	2.02	-2.23	ⅤCOE	2.04	-2.25
ⅠEO	1.98	-2.19	ⅣCOM	2.16	-2.39	ⅤCOF	1.95	-2.16
ⅡB	2.08	-2.30	ⅣDO	1.97	-2.17	ⅤCOG	2.11	-2.33
ⅡC	1.91	-2.11	ⅣD	2.27	-2.51	ⅤCOM	2.21	-2.45
ⅡD	2.01	-2.23	ⅣEO	2.22	-2.46	ⅤDO	2.15	-2.38
ⅡE	2.05	-2.27	ⅣE	2.23	-2.47	ⅤD	2.40	-2.65
ⅢB1	2.04	-2.25	ⅣIA	2.30	-2.54	ⅤEO	2.38	-2.63
ⅢB2	2.09	-2.32	ⅣIAO	2.02	-2.23	ⅤE	2.48	-2.75
ⅢC	1.98	-2.19	ⅣIB	2.06	-2.28	ⅤIA	2.49	-2.75

Mixture type	Shift factors		Mixture type	Shift factors		Mixture type	Shift factors	
	4°C (39.2°F)	45°C (113°F)		4°C (39.2°F)	45°C (113°F)		4°C (39.2°F)	45°C (113°F)
ⅢCO	2.03	-2.24	ⅣIBO	1.99	-2.21	ⅤIAO	2.03	-2.25
ⅢD	2.01	-2.22	ⅣIC	1.97	-2.18	ⅤIB	2.07	-2.29
ⅢDO	2.12	-2.34	ⅣICO	2.03	-2.25	ⅤIBO	2.06	-2.28
ⅢE	2.12	-2.34	ⅣSA	2.02	-2.23	ⅤIC	1.96	-2.17
ⅢEO	2.10	-2.32	ⅣSAO	1.95	-2.16	ⅤICO	2.10	-2.32
ⅣBON	2.10	-2.32	ⅣSB	1.75	-1.93	ⅤSA	2.02	-2.24
ⅣB	2.12	-2.35	ⅣSBO	1.92	-2.13	ⅤSAO	2.13	-2.35
ⅣBG	2.22	-2.45	ⅤBO	1.98	-2.19	ⅤSB	1.96	-2.17
ⅣBN	2.05	-2.27	ⅤB	2.44	-2.69	ⅤSBO	2.10	-2.32
ⅣBOG	2.12	-2.35	ⅤBG	1.99	-2.20	ⅥB	2.02	-2.23
ⅣBO	2.12	-2.34	ⅤBN	2.24	-2.47	ⅥBO	2.09	-2.31
ⅣCO	2.21	-2.45	ⅤBOG	1.99	-2.20	ⅥC	2.04	-2.26
ⅣC	2.18	-2.41	ⅤBON	2.15	-2.38	ⅥCO	1.99	-2.20
ⅣCA	2.15	-2.37	ⅤCO	1.94	-2.15	ⅥD	1.96	-2.17
ⅣCE	2.03	-2.25	ⅤC	2.25	-2.49	ⅥDO	2.00	-2.21
ⅣCF	2.03	-2.24	ⅤCA	2.23	-2.47	ⅥE	2.01	-2.23
IIIB	1.97	-2.17	VIIIB	2.02	-2.23			

6.3.2 Sample Developed Master Curves

Figure 6-112 shows an example of a dynamic modulus master curve for Surface Type A using aggregate source I. It is important to note that the curve in red provides the data points for inputting into the MEPDG. As shown in Figure 6-112, these shifted curves can be used to determine the dynamic modulus values, which were not tested in the laboratory, but should be employed at the MEPDG requiring higher and lower test temperatures.

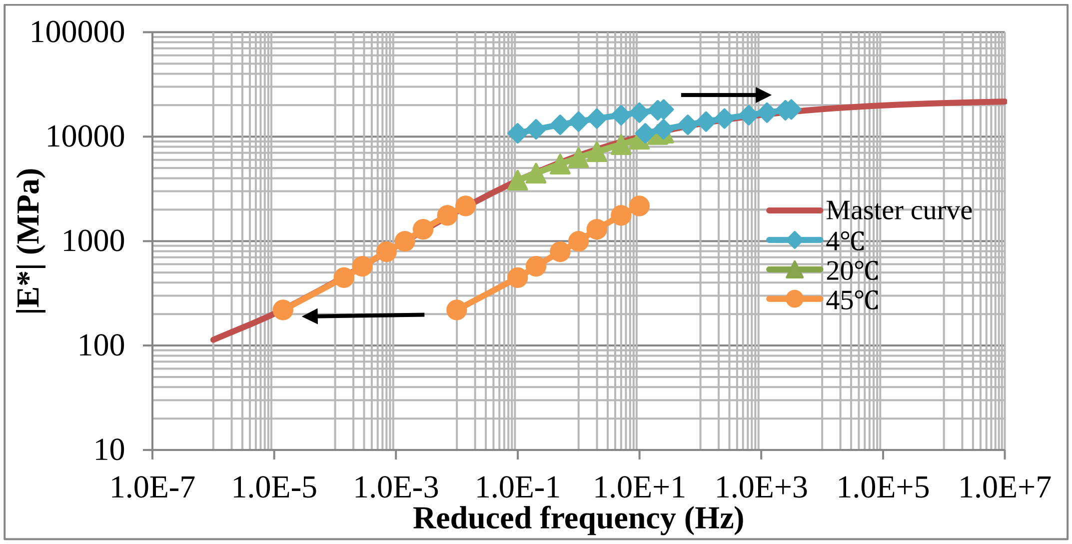

Figure 6-112 Typical Master Curve of Dynamic Modulus for Surface A Mixture Made With Aggregate Source I

6.3.3 Results of Master Curve Development

The master curves of dynamic modulus values for various mixtures are shown in Appendix D. The following results were noted with respect to dynamic modulus:

- In general, the master dynamic modulus curves of different Surface Course types and different aggregate sources showed different trends. It can be noted that the dynamic modulus values of aggregate sources V and II and containing RAP were the highest and the lowest in most cases, respectively. However, it can also be noted that aggregate sources V and IV and containing no RAP showed the highest and the lowest values, respectively.
- As for Intermediate and Base Courses, the dynamic modulus values of the mixtures made with aggregate source V were mostly higher than those of the mixtures containing aggregate source IV. For Intermediate Type B Special mixtures, dynamic modulus values were similar, regardless of aggregate source.
- The dynamic modulus values of Surface Type C mixtures made with aggregate sources IV and V, containing RAP, and using WMA technologies were similar. However, Surface Type C mixtures using WMA technologies with those same two aggregate sources without RAP showed significant difference.

- The dynamic modulus values of Surface Type C mixtures containing aggregate source V were higher than those of aggregate source IV regardless of liquid ASA type when these mixtures both contained RAP. However, for those same mixtures without RAP, the dynamic modulus values for both aggregate sources (IV and V) were similar.
- For Surface Type A mixtures containing RAP and conditioned with a long-term aging procedure, the dynamic modulus values were similar for both aggregate sources. However, for those same mixtures without RAP, aggregate source V showed higher values than aggregate source IV. This effect was more pronounced at lower values of reduced frequency. Surface Type B and C aged mixtures showed a different trend than the Surface Type A aged mixtures. The aged mixtures without RAP exhibited similar dynamic modulus values for both aggregate sources, while aggregate source V exhibited higher values than aggregate source IV for those same mixtures containing RAP. Again, this effect was more pronounced at lower values of reduced frequency.

With respect to the phase angle, the following trends were observed:

- The master curves of phase angles from various Surface Course types and different aggregate sources showed different trends. The phase angle values of the mixtures from aggregate source V with or without RAP were the lowest in most cases under a reduced frequency.
- As for the Intermediate and Base courses, the aggregate source did not affect the phase angle values in terms of the mixtures made with aggregate sources IV and V. Intermediate Type B special mixtures made with aggregate sources II and IIV also showed similar trends.
- The phase angle values of Surface Type C mixtures using the WMA chemical additive technology were slightly higher than those values of Surface Type C mixes using WMA-foaming technology.

6.4 Model Development

6.4.1 Data summary and analysis

In order to develop and calibrate the models for predicting dynamic modulus and flow numbers for the materials tested for this project, a large amount of experimental data was acquired. The data, for the most part, included the dynamic modulus and flow number test data. The parameters used to calculate the dynamic modulus and flow numbers were divided into model parameters and non-model parameters.

As for the Witczak model, as shown in previous chapters, the model parameters included test temperature, loading frequency, volumetric properties of asphalt mixture, complex shear modulus, and phase angle of binder. The non-model parameters consisted of the six Surface Course types, three Intermediate Course types, two Base Course types, two binder sources, two warm mix asphalt (WMA) technologies, two liquid anti-strip additives (ASAs), and the long-term aging affects.

The parameters considered in the Hirsch model were same as those in the Witczak model except that the phase angle of the used binder was not regarded as a model parameter. In addition, Kaloush (2001) flow number prediction model was used to simulate flow number in this study.

6.4.2 Data processing of Witczak model

All data points of each parameter were summarized from the dynamic modulus test data and job mix design sheets provide by SCDOT. The following steps were followed to develop the model.

Step 1: Obtain the measured dynamic modulus value.

At first, the measured values of dynamic modulus values were collected from the original data in terms of different temperatures and frequencies. There were some small differences in these dynamic modulus values for various Surface Course mixture types due to different binder grades used for this portion of the research study. For example, because the Surface Type A mixtures contained PG 76-22 binder, the test temperatures for those mixtures included 4°C (39.2°F)， 20°C (68°F), and 45 ℃. However, for all of the mixture types containing PG 64-22 binder (Surface Types B, C, D, and E; all Intermediate Course mixtures; and all Base Course mixtures), the test temperatures used consisted of 4°C (39.2°F), 20°C (68°F), and 40°C (104°F). All detailed information is shown in Table 6-3**.**

Table 6-3 Classification System of the Measured Value of Dynamic Modulus

Witczak model	Surface Type A	Surface Types B, C, D, and E; Base mixes; Intermediate mixes
Temperature ℃ (°F)	4, 20, 45 (39.2, 68, 113)	4, 20, 40 (39.2, 68, 104)
Frequency (Hz)	0.1, 0.2, 0.5, 1, 2, 5, 10, 20, 25	0.01, 0.1 ,0.2, 0.5, 1, 2, 5, 10
Binder grade	PG 76-22	PG 64-22

Step 2: Acquire the volumetric properties of asphalt mixture.

Some parameters such as percent void content, the passing rate, and the accumulated screening rate were collected from the job mix designs directly. However, effective asphalt contents (by volume of the mixture) were calculated as the steps listed in Figure 6-113. In addition, the dynamic modulus and the flow number testing were conducted for each asphalt mixture at three target air void levels.

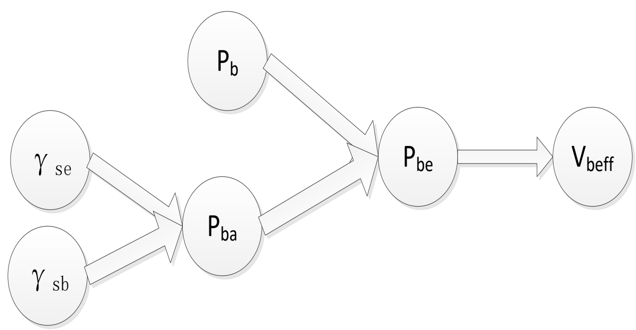

Where： γ_{se}: effective relative density of aggregates;

R_{sb}: bulk specific gravity; P_{ba}: asphalt content which was absorbed by aggregates; P_b: asphalt content (is not equal to the OAC); P_{be}: effective asphalt content, % by gravity; V_{beff}: effective asphalt content, % by volume.

Figure 6-113 Flow Chart of Calculating the Effective Asphalt Content by Volume

Step 3: Determine the complex shear modulus and the phase angle of the binder.

The model also needed to consider the properties of binder at different temperatures and frequencies. In other words, the rheological behaviors of the binders at different temperatures and frequencies can also influence the dynamic modulus of asphalt mixtures. The fitting of formulas to calculate the complex shear modulus and phase angle at different frequencies and various temperatures was conducted according to the test results from dynamic shear rheometer. The conducted test results are summarized in Table 6-4 to Table 6-9.

Step 4: Determine the predicted values of dynamic modulus.

The Witczak model has been mentioned above, so the predicted values of dynamic modulus can be obtained after inputting the required parameters. Table 6-10 to Table 6-12 show the measured values of dynamic modulus of IA mixtures at 4, 20, and 45℃ (39.2, 68, and 113°F).

Table 6-4 G* Values and Phase Angles of PG 76-22 at 4°C (39.2°F)

	G*	δ								
Slope	0.36	-7.27								
Intercept	7.65	34.41								
Frequency(Hz)	0.01	0.1	0.2	0.5	1	2	5	10	20	25
Log (F)	-2.00	-1.00	-0.70	-0.30	0.00	0.30	0.70	1.00	1.30	1.40
Log (G*)	6.93	7.29	7.40	7.55	7.65	7.76	7.91	8.01	8.12	8.16
G* (Pa)	8.60E+06	1.97E+07	2.53E+07	3.52E+07	4.51E+07	5.79E+07	8.05E+07	1.03E+08	1.33E+08	1.44E+08
G* (Psi)	1.25E+03	2.86E+03	3.67E+03	5.10E+03	6.54E+03	8.40E+03	1.17E+04	1.49E+04	1.93E+04	2.09E+04
Phase Angle	48.96	41.69	39.50	36.60	34.41	32.22	29.33	27.14	24.95	24.24

Table 6-5 G* Values and Phase Angles of PG 76-22 at 20°C (68°F)

	G*	δ								
Slope	0.60	-7.74								
Intercept	6.48	55.60								
Frequency(Hz)	0.01	0.1	0.2	0.5	1	2	5	10	20	25
Log (F)	-2.00	-1.00	-0.70	-0.30	0.00	0.30	0.70	1.00	1.30	1.40
Log (G*)	5.28	5.88	6.06	6.30	6.48	6.66	6.90	7.08	7.26	7.32
G* (Pa)	1.89E+05	7.53E+05	1.14E+06	1.98E+06	3.00E+06	4.54E+06	7.88E+06	1.19E+07	1.81E+07	2.07E+07
G* (Psi)	2.74E+01	1.09E+02	1.65E+02	2.87E+02	4.35E+02	6.58E+02	1.14E+03	1.73E+03	2.62E+03	3.00E+03
Phase Angle	71.07	63.33	61.00	57.93	55.60	53.27	50.19	47.86	45.53	44.78

Table 6-6 G* Values and Phase Angles of PG 76-22 at 45°C (113°F)

	G*	δ								
Slope	0.74	2.45								
Intercept	4.46	66.21								
Frequency(Hz)	0.01	0.1	0.2	0.5	1	2	5	10	20	25
Log (F)	-2.00	-1.00	-0.70	-0.30	0.00	0.30	0.70	1.00	1.30	1.40
Log (G*)	2.98	3.72	3.94	4.24	4.46	4.68	4.98	5.20	5.42	5.49
G* (Pa)	9.51E+02	5.23E+03	8.74E+03	1.72E+04	2.88E+04	4.80E+04	9.47E+04	1.58E+05	2.64E+05	3.12E+05
G* (Psi)	1.38E-01	7.58E-01	1.27E+00	2.49E+00	4.18E+00	6.96E+00	1.37E+01	2.29E+01	3.83E+01	4.52E+01
Phase Angle	61.32	63.77	64.50	65.48	66.21	66.95	67.92	68.66	69.40	69.63

Table 6-7 G* Values and Phase Angles of PG 64-22 at 4°C (39.2°F)

	G*	δ								
Slope	0.36	-8.58								
Intercept	7.77	35.38								
Frequency(Hz)	0.01	0.1	0.2	0.5	1	2	5	10	20	25
Log (F)	-2.00	-1.00	-0.70	-0.30	0.00	0.30	0.70	1.00	1.30	1.40
Log (G*)	7.05	7.41	7.52	7.66	7.77	7.87	8.01	8.12	8.23	8.26
G* (Pa)	1.13E+07	2.56E+07	3.28E+07	4.55E+07	5.82E+07	7.46E+07	1.03E+08	1.32E+08	1.70E+08	1.84E+08
G* (Psi)	1.64E+03	3.71E+03	4.76E+03	6.60E+03	8.44E+03	1.08E+04	1.49E+04	1.91E+04	2.47E+04	2.67E+04
Phase Angle	52.53	43.95	41.37	37.96	35.38	32.79	29.38	26.80	24.22	23.38

Table 6-8 G* Values and Phase Angles of PG 64-22 at 20°C (68°F)

	G*	δ								
Slope	0.66	-10.38								
Intercept	6.47	62.02								
Frequency(Hz)	0.01	0.1	0.2	0.5	1	2	5	10	20	25
Log (F)	-2.00	-1.00	-0.70	-0.30	0.00	0.30	0.70	1.00	1.30	1.40
Log (G*)	5.15	5.81	6.01	6.27	6.47	6.67	6.93	7.13	7.32	7.39
G* (Pa)	1.42E+05	6.47E+05	1.02E+06	1.87E+06	2.94E+06	4.64E+06	8.48E+06	1.34E+07	2.11E+07	2.44E+07
G* (Psi)	2.06E+01	9.38E+01	1.48E+02	2.71E+02	4.26E+02	6.73E+02	1.23E+03	1.94E+03	3.06E+03	3.54E+03
Phase Angle	82.78	72.40	69.27	65.14	62.02	58.89	54.76	51.64	48.51	47.50

Table 6-9 G* Values and Phase Angles of PG 64-22 at 40°C (104°F)

	G*	δ								
Slope	0.92	-4.32								
Intercept	4.48	83.28								
Frequency(Hz)	0.01	0.1	0.2	0.5	1	2	5	10	20	25
Log (F)	-2.00	-1.00	-0.70	-0.30	0.00	0.30	0.70	1.00	1.30	1.40
Log (G*)	2.64	3.56	3.84	4.20	4.48	4.75	5.12	5.39	5.67	5.76
G* (Pa)	4.38E+02	3.62E+03	6.85E+03	1.59E+04	3.00E+04	5.66E+04	1.31E+05	2.48E+05	4.68E+05	5.75E+05
G* (Psi)	6.35E-02	5.25E-01	9.93E-01	2.31E+00	4.35E+00	8.21E+00	1.90E+01	3.60E+01	6.79E+01	8.34E+01
Phase Angle	91.93	87.60	86.30	84.58	83.28	81.98	80.26	78.95	77.65	77.23

Table 6-10 Typical Measured and Predicted Values of Dynamic Modulus of IA at 4°C (39.2°F) based on Witczak model

	Frequency (Hz)	Measured value of |E*| (MPa)	Measured value of |E*| (psi)	ρ_{200}	ρ_4	ρ_{38}	ρ_{34}	V_a	V_{beff}	G_{b*} (psi)	δ	Predicted value of |E*| (log, psi)	Measured value of |E*| (log, psi)
IA	25	19074	2765730	4.85	39	11	0	6.32	11.55	20828.85	24.24	6.10	6.44
		18248	2645960	4.85	39	11	0	5.78	11.55	20828.85	24.24	6.11	6.42
		17371	2518795	4.85	39	11	0	6.44	11.55	20828.85	24.24	6.10	6.40
	20	18805	2726725	4.85	39	11	0	6.32	11.55	19221.79	24.95	6.09	6.44
		17906	2596370	4.85	39	11	0	5.78	11.55	19221.79	24.95	6.10	6.41
		17106	2480370	4.85	39	11	0	6.44	11.55	19221.79	24.95	6.09	6.39
	10	17783	2578535	4.85	39	11	0	6.32	11.55	14978.67	27.14	6.06	6.41
		17042	2471090	4.85	39	11	0	5.78	11.55	14978.67	27.14	6.07	6.39
		16242	2355090	4.85	39	11	0	6.44	11.55	14978.67	27.14	6.06	6.37
	5	16801	2436145	4.85	39	11	0	6.32	11.55	11672.19	29.33	6.03	6.39
		16137	2339865	4.85	39	11	0	5.78	11.55	11672.19	29.33	6.04	6.37
		15332	2223140	4.85	39	11	0	6.44	11.55	11672.19	29.33	6.03	6.35
	2	15543	2253735	4.85	39	11	0	6.32	11.55	8393.83	32.22	5.99	6.35
		14985	2172825	4.85	39	11	0	5.78	11.55	8393.83	32.22	6.00	6.34
		14165	2053925	4.85	39	11	0	6.44	11.55	8393.83	32.22	5.98	6.31

	Frequency (Hz)	Measured value of |E*| (MPa)	Measured value of |E*| (psi)	ρ_{200}	ρ_4	ρ_{38}	ρ_{34}	V_a	V_{beff}	G_{b*} (psi)	δ	Predicted value of |E*| (log, psi)	Measured value of |E*| (log, psi)
IA	1	14566	2112070	4.85	39	11	0	6.32	11.55	6540.93	34.41	5.95	6.32
		14054	2037830	4.85	39	11	0	5.78	11.55	6540.93	34.41	5.97	6.31
		13235	1919075	4.85	39	11	0	6.44	11.55	6540.93	34.41	5.95	6.28
	0.5	13526	1961270	4.85	39	11	0	6.32	11.55	5097.05	36.60	5.92	6.29
		13191	1912695	4.85	39	11	0	5.78	11.55	5097.05	36.60	5.93	6.28
		12318	1786110	4.85	39	11	0	6.44	11.55	5097.05	36.60	5.91	6.25
	0.2	12153	1762185	4.85	39	11	0	6.32	11.55	3665.45	39.50	5.87	6.25
		11996	1739420	4.85	39	11	0	5.78	11.55	3665.45	39.50	5.88	6.24
		11128	1613560	4.85	39	11	0	6.44	11.55	3665.45	39.50	5.86	6.21
	0.1	11102	1609790	4.85	39	11	0	6.32	11.55	2856.32	41.69	5.82	6.21
		11067	1604715	4.85	39	11	0	5.78	11.55	2856.32	41.69	5.84	6.21
		10173	1475085	4.85	39	11	0	6.44	11.55	2856.32	41.69	5.82	6.17

Table 6-11 Typical Measured and Predicted Values of Dynamic Modulus of IA at 20°C (68°F) based on Witczak model

	Frequency (Hz)	Measured value of |E*| (MPa)	Measured value of |E*| (psi)	ρ_{200}	ρ_4	ρ_{38}	ρ_{34}	V_a	V_{beff}	G_{b*} (psi)	δ	Predicted value of |E*| (log, psi)	Measured value of |E*| (log, psi)
IA	25	11105	1610225	4.85	39	11	0	6.32	11.55	3000.88	44.78	5.82	6.21
		11129	1613705	4.85	39	11	0	5.78	11.55	3000.88	44.78	5.83	6.21
		10342	1499590	4.85	39	11	0	6.44	11.55	3000.88	44.78	5.81	6.18
	20	10773	1562085	4.85	39	11	0	6.32	11.55	2624.73	45.53	5.80	6.19
		10803	1566435	4.85	39	11	0	5.78	11.55	2624.73	45.53	5.81	6.20
		9989	1448405	4.85	39	11	0	6.44	11.55	2624.73	45.53	5.79	6.16
	10	9626	1395770	4.85	39	11	0	6.32	11.55	1731.44	47.86	5.73	6.14
		9762	1415490	4.85	39	11	0	5.78	11.55	1731.44	47.86	5.74	6.15
		8982	1302390	4.85	39	11	0	6.44	11.55	1731.44	47.86	5.73	6.11
	5	8565	1241925	4.85	39	11	0	6.32	11.55	1142.17	50.19	5.66	6.09
		8737	1266865	4.85	39	11	0	5.78	11.55	1142.17	50.19	5.67	6.10
		8007	1161015	4.85	39	11	0	6.44	11.55	1142.17	50.19	5.66	6.06
	2	7246	1050670	4.85	39	11	0	6.32	11.55	659.01	53.27	5.56	6.02
		7484	1085180	4.85	39	11	0	5.78	11.55	659.01	53.27	5.58	6.04
		6809	987305	4.85	39	11	0	6.44	11.55	659.01	53.27	5.56	5.99

	Frequency (Hz)	Measured value of |E*| (MPa)	Measured value of |E*| (psi)	ρ_{200}	ρ_4	ρ_{38}	ρ_{34}	V_a	V_{beff}	G_{b^*} (psi)	δ	Predicted value of |E*| (log, psi)	Measured value of |E*| (log, psi)
IA	1	6329	917705	4.85	39	11	0	6.32	11.55	434.73	55.60	5.48	5.96
		6594	956130	4.85	39	11	0	5.78	11.55	434.73	55.60	5.50	5.98
		5974	866230	4.85	39	11	0	6.44	11.55	434.73	55.60	5.48	5.94
	0.5	5460	791700	4.85	39	11	0	6.32	11.55	286.77	57.93	5.40	5.90
		5756	834620	4.85	39	11	0	5.78	11.55	286.77	57.93	5.42	5.92
		5192	752840	4.85	39	11	0	6.44	11.55	286.77	57.93	5.40	5.88
	0.2	4428	642060	4.85	39	11	0	6.32	11.55	165.46	61.00	5.29	5.81
		4744	687880	4.85	39	11	0	5.78	11.55	165.46	61.00	5.30	5.84
		4252	616540	4.85	39	11	0	6.44	11.55	165.46	61.00	5.29	5.79
	0.1	3766	546070	4.85	39	11	0	6.32	11.55	109.15	63.33	5.20	5.74
		4089	592905	4.85	39	11	0	5.78	11.55	109.15	63.33	5.22	5.77
		3651	529395	4.85	39	11	0	6.44	11.55	109.15	63.33	5.20	5.72

Table 6-12 Typical Measured and Predicted Values of Dynamic Modulus of IA at 45°C (113°F) Based on Witczak model

	Frequency (Hz)	Measured value of |E*| (MPa)	Measured value of |E*| (psi)	ρ_{200}	ρ_{4}	ρ_{38}	ρ_{34}	V_a	V_{beff}	G_{b^*} (psi)	δ	Predicted value of |E*| (log, psi)	Measured value of |E*| (log, psi)
IA	10	2130	308850	4.85	39	11	0	6.32	11.55	22.93	68.66	4.88	5.49
		2310	334950	4.85	39	11	0	5.78	11.55	22.93	68.66	4.89	5.53
		2089	302905	4.85	39	11	0	6.44	11.55	22.93	68.66	4.87	5.48
	5	1713	248385	4.85	39	11	0	6.32	11.55	13.73	67.92	4.78	5.40
		1884	273180	4.85	39	11	0	5.78	11.55	13.73	67.92	4.80	5.44
		1691	245195	4.85	39	11	0	6.44	11.55	13.73	67.92	4.78	5.39
	2	1243	180235	4.85	39	11	0	6.32	11.55	6.97	66.95	4.66	5.26
		1400	203000	4.85	39	11	0	5.78	11.55	6.97	66.95	4.67	5.31
		1249	181105	4.85	39	11	0	6.44	11.55	6.97	66.95	4.65	5.26
	1	949	137649	4.85	39	11	0	6.32	11.55	4.17	66.21	4.57	5.14
		1081	156745	4.85	39	11	0	5.78	11.55	4.17	66.21	4.58	5.20
		956	138548	4.85	39	11	0	6.44	11.55	4.17	66.21	4.56	5.14
	0.5	746	108170	4.85	39	11	0	6.32	11.55	2.50	65.48	4.48	5.03
		864	125237	4.85	39	11	0	5.78	11.55	2.50	65.48	4.49	5.10
		765	110911	4.85	39	11	0	6.44	11.55	2.50	65.48	4.48	5.05

	Frequency (Hz)	Measured value of |E*| (MPa)	Measured value of |E*| (psi)	ρ_{200}	ρ_4	ρ_{38}	ρ_{34}	V_a	V_{beff}	G_{b^*} (psi)	δ	Predicted value of |E*| (log, psi)	Measured value of |E*| (log, psi)
IA	0.2	536	77706	4.85	39	11	0	6.32	11.55	1.27	64.50	4.37	4.89
		628	91046	4.85	39	11	0	5.78	11.55	1.27	64.50	4.38	4.96
		558	80910	4.85	39	11	0	6.44	11.55	1.27	64.50	4.36	4.91
	0.1	415	60161	4.85	39	11	0	6.32	11.55	0.76	63.77	4.29	4.78
		491	71253	4.85	39	11	0	5.78	11.55	0.76	63.77	4.30	4.85
		437	63365	4.85	39	11	0	6.44	11.55	0.76	63.77	4.28	4.80
	0.01	203	29493	4.85	39	11	0	6.32	11.55	0.14	61.32	4.06	4.47
		240	34815	4.85	39	11	0	5.78	11.55	0.14	61.32	4.07	4.54
		215	31132	4.85	39	11	0	6.44	11.55	0.14	61.32	4.06	4.49

6.4.3 Data processing of Hirsch model

The Hirsch model, as described previously, was also conducted to determine the predicted dynamic modulus as part of this research. In this process, similar methodology to the Witczak model was employed. However, some new parameters were involved in developing the Hirsch model.

Step 1: Collect the measured value of dynamic modulus.

This step was the same as Witczak model.

Step 2: Obtain the volumetric properties of asphalt mixtures.

Obtaining void content, the passing rate, and the accumulated screening rate was the same as the Witczak model. However, when calculating the effective asphalt content, the equations for VMA and VFA listed below were utilized.

$$\boldsymbol{V_{beff} = \frac{\gamma_f \times OAC}{\gamma_b}} \qquad \textbf{(Equation 6-6)}$$

Where,

- γ_f: Bulk specific gravity of asphalt mixture;
- γ_b: Specific gravity of binder.

$$\mathbf{VMA} = \boldsymbol{V_{beff} + VV} \qquad \textbf{(Equation 6-7)}$$

Where,

- *VMA*: voids in the mineral aggregate
- VV: void content.

$$\boldsymbol{VFA = \frac{V_{beff} \times 100}{\mathbf{VMA}}} \qquad \textbf{(Equation 6-8)}$$

Where,

- VFA: voids filled with asphalt

Step 3: Determine the complex shear modulus of binder.

This model only needed the complex shear modulus of the binder, unlike the Witczak model, which also required phase angle.

Step 4: Determine the predicted value of dynamic modulus.

The predicted values of dynamic modulus from the Hirsch model were obtained after inputting several testing values and the required parameters. The typical obtained values are shown in Table 6-13 to Table 6-15.

Table 6-13 Typical Measured and Predicted Values of Dynamic Modulus of IA at 4°C (39.2°F) Based on Hirsch Model

	Frequency (Hz)	Measured value of |E*| (MPa)	Measured value of |E*| (psi)	V_{beff}	VMA	VFA	P_c	VV	G_b* (psi)	Predicted value of |E*| (psi)
IA	25	19074	2765730	11.25	17.57	64.02	0.66	6.32	20828.85	2374500.61
		18248	2645960	11.25	17.03	66.05	0.67	5.78	20828.85	2420246.05
		17371	2518795	11.25	17.69	63.59	0.66	6.44	20828.85	2364474.96
	20	18805	2726725	11.25	17.57	64.02	0.65	6.32	19221.79	2334476.02
		17906	2596370	11.25	17.03	66.05	0.66	5.78	19221.79	2380330.76
		17106	2480370	11.25	17.69	63.59	0.65	6.44	19221.79	2324430.60
	10	17783	2578535	11.25	17.57	64.02	0.62	6.32	14978.67	2207842.68
		17042	2471090	11.25	17.03	66.05	0.63	5.78	14978.67	2253866.38
		16242	2355090	11.25	17.69	63.59	0.62	6.44	14978.67	2197773.61
	5	16801	2436145	11.25	17.57	64.02	0.58	6.32	11672.19	2078410.32
		16137	2339865	11.25	17.03	66.05	0.59	5.78	11672.19	2124324.22
		15332	2223140	11.25	17.69	63.59	0.58	6.44	11672.19	2068379.07
	2	15543	2253735	11.25	17.57	64.02	0.54	6.32	8393.83	1904742.18
		14985	2172825	11.25	17.03	66.05	0.55	5.78	8393.83	1950047.42
		14165	2053925	11.25	17.69	63.59	0.54	6.44	8393.83	1894862.50

	Frequency (Hz)	Measured value of |E*| (MPa)	Measured value of |E*| (psi)	V_{beff}	VMA	VFA	P_c	VV	G_b* (psi)	Predicted value of |E*| (psi)
IA	1	14566	2112070	11.25	17.57	64.02	0.50	6.32	6540.93	1772879.69
		14054	2037830	11.25	17.03	66.05	0.51	5.78	6540.93	1817359.59
		13235	1919075	11.25	17.69	63.59	0.50	6.44	6540.93	1763194.11
	0.5	13526	1961270	11.25	17.57	64.02	0.47	6.32	5097.05	1641921.93
		13191	1912695	11.25	17.03	66.05	0.47	5.78	5097.05	1685263.55
		12318	1786110	11.25	17.69	63.59	0.46	6.44	5097.05	1632498.07
	0.2	12153	1762185	11.25	17.57	64.02	0.42	6.32	3665.45	1472232.54
		11996	1739420	11.25	17.03	66.05	0.43	5.78	3665.45	1513615.73
		11128	1613560	11.25	17.69	63.59	0.42	6.44	3665.45	1463251.94
	0.1	11102	1609790	11.25	17.57	64.02	0.38	6.32	2856.32	1347926.42
		11067	1604715	11.25	17.03	66.05	0.39	5.78	2856.32	1387521.34
		10173	1475085	11.25	17.69	63.59	0.38	6.44	2856.32	1339346.27

Table 6-14 Typical Measured and Predicted Values of Dynamic Modulus of IA at 20°C (68°F) Based on Hirsch Model

	Frequency (Hz)	Measured value of |E*| (MPa)	Measured value of |E*| (psi)	V_{beff}	VMA	VFA	P_c	VV	G_b* (psi)	Predicted value of |E*| (psi)
IA	25	11105	1610225	11.25	17.57	64.02	0.39	6.32	3000.88	1372195.86
		11129	1613705	11.25	17.03	66.05	0.40	5.78	3000.88	1412163.71
		10342	1499590	11.25	17.69	63.59	0.39	6.44	3000.88	1363532.45
	20	10773	1562085	11.25	17.57	64.02	0.37	6.32	2624.73	1306790.02
		10803	1566435	11.25	17.03	66.05	0.38	5.78	2624.73	1345726.32
		9989	1448405	11.25	17.69	63.59	0.37	6.44	2624.73	1298356.66
	10	9626	1395770	11.25	17.57	64.02	0.32	6.32	1731.44	1113314.34
		9762	1415490	11.25	17.03	66.05	0.33	5.78	1731.44	1148700.58
		8982	1302390	11.25	17.69	63.59	0.32	6.44	1731.44	1105667.40
	5	8565	1241925	11.25	17.57	64.02	0.27	6.32	1142.17	937049.60
		8737	1266865	11.25	17.03	66.05	0.28	5.78	1142.17	968541.95
		8007	1161015	11.25	17.69	63.59	0.27	6.44	1142.17	930258.49
	2	7246	1050670	11.25	17.57	64.02	0.21	6.32	659.01	733863.62
		7484	1085180	11.25	17.03	66.05	0.22	5.78	659.01	760070.74
		6809	987305	11.25	17.69	63.59	0.21	6.44	659.01	728226.19

	Frequency (Hz)	Measured value of |E*| (MPa)	Measured value of |E*| (psi)	V_{beff}	VMA	VFA	P_c	VV	G_b* (psi)	Predicted value of |E*| (psi)
IA	1	6329	917705	11.25	17.57	64.02	0.17	6.32	434.73	603443.60
		6594	956130	11.25	17.03	66.05	0.18	5.78	434.73	625800.03
		5974	866230	11.25	17.69	63.59	0.17	6.44	434.73	598642.22
	0.5	5460	791700	11.25	17.57	64.02	0.14	6.32	286.77	492396.44
		5756	834620	11.25	17.03	66.05	0.15	5.78	286.77	511185.93
		5192	752840	11.25	17.69	63.59	0.14	6.44	286.77	488366.70
	0.2	4428	642060	11.25	17.57	64.02	0.11	6.32	165.46	372820.64
		4744	687880	11.25	17.03	66.05	0.11	5.78	165.46	387465.08
		4252	616540	11.25	17.69	63.59	0.11	6.44	165.46	369684.64
	0.1	3766	546070	11.25	17.57	64.02	0.09	6.32	109.15	300503.82
		4089	592905	11.25	17.03	66.05	0.09	5.78	109.15	312482.28
		3651	529395	11.25	17.69	63.59	0.09	6.44	109.15	297941.13

Table 6-15 Typical Measured and Predicted Values of Dynamic Modulus of IA at 40°C (104°F) Based on Hirsch Model

	Frequency (Hz)	Measured value of |E*| (MPa)	Measured value of |E*| (psi)	V_{beff}	VMA	VFA	P_c	VV	G_b* (psi)	Predicted value of |E*| (psi)
IA	10	11.25	1631.25	17.57	64.02	0.04	6.32	22.93	132409.93	912.93
		11.25	1631.25	17.03	66.05	0.04	5.78	22.93	137654.13	949.09
		11.25	1631.25	17.69	63.59	0.04	6.44	22.93	131290.78	905.22
	5	11.25	1631.25	17.57	64.02	0.03	6.32	13.73	102041.57	703.55
		11.25	1631.25	17.03	66.05	0.03	5.78	13.73	105954.35	730.53
		11.25	1631.25	17.69	63.59	0.03	6.44	13.73	101207.08	697.80
	2	11.25	1631.25	17.57	64.02	0.02	6.32	6.97	73933.23	509.75
		11.25	1631.25	17.03	66.05	0.02	5.78	6.97	76546.65	527.77
		11.25	1631.25	17.69	63.59	0.02	6.44	6.97	73376.28	505.91
	1	11.25	1631.25	17.57	64.02	0.02	6.32	4.17	59490.80	410.17
		11.25	1631.25	17.03	66.05	0.02	5.78	4.17	61391.59	423.28
		11.25	1631.25	17.69	63.59	0.02	6.44	4.17	59085.87	407.38
	0.5	11.25	1631.25	17.57	64.02	0.01	6.32	2.50	49376.73	340.44
		11.25	1631.25	17.03	66.05	0.01	5.78	2.50	50745.41	349.88
		11.25	1631.25	17.69	63.59	0.01	6.44	2.50	49085.11	338.43

	Frequency (Hz)	Measured value of |E*| (MPa)	Measured value of |E*| (psi)	V_{beff}	VMA	VFA	P_c	VV	G_b* (psi)	Predicted value of |E*| (psi)
IA	0.2	11.25	1631.25	17.57	64.02	0.01	6.32	1.27	40800.41	281.31
		11.25	1631.25	17.03	66.05	0.01	5.78	1.27	41682.00	287.39
		11.25	1631.25	17.69	63.59	0.01	6.44	1.27	40612.24	280.01
	0.1	11.25	1631.25	17.57	64.02	0.01	6.32	0.76	36830.91	253.94
		11.25	1631.25	17.03	66.05	0.01	5.78	0.76	37469.76	258.34
		11.25	1631.25	17.69	63.59	0.01	6.44	0.76	36694.11	253.00
	0.01	11.25	1631.25	17.57	64.02	0.01	6.32	0.14	31514.66	217.29
		11.25	1631.25	17.03	66.05	0.01	5.78	0.14	31801.93	219.27
		11.25	1631.25	17.69	63.59	0.01	6.44	0.14	31451.95	216.85

6.4.4 Data Processing of Kaloush Model

In this portion of the study, the Kaloush model, as described previously, was used to conduct the predicted flow number of various mixtures.

Step 1: Collect measured value of flow number.

The measured value of flow number was summarized from the original data.

Step 2: Obtain the volumetric properties of asphalt mixture.

VV and V_{beff} were obtained in the same manner as for the Witczak model.

Step 3: Determine the viscosity of binders.

The viscosity values of two binders at the test temperatures of flow tests for various mixtures were obtained, as shown in Table 6-16.

Table 6-16 Viscosity Values of Two Binders

	Viscosity (10^6 p)
PG 76-22	0.89
PG 64-22	0.08

Step 4: Determine the predicted flow number value.

The predicted flow number values (Figure 6-114) were obtained after inputting the required parameters to the model. Table 6-17 shows the typical measured and predicted values of flow numbers of AA and AB mixtures at 59°C (138.2F).

Table 6-17 Typical Measured and Predicted Flow Number Values of ID and IE at 59°C (138.2°F) Based on Kaloush Model

	Measured value(circle)	T(℃)	Viscosity (10^6 p)	VV	V_{beff}	Predicted value(circle)
ID	245	59	0.08	5.67	12.26	23.02
	286	59	0.08	6.14	12.26	22.74
	211	59	0.08	5.66	12.26	23.03
IE	228	59	0.08	6.45	12.26	22.57
	638	59	0.08	6.87	12.26	22.36
	217	59	0.08	7.23	12.26	22.18

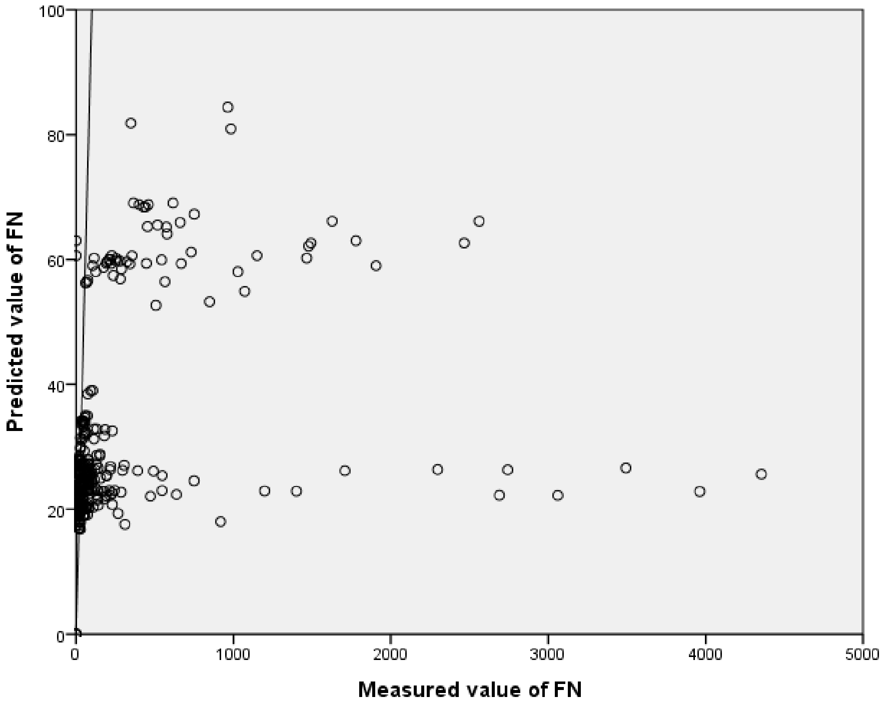

(a)

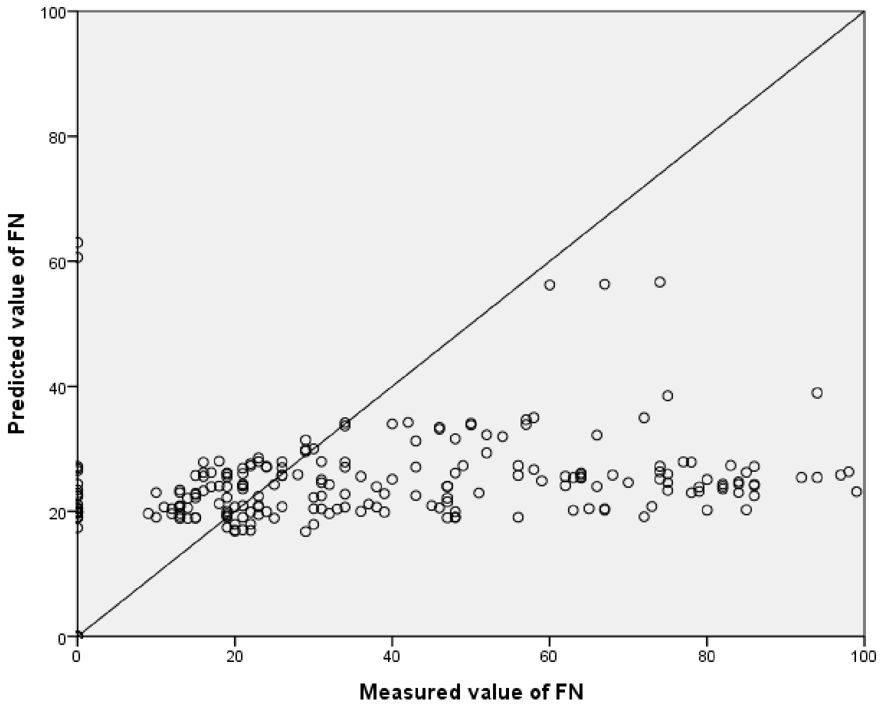

(b)

Figure 6-114 Comparison between Predicted Values and Measured Values of Flow Number：(a) All Data Points; (b) Partial Points (less than 100)

6.5 Calibration of Predictive Dynamic Modulus Models

In this study, Se/Sy and R^2 were used to judge the accuracy of these two dynamic models based on the criteria shown in
Table 6-18. The formulas used to compute these values are shown below. Furthermore, the S_e/S_y and R^2 of the developed predictive models are listed in Table 6-19.

$$S_e = \sqrt{\frac{\sum_1^n (\hat{y}_i - y_i)^2}{n-k-1}} \quad \textbf{(Equation 6-9)}$$

$$S_y = \sqrt{\frac{\sum_1^n (y_i - \bar{y})^2}{n-1}} \quad \textbf{(Equation 6-10)}$$

$$R^2 = 1 - \frac{(n-k-1)}{(n-1)} \left(\frac{S_e}{S_y}\right)^2 \quad \textbf{(Equation 6-11)}$$

Where:

- R^2: correlation coefficient
- S_e: standard error of estimate
- S_y: standard deviation
- y_i: measured dynamic modulus
- $\bar{y}$: mean value of measured dynamic modulus
- n: sample size
- k: number of independent variables used in model
- $\hat{y}_i$: predicted dynamic modulus

Table 6-18 Criteria for Goodness of Fit Statistical Parameters

Criteria	R	S_e/S_y
Excellent	>=0.9	<=0.35
Good	0.7-0.89	0.36-0.55
Fair	0.4-0.69	0.56-0.75
Poor	0.2-0.39	0.76-0.89
Very poor	<=0.19	>=0.90

Table 6-19 Comparison of Dynamic Modulus Prediction Models

Parameters	|E*| Predictive Models	
	Witczak model	Hirsch model
Measured and predicted data points	8627	8553
Goodness of Fit in Logarithmic Scale		
S_e/S_y	0.65	0.34
R^2	0.58	0.89

6.5.1 Modification of Witczak Model

After a very extensive trial and error process, the optimum coefficients were determined. The value of constant "-0.349" was adjusted into "-0.345," and the "0.754" was revised to "0.822." These changes caused the R^2 value of the predictive Witczak model to increase from 0.58 to 0.8635, which is shown in Table 6-20. Figure 6-115(a) and Figure 6-115(b) show the predicted and measured values based on the initial and modified Witczak models, respectively.

Table 6-20 Comparisons between the Initial and Modified Witczak Models

Parameters	|E*| Predictive Models	
	Initial Witczak model	Modified Witczak model
Adjustment of coefficients	-0.349, 0.754	-0.345, 0.822
Goodness of Fit in Logarithmic Scale		
S_e/S_y	0.65	0.40
R^2	0.58	0.86

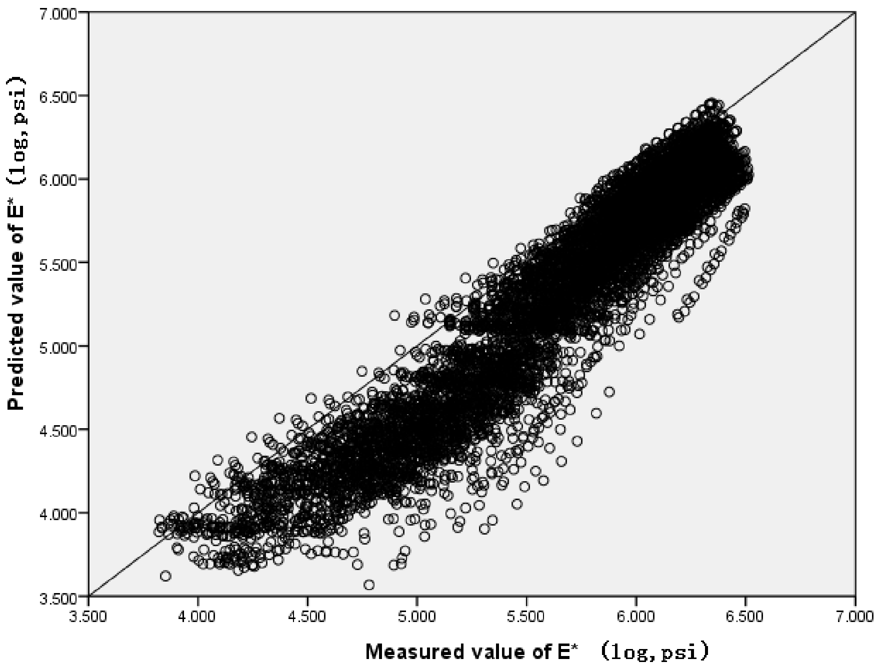

(a)

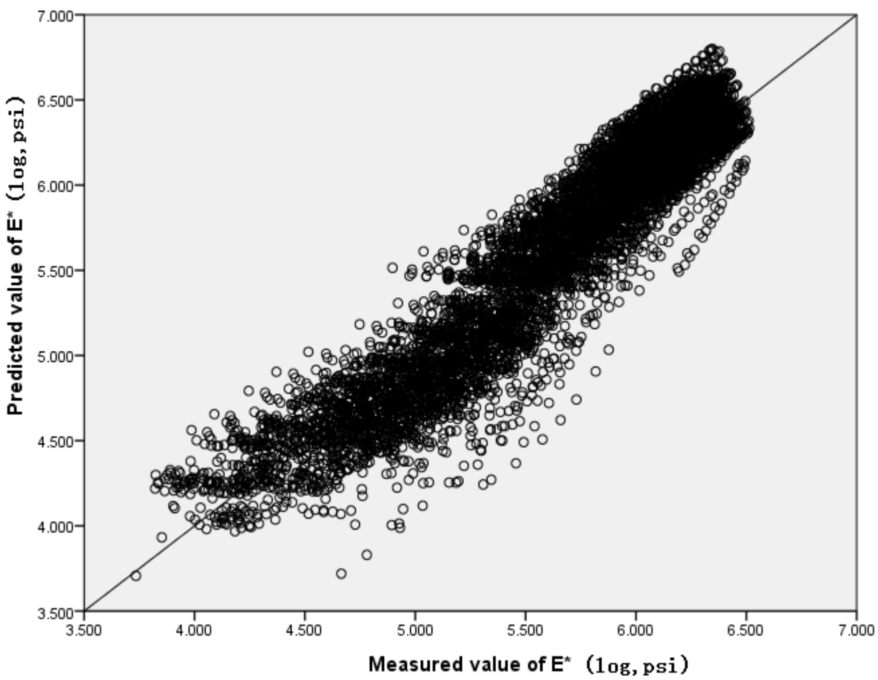

(b)

Figure 6-115 Predicted and Measured Dynamic Modulus Values, (a) Witczak Model; (b) Modified Witczak Model

6.5.2 Modification of Hirsch Model

A similar process was used to modify the Hirsch model, and the optimum coefficients were determined. The constant value of "4,200,000" was changed to "3,960,000." These changes caused the R^2 value to increase from 0.89 to 0.90 as shown in Table 6-21. The measured and predicted dynamic modulus values of various mixtures are shown in Figure 6-116. In addition, it can be noted that both the initial and modified Hirsch models exhibited good R^2 values, which were 0.89 and 0.90, respectively. Thus, both of these models provided relatively accurate predictions for these dynamic modulus values.

Table 6-21 Comparisons between the Initial and Modified Hirsch Models

Parameters	|E*| Predictive Models	
	Hirsch model	Modifier of Hirsch model
Adjustment of coefficients	4200000	3960000
Goodness of Fit in Logarithmic Scale		
S_e/S_y	0.34	0.32
R^2	0.89	0.90

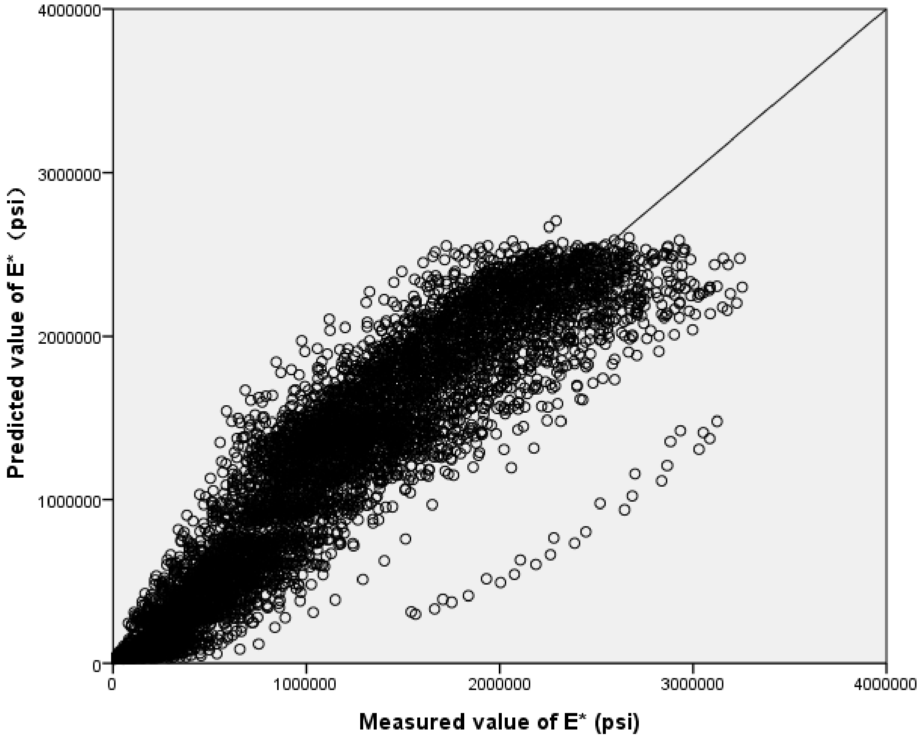

(a)

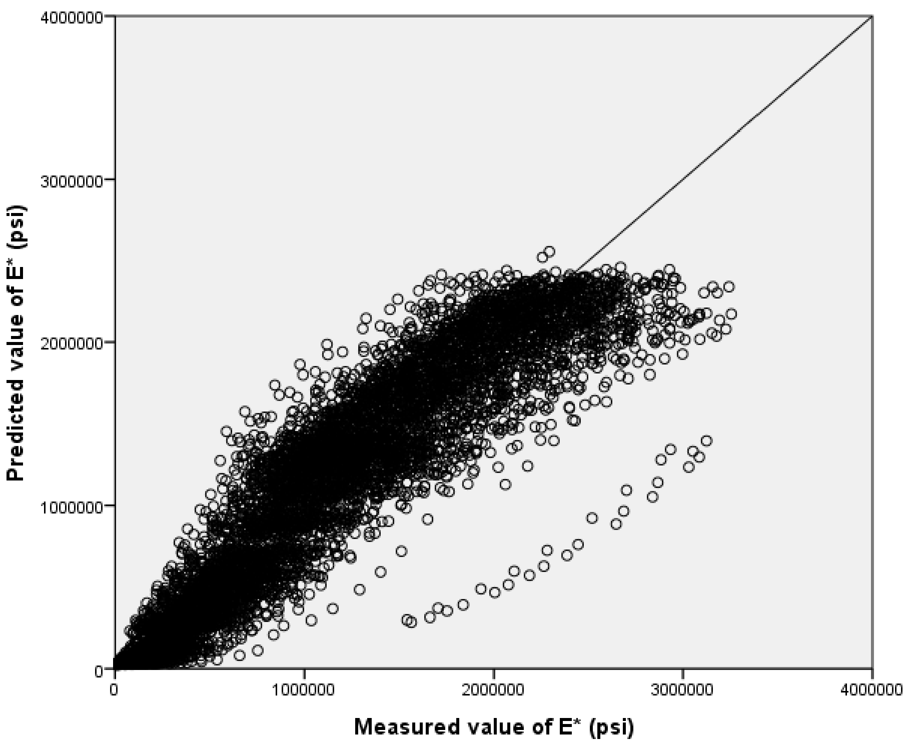

(b)

Figure 6-116 Predicted and Measured Dynamic Modulus Values, (a) Hirsch Model; (b) Modified Hirsch Model

6.5.3 Modification of Kaloush Model

In this study, it can be noted that the predicted flow number values from the Kaloush model ranged from 16 to 84; however, the measured values ranged from 0 to 4354. Therefore, this model was not suitable for predicting flow number. Based on the literature, it was found that flow number values of various mixtures were generally difficult to predict. Meanwhile, no proper predicted models could be found effectively. Consequently, the modification was not performed.

7 Summary, Conclusions, and Recommendations

7.1 Summary

For this research project, the following tasks were completed, and the data was analyzed and reported in previous chapters. In addition, the conclusions are included in the following section. Recommendations are also being made for future research work needed to further the findings of this research project.

1. The dynamic modulus (|E*|), phase angle (δ), and flow number (FN) were determined at various temperatures and frequencies for many mixtures used by SCDOT.

    a) Mix types tested included the following: Surface Type A, Surface Type B, Surface Type C, Surface Type D, Surface Type E, Intermediate Type A, Intermediate Type B, Intermediate Type B Special, Intermediate Type C, Base Type A and Base Type B.

    b) Variables included seven different aggregate sources from various regions around SC; two RAP percentages (0% RAP and the % RAP from each approved mix design); two binder sources typically used in SC; two binder grades (PG 76-22 and PG 64-22 as required per mix type per SCDOT specifications); two commonly-used warm mix asphalt (WMA) technologies (foaming and Evotherm® chemical additive); two commonly-used liquid anti-stripping agents (Adhere® and Morlife®); and a long-term aging procedure (AASHTO R30).

    c) The optimum asphalt binder contents for each mixture as determined by Superpave mix design procedures were provided by SCDOT.

    d) Various frequencies including 0.1, 0.2, 0.5, 1, 2, 5, 10, 20 and 25 Hz were used for the dynamic modulus testing. In addition, these tests were performed at various temperatures including 4, 20, 40, and 45°C (39.2, 68, 104, and 113°F).

    e) The flow number tests were performed at 59°C (138.2 °F).

2. The performance of the various mixtures tested under the conditions stated above were evaluated with respect to multiple variables.

    a) The impact of mixture type on |E*| and FN was studied for Surface Course mixture types, Intermediate Course mixture types, and Base Course mixture types.

    b) The impact of binder source (two different grades and two different sources) on |E*| and FN of mixtures was evaluated.

    c) The |E*| and FN values of mixtures containing typical warm mix asphalt technologies (chemical additive and foaming) were studied.

d) Assessment of |E*| and FN values of mixtures containing various ASAs (lime and liquid ASAs) was also completed.

e) The |E*| and FN values of mixtures after a long-term aging procedure (AASHTO R30) were also studied.

3. Master curves of the various mixtures included in this study were effectively constructed in predicting the dynamic modulus and phase angle values of various mixtures.

4. Calibration and development of dynamic modulus and flow number predictive models (including Witczak and Hirsch models) from the MEPDG based on the data obtained from this study were finalized.

5. Input tables for use by SCDOT engineers with the new MEPDG pavement design system were developed for all of the mix types and material types included in this study.

6. The evaluation of field cores using AMPT was not included in this project based on recommendations from the Steering Committee to include that testing in a different research project.

7.2 Conclusions

The researchers compiled the following conclusions from the results of this study:

1. Conclusions relating to dynamic modulus and phase angle values included:

    a) For the temperatures tested, increasing frequency resulted in an increase of dynamic modulus values at various test temperatures and a reduction of phase angle values at 4°C (39.2°F) and 20°C (68°F) regardless of binder type, aggregate type, Surface Course mixture type, Intermediate Course mixture type, Base Course mixture type, binder source, WMA technology type, liquid ASA type, and aged state. In addition, it was observed that with the increase of temperature, the dynamic modulus values generally decreased and phase angle values generally increased regardless of other variables.

    b) Aggregate source generally impacted the dynamic modulus values and phase angle values of various mixtures irrespective of Surface Course mixture type, Intermediate Course mixture type, Base Course mixture type, binder source, WMA technology type, liquid ASA type, and aged state.

        i. Specifically, aggregate sources I and V generally produced mixtures with higher dynamic modulus and lower phase angle values compared to other aggregate sources. It is hypothesized that several aggregate-related properties, such as gradation and the physical characteristics of the aggregates, contributed to producing these differences. The scope of this study did not allow for further investigation of these differences. However, the tables and graphs shown in Appendix E could still be used to select the proper materials for the best outcome of any pavement design in the near future.

c) Surface Course mixture type significantly affected the dynamic modulus values and phase angle values of the mixtures. As expected, the Surface Type A and B mixtures, which were designed for higher-volume pavements, generally exhibited greater dynamic modulus values and lower phase angle values than Surface Type D and E mixtures for all aggregate sources.

d) Intermediate mixture type (e.g., Type A vs. Type C) also had a significant influence on the dynamic modulus values and phase angle values of various mixtures regardless of aggregate type. As expected, Intermediate Type A mixtures generally exhibited greater dynamic modulus values and lower phase angle values, while Intermediate Type C mixtures generally exhibited lower dynamic modulus values and the higher phase angle values for all aggregate sources.

e) Base mixture type only slightly affected the dynamic modulus values and phase angle values of various mixtures regardless of aggregate type. Base Type A mixtures generally produced slightly higher dynamic modulus values and slightly lower phase angle values than Base Type B mixtures, but overall the values were very similar for these two mixture types.

f) Binder source only slightly affected the dynamic modulus values and phase angle values of various mixtures regardless of aggregate type. Binder source 2 exhibited slightly lower dynamic modulus values and slightly higher phase angle values than binder source 1 regardless of aggregate type, loading frequency and test temperature.

g) WMA technology type had a slight influence on the dynamic modulus values and phase angle of various mixtures, but this effect varied with aggregate type and the use of RAP. For instance, for aggregate source IV with RAP, the WMA foaming technology produced slightly higher dynamic modulus and slightly lower phase angle values than the WMA chemical additive. However, these results were reversed for aggregate source V without RAP.

h) Liquid ASA type generally had little influence on the dynamic modulus values and phase angle values of various mixtures regardless of aggregate type.

i) The long-term aging procedure had no noticeable impact on the dynamic modulus values and phase angle values of various mixtures in terms of aggregate type.

j) The inclusion of RAP did affect the dynamic modulus and phase angle values of various mixtures. Mixtures with RAP generally exhibited higher dynamic modulus values and lower phase angle values than corresponding mixtures without RAP. However, these trends were also influenced by aggregate source in a few cases when other variables were involved including binder source 2, WMA chemical additive, and aging. In those cases with certain aggregate sources, the dynamic modulus and phase angle values were similar for corresponding mixtures both with and without RAP.

2. Conclusions relating to flow number values included:

    a) Aggregate source generally impacted the flow number values of various mixtures irrespective of Surface Course mixture type, Intermediate Course mixture type, Base Course mixture type, binder source, WMA technology type, liquid ASA type, and aged state.

        i. In addition, aggregate sources I and V generally produced mixtures with higher flow number values compared to other aggregate sources. It is hypothesized that several aggregate-related properties, such as gradation and the physical characteristics of the aggregates, contributed to producing these differences. The scope of this study did not allow for further investigation of these differences. However, the tables and graphs shown in Appendix E could still be used to select the proper materials for the best outcome of any pavement design in the near future.

    b) Surface Course mixture type significantly affected the flow number values of the mixtures. As expected, the Surface Type A and B mixtures, which were designed for higher-volume pavements, generally exhibited greater flow number values than Surface Type D and E mixtures for all aggregate sources.

    c) Intermediate mixture type also had a significant influence on the flow number values of various mixtures regardless of aggregate type. Generally, Intermediate Type A mixtures exhibited the highest flow number values, while Intermediate Type C mixtures generally exhibited the lowest flow number values for all aggregate sources.

        i. In addition, the Intermediate Type B Special mixtures exhibited the highest flow number values compared to all of the other Intermediate mixture types; however, it is difficult to conclude whether this is due to mixture type because the Intermediate Type B Special mixtures were made with different aggregate sources than all of the other Intermediate mixtures. Testing of the Intermediate Type B Special mixtures was added towards the end of the project, and the aggregate sources were selected by the Steering Committee based on field pilot projects. The scope of this study did not allow for further investigation of the causes of these differences in flow number values.

        ii. All Intermediate Type A and B mixtures tested in this project exhibited flow number values below AASHTO minimum recommendation of 190 for higher volume pavements. Although the utilization of RAP resulted in somewhat higher flow number values, they still did not reach the minimum recommended value. The scope of this study did not allow for further investigation into the cause of this result.

d) Base mixture type only slightly affected the flow number values of various mixtures, and this effect varied based on aggregate type.

e) Binder source significantly affected the flow number values of various mixtures; however, aggregate source/binder source interaction had an even greater effect. For example, although binder source 1 generated higher flow numbers than binder source 2 in every case, the flow number differences between binder source 1 and 2 were significantly greater for aggregate source V than for aggregate source IV.

   i. In addition, binder grade also influenced flow number values more than binder source. In general, the mixtures in this study containing PG 76-22 exhibited higher flow number values than the mixtures containing PG 64-22 binders. The only exception was aggregate source V with asphalt source 1. This seems to validate the use of a higher binder grade (PG 76-22 vs. PG 64-22) on higher volume routes.

f) Although WMA type did not affect flow number values when comparing WMA technology types to each other (chemical additive vs. foaming), inclusion of WMA technologies did affect flow number values when compared to corresponding mixtures that did not utilize WMA. Flow number values for mixtures without WMA were higher than the corresponding mixtures utilizing either WMA technology type in all cases. This effect was especially pronounced with aggregate source IV. In addition, the flow numbers of all mixtures made with either WMA technology type were very low and did not meet the recommendations from AASHTO TP 79.

g) Although liquid ASA type generally had little influence on the flow number values of various mixtures, inclusion of liquid ASA did affect flow number values when compared to mixtures without liquid ASAs. In addition, these differences were affected by aggregate source. When liquid ASAs were utilized, regardless of liquid ASA type, aggregate source IV showed slightly lower flow number values while aggregate source V showed significantly higher flow number values when compared to mixtures without liquid ASAs.

h) The long-term aging procedure had noticeable impact on the flow number values of various mixtures in terms of both aggregate type and mixture type. For aggregate source IV, flow number values of all three types of Surface mixtures were either similar or slightly higher after aging. However, for aggregate source V, Surface Type A and B mixtures exhibited significantly lower flow number values after aging, while Surface Type C mixtures exhibited the opposite. The scope of this study did not allow for further investigation of the causes of these differences.

i) The inclusion of RAP affected the flow number values of some mixtures, but the effect of RAP seemed to be related to mixture type more than aggregate source. For example, regardless of aggregate source, Surface Type A, C, D and E mixtures containing RAP generally exhibited higher flow number values compared to the corresponding mixtures without RAP; however, Surface Type B mixtures from all aggregate sources exhibited very similar flow number values when comparing mixtures with RAP to those without RAP. The scope of this study did not allow for further investigation of the causes of these differences.

j) Although several mixtures in this study did not meet the minimum flow number values recommended by AASHTO, most notably the mixtures containing WMA technologies, the scope of this study did not allow for further investigation of these low flow numbers. However, the tables and graphs shown in Appendix E could still be used to select the proper materials for the best outcome of any pavement design in the near future.

3. Conclusions relating to the master curve development included:

   a) In this research project, the master curves of various mixtures were effectively constructed in predicting the dynamic modulus and phase angle values of various mixtures. These curves could be used by SCDOT engineers to input the proper testing values in the MEPDG program for the future pavement design process. These curves were obtained by considering multiple frequencies and temperatures. These two parameters play a major role in the performance of any pavement.

4. Conclusions relating to the design models in |E*| prediction for local mixtures included:

   a) The tables and inputs included in Appendix E may be used in the new MEPDG pavement design procedures. These tables contain all the necessary input data for the MEPDG software program. The numbers in these tables might have to be adjusted for future changes in variables (e.g., higher percentages of RAP use).

5. Conclusions relating to different parameters sensitive to variations in |E*| included:

   a) Based on the literature review, the following parameters were found to be sensitive to variations in |E*|:

      i. rutting (asphaltic concrete layers; unbound base, subbase, and subgrade layers; and total rut depth);

      ii. fatigue cracking (surface-down longitudinal cracking and bottom-up alligator cracking);

      iii. transverse (thermal) cracking; and

      iv. IRI prediction.

   b) Based on the literature review, the current MEPDG prediction model for surface-down (longitudinal cracking) was found to be unreliable.

6. Conclusions relating to the prediction models included:

a) The original Witczak model could not effectively predict the dynamic modulus values of the various mixtures and materials used in this research project. However, by adjusting some constants from the original model, the revised model could predict the dynamic modulus values effectively for the materials tested in this project.

b) The Hirsch model could generally be used to predict the dynamic modulus values for SCDOT mixtures in terms of the model's coefficient and variation. The adjusted model also exhibited some slight improvements.

c) It is recommended for SCDOT to use the following revised Witczak and Hirsch models in the future for predicting dynamic modulus values:

Revised Witczak model for SCDOT:

$$\log(|E^*|) = -0.345 + 0.822\left(|G_b^*|^{-0.0052}\right)\cdot\left(\begin{array}{l} 6.65 - 0.032\rho_{200} + 0.0027\rho_{200}^{2} - 0.011\rho_4 - 0.0001\rho_4^{2} \\ + 0.006\rho_{38} - 0.00014\rho_{38}^{2} - 0.08V_a - 1.06\left(\dfrac{V_{beff}}{V_a + V_{beff}}\right) \end{array}\right) + \frac{2.558 + 0.032V_a + 0.713\left(\dfrac{V_{beff}}{V_a + V_{beff}}\right) + 0.0124\rho_{38} + 0.0001\rho_{38}^{2} - 0.0098\rho_{34}}{1 + e^{\left(-0.7814 - 0.5785\log|G_b^*| + 0.8834\log(\delta_b)\right)}}$$

Revised Hirsch model for SCDOT:

$$|E^*| = Pc\left[3960000\left(1 - \frac{VMA}{100}\right) + 3|G^*|_{binder}\left(\frac{VFA \cdot VMA}{10{,}000}\right)\right] + (1 - Pc)\left[\frac{1 - \dfrac{VMA}{100}}{4{,}200{,}000} + \frac{VMA}{VFA \cdot 3|G^*|_{binder}}\right]^{-1}$$

d) Flow number values of the various mixtures included in this study could not be predicted effectively in terms of the current models considered in this study. Many other researchers around the country have indicated inconsistencies with the current models as well; however, more effective models might be developed in the future.

7. Additional conclusions included:

a) In the original proposal, one of the objectives was to test samples in the indirect tension (IDT) mode and compare the results to those from the axial test mode. However, the original proposal also assumed one testing temperature but allowed for input from the Steering Committee to choose additional testing temperatures. Near the beginning of the project, the Steering Committee selected two additional testing temperatures for dynamic modulus and phase angle. Due to the large amount of time it takes to test samples at multiple temperatures, the IDT mode testing could not be completed to allow for the additional requested testing temperatures to be completed. Additionally, the literature review for this project revealed evidence of a strong correlation between |E*| values obtained by axial and IDT testing, so testing in both modes may not be necessary.

b) For the mixtures in this study, the current SCDOT mix design procedures did not exhibit a need to be changed for the RAP percentages from 0% to 35%. However, it might be necessary to change the constants for the models for RAP percentages higher than 35% since higher RAP percentages were not examined in this study. This would require more in-depth testing to determine the appropriate values.

c) The results of this study did not show a need for changes to the existing approved materials list for the selection of qualified materials for various asphalt mixtures in SC. Some of these values could be used as an input into the MEPDG program without any modifications to the mix design.

d) Evaluation of field cores using AMPT was assigned by SCDOT to a different research project.

7.3 Recommendations

The researchers offered the following recommendations based on the results of this study:

1. Because only RAP percentages currently used by SCDOT were utilized in this study, it might be necessary in the future to change the constants for the models for higher RAP percentages than those currently allowed by SCDOT. This would require more in-depth testing to determine the appropriate values.

2. It is recommended that SCDOT engineers use the tables and inputs in Appendix E for use in the new MEPDG pavement design procedures. These tables contain all the necessary input data for the MEPDG software program. The numbers in these tables might have to be adjusted for future changes in variables (e.g., higher percentages of RAP use).

3. It is recommended that the SCDOT use the existing approved materials list for the selection of qualified materials for various mixtures around the state. Some of these values could be used as an input into the MEPDG program without any modifications to the mix design.

4. There is much more research needed to calibrate more models with respect to the AMPT system for use in the MEPDG program (e.g., base materials, subbase materials, open-graded friction course mixtures).

5. A comprehensive laboratory study of field mixtures should be completed to correlate the field mixture data to the laboratory mixture data from this study. These mixtures should

include all types of mixtures (e.g., Surface, Intermediate, and Base), RAP materials, liquid anti-stripping agents (ASAs), and warm mix asphalt (WMA) technologies.

8 References Cited or Reviewed

1. “AASHO Road Test, History and Description of Project”, Highway Research Board (HRB) Special Report 61A, National Academy of Sciencs, Washington, D.C., 1961.
2. “AASHO Road Test”, http://www.pavementinteractive.org/article/aasho-road-test/
3. “AASHTO Interim Guide for Design of Pavement Structures”, American Association of State Highway and Transportation Officials, Washington, D.C., 1972.
4. “AASHTO Interim Guide for Design of Pavement Structures Chapter III Revised”, American Association of State Highway and Transportation Officials, Washington, D.C., 1981.
5. “AASHTO Guide for Design of Pavement Structures Volume 2”, American Association of State Highway and Transportation Officials, Washington, D.C., 1986.
6. “AASHTO Guide for Design of Pavement Structures 1993”, American Association of State Highway and Transportation Officials, Washington, D.C., 1993.
7. “AASHTO Mechanisitic-Empirical Pavement Design Guide: A Manual of Practice, Interim Edition”, American Association of State Highway and Transportation Officials, Washington, D.C., 2008.
8. “AASHTO R30, Mixture Conditioning of Hot Mix Asphalt (HMA)”, American Association of State Highway and Transportation Officials, AASHTO
9. “AASHTO T 322-07, Standard Method of Test for Determining the Creep Compliance and Strength of Hot-Mix Asphalt (HMA) Using the Indirect Tensile Test Device”, American Association of State Highway and Transportation Officials, AASHTO
10. “AASHTO T 342-11, Standard Method of Test for Determining Dynamic Modulus of Hot-Mix Asphalt”, American Association of State Highway and Transportation Officials, AASHTO
11. “AASHTO TP 79-13, Standard Method of Test for Determining Dynamic Modulus and Flow Number for Asphalt Mixtures Using the Asphalt Mixture Performance Tester (AMPT)”, American Association of State Highway and Transportation Officials, AASHTO
12. Abdo, A. Abu., F. Bayomy, R. Nielsen, T. Weaver, S.J. Jung, M.J. Santi (2009). Prediction of the dynamic modulus of Superpave mixes, proceedings of Bearing Capacity of Roads, Railways and Airfields, Taylor & Francis Group, London, ISBN 978-0-415-87199-0
13. Amirkhanian S., Xiao F., and Herndon D., 2014, “The Evaluation and Specification Development of Alternate Modified Asphalt Binders in South Carolina”, Report No. FHWA-SC-14-03, South Carolina Department of Transportation, 1406 Shop Road, Columbia, SC 29201.
14. Bari, J., and Witczak, M. W. (2006). “ Development of a New Revised Version of the Witczak |E*| Predictive Model for Hot Mix Asphalt Mixtures.” Journal of the Association of Asphalt Paving Technologists, Volume 75.
15. Baus, R.L. and Stires, N.R., 2010, “Mechanistic-Empirical Pavement Design Guide Implementation”, Report No. FHWA-SC-10-01, South Carolina Department of Transportation, 1406 Shop Road, Columbia, SC 29201.
16. Bhasin, A., Button, J.W., and Chowdhury, A., 2005, “Evaluation of Selected Laboratory Procedures and Development of Databases for HMA”, Report No. 0-4203-3, Texas Transportation Institute, College Station, TX.

17. Bennert T., 2010, “Dynamic Modulus of Hot Mix Asphalt”, Report No. FHWA-NJ-2009-011, New Jersey Department of Transportation.
18. Birgisson, B. and Roque, R., 2005, “Evaluation of the Gradation Effect on the Dynamic Modulus”, Transportation Research Record: Journal of the Transportation Research Board, No. 1929, pp. 193 – 199.
19. Bonaquist, R., 2008, “Refining the Simple Performance Tester for Use in Routine Practice”, NCHRP Report 614, National Cooperative Highway Research Program, Washington, D.C.
20. Bonaquist, R.F. (2008), NCHRP Report 629: Ruggedness Testing of the Dynamic Modulus and Flow Number Tests with the Simple Performance Tester, National Cooperative Highway Research Program, Washington, D.C.
21. Birgisson, B., Sholar, G. and Roque, R., 2005, "Evaluation of a Predicted Dynamic Modulus for Florida Mixtures," 84th Annual Meeting of the Transportation Research Board, Washington D.C..
22. Bonaquist, R. and Christensen, D., 2005, “Practical Procedure for Developing Dynamic Modulus Master Curves for Pavement Structural Design”, Transportation Research Record: Journal of the Transportation Research Board, No. 1929, pp. 208 – 217.
23. Christensen, D.W., Pellinen, T. and Bonaquist, R., 2003, “Hirsch Model for Estimating the Modulus of Asphalt Concrete”, Asphalt Paving Technology, Association of Asphalt Paving Technologists, Vol. 72, pp. 97 – 121.
24. Christensen, D. et al., 2009, “A Mix Design Manual for Hot-Mix Asphalt”, NCHRP Report 9-33, Transportation Research Board, National Research Council, Washington, D.C.
25. Cross, S.A., Jakatimath, Y. and Sumesh, K.C., 2007, “Determination of Dynamic Modulus Master Curves for Oklahoma HMA Mixtures”, Oklahoma Department of Transportation, Planning & Research Division, 200 N.E. 21st Street, Room 3A7, Oklahoma City, OK 73105.
26. Dougan, E.C., Stephens, E.J., Mahoney, J., and Hansen, S., 2003, “Dynamic Modulus Test Protocol – Problems and Solutions”, University of Connecticut, 179 Middle Turnpike, U-202, Storrs, CT 06269-5202.
27. Flintsch, G.W., Loulizi, A., Diefenderfer, S.D., Diefenderfer, B.K, and Galal, K. A., 2008, “Asphalt Materials Characterization in Support of the Mechanistic-Empirical Pavement Design Guide Implementation Efforts in Virginia”, Transportation Research Record, Vol. 2057, pp. 114-125.
28. Huang, Y. H., *Pavement Analysis and Design*, Prentice-Hall, Inc., Englewood Cliffs, NJ, 1993.
29. Hall, K.D., Xiao, D.X. and Wang, K., 2011, “Calibration of the MEPDG for Flexible Pavement Design in Arkansas”, 2011 Transportation Research Board CD-ROM, Transportation Research Board.
30. Harman, T., “Using the Dynamic Modulus Test to Assess the Mix Strength of HMA”, Public Roads, May/June, Vol. 64 · No. 6, 2001.
31. Kaloush, K.E., 2001, “Simple Performance Test for Permanent Deformation of Asphalt Mixtures”, Doctoral Dissertation, Department of Civil and Environmental Engineering, Arizona State University, Tempe, AZ.

32. Kim, Y.R., King, M., and Mostafa, M., 2004, “Typical Dynamic Moduli Values of Hot Mix Asphalt in North Carolina and Their Prediction.” Transportation Research Board Annual Meeting CD-ROM, Washington, D.C.
33. Kvanak et al.(2007), Statistical development of a flow number predictive equation for the Mechanistic-Empirical Pavement Design Guide TRB Annual Meeting Paper 07-1000,.
34. King, M., 2004, “Determination of Dynamic Moduli in Uniaxial Compression for North Carolina Hot Mix Asphalt Concrete”, A Thesis Submitted in Partial Fulfillment of the Requirements for the Degree of Master of Science, North Carolina State University.
35. Kvanak et al., 2007, “Statistical Development of a Flow Number Predictive Equation for the Mechanistic-Empirical Pavement Design Guide”, TRB Annual Meeting, Paper 07-1000.
36. Mohammad, L., Kim, M., Raghavendra, A., and Obulareddy, S., 2014, “Characterization of Louisiana Asphalt Mixtures Using Simple Performance Tests and MEPDG”, LTRC Project No. 04-6B, Louisiana Transportation Research Center, Baton Rouge, LA 70808.
37. “NCHRP Report 1-37A: Guide for Mechanistic-Empirical Design of New and Rehabilitated Pavement Structures”, National Cooperative Highway Research Program, Transportation Research Board, National Research Council, Washington, D.C., 2004.
38. “SCDOT Pavement Design Guidelines”, South Carolina Department of Transportaiton, Office of Materials and Research, Pavement Design Unit, July 2008.
39. Shah, A., McDaniel, R., and Gallivan, V., 2005, “Evaluation of Mixtures Using Dynamic Modulus Tester: Results and Practical Considerations”, Electronic Journal of the Asphalt Paving Technology, Association of Asphalt Paving Technologists, Vol. 74E.
40. Shen, S. and Yu, H., 2012, “An Investigation of Dynamic Modulus and Flow Number Properties of Asphalt Mixtures in Washington State”, Transportation Northwest (TransNow), University of Washington, 135 More Hall, Seattle, WA 98195-2700
41. Tran, N. and Hall, K., 2006, “Dynamic Modulus of Hot-Mix Asphalt”, Transportation Research Record: Journal of the Transportation Research Board, No. 1970, Transportation Research Board, Washington, D.C., pp. 126 – 132.
42. Von Quintus, Harold L. and Moulthrop, James S., 2007, “Mechanistic-Empirical Pavement Design Guide Flexible Pavement Performance Prediction Models, Volume III Field Guide – Calibration and User’s Guide for the Mechanistic-Empirical Pavement Design Guide”, Montana Department of Transportation.
43. Witczak, M.W., 2007, “NCHRP Report 580: Specification Criteria for Simple Performance Tests for Rutting”, Transportation Research Board, National Research Council, Washington, DC.
44. Witczak, M.W., Kaloush, K.E., Pellien, T.K., El-Basyouny, M. and Von Quintus, H.L., 2002, “NCHRP Report 465: Simple Performance Test for Superpave Mix Design”, Transportation Research Board, National Research Council, Washington, DC.
45. Witczak, M.W. and Fonseca, O.A., 1996, “Revised Predictive Model for Dynamic (Complex) Modulus of Asphalt Mixtures”, Transportation Research Record 1540, pp. 15–23.
46. Yang, Enhui., Ping, W. V., Xiao, Y., and Qiu, Y., 2011, “A Simplified Predictive Model of Dynamic Modulus for Characterizing Florida Hot Mix Asphalt Mixtures”, 2011 Transportation Research Board CD-ROM, TRB Paper No. 11-1565.
47. Yu, J., 2012, “Modification of Dynamic Modulus Predictive Models for Asphalt Mixtures Containing Recycled Asphalt Shingles”, Dissertation, Iowa State University.

9 Appendix A - Dynamic Modulus and Phase Angle Values of Various Mixtures in Terms of Aggregate Source

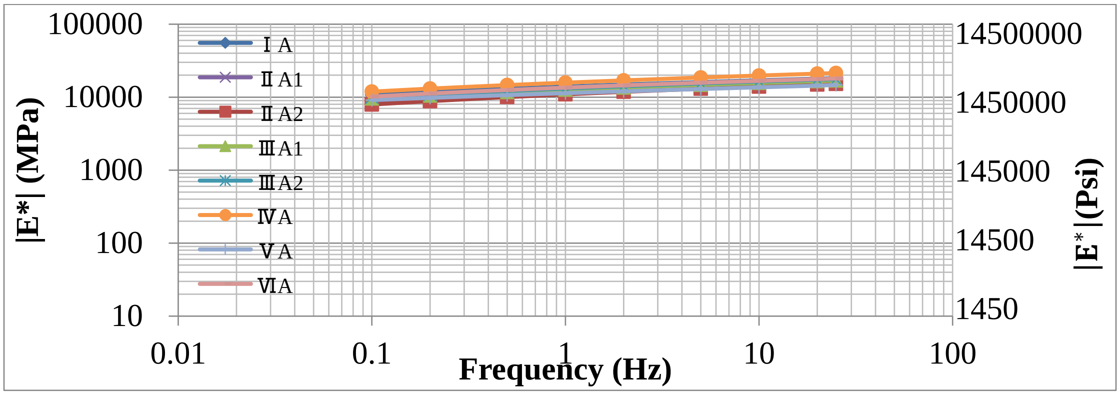

(a)

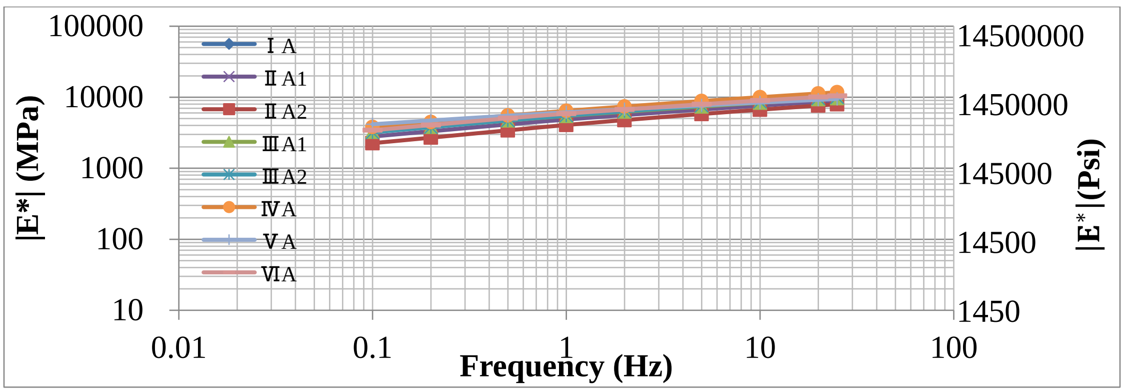

(b)

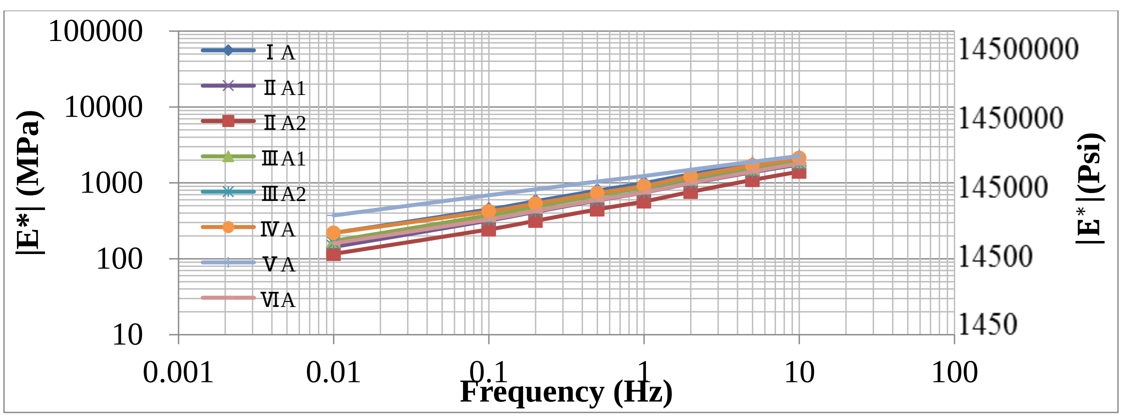

(c)

Figure 9-1 Dynamic Modulus Values of Various Surface Type A Mixtures with RAP in Terms of Aggregate Source, (a) at 4°C (39.2°F), (b) at 20°C (68°F), (c) at 40°C (104°F)

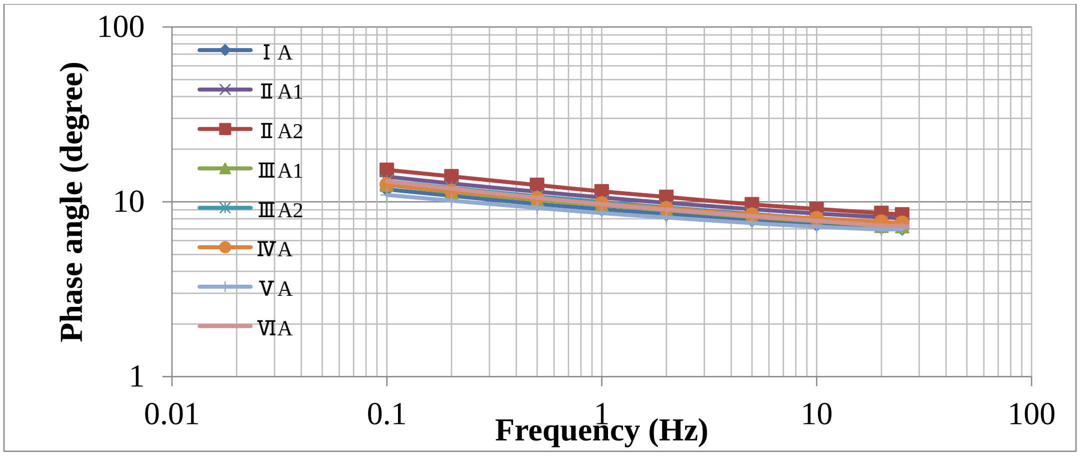

(a)

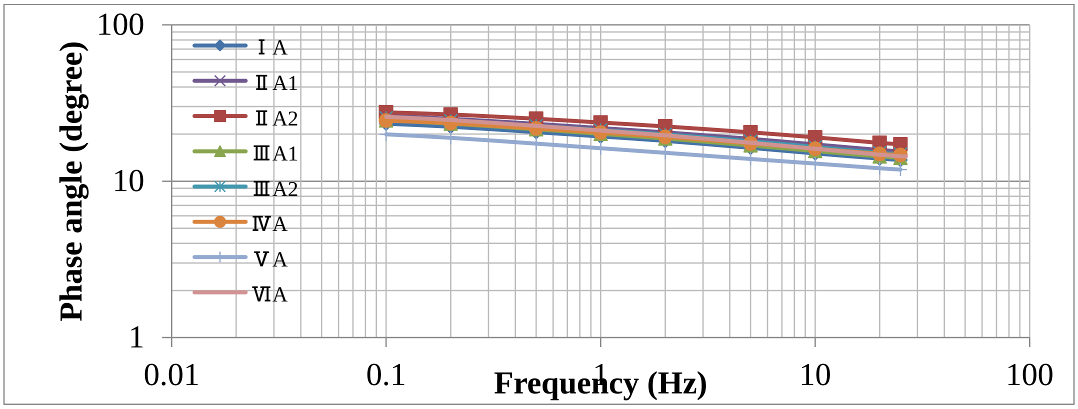

(b)

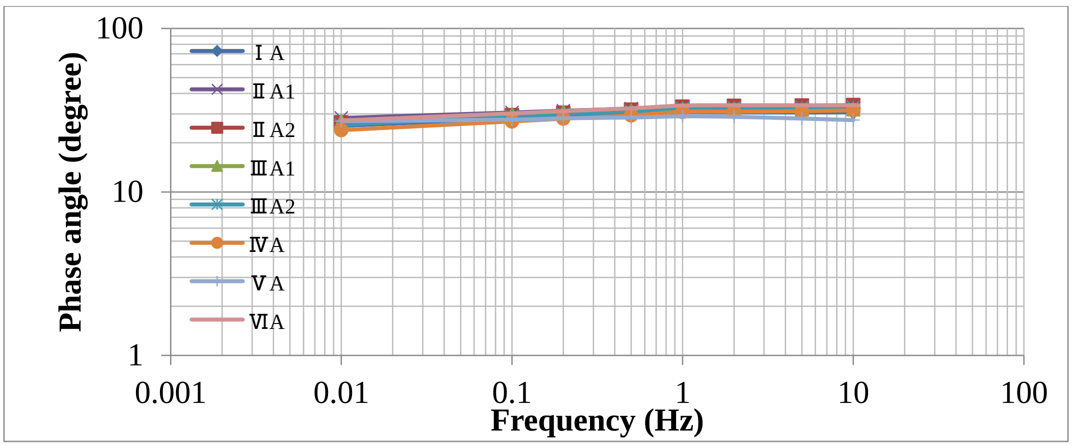

(c)

Figure 9-2 Phase Angle Values of Various Surface Type A Mixtures with RAP in Terms of Aggregate Source, (a) at 4°C (39.2°F), (b) at 20°C (68°F), (c) at 40°C (104°F)

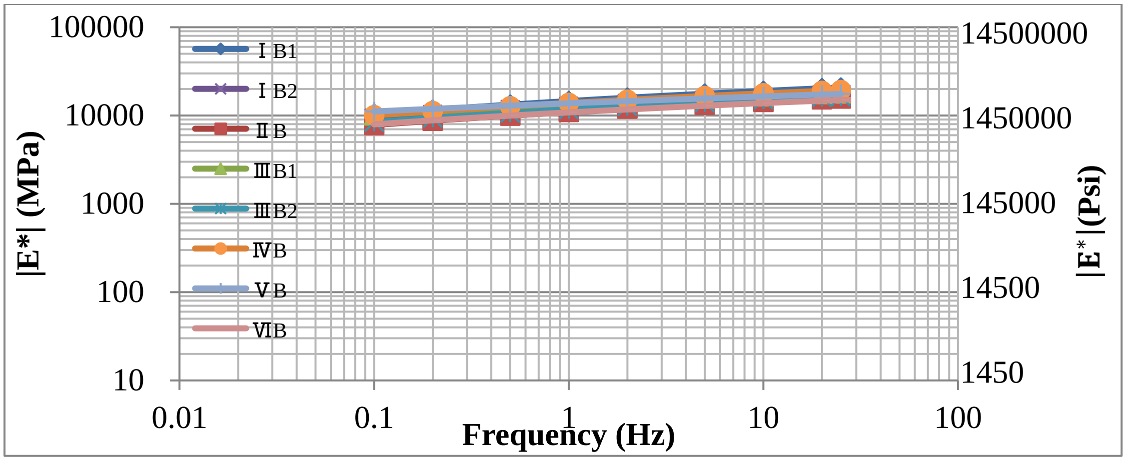

(a)

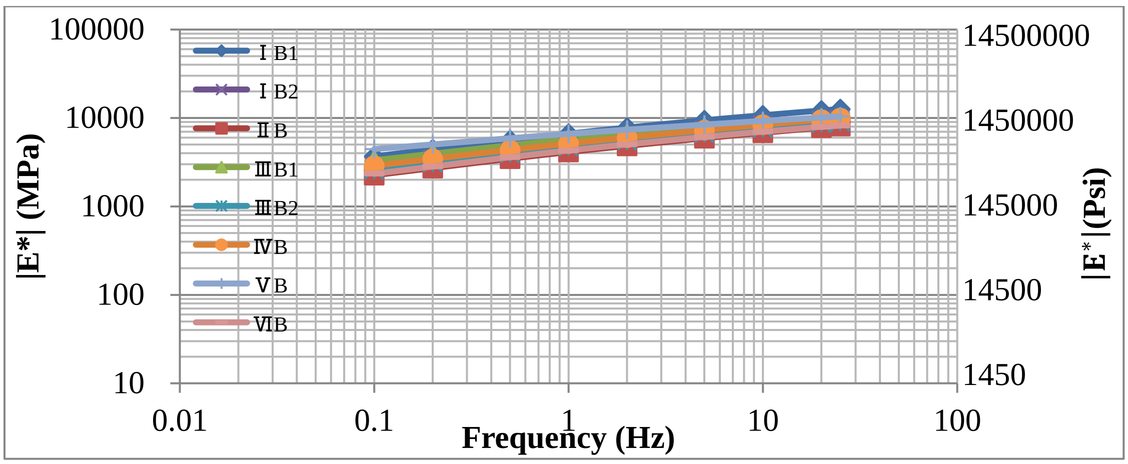

(b)

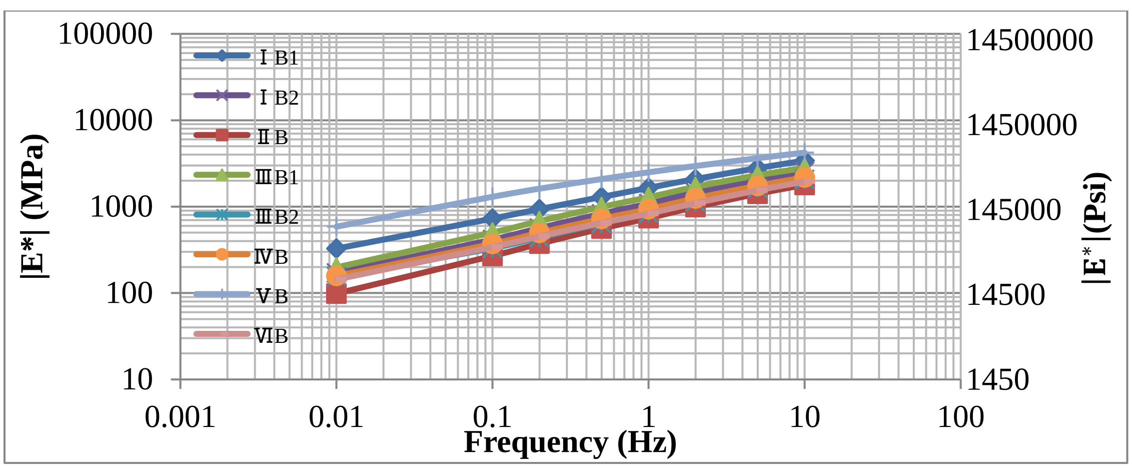

(c)

Figure 9-3 Dynamic Modulus Values of Various Surface Type B Mixtures with RAP in Terms of Aggregate Source, (a) at 4°C (39.2F), (b) at 20°C (68°F), (c) at 40°C (104°F)

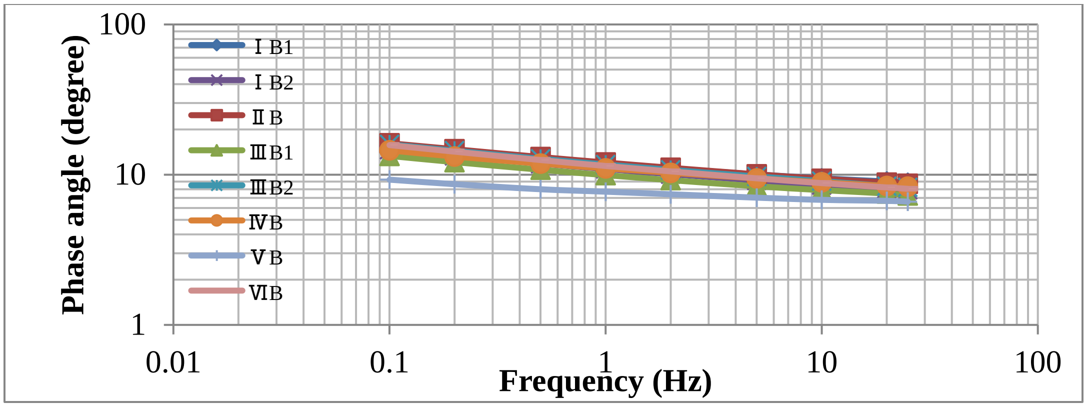

(a)

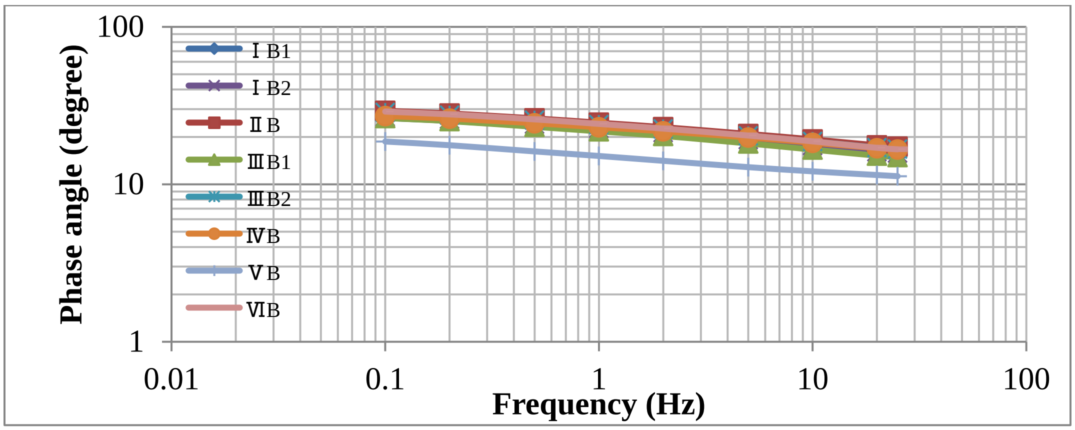

(b)

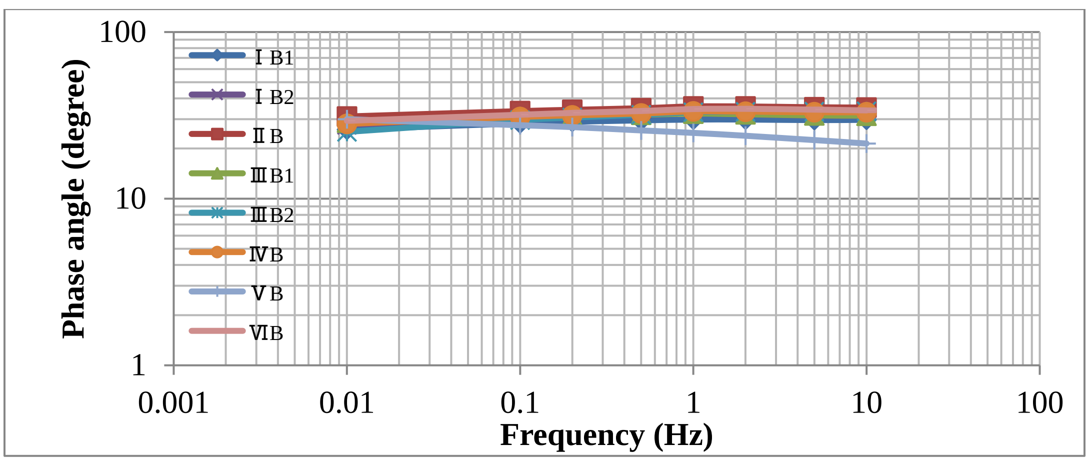

(c)

Figure 9-4 Phase Angle Values of Various Surface Type B Mixtures with RAP in Terms of Aggregate Source, (a) at 4°C (39.2°F), (b) at 20°C (68°F), (c) at 40°C (104°F)

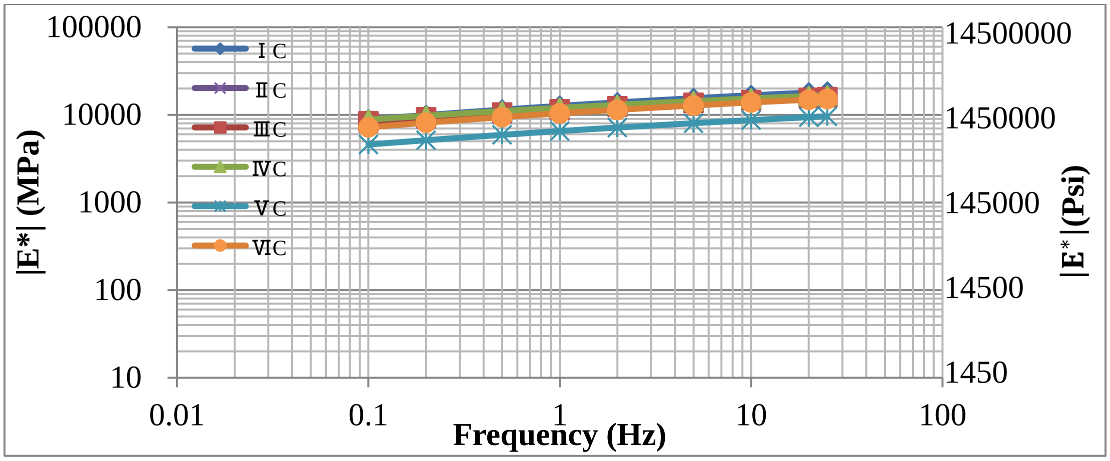

(a)

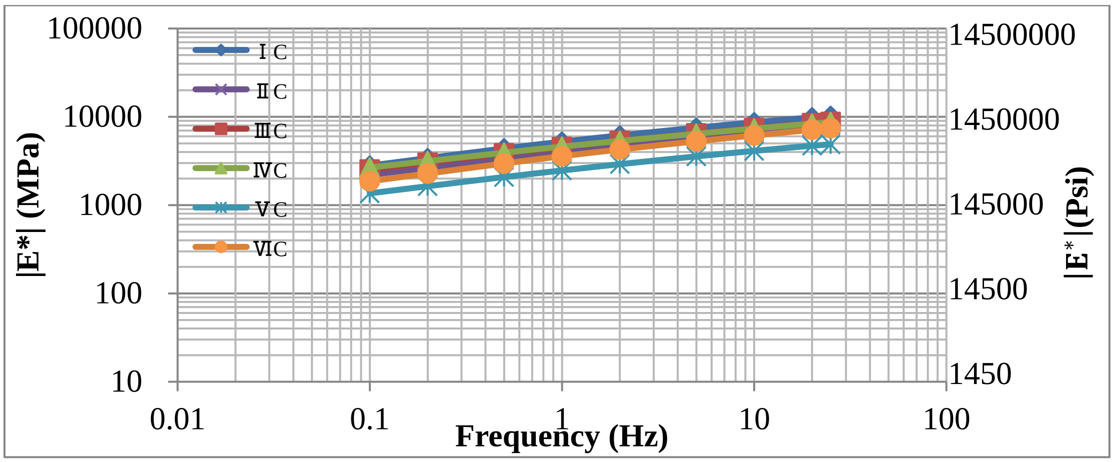

(b)

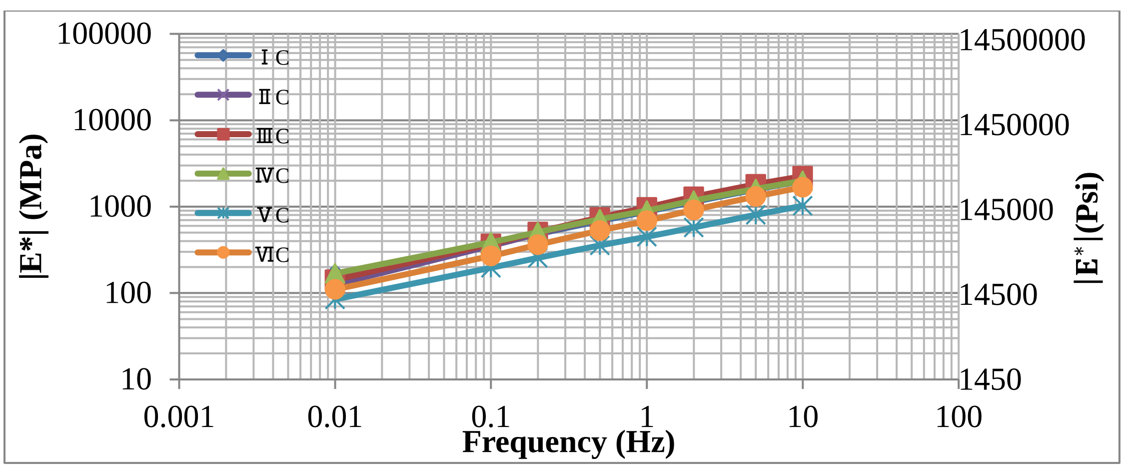

(c)

Figure 9-5 Dynamic Modulus Values of Various Surface Type C Mixtures with RAP in Terms of Aggregate Source, (a) at 4°C (39.2°F), (b) at 20°C (68°F), (c) at 40°C (104°F)

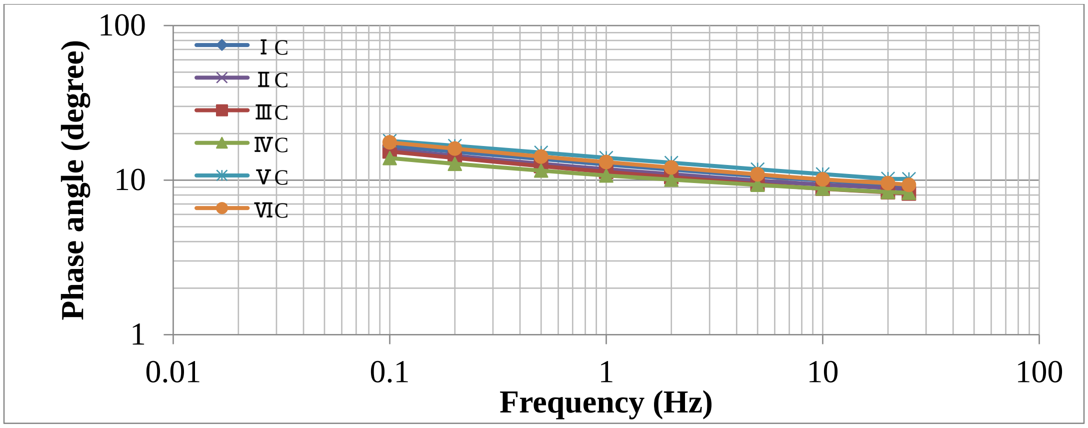

(a)

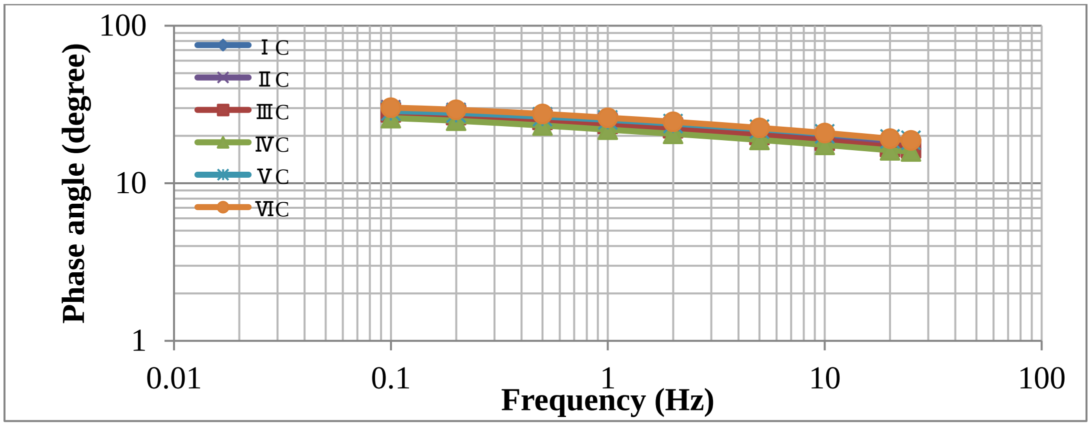

(b)

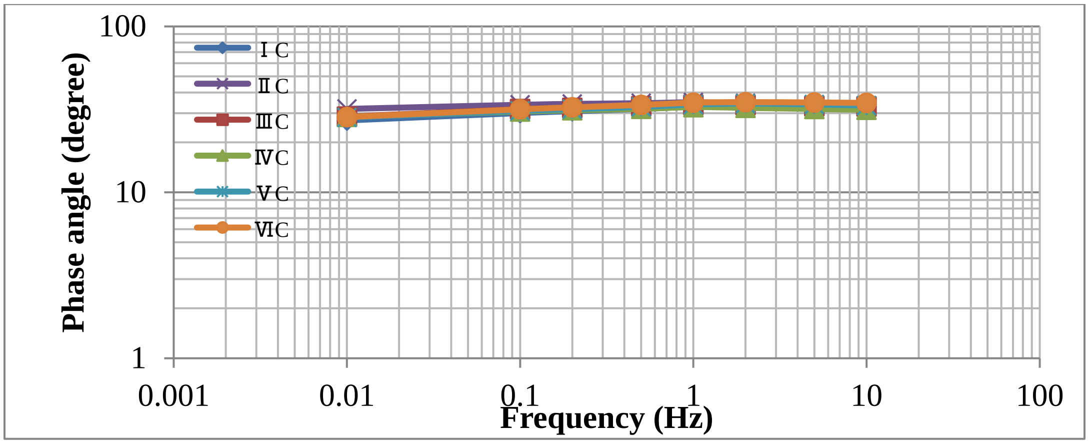

(c)

Figure 9-6 Phase Angle Values of Various Surface Type C Mixtures with RAP in Terms of Aggregate Source, (a) at 4°C (39.2°F), (b) at 20°C (68°F), (c) at 40°C (104°F)

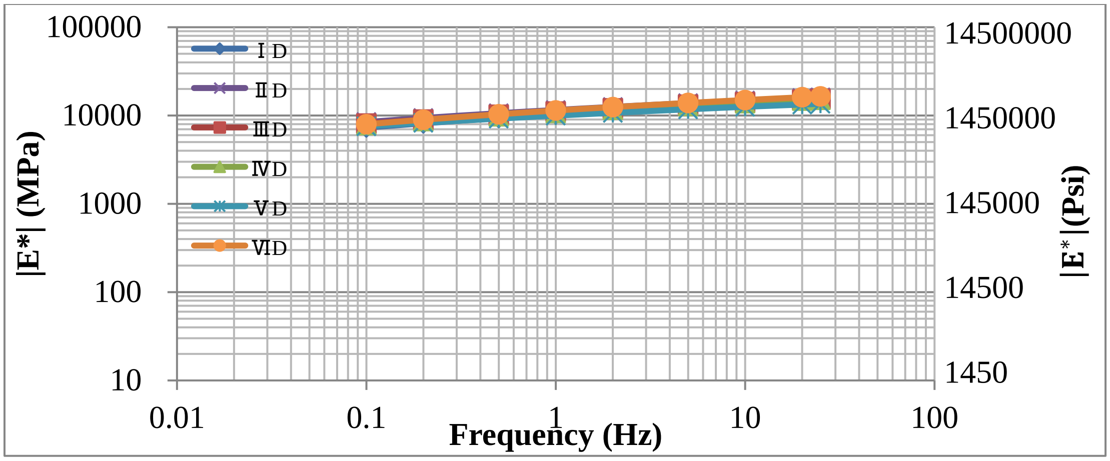

(a)

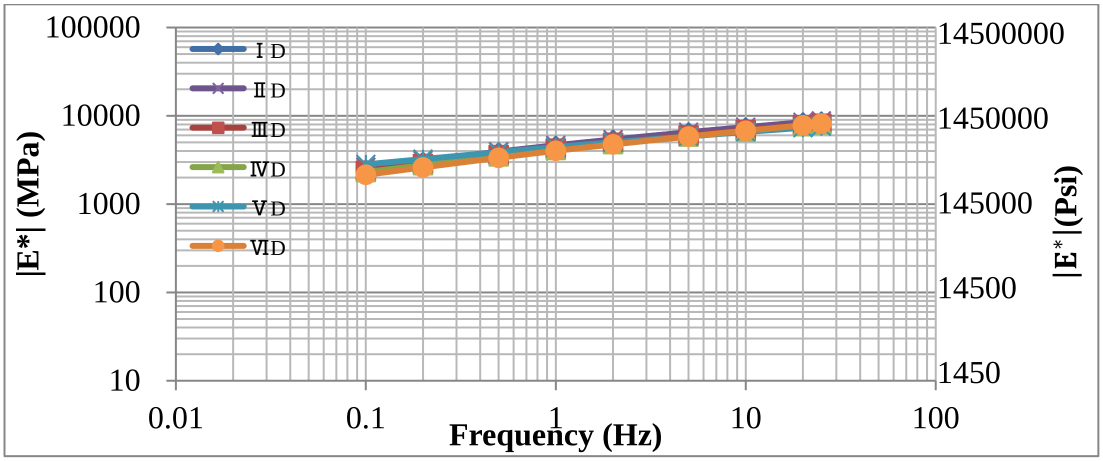

(b)

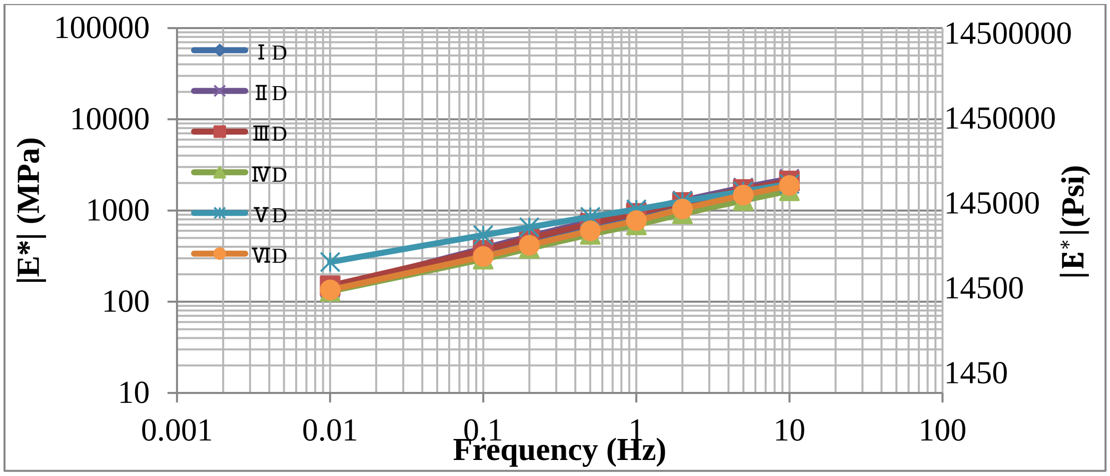

(c)

Figure 9-7 Dynamic Modulus Values of Various Surface Type D Mixtures with RAP in Terms of Aggregate Source, (a) at 4°C (39.2°F), (b) at 20°C (68°F), (c) at 40°C (104°F)

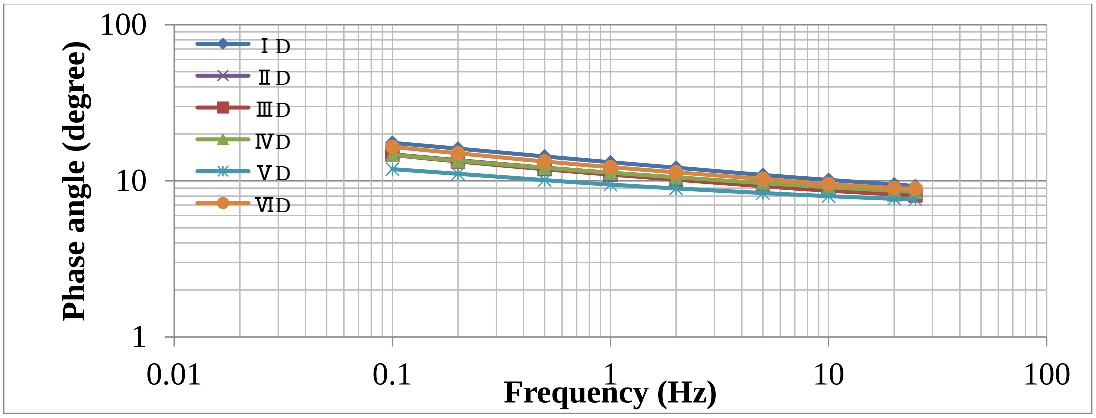

(a)

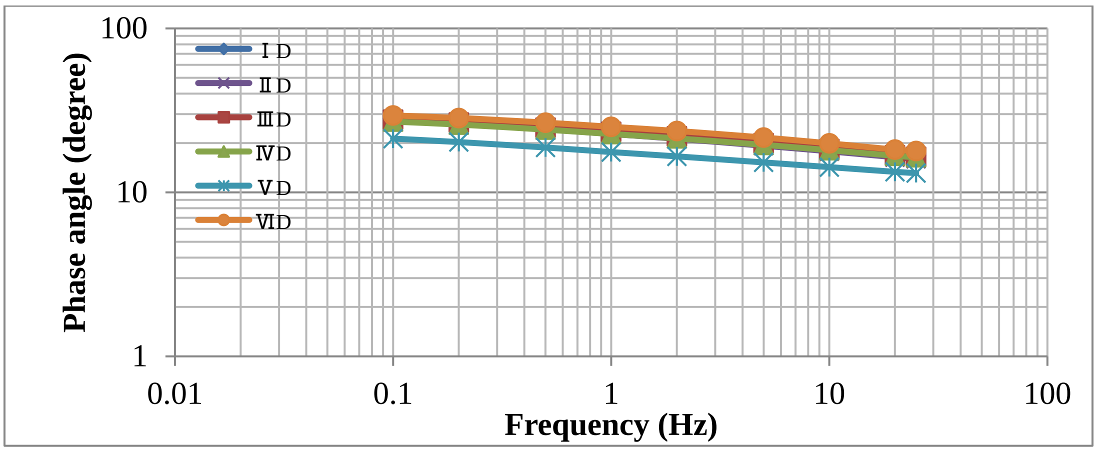

(b)

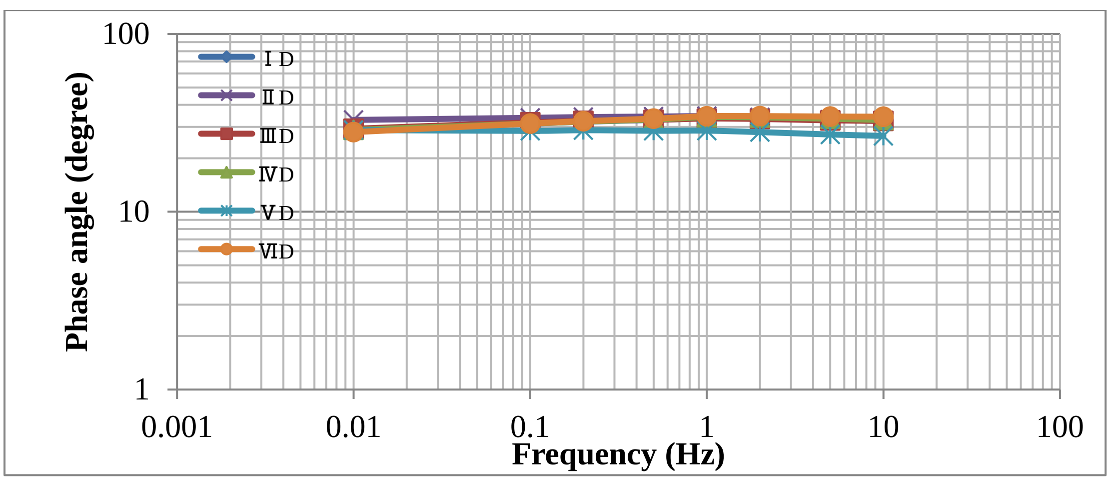

(c)

Figure 9-8 Phase Angle Values of Various Surface Type D Mixtures with RAP in Terms of Aggregate Source, (a) at 4°C (39.2°F), (b) at 20°C (68°F), (c) at 40°C (104°F)

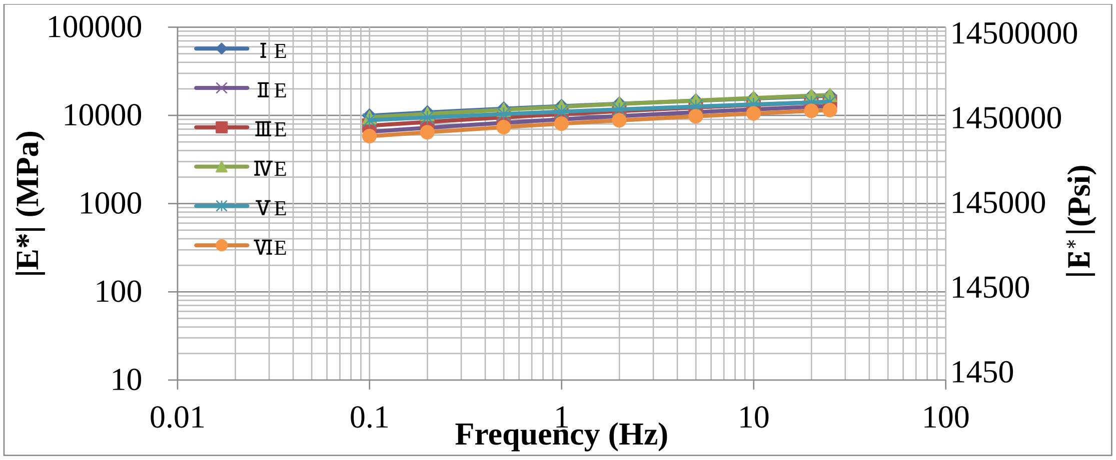

(a)

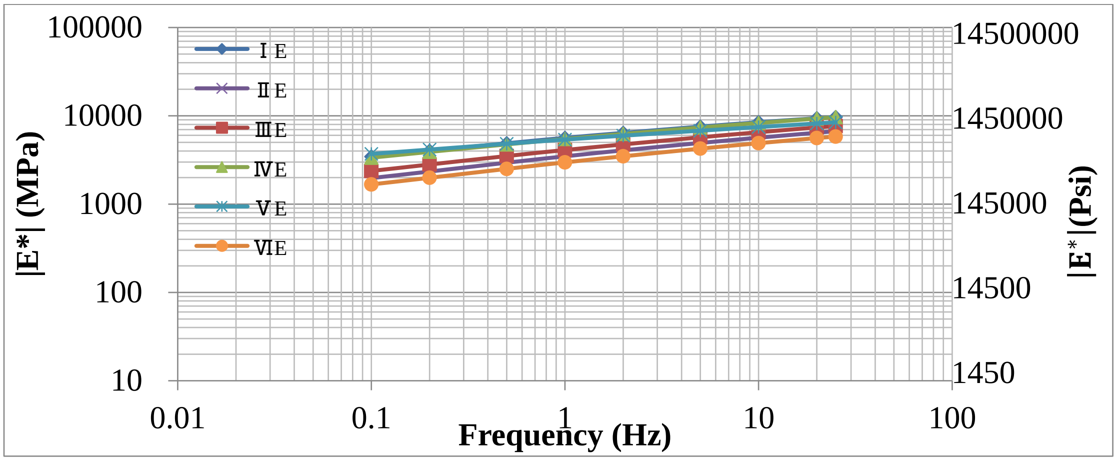

(b)

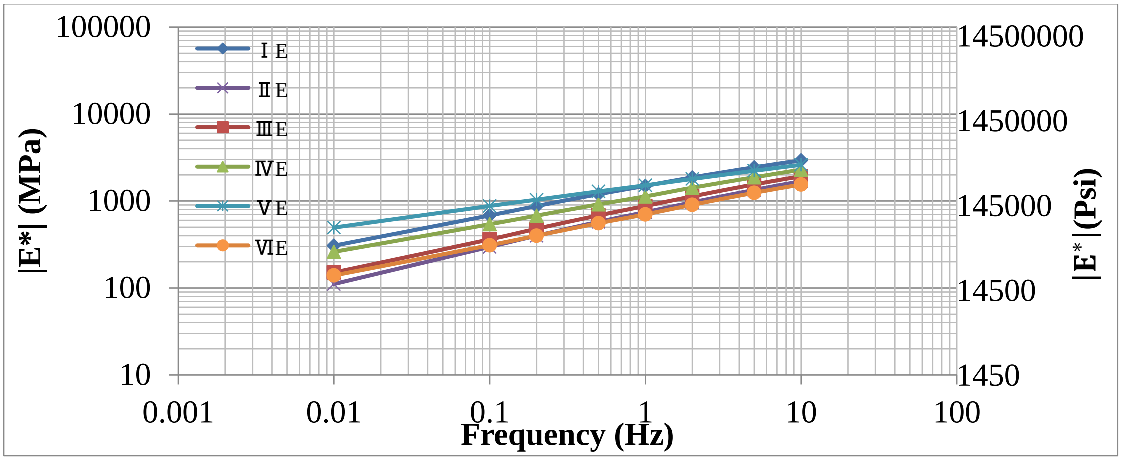

(c)

Figure 9-9 Dynamic Modulus Values of Various Surface Type E Mixtures with RAP in Terms of Aggregate Source, (a) at 4°C (39.2°F), (b) at 20°C (68°F), (c) at 40°C (104°F)

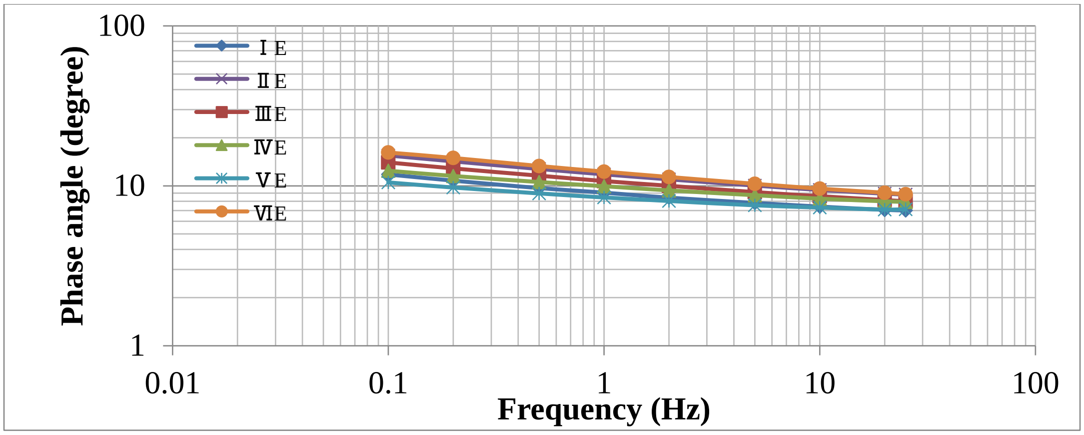

(a)

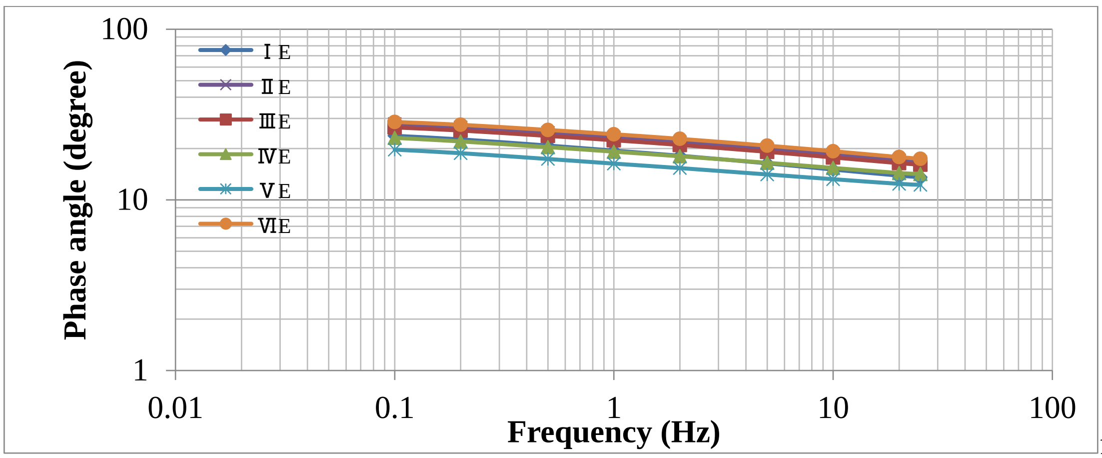

f

(b)

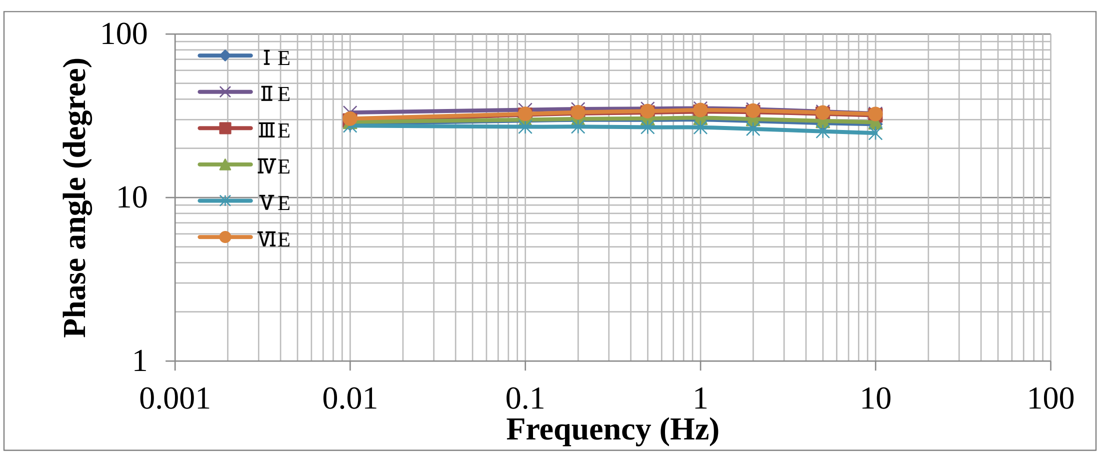

(c)

Figure 9-10 Phase Angle Values of Various Surface Type E Mixtures with RAP in Terms of Aggregate Source, (a) at 4°C (39.2°F), (b) at 20°C (68°F), (c) at 40°C (104°F)

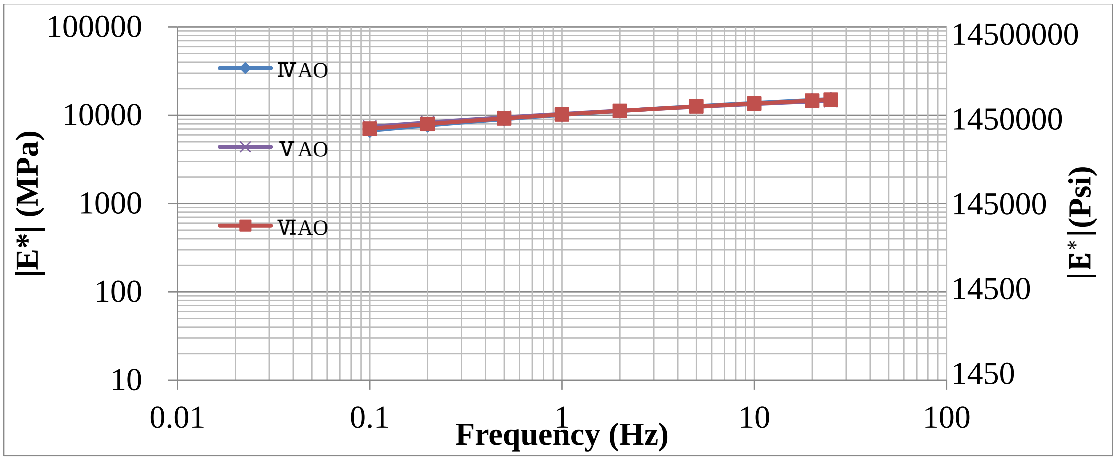

(a)

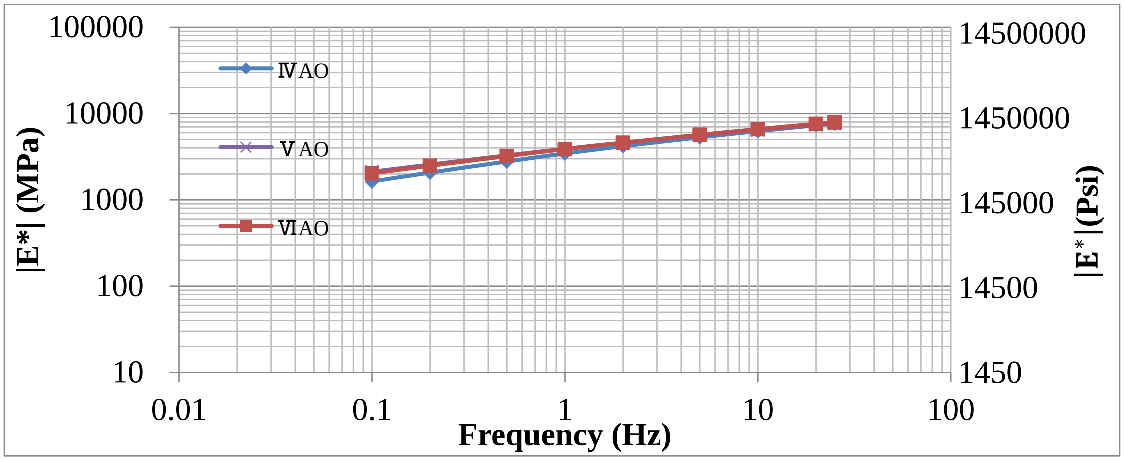

(b)

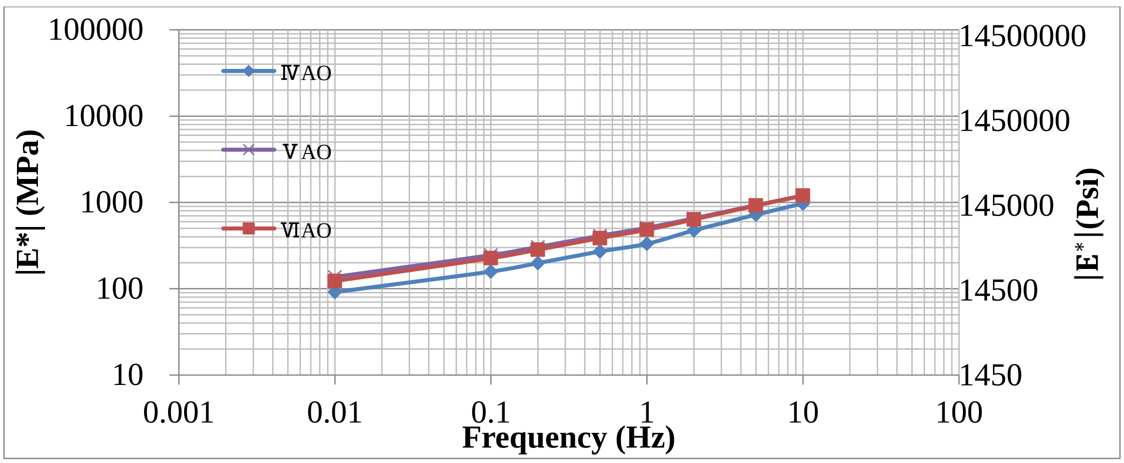

(c)

Figure 9-11 Dynamic Modulus Values of Various Surface Type A Mixtures without RAP in Terms of Aggregate Source, (a) at 4°C (39.2°F), (b) at 20°C (68°F), (c) at 45°C (113°F)

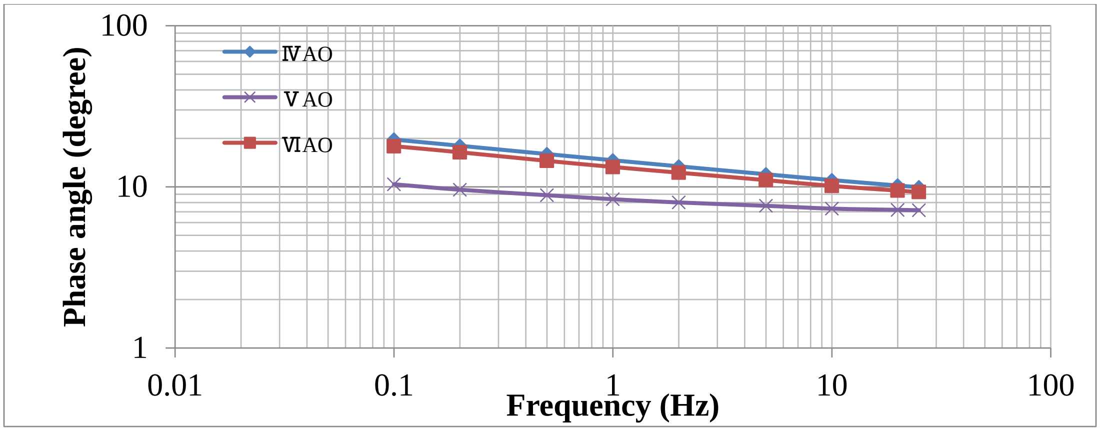

(a)

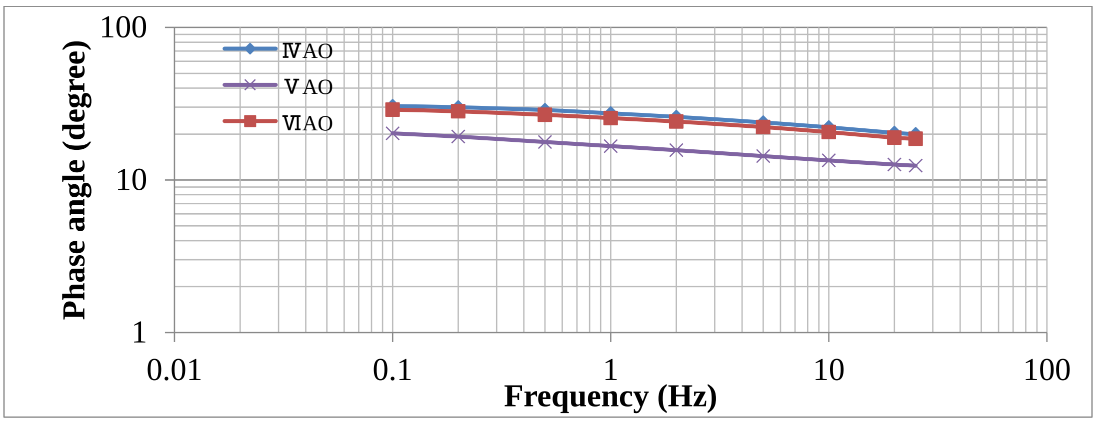

(b)

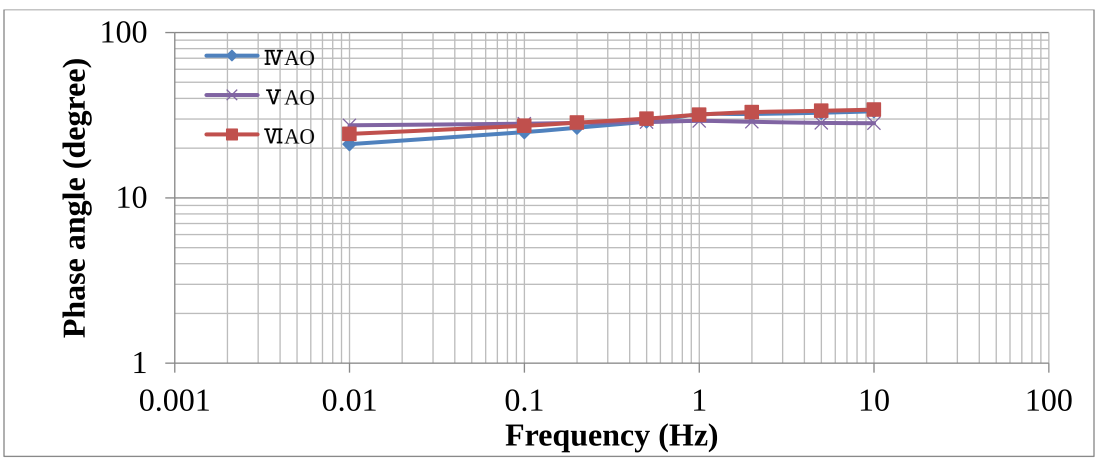

(c)

Figure 9-12 Phase Angle Values of Various Surface Type A Mixtures without RAP in Terms of Aggregate Source, (a) at 4°C (39.2°F), (b) at 20°C (68°F), (c) at 45°C (113°F)

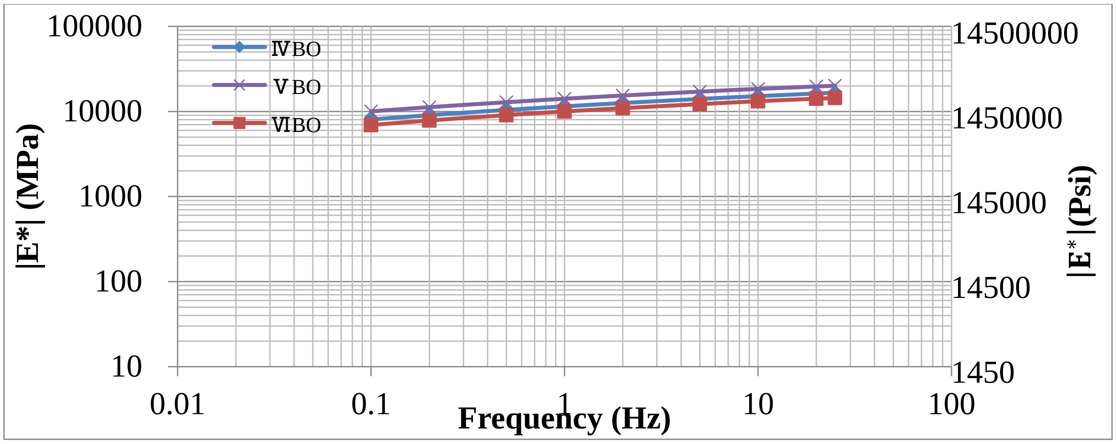

(a)

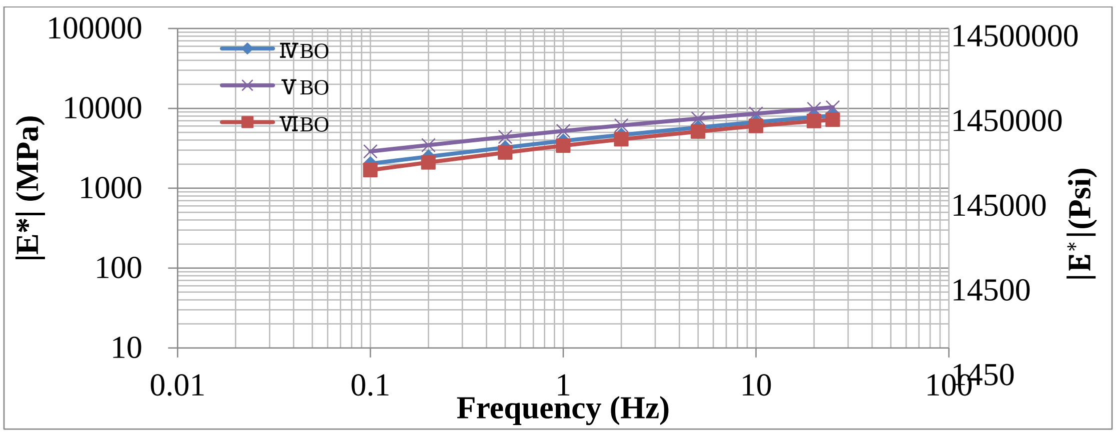

(b)

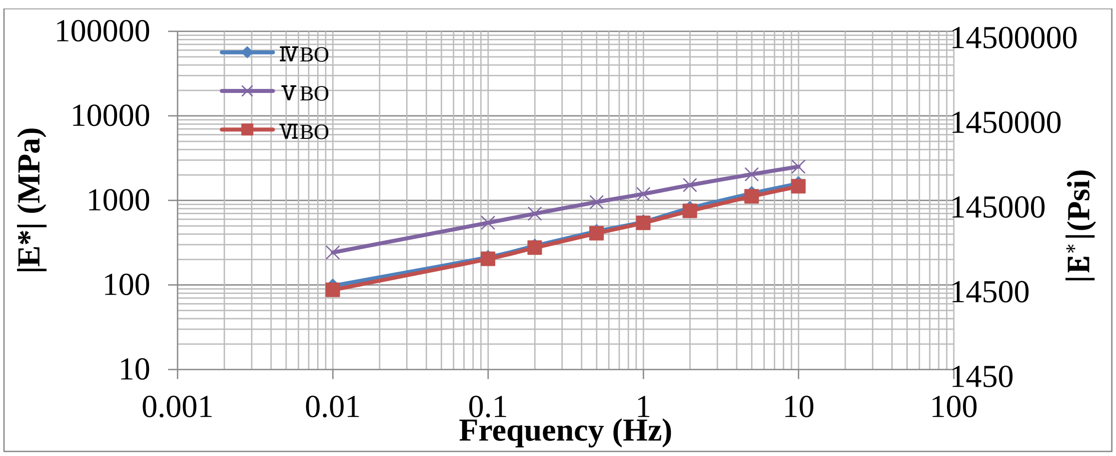

(c)

Figure 9-13 Dynamic Modulus Values of Various Surface Type B Mixtures without RAP in Terms of Aggregate Source, (a) at 4°C (39.2°F), (b) at 20°C (68°F), (c) at 40°C (104°F)

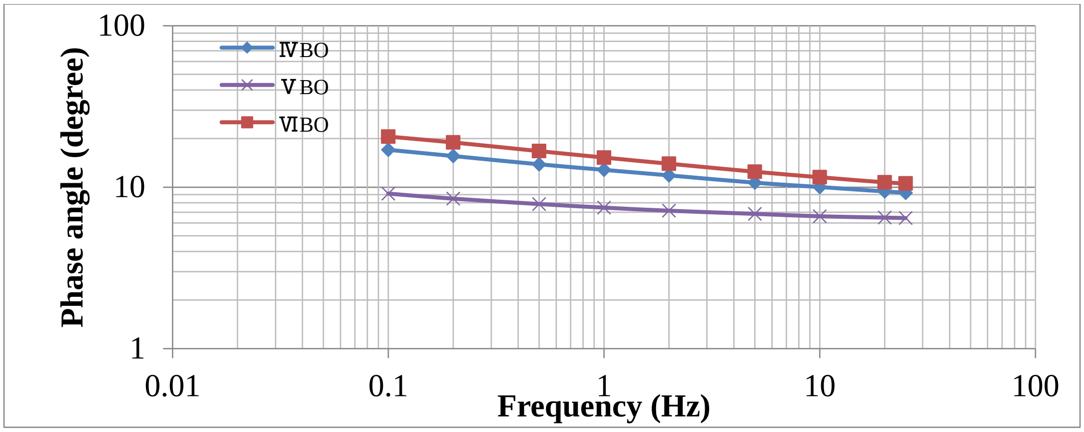

(a)

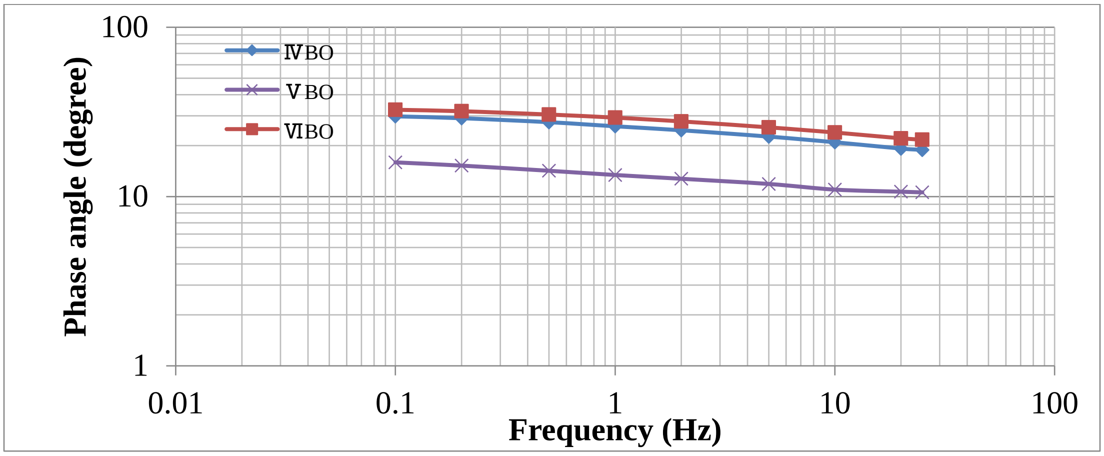

(b)

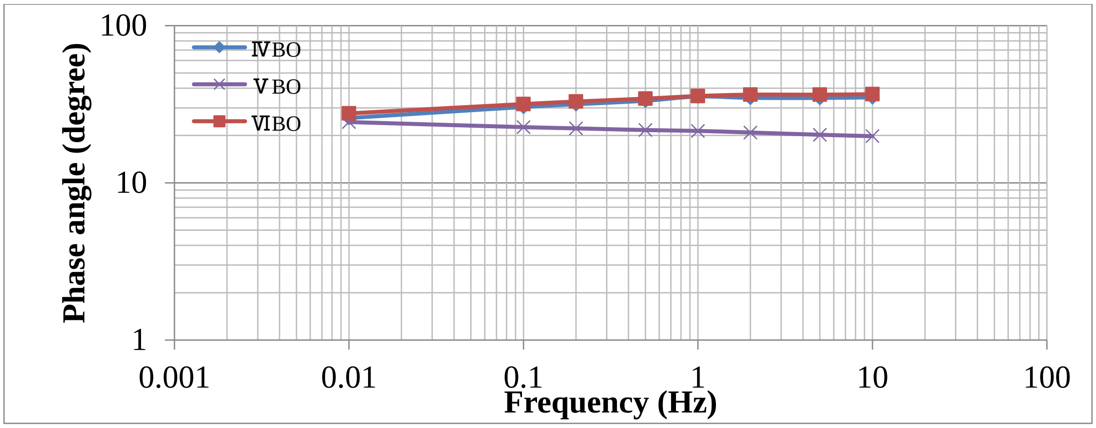

(c)

Figure 9-14 Phase Angle Values of Various Surface Type B Mixtures without RAP in Terms of Aggregate Source, (a) at 4°C (39.2°F), (b) at 20°C (68°F), (c) at 40°C (104°F)

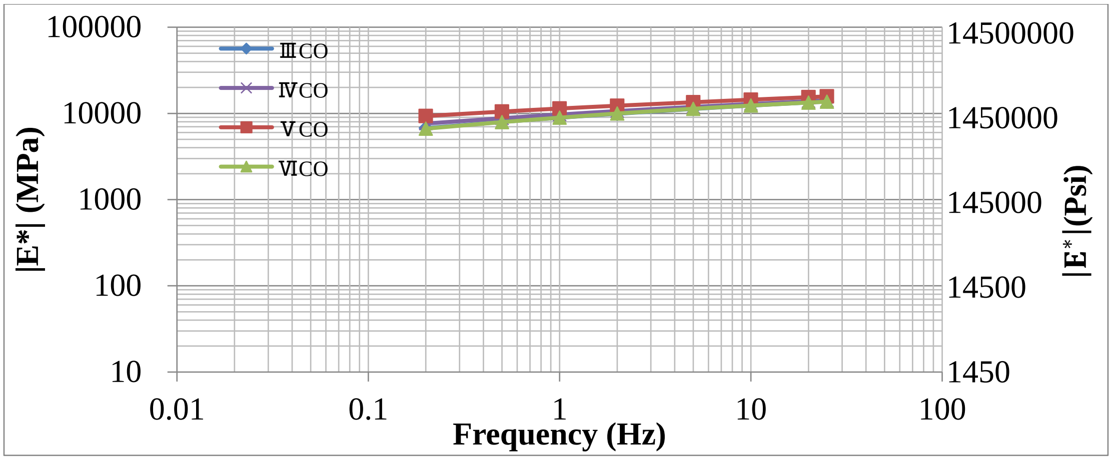

(a)

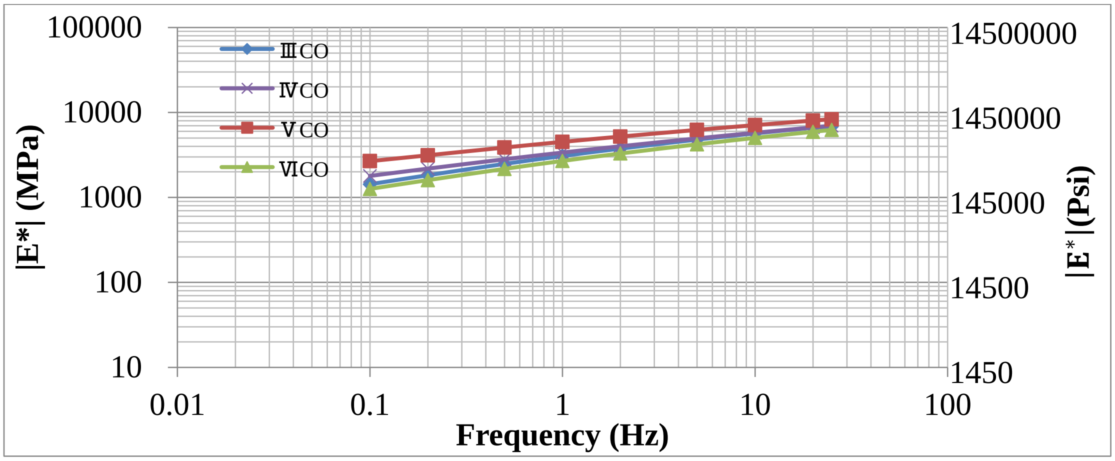

(b)

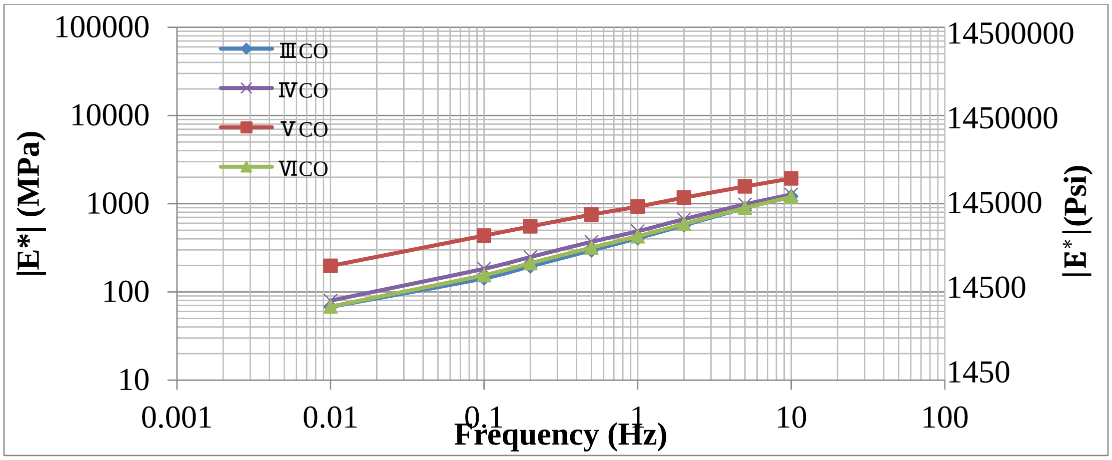

(c)

Figure 9-15 Dynamic Modulus Values of Various Surface Type C mixtures without RAP in Terms of Aggregate Source, (a) at 4°C (39.2°F), (b) at 20°C (68°F), (c) at 40°C (104°F)

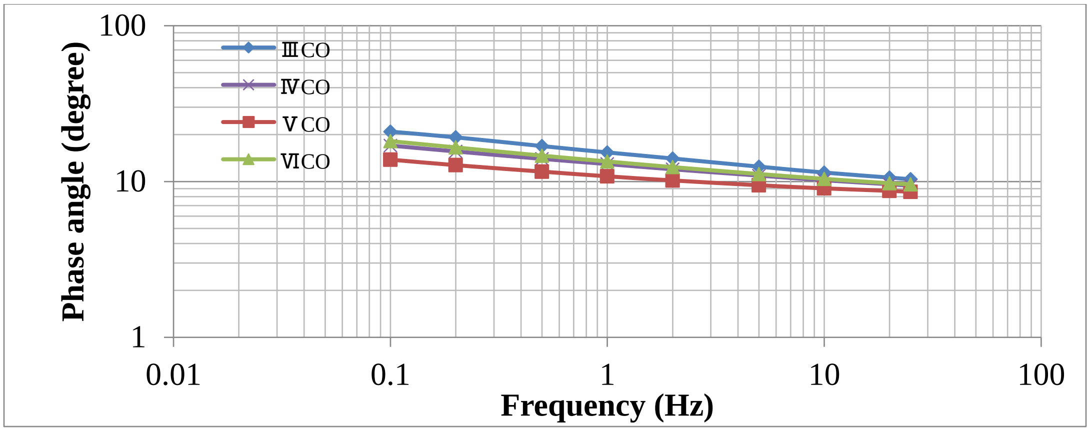

(a)

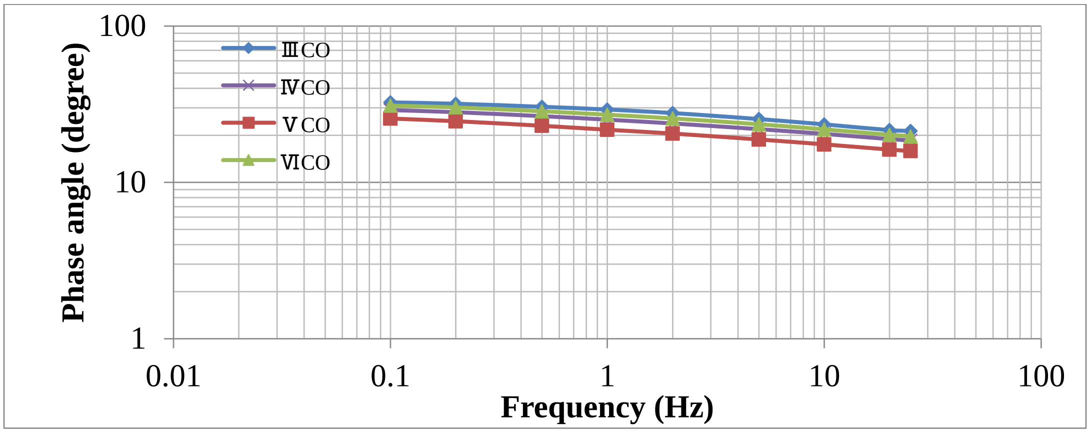

(b)

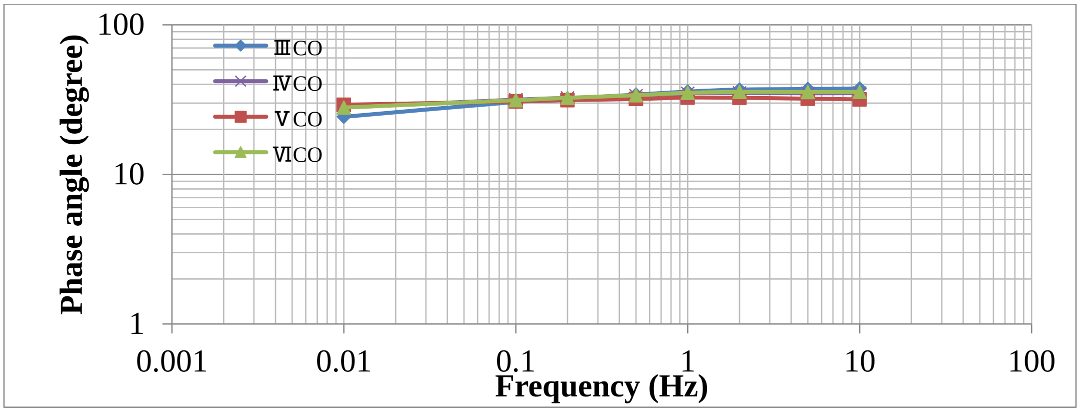

(c)

Figure 9-16 Phase Angle Values of Various Surface Type C Mixtures without RAP in Terms of Aggregate Source, (a) at 4°C (39.2°F), (b) at 20°C (68°F), (c) at 40°C (104°F)

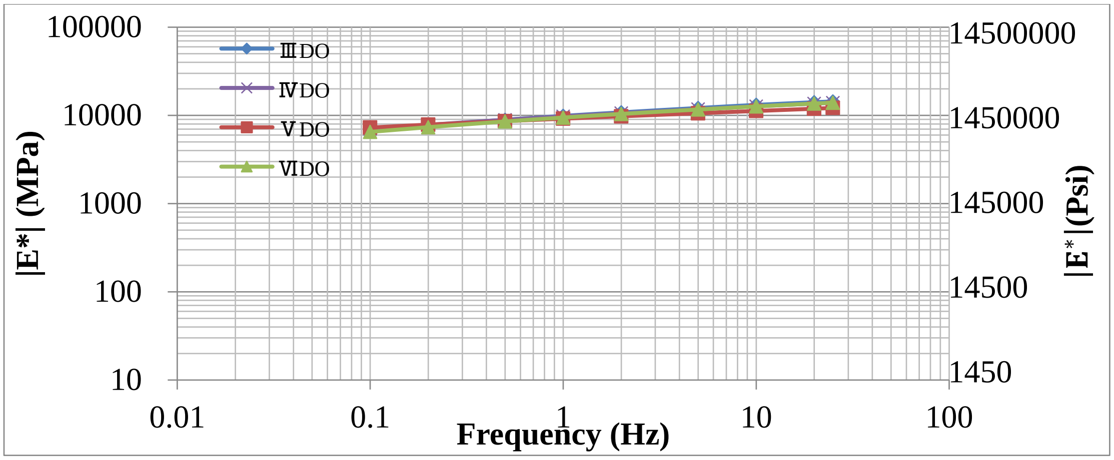

(a)

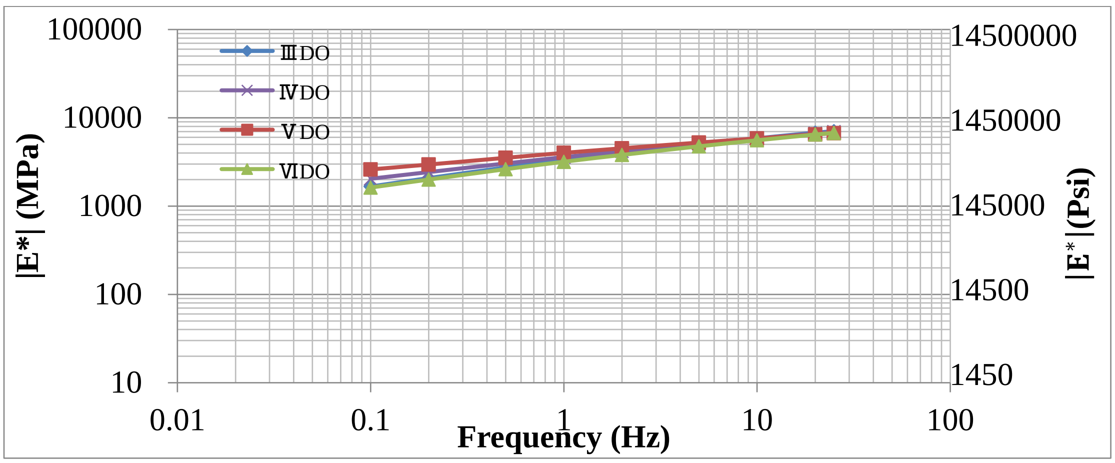

(b)

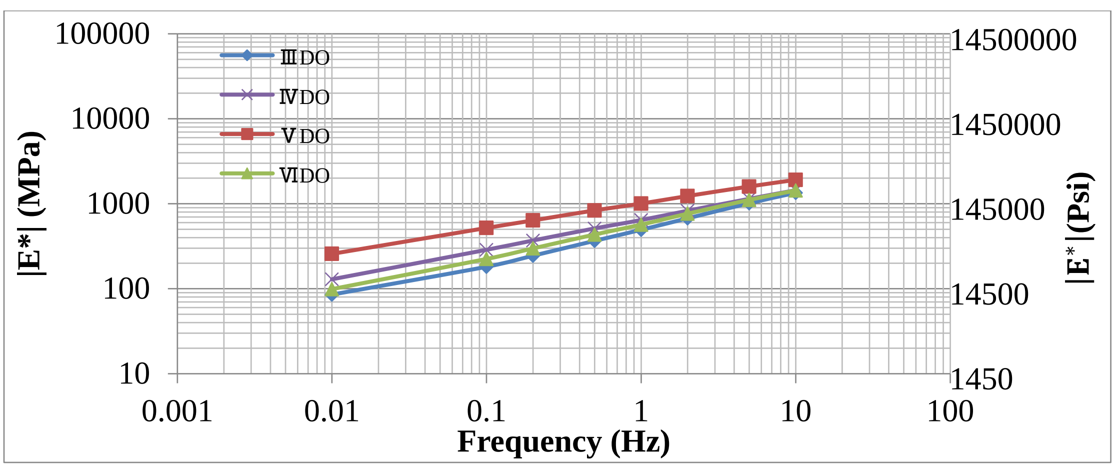

(c)

Figure 9-17 Dynamic Modulus Values of Various Surface Type D Mixtures without RAP in Terms of Aggregate Source, (a) at 4°C (39.2°F), (b) at 20°C (68°F), (c) at 40°C (104°F)

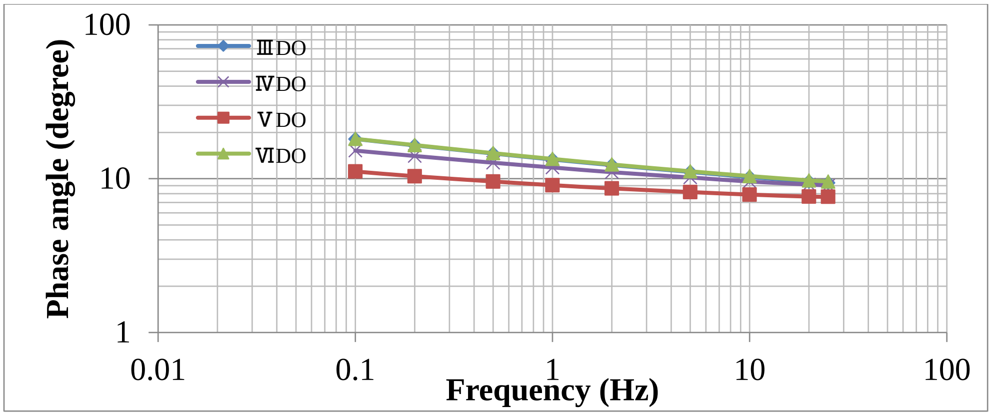

(a)

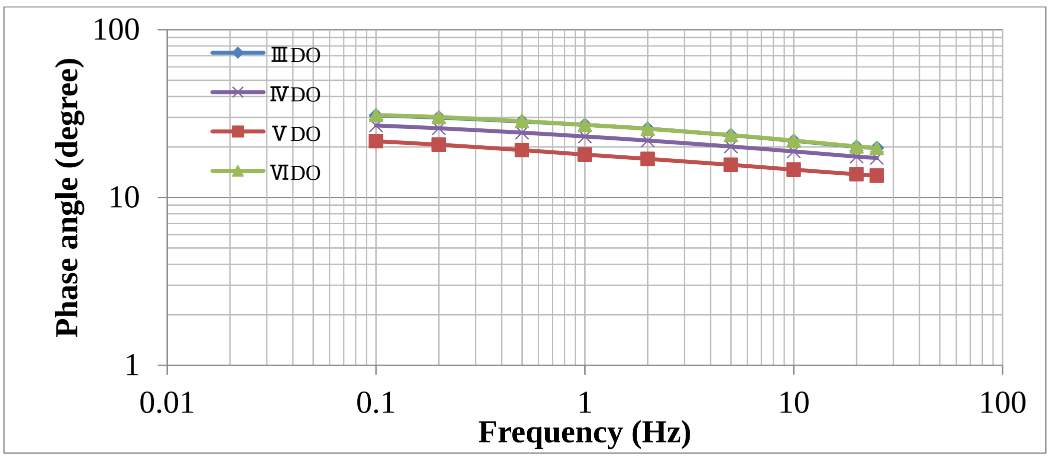

(b)

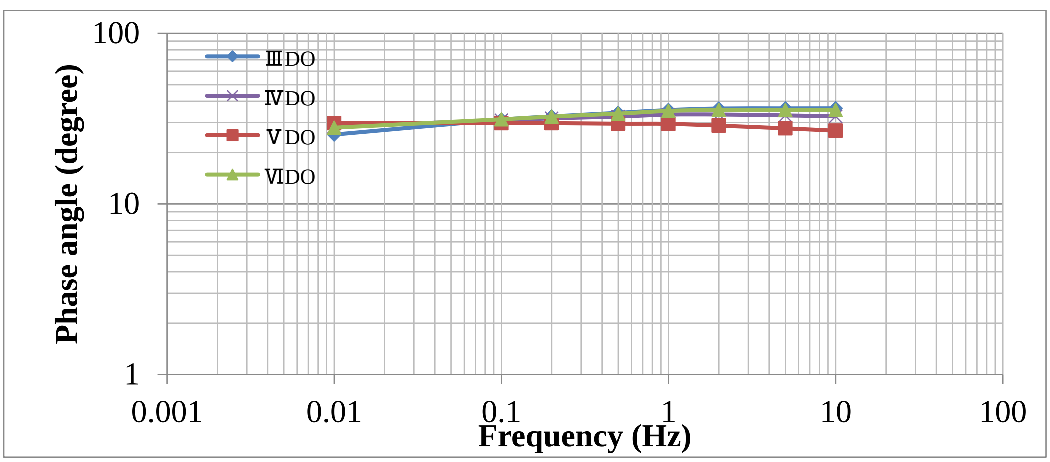

(c)

Figure 9-18 Phase Angle Values of Various Surface Type D Mixtures without RAP in Terms of Aggregate Source, (a) at 4°C (39.2°F), (b) at 20°C (68°F), (c) at 40°C (104°F)

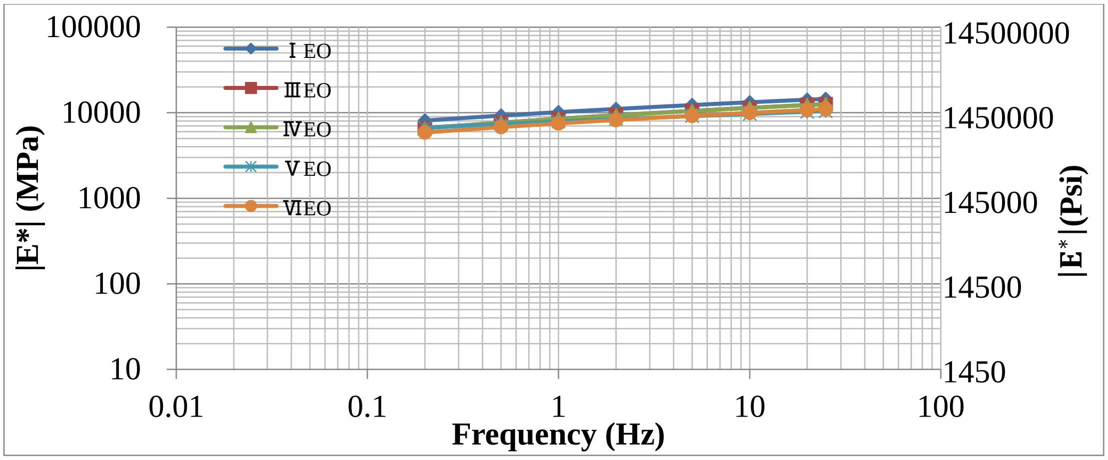

(a)

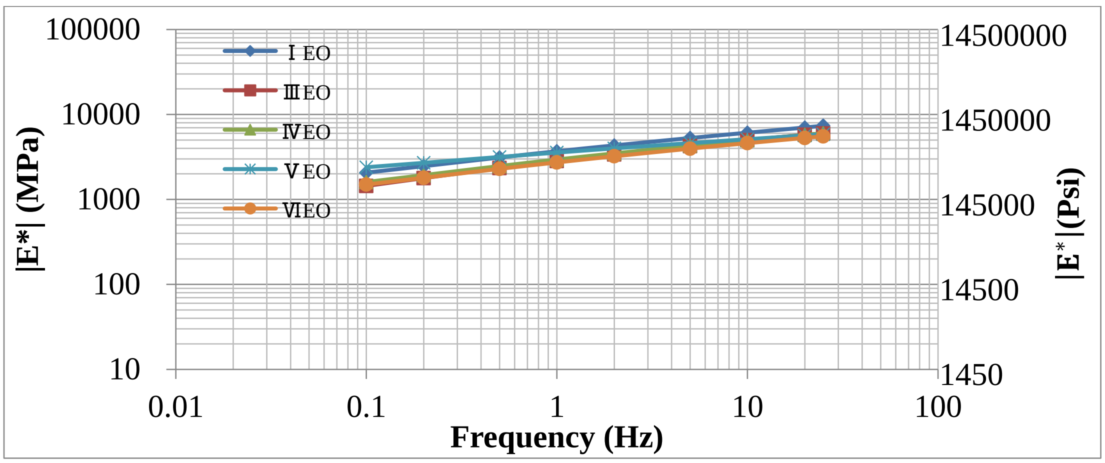

(b)

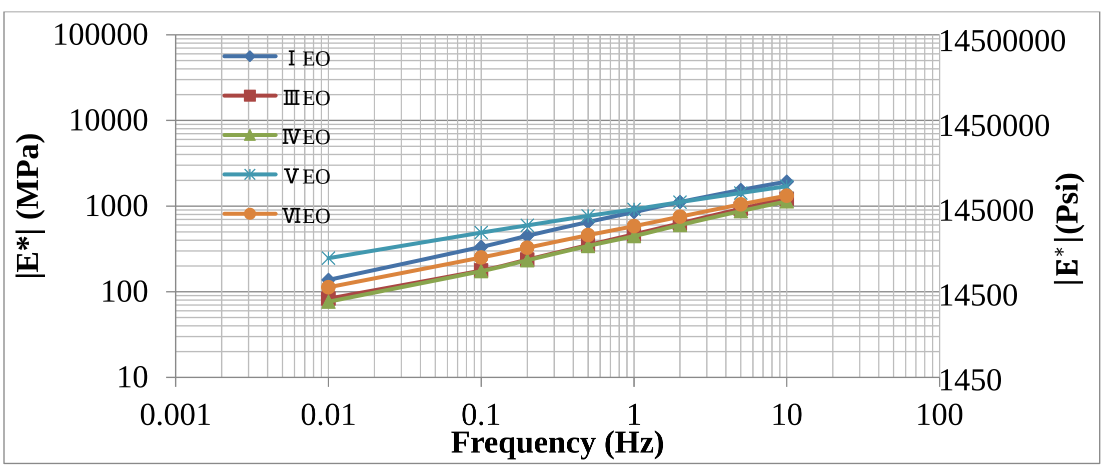

(c)

Figure 9-19 Dynamic Modulus Values of Various Surface Type E Mixtures without RAP in Terms of Aggregate Source, (a) at 4°C (39.2°F), (b) at 20°C (68°F), (c) at 40°C (104°F)

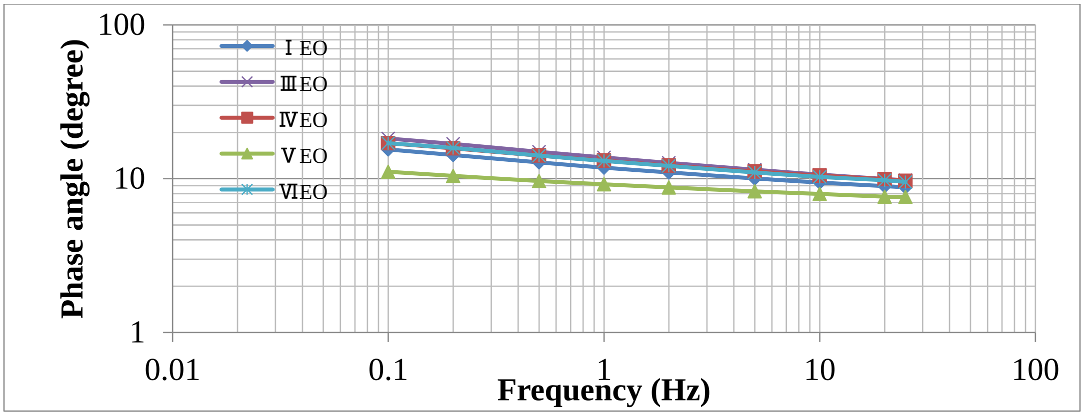

(a)

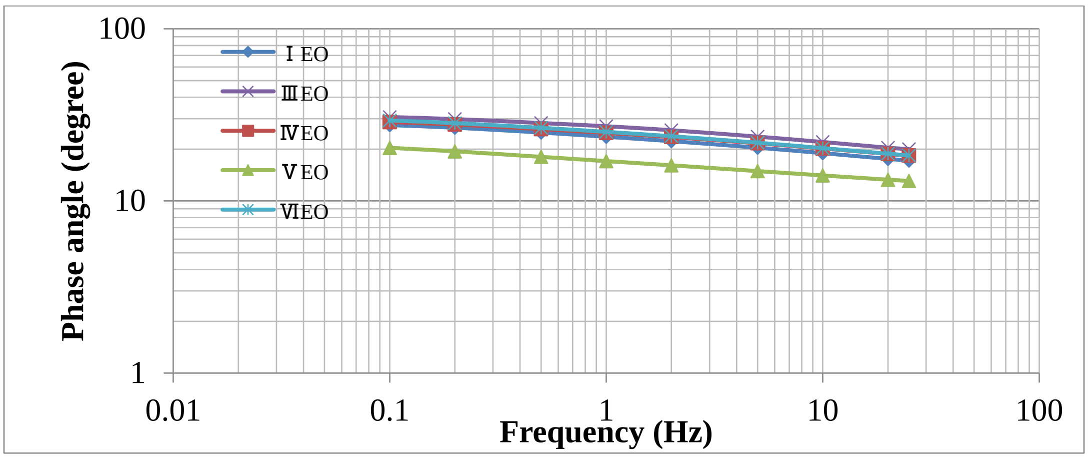

(b)

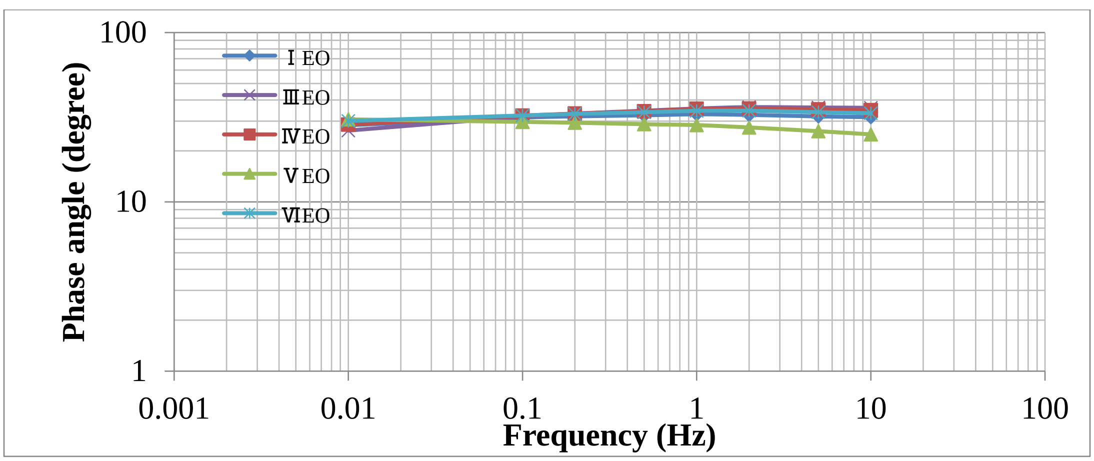

(c)

Figure 9-20 Phase Angle Values of Various Surface Type E Mixtures without RAP in Terms of Aggregate Source, (a) at 4°C (39.2°F), (b) at 20°C (68°F), (c) at 40°C (104°F)

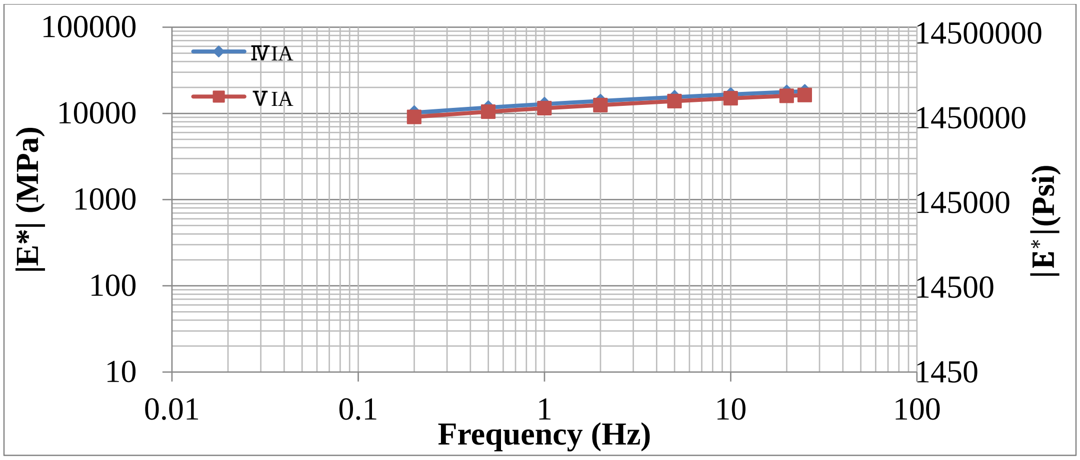

(a)

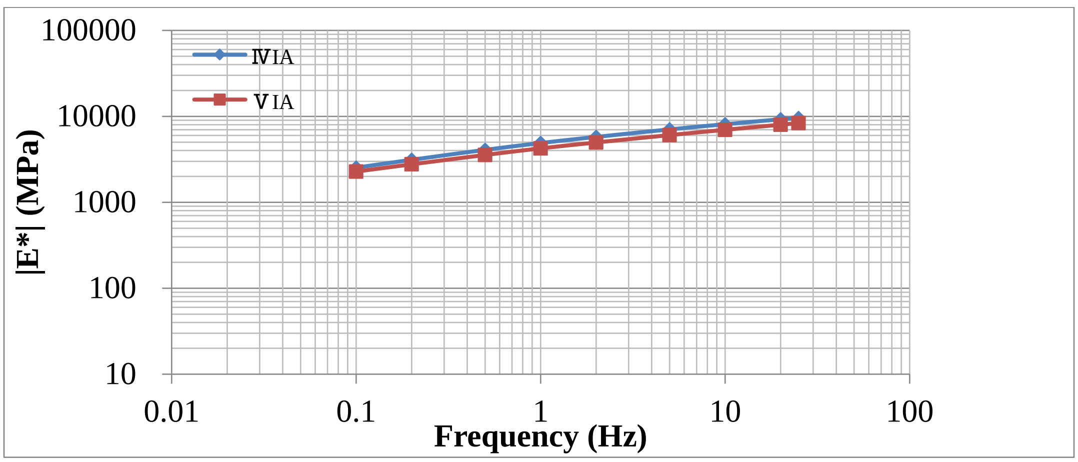

(b)

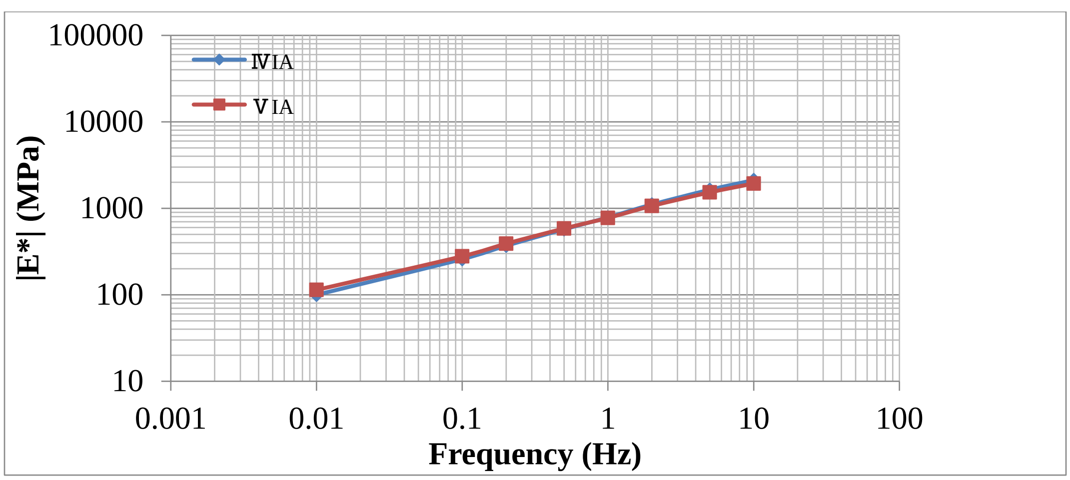

(c)

Figure 9-21 Dynamic Modulus Values of Various Intermediate Type A Mixtures with RAP in Terms of Aggregate Source, (a) at 4°C (39.2°F), (b) at 20°C (68°F), (c) at 40°C (104°F)

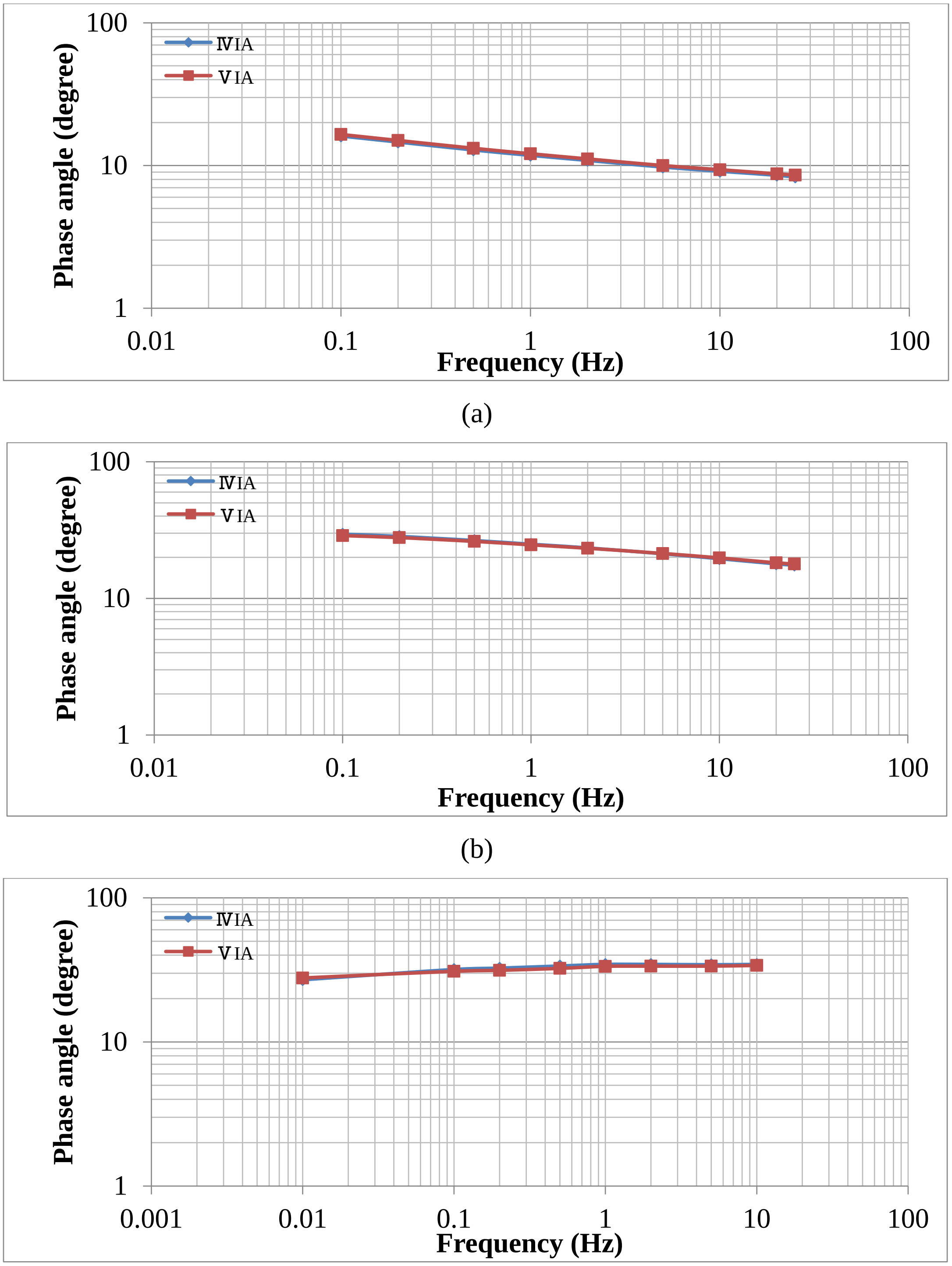

(c)

Figure 9-22 Phase Angle Values of Various Intermediate Type A Mixtures with RAP in Terms of Aggregate Source, (a) at 4°C (39.2°F), (b) at 20°C (68°F), (c) at 40°C (104°F)

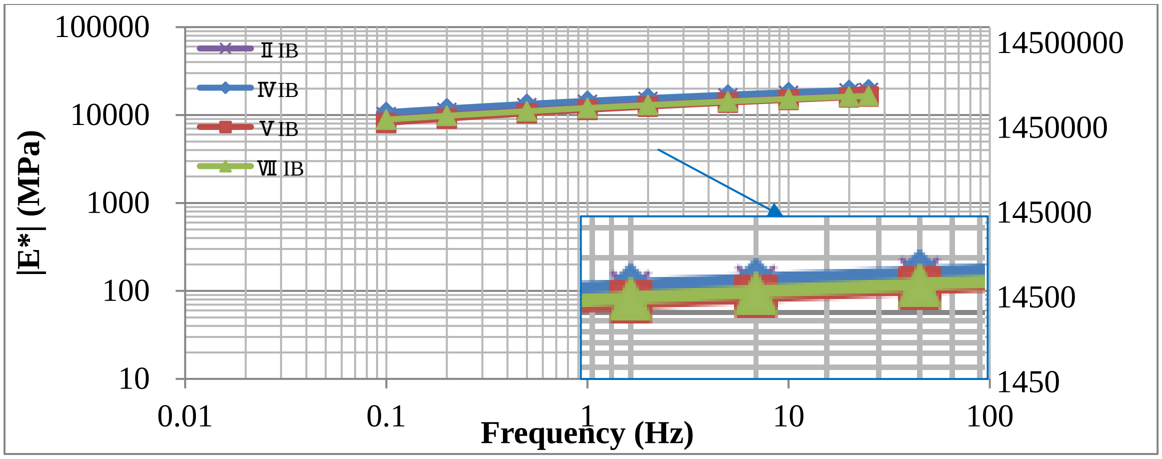

(a)

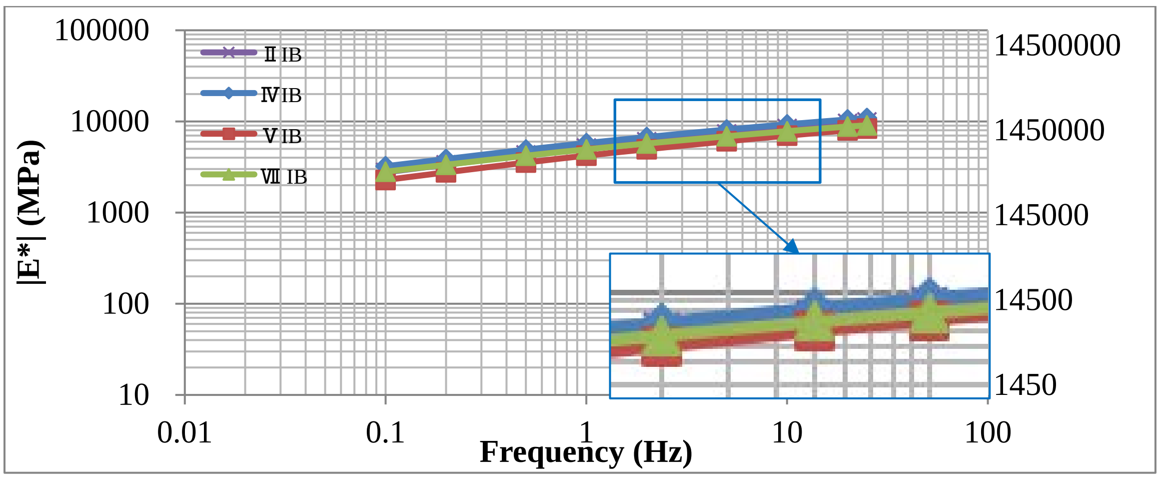

(b)

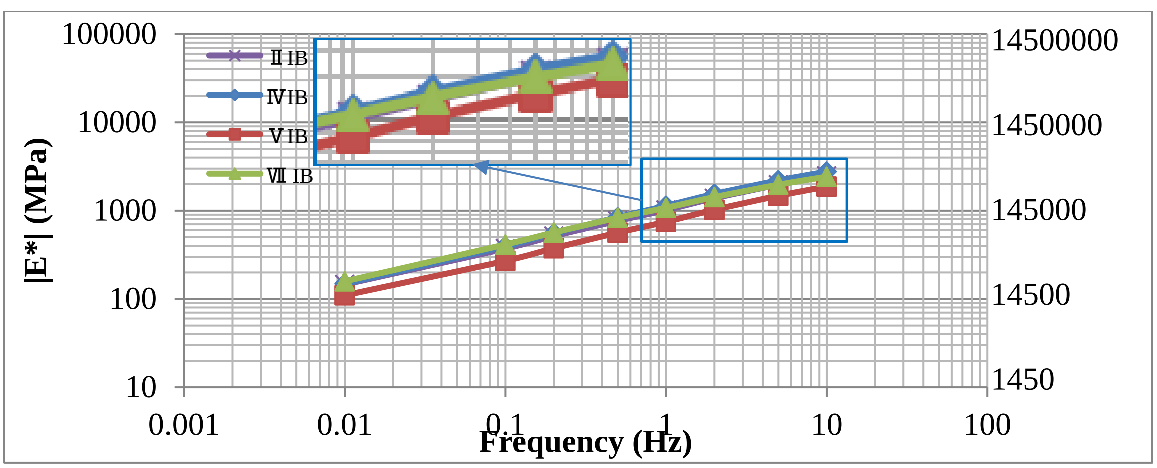

(c)

Figure 9-23 Dynamic Modulus Values of Various Intermediate Type B Mixtures with RAP in Terms of Aggregate Source, (a) at 4°C (39.2°F), (b) at 20°C (68°F), (c) at 40°C (104°F)

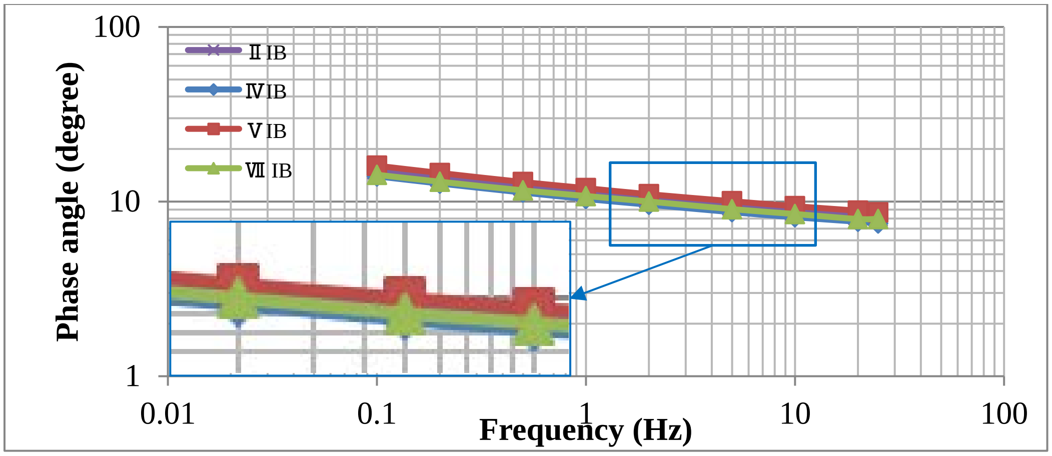

(a)

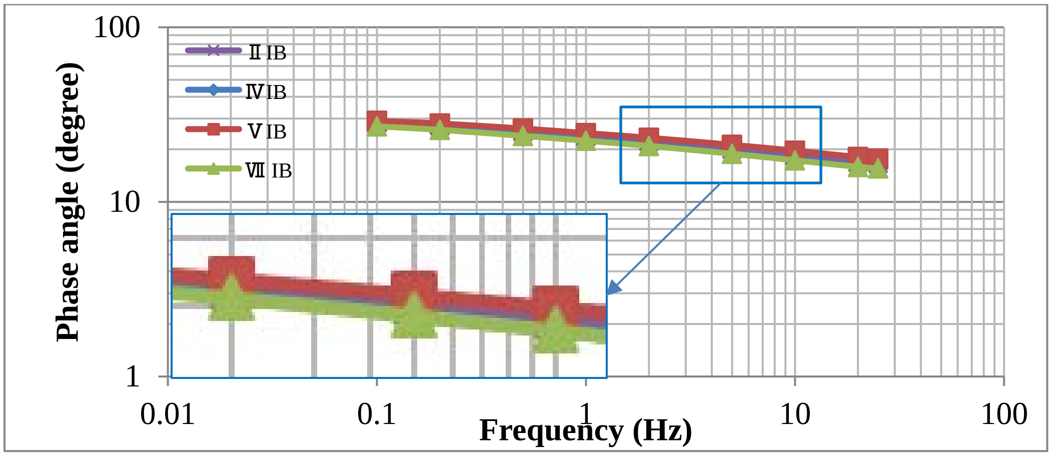

(b)

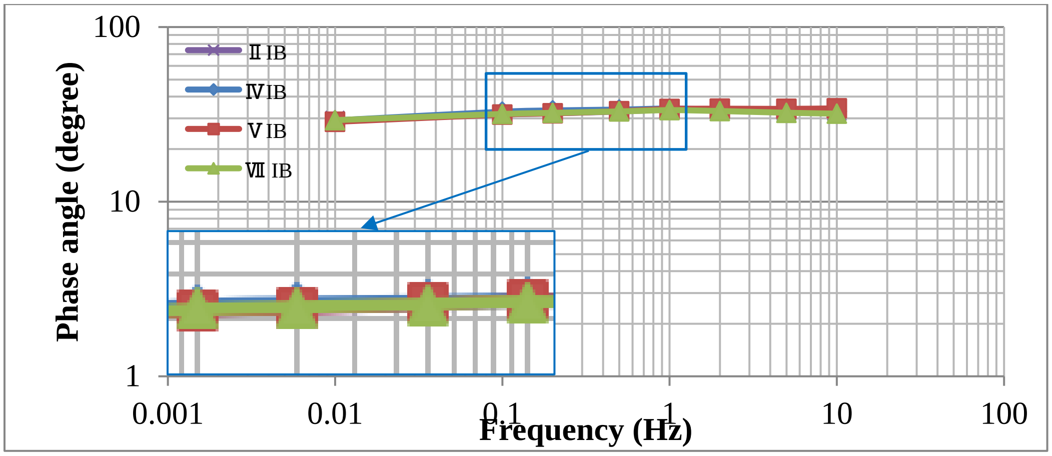

(c)

Figure 9-24 Phase Angle Values of Various Intermediate Type B Mixtures with RAP in Terms of Aggregate Source, (a) at 4°C (39.2°F), (b) at 20°C (68°F), (c) at 40°C (104°F)

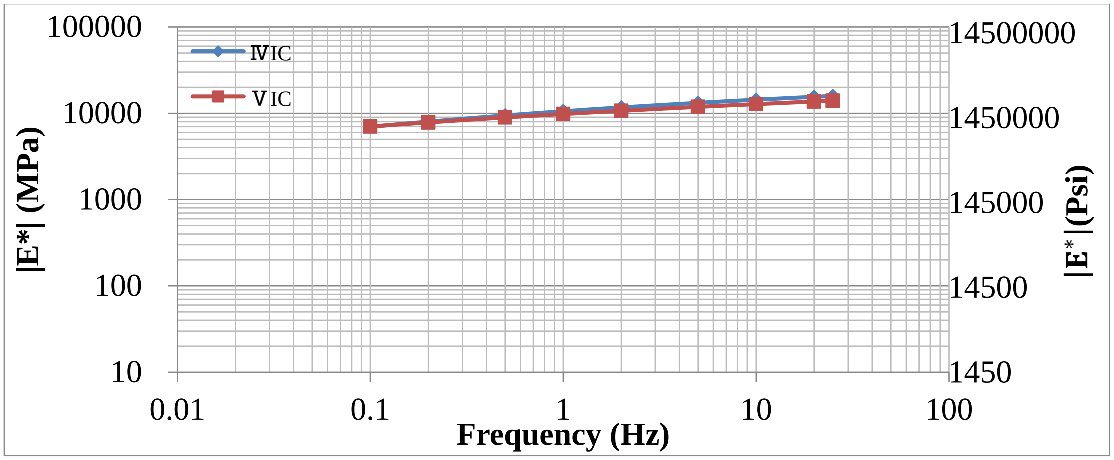

(a)

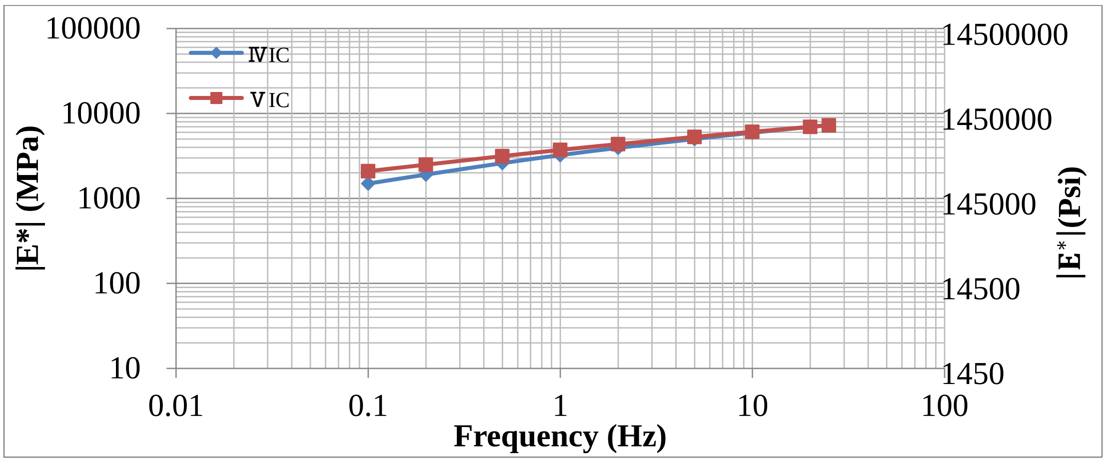

(b)

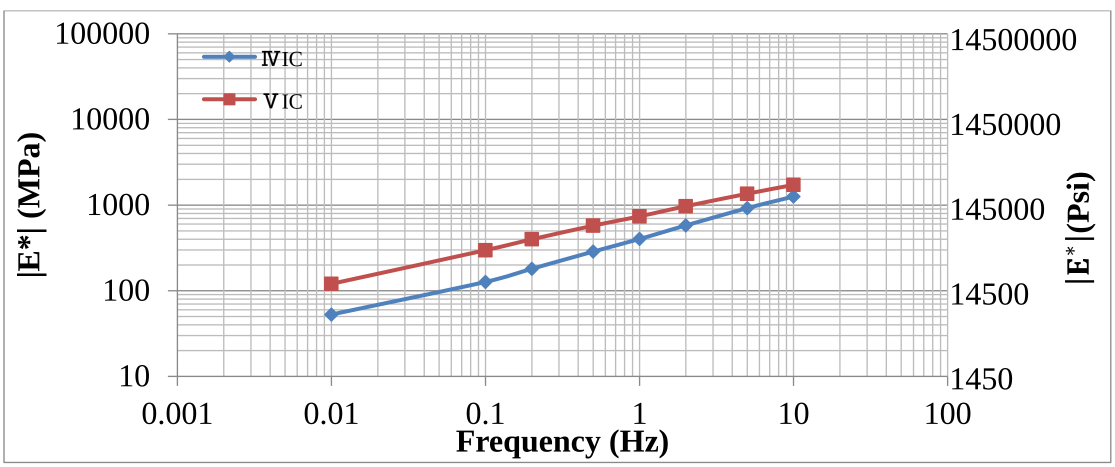

(c)

Figure 9-25 Dynamic Modulus Values of Various Intermediate Type C Mixtures with RAP in Terms of Aggregate Source, (a) at 4°C (39.2°F), (b) at 20°C (68°F), (c) at 40°C (104°F)

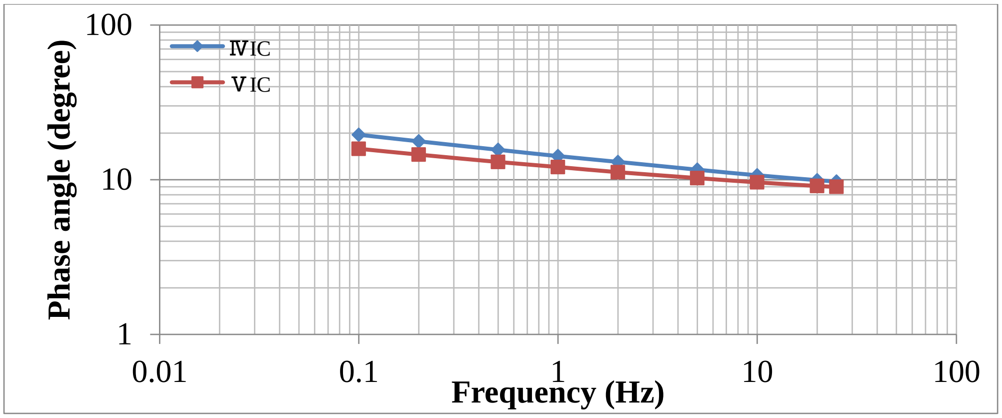

(a)

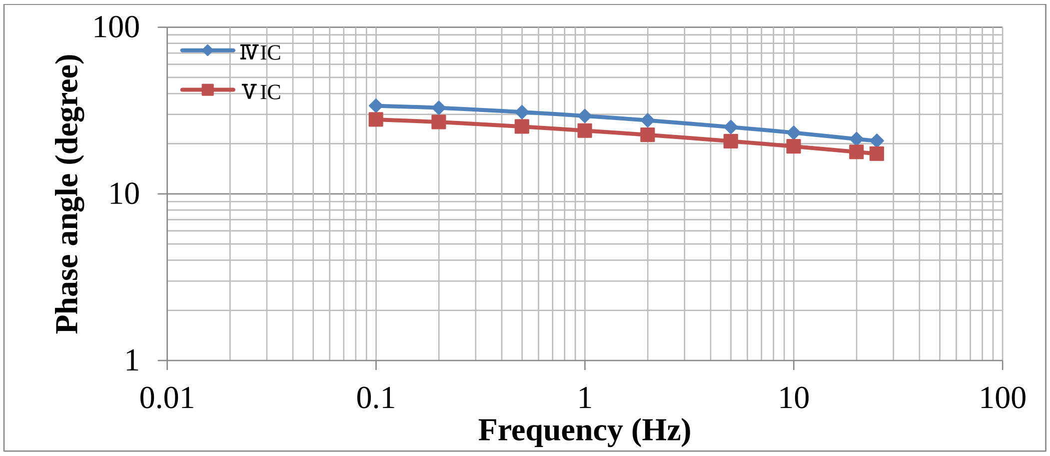

(b)

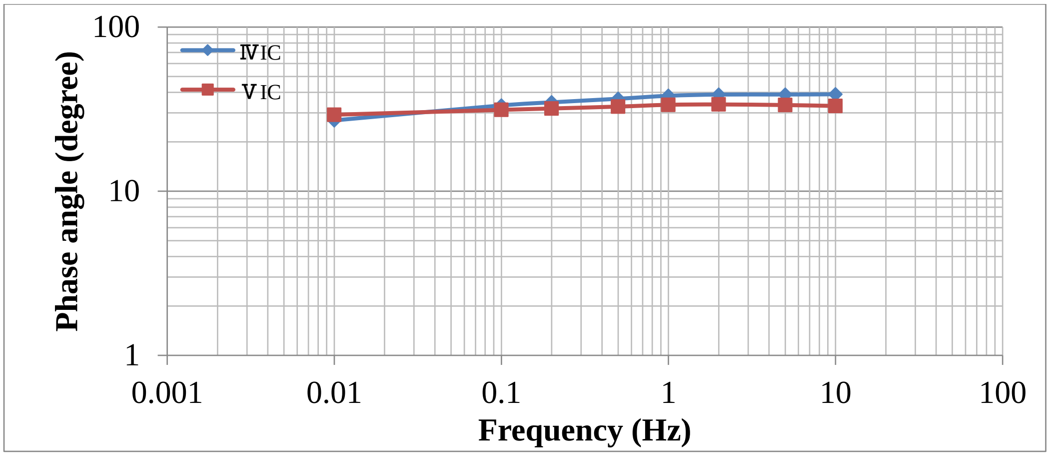

(c)

Figure 9-26 Phase Angle Values of Various Intermediate Type C Mixtures with RAP in Terms of Aggregate Source, (a) at 4°C (39.2°F), (b) at 20°C (68°F), (c) at 40°C (104°F)

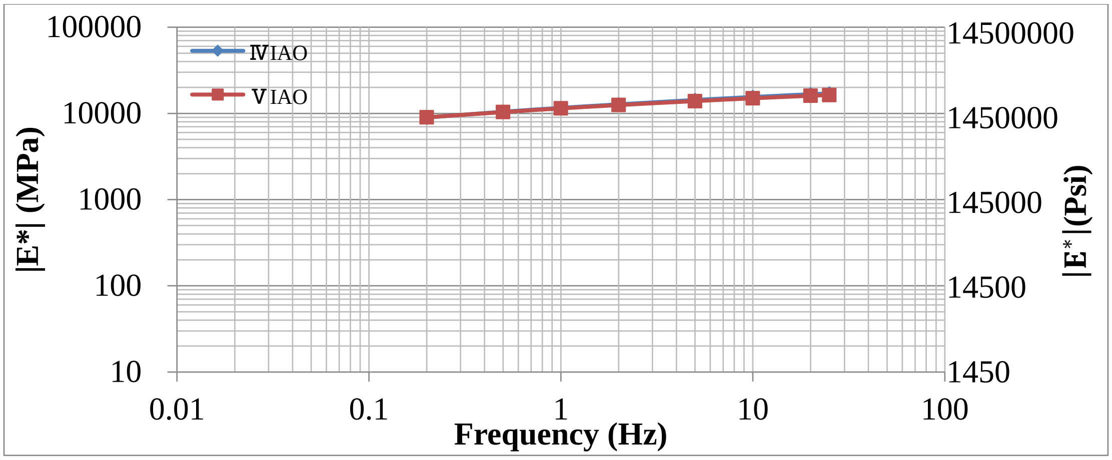

(a)

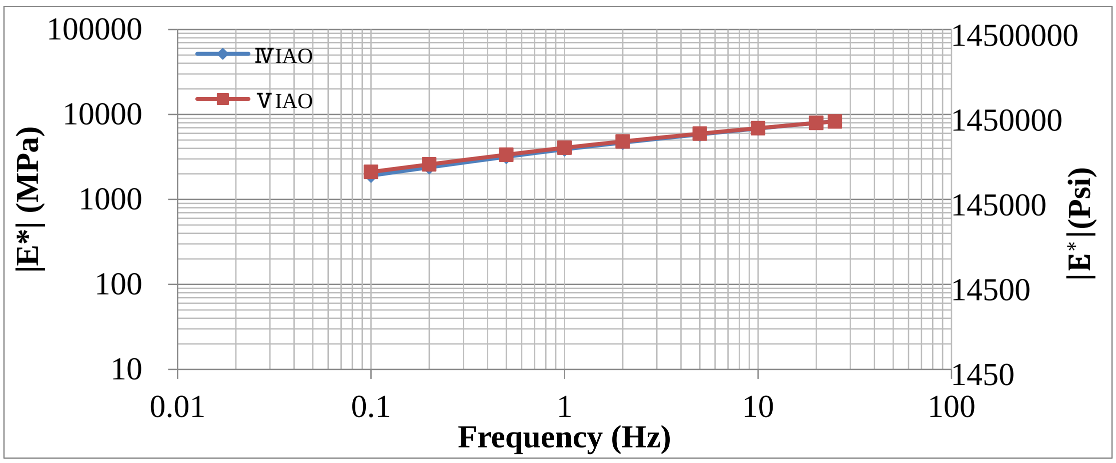

(b)

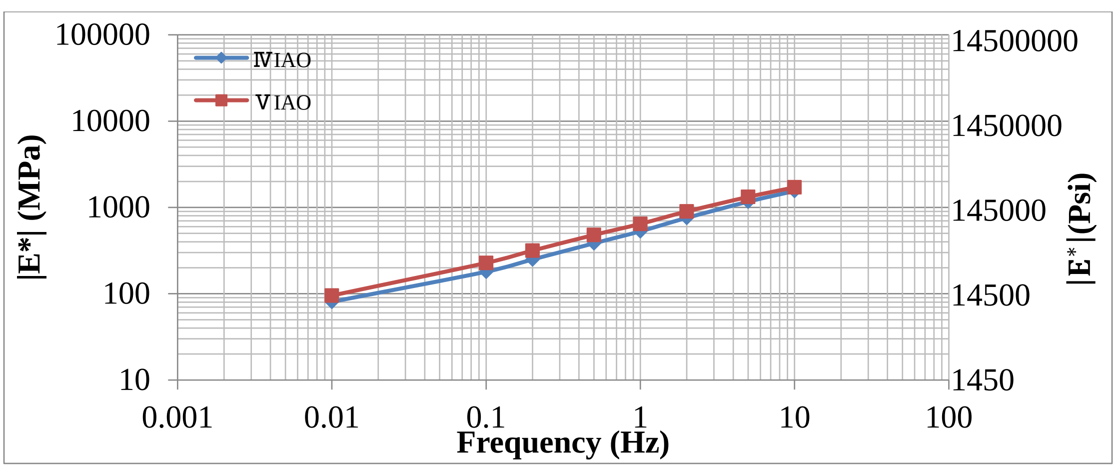

(c)

Figure 9-27 Dynamic Modulus Values of Various Intermediate Type A Mixtures without RAP in Terms of Aggregate Source, (a) at 4°C (39.2°F), (b) at 20°C (68°F), (c) at 40°C (104°F)

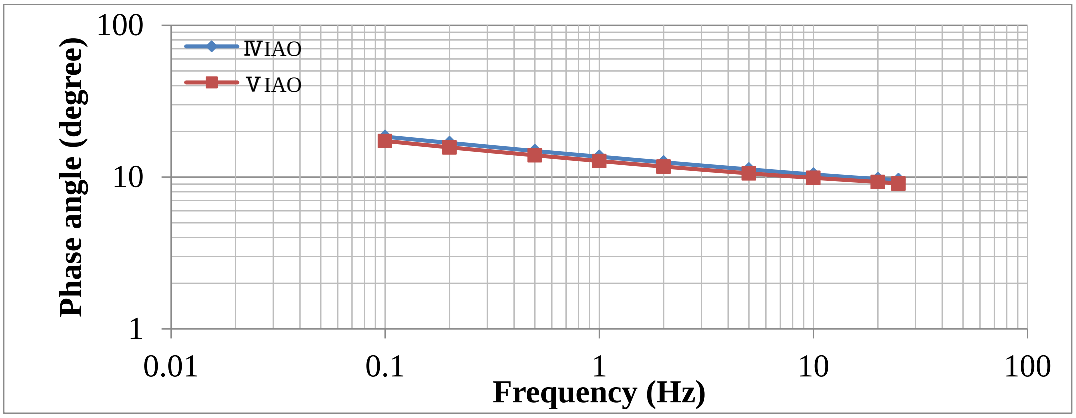

(a)

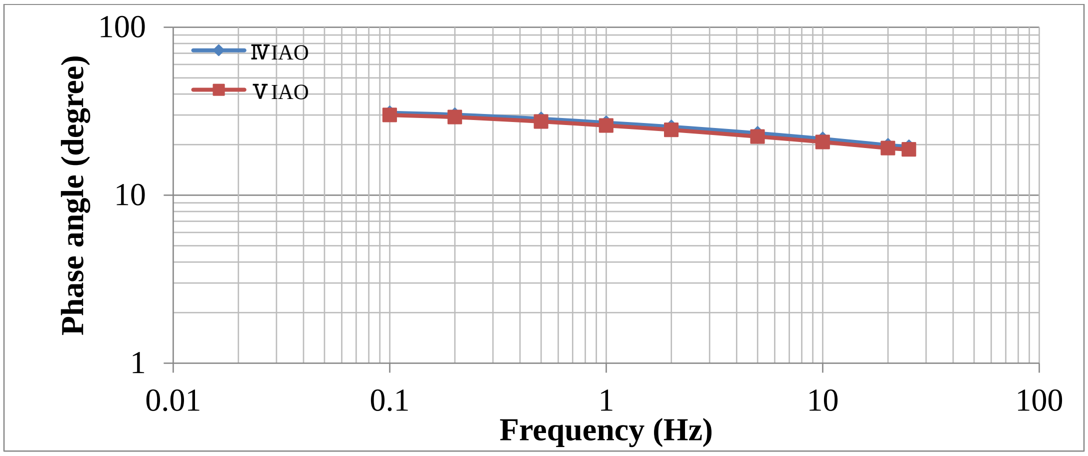

(b)

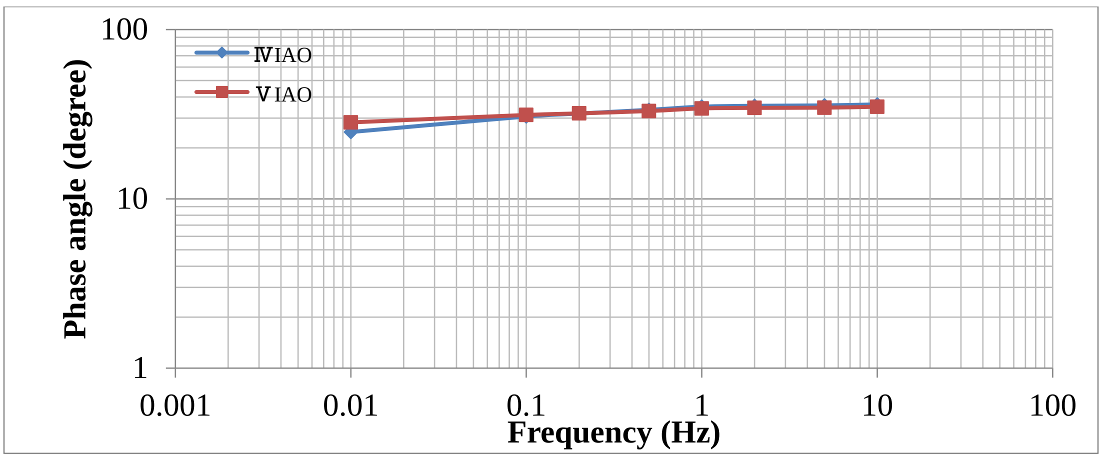

(c)

Figure 9-28 Phase Angle Values of Various Intermediate Type A Mixtures without RAP in Terms of Aggregate Source, (a) at 4°C (39.2°F), (b) at 20°C (68°F), (c) at 40°C (104°F)

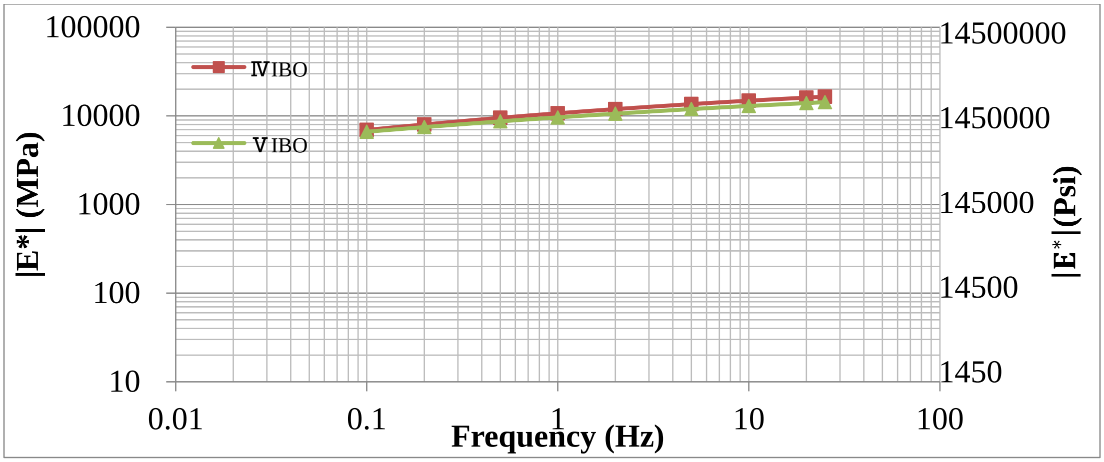

(a)

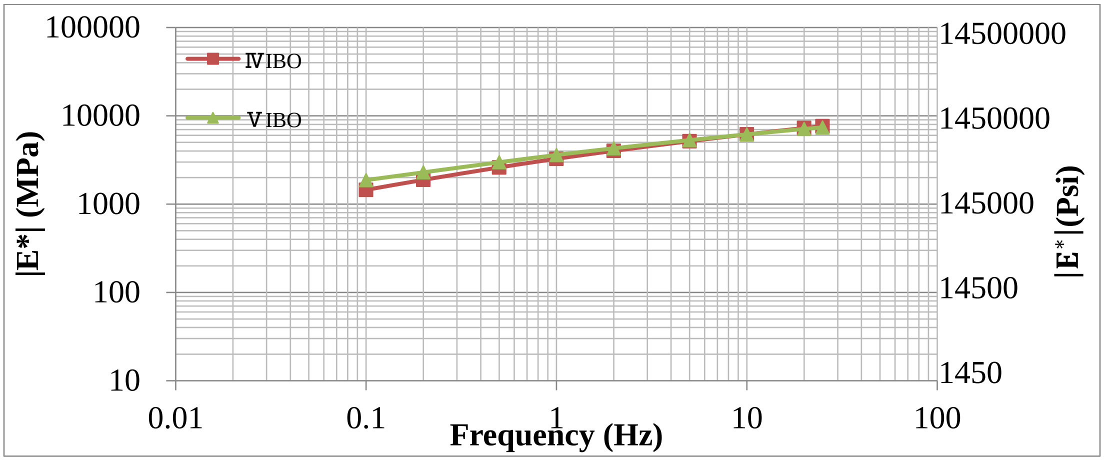

(b)

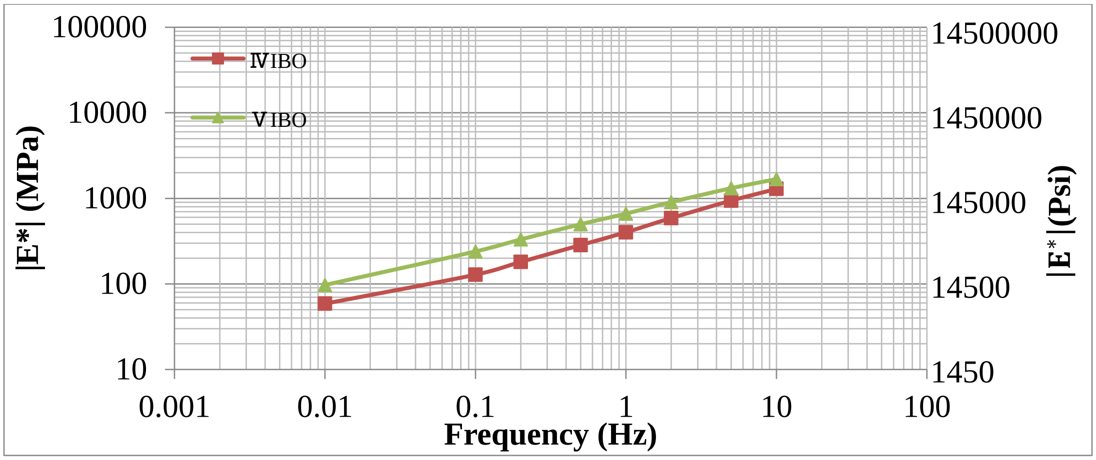

(c)

Figure 9-29 Dynamic Modulus Values of Various Intermediate Type B Mixtures without RAP in Terms of Aggregate Source, (a) at 4°C (39.2°F), (b) at 20°C (68°F), (c) at 40°C (104°F)

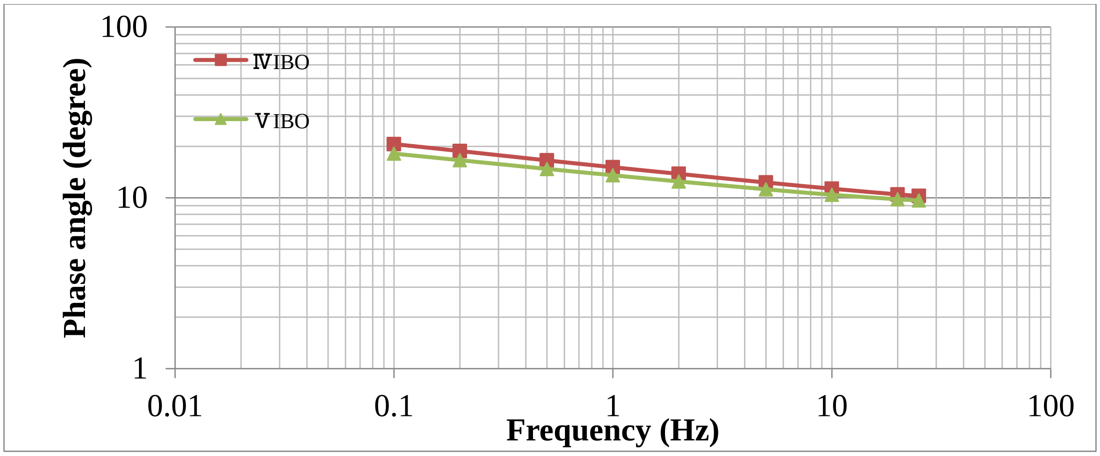

(a)

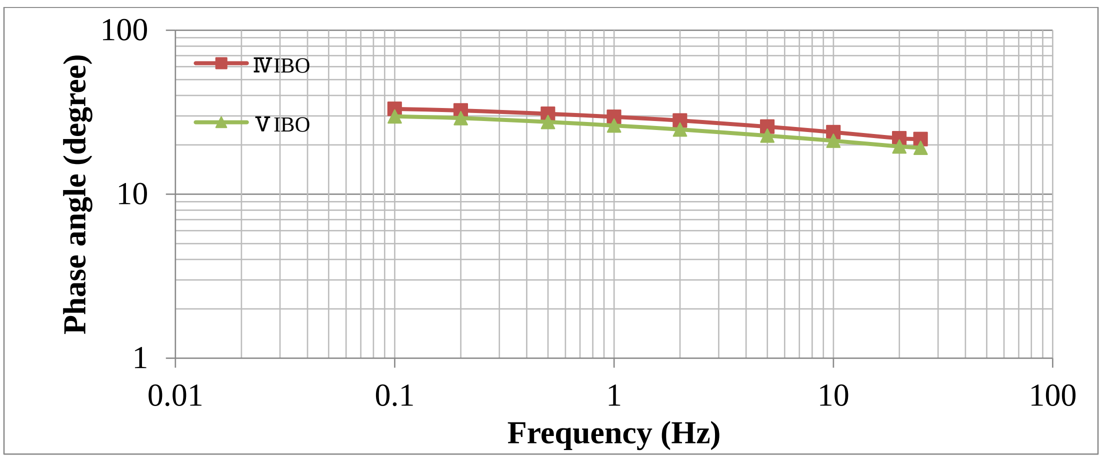

(b)

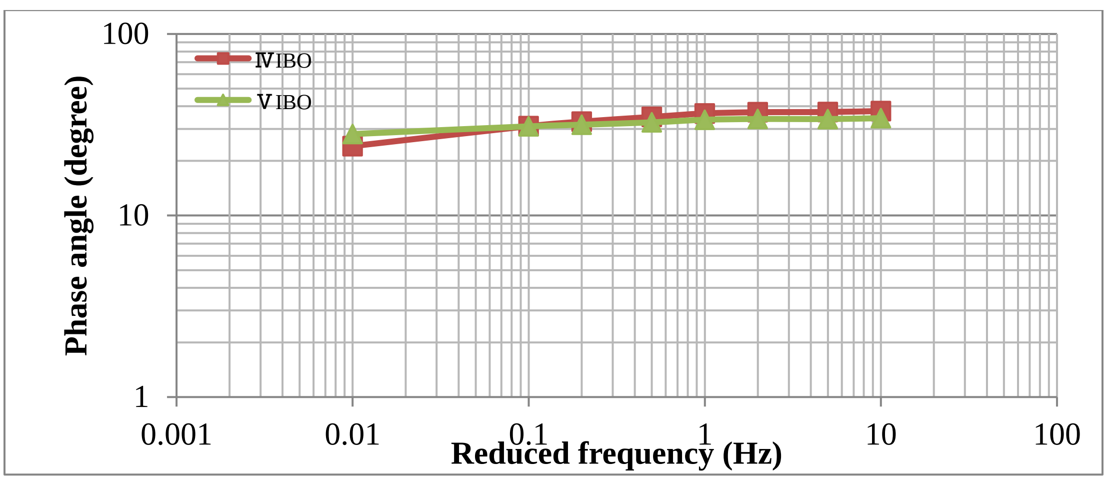

(c)

Figure 9-30 Phase Angle Values of Various Intermediate Type B Mixtures without RAP in Terms of Aggregate Source, (a) at 4°C (39.2°F), (b) at 20°C (68°F), (c) at 40°C (104°F)

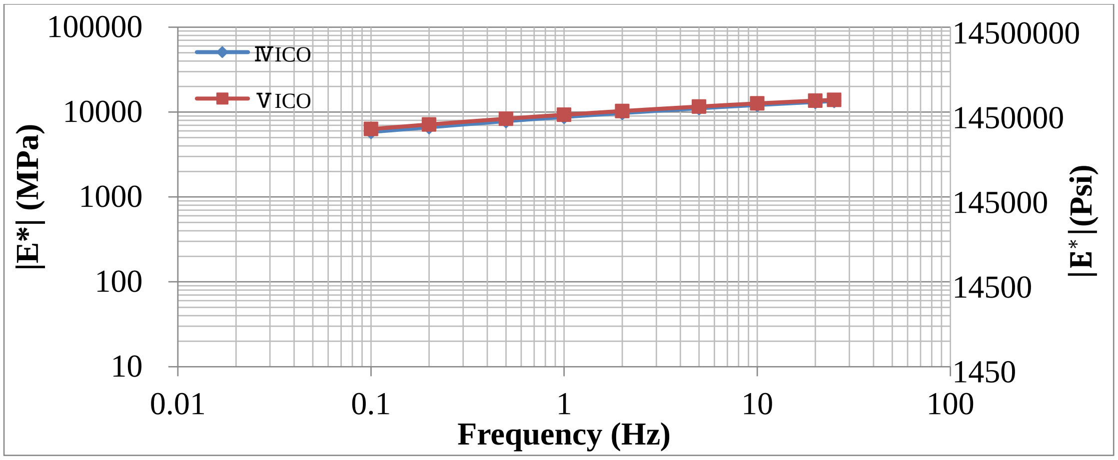

(a)

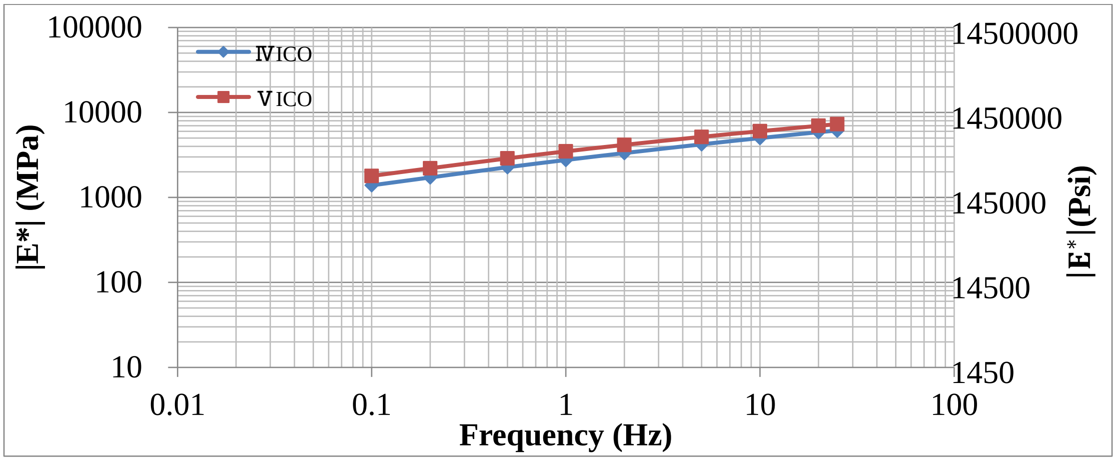

(b)

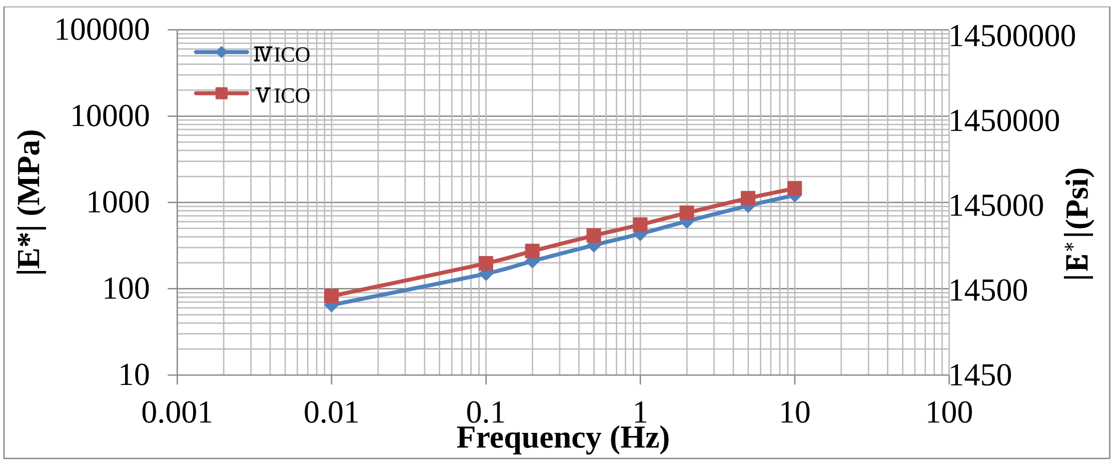

(c)

Figure 9-31 Dynamic Modulus Values of Various Intermediate Type C Mixtures without RAP in Terms of Aggregate Source, (a) at 4°C (39.2°F), (b) at 20°C (68°F), (c) at 40°C (104°F)

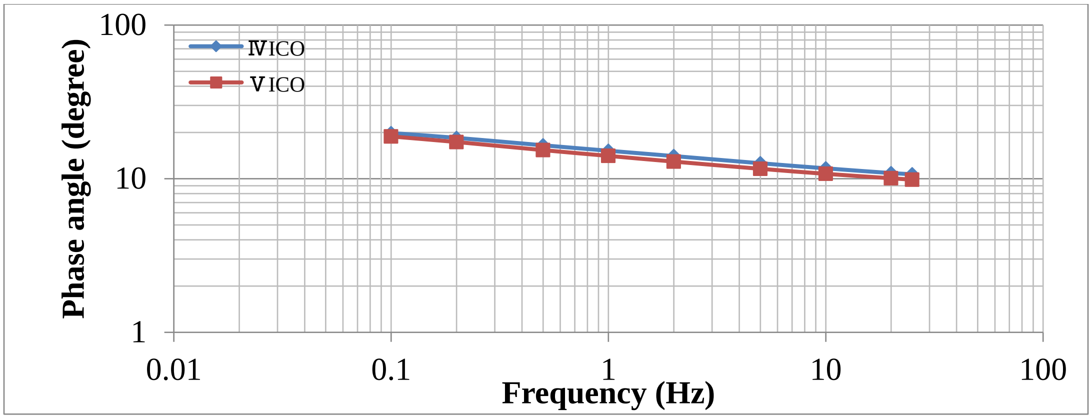

(a)

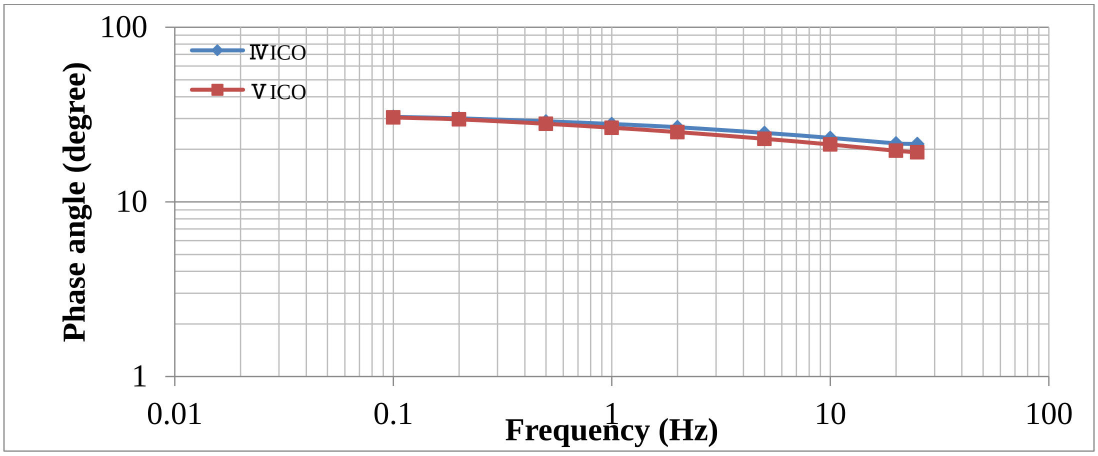

(b)

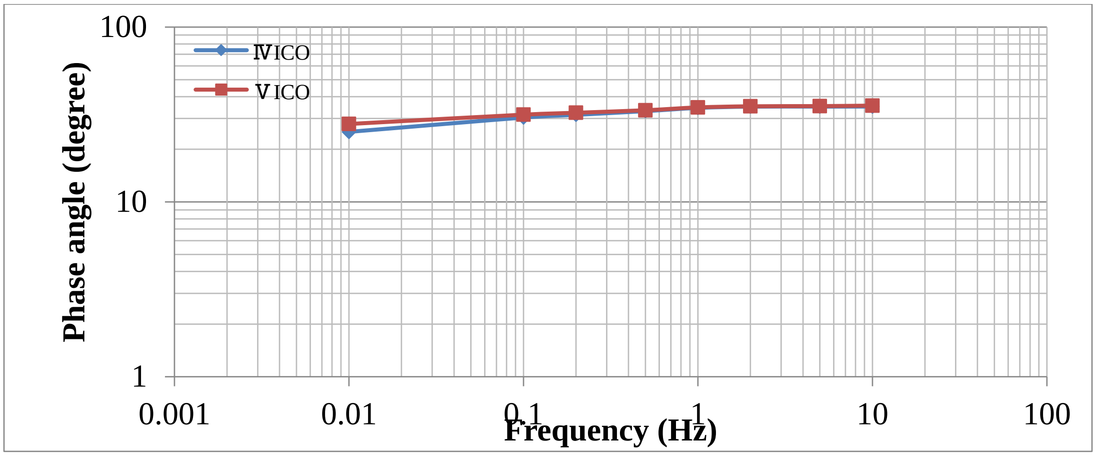

(c)

Figure 9-32 Phase Angle Values of Various Intermediate Type C Mixtures without RAP in Terms of Aggregate Source, (a) at 4°C (39.2°F), (b) at 20°C (68°F), (c) at 40°C (104°F)

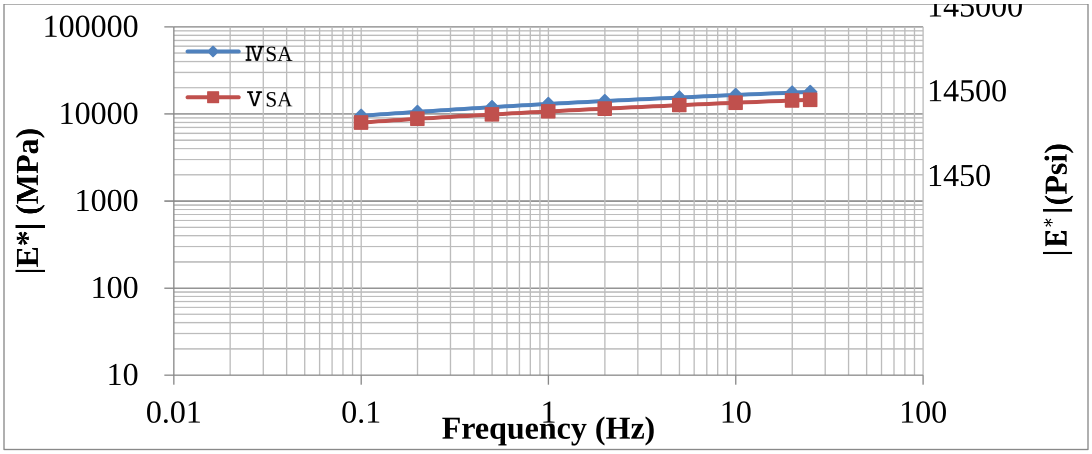

(a)

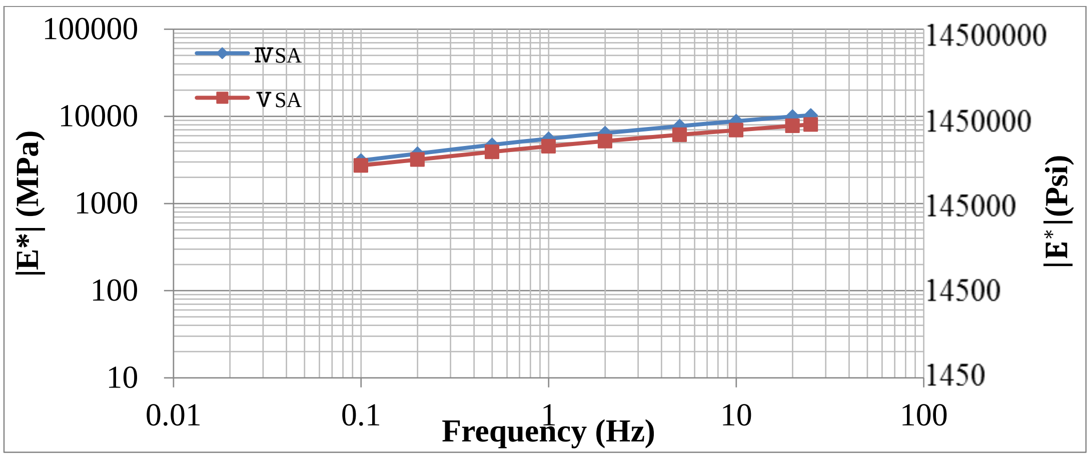

(b)

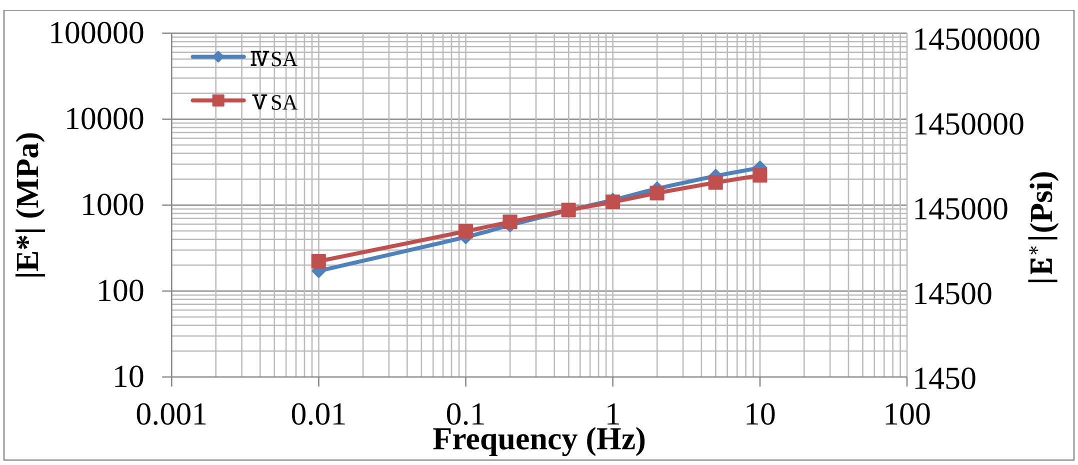

(c)

Figure 9-33 Dynamic Modulus Values of Various Base Type A Mixtures with RAP in Terms of Aggregate Source, (a) at 4°C (39.2°F), (b) at 20°C (68°F), (c) at 40°C (104°F)

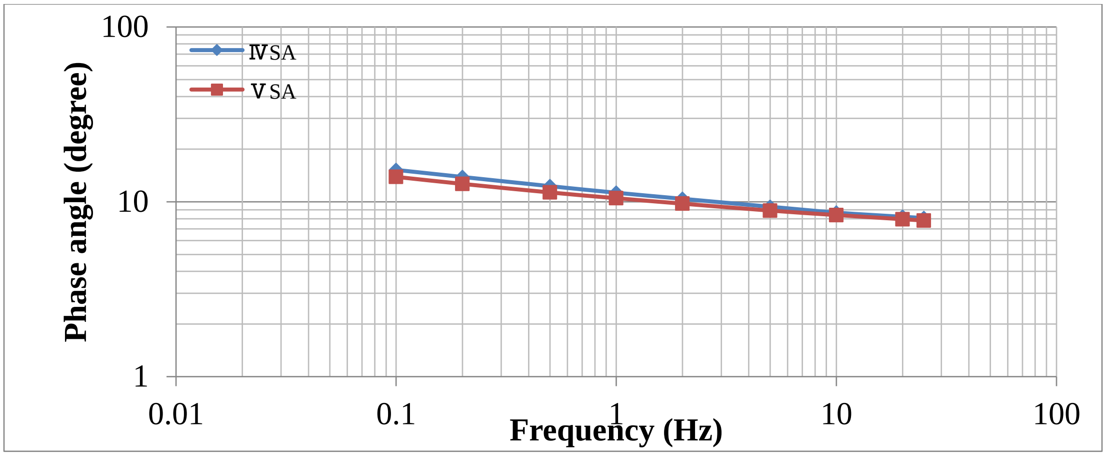

(a)

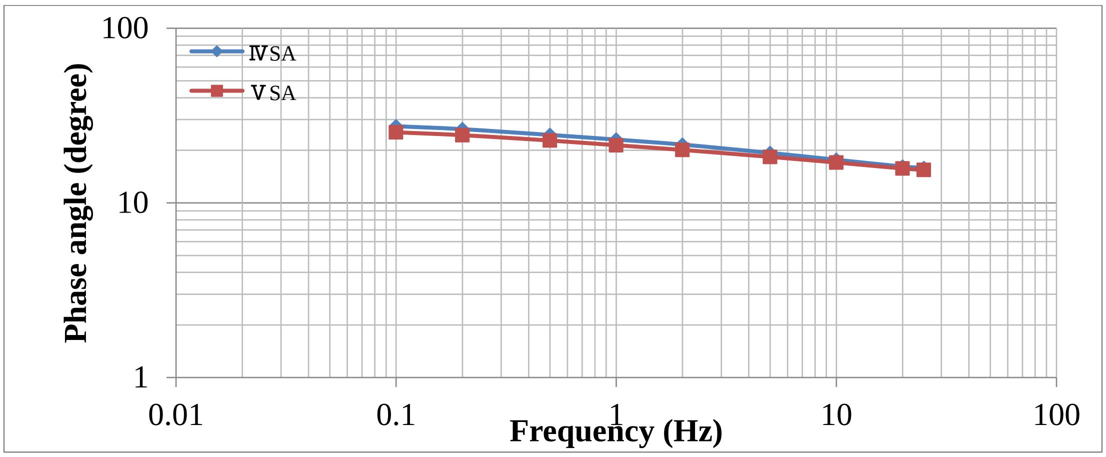

(b)

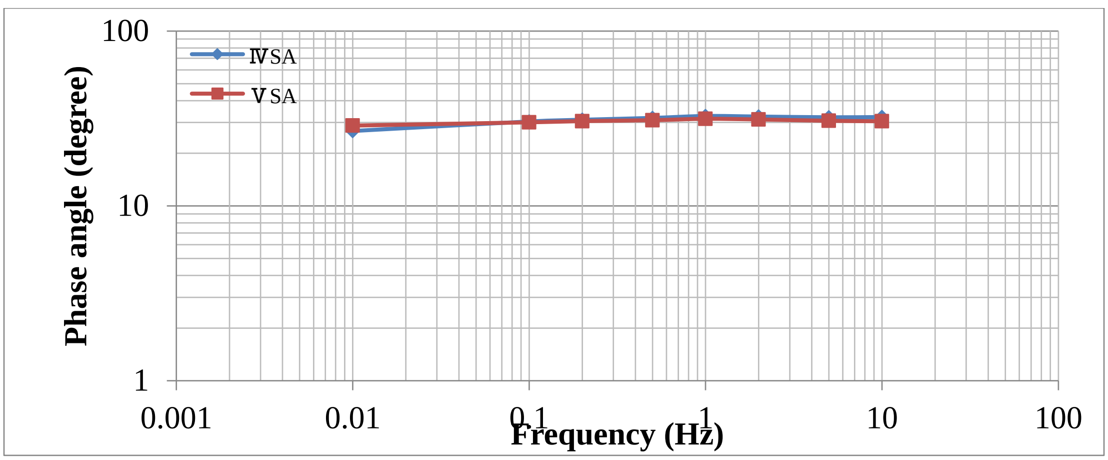

(c)

Figure 9-34 Phase Angle Values of Various Base Type A Mixtures with RAP in Terms of Aggregate Source, (a) at 4°C (39.2°F), (b) at 20°C (68°F), (c) at 40°C (104°F)

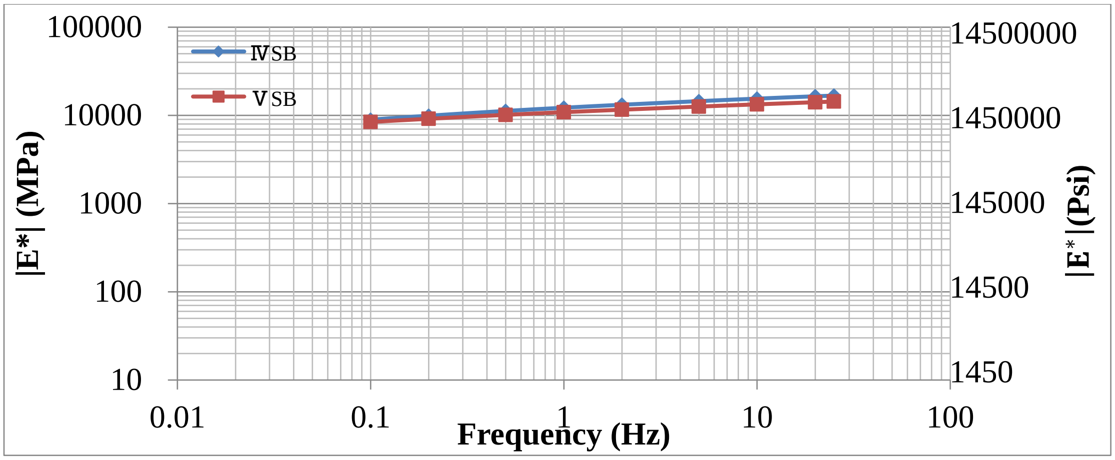

(a)

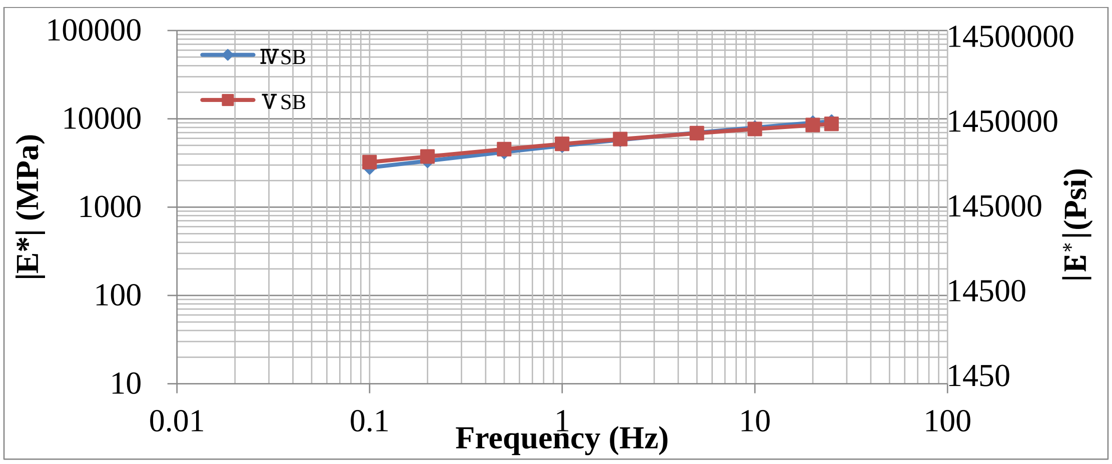

(b)

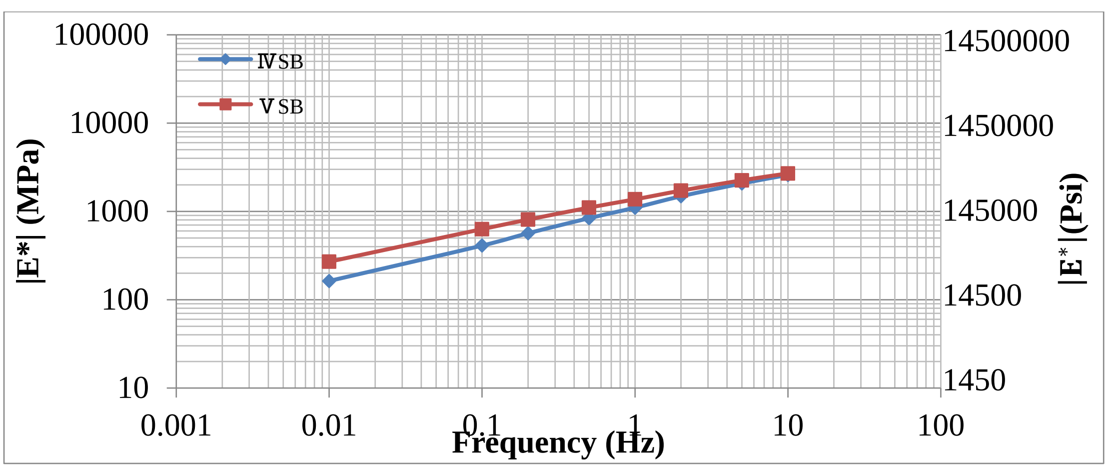

(c)

Figure 9-35 Dynamic Modulus Values of Various Base Type B Mixtures with RAP in Terms of Aggregate Source, (a) at 4°C (39.2°F), (b) at 20°C (68°F), (c) at 40°C (104°F)

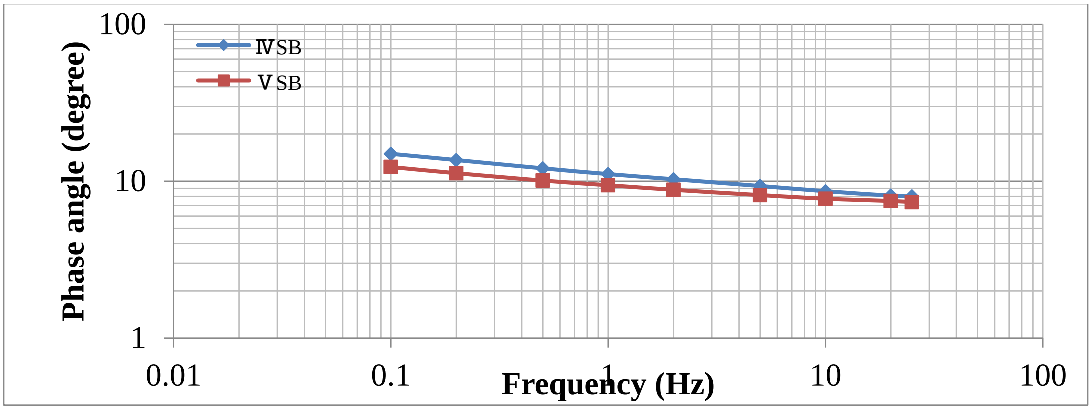

(a)

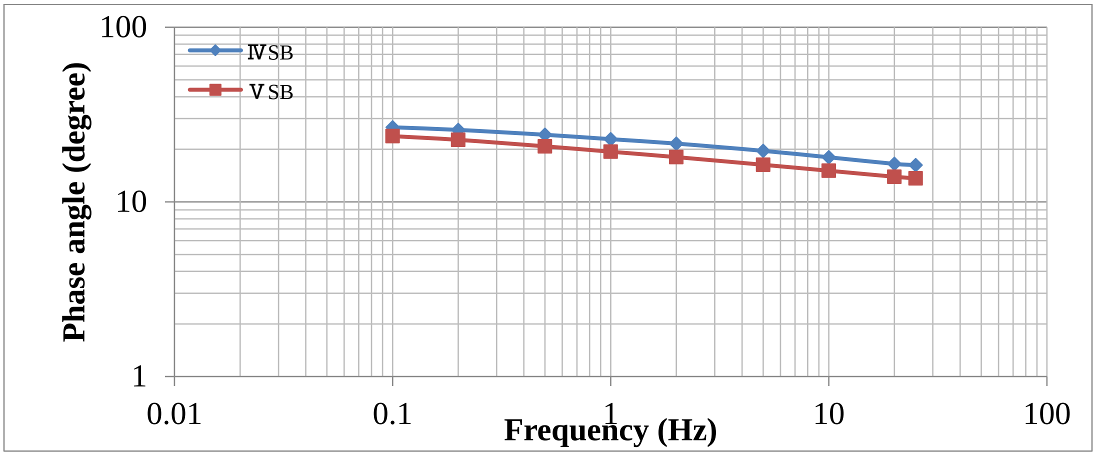

(b)

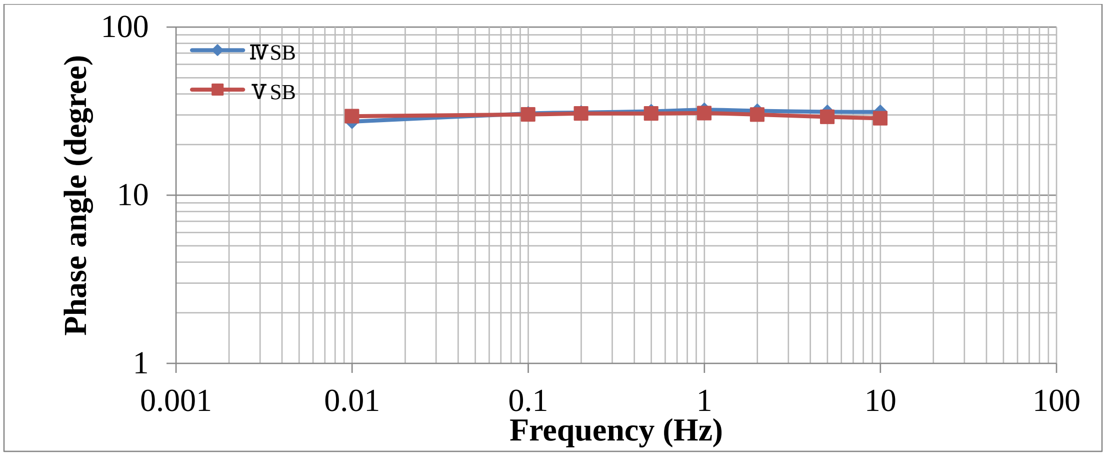

(c)

Figure 9-36 Phase Angle Values of Various Base Type B Mixtures with RAP in Terms of Aggregate Source, (a) at 4°C (39.2°F), (b) at 20°C (68°F), (c) at 40°C (104°F)

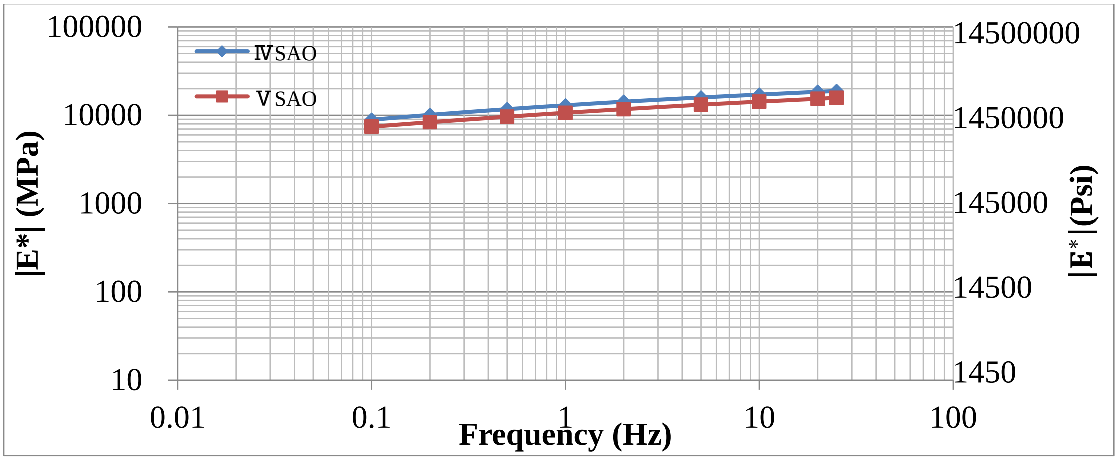

(a)

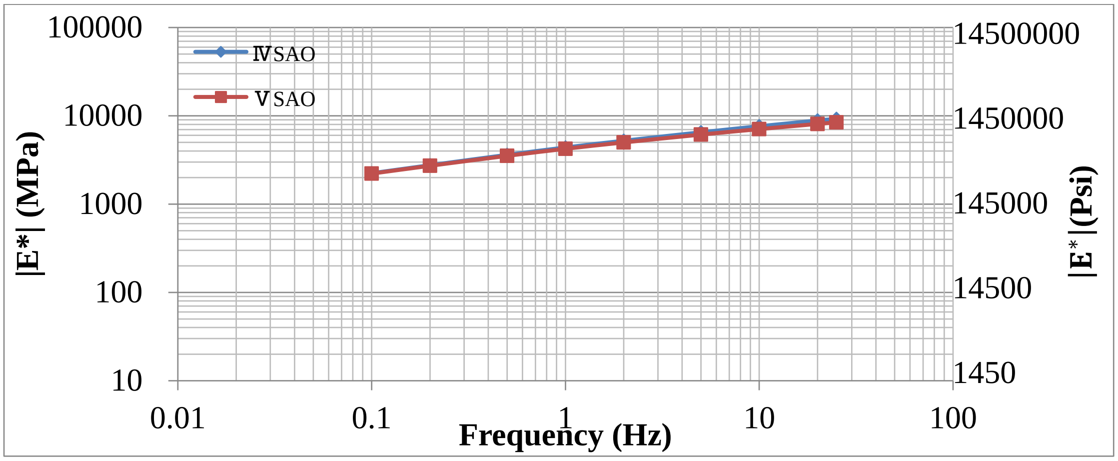

(b)

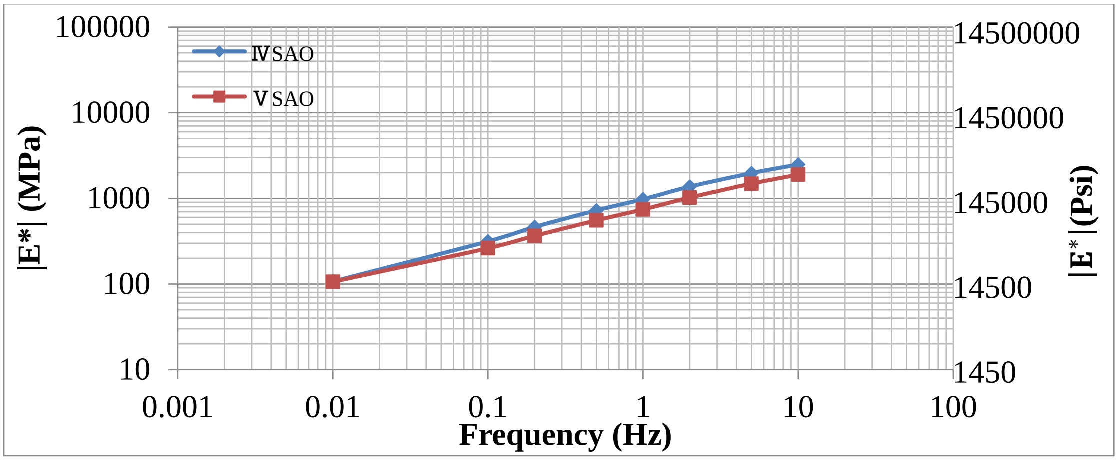

(c)

Figure 9-37 Dynamic Modulus Values of Various Base Type A Mixtures without RAP in Terms of Aggregate Source, (a) at 4°C (39.2°F), (b) at 20°C (68°F), (c) at 40°C (104°F)

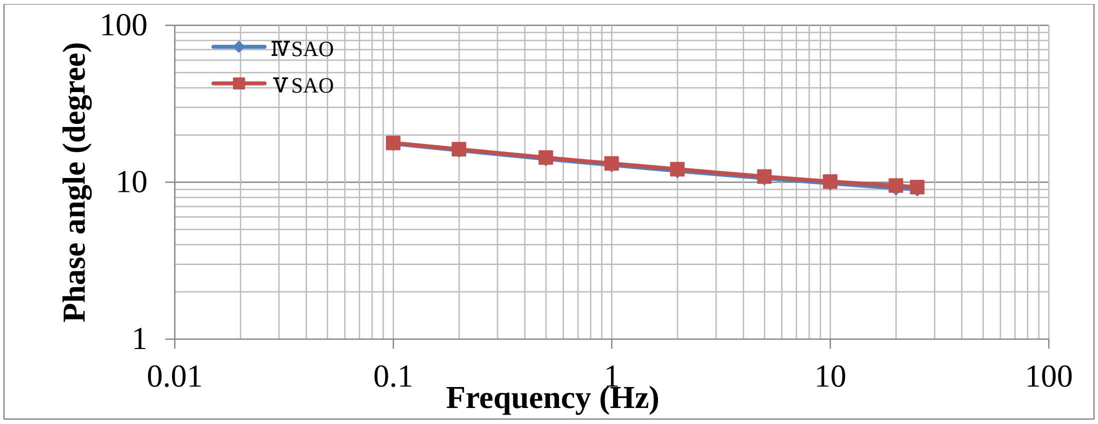

(a)

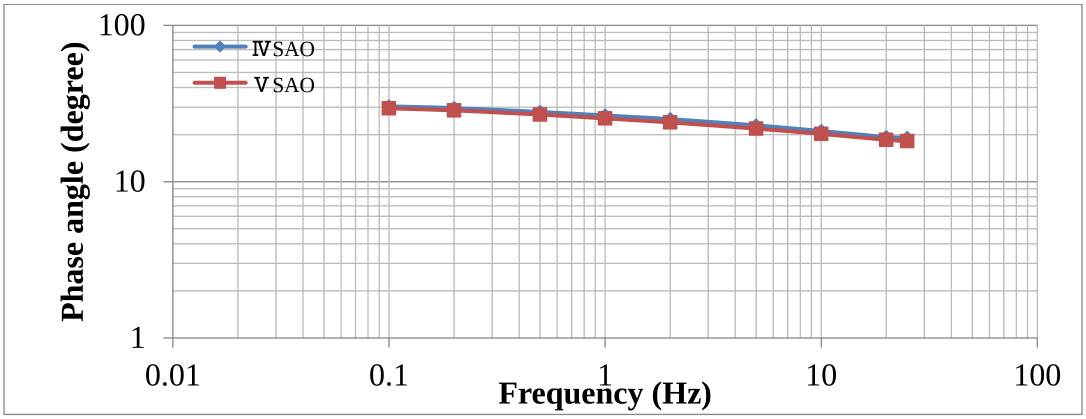

(b)

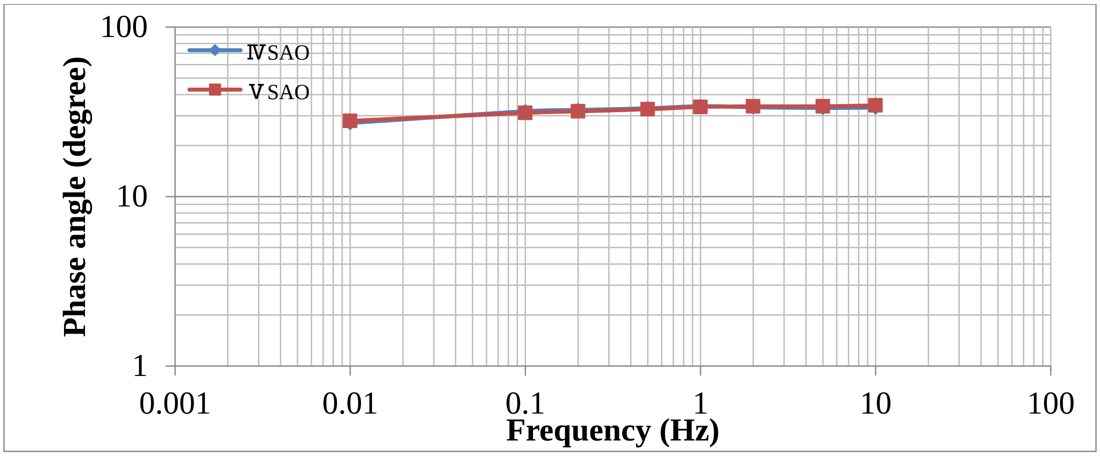

(c)

Figure 9-38 Phase Angle Values of Various Base Type A Mixtures without RAP in Terms of Aggregate Source, (a) at 4°C (39.2°F), (b) at 20°C (68°F), (c) at 40°C (104°F)

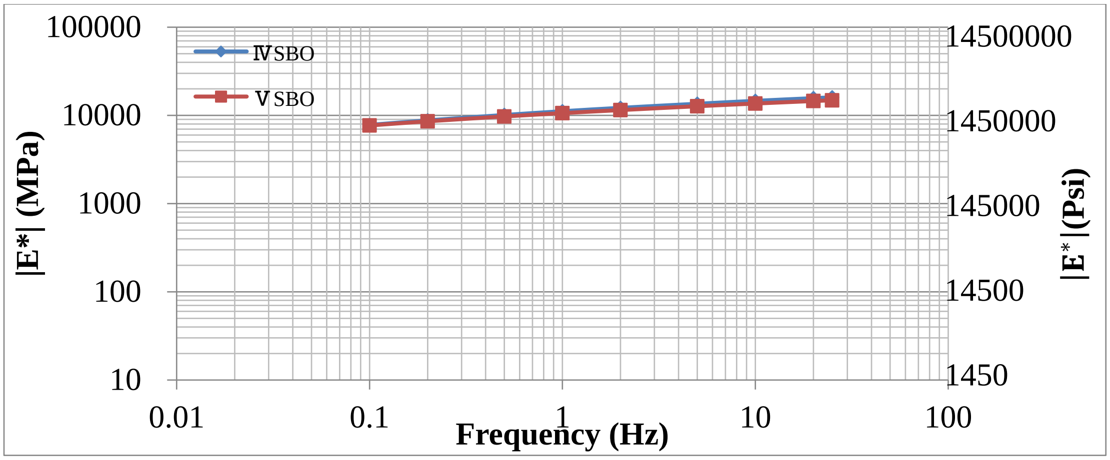

(a)

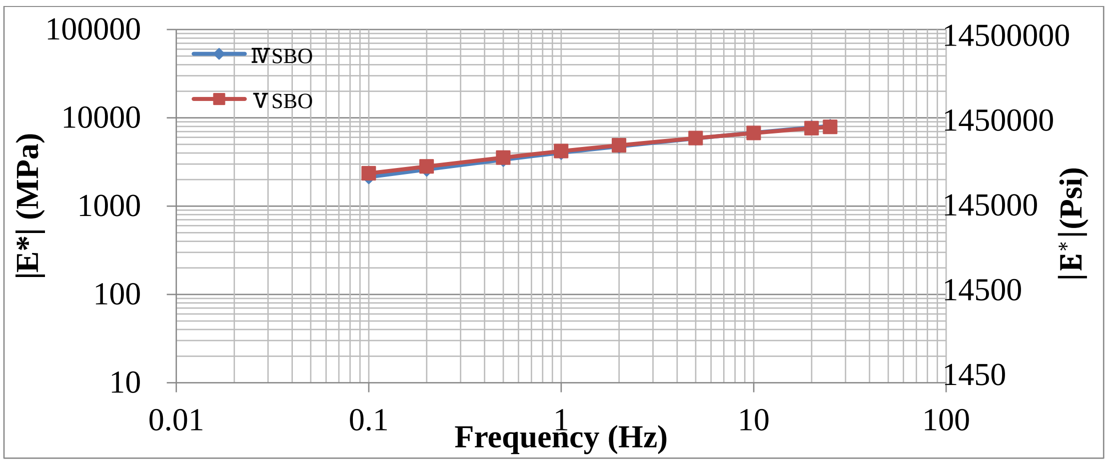

(b)

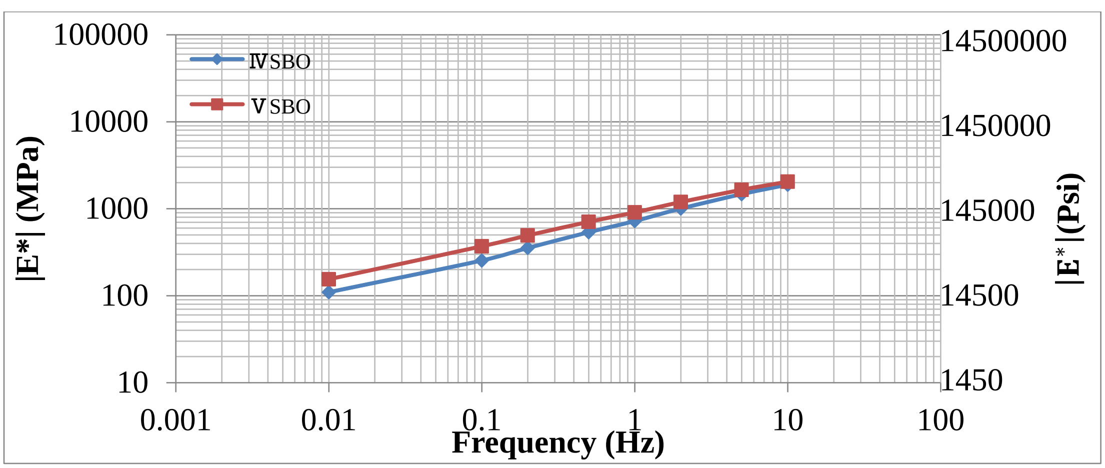

(c)

Figure 9-39 Dynamic Modulus Values of Various Base Type B Mixtures without RAP in Terms of Aggregate Source, (a) at 4°C (39.2°F), (b) at 20°C (68°F), (c) at 40°C (104°F)

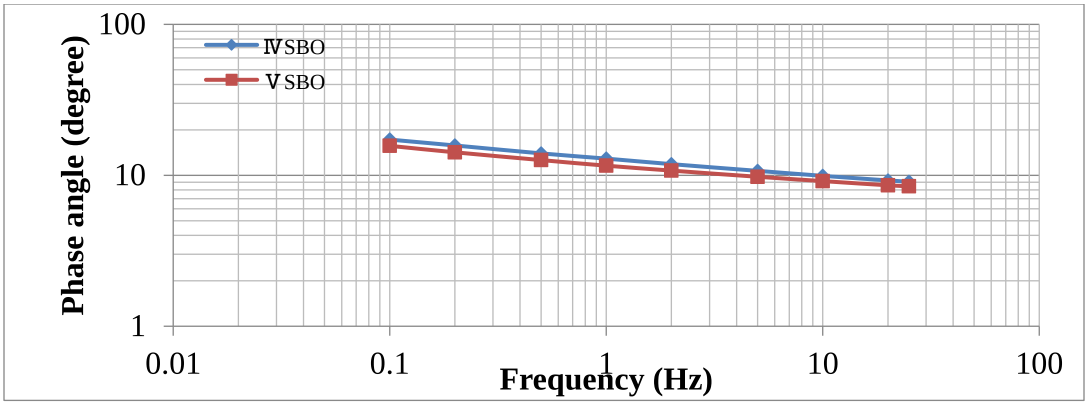

(a)

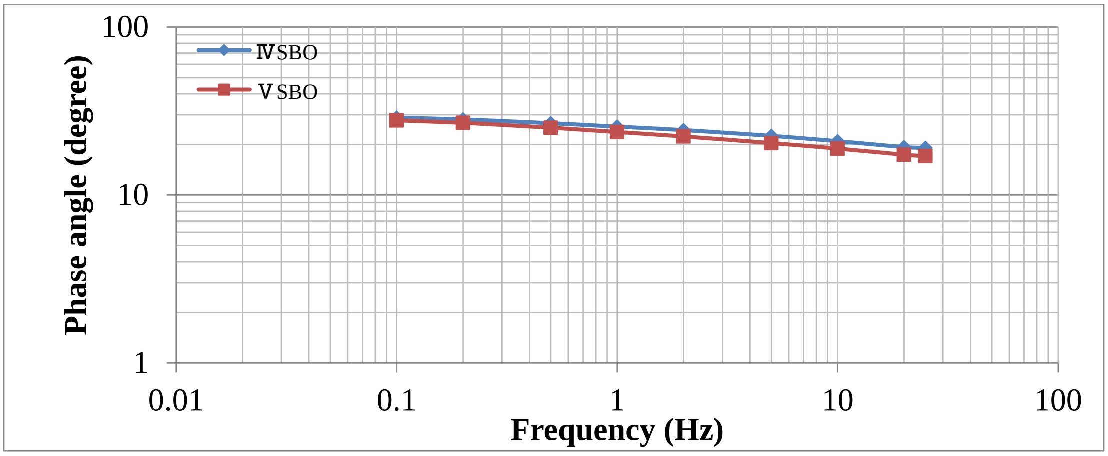

(b)

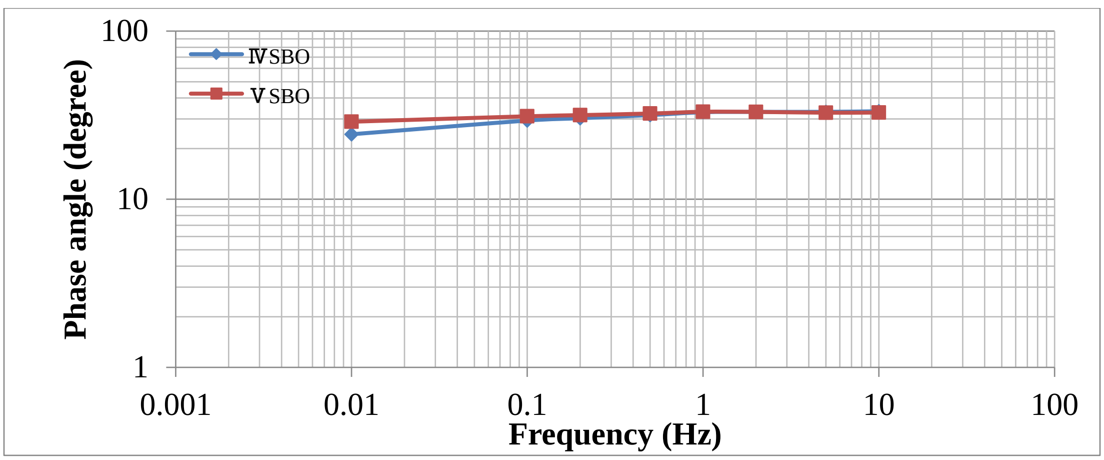

(c)

Figure 9-40 Phase Angle Values of Various Base Type B Mixtures without RAP in Terms of Aggregate Source, (a) at 4°C (39.2°F), (b) at 20°C (68°F), (c) at 40°C (104°F)

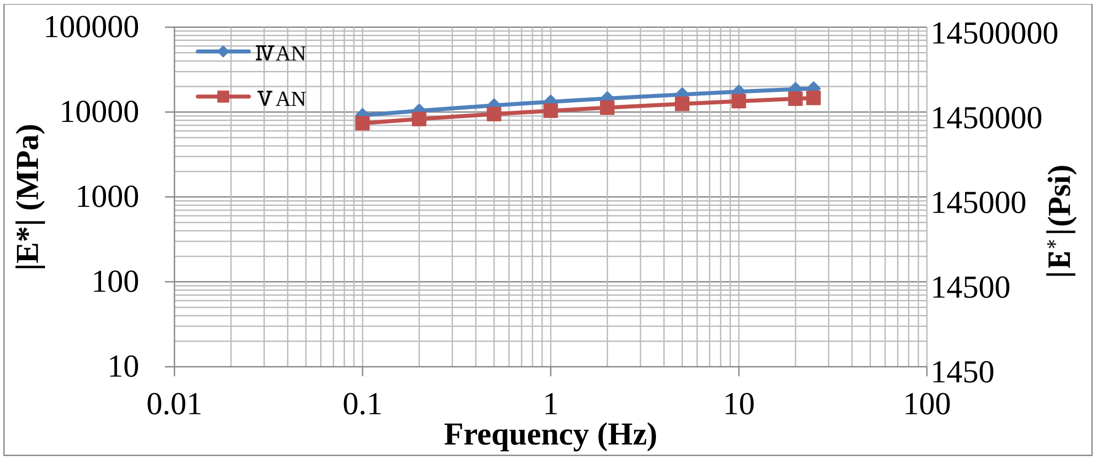

(a)

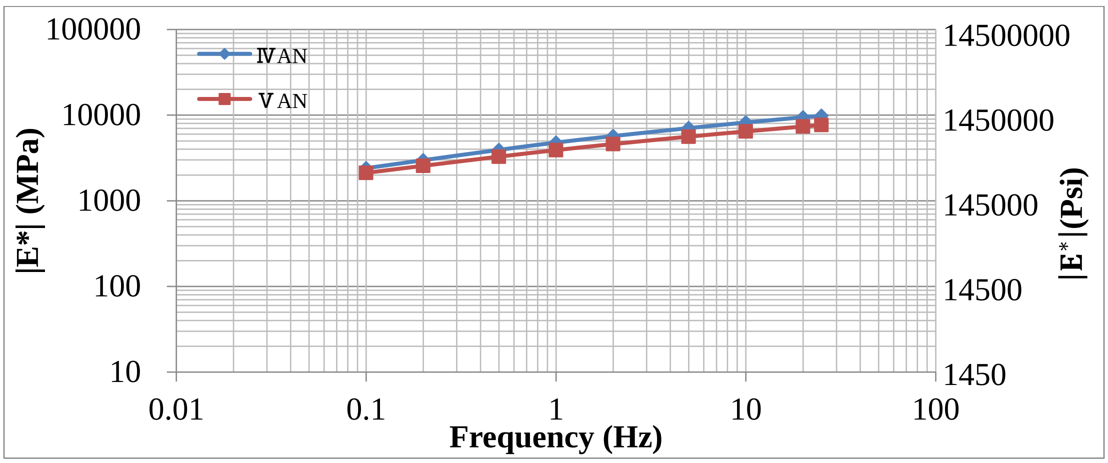

(b)

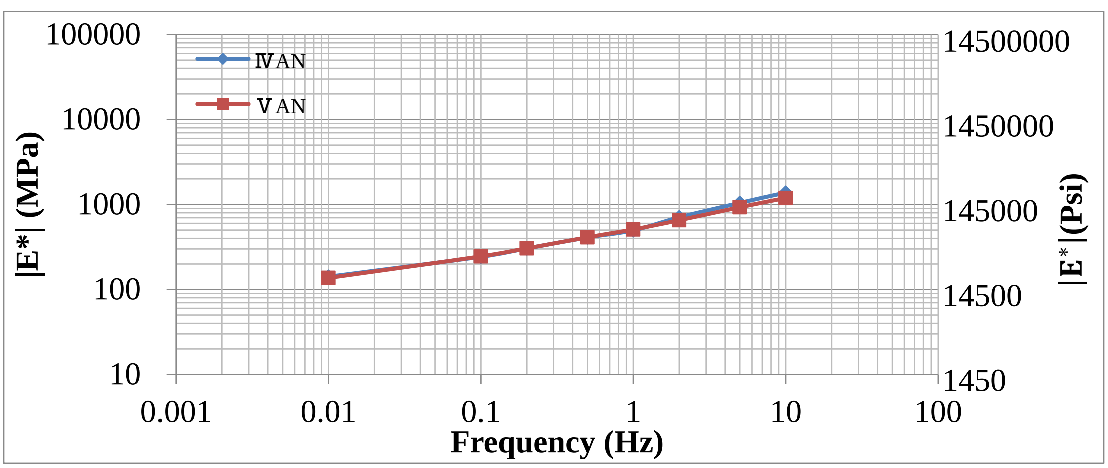

(c)

Figure 9-41 Dynamic Modulus Values of Various Surface Type A Mixtures with RAP and Asphalt Source 2 in Terms of Aggregate Source, (a) at 4°C (39.2°F), (b) at 20°C (68°F), (c) at 40°C (104°F)

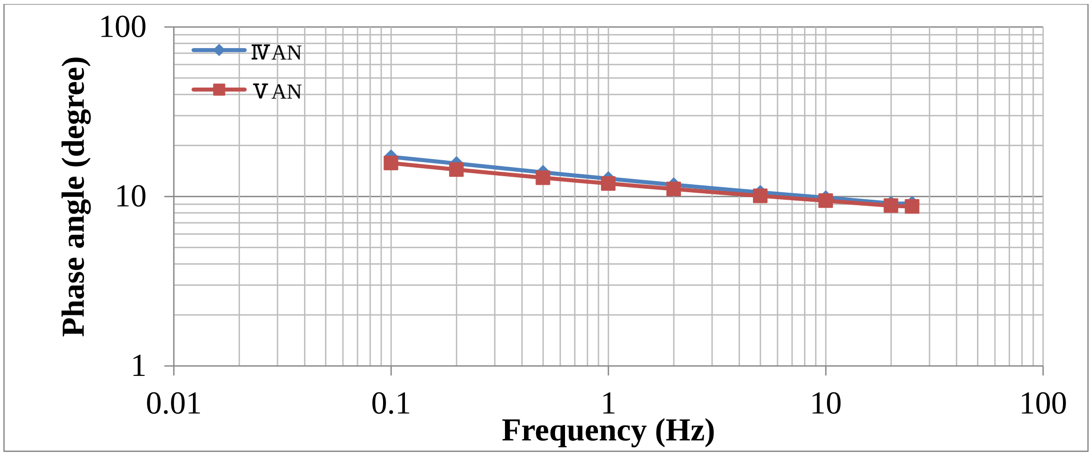

(a)

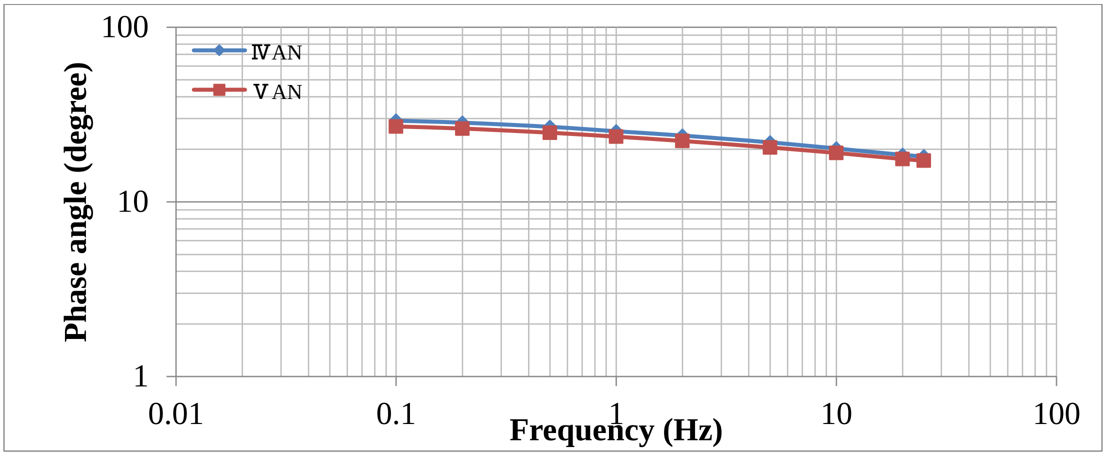

(b)

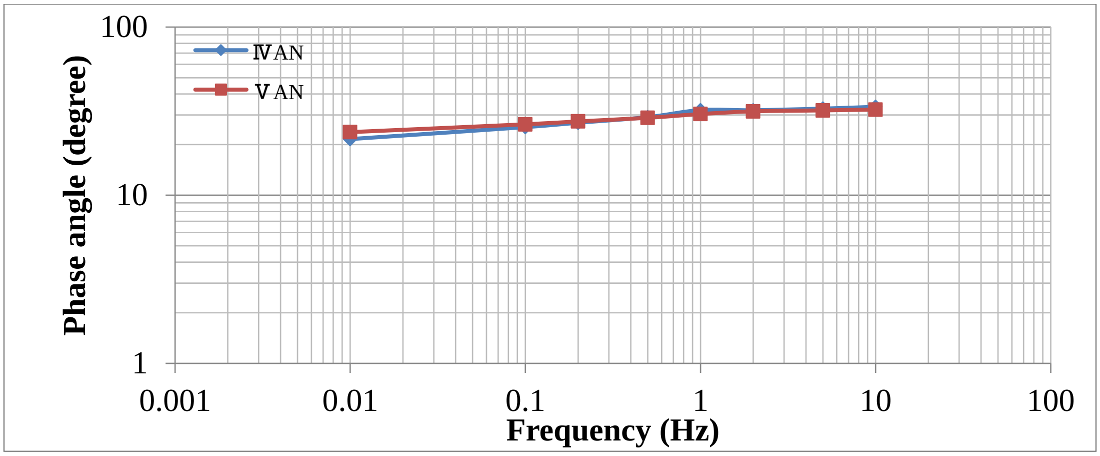

(c)

Figure 9-42 Phase Angle Values of Various Surface Type A Mixtures with RAP and Asphalt Source 2 in Terms of Aggregate Source, (a) at 4°C (39.2°F), (b) at 20°C (68°F), (c) at 40°C (104°F)

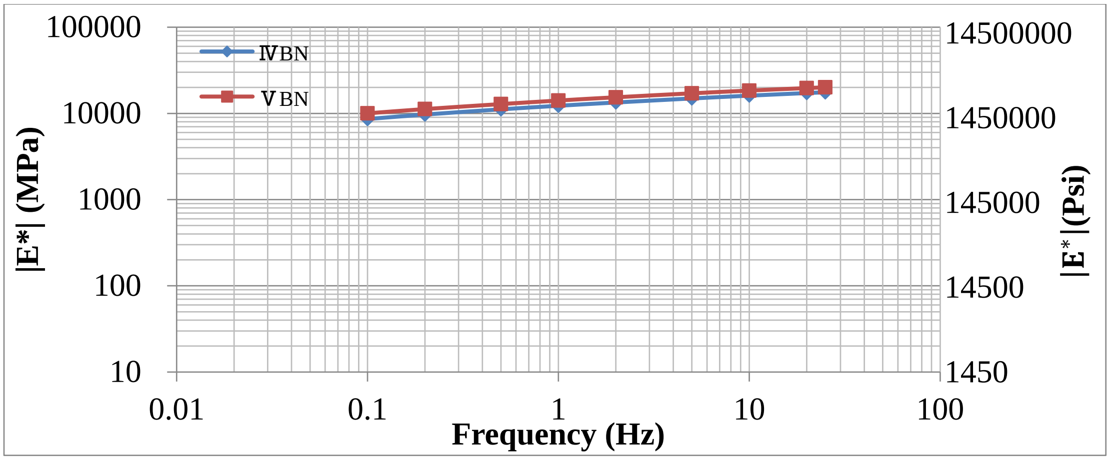

(a)

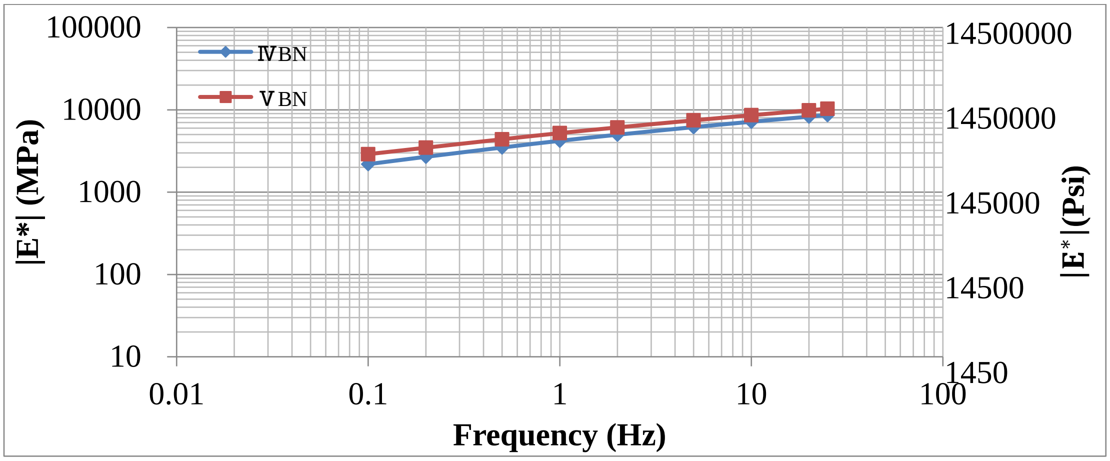

(b)

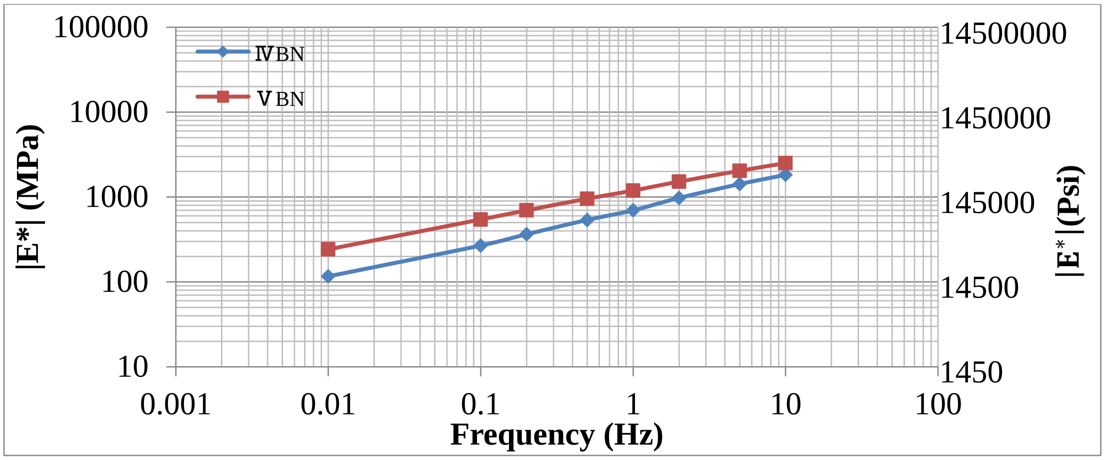

(c)

Figure 9-43 Dynamic Modulus Values of Various Surface Type B Mixtures with RAP and Asphalt Source 2 in Terms of Aggregate Source, (a) at 4°C (39.2°F), (b) at 20°C (68°F), (c) at 40°C (104°F)

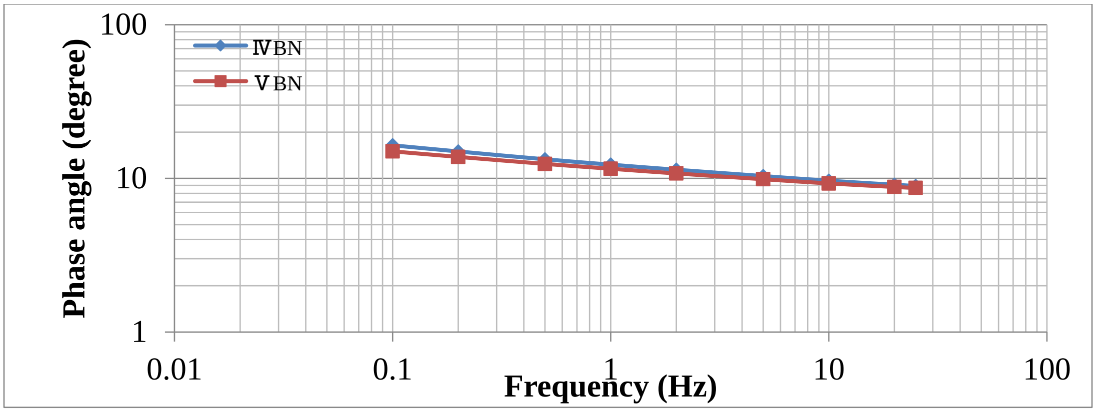

(a)

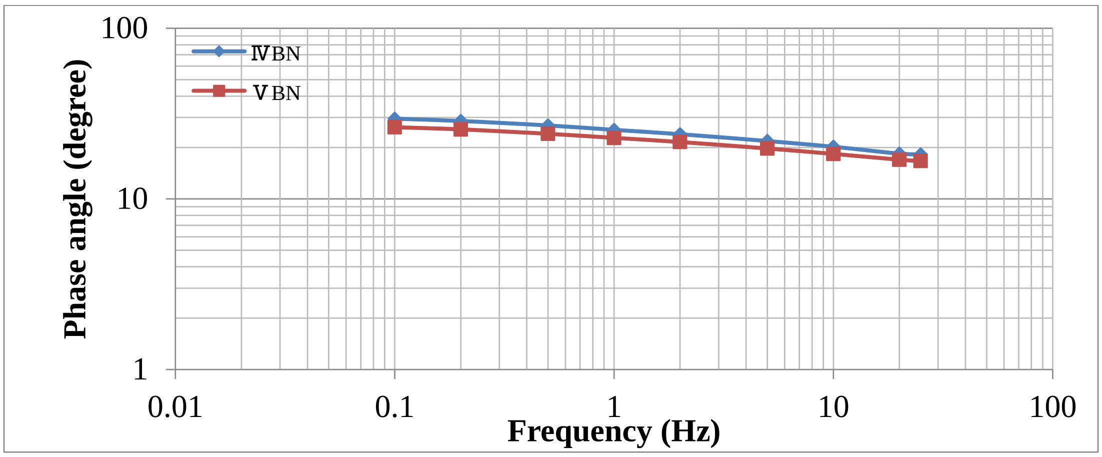

(b)

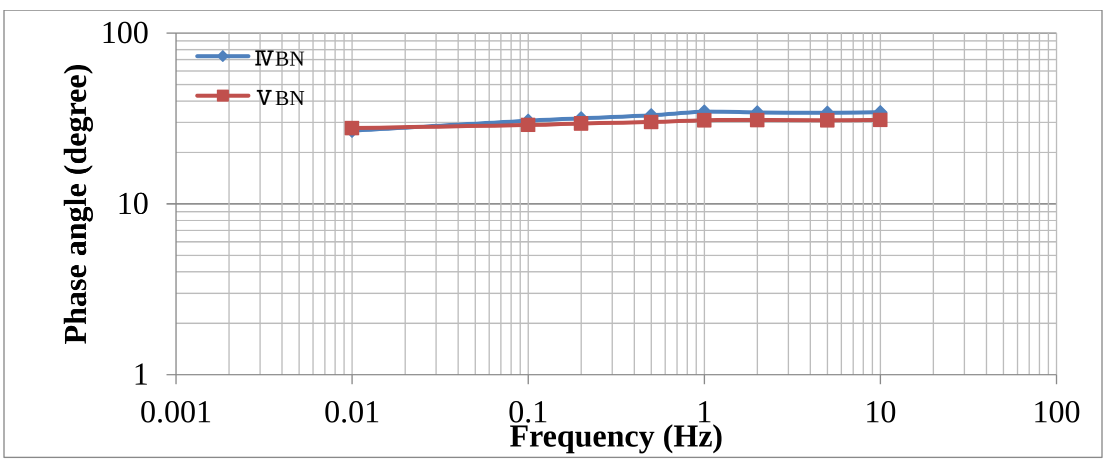

(c)

Figure 9-44 Phase Angle Values of Various Surface Type B Mixtures with RAP and Asphalt Source 2 in Terms of Aggregate Source, (a) at 4°C (39.2°F), (b) at 20°C (68°F), (c) at 40°C (104°F)

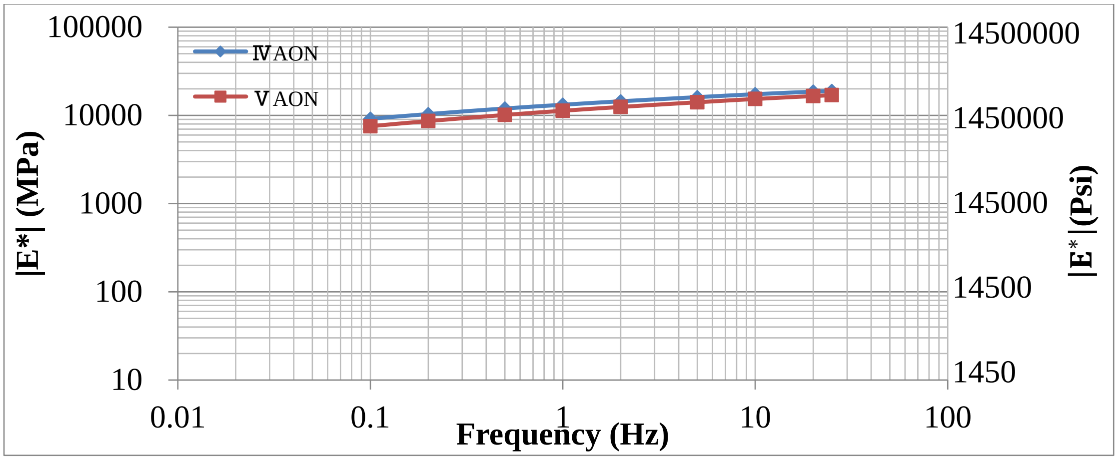

(a)

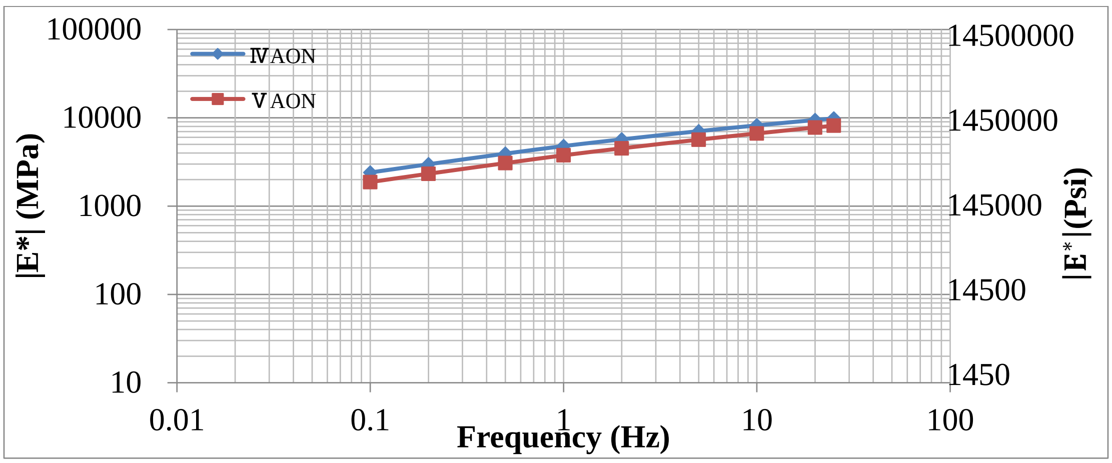

(b)

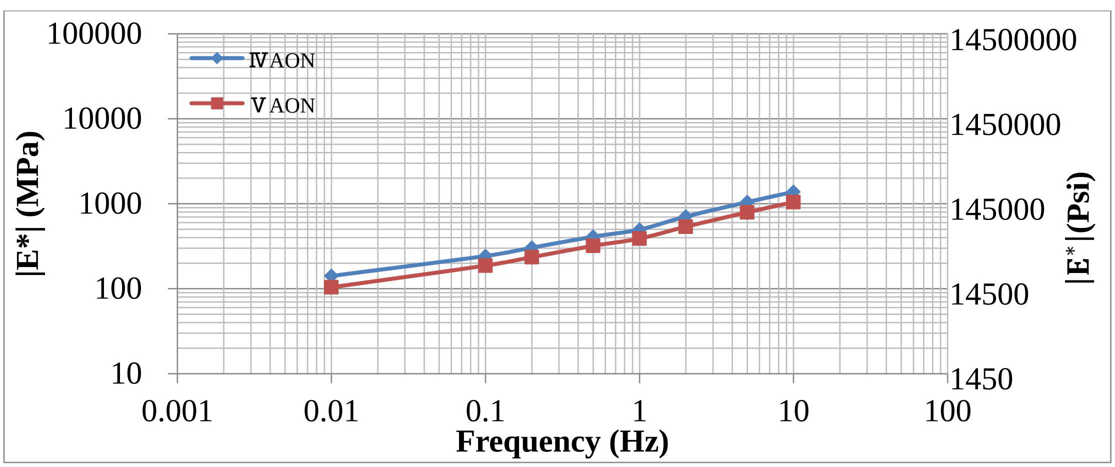

(c)

Figure 9-45 Dynamic Modulus Values of Various Surface Type A Mixtures using Asphalt Source 2 without RAP in Terms of Aggregate Source, (a) at 4°C (39.2°F), (b) at 20°C (68°F), (c) at 45°C (113°F)

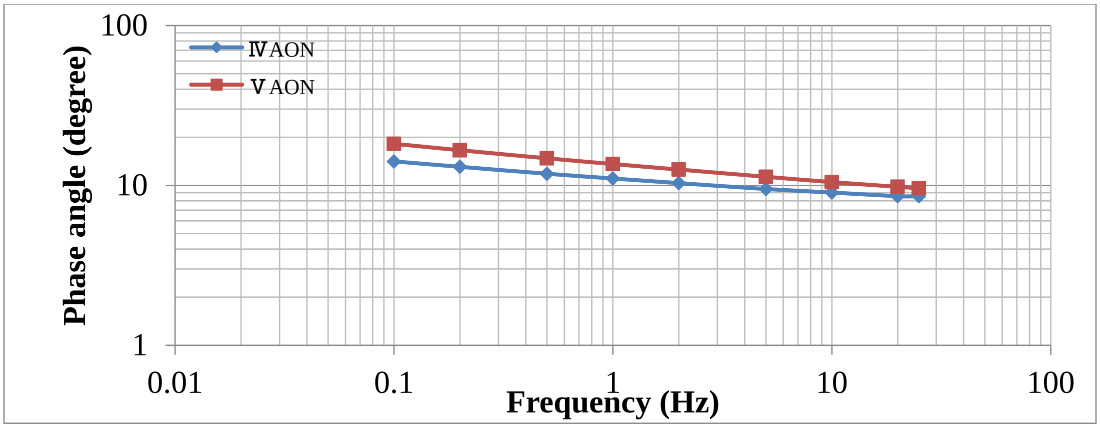

(a)

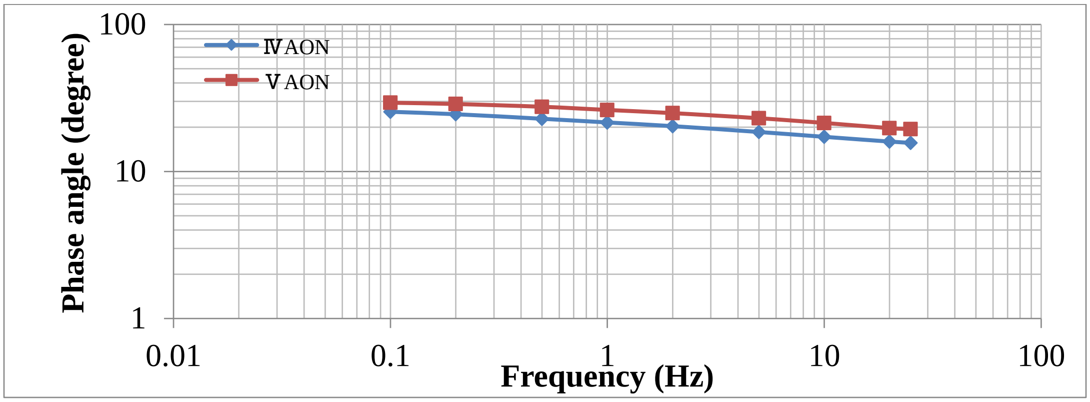

(b)

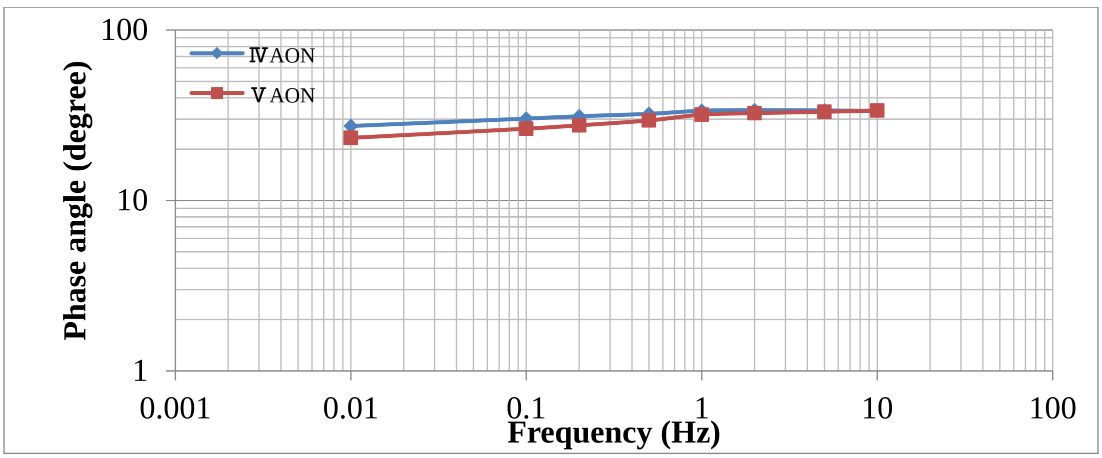

(c)

Figure 9-46 Phase Angle Values of Various Surface Type A Mixtures using Asphalt Source 2 without RAP in Terms of Aggregate Source, (a) at 4°C (39.2°F), (b) at 20°C (68°F), (c) at 45°C (113°F)

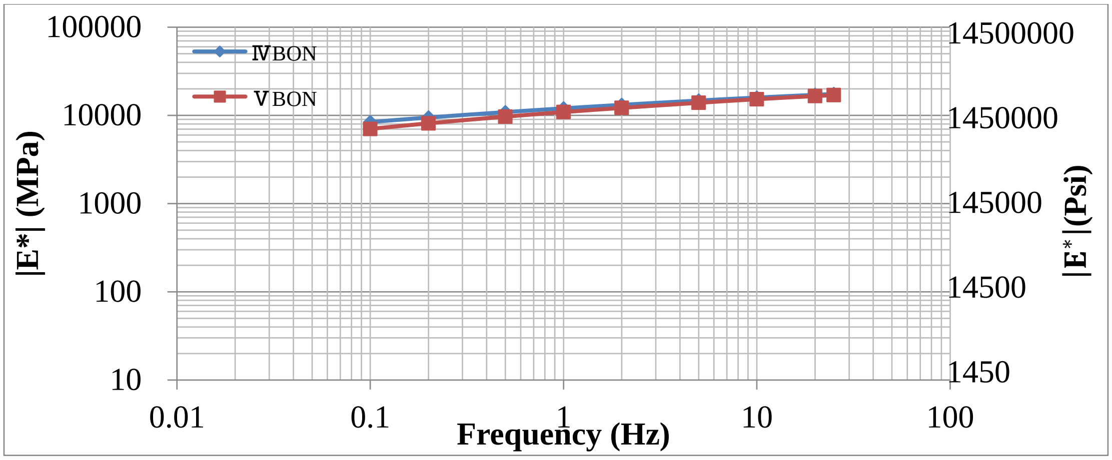

(a)

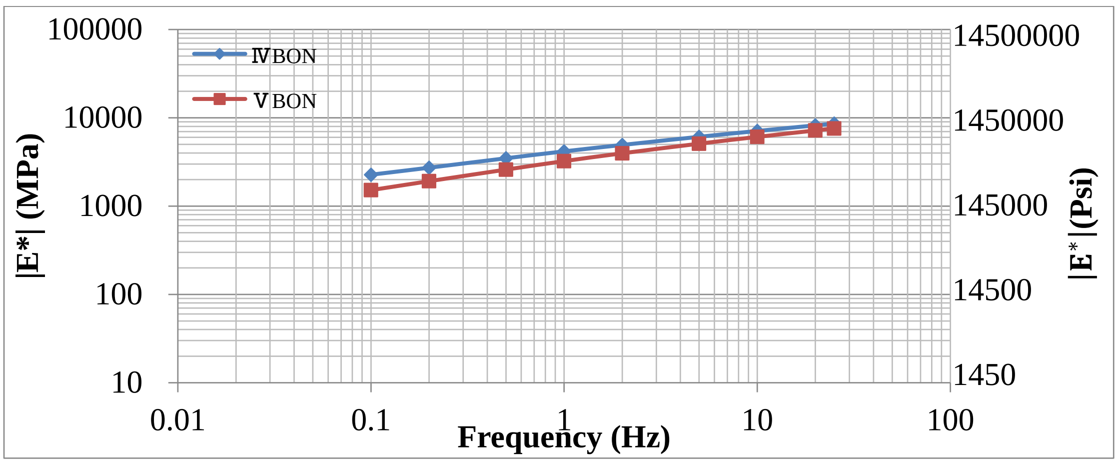

(b)

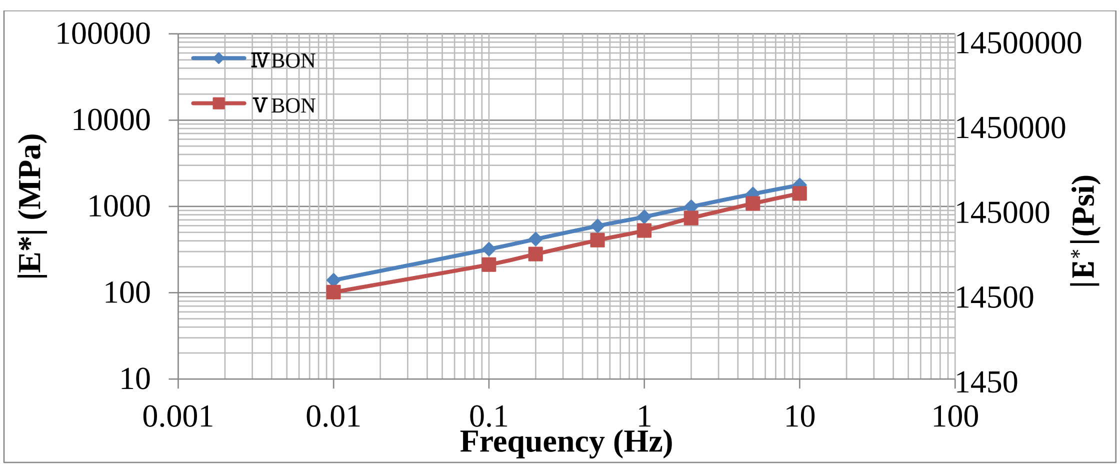

(c)

Figure 9-47 Dynamic Modulus Values of Various Surface Type B Mixtures using Asphalt Source 2 without RAP in Terms of Aggregate Source, (a) at 4°C (39.2°F), (b) at 20°C (68°F), (c) at 40°C (104°F)

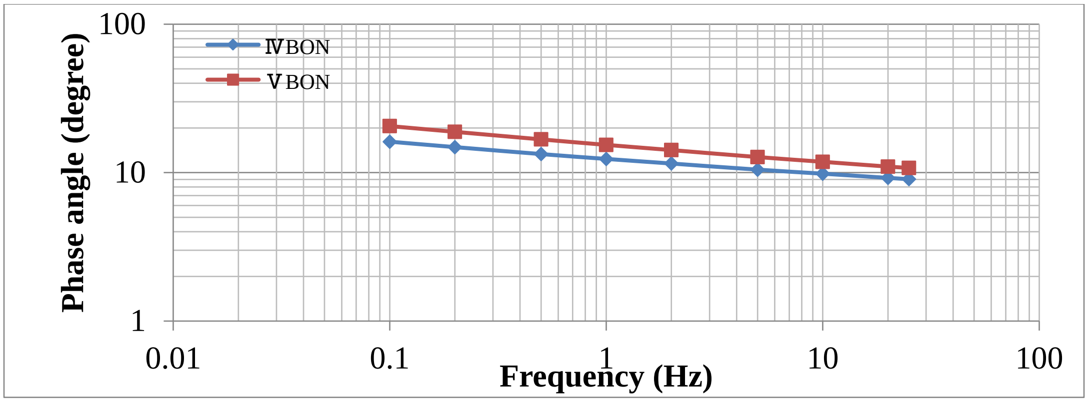

(a)

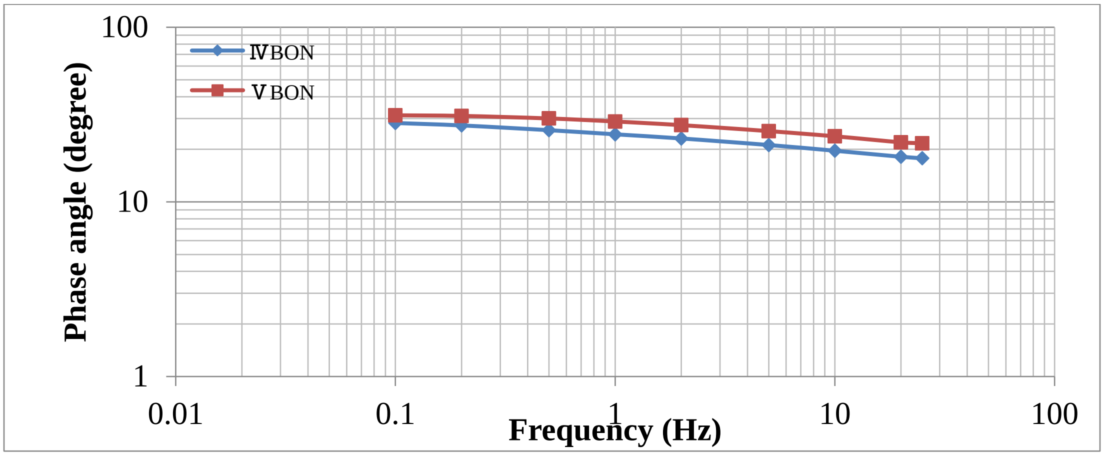

(b)

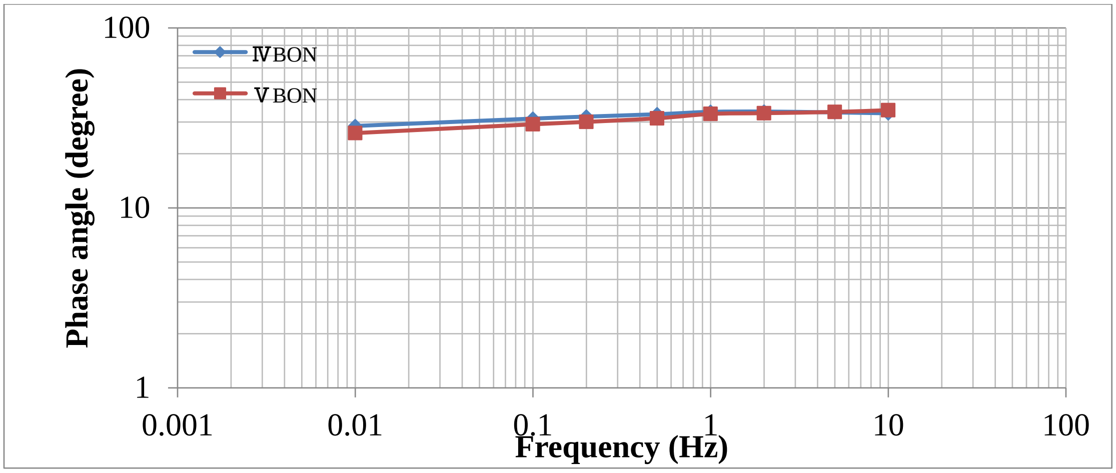

(c)

Figure 9-48 Phase Angle Values of Various Mixtures from Surface Type B using Asphalt Source 2 without RAP in Terms of Aggregate Source, (a) at 4°C (39.2°F), (b) at 20°C (68°F), (c) at 40°C (104°F)

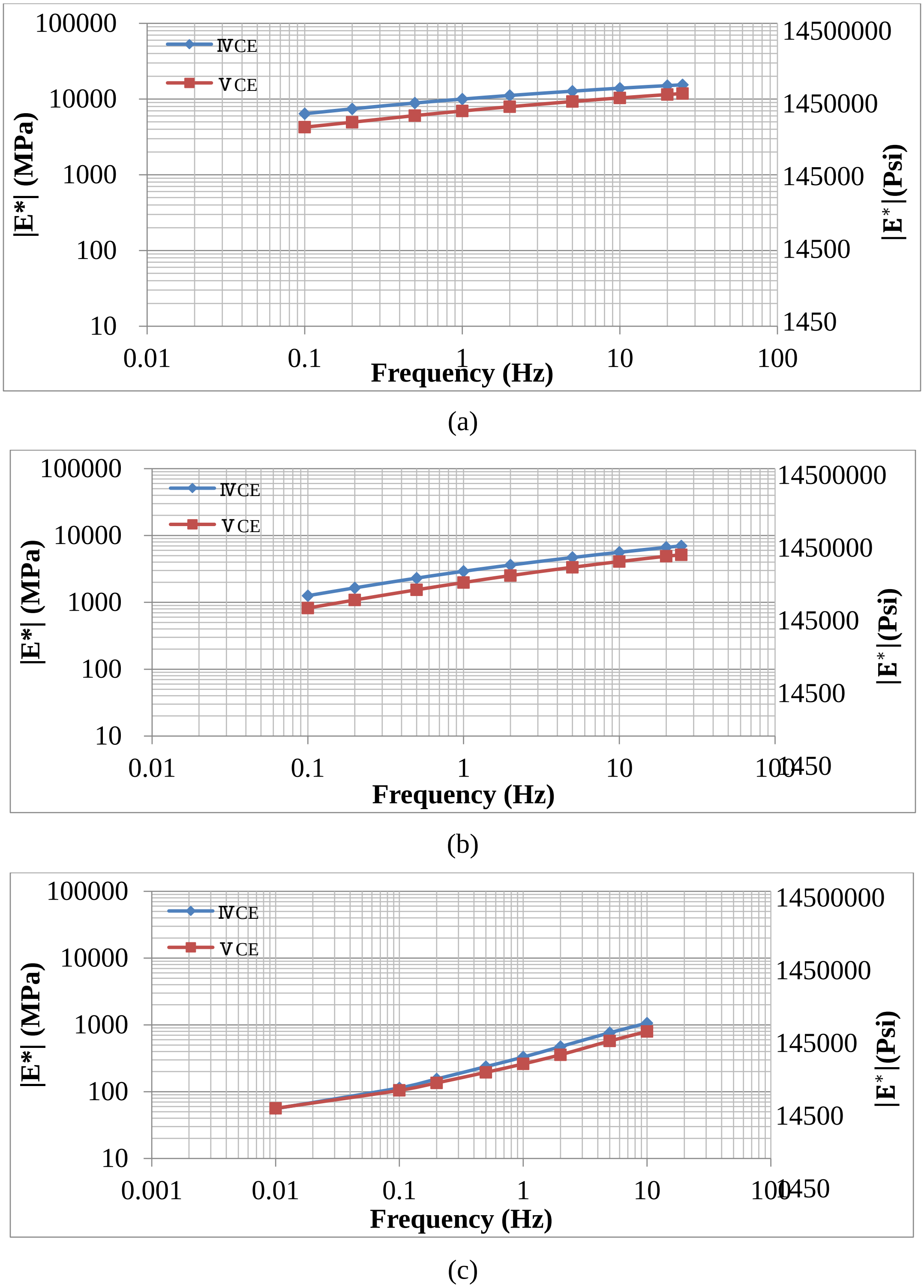

Figure 9-49 Dynamic Modulus Values of Various Mixtures from Surface Type C with RAP and WMA-Chemical Additive in Terms of Aggregate Source, (a) at 4°C (39.2°F), (b) at 20°C (68°F), (c) at 40°C (104°F)

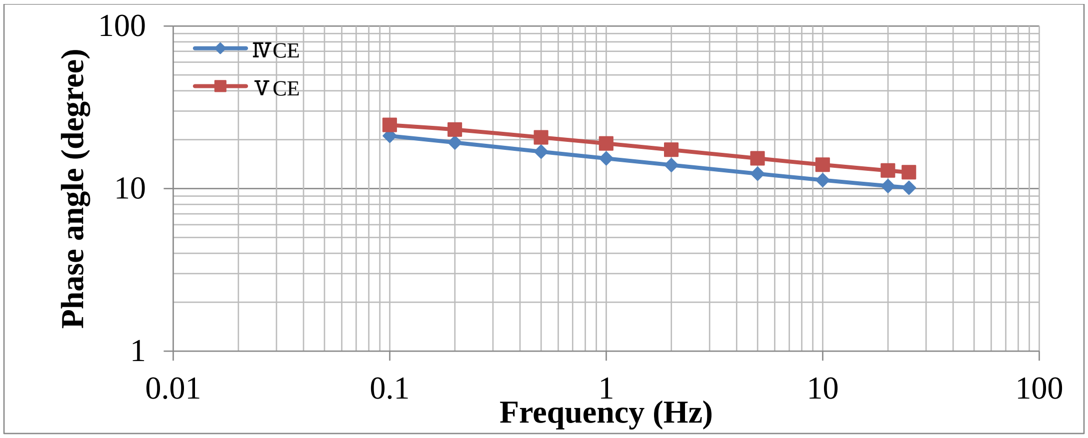

(a)

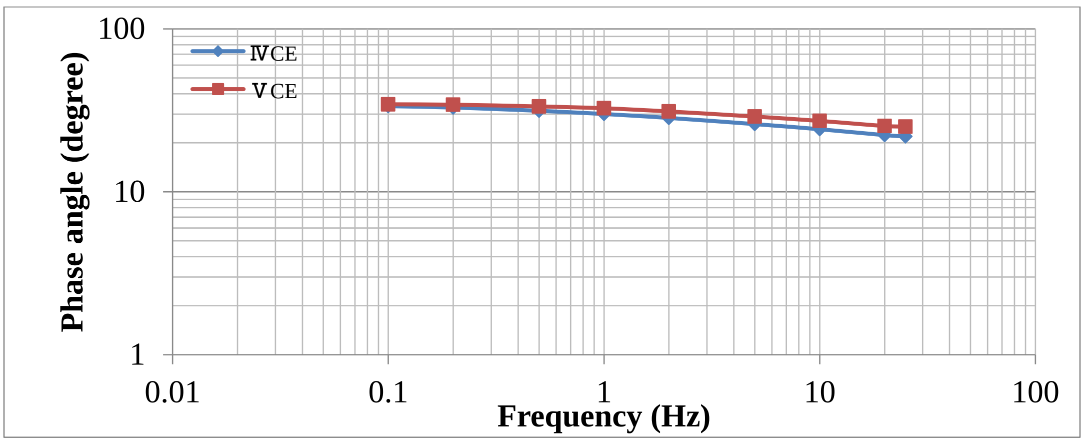

(b)

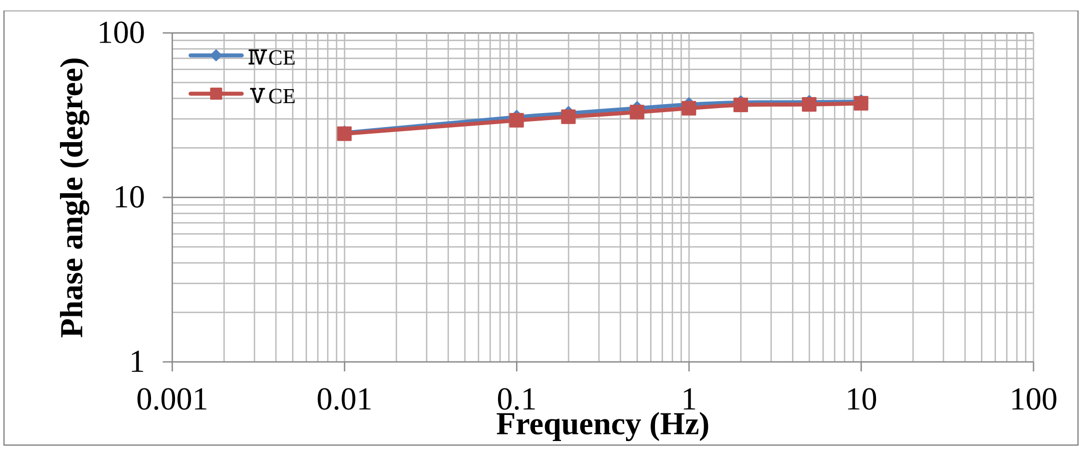

(c)

Figure 9-50 Phase Angle Values of Various Mixtures from Surface Type C with RAP and WMA-Chemical Additive in Terms of Aggregate Source, (a) at 4°C (39.2°F), (b) at 20°C (68°F), (c) at 40°C (104°F)

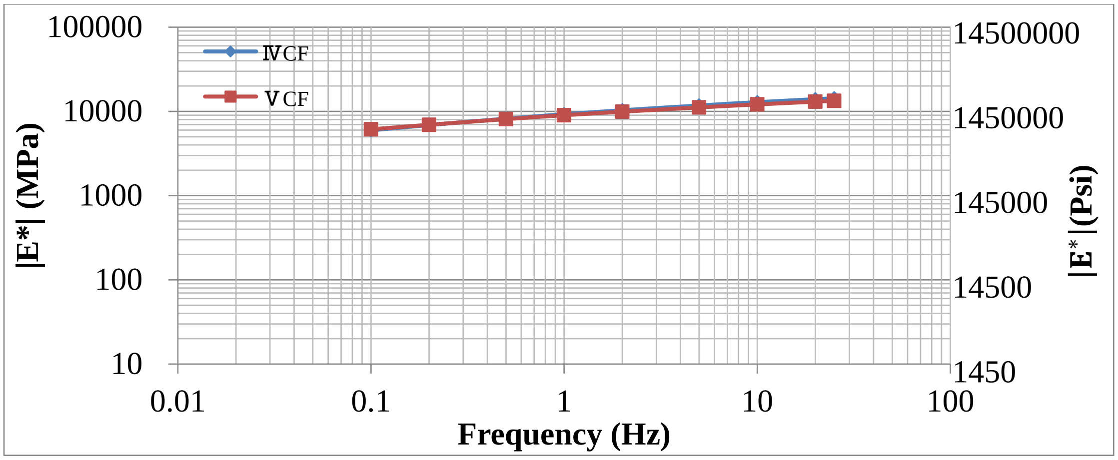

(a)

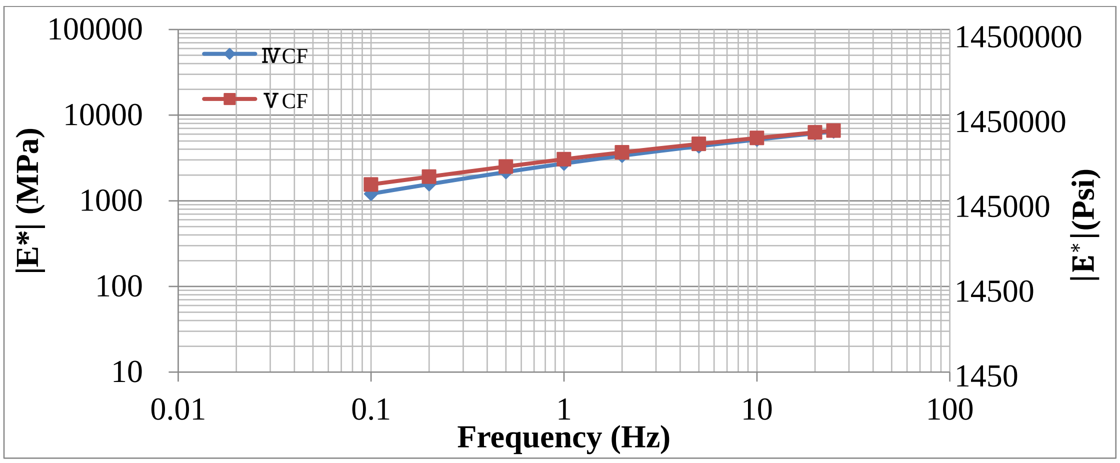

(b)

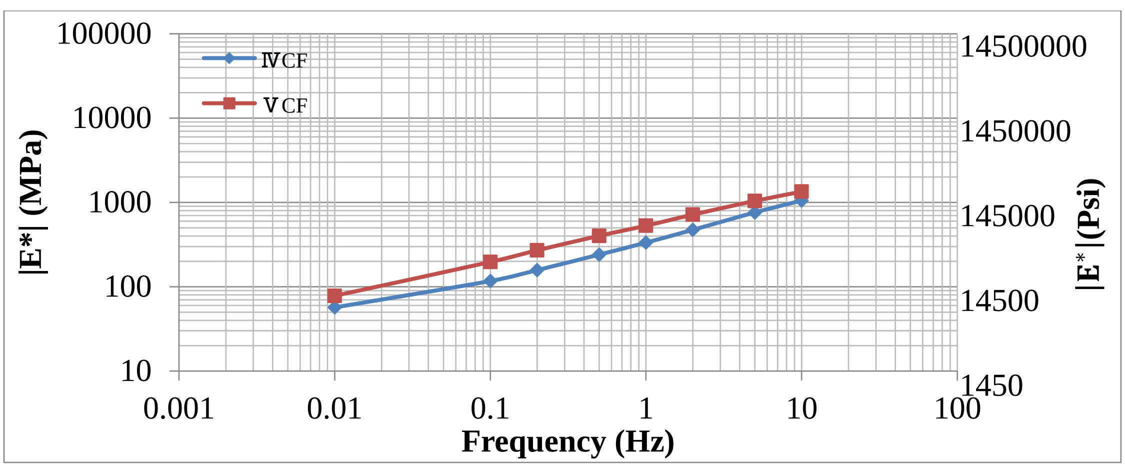

(c)

Figure 9-51 Dynamic Modulus Values of Various Mixtures from Surface Type C with RAP and WMA-Foaming in Terms of Aggregate Source, (a) at 4°C (39.2°F), (b) at 20°C (68°F), (c) at 40°C (104°F)

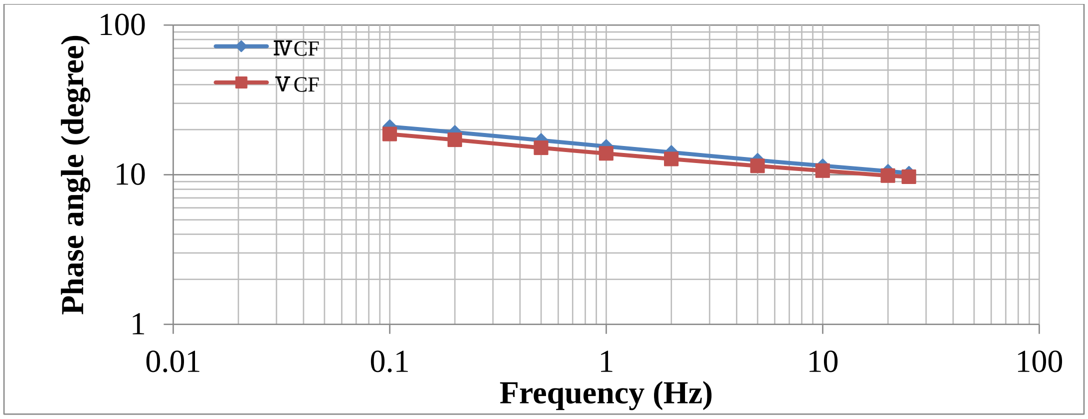

(a)

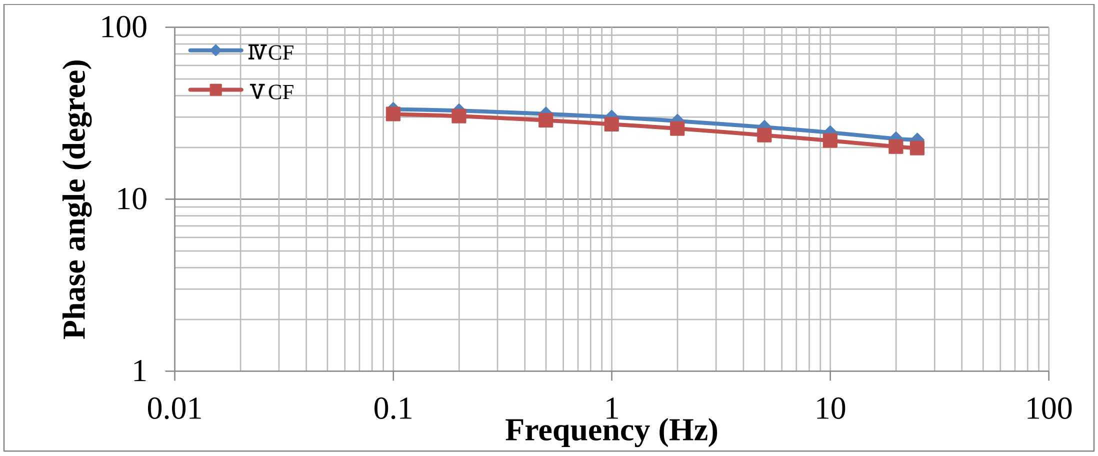

(b)

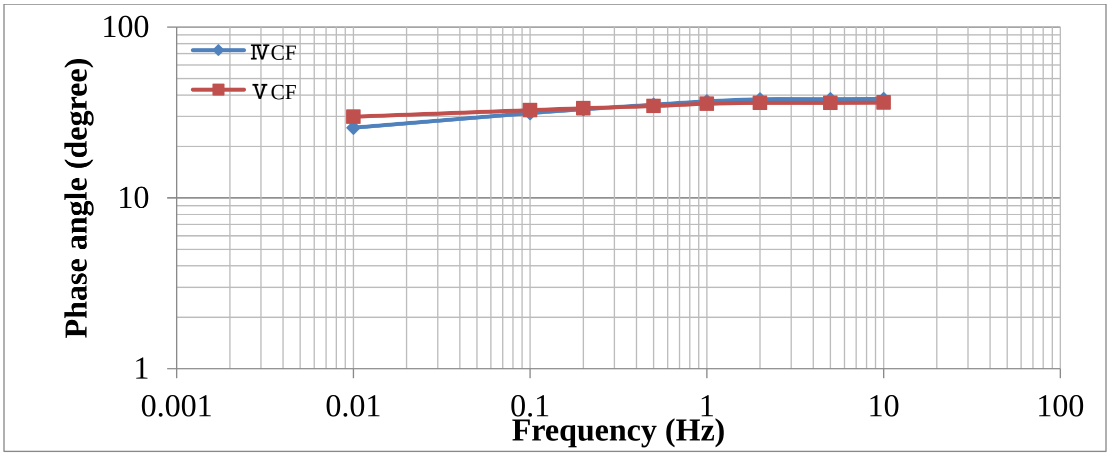

(c)

Figure 9-52 Phase Angle Values of Various Mixtures from Surface Type C with RAP and WMA-Foaming in Terms of Aggregate Source, (a) at 4°C (39.2°F), (b) at 20°C (68°F), (c) at 40°C (104°F)

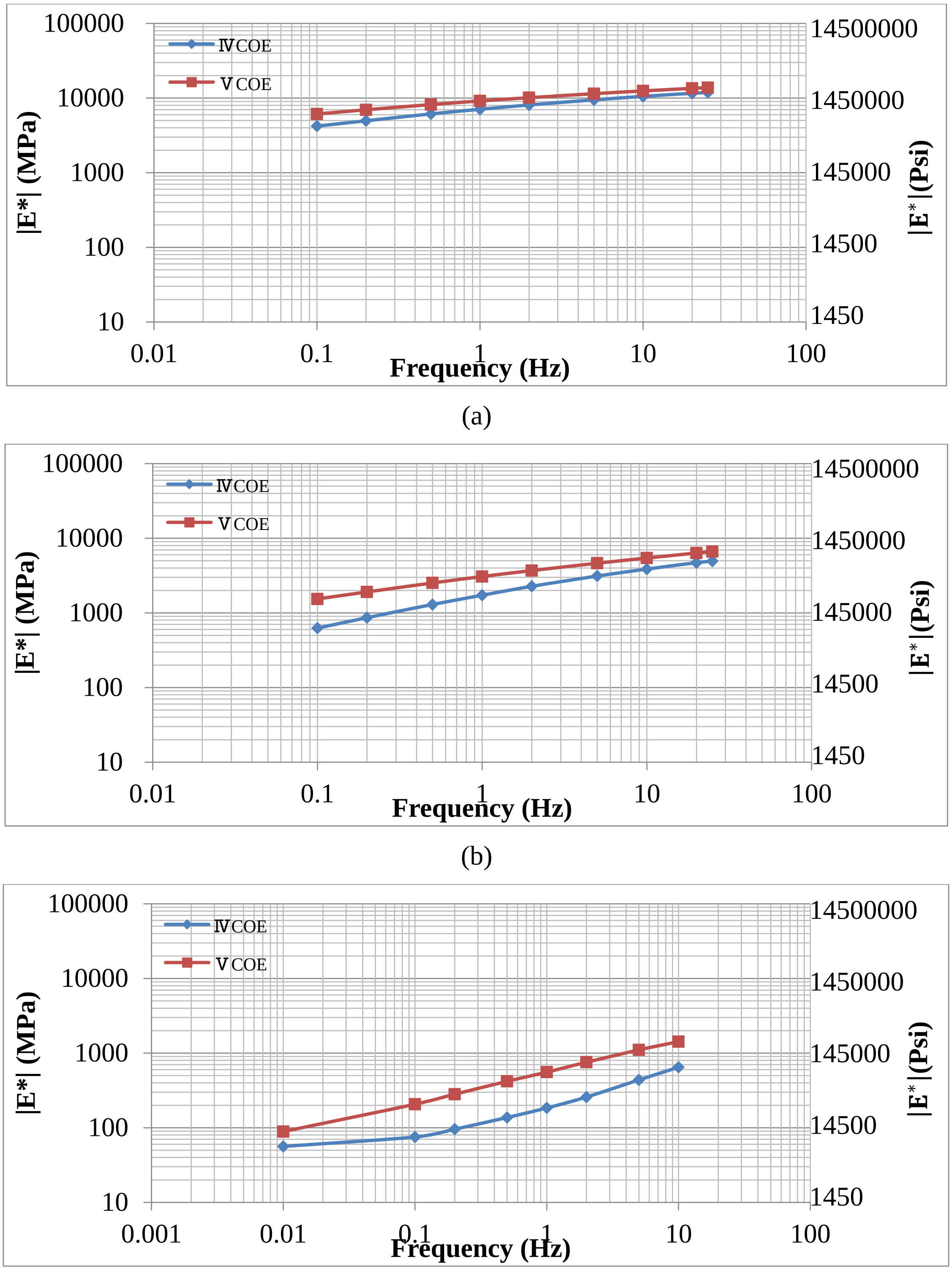

(a)

(b)

(c)

Figure 9-53 Dynamic Modulus Values of Various Mixtures from Surface Type C using WMA-Chemical Additive without RAP in Terms of Aggregate Source, (a) at 4°C (39.2°F), (b) at 20°C (68°F), (c) at 40°C (104°F)

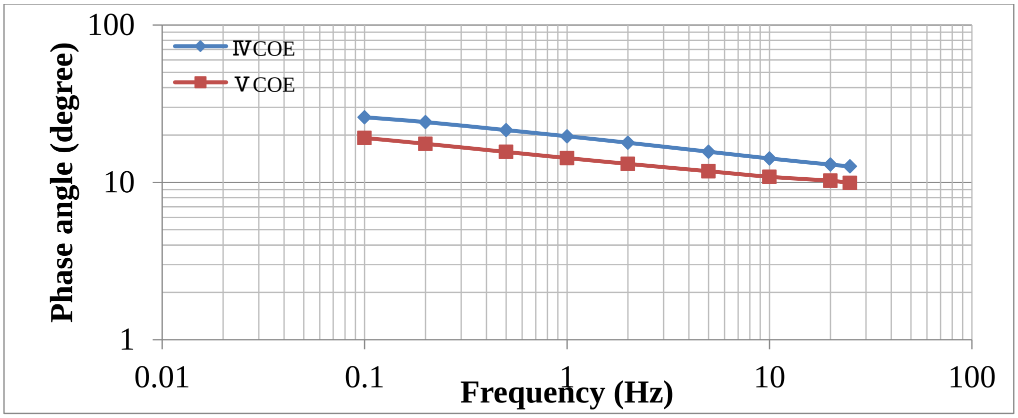

(a)

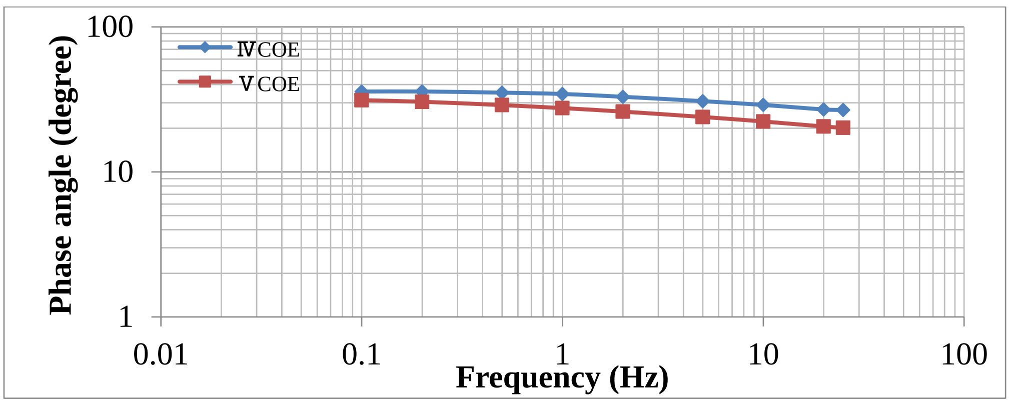

(b)

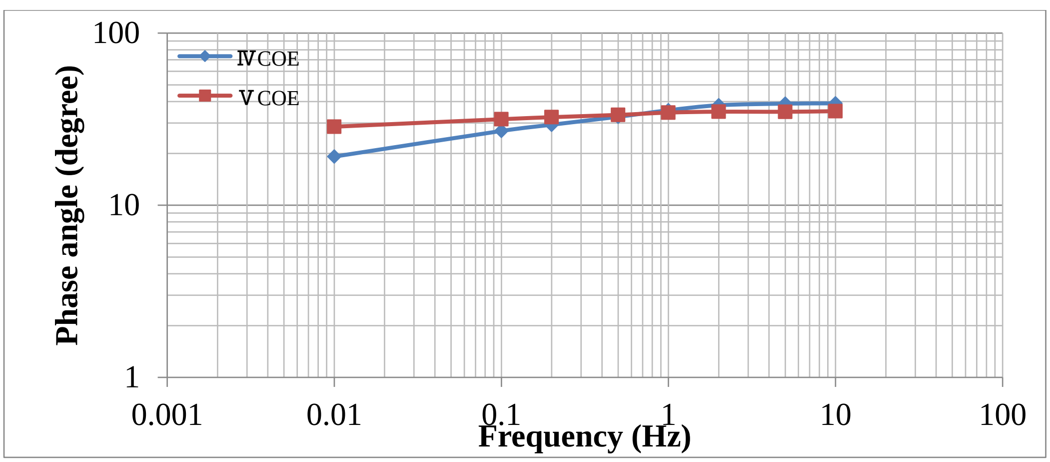

(c)

Figure 9-54 Phase Angle Values of Various Mixtures from Surface Type C using WMA-Chemical Additive without RAP in Terms of Aggregate Source, (a) at 4°C (39.2°F), (b) at 20°C (68°F), (c) at 40°C (104°F)

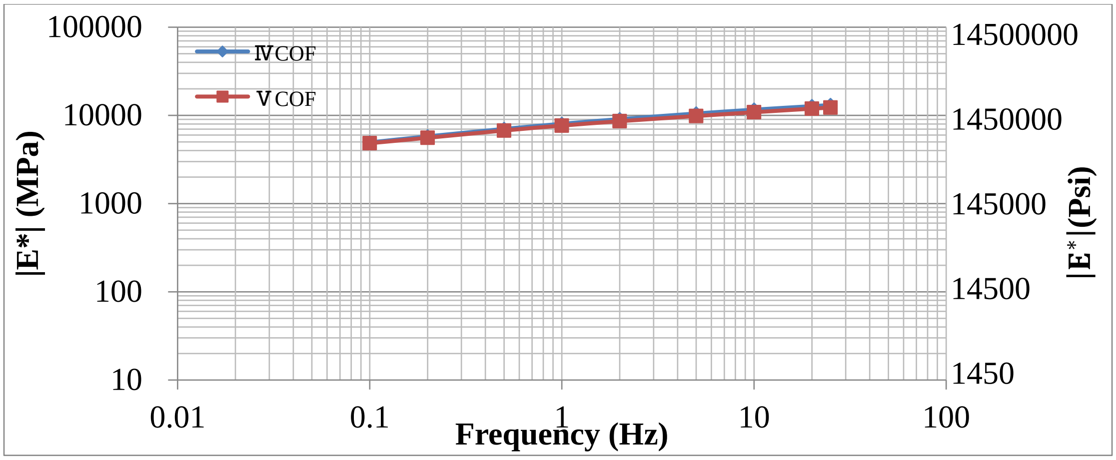

(a)

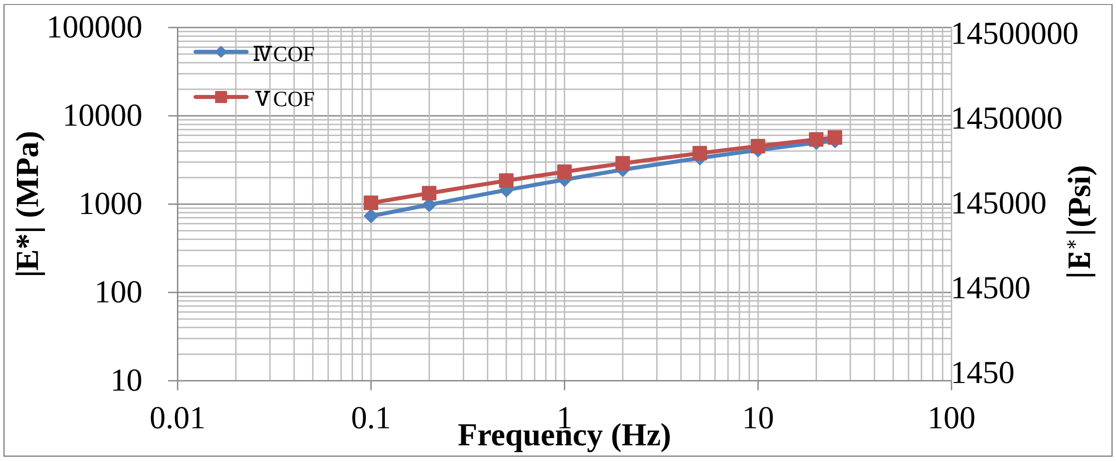

(b)

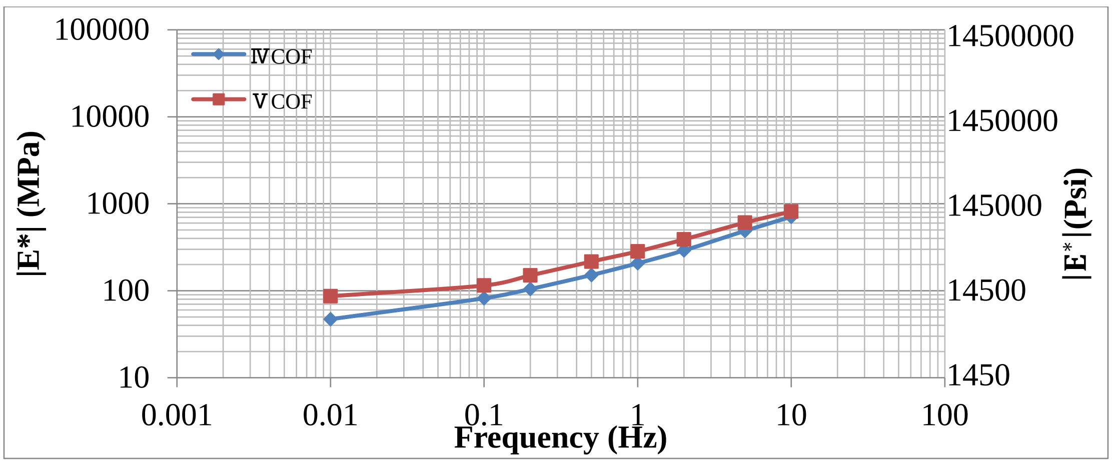

(c)

Figure 9-55 Dynamic Modulus Values of Various Mixtures from Surface Type C using WMA-Foaming without RAP in Terms of Aggregate Source, (a) at 4°C (39.2°F), (b) at 20°C (68°F), (c) at 40°C (104°F)

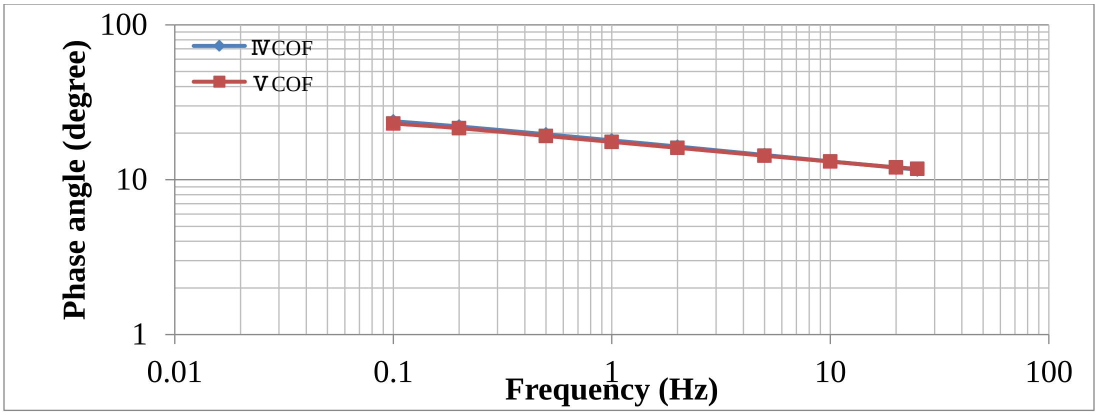

(a)

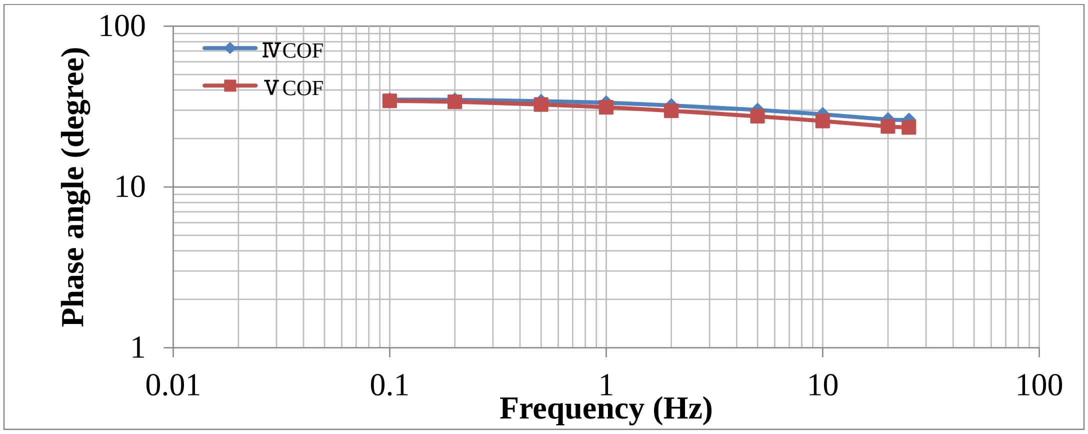

(b)

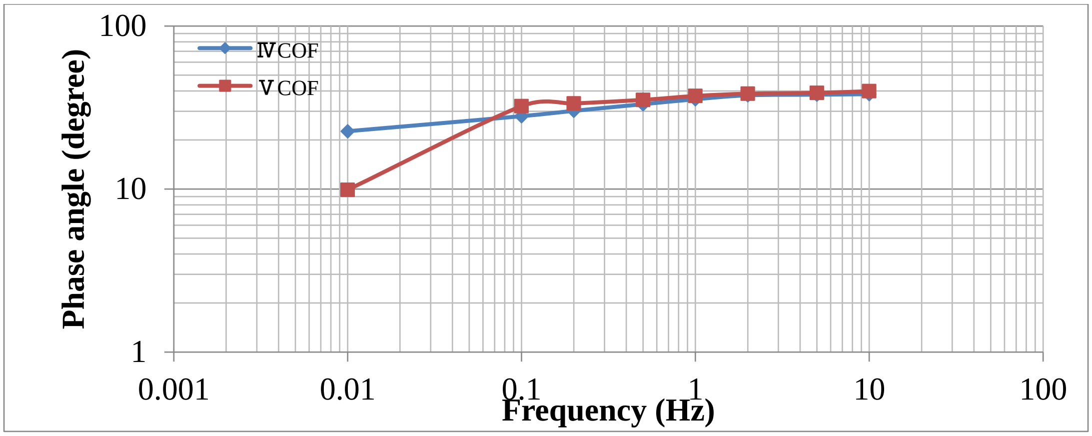

(c)

Figure 9-56 Phase Angle Values of Various Mixtures from Surface Type C using WMA-Foaming without RAP in Terms of Aggregate Source, (a) at 4°C (39.2°F), (b) at 20°C (68°F), (c) at 40°C (104°F)

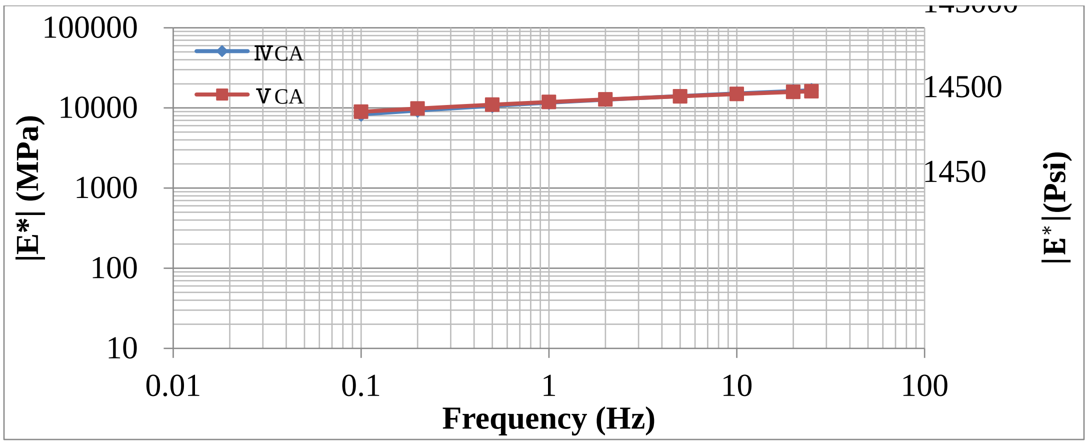

(a)

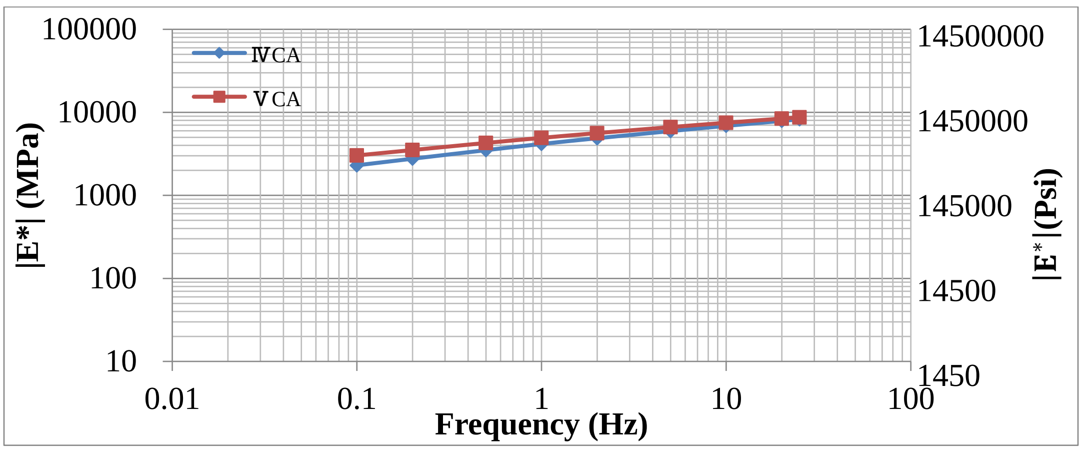

(b)

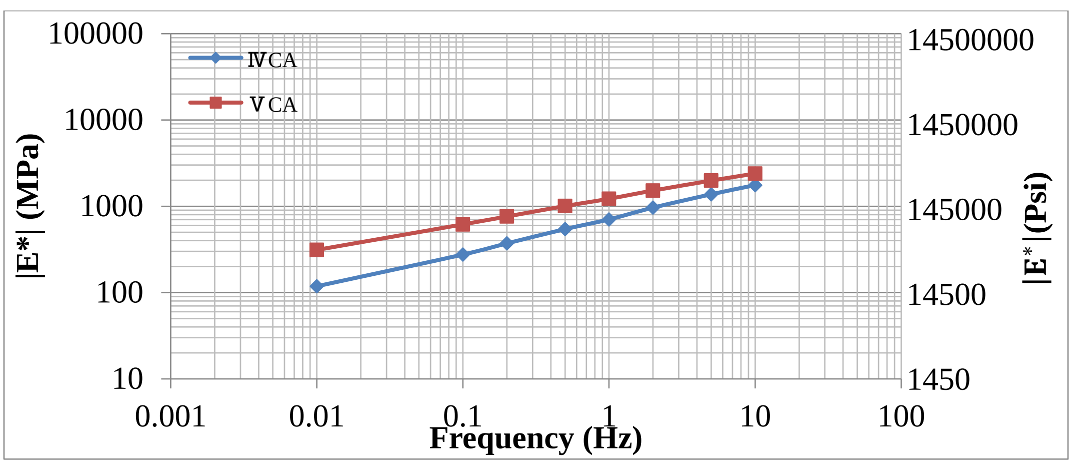

(c)

Figure 9-57 Dynamic Modulus Values of Various Mixtures from Surface Type C with RAP and Liquid ASA1 in Terms of Aggregate Source, (a) at 4°C (39.2°F), (b) at 20°C (68°F), (c) at 40°C (104°F)

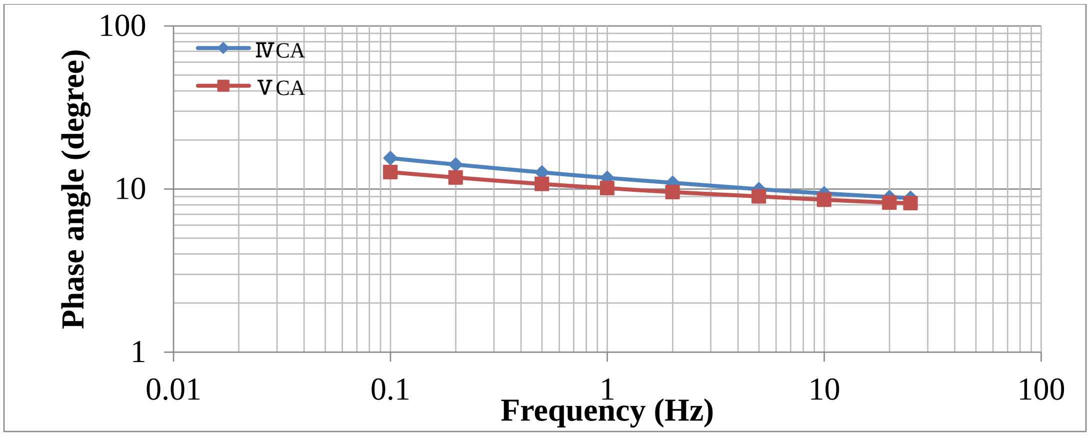

(a)

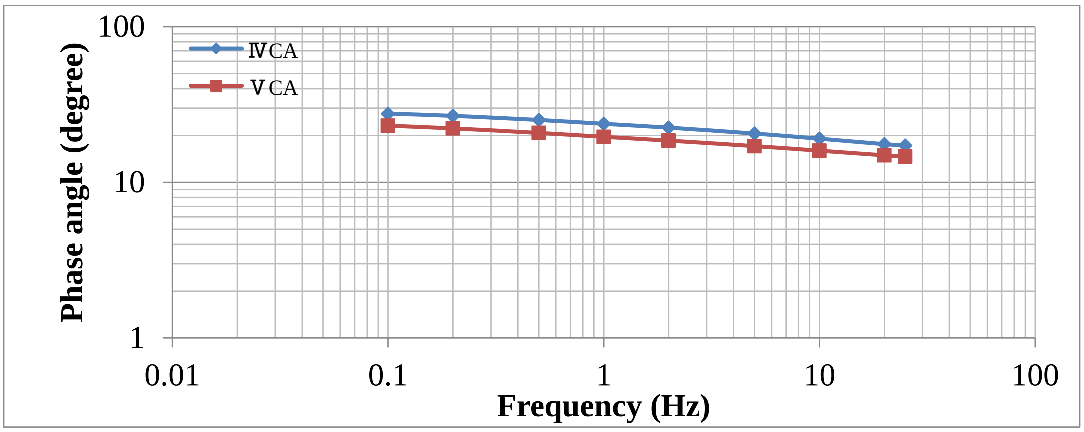

(b)

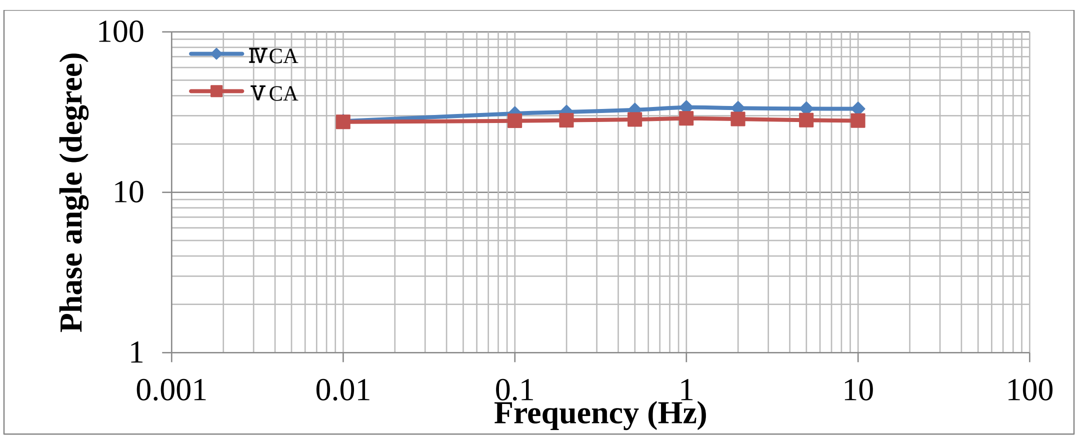

(c)

Figure 9-58 Phase Angle Values of Various Mixtures from Surface Type C with RAP and Liquid ASA1 in Terms of Aggregate Source, (a) at 4°C (39.2°F), (b) at 20°C (68°F), (c) at 40°C (104°F)

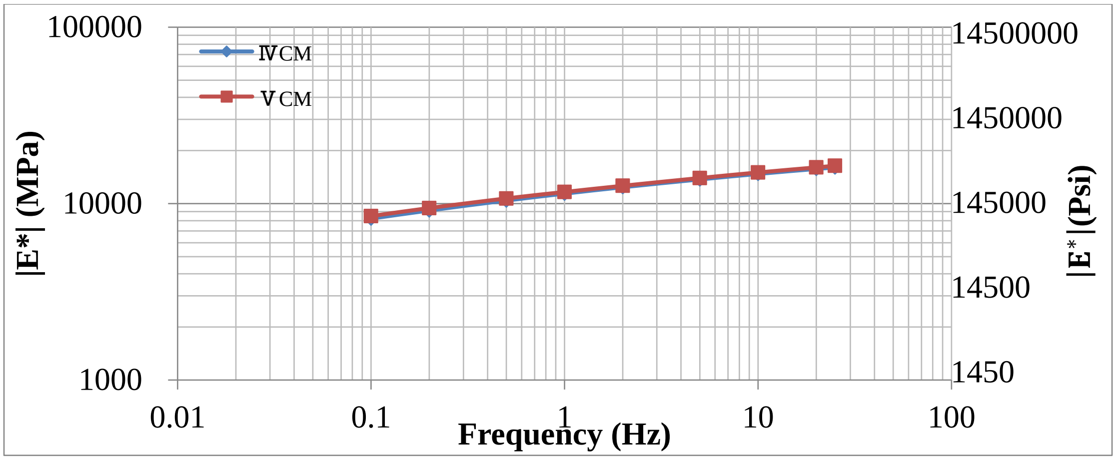

(a)

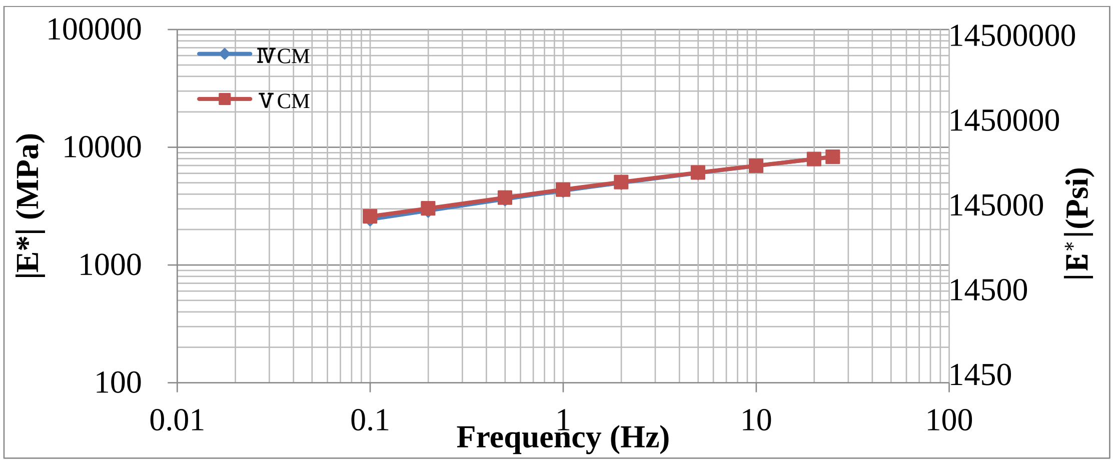

(b)

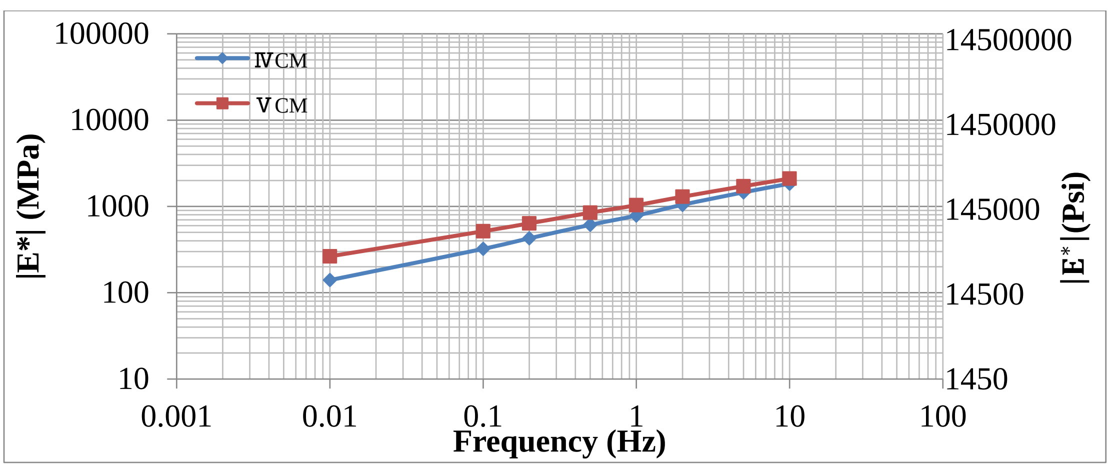

(c)

Figure 9-59 Dynamic Modulus Values of Various Mixtures from Surface Type C with RAP and Liquid ASA2 in Terms of Aggregate Source, (a) at 4°C (39.2°F), (b) at 20°C (68°F), (c) at 40°C (104°F)

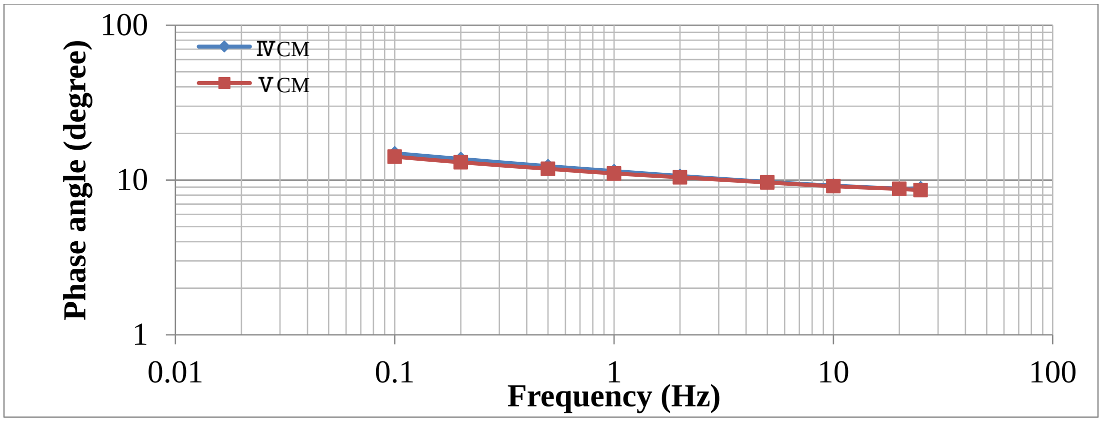

(a)

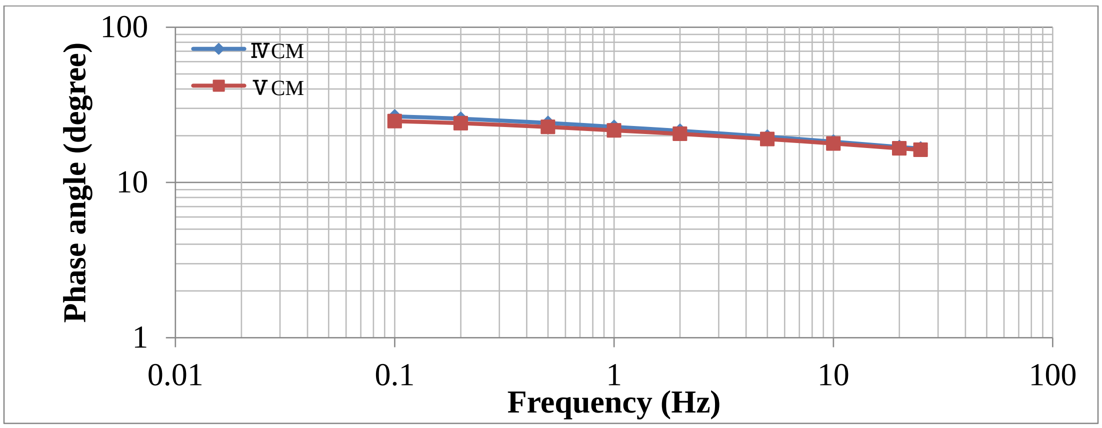

(b)

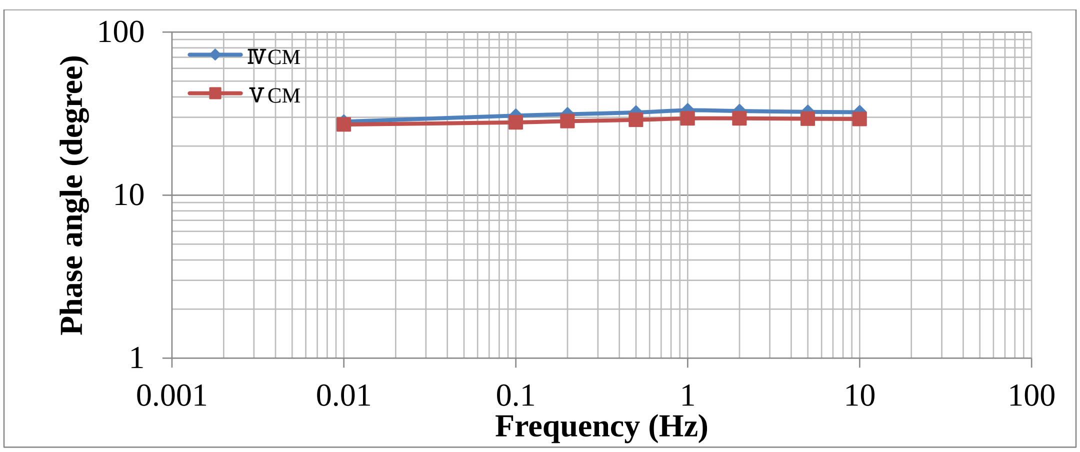

(c)

Figure 9-60 Phase Angle Values of Various Mixtures from Surface Type C with RAP and Liquid ASA2 in Terms of Aggregate Source, (a) at 4°C (39.2°F), (b) at 20°C (68°F), (c) at 40°C (104°F)

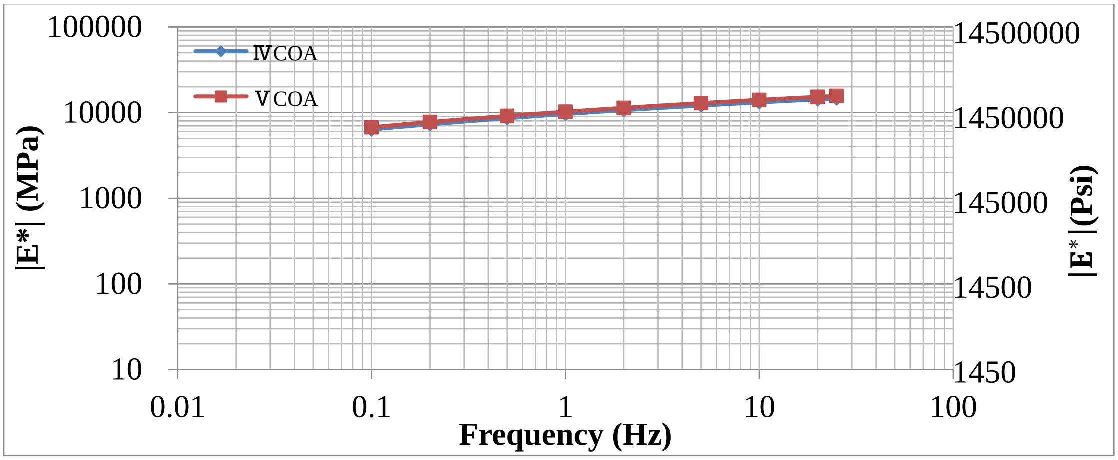

(a)

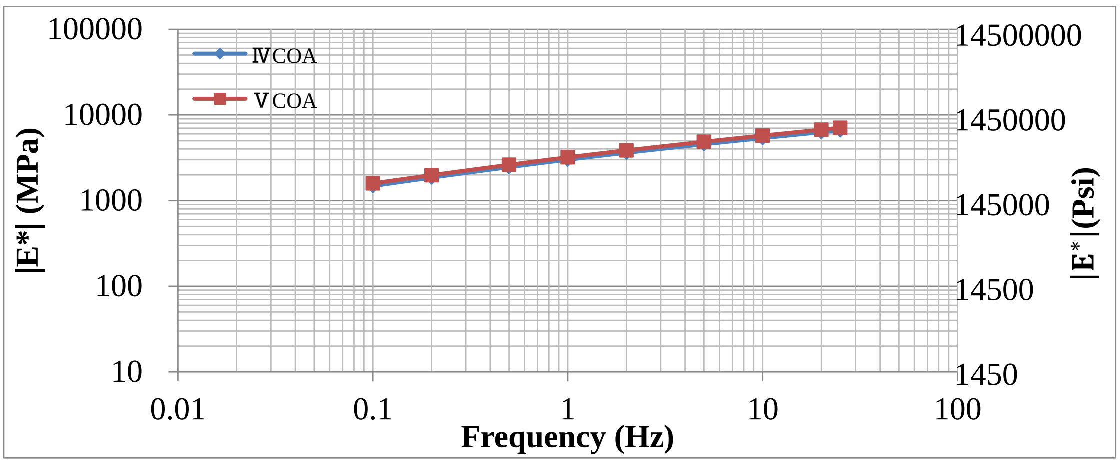

(b)

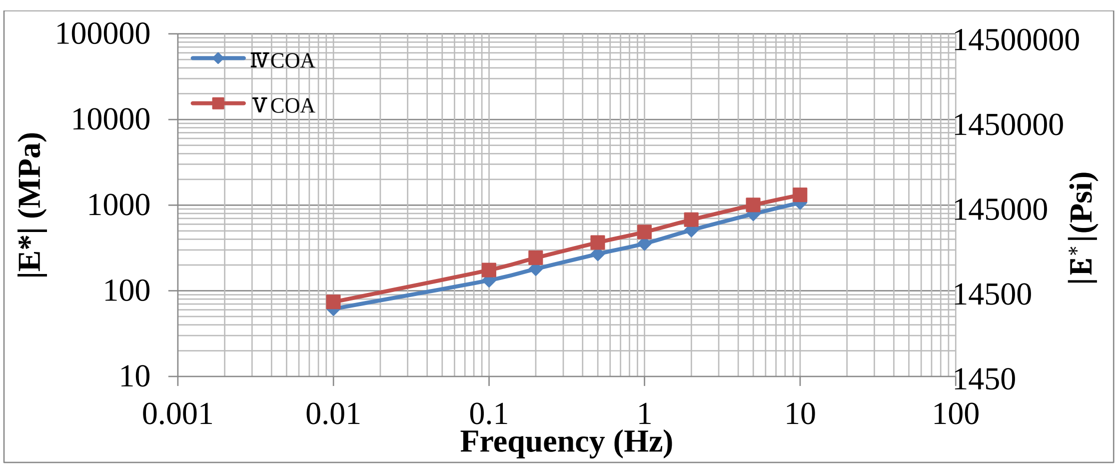

(c)

Figure 9-61 Dynamic Modulus Values of Various Mixtures from Surface Type C using Liquid ASA1 without RAP in Terms of Aggregate Source, (a) at 4°C (39.2°F), (b) at 20°C (68°F), (c) at 40°C (104°F)

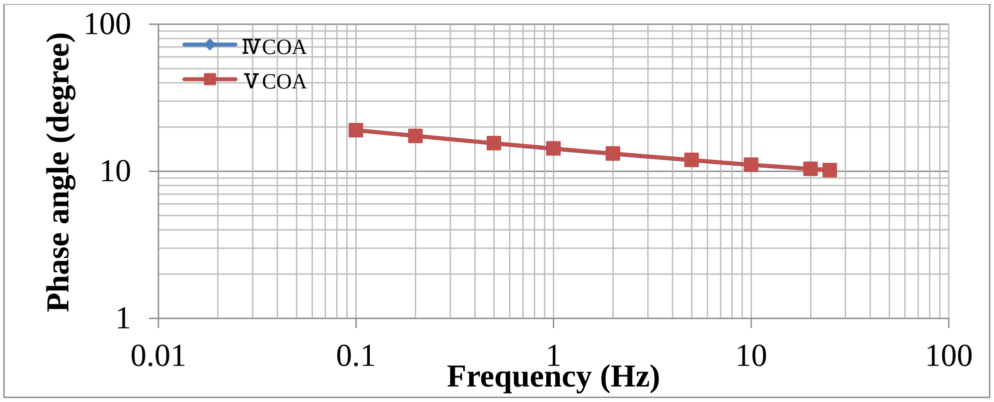

(a)

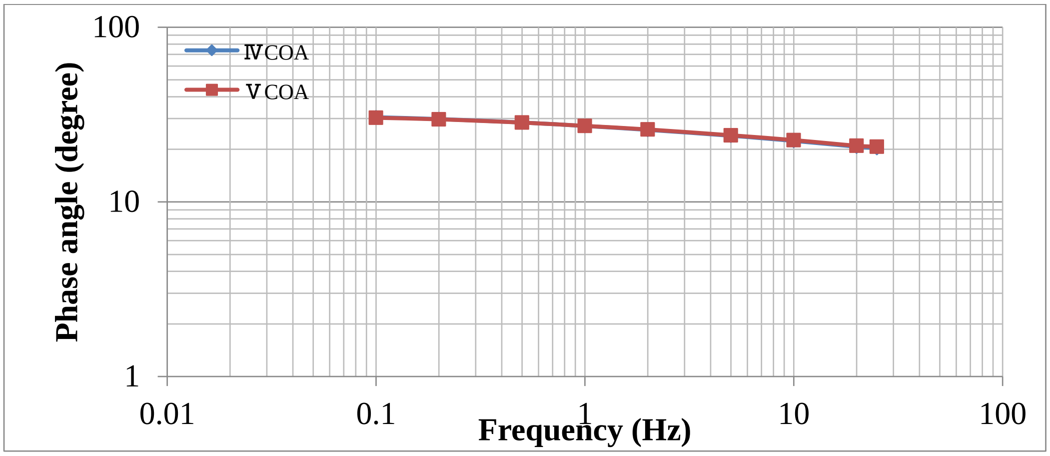

(b)

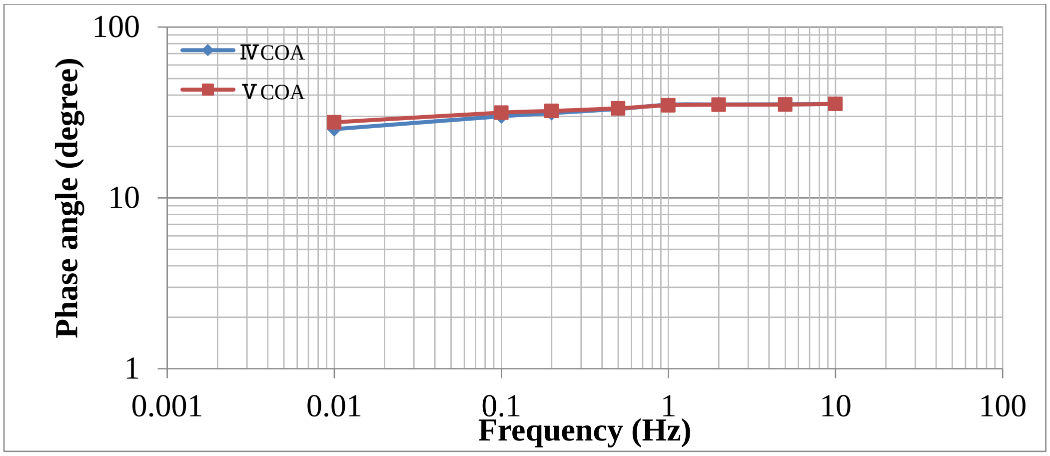

(c)

Figure 9-62 Phase Angle Values of Various Mixtures from Surface Type C using Liquid ASA1 without RAP in Terms of Aggregate Source, (a) at 4°C (39.2°F), (b) at 20°C (68°F), (c) at 40°C (104°F)

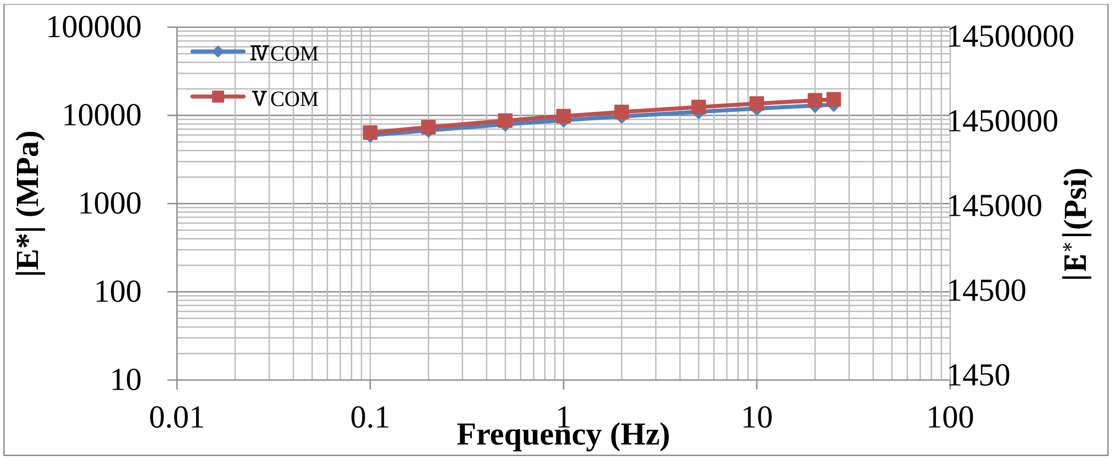

(a)

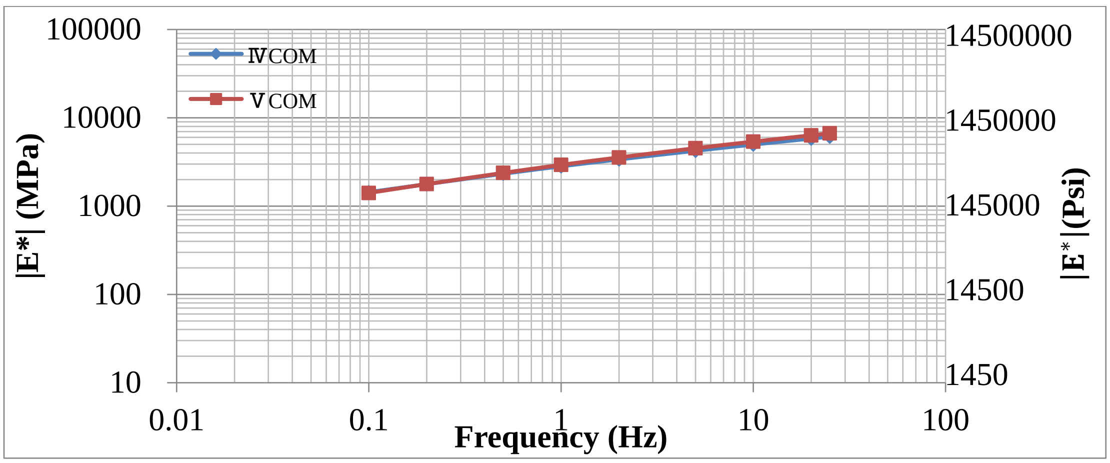

(b)

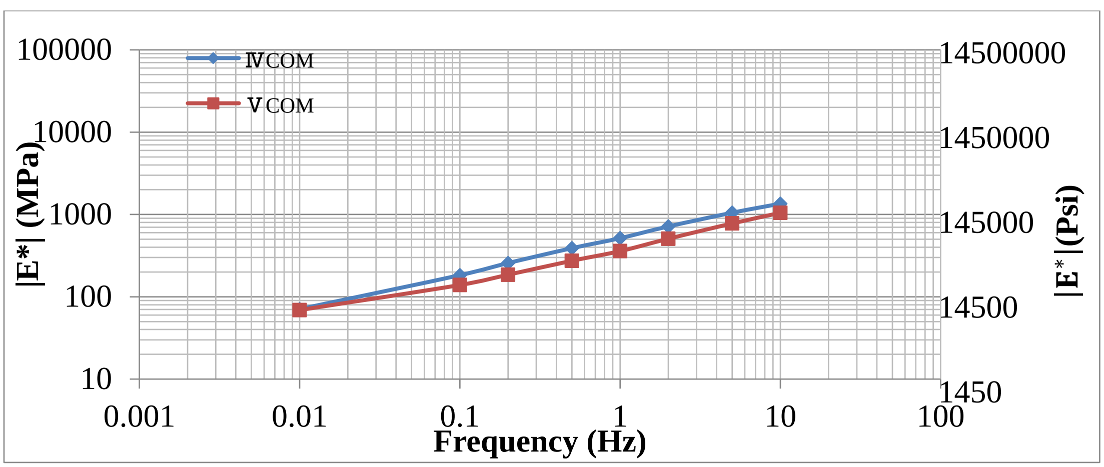

(c)

Figure 9-63 Dynamic Modulus Values of Various Mixtures from Surface Type C using Liquid ASA2 without RAP in Terms of Aggregate Source, (a) at 4°C (39.2°F), (b) at 20°C (68°F), (c) at 40°C (104°F)

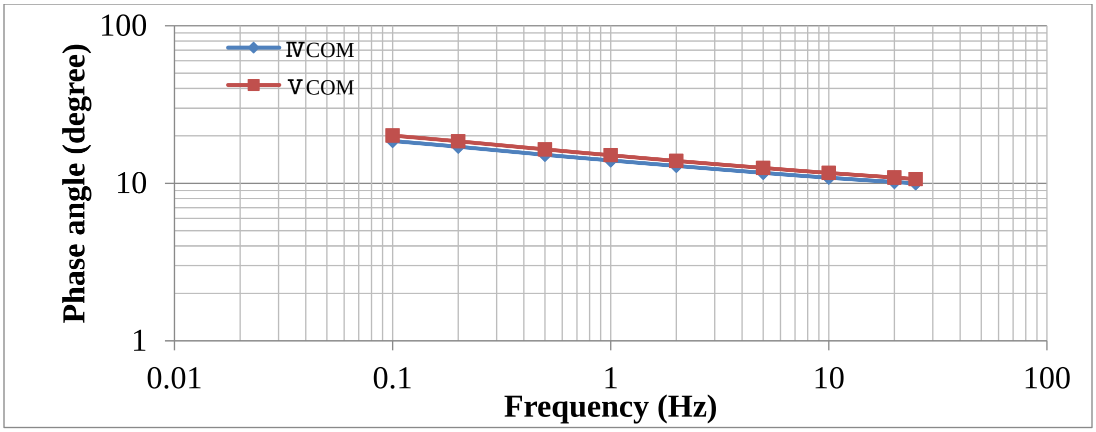

(a)

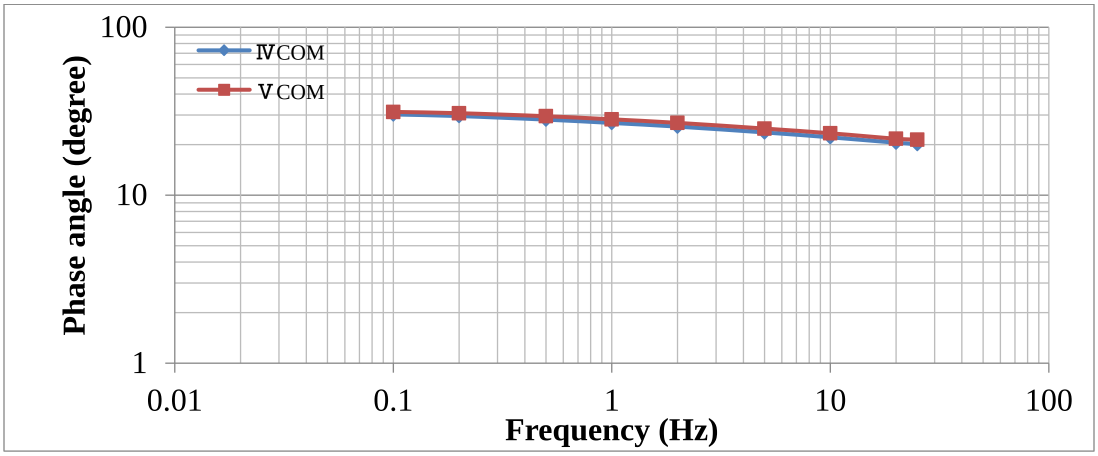

(b)

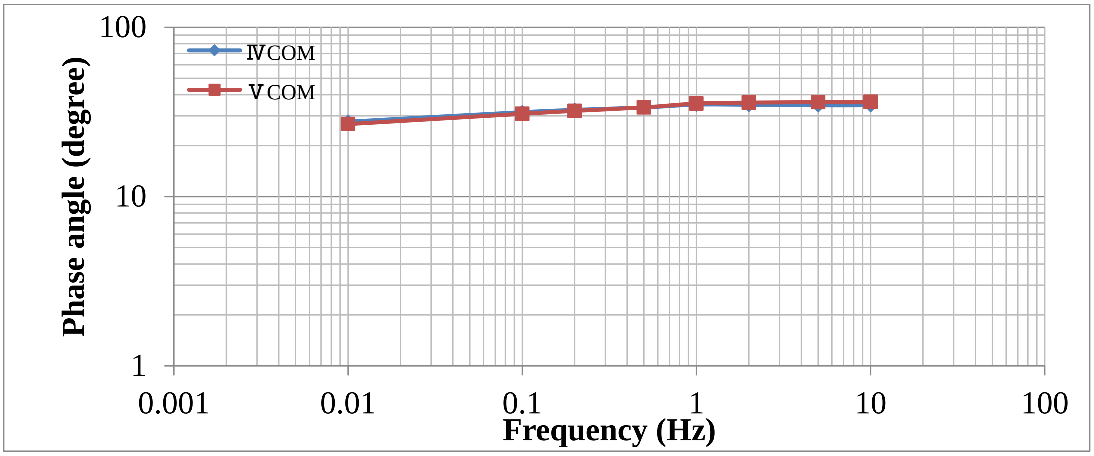

(c)

Figure 9-64 Phase Angle Values of Various Mixtures from Surface Type C using Liquid ASA2 without RAP in Terms of Aggregate Source, (a) at 4°C (39.2°F), (b) at 20°C (68°F), (c) at 40°C (104°F)

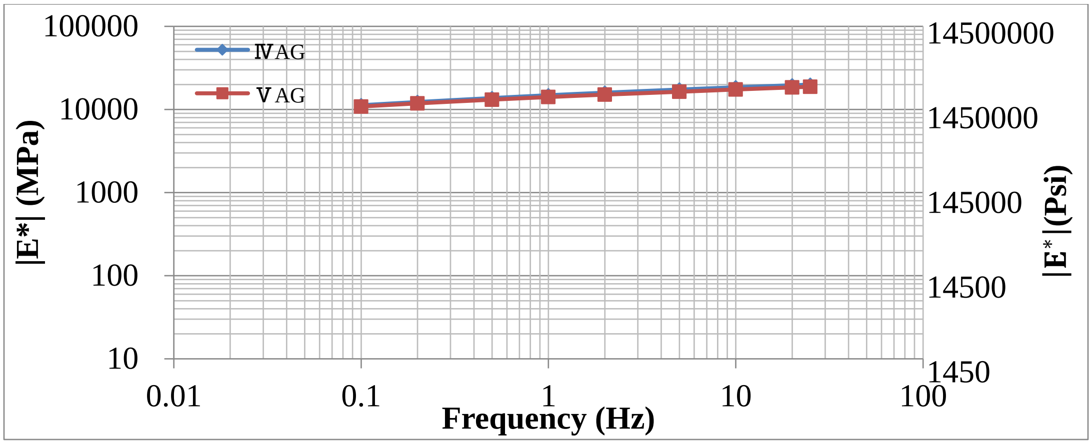

(a)

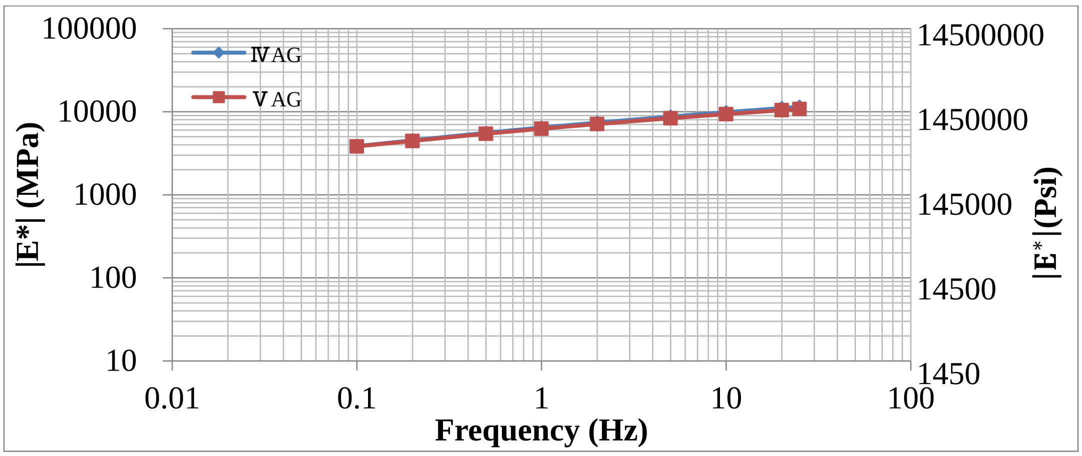

(b)

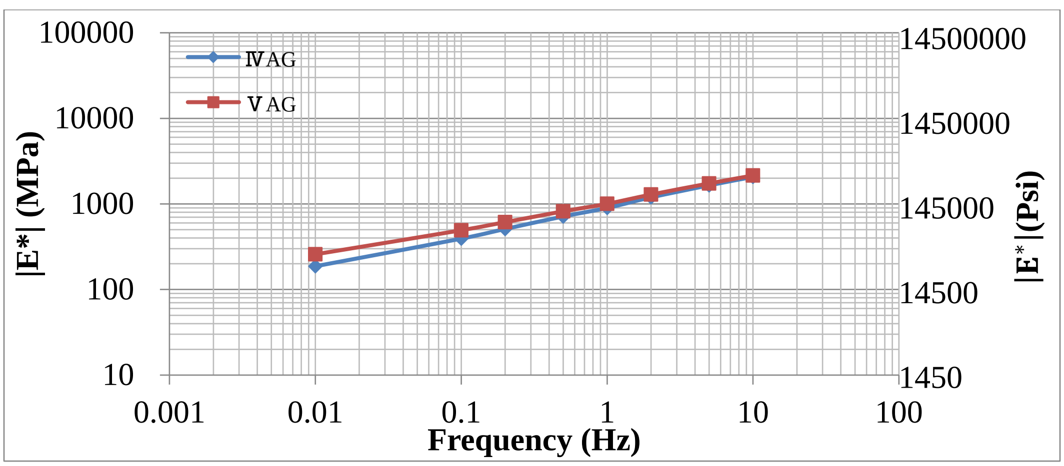

(c)

Figure 9-65 Dynamic Modulus Values of Various Mixtures from Surface Type A with RAP after Long-Term Aging in Terms of Aggregate Source, (a) at 4°C (39.2°F), (b) at 20°C (68°F), (c) at 40°C (104°F)

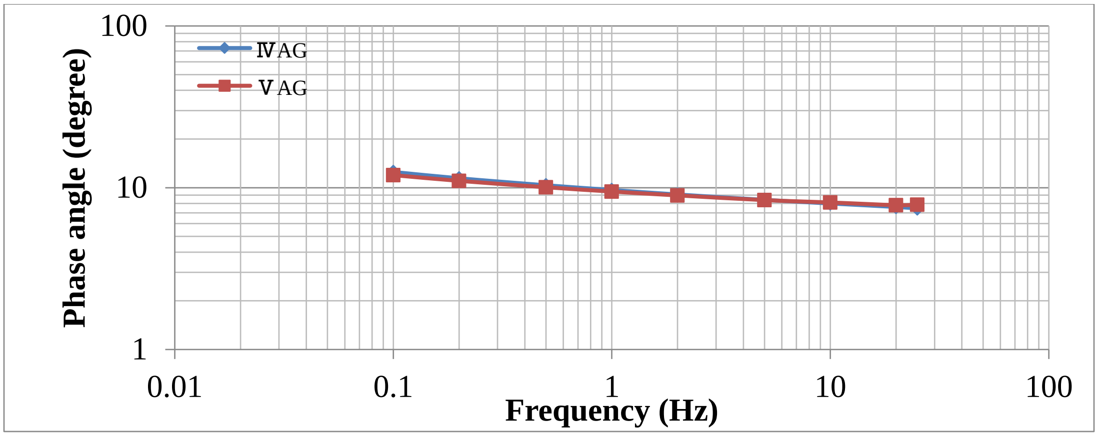

(a)

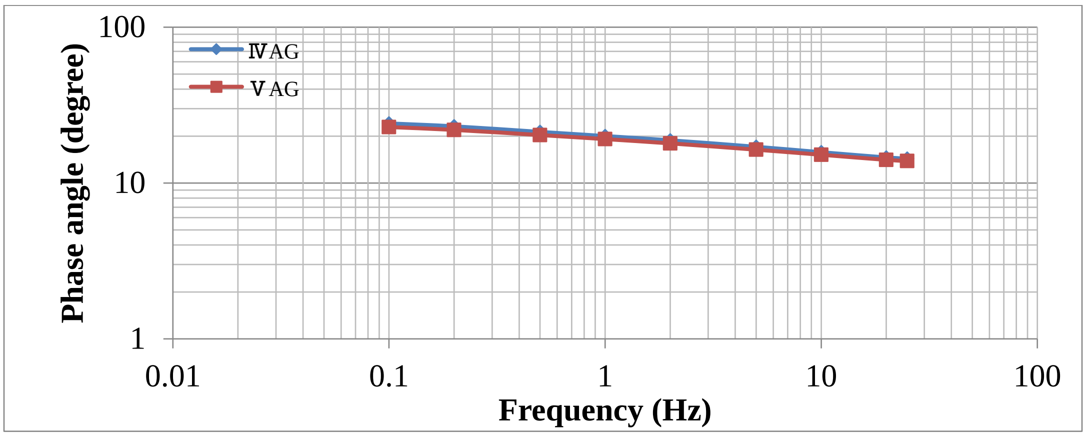

(b)

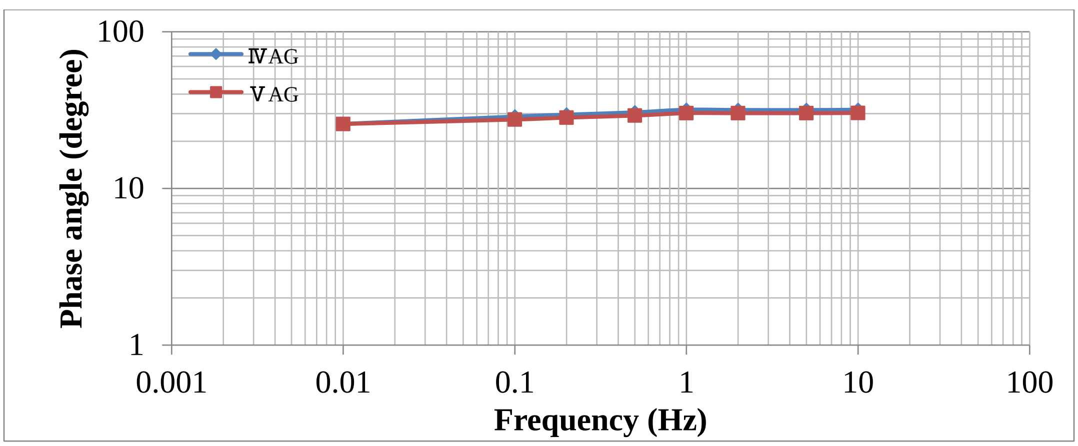

(c)

Figure 9-66 Phase Angle Values of Various Mixtures from Surface Type A with RAP after Long-Term Aging in Terms of Aggregate Source, (a) at 4°C (39.2°F), (b) at 20°C (68°F), (c) at 40°C (104°F)

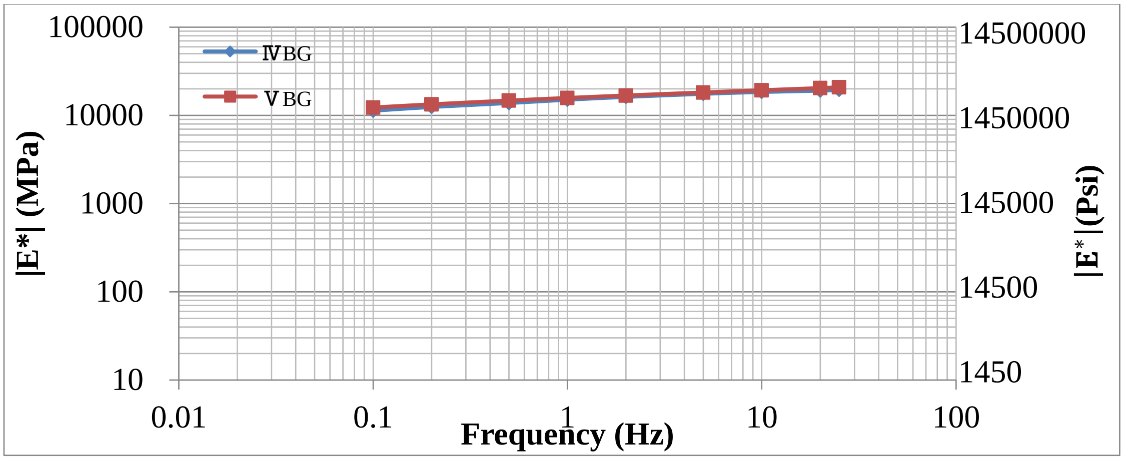

(a)

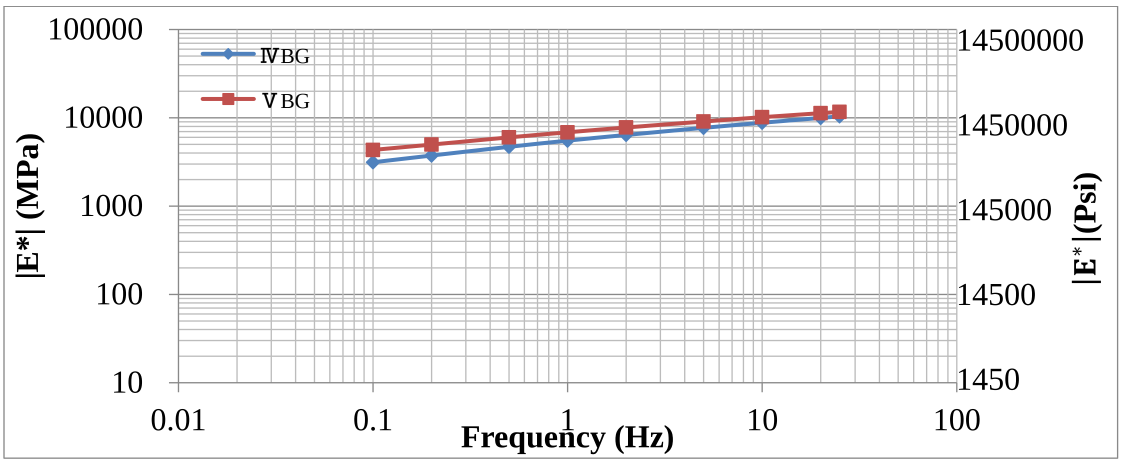

(b)

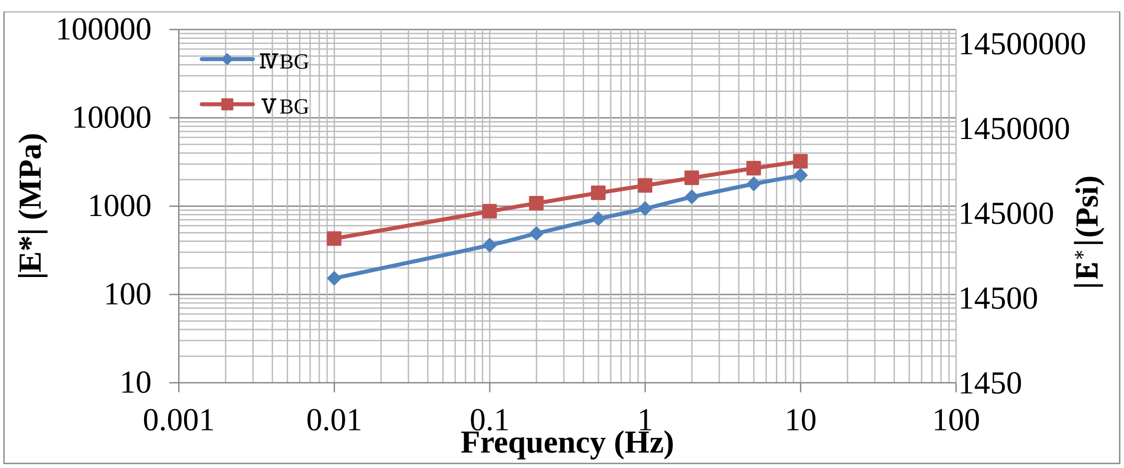

(c)

Figure 9-67 Dynamic Modulus Values of Various Mixtures from Surface Type B with RAP after Long-Term Aging in Terms of Aggregate Source, (a) at 4°C (39.2°F), (b) at 20°C (68°F), (c) at 40°C (104°F)

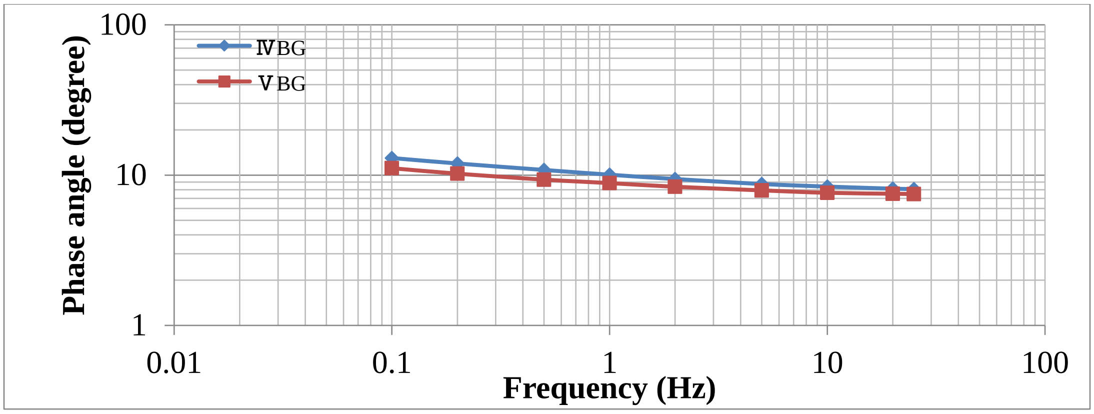

(a)

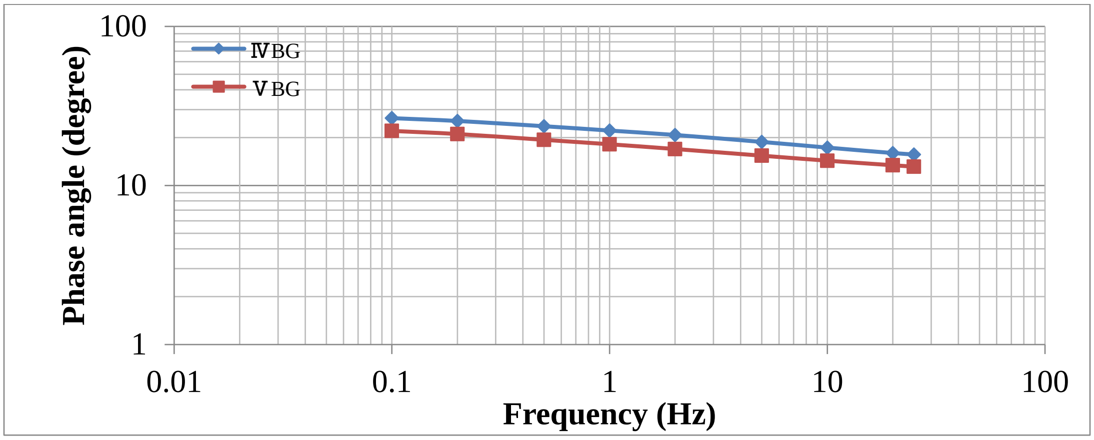

(b)

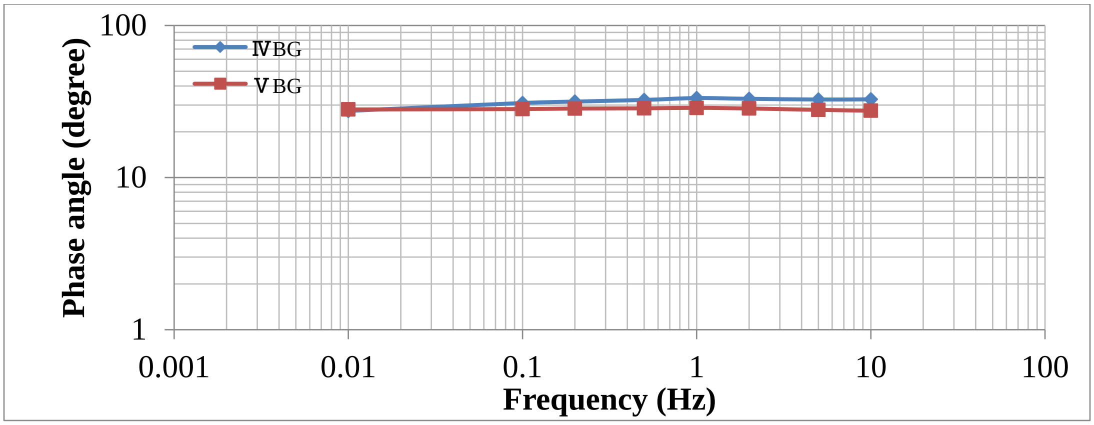

(c)

Figure 9-68 Phase Angle Values of Various Mixtures from Surface Type B with RAP after Long-Term Aging in Terms of Aggregate Source, (a) at 4°C (39.2°F), (b) at 20°C (68°F), (c) at 40°C (104°F)

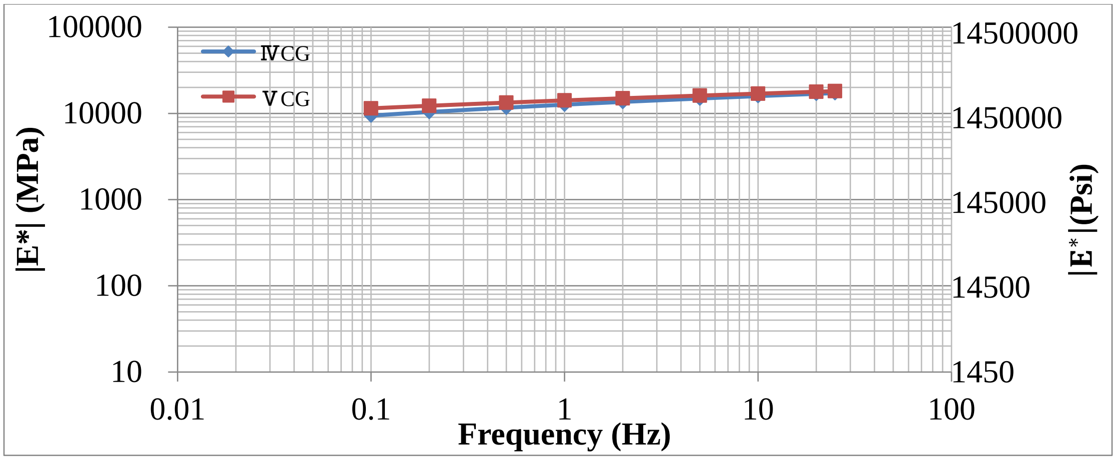

(a)

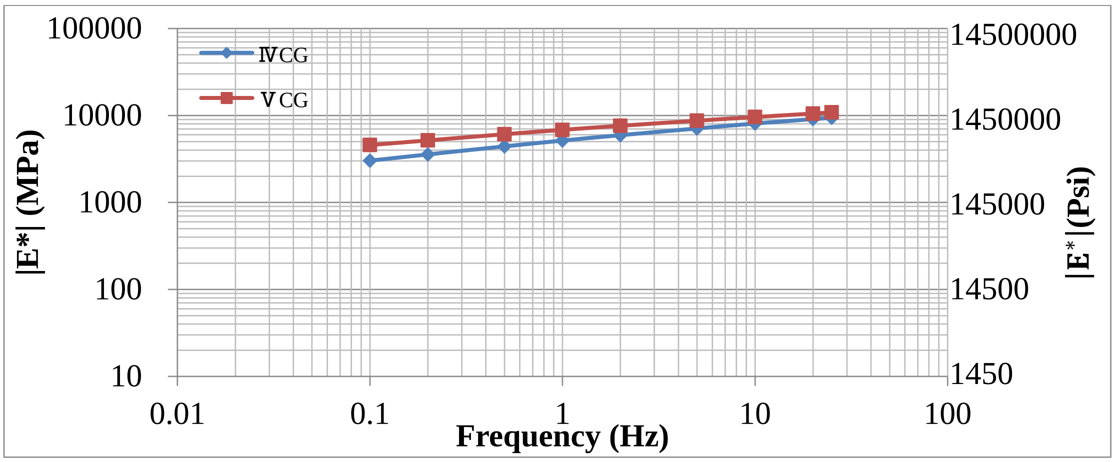

(b)

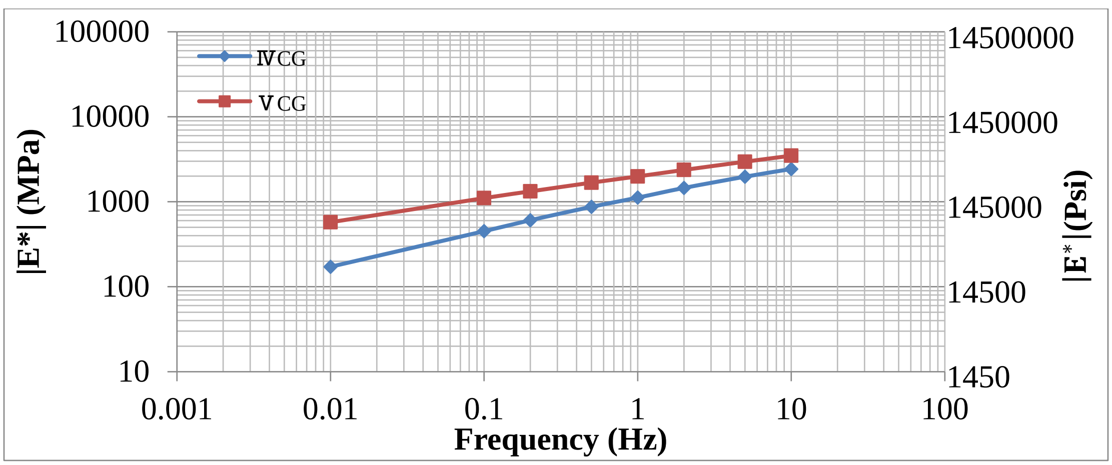

(c)

Figure 9-69 Dynamic Modulus Values of Various Mixtures from Surface Type C with RAP after Long-Term Aging in Terms of Aggregate Source, (a) at 4°C (39.2°F), (b) at 20°C (68°F), (c) at 40°C (104°F)

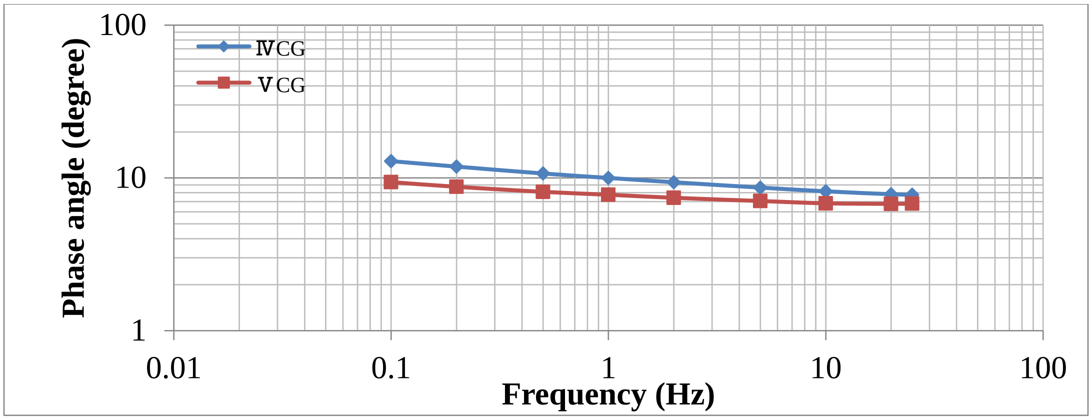

(a)

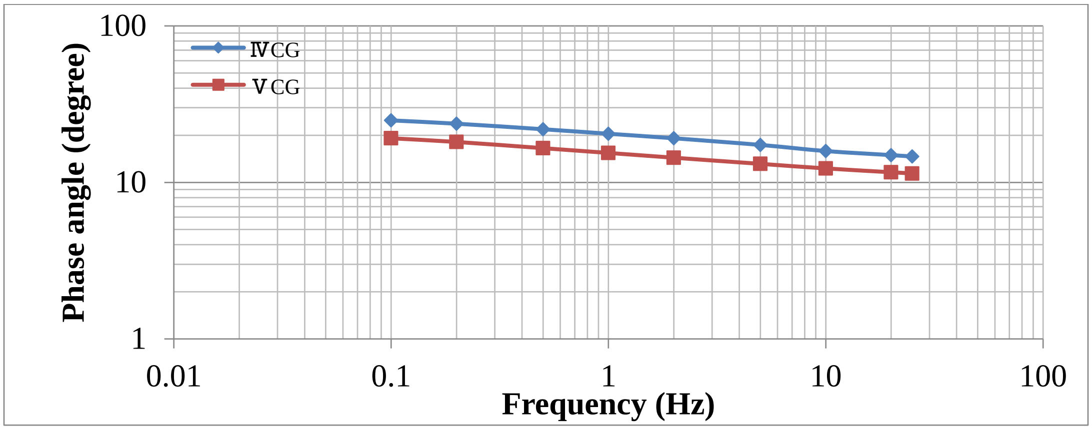

(b)

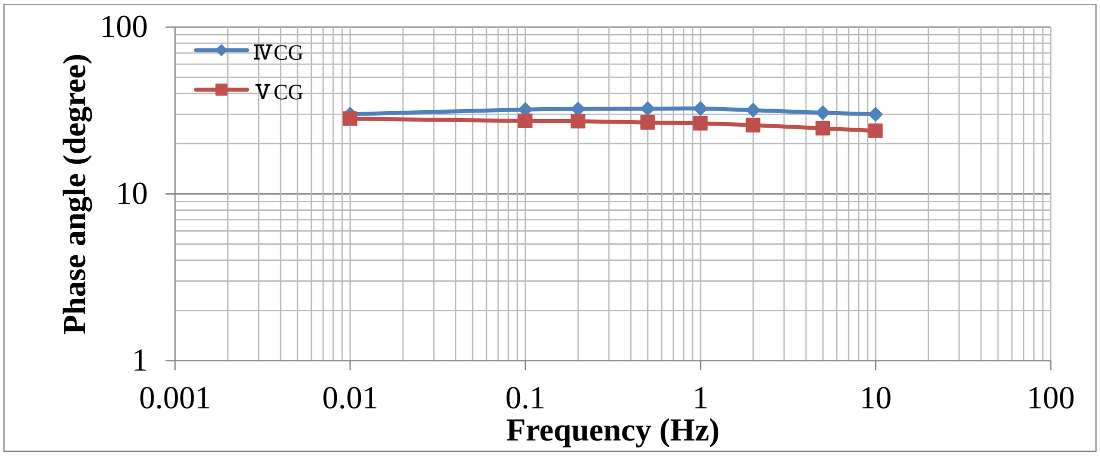

(c)

Figure 9-70 Phase Angle Values of Various Mixtures from Surface Type C with RAP after Long-Term Aging in Terms of Aggregate Source, (a) at 4°C (39.2°F), (b) at 20°C (68°F), (c) at 40°C (104°F)

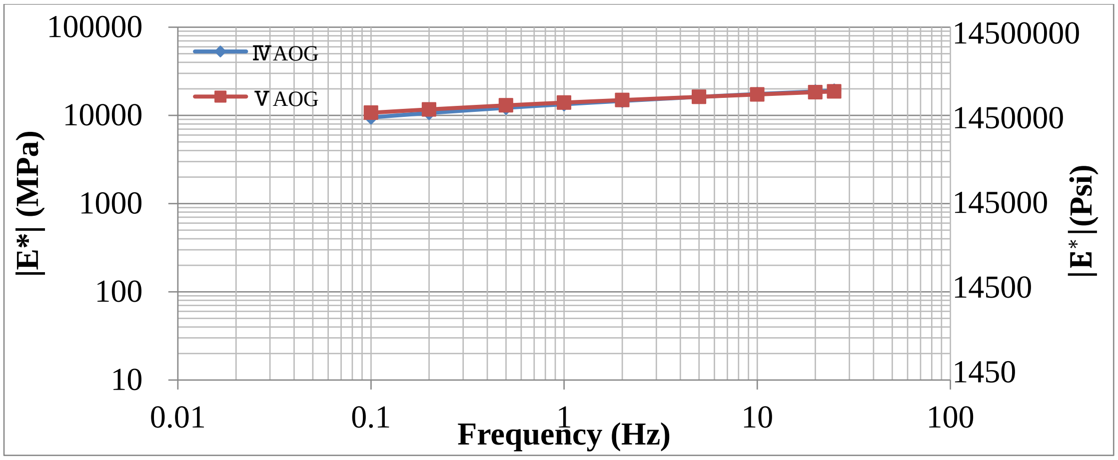

(a)

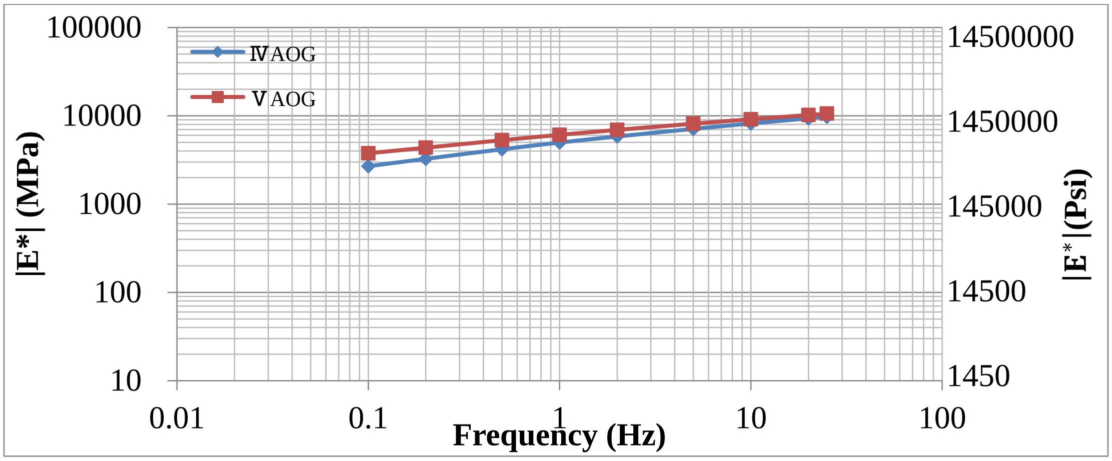

(b)

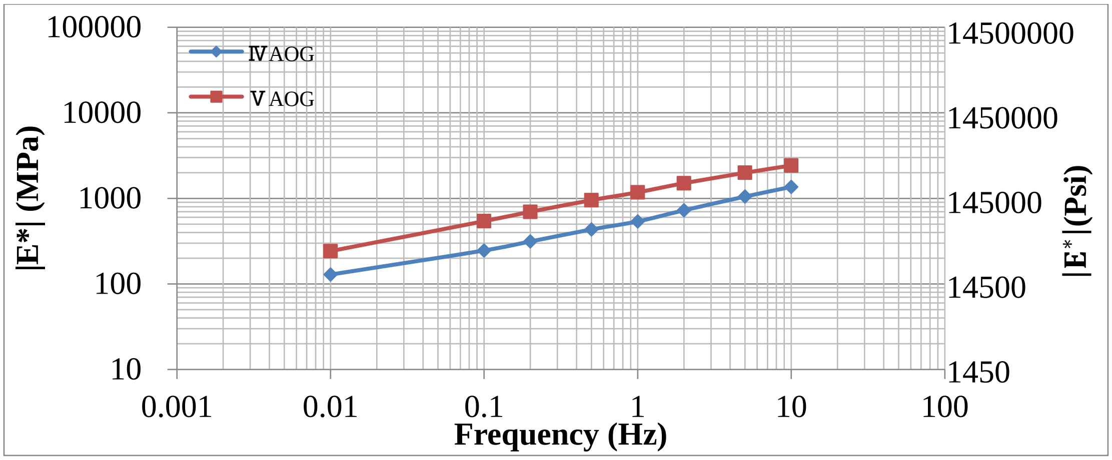

(c)

Figure 9-71 Dynamic Modulus Values of Various Mixtures from Surface Type A without RAP after Long-Term Aging in Terms of Aggregate Source, (a) at 4°C (39.2°F), (b) at 20°C (68°F), (c) at 45°C (113°F)

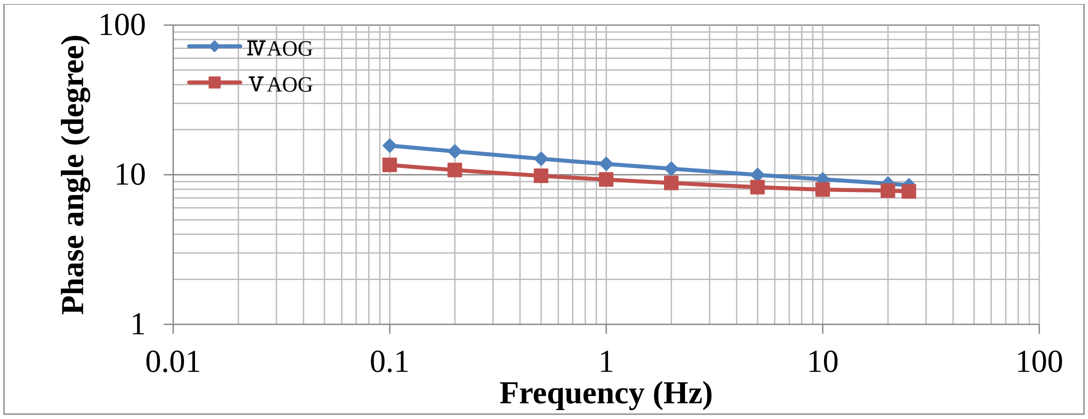

(a)

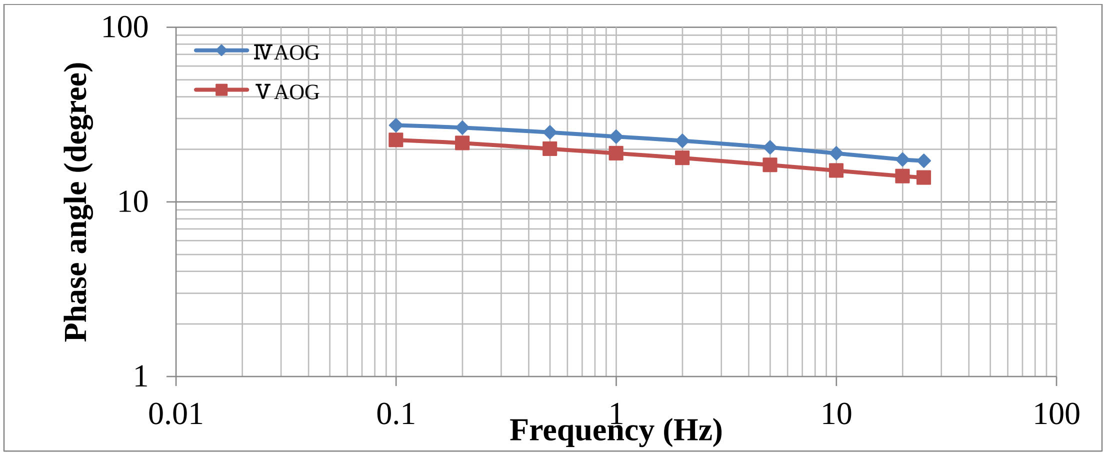

(b)

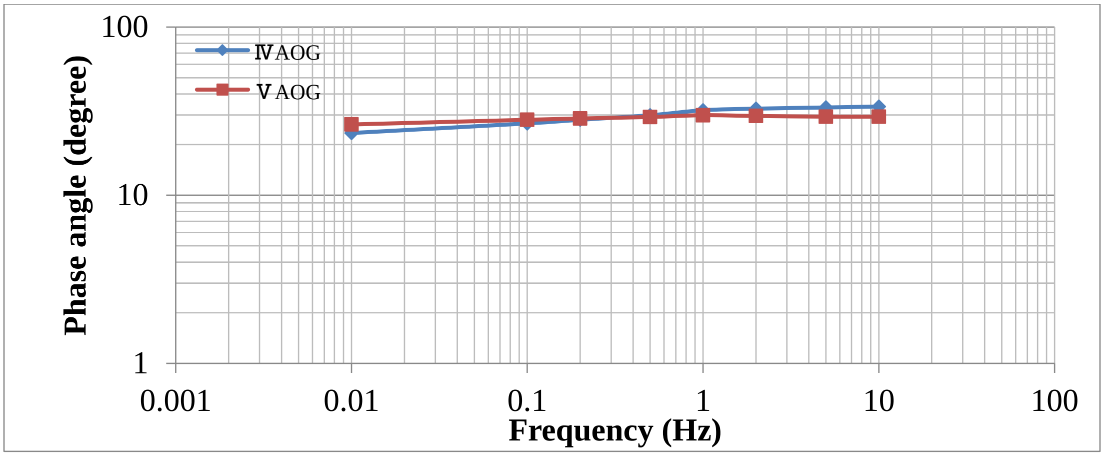

(c)

Figure 9-72 Phase Angle Values of Various Mixtures from Surface Type A without RAP after Long-Term Aging in Terms of Aggregate Source, (a) at 4°C (39.2°F), (b) at 20°C (68°F), (c) at 45°C (113°F)

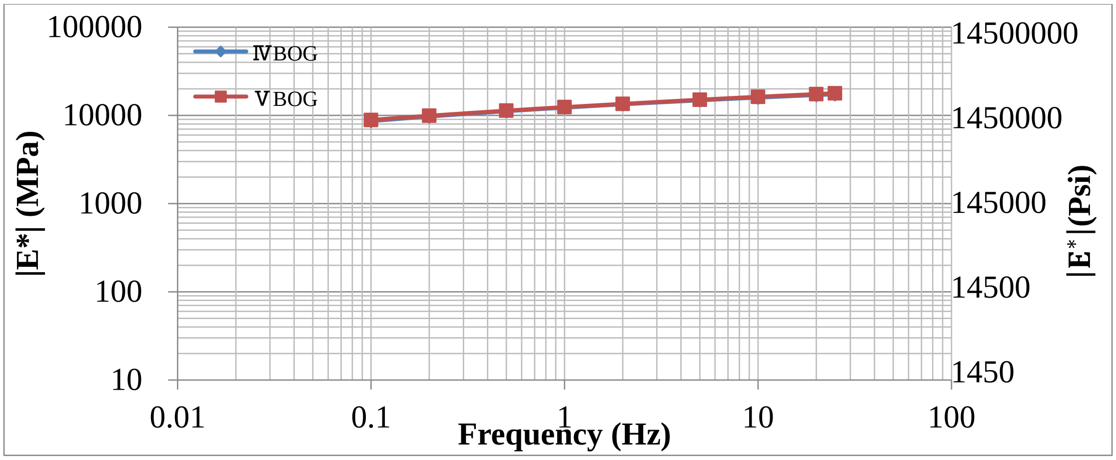

(a)

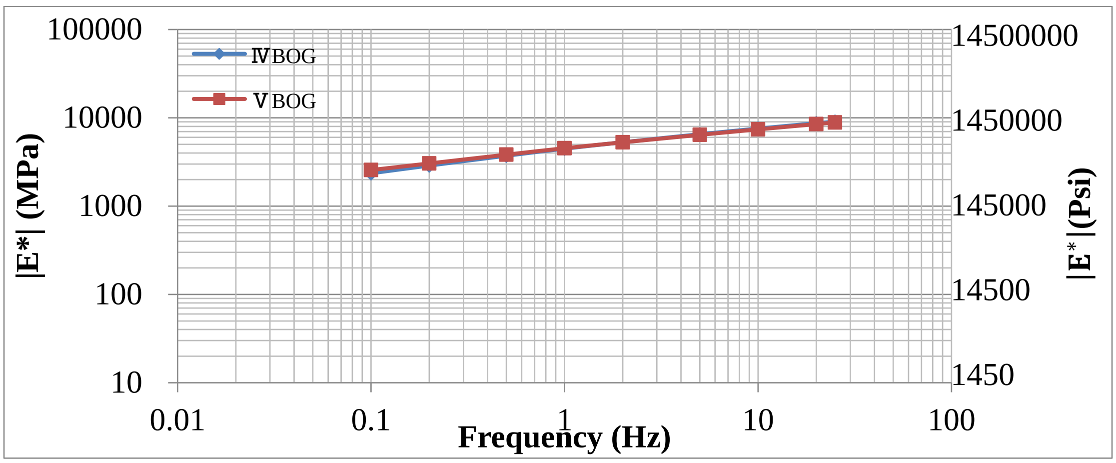

(b)

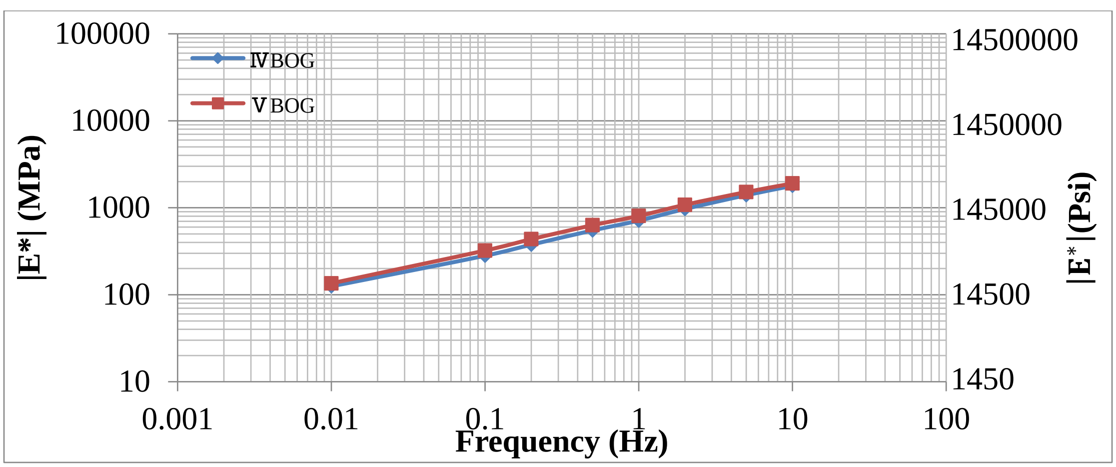

(c)

Figure 9-73 Dynamic Modulus Values of Various Mixtures from Surface Type B without RAP after Long-Term Aging in Terms of Aggregate Source, (a) at 4°C (39.2°F), (b) at 20°C (68°F), (c) at 40°C (104°F)

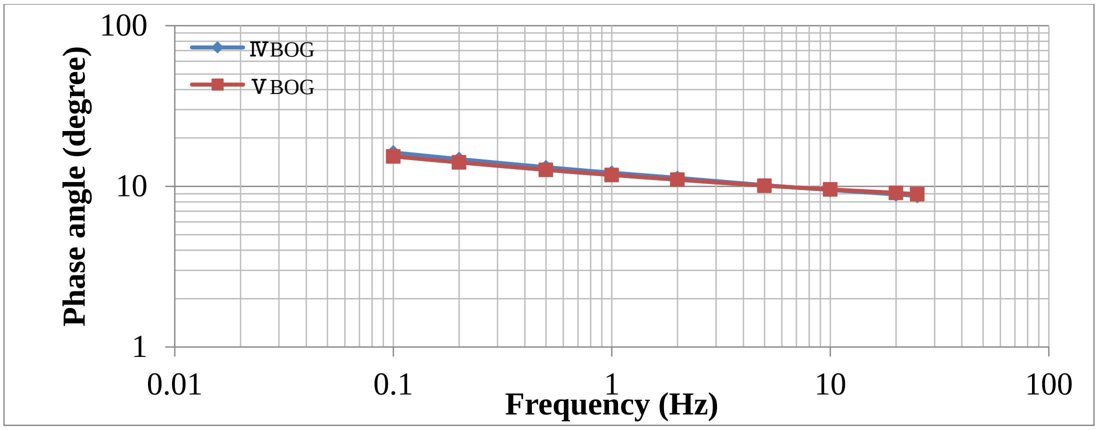

(a)

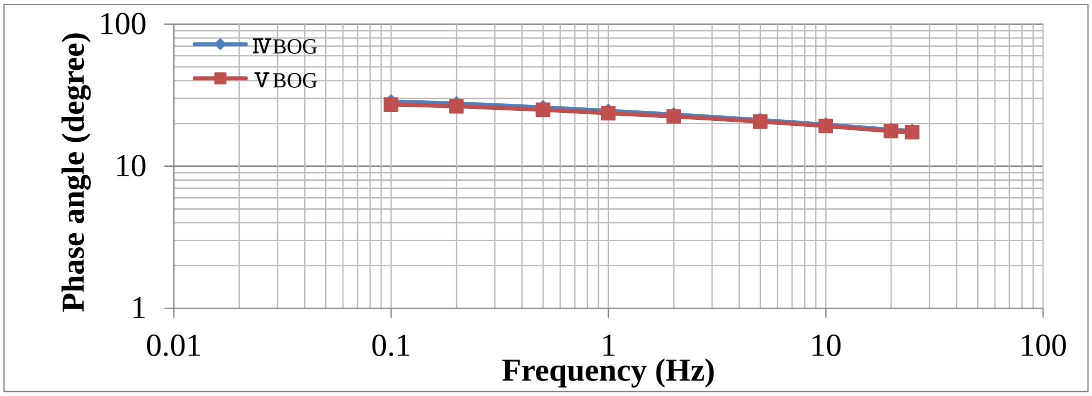

(b)

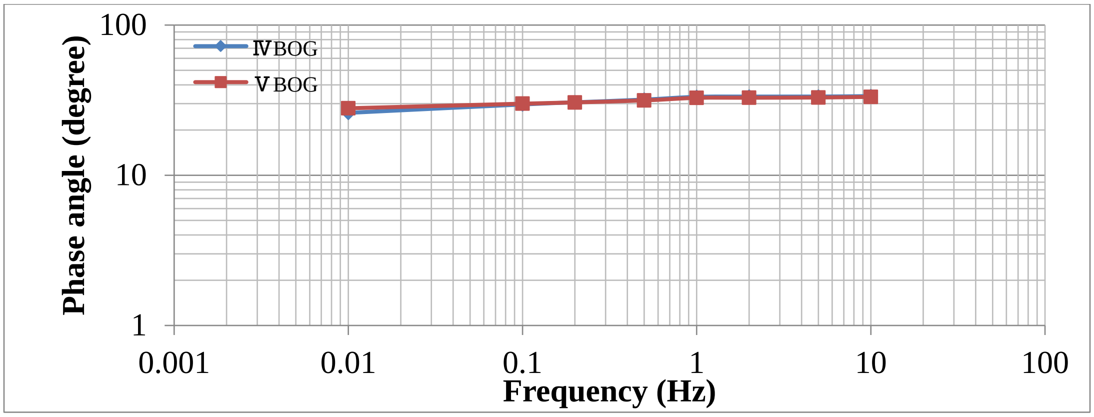

(c)

Figure 9-74 Phase Angle Values of Various Mixtures from Surface Type B without RAP after Long-Term Aging in Terms of Aggregate Source, (a) at 4°C (39.2°F), (b) at 20°C (68°F), (c) at 40°C (104°F)

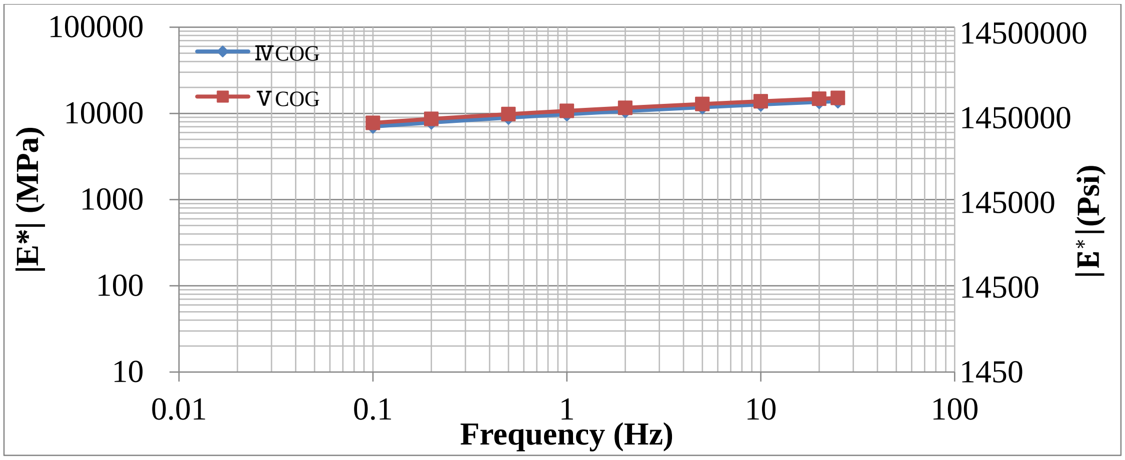

(a)

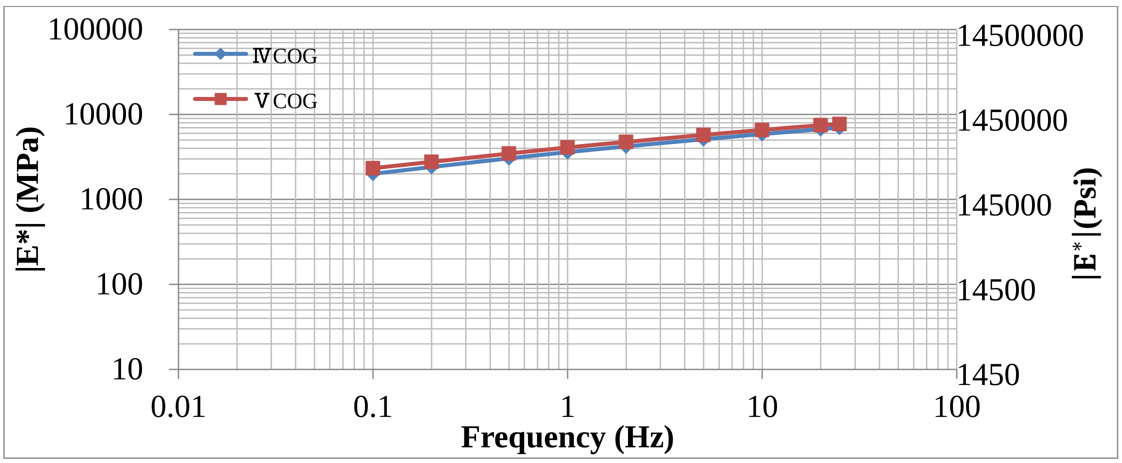

(b)

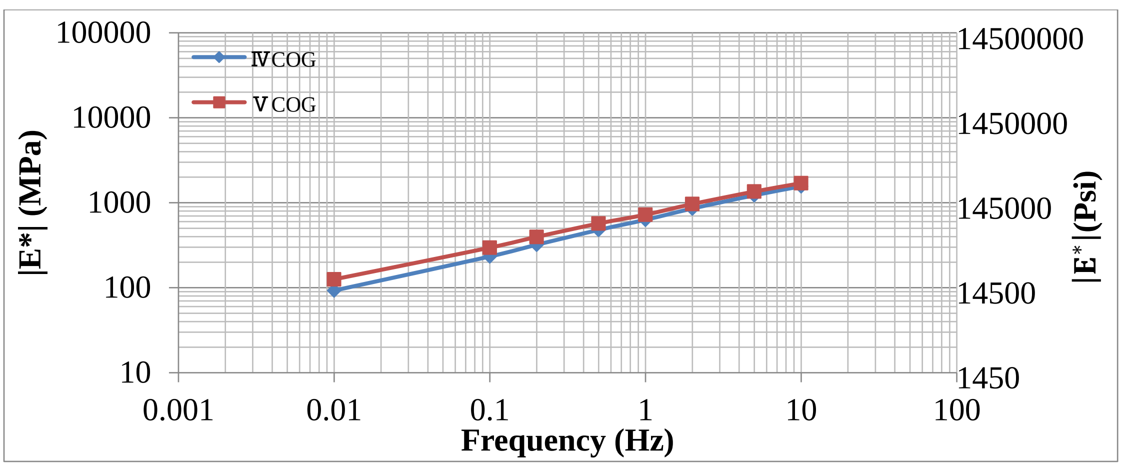

(c)

Figure 9-75 Dynamic Modulus Values of Various Mixtures from Surface Type C without RAP after Long-Term Aging in Terms of Aggregate Source, (a) at 4°C (39.2°F), (b) at 20°C (68°F), (c) at 40°C (104°F)

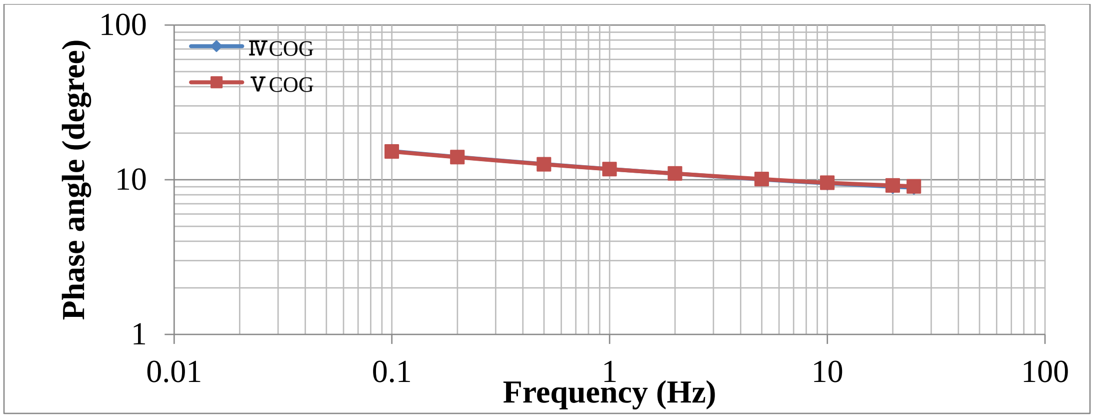

(a)

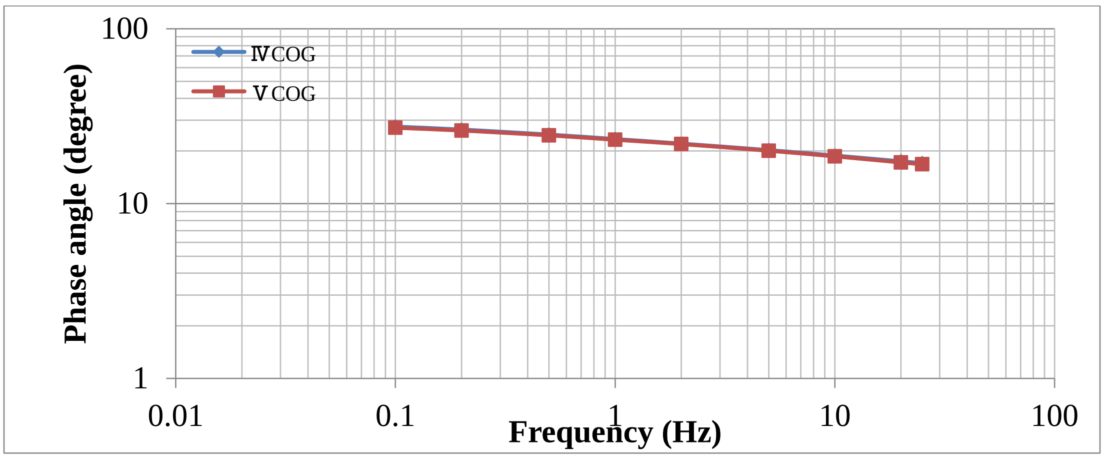

(b)

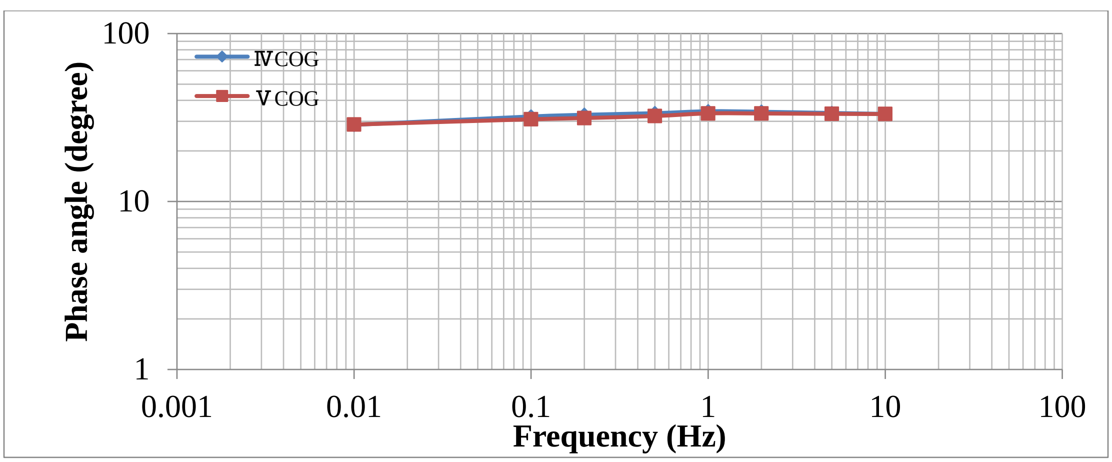

(c)

Figure 9-76 Phase Angle Values of Various Mixtures from Surface Type C without RAP after Long-Term Aging in Terms of Aggregate Source, (a) at 4°C (39.2°F), (b) at 20°C (68°F), (c) at 40°C (104°F)

10 Appendix B - Dynamic Modulus and Phase Angle Values of Various Mixtures in Terms of Mixture Type and Other Variables

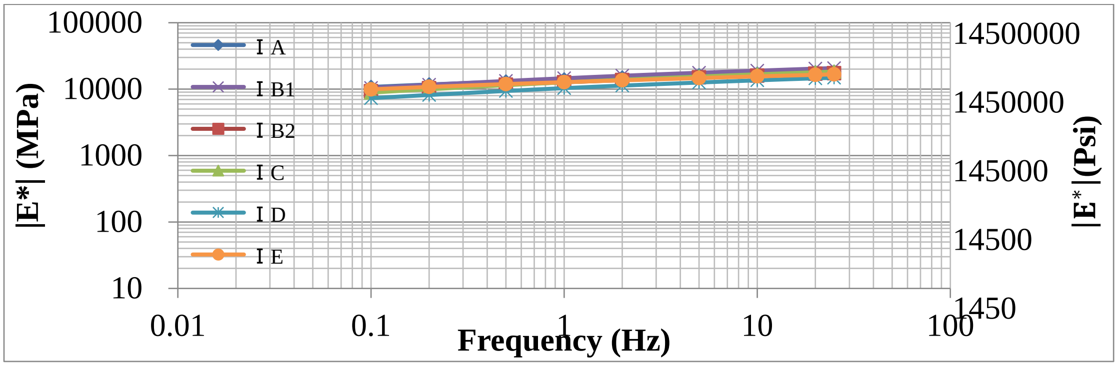

(a)

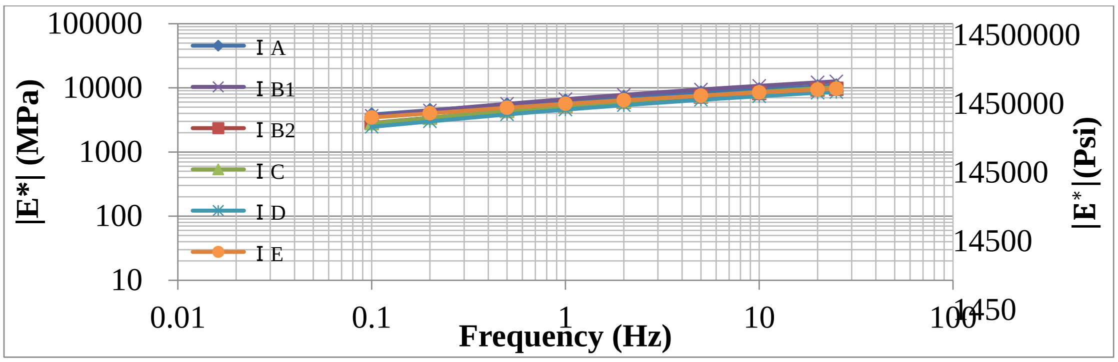

(b)

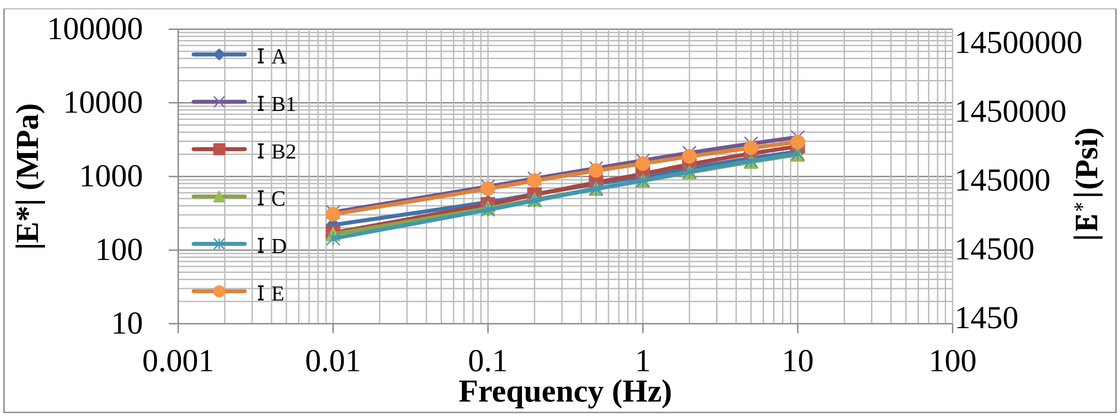

(c)

Figure 10-1 Dynamic Modulus Values of Various Mixtures from Aggregate I with RAP in Terms of Surface Mixture Type, (a) at 4°C (39.2°F), (b) at 20°C (68°F), (c) at 45°C (113°F) (Surface A), 40°C (104°F) (Surface B, C, D, and E)

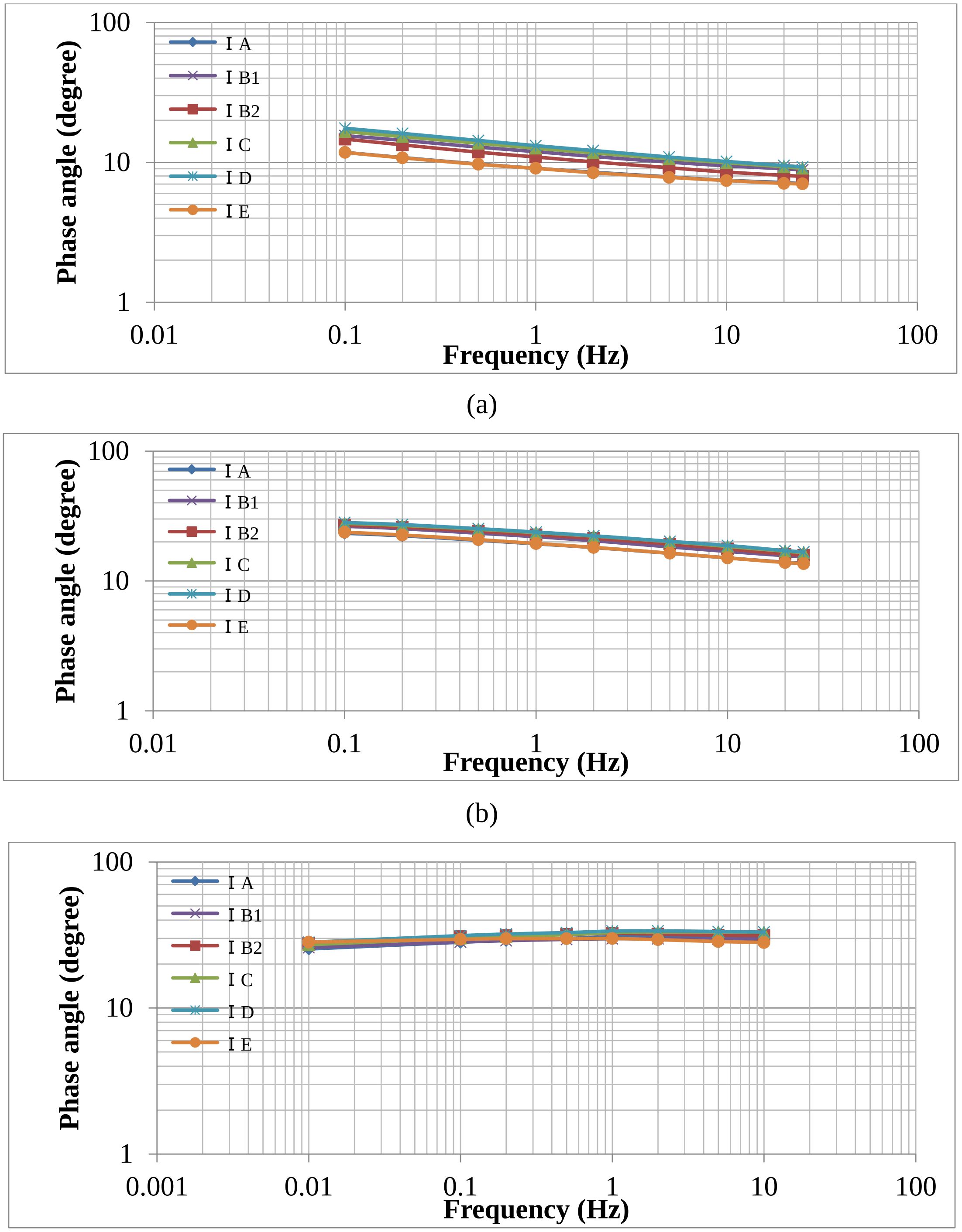

(a)

(b)

(c)

Figure 10-2 Phase Angle Values of Various Mixtures from Aggregate I with RAP in Terms of Surface Mixture Type, (a) at 4°C (39.2°F), (b) at 20°C (68°F), (c) at 45°C (113°F) (Surface A), 40°C (104°F) (Surface B, C, D, and E)

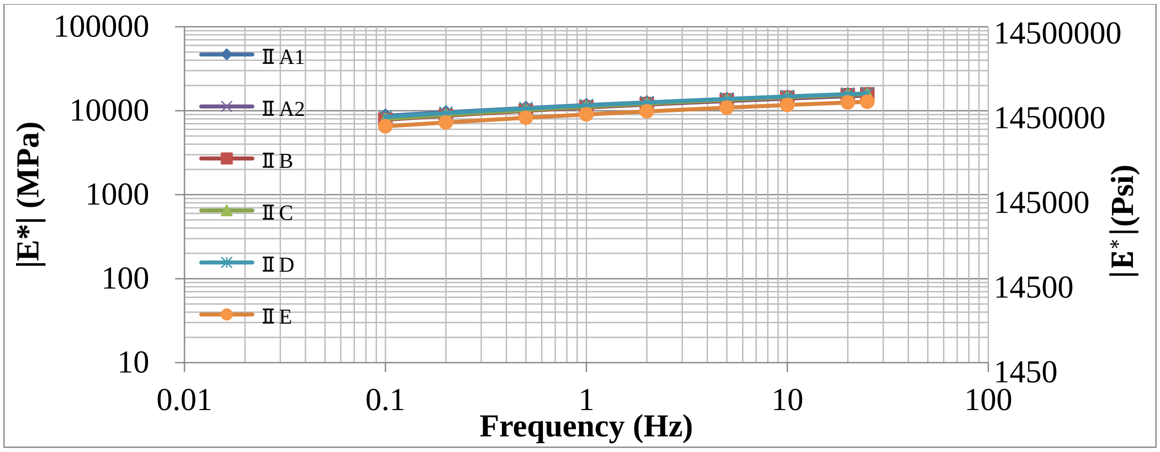

(a)

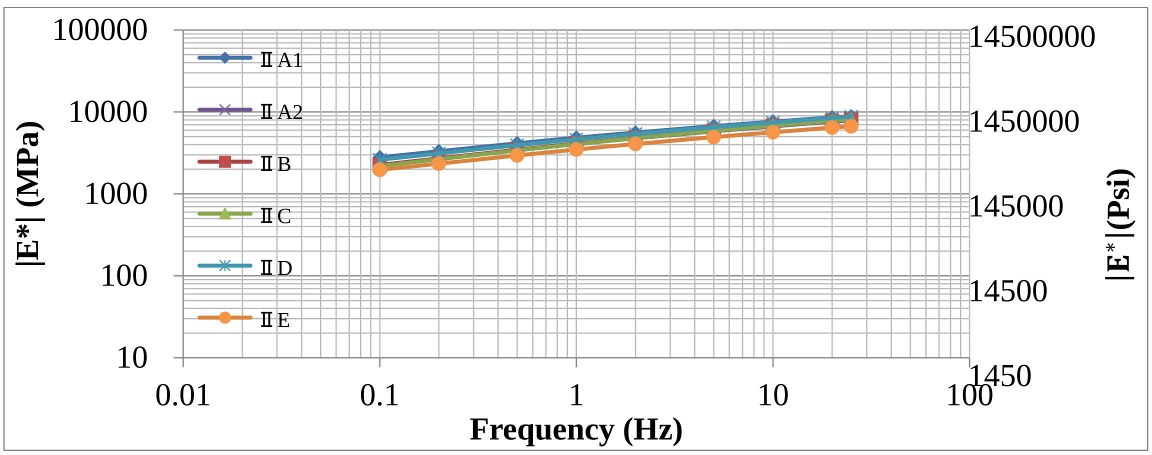

(b)

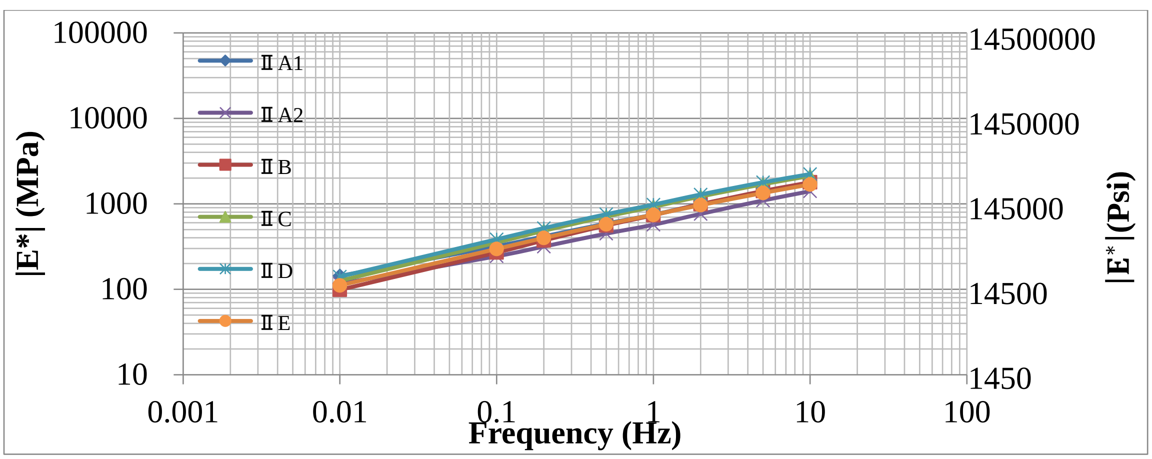

(c)

Figure 10-3 Dynamic Modulus Values of Various Mixtures from Aggregate II with RAP in Terms of Surface Mixture Type, (a) at 4°C (39.2°F), (b) at 20C (68°F), (c) at 45°C (113°F) (Surface A), 40°C (104°F) (Surface B, C, D, and E)

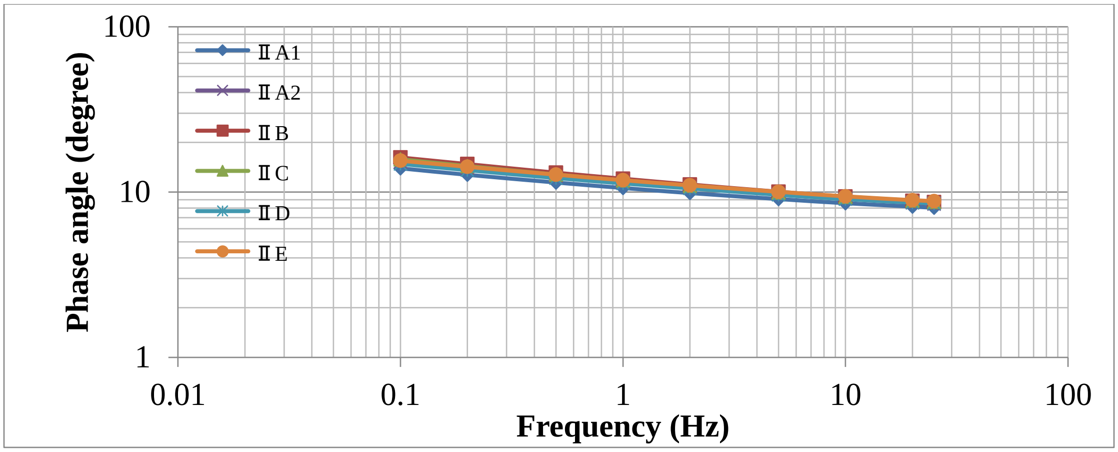

(a)

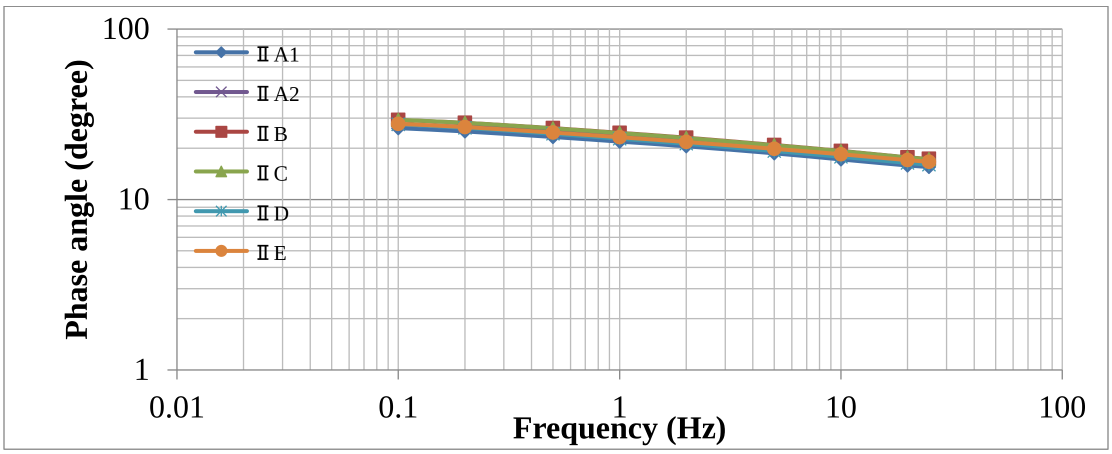

(b)

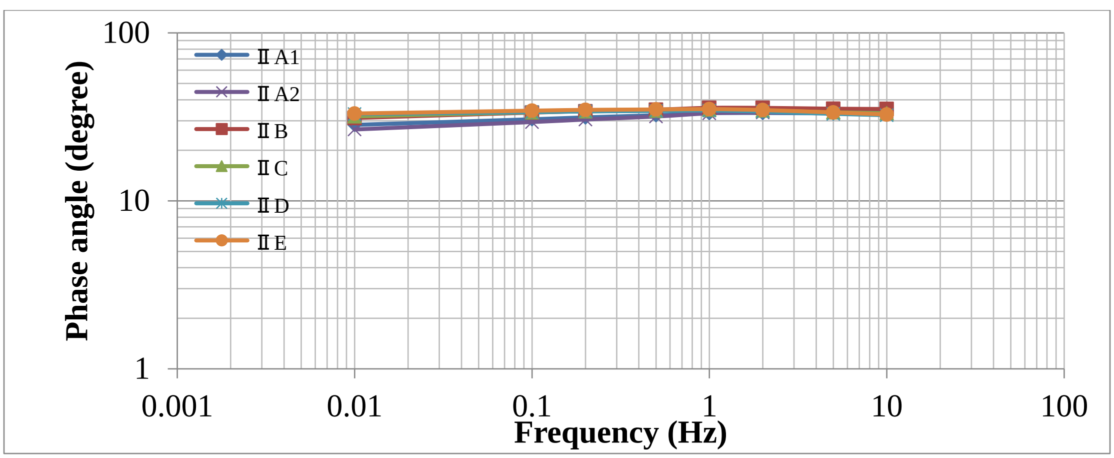

(c)

Figure 10-4 Phase Angle Values of Various Mixtures from Aggregate II with RAP in Terms of Surface Mixture Type, (a) at 4°C (39.2°F), (b) at 20°C (68°F), (c) at 45°C (113°F) (Surface A), 40°C (104°F) (Surface B, C, D, and E)

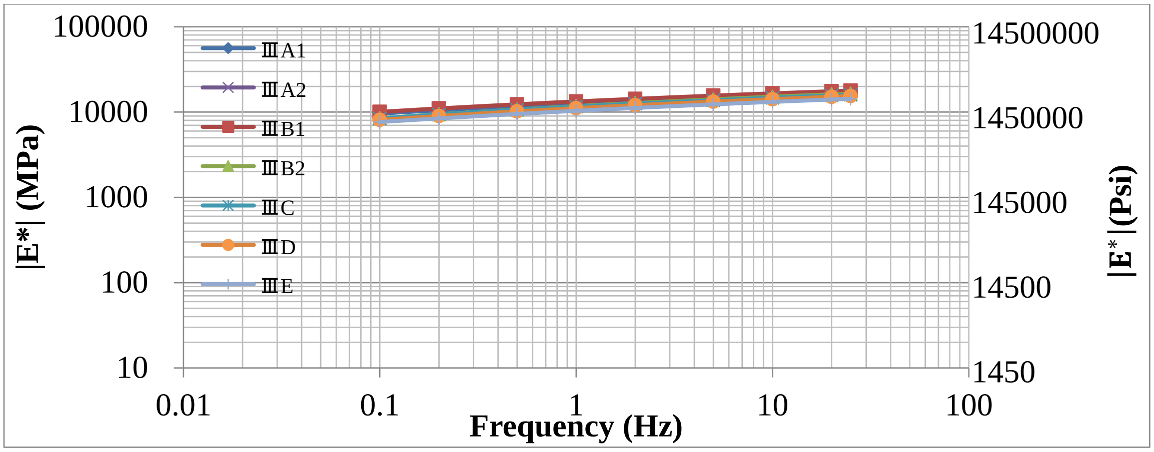

(a)

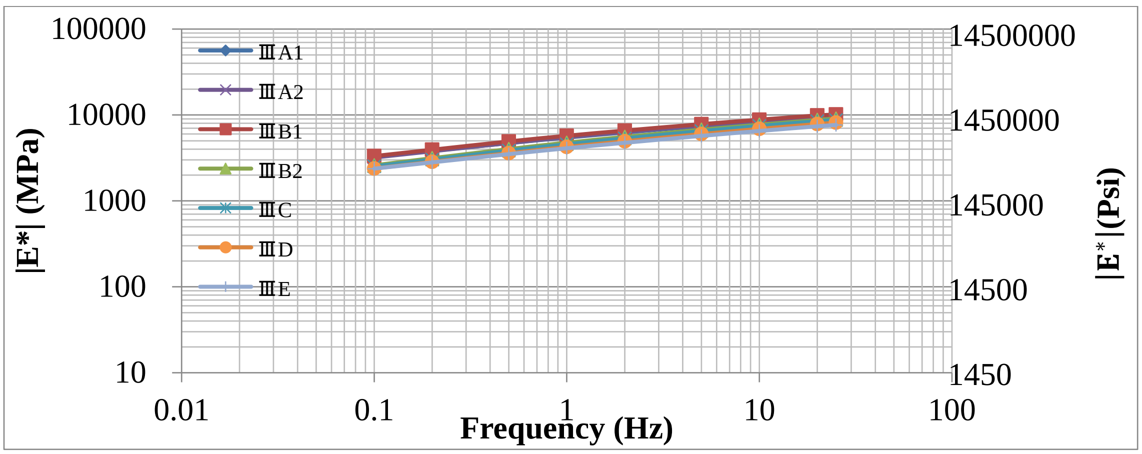

(b)

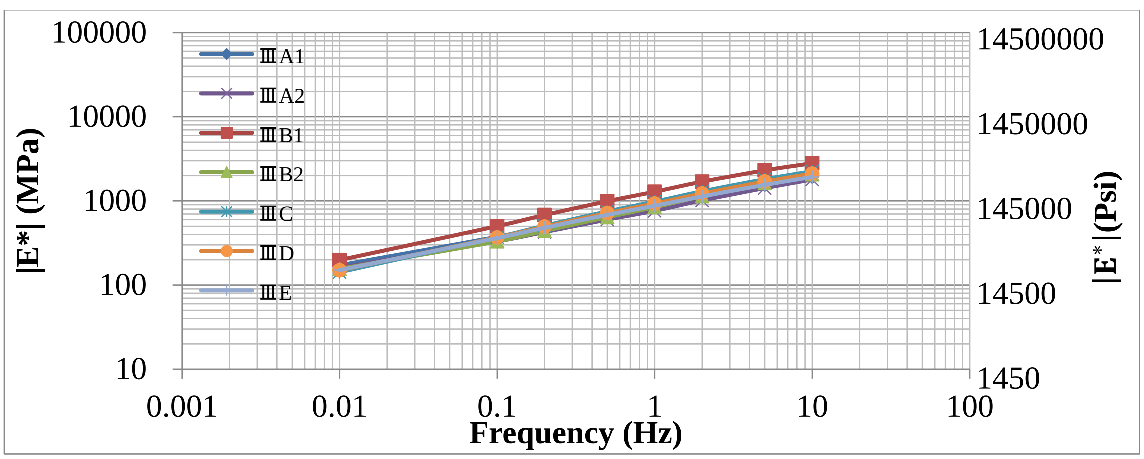

(c)

Figure 10-5 Dynamic Modulus Values of Various Mixtures from Aggregate III with RAP in Terms of Surface Mixture Type, (a) at 4°C (39.2°F), (b) at 20°C (68°F), (c) at 45°C (113°F) (Surface A), 40°C (104°F) (Surface B, C, D, and E)

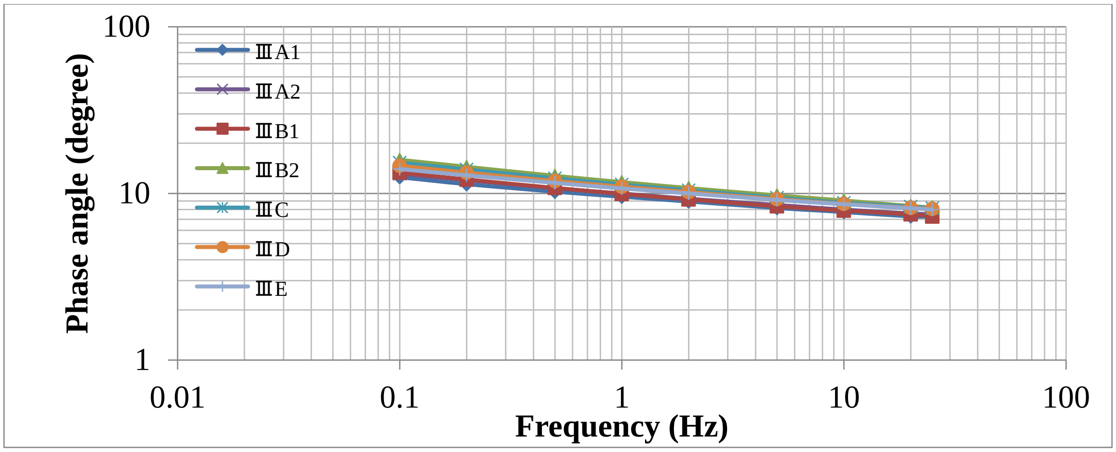

(a)

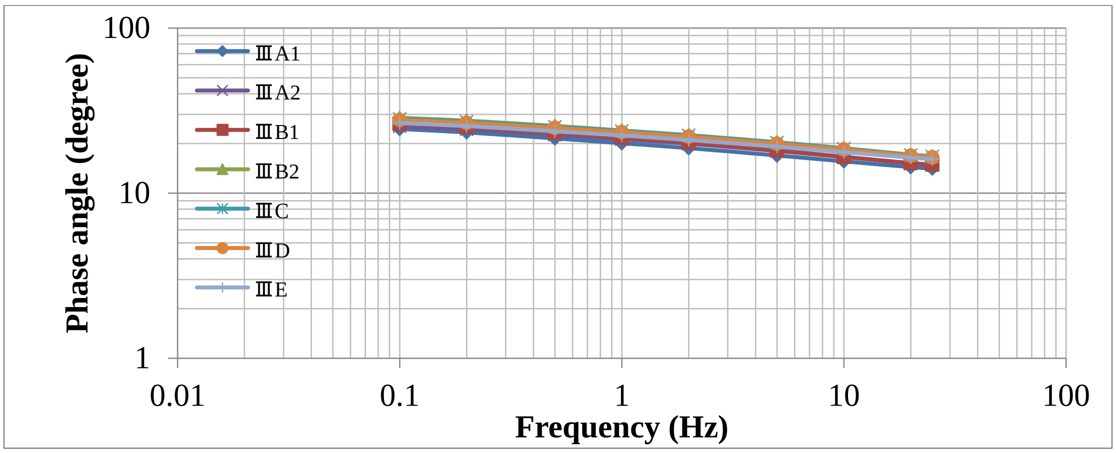

(b)

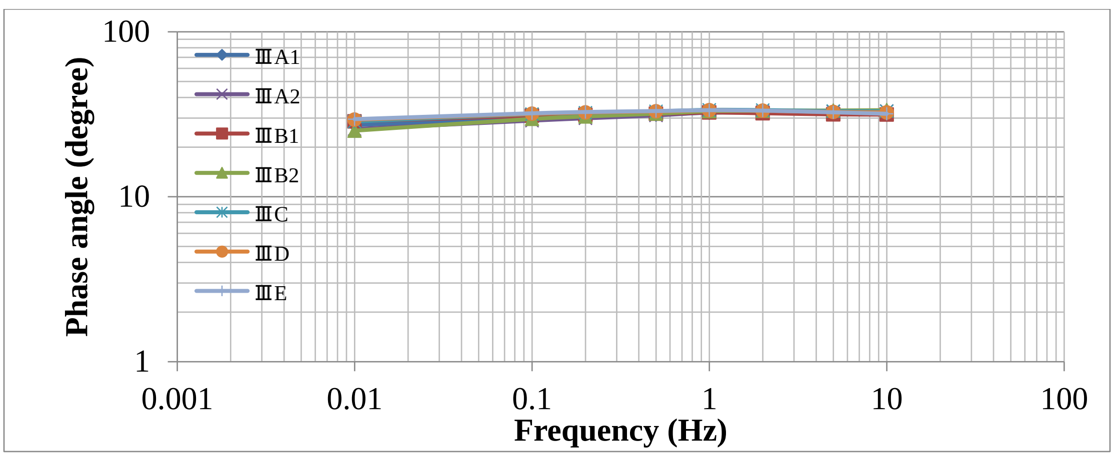

(c)

Figure 10-6 Phase Angle Values of Various Mixtures from Aggregate III with RAP in Terms of Surface Mixture Type, (a) at 4°C (39.2°F), (b) at 20°C (68°F), (c) at 45°C (113°F) (Surface A), 40°C (104°F) (Surface B, C, D, and E)

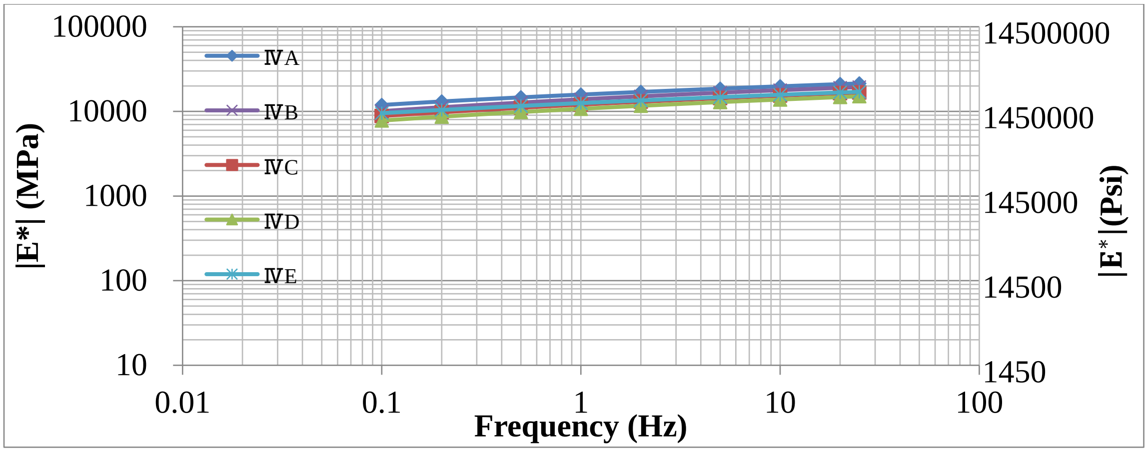

(a)

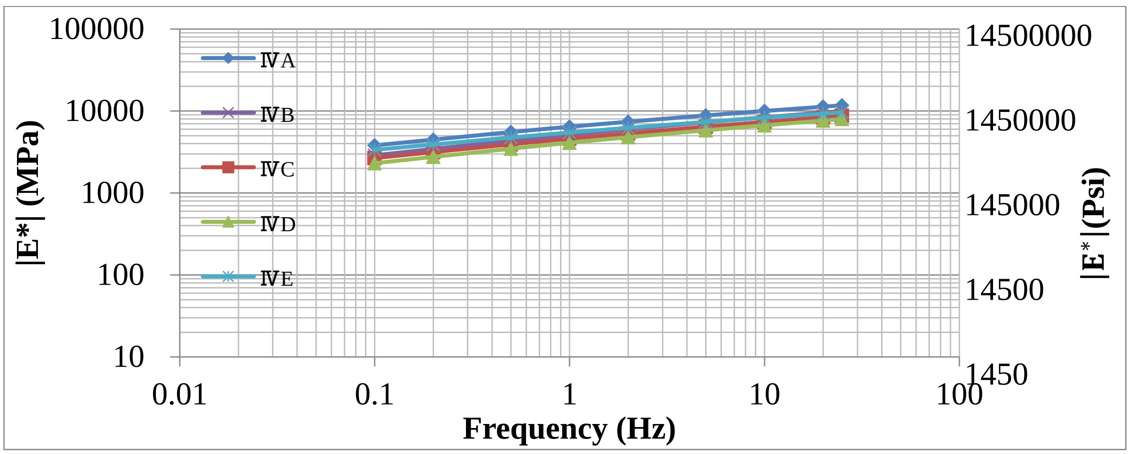

(b)

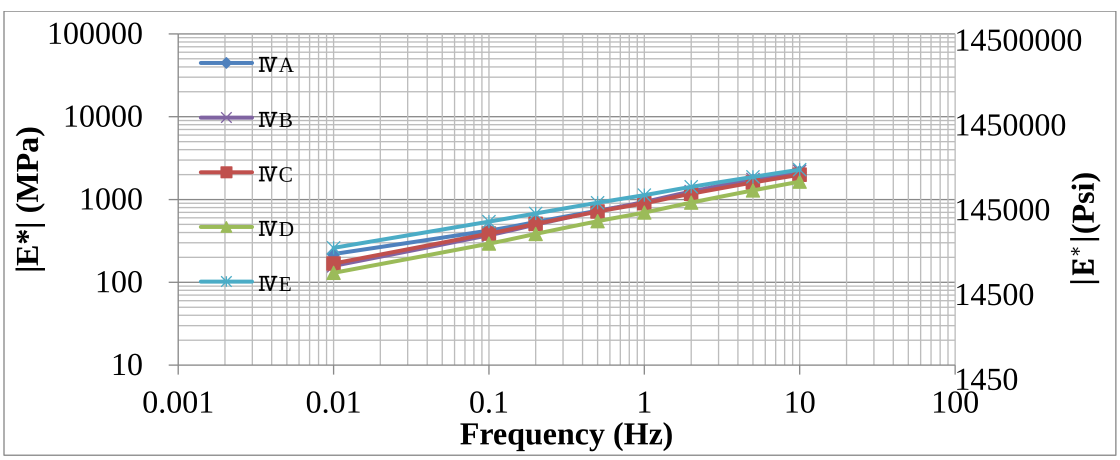

(c)

Figure 10-7 Dynamic Modulus Values of Various Mixtures from Aggregate IV with RAP in Terms of Surface Mixture Type, (a) at 4°C (39.2°F), (b) at 20°C (68°F), (c) at 45°C (113°F) (Surface A), 40°C (104°F) (Surface B, C, D, and E)

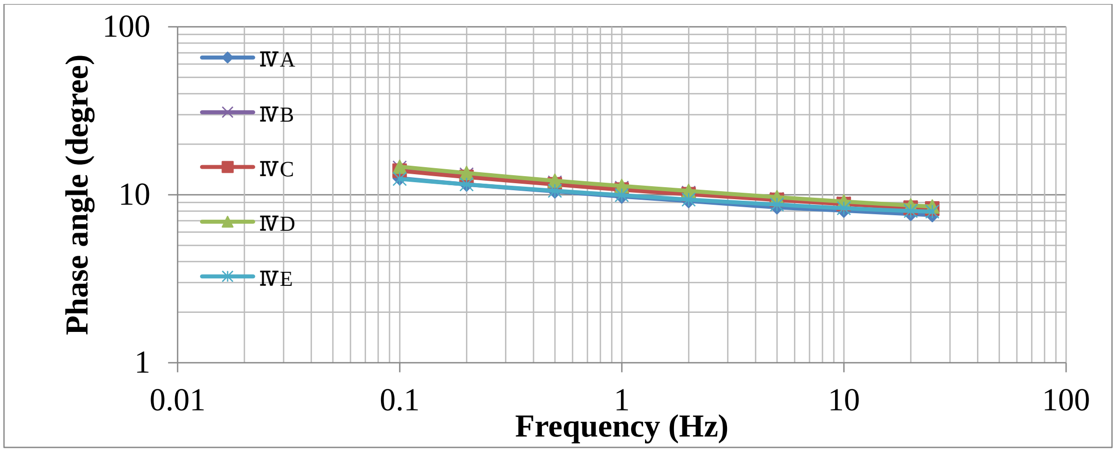

(a)

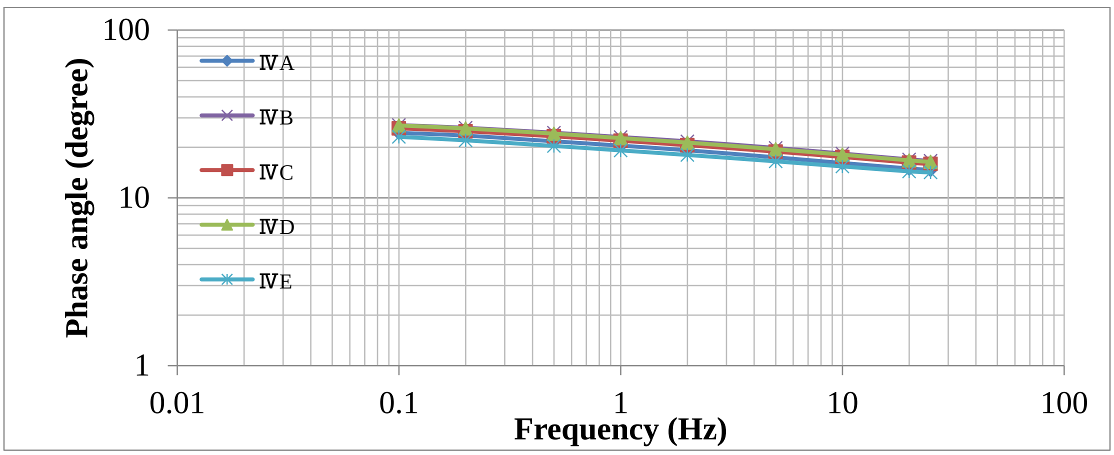

(b)

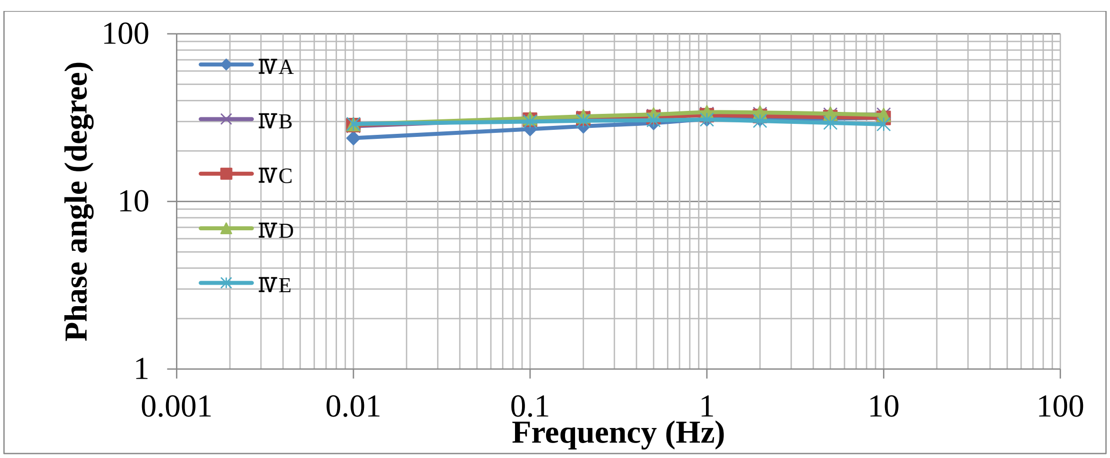

(c)

Figure 10-8 Phase Angle Values of Various Mixtures from Aggregate IV with RAP in Terms of Surface Mixture Type, (a) at 4°C (39.2°F), (b) at 20°C (68°F), (c) at 45°C (113°F) (Surface A), 40°C (104°F) (Surface B, C, D, and E)

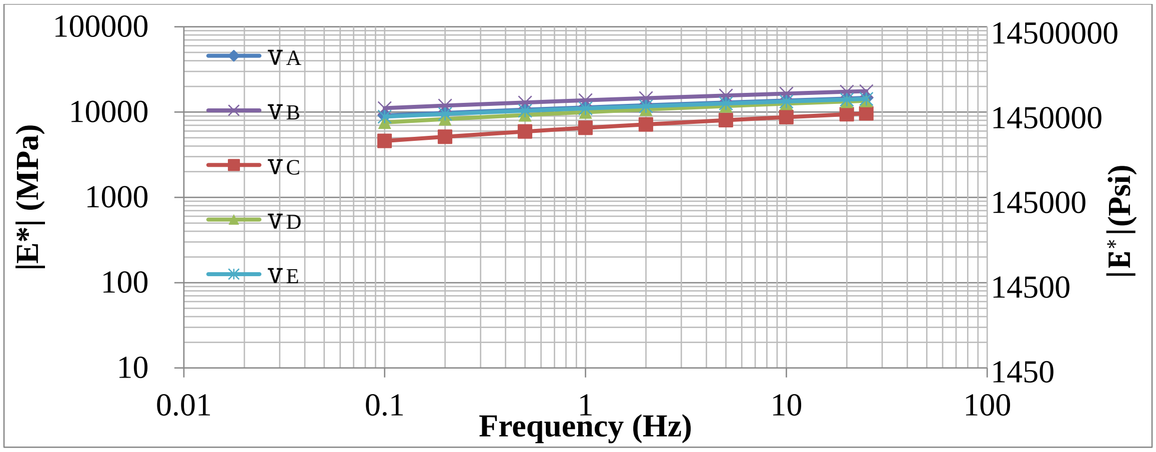

(a)

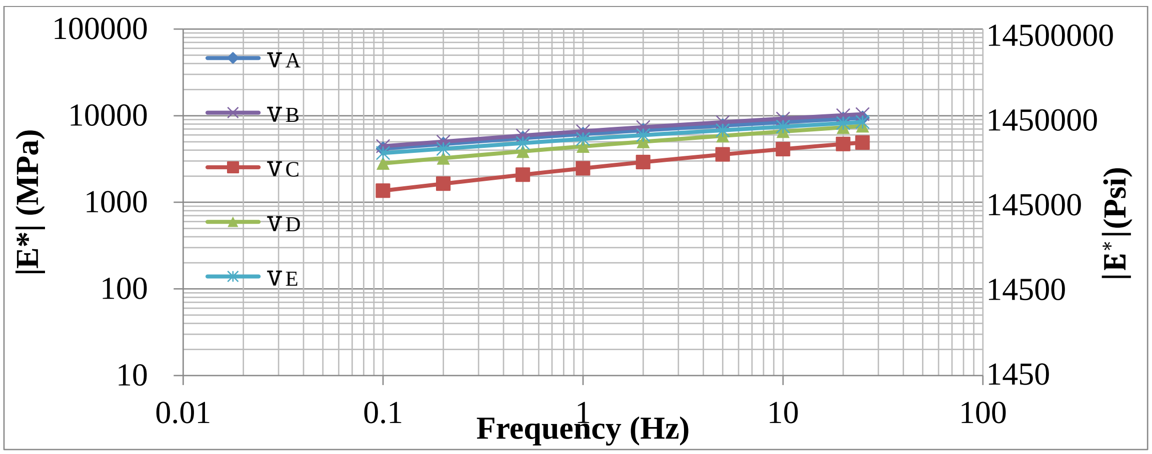

(b)

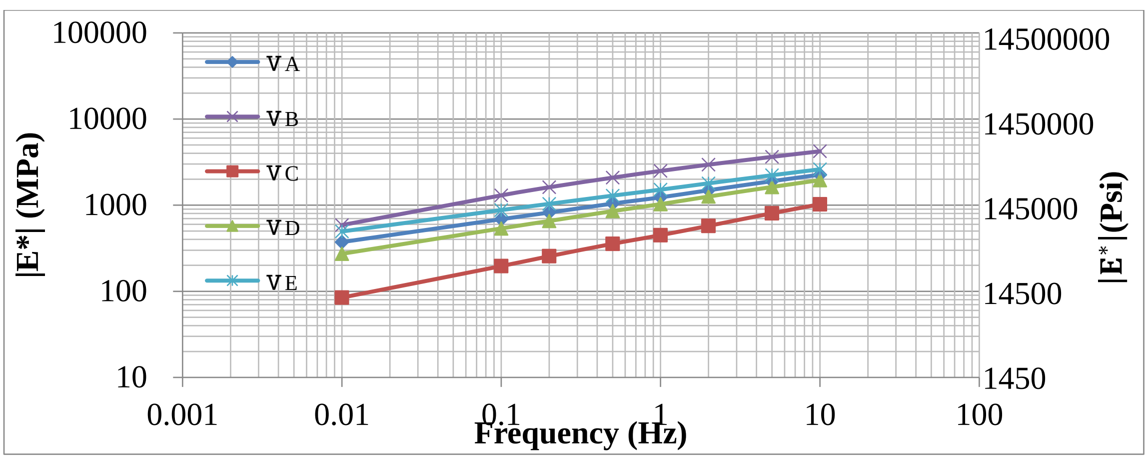

(c)

Figure 10-9 Dynamic Modulus Values of Various Mixtures from Aggregate V with RAP in Terms of Surface Mixture Type, (a) at 4°C (39.2°F), (b) at 20°C (68°F), (c) at 45°C (113°F) (Surface A), 40°C (104°F) (Surface B, C, D, and E)

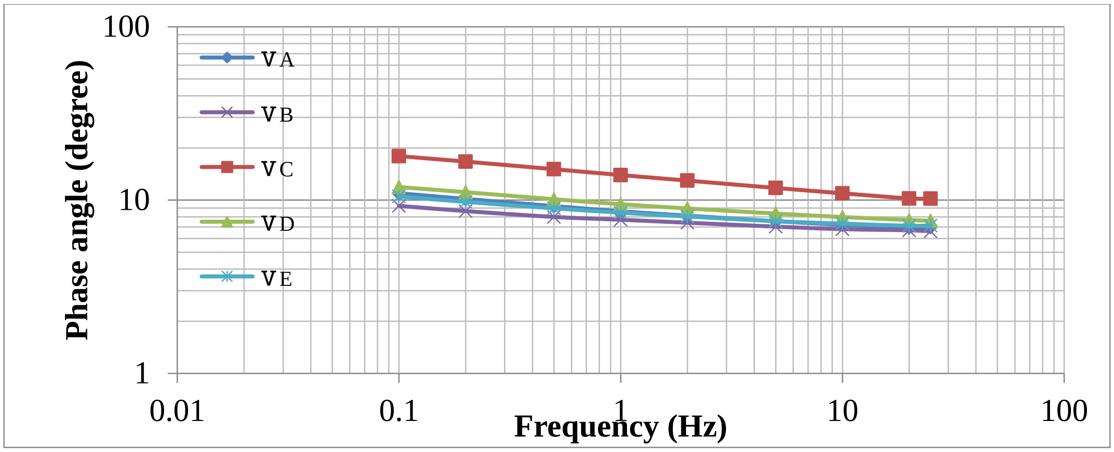

(a)

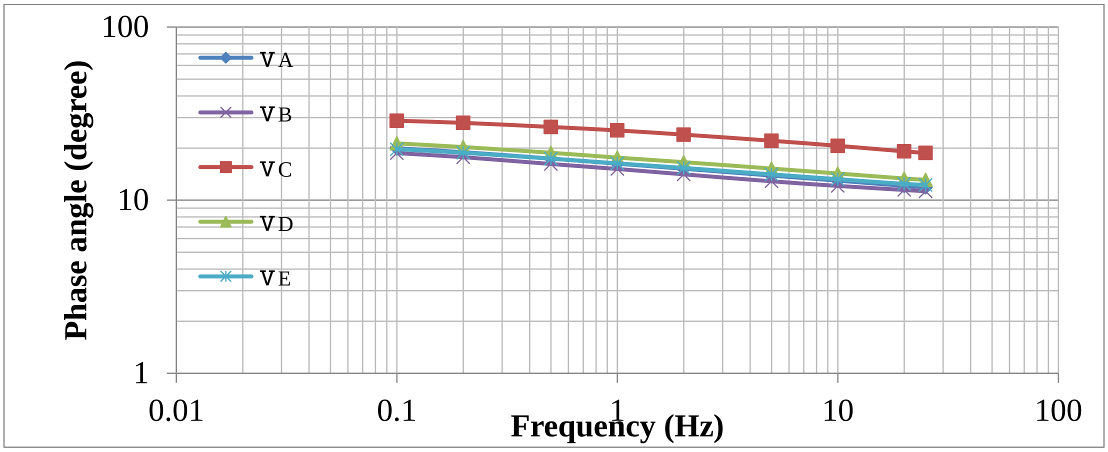

(b)

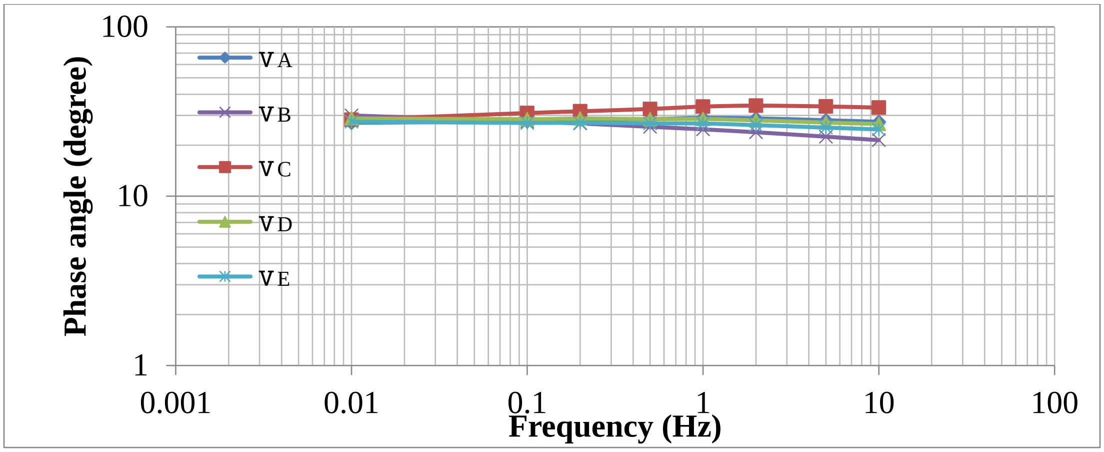

(c)

Figure 10-10 Phase Angle Values of Various Mixtures from Aggregate V with RAP in Terms of Surface Mixture Type, (a) at 4°C (39.2°F), (b) at 20°C (68°F), (c) at 45°C (113°F) (Surface A), 40°C (104°F) (Surface B, C, D, and E)

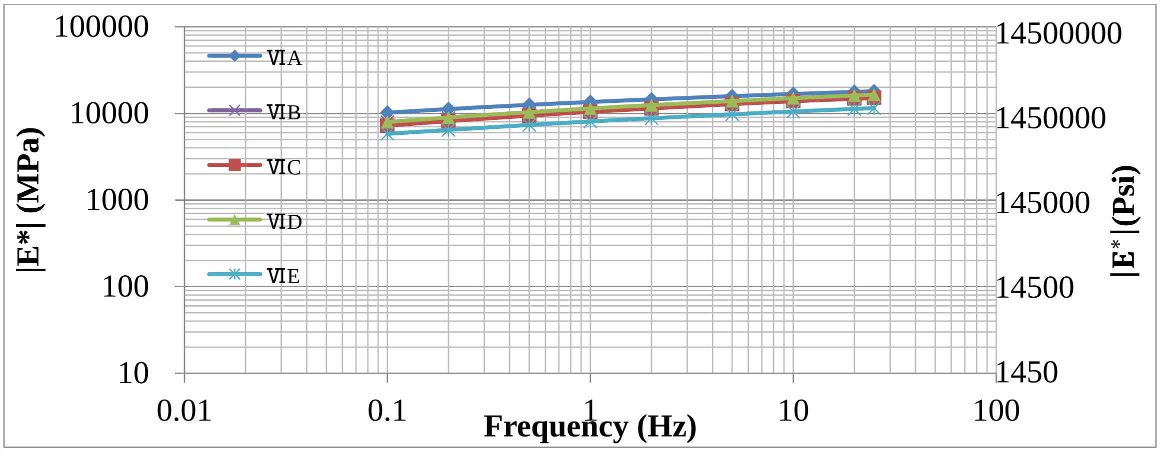

(a)

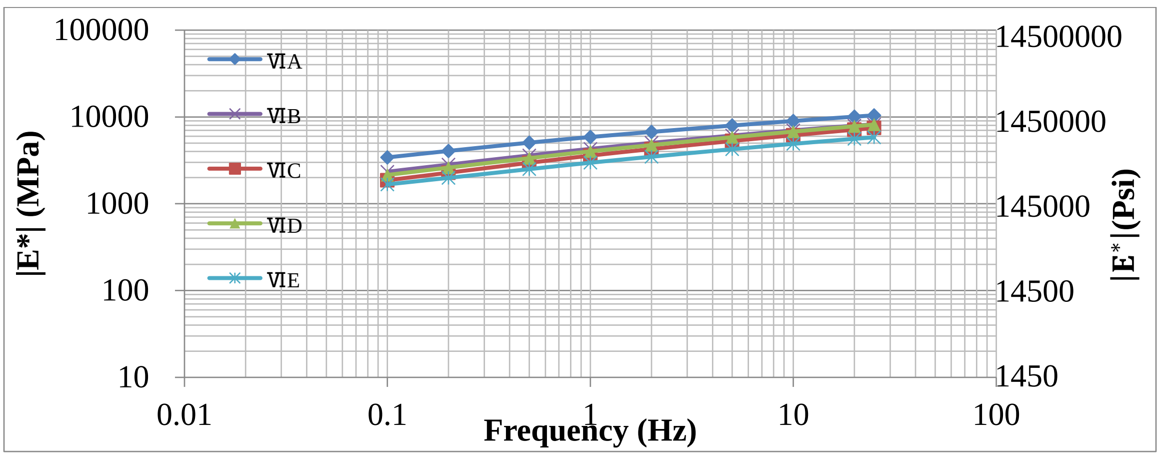

(b)

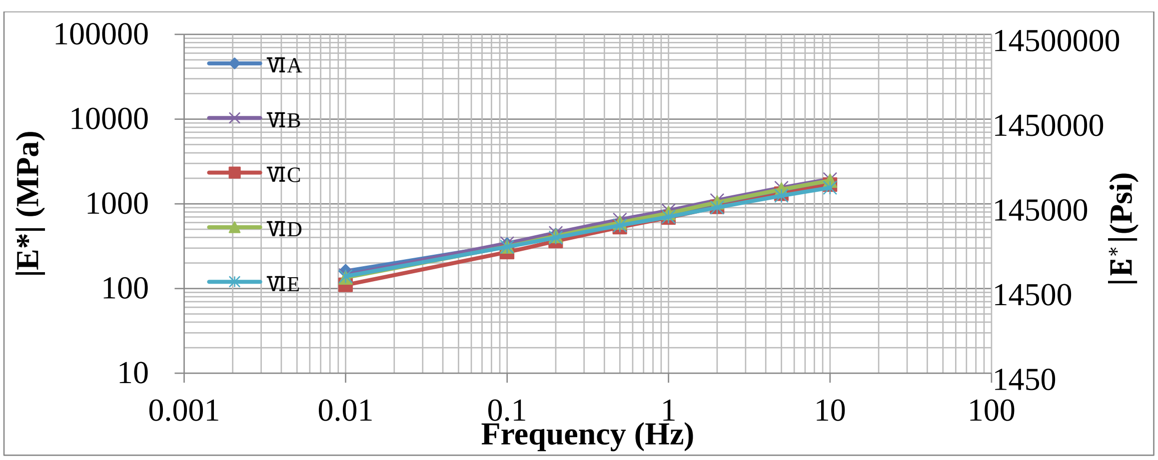

(c)

Figure 10-11 Dynamic Modulus Values of Various Mixtures from Aggregate VI with RAP in Terms of Surface Mixture Type, (a) at 4°C (39.2°F), (b) at 20°C (68°F), (c) at 45°C (113°F) (Surface A), 40°C (104°F) (Surface B, C, D, and E)

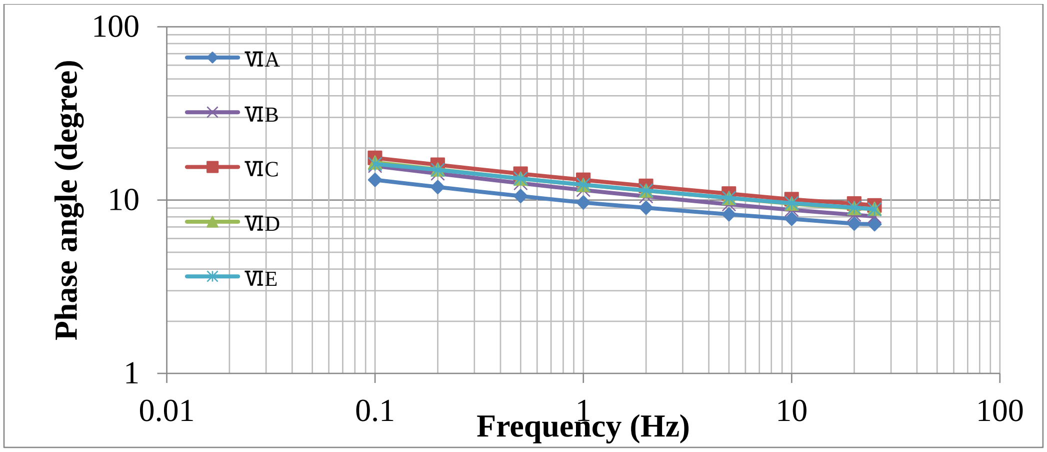

(a)

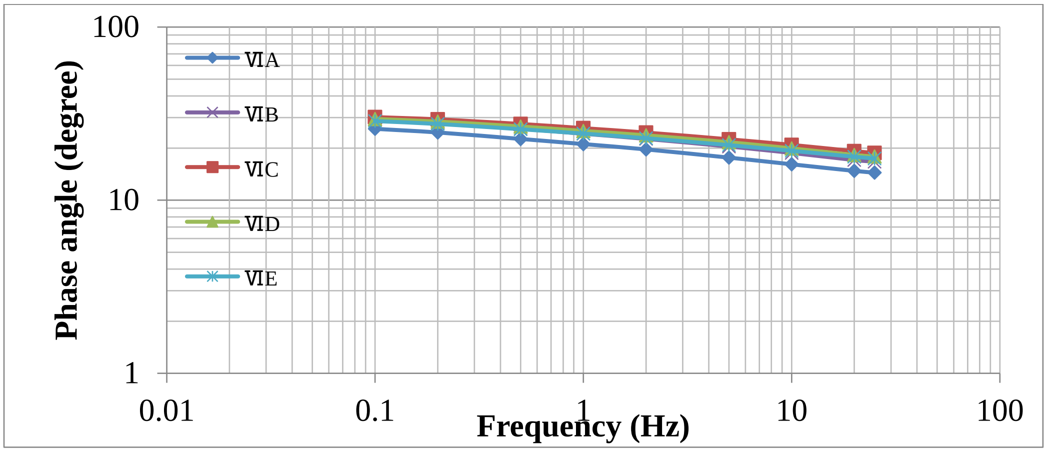

(b)

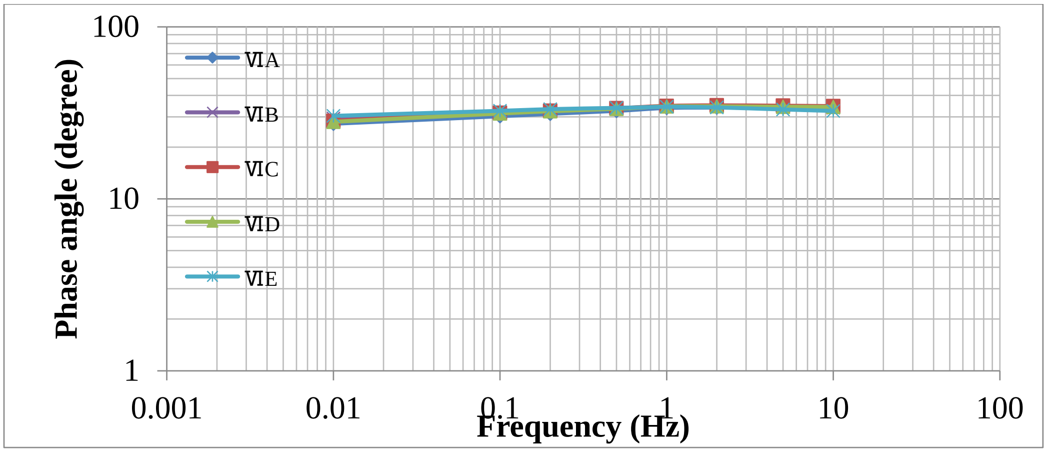

(c)

Figure 10-12 Phase Angle Values of Various Mixtures from Aggregate VI with RAP in Terms of Surface Mixture Type, (a) at 4°C (39.2°F), (b) at 20°C (68°F), (c) at 45°C (113°F) (Surface A), 40°C (104°F) (Surface B, C, D, and E)

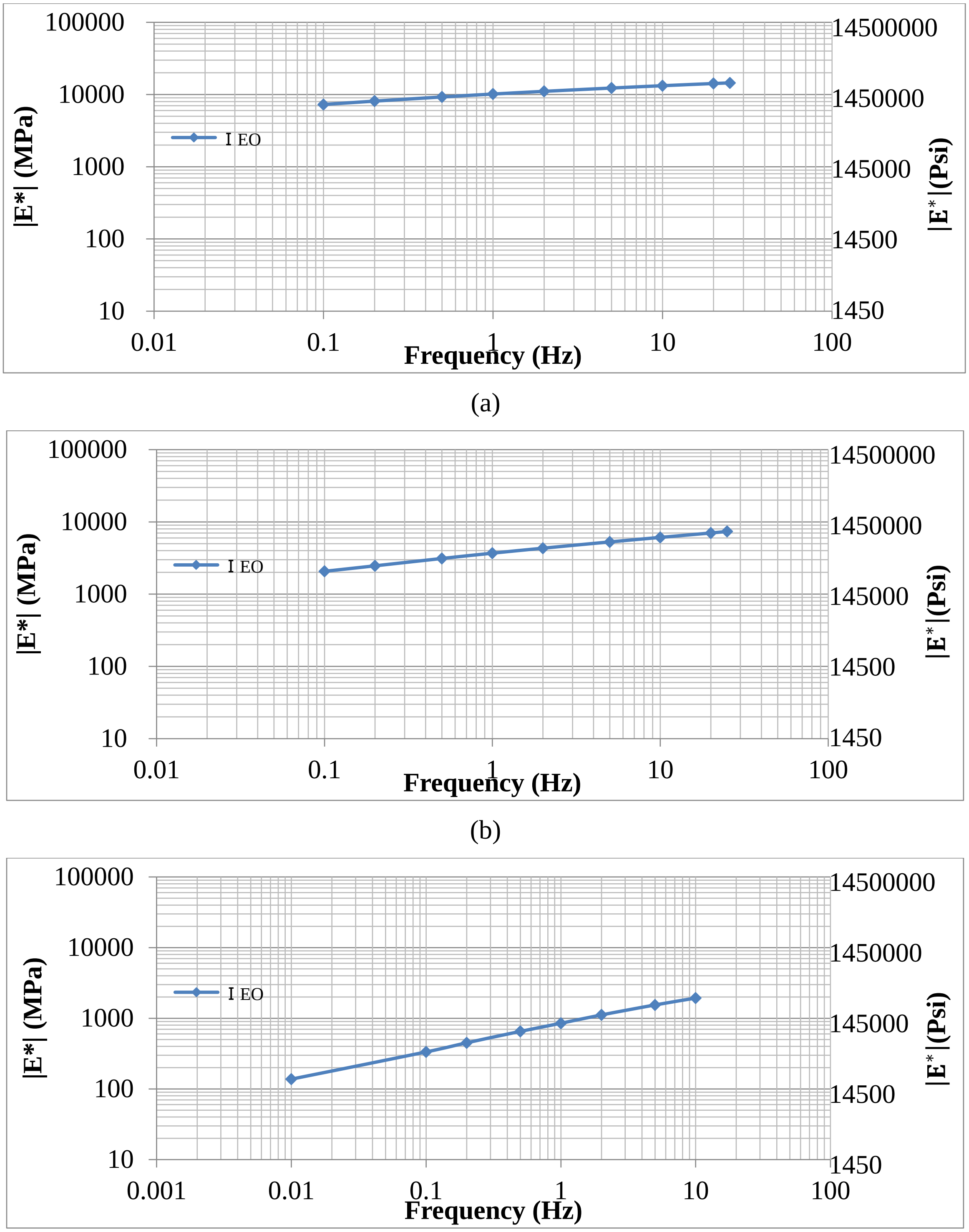

(a)

(b)

(c)

Figure 10-13 Dynamic Modulus Values of Various Mixtures from Aggregate I without RAP in Terms of Surface Mixture Type, (a) at 4°C (39.2°F), (b) at 20°C (68°F), (c) at 45°C (113°F) (Surface A), 40°C (104°F) (Surface B, C, D, and E)

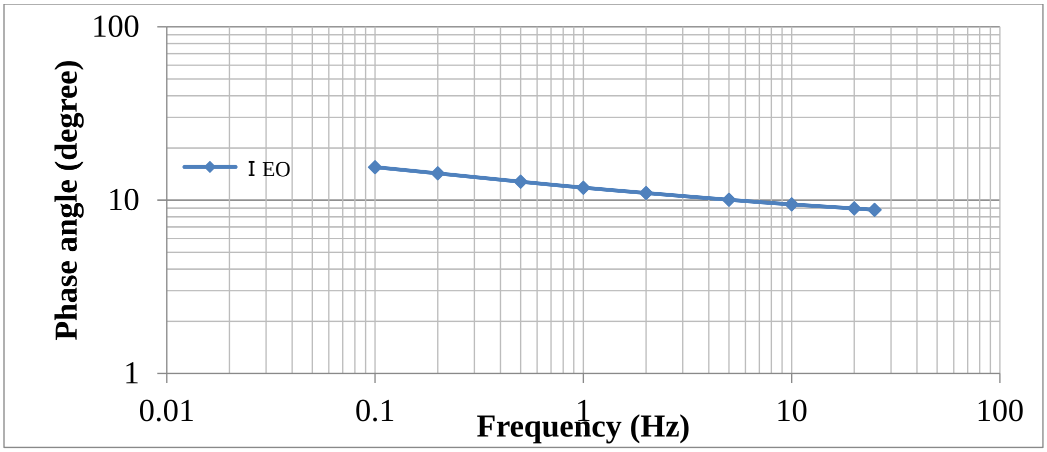

(a)

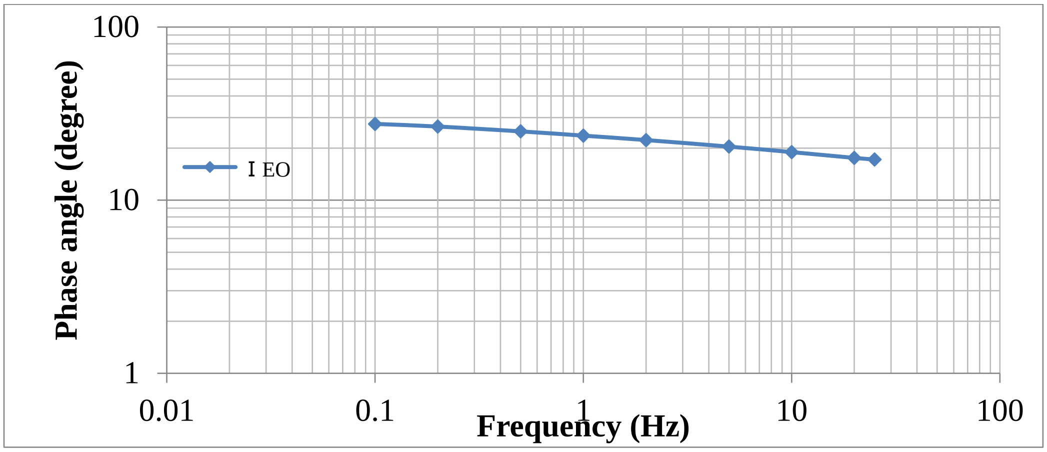

(b)

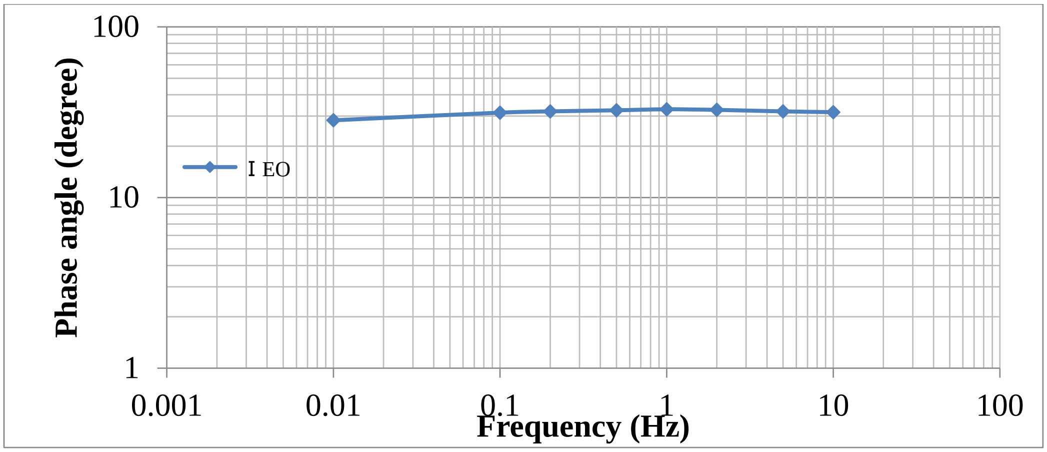

(c)

Figure 10-14 Phase Angle Values of Various Mixtures from Aggregate I without RAP in Terms of Surface Mixture Type, (a) at 4°C (39.2°F), (b) at 20°C (68°F), (c) at 45°C (113°F) (Surface A), 40°C (104°F) (Surface B, C, D, and E)

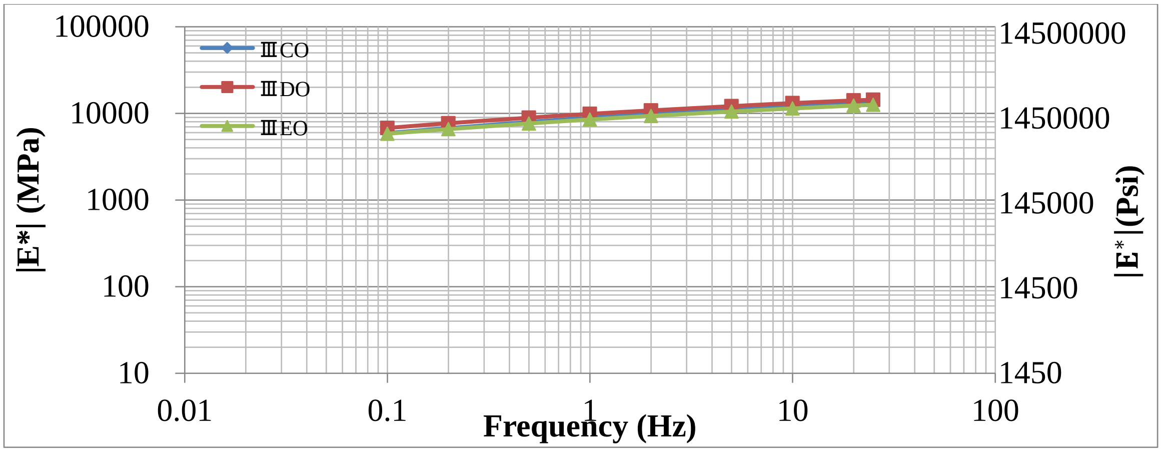

(a)

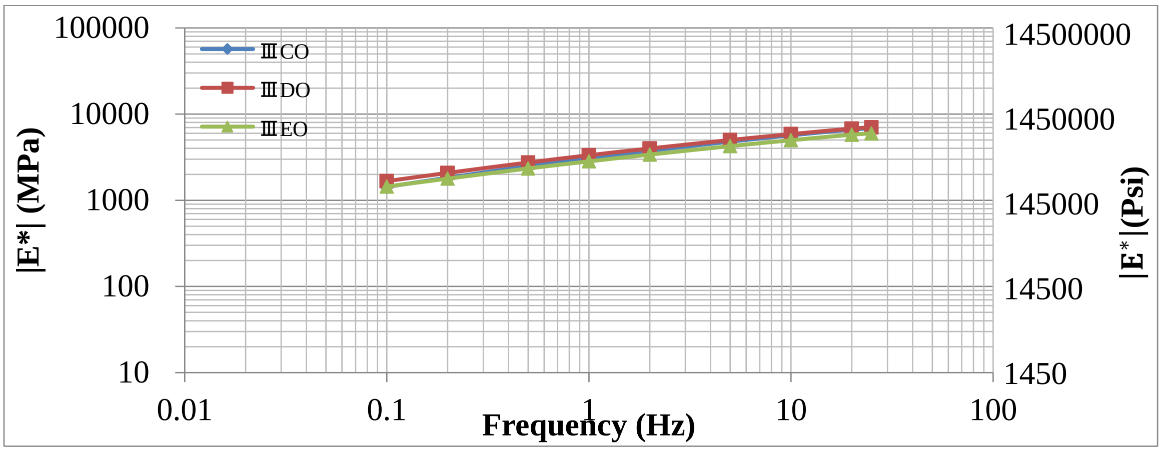

(b)

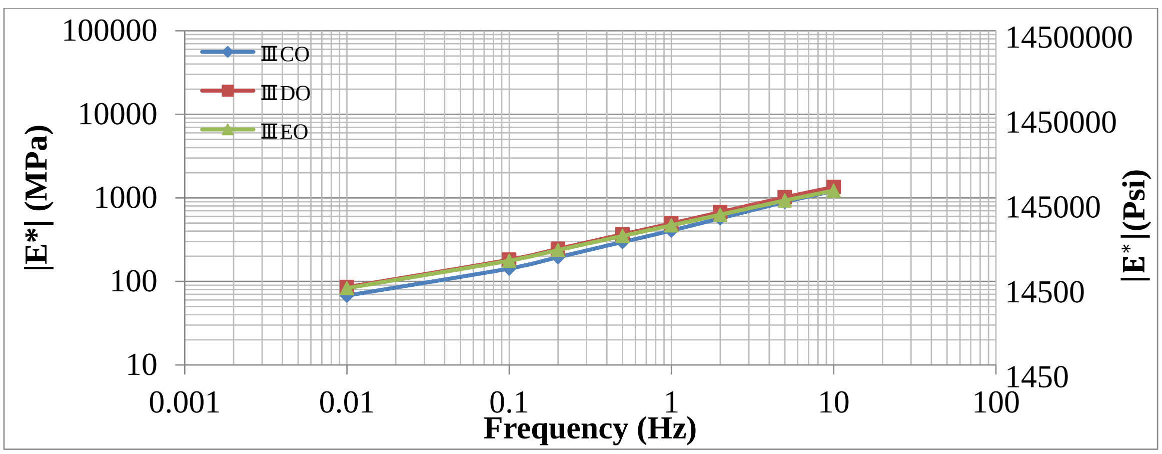

(c)

Figure 10-15 Dynamic Modulus Values of Various Mixtures from Aggregate III without RAP in Terms of Surface Mixture Type, (a) at 4°C (39.2°F), (b) at 20°C (68°F), (c) at 45°C (113°F) (Surface A), 40°C (104°F) (Surface B, C, D, and E)

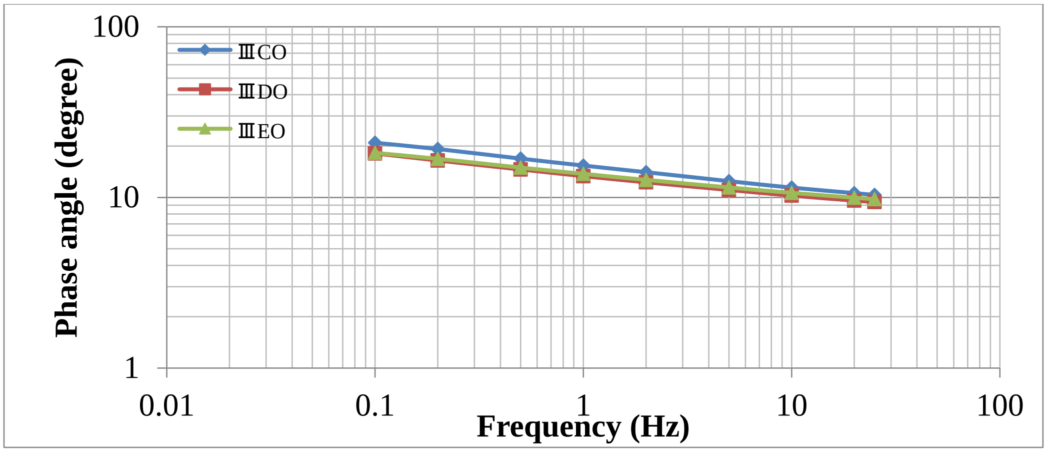

(a)

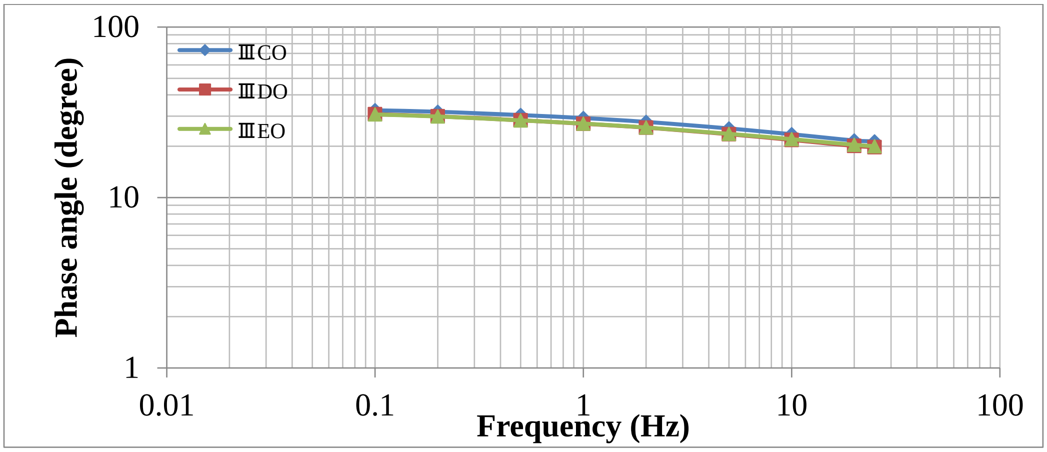

(b)

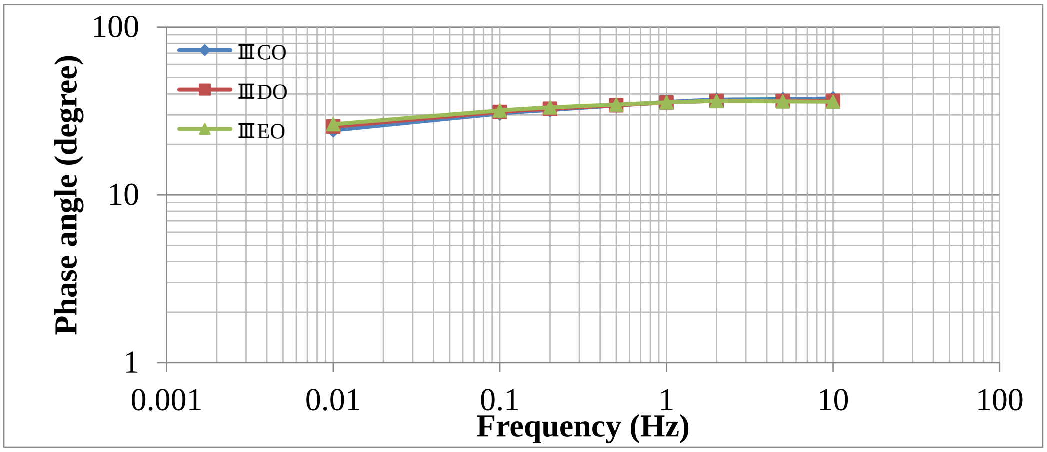

(c)

Figure 10-16 Phase Angle Values of Various Mixtures from Aggregate III without RAP in Terms of Surface Mixture Type, (a) at 4°C (39.2°F), (b) at 20°C (68°F), (c) at 45°C (113°F) (Surface A), 40°C (104°F) (Surface B, C, D, and E)

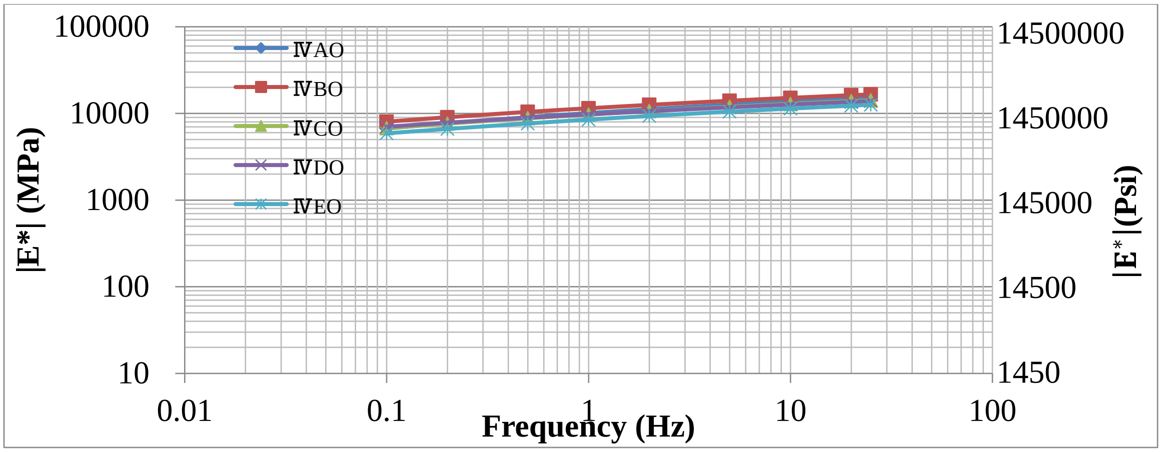

(a)

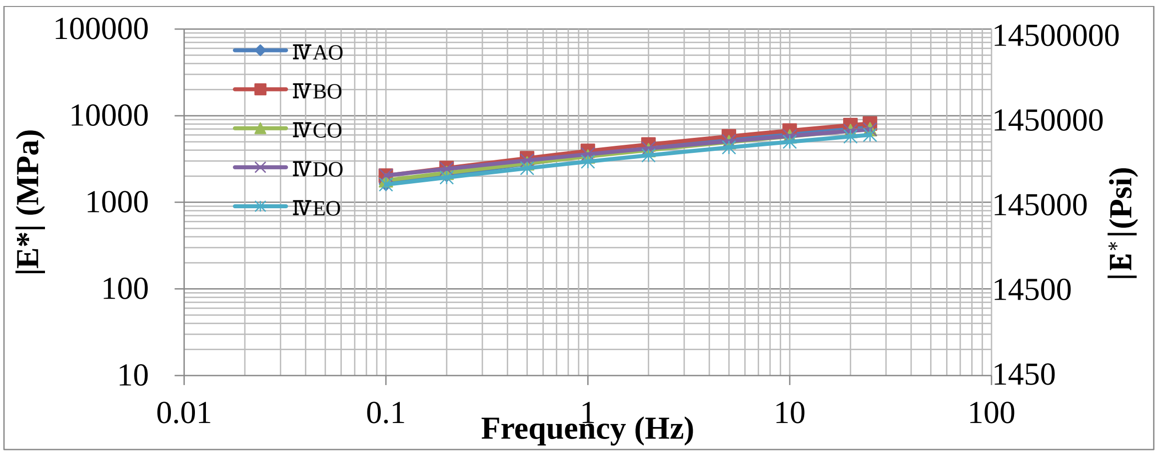

(b)

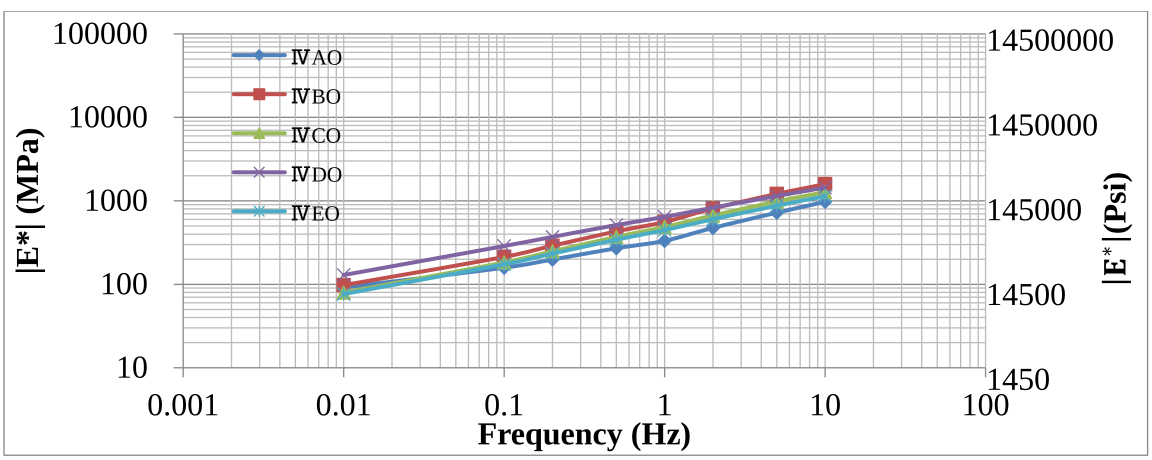

(c)

Figure 10-17 Dynamic Modulus Values of Various Mixtures from Aggregate IV without RAP in Terms of Surface Mixture Type, (a) at 4°C (39.2°F), (b) at 20°C (68°F), (c) at 45°C (113°F) (Surface A), 40°C (104°F) (Surface B, C, D, and E)

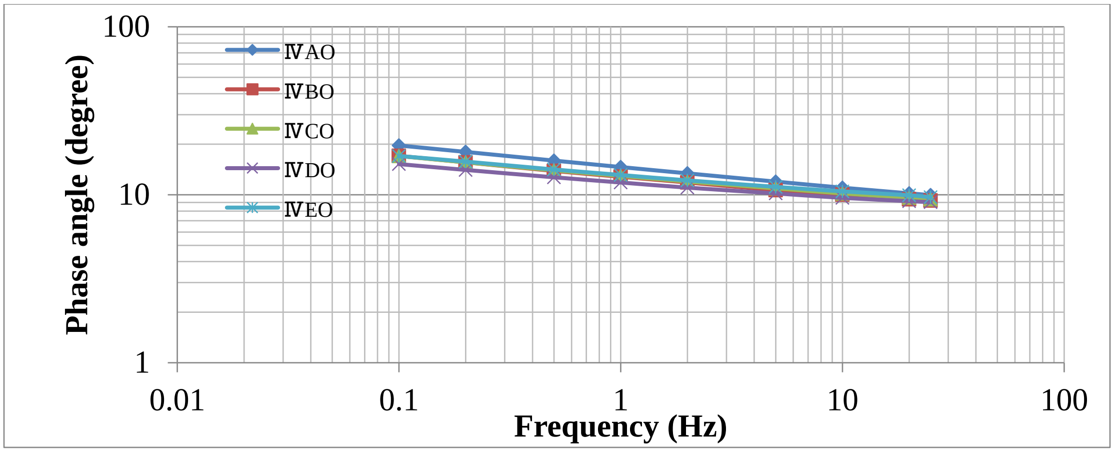

(a)

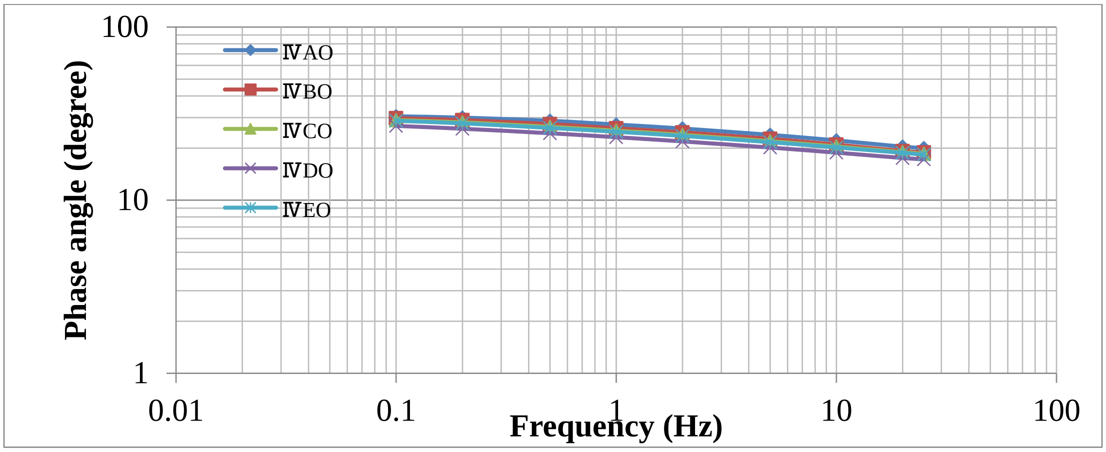

(b)

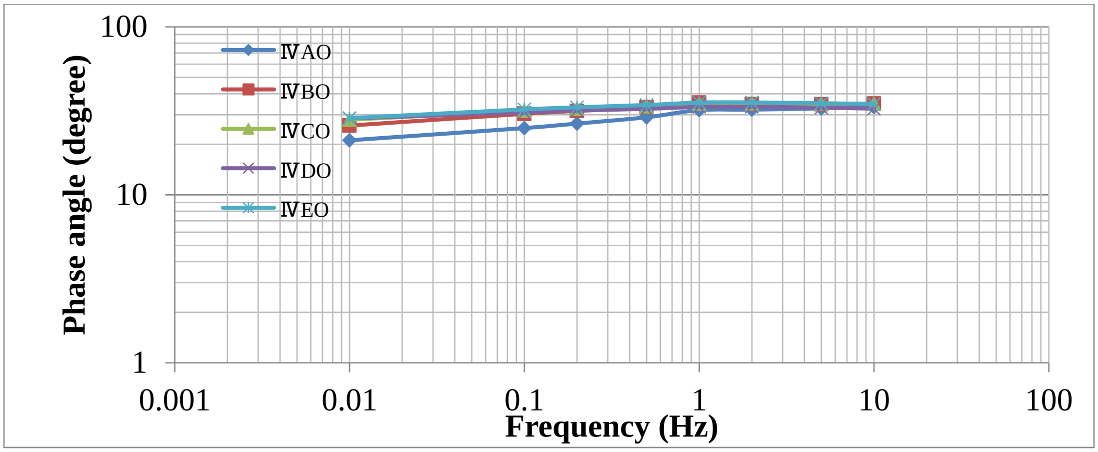

(c)

Figure 10-18 Phase Angle Values of Various Mixtures from Aggregate IV without RAP in Terms of Surface Mixture Type, (a) at 4°C (39.2°F), (b) at 20°C (68°F), (c) at 45°C (113°F) (Surface A), 40°C (104°F) (Surface B, C, D, and E)

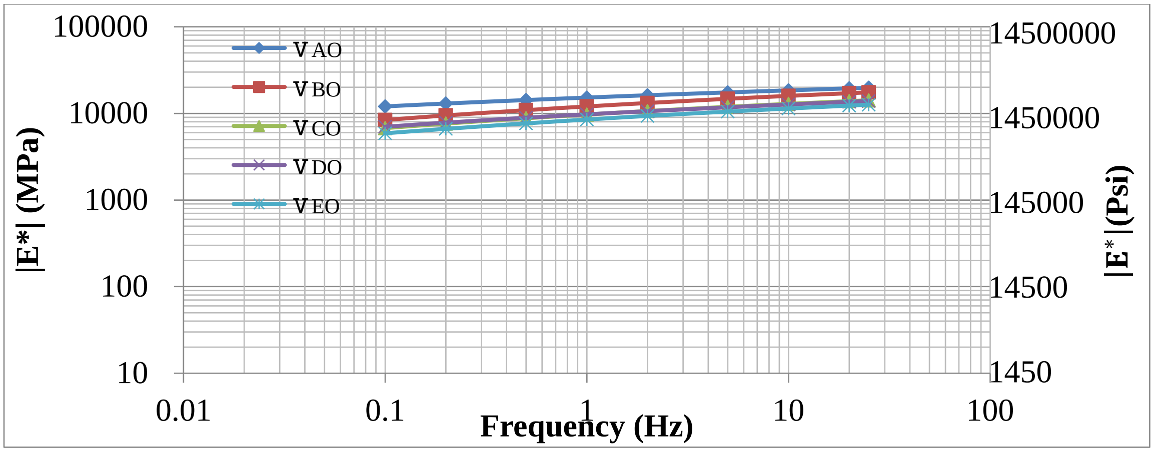

(a)

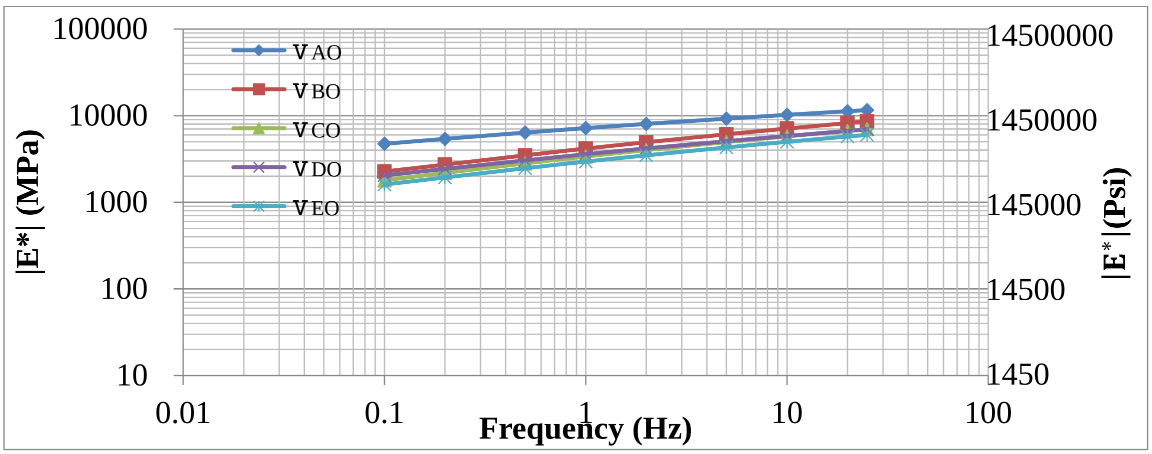

(b)

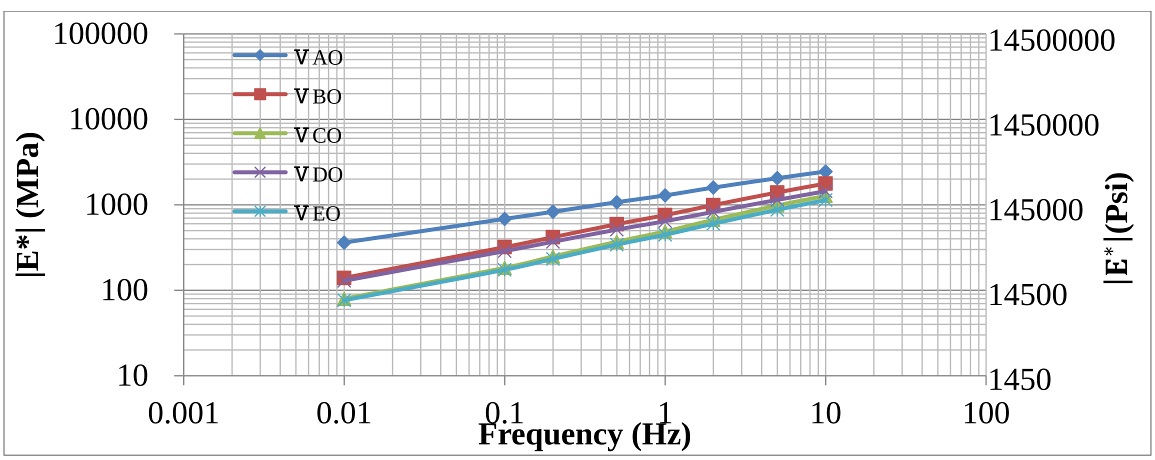

(c)

Figure 10-19 Dynamic Modulus Values of Various Mixtures from Aggregate V without RAP in Terms of Surface Mixture Type, (a) at 4°C (39.2°F), (b) at 20°C (68°F), (c) at 45°C (113°F) (Surface A), 40°C (104°F) (Surface B, C, D, and E)

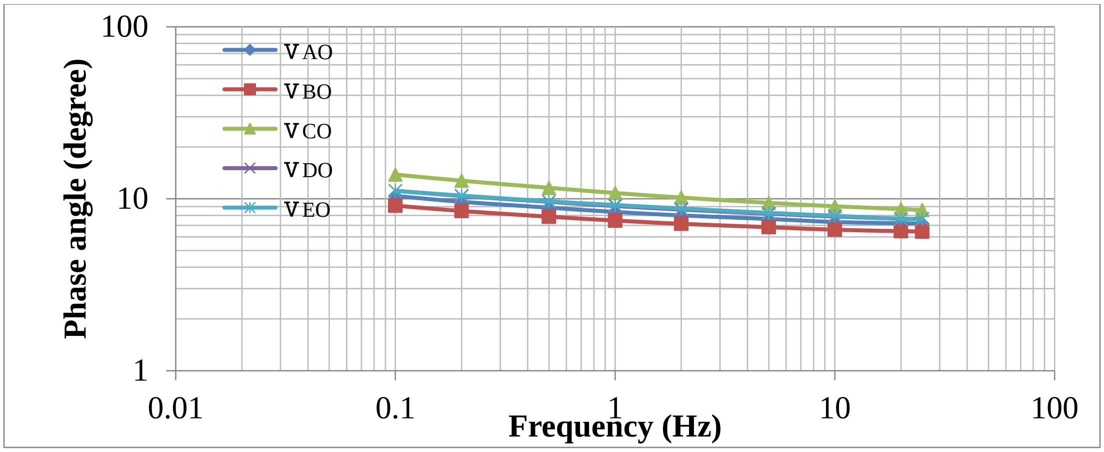

(a)

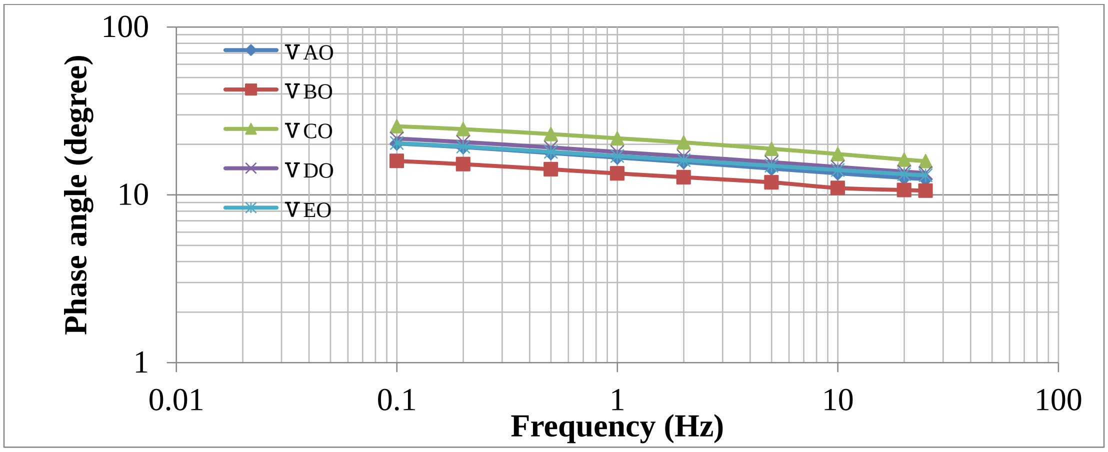

(b)

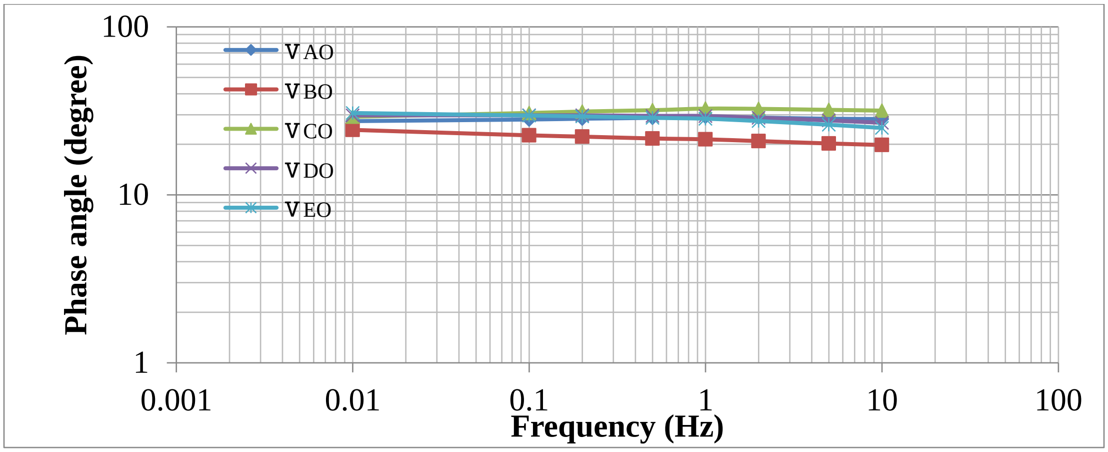

(c)

Figure 10-20 Phase Angle Values of Various Mixtures from Aggregate V without RAP in Terms of Surface Mixture Type, (a) at 4°C (39.2°F), (b) at 20°C (68°F), (c) at 45°C (113°F) (Surface A), 40°C (104°F) (Surface B, C, D, and E)

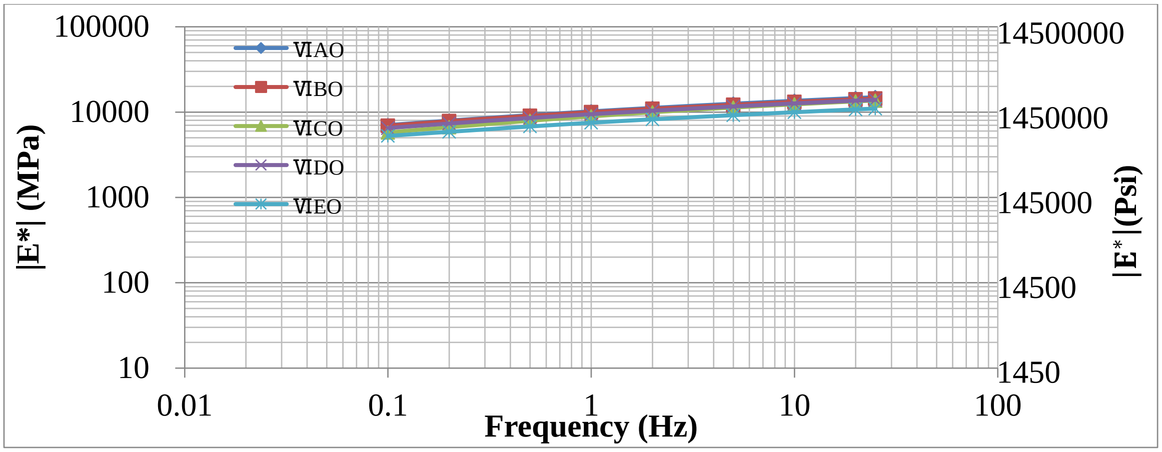

(a)

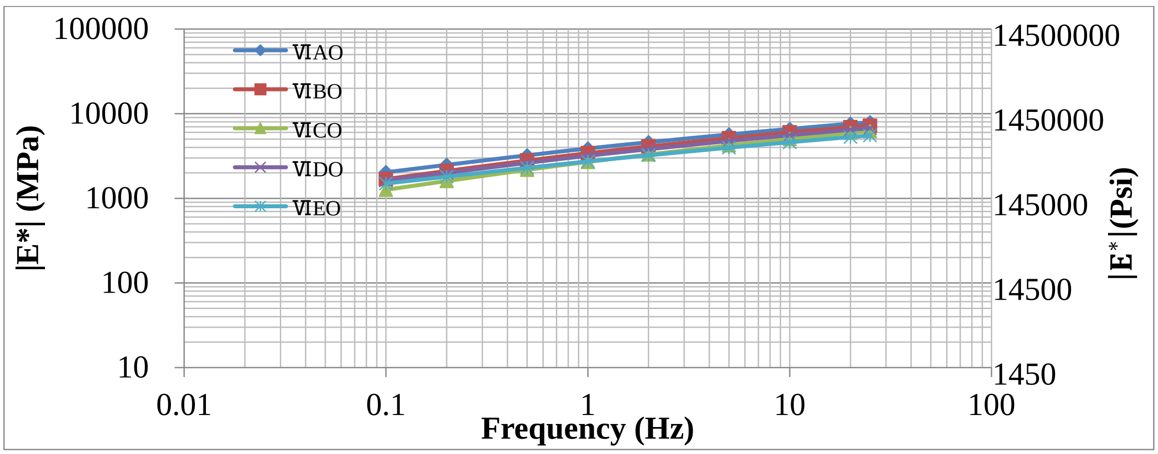

(b)

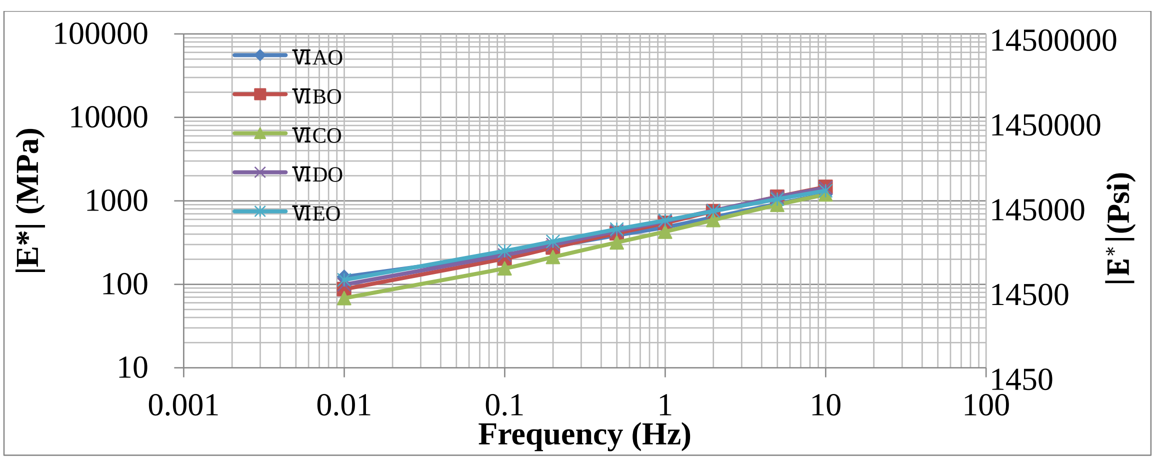

(c)

Figure 10-21 Dynamic Modulus Values of Various Mixtures from Aggregate VI without RAP in Terms of Surface Mixture Type, (a) at 4°C (39.2°F), (b) at 20°C (68°F), (c) at 45°C (113°F) (Surface A), 40°C (104°F) (Surface B, C, D, and E)

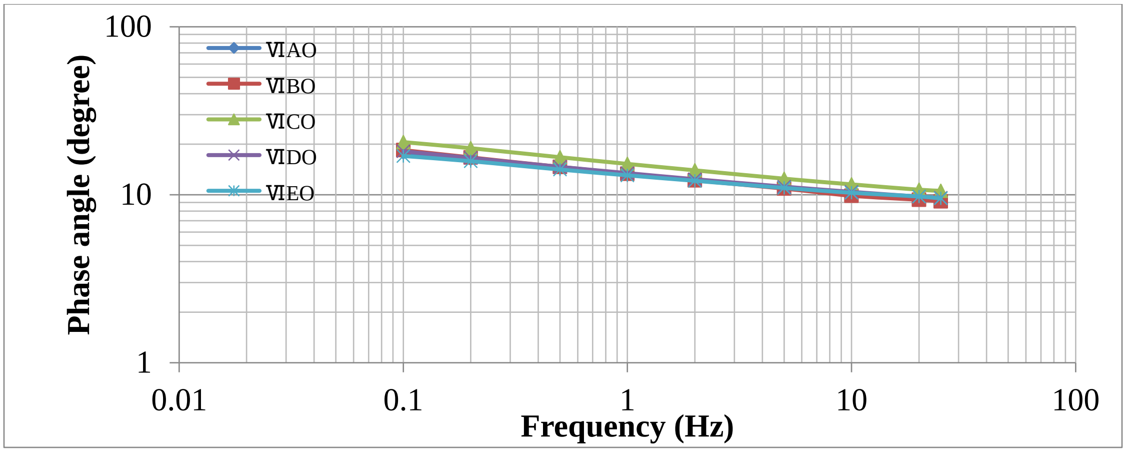

(a)

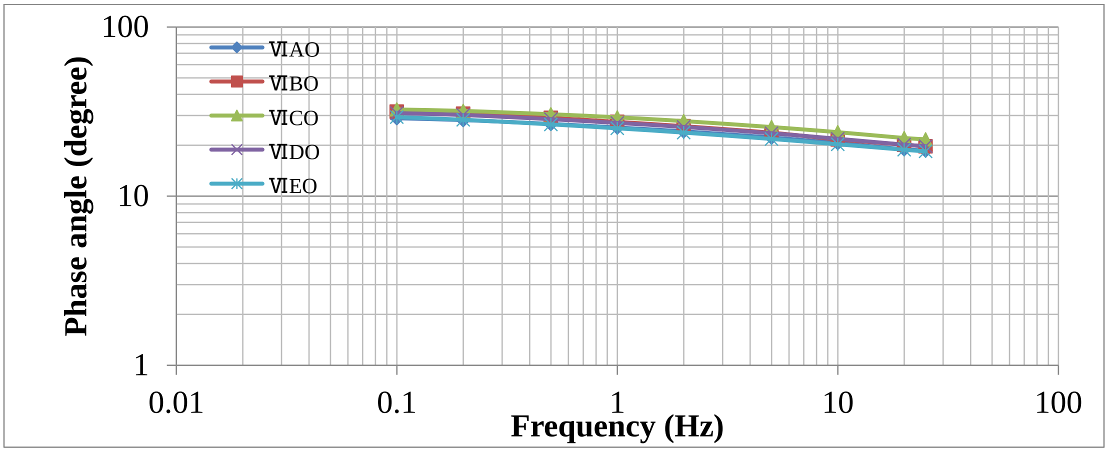

(b)

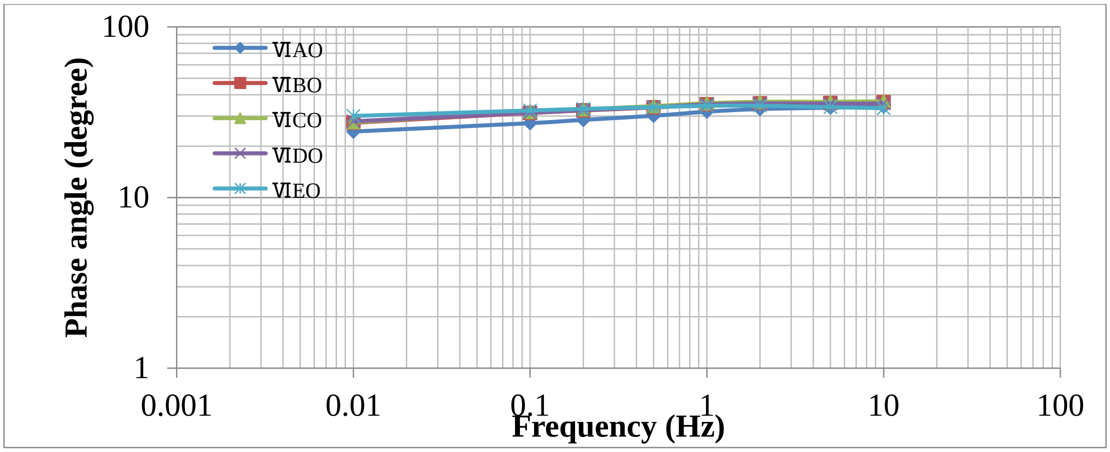

(c)

Figure 10-22 Phase Angle Values of Various Mixtures from Aggregate VI without RAP in Terms of Surface Mixture Type, (a) at 4°C (39.2°F), (b) at 20°C (68°F), (c) at 45°C (113°F) (Surface A), 40°C (104°F) (Surface B, C, D, and E)

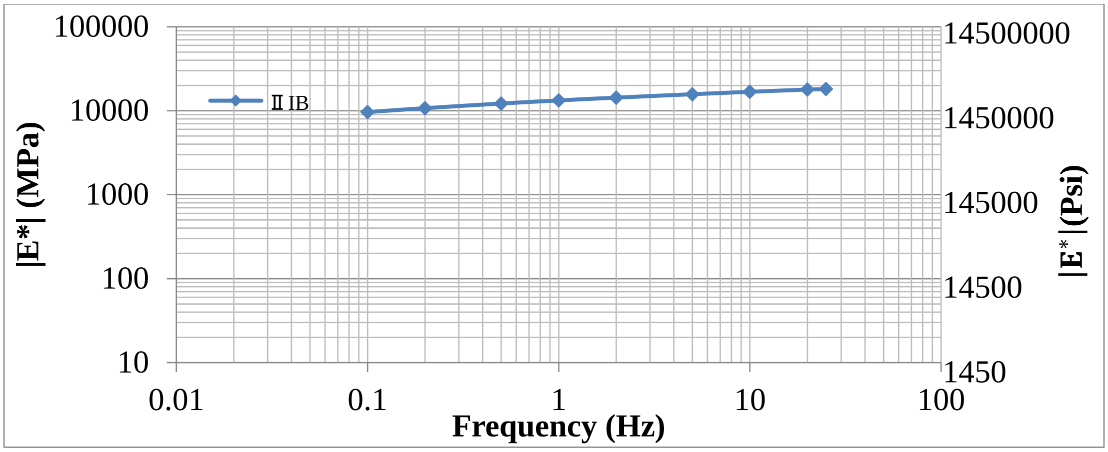

(a)

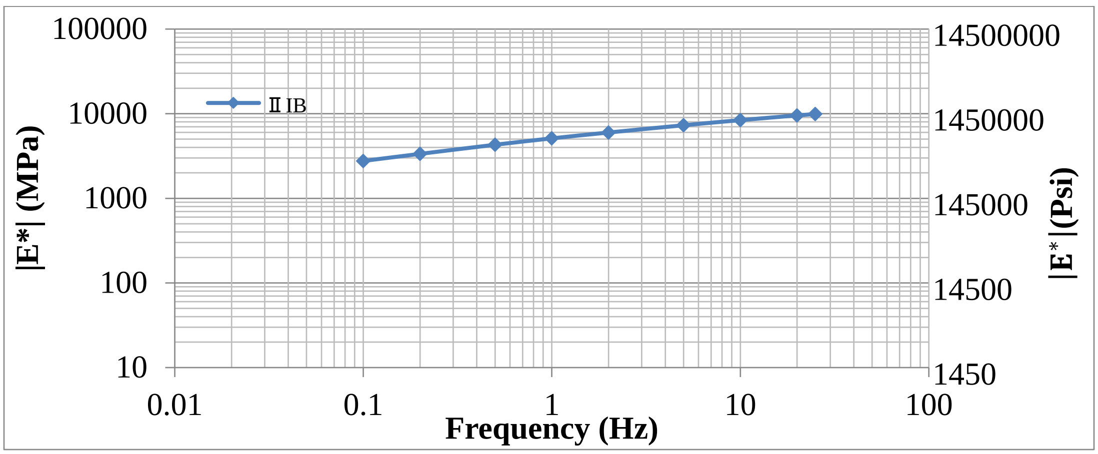

(b)

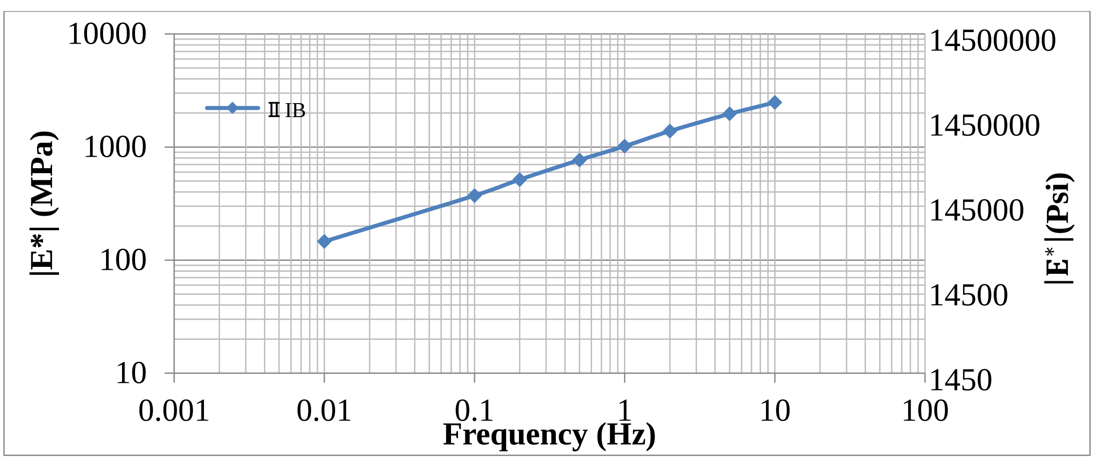

(c)

Figure 10-23 Dynamic Modulus Values of Various Mixtures from Aggregate II with RAP in Terms of Intermediate Mixture Type, (a) at 4°C (39.2°F), (b) at 20°C (68°F), (c) at 40°C (104°F)

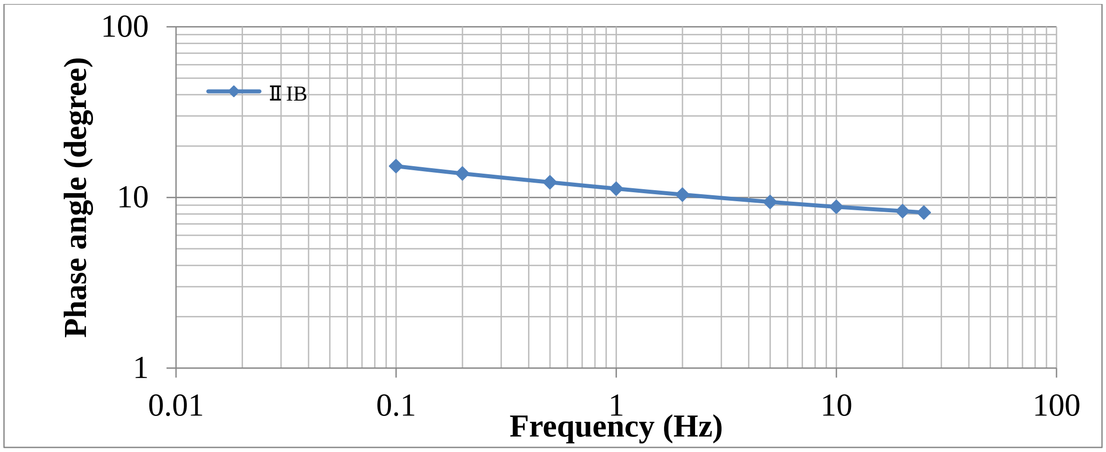

(a)

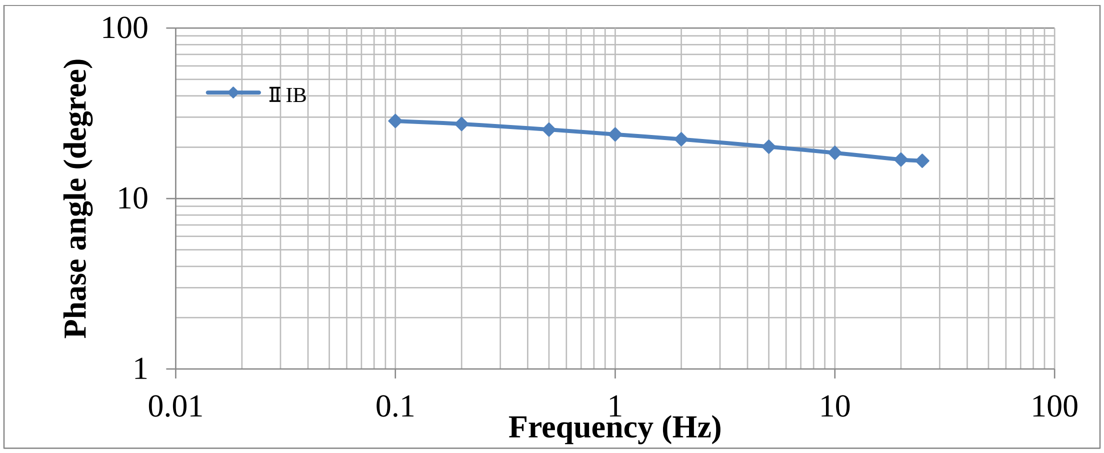

(b)

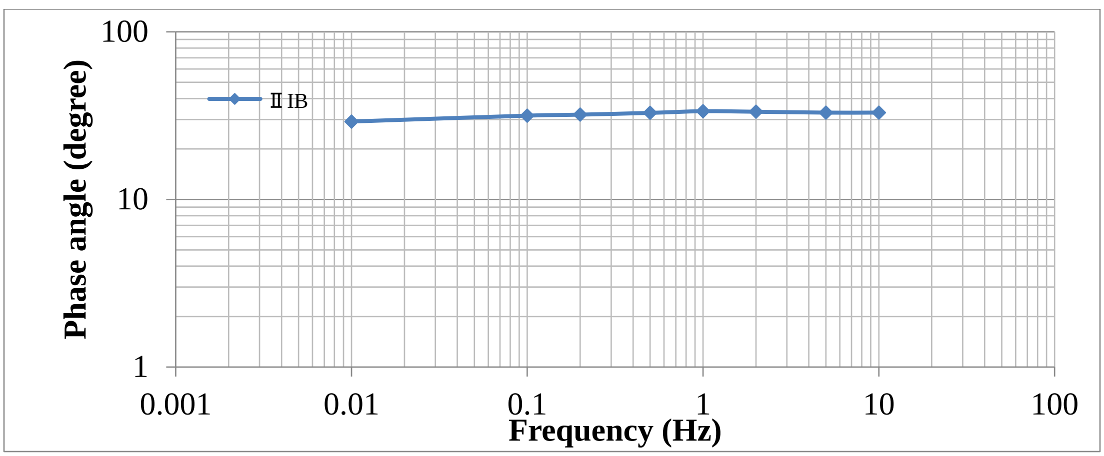

(c)

Figure 10-24 Phase Angle Values of Various Mixtures from Aggregate II with RAP in Terms of Intermediate Mixture Type, (a) at 4°C (39.2°F), (b) at 20°C (68°F), (c) at 40°C (104°F)

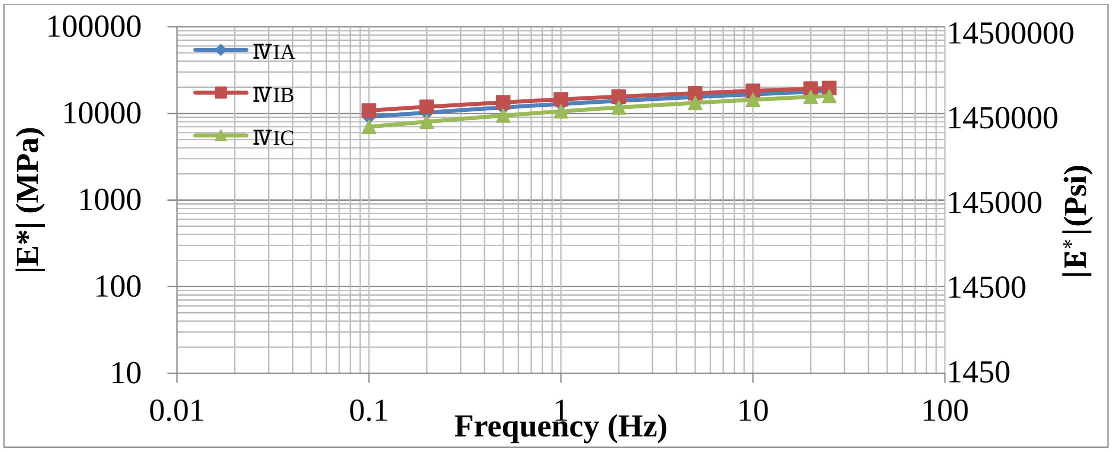

(a)

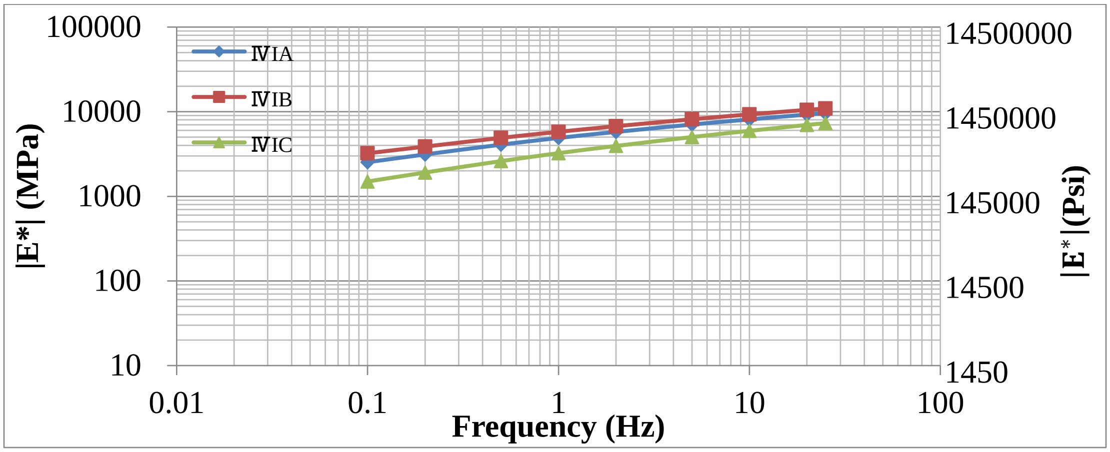

(b)

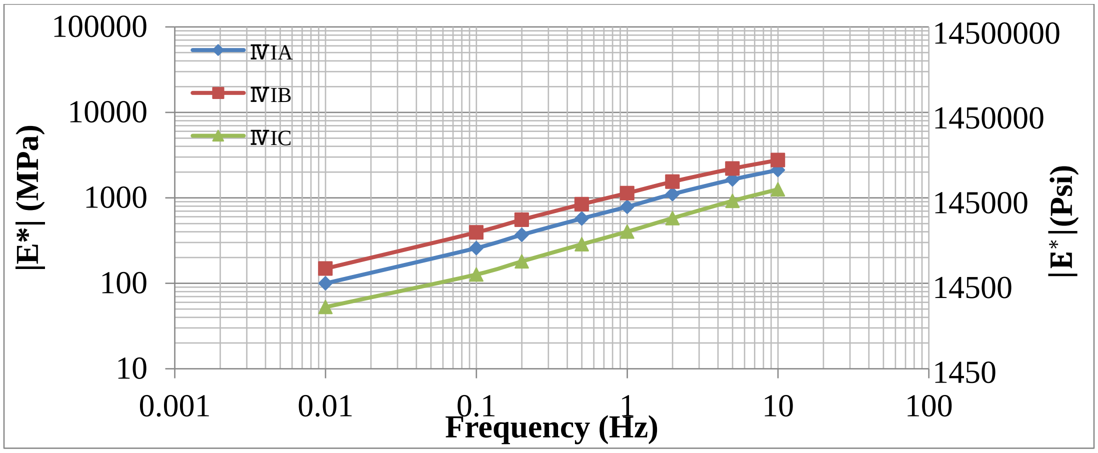

(c)

Figure 10-25 Dynamic Modulus Values of Various Mixtures from Aggregate IV with RAP in Terms of Intermediate Mixture Type, (a) at 4°C (39.2°F), (b) at 20°C (68°F), (c) at 40°C (104°F)

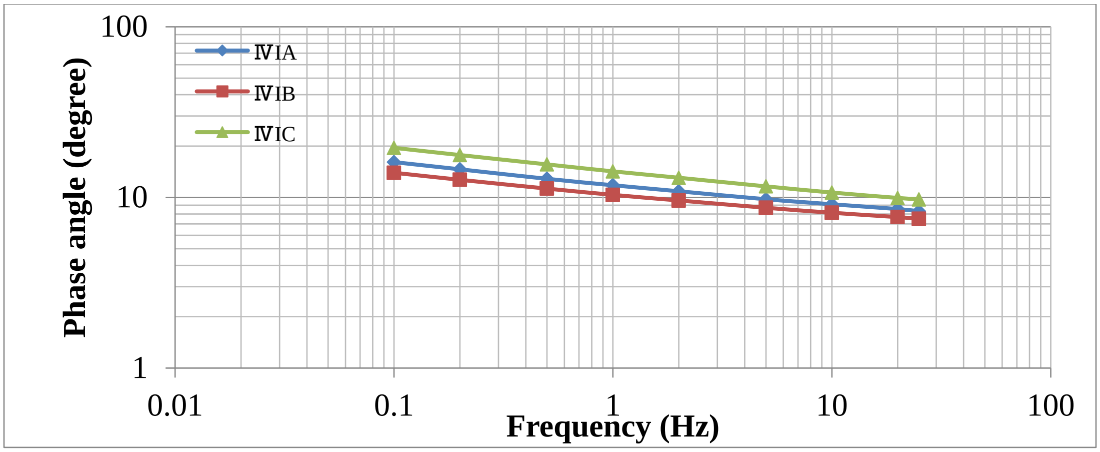

(a)

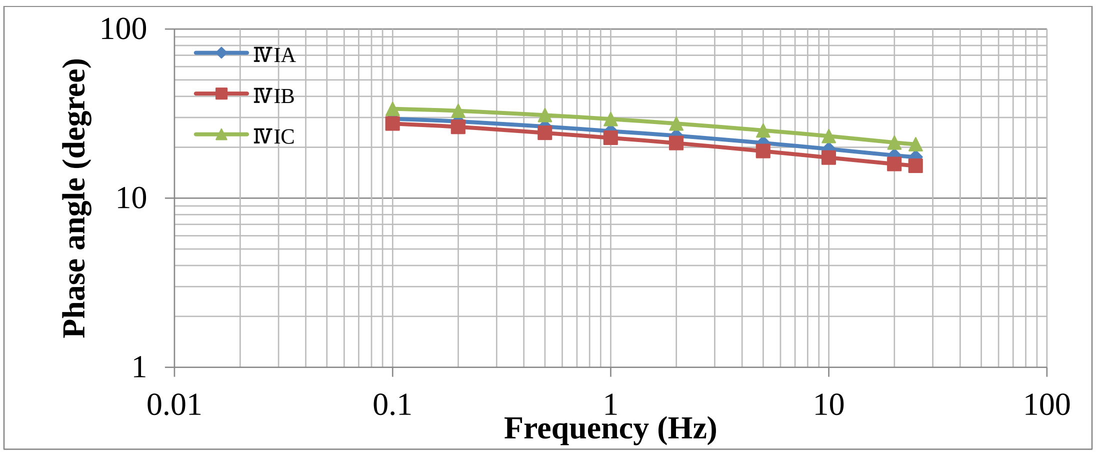

(b)

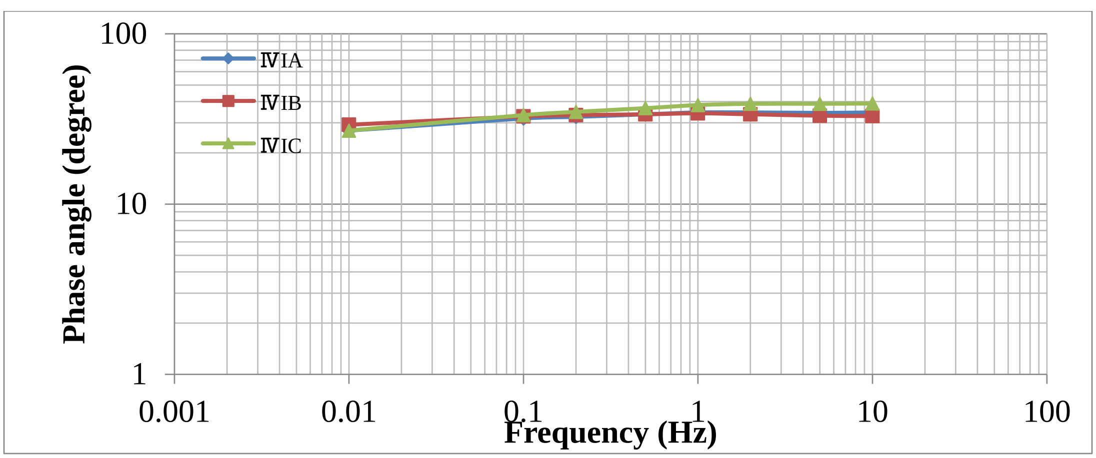

(c)

Figure 10-26 Phase Angle Values of Various Mixtures from Aggregate IV with RAP in Terms of Intermediate Mixture Type, (a) at 4°C (39.2°F), (b) at 20°C (68°F), (c) at 40°C (104°F)

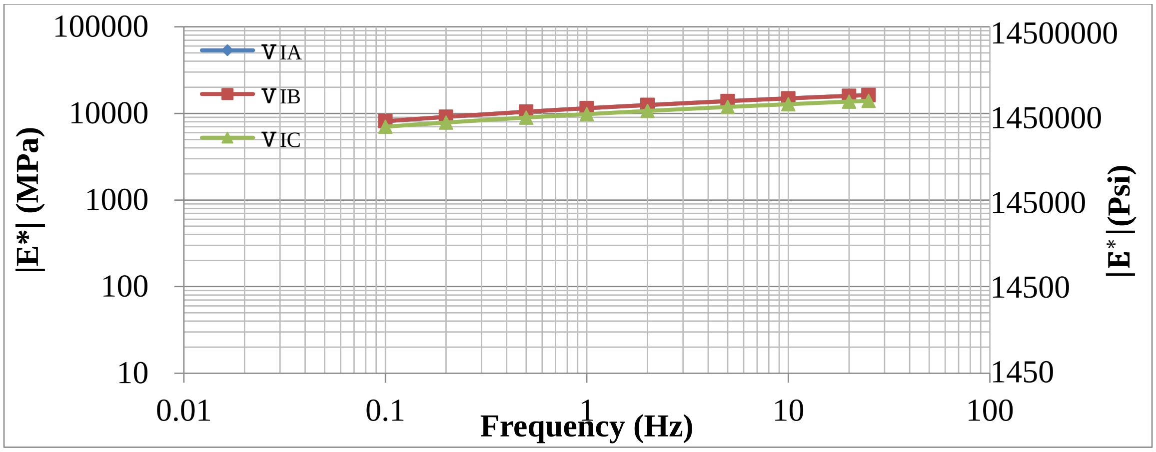

(a)

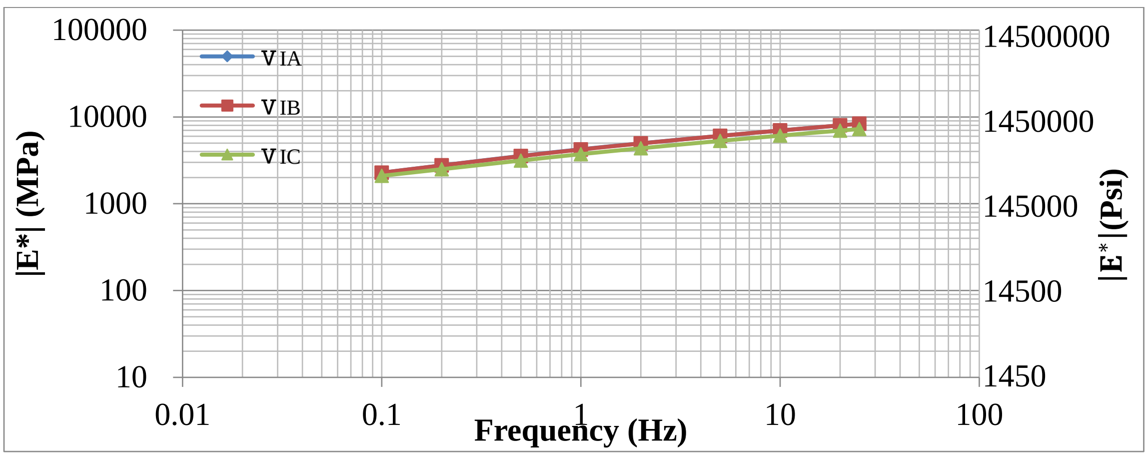

(b)

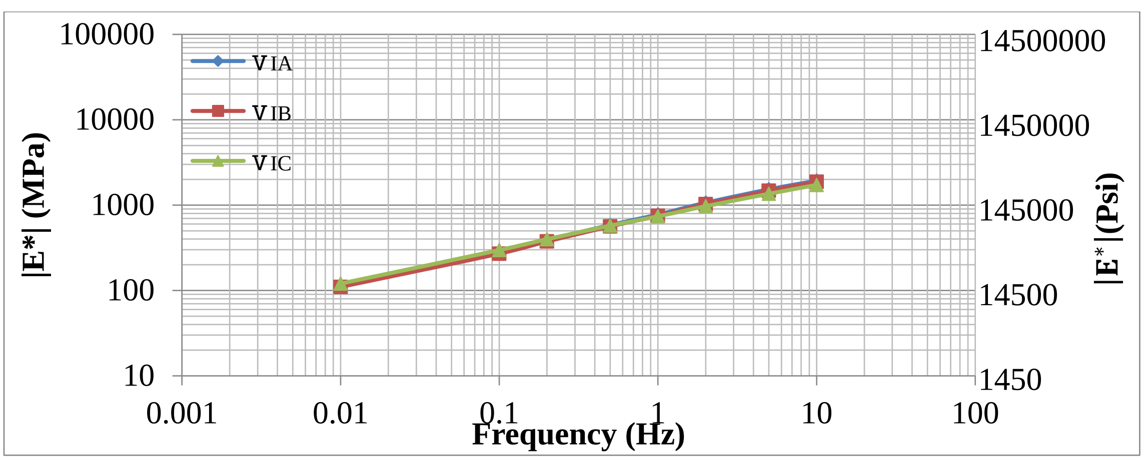

(c)

Figure 10-27 Dynamic Modulus Values of Various Mixtures from Aggregate V with RAP in Terms of Intermediate Mixture Type, (a) at 4°C (39.2°F), (b) at 20°C (68°F), (c) at 40°C (104°F)

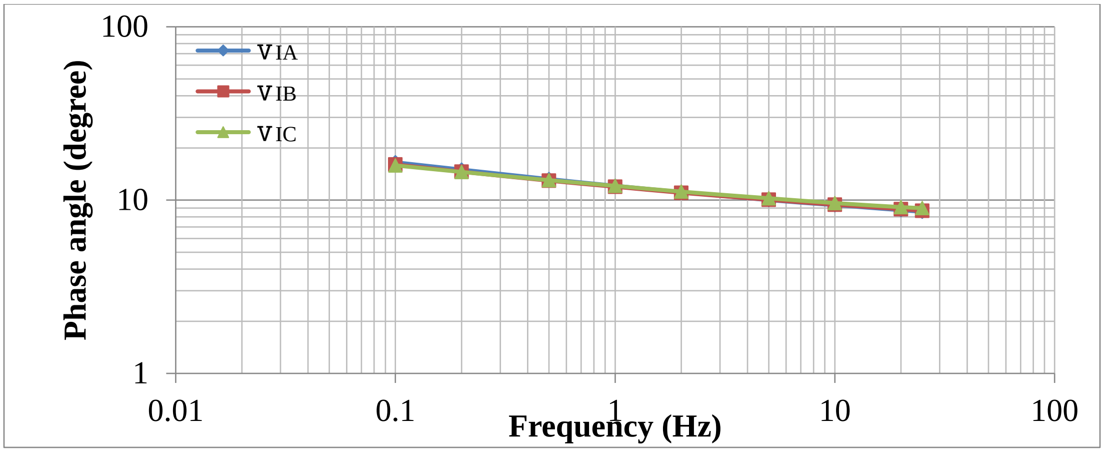

(a)

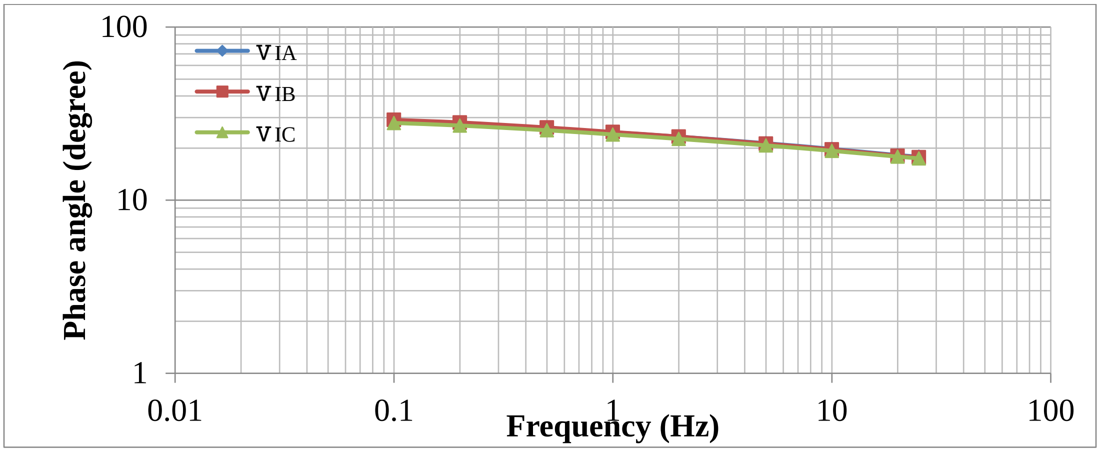

(b)

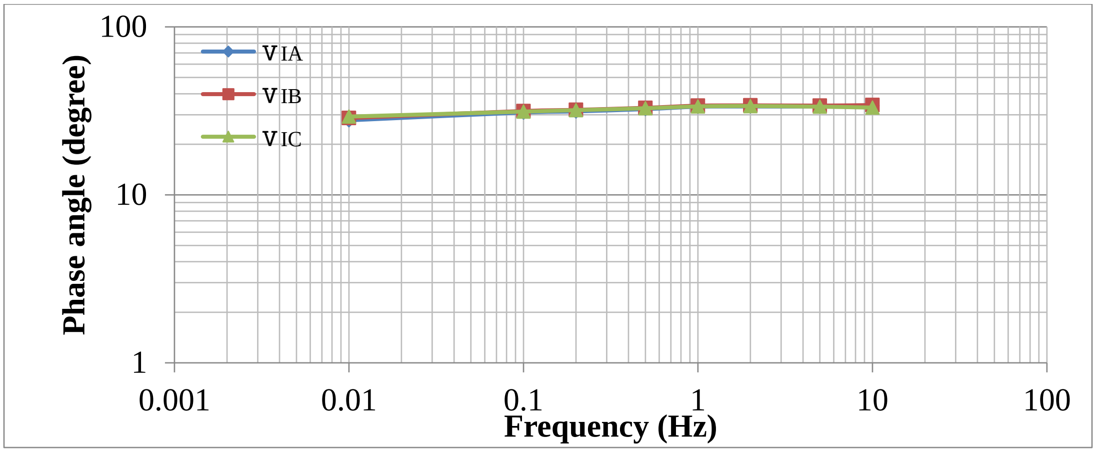

(c)

Figure 10-28 Phase Angle Values of Various Mixtures from Aggregate V with RAP in Terms of Intermediate Mixture Type, (a) at 4°C (39.2°F), (b) at 20°C (68°F), (c) at 40°C (104°F)

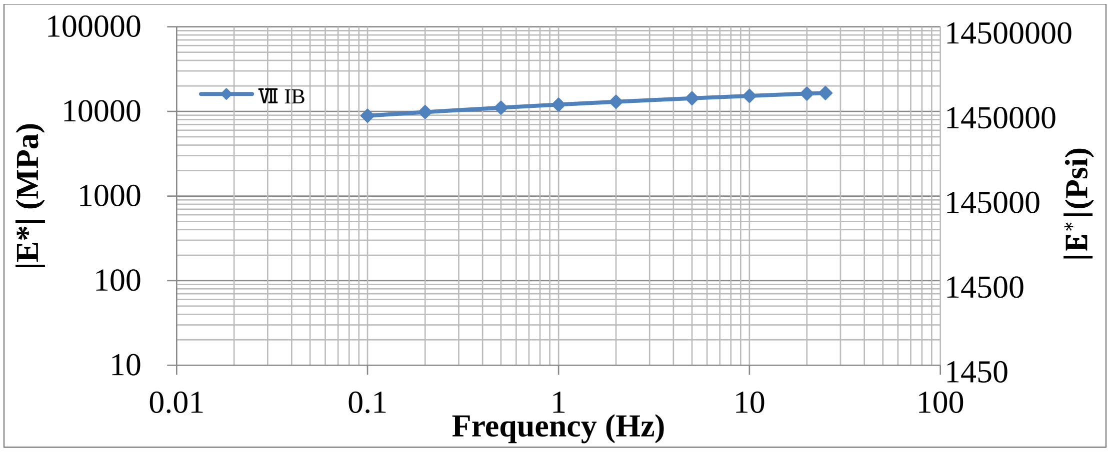

(a)

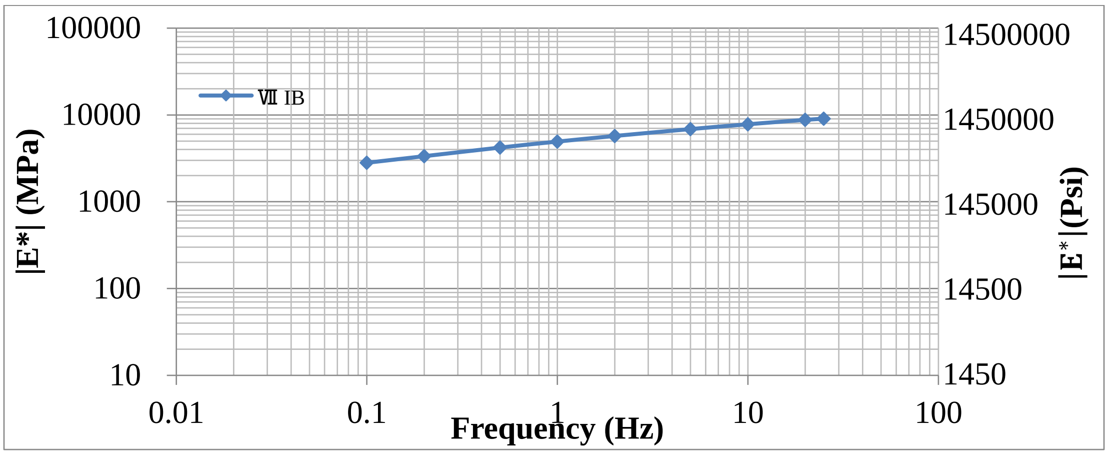

(b)

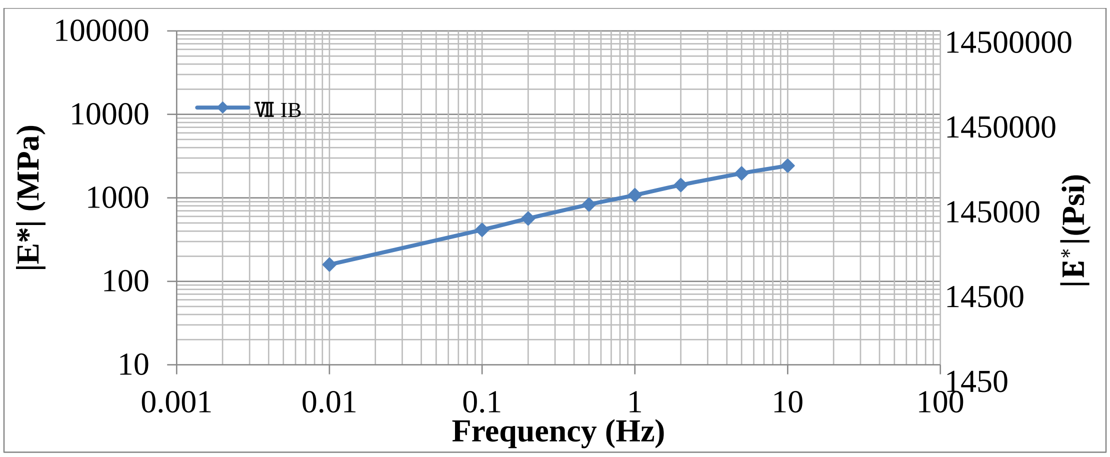

(c)

Figure 10-29 Dynamic Modulus Values of Various Mixtures from Aggregate VII with RAP in Terms of Intermediate Mixture Type, (a) at 4°C (39.2°F), (b) at 20°C (68°F), (c) at 40°C (104°F)

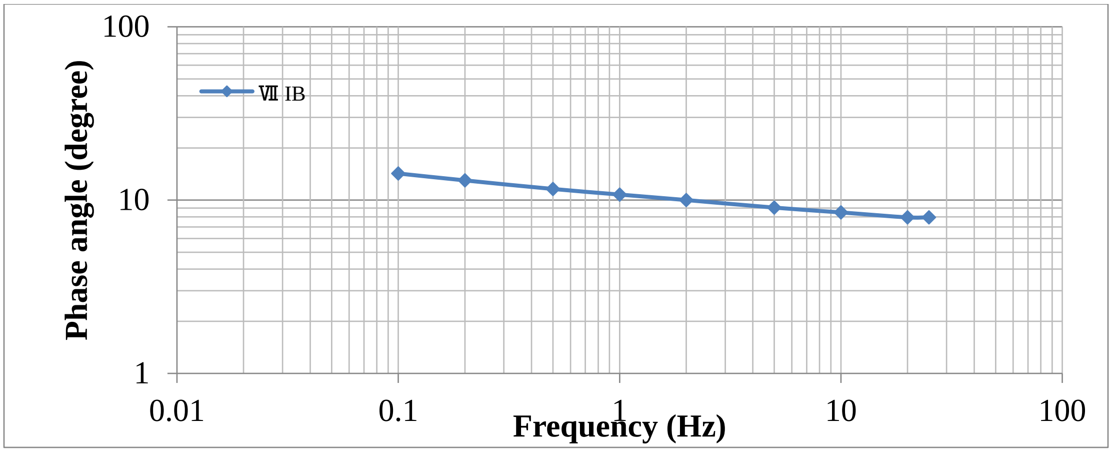

(a)

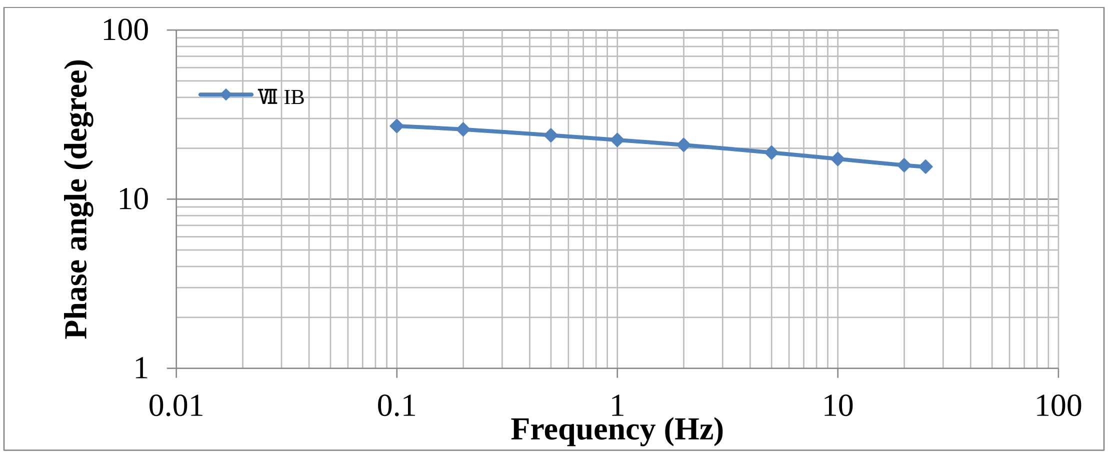

(b)

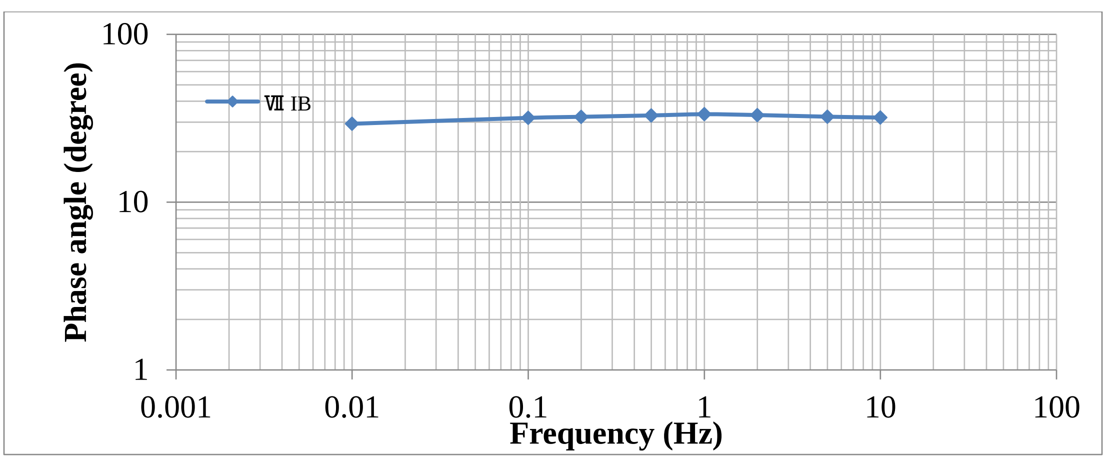

(c)

Figure 10-30 Phase Angle Values of Various Mixtures from Aggregate VII with RAP in Terms of Intermediate Mixture Type, (a) at 4°C (39.2°F), (b) at 20°C (68°F), (c) at 40°C (104°F)

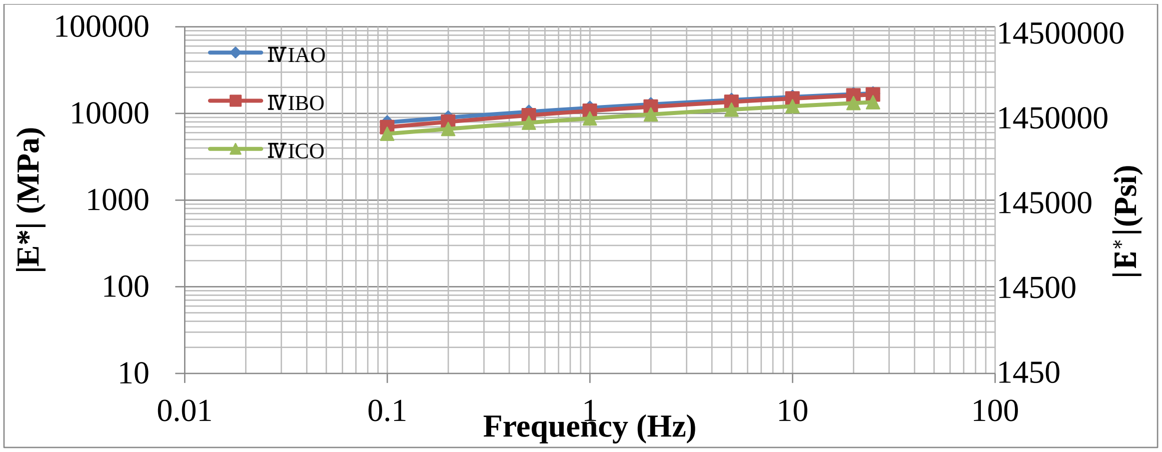

(a)

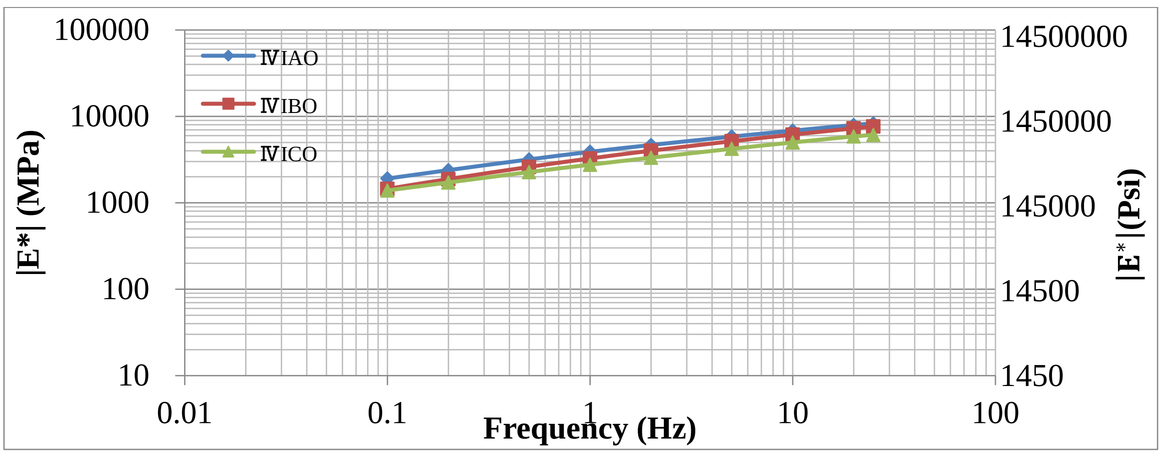

(b)

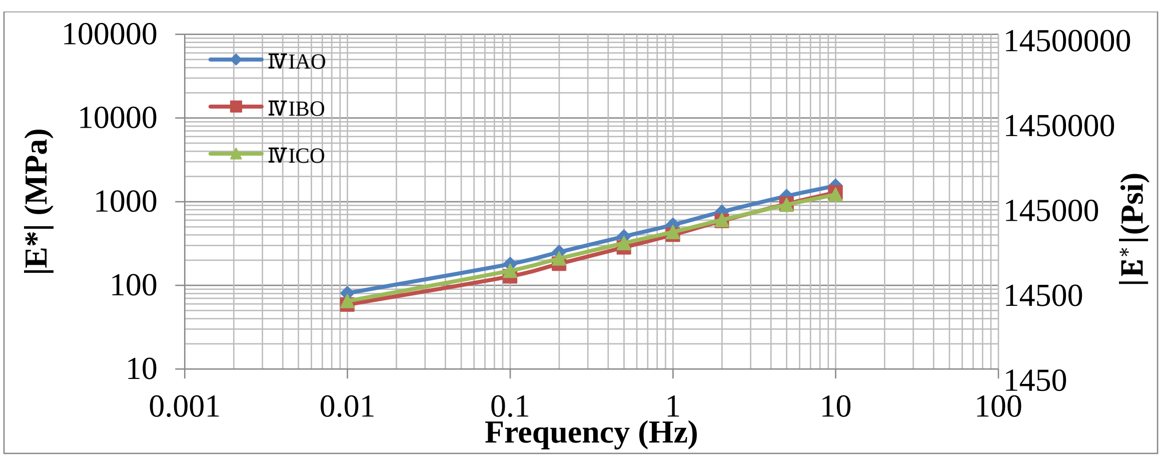

(c)

Figure 10-31 Dynamic Modulus Values of Various Mixtures from Aggregate IV without RAP in Terms of Intermediate Mixture Type, (a) at 4°C (39.2°F), (b) at 20°C (68°F), (c) at 40°C (104°F)

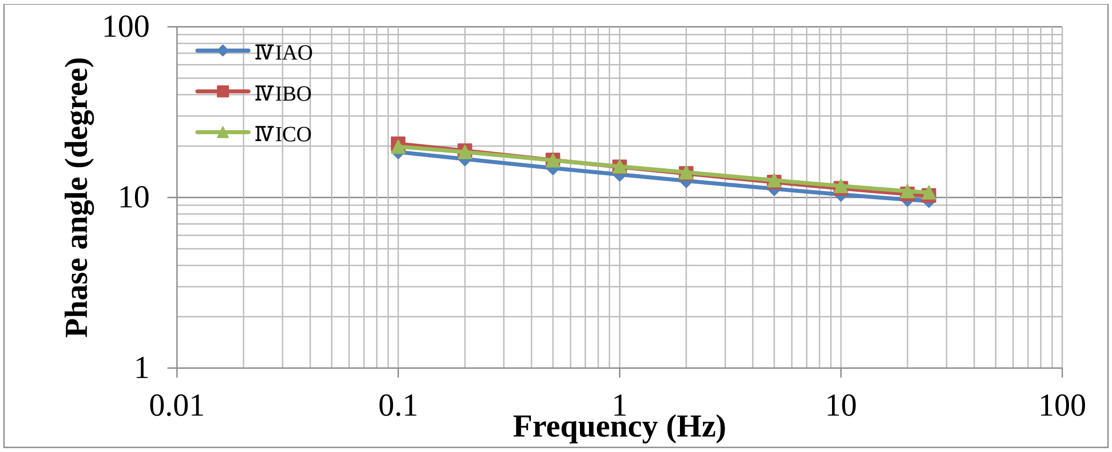

(a)

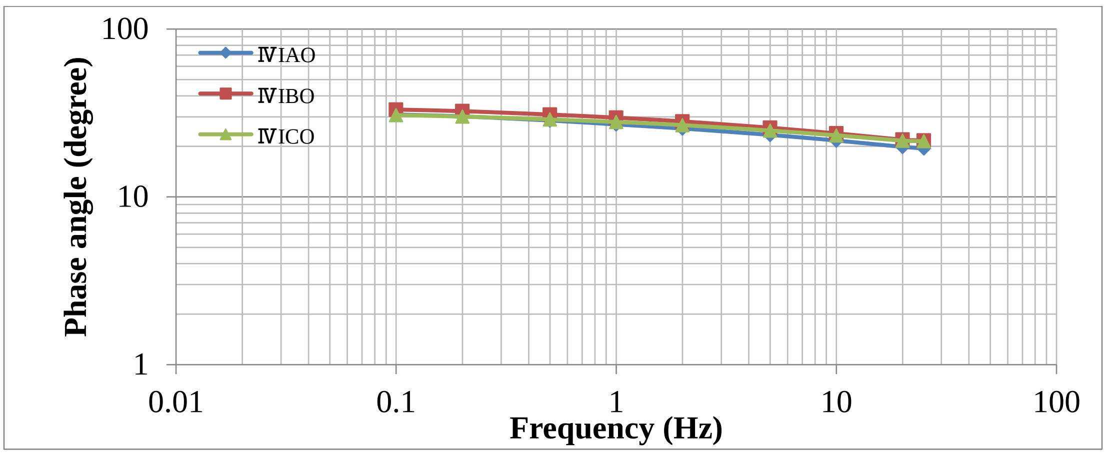

(b)

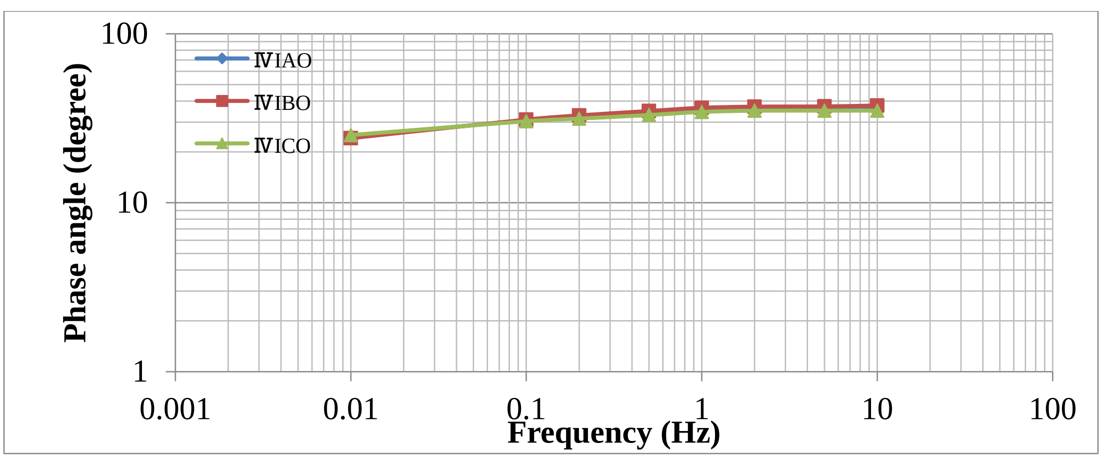

(c)

Figure 10-32 Phase Angle Values of Various Mixtures from Aggregate IV without RAP in Terms of Intermediate Mixture Type, (a) at 4°C (39.2°F), (b) at 20°C (68°F), (c) at 40°C (104°F)

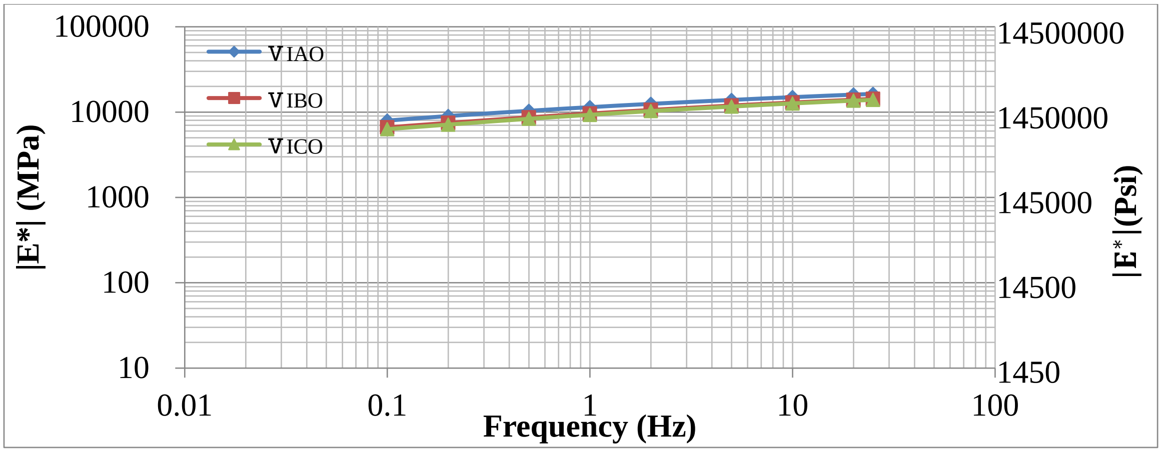

(a)

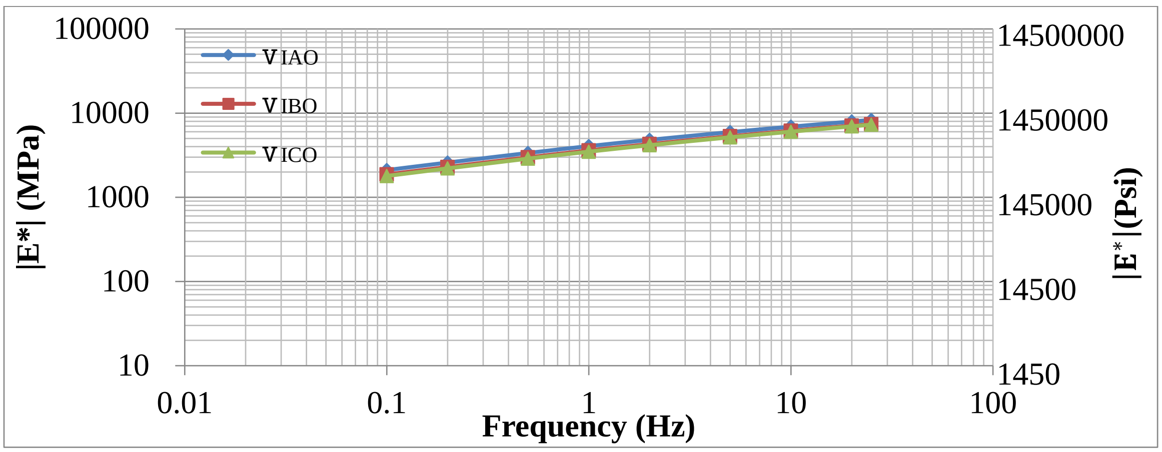

(b)

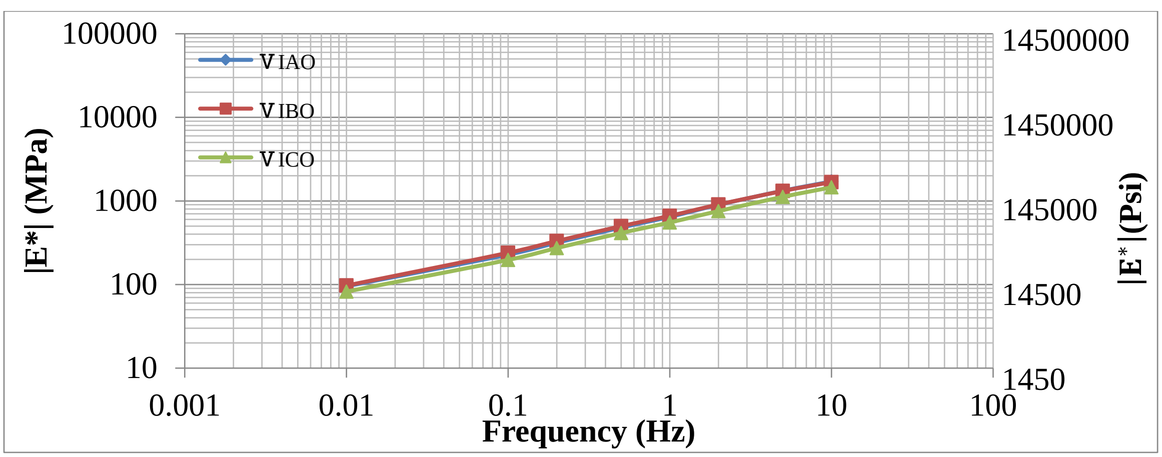

(c)

Figure 10-33 Dynamic Modulus Values of Various Mixtures from Aggregate V without RAP in Terms of Intermediate Mixture Type, (a) at 4°C (39.2°F), (b) at 20°C (68°F), (c) at 40°C (104°F)

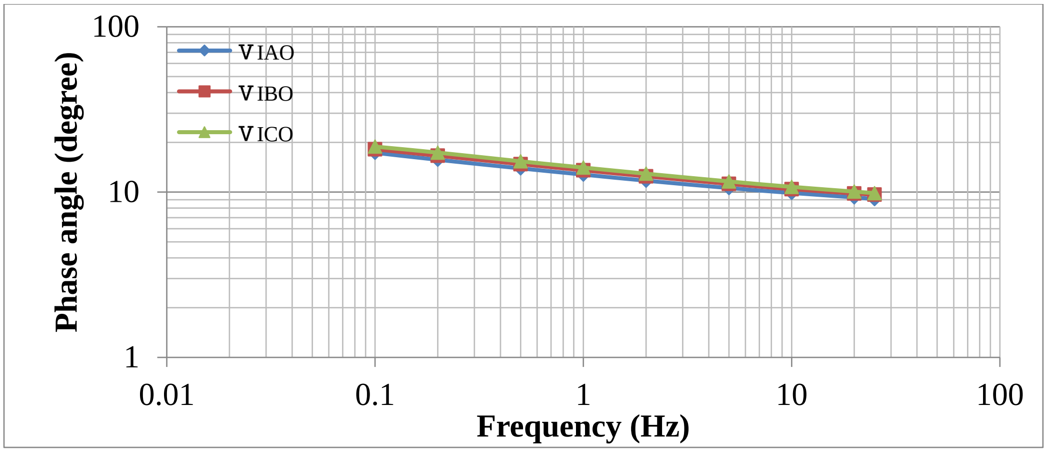

(a)

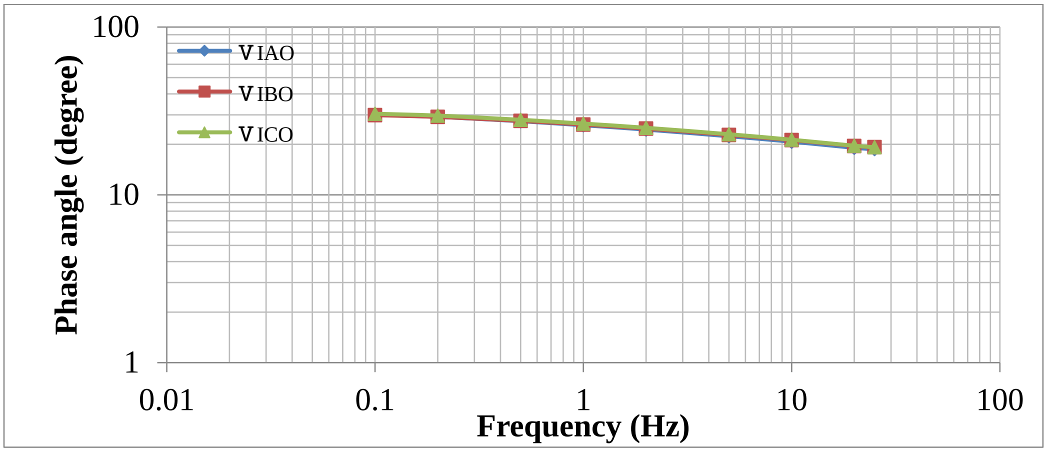

(b)

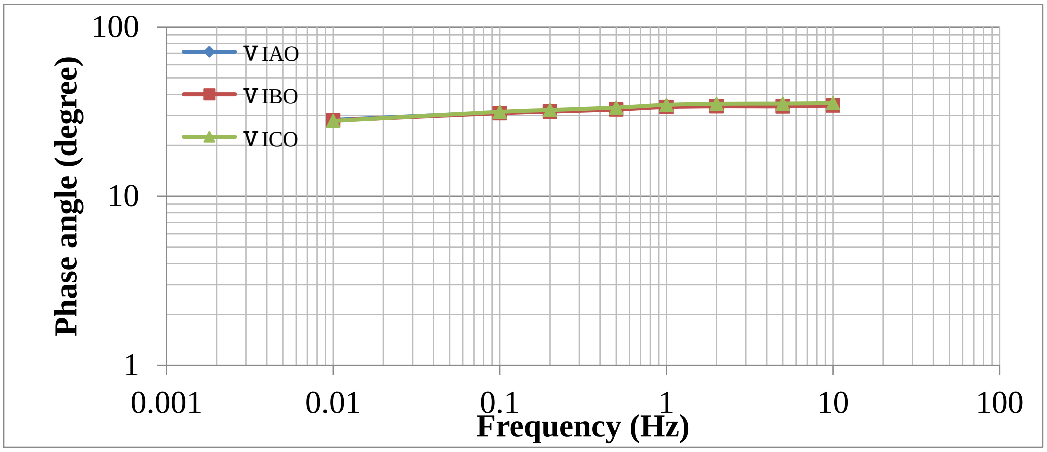

(c)

Figure 10-34 Phase Angle Values of Various Mixtures from Aggregate V without RAP in Terms of Intermediate Mixture Type, (a) at 4°C (39.2°F), (b) at 20°C (68°F), (c) at 40°C (104°F)

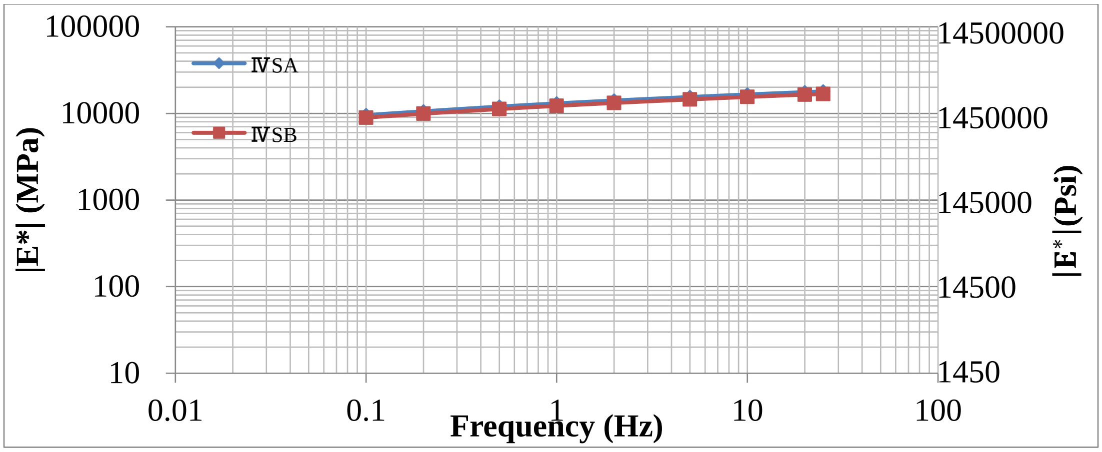

(a)

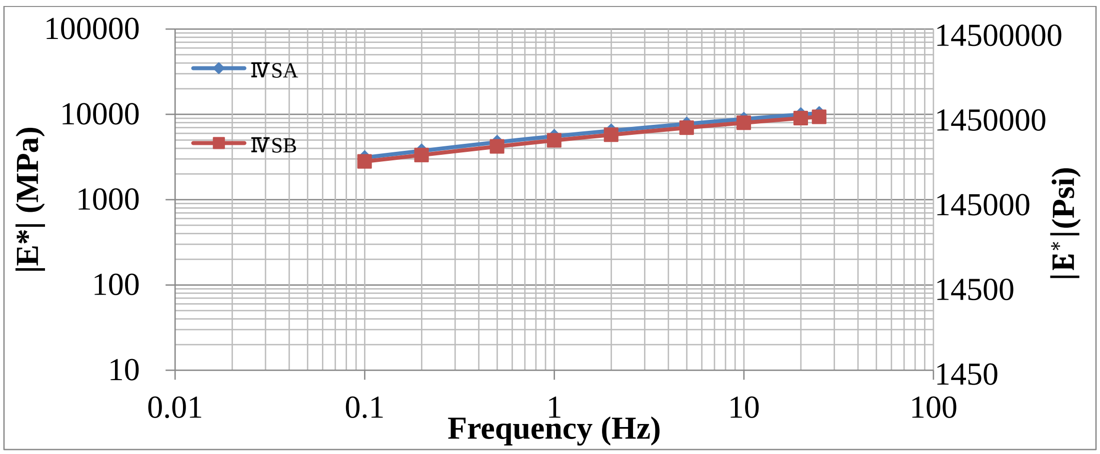

(b)

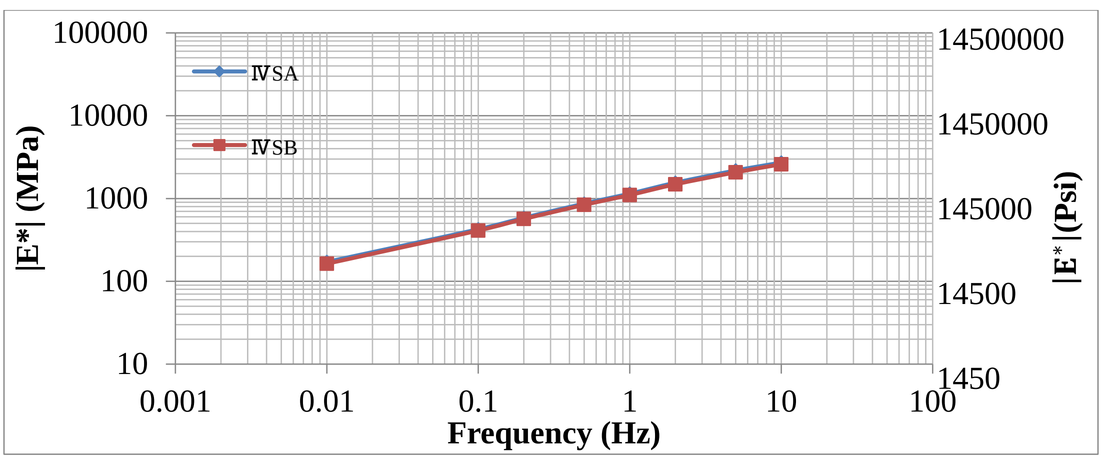

(c)

Figure 10-35 Dynamic Modulus Values of Various Mixtures from Aggregate IV with RAP in Terms of Base Mixture Type, (a) at 4°C (39.2°F), (b) at 20°C (68°F), (c) at 40°C (104°F)

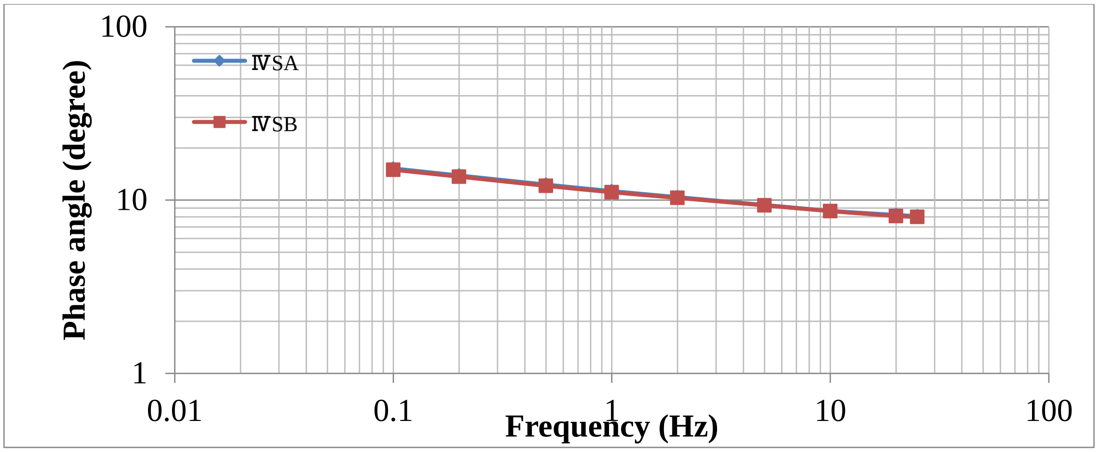

(a)

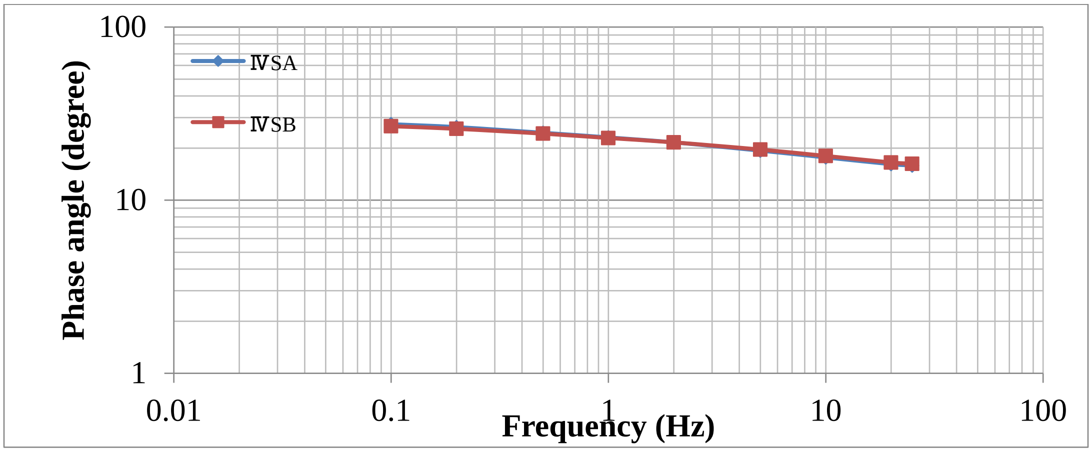

(b)

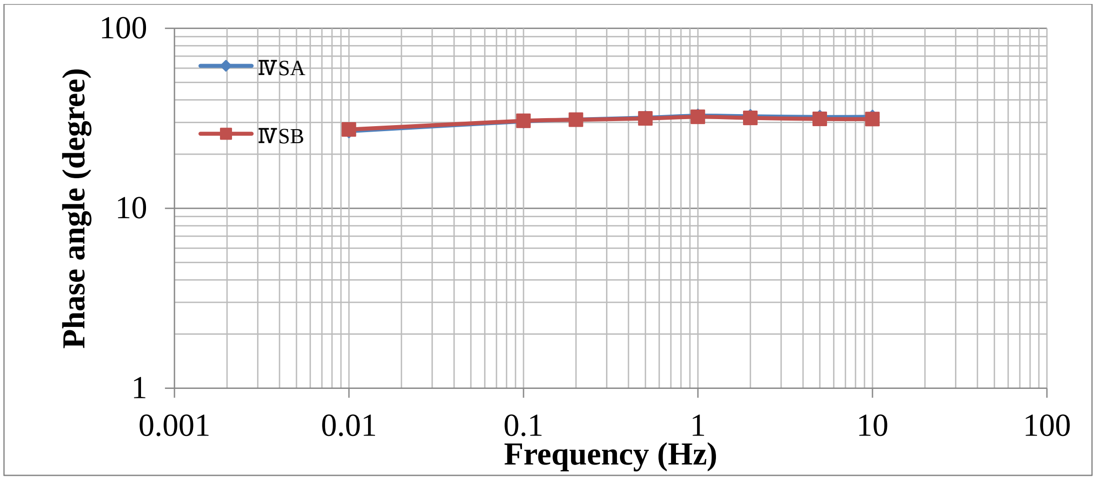

(c)

Figure 10-36 Phase Angle Values of Various Mixtures from Aggregate IV with RAP in Terms of Base Mixture Type, (a) at 4°C (39.2°F), (b) at 20°C (68°F), (c) at 40°C (104°F)

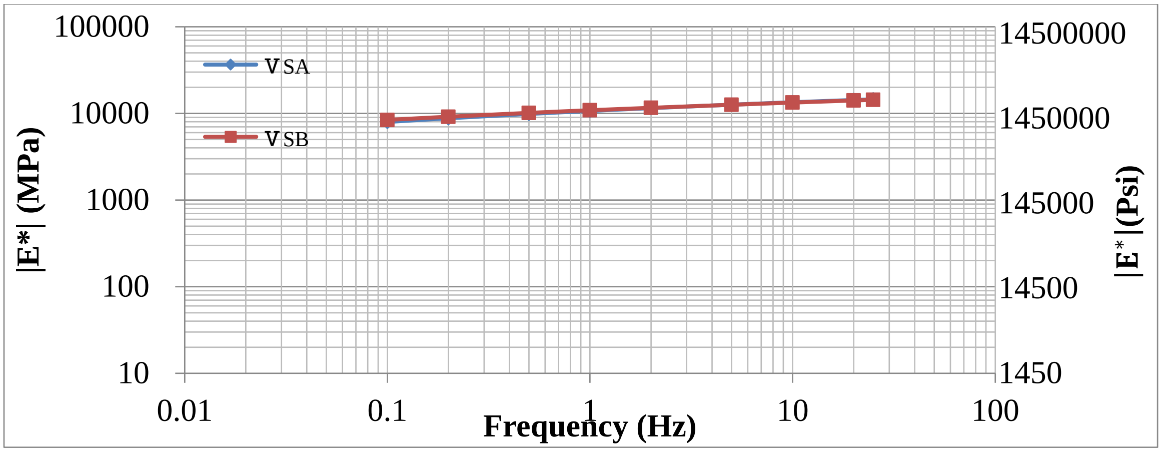

(a)

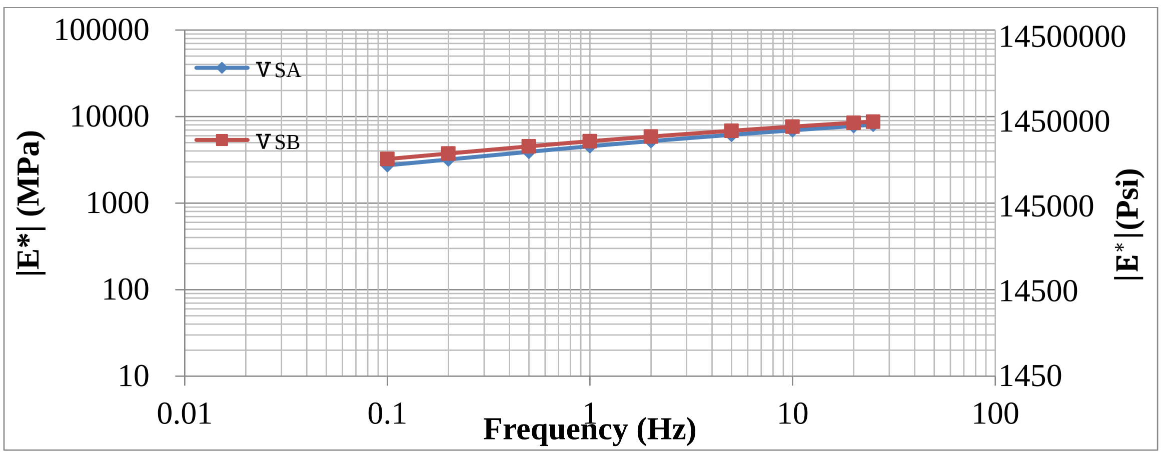

(b)

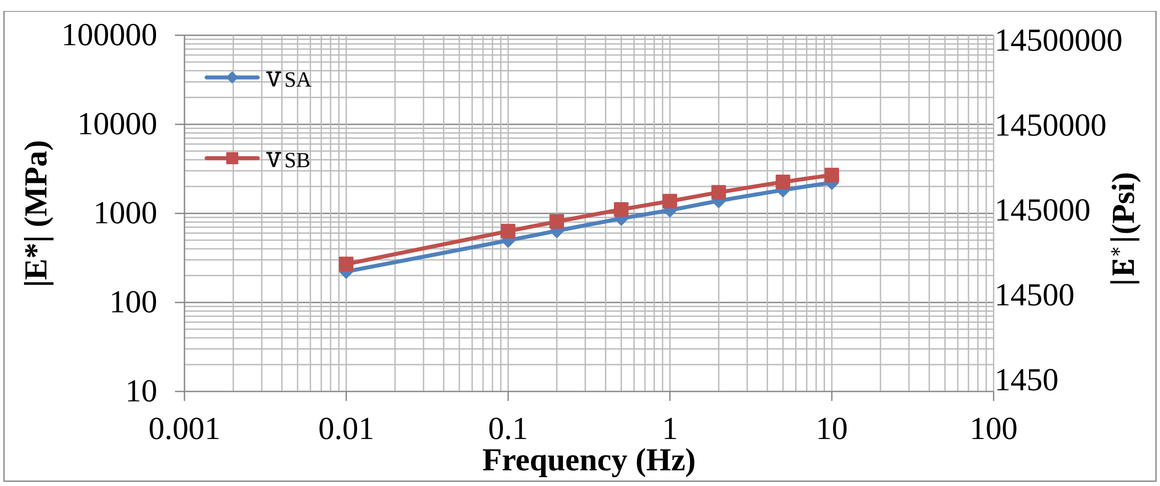

(c)

Figure 10-37 Dynamic Modulus Values of Various Mixtures from Aggregate V with RAP in Terms of Base Mixture Type, (a) at 4°C (39.2°F), (b) at 20°C (68°F), (c) at 40°C (104°F)

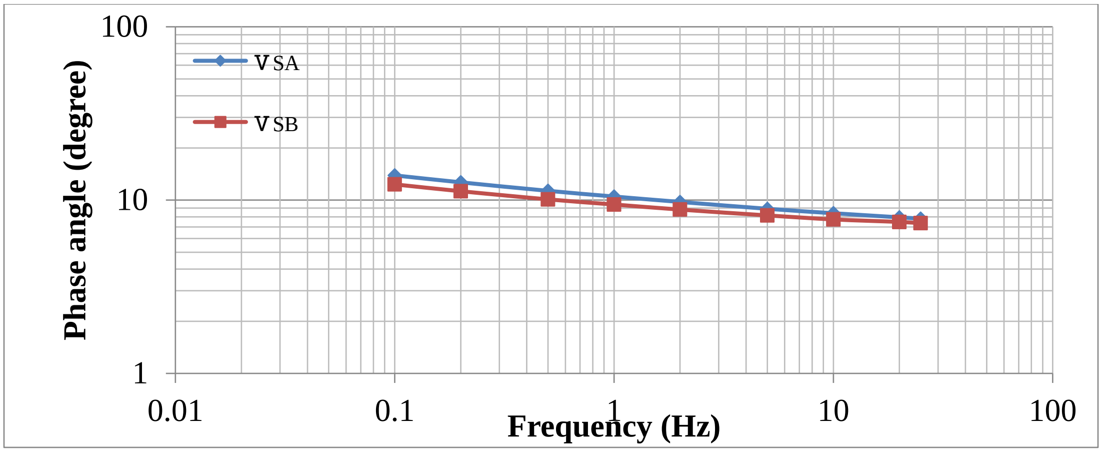

(a)

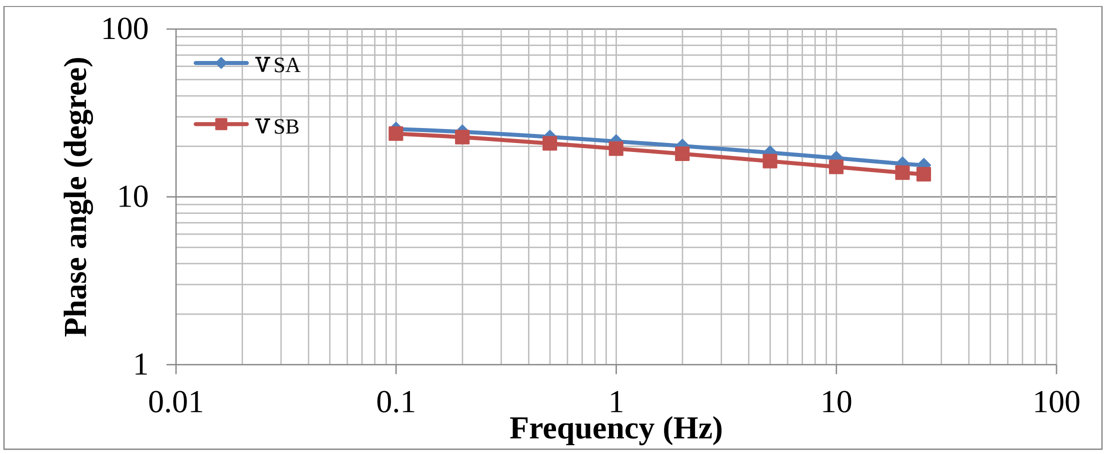

(b)

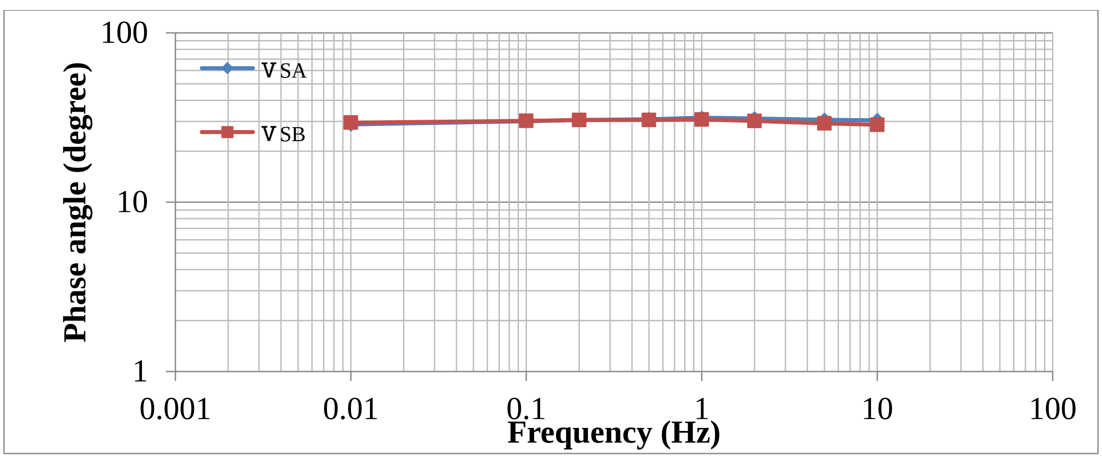

(c)

Figure 10-38 Phase Angle Values of Various Mixtures from Aggregate V with RAP in Terms of Base Mixture Type, (a) at 4°C (39.2°F), (b) at 20°C (68°F), (c) at 40°C (104°F)

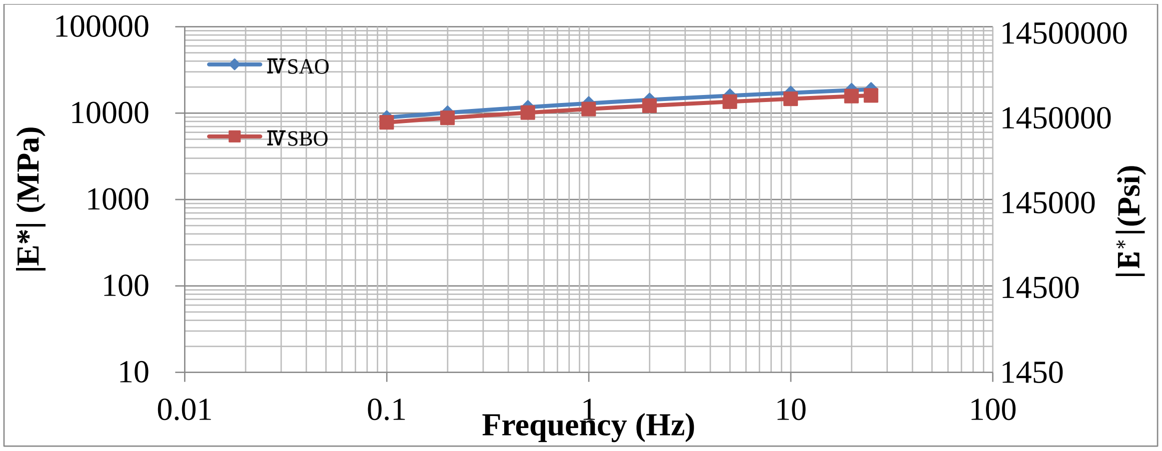

(a)

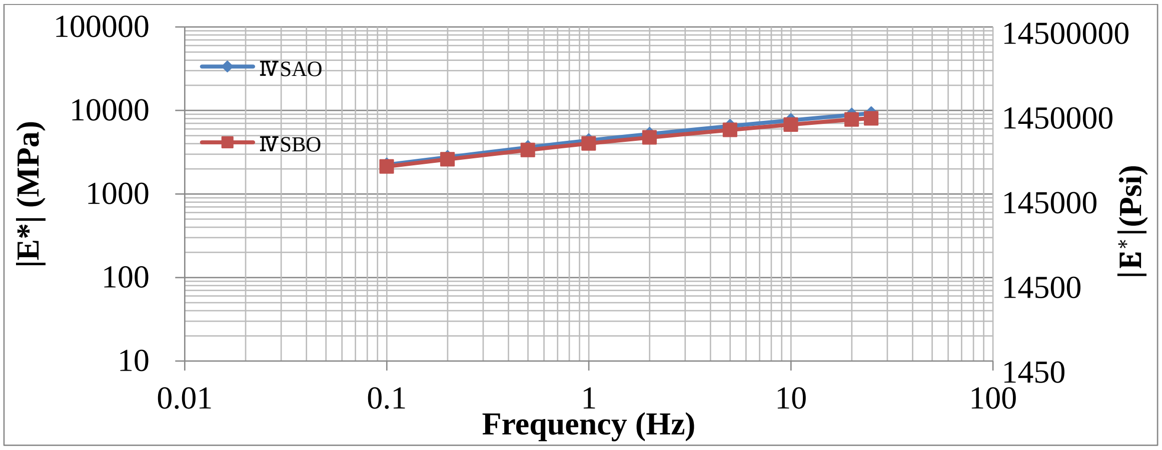

(b)

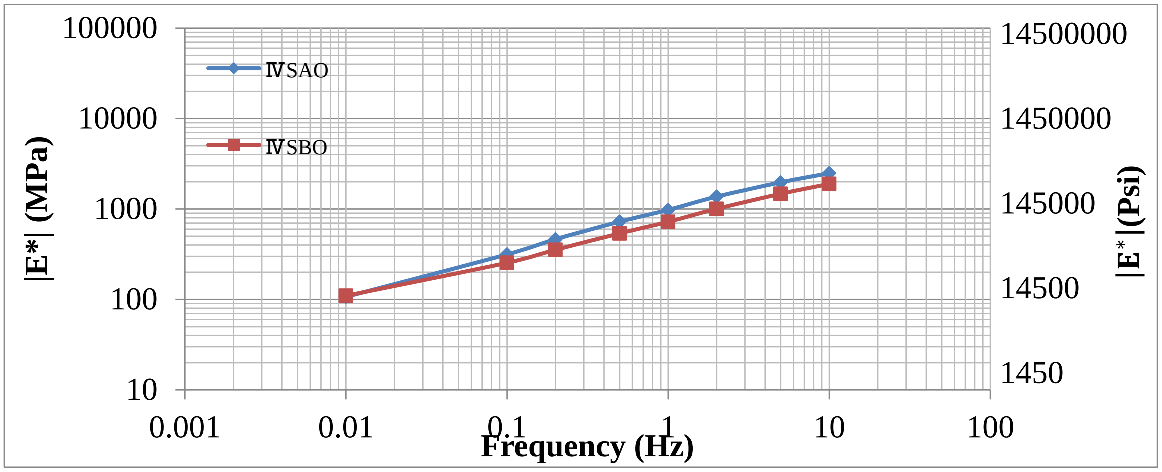

(c)

Figure 10-39 Dynamic Modulus Values of Various Mixtures from Aggregate IV without RAP in Terms of Base Mixture Type, (a) at 4°C (39.2°F), (b) at 20°C (68°F), (c) at 40°C (104°F)

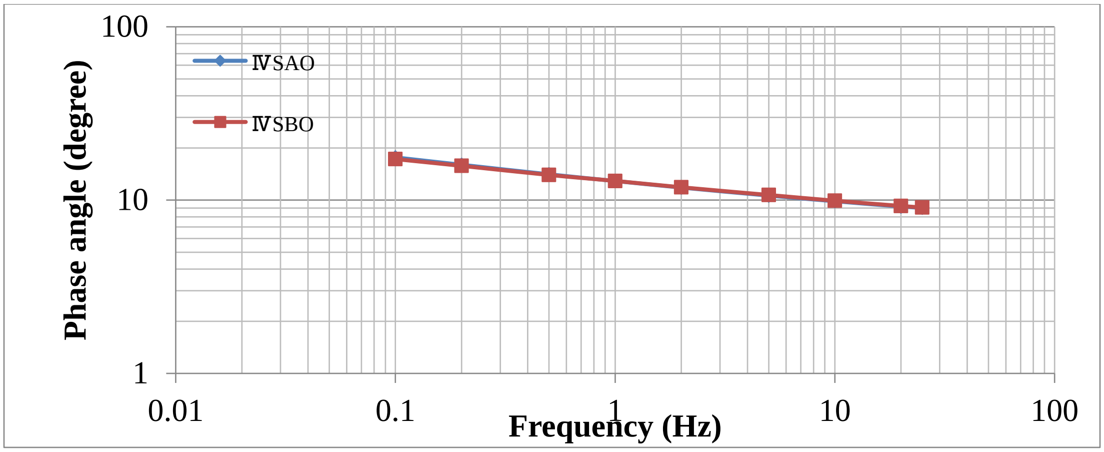

(a)

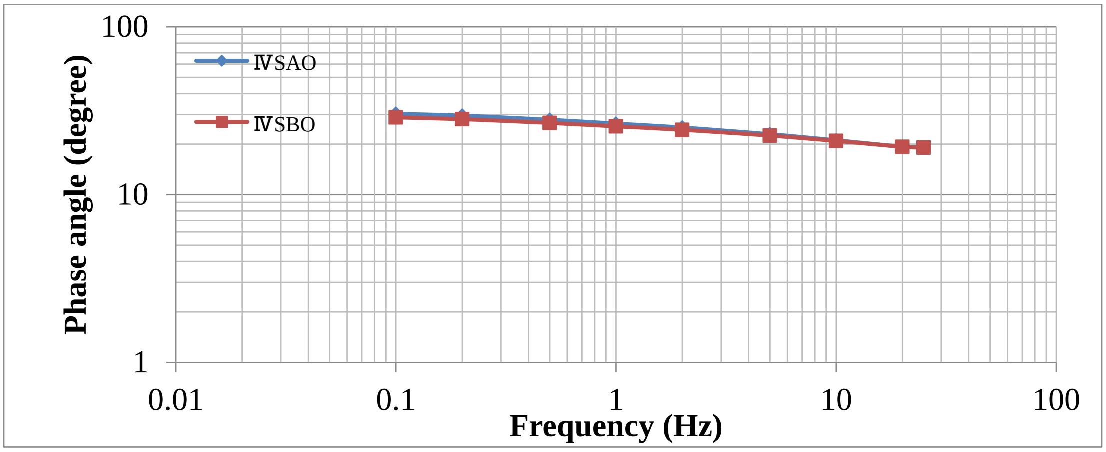

(b)

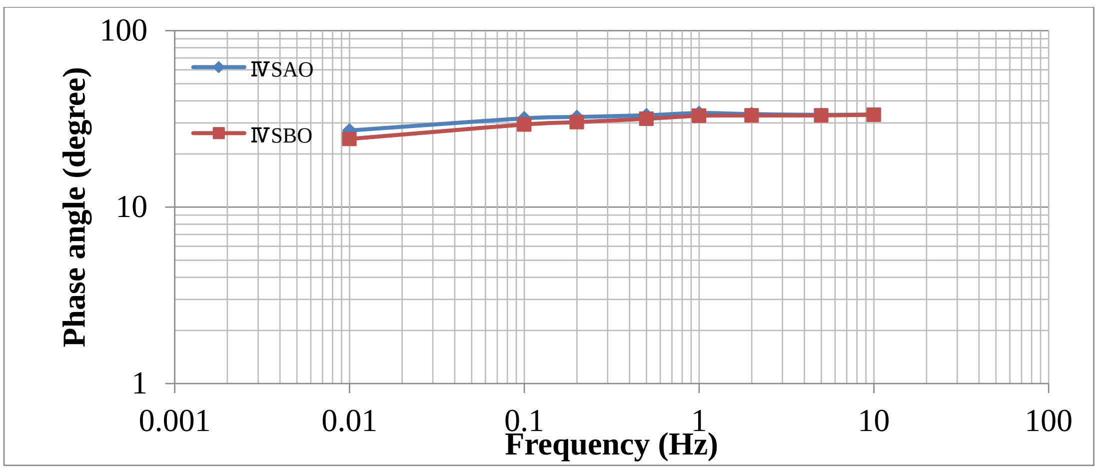

(c)

Figure 10-40 Phase Angle Values of Various Mixtures from Aggregate IV without RAP in Terms of Base Mixture Type, (a) at 4°C (39.2°F), (b) at 20°C (68°F), (c) at 40°C (104°F)

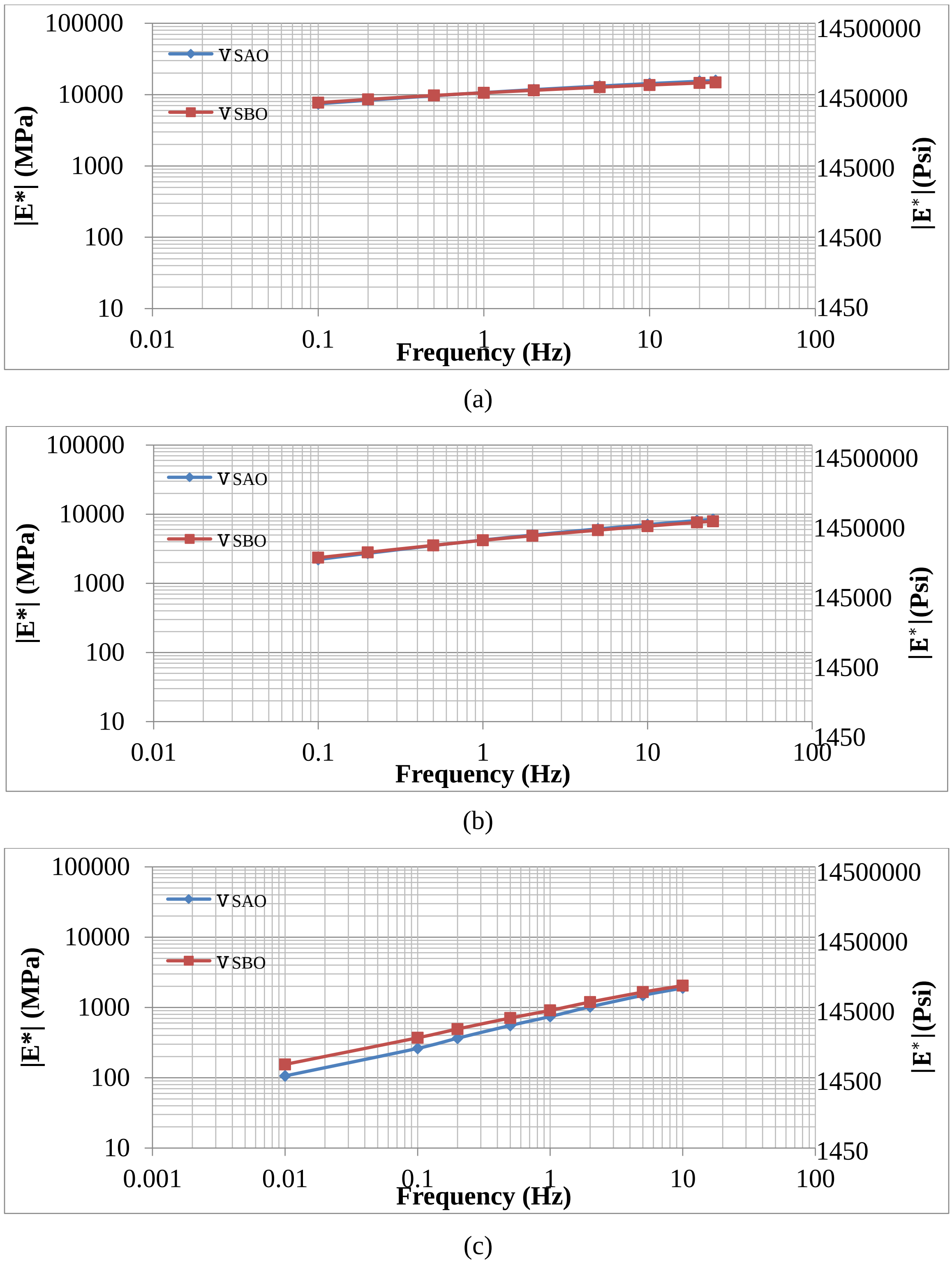

Figure 10-41 Dynamic Modulus Values of Various Mixtures from Aggregate V without RAP in Terms of Base Mixture Type, (a) at 4°C (39.2°F), (b) at 20°C (68°F), (c) at 40°C (104°F)

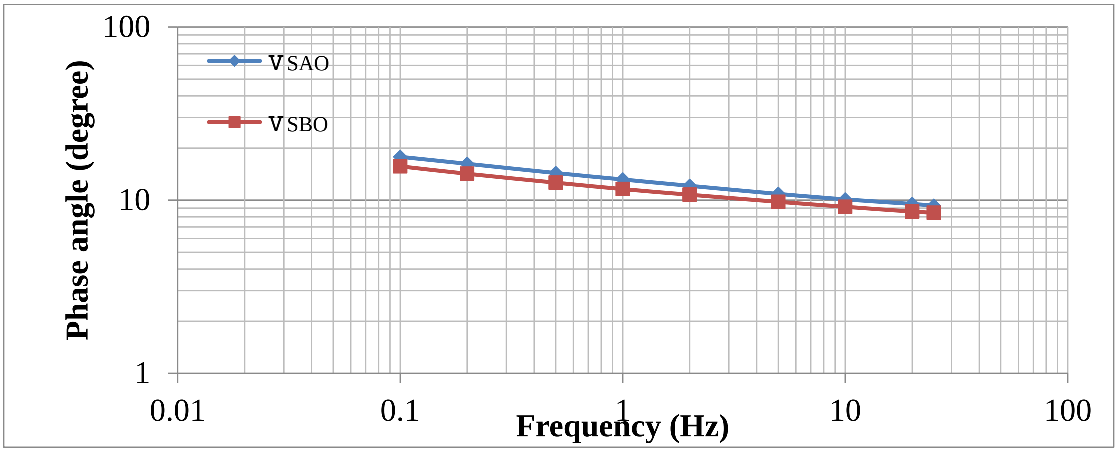

(a)

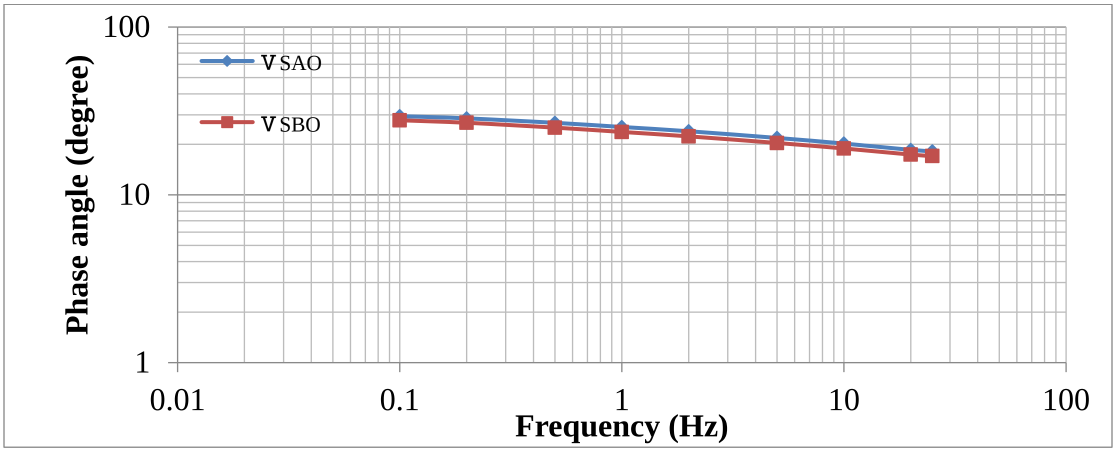

(b)

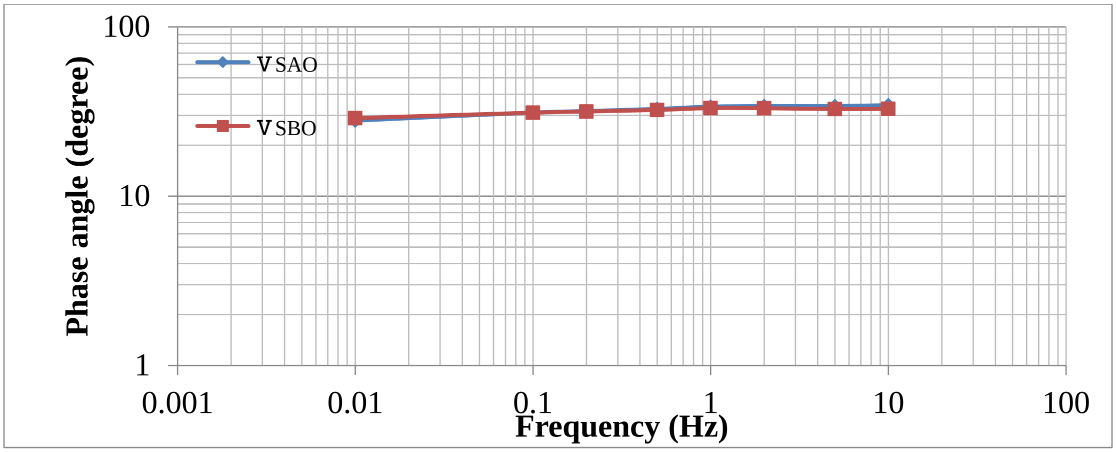

(c)

Figure 10-42 Phase Angle Values of Various Mixtures from Aggregate V without RAP in Terms of Base Mixture Type, (a) at 4°C (39.2°F), (b) at 20°C (68°F), (c) at 40°C (104°F)

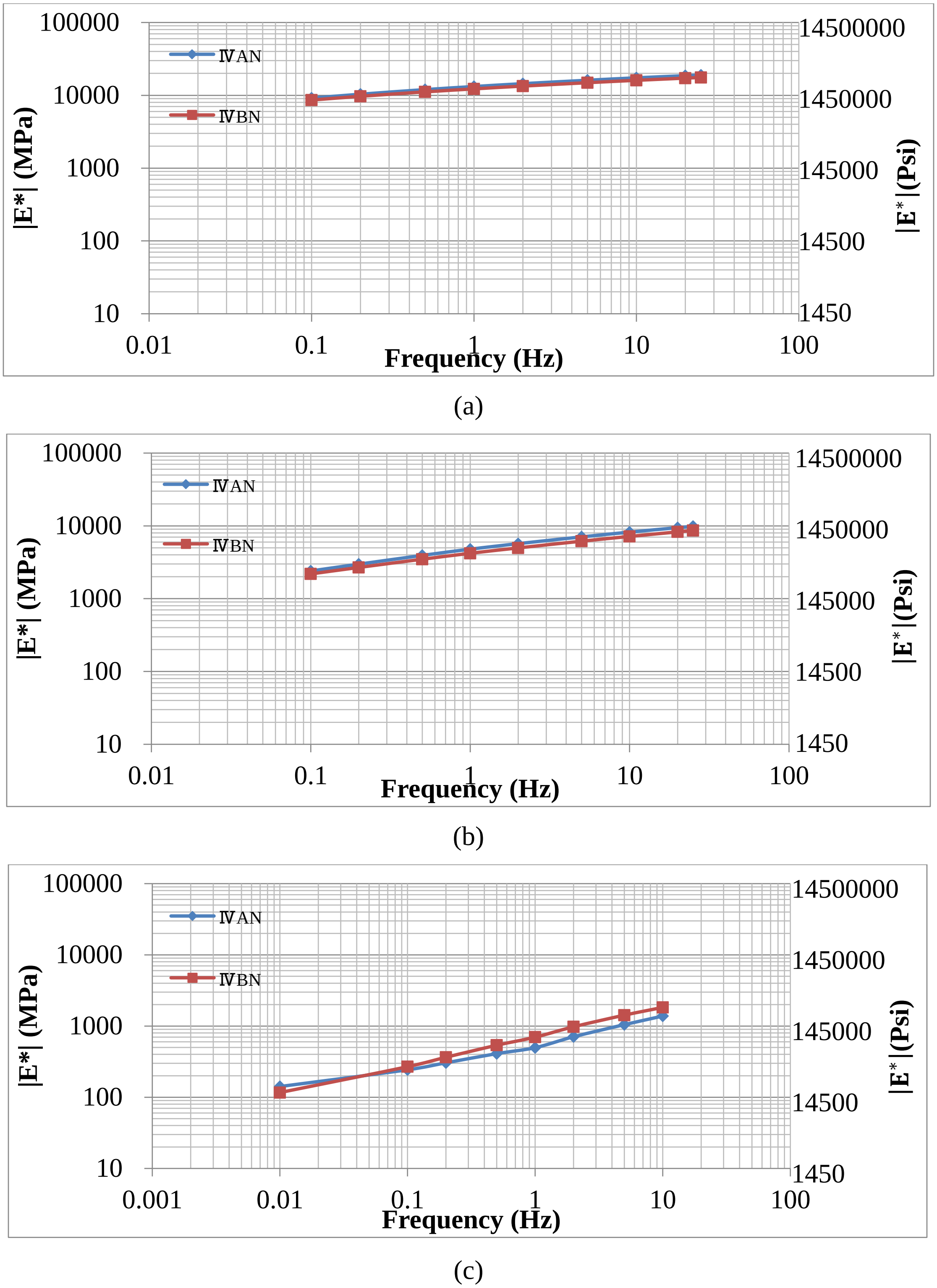

Figure 10-43 Dynamic Modulus Values of Various Mixtures from Aggregate IV with RAP and Asphalt Source 2 in Terms of Surface Mixture Type, (a) at 4°C (39.2°F), (b) at 20°C (68°F), (c) at 45°C (113°F) (Surface A), 40C (104°F) (Surface B)

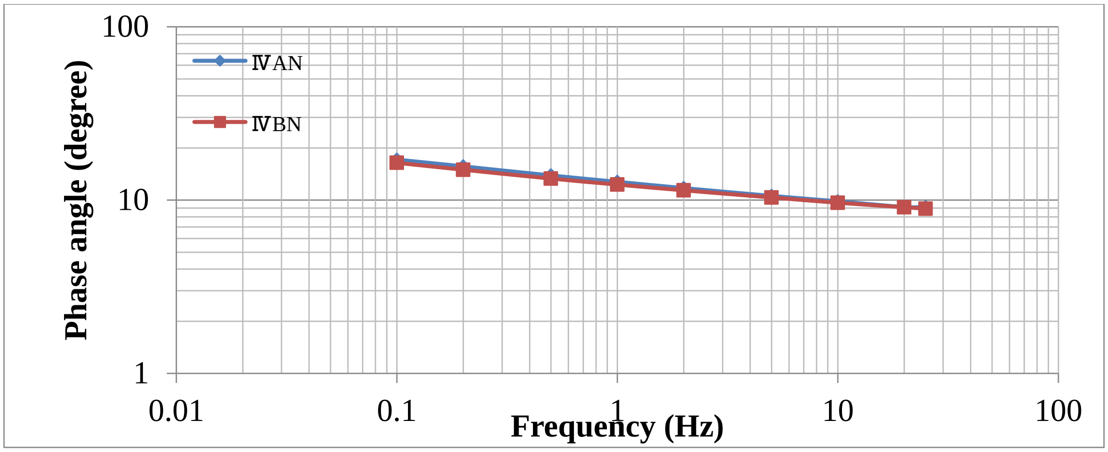

(a)

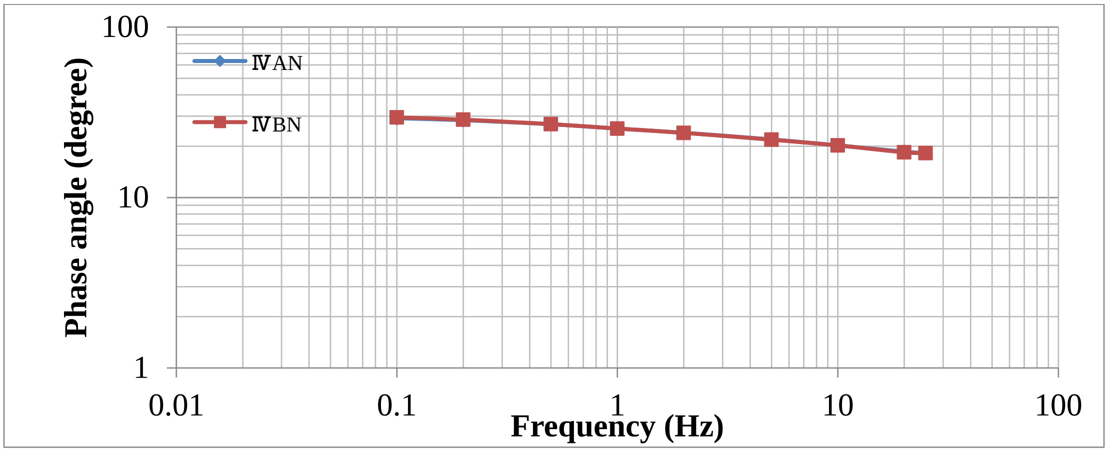

(b)

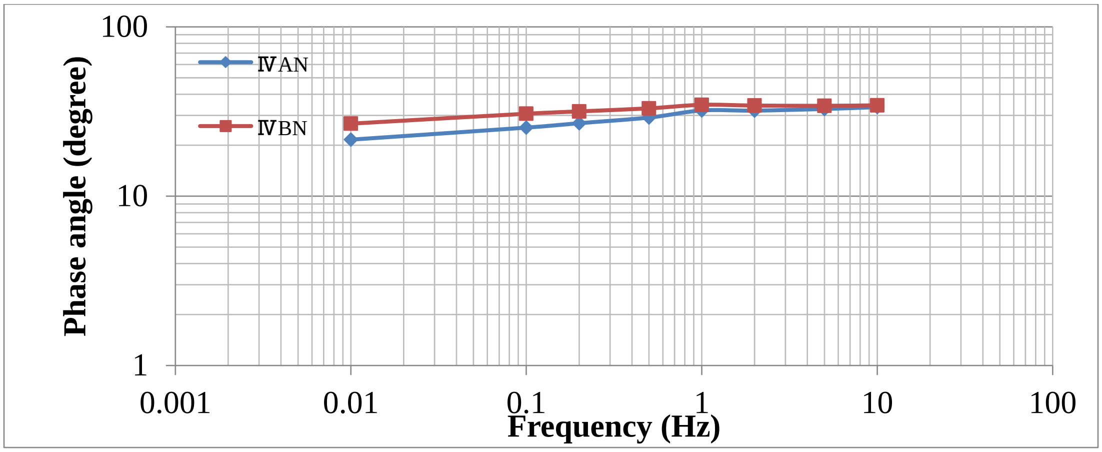

(c)

Figure 10-44 Phase Angle Values of Various Mixtures from Aggregate IV with RAP and Asphalt Source 2 in Terms of Surface Mixture Type, (a) at 4°C (39.2°F), (b) at 20°C (68°F), (c) at 45°C (113°F) (Surface A), 40°C (104°F) (Surface B)

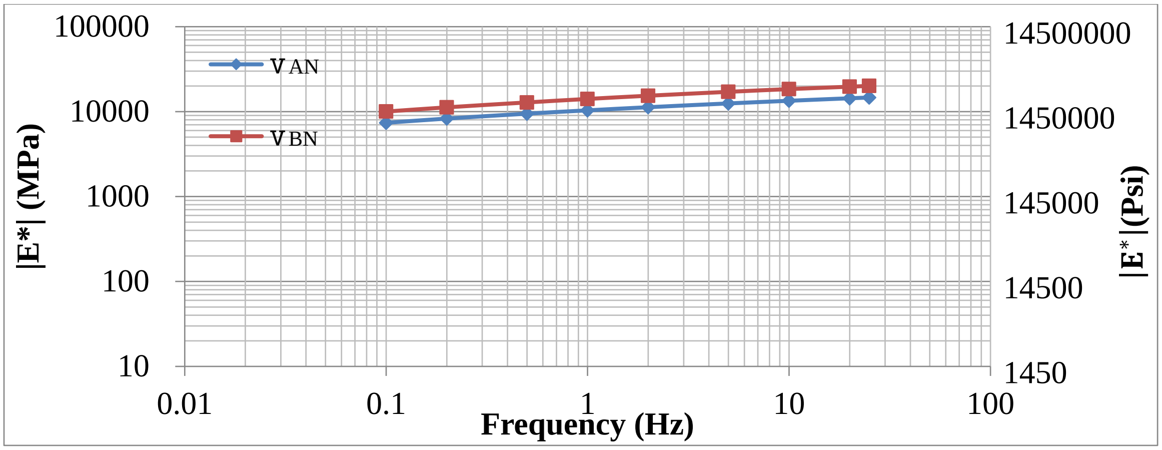

(a)

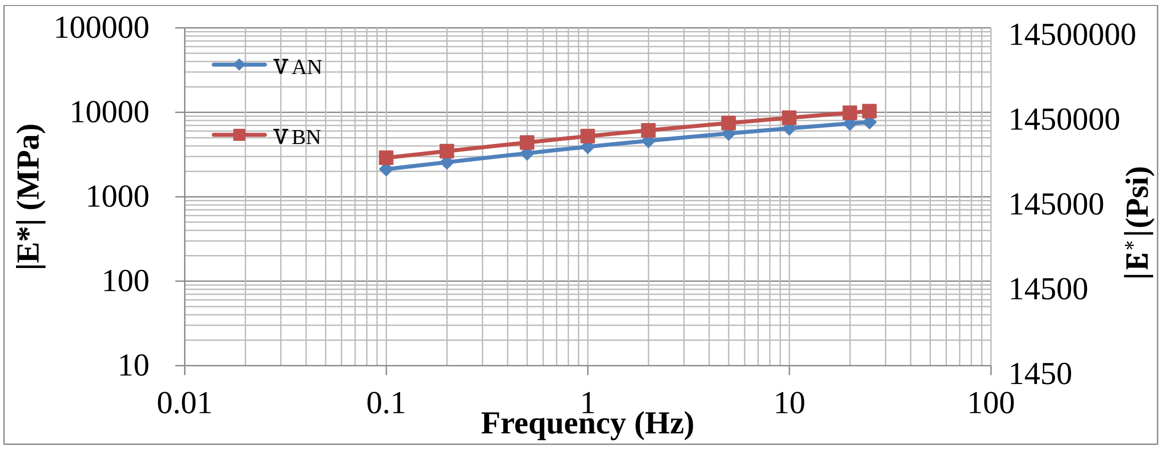

(b)

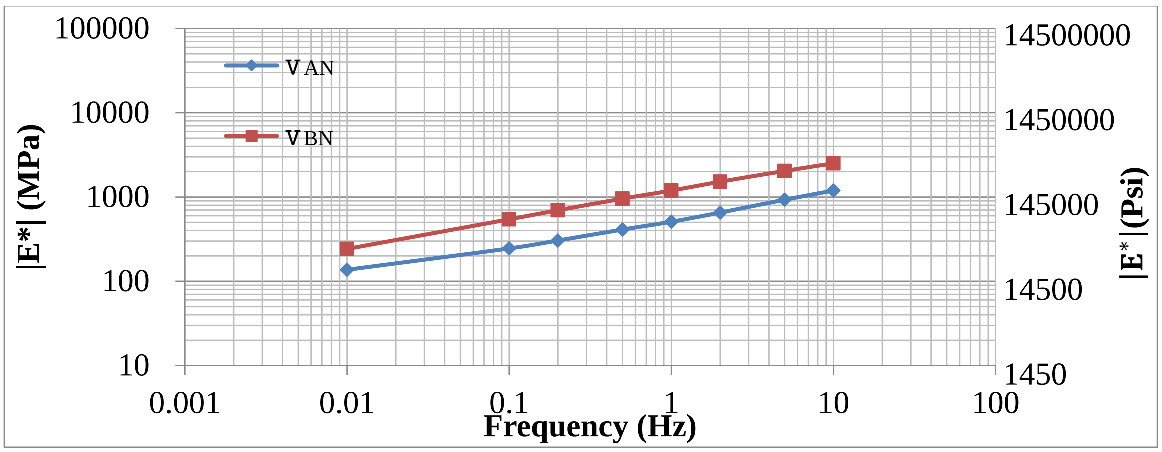

(c)

Figure 10-45 Dynamic Modulus Values of Various Mixtures from Aggregate V with RAP and Asphalt Source 2 in Terms of Surface Mixture Type, (a) at 4°C (39.2°F), (b) at 20°C (68°F), (c) at 45°C (113°F) (Surface A), 40C (104°F) (Surface B)

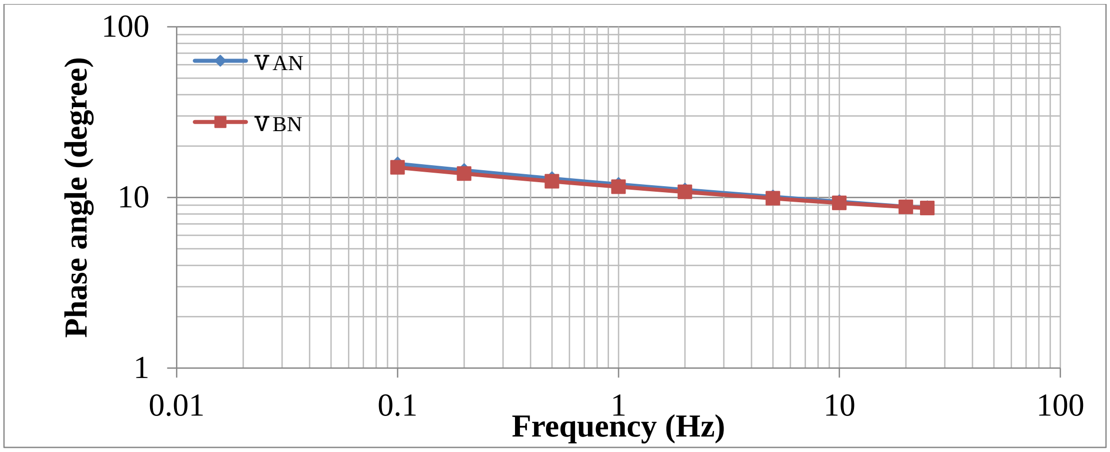

(a)

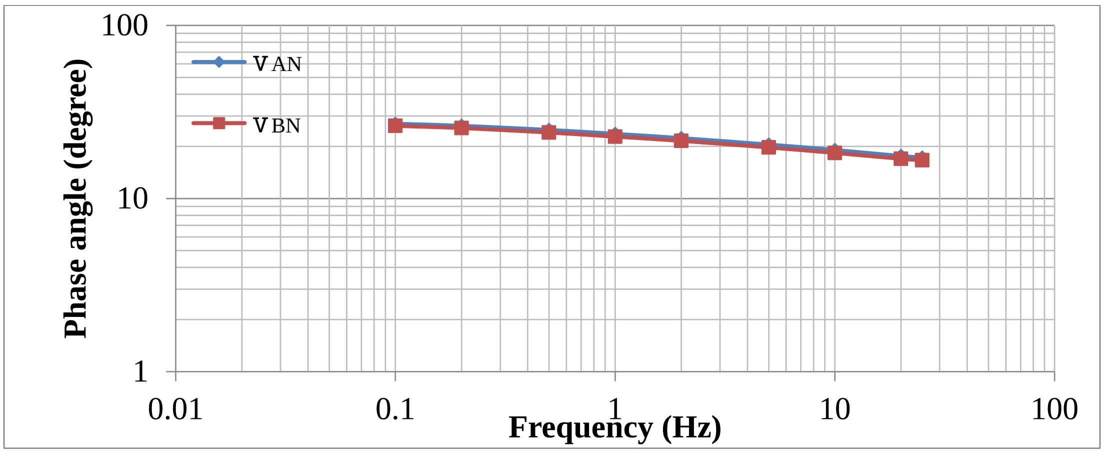

(b)

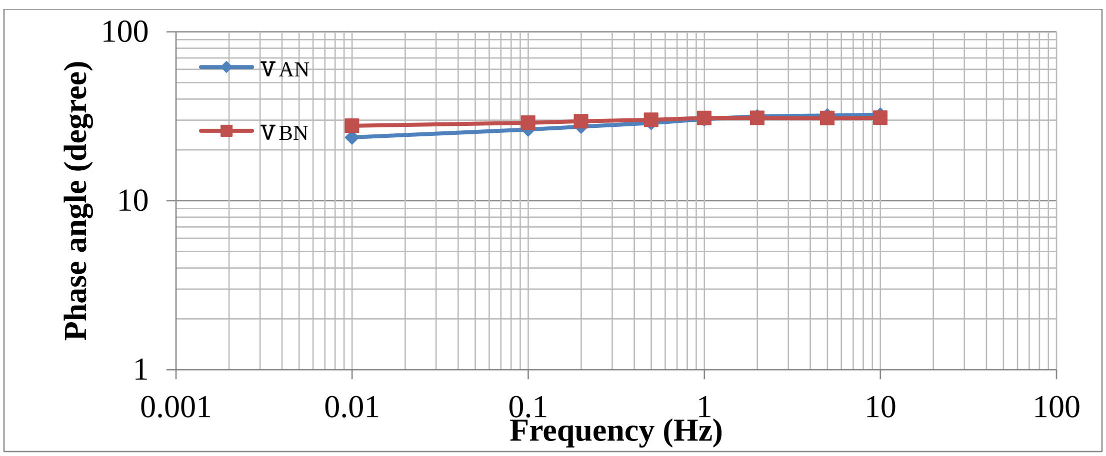

(c)

Figure 10-46 Phase Angle Values of Various Mixtures from Aggregate V with RAP and Asphalt Source 2 in Terms of Surface Mixture Type, (a) at 4°C (39.2°F), (b) at 20°C (68°F), (c) at 45°C (113°F) (Surface A), 40°C (104°F) (Surface B)

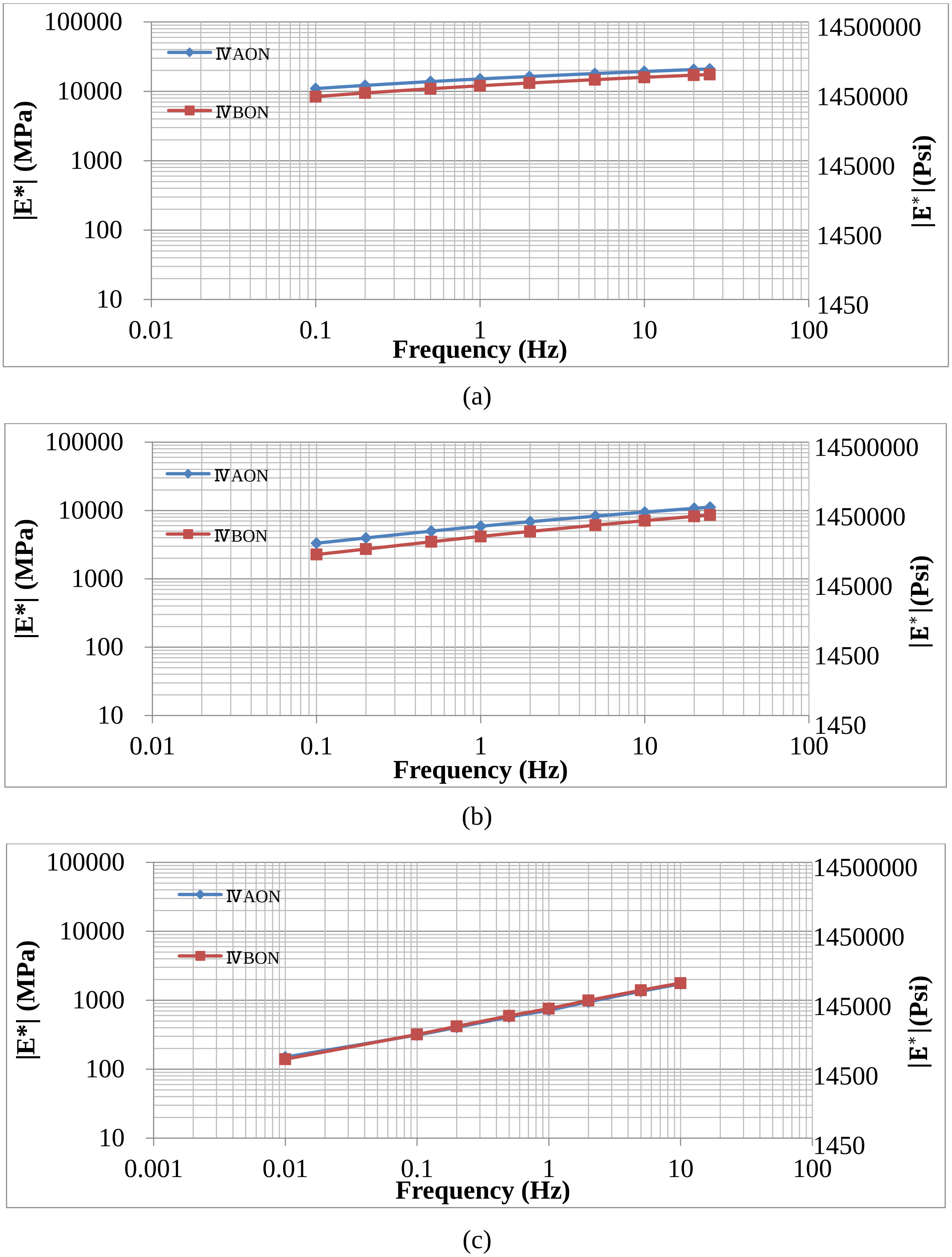

Figure 10-47 Dynamic Modulus Values of Various Mixtures from Aggregate IV using Asphalt Source 2 without RAP in Terms of Surface Mixture Type, (a) at 4°C (39.2°F), (b) at 20°C (68°F), (c) at 45°C (113F) (Surface A), 40°C (104°F) (Surface B)

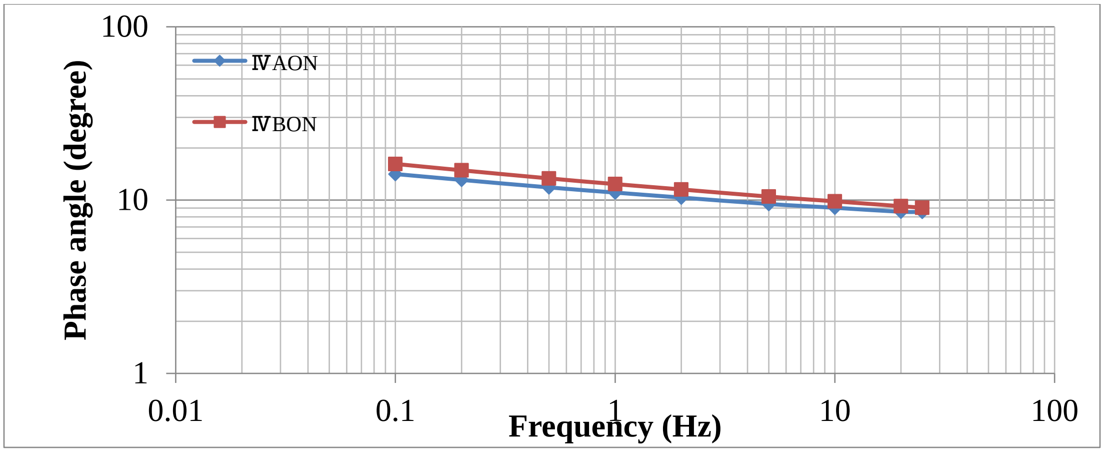

(a)

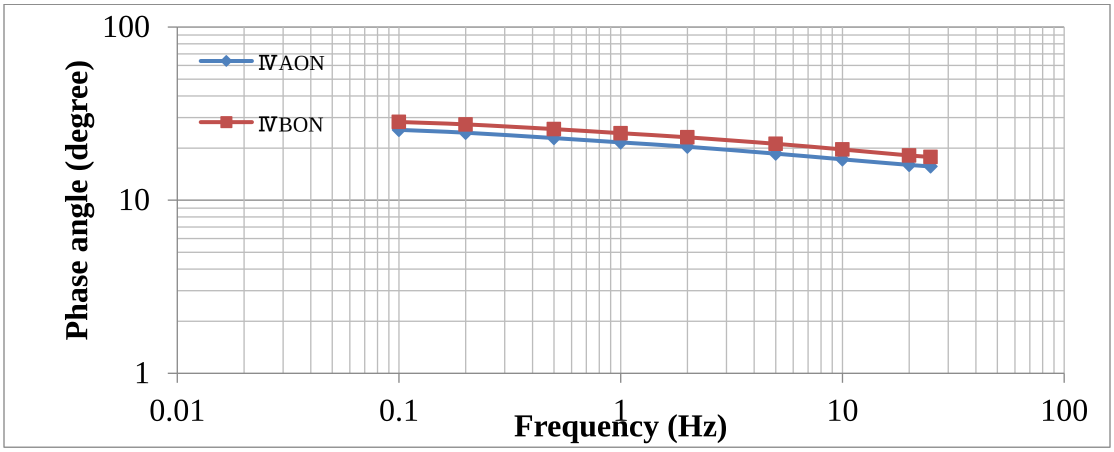

(b)

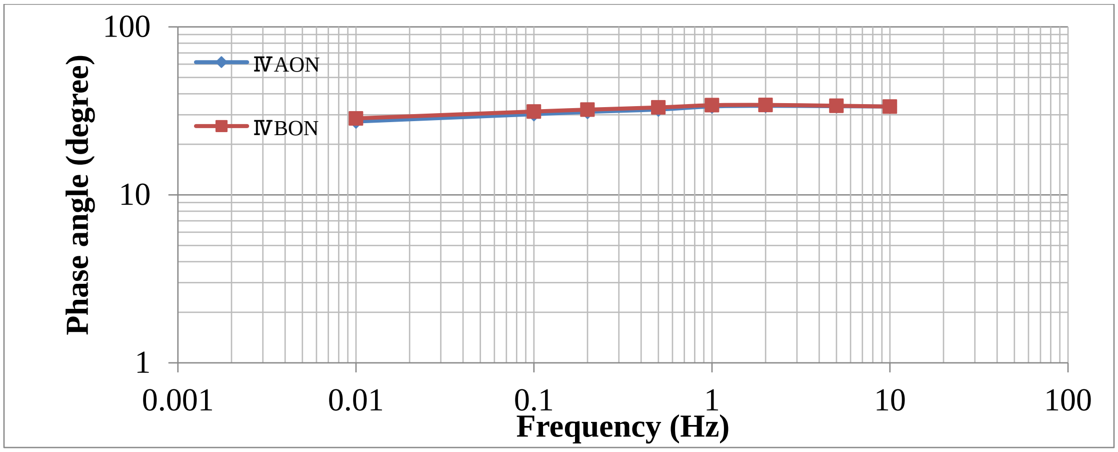

(c)

Figure 10-48 Phase Angle Values of Various Mixtures from Aggregate IV using Asphalt Source 2 without RAP in Terms of Surface Mixture Type, (a) at 4°C (39.2°F), (b) at 20°C (68°F), (c) at 45°C (113°F) (Surface A), 40°C (104°F) (Surface B)

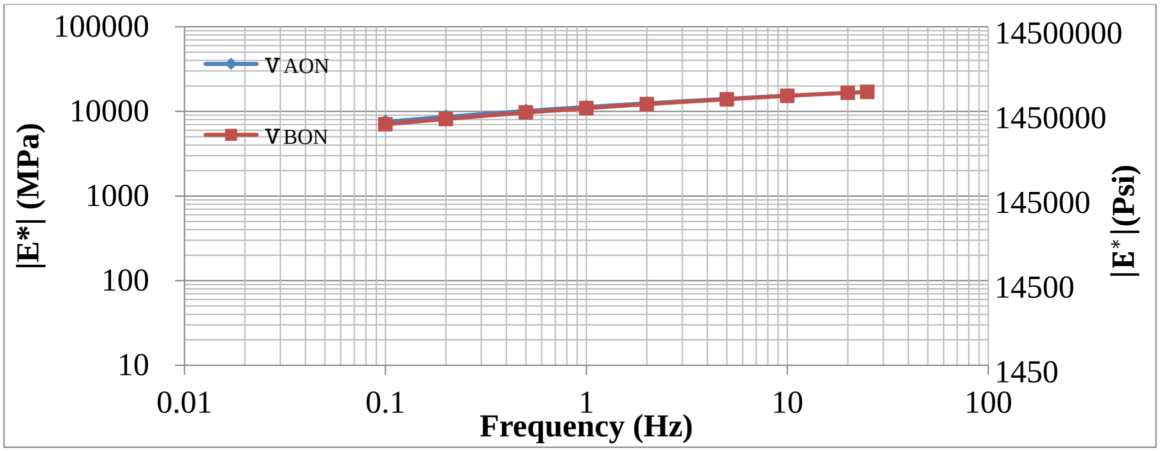

(a)

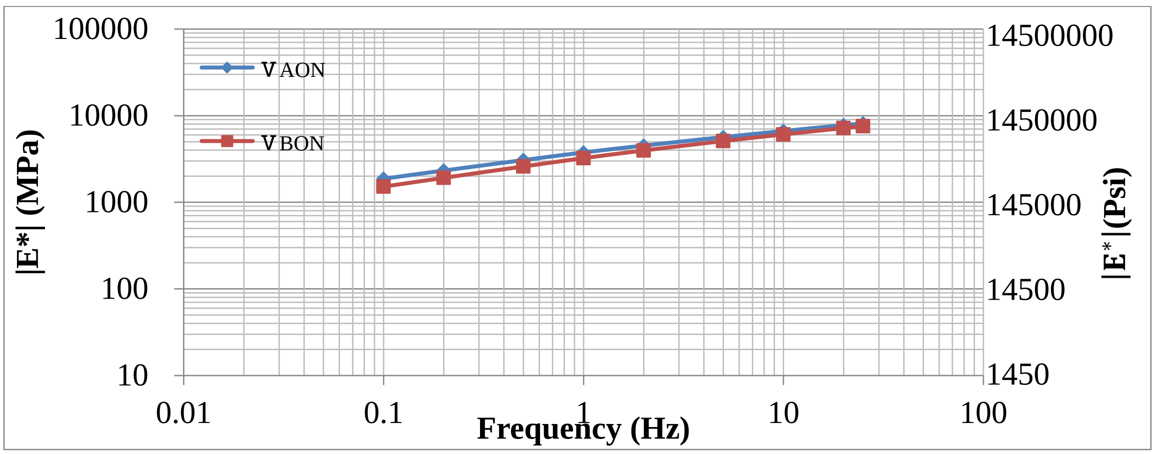

(b)

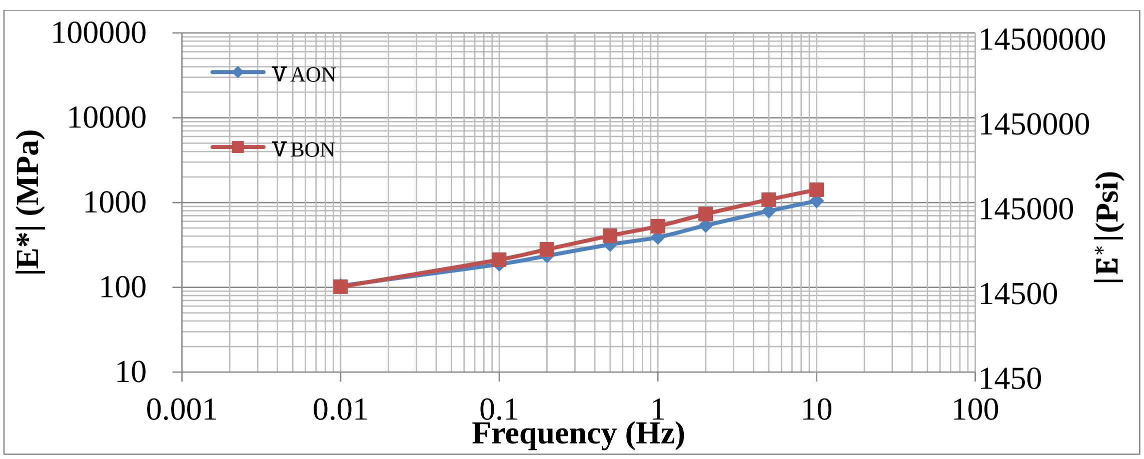

(c)

Figure 10-49 Dynamic Modulus Values of Various Mixtures from Aggregate V using Asphalt Source 2 without RAP in Terms of Surface Mixture Type, (a) at 4°C (39.2°F), (b) at 20°C (68°F), (c) at 45°C (113°F) (Surface A), 40°C (104°F) (Surface B)

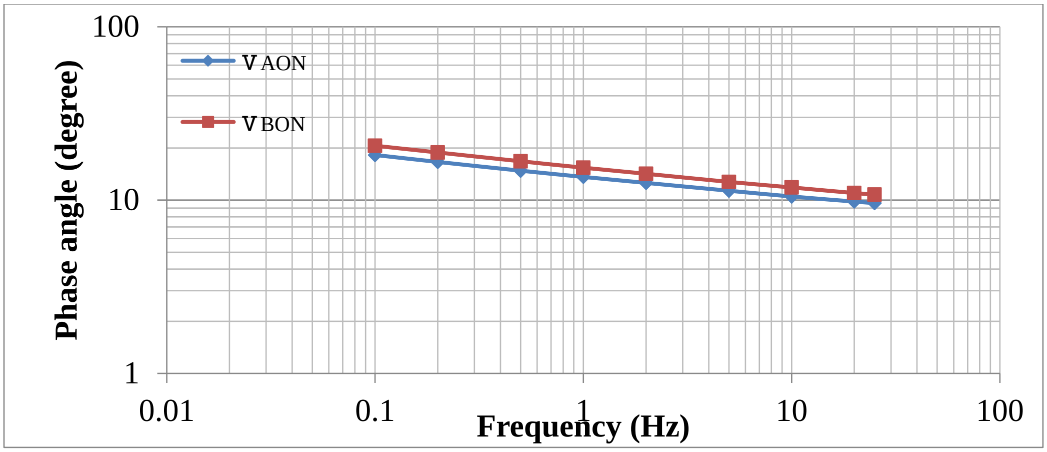

(a)

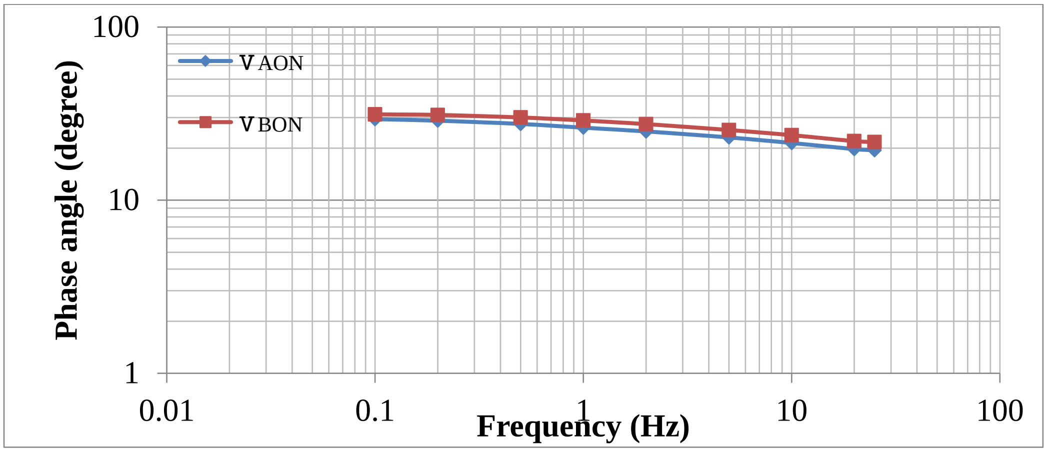

(b)

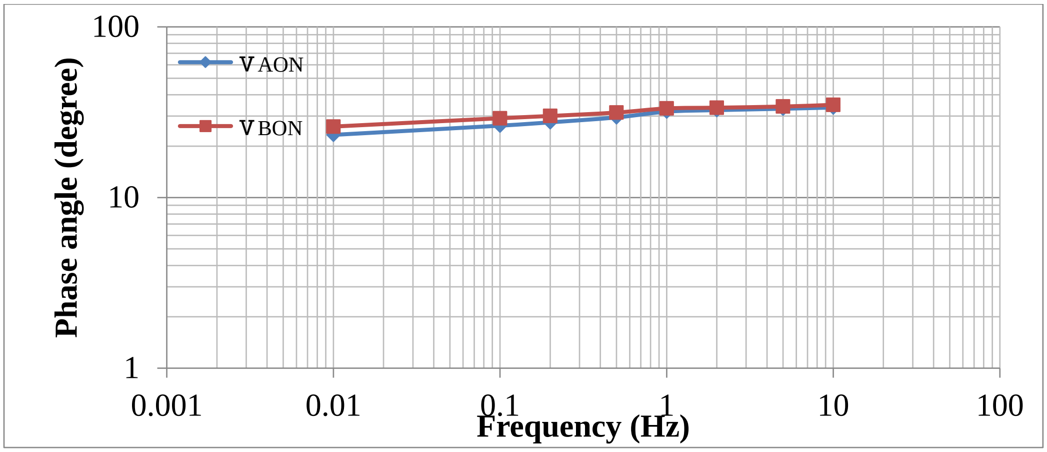

(c)

Figure 10-50 Phase Angle Values of Various Mixtures from Aggregate V using Asphalt Source 2 without RAP in Terms of Surface Mixture Type, (a) at 4°C (39.2°F), (b) at 20°C (68°F), (c) at 45°C (113°F) (Surface A), 40°C (104°F) (Surface B)

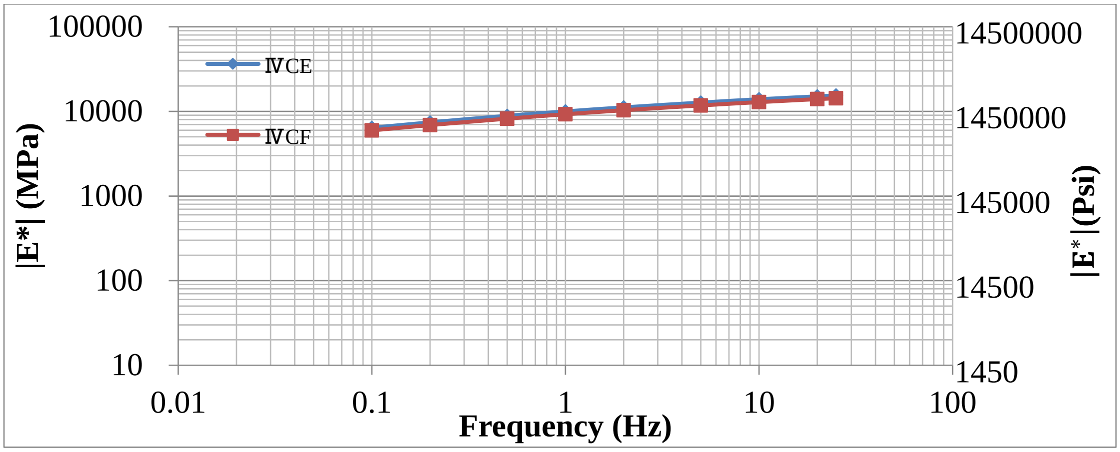

(a)

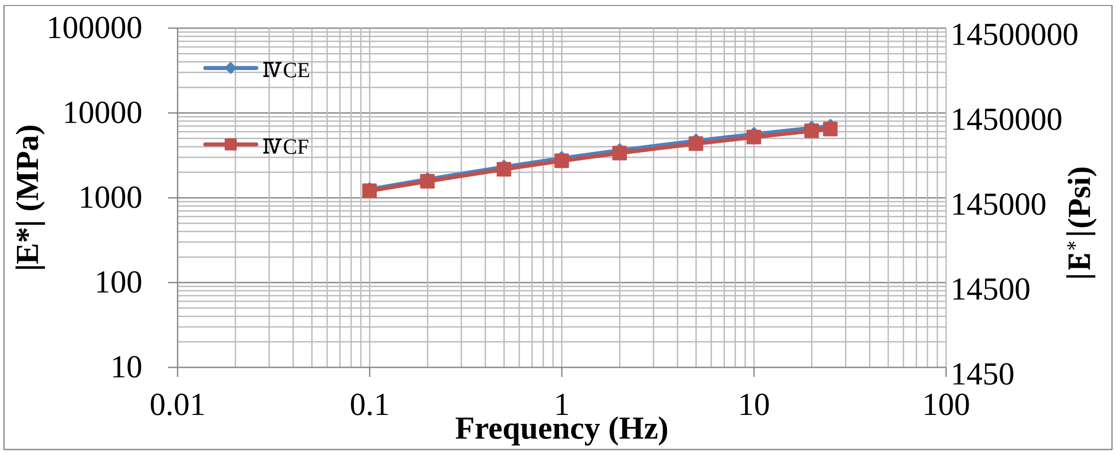

(b)

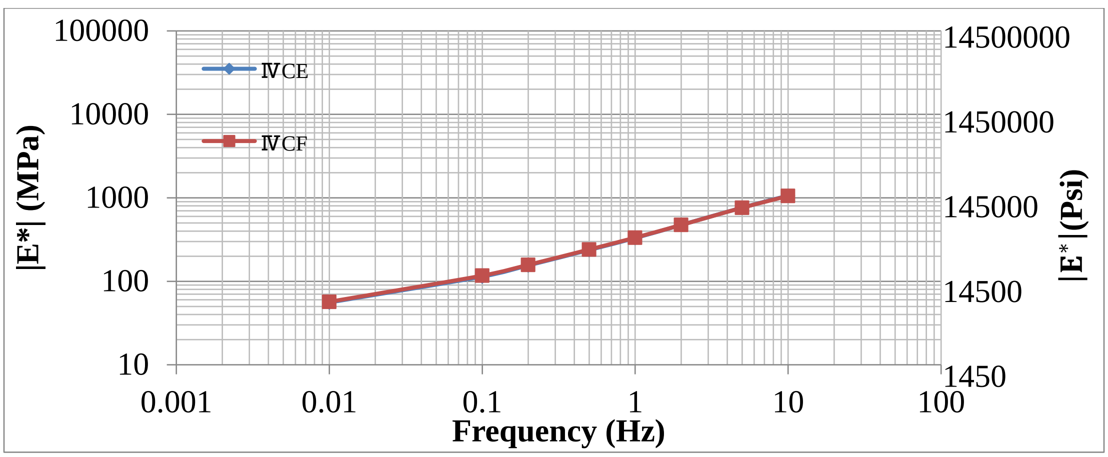

(c)

Figure 10-51 Dynamic Modulus Values of Various Surface Type C Mixtures from Aggregate IV with RAP in Terms of WMA Technology Type, (a) at 4°C (39.2°F), (b) at 20°C (68°F), (c) at 40°C (104°F)

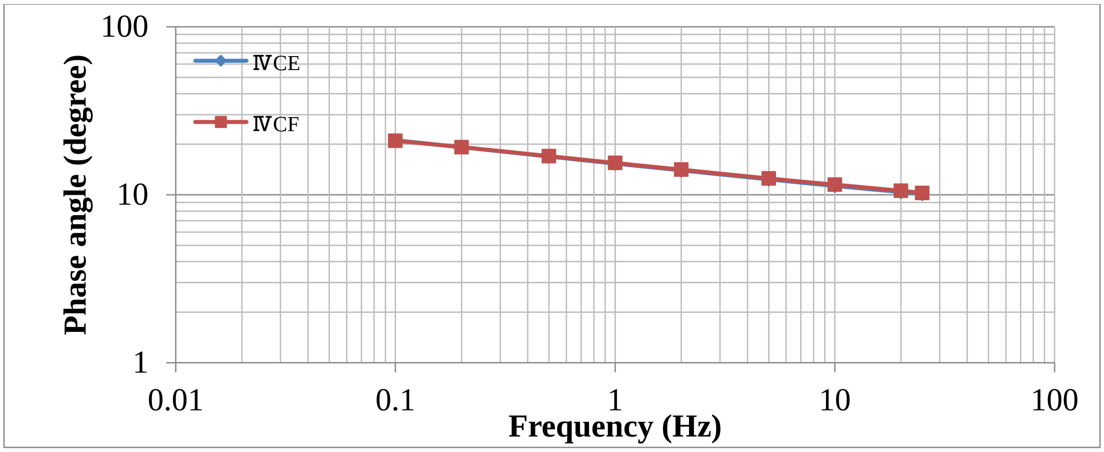

(a)

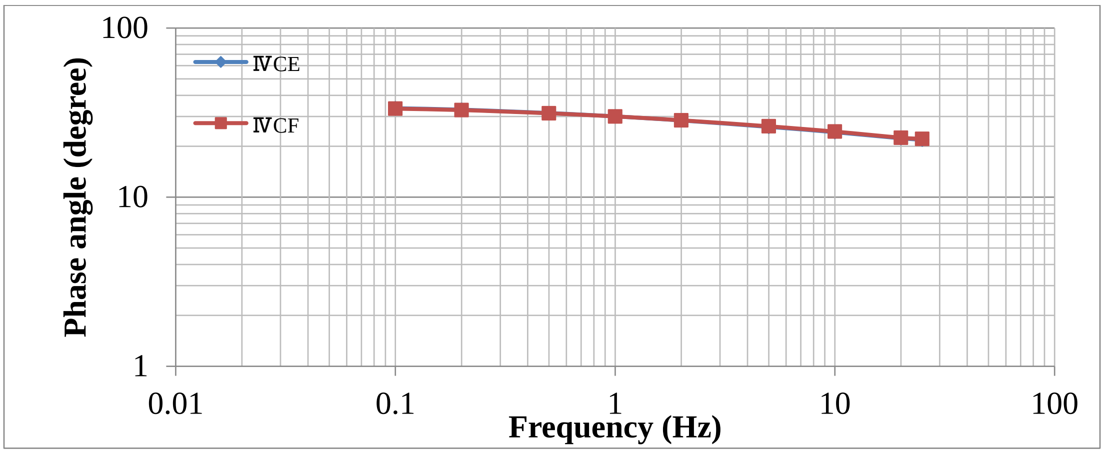

(b)

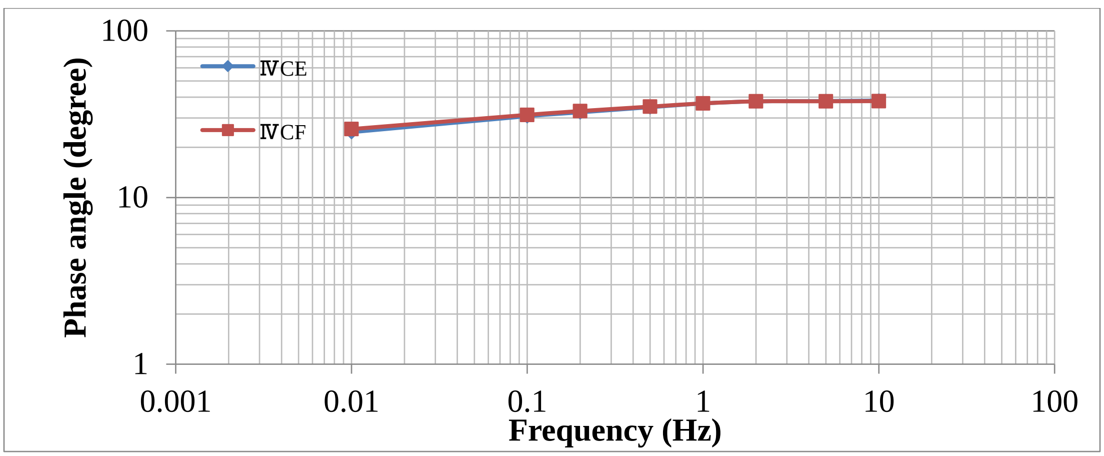

(c)

Figure 10-52 Phase Angle Values of Various Surface Type C Mixtures from Aggregate IV with RAP in Terms of WMA Technology Type, (a) at 4°C (39.2°F), (b) at 20°C (68°F), (c) at 40°C (104°F)

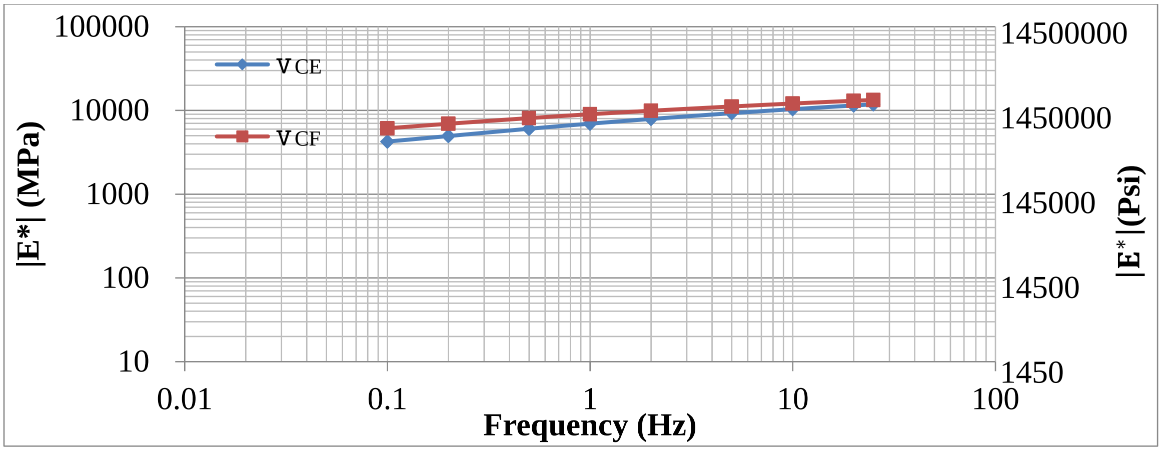

(a)

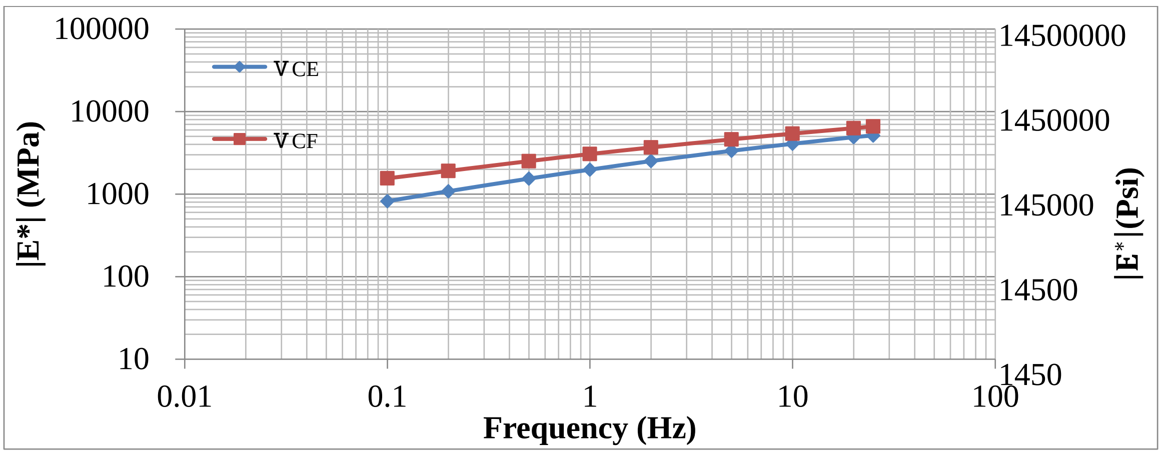

(b)

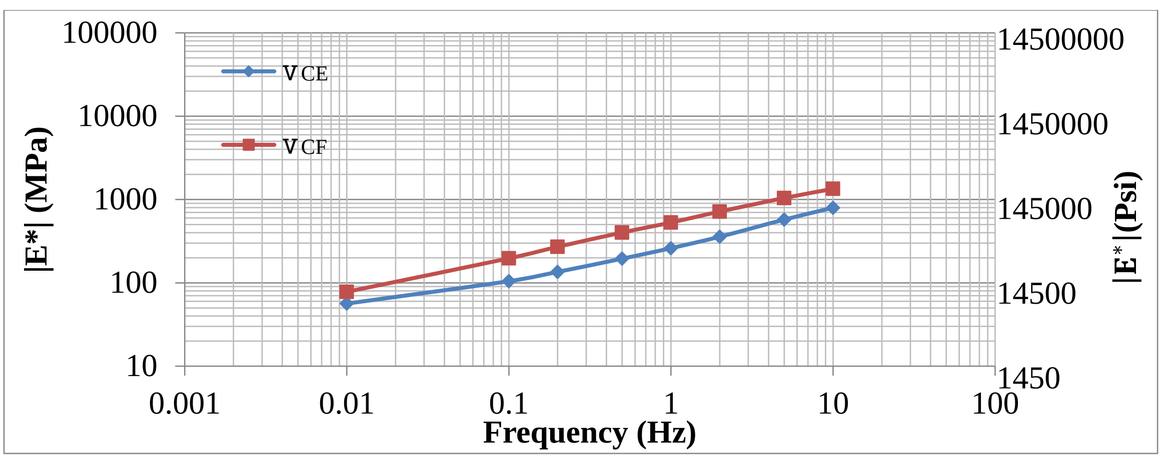

(c)

Figure 10-53 Dynamic Modulus Values of Various Surface Type C Mixtures from Aggregate V with RAP in Terms of WMA Technology Type, (a) at 4°C (39.2°F), (b) at 20°C (68°F), (c) at 40°C (104°F)

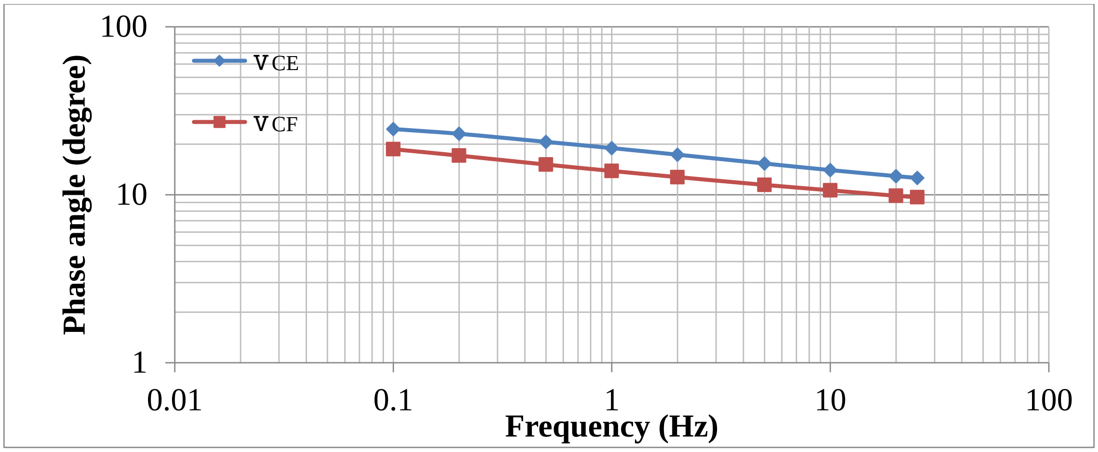

(a)

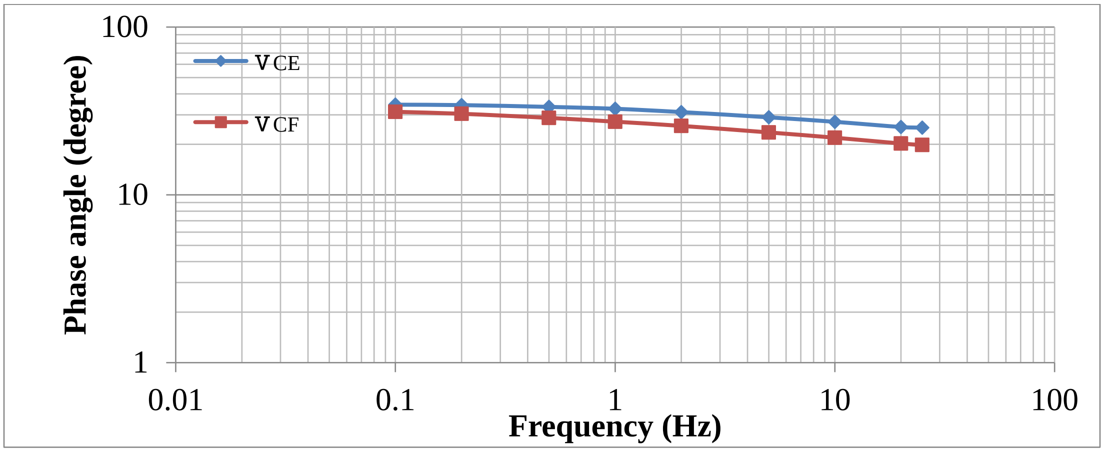

(b)

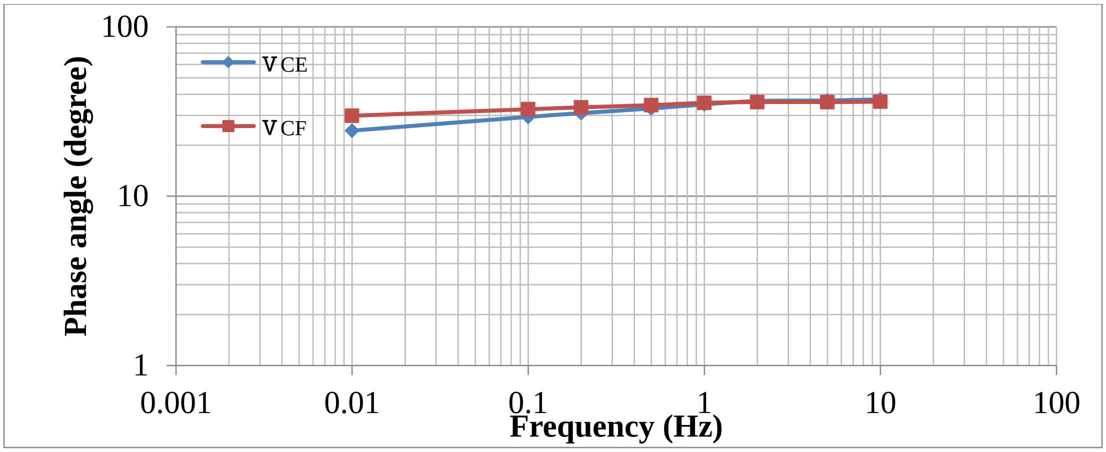

(c)

Figure 10-54 Phase Angle Values of Various Surface Type C Mixtures from Aggregate V with RAP in Terms of WMA Technology Type, (a) at 4°C (39.2°F), (b) at 20°C (68°F), (c) at 40°C (104°F)

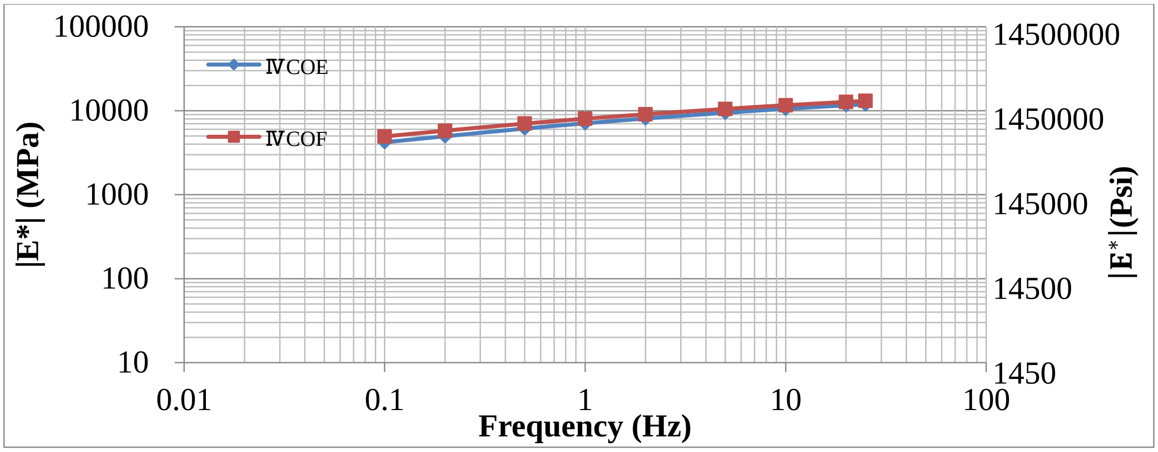

(a)

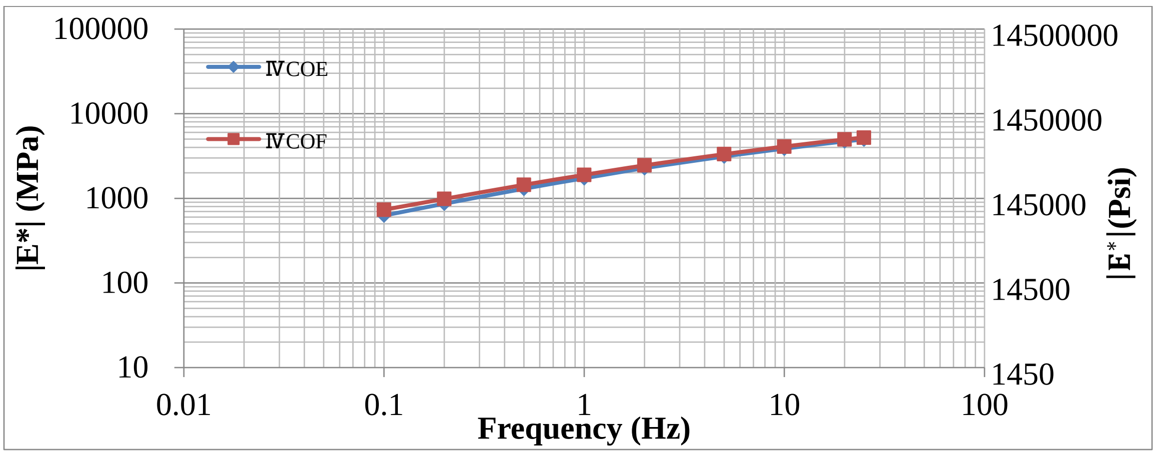

(b)

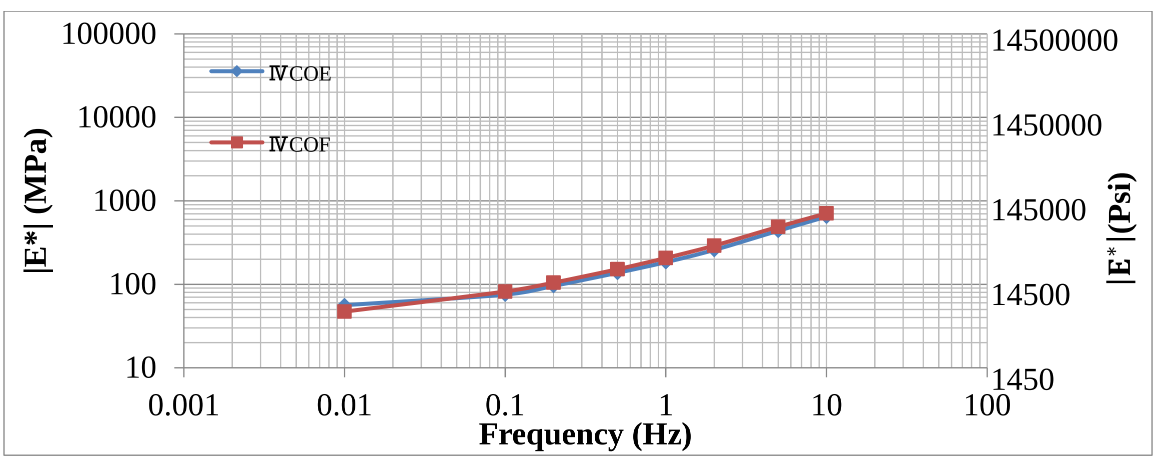

(c)

Figure 10-55 Dynamic Modulus Values of Various Surface Type C Mixtures from Aggregate IV without RAP in Terms of WMA Technology Type, (a) at 4°C (39.2°F), (b) at 20°C (68°F), (c) at 40°C (104°F)

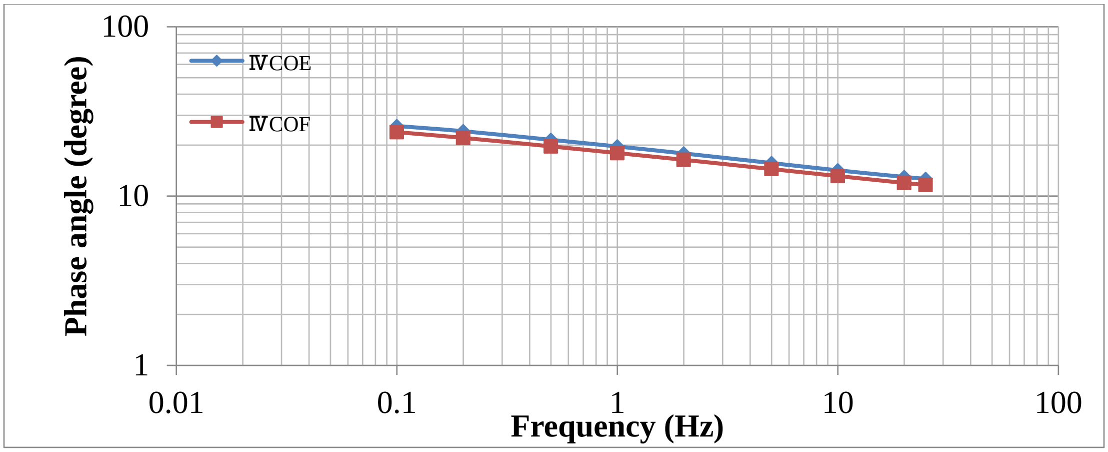

(a)

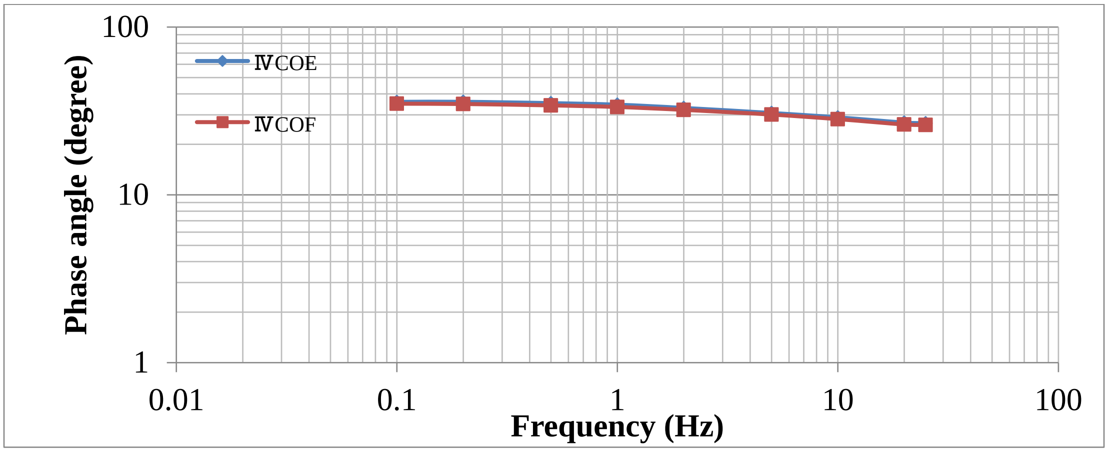

(b)

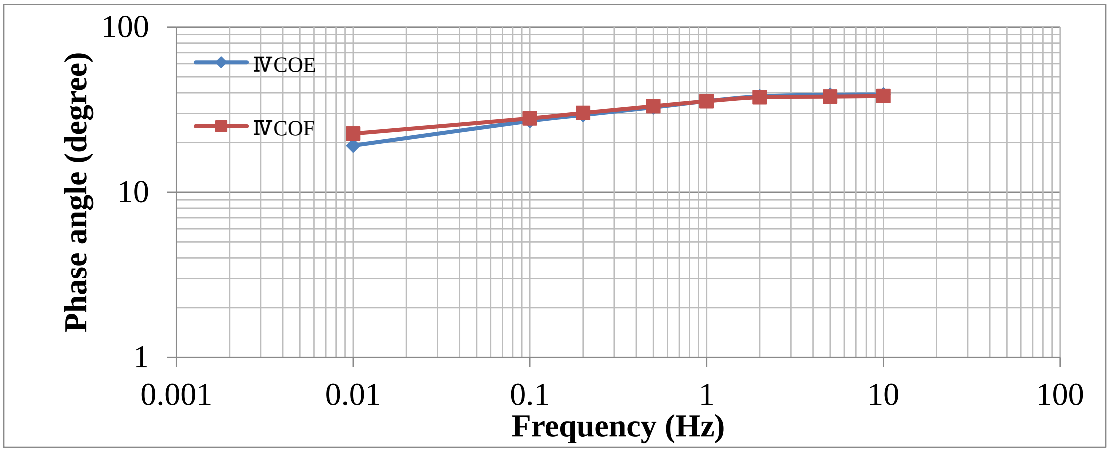

(c)

Figure 10-56 Phase Angle Values of Various Surface Type C Mixtures from Aggregate IV without RAP in Terms of WMA Technology Type, (a) at 4°C (39.2°F), (b) at 20°C (68°F), (c) at 40°C (104°F)

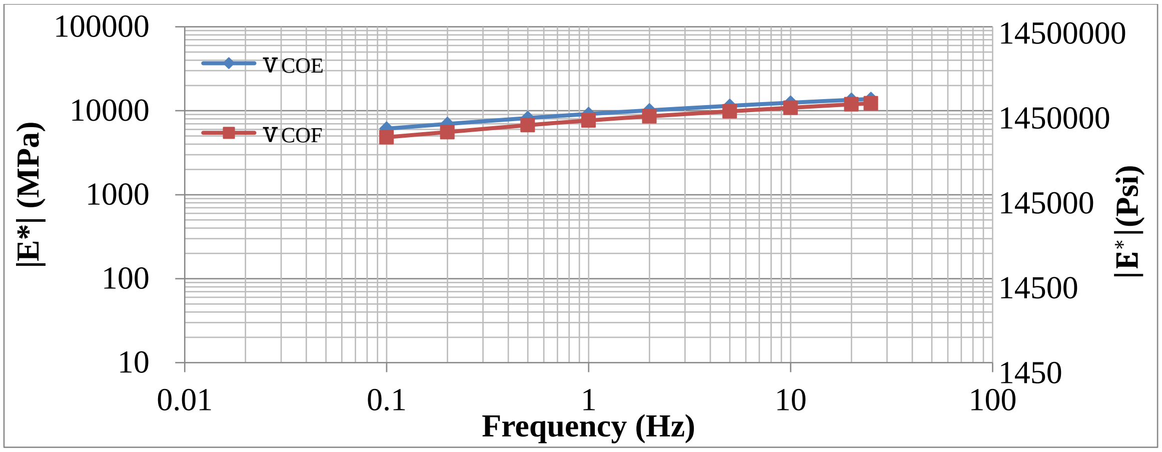

(a)

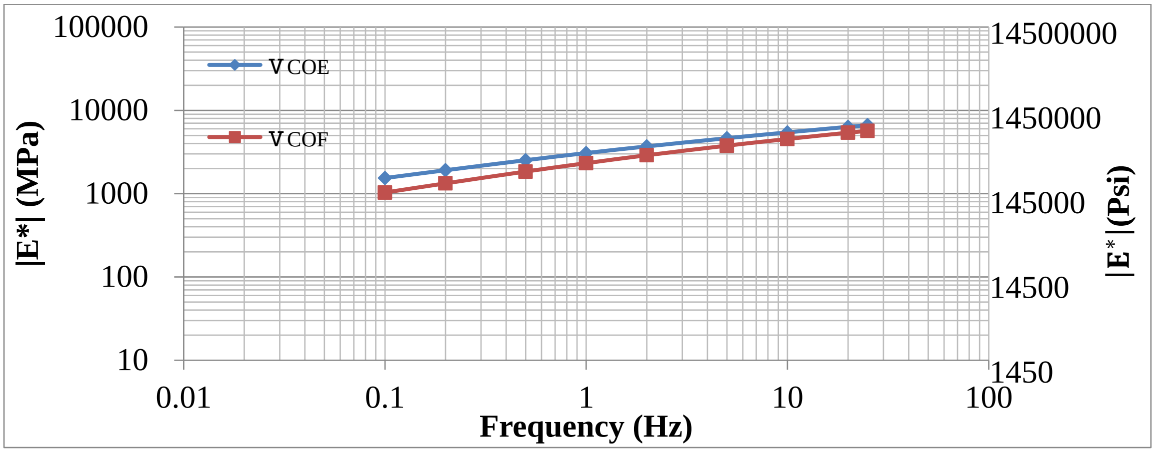

(b)

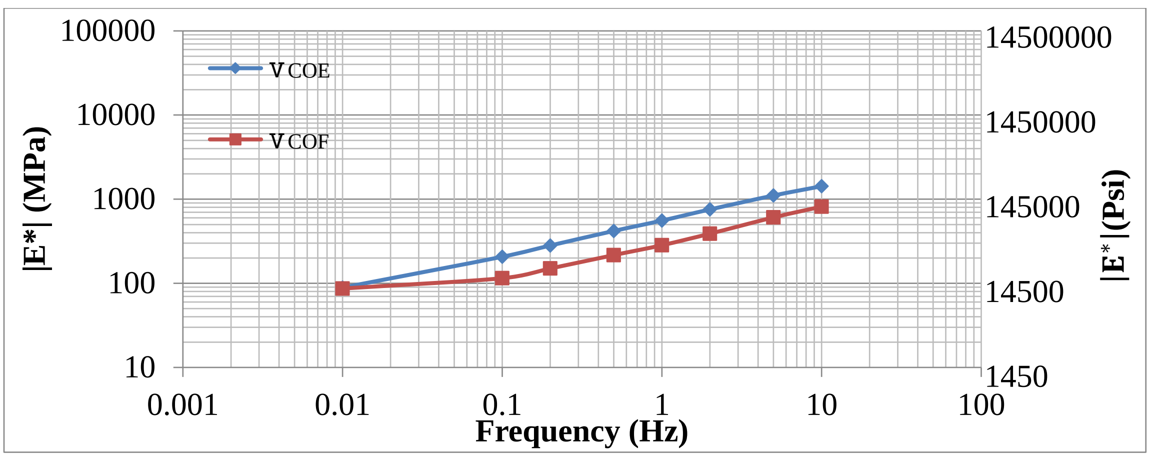

(c)

Figure 10-57 Dynamic Modulus Values of Various Surface Type C Mixtures from Aggregate V without RAP in Terms of WMA Technology Type, (a) at 4°C (39.2°F), (b) at 20°C (68°F), (c) at 40°C (104°F)

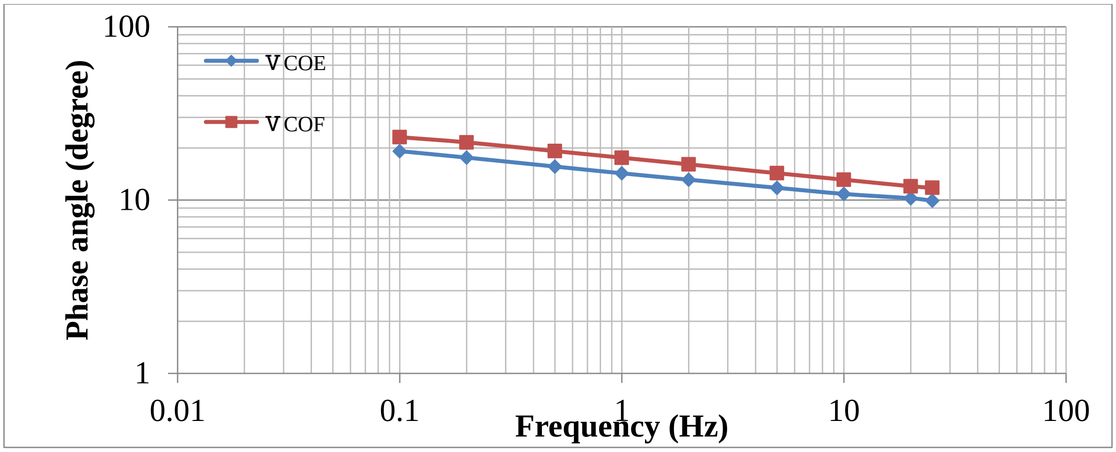

(a)

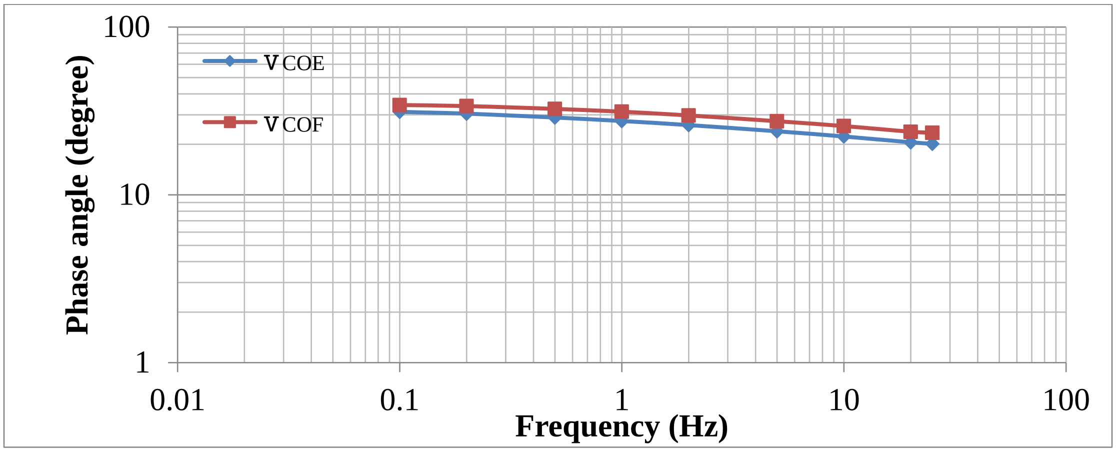

(b)

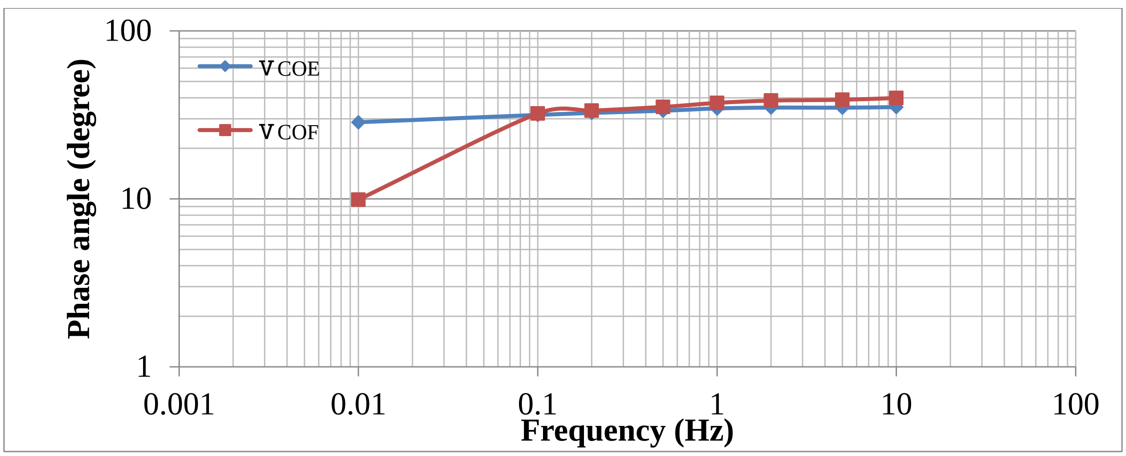

(c)

Figure 10-58 Phase Angle Values of Various Surface Type C Mixtures from Aggregate V without RAP in Terms of WMA Technology Type, (a) at 4°C (39.2°F), (b) at 20°C (68°F), (c) at 40°C (104°F)

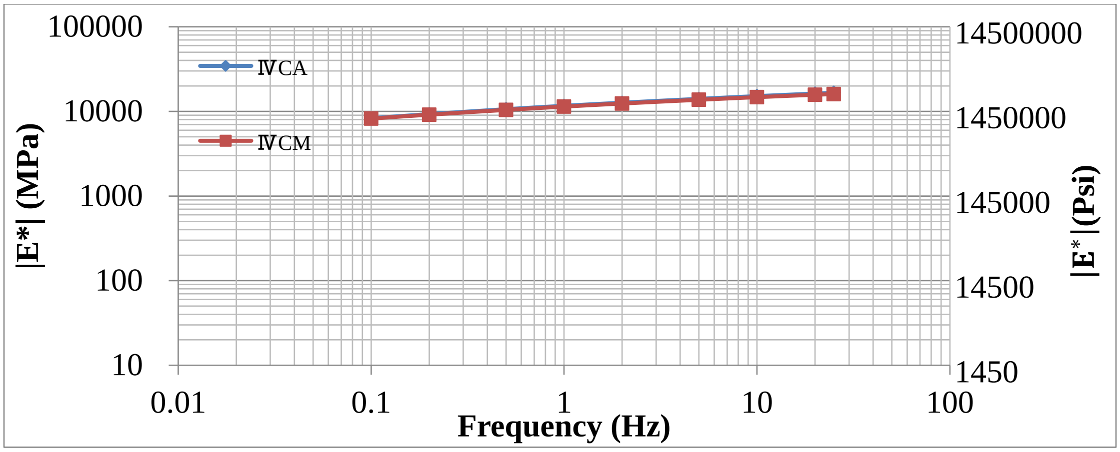

(a)

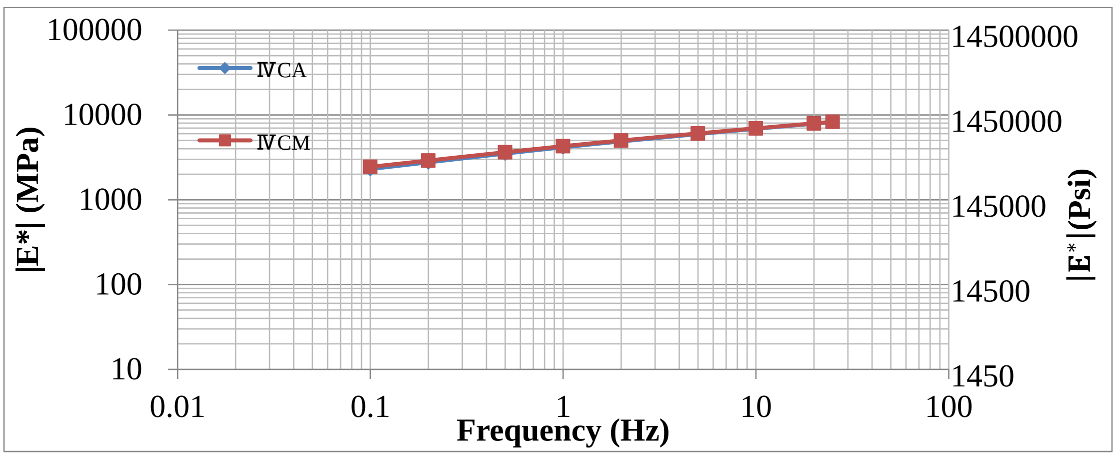

(b)

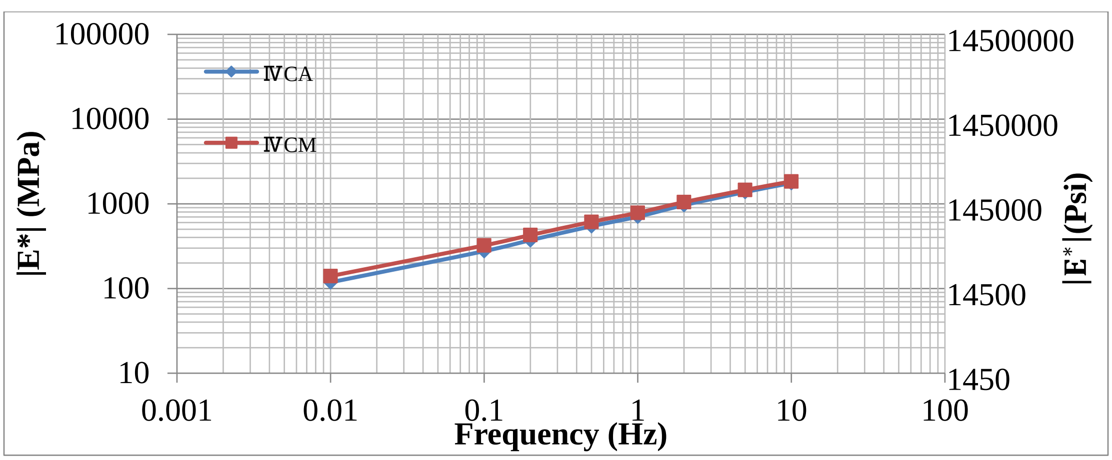

(c)

Figure 10-59 Dynamic Modulus Values of Various Surface Type C Mixtures from Aggregate IV with RAP in Terms of Liquid ASA Type, (a) at 4°C (39.2°F), (b) at 20°C (68°F), (c) at 40°C (104°F)

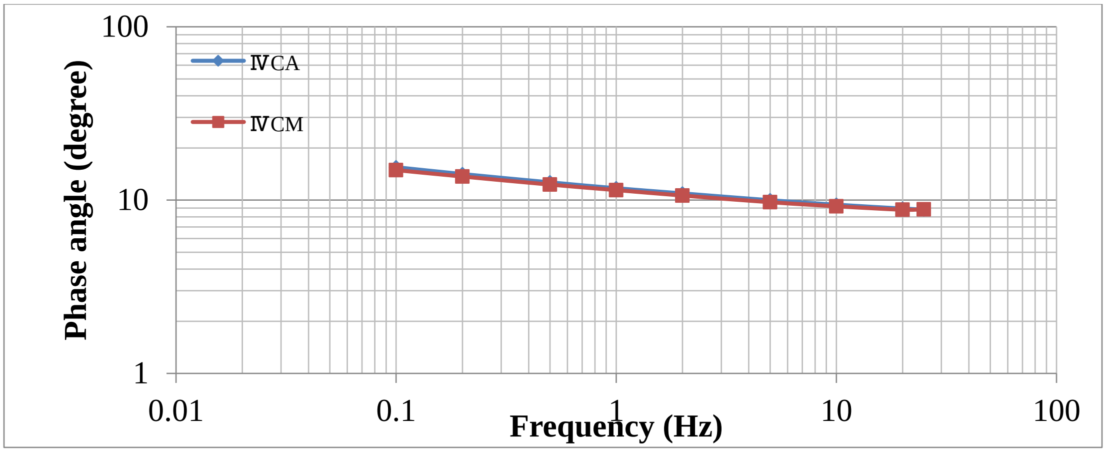

(a)

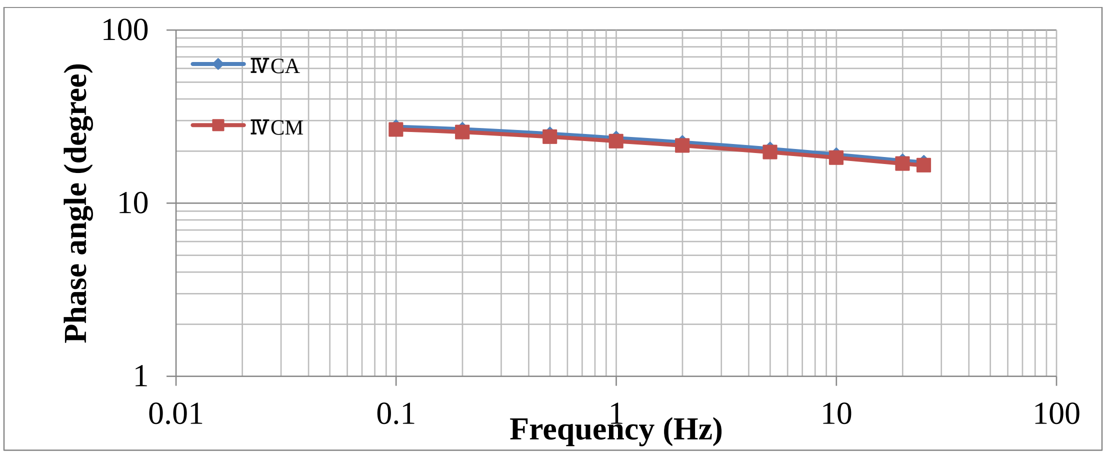

(b)

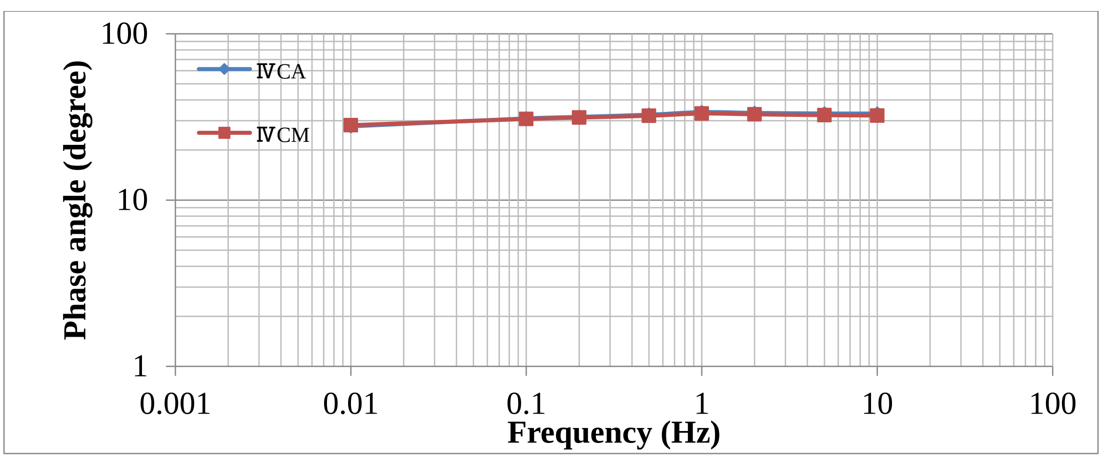

(c)

Figure 10-60 Phase Angle Values of Various Surface Type C Mixtures from Aggregate IV with RAP in Terms of Liquid ASA Type, (a) at 4°C (39.2°F), (b) at 20°C (68°F), (c) at 40°C (104°F)

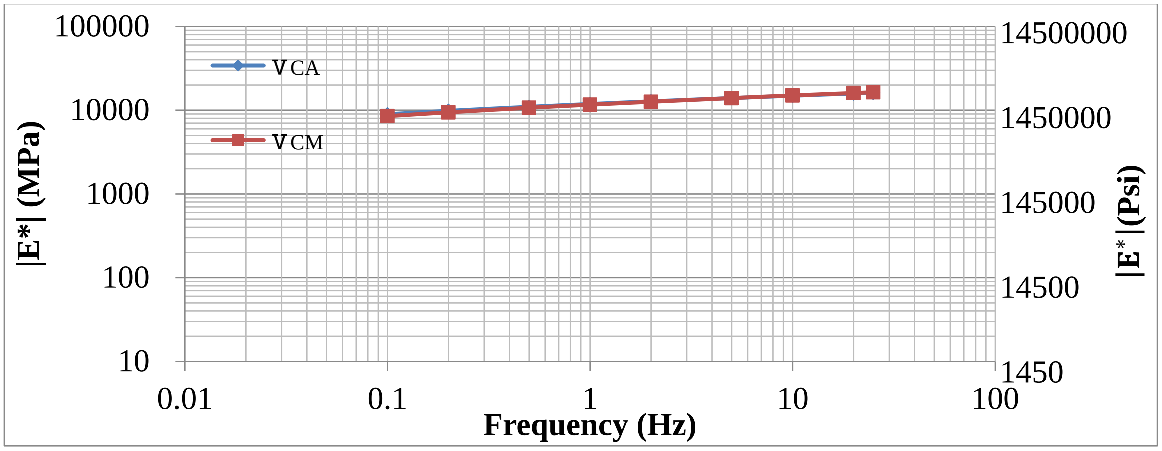

(a)

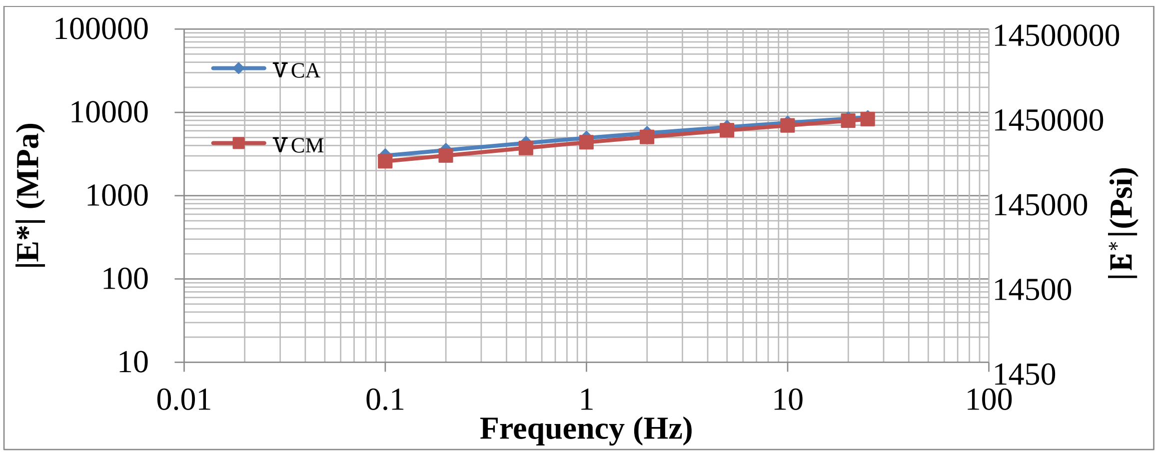

(b)

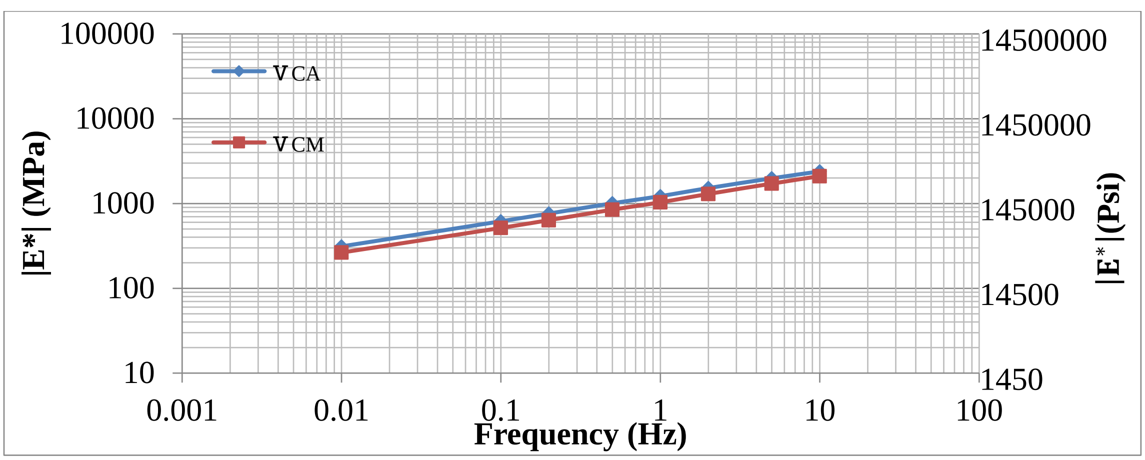

(c)

Figure 10-61 Dynamic Modulus Values of Various Surface Type C Mixtures from Aggregate V with RAP in Terms of Liquid ASA Type, (a) at 4°C (39.2°F), (b) at 20°C (68°F), (c) at 40°C (104°F)

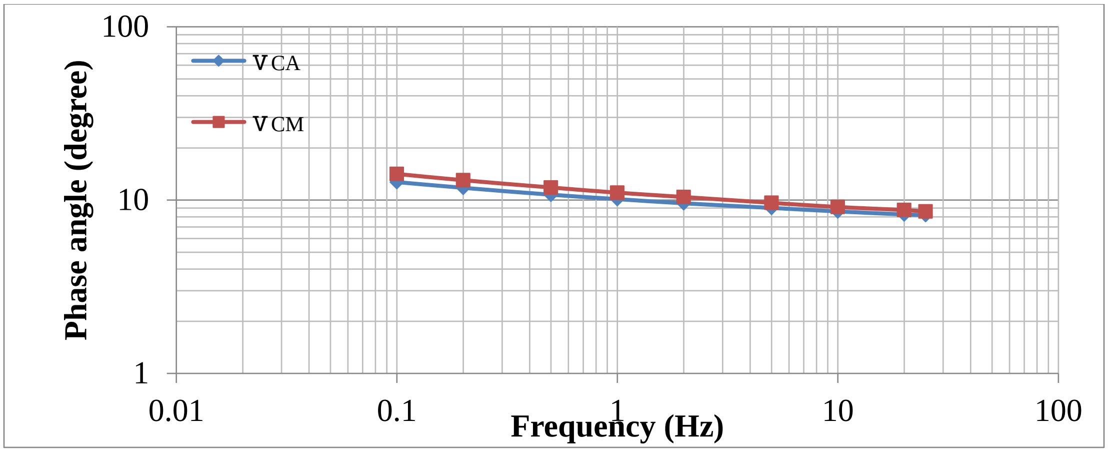

(a)

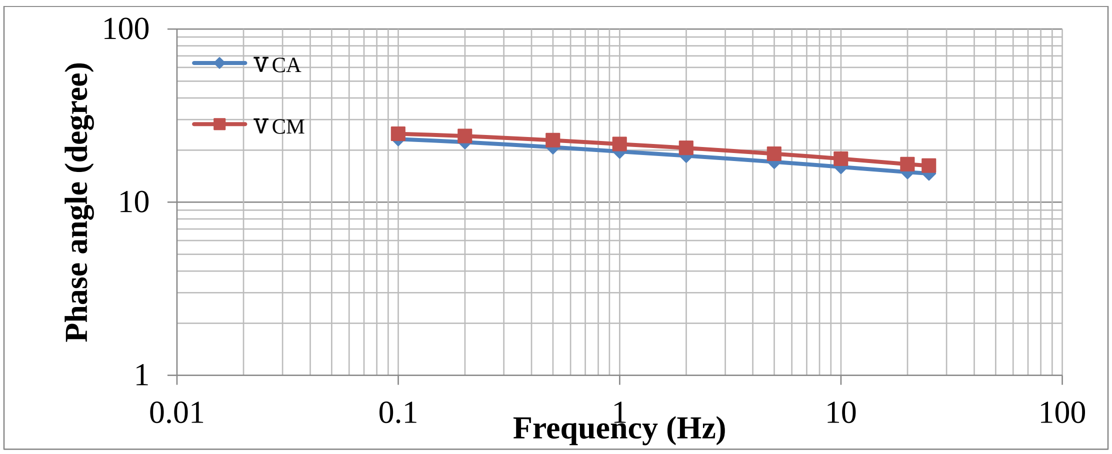

(b)

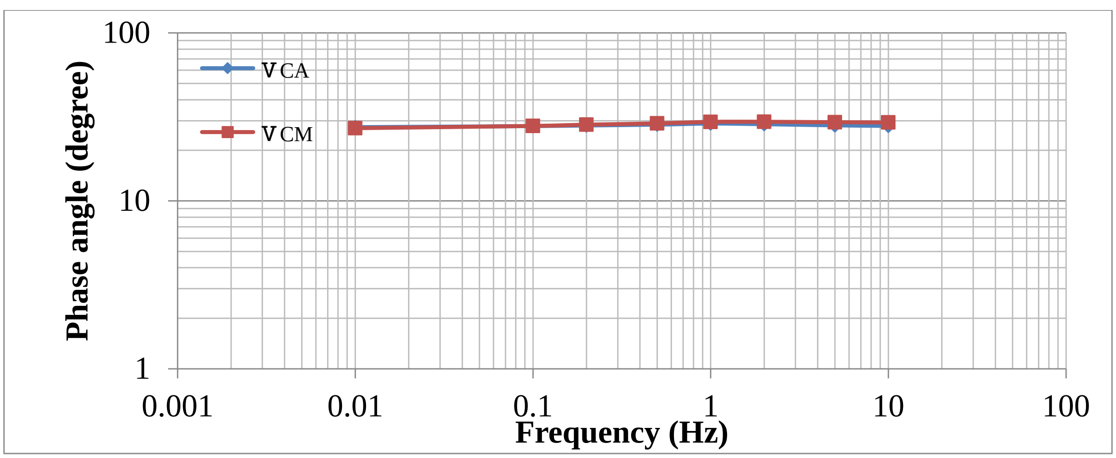

(c)

Figure 10-62 Phase Angle Values of Various Surface Type C Mixtures from Aggregate V with RAP in Terms of Liquid ASA Type, (a) at 4°C (39.2°F), (b) at 20°C (68°F), (c) at 40°C (104°F)

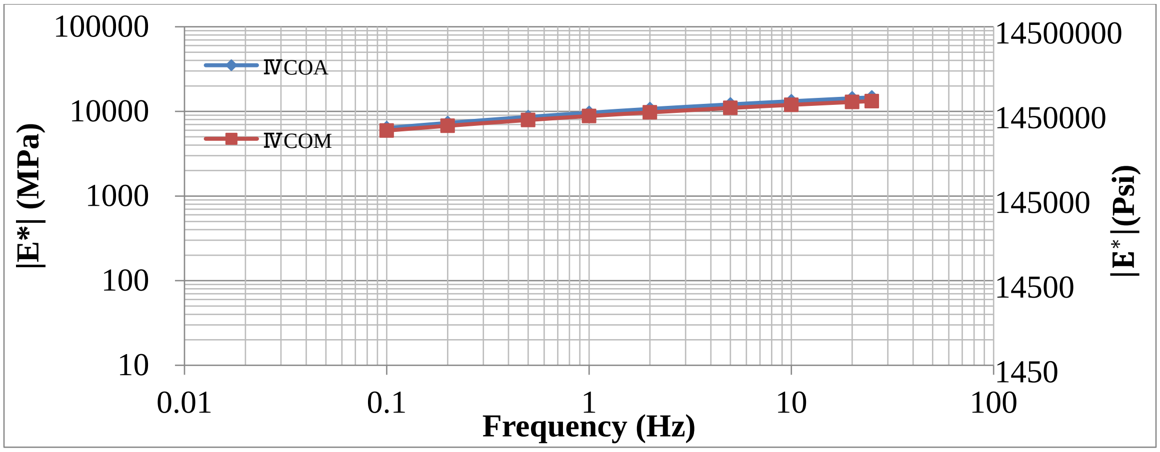

(a)

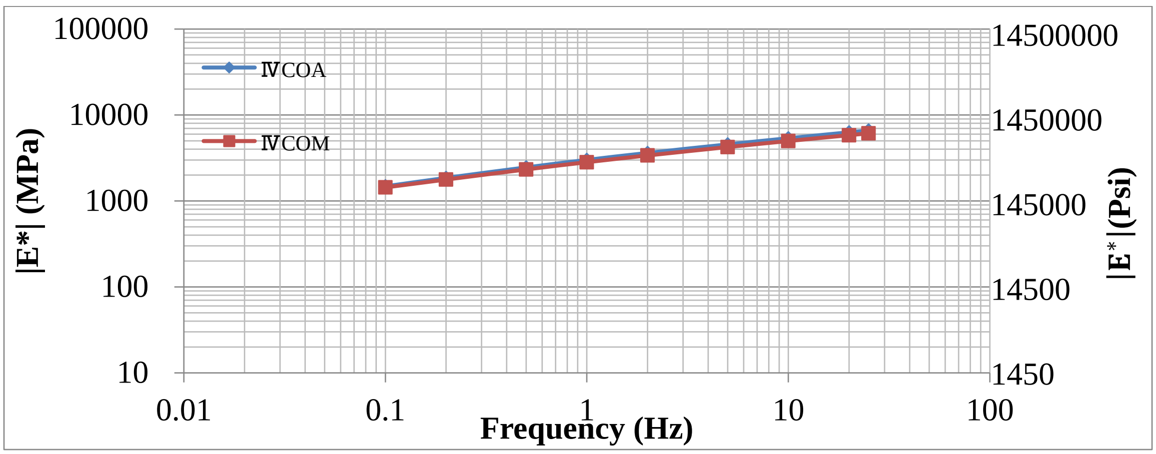

(b)

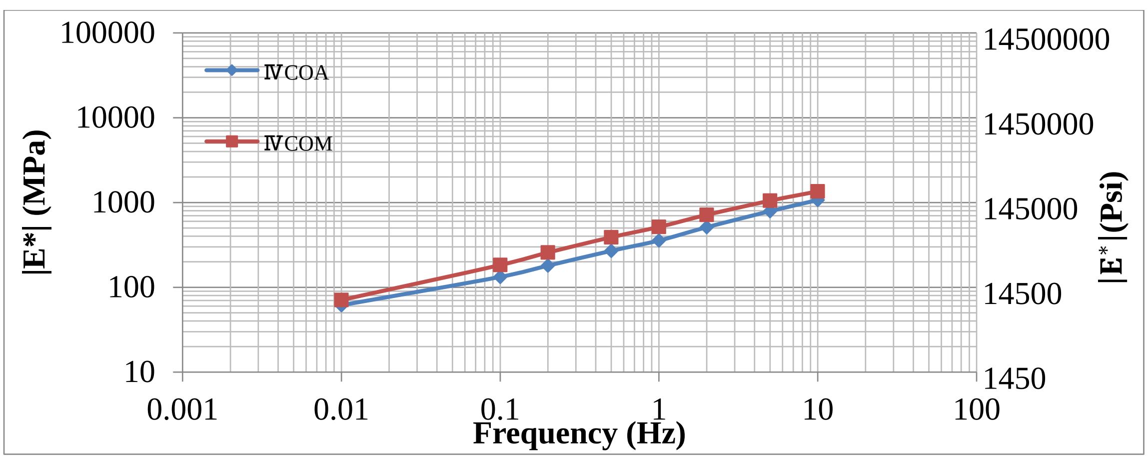

(c)

Figure 10-63 Dynamic Modulus Values of Various Surface Type C Mixtures from Aggregate IV without RAP in Terms of Liquid ASA Type, (a) at 4°C (39.2°F), (b) at 20°C (68°F), (c) at 40°C (104°F)

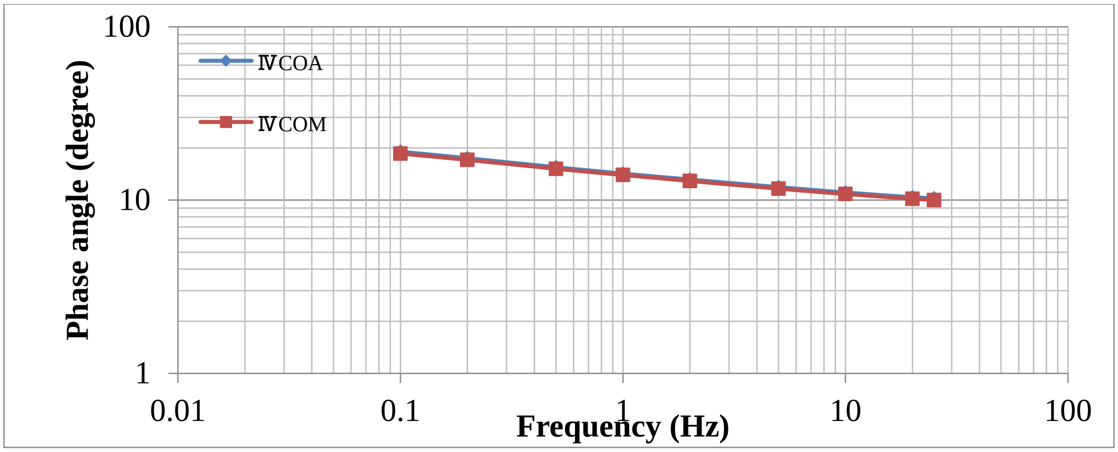

(a)

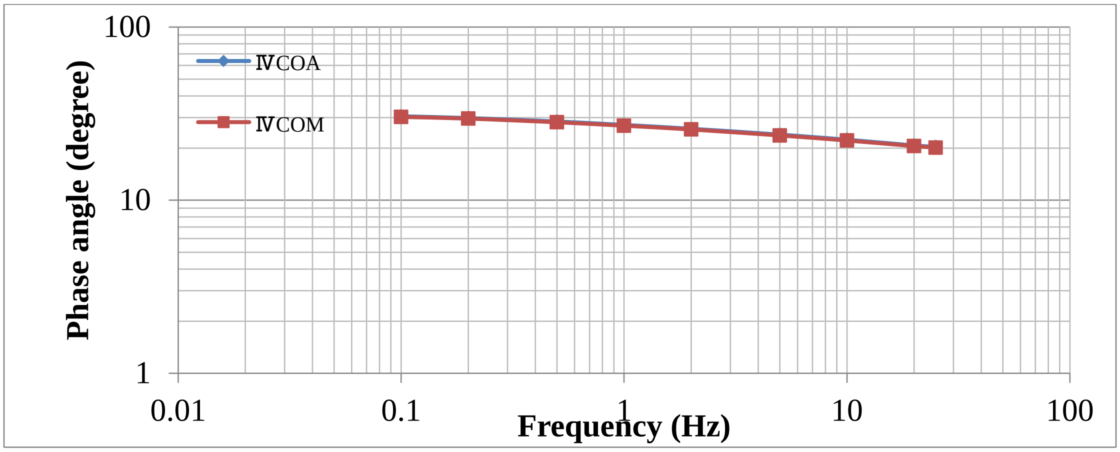

(b)

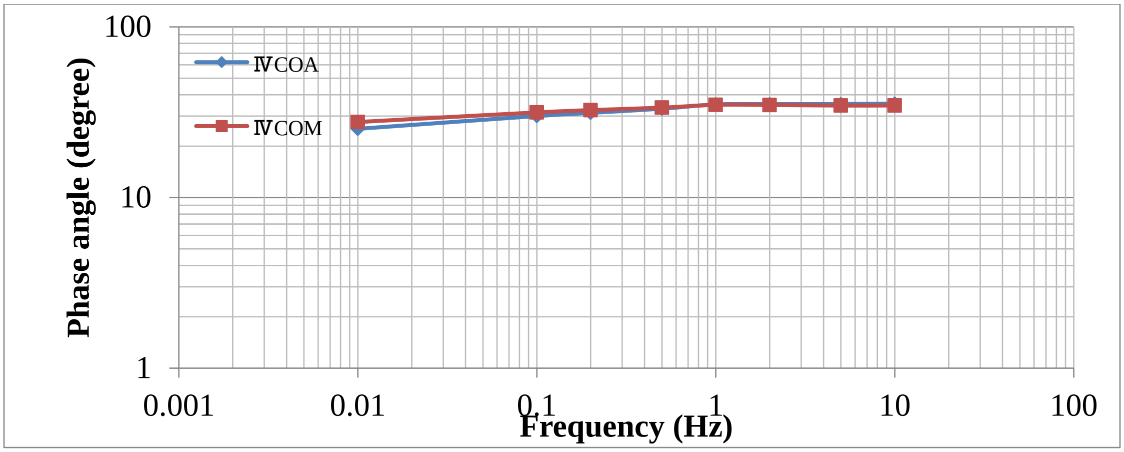

(c)

Figure 10-64 Phase Angle Values of Various Surface Type C Mixtures from Aggregate IV without RAP in Terms of Liquid ASA Type, (a) at 4°C (39.2°F), (b) at 20°C (68°F), (c) at 40°C (104°F)

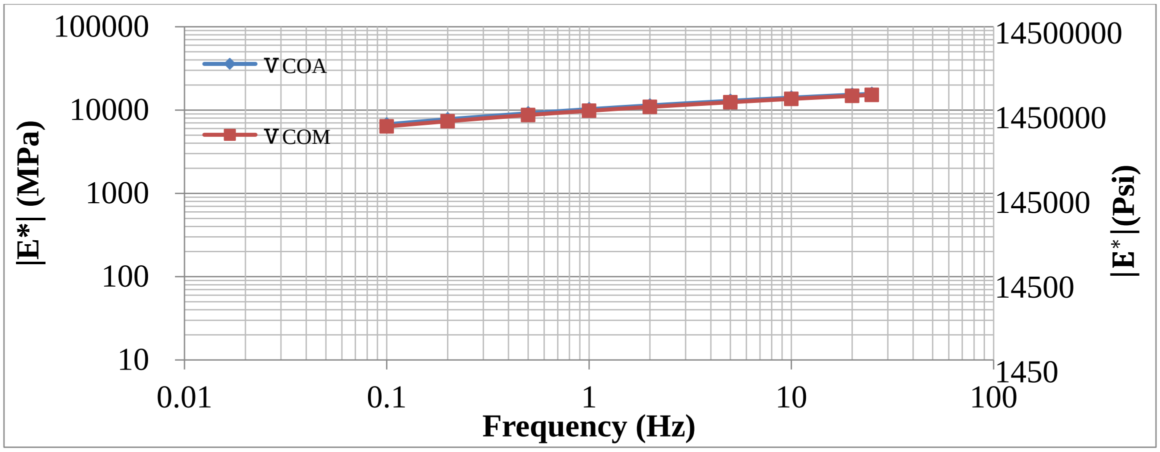

(a)

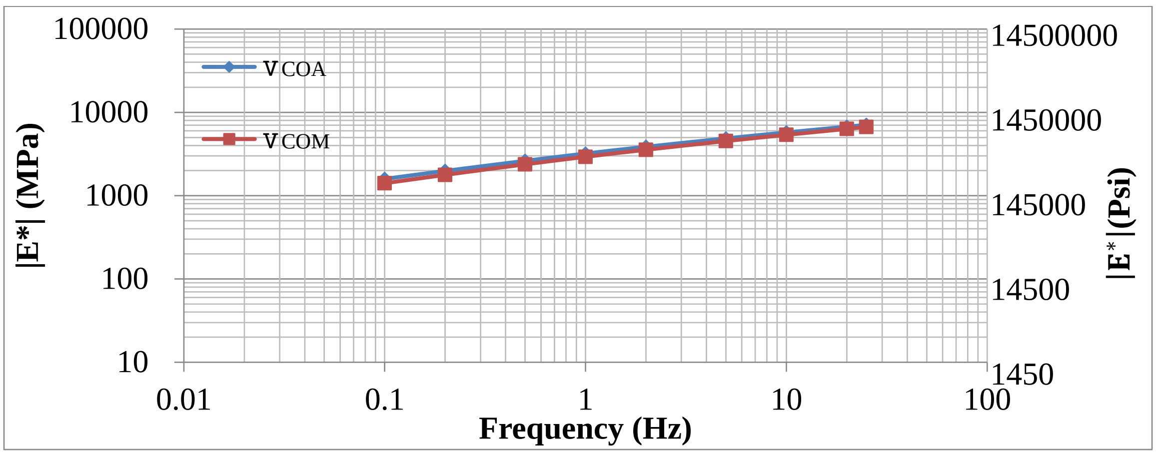

(b)

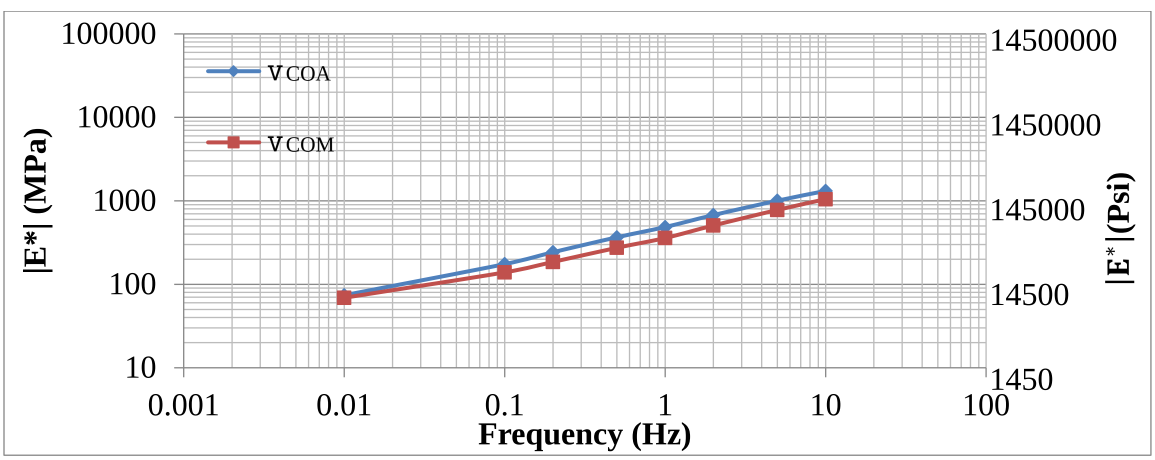

(c)

Figure 10-65 Dynamic Modulus Values of Various Surface Type C Mixtures from Aggregate V without RAP in Terms of Liquid ASA Type, (a) at 4°C (39.2°F), (b) at 20°C (68°F), (c) at 40°C (104°F)

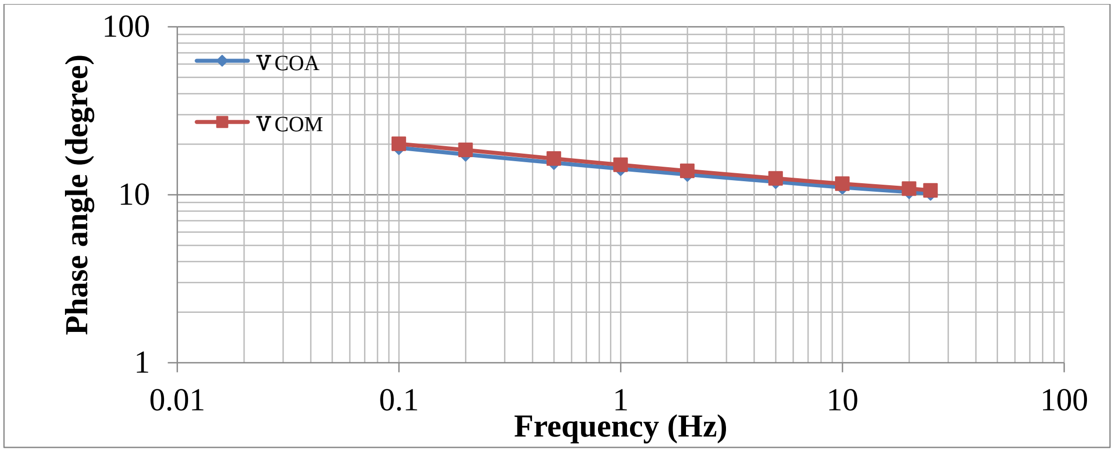

(a)

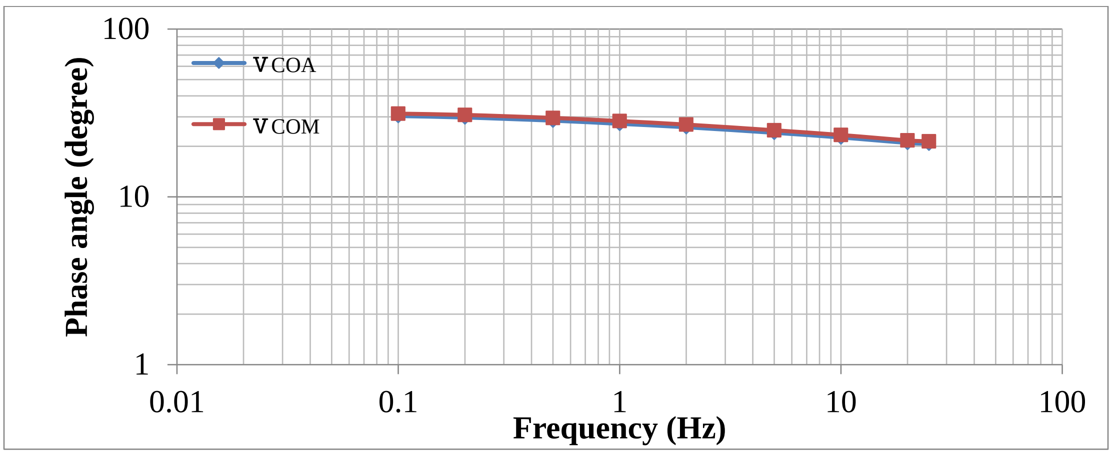

(b)

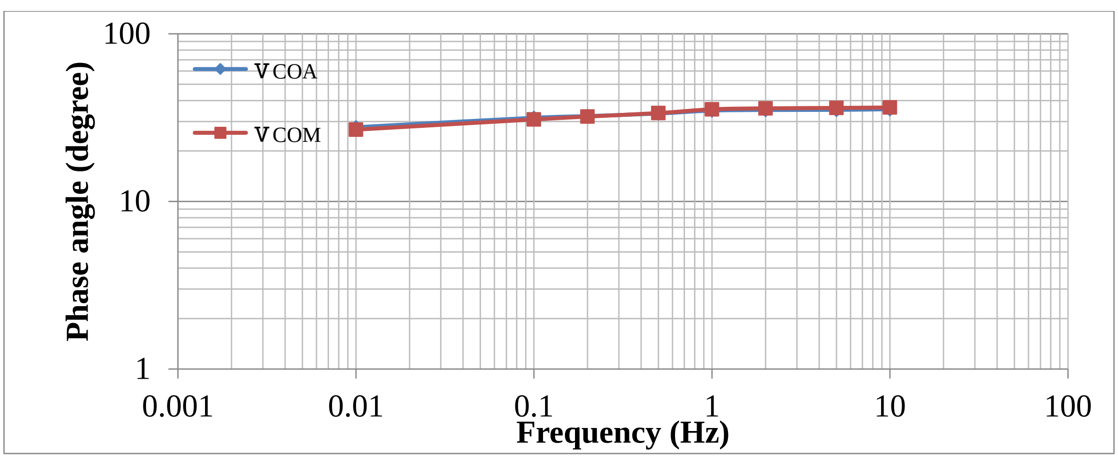

(c)

Figure 10-66 Phase Angle Values of Various Surface Type C Mixtures from Aggregate V without RAP in Terms of Liquid ASA Type, (a) at 4°C (39.2°F), (b) at 20°C (68°F), (c) at 40°C (104°F)

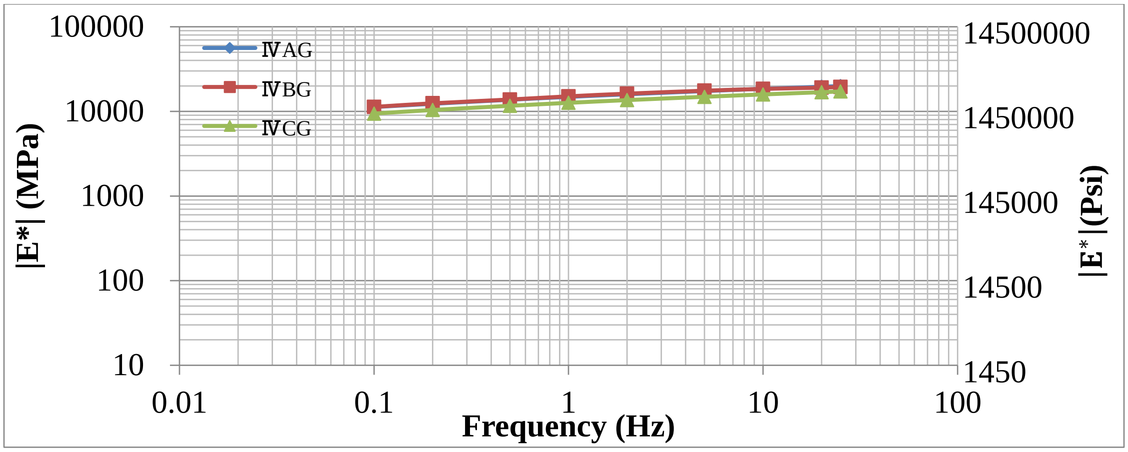

(a)

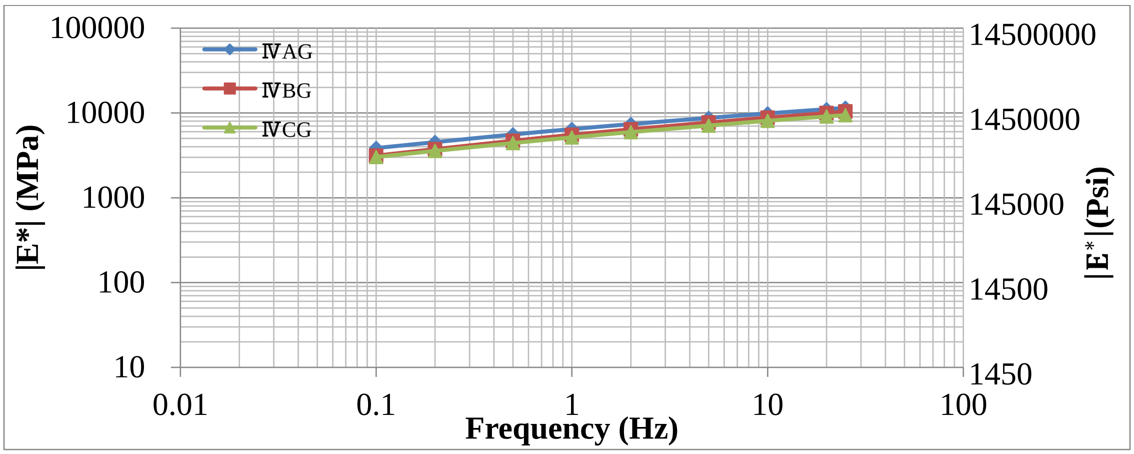

(b)

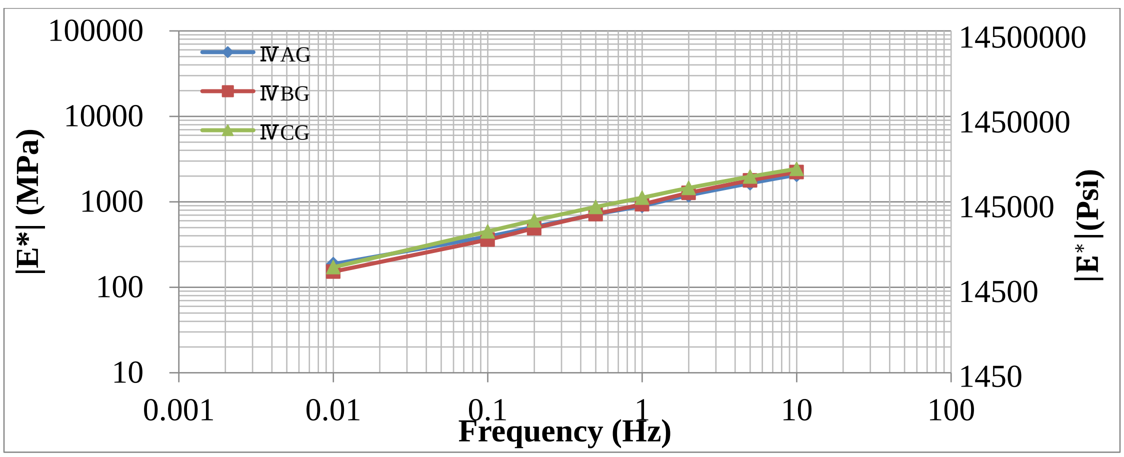

(c)

Figure 10-67 Dynamic Modulus Values of Various Mixtures from Aggregate IV with RAP after Long-Term Aging in Terms of Surface Mixture Type, (a) at 4°C (39.2°F), (b) at 20°C (68°F), (c) at 45°C (113°F) (Surface A), 40°C (104°F) (Surface B and C)

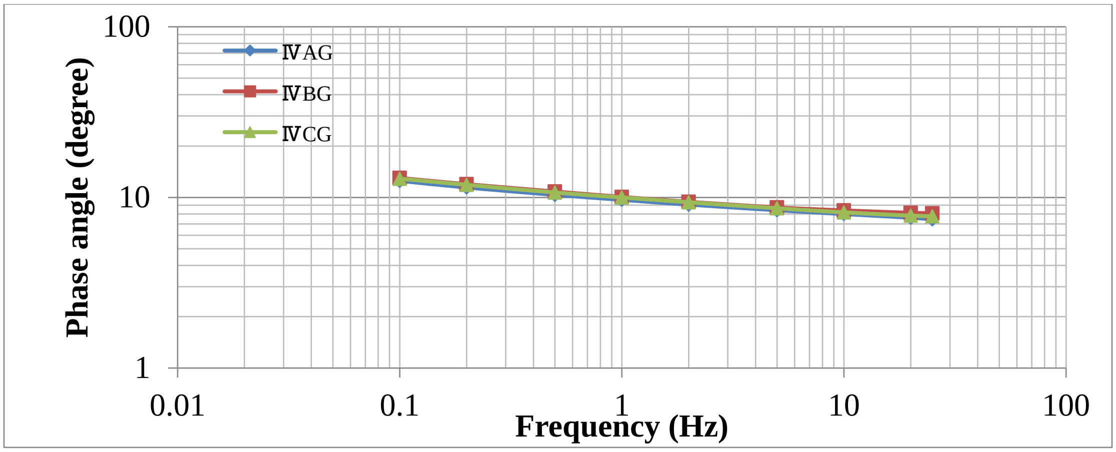

(a)

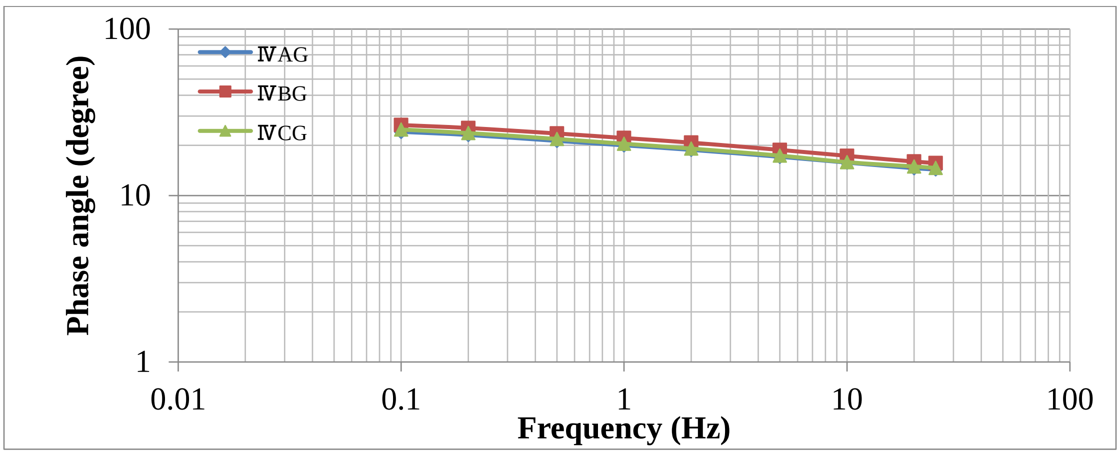

(b)

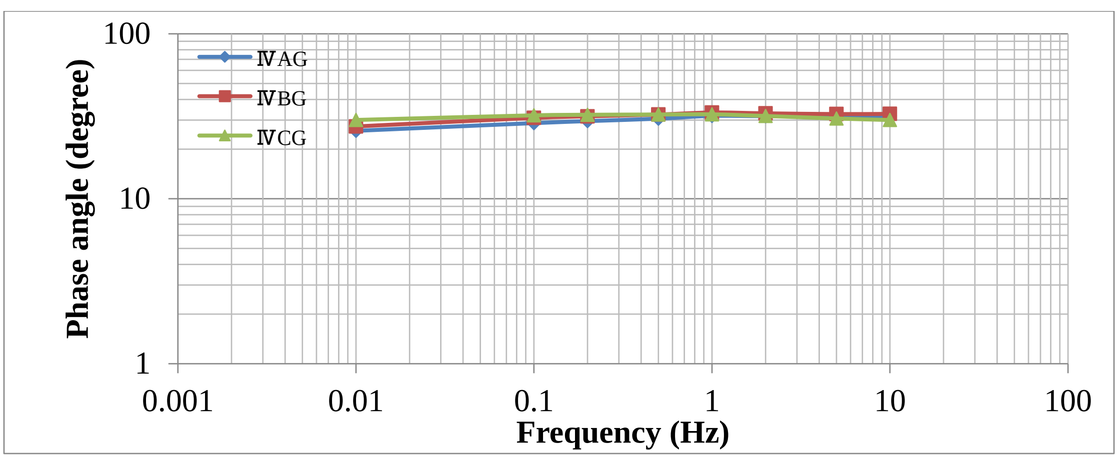

(c)

Figure 10-68 Phase Angle Values of Various Mixtures from Aggregate IV with RAP after Long-Term Aging in Terms of Surface Mixture Type, (a) at 4°C (39.2°F), (b) at 20°C (68°F), (c) at 45°C (113°F) (Surface A), 40°C (104°F) (Surface B and C)

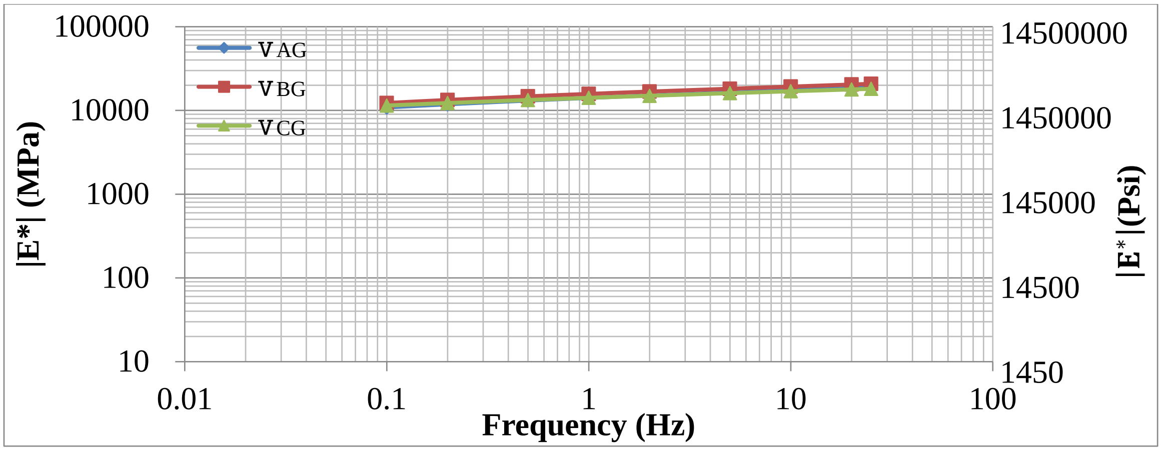

(a)

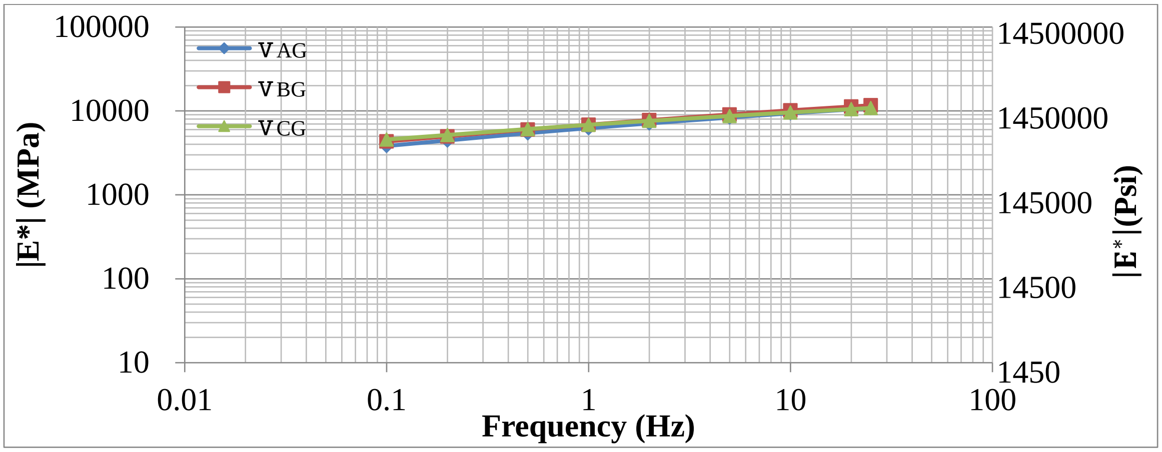

(b)

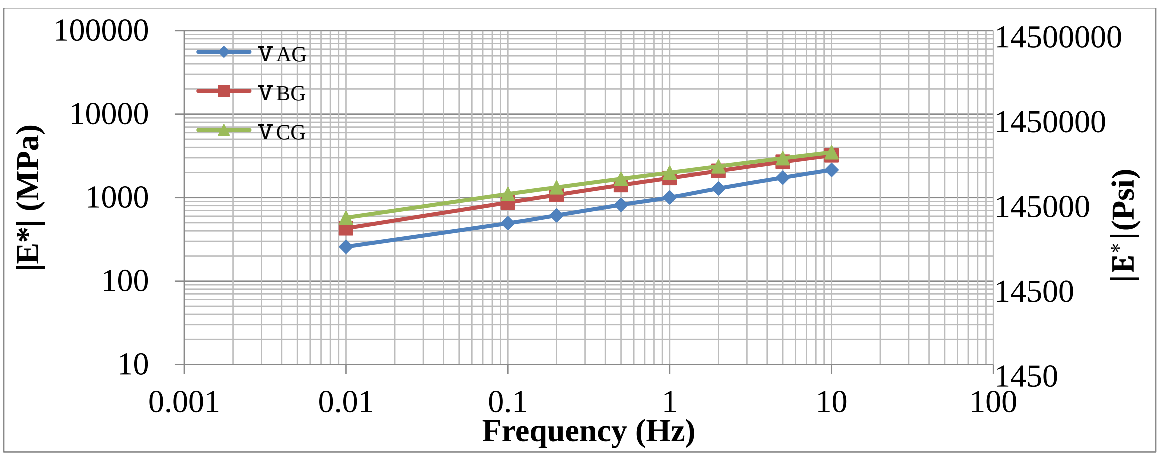

(c)

Figure 10-69 Dynamic Modulus Values of Various Mixtures from Aggregate V with RAP after Long-Term Aging in Terms of Surface Mixture Type, (a) at 4°C (39.2°F), (b) at 20°C (68°F), (c) at 45°C (113°F) (Surface A), 40°C (104°F) (Surface B and C)

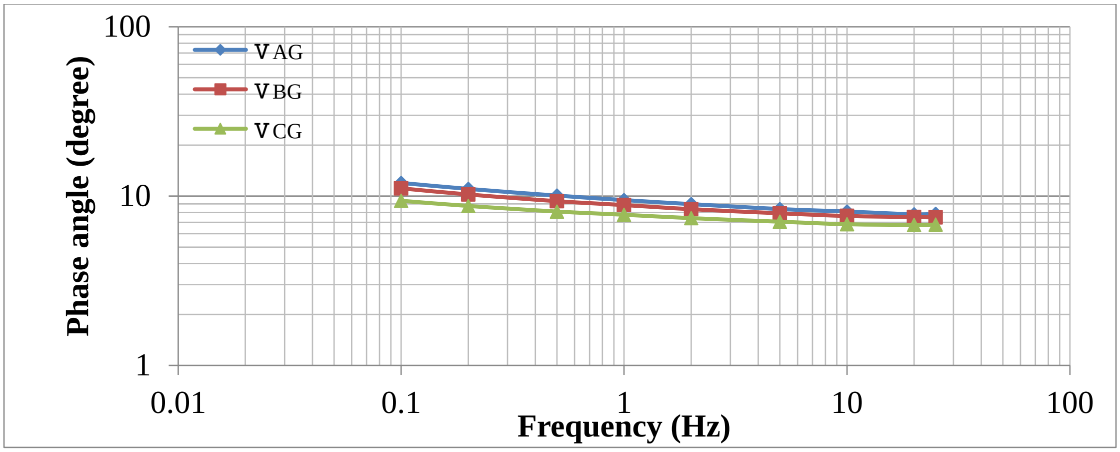

(a)

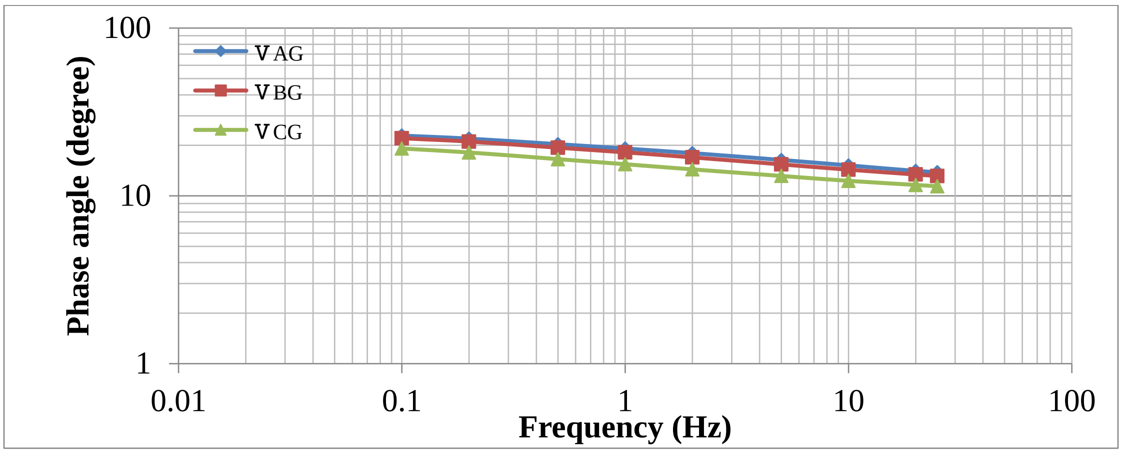

(b)

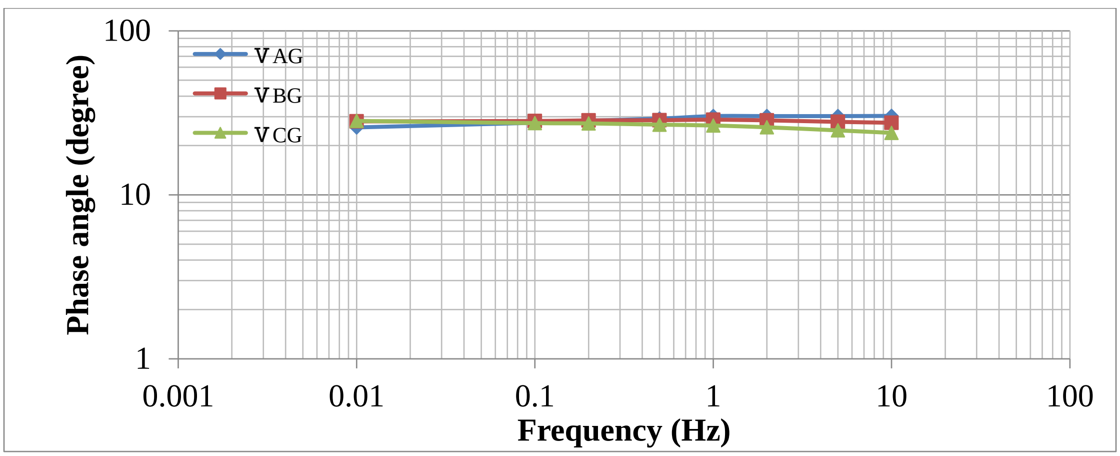

(c)

Figure 10-70 Phase Angle Values of Various Mixtures from Aggregate V with RAP after Long-Term Aging in Terms of Surface Mixture Type, (a) at 4°C (39.2°F), (b) at 20°C (68°F), (c) at 45°C (113°F) (Surface A), 40°C (104°F) (Surface B and C)

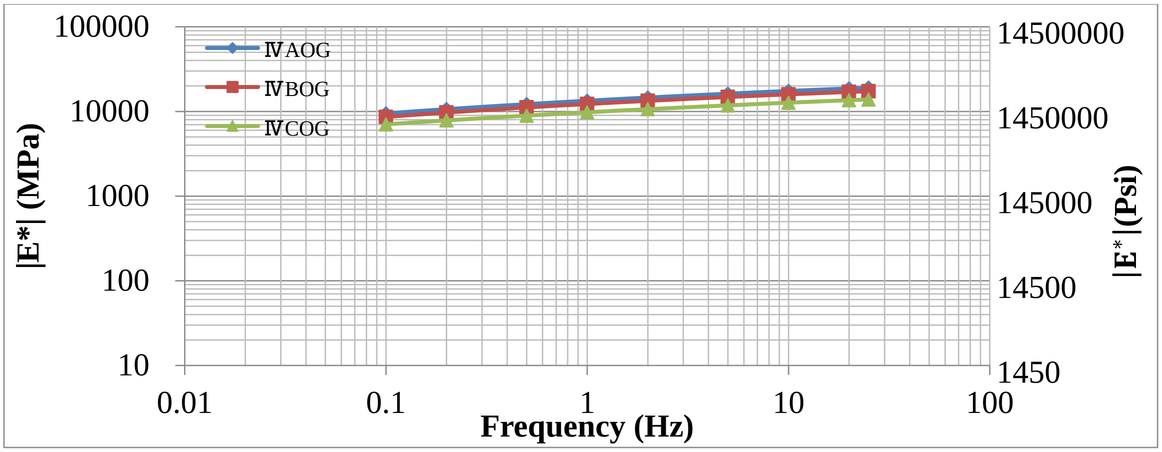

(a)

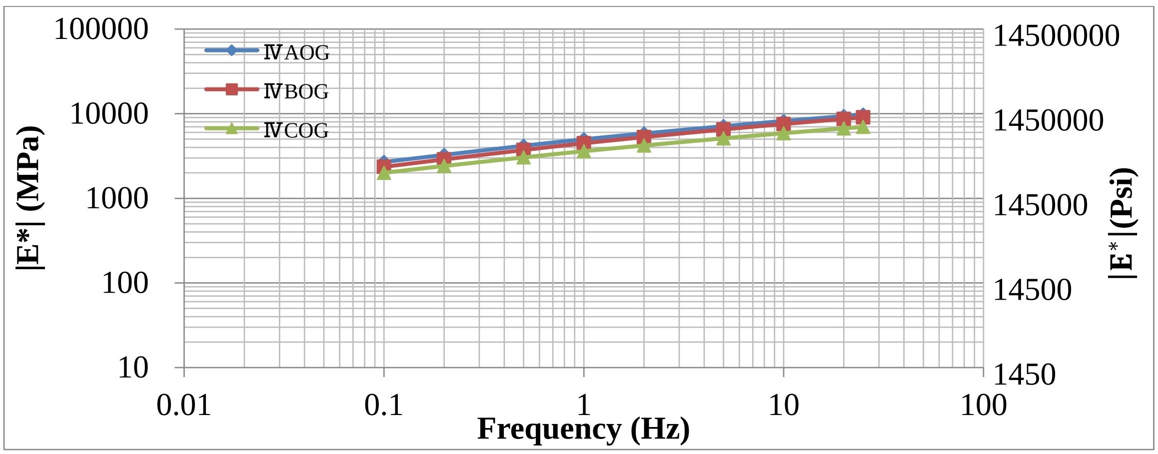

(b)

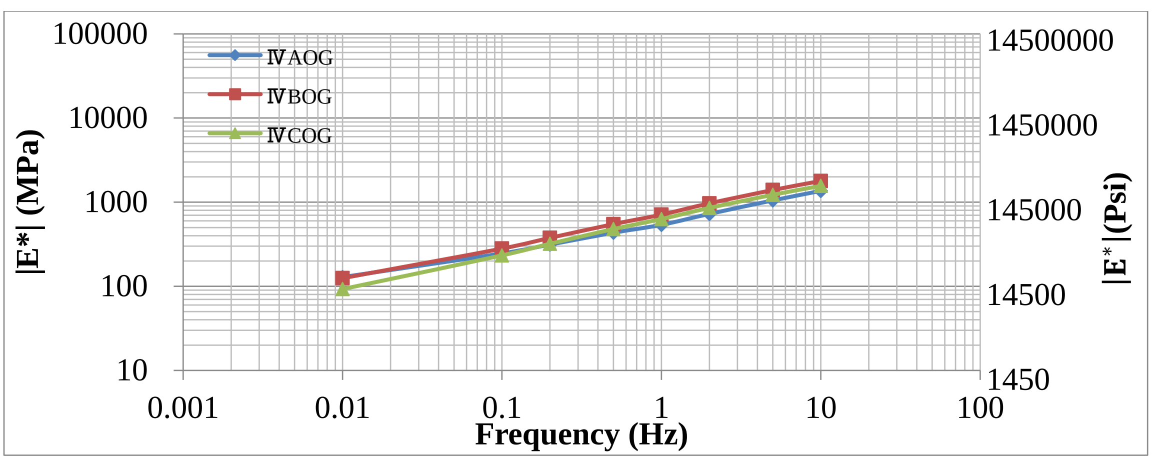

(c)

Figure 10-71 Dynamic Modulus Values of Various Mixtures from Aggregate IV without RAP after Long-Term Aging in Terms of Surface Mixture Type, (a) at 4°C (39.2°F), (b) at 20°C (68°F), (c) at 45°C (113°F) (Surface A), 40°C (104°F) (Surface B and C)

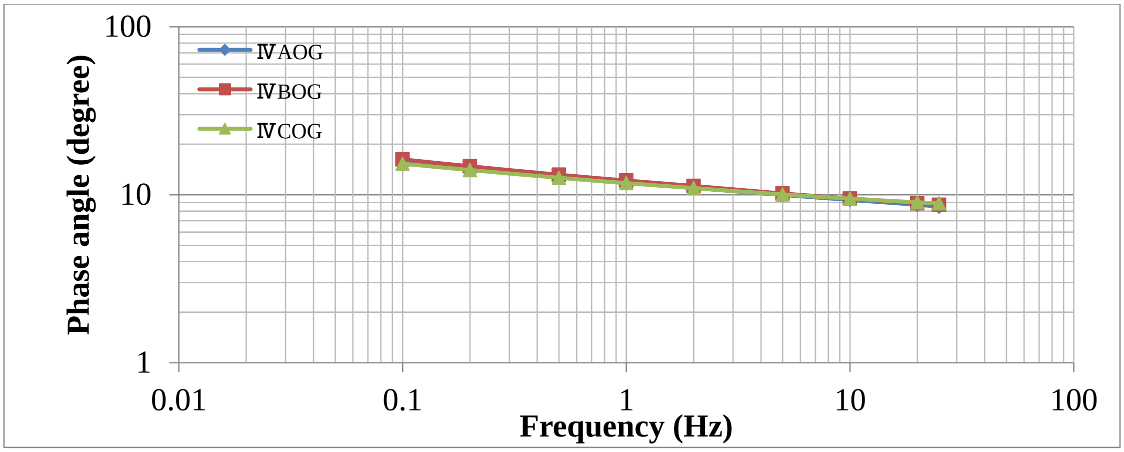

(a)

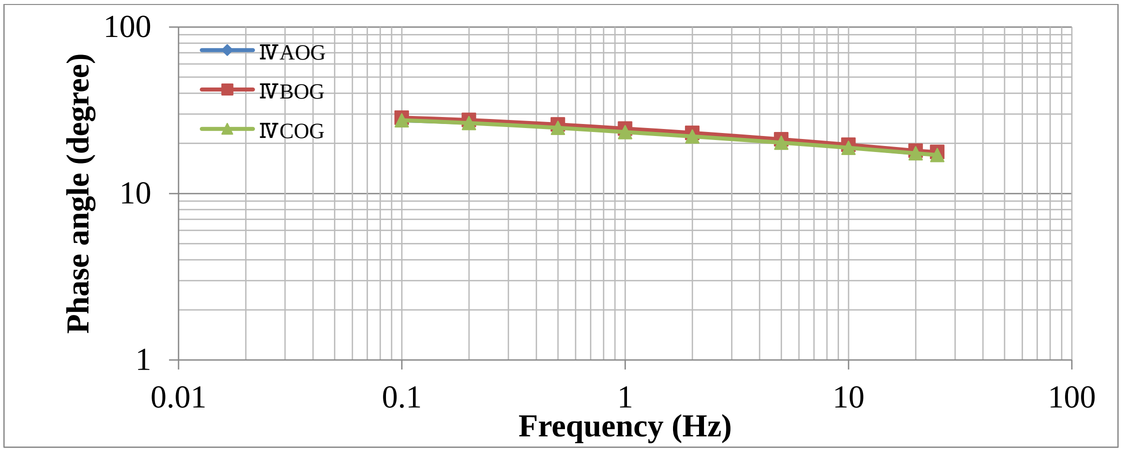

(b)

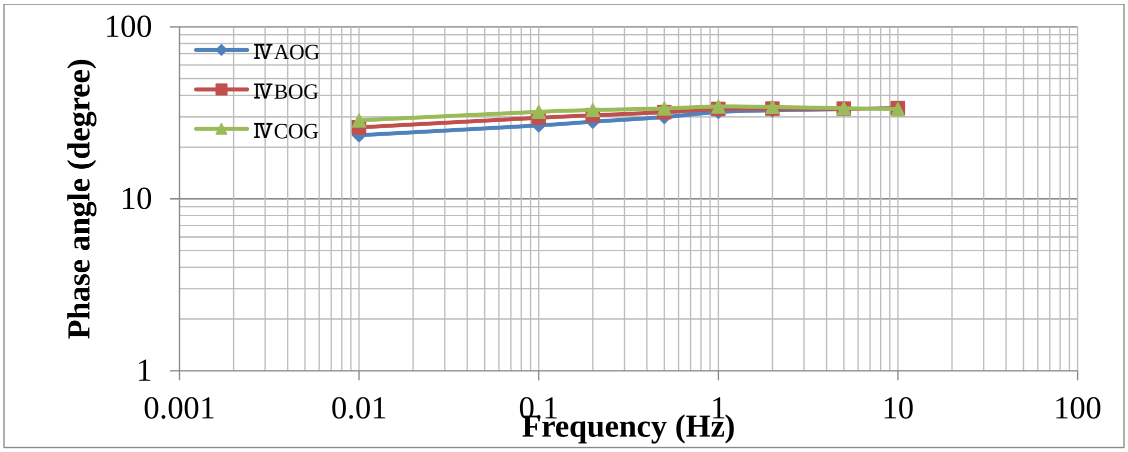

(c)

Figure 10-72 Phase Angle Values of Various Mixtures from Aggregate IV without RAP after Long-Term Aging in Terms of Surface Mixture Type, (a) at 4°C (39.2°F), (b) at 20°C (68°F), (c) at 45°C (113°F) (Surface A), 40°C (104°F) (Surface B and C)

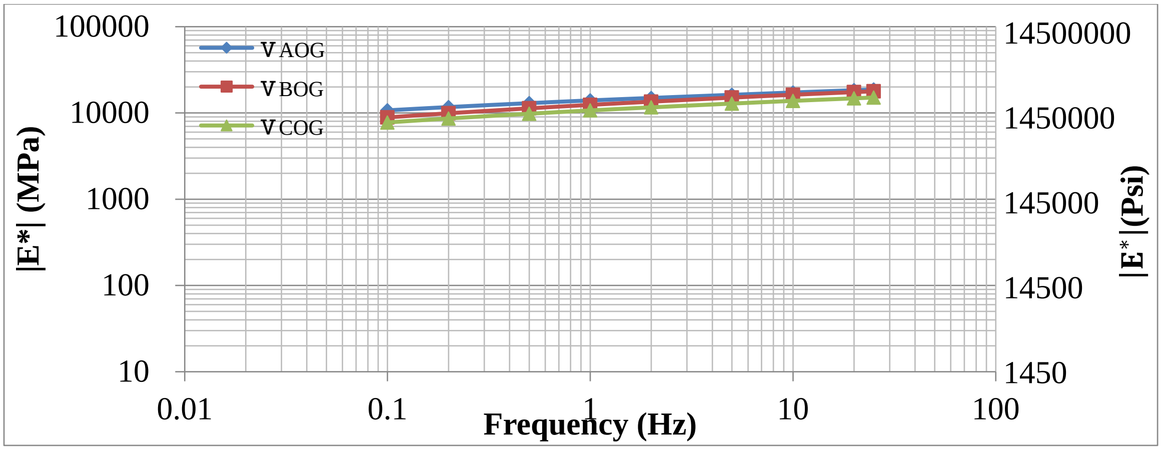

(a)

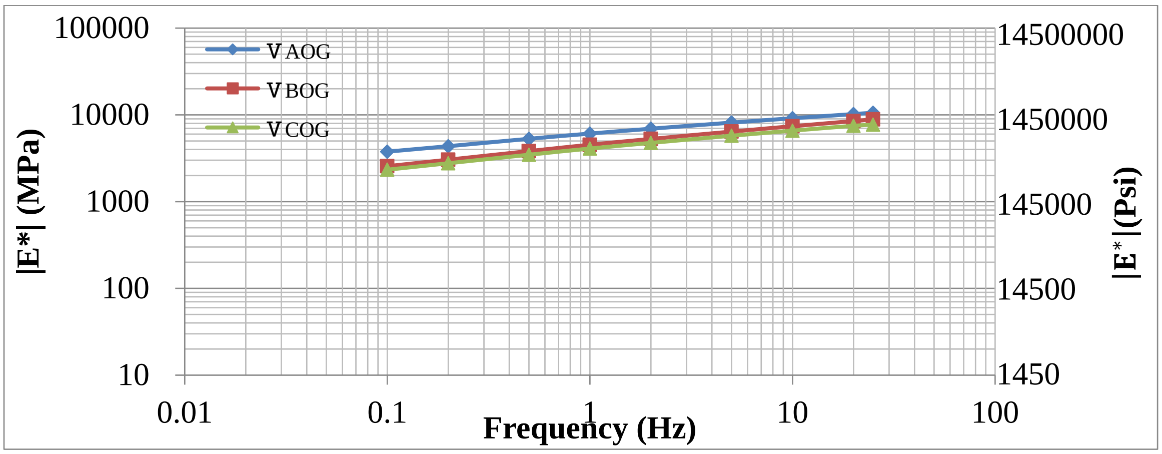

(b)

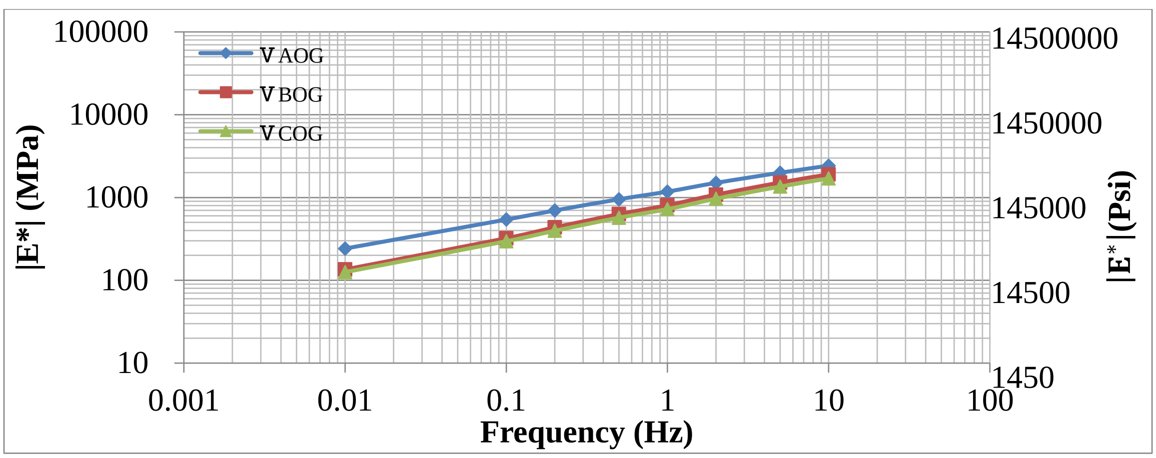

(c)

Figure 10-73 Dynamic Modulus Values of Various Mixtures from Aggregate V without RAP after Long-Term Aging in Terms of Surface Mixture Type, (a) at 4°C (39.2°F), (b) at 20°C (68°F), (c) at 45°C (113°F) (Surface A), 40°C (104°F) (Surface B, C)

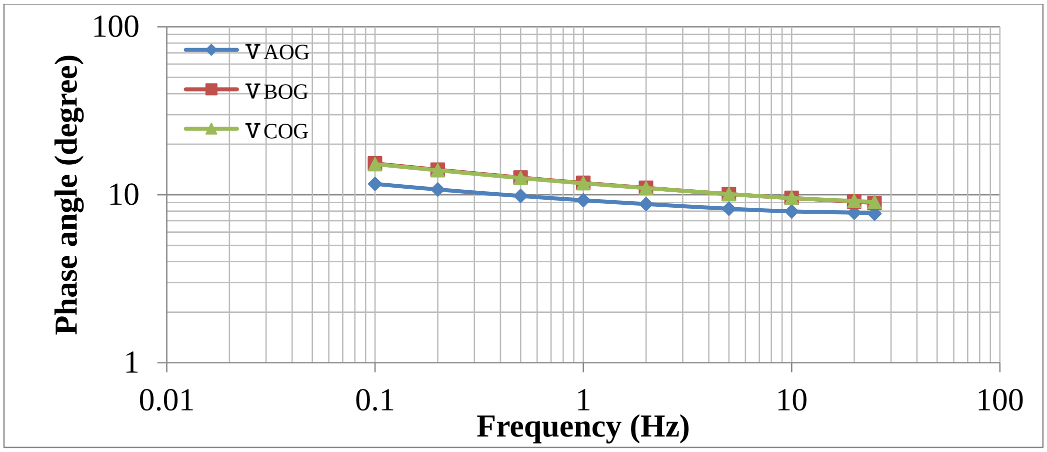

(a)

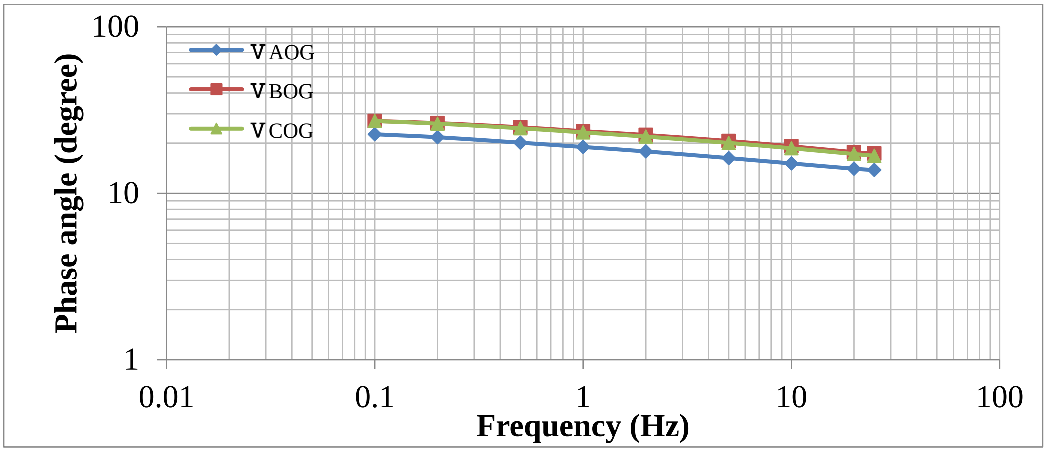

(b)

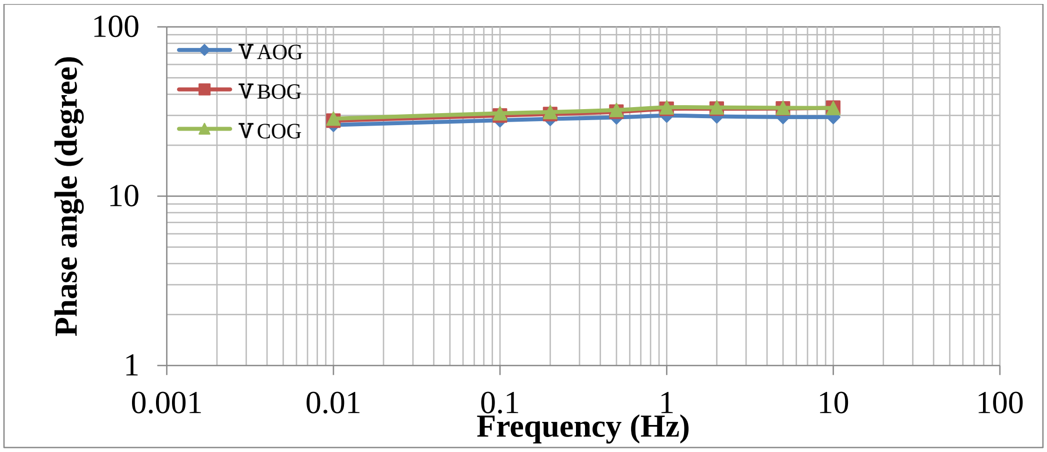

(c)

Figure 10-74 Phase Angle Values of Various Mixtures from Aggregate V without RAP after Long-Term Aging in Terms of Surface Mixture Type, (a) at 4°C (39.2°F), (b) at 20°C (68°F), (c) at 45°C (113°F) (Surface A), 40°C (104°F) (Surface B and C)

11 Appendix C - Flow Numbers of Various Mixtures Tested

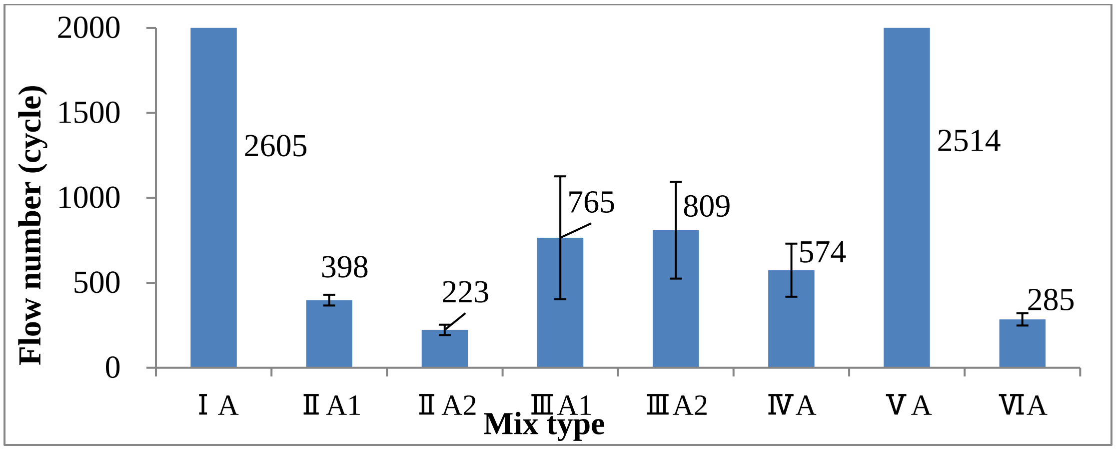

Figure 11-1 Flow Numbers of Various Surface Type A Mixtures with RAP in Terms of Aggregate Source at 59°C (138.2°F)

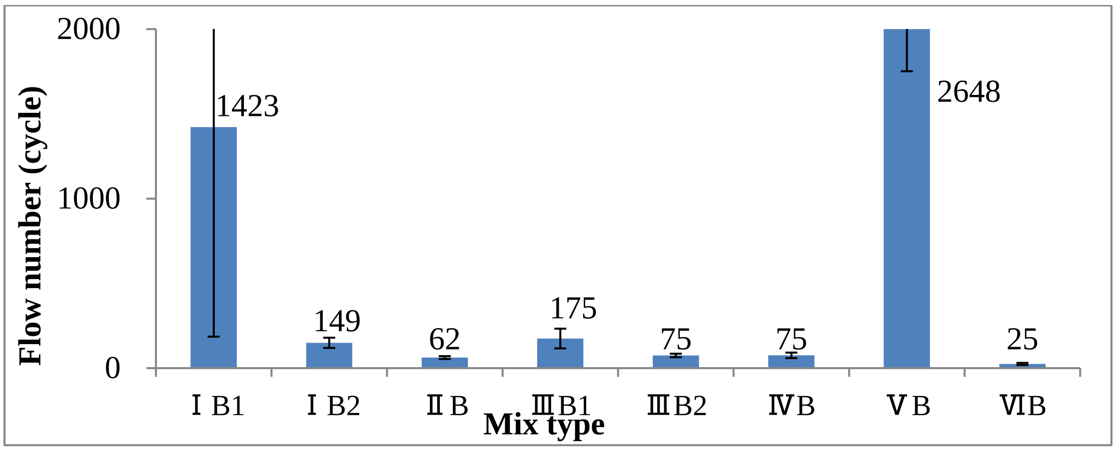

Figure 11-2 Flow Numbers of Various Surface Type B Mixtures with RAP in Terms of Aggregate Source at 59°C (138.2°F)

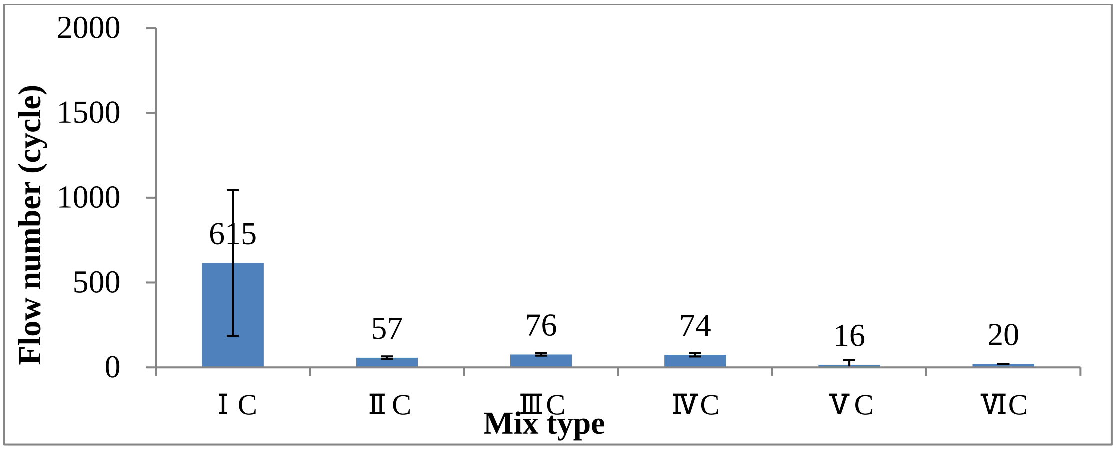

Figure 11-3 Flow Numbers of Various Surface Type C Mixtures with RAP in Terms of Aggregate Source at 59°C (138.2°F)

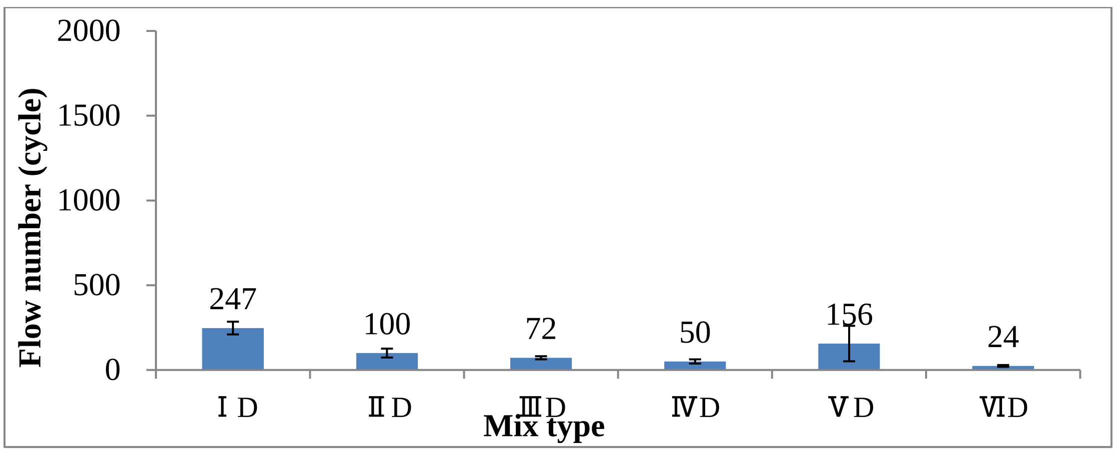

Figure 11-4 Flow Numbers of Various Surface Type D Mixtures with RAP in Terms of Aggregate Source at 59°C (138.2°F)

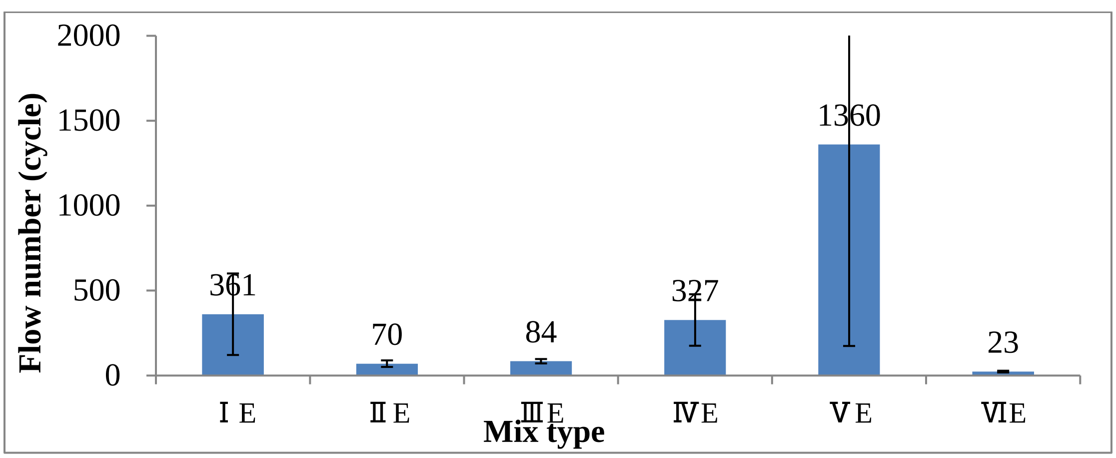

Figure 11-5 Flow Numbers of Various Surface Type E Mixtures with RAP in Terms of Aggregate Source 59°C (138.2°F)

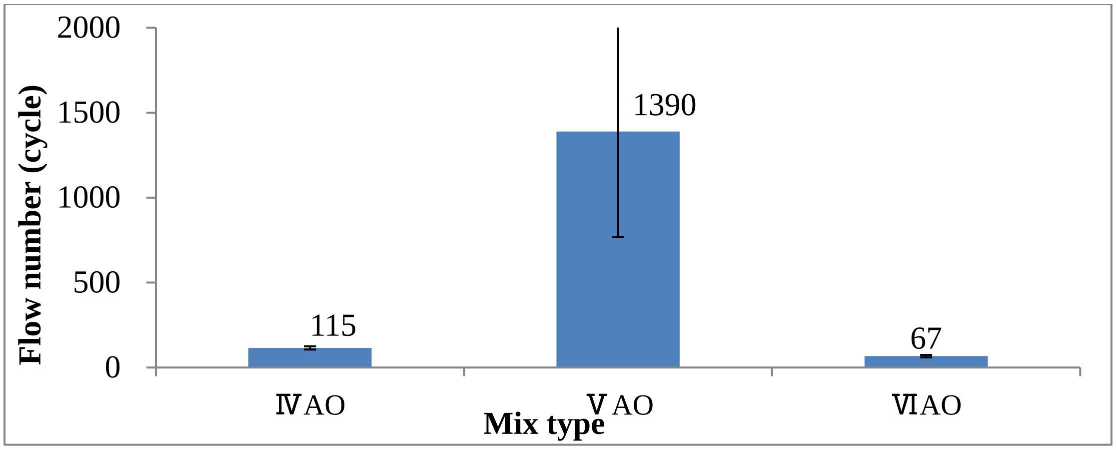

Figure 11-6 Flow Numbers of Various Surface Type A Mixtures without RAP in Terms of Aggregate Source at 59°C (138.2°F)

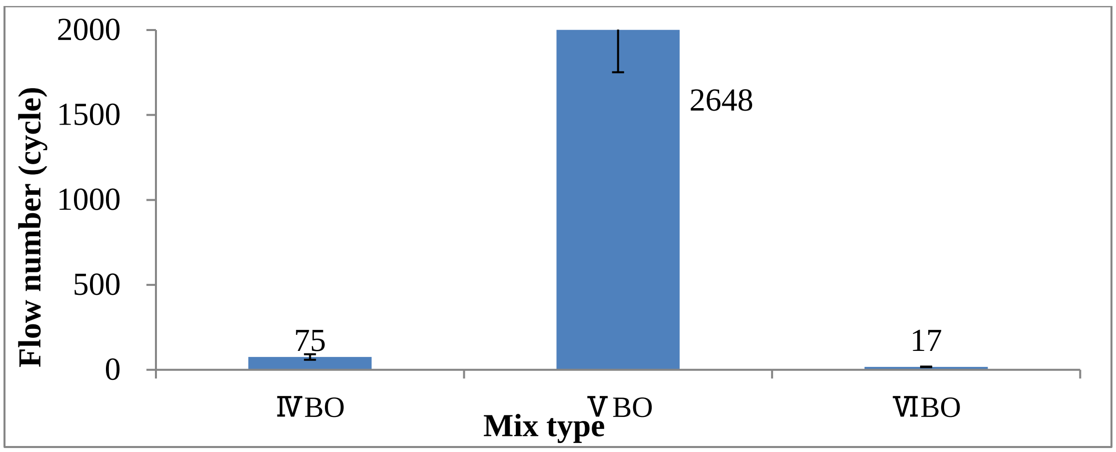

Figure 11-7 Flow Numbers of Various Surface Type B Mixtures without RAP in Terms of Aggregate Source at 59°C (138.2°F)

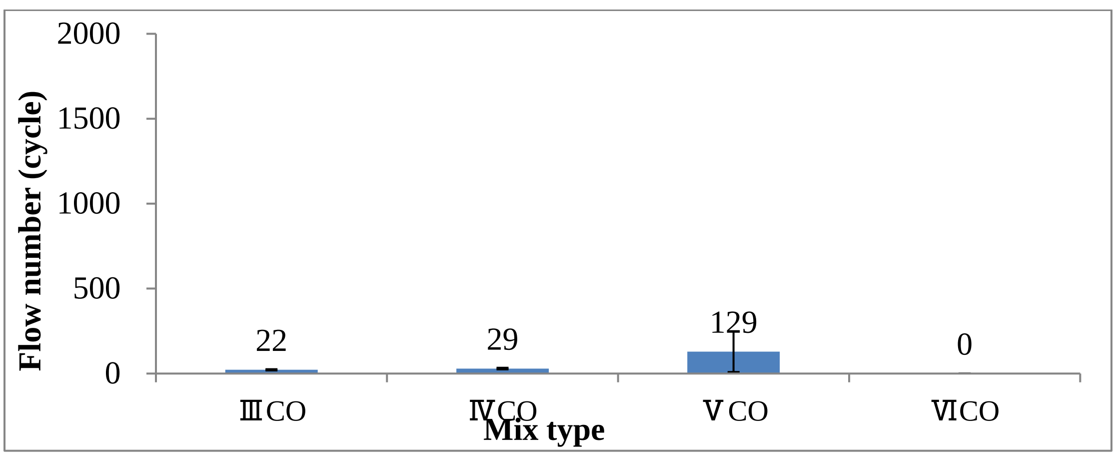

Figure 11-8 Flow Numbers of Various Surface Type C Mixtures without RAP in Terms of Aggregate Source at 59°C (138.2°F)

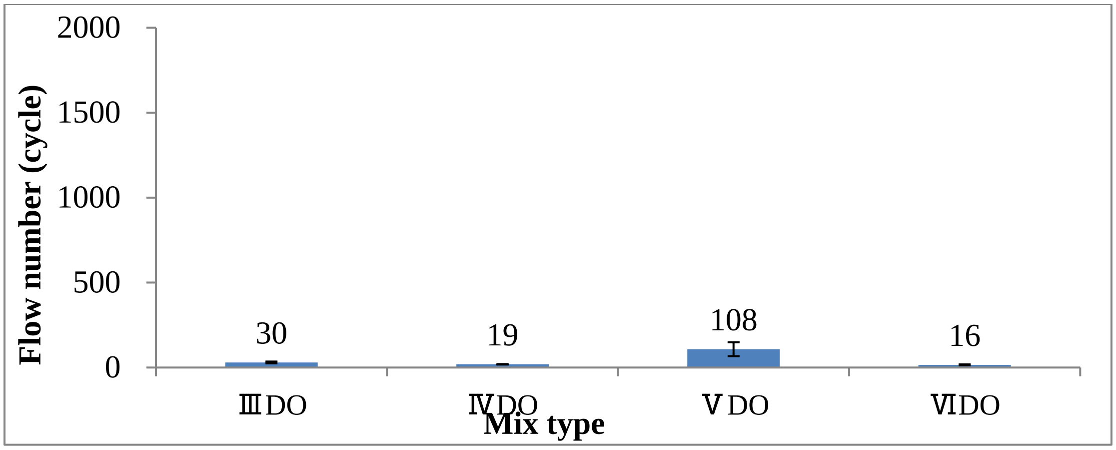

Figure 11-9 Flow Numbers of Various Surface Type D Mixtures without RAP in Terms of Aggregate Source at 59°C (138.2°F)

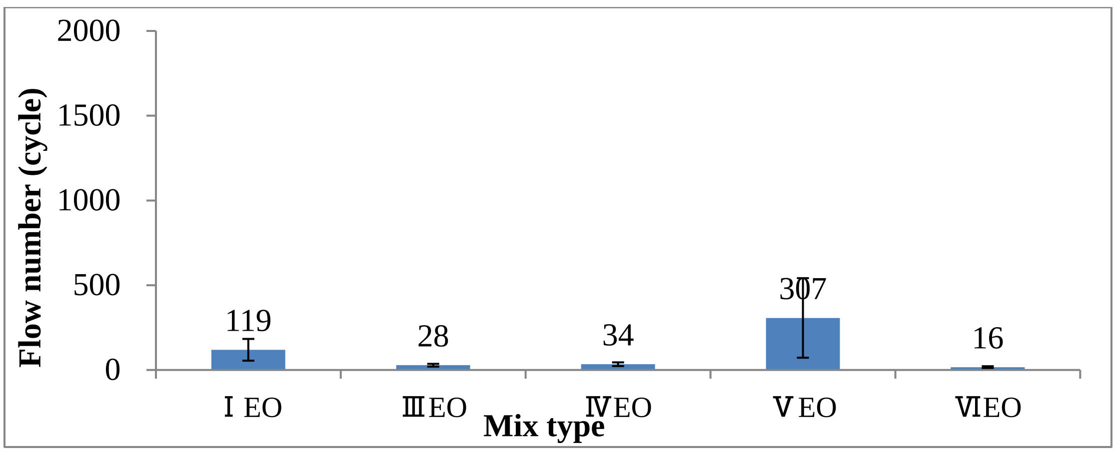

Figure 11-10 Flow Numbers of Various Surface Type E Mixtures without RAP in Terms of Aggregate Source at 59°C (138.2°F)

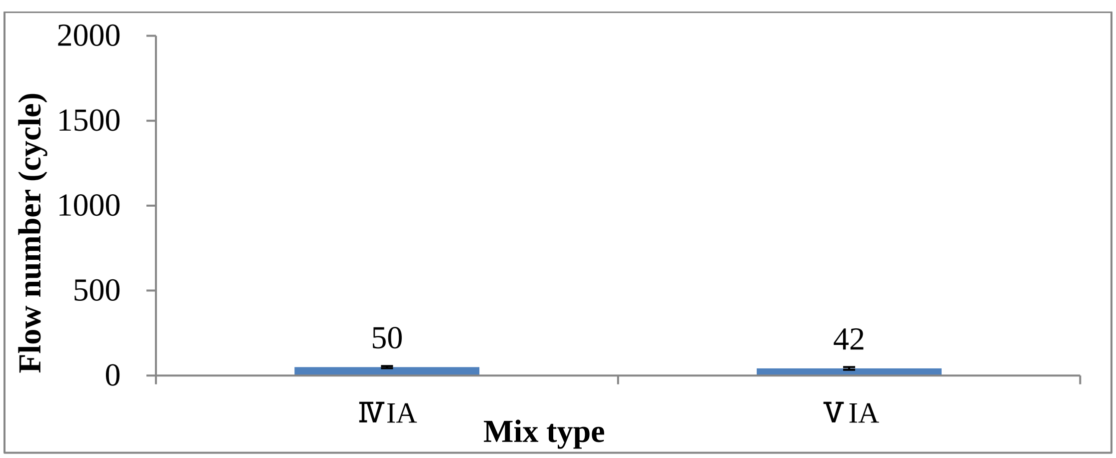

Figure 11-11 Flow Numbers of Various Intermediate Type A Mixtures with RAP in Terms of Aggregate Source at 59°C (138.2°F)

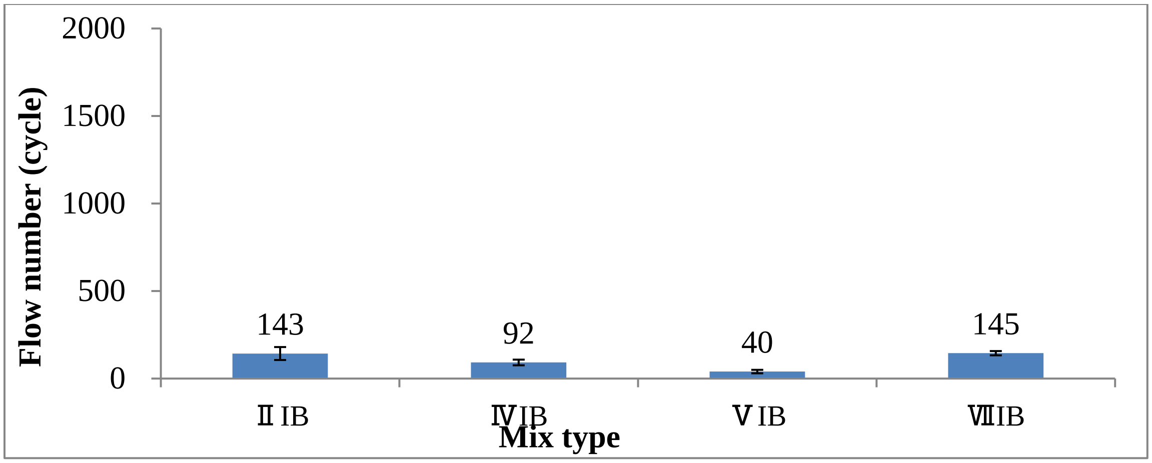

Figure 11-12 Flow Numbers of Various Intermediate Type B Mixtures with RAP in Terms of Aggregate Source at 59°C (138.2°F)

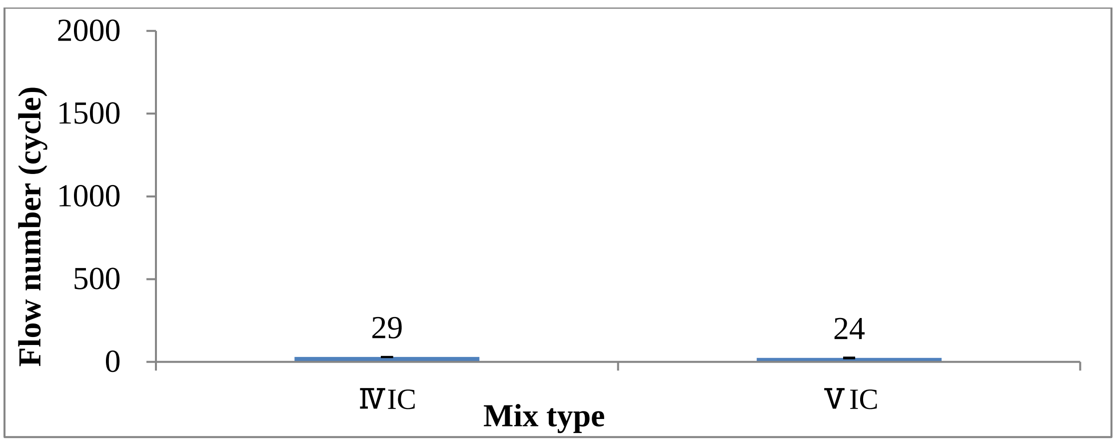

Figure 11-13 Flow Numbers of Various Intermediate Type C Mixtures with RAP in Terms of Aggregate Source at 59°C (138.2°F)

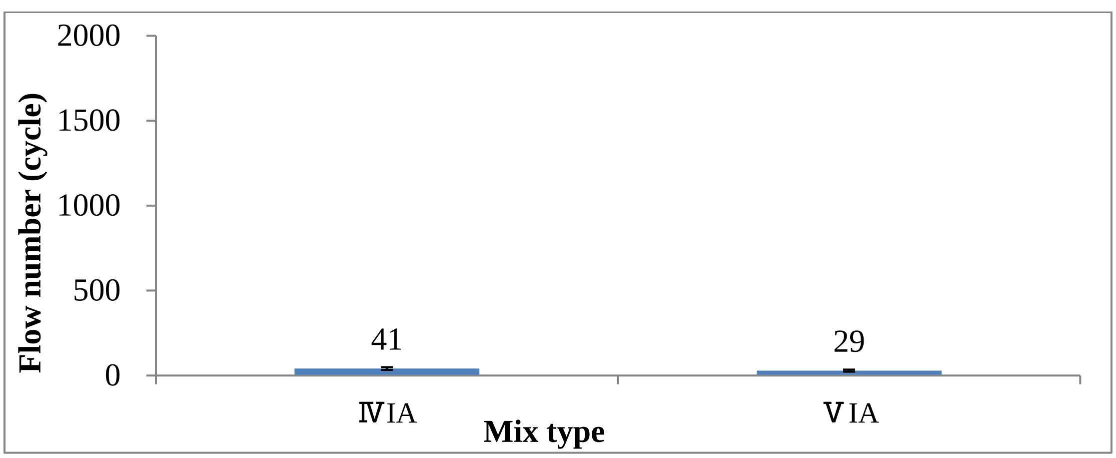

Figure 11-14 Flow Numbers of Various Intermediate Type A Mixtures without RAP in Terms of Aggregate Source at 59°C (138.2°F)

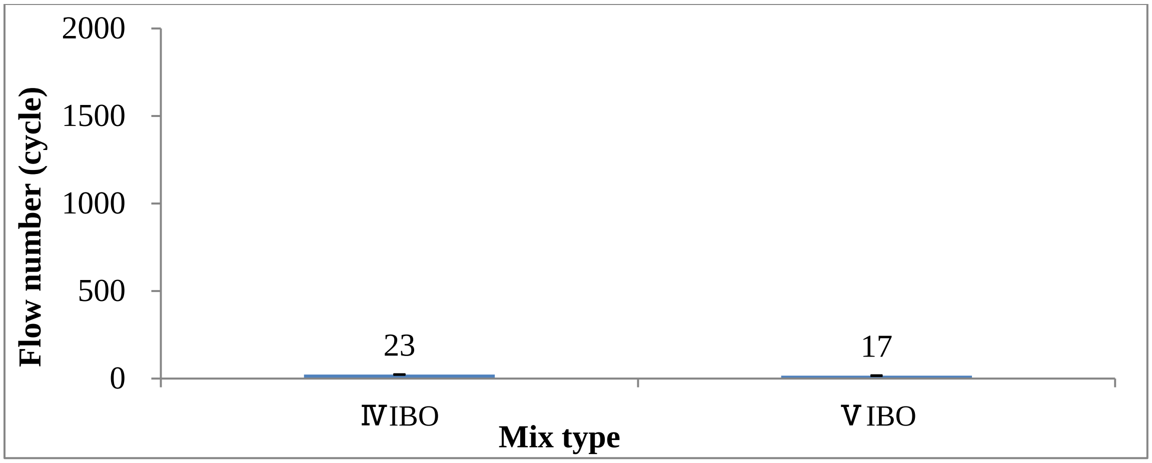

Figure 11-15 Flow Numbers of Various Intermediate Type B Mixtures without RAP in Terms of Aggregate Source at 59°C (138.2°F)

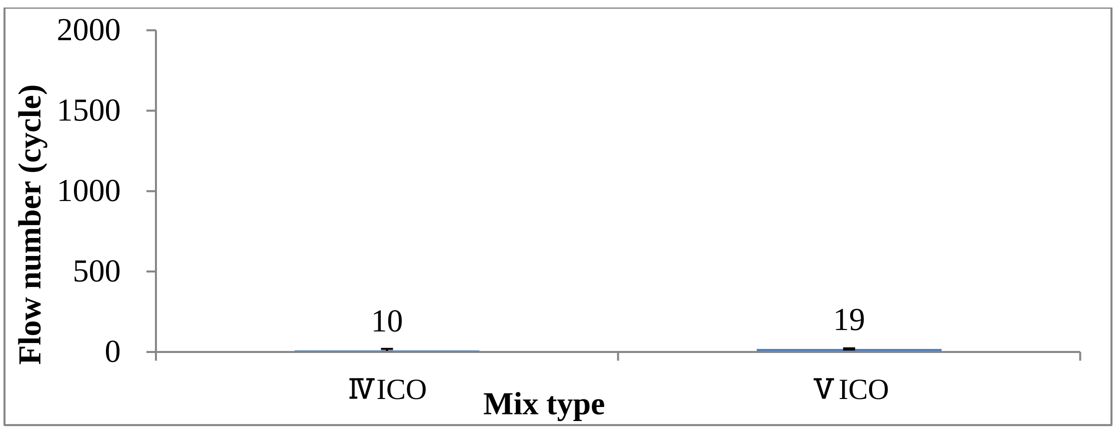

Figure 11-16 Flow Numbers of Various Intermediate Type C Mixtures without RAP in Terms of Aggregate Source at 59°C (138.2°F)

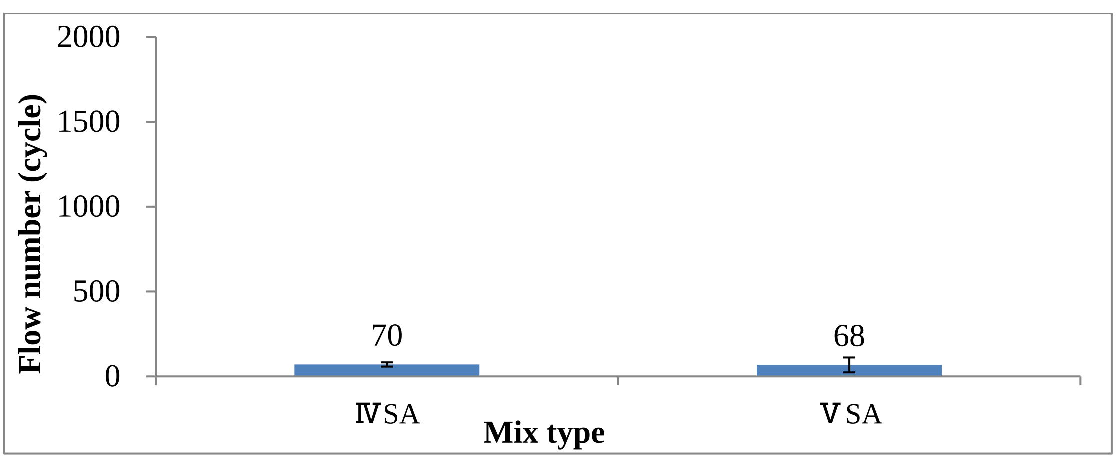

Figure 11-17 Flow Numbers of Various Base Type A Mixtures with RAP in Terms of Aggregate Source at 59°C (138.2°F)

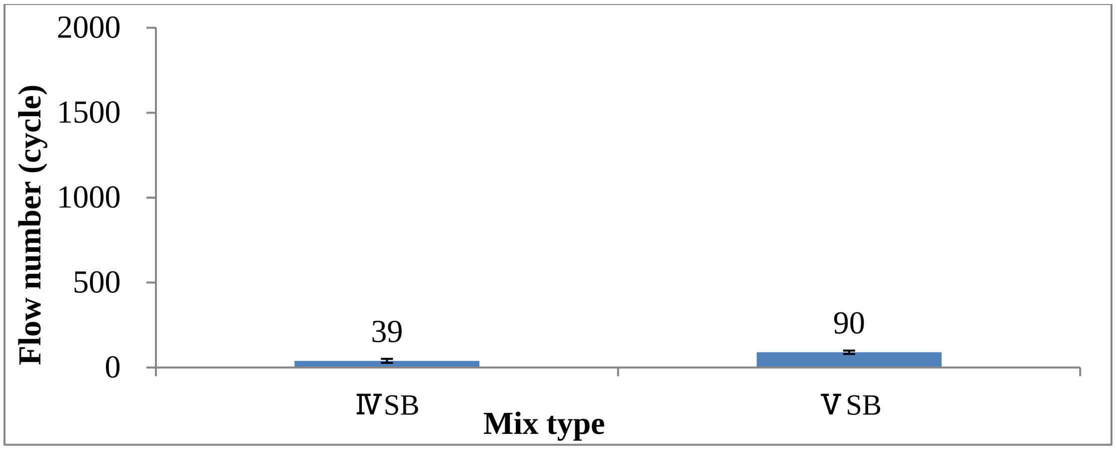

Figure 11-18 Flow Numbers of Various Base Type B Mixtures with RAP in Terms of Aggregate Source at 59°C (138.2°F)

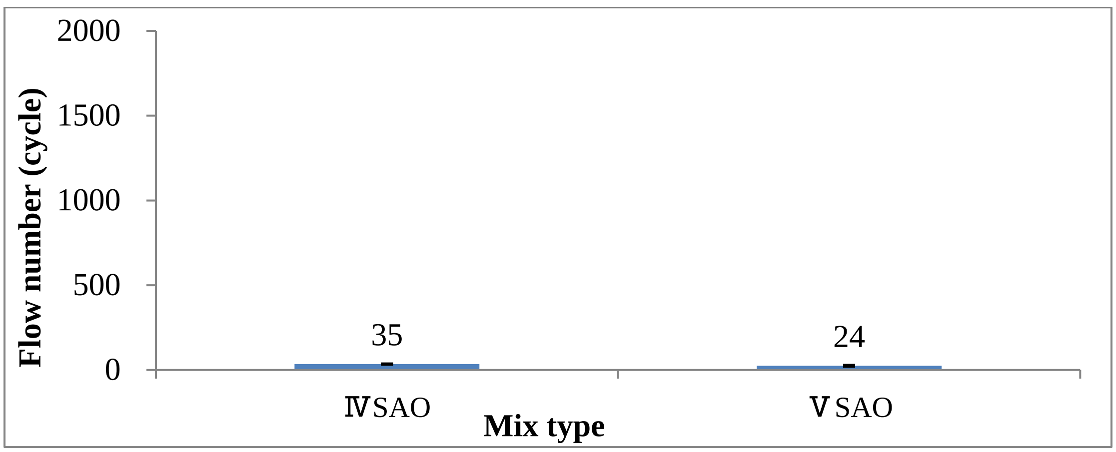

Figure 11-19 Flow Numbers of Various Base Type A Mixtures without RAP in Terms of Aggregate Source at 59°C (138.2°F)

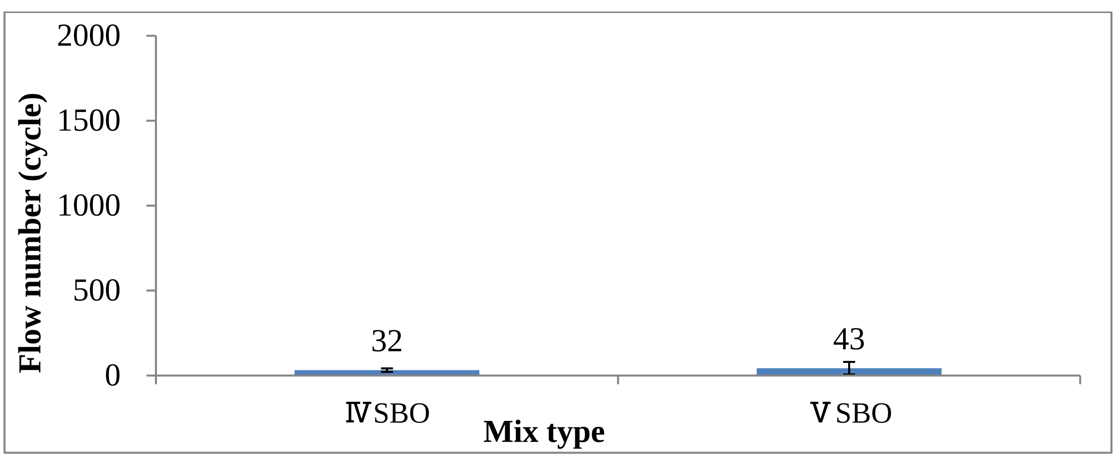

Figure 11-20 Flow Numbers of Various Base Type B Mixtures without RAP in Terms of Aggregate Source at 59°C (138.2°F)

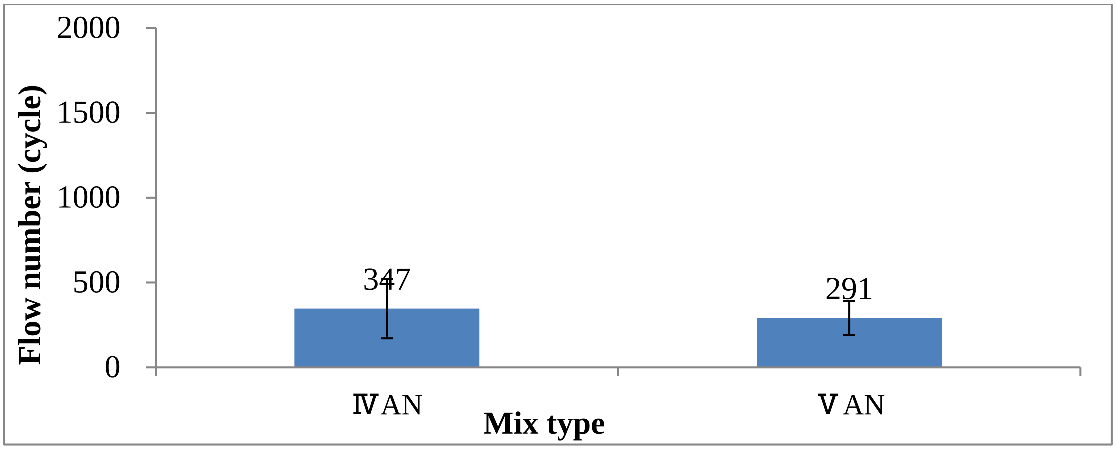

Figure 11-21 Flow Numbers of Various Surface Type A Mixtures with RAP and Asphalt Source 2 in Terms of Aggregate Source at 59°C (138.2°F)

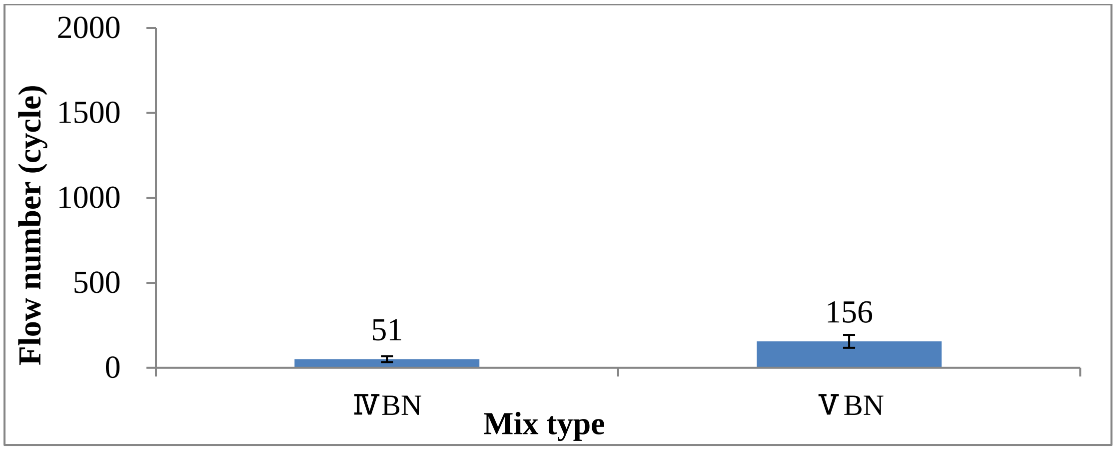

Figure 11-22 Flow Numbers of Various Surface Type B Mixtures with RAP and Asphalt Source 2 in Terms of Aggregate Source at 59°C (138.2°F)

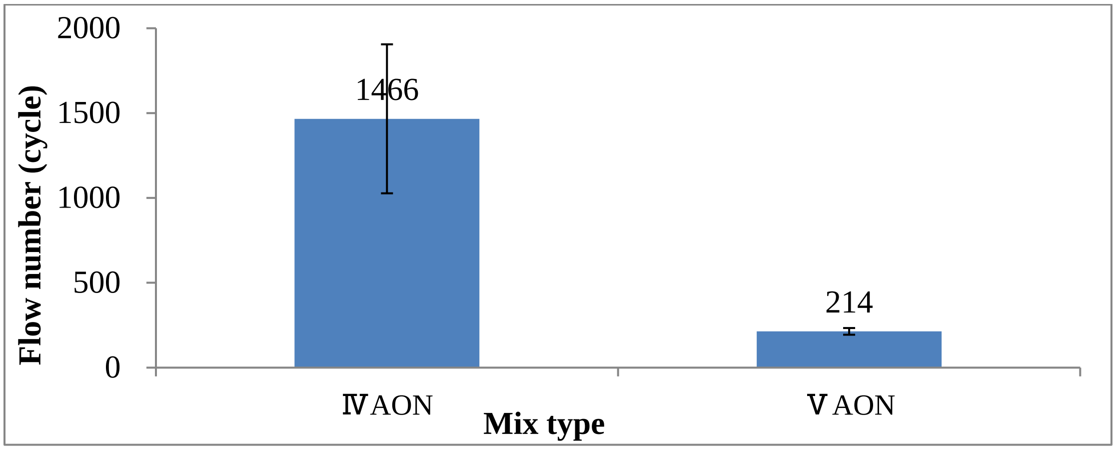

Figure 11-23 Flow Numbers of Various Surface Type A Mixtures using Asphalt Source 2 without RAP in Terms of Aggregate Source at 59°C (138.2°F)

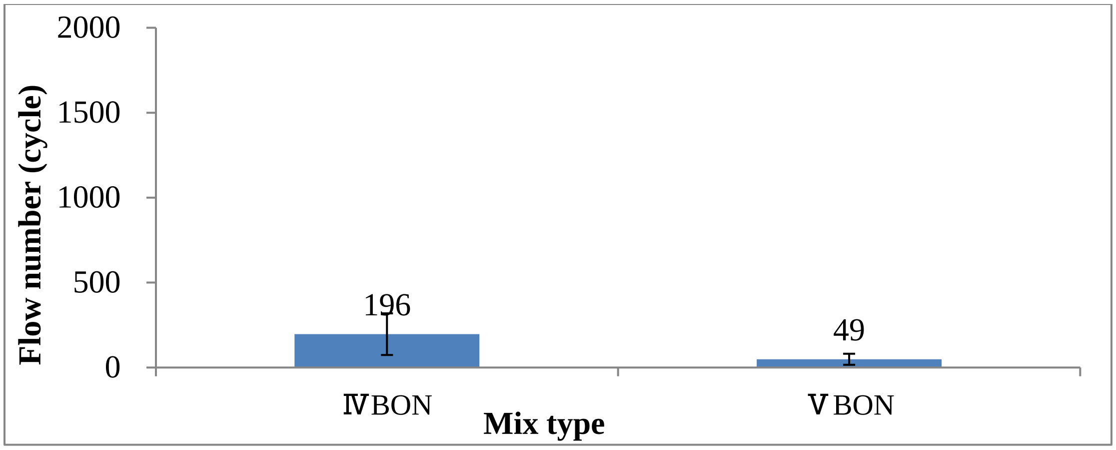

Figure 11-24 Flow Numbers of Various Surface Type B Mixtures using Asphalt Source 2 without RAP in Terms of Aggregate Source at 59°C (138.2°F)

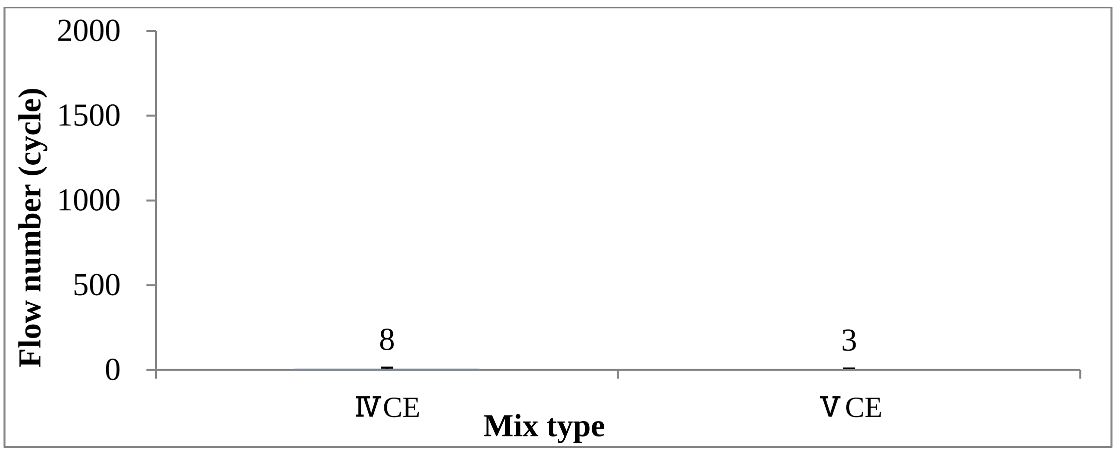

Figure 11-25 Flow Numbers of Various Surface Type C Mixtures with RAP and WMA-Chemical Additive in Terms of Aggregate Source at 59°C (138.2°F)

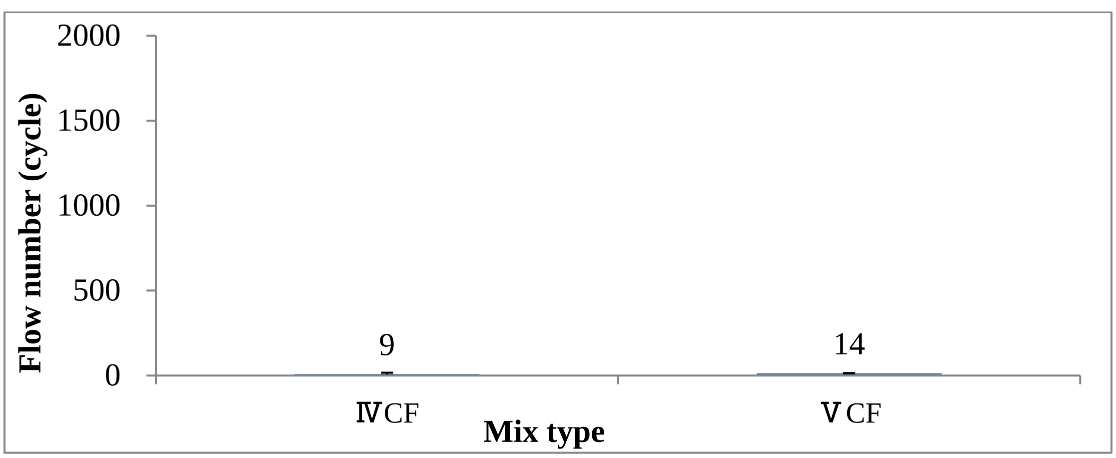

Figure 11-26 Flow Numbers of Various Surface Type C Mixtures with RAP and WMA-Foaming in Terms of Aggregate Source at 59°C (138.2°F)

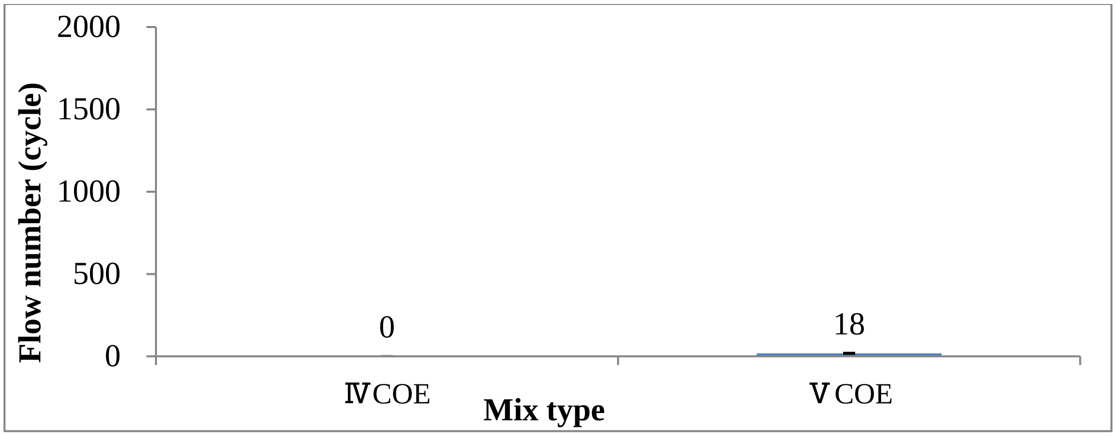

Figure 11-27 Flow Numbers of Various Surface Type C Mixtures using WMA-Chemical Additive without RAP in Terms of Aggregate Source at 59°C (138.2°F)

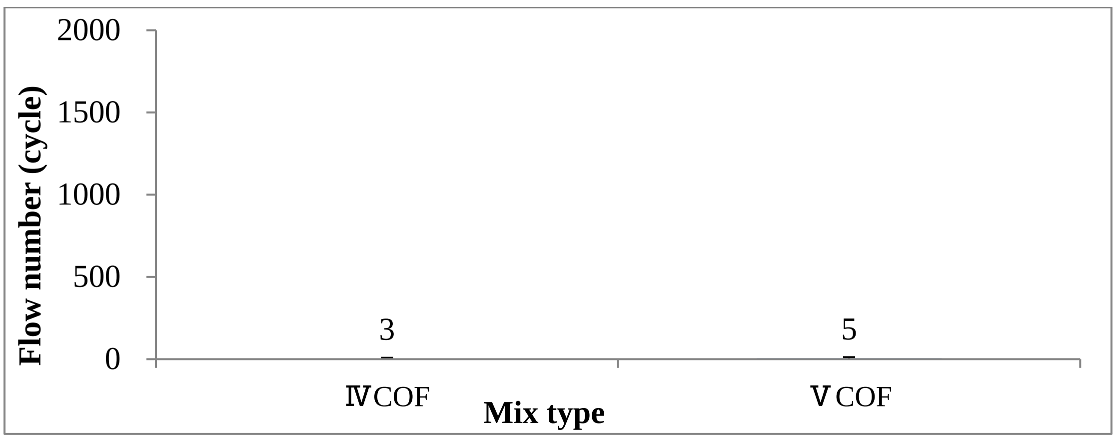

Figure 11-28 Flow Numbers of Various Surface Type C Mixtures using WMA-Foaming without RAP in Terms of Aggregate Source at 59°C (138.2°F)

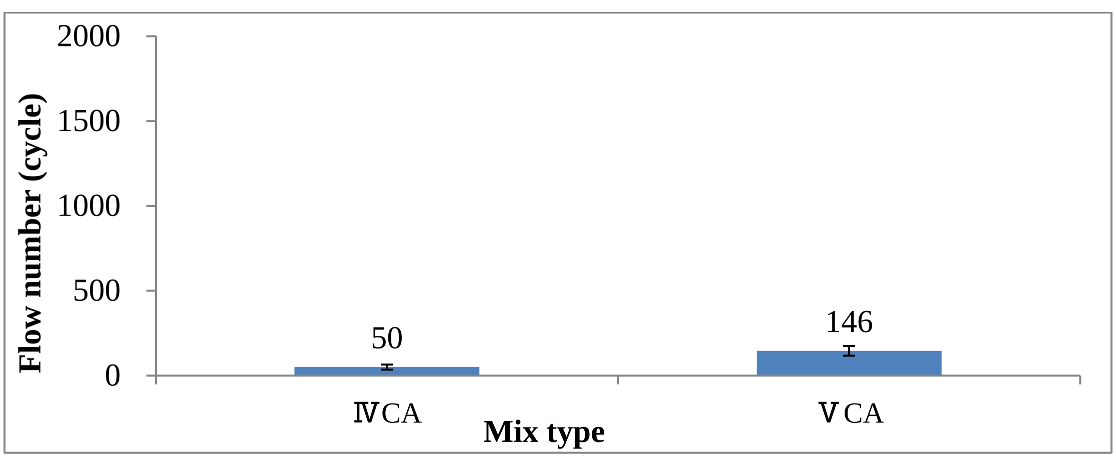

Figure 11-29 Flow Numbers of Various Surface Type C Mixtures with RAP and Liquid ASA1 in Terms of Aggregate Source at 59°C (138.2°F)

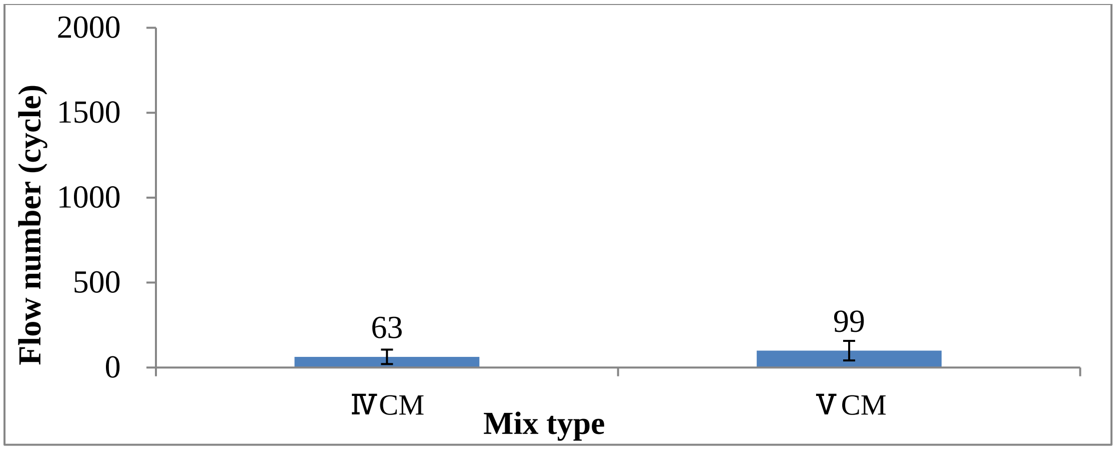

Figure 11-30 Flow Numbers of Various Surface Type C Mixtures with RAP and Liquid ASA2 in Terms of Aggregate Source at 59°C (138.2°F)

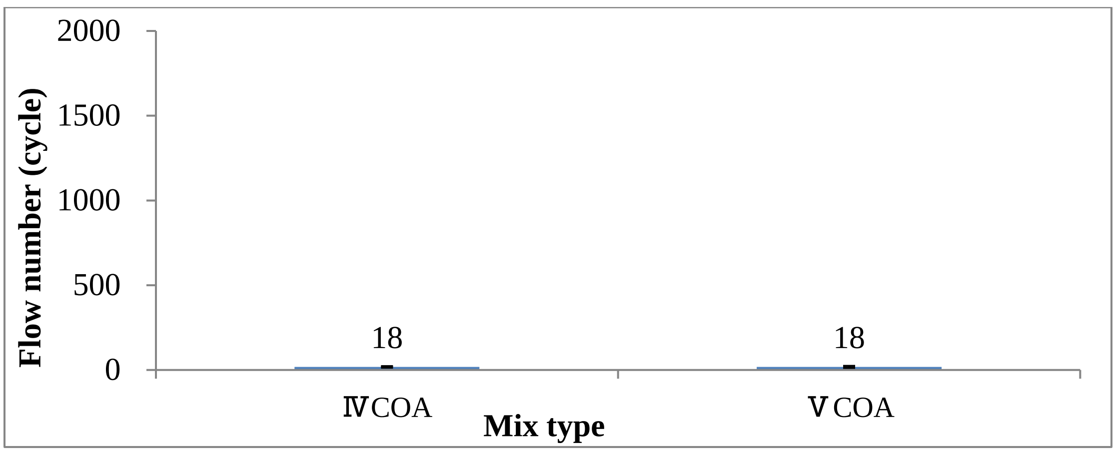

Figure 11-31 Flow Numbers of Various Surface Type C Mixtures using Liquid ASA1 without RAP in Terms of Aggregate Source at 59°C (138.2°F)

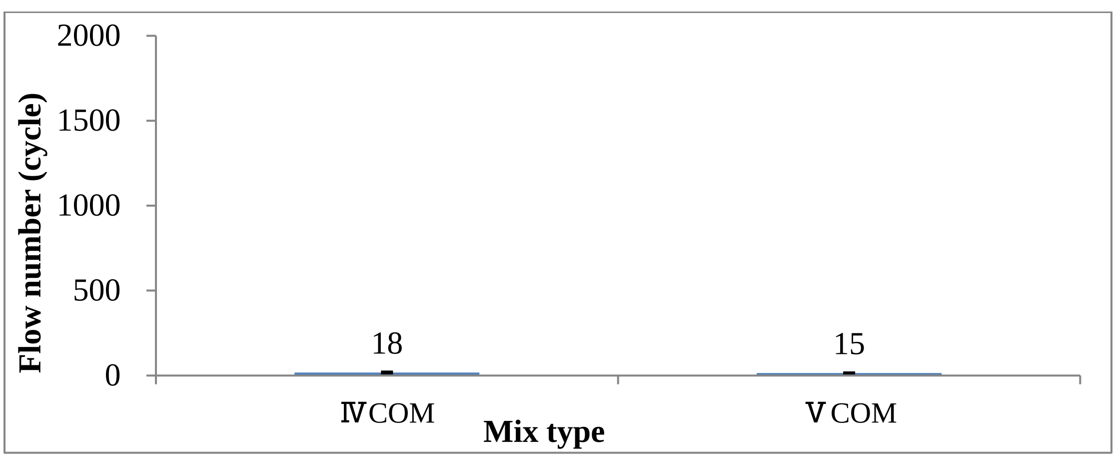

Figure 11-32 Flow Numbers of Various Surface Type C Mixtures using Liquid ASA2 without RAP in Terms of Aggregate Source at 59°C (138.2°F)

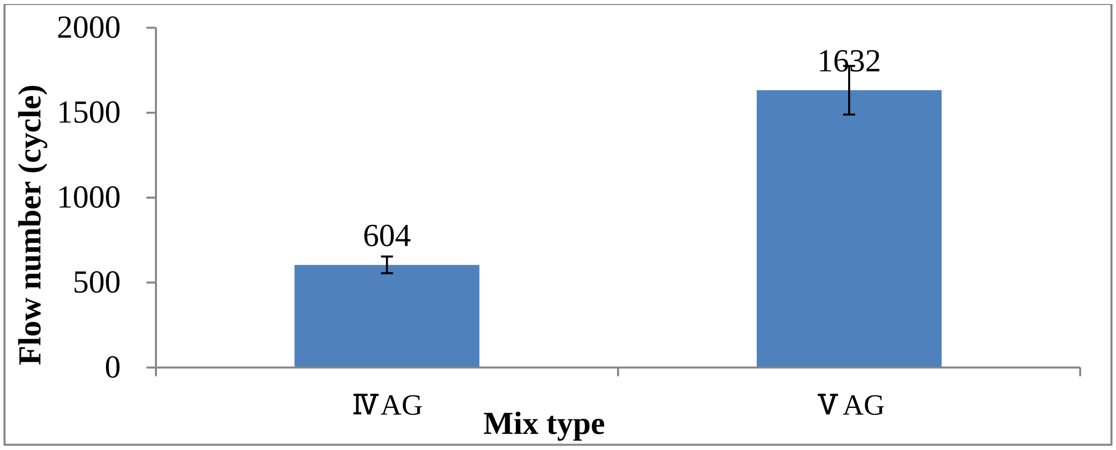

Figure 11-33 Flow Numbers of Various Surface Type A Mixtures with RAP after Long-Term Aging in Terms of Aggregate Source at 59°C (138.2°F)

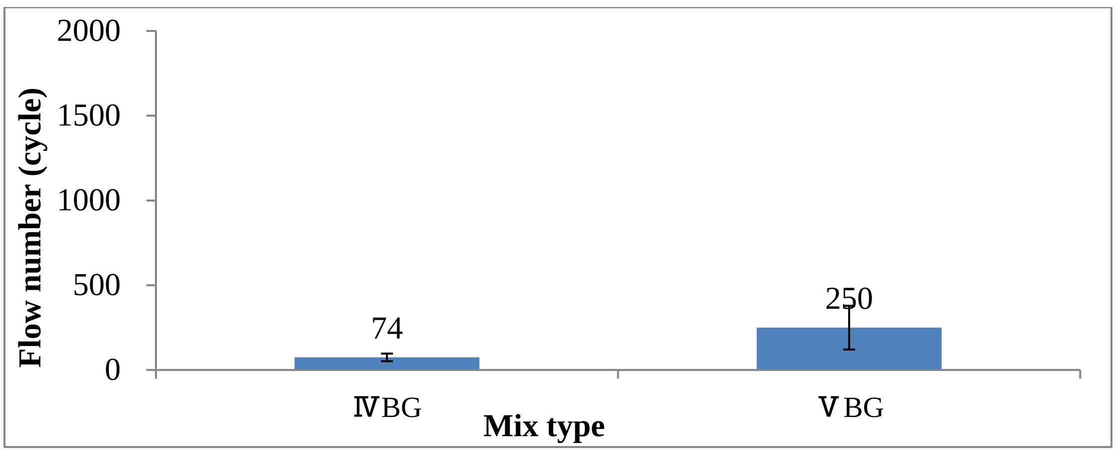

Figure 11-34 Flow Numbers of Various Surface Type B Mixtures with RAP after Long-Term Aging in Terms of Aggregate Source at 59°C (138.2°F)

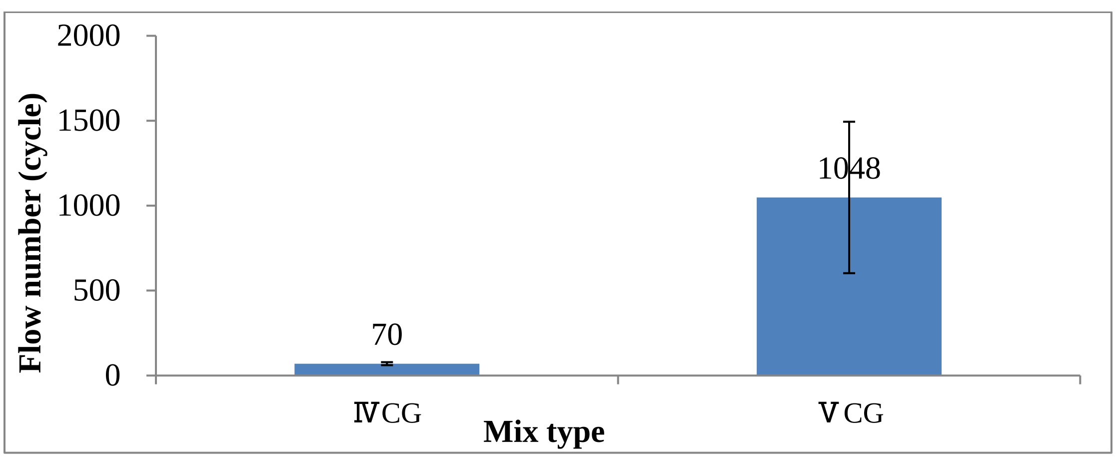

Figure 11-35 Flow Numbers of Various Surface Type C Mixtures with RAP after Long-Term Aging in Terms of Aggregate Source at 59°C (138.2°F)

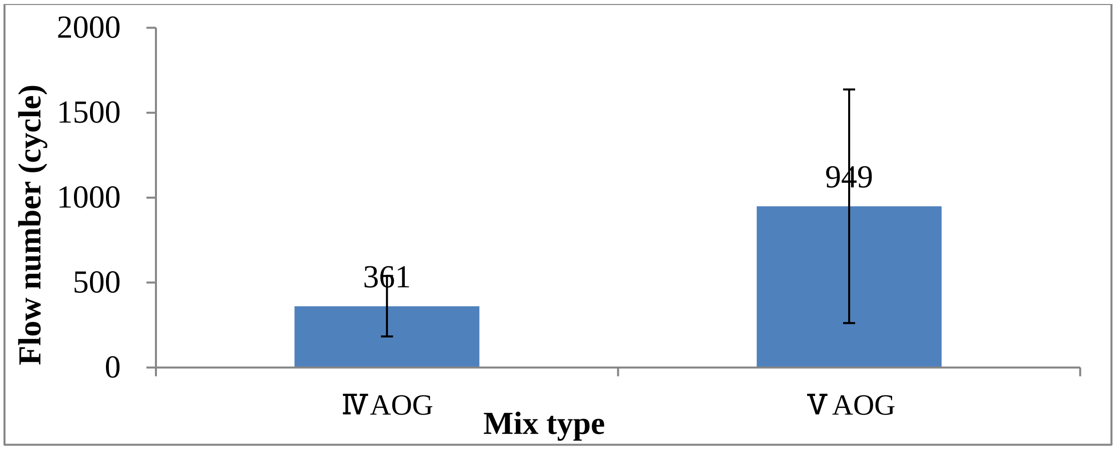

Figure 11-36 Flow Numbers of Various Surface Type A Mixtures without RAP after Long-Term Aging in Terms of Aggregate Source at 59°C (138.2°F)

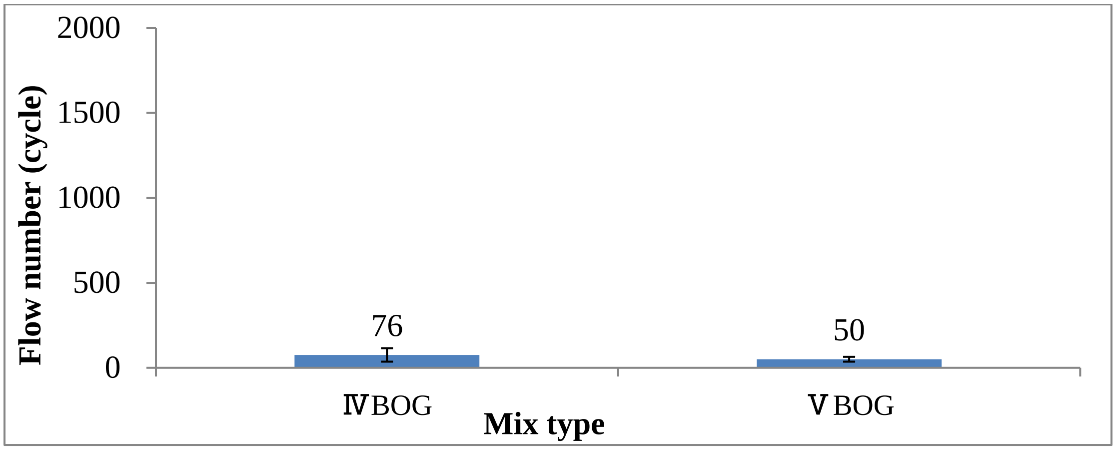

Figure 11-37 Flow Numbers of Various Surface Type B Mixtures without RAP after Long-Term Aging in Terms of Aggregate Source at 59°C (138.2°F)

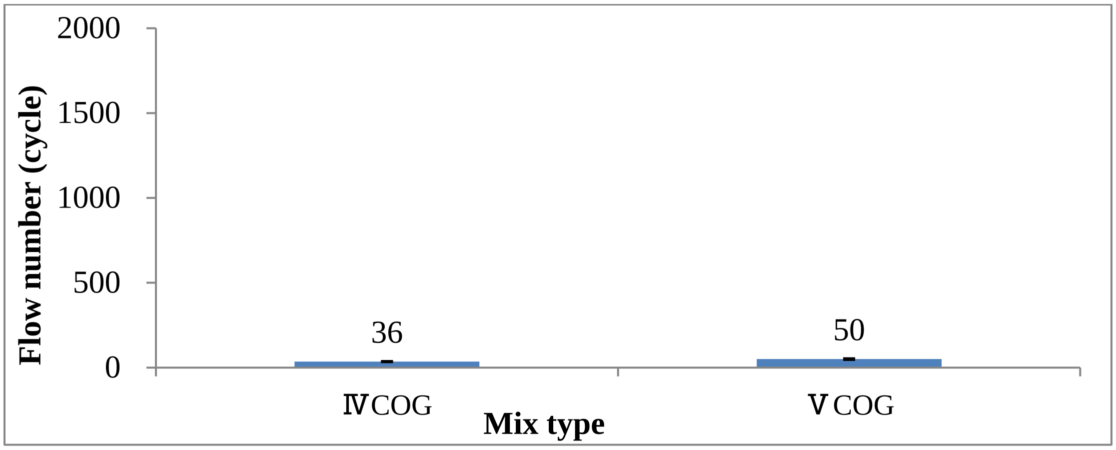

Figure 11-38 Flow Numbers of Various Surface Type C mixtures without RAP after Long-Term Aging in Terms of Aggregate Source at 59°C (138.2°F)

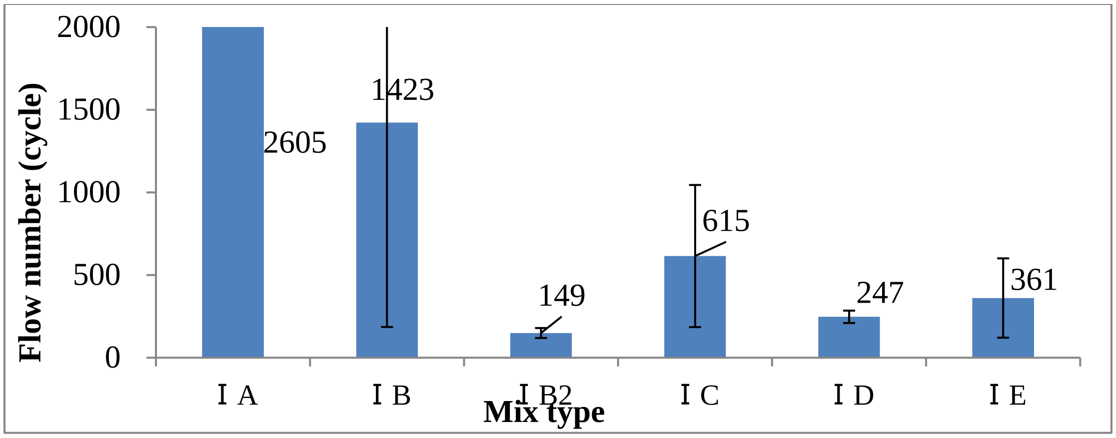

Figure 11-39 Flow Numbers of Various Mixtures from Aggregate I with RAP in Terms of Surface Mixture Type at 59°C (138.2°F)

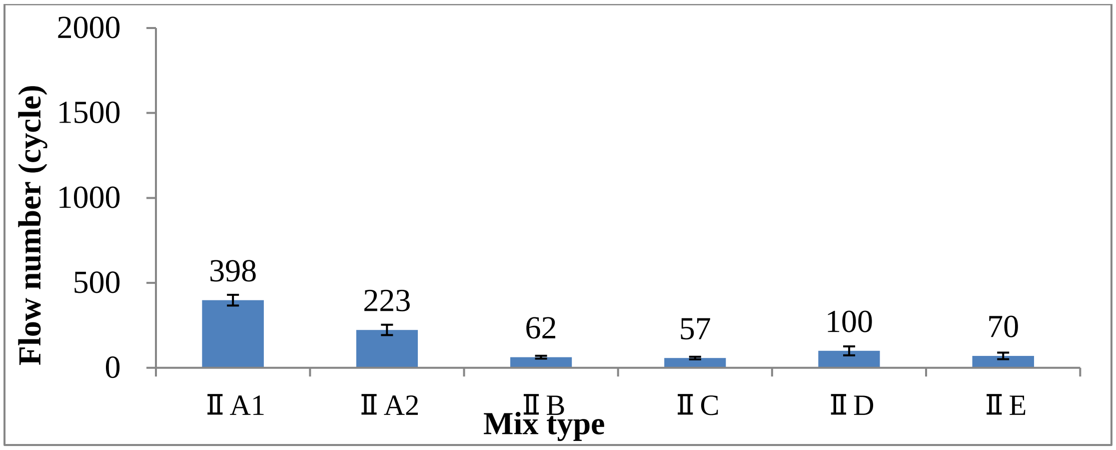

Figure 11-40 Flow Numbers of Various Mixtures from Aggregate II with RAP in Terms of Surface Mixture Type at 59°C (138.2°F)

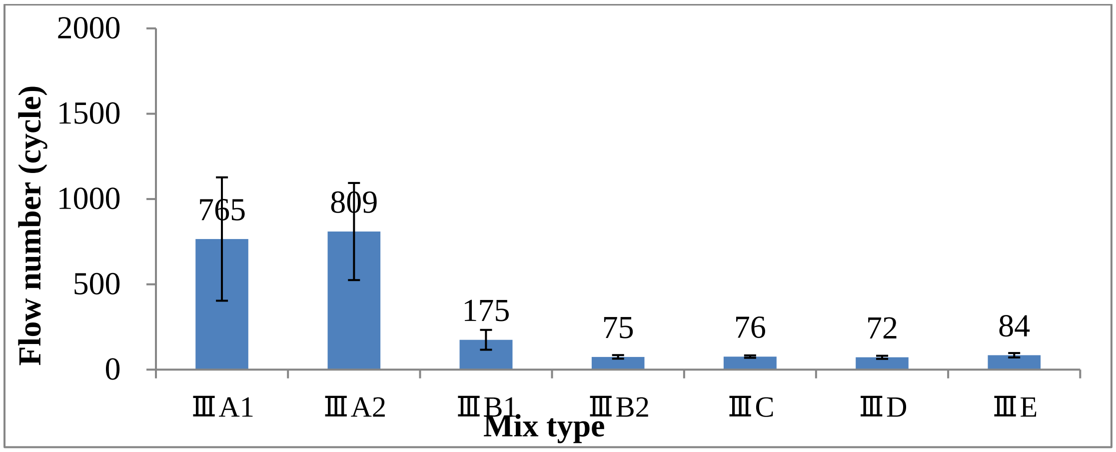

Figure 11-41 Flow Numbers of Various Mixtures from Aggregate III with RAP in Terms of Surface Mixture Type at 59°C (138.2°F)

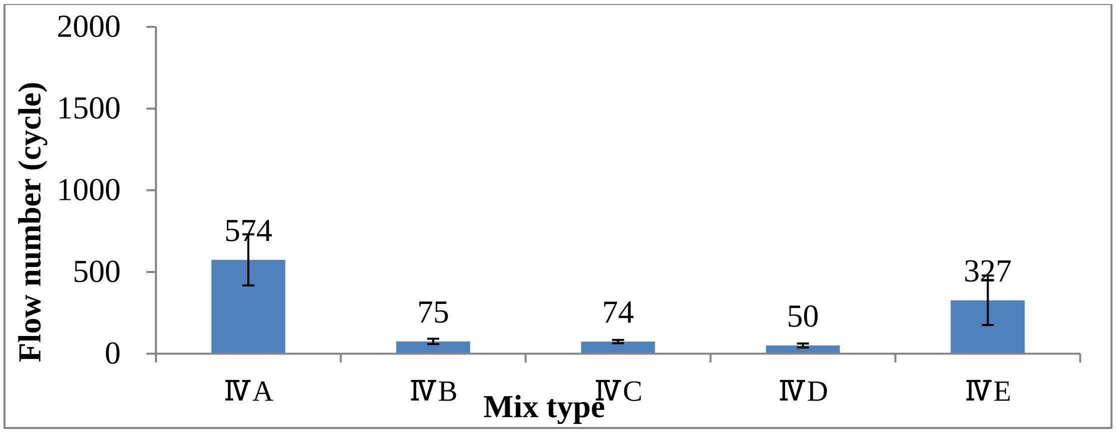

Figure 11-42 Flow Numbers of Various Mixtures from Aggregate IV with RAP in Terms of Surface Mixture Type at 59°C (138.2°F)

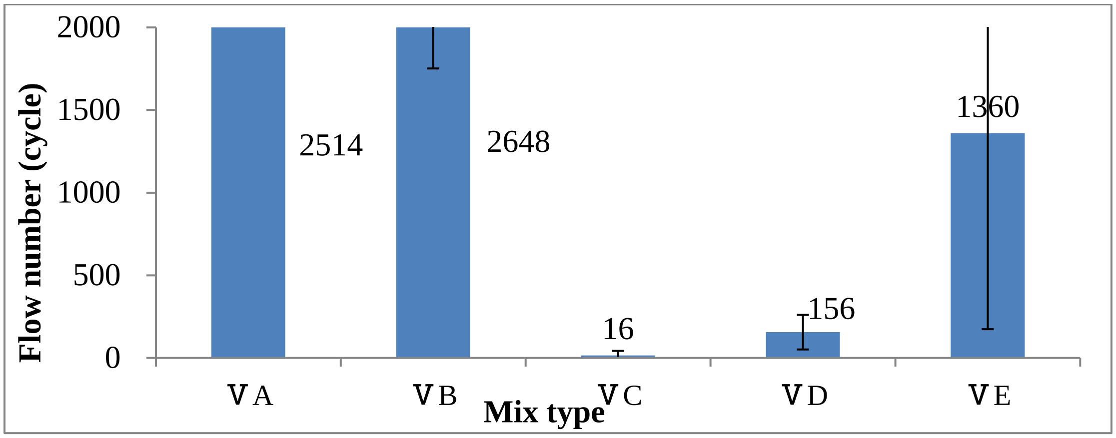

Figure 11-43 Flow Numbers of Various Mixtures from Aggregate V with RAP in Terms of Surface Mixture Type at 59°C (138.2°F)

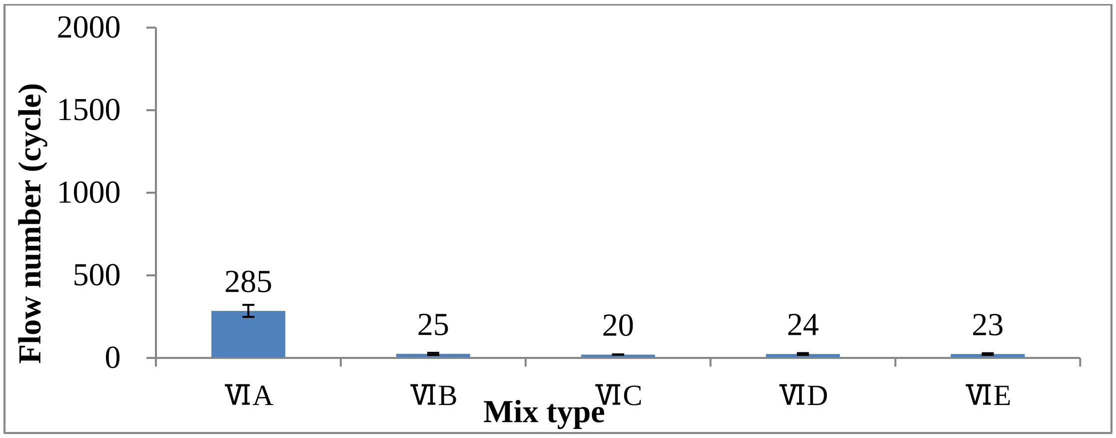

Figure 11-44 Flow Numbers of Various Mixtures from Aggregate VI with RAP in Terms of Surface Mixture Type at 59°C (138.2°F)

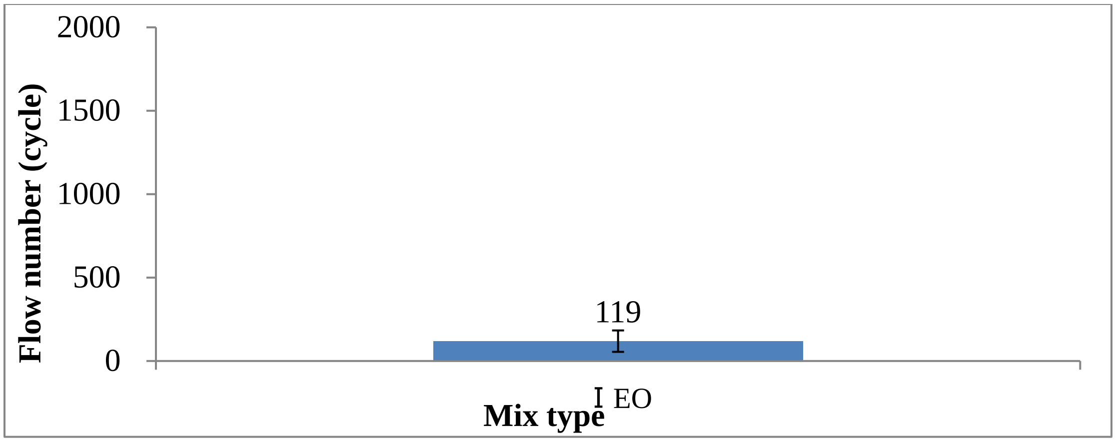

Figure 11-45 Flow Numbers of Various Mixtures from Aggregate I without RAP in Terms of Surface Mixture Type at 59°C (138.2°F)

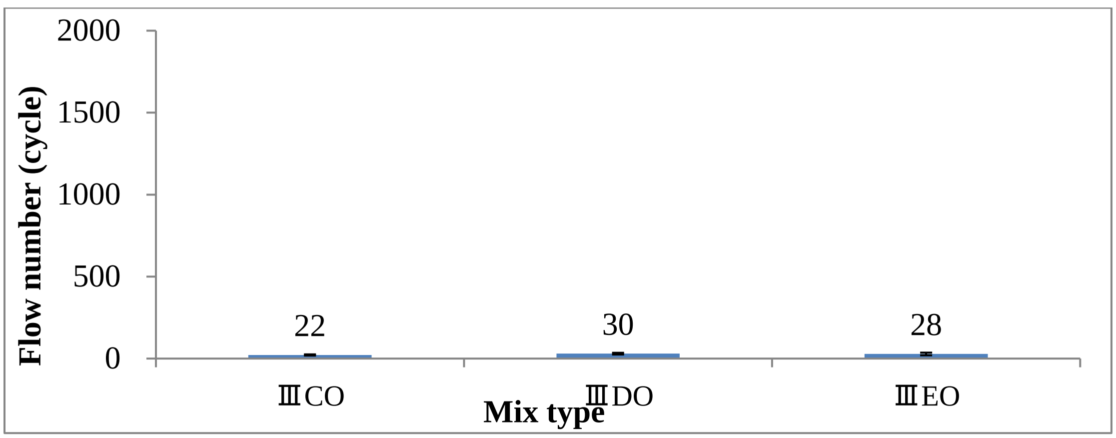

Figure 11-46 Flow Numbers of Various Mixtures from Aggregate III without RAP in Terms of Surface Mixture Type at 59°C (138.2°F)

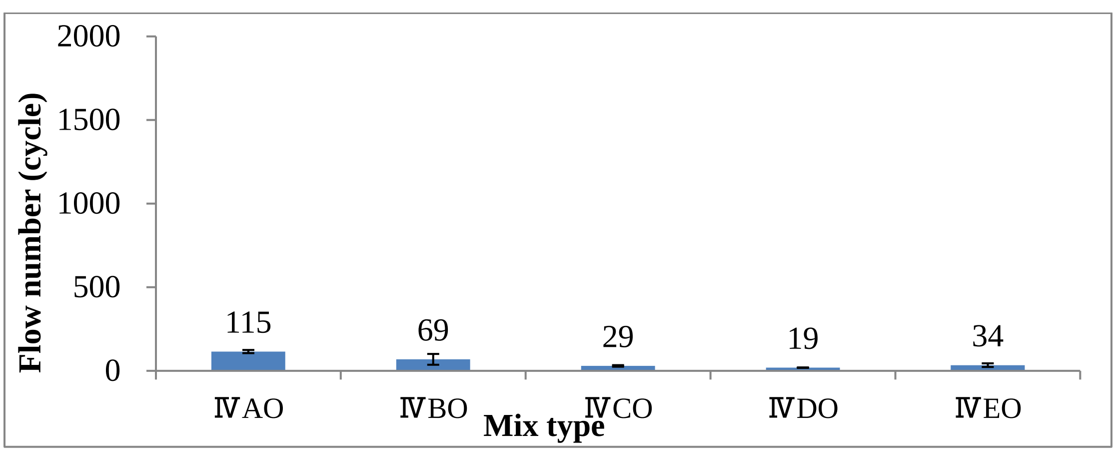

Figure 11-47 Flow Numbers of Various Mixtures from Aggregate IV without RAP in Terms of Surface Mixture Type at 59°C (138.2°F)

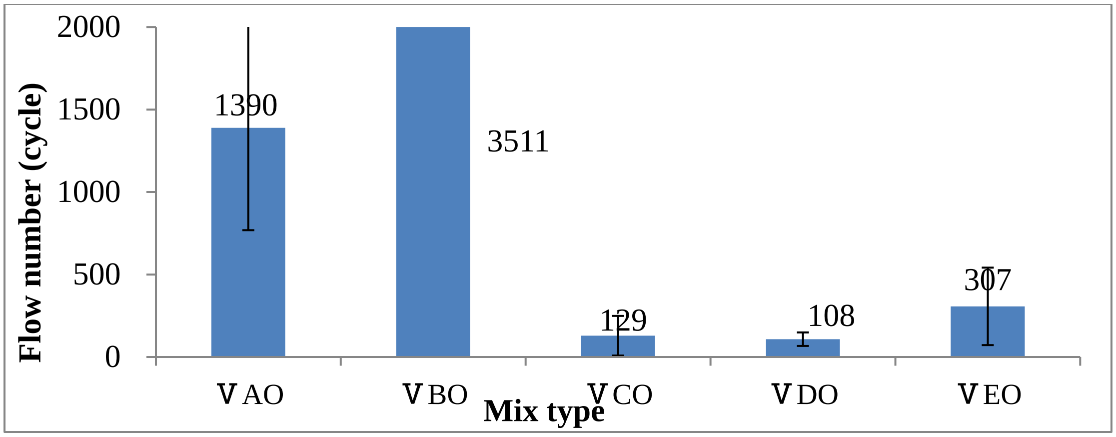

Figure 11-48 Flow Numbers of Various Mixtures from Aggregate V without RAP in Terms of Surface Mixture Type at 59°C (138.2°F)

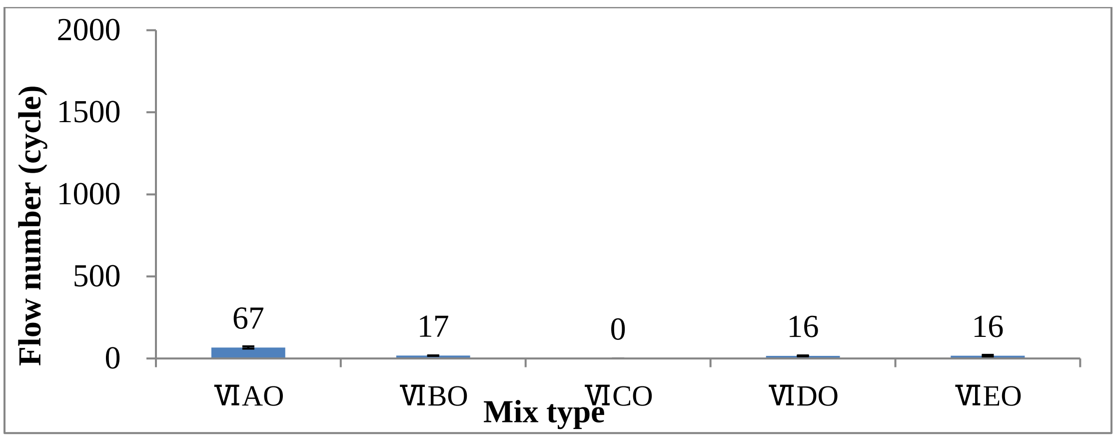

Figure 11-49 Flow Numbers of Various Mixtures from Aggregate VI without RAP in Terms of Surface Mixture Type at 59°C (138.2°F)

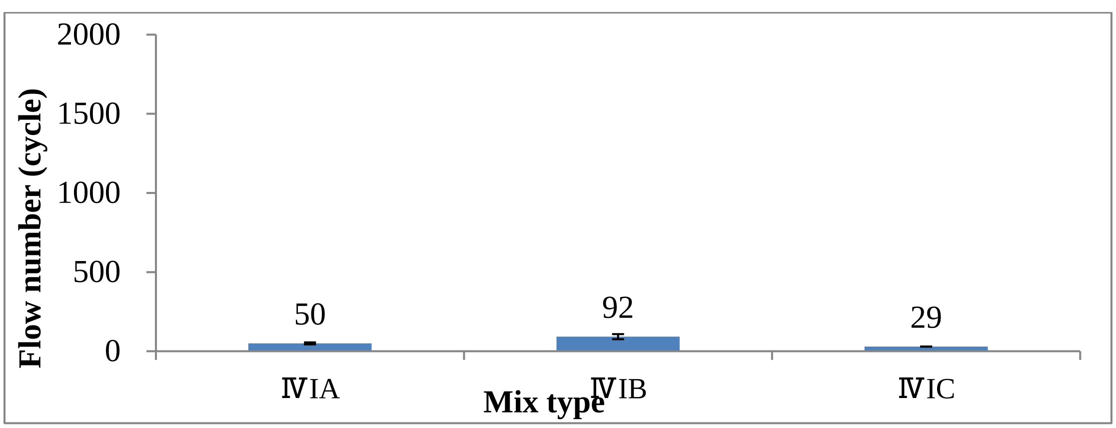

Figure 11-50 Flow Numbers of Various Mixtures from Aggregate IV with RAP in Terms of Intermediate Mixture Type at 59°C (138.2°F)

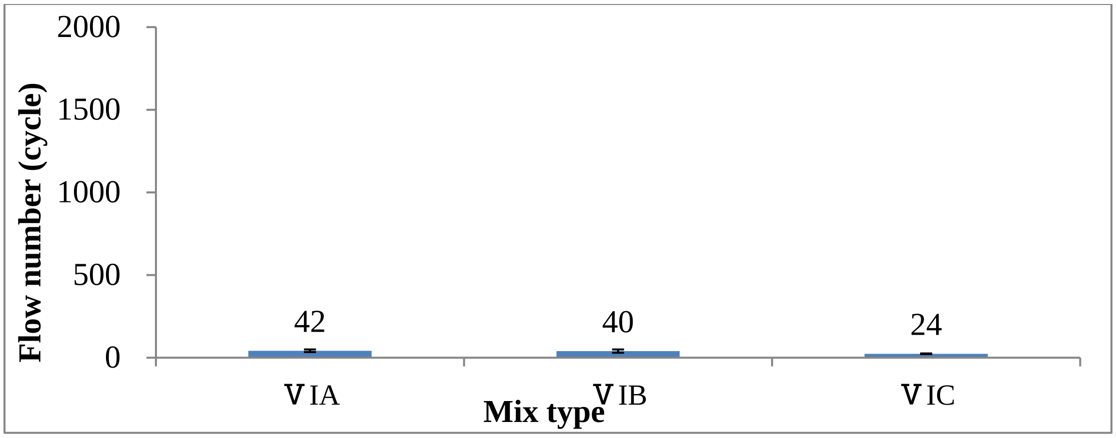

Figure 11-51 Flow Numbers of Various Mixtures from Aggregate V with RAP in Terms of Intermediate Mixture Type at 59°C (138.2°F)

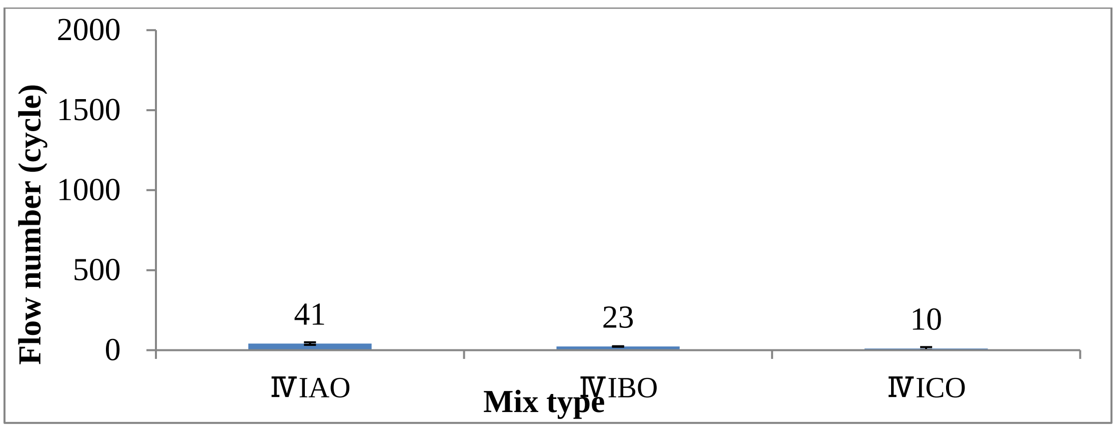

Figure 11-52 Flow Numbers of Various Mixtures from Aggregate IV without RAP in Terms of Intermediate Mixture Type at 59°C (138.2°F)

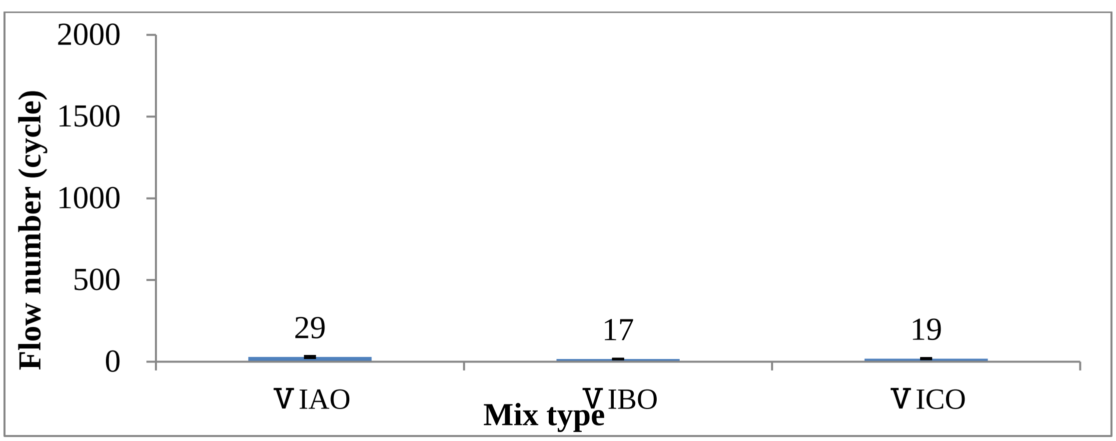

Figure 11-53 Flow Numbers of Various Mixtures from Aggregate V without RAP in Terms of Intermediate Mixture Type at 59°C (138.2°F)

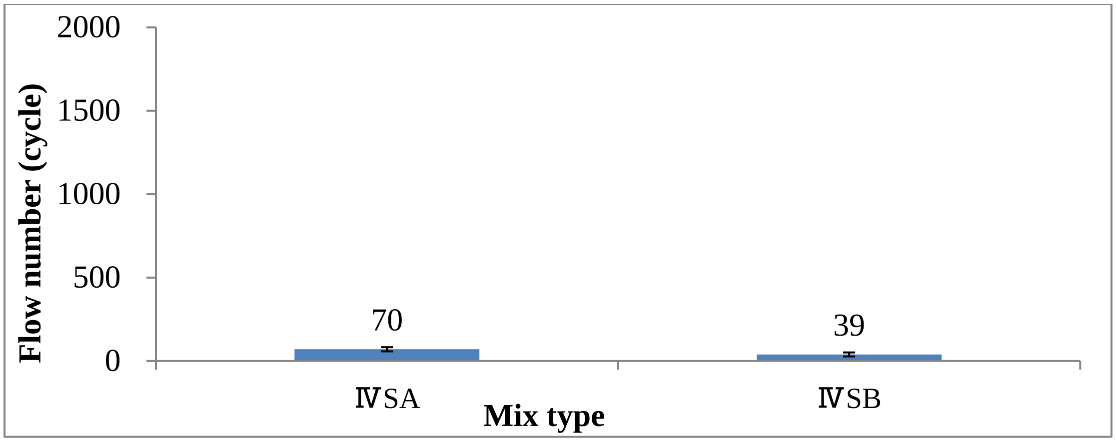

Figure 11-54 Flow Numbers of Various Mixtures from Aggregate IV with RAP in Terms of Base Mixture Type at 59°C (138.2°F)

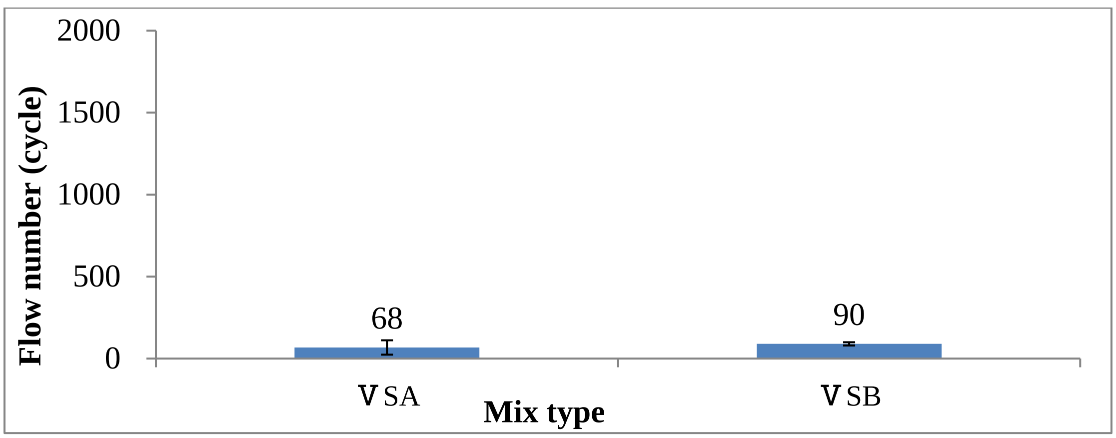

Figure 11-55 Flow Numbers of Various Mixtures from Aggregate V with RAP in Terms of Base Mixture Type at 59°C (138.2°F)

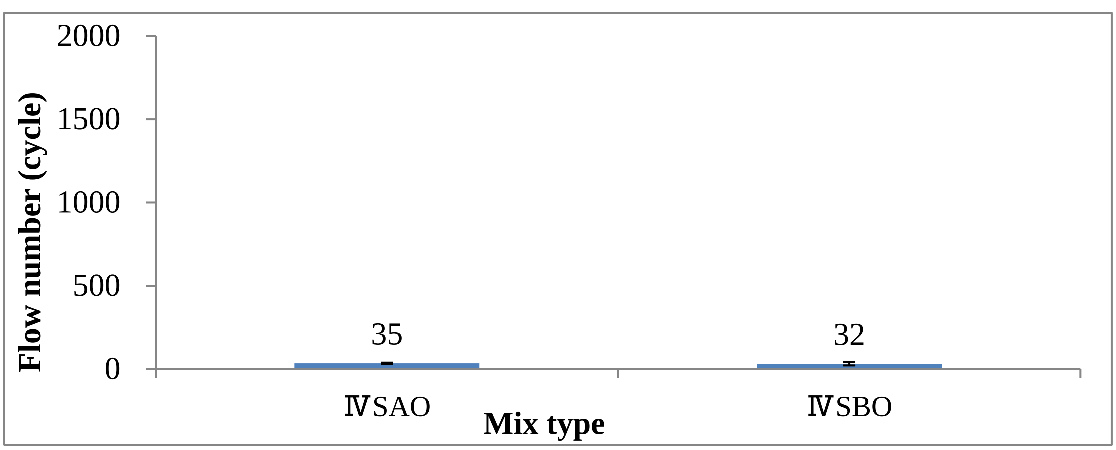

Figure 11-56 Flow Numbers of Various Mixtures from Aggregate IV without RAP in Terms of Base Mixture Type at 59°C (138.2°F)

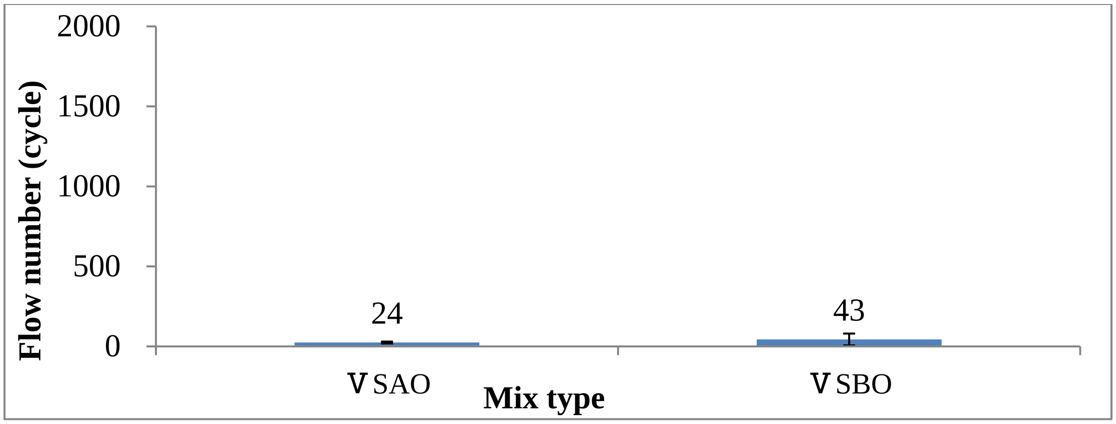

Figure 11-57 Flow Numbers of Various Mixtures from Aggregate V without RAP in Terms of Base Mixture Type at 59°C (138.2°F)

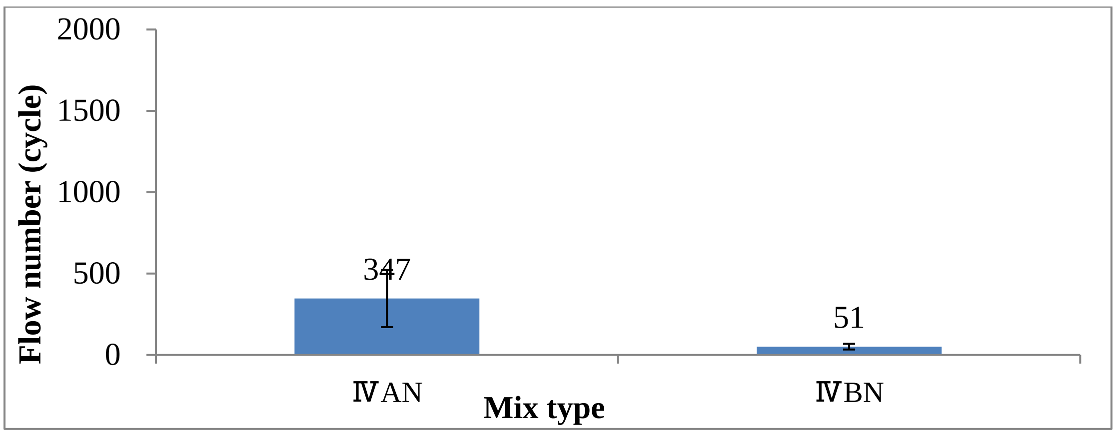

Figure 11-58 Flow Numbers of Various Mixtures from Aggregate IV with RAP and Asphalt Source 2 in Terms of Surface Mixture Type at 59°C (138.2°F)

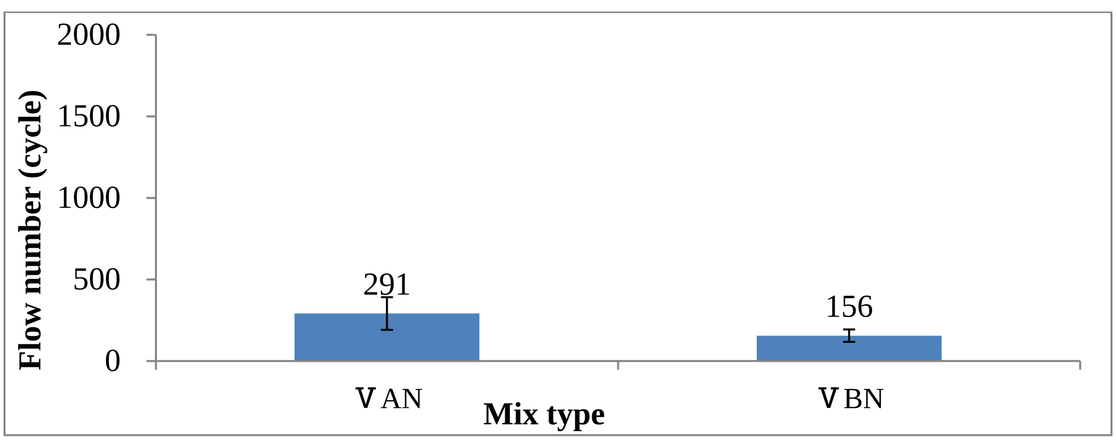

Figure 11-59 Flow Numbers of Various Mixtures from Aggregate V with RAP and Asphalt Source 2 in Terms of Surface Mixture Type at 59°C (138.2°F)

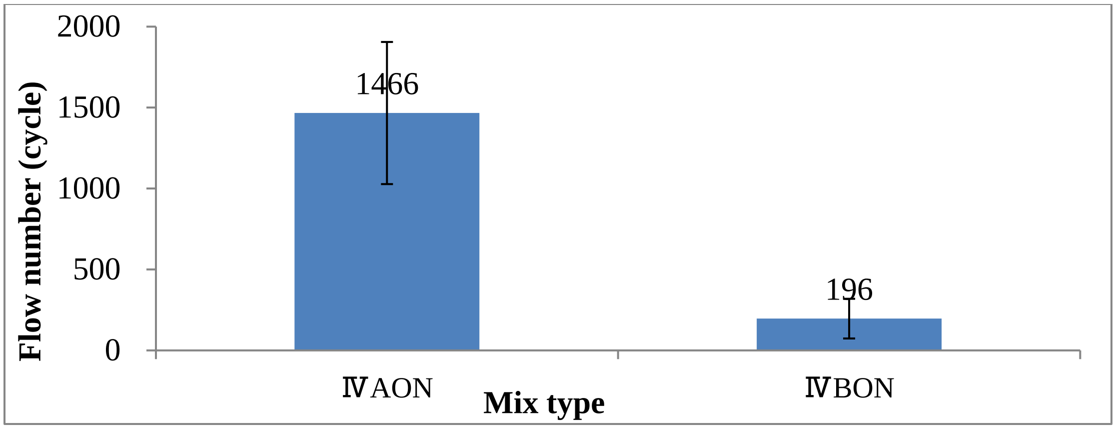

Figure 11-60 Flow Numbers of Various Mixtures from Aggregate IV using Asphalt Source 2 without RAP in Terms of Surface Mixture Type at 59°C (138.2°F)

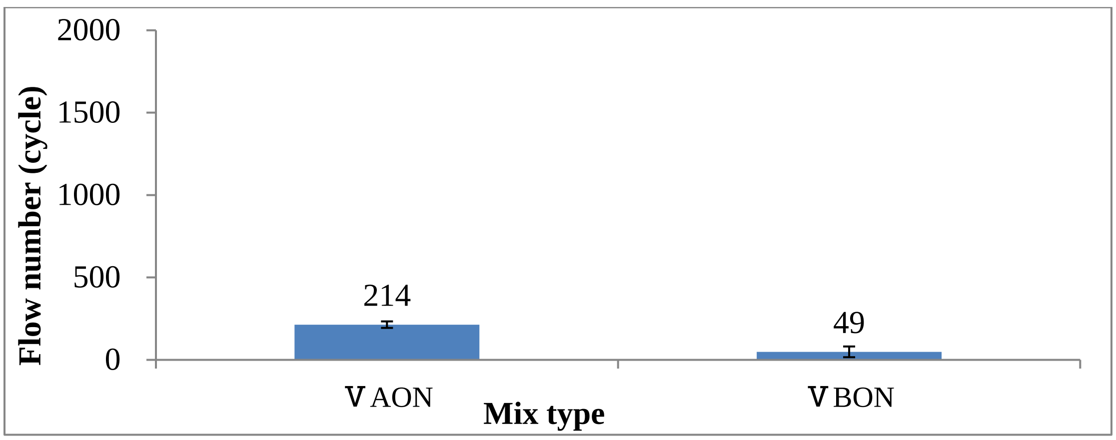

Figure 11-61 Flow Numbers of Various Mixtures from Aggregate V using Asphalt Source 2 without RAP in Terms of Surface Mixture Type at 59°C (138.2°F)

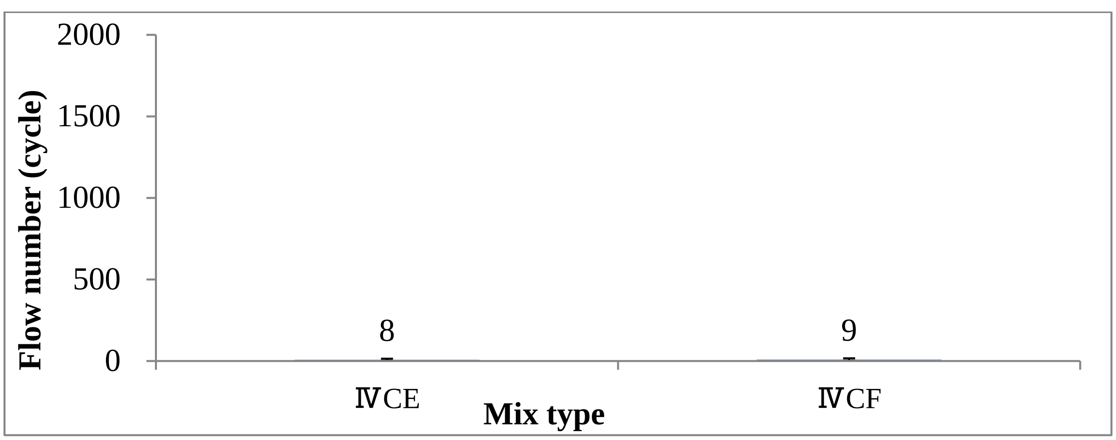

Figure 11-62 Flow Numbers of Various Surface Type C Mixtures from Aggregate IV with RAP in Terms of WMA Technology Type at 59°C (138.2°F)

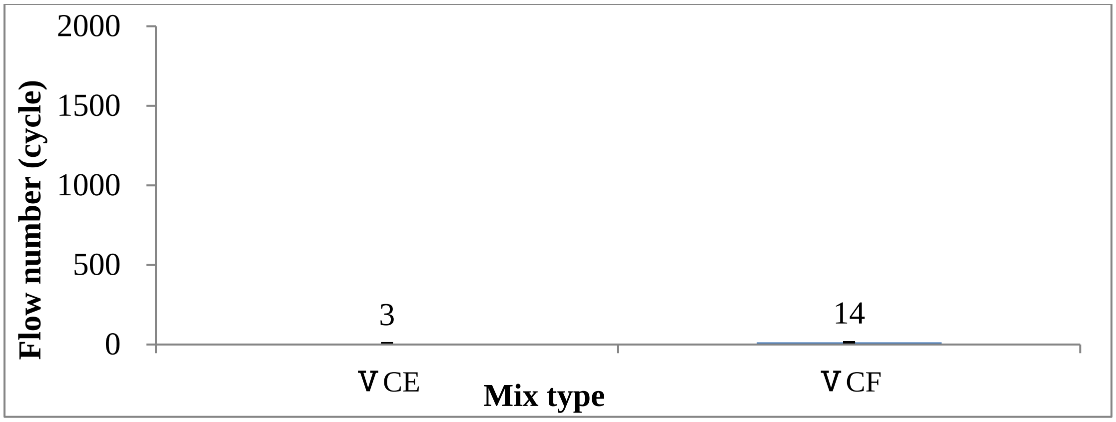

Figure 11-63 Flow Numbers of Various Surface Type C Mixtures from Aggregate V with RAP in Terms of WMA Technology Type at 59°C (138.2°F)

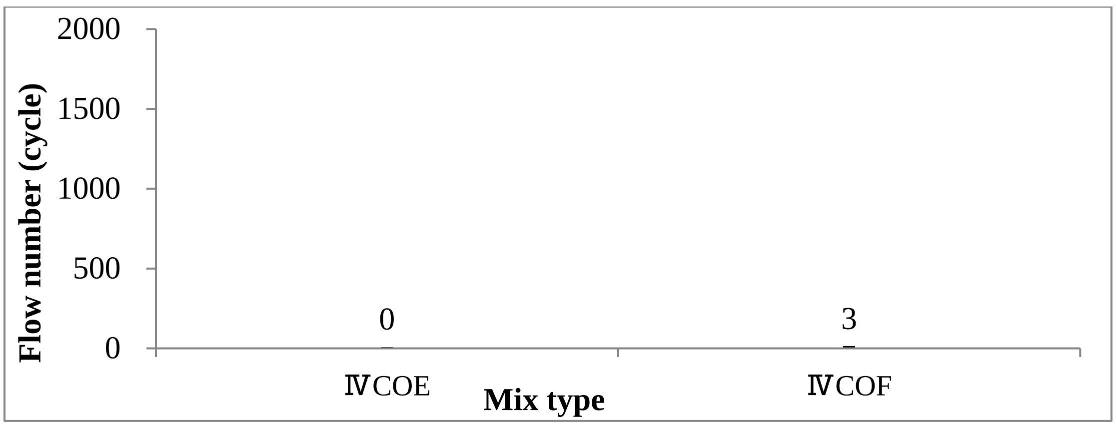

Figure 11-64 Flow Numbers of Various Surface Type C Mixtures from Aggregate IV without RAP in Terms of WMA Technology Type at 59°C (138.2°F)

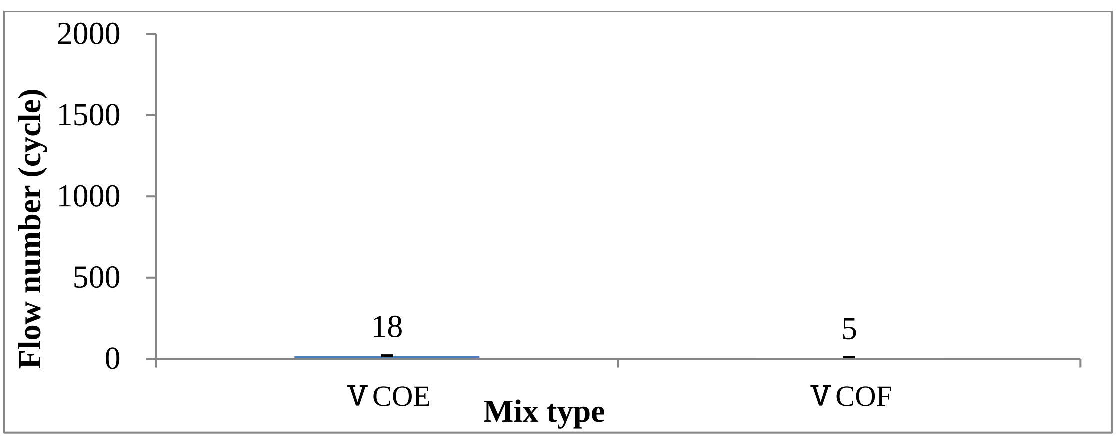

Figure 11-65 Flow Numbers of Various Surface Type C Mixtures from Aggregate V without RAP in Terms of WMA Technology Type at 59°C (138.2°F)

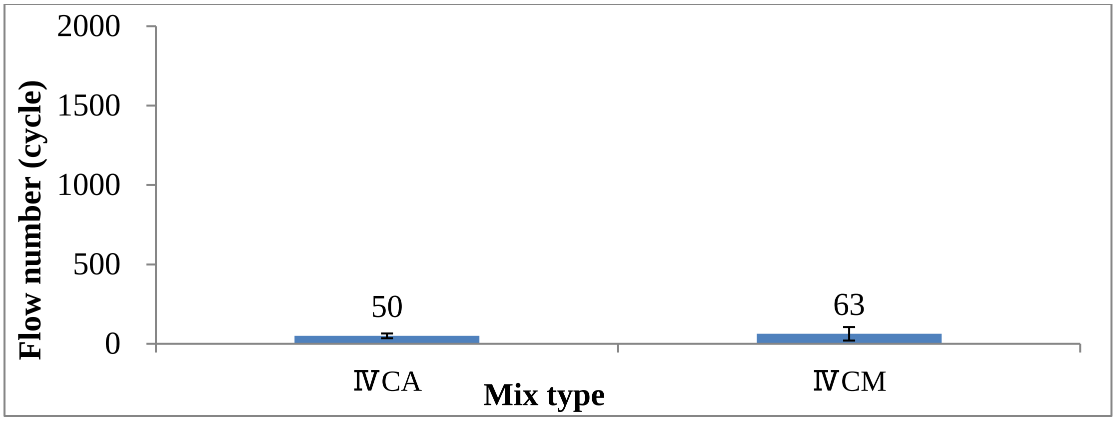

Figure 11-66 Flow Numbers of Various Surface Type C Mixtures from Aggregate IV with RAP in Terms of Liquid ASA Type at 59°C (138.2°F)

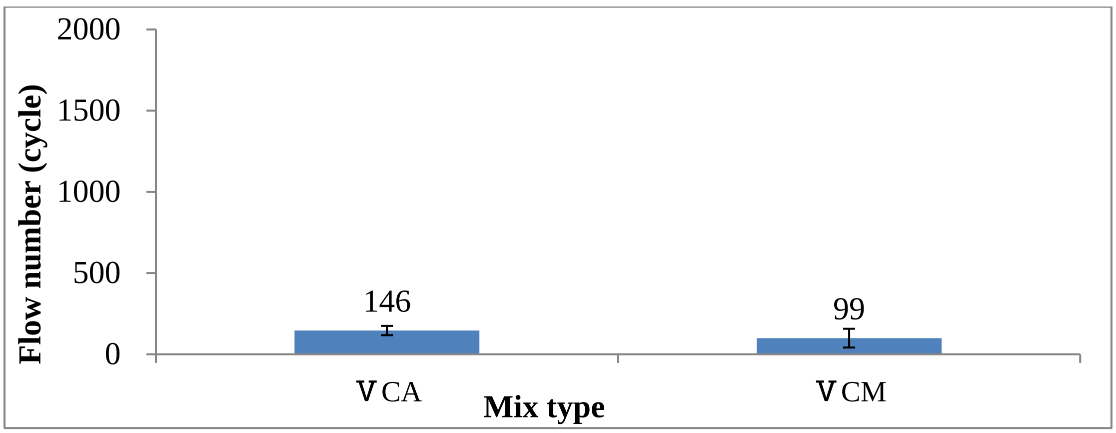

Figure 11-67 Flow Numbers of Various Surface Type C Mixtures from Aggregate V with RAP in Terms of Liquid ASA Type at 59°C (138.2°F)

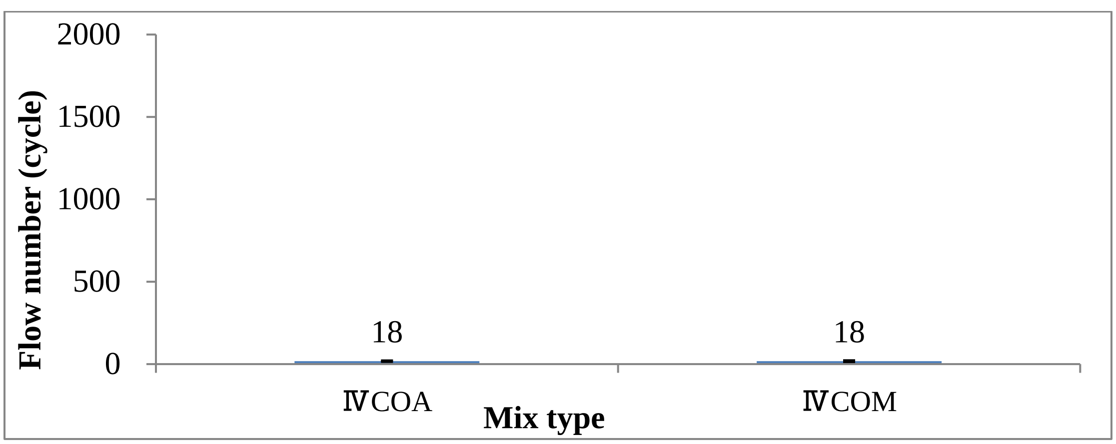

Figure 11-68 Flow Numbers of Various Surface Type C Mixtures from Aggregate IV without RAP in Terms of Liquid ASA Type at 59°C (138.2°F)

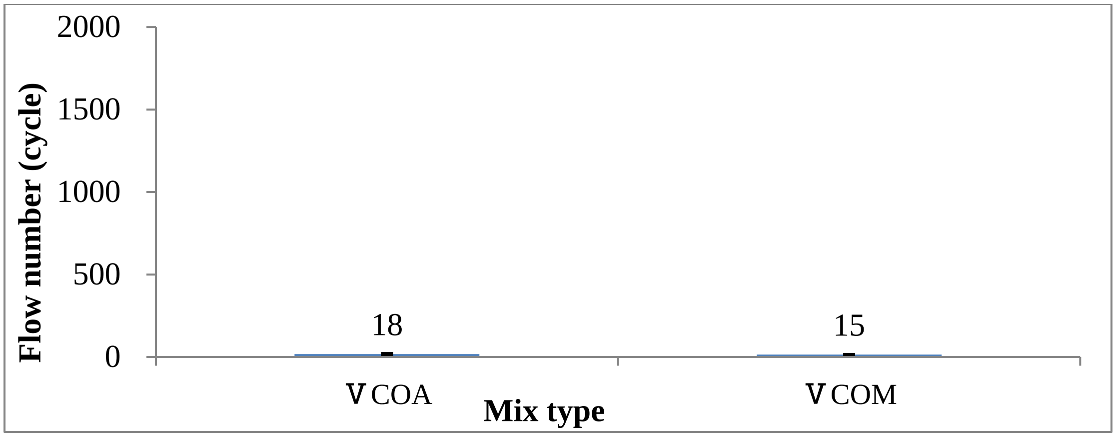

Figure 11-69 Flow Numbers of Various Surface Type C Mixtures from Aggregate V without RAP in Terms of Liquid ASA Type at 59°C (138.2°F)

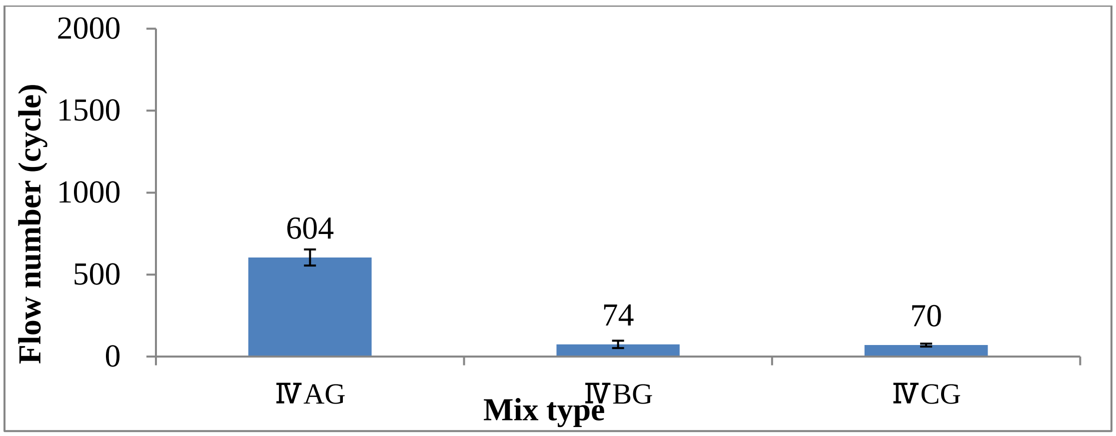

Figure 11-70 Flow Numbers of Various Mixtures from Aggregate IV with RAP after Long-Term Aging in Terms of Surface Mixture Type at 59°C (138.2°F)

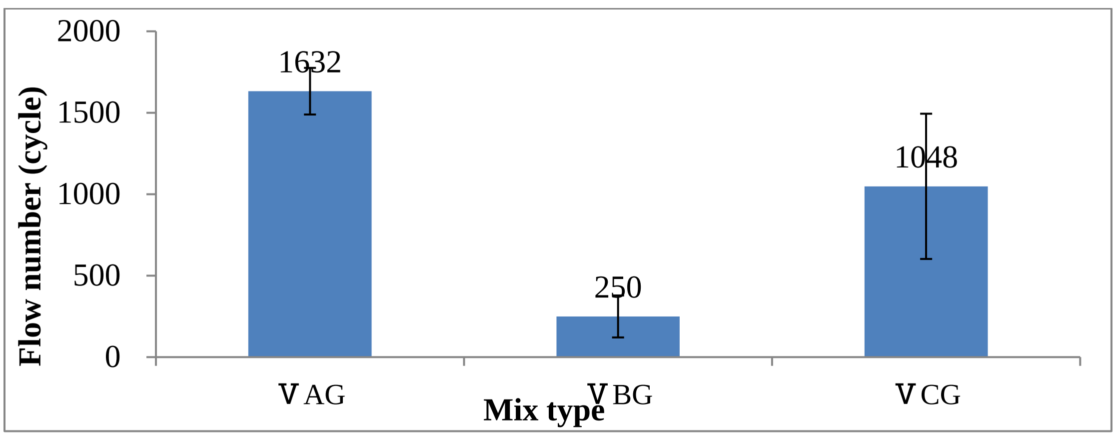

Figure 11-71 Flow Numbers of Various Mixtures from Aggregate V with RAP after Long-Term Aging in Terms of Surface Mixture Type at 59°C (138.2°F)

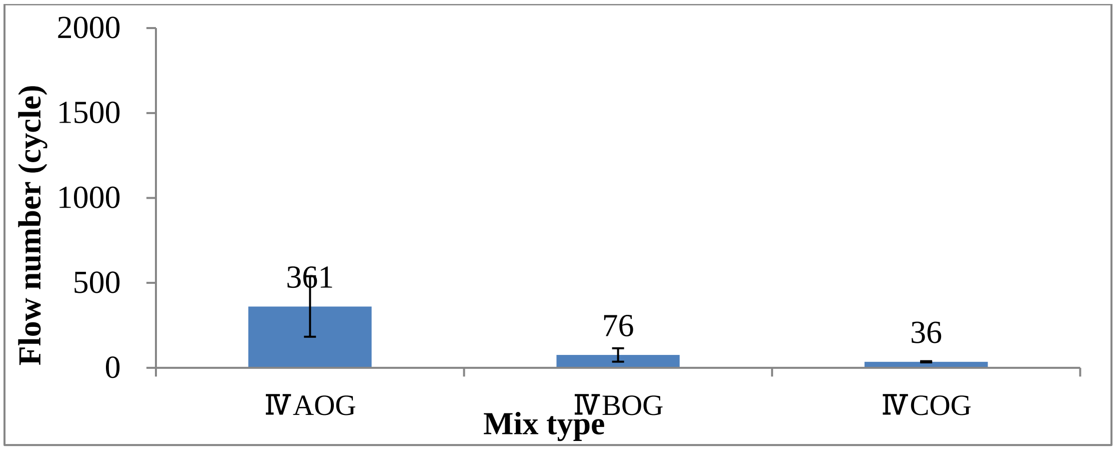

Figure 11-72 Flow Numbers of Various Mixtures from Aggregate IV without RAP after Long-Term Aging in Terms of Surface Mixture Type at 59°C (138.2°F)

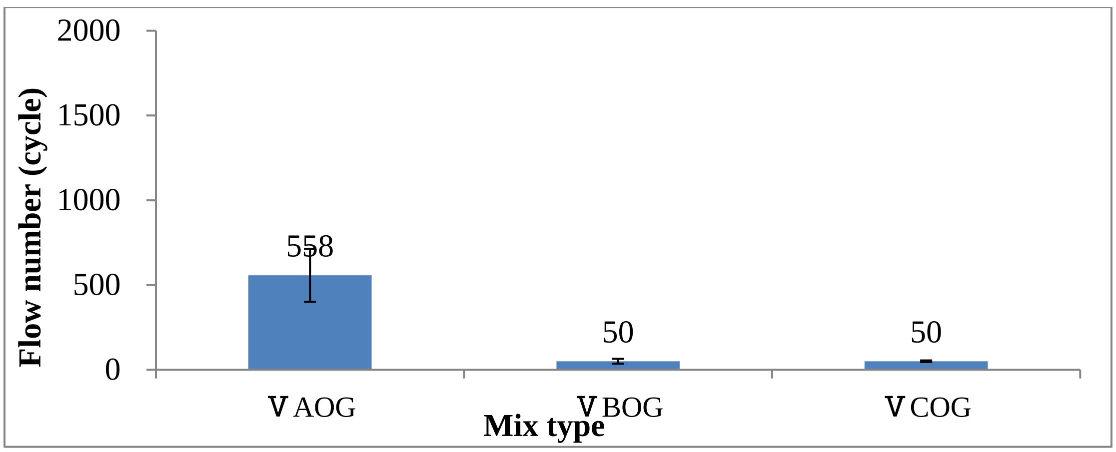

Figure 11-73 Flow Numbers of Various Mixtures from Aggregate V without RAP after Long-Term Aging in Terms of Surface Mixture Type at 59°C (138.2°F)

12 Appendix D - Master Curve Development for All Mixtures Designed and Tested for This Research Project

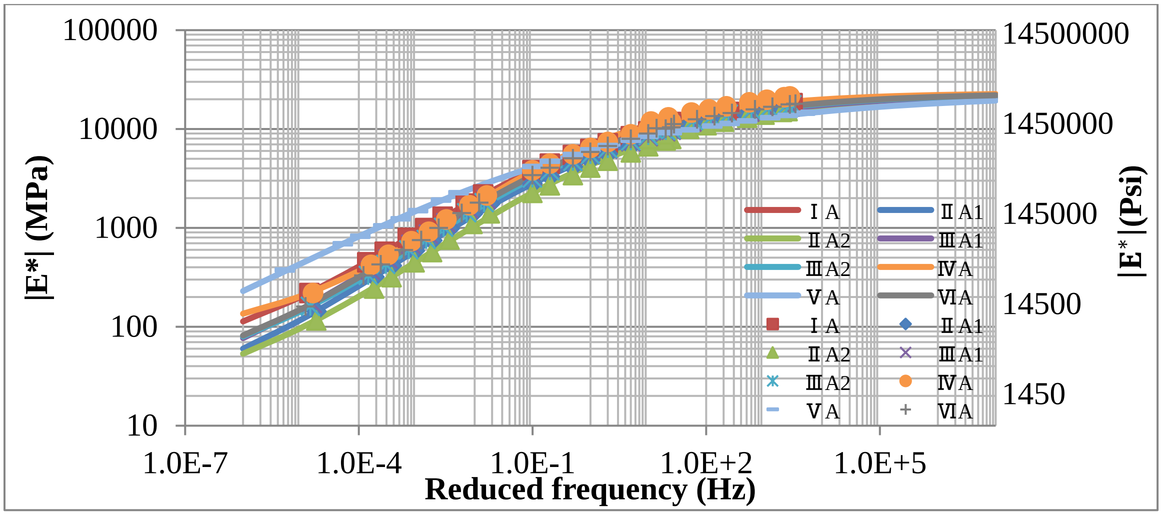

Figure 12-1 Master Dynamic Modulus Curves for Surface Type A Mixtures with RAP in Terms of Aggregate Source

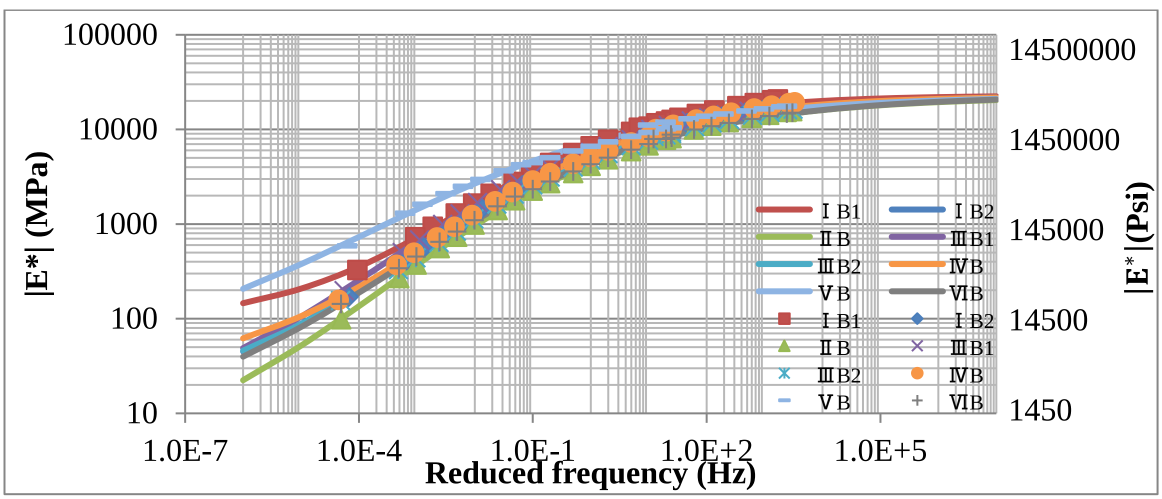

Figure 12-2 Master Dynamic Modulus Curves for Surface Type B Mixtures with RAP in Terms of Aggregate Source

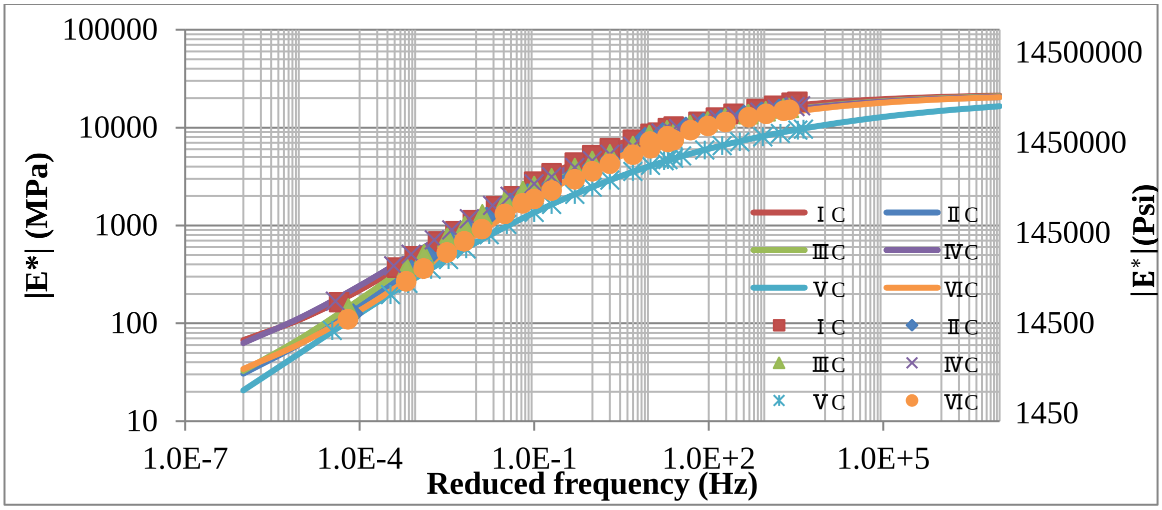

Figure 12-3 Master Dynamic Modulus Curves for Surface Type C Mixtures with RAP in Terms of Aggregate Source

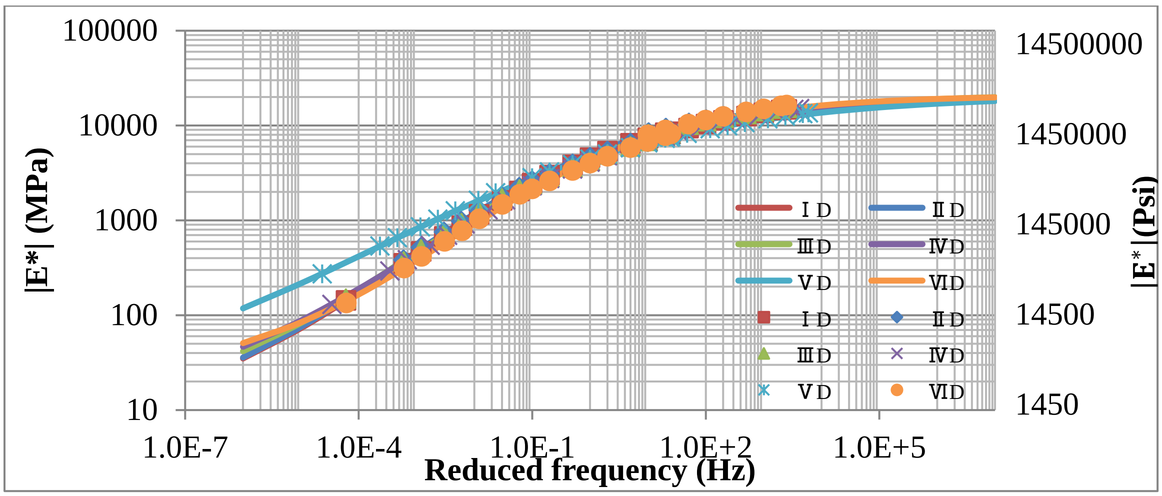

Figure 12-4 Master Dynamic Modulus Curves for Surface Type D Mixtures with RAP in Terms of Aggregate Source

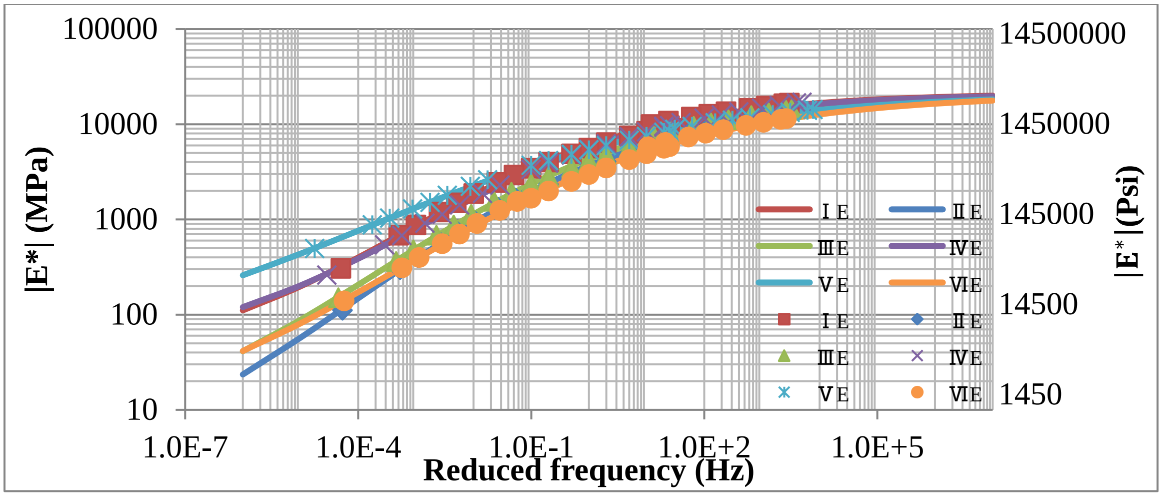

Figure 12-5 Master Dynamic Modulus Curves for Surface Type E Mixtures with RAP in Terms of Aggregate Source

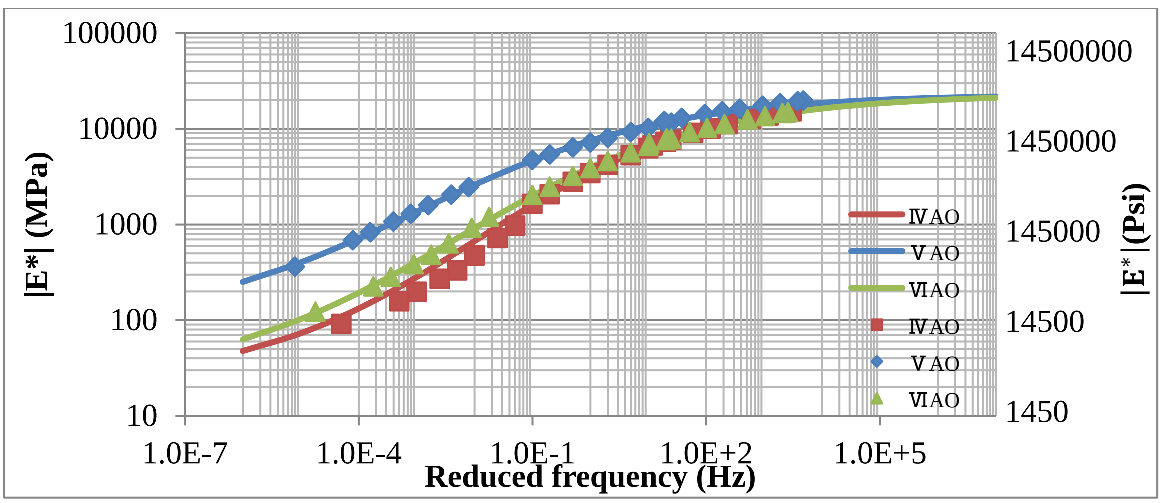

Figure 12-6 Master Dynamic Modulus Curves for Surface Type A Mixtures without RAP in Terms of Aggregate Source

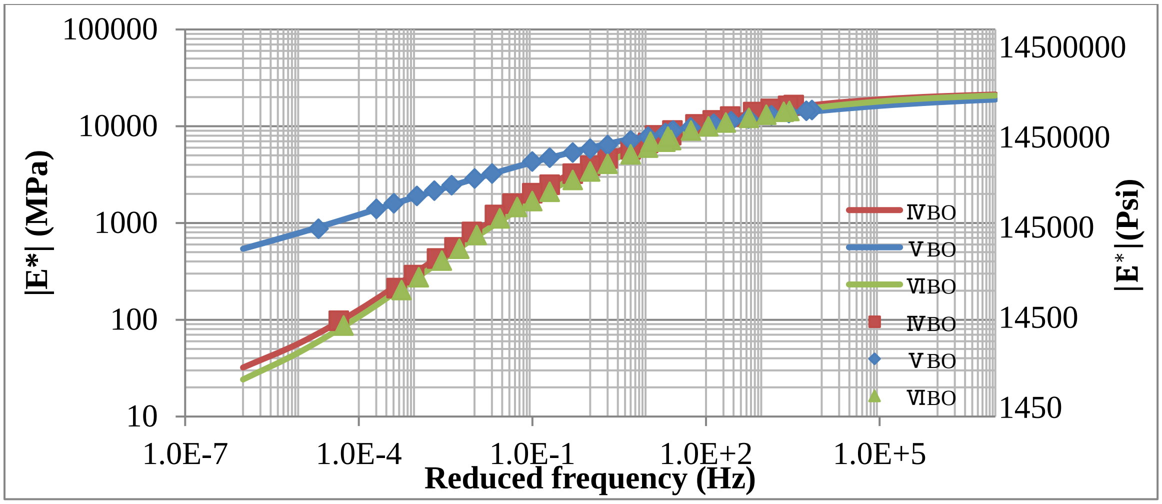

Figure 12-7 Master Dynamic Modulus Curves for Surface Type B Mixtures without RAP in Terms of Aggregate Source

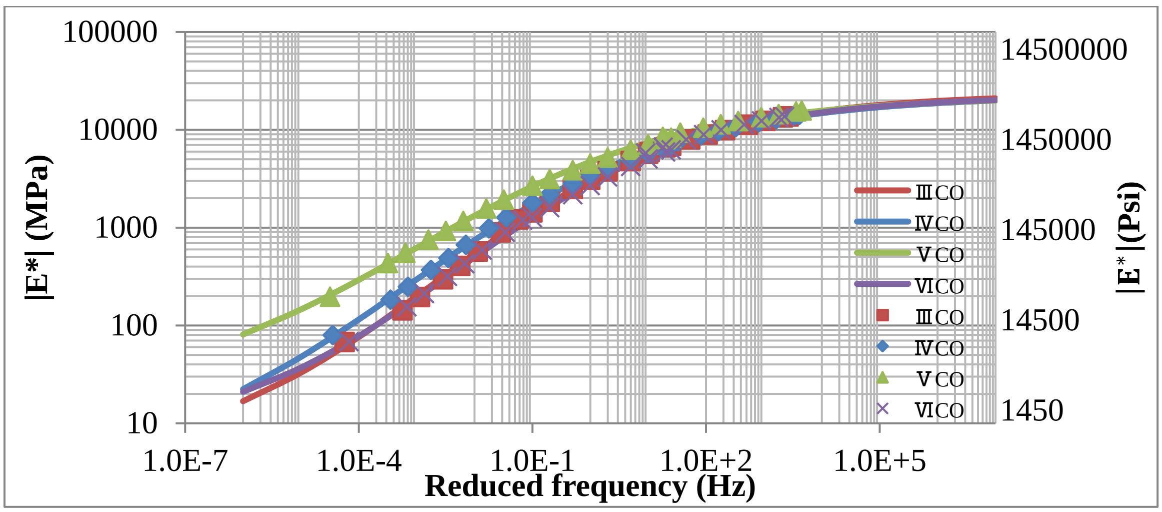

Figure 12-8 Master Dynamic Modulus Curves for Surface Type C Mixtures without RAP in Terms of Aggregate Source

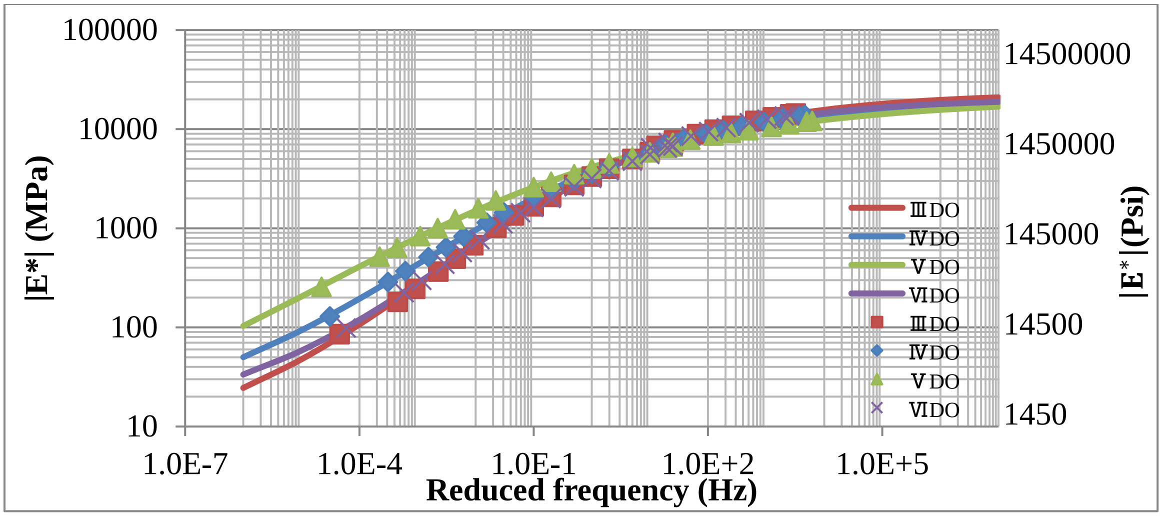

Figure 12-9 Master Dynamic Modulus Curves for Surface Type D Mixtures without RAP in Terms of Aggregate Source

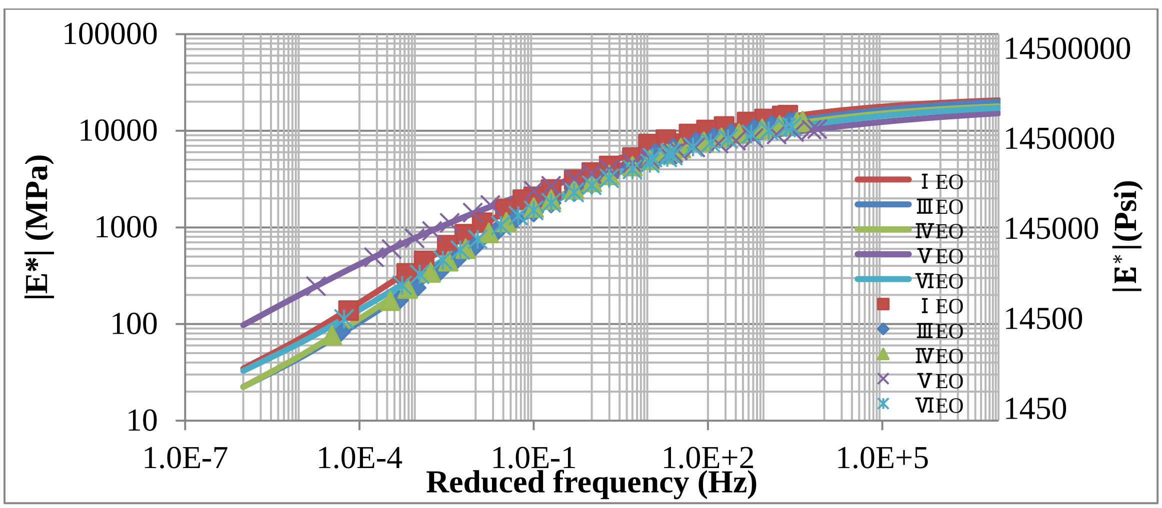

Figure 12-10 Master Dynamic Modulus Curves for Surface Type E Mixtures without RAP in Terms of Aggregate Source

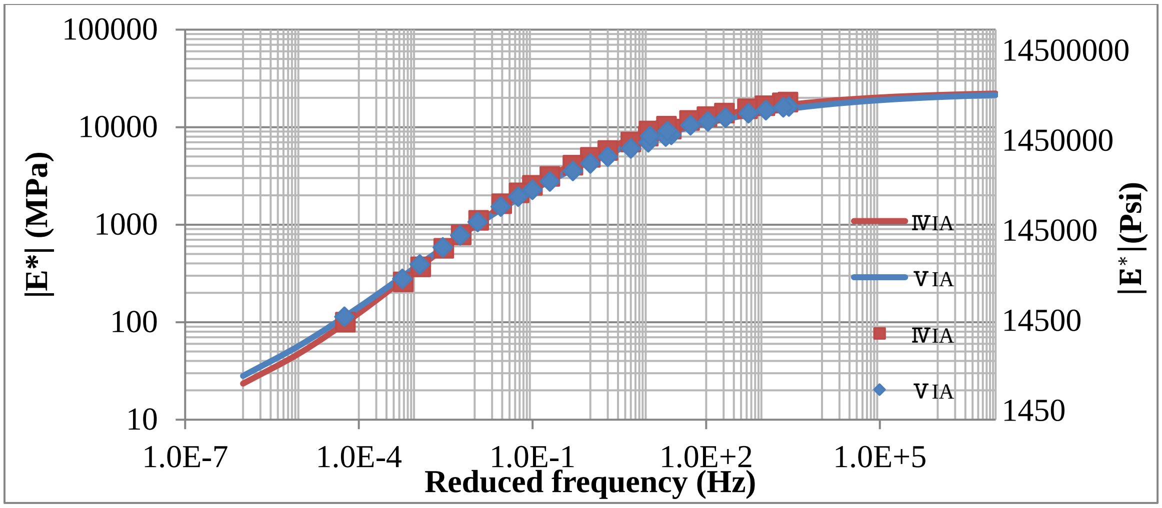

Figure 12-11 Master Dynamic Modulus Curves of Intermediate Type A Mixtures with RAP in Terms of Aggregate Source

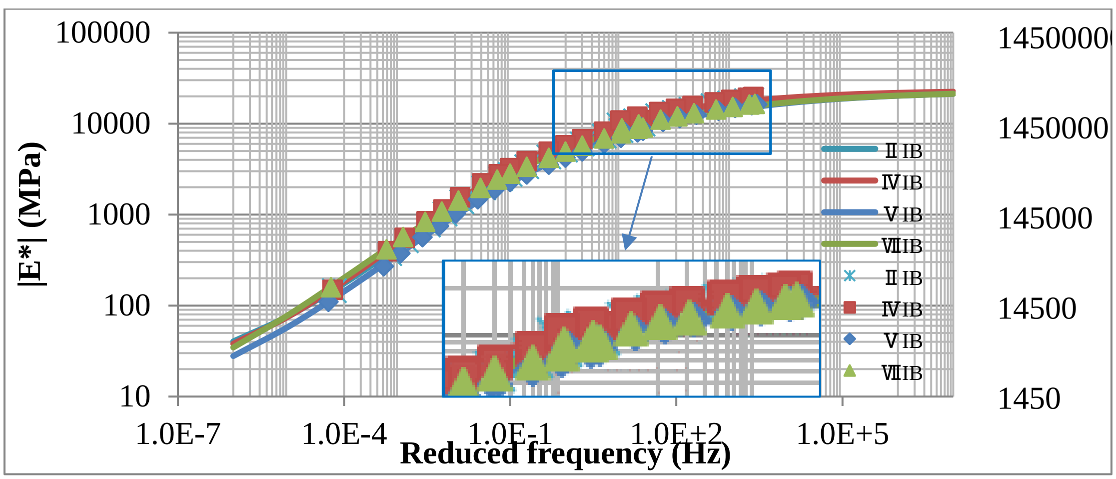

Figure 12-12 Master Dynamic Modulus Curves of Intermediate Type B Mixtures with RAP in Terms of Aggregate Source

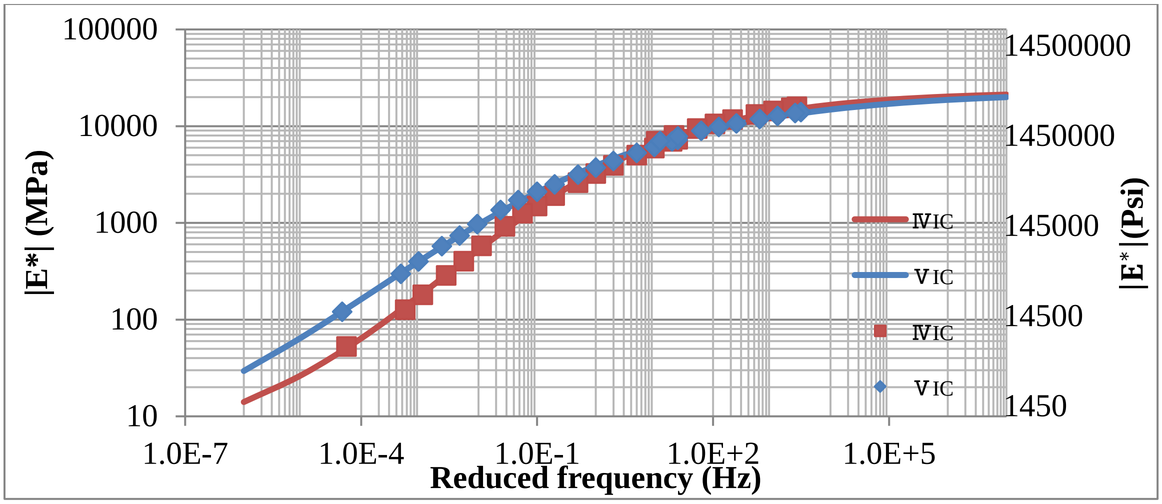

Figure 12-13 Master Dynamic Modulus Curves of Intermediate Type C Mixtures with RAP in Terms of Aggregate Source

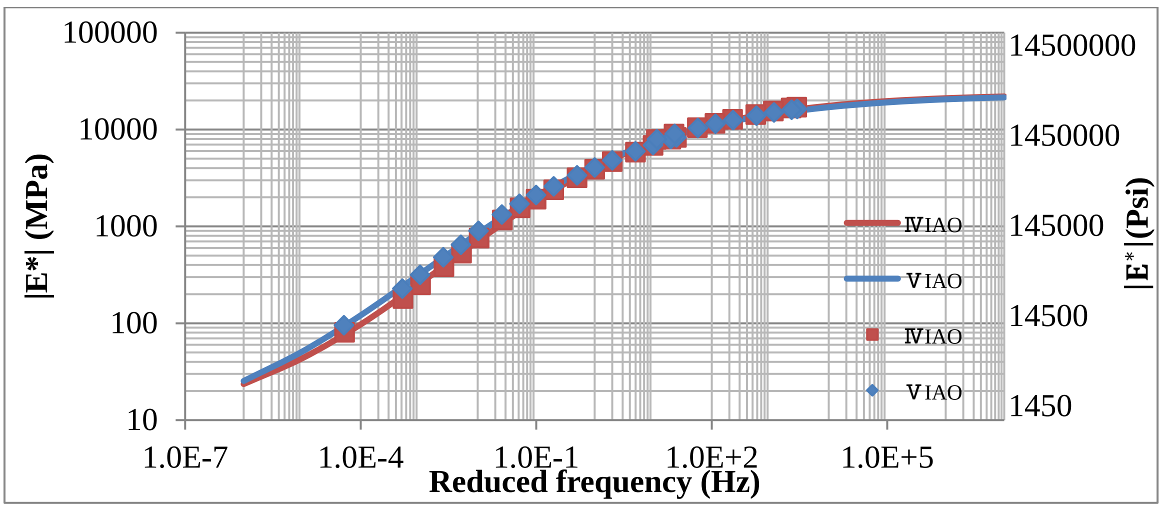

Figure 12-14 Master Dynamic Modulus Curves of Intermediate Type A Mixtures without RAP in Terms of Aggregate Source

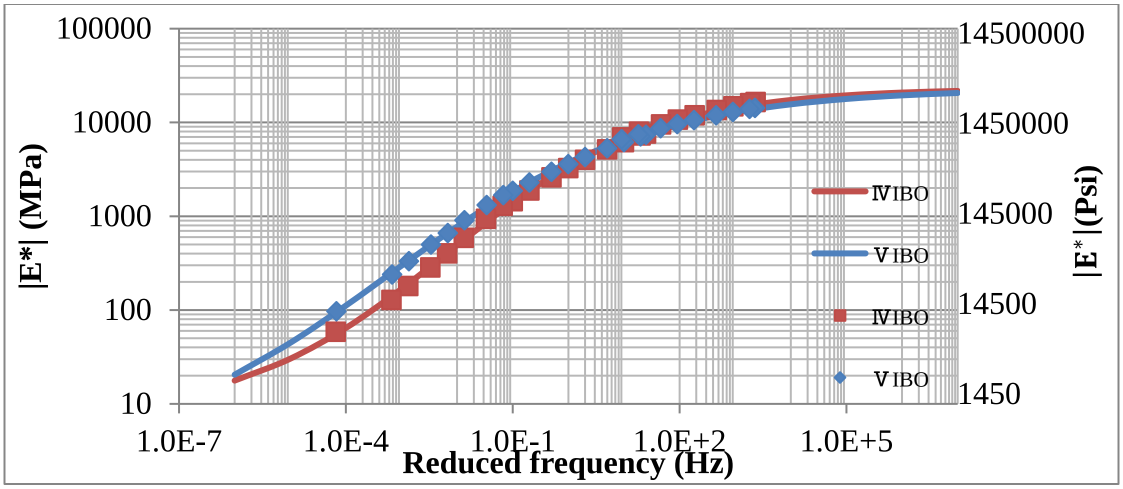

Figure 12-15 Master Dynamic Modulus Curves of Intermediate Type B Mixtures without RAP in Terms of Aggregate Source

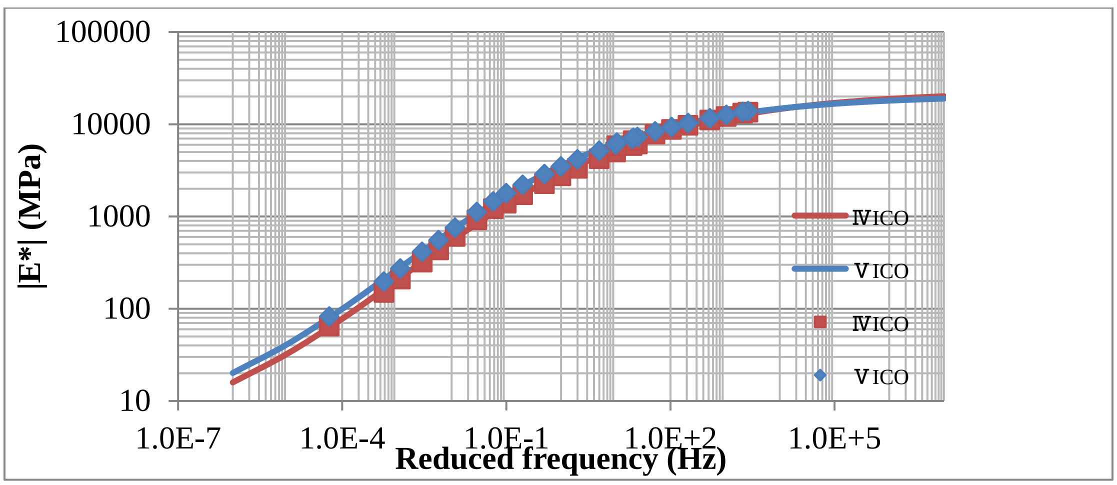

Figure 12-16 Master Dynamic Modulus Curves of Intermediate Type C Mixtures without RAP in Terms of Aggregate Source

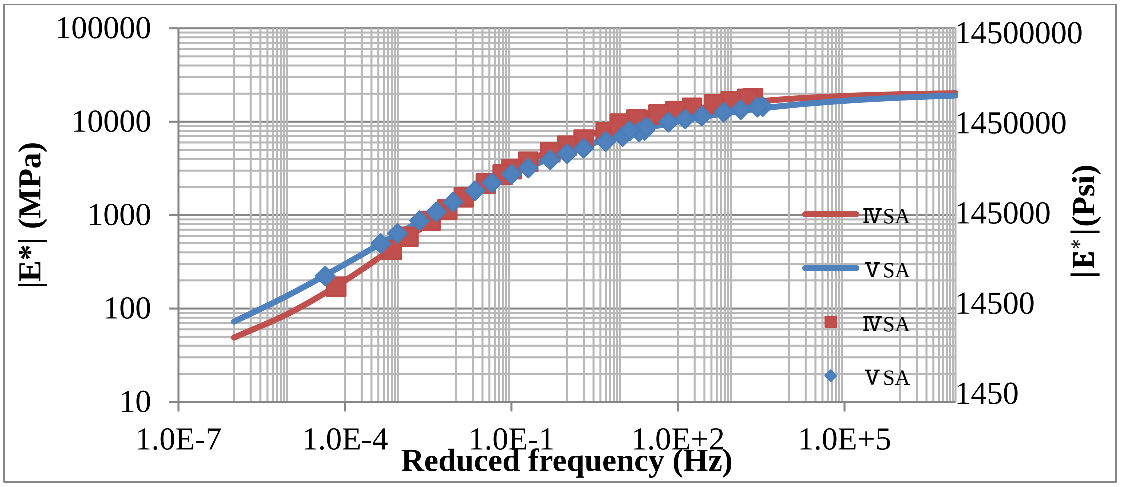

Figure 12-17 Master Dynamic Modulus Curves of Base Type A Mixtures with RAP in Terms of Aggregate Source

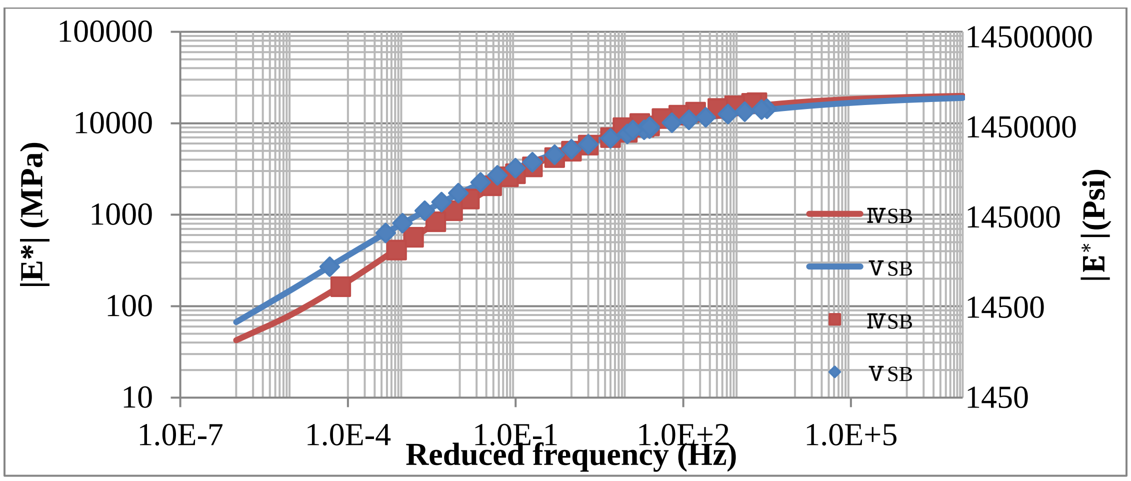

Figure 12-18 Master Dynamic Modulus Curves of Base Type B Mixtures with RAP in Terms of Aggregate Source

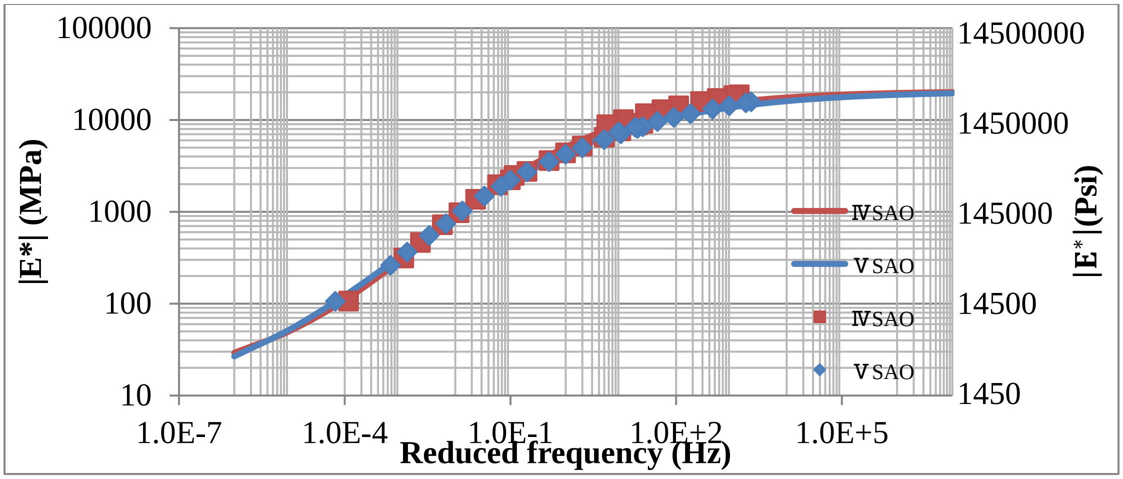

Figure 12-19 Master Dynamic Modulus Curves of Base Type A Mixtures without RAP in Terms of Aggregate Source

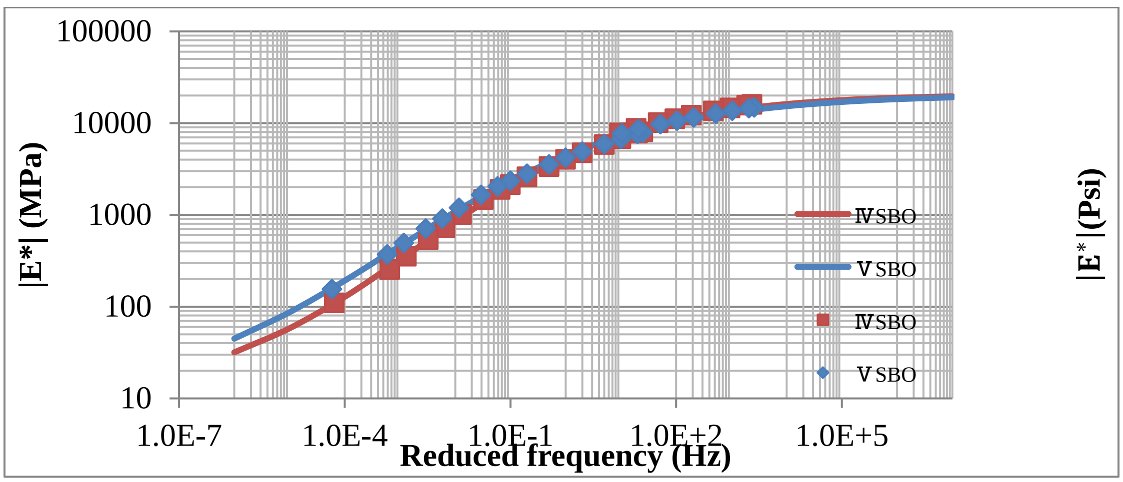

Figure 12-20 Master Dynamic Modulus Curves of Base Type B Mixtures without RAP in Terms of Aggregate Source

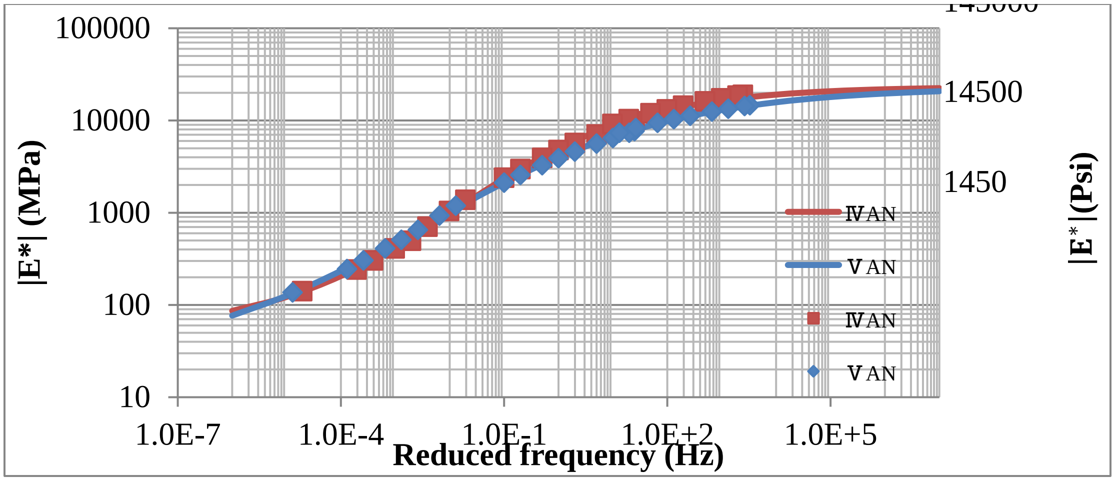

Figure 12-21 Master Dynamic Modulus Curves of Surface Type A Mixtures with RAP and Asphalt Source 2 in Terms of Aggregate Source

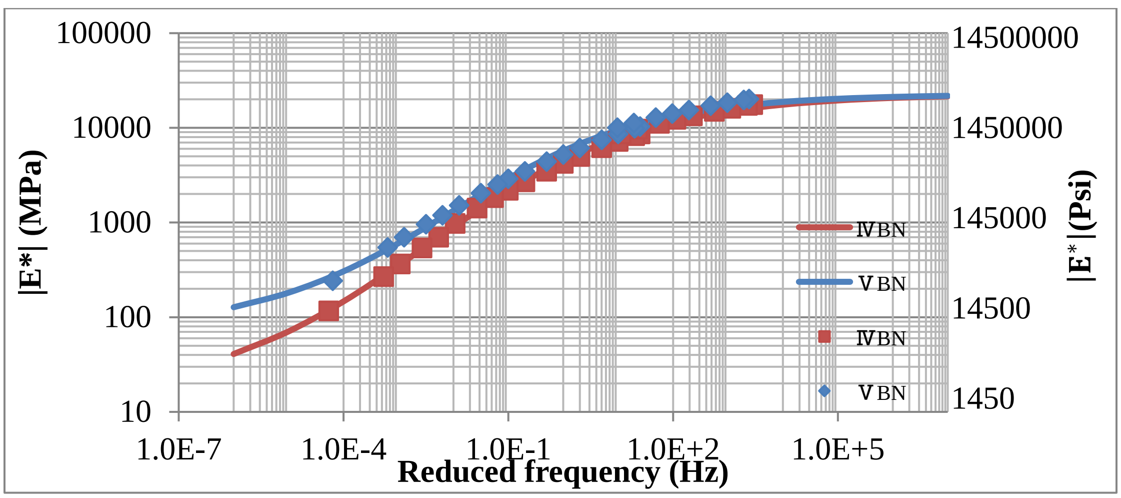

Figure 12-22 Master Dynamic Modulus Curves of Surface Type B Mixtures with RAP and Asphalt Source 2 in Terms of Aggregate Source

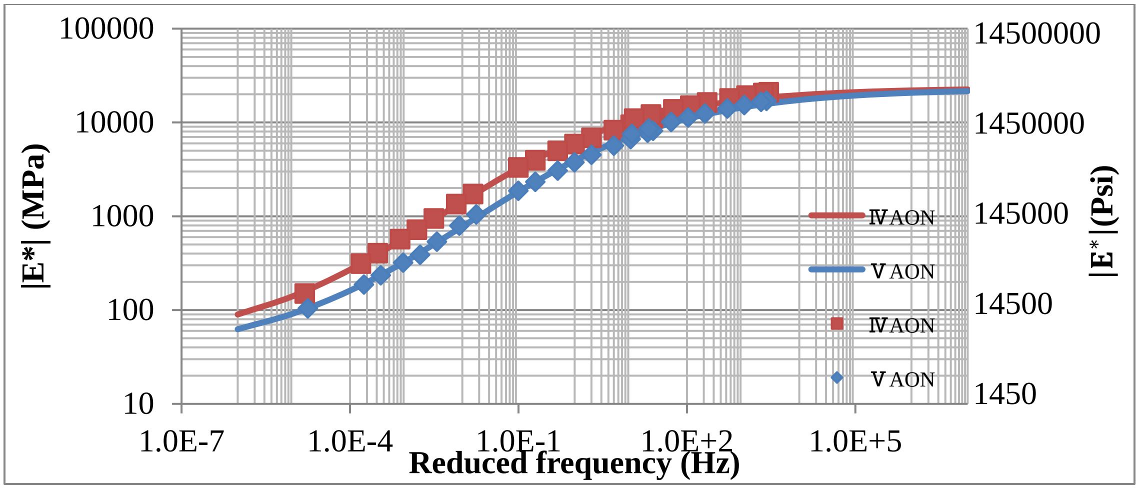

Figure 12-23 Master Dynamic Modulus Curves of Surface Type A Mixtures without RAP using Asphalt Source 2 in Terms of Aggregate Source

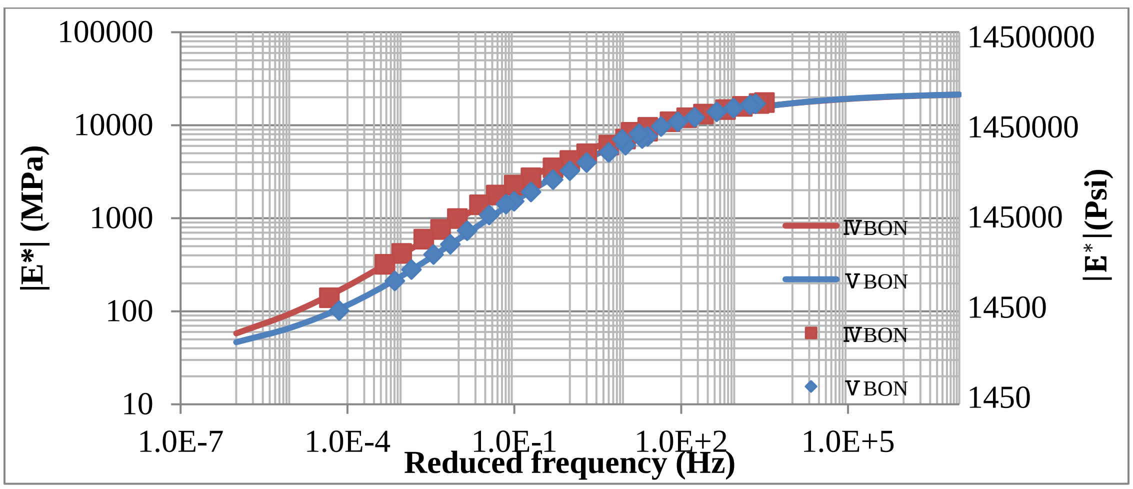

Figure 12-24 Master Dynamic Modulus Curves of Surface Type B Mixtures without RAP using Asphalt Source 2 in Terms of Aggregate Source

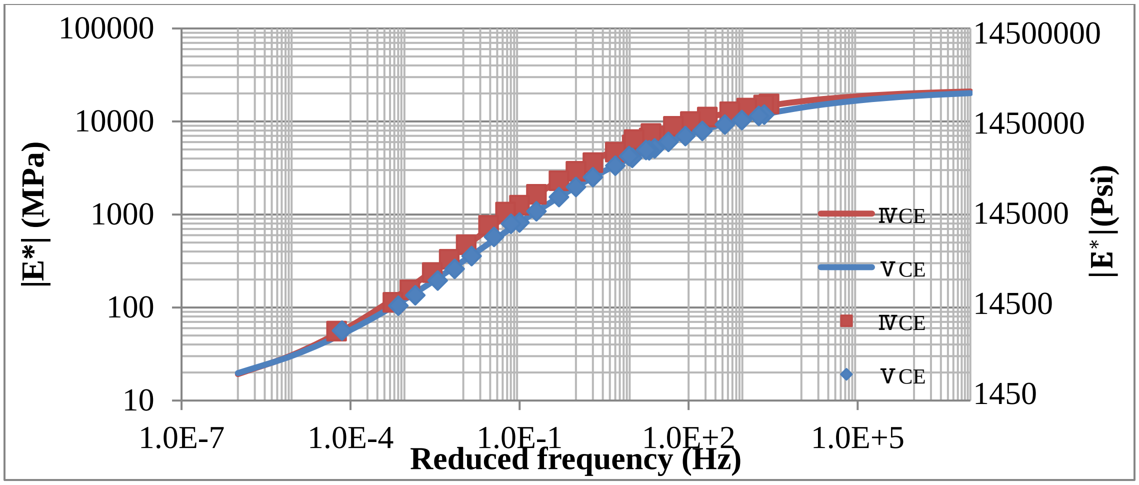

Figure 12-25 Master Dynamic Modulus Curves of Surface Type C Mixtures with RAP and WMA-Chemical Additive in Terms of Aggregate Source

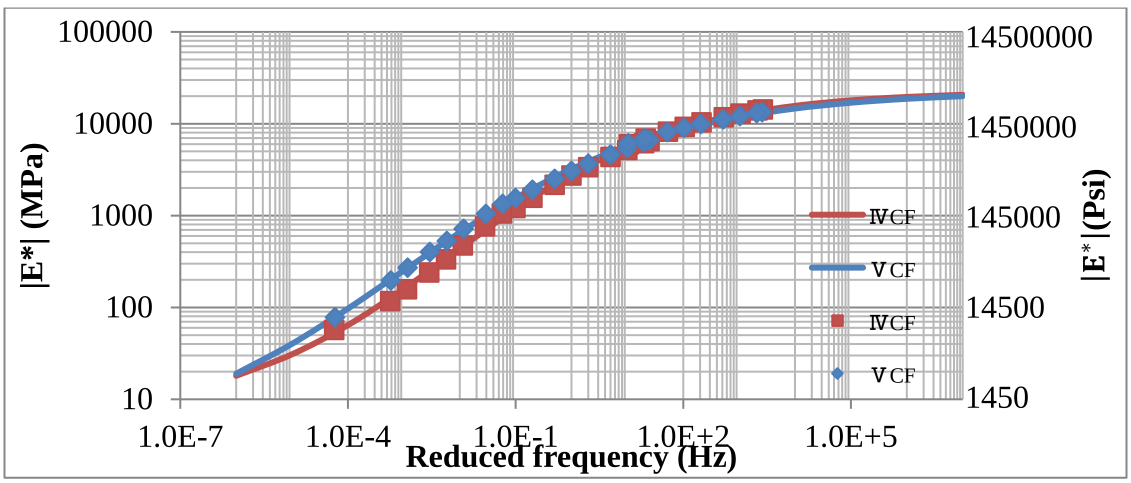

Figure 12-26 Master Dynamic Modulus Curves of Surface Type C Mixtures with RAP and WMA-Foaming in Terms of Aggregate Source

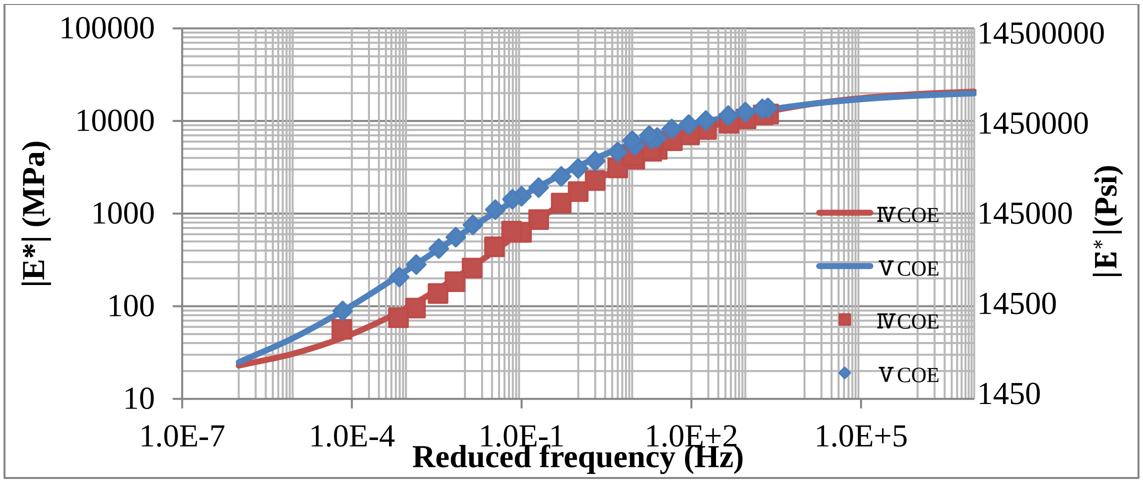

Figure 12-27 Master Dynamic Modulus Curves of Surface Type C Mixtures without RAP using WMA-Chemical Additive in Terms of Aggregate Source

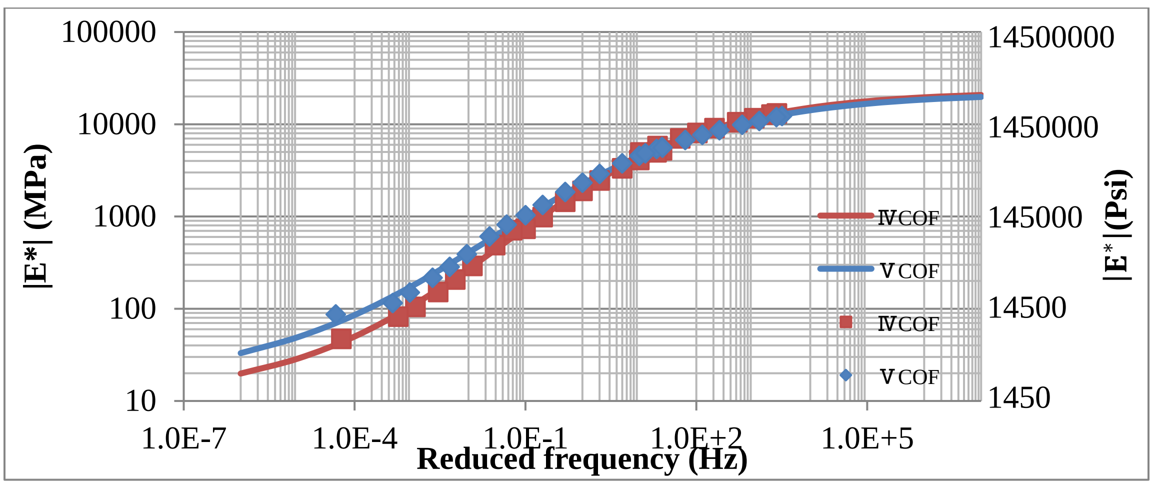

Figure 12-28 Master Dynamic Modulus Curves of Surface Type C Mixtures without RAP using WMA-Foaming in Terms of Aggregate Source

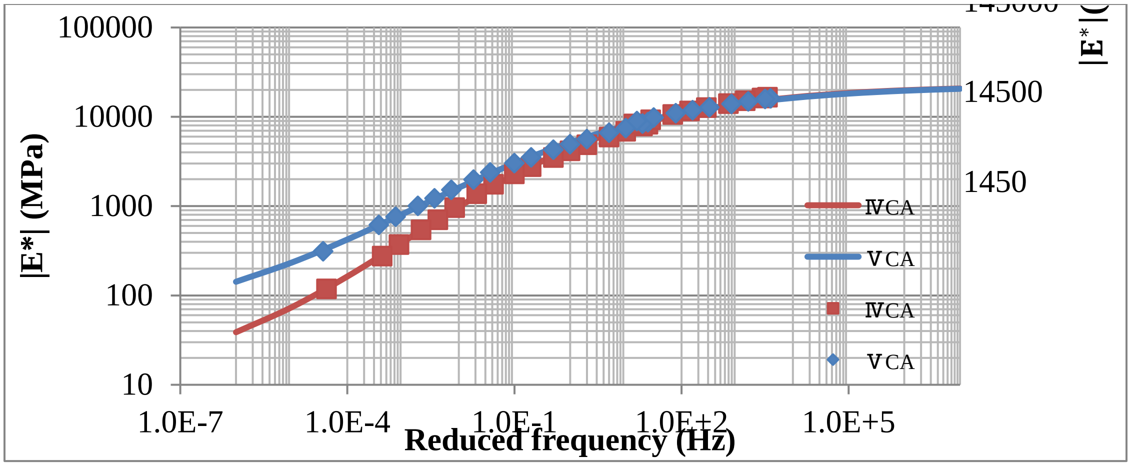

Figure 12-29 Master Dynamic Modulus Curves of Surface Type C Mixtures with RAP and Liquid ASA1 in Terms of Aggregate Source

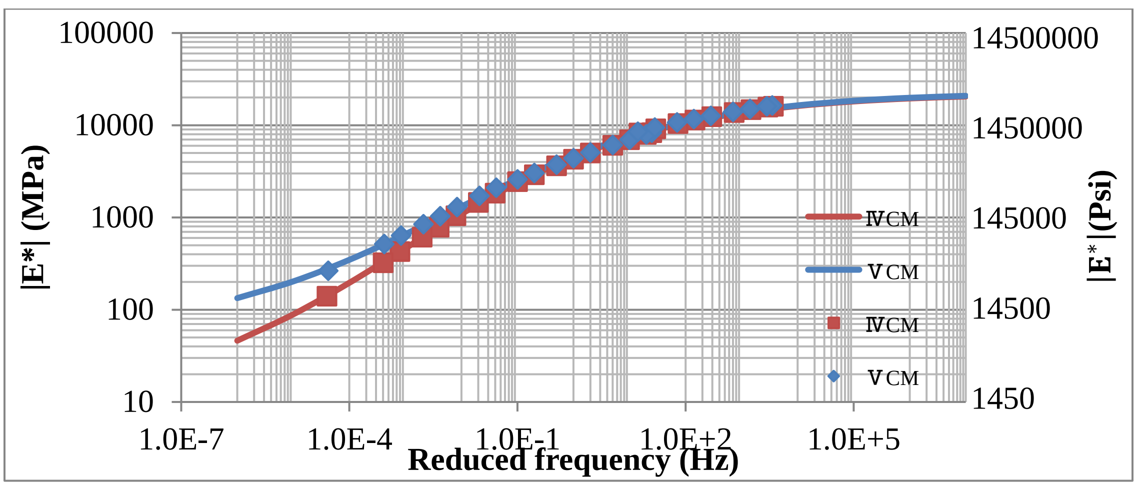

Figure 12-30 Master Dynamic Modulus Curves of Surface Type C Mixtures with RAP and Liquid ASA2 in Terms of Aggregate Source

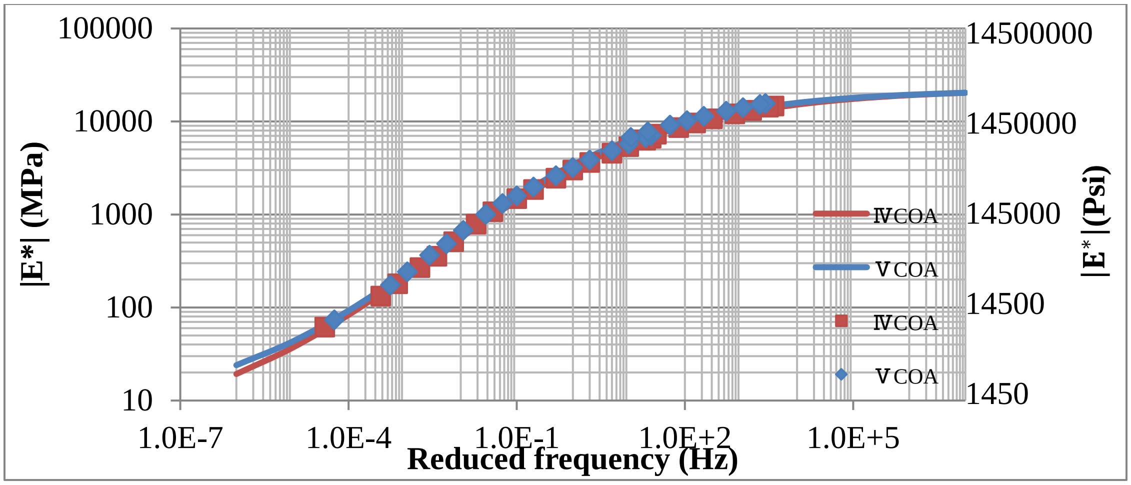

Figure 12-31 Master Dynamic Modulus Curves of Surface Type C Mixtures without RAP using Liquid ASA1 in Terms of Aggregate Source

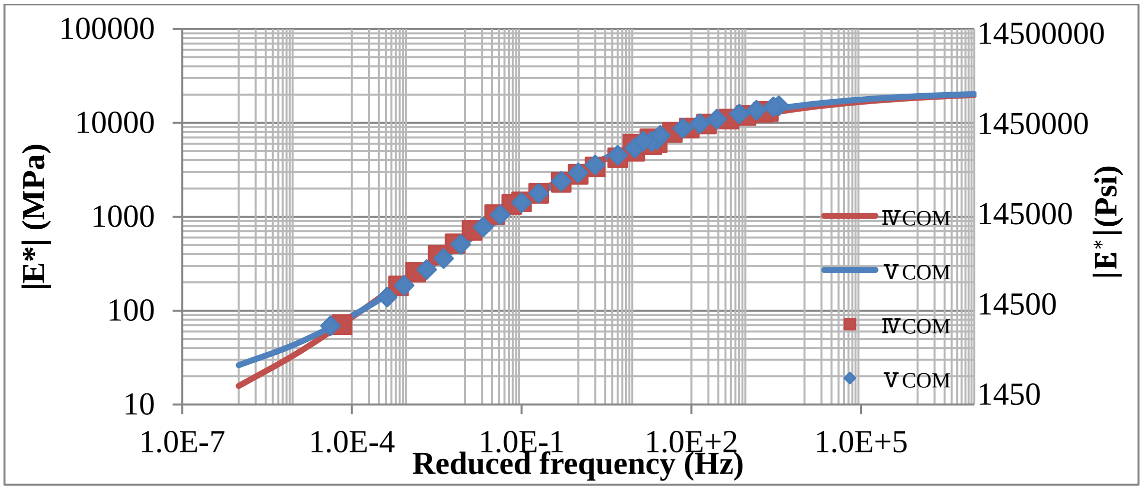

Figure 12-32 Master Dynamic Modulus Curves of Surface Type C Mixtures without RAP using Liquid ASA2 in Terms of Aggregate Source

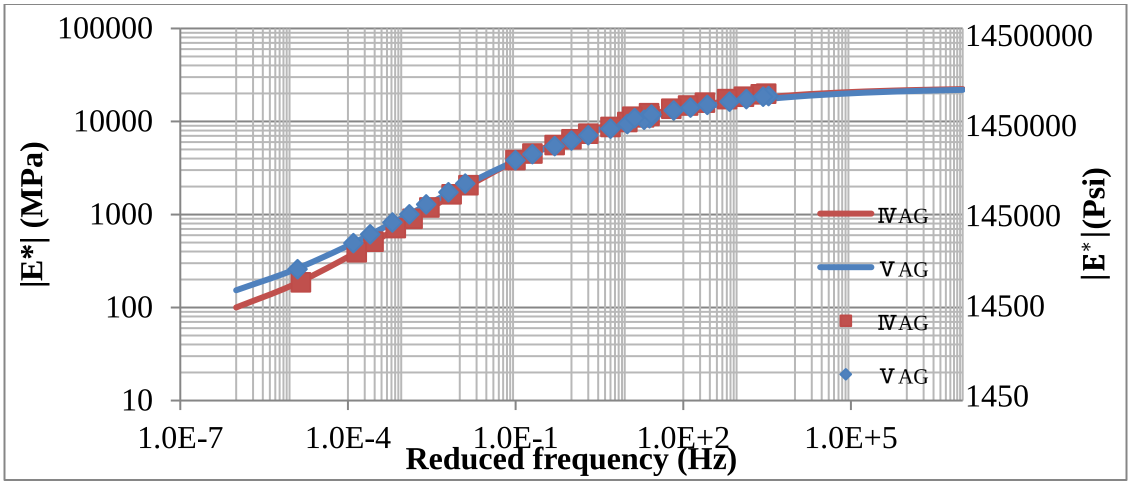

Figure 12-33 Master Dynamic Modulus Curves of Surface Type A Mixtures with RAP after Long-Term Aging in Terms of Aggregate Source

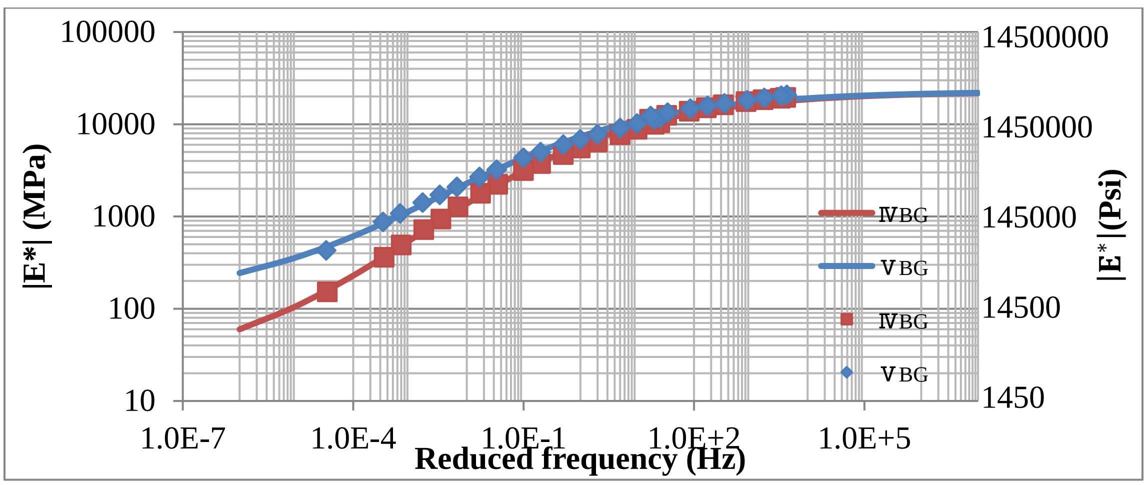

Figure 12-34 Master Dynamic Modulus Curves of Surface Type B Mixtures with RAP after Long-Term Aging in Terms of Aggregate Source

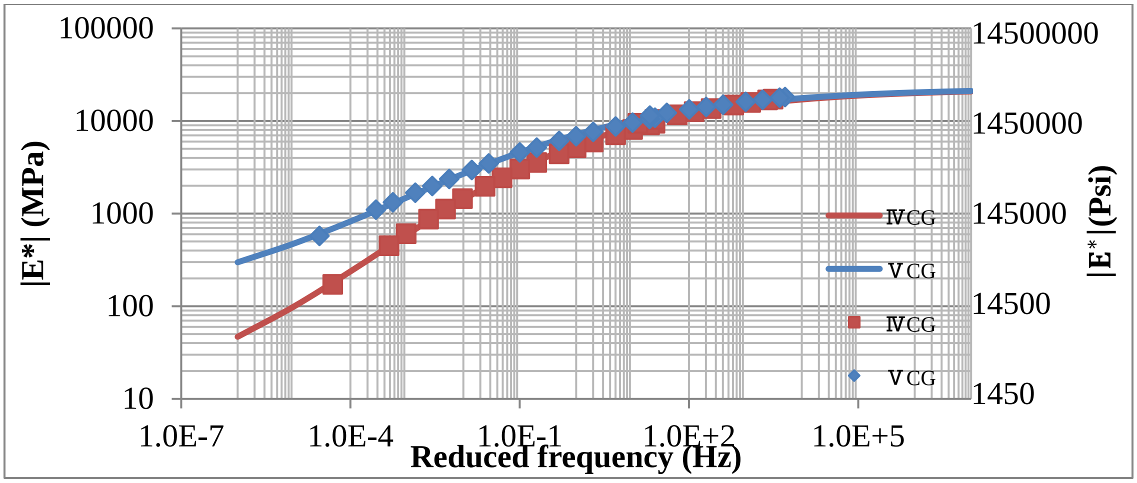

Figure 12-35 Master Dynamic Modulus Curves of Surface Type C Mixtures with RAP after Long-Term Aging in Terms of Aggregate Source

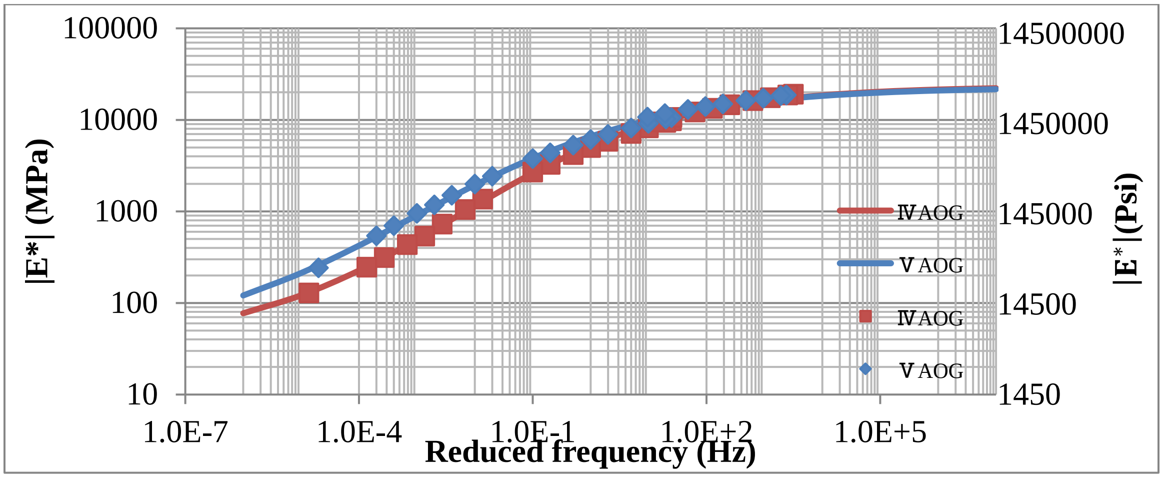

Figure 12-36 Master Dynamic Modulus Curves of Surface Type A Mixtures without RAP after Long-Term Aging in Terms of Aggregate Source

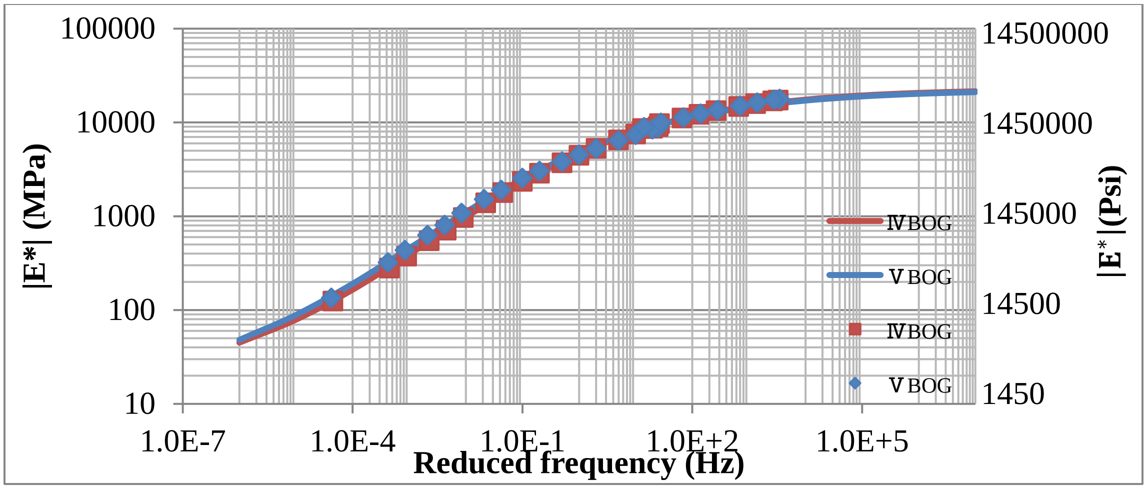

Figure 12-37 Master Dynamic Modulus Curves of Surface Type B mixtures without RAP after Long-Term Aging in Terms of Aggregate Source

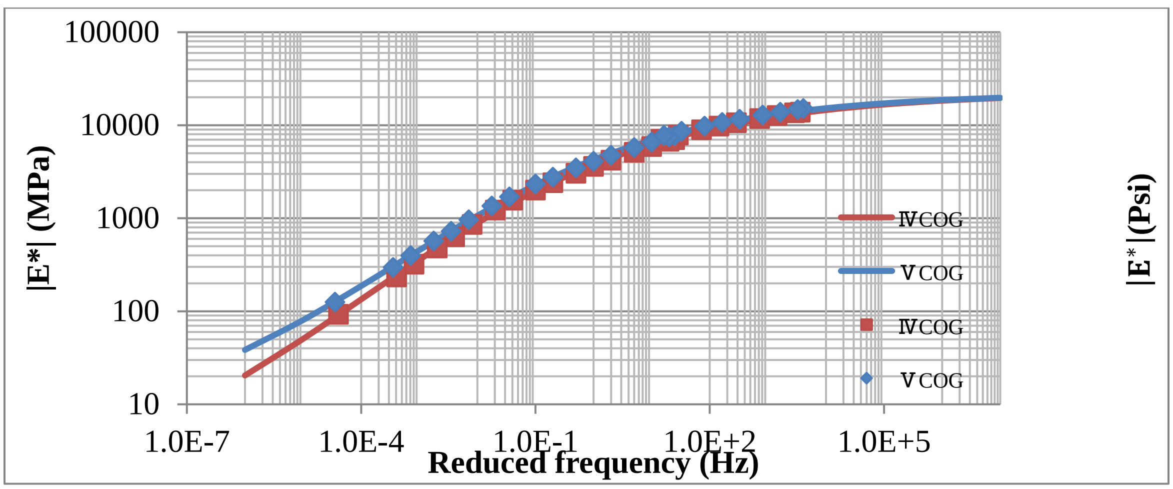

Figure 12-38 Master Dynamic Modulus Curves of Surface Type C Mixtures without RAP after Long-Term Aging in Terms of Aggregate Source

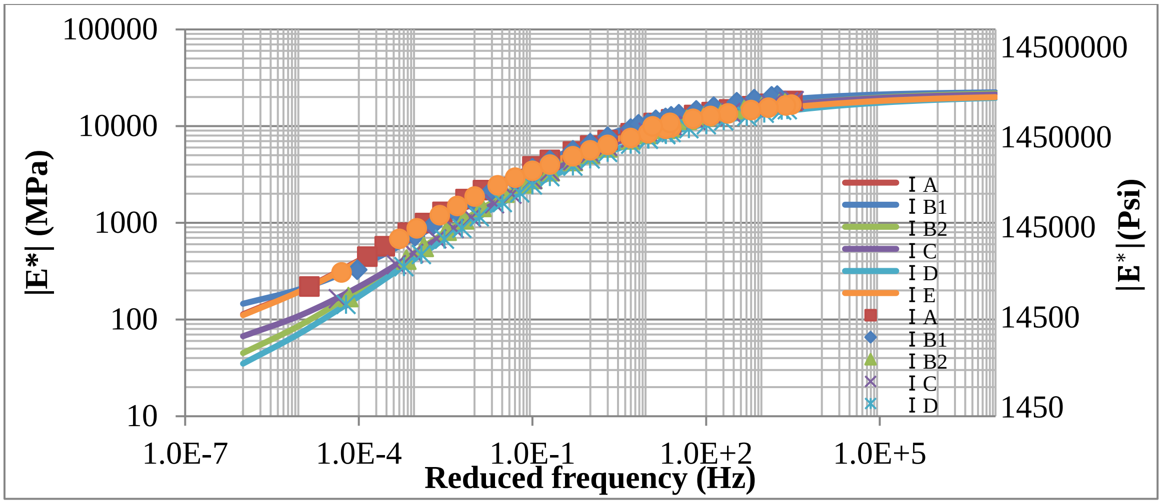

Figure 12-39 Master Dynamic Modulus Curves of Mixtures from Aggregate I with RAP in Terms of Surface Mixture Type

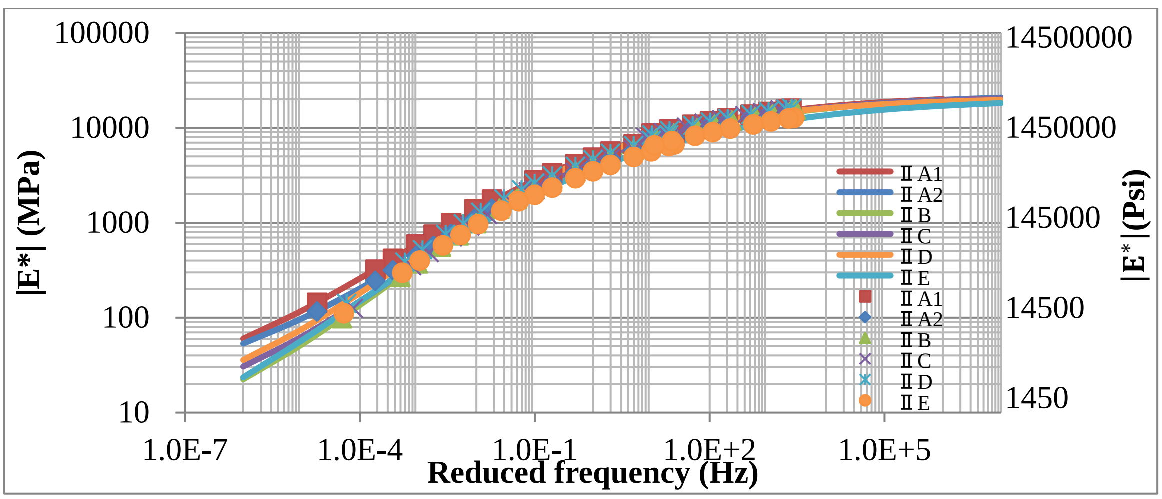

Figure 12-40 Master Dynamic Modulus Curves of Mixtures from Aggregate II with RAP in Terms of Surface Mixture Type

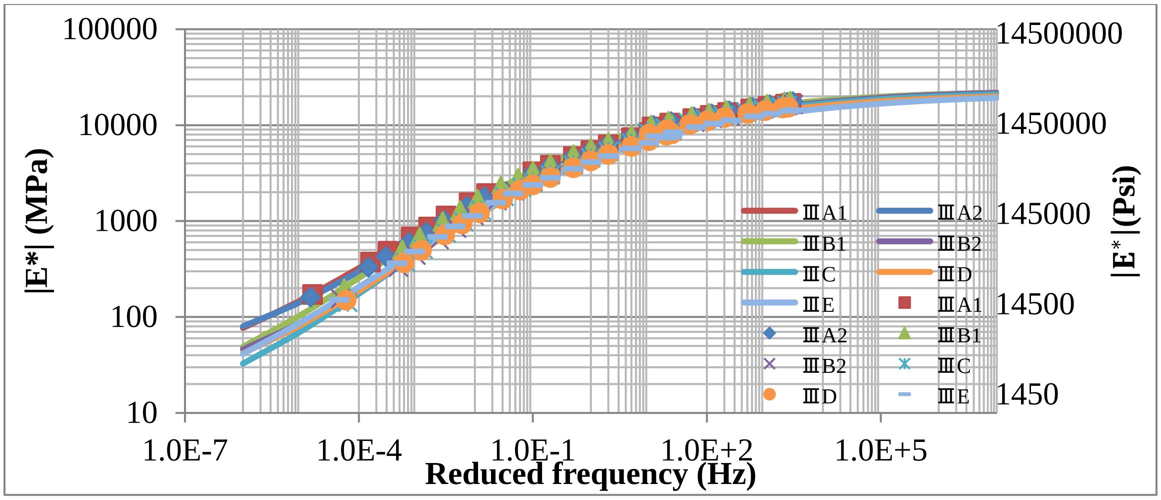

Figure 12-41 Master Dynamic Modulus Curves of Mixtures from Aggregate III with RAP in Terms of Surface Mixture Type

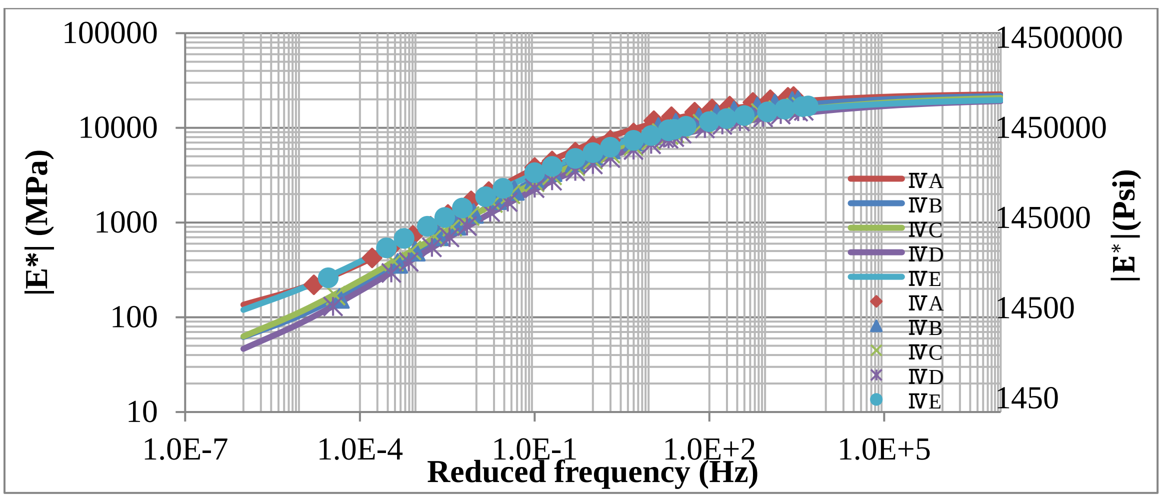

Figure 12-42 Master Dynamic Modulus Curves of Mixtures from Aggregate IV with RAP in Terms of Surface Mixture Type

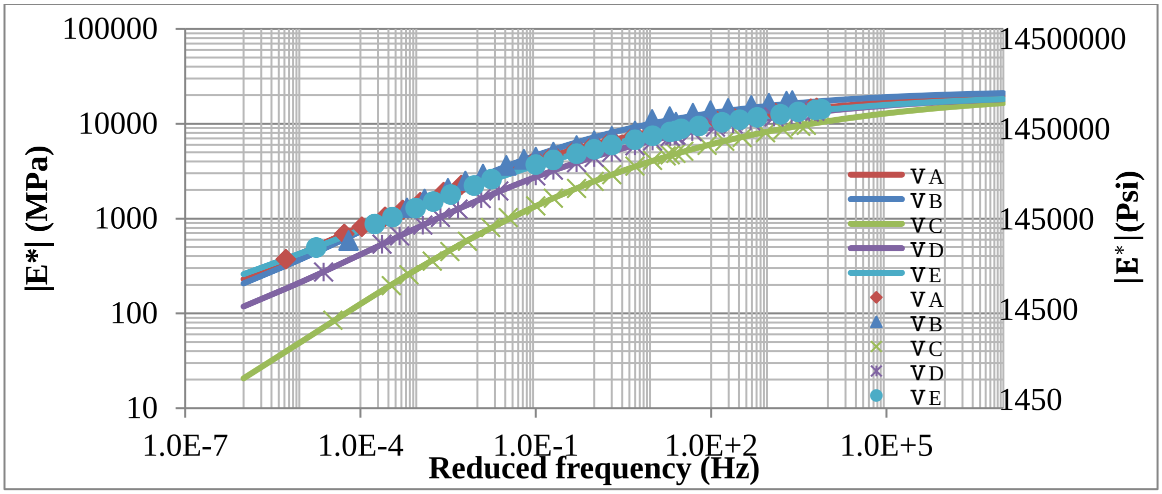

Figure 12-43 Master Dynamic Modulus Curves of Mixtures from Aggregate V with RAP in Terms of Surface Mixture Type

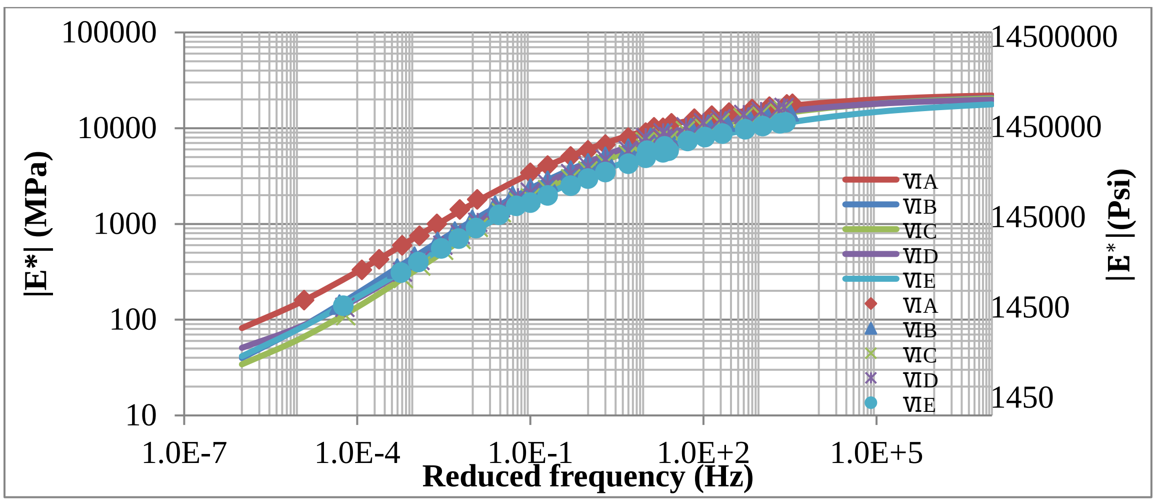

Figure 12-44 Master Dynamic Modulus Curves of Mixtures from Aggregate VI with RAP in Terms of Surface Mixture Type

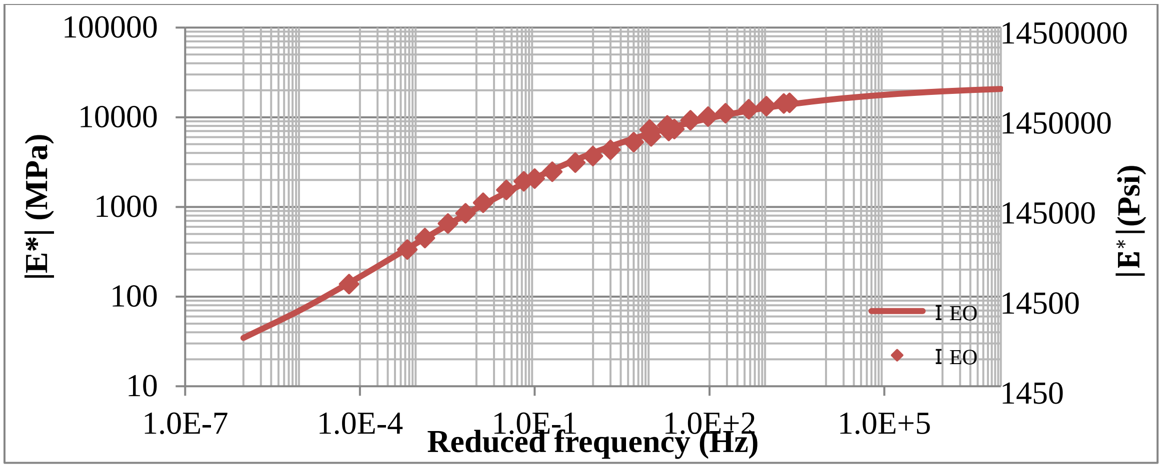

Figure 12-45 Master Dynamic Modulus Curves of Mixtures from Aggregate I without RAP in Terms of Surface Mixture Type

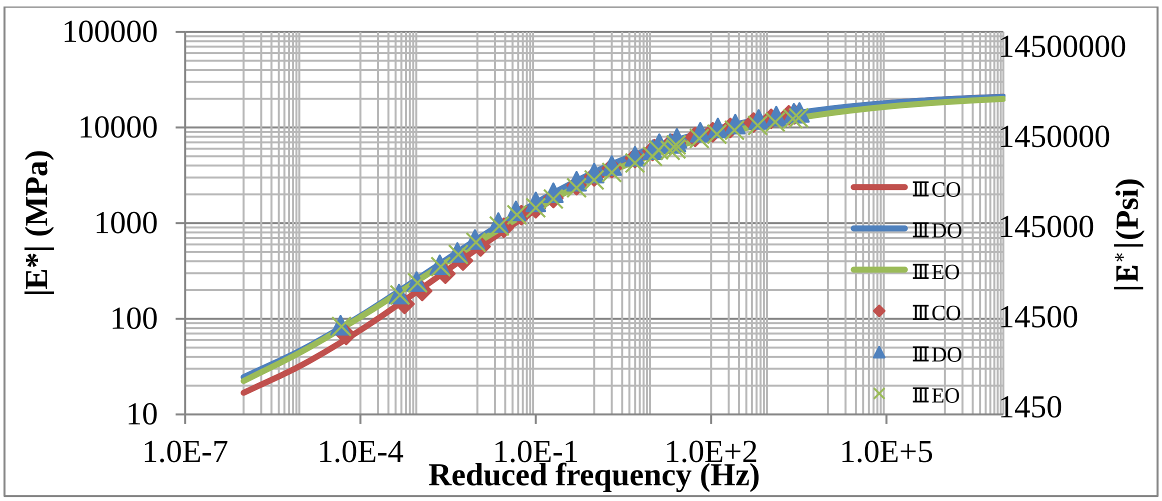

Figure 12-46 Master Dynamic Modulus Curves of Mixtures from Aggregate III without RAP in Terms of Surface Mixture Type

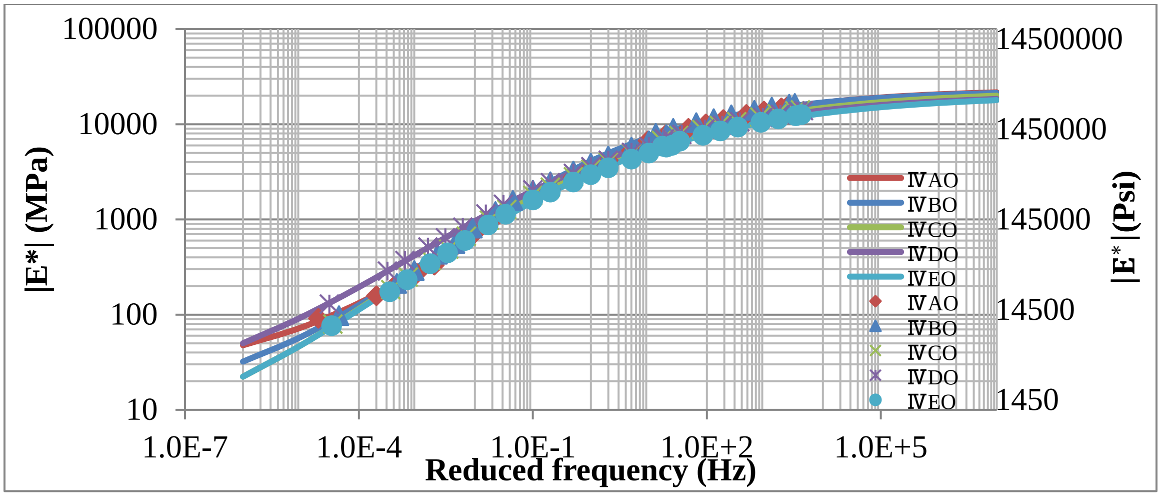

Figure 12-47 Master Dynamic Modulus Curves of Mixtures from Aggregate IV without RAP in Terms of Surface Mixture Type

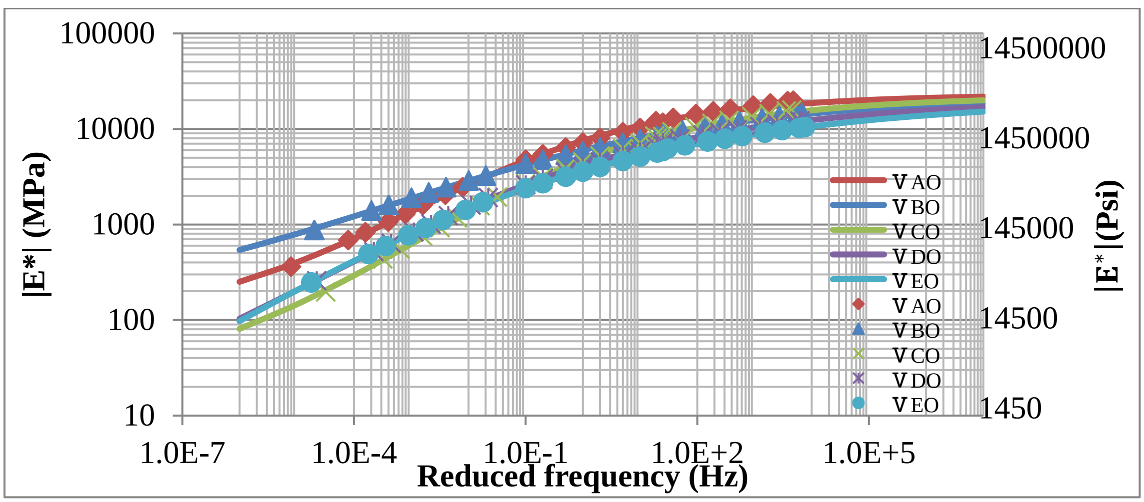

Figure 12-48 Master Dynamic Modulus Curves of Mixtures from Aggregate V without RAP in Terms of Surface Mixture Type

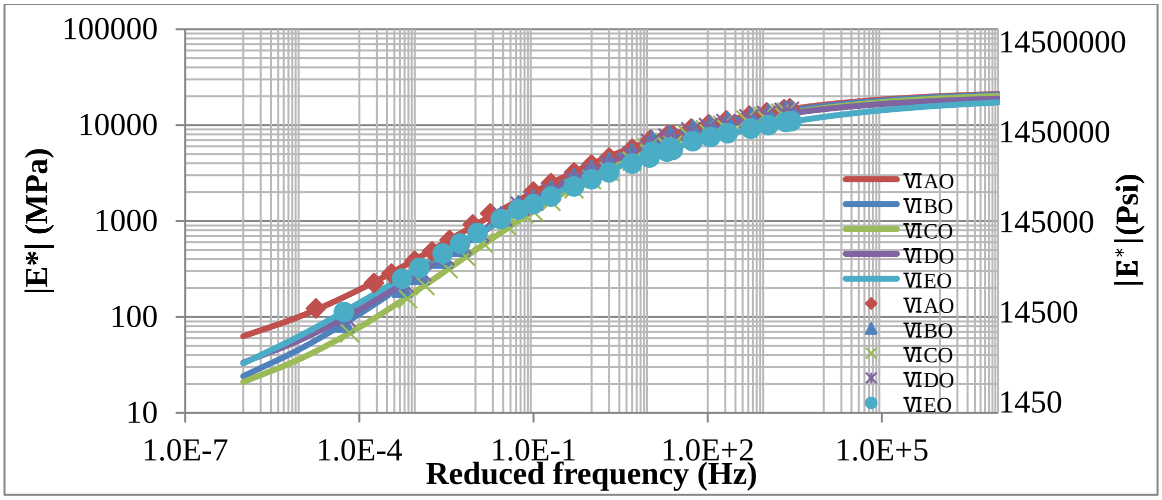

Figure 12-49 Master Dynamic Modulus Curves of Mixtures from Aggregate VI without RAP in Terms of Surface Mixture Type

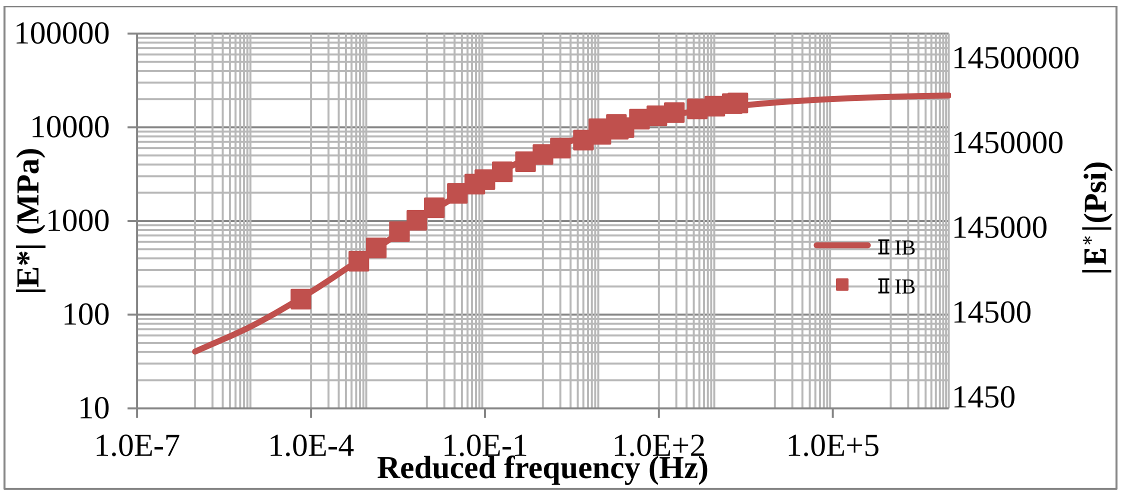

Figure 12-50 Master Dynamic Modulus Curves of Mixtures from Aggregate II with RAP in Terms of Intermediate Mixture Type

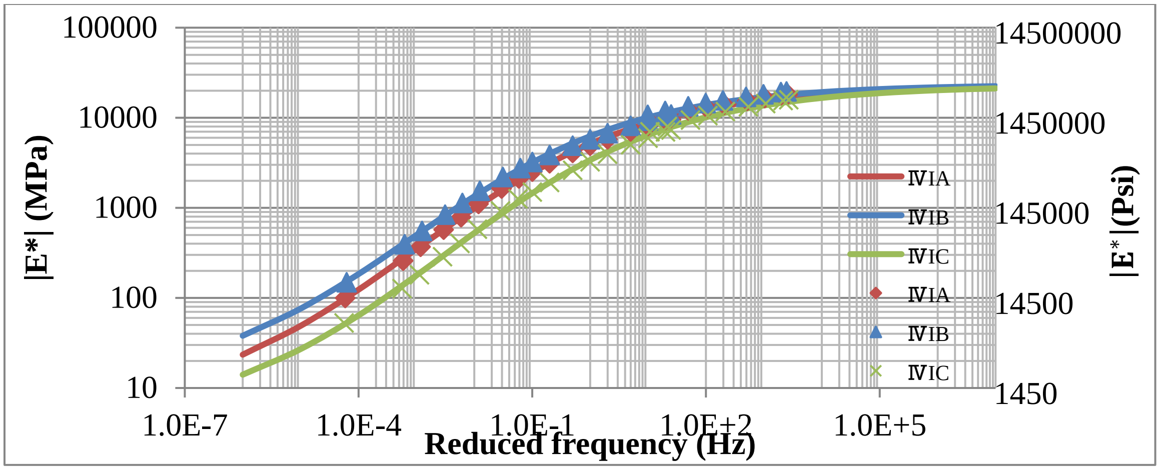

Figure 12-51 Master Dynamic Modulus Curves of Mixtures from Aggregate IV with RAP in Terms of Intermediate Mixture Type

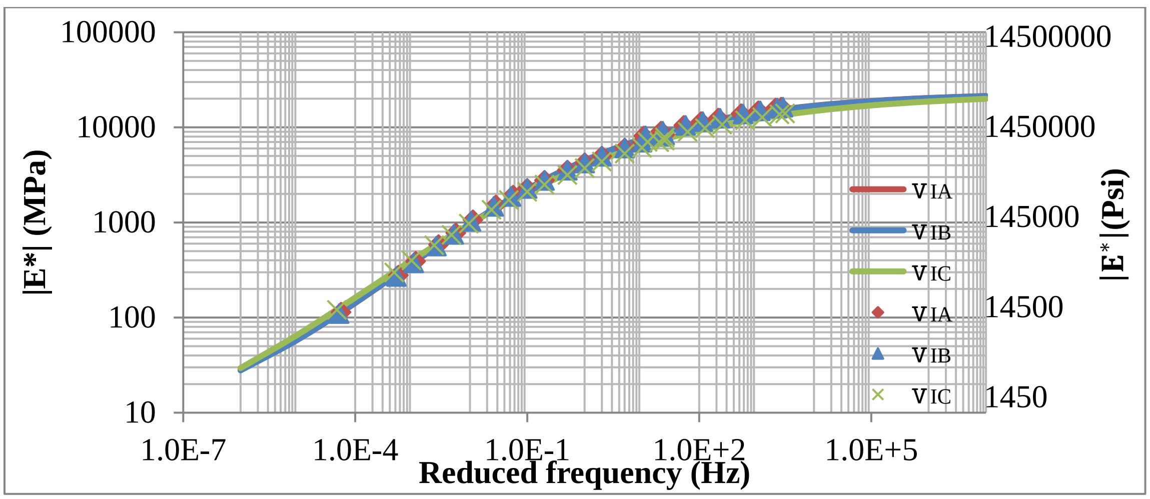

Figure 12-52 Master Dynamic Modulus Curves of Mixtures from Aggregate V with RAP in Terms of Intermediate Mixture Type

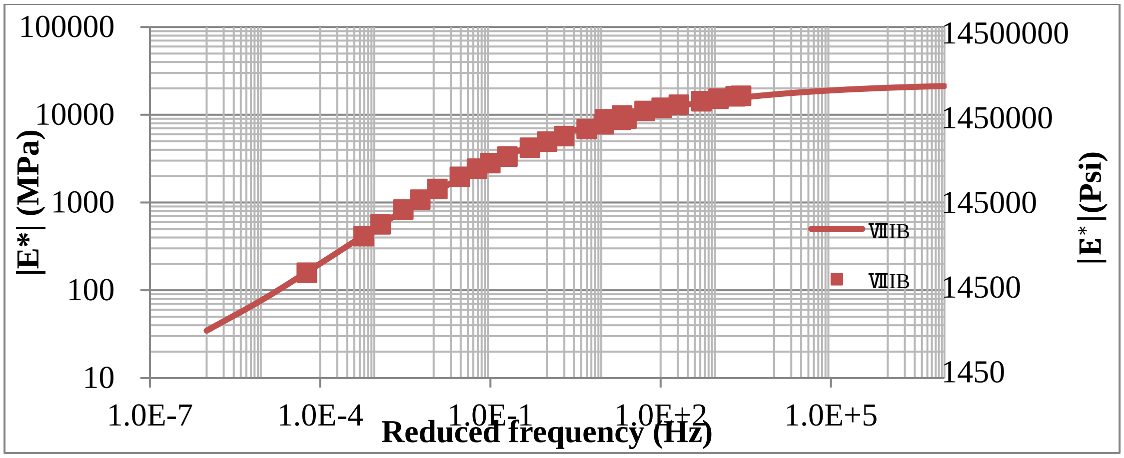

Figure 12-53 Master Dynamic Modulus Curves of Mixtures from Aggregate VII with RAP in Terms of Intermediate Mixture Type

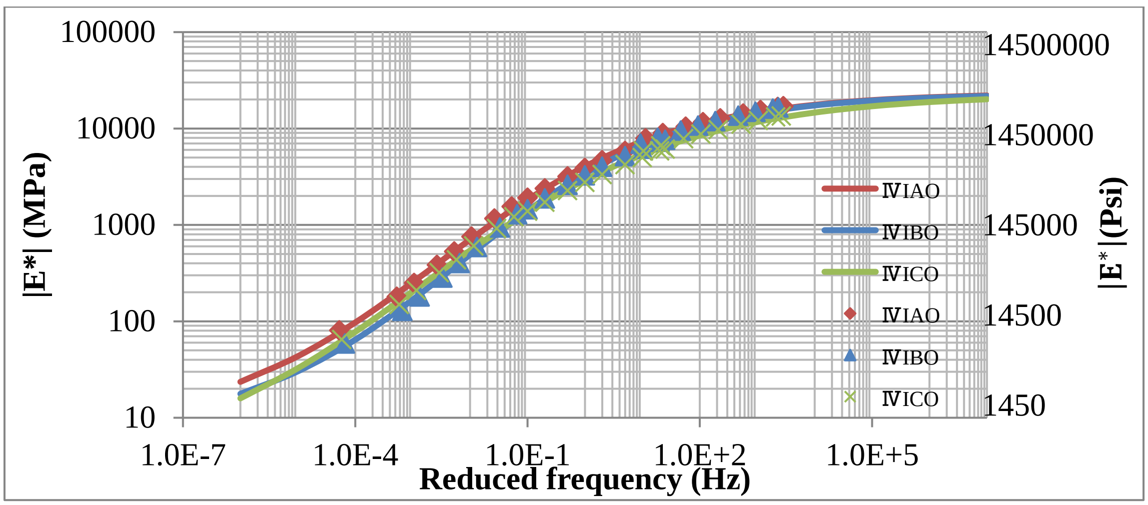

Figure 12-54 Master Dynamic Modulus Curves of Mixtures from Aggregate IV without RAP in Terms of Intermediate Mixture Type

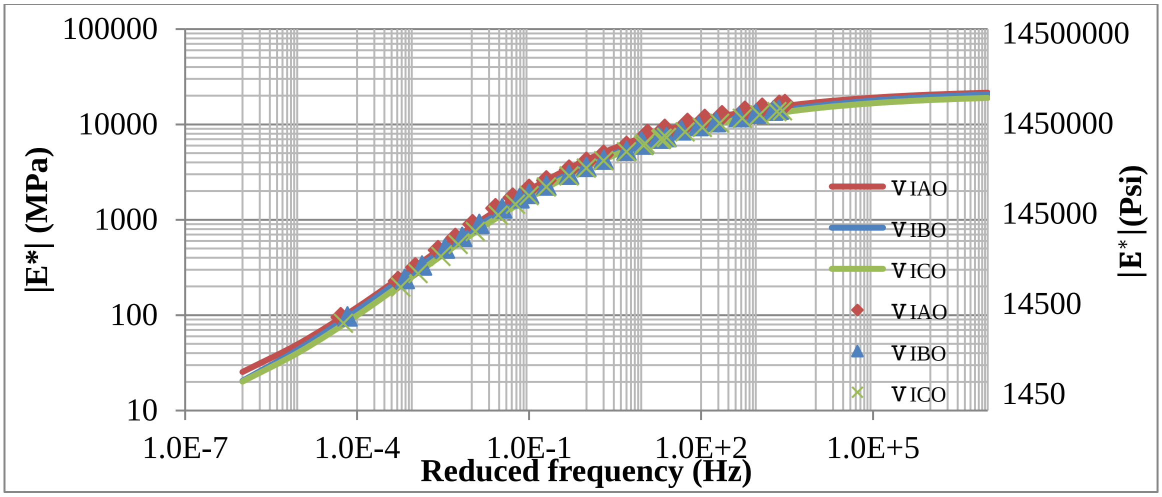

Figure 12-55 Master Dynamic Modulus Curves of Mixtures from Aggregate V without RAP in Terms of Intermediate Mixture Type

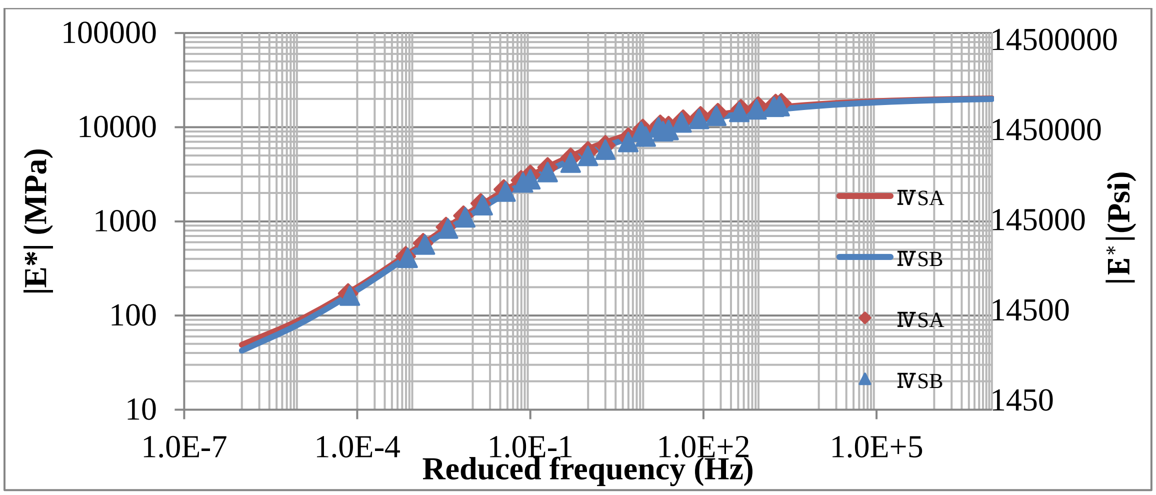

Figure 12-56 Master Dynamic Modulus Curves of Mixtures from Aggregate IV with RAP in Terms of Base Mixture Type

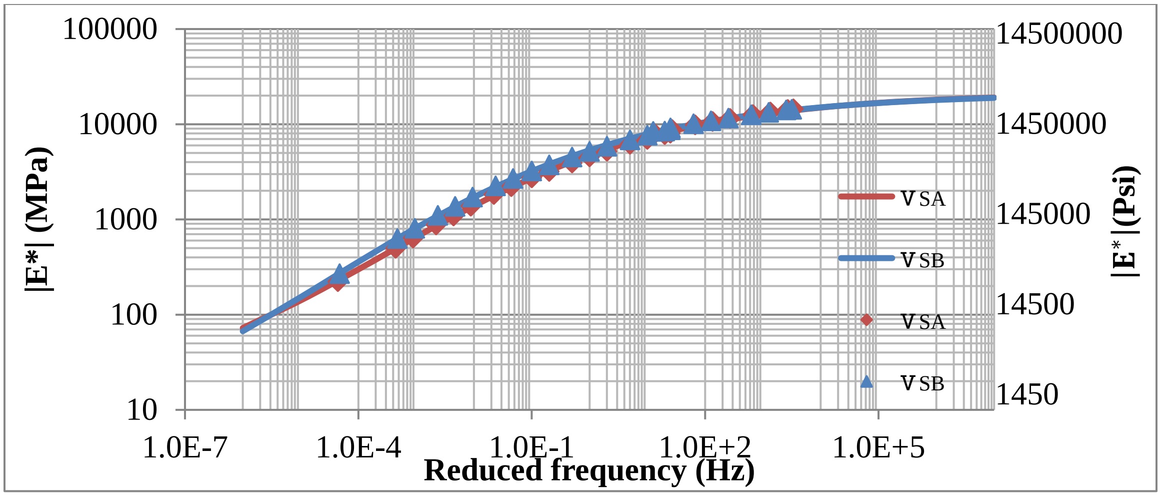

Figure 12-57 Master Dynamic Modulus Curves of Mixtures from Aggregate V with RAP in Terms of Base Mixture Type

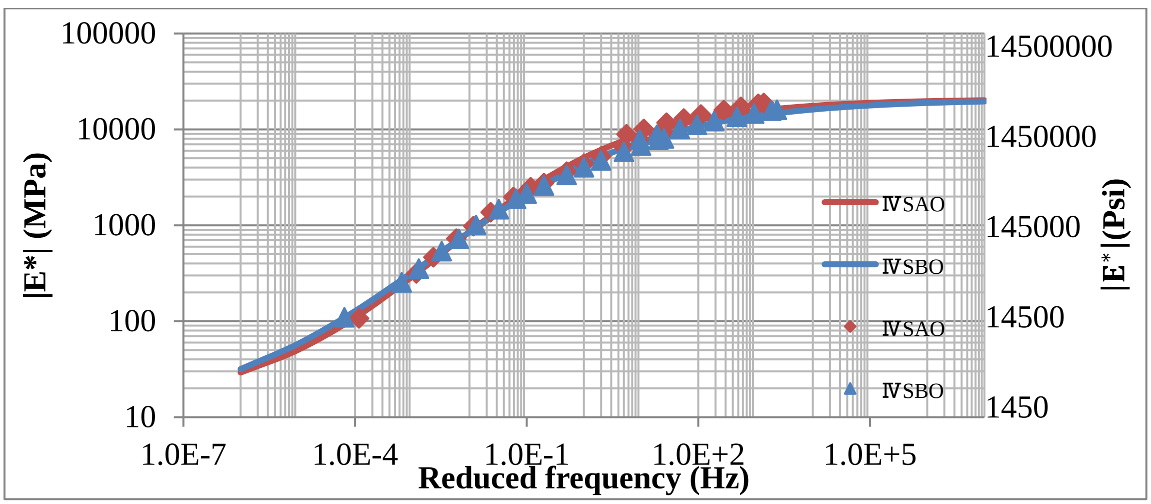

Figure 12-58 Master Dynamic Modulus Curves of Mixtures from Aggregate IV without RAP in Terms of Base Type

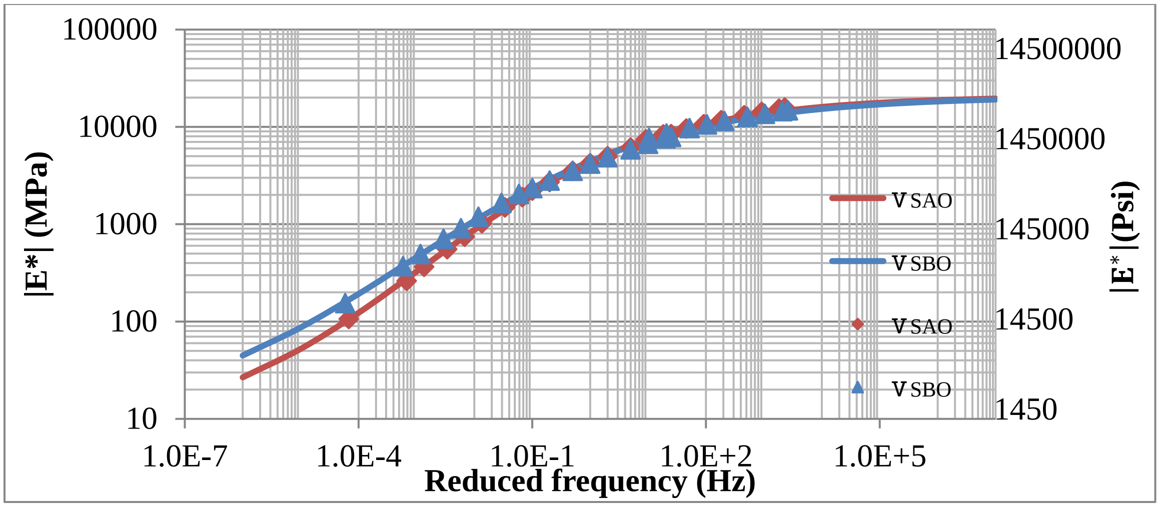

Figure 12-59 Master Dynamic Modulus Curves of Mixtures from Aggregate V without RAP in Terms of Base Mixture Type

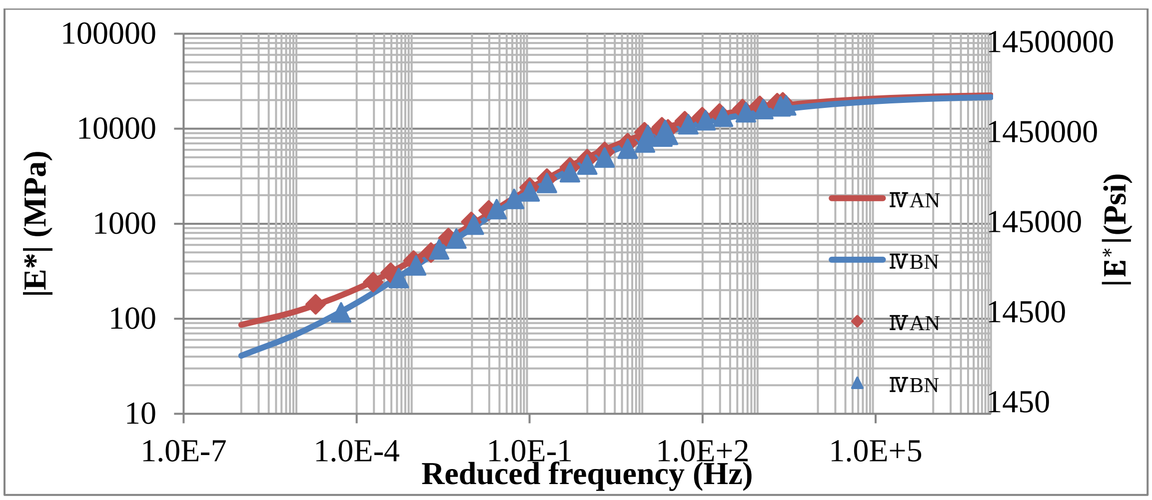

Figure 12-60 Master Dynamic Modulus Curves of Mixtures from Aggregate IV with RAP and Asphalt Source 2 in Terms of Surface Mixture Type

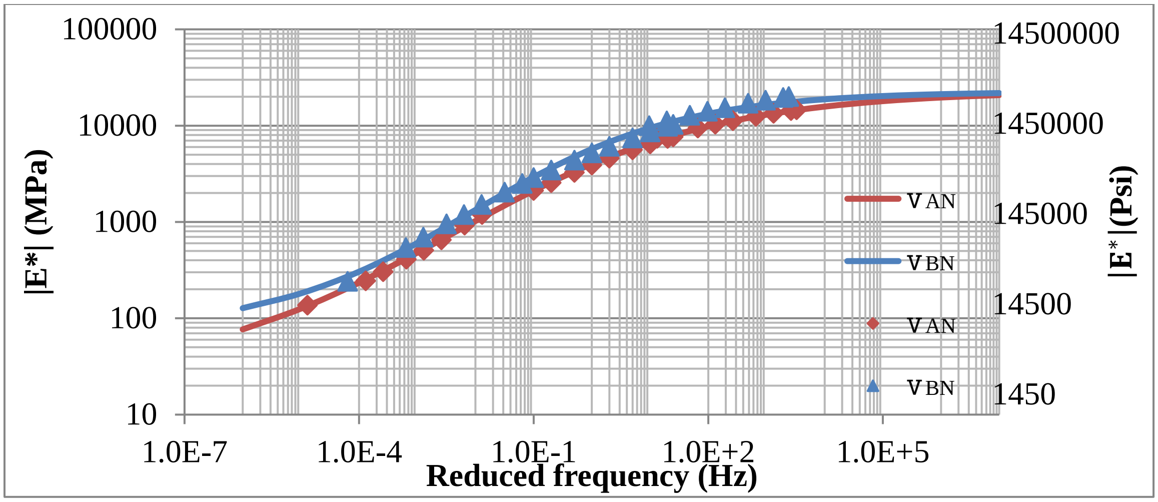

Figure 12-61 Master Dynamic Modulus Curves of Mixtures from Aggregate V with RAP and Asphalt Source 2 in Terms of Surface Mixture Type

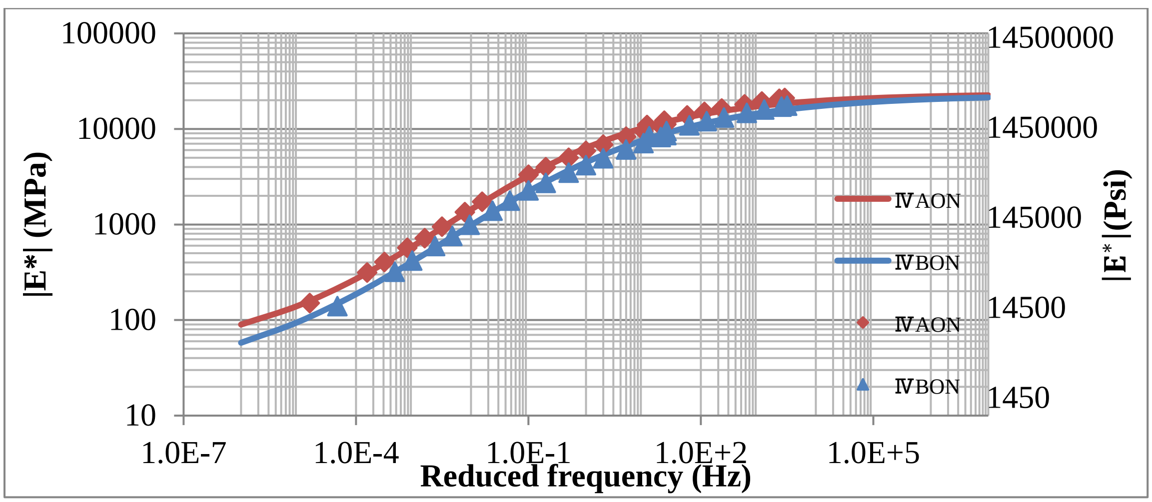

Figure 12-62 Master Dynamic Modulus Curves of Mixtures from Aggregate IV without RAP using Asphalt Source 2 in Terms of Surface Mixture Type

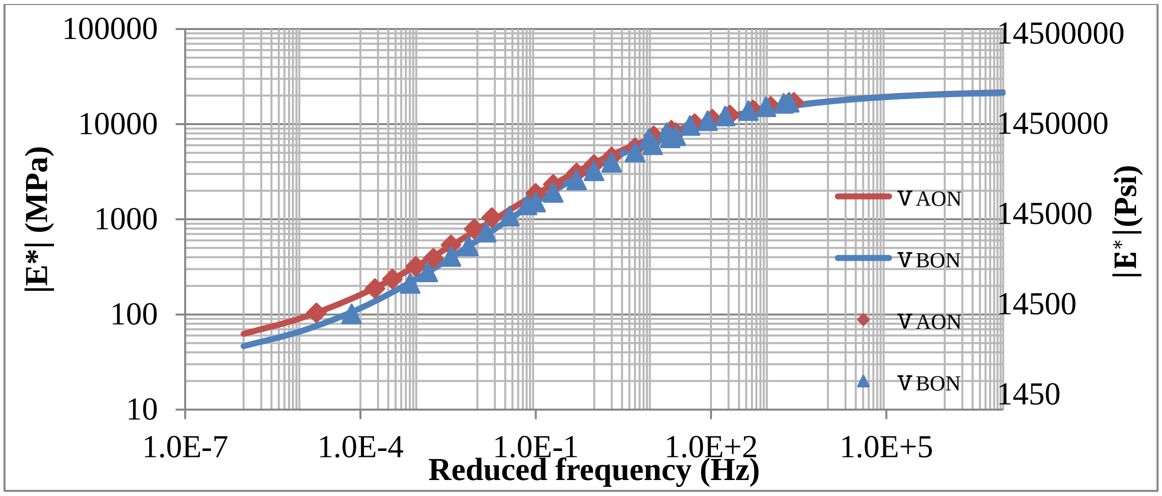

Figure 12-63 Master Dynamic Modulus Curves of Mixtures from Aggregate V without RAP using Asphalt Source 2 in Terms of Surface Mixture Type

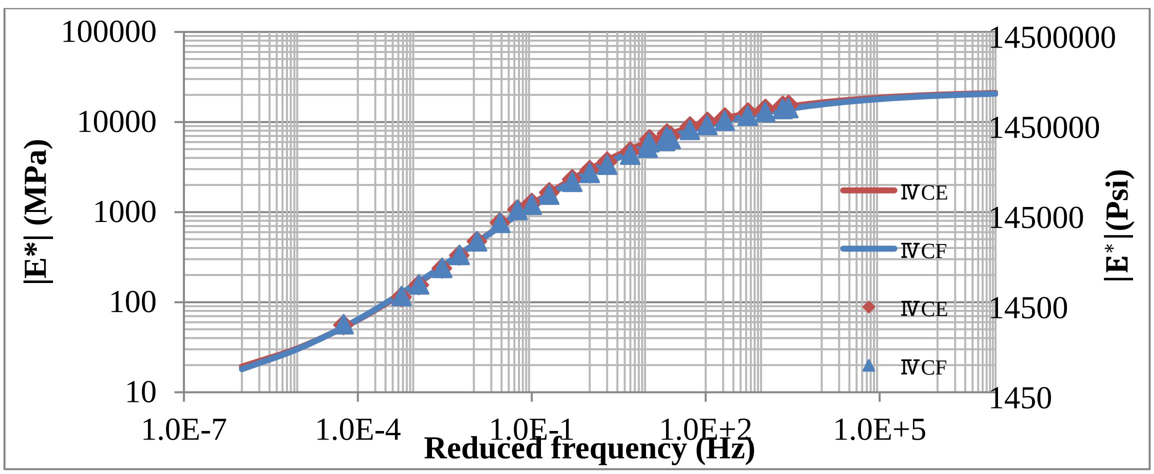

Figure 12-64 Master Dynamic Modulus Curves of Surface Type C Mixtures from Aggregate IV with RAP in Terms of WMA Technology Type

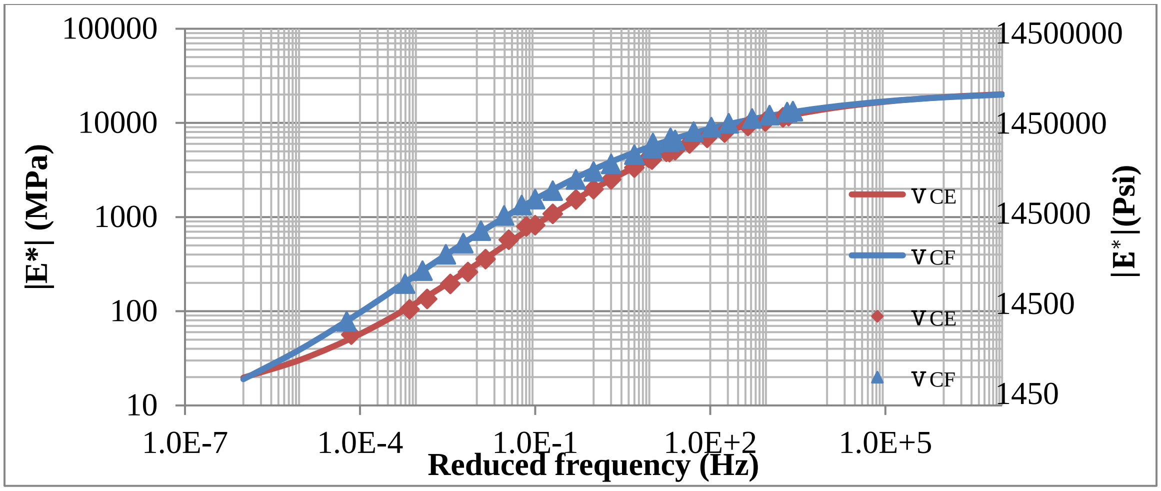

Figure 12-65 Master Dynamic Modulus Curves of Surface Type C Mixtures from Aggregate V with RAP in Terms of WMA Technology Type

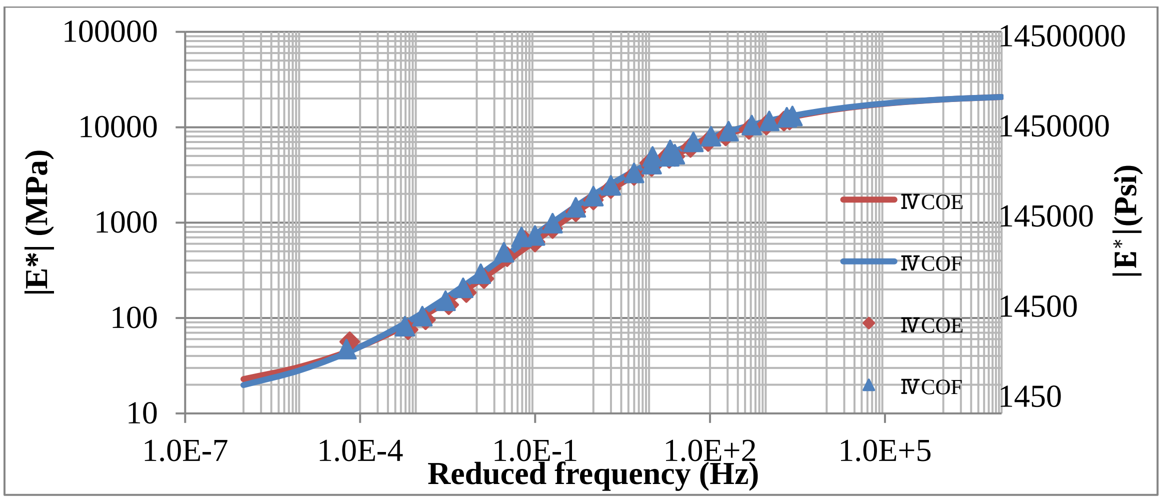

Figure 12-66 Master Dynamic Modulus Curves of Surface Type C Mixtures from Aggregate IV without RAP in Terms of WMA Technology Type

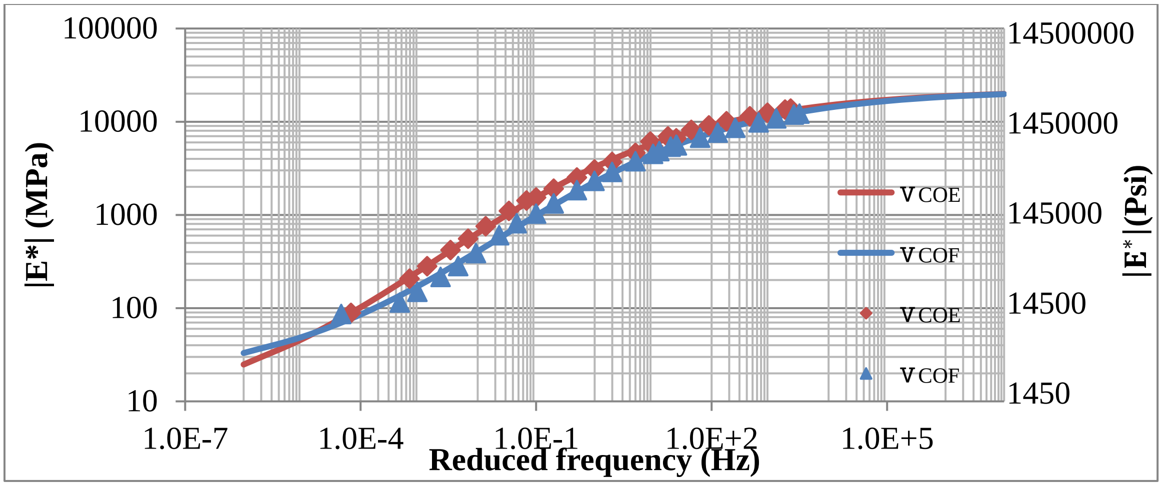

Figure 12-67 Master Dynamic Modulus Curves of Surface Type C Mixtures from Aggregate V without RAP in Terms of WMA Technology Type

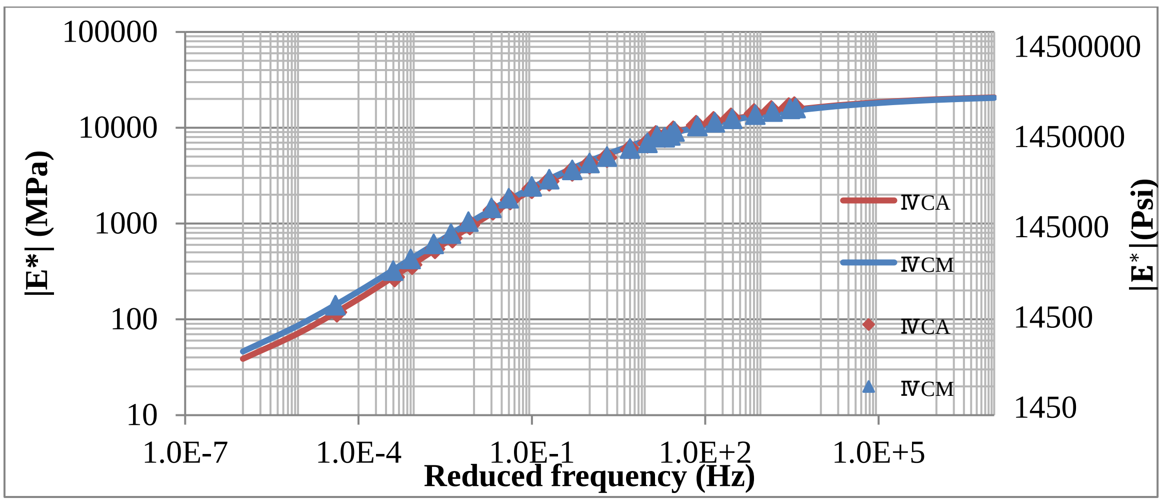

Figure 12-68 Master Dynamic Modulus Curves of Surface Type C Mixtures from Aggregate IV with RAP in Terms of Liquid ASA Type

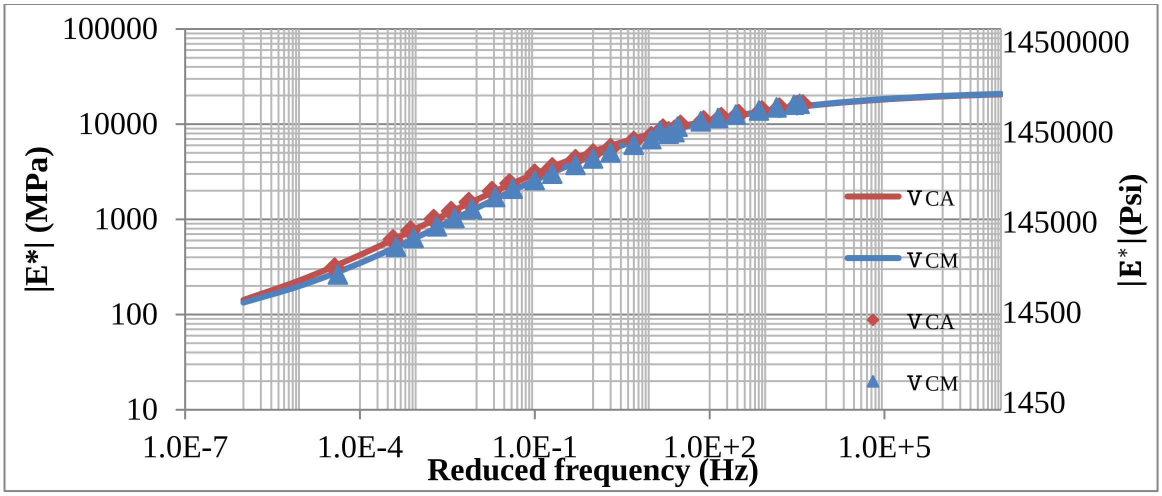

Figure 12-69 Master Dynamic Modulus Curves of Surface Type C Mixtures from Aggregate V with RAP in Terms of Liquid ASA Type

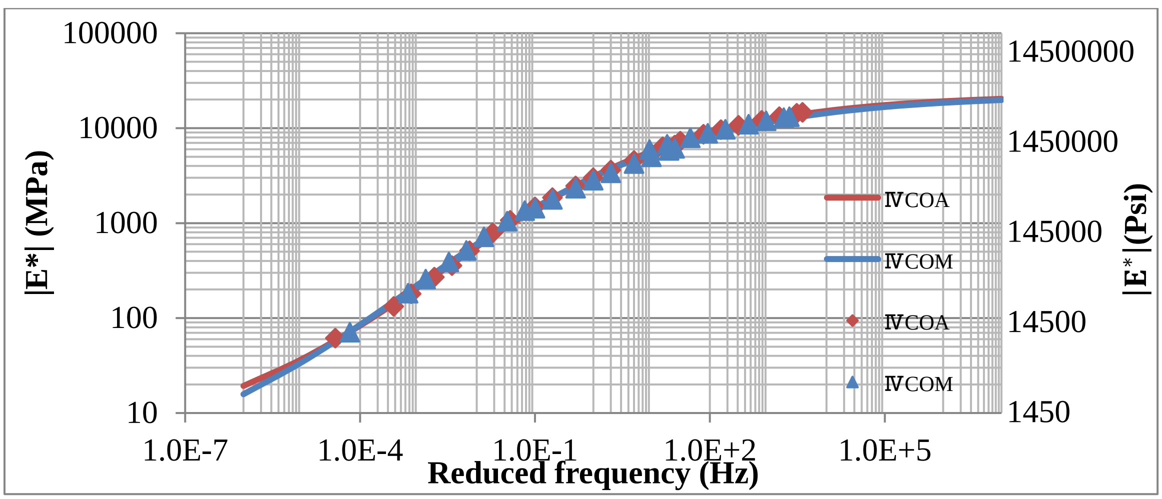

Figure 12-70 Master Dynamic Modulus Curves of Surface Type C Mixtures from Aggregate IV without RAP in Terms of Liquid ASA Type

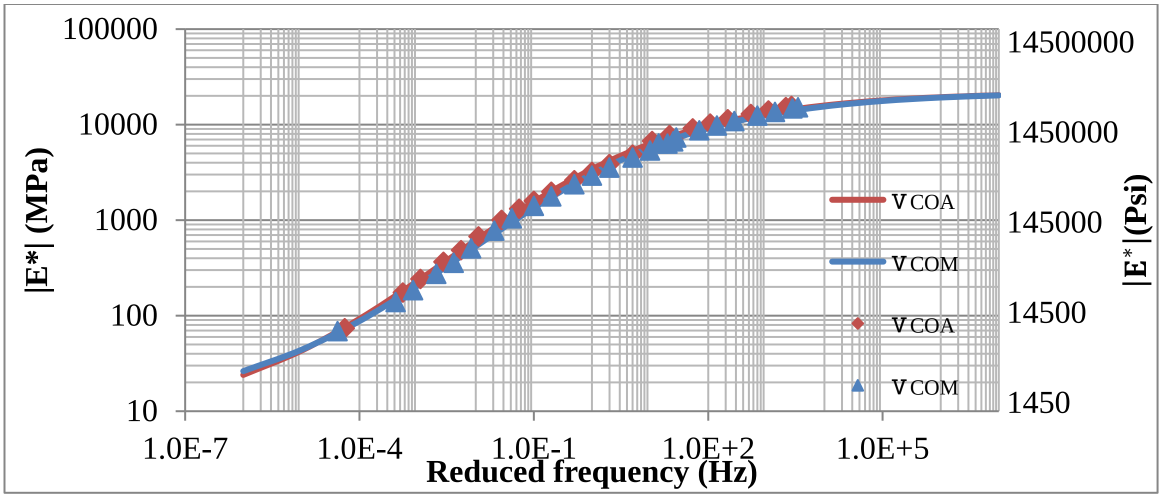

Figure 12-71 Master Dynamic Modulus Curves of Surface Type C Mixtures from Aggregate V without RAP in Terms of Liquid ASA Type

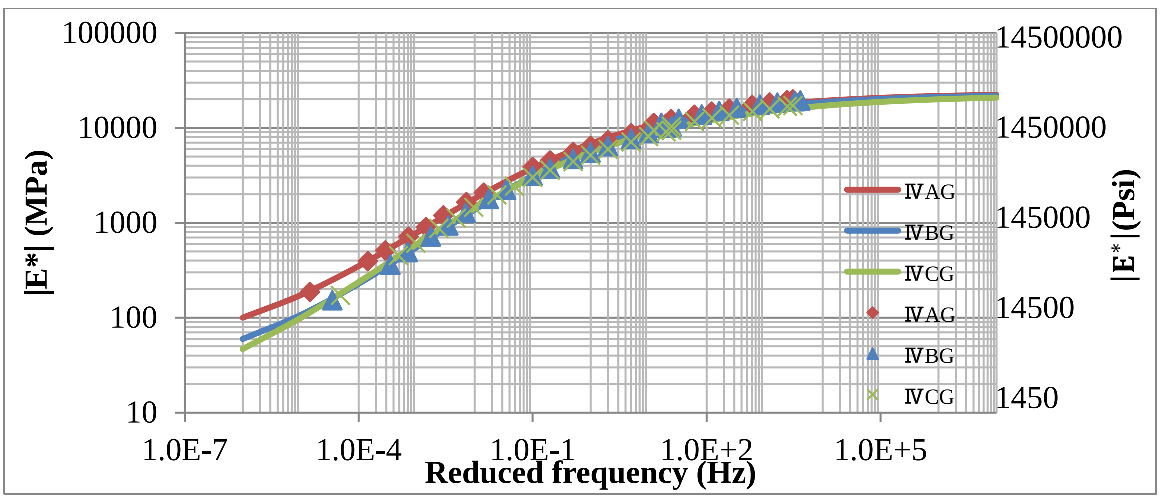

Figure 12-72 Master Dynamic Modulus Curves of Mixtures from Aggregate IV with RAP after Long-Term Aging in Terms of Surface Mixture Type

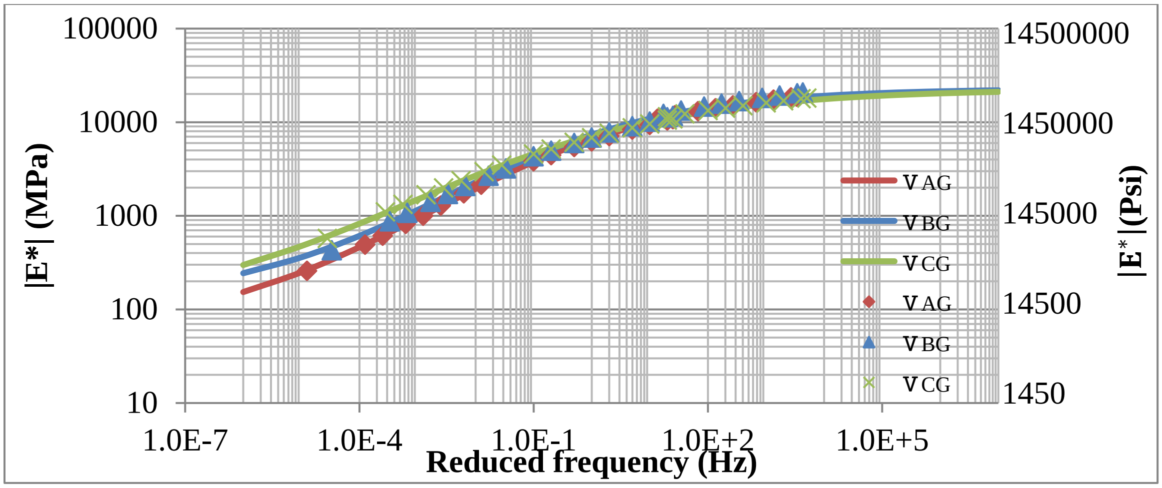

Figure 12-73 Master Dynamic Modulus Curves of Mixtures from Aggregate V with RAP after Long-Term Aging in Terms of Surface Mixture Type

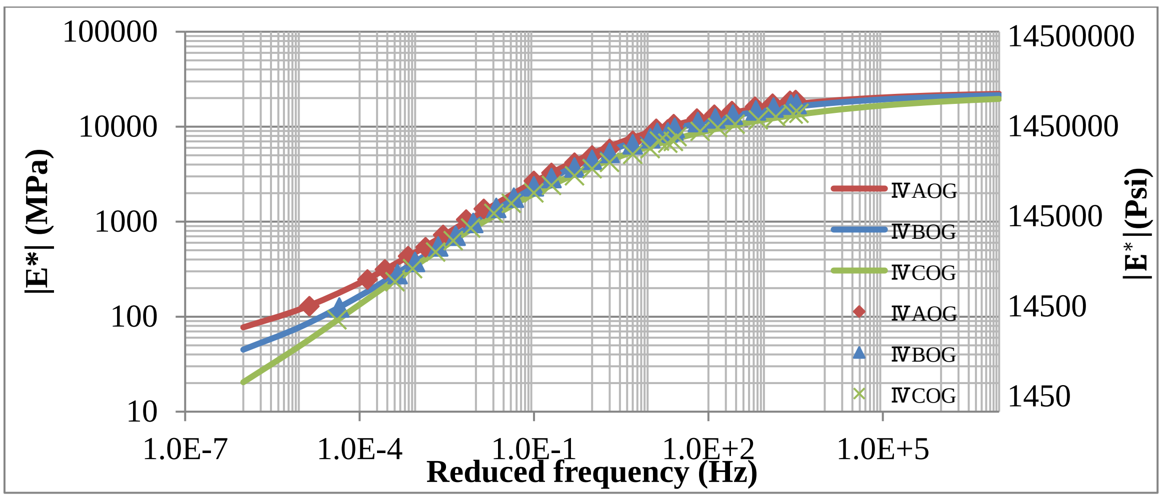

Figure 12-74 Master Dynamic Modulus Curves of Mixtures from Aggregate IV without RAP after Long-Term Aging in Terms of Surface Mixture Type

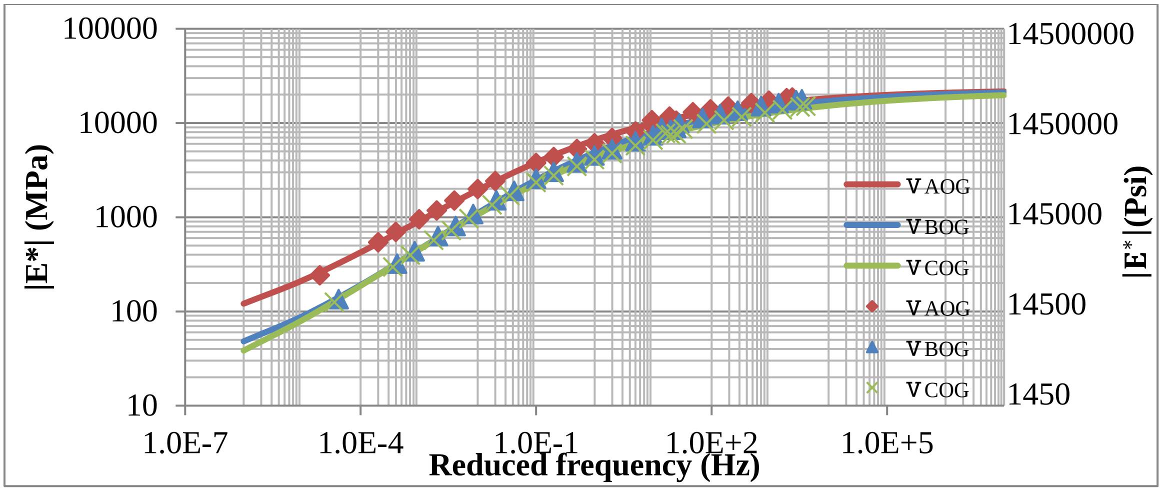

Figure 12-75 Master Dynamic Modulus Curves of Mixtures from Aggregate V without RAP after Long-Term Aging in Terms of Surface Mixture Type

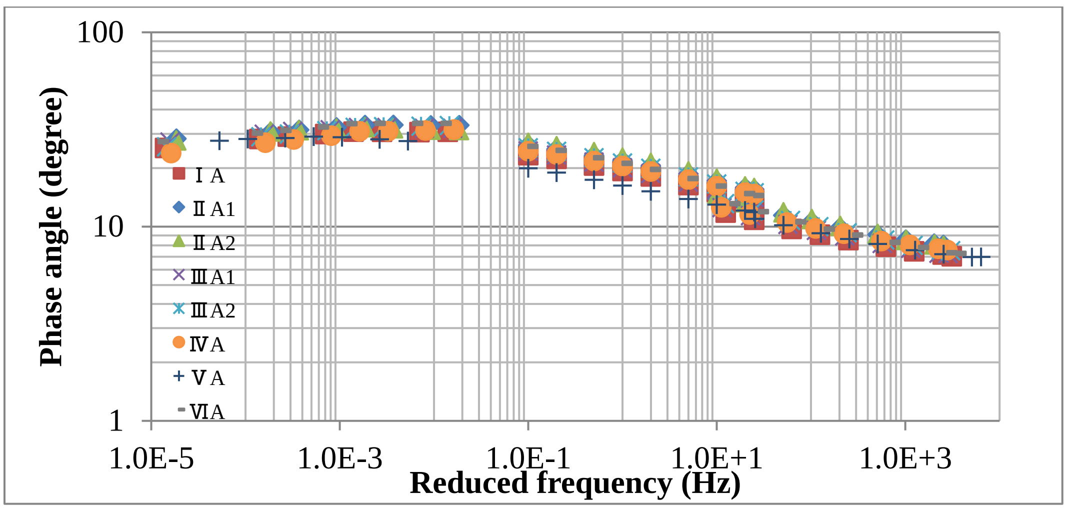

Figure 12-76 Master Phase Angle Curves for Surface Type A Mixtures with RAP in Terms of Aggregate Source

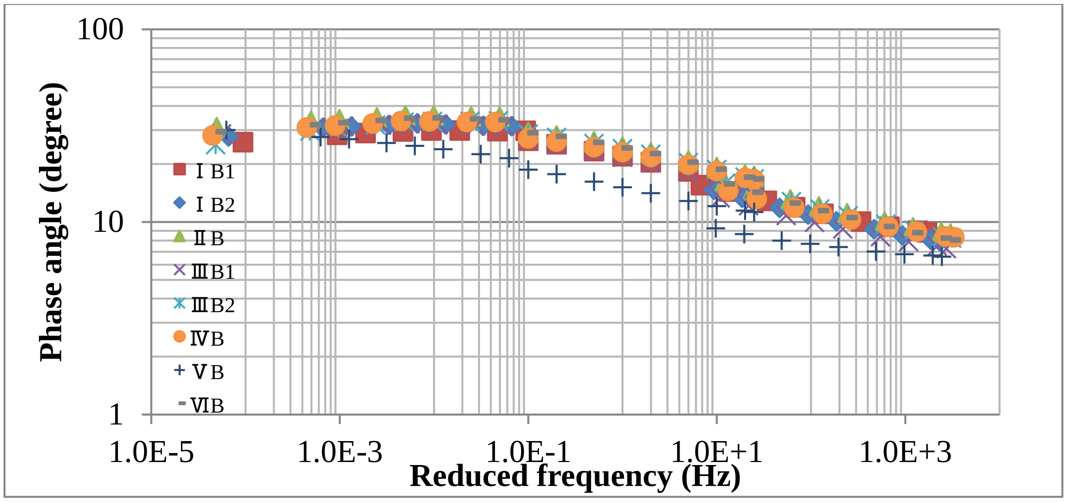

Figure 12-77 Master Phase Angle Curves for Surface Type B Mixtures with RAP in Terms of Aggregate Source

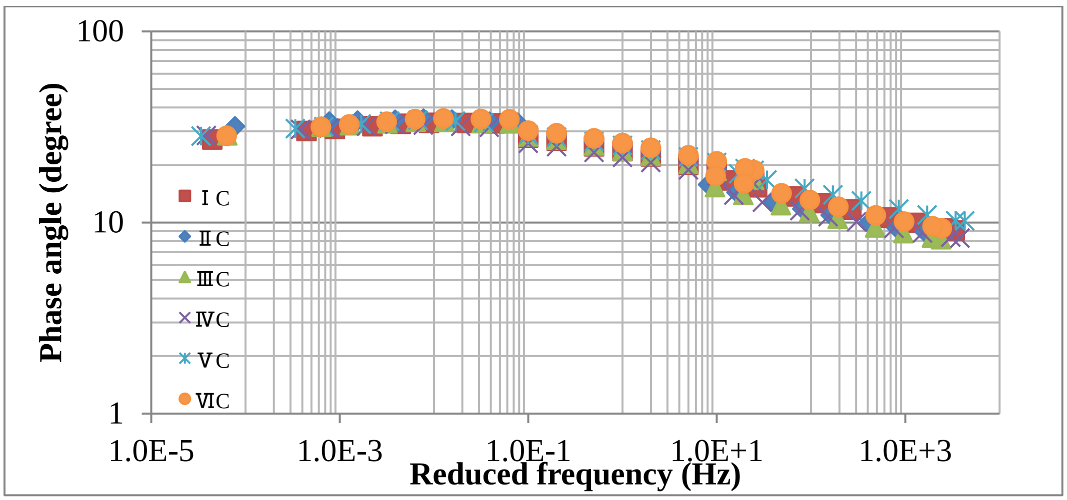

Figure 12-78 Master Phase Angle Curves for Surface Type C Mixtures with RAP in Terms of Aggregate Source

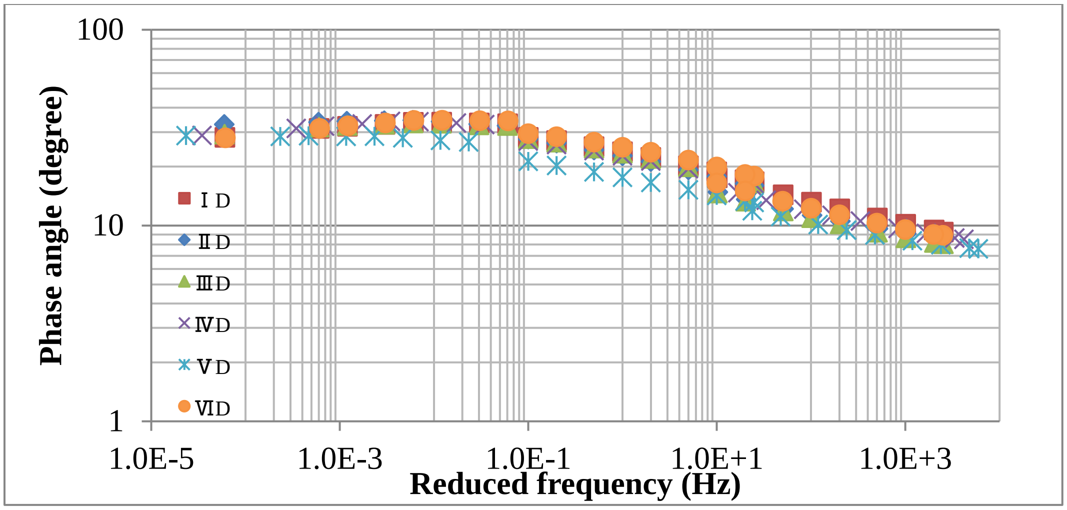

Figure 12-79 Master Phase Angle Curves for Surface Type D Mixtures with RAP in Terms of Aggregate Source

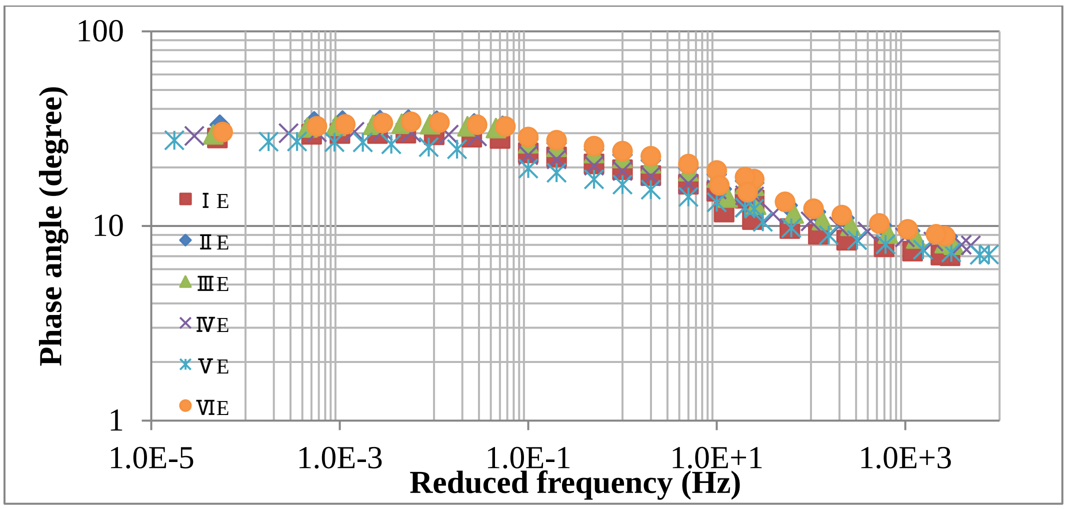

Figure 12-80 Master Phase Angle Curves for Surface Type E Mixtures with RAP in Terms of Aggregate Source

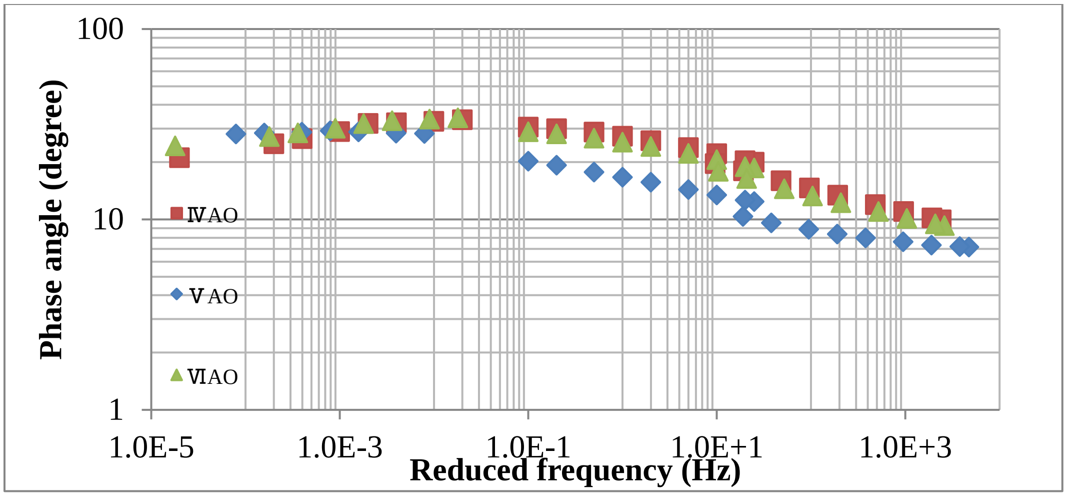

Figure 12-81 Master Phase Angle Curves for Surface Type A Mixtures without RAP in Terms of Aggregate Source

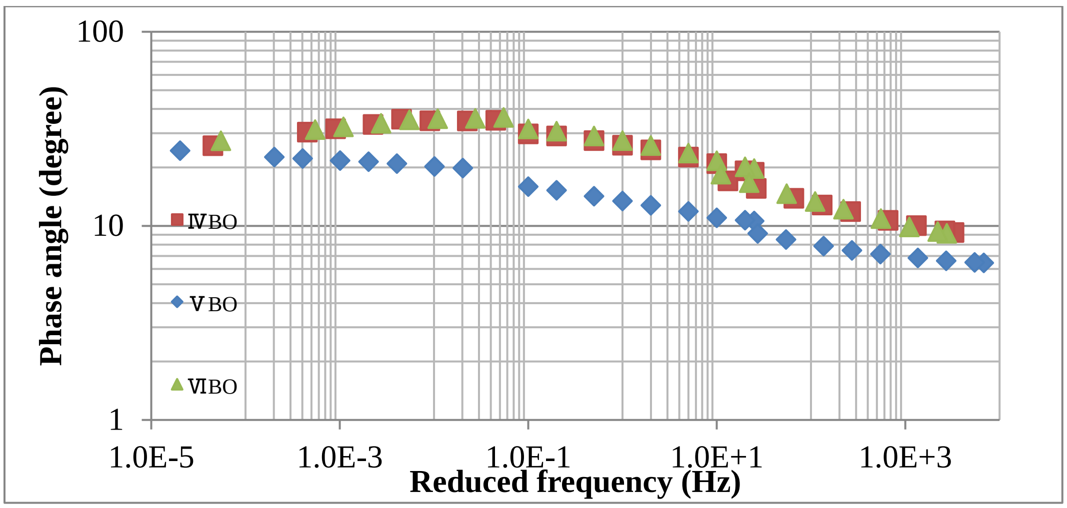

Figure 12-82 Master Phase Angle Curves for Surface Type B Mixtures without RAP in Terms of Aggregate Source

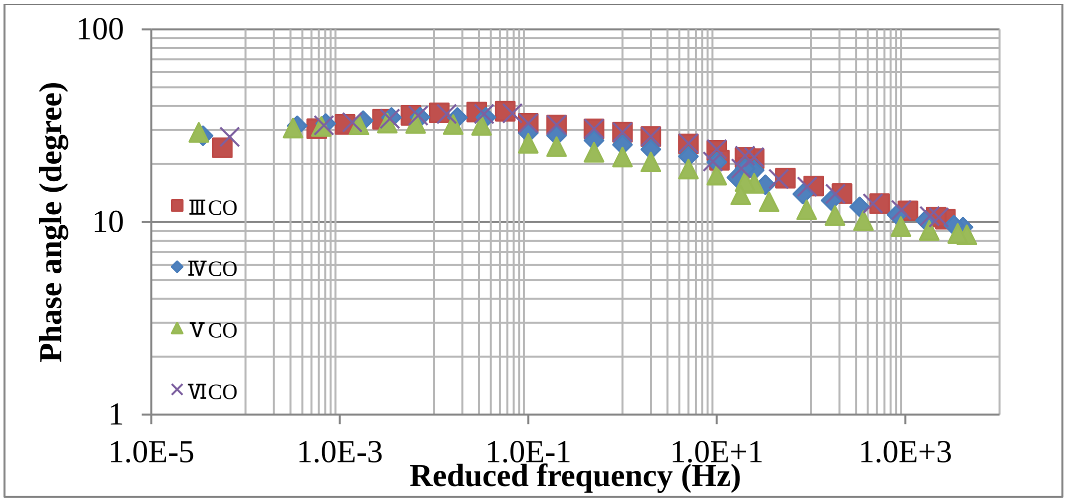

Figure 12-83 Master Phase Angle Curves for Surface Type C Mixtures without RAP in Terms of Aggregate Source

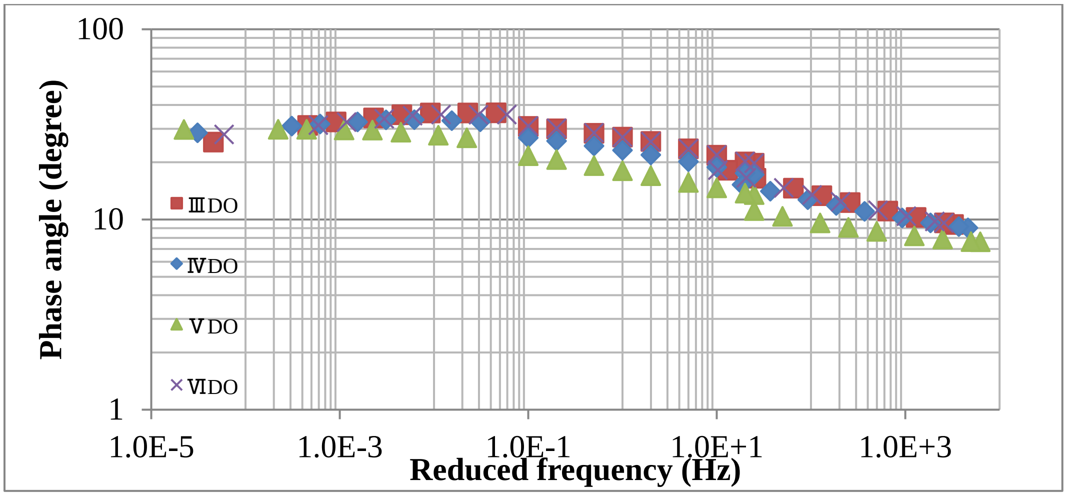

Figure 12-84 Master Phase Angle Curves for Surface Type D Mixtures without RAP in Terms of Aggregate Source

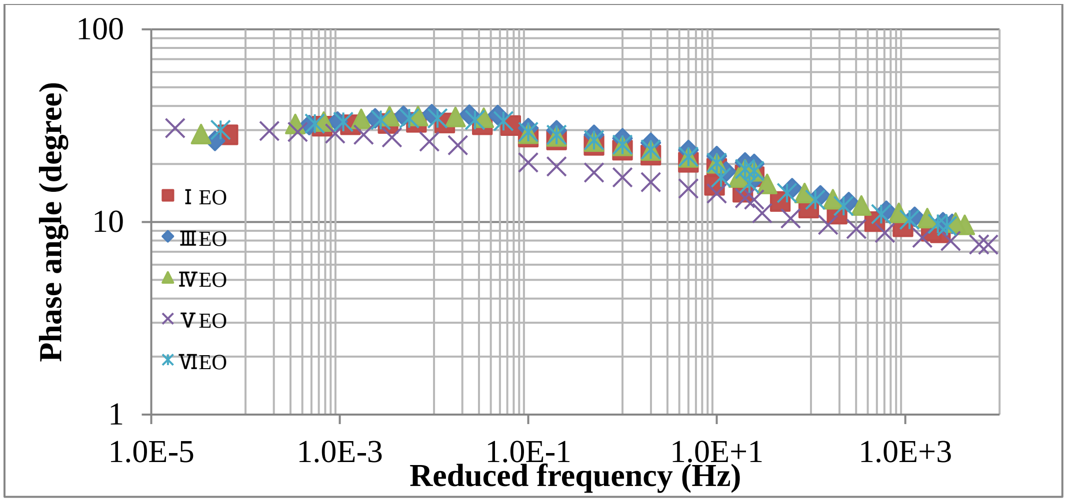

Figure 12-85 Master Phase Angle Curves for Surface Type E Mixtures without RAP in Terms of Aggregate Source

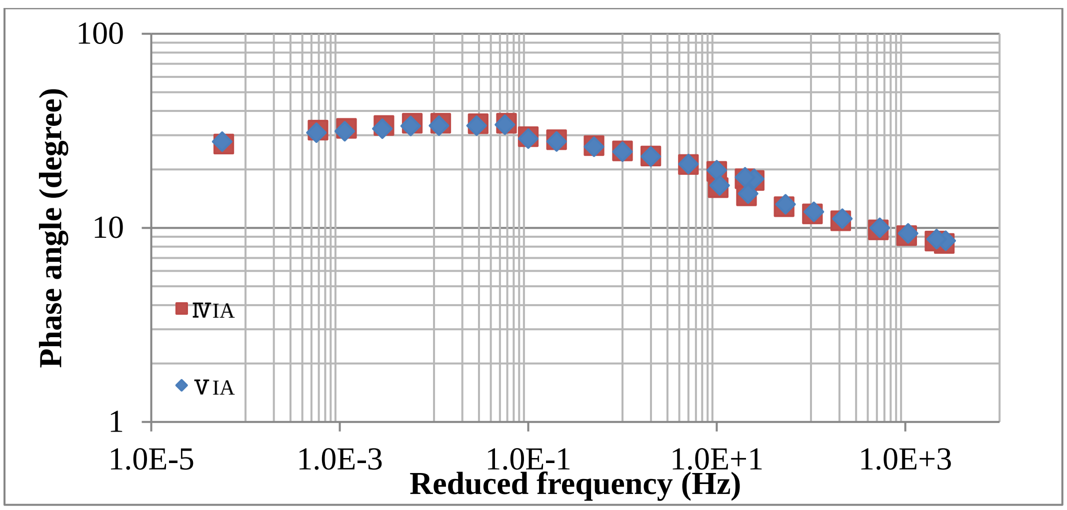

Figure 12-86 Master Phase Angle Curves for Intermediate Type A Mixtures with RAP in Terms of Aggregate Source

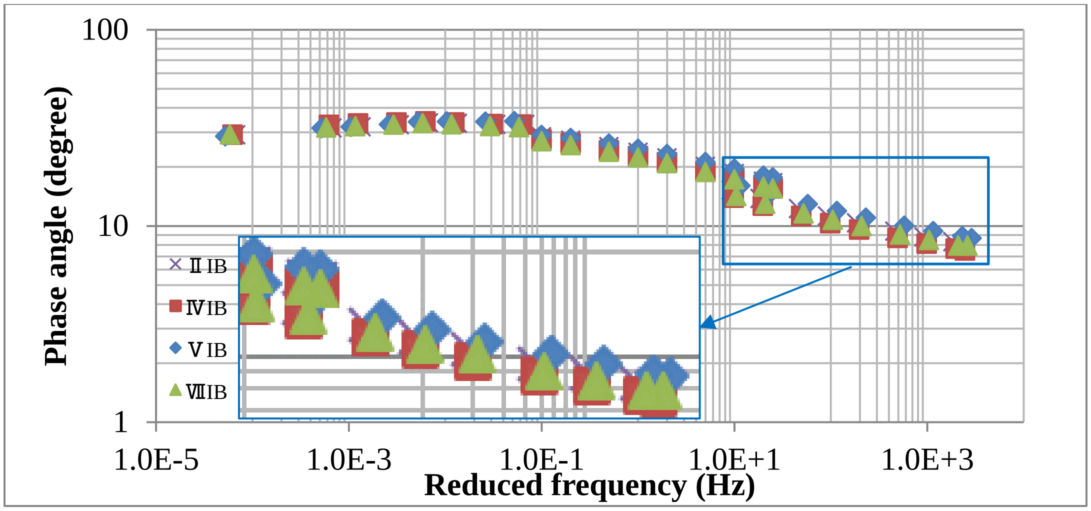

Figure 12-87 Master Phase Angle Curves for Intermediate Type B Mixtures with RAP in Terms of Aggregate Source

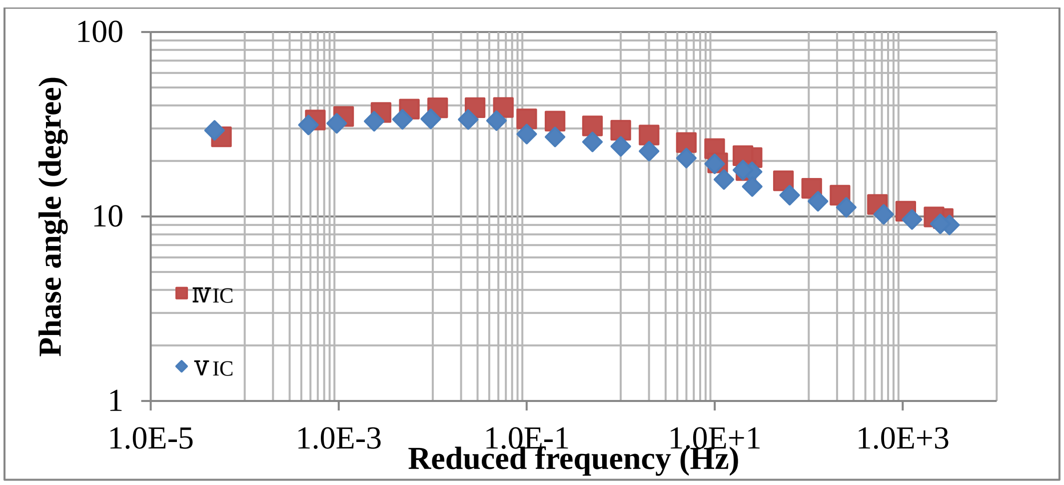

Figure 12-88 Master Phase Angle Curves for Intermediate Type C Mixtures with RAP in Terms of Aggregate Source

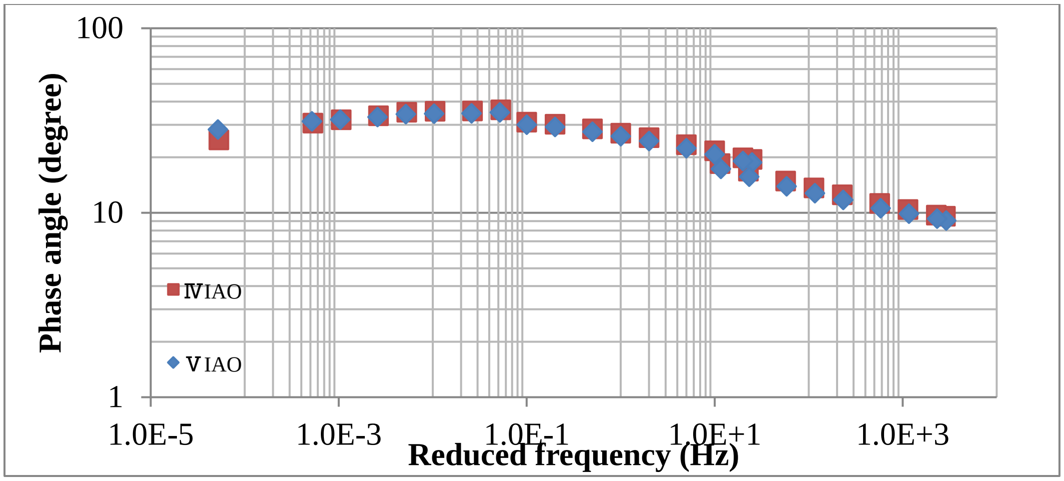

Figure 12-89 Master Phase Angle Curves for Intermediate Type A Mixtures without RAP in Terms of Aggregate Source

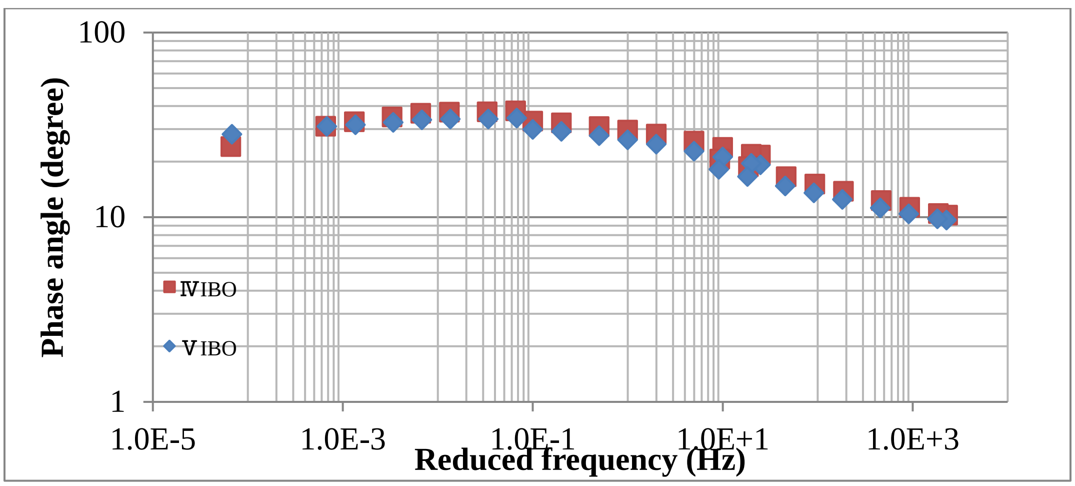

Figure 12-90 Master Phase Angle Curves for Intermediate Type B Mixtures without RAP in Terms of Aggregate Source

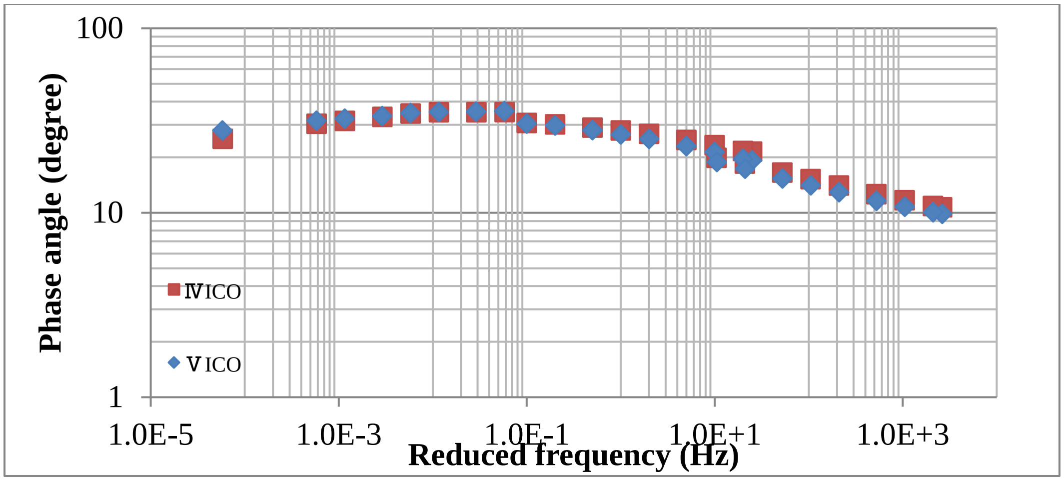

Figure 12-91 Master Phase Angle Curves for Intermediate Type C Mixtures without RAP in Terms of Aggregate Source

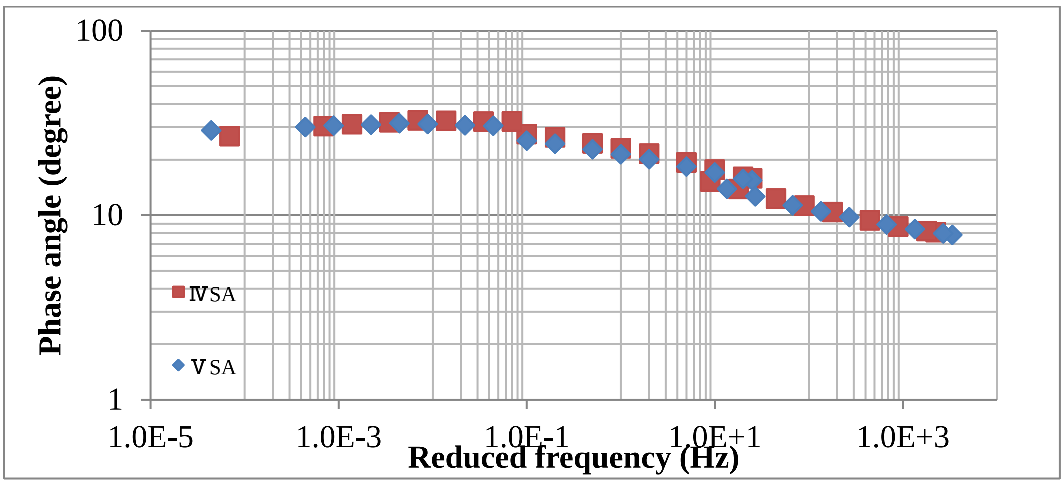

Figure 12-92 Master Phase Angle Curves for Base Type A Mixtures with RAP in Terms of Aggregate Source

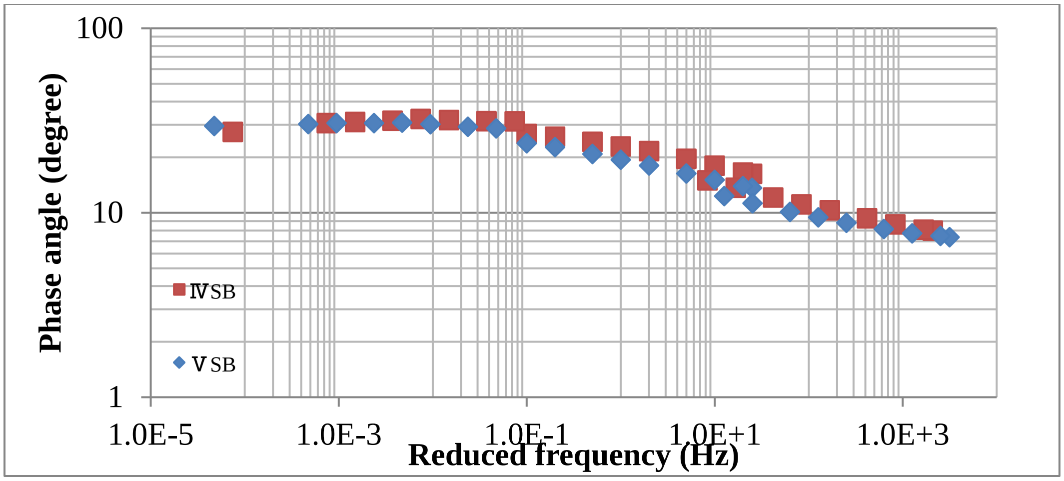

Figure 12-93 Master Phase Angle Curves for Base Type B Mixtures with RAP in Terms of Aggregate Source

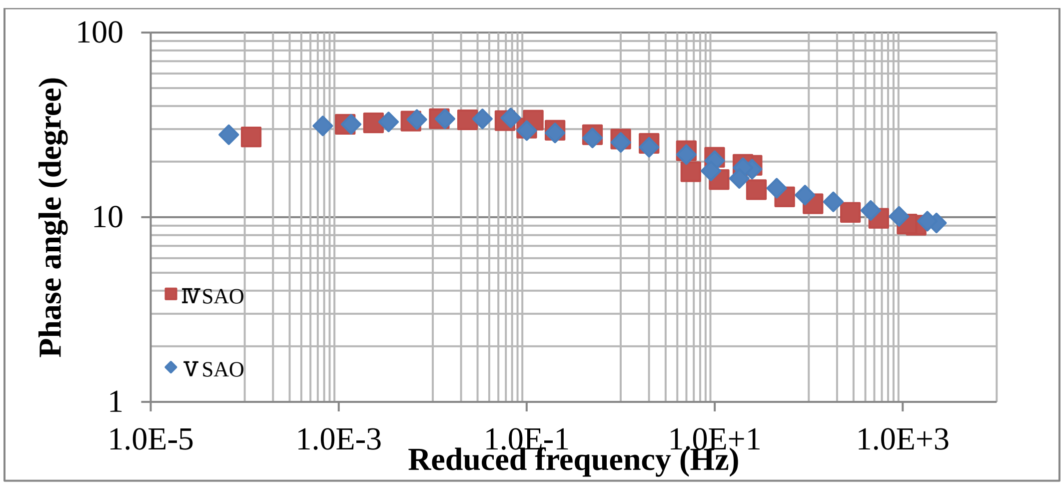

Figure 12-94 Master Phase Angle Curves for Base Type A Mixtures without RAP in Terms of Aggregate Source

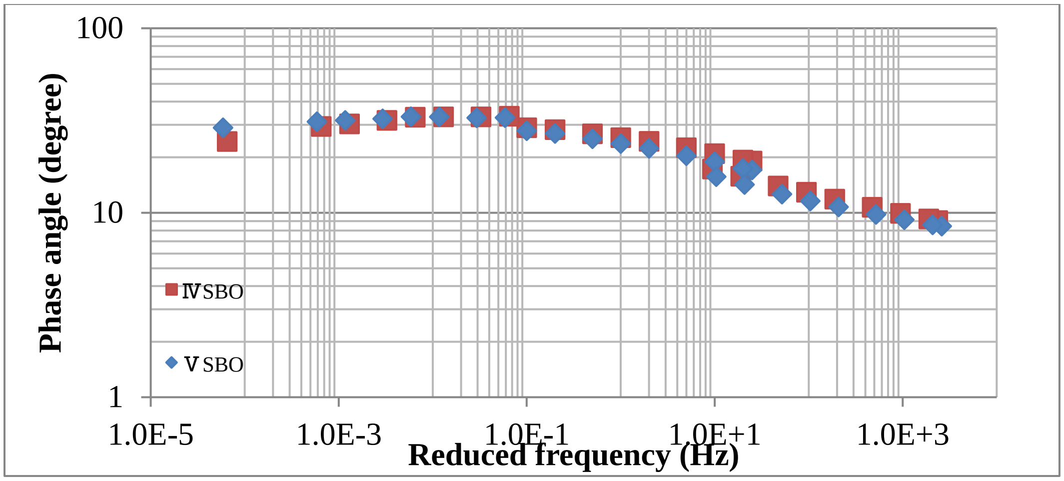

Figure 12-95 Master Phase Angle Curves for Base Type B Mixtures without RAP in Terms of Aggregate Source

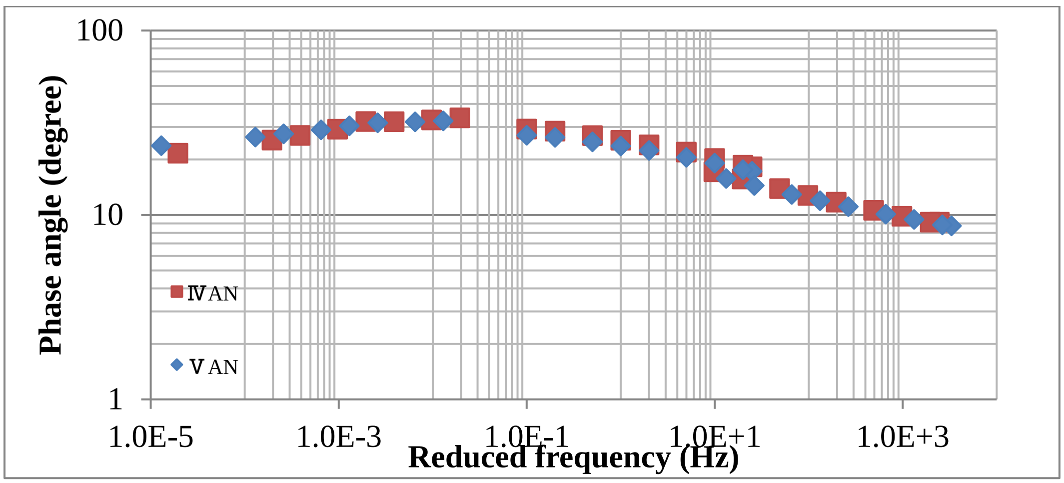

Figure 12-96 Master Phase Angle Curves for Surface Type A Mixtures with RAP and Asphalt Source 2 in Terms of Aggregate Source

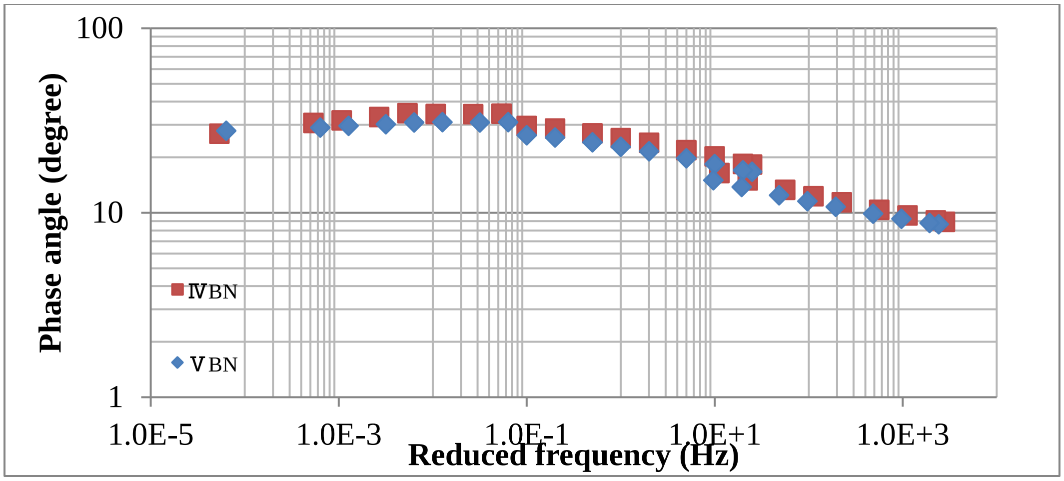

Figure 12-97 Master Phase Angle Curves for Surface Type B Mixtures with RAP and Asphalt Source 2 in Terms of Aggregate Source

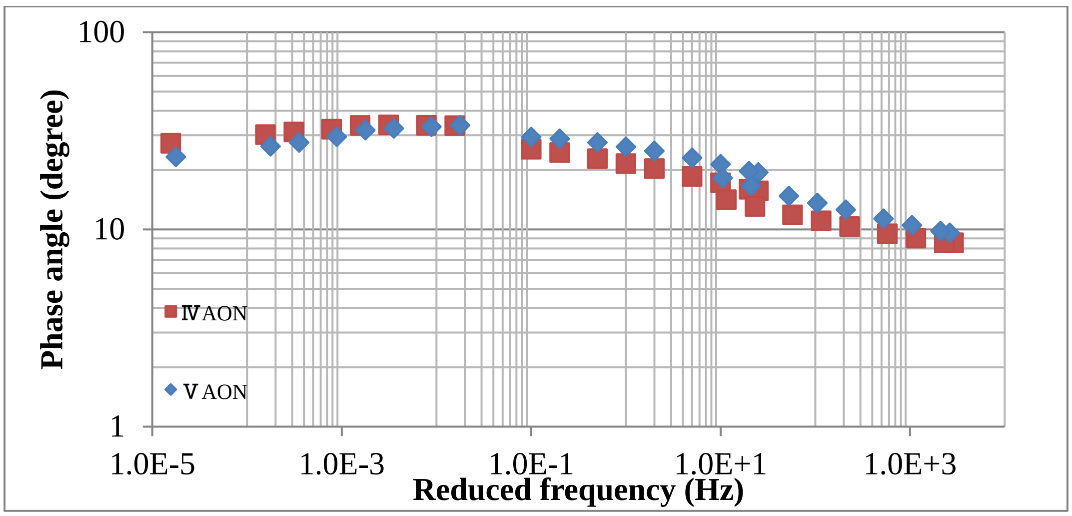

Figure 12-98 Master Phase Angle Curves for Surface Type A Mixtures without RAP using Asphalt Source 2 in Terms of Aggregate Source

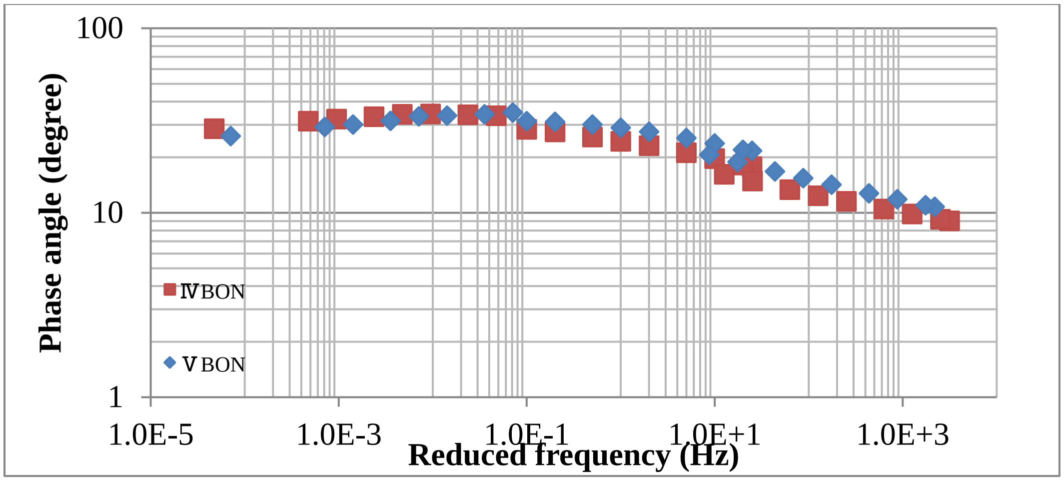

Figure 12-99 Master Phase Angle Curves for Surface Type B Mixtures without RAP using Asphalt Source 2 in Terms of Aggregate Source

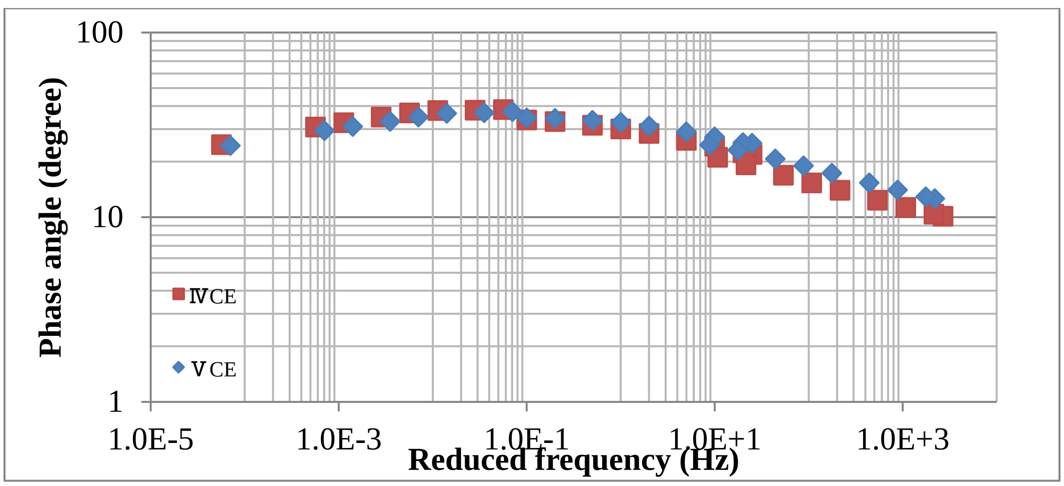

Figure 12-100 Master Phase Angle Curves for Surface Type C Mixtures with RAP and WMA-Chemical Additive in Terms of Aggregate Source

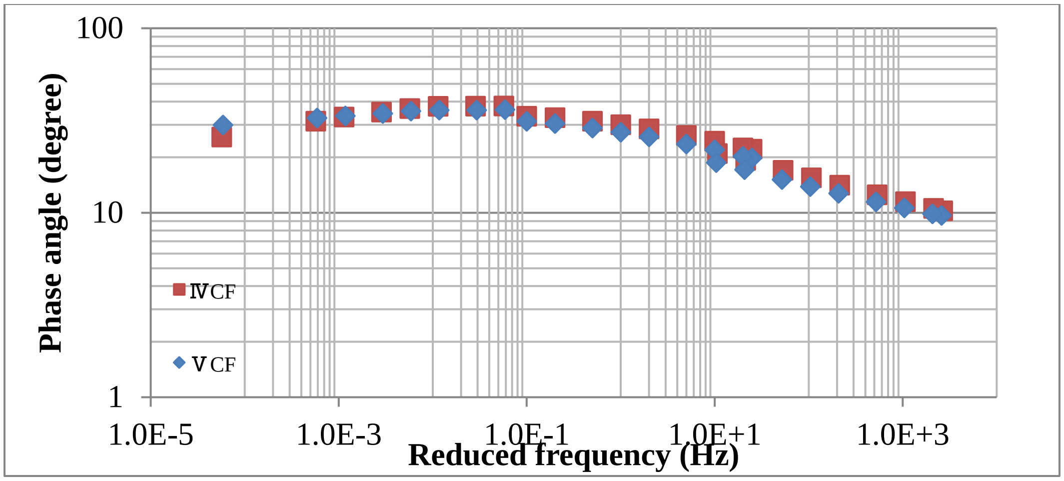

Figure 12-101 Master Phase Angle Curves for Surface Type C Mixtures with RAP and WMA-Foaming in Terms of Aggregate Source

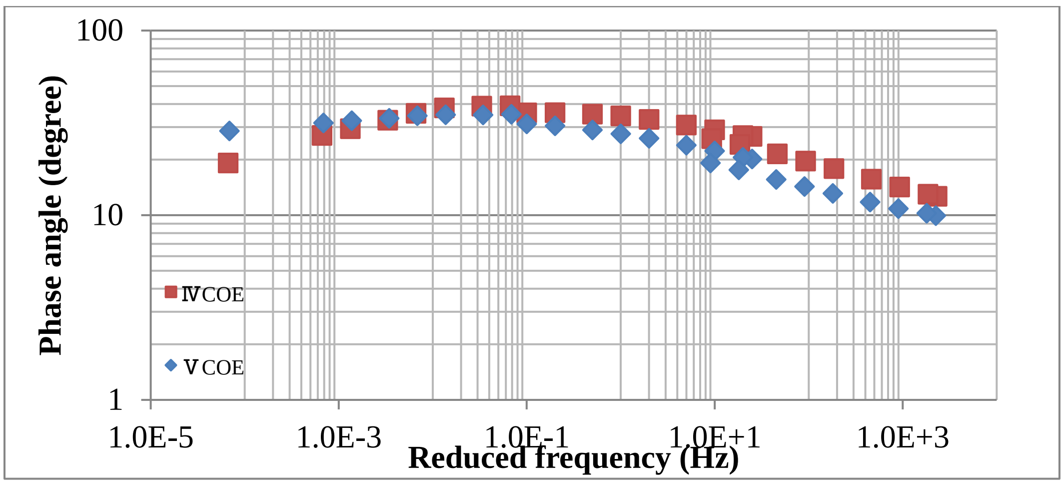

Figure 12-102 Master Phase Angle Curves for Surface Type C Mixtures without RAP using WMA-Chemical Additive in Terms of Aggregate Source

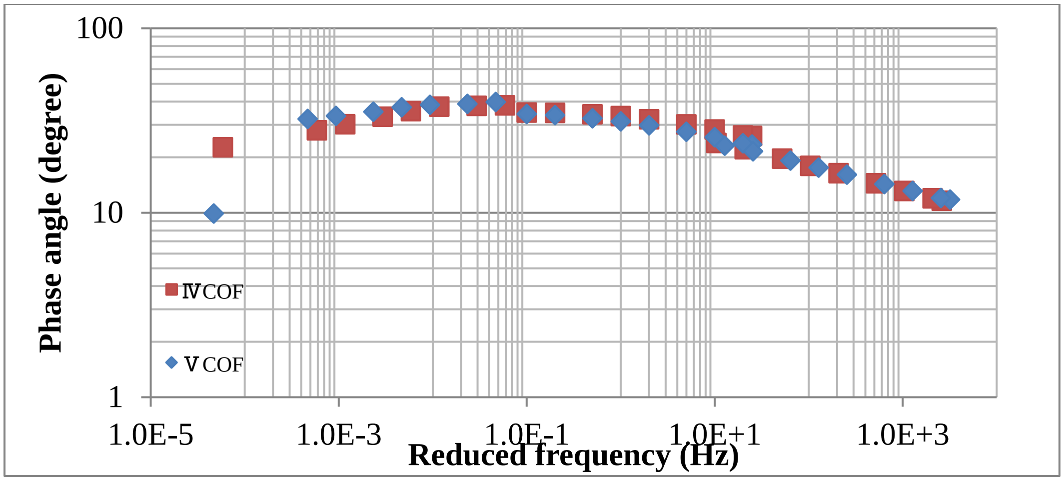

Figure 12-103 Master Phase Angle Curves for Surface Type C Mixtures without RAP using WMA-Foaming in Terms of Aggregate Source

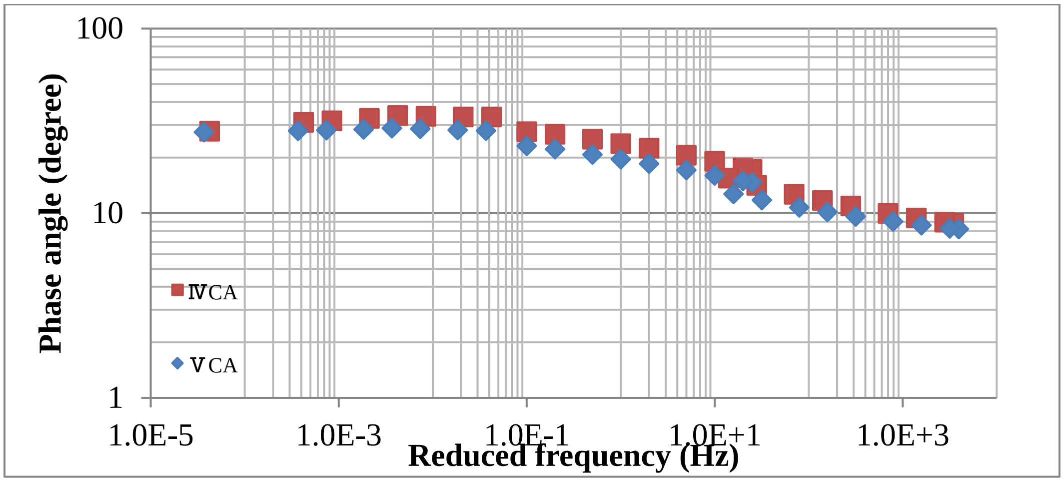

Figure 12-104 Master Phase Angle Curves for Surface Type C Mixtures with RAP and Liquid ASA1 in Terms of Aggregate Source

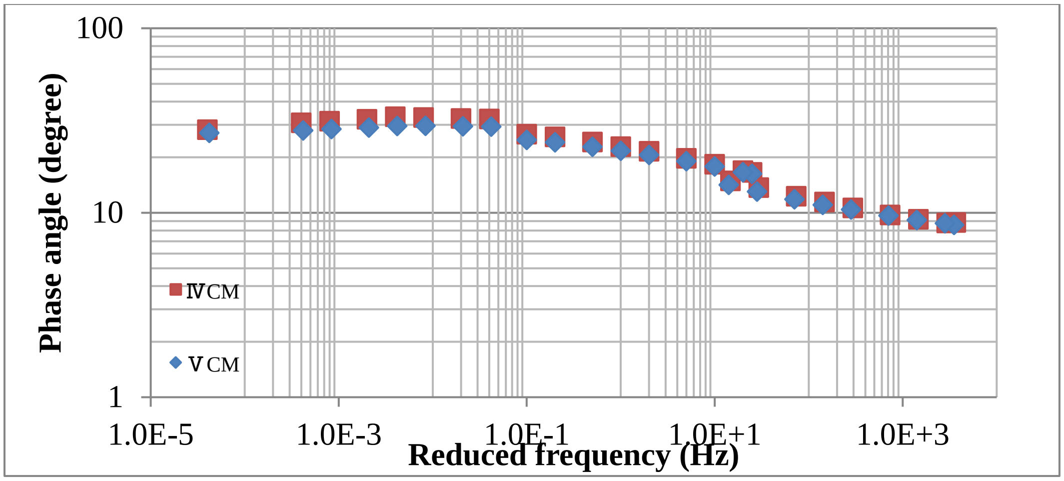

Figure 12-105 Master Phase Angle Curves for Surface Type C Mixtures with RAP and Liquid ASA2 in Terms of Aggregate Source

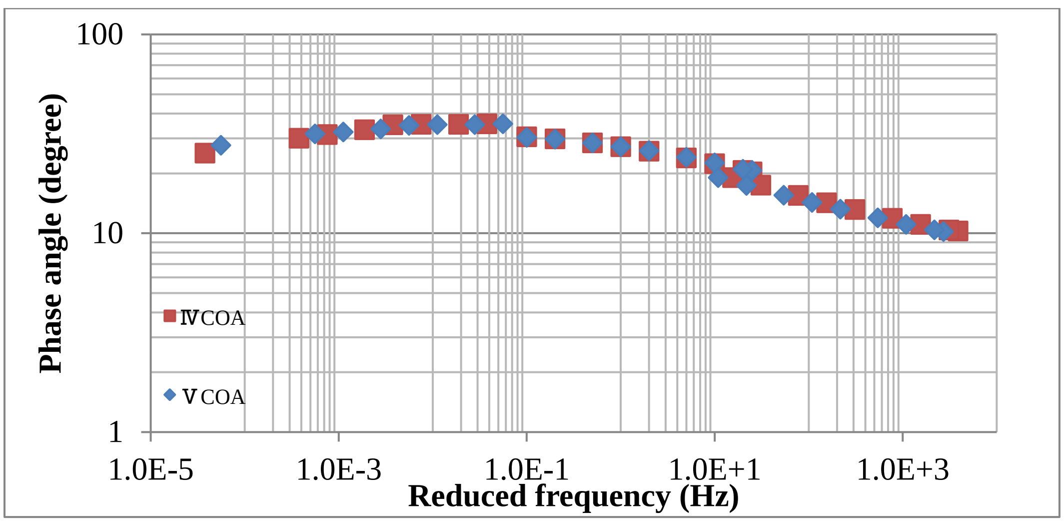

Figure 12-106 Master Phase Angle Curves for Surface Type C Mixtures without RAP using Liquid ASA1 in Terms of Aggregate Source

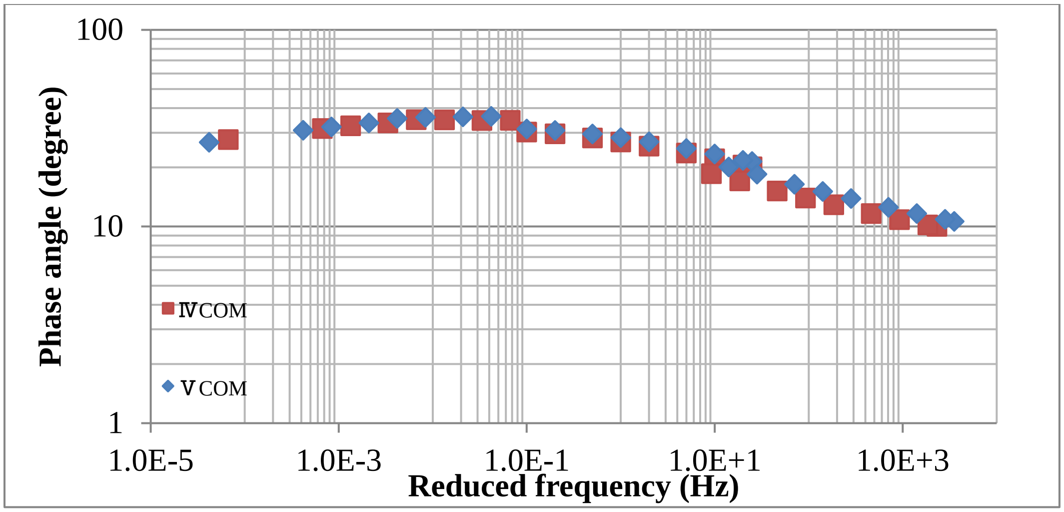

Figure 12-107 Master Phase Angle Curves for Surface Type C Mixtures without RAP using Liquid ASA2 in Terms of Aggregate Source

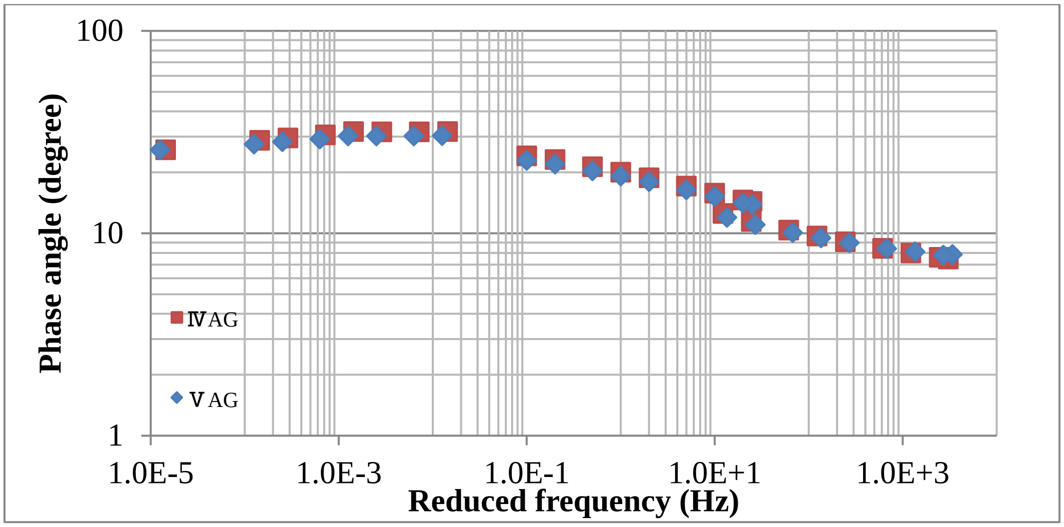

Figure 12-108 Master Phase Angle Curves for Surface Type A Mixtures with RAP after Long-Term Aging in Terms of Aggregate Source

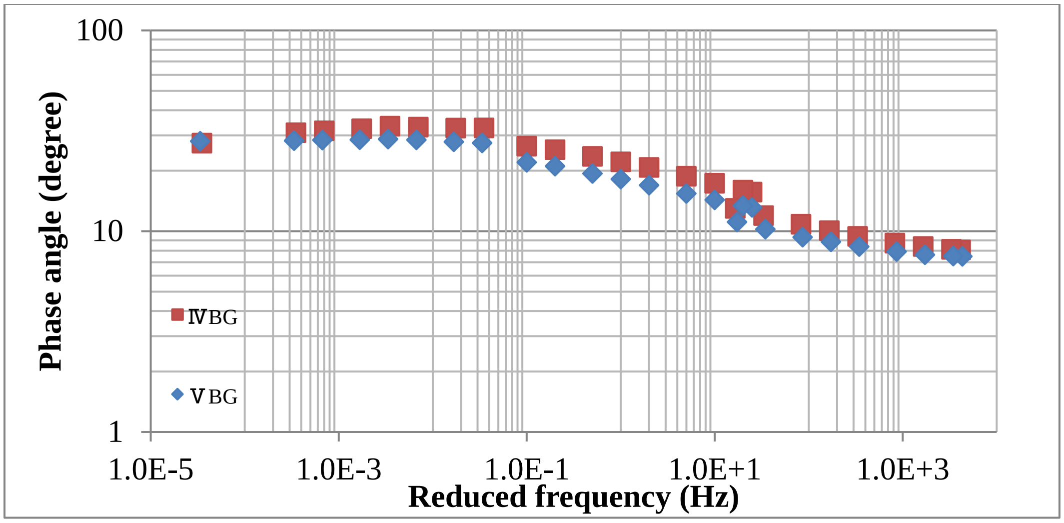

Figure 12-109 Master Phase Angle Curves for Surface Type B Mixtures with RAP after Long-Term Aging in Terms of Aggregate Source

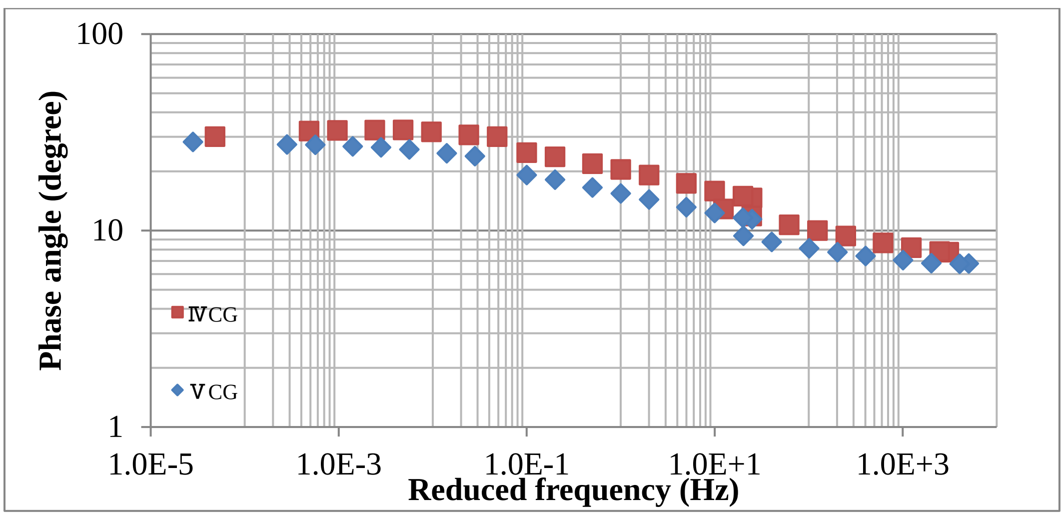

Figure 12-110 Master Phase Angle Curves for Surface Type C Mixtures with RAP after Long-Term Aging in Terms of Aggregate Source

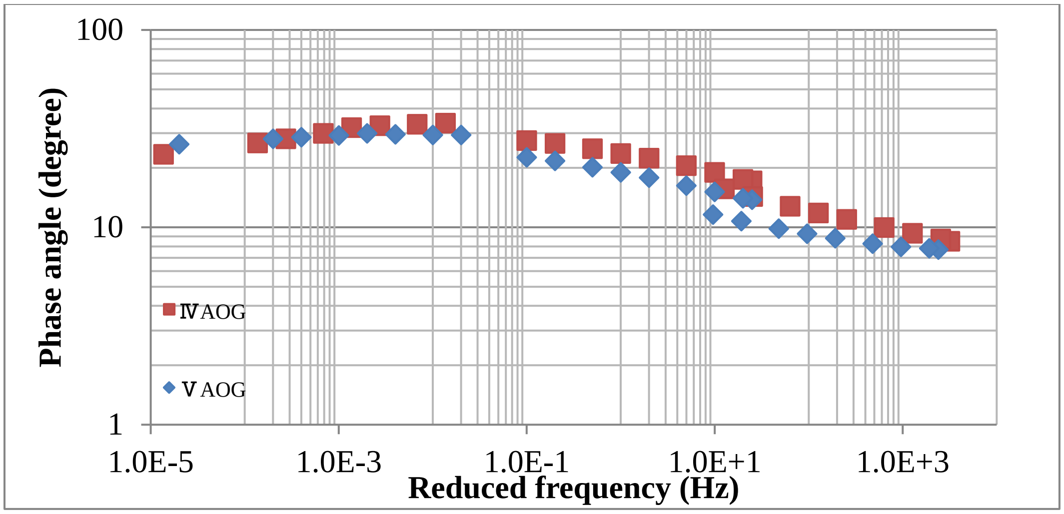

Figure 12-111 Master Phase Angle Curves for Surface Type A without RAP after Long-Term Aging in Terms of Aggregate Source

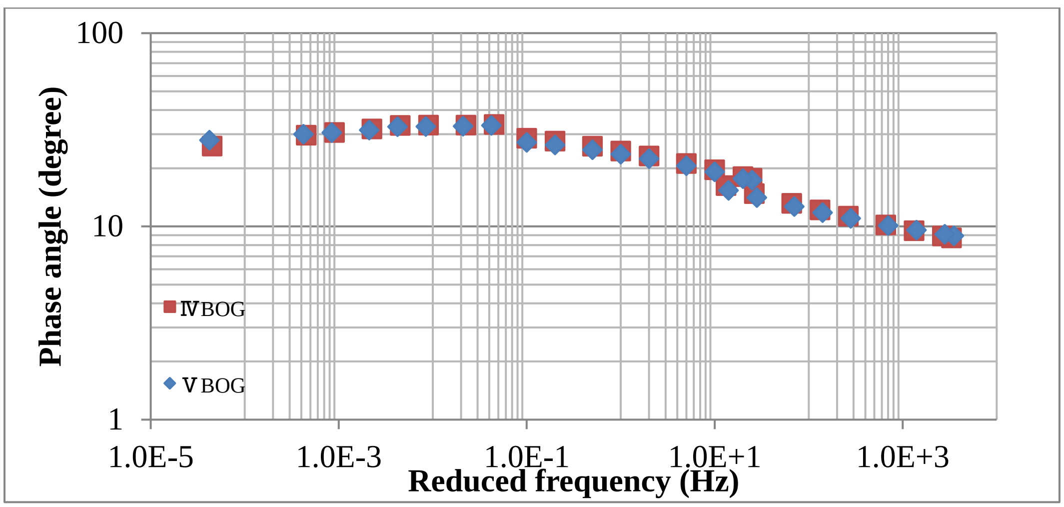

Figure 12-112 Master Phase Angle Curves for Surface Type B Mixtures without RAP after Long-Term Aging in Terms of Aggregate Source

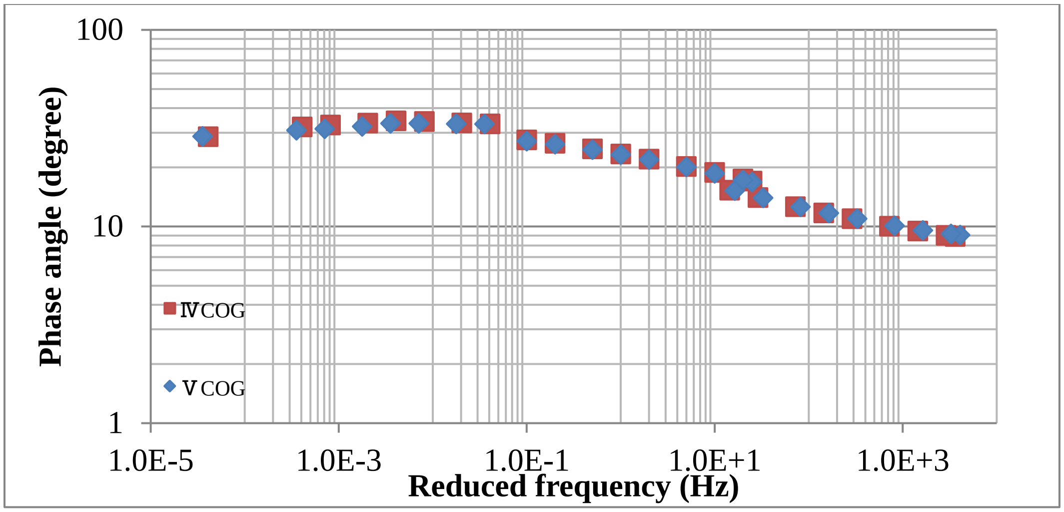

Figure 12-113 Master Phase Angle Curves for Surface Type C Mixtures without RAP after Long-Term Aging in Terms of Aggregate Source

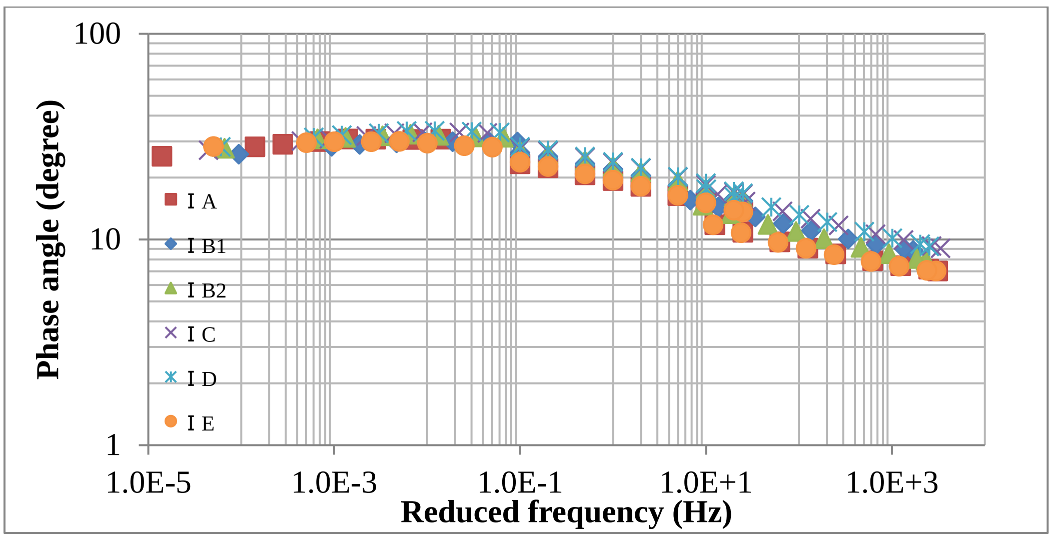

Figure 12-114 Master Phase Angle Curves of Mixtures from Aggregate I with RAP in Terms of Surface Mixture Type

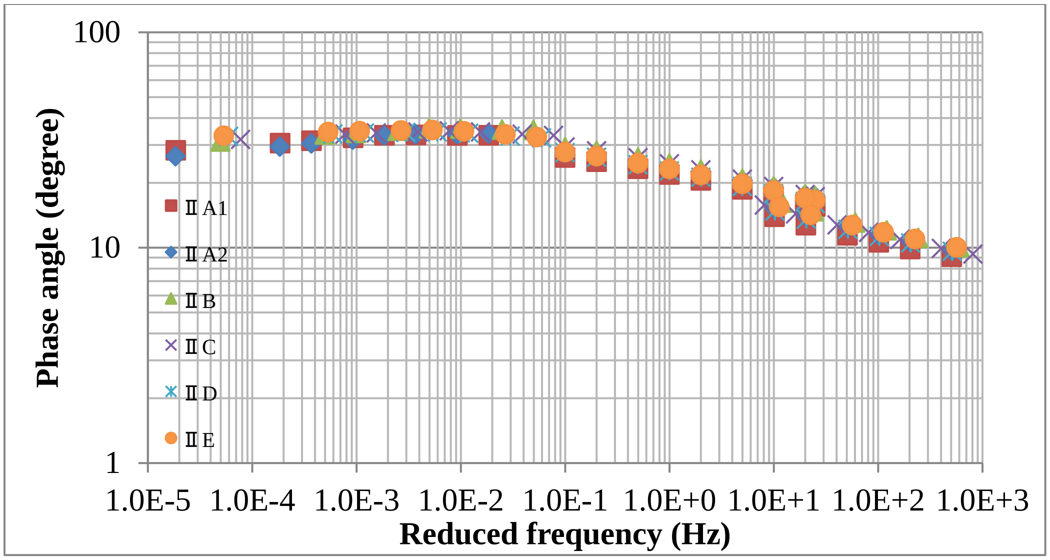

Figure 12-115 Master Phase Angle Curves of Mixtures from Aggregate II with RAP in Terms of Surface Mixture Type

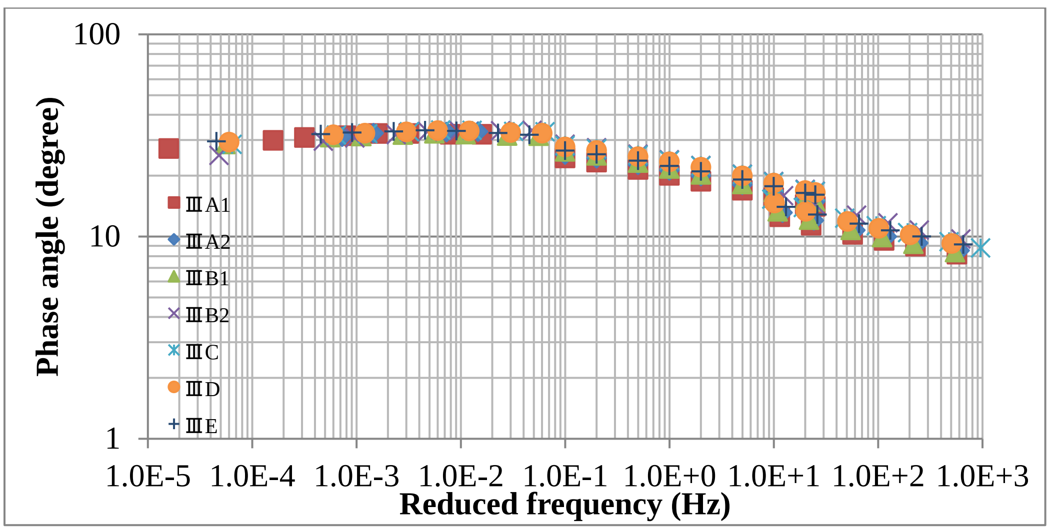

Figure 12-116 Master Phase Angle Curves of Mixtures from Aggregate III with RAP in Terms of Surface Mixture Type

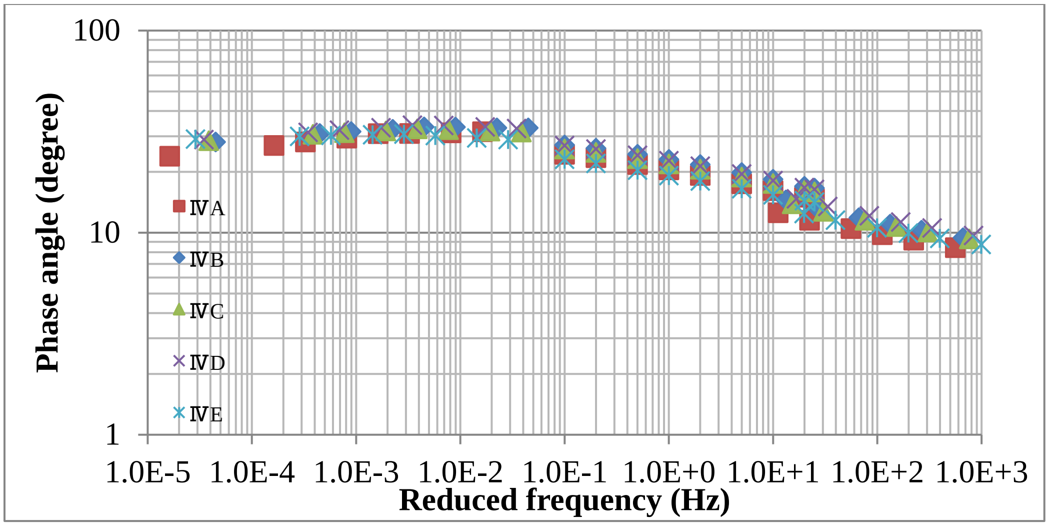

Figure 12-117 Master Phase Angle Curves of Mixtures from Aggregate IV with RAP in Terms of Surface Mixture Type

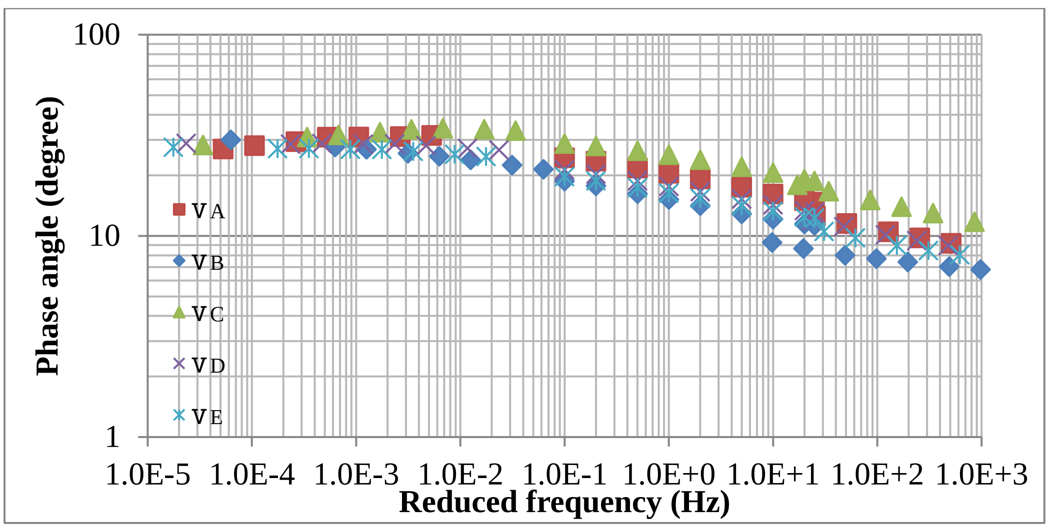

Figure 12-118 Master Phase Angle Curves of Mixtures from Aggregate V with RAP in Terms of Surface Mixture Type

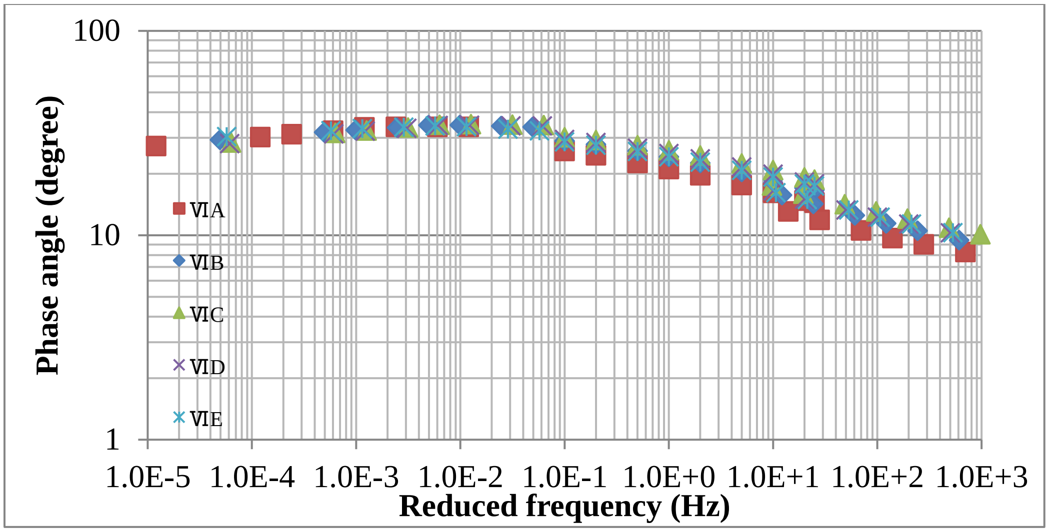

Figure 12-119 Master Phase Angle Curves of Mixtures from Aggregate VI with RAP in Terms of Surface Mixture Type

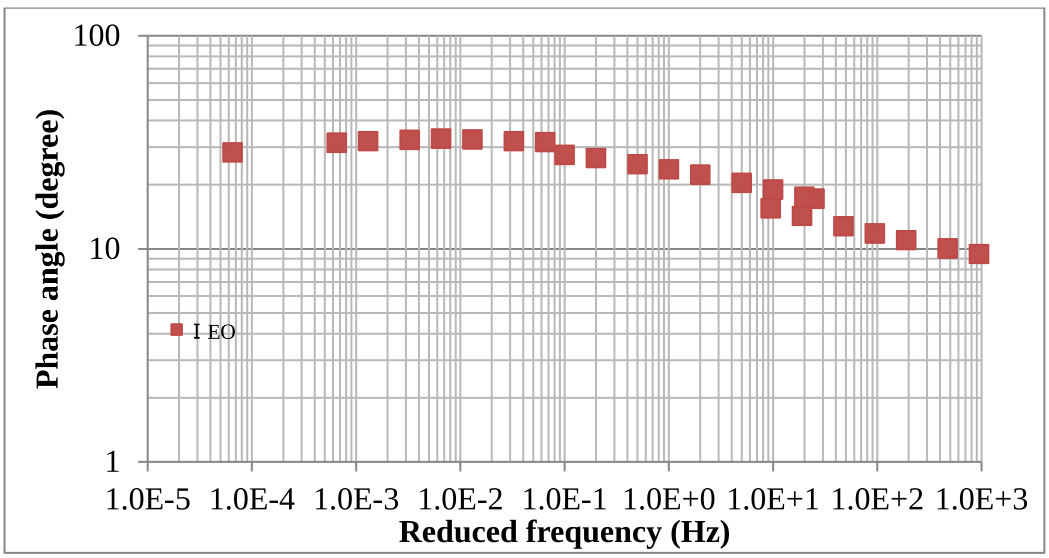

Figure 12-120 Master Phase Angle Curves of Mixtures from Aggregate I without RAP in Terms of Surface Mixture Type

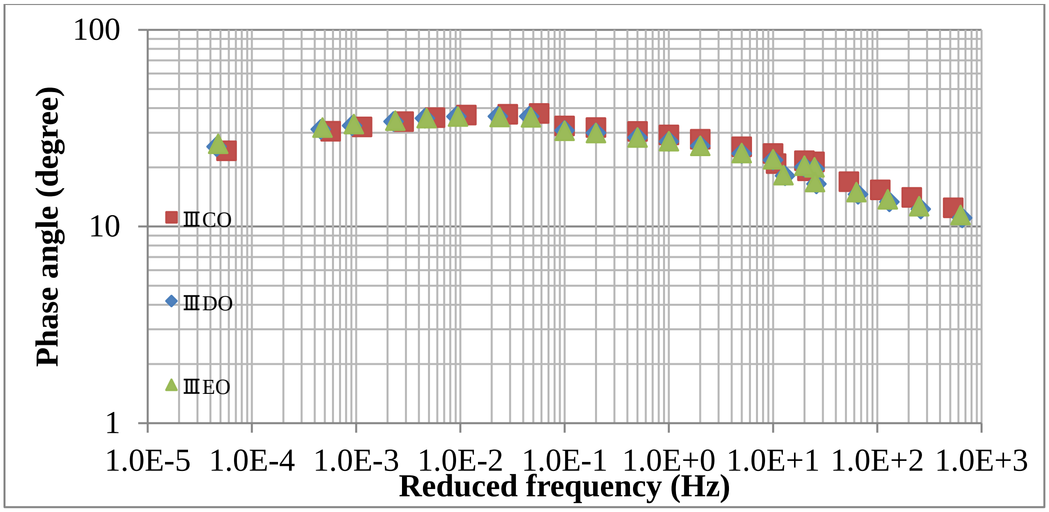

Figure 12-121 Master Phase Angle Curves of Mixtures from Aggregate III without RAP in Terms of Surface Mixture Type

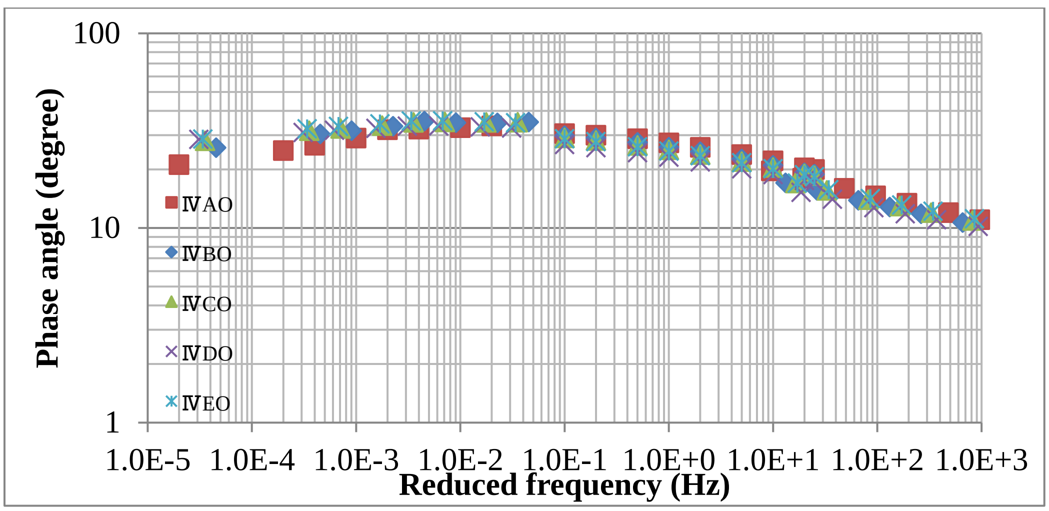

Figure 12-122 Master Phase Angle Curves of Mixtures from Aggregate IV without RAP in Terms of Surface Mixture Type

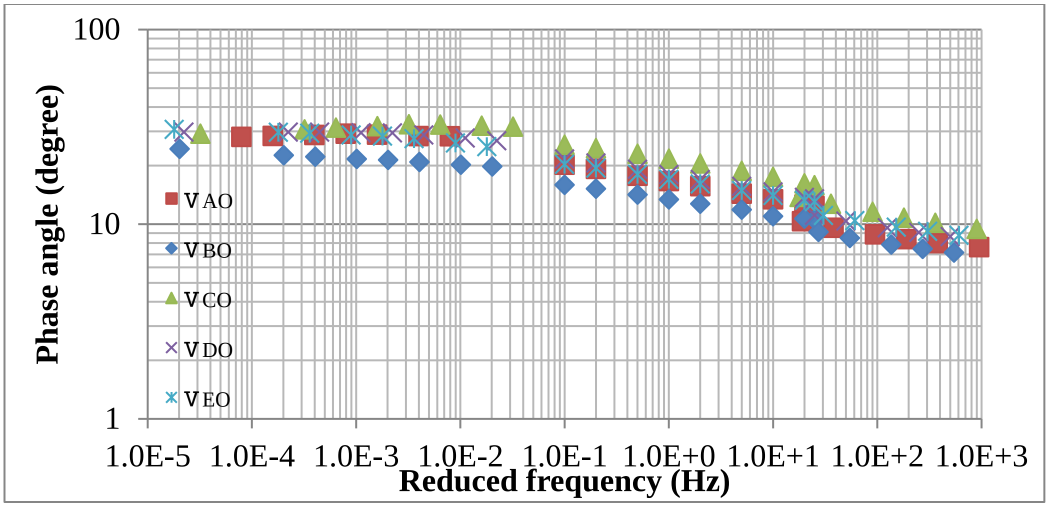

Figure 12-123 Master Phase Angle Curves of Mixtures from Aggregate V without RAP in Terms of Surface Mixture Type

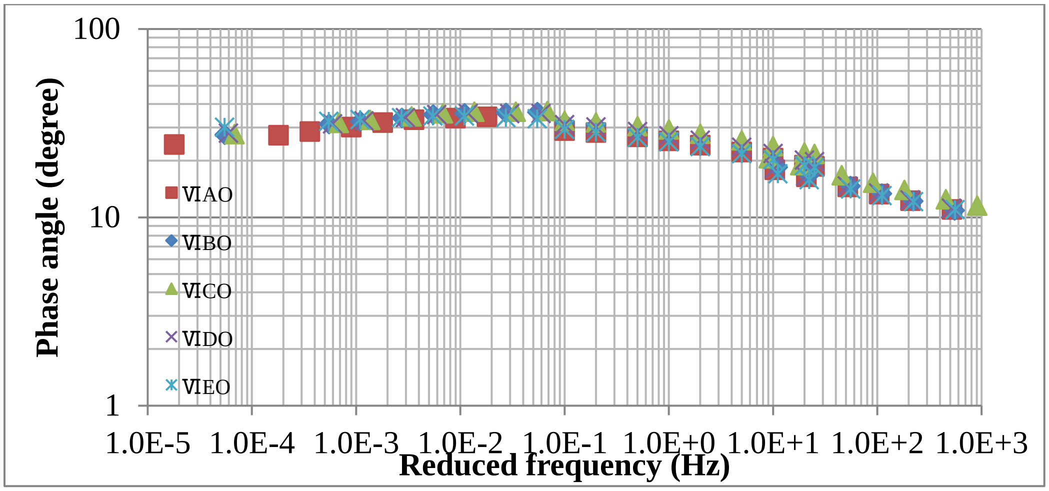

Figure 12-124 Master Phase Angle Curves of Mixtures from Aggregate VI without RAP in Terms of Surface Mixture Type

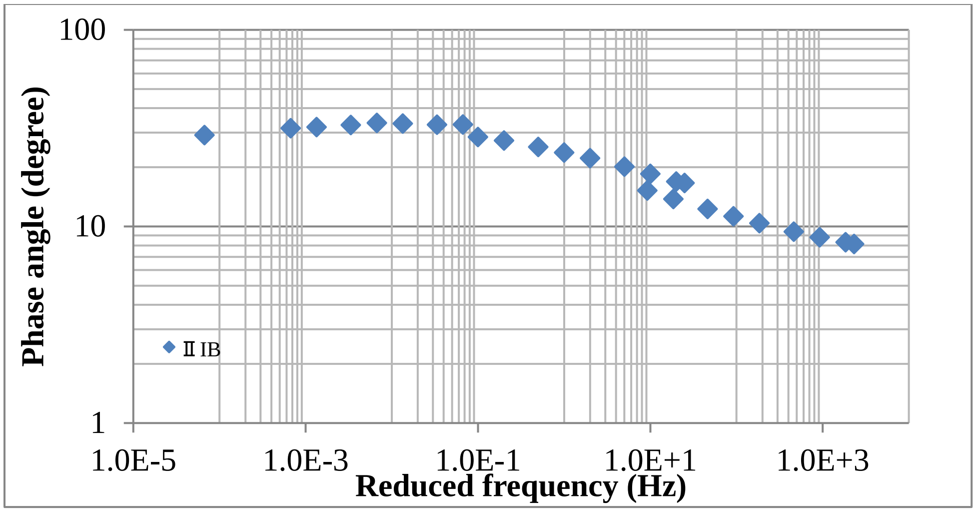

Figure 12-125 Master Phase Angle Curves of Mixtures from Aggregate II with RAP in Terms of Intermediate Mixture Type

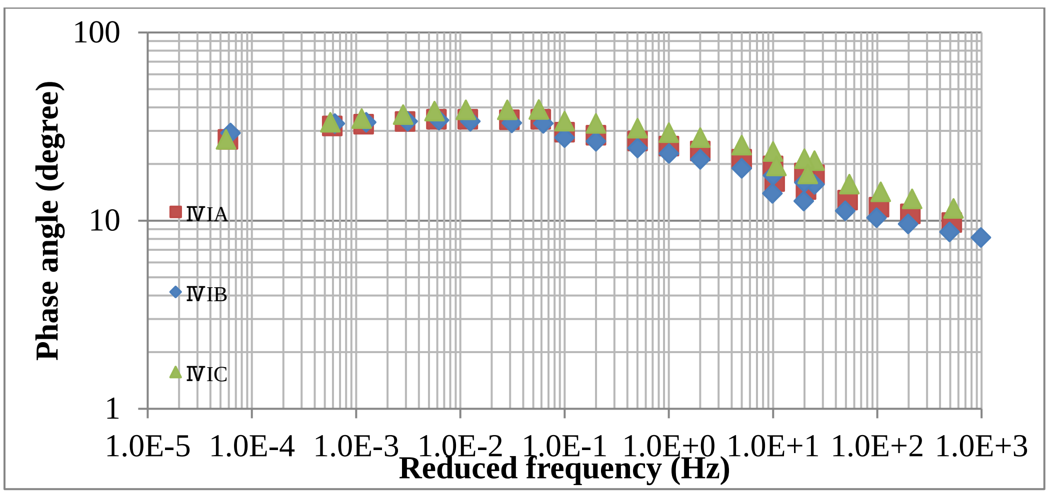

Figure 12-126 Master Phase Angle Curves of Mixtures from Aggregate IV with RAP in Terms of Intermediate Mixture Type

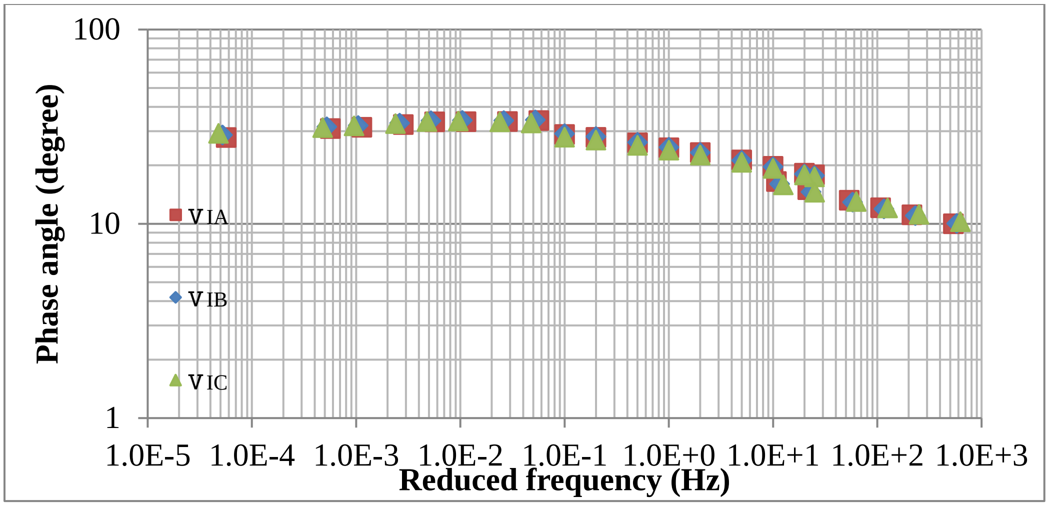

Figure 12-127 Master Phase Angle Curves of Mixtures from Aggregate V with RAP in Terms of Intermediate Mixture Type

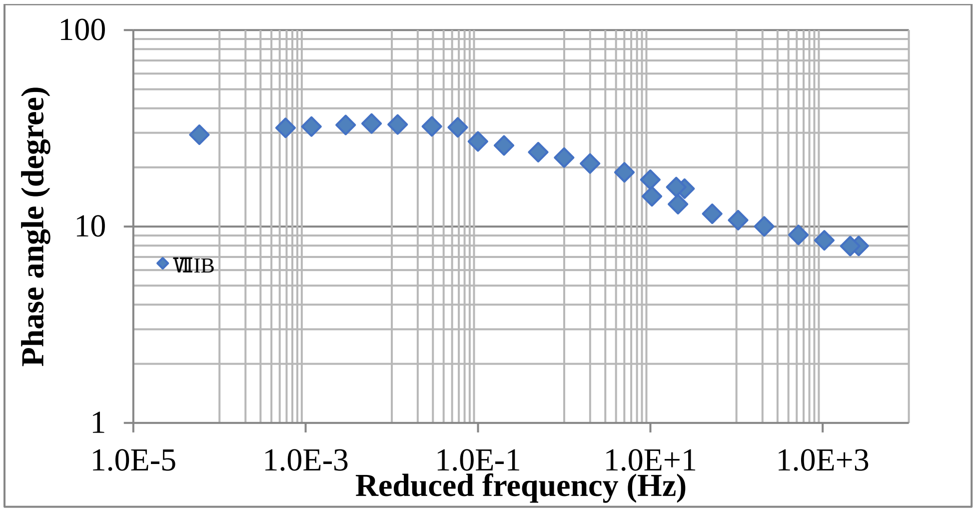

Figure 12-128 Master Phase Angle Curves of Mixtures from Aggregate VII with RAP in Terms of Intermediate Mixture Type

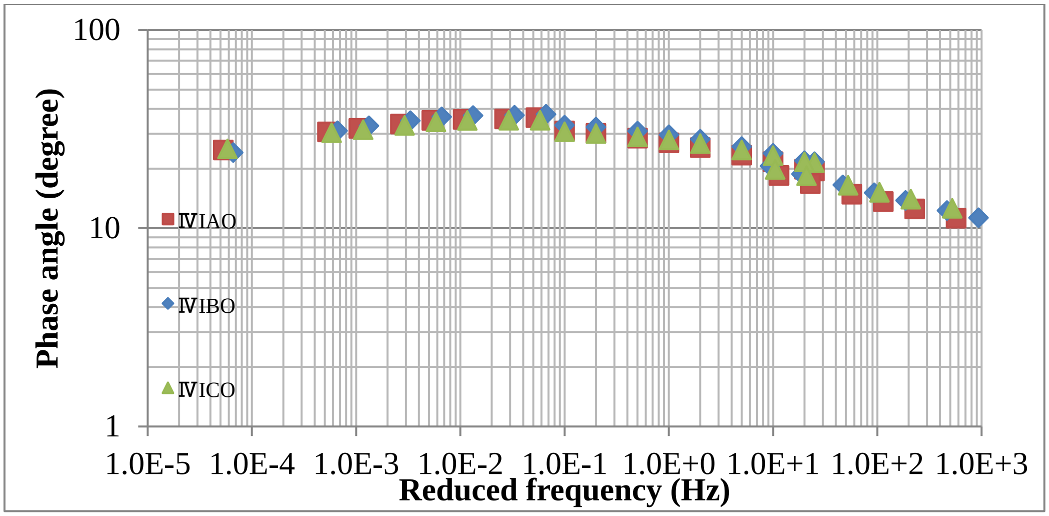

Figure 12-129 Master Phase Angle Curves of Mixtures from Aggregate IV without RAP in Terms of Intermediate Mixture Type

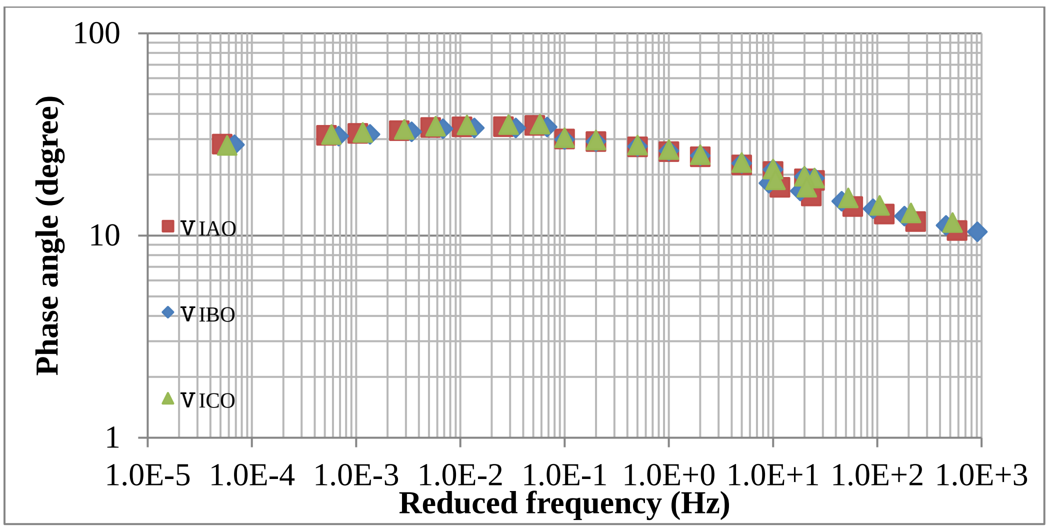

Figure 12-130 Master Phase Angle Curves of Mixtures from Aggregate V without RAP in Terms of Intermediate Mixture Type

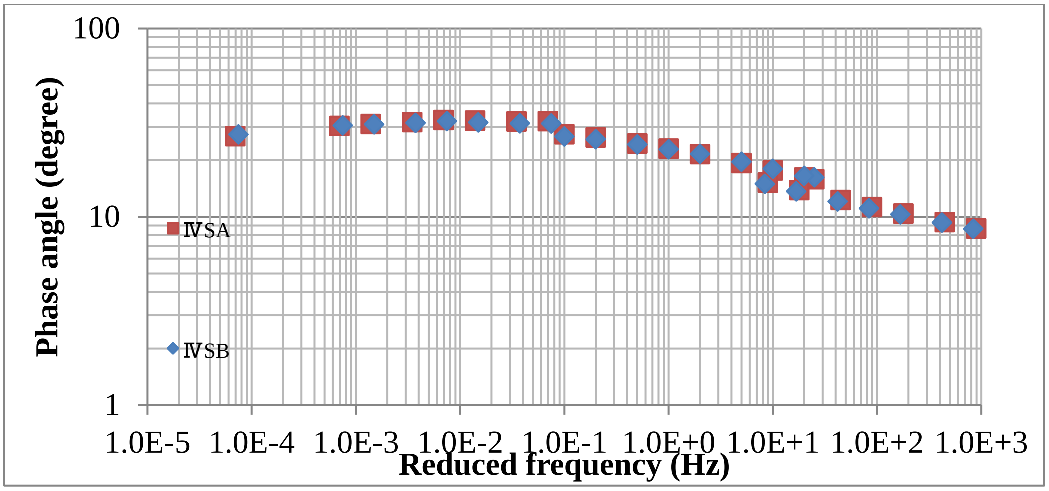

Figure 12-131 Master Phase Angle Curves of Mixtures from Aggregate IV with RAP in Terms of Base Mixture Type

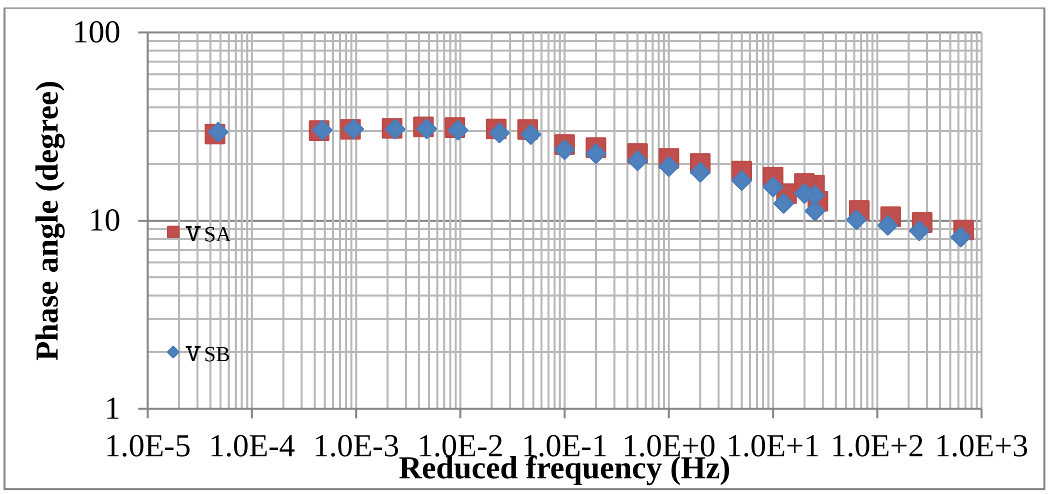

Figure 12-132 Master Phase Angle Curves of Mixtures from Aggregate V with RAP in Terms of Base Mixture Type

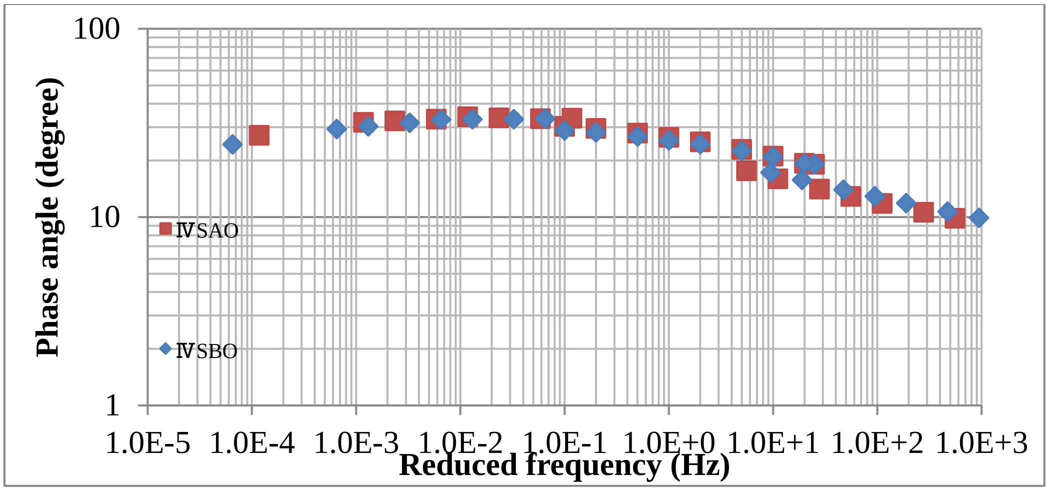

Figure 12-133 Master Phase Angle Curves of Mixtures from Aggregate IV without RAP in Terms of Base Mixture Type

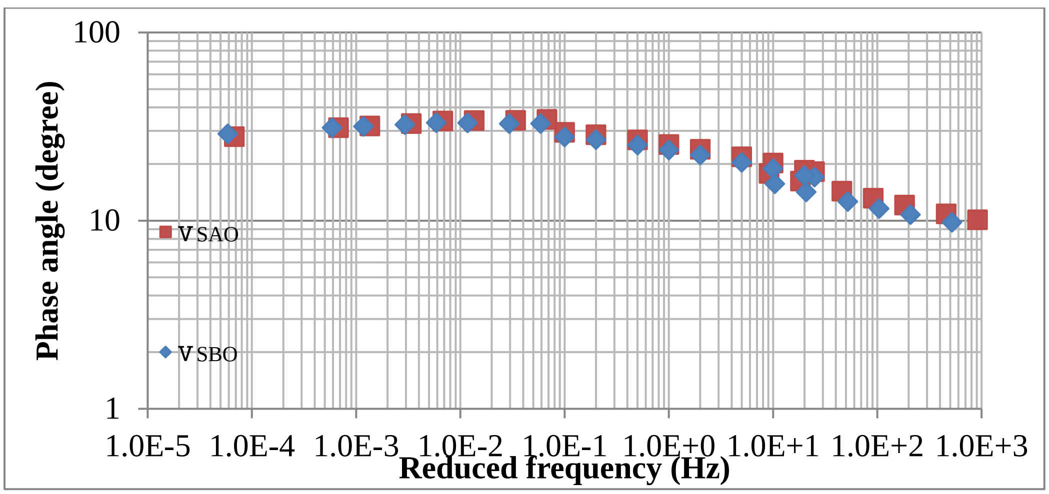

Figure 12-134 Master Phase Angle Curves of Mixtures from Aggregate V without RAP in Terms of Base Mixture Type

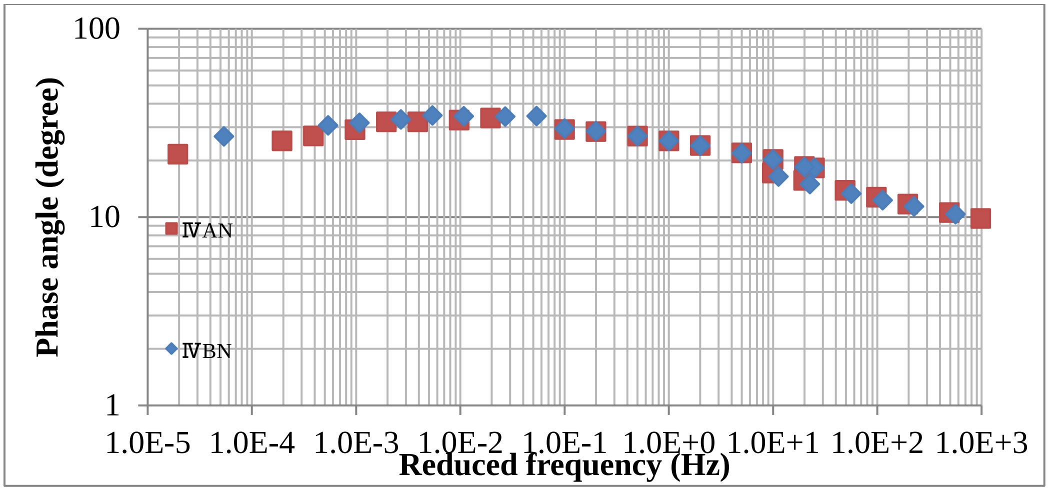

Figure 12-135 Master Phase Angle Curves of Mixtures from Aggregate IV with RAP and Asphalt Source 2 in Terms of Surface Mixture Type

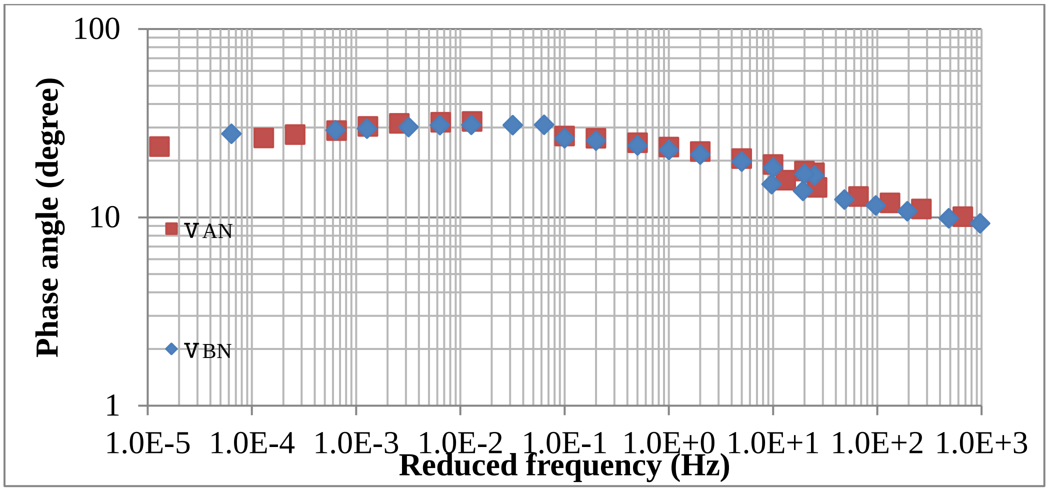

Figure 12-136 Master Phase Angle Curves of Mixtures from Aggregate V with RAP and Asphalt Source 2 in Terms of Surface Type

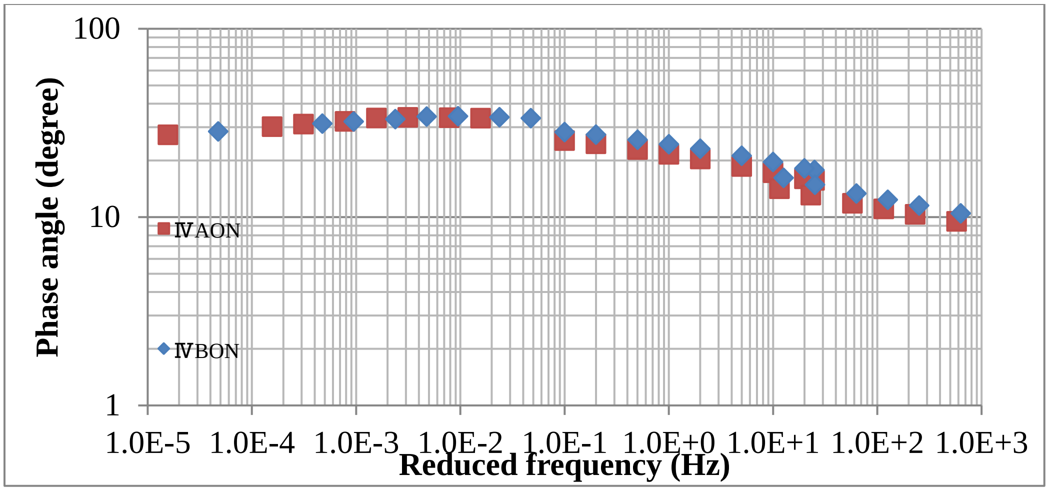

Figure 12-137 Master Phase Angle Curves of Mixtures from Aggregate IV without RAP using Asphalt Source 2 in Terms of Surface Mixture Type

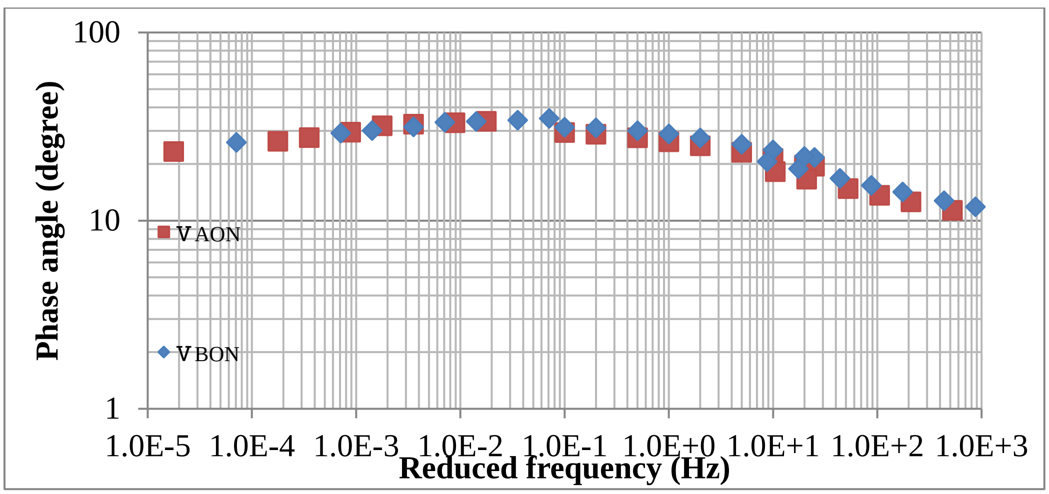

Figure 12-138 Master Phase Angle Curves of Mixtures from Aggregate V without RAP using Asphalt Source 2 in Terms of Surface Mixture Type

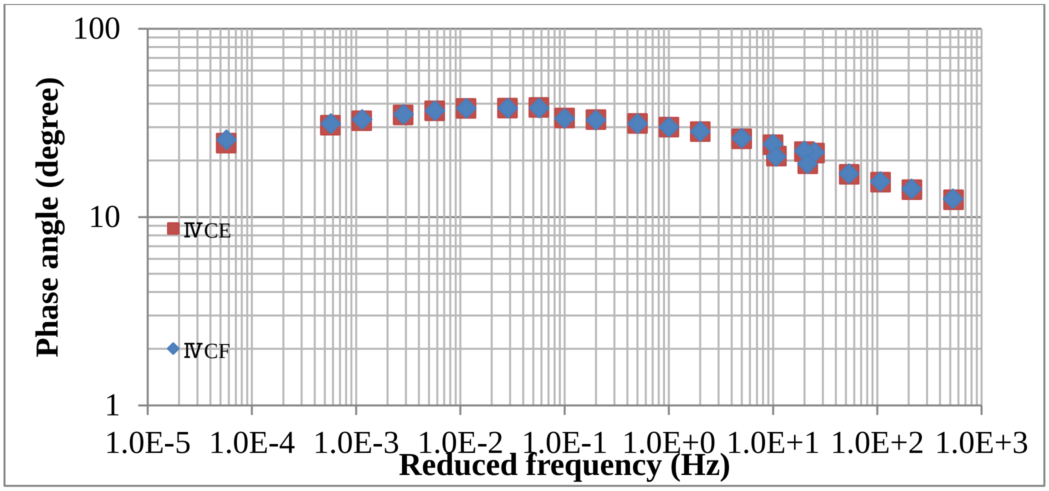

Figure 12-139 Master Phase Angle Curves of Surface Type C Mixtures from Aggregate IV with RAP in Terms of WMA Technology Type

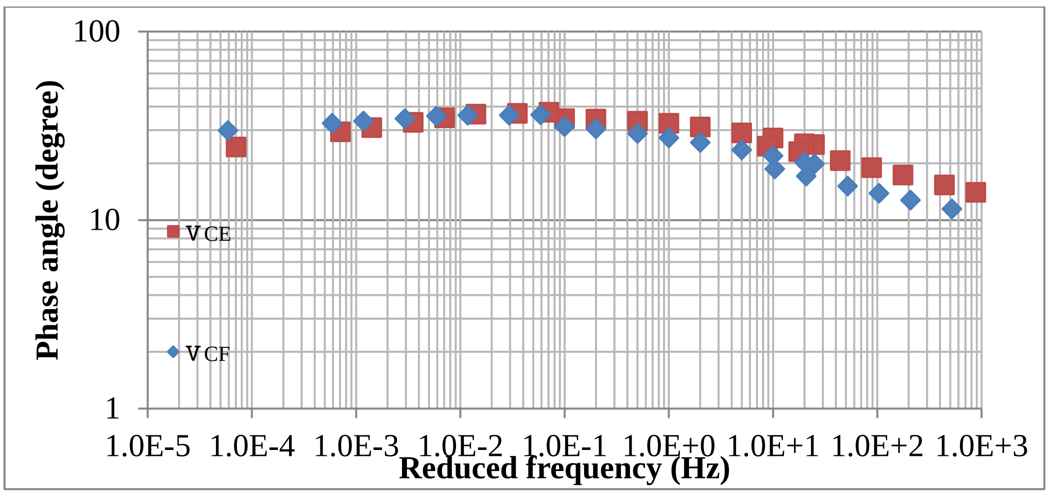

Figure 12-140 Master Phase Angle Curves of Surface Type C Mixtures from Aggregate V with RAP in Terms of WMA Technology Type

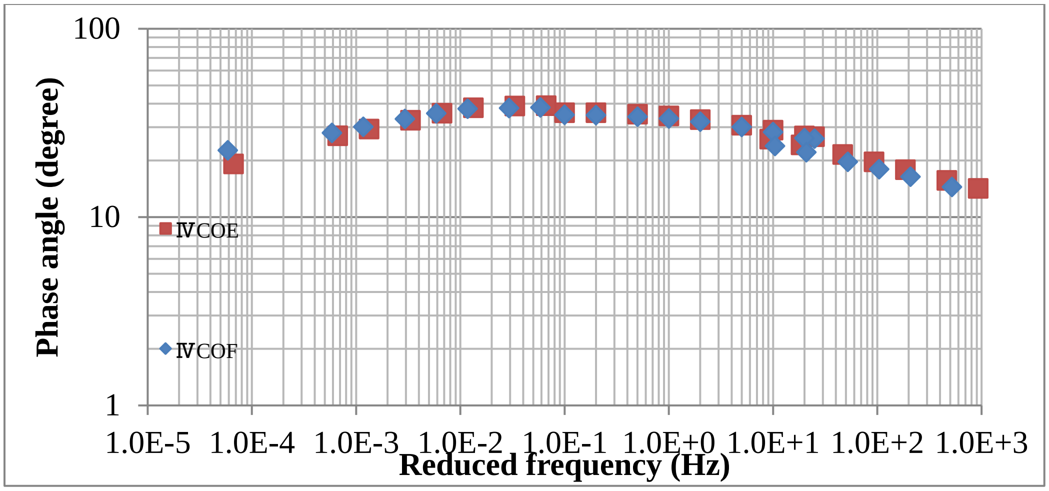

Figure 12-141 Master Phase Angle Curves of Surface Type C Mixtures from Aggregate IV without RAP in Terms of WMA Technology Type

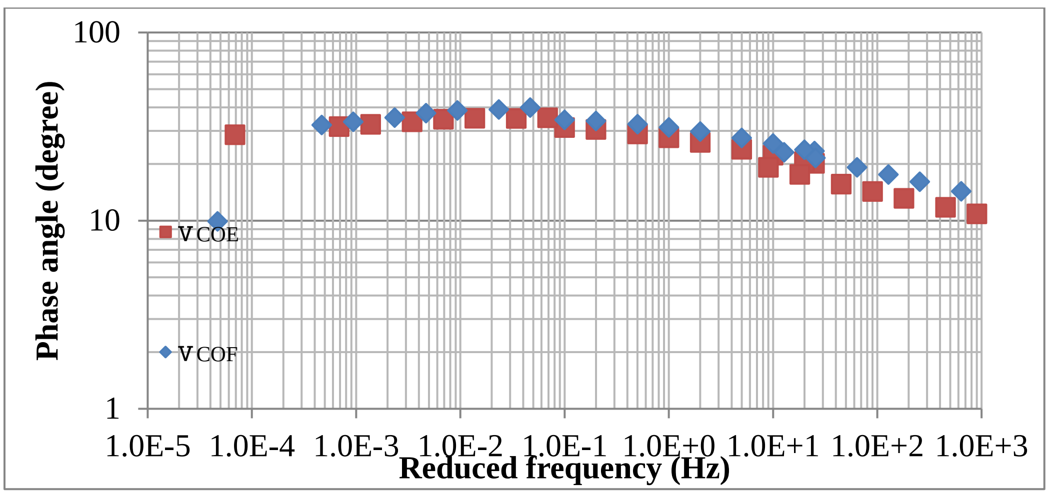

Figure 12-142 Master Phase Angle Curves of Surface Type C Mixtures from Aggregate V without RAP in Terms of WMA Technology Type

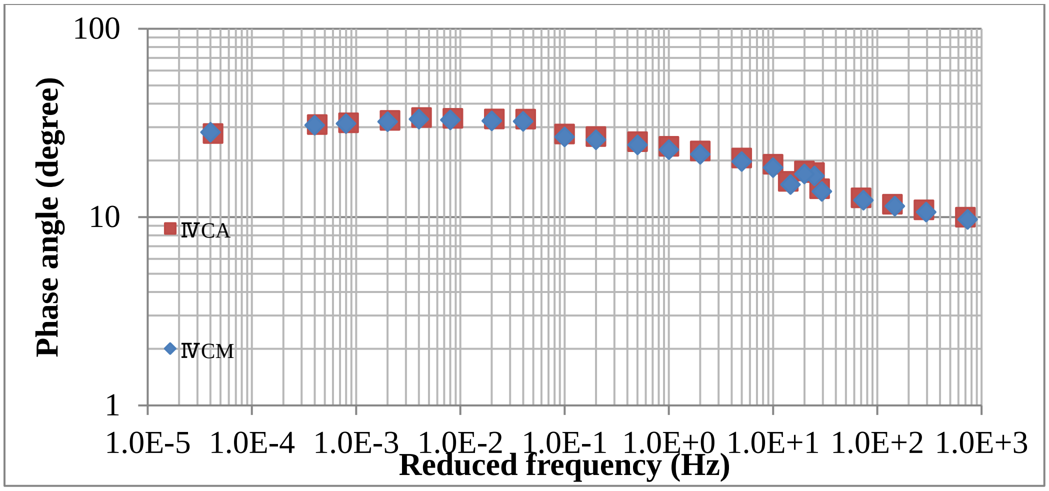

Figure 12-143 Master Phase Angle Curves of Surface Type C Mixtures from Aggregate IV with RAP in Terms of Liquid ASA Type

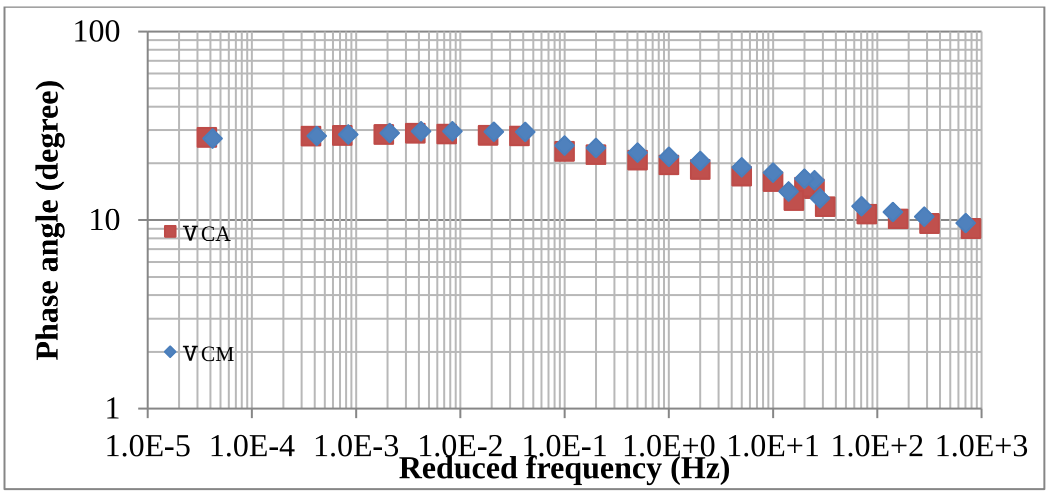

Figure 12-144 Master Phase Angle Curves of Surface Type C Mixtures from Aggregate V with RAP in Terms of Liquid ASA Type

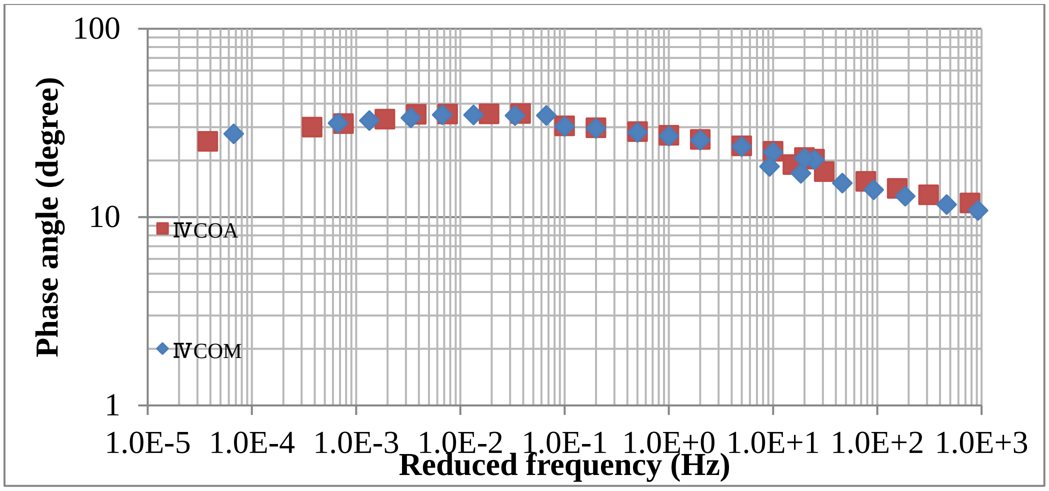

Figure 12-145 Master Phase Angle Curves of Surface Type C Mixtures from Aggregate IV without RAP in Terms of Liquid ASA Type

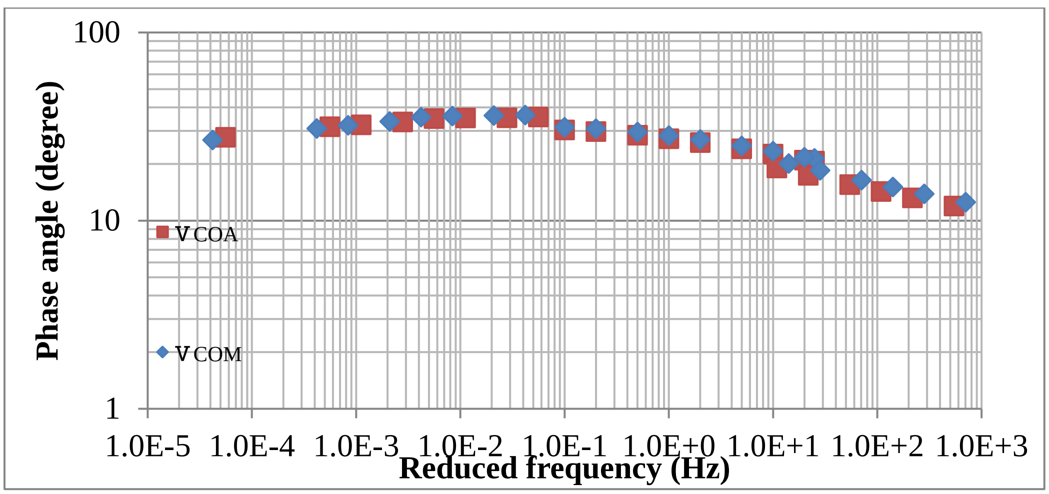

Figure 12-146 Master Phase Angle Curves of Surface Type C Mixtures from Aggregate V without RAP in Terms of Liquid ASA Type

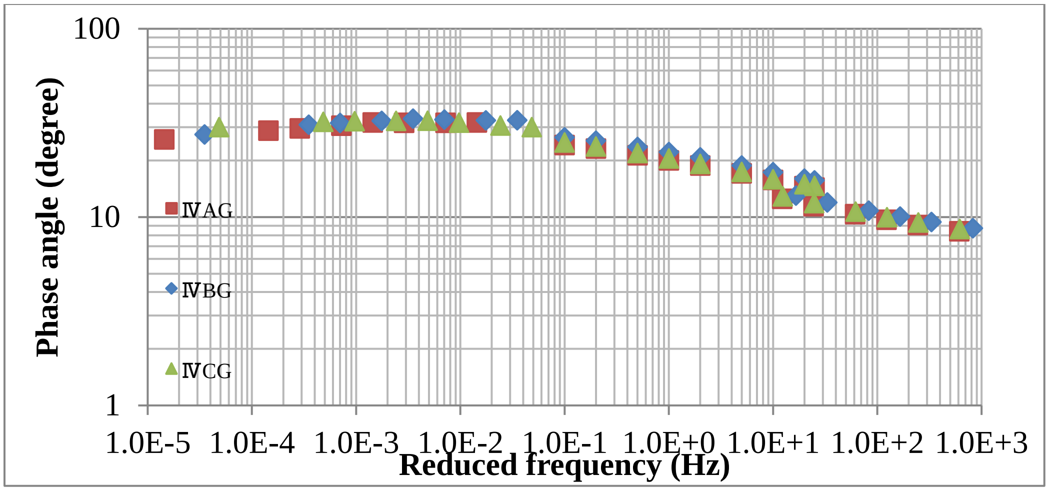

Figure 12-147 Master Phase Angle Curves of Mixtures from Aggregate IV with RAP after Long-Term Aging in Terms of Surface Mixture Type

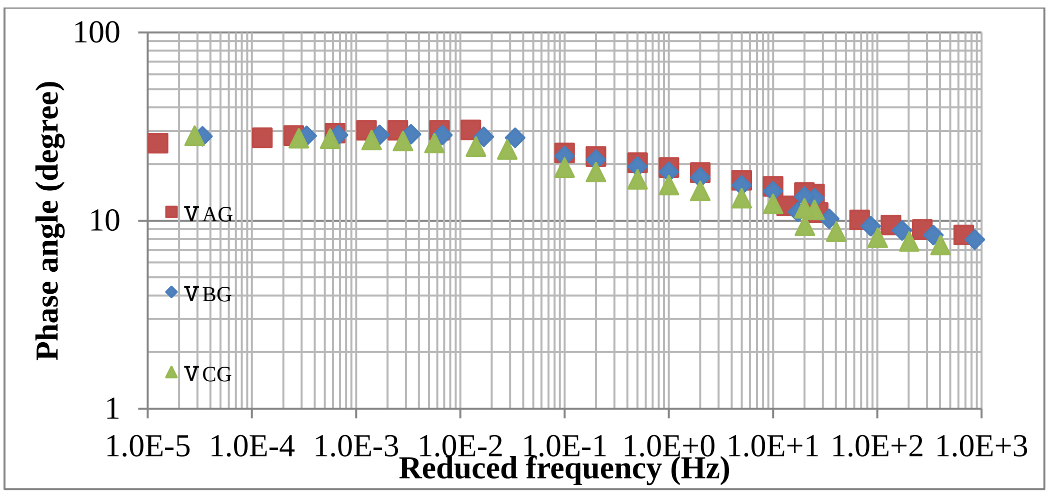

Figure 12-148 Master Phase Angle Curves of Mixtures from Aggregate V with RAP after Long-Term Aging in Terms of Surface Mixture Type

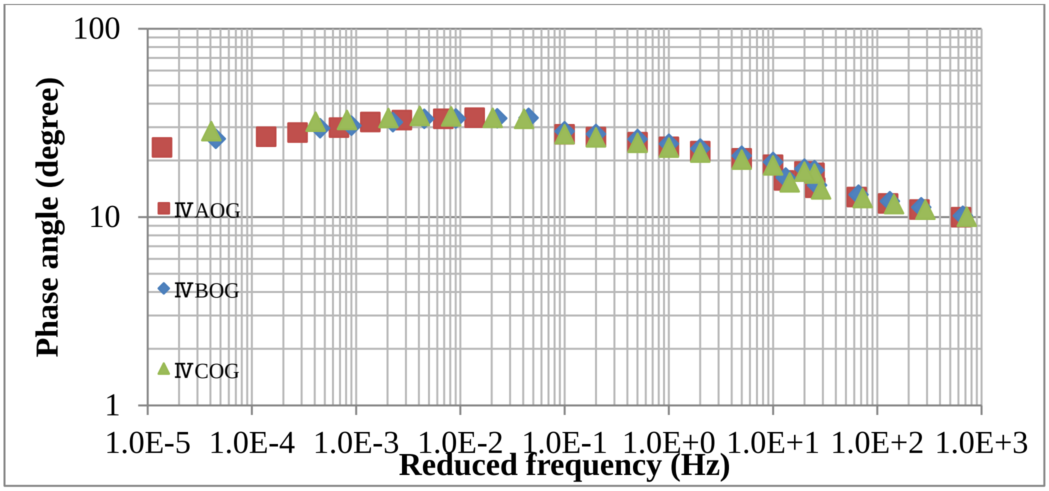

Figure 12-149 Master Phase Angle Curves of Mixtures from Aggregate IV without RAP after Long-Term Aging in Terms of Surface Type

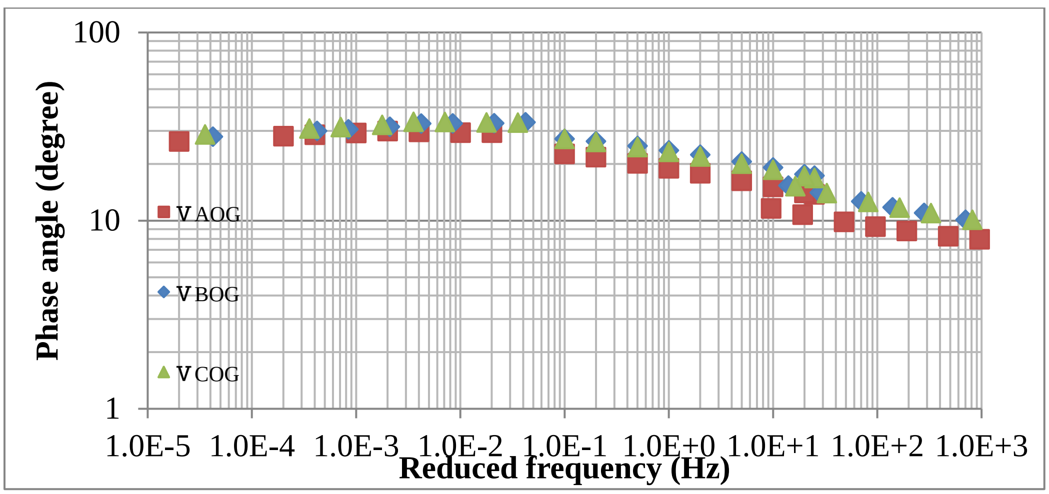

Figure 12-150 Master Phase Angle Curves of Mixtures from Aggregate V without RAP after Long-Term Aging in Terms of Surface Type

13 Appendix E - MEPEG Level 1, 2 and 3 Inputs for Mixtures

Figure 13-1: Mixture Type: I A (Augusta Surface Type A with RAP)

Level 1

Asphalt Mix: Dynamic Modulus Table						
Temperature (°F)	Mixture |E*| (psi)					
	0.1 Hz	0.5 Hz	1 Hz	5 Hz	10 Hz	25 Hz
14	2269976	2620315	2739011	2949458	3016469	3087685
40	1281595	1792070	1998771	2414201	2560850	2724921
70	405384	751564	942085	1441266	1662247	1942447
100	104809	215942	294345	573482	738457	992494
130	36645	65322	86912	177415	242661	362909

Asphalt Binder: Superpave Binder Test Data		
Temperature (°F)	Angular freq. = 10 rad/sec	
	G* (Pa)	Delta (degree)
158.0	2995	63.7
168.8	1501	61.9
179.6	750	60.0

Asphalt General: Volumetric Properties as Built	
Effective Binder (%)	10.69
Air Voids (%)	7.59
Total unit weight	165.62

Level 2

Asphalt Mix: Aggregate Gradation	
Cumulative % Retained ¾" sieve	0
Cumulative % Retained ⅜" sieve	11
Cumulative % Retained #4 sieve	39
% Passing #200 sieve	4.85

Level 3

Asphalt Binder: Superpave Binder Grading	PG 76-22

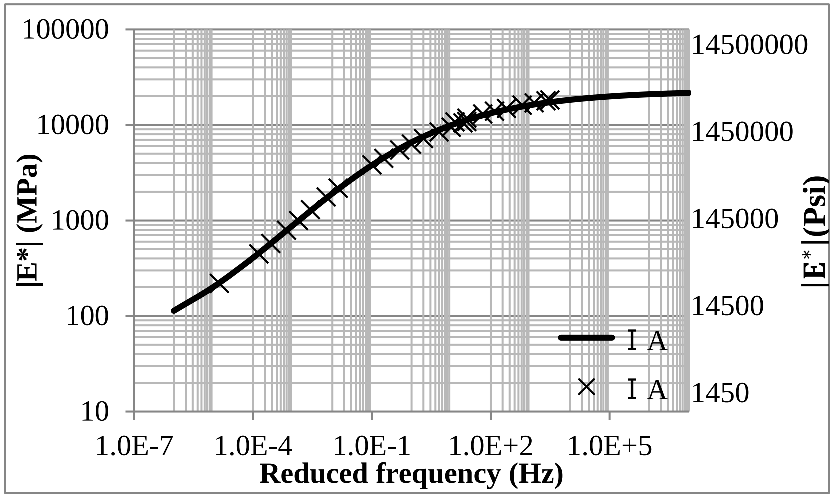

Master Dynamic Modulus Curves for Mixtures from Augusta Surface Type A with RAP

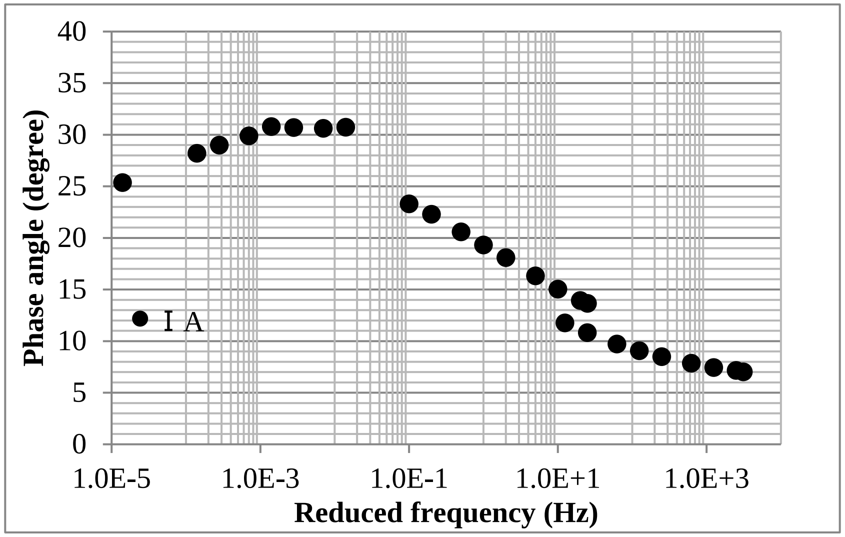

Master Phase Angle Curves for Mixtures from Augusta Surface Type A with RAP

Figure 13-2: Mixture Type: I B1 (Augusta Surface Type B, Mix Design 1 with RAP)

Level 1

Asphalt Mix: Dynamic Modulus Table						
Temperature (°F)	Mixture |E*| (psi)					
	0.1 Hz	0.5 Hz	1 Hz	5 Hz	10 Hz	25 Hz
14	2247433	2652087	2783518	3004878	3071152	3138599
40	1237523	1822610	2058088	2515733	2669336	2834246
70	392083	773906	992739	1569530	1819552	2126835
100	115082	238131	329234	666866	869394	1178355
130	49166	83400	110021	226518	313285	475437

Asphalt Binder: Superpave Binder Test Data		
Temperature (°F)	Angular freq. = 10 rad/sec	
	G* (Pa)	Delta (degree)
158.0	792.60	88.98
168.8	299.28	89.22
179.6	150.21	89.46

Asphalt General: Volumetric Properties as Built	
Effective Binder (%)	11.55
Air Voids (%)	7.59
Total unit weight (pcf)	165.63

Level 2

Asphalt Mix: Aggregate Gradation	
Cumulative % Retained ¾” sieve	0
Cumulative % Retained ⅜” sieve	11
Cumulative % Retained #4 sieve	39
% Passing #200 sieve	4.85

Level 3

Asphalt Binder: Superpave Binder Grading	PG 64-22

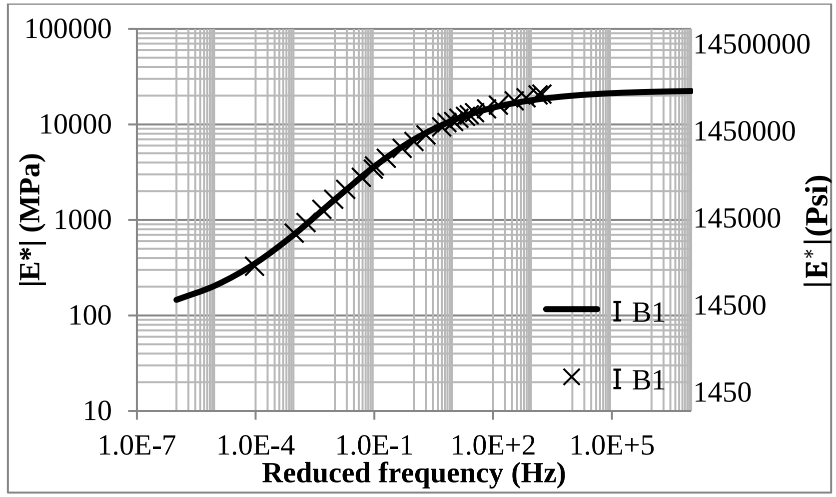

Master Dynamic Modulus Curves for Mixtures from Augusta Surface B Mix Design 1 with RAP

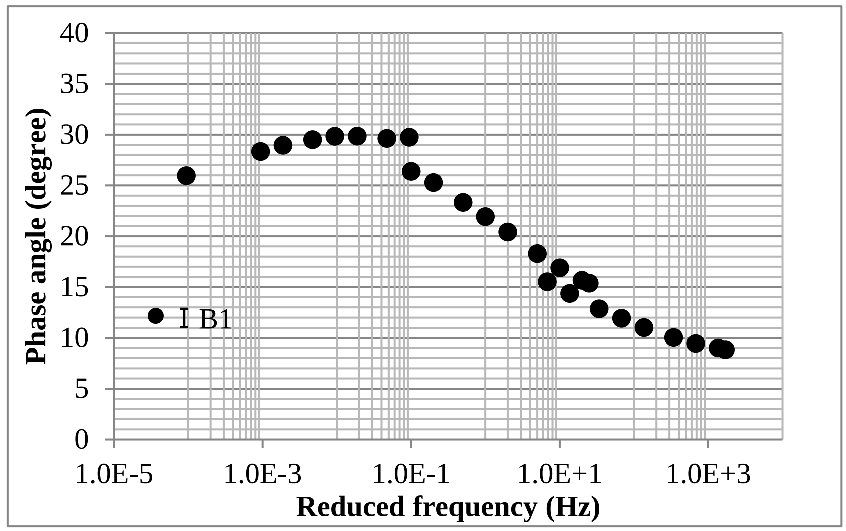

Master Phase Angle Curves for Mixtures from Augusta Surface B Mix Design 1 with RAP

Figure 13-3: Mixture Type: I B2 (Augusta Surface Type B, Mix Design 2 with RAP)

Level 1

Asphalt Mix: Dynamic Modulus Table						
Temperature (°F)	Mixture |E*| (psi)					
	0.1 Hz	0.5 Hz	1 Hz	5 Hz	10 Hz	25 Hz
14	1975436	2398321	2549029	2826506	2917918	3016922
40	1013545	1522236	1741930	2207493	2379791	2577834
70	296892	593058	765455	1242983	1465232	1756150
100	72995	163787	230591	478992	631241	871643
130	23388	46546	64807	145045	204870	317374

Asphalt Binder: Superpave Binder Test Data		
Temperature (°F)	Angular freq. = 10 rad/sec	
	G* (Pa)	Delta (degree)
158.0	792.60	88.98
168.8	299.28	89.22
179.6	150.21	89.46

Asphalt General: Volumetric Properties as Built	
Effective Binder (%)	12.30
Air Voids (%)	7.59
Total unit weight	165.63

Level 2

Asphalt Mix: Aggregate Gradation	
Cumulative % Retained ¾” sieve	0
Cumulative % Retained ⅜” sieve	11
Cumulative % Retained #4 sieve	39
% Passing #200 sieve	4.85

Level 3

Asphalt Binder: Superpave Binder Grading	PG 64-22

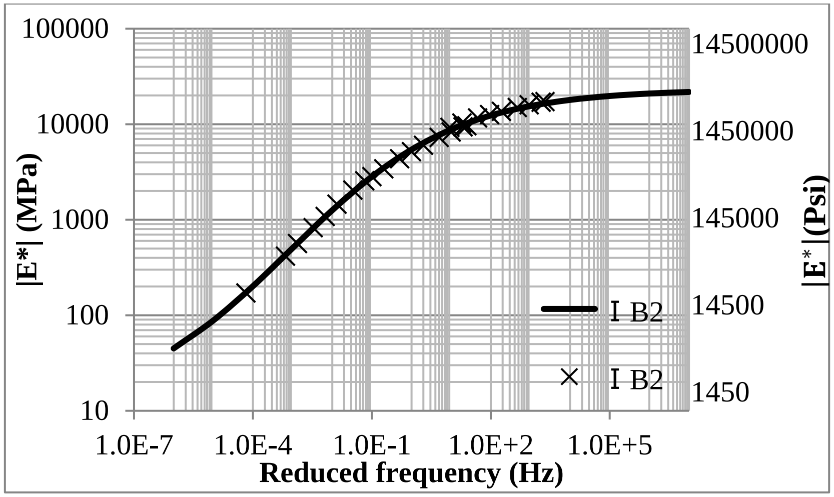

Master Dynamic Modulus Curves for Mixtures from Augusta Surface B Mix Design 2 with RAP

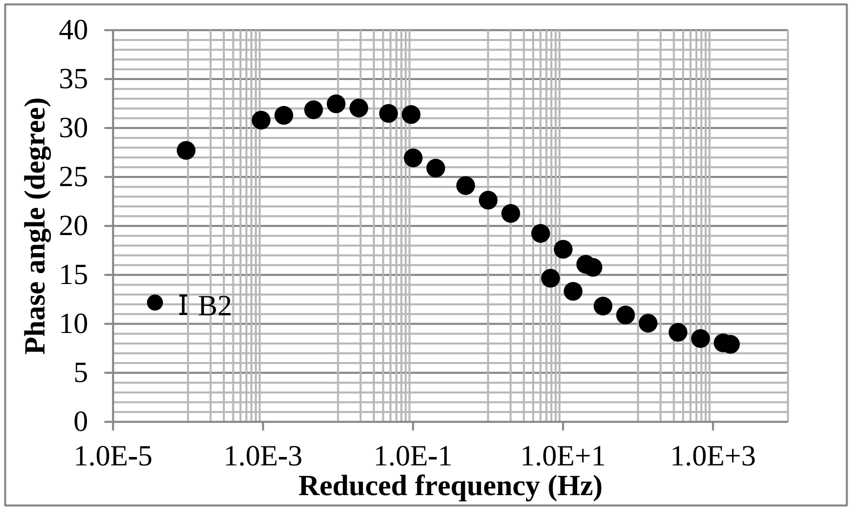

Master Phase Angle Curves for Mixtures from Augusta Surface B Mix Design 2 with RAP

Figure 13-4: Mixture Type: I C (Augusta Surface Type C with RAP)

Level 1

Asphalt Mix: Dynamic Modulus Table						
Temperature (°F)	Mixture |E*| (psi)					
	0.1 Hz	0.5 Hz	1 Hz	5 Hz	10 Hz	25 Hz
14	2078150	2479854	2615069	2850844	2924164	3000657
40	1041541	1584469	1812856	2277694	2441509	2623119
70	267847	565059	745241	1253668	1489922	1794893
100	61488	136898	195584	430103	582359	830492
130	22024	39248	52970	115948	165608	264058

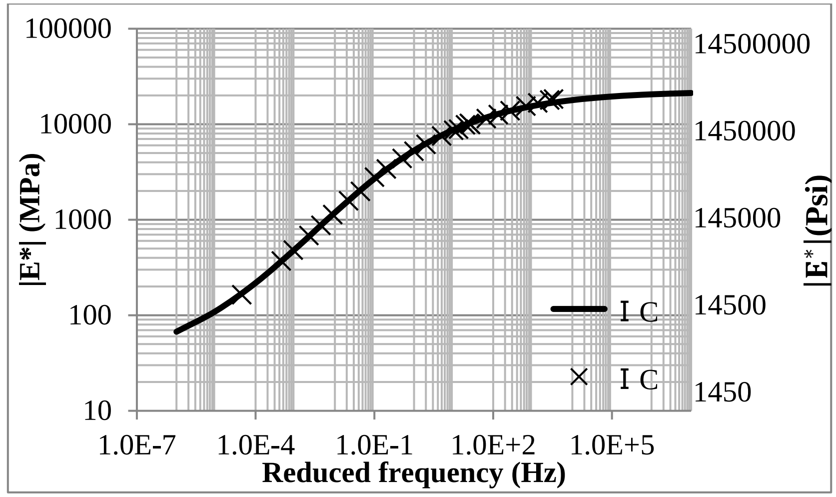

Master Dynamic Modulus Curves for Mixtures from Augusta Surface Type C with RAP

Asphalt Binder: Superpave Binder Test Data		
Temperature (°F)	Angular freq. = 10 rad/sec	
	G* (Pa)	Delta (degree)
158.0	792.60	88.98
168.8	299.28	89.22
179.6	150.21	89.46

Asphalt General: Volumetric Properties as Built	
Effective Binder (%)	13.33
Air Voids (%)	7.51
Total unit weight (pcf)	166.13

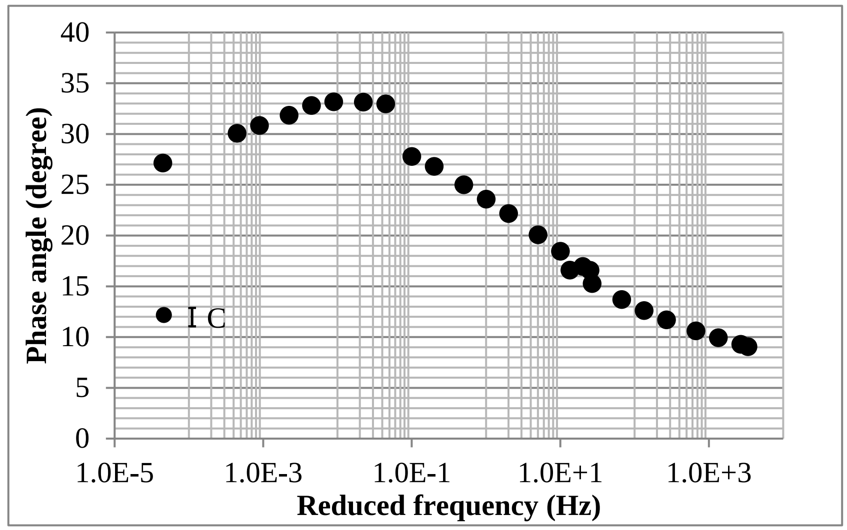

Master Phase Angle Curves for Mixtures from Augusta Surface Type C with RAP

Level 2

Asphalt Mix: Aggregate Gradation	
Cumulative % Retained ¾” sieve	0
Cumulative % Retained ⅜” sieve	3
Cumulative % Retained #4 sieve	29
% Passing #200 sieve	5.64

Level 3

Asphalt Binder: Superpave Binder Grading	PG 64-22

Figure 13-5: Mixture Type: I D (Augusta Surface Type D with RAP)

Level 1

Asphalt Mix: Dynamic Modulus Table						
Temperature (°F)	Mixture |E*| (psi)					
	0.1 Hz	0.5 Hz	1 Hz	5 Hz	10 Hz	25 Hz
14	1701824	2092927	2236406	2507810	2599748	2701120
40	853382	1292552	1486855	1910104	2071429	2260653
70	249585	495446	639409	1044654	1237366	1494344
100	61693	137602	192932	397876	523924	724627
130	19322	38995	54373	121112	170411	262748

Asphalt Binder: Superpave Binder Test Data		
Temperature (°F)	Angular freq. = 10 rad/sec	
	G* (Pa)	Delta (degree)
158.0	792.60	88.98
168.8	299.28	89.22
179.6	150.21	89.46

Asphalt General: Volumetric Properties as Built	
Effective Binder (%)	12.26
Air Voids (%)	5.82
Total unit weight (pcf)	167.31

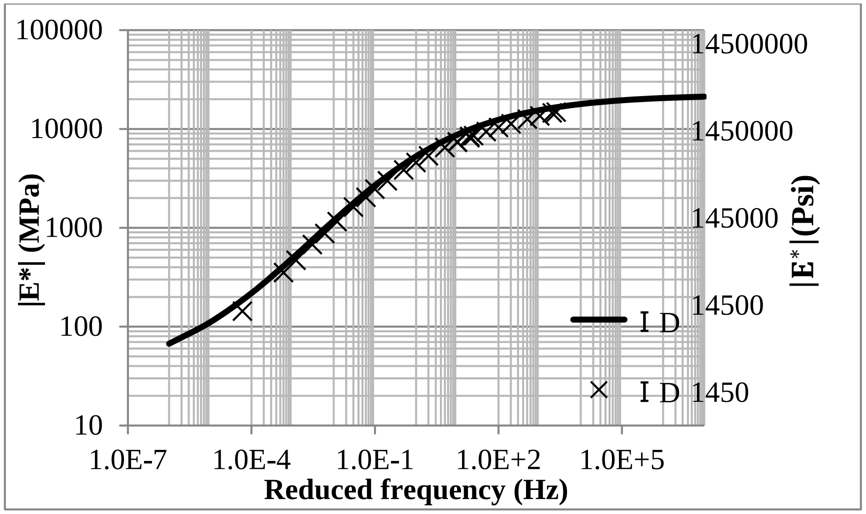

Master Dynamic Modulus Curves for Mixtures from Augusta Surface Type D with RAP

Level 2

Asphalt Mix: Aggregate Gradation	
Cumulative % Retained ¾” sieve	0
Cumulative % Retained ⅜” sieve	2
Cumulative % Retained #4 sieve	18
% Passing #200 sieve	6

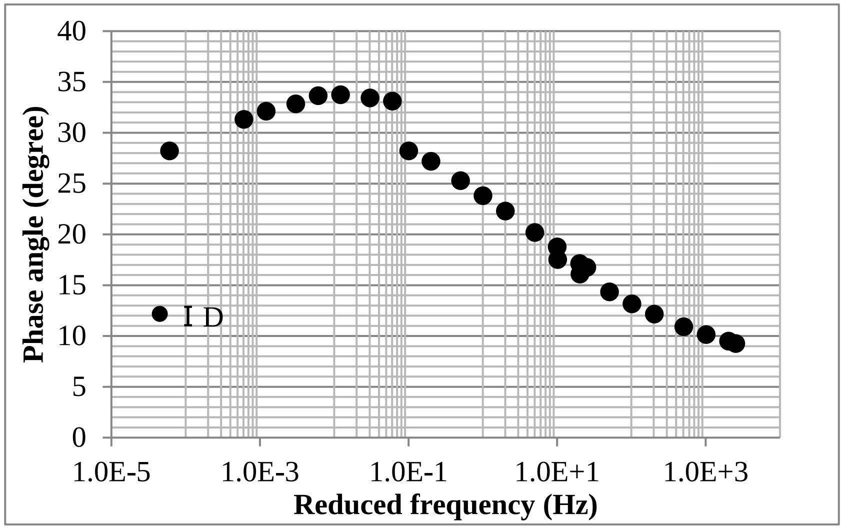

Master Phase Angle Curves for Mixtures from Augusta Surface Type D with RAP

Level 3

Asphalt Binder: Superpave Binder Grading	PG 64-22

Figure 13-6: Mixture Type: I E Augusta Surface Type E with RAP)

Level 1

Asphalt Mix: Dynamic Modulus Table						
Temperature (°F)	Mixture |E*| (psi)					
	0.1 Hz	0.5 Hz	1 Hz	5 Hz	10 Hz	25 Hz
14	1951357	2294890	2416204	2639252	2712931	2793050
40	1101468	1546803	1732797	2119603	2261229	2423634
70	383489	683970	847461	1277291	1470099	1718257
100	113884	224609	299328	554095	700198	922174
130	42146	75427	99635	195995	262091	379366

Asphalt Binder: Superpave Binder Test Data		
Temperature (°F)	Angular freq. = 10 rad/sec	
	G* (Pa)	Delta (degree)
158.0	792.60	88.98
168.8	299.28	89.22
179.6	150.21	89.46

Asphalt General: Volumetric Properties as Built	
Effective Binder (%)	12.26
Air Voids (%)	6.85
Total unit weight	167.31

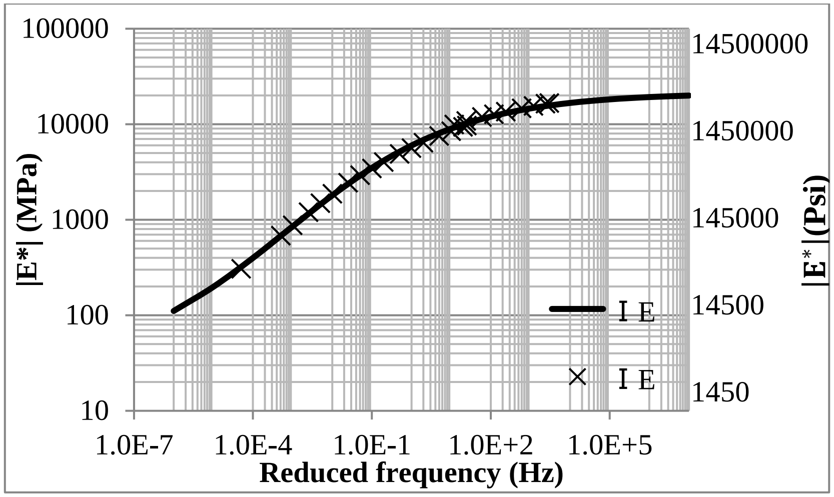

Master Dynamic Modulus Curves for Mixtures from Augusta Surface Type E with RAP

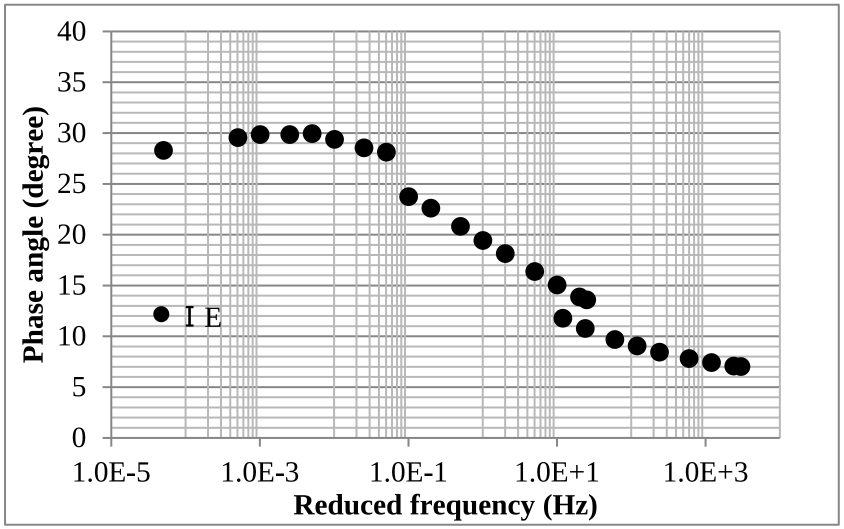

Master Phase Angle Curves for Mixtures from Augusta Surface Type E with RAP

Level 2

Asphalt Mix: Aggregate Gradation	
Cumulative % Retained ¾” sieve	0
Cumulative % Retained ⅜” sieve	2
Cumulative % Retained #4 sieve	18
% Passing #200 sieve	6

Level 3

Asphalt Binder: Superpave Binder Grading	PG 64-22

Figure 13-7: Mixture Type: I EO (Augusta Surface Type E, no RAP)

Level 1

Asphalt Mix: Dynamic Modulus Table						
Temperature	Mixture |E*| (psi)					
(°F)	0.1 Hz	0.5 Hz	1 Hz	5 Hz	10 Hz	25 Hz
14	1553140	1977131	2143941	2481148	2603392	2744238
40	748185	1152695	1341471	1779378	1957960	2177612
70	226656	439006	564084	926396	1106011	1354818
100	59736	129513	178804	357529	466969	642893
130	18562	38257	53217	115575	160121	241910

Asphalt Binder: Superpave Binder Test Data		
Temperature	Angular freq. = 10 rad/sec	
(°F)	G* (Pa)	Delta (degree)
158.0	792.60	88.98
168.8	299.28	89.22
179.6	150.21	89.46

Asphalt General: Volumetric Properties as Built	
Effective Binder (%)	12.26
Air Voids (%)	6.60
Total unit weight	• 167.31

Level 2

Asphalt Mix: Aggregate Gradation	
Cumulative % Retained ¾" sieve	0
Cumulative % Retained ⅜" sieve	10
Cumulative % Retained #4 sieve	37
% Passing #200 sieve	4

Level 3

Asphalt Binder: Superpave Binder Grading	PG 64-22

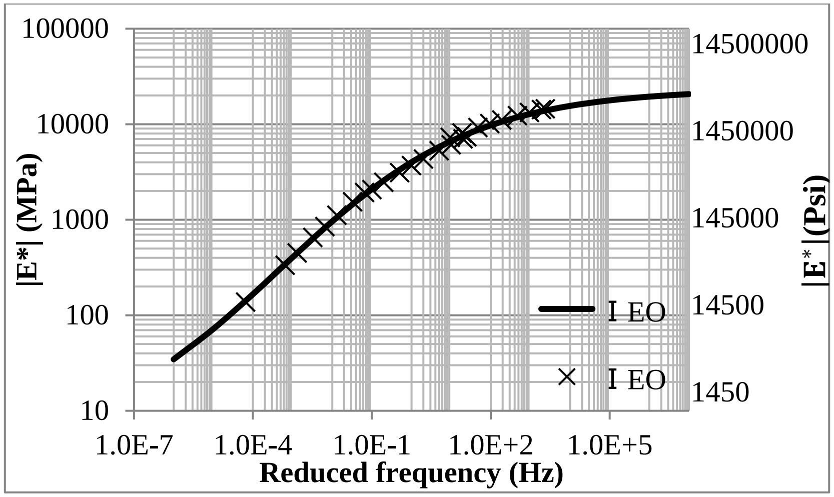

Master Dynamic Modulus Curves for Mixtures from Augusta Surface Type E no RAP

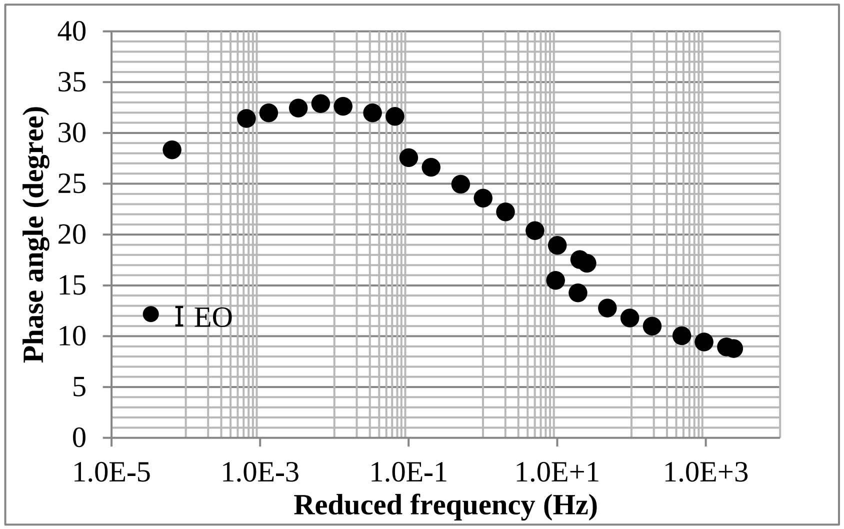

Master Phase Angle Curves for Mixtures from Augusta Surface Type E no RAP

Figure 13-8: Mixture Type: II A1 (Blacksburg Surface Type A, Mix Design 1 with RAP)

Level 1

Asphalt Mix: Dynamic Modulus Table						
Temperature	Mixture |E*| (psi)					
(°F)	0.1 Hz	0.5 Hz	1 Hz	5 Hz	10 Hz	25 Hz
14	1900562	2299005	2445689	2725506	2821412	2928150
40	984581.2	1442258	1642706	2079166	2246421	2443944
70	303138.3	571154.2	723701.9	1145749	1344943	1610720
100	78137.64	165169.7	226219.1	444538.1	575739.9	782594
130	24903.69	48323.92	65968.36	139295	191642.1	287633.3

Asphalt Binder: Superpave Binder Test Data		
Temperature	Angular freq. = 10 rad/sec	
(°F)	G* (Pa)	Delta (degree)
158.0	2995.00	63.70
168.8	1501.00	61.90
179.6	750.50	60.00

Asphalt General: Volumetric Properties as Built	
Effective Binder (%)	10.69
Air Voids (%)	6.33
Total unit weight	164.31

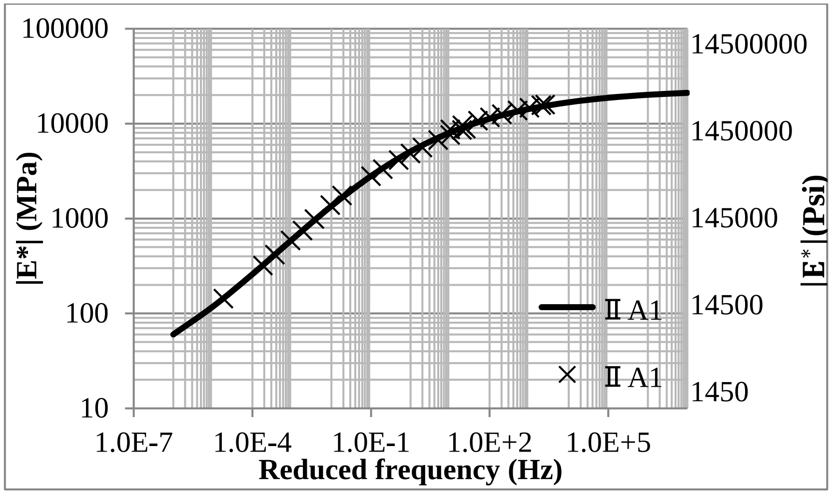

Master Dynamic Modulus Curves for Mixtures from Blacksburg Surface A Mix Design 1 with RAP

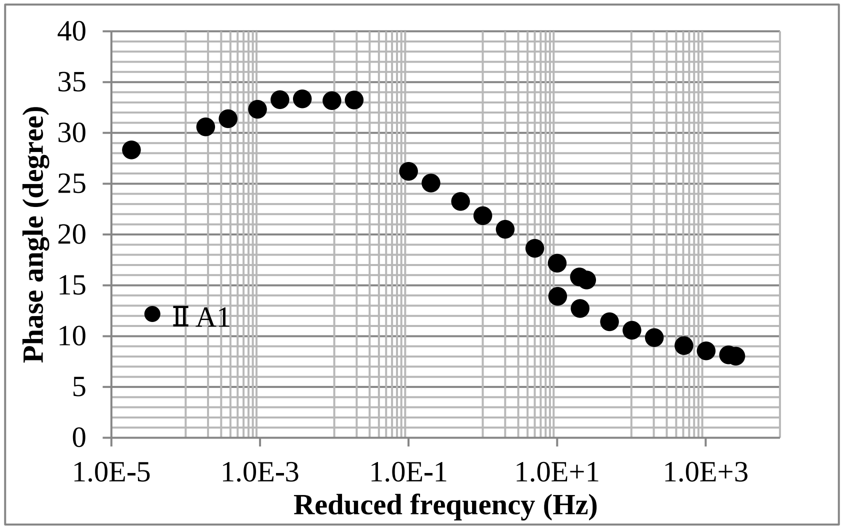

Master Phase Angle Curves for Mixtures from Blacksburg Surface A Mix Design 1 with RAP

Level 2

Asphalt Mix: Aggregate Gradation	
Cumulative % Retained ¾" sieve	0
Cumulative % Retained ⅜" sieve	18
Cumulative % Retained #4 sieve	49
% Passing #200 sieve	5

Level 3

Asphalt Binder: Superpave Binder Grading	PG 76-22

Figure 13-9: Mixture Type: II A2 (Blacksburg Surface Type A, Mix Design 2 with RAP)

Level 1

Asphalt Mix: Dynamic Modulus Table						
Temperature (°F)	Mixture |E*| (psi)					
	0.1 Hz	0.5 Hz	1 Hz	5 Hz	10 Hz	25 Hz
14	1769583	2189057	2345684	2646993	2750853	2866670
40	856675	1306068	1509038	1961206	2137583	2347686
70	241523	476056	615446	1017587	1214160	1481884
100	59738	128684	178717	365930	483282	674010
130	19381	37146	50711	108643	151298	231755

Asphalt Binder: Superpave Binder Test Data		
Temperature (°F)	Angular freq. = 10 rad/sec	
	G* (Pa)	Delta (degree)
158.0	2995.00	63.70
168.8	1501.00	61.90
179.6	750.50	60.00

Asphalt General: Volumetric Properties as Built	
Effective Binder (%)	11.26
Air Voids (%)	6.33
Total unit weight (pcf)	164.31

Level 2

Asphalt Mix: Aggregate Gradation	
Cumulative % Retained ¾" sieve	0
Cumulative % Retained ⅜" sieve	13
Cumulative % Retained #4 sieve	39
% Passing #200 sieve	5.97

Level 3

Asphalt Binder: Superpave Binder Grading	PG 76-22

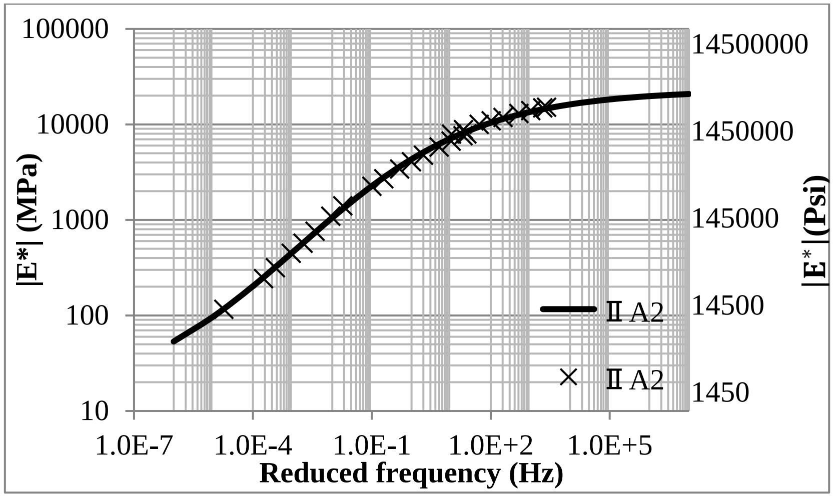

Master Dynamic Modulus Curves for Mixtures from Blacksburg Surface Type A Mix Design 2 with RAP

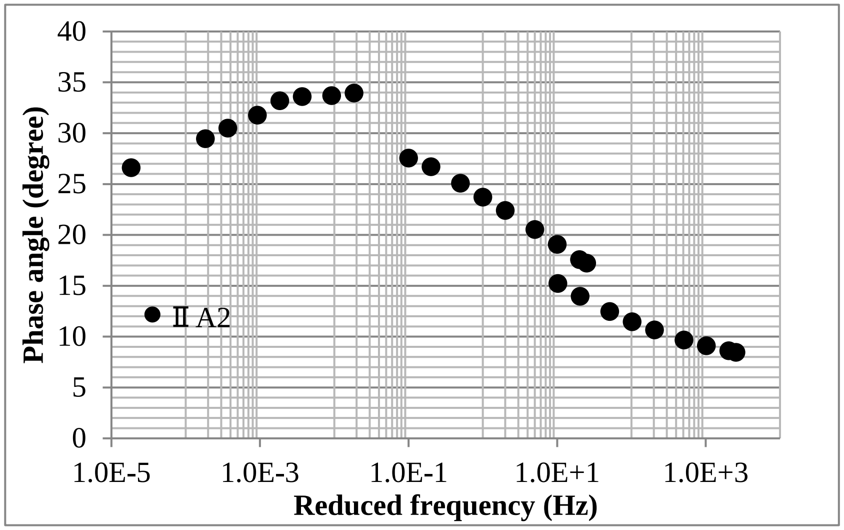

Master Phase Angle Curves for Mixtures from Blacksburg Surface Type A Mix Design 2 with RAP

Figure 13-10: Mixture Type: II B (Blacksburg Surface Type B with RAP)

Level 1

Asphalt Mix: Dynamic Modulus Table						
Temperature (°F)	Mixture |E*| (psi)					
	0.1 Hz	0.5 Hz	1 Hz	5 Hz	10 Hz	25 Hz
14	1751711	2166111	2319650	2613060	2713561	2825216
40	844506	1298311	1501560	1950017	2123263	2328366
70	225165	464076	606821	1016884	1215630	1484197
100	48276	114738	164736	356142	477184	673769
130	13014	28221	40551	96401	139152	221391

Asphalt Binder: Superpave Binder Test Data		
Temperature (°F)	Angular freq. = 10 rad/sec	
	G* (Pa)	Delta (degree)
158.0	792.60	88.98
168.8	299.28	89.22
179.6	150.21	89.46

Asphalt General: Volumetric Properties as Built	
Effective Binder (%)	10.37
Air Voids (%)	6.88
Total unit weight	165.94

Level 2

Asphalt Mix: Aggregate Gradation	
Cumulative % Retained ¾” sieve	0
Cumulative % Retained ⅜” sieve	13
Cumulative % Retained #4 sieve	12
% Passing #200 sieve	6.21

Level 3

Asphalt Binder: Superpave Binder Grading	PG 64-22

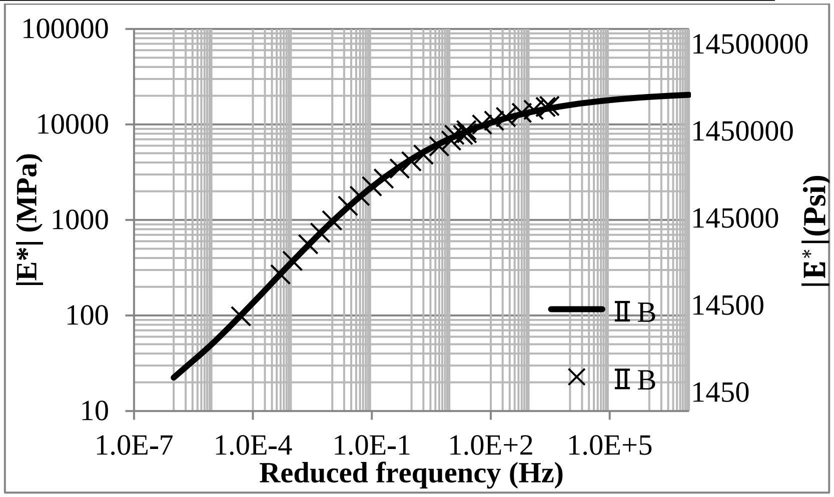

Master Dynamic Modulus Curves for Mixtures from Blacksburg Surface Type B with RAP

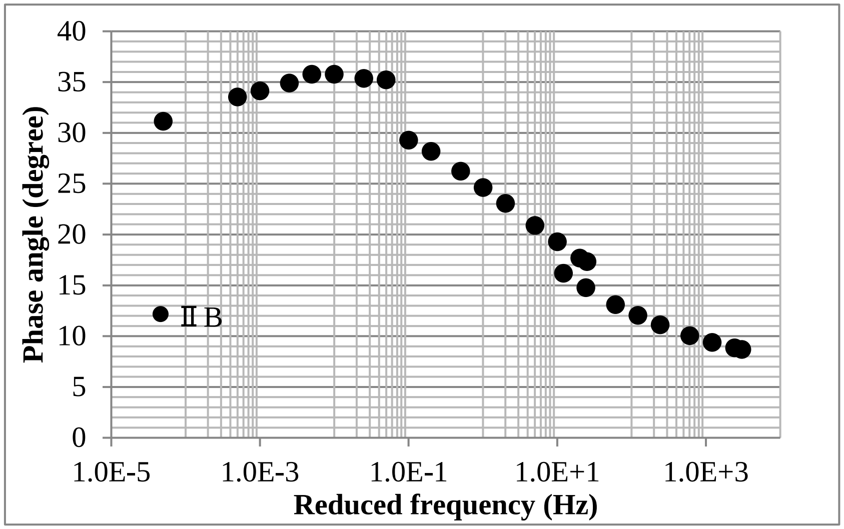

Master Phase Angle Curves for Mixtures from Blacksburg Surface Type B with RAP

Figure 13-11: Mixture Type: II C (Blacksburg Surface Type C with RAP)

Level 1

Asphalt Mix: Dynamic Modulus Table						
Temperature (°F)	Mixture |E*| (psi)					
	0.1 Hz	0.5 Hz	1 Hz	5 Hz	10 Hz	25 Hz
14	1671366	2088693	2244696	2544472	2647557	2762253
40	824714	1269475	1469629	1912799	2084417	2287766
70	241885	486158	630297	1039882	1236609	1500956
100	59921	136653	192795	401075	529290	733654
130	18225	38401	54353	124029	175548	271845

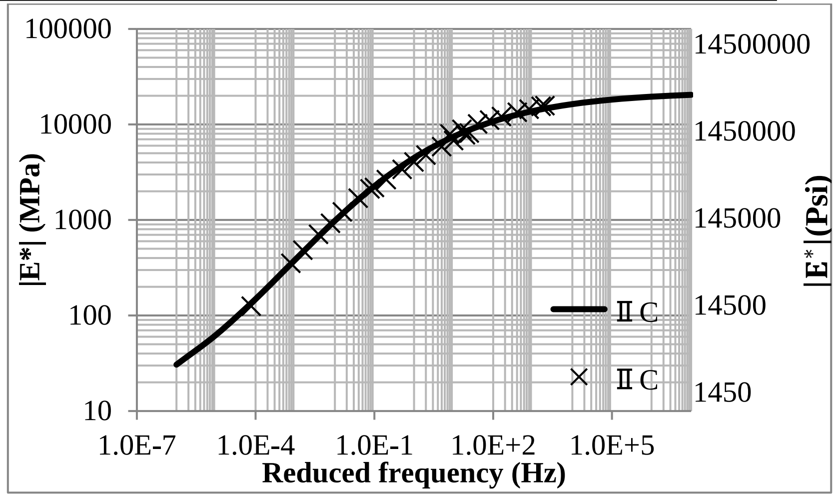

Master Dynamic Modulus Curves for Mixtures from Blacksburg Surface Type C with RAP

Asphalt Binder: Superpave Binder Test Data		
Temperature (°F)	Angular freq. = 10 rad/sec	
	G* (Pa)	Delta (degree)
158.0	792.60	88.98
168.8	299.28	89.22
179.6	150.21	89.46

Asphalt General: Volumetric Properties as Built	
Effective Binder (%)	10.67
Air Voids (%)	7.13
Total unit weight	167.06

Level 2

Asphalt Mix: Aggregate Gradation	
Cumulative % Retained ¾” sieve	0
Cumulative % Retained ⅜” sieve	10
Cumulative % Retained #4 sieve	31
% Passing #200 sieve	6.59

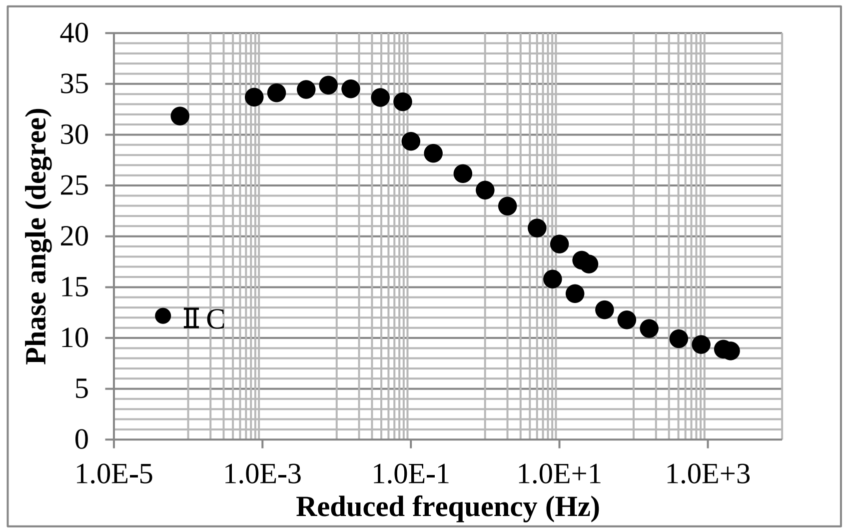

Master Phase Angle Curves for Mixtures from Blacksburg Surface Type C with RAP

Level 3

Asphalt Binder: Superpave Binder Grading	PG 64-22

Figure 13-12: Mixture Type: II D (Blacksburg Surface Type D with RAP)

Level 1

Asphalt Mix: Dynamic Modulus Table						
Temperature (°F)	Mixture |E*| (psi)					
	0.1 Hz	0.5 Hz	1 Hz	5 Hz	10 Hz	25 Hz
14	1795242	2171876	2306853	2557224	2640456	2731196
40	927952	1381327	1576813	1992274	2146907	2325596
70	273102	541034	695529	1121068	1318807	1578055
100	65333	148141	208673	431713	567452	781082
130	19719	40470	56888	128921	182409	282574

Asphalt Binder: Superpave Binder Test Data		
Temperature (°F)	Angular freq. = 10 rad/sec	
	G* (Pa)	Delta (degree)
158.0	792.60	88.98
168.8	299.28	89.22
179.6	150.21	89.46

Asphalt General: Volumetric Properties as Built	
Effective Binder (%)	11.34
Air Voids (%)	7.33
Total unit weight	167.56

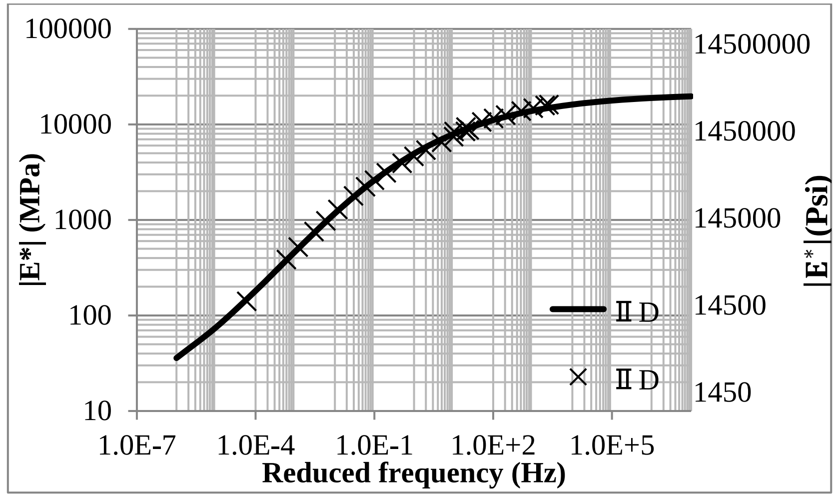

Master Dynamic Modulus Curves for Mixtures from Blacksburg Surface Type D with RAP

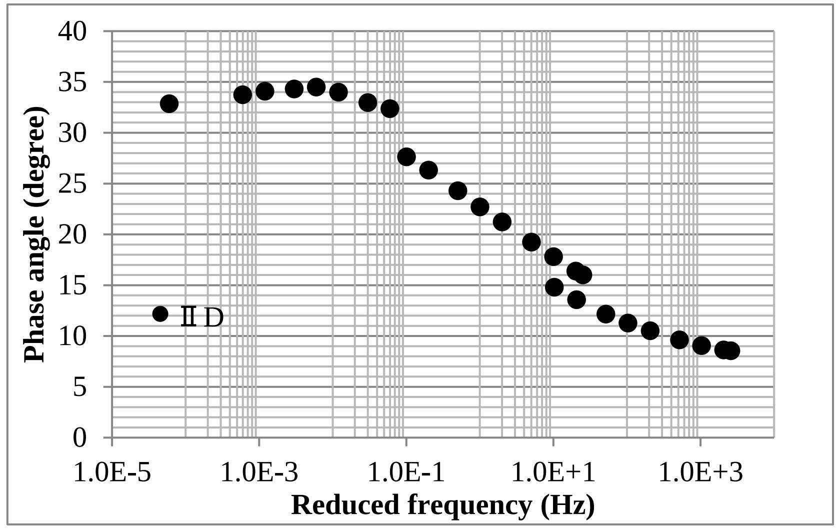

Master Phase Angle Curves for Mixtures from Blacksburg Surface Type D with RAP

Level 2

Asphalt Mix: Aggregate Gradation	
Cumulative % Retained ¾" sieve	0
Cumulative % Retained ⅜" sieve	0
Cumulative % Retained #4 sieve	17
% Passing #200 sieve	7.27

Level 3

Asphalt Binder: Superpave Binder Grading	PG 64-22

Figure 13-13: Mixture Type: II E (Blacksburg Surface Type E with RAP)

Level 1

Asphalt Mix: Dynamic Modulus Table						
Temperature (°F)	Mixture |E*| (psi)					
	0.1 Hz	0.5 Hz	1 Hz	5 Hz	10 Hz	25 Hz
14	1421402	1788449	1932865	2226106	2333188	2457360
40	695188	1051908	1216737	1597702	1753164	1944979
70	210551	403026	514591	833573	990413	1207131
100	52661	116072	160506	319604	415946	569778
130	14756	31932	45084	99959	139018	210390

Asphalt Binder: Superpave Binder Test Data		
Temperature (°F)	Angular freq. = 10 rad/sec	
	G* (Pa)	Delta (degree)
158.0	792.60	88.98
168.8	299.28	89.22
179.6	150.21	89.46

Asphalt General: Volumetric Properties as Built	
Effective Binder (%)	11.34
Air Voids (%)	10.97
Total unit weight	167.56

Level 2

Asphalt Mix: Aggregate Gradation	
Cumulative % Retained ¾" sieve	0
Cumulative % Retained ⅜" sieve	0
Cumulative % Retained #4 sieve	1
% Passing #200 sieve	8.72

Level 3

Asphalt Binder: Superpave Binder Grading	PG 64-22

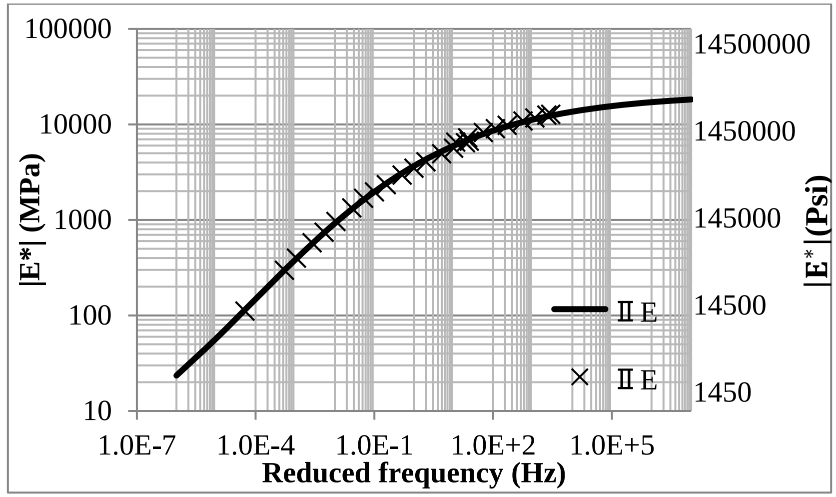

Master Dynamic Modulus Curves for Mixtures from Blacksburg Surface Type E with RAP

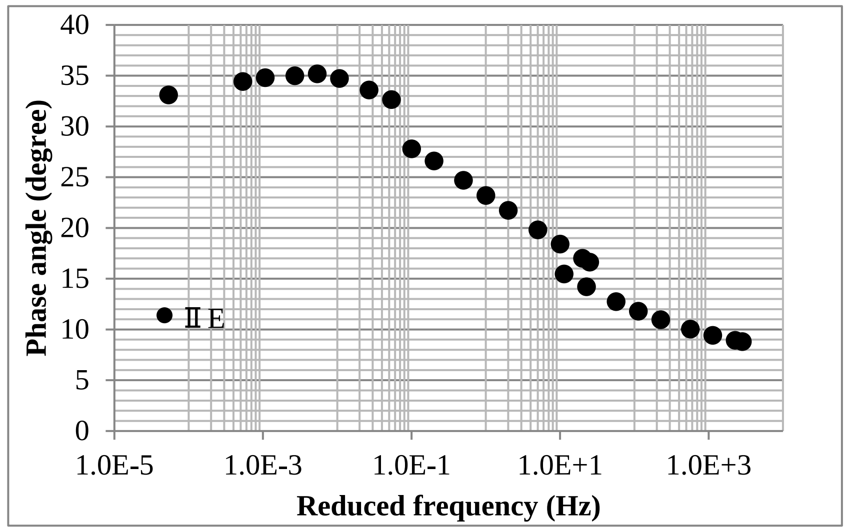

Master Phase Angle Curves for Mixtures from Blacksburg Surface Type E with RAP

Figure 13-14: Mixture Type: II IB (Blacksburg Intermediate Type B Special with RAP)

Level 1

Asphalt Mix: Dynamic Modulus Table						
Temperature (°F)	Mixture |E*| (psi)					
	0.1 Hz	0.5 Hz	1 Hz	5 Hz	10 Hz	25 Hz
14	2262615	2529447	2627009	2815943	2882590	2958764
40	1263119	1643264	1801927	2142441	2273740	2431402
70	362247	606619	736417	1082074	1243350	1460486
100	68808	134982	178753	328905	417812	559146
130	15451	28307	37439	73356	98226	143637

Asphalt Binder: Superpave Binder Test Data		
Temperature (°F)	Angular freq. = 10 rad/sec	
	G* (Pa)	Delta (degree)
158.0	792.60	88.98
168.8	299.28	89.22
179.6	150.21	89.46

Asphalt General: Volumetric Properties as Built	
Effective Binder (%)	12.48
Air Voids (%)	7.72
Total unit weight	165.00

Level 2

Asphalt Mix: Aggregate Gradation	
Cumulative % Retained ¾" sieve	1
Cumulative % Retained ⅜" sieve	17
Cumulative % Retained #4 sieve	49
% Passing #200 sieve	5.15

Level 3

Asphalt Binder: Superpave Binder Grading	PG 64-22

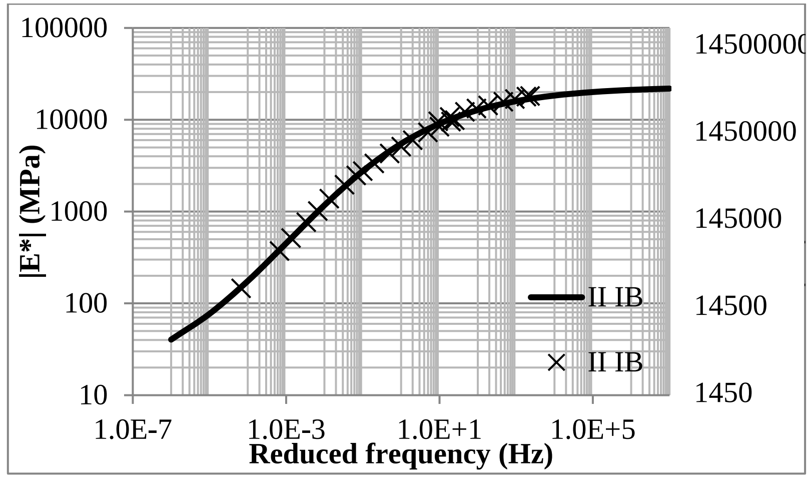

Master Dynamic Modulus Curves for Mixtures from Blacksburg Intermediate Type B Special with RAP

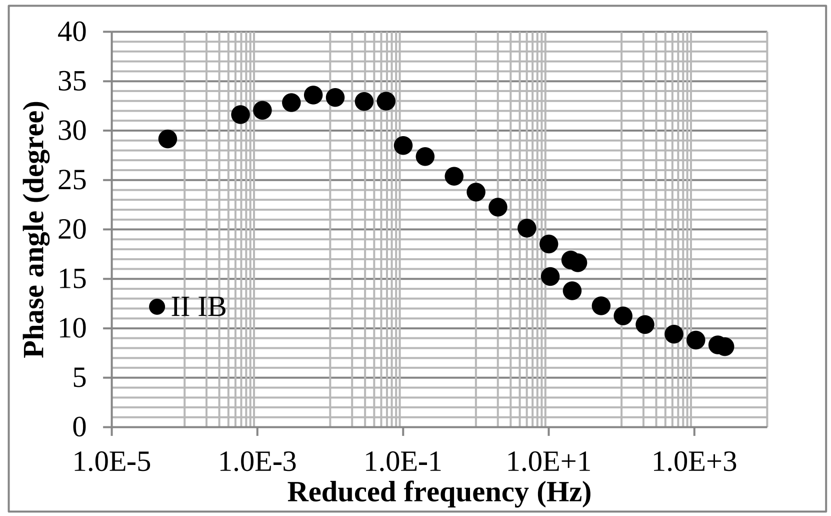

Master Phase Angle Curves for Mixtures from Blacksburg Intermediate Type B Special with RAP

Figure 13-15: Mixture Type: III A1 (Columbia Surface Type A, Mix Design 1 with RAP)

Level 1

Asphalt Mix: Dynamic Modulus Table						
Temperature (°F)	Mixture |E*| (psi)					
	0.1 Hz	0.5 Hz	1 Hz	5 Hz	10 Hz	25 Hz
14	2061881	2447035	2585509	2844532	2931668	3027562
40	1108476	1586278	1790051	2222995	2385070	2573712
70	349752	647227	813280	1262350	1469540	1741589
100	90668	188879	257161	498246	641150	863817
130	29316	55625	75318	156588	214242	319384

Asphalt Binder: Superpave Binder Test Data		
Temperature (°F)	Angular freq. = 10 rad/sec	
	G* (Pa)	Delta (degree)
158.0	792.60	88.98
168.8	299.28	89.22
179.6	150.21	89.46

Asphalt General: Volumetric Properties as Built	
Effective Binder (%)	9.97
Air Voids (%)	6.57
Total unit weight	164.81

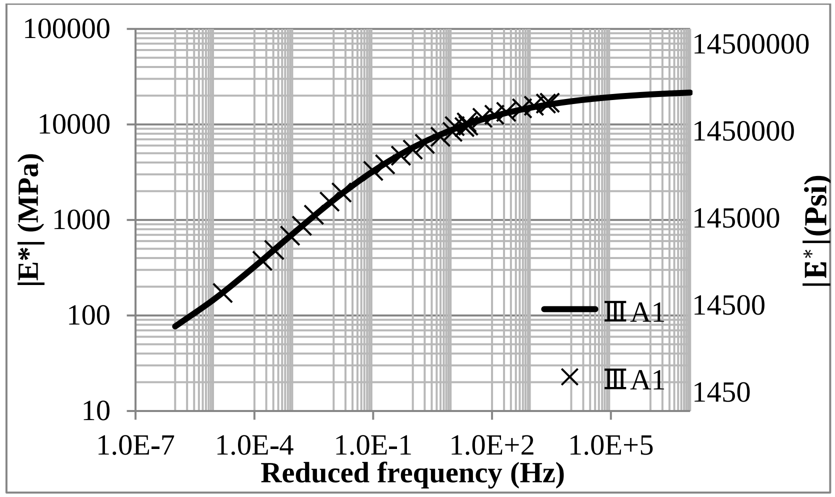

Master Dynamic Modulus Curves for Mixtures from Columbia Surface Type A, Mix Design 1 with RAP

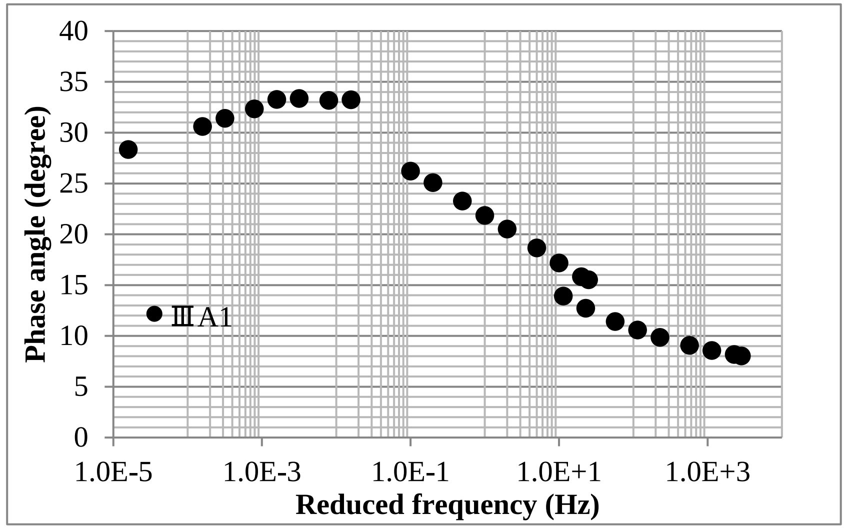

Master Phase Angle Curves for Mixtures from Columbia Surface Type A, Mix Design 1 with RAP

Level 2

Asphalt Mix: Aggregate Gradation	
Cumulative % Retained ¾” sieve	0
Cumulative % Retained ⅜” sieve	20
Cumulative % Retained #4 sieve	50
% Passing #200 sieve	3.77

Level 3

Asphalt Binder: Superpave Binder Grading	PG 76-22

Figure 13-16: Mixture Type: III A2 (Columbia Surface Type A, Mix Design 2 with RAP)

Level 1

Asphalt Mix: Dynamic Modulus Table						
Temperature (°F)	Mixture |E*| (psi)					
	0.1 Hz	0.5 Hz	1 Hz	5 Hz	10 Hz	25 Hz
14	2162927	2549917	2684023	2925906	3004156	3088067
40	1144951	1661510	1878008	2325610	2487673	2671640
70	331448	643562	822375	1310242	1534258	1824922
100	79800	171139	237673	484340	635764	875578
130	26546	48853	66005	140120	195160	299190

Asphalt Binder: Superpave Binder Test Data		
Temperature (°F)	Angular freq. = 10 rad/sec	
	G* (Pa)	Delta (degree)
158.0	792.60	88.98
168.8	299.28	89.22
179.6	150.21	89.46

Asphalt General: Volumetric Properties as Built	
Effective Binder (%)	11.72
Air Voids (%)	6.57
Total unit weight	165.25

Level 2

Asphalt Mix: Aggregate Gradation	
Cumulative % Retained ¾" sieve	0
Cumulative % Retained ⅜" sieve	10
Cumulative % Retained #4 sieve	37
% Passing #200 sieve	4.85

Level 3

Asphalt Binder: Superpave Binder Grading	PG 76-22

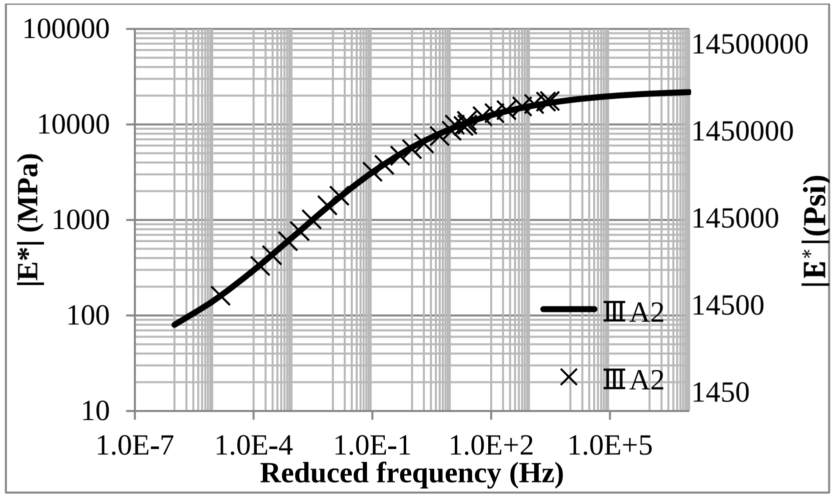

Master Dynamic Modulus Curves for Mixtures from Columbia Surface Type A, Mix Design 2 with RAP

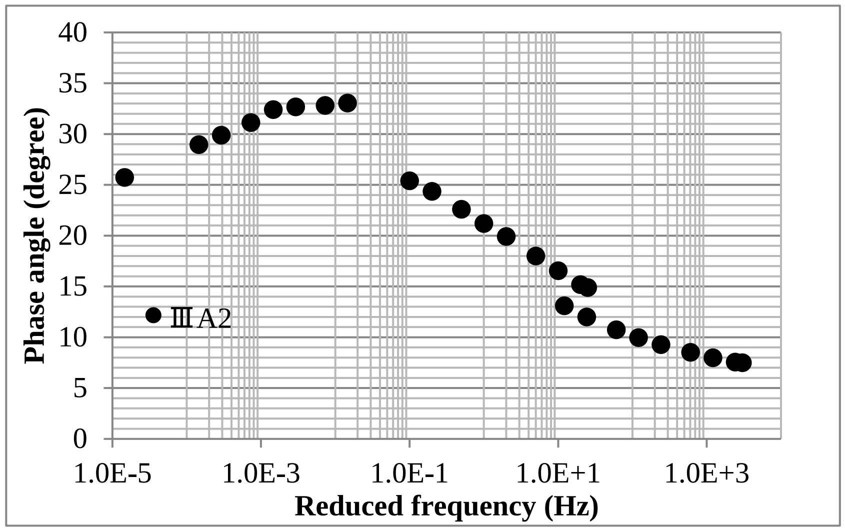

Master Phase Angle Curves for Mixtures from Columbia Surface Type A, Mix Design 2 with RAP

Figure 13-17: Mixture Type: III B1 (Columbia Surface Type B, Mix Design 1 with RAP)

Level 1

Asphalt Mix: Dynamic Modulus Table						
Temperature (°F)	Mixture |E*| (psi)					
	0.1 Hz	0.5 Hz	1 Hz	5 Hz	10 Hz	25 Hz
14	2076797	2469520	2608378	2863590	2947795	3039252
40	1123893	1624162	1834896	2274877	2436251	2621301
70	351580	671076	849780	1328170	1545191	1825740
100	87868	193255	268238	535799	694099	938443
130	27088	54511	75809	166822	232746	353763

Asphalt Binder: Superpave Binder Test Data		
Temperature (°F)	Angular freq. = 10 rad/sec	
	G* (Pa)	Delta (degree)
158.0	792.60	88.98
168.8	299.28	89.22
179.6	150.21	89.46

Asphalt General: Volumetric Properties as Built	
Effective Binder (%)	10.81
Air Voids (%)	6.21
Total unit weight	164.81

Level 2

Asphalt Mix: Aggregate Gradation	
Cumulative % Retained ¾" sieve	0
Cumulative % Retained ⅜" sieve	10
Cumulative % Retained #4 sieve	37
% Passing #200 sieve	4

Level 3

Asphalt Binder: Superpave Binder Grading	PG 64-22

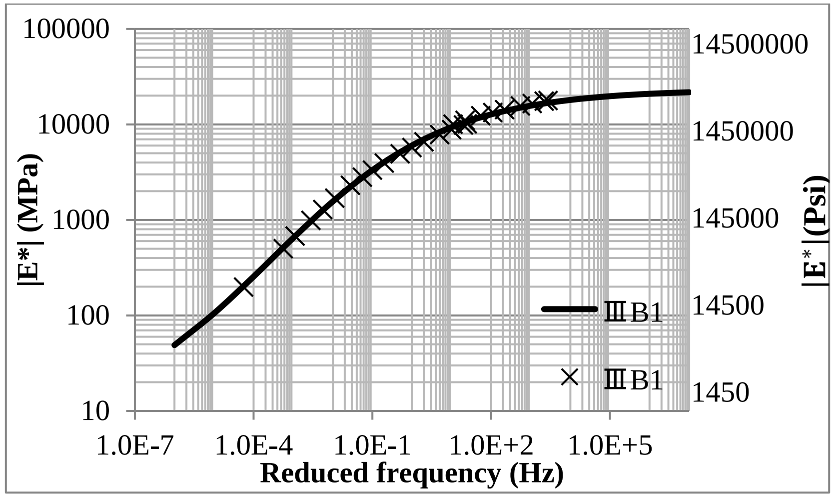

Master Dynamic Modulus Curves for Mixtures from Columbia Surface Type B, Mix Design 1 with RAP

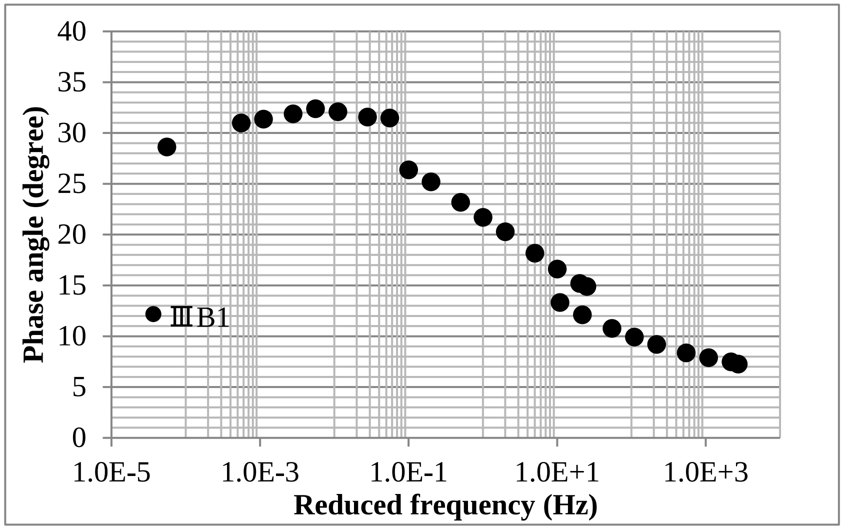

Master Phase Angle Curves for Mixtures from Columbia Surface Type B, Mix Design 1 with RAP

Figure 13-18: Mixture Type: III B2 (Columbia Surface Type B, Mix Design 2 with RAP)

Level 1

Asphalt Mix: Dynamic Modulus Table						
Temperature (°F)	Mixture |E*| (psi)					
	0.1 Hz	0.5 Hz	1 Hz	5 Hz	10 Hz	25 Hz
14	1924350	2358932	2515986	2808563	2906051	3012365
40	938570	1437613	1658320	2136168	2316575	2526441
70	254876	518958	677302	1131353	1349768	1642046
100	60133	133895	189044	400661	534992	753435
130	19473	37471	51581	114003	161338	252322

Asphalt Binder: Superpave Binder Test Data		
Temperature (°F)	Angular freq. = 10 rad/sec	
	G* (Pa)	Delta (degree)
158.0	792.60	88.98
168.8	299.28	89.22
179.6	150.21	89.46

Asphalt General: Volumetric Properties as Built	
Effective Binder (%)	11.53
Air Voids (%)	7.24
Total unit weight	164.81

Level 2

Asphalt Mix: Aggregate Gradation	
Cumulative % Retained ¾” sieve	0
Cumulative % Retained ⅜” sieve	10
Cumulative % Retained #4 sieve	37
% Passing #200 sieve	4

Level 3

Asphalt Binder: Superpave Binder Grading	PG 64-22

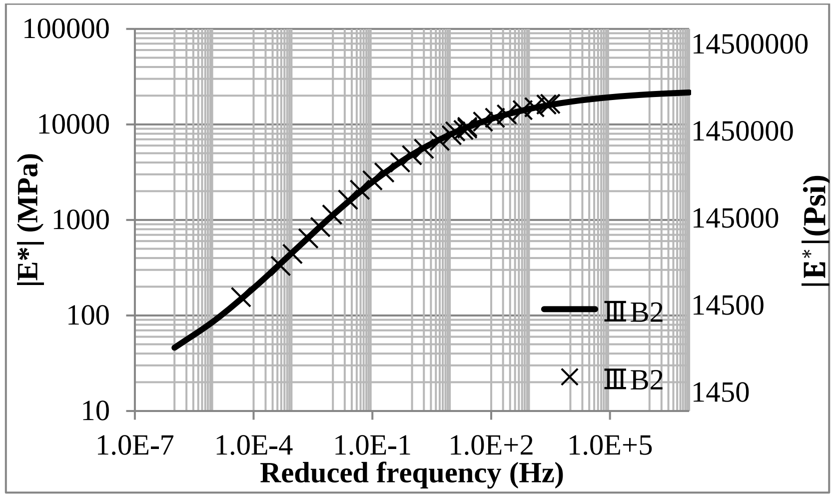

Master Dynamic Modulus Curves for Mixtures from Columbia Surface Type B, Mix Design 2 with RAP

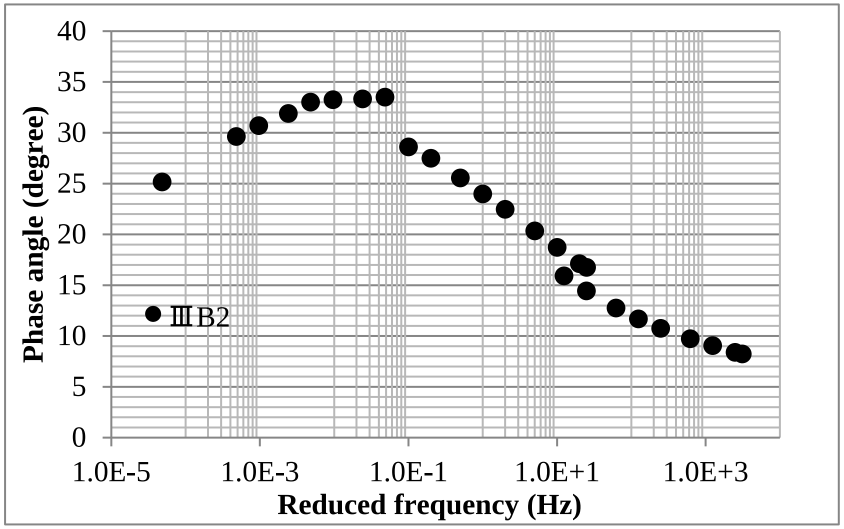

Master Phase Angle Curves for Mixtures from Columbia Surface Type B, Mix Design 2 with RAP

Figure 13-19: Mixture Type: III C (Columbia Surface Type C with RAP)

Level 1

Asphalt Mix: Dynamic Modulus Table						
Temperature (°F)	Mixture |E*| (psi)					
	0.1 Hz	0.5 Hz	1 Hz	5 Hz	10 Hz	25 Hz
14	1800240	2214545	2367631	2659552	2759344	2870076
40	908338	1369597	1573818	2020430	2191683	2393590
70	268848	530806	683014	1109316	1311660	1581717
100	65661	148164	207939	427236	560979	772874
130	19597	40929	57683	130293	183650	282979

Asphalt Binder: Superpave Binder Test Data		
Temperature (°F)	Angular freq. = 10 rad/sec	
	G* (Pa)	Delta (degree)
158.0	792.60	88.98
168.8	299.28	89.22
179.6	150.21	89.46

Asphalt General: Volumetric Properties as Built	
Effective Binder (%)	11.79
Air Voids (%)	7.13
Total unit weight	165.00

Level 2

Asphalt Mix: Aggregate Gradation	
Cumulative % Retained ¾" sieve	0
Cumulative % Retained ⅜" sieve	8
Cumulative % Retained #4 sieve	30
% Passing #200 sieve	5.46

Level 3

Asphalt Binder: Superpave Binder Grading	PG 64-22

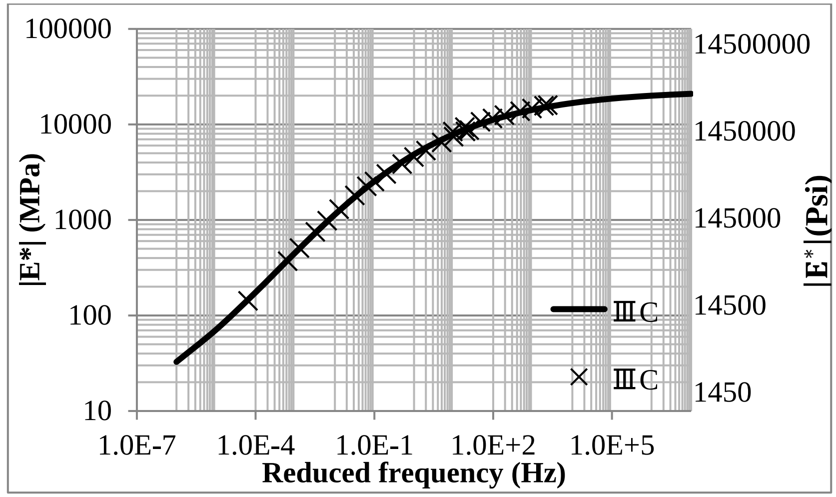

Master Dynamic Modulus Curves for Mixtures from Columbia Surface Type C with RAP

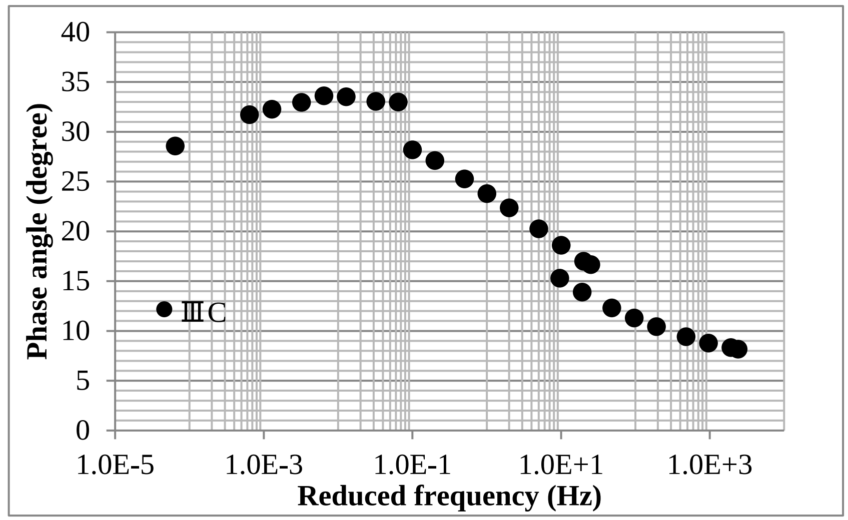

Master Phase Angle Curves for Mixtures from Columbia Surface Type C with RAP

Figure 13-20: Mixture Type: III CO (Columbia Surface Type C, no RAP)

Level 1

Asphalt Mix: Dynamic Modulus Table						
Temperature (°F)	Mixture |E*| (psi)					
	0.1 Hz	0.5 Hz	1 Hz	5 Hz	10 Hz	25 Hz
14	1518561	2004136	2192005	2560826	2689602	2833757
40	616020	1055207	1269071	1772054	1976289	2224128
70	135003	310443	426929	799213	996408	1277384
100	27365	67291	99591	236915	332681	499944
130	8002	16664	23836	58135	86138	143464

Asphalt Binder: Superpave Binder Test Data		
Temperature (°F)	Angular freq. = 10 rad/sec	
	G* (Pa)	Delta (degree)
158.0	792.60	88.98
168.8	299.28	89.22
179.6	150.21	89.46

Asphalt General: Volumetric Properties as Built	
Effective Binder (%)	11.53
Air Voids (%)	7.60
Total unit weight	165.00

Level 2

Asphalt Mix: Aggregate Gradation	
Cumulative % Retained ¾” sieve	0
Cumulative % Retained ⅜” sieve	8
Cumulative % Retained #4 sieve	30
% Passing #200 sieve	5.46

Level 3

Asphalt Binder: Superpave Binder Grading	PG 64-22

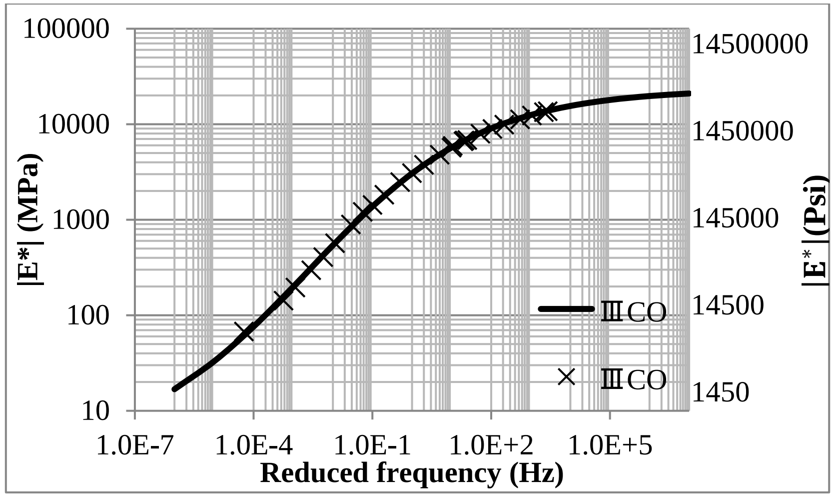

Master Dynamic Modulus Curves for Mixtures from Columbia Surface Type C, no RAP

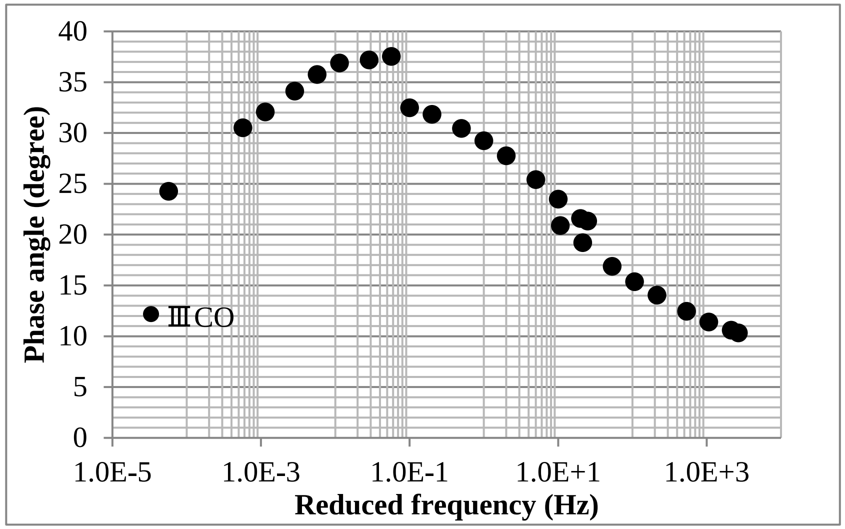

Master Phase Angle Curves for Mixtures from Columbia Surface Type C, no RAP

Figure 13-21: Mixture Type: III D (Columbia Surface Type D with RAP)

Level 1

Asphalt Mix: Dynamic Modulus Table						
Temperature	Mixture |E*| (psi)					
(°F)	0.1 Hz	0.5 Hz	1 Hz	5 Hz	10 Hz	25 Hz
14	1708787	2104078	2250141	2528438	2623439	2728727
40	857542	1295248	1489730	1915997	2079656	2272644
70	254270	499157	642087	1044702	1236793	1493937
100	64143	141008	196496	400429	525355	724169
130	20333	40664	56393	123824	173159	265030

Asphalt Binder: Superpave Binder Test Data		
Temperature	Angular freq. = 10 rad/sec	
(°F)	G* (Pa)	Delta (degree)
158.0	792.60	88.98
168.8	299.28	89.22
179.6	150.21	89.46

Asphalt General: Volumetric Properties as Built	
Effective Binder (%)	11.94
Air Voids (%)	5.10
Total unit weight	165.06

Level 2

Asphalt Mix: Aggregate Gradation	
Cumulative % Retained ¾” sieve	0
Cumulative % Retained ⅜” sieve	7
Cumulative % Retained #4 sieve	14
% Passing #200 sieve	6.25

Level 3

Asphalt Binder: Superpave Binder Grading	PG 64-22

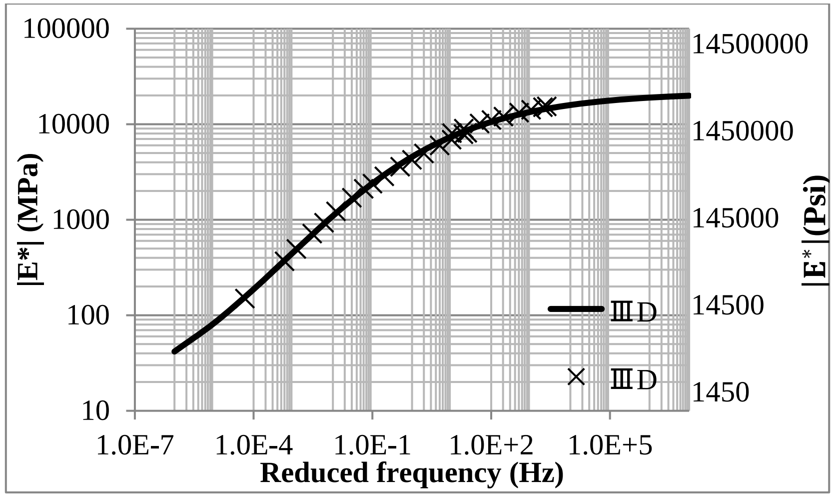

Master Dynamic Modulus Curves for Mixtures from Columbia Surface Type D with RAP

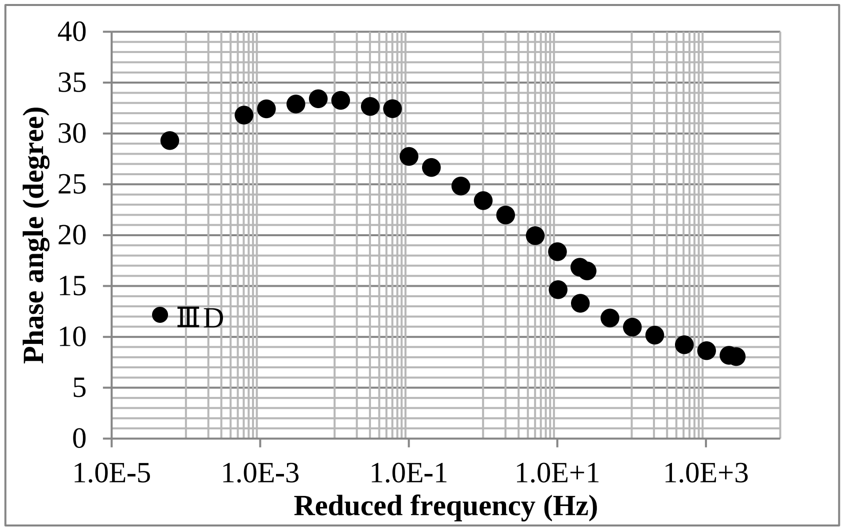

Master Phase Angle Curves for Mixtures from Columbia Surface Type D with RAP

Figure 13-22: Mixture Type: III DO (Columbia Surface Type D, no RAP)

Level 1

Asphalt Mix: Dynamic Modulus Table						
Temperature (°F)	Mixture |E*| (psi)					
	0.1 Hz	0.5 Hz	1 Hz	5 Hz	10 Hz	25 Hz
14	1628170	2093170	2270424	2615457	2735281	2869201
40	696829	1144845	1357190	1847026	2043156	2279675
70	162098	354889	478536	861352	1059288	1337634
100	34046	80293	116520	264948	365455	537678
130	10122	20439	28760	67203	97676	158693

Asphalt Binder: Superpave Binder Test Data		
Temperature (°F)	Angular freq. = 10 rad/sec	
	G* (Pa)	Delta (degree)
158.0	792.60	88.98
168.8	299.28	89.22
179.6	150.21	89.46

Asphalt General: Volumetric Properties as Built	
Effective Binder (%)	11.53
Air Voids (%)	7.98
Total unit weight	165.06

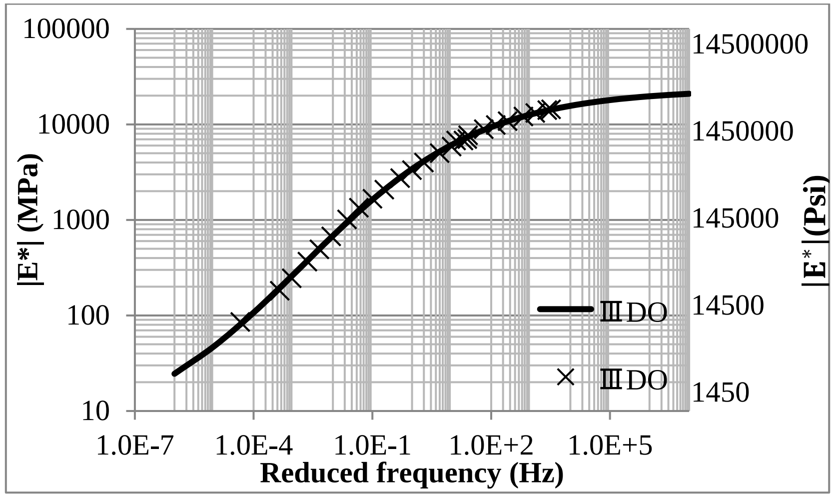

Master Dynamic Modulus Curves for Mixtures from Columbia Surface Type D, no RAP

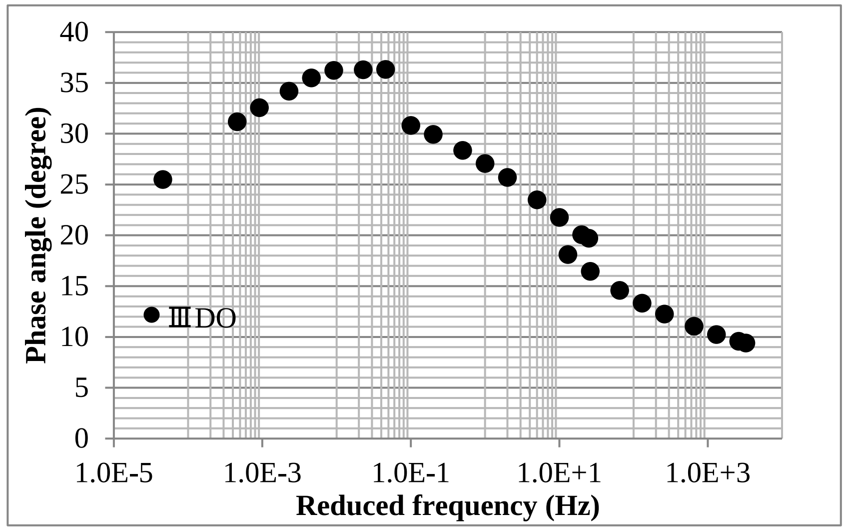

Master Phase Angle Curves for Mixtures from Columbia Surface Type D, no RAP

Level 2

Asphalt Mix: Aggregate Gradation	
Cumulative % Retained ¾” sieve	0
Cumulative % Retained ⅜” sieve	7
Cumulative % Retained #4 sieve	14
% Passing #200 sieve	6.25

Level 3

Asphalt Binder: Superpave Binder Grading	PG 64-22

Figure 13-23: Mixture Type: III E (Columbia Surface Type E with RAP)

Level 1

Asphalt Mix: Dynamic Modulus Table						
Temperature (°F)	Mixture |E*| (psi)					
	0.1 Hz	0.5 Hz	1 Hz	5 Hz	10 Hz	25 Hz
14	1638399	2016277	2159551	2440385	2539316	2651370
40	823997	1225627	1406093	1810075	1969406	2161307
70	250672	475311	604523	968363	1143739	1381828
100	63977	136877	187985	371210	482001	658107
130	19546	39256	54148	116006	160104	240942

Asphalt Binder: Superpave Binder Test Data		
Temperature (°F)	Angular freq. = 10 rad/sec	
	G* (Pa)	Delta (degree)
158.0	792.60	88.98
168.8	299.28	89.22
179.6	150.21	89.46

Asphalt General: Volumetric Properties as Built	
Effective Binder (%)	11.94
Air Voids (%)	7.91
Total unit weight	165.06

Level 2

Asphalt Mix: Aggregate Gradation	
Cumulative % Retained ¾” sieve	0
Cumulative % Retained ⅜” sieve	0
Cumulative % Retained #4 sieve	5
% Passing #200 sieve	7.8

Level 3

Asphalt Binder: Superpave Binder Grading	PG 64-22

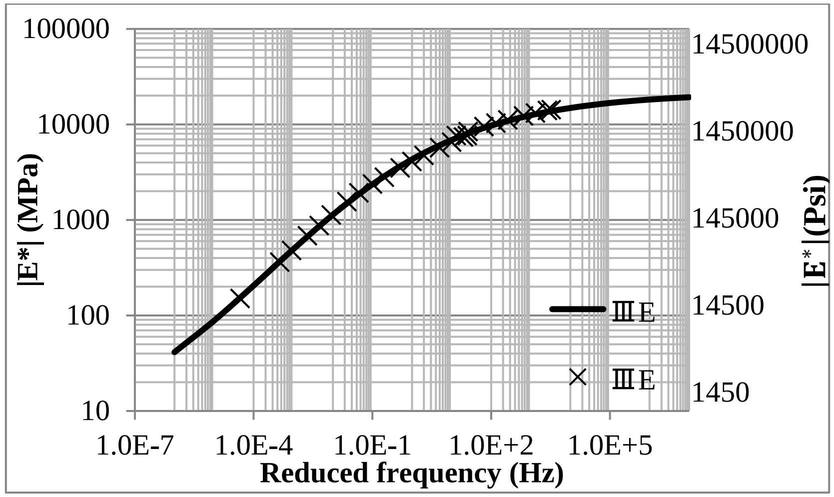

Master Dynamic Modulus Curves for Mixtures from Columbia Surface Type E with RAP

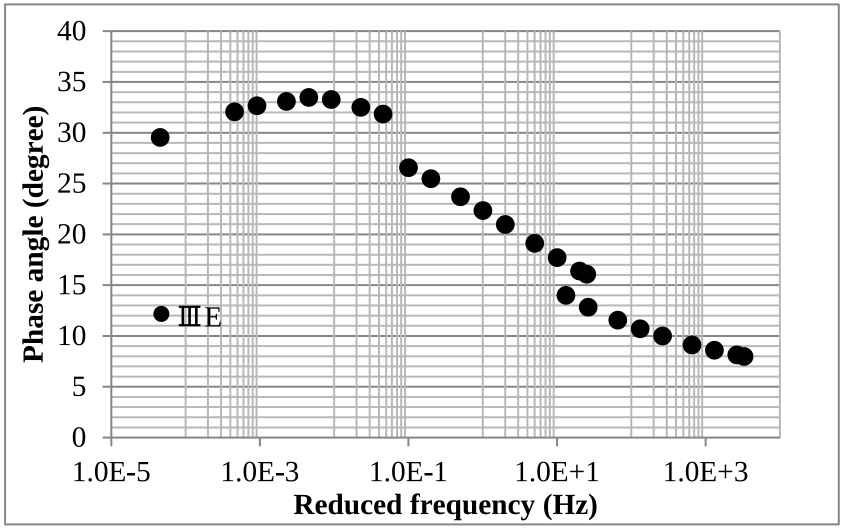

Master Phase Angle Curves for Mixtures from Columbia Surface Type E with RAP

Figure 13-24: Mixture Type: III EO (Columbia Surface Type E, no RAP)

Level 1

Asphalt Mix: Dynamic Modulus Table						
Temperature (°F)	Mixture |E*| (psi)					
	0.1 Hz	0.5 Hz	1 Hz	5 Hz	10 Hz	25 Hz
14	1384803	1824068	2001382	2366739	2501318	2657689
40	586840	961878	1145710	1590165	1777870	2013365
70	147400	308289	409781	725337	891723	1131467
100	33544	76426	108598	234926	318264	459911
130	9830	20324	28551	64833	92373	145769

Asphalt Binder: Superpave Binder Test Data		
Temperature (°F)	Angular freq. = 10 rad/sec	
	G* (Pa)	Delta (degree)
158.0	792.60	88.98
168.8	299.28	89.22
179.6	150.21	89.46

Asphalt General: Volumetric Properties as Built	
Effective Binder (%)	12.34
Air Voids (%)	9.40
Total unit weight	165.06

Level 2

Asphalt Mix: Aggregate Gradation	
Cumulative % Retained ¾" sieve	0
Cumulative % Retained ⅜" sieve	0
Cumulative % Retained #4 sieve	5
% Passing #200 sieve	7.8

Level 3

Asphalt Binder: Superpave Binder Grading	PG 64-22

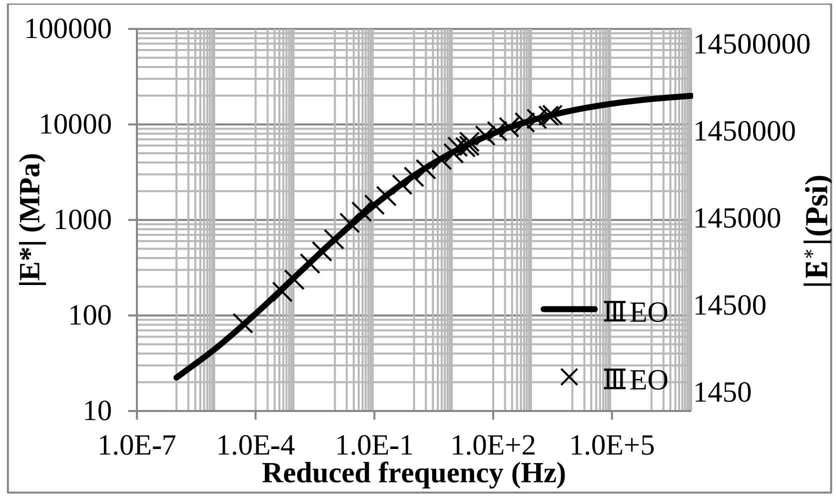

Master Dynamic Modulus Curves for Mixtures from Columbia Surface Type E, no RAP

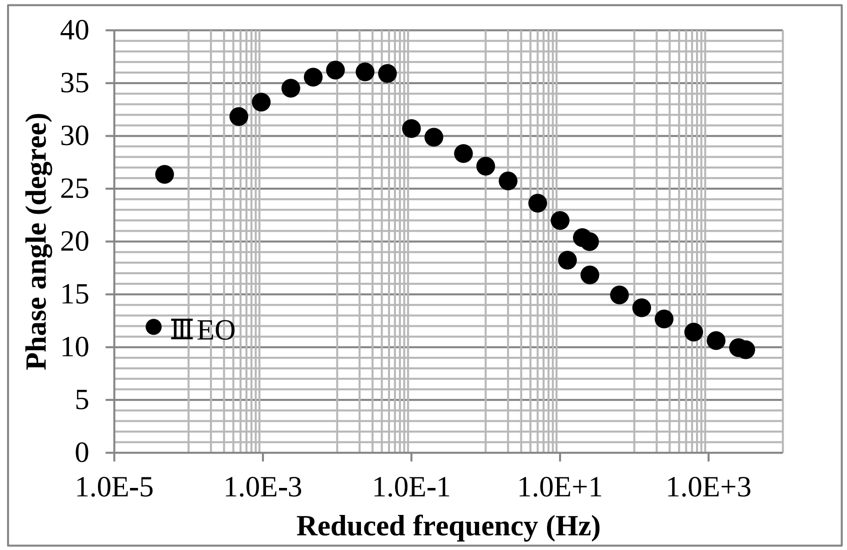

Master Phase Angle Curves for Mixtures from Columbia Surface Type E, no RAP

Figure 13-25: Mixture Type: IV A (Jefferson Surface Type A with RAP)

Level 1

Asphalt Mix: Dynamic Modulus Table						
Temperature (°F)	Mixture |E*| (psi)					
	0.1 Hz	0.5 Hz	1 Hz	5 Hz	10 Hz	25 Hz
14	2481673	2834189	2944498	3125745	3178872	3232362
40	1385279	1984186	2215768	2651869	2794259	2944903
70	386081	783240	1011634	1611178	1869096	2183965
100	92771	198627	279997	596041	793428	1102572
130	36295	60439	79539	166488	234438	367561

Asphalt Binder: Superpave Binder Test Data		
Temperature (°F)	Angular freq. = 10 rad/sec	
	G* (Pa)	Delta (degree)
158.0	2995.00	63.70
168.8	1501.00	61.90
179.6	750.50	60.00

Asphalt General: Volumetric Properties as Built	
Effective Binder (%)	10.90
Air Voids (%)	5.91
Total unit weight	165.31

Level 2

Asphalt Mix: Aggregate Gradation	
Cumulative % Retained ¾” sieve	3
Cumulative % Retained ⅜” sieve	14
Cumulative % Retained #4 sieve	48
% Passing #200 sieve	4.26

Level 3

Asphalt Binder: Superpave Binder Grading	PG 76-22

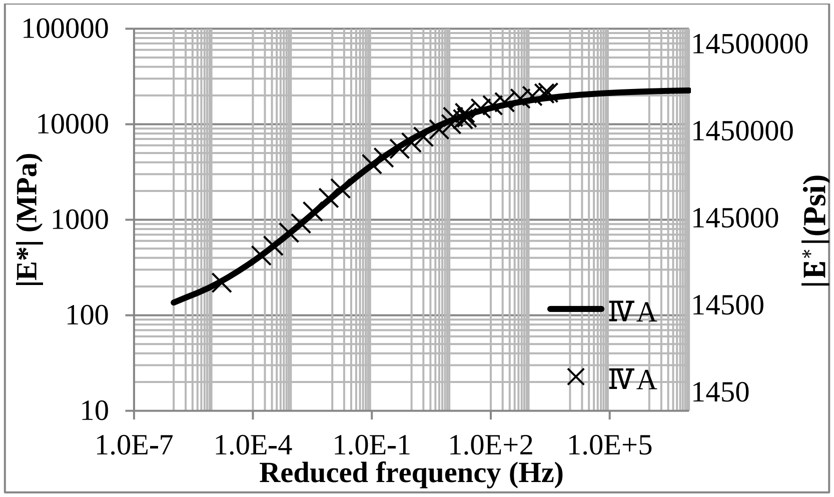

Master Dynamic Modulus Curves for Mixtures from Jefferson Surface Type A with RAP

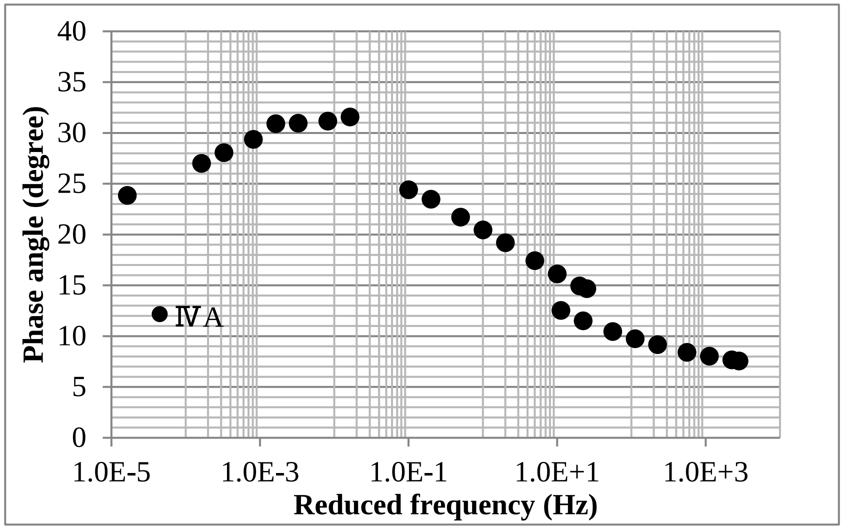

Master Phase Angle Curves for Mixtures from Jefferson Surface Type A with RAP

Figure 13-26: Mixture Type: IV AG (Jefferson Surface Type A with Long-Term Aging and RAP)

Level 1

Asphalt Mix: Dynamic Modulus Table

Temperature (°F)	Mixture |E*| (psi)					
	0.1 Hz	0.5 Hz	1 Hz	5 Hz	10 Hz	25 Hz
14	2405905	2757871	2872529	3068445	3128411	3190526
40	1349326	1907837	2128441	2557529	2703335	2862126
70	391891	767900	979223	1532847	1774410	2075141
100	91596	198850	278599	576856	758623	1041333
130	31608	56384	75800	162042	227551	352880

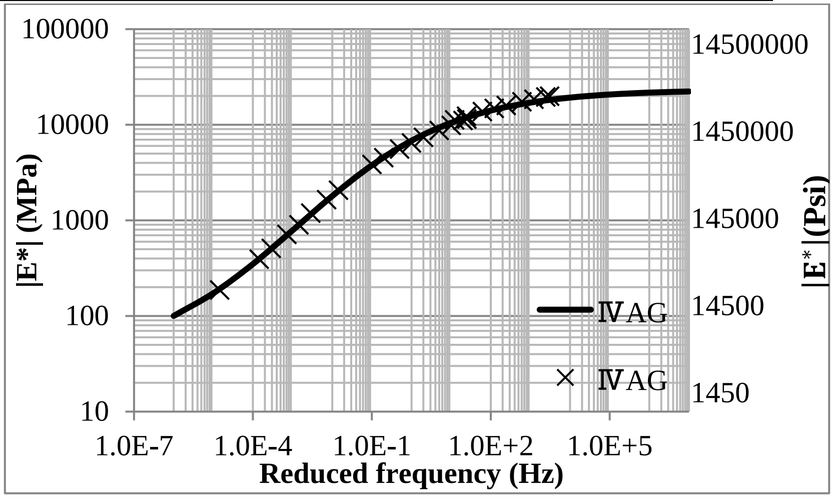

Master Dynamic Modulus Curves for Mixtures from Jefferson Surface Type A with Long-Term Aging and RAP

Asphalt Binder: Superpave Binder Test Data

Temperature (°F)	Angular freq. = 10 rad/sec	
	G* (Pa)	Delta (degree)
158.0	2995.00	63.70
168.8	1501.00	61.90
179.6	750.50	60.00

Asphalt General: Volumetric Properties as Built

Effective Binder (%)	10.90
Air Voids (%)	6.47
Total unit weight	165.31

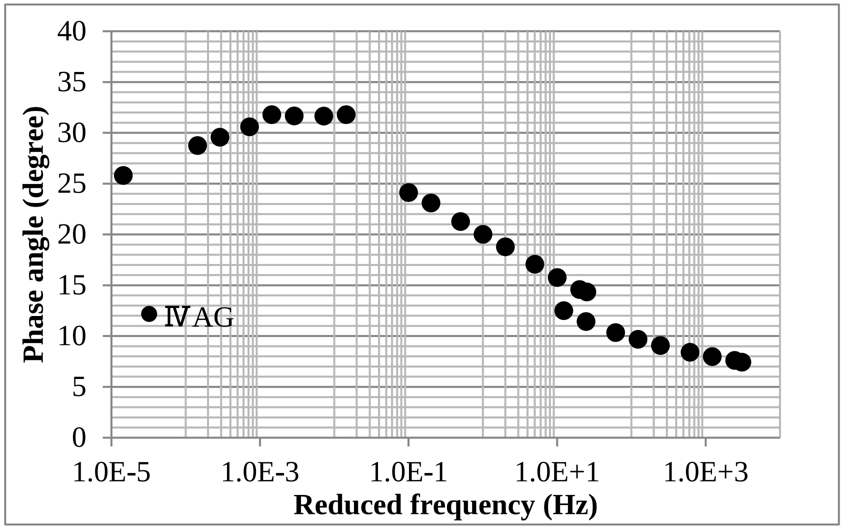

Master Phase Angle Curves for Mixtures from Jefferson Surface Type A with Long-Term Aging and RAP

Level 2

Asphalt Mix: Aggregate Gradation

Cumulative % Retained ¾" sieve	3
Cumulative % Retained ⅜" sieve	14
Cumulative % Retained #4 sieve	48
% Passing #200 sieve	4.26

Level 3

Asphalt Binder: Superpave Binder Grading	PG 76-22

Figure 13-27: Mixture Type: IV AN (Jefferson Surface Type A with Asphalt Source 2 and RAP)

Level 1

Asphalt Mix: Dynamic Modulus Table						
Temperature (°F)	Mixture |E*| (psi)					
	0.1 Hz	0.5 Hz	1 Hz	5 Hz	10 Hz	25 Hz
14	2178293	2626389	2773194	3021276	3095632	3171265
40	1027534	1637923	1896920	2418011	2597429	2792184
70	234841	531549	722714	1285559	1552472	1897104
100	53626	118975	172607	403319	562510	831519
130	21533	35863	47451	102770	148521	243432

Asphalt Binder: Superpave Binder Test Data		
Temperature (°F)	Angular freq. = 10 rad/sec	
	G* (Pa)	Delta (degree)
158.0	2995.00	63.70
168.8	1501.00	61.90
179.6	750.50	60.00

Asphalt General: Volumetric Properties as Built	
Effective Binder (%)	11.39
Air Voids (%)	5.46
Total unit weight	165.31

Level 2

Asphalt Mix: Aggregate Gradation	
Cumulative % Retained ¾” sieve	0
Cumulative % Retained ⅜” sieve	12
Cumulative % Retained #4 sieve	42
% Passing #200 sieve	4.44

Level 3

Asphalt Binder: Superpave Binder Grading	PG 76-22

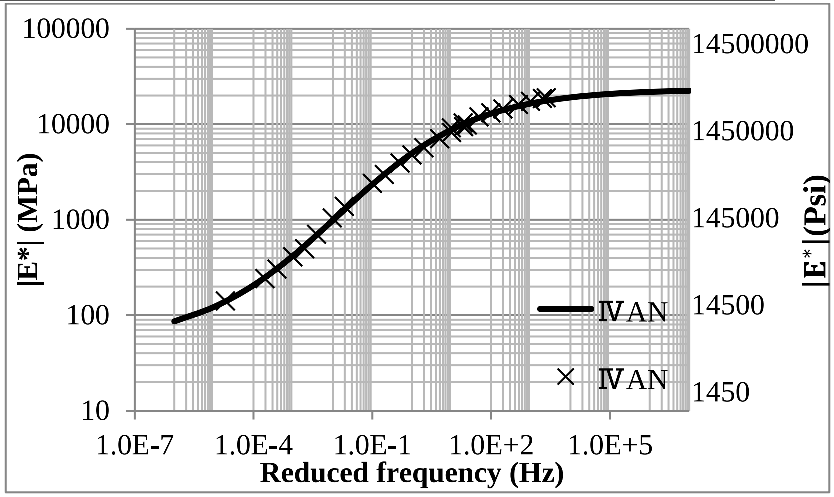

Master Dynamic Modulus Curves for Mixtures from Jefferson Surface Type A with Asphalt Source 2 and RAP

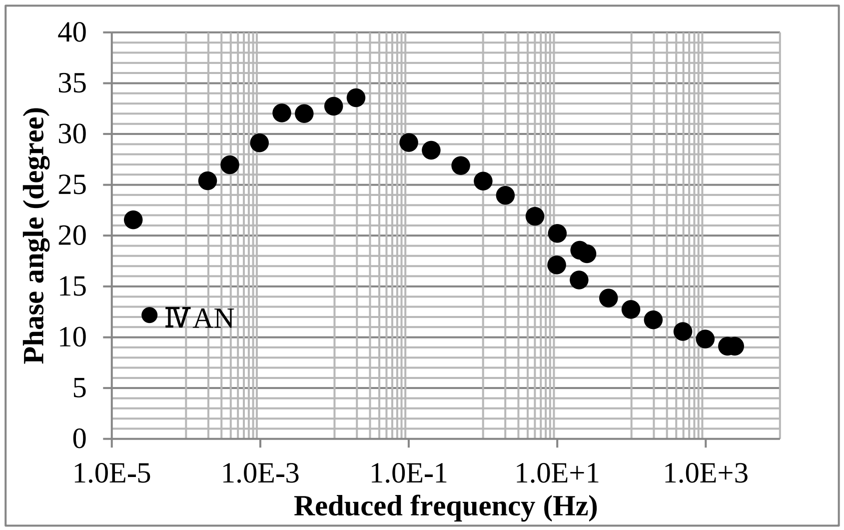

Master Phase Angle Curves for Mixtures from Jefferson Surface Type A with Asphalt Source 2 and RAP

Figure 13-28: Mixture Type: IV AO (Jefferson Surface Type A, no RAP)

Level 1

Asphalt Mix: Dynamic Modulus Table						
Temperature (°F)	Mixture |E*| (psi)					
	0.1 Hz	0.5 Hz	1 Hz	5 Hz	10 Hz	25 Hz
14	1727731	2219492	2400263	2737948	2849912	2971099
40	725268	1220983	1454748	1981844	2185959	2425230
70	163062	366586	501460	927319	1148189	1455907
100	37185	83541	120655	278430	388638	580781
130	13478	24197	32725	72289	104179	169361

Asphalt Binder: Superpave Binder Test Data		
Temperature (°F)	Angular freq. = 10 rad/sec	
	G* (Pa)	Delta (degree)
158.0	2995.00	63.70
168.8	1501.00	61.90
179.6	750.50	60.00

Asphalt General: Volumetric Properties as Built	
Effective Binder (%)	11.39
Air Voids (%)	5.46
Total unit weight	164.06

Level 2

Asphalt Mix: Aggregate Gradation	
Cumulative % Retained ¾" sieve	0
Cumulative % Retained ⅜" sieve	12
Cumulative % Retained #4 sieve	42
% Passing #200 sieve	44.4

Level 3

Asphalt Binder: Superpave Binder Grading	PG 76-22

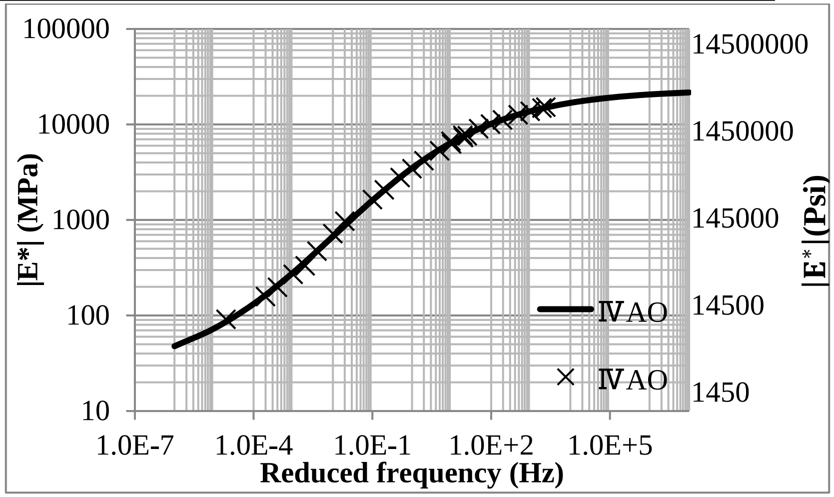

Master Dynamic Modulus Curves for Mixtures from Jefferson Surface Type A, no RAP

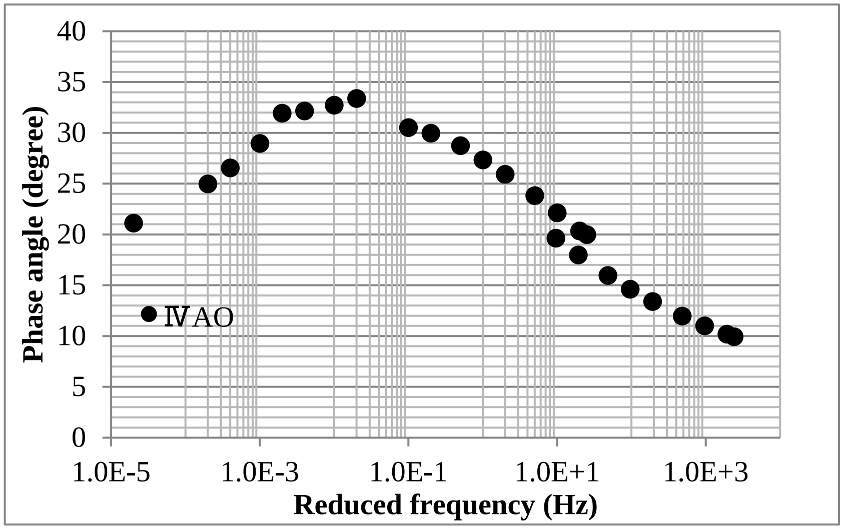

Master Phase Angle Curves for Mixtures from Jefferson Surface Type A, no RAP

Figure 13-29: Mixture Type: IV AOG (Jefferson Surface Type A with Long-Term Aging, no RAP)

Level 1

Asphalt Mix: Dynamic Modulus Table						
Temperature (°F)	Mixture |E*| (psi)					
	0.1 Hz	0.5 Hz	1 Hz	5 Hz	10 Hz	25 Hz
14	2212665	2628198	2766481	3005222	3078716	3154910
40	1089909	1667752	1910097	2400527	2572104	2761287
70	261520	564997	752356	1288487	1539789	1865102
100	56648	126913	182752	412694	566057	820683
130	20338	35442	47529	103886	149265	241215

Asphalt Binder: Superpave Binder Test Data		
Temperature (°F)	Angular freq. = 10 rad/sec	
	G* (Pa)	Delta (degree)
158.0	2995.00	63.70
168.8	1501.00	61.90
179.6	750.50	60.00

Asphalt General: Volumetric Properties as Built	
Effective Binder (%)	11.39
Air Voids (%)	7.26
Total unit weight	164.06

Level 2

Asphalt Mix: Aggregate Gradation	
Cumulative % Retained ¾” sieve	0
Cumulative % Retained ⅜” sieve	12
Cumulative % Retained #4 sieve	42
% Passing #200 sieve	44.4

Level 3

Asphalt Binder: Superpave Binder Grading	PG 76-22

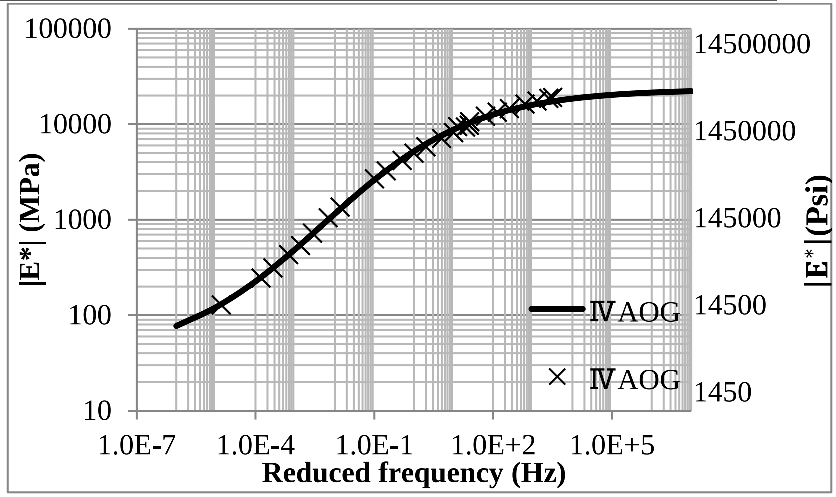

Master Dynamic Modulus Curves for Mixtures from Jefferson Surface Type A with Long-Term Aging, no RAP

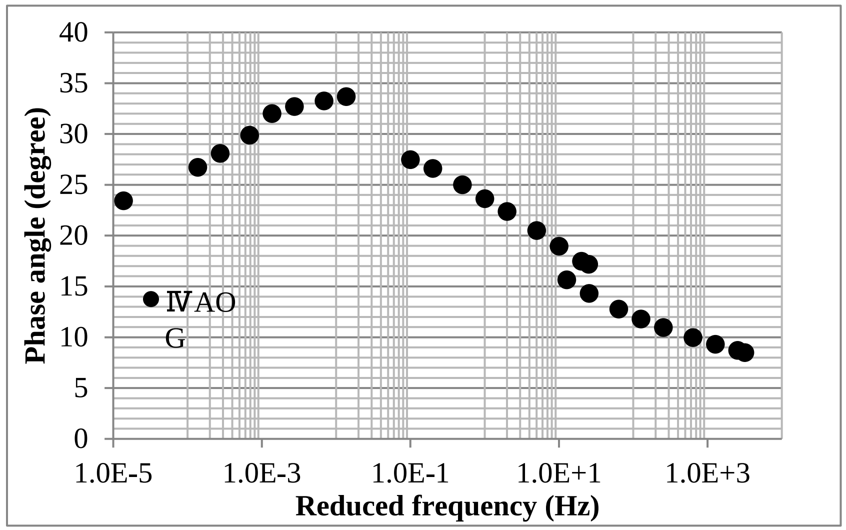

Master Phase Angle Curves for Mixtures from Jefferson Surface Type A with Long-Term Aging, no RAP

Figure 13-30: Mixture Type: IV AON (Jefferson Surface Type A with Asphalt Source 2, no RAP)

Level 1

Asphalt Mix: Dynamic Modulus Table						
Temperature (°F)	Mixture |E*| (psi)					
	0.1 Hz	0.5 Hz	1 Hz	5 Hz	10 Hz	25 Hz
14	2409944	2783250	2901791	3098833	3157256	3216482
40	1286418	1889614	2128114	2585555	2737494	2899852
70	328281	696808	915204	1505591	1766333	2089908
100	70887	160415	231428	517670	702316	998294
130	25444	44362	59697	131942	190201	307293

Asphalt Binder: Superpave Binder Test Data		
Temperature (°F)	Angular freq. = 10 rad/sec	
	G* (Pa)	Delta (degree)
158.0	2995.00	63.70
168.8	1501.00	61.90
179.6	750.50	60.00

Asphalt General: Volumetric Properties as Built	
Effective Binder (%)	11.39
Air Voids (%)	5.70
Total unit weight	164.06

Level 2

Asphalt Mix: Aggregate Gradation	
Cumulative % Retained ¾” sieve	0
Cumulative % Retained ⅜” sieve	12
Cumulative % Retained #4 sieve	42
% Passing #200 sieve	44.4

Level 3

Asphalt Binder: Superpave Binder Grading	PG 76-22

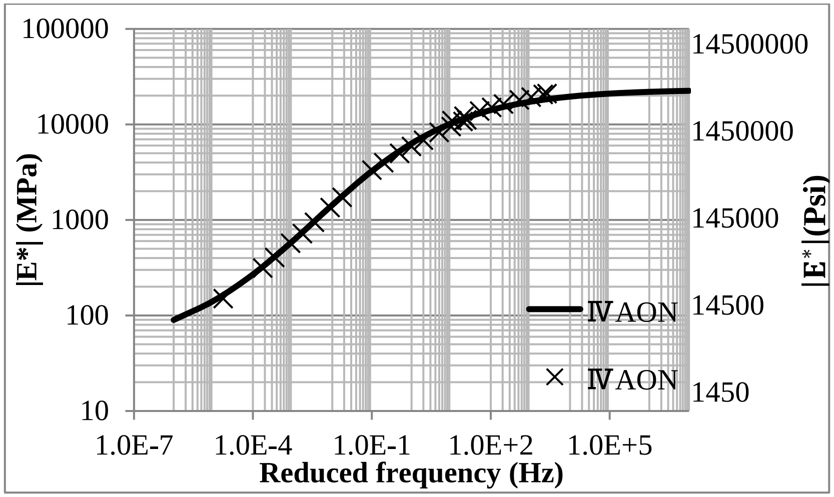

Master Dynamic Modulus Curves for Mixtures from Jefferson Surface Type A with Asphalt Source 2, no RAP

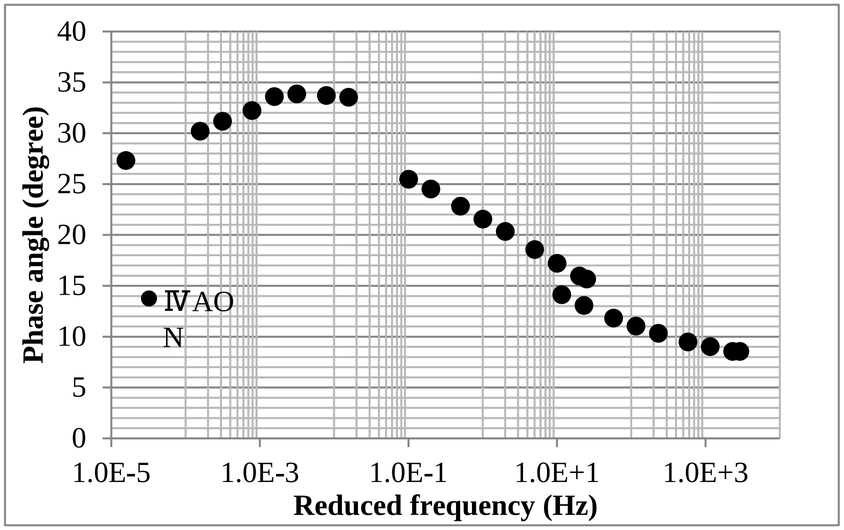

Master phase Angle Curves for Mixtures from Jefferson Surface Type A with Asphalt Source 2, no RAP

Figure 13-31: Mixture Type: IV B (Jefferson Surface Type B with RAP)

Level 1

Asphalt Mix: Dynamic Modulus Table						
Temperature	Mixture |E*| (psi)					
(°F)	0.1 Hz	0.5 Hz	1 Hz	5 Hz	10 Hz	25 Hz
14	2146965	2547658	2682245	2916927	2989991	3066322
40	1093618	1646082	1876354	2342494	2506242	2687647
70	283642	596282	783508	1305211	1545187	1853339
100	62921	143037	205308	452183	610891	867447
130	21321	39211	53593	120006	172420	276029

Asphalt Binder: Superpave Binder Test Data		
Temperature	Angular freq. = 10 rad/sec	
(°F)	G* (Pa)	Delta (degree)
158.0	792.60	88.98
168.8	299.28	89.22
179.6	150.21	89.46

Asphalt General: Volumetric Properties as Built	
Effective Binder (%)	11.73
Air Voids (%)	5.89
Total unit weight	164.69

Level 2

Asphalt Mix: Aggregate Gradation	
Cumulative % Retained ¾" sieve	0
Cumulative % Retained ⅜" sieve	7
Cumulative % Retained #4 sieve	32
% Passing #200 sieve	5.88

Level 3

Asphalt Binder: Superpave Binder Grading	PG 64-22

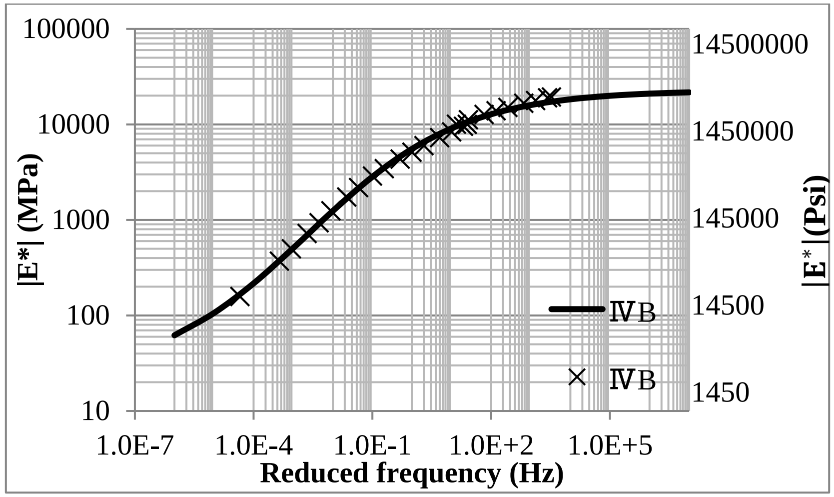

Master Dynamic Modulus Curves for Mixtures from Jefferson Surface Type B with RAP

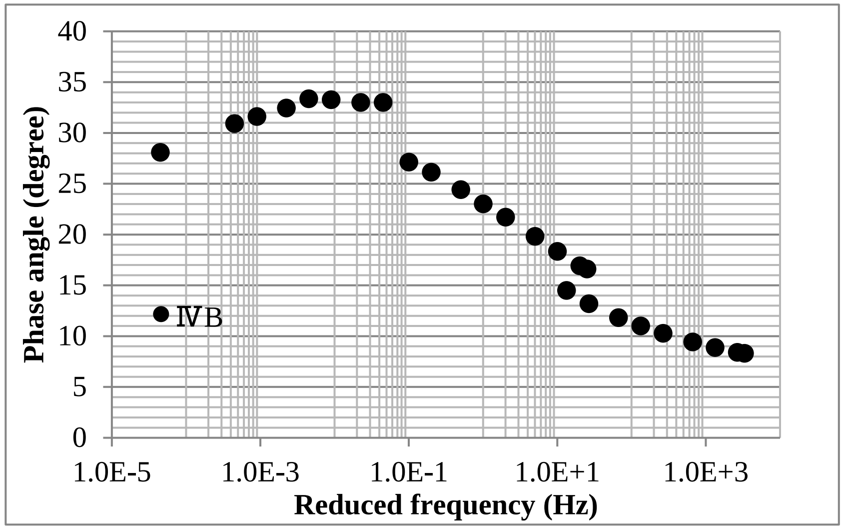

Master Phase Angle Curves for Mixtures from Jefferson Surface Type B with RAP

Figure 13-32: Mixture Type: IV BG (Jefferson Surface Type B with Long-Term Aging and RAP)

Level 1

Asphalt Mix: Dynamic Modulus Table						
Temperature (°F)	Mixture |E*| (psi)					
	0.1 Hz	0.5 Hz	1 Hz	5 Hz	10 Hz	25 Hz
14	2302663	2668739	2787638	2989643	3050996	3114179
40	1215022	1783440	2011636	2458304	2610268	2775429
70	305060	645728	847254	1396590	1642973	1953368
100	61807	143523	208095	467376	634808	904842
130	20092	36731	50284	114246	165787	269334

Asphalt Binder: Superpave Binder Test Data		
Temperature (°F)	Angular freq. = 10 rad/sec	
	G* (Pa)	Delta (degree)
158.0	792.60	88.98
168.8	299.28	89.22
179.6	150.21	89.46

Asphalt General: Volumetric Properties as Built	
Effective Binder (%)	11.73
Air Voids (%)	6.47
Total unit weight	165.63

Level 2

Asphalt Mix: Aggregate Gradation	
Cumulative % Retained ¾” sieve	0
Cumulative % Retained ⅜” sieve	7
Cumulative % Retained #4 sieve	32
% Passing #200 sieve	5.88

Level 3

Asphalt Binder: Superpave Binder Grading	PG 64-22

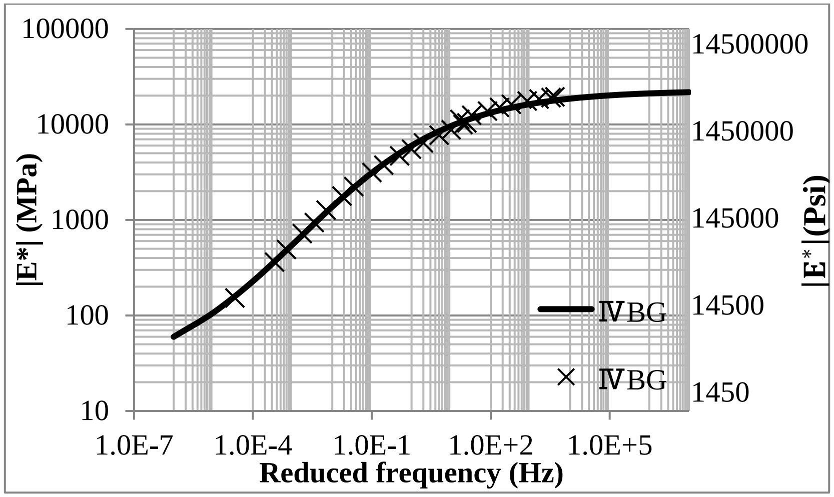

Master Dynamic Modulus Curves for Mixtures from Jefferson Surface Type B with Long-Term Aging and RAP

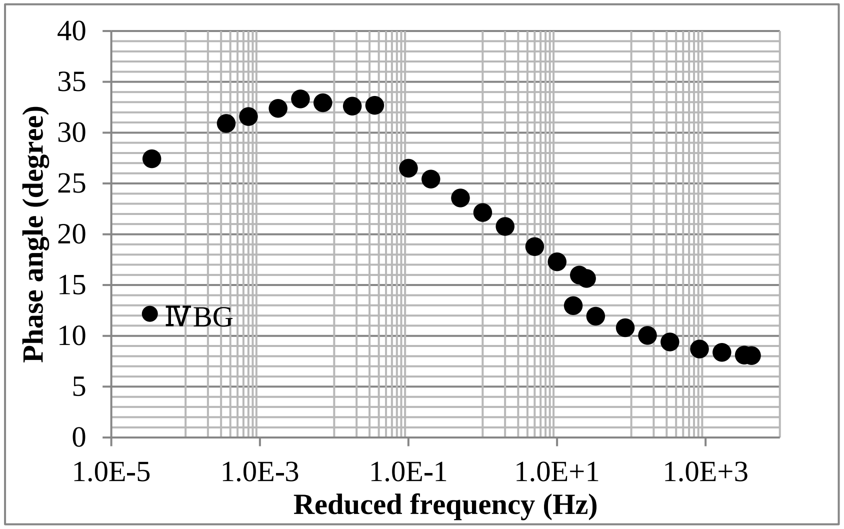

Master Phase Angle Curves for Mixtures from Jefferson Surface Type B with Long-Term Aging and RAP

Figure 13-33: Mixture Type: IV BN (Jefferson Surface Type B with Asphalt Source 2 and RAP)

Level 1

Asphalt Mix: Dynamic Modulus Table						
Temperature (°F)	Mixture |E*| (psi)					
	0.1 Hz	0.5 Hz	1 Hz	5 Hz	10 Hz	25 Hz
14	1914517	2362047	2519853	2805770	2898076	2996567
40	893696	1419079	1651561	2147939	2331220	2540402
70	216815	474830	636482	1112280	1343240	1651079
100	46981	110073	160076	364652	500756	727548
130	15342	29409	40858	94591	137672	224140

Asphalt Binder: Superpave Binder Test Data		
Temperature (°F)	Angular freq. = 10 rad/sec	
	G* (Pa)	Delta (degree)
158.0	792.60	88.98
168.8	299.28	89.22
179.6	150.21	89.46

Asphalt General: Volumetric Properties as Built	
Effective Binder (%)	11.73
Air Voids (%)	6.91
Total unit weight	164.69

Level 2

Asphalt Mix: Aggregate Gradation	
Cumulative % Retained ¾” sieve	0
Cumulative % Retained ⅜” sieve	7
Cumulative % Retained #4 sieve	32
% Passing #200 sieve	5.88

Level 3

Asphalt Binder: Superpave Binder Grading	PG 64-22

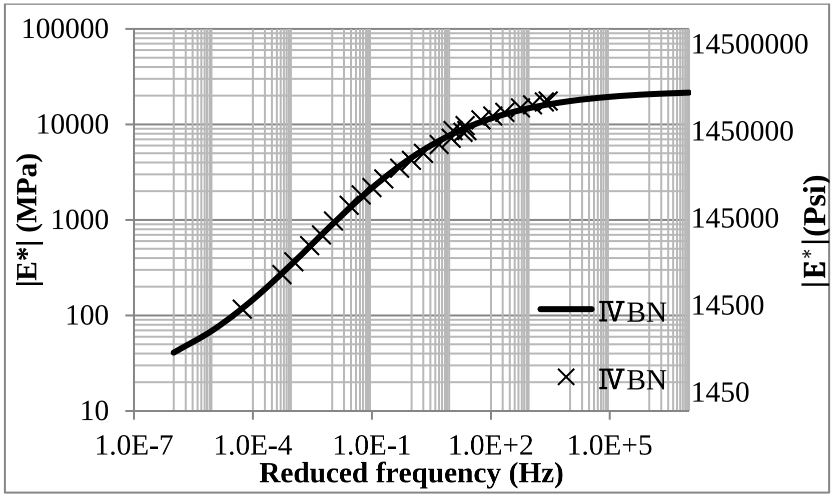

Master Dynamic Modulus Curves for Mixtures from Jefferson Surface Type B with Asphalt Source 2 and RAP

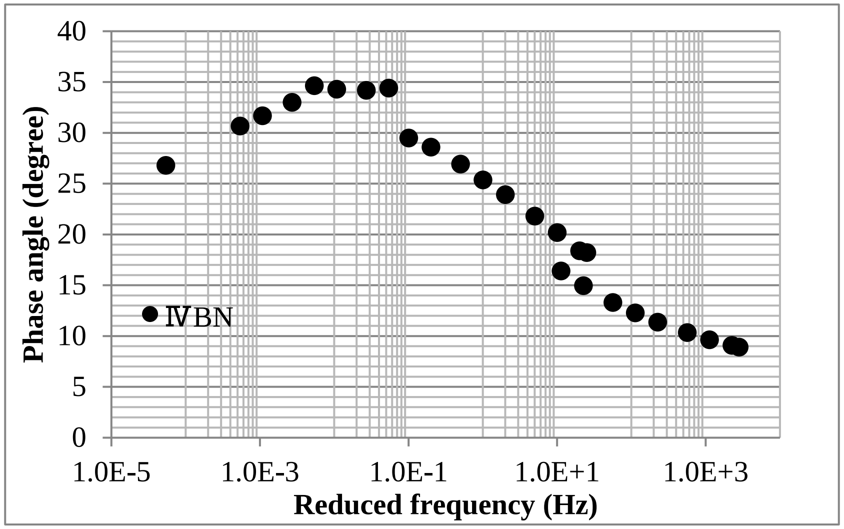

Master Phase Angle Curves for Mixtures from Jefferson Surface Type B with Asphalt Source 2 and RAP

Figure 13-34: Mixture Type: IV BO (Jefferson Surface Type B, no RAP)

Level 1

Asphalt Mix: Dynamic Modulus Table						
Temperature (°F)	Mixture |E*| (psi)					
	0.1 Hz	0.5 Hz	1 Hz	5 Hz	10 Hz	25 Hz
14	1858233	2309965	2471368	2767345	2864087	2968125
40	836405	1347214	1577088	2076236	2263662	2479907
70	190676	426048	576239	1028361	1252777	1556703
100	38744	92511	135721	316329	439176	647792
130	12061	23446	32777	77136	113229	186776

Asphalt Binder: Superpave Binder Test Data		
Temperature (°F)	Angular freq. = 10 rad/sec	
	G* (Pa)	Delta (degree)
158.0	792.60	88.98
168.8	299.28	89.22
179.6	150.21	89.46

Asphalt General: Volumetric Properties as Built	
Effective Binder (%)	11.51
Air Voids (%)	7.04
Total unit weight	164.69

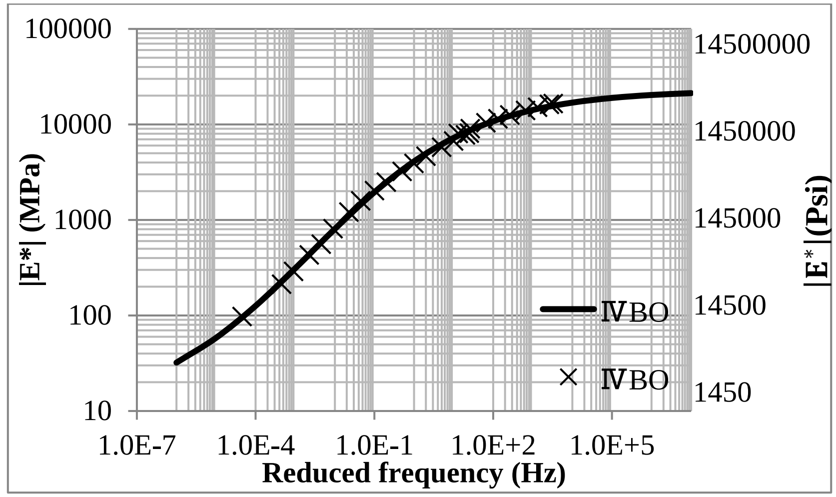

Master Dynamic Modulus Curves for Mixtures from Jefferson Surface Type B, no RAP

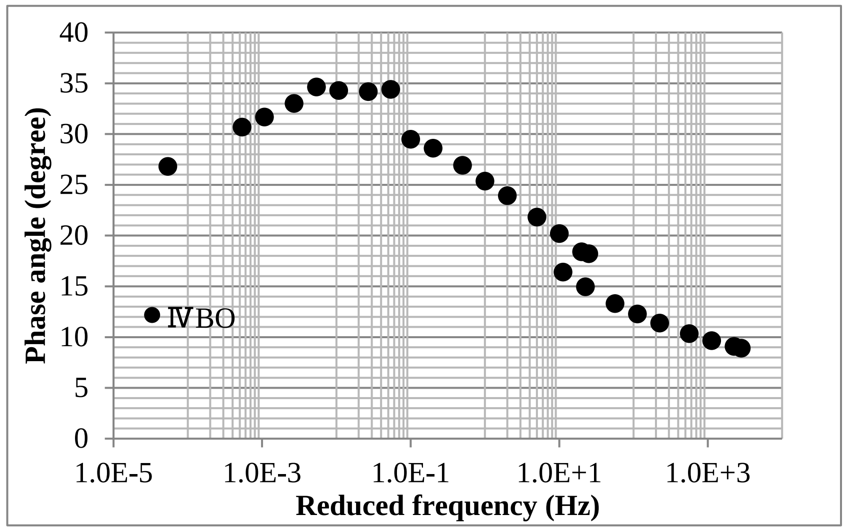

Master Phase Angle Curves for Mixtures from Jefferson Surface Type B, no RAP

Level 2

Asphalt Mix: Aggregate Gradation	
Cumulative % Retained ¾” sieve	0
Cumulative % Retained ⅜” sieve	9
Cumulative % Retained #4 sieve	40
% Passing #200 sieve	4.53

Level 3

Asphalt Binder: Superpave Binder Grading	PG 64-22

Figure 13-35: Mixture Type: IV BOG (Jefferson Surface Type B with Long-Term Aging, no RAP)

Level 1

Asphalt Mix: Dynamic Modulus Table						
Temperature (°F)	Mixture |E*| (psi)					
	0.1 Hz	0.5 Hz	1 Hz	5 Hz	10 Hz	25 Hz
14	1973618	2407805	2559525	2832776	2920568	3014025
40	935475	1463728	1694747	2183605	2362798	2566548
70	227359	491676	655821	1134990	1366039	1672813
100	48934	113040	163525	368965	505193	731853
130	16062	30199	41604	94690	137050	221938

Asphalt Binder: Superpave Binder Test Data		
Temperature (°F)	Angular freq. = 10 rad/sec	
	G* (Pa)	Delta (degree)
158.0	792.60	88.98
168.8	299.28	89.22
179.6	150.21	89.46

Asphalt General: Volumetric Properties as Built	
Effective Binder (%)	11.51
Air Voids (%)	6.91
Total unit weight	164.69

Level 2

Asphalt Mix: Aggregate Gradation	
Cumulative % Retained ¾” sieve	0
Cumulative % Retained ⅜” sieve	9
Cumulative % Retained #4 sieve	40
% Passing #200 sieve	4.53

Level 3

Asphalt Binder: Superpave Binder Grading	PG 64-22

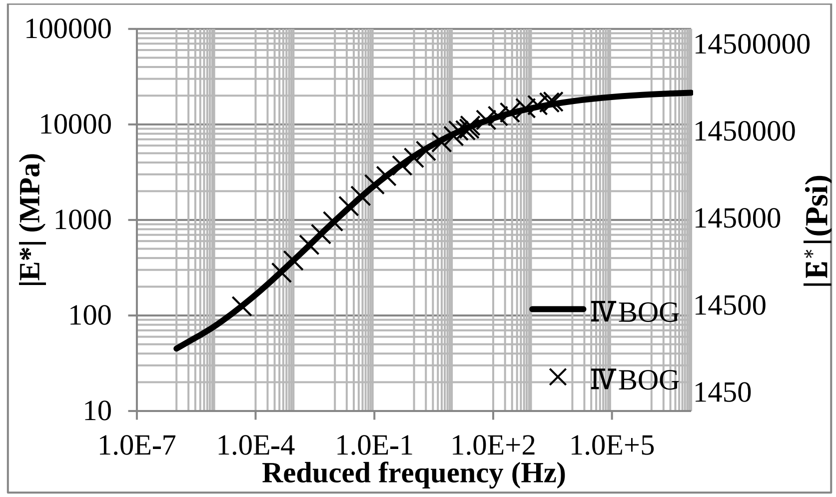

Master Dynamic Modulus Curves for Mixtures from Jefferson Surface Type B with Long-Term Aging, no RAP

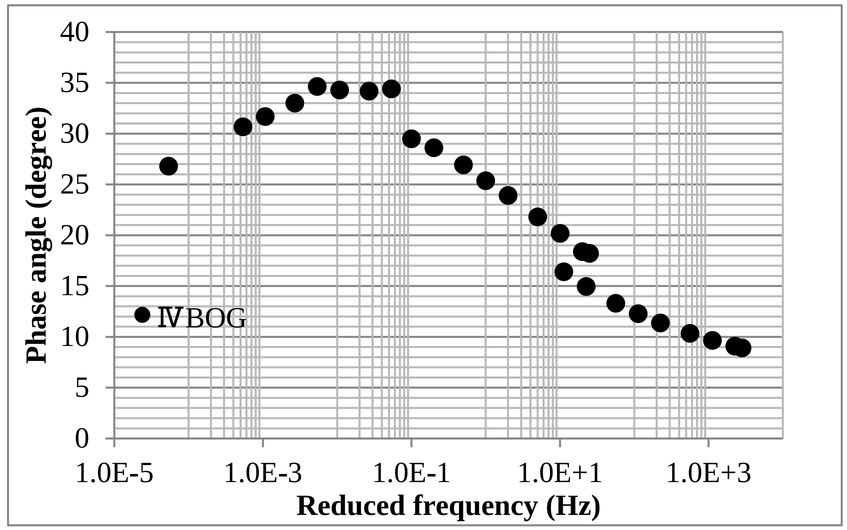

Master Phase Angle Curves for Mixtures from Jefferson Surface Type B with Long-Term Aging, no RAP

Figure 13-36: Mixture Type: IV BON (Jefferson Surface Type B with Asphalt Source 2, no RAP)

Level 1

Asphalt Mix: Dynamic Modulus Table						
Temperature (°F)	Mixture |E*| (psi)					
	0.1 Hz	0.5 Hz	1 Hz	5 Hz	10 Hz	25 Hz
14	1879053	2320018	2477953	2768583	2863983	2966890
40	885878	1389197	1613693	2099444	2281704	2492188
70	227663	477639	631981	1084960	1305997	1603045
100	53727	118925	168849	366996	496552	711288
130	18645	34305	46612	101907	144733	228785

Asphalt Binder: Superpave Binder Test Data		
Temperature (°F)	Angular freq. = 10 rad/sec	
	G* (Pa)	Delta (degree)
158.0	792.60	88.98
168.8	299.28	89.22
179.6	150.21	89.46

Asphalt General: Volumetric Properties as Built	
Effective Binder (%)	11.73
Air Voids (%)	6.91
Total unit weight	164.69

Level 2

Asphalt Mix: Aggregate Gradation	
Cumulative % Retained ¾” sieve	0
Cumulative % Retained ⅜” sieve	9
Cumulative % Retained #4 sieve	40
% Passing #200 sieve	4.53

Level 3

Asphalt Binder: Superpave Binder Grading	PG 64-22

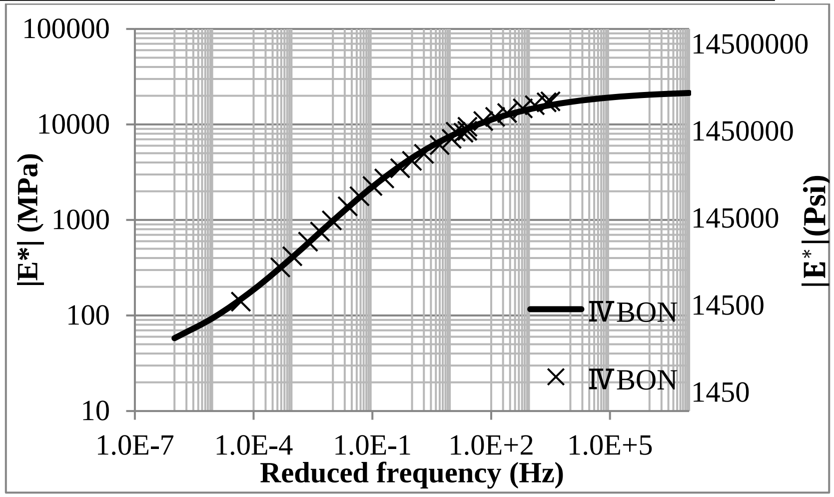

Master Dynamic Modulus Curves for Mixtures from Jefferson Surface Type B with Asphalt Source 2, no RAP

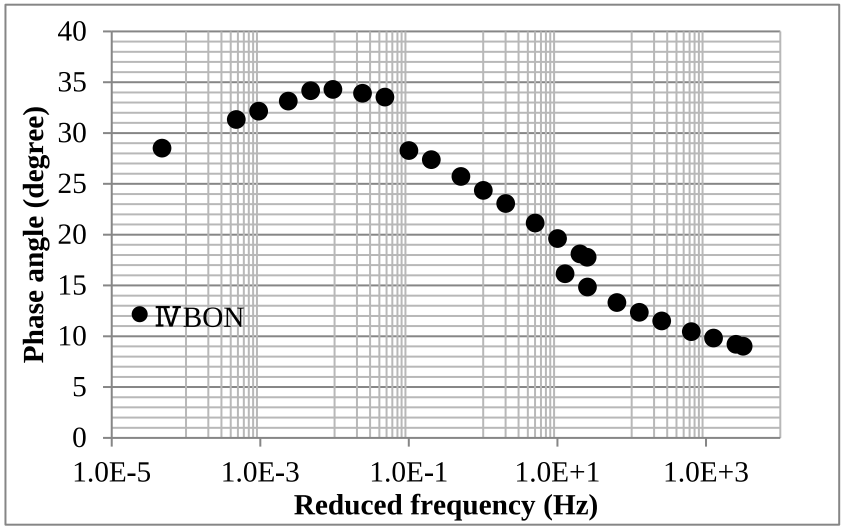

Master Phase Angle Curves for Mixtures from Jefferson Surface Type B with Asphalt Source 2, no RAP

Figure 13-37: Mixture Type: IV C (Jefferson Surface Type C with RAP)

Level 1

Asphalt Mix: Dynamic Modulus Table						
Temperature (°F)	Mixture |E*| (psi)					
	0.1 Hz	0.5 Hz	1 Hz	5 Hz	10 Hz	25 Hz
14	1900729	2298917	2442411	2709947	2799350	2897140
40	955922	1427131	1632985	2076040	2242943	2437233
70	271399	532331	685251	1116308	1321411	1594772
100	66378	142458	197845	404745	533534	740764
130	21939	41066	55707	118598	165139	253128

Asphalt Binder: Superpave Binder Test Data		
Temperature (°F)	Angular freq. = 10 rad/sec	
	G* (Pa)	Delta (degree)
158.0	792.60	88.98
168.8	299.28	89.22
179.6	150.21	89.46

Asphalt General: Volumetric Properties as Built	
Effective Binder (%)	12.52
Air Voids (%)	8.37
Total unit weight	165.81

Level 2

Asphalt Mix: Aggregate Gradation	
Cumulative % Retained ¾" sieve	0
Cumulative % Retained ⅜" sieve	7
Cumulative % Retained #4 sieve	30
% Passing #200 sieve	5.09

Level 3

Asphalt Binder: Superpave Binder Grading	PG 64-22

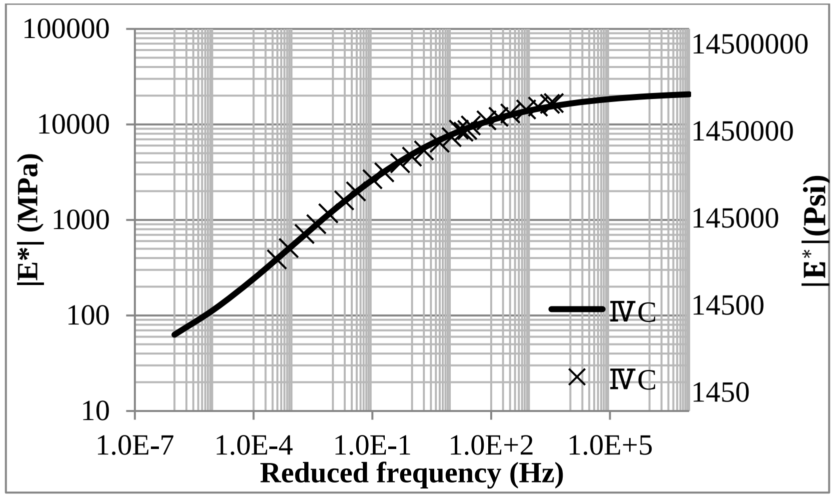

Master Dynamic Modulus Curves for Mixtures from Jefferson Surface Type C with RAP

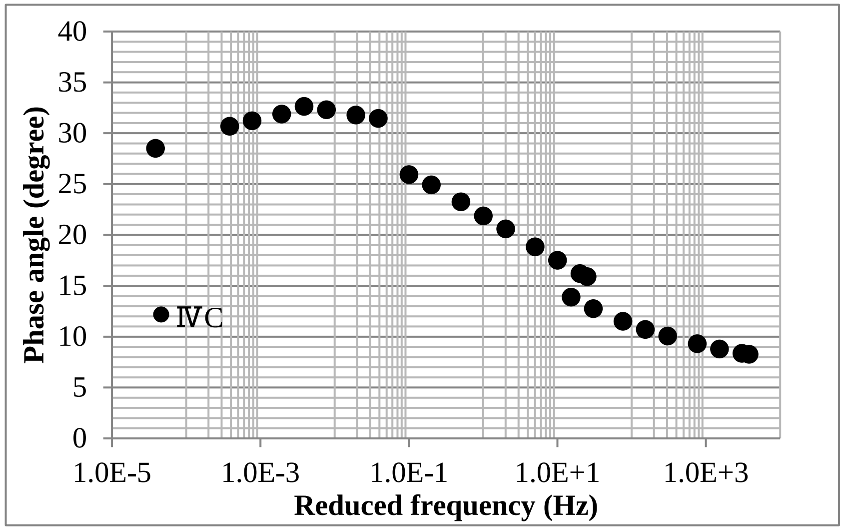

Master Phase Angle Curves for Mixtures from Jefferson Surface Type C with RAP

Figure 13-38: Mixture Type: IV CO (Jefferson Surface Type C, no RAP)

Level 1

Asphalt Mix: Dynamic Modulus Table						
Temperature (°F)	Mixture |E*| (psi)					
	0.1 Hz	0.5 Hz	1 Hz	5 Hz	10 Hz	25 Hz
14	1622894	2052953	2216433	2535440	2646849	2772037
40	715337	1143527	1343350	1800816	1983562	2204299
70	169377	362091	482833	849210	1036110	1297534
100	34229	81074	117245	262460	359095	522868
130	9405	19539	27710	65175	94571	152868

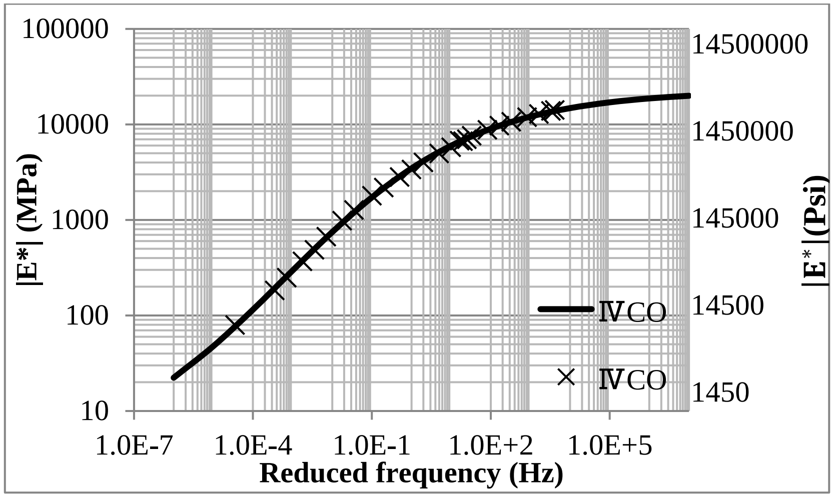

Master Dynamic Modulus Curves for Mixtures from Jefferson Surface Type C, no RAP

Asphalt Binder: Superpave Binder Test Data		
Temperature (°F)	Angular freq. = 10 rad/sec	
	G* (Pa)	Delta (degree)
158.0	792.60	88.98
168.8	299.28	89.22
179.6	150.21	89.46

Asphalt General: Volumetric Properties as Built	
Effective Binder (%)	12.70
Air Voids (%)	7.15
Total unit weight	164.44

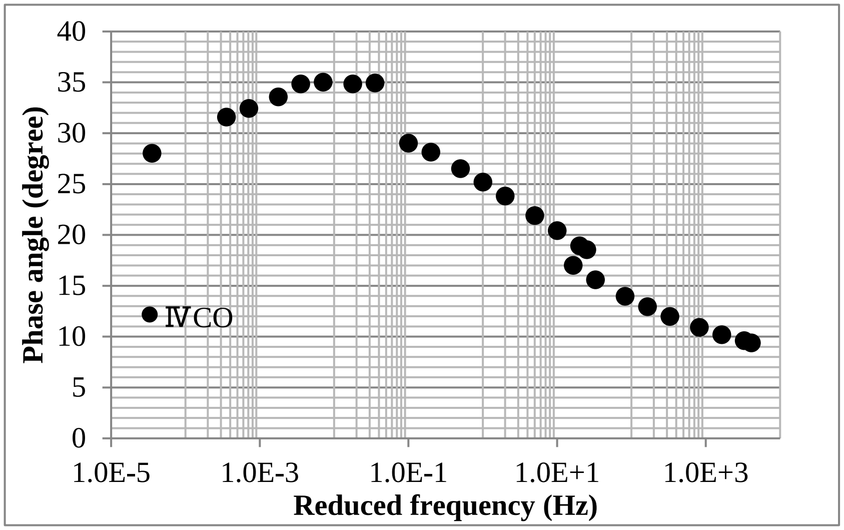

Master Phase Angle Curves for Mixtures from Jefferson Surface Type C, no RAP

Level 2

Asphalt Mix: Aggregate Gradation	
Cumulative % Retained ¾" sieve	0
Cumulative % Retained ⅜" sieve	6
Cumulative % Retained #4 sieve	27
% Passing #200 sieve	5.91

Level 3

Asphalt Binder: Superpave Binder Grading	PG 64-22

Figure 13-39: Mixture Type: IV CA (Jefferson Surface Type C with LASA 2 (Adhere®) and RAP)

Level 1

Asphalt Mix: Dynamic Modulus Table						
Temperature (°F)	Mixture |E*| (psi)					
	0.1 Hz	0.5 Hz	1 Hz	5 Hz	10 Hz	25 Hz
14	1851218	2271235	2422409	2702884	2795936	2897122
40	882154	1366289	1580941	2045656	2220860	2424341
70	224360	470471	620541	1056534	1268143	1552449
100	48913	112512	161249	353476	478228	683977
130	15067	29506	41044	93516	134341	214450

Asphalt Binder: Superpave Binder Test Data		
Temperature (°F)	Angular freq. = 10 rad/sec	
	G* (Pa)	Delta (degree)
158.0	792.60	88.98
168.8	299.28	89.22
179.6	150.21	89.46

Asphalt General: Volumetric Properties as Built	
Effective Binder (%)	12.52
Air Voids (%)	8.17
Total unit weight	165.81

Level 2

Asphalt Mix: Aggregate Gradation	
Cumulative % Retained ¾” sieve	0
Cumulative % Retained ⅜” sieve	7
Cumulative % Retained #4 sieve	30
% Passing #200 sieve	5.09

Level 3

Asphalt Binder: Superpave Binder Grading	PG 64-22

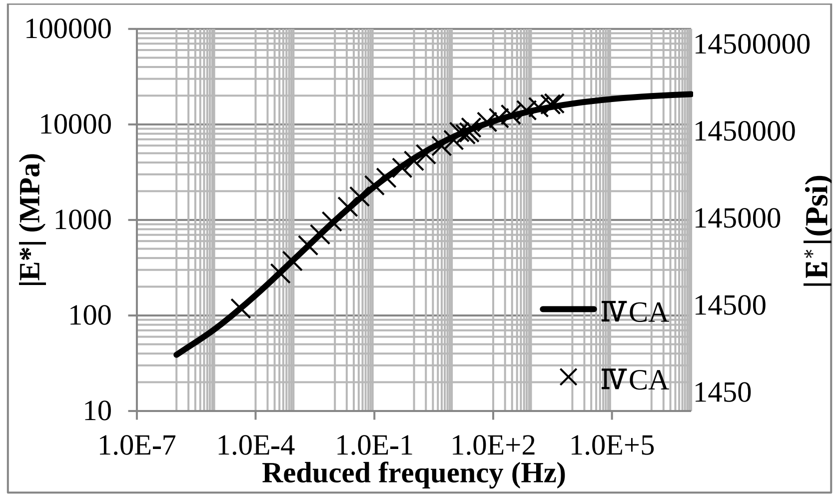

Master Dynamic Modulus Curves for Mixtures from Jefferson Surface Type C with Adhere® and RAP

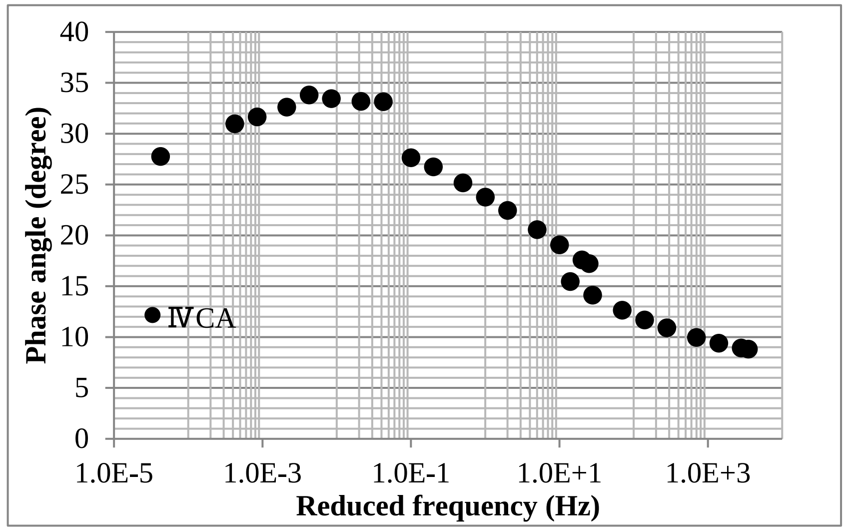

Master Phase Angle Curves for Mixtures from Jefferson Surface Type C with Adhere® and RAP

Figure 13-40: Mixture Type: IV CE (Jefferson Surface Type C with Evotherm® WMA Chemical Additive and RAP)

Level 1

Asphalt Mix: Dynamic Modulus Table						
Temperature (°F)	Mixture |E*| (psi)					
	0.1 Hz	0.5 Hz	1 Hz	5 Hz	10 Hz	25 Hz
14	1644237	2148556	2331424	2666788	2775560	2891470
40	632734	1134864	1375491	1917357	2124955	2365416
70	115048	294968	422803	847047	1073047	1389979
100	20968	53783	82647	218776	321297	507922
130	6678	12979	18384	46274	70948	125102

Asphalt Binder: Superpave Binder Test Data		
Temperature (°F)	Angular freq. = 10 rad/sec	
	G* (Pa)	Delta (degree)
158.0	792.60	88.98
168.8	299.28	89.22
179.6	150.21	89.46

Asphalt General: Volumetric Properties as Built	
Effective Binder (%)	12.52
Air Voids (%)	8.17
Total unit weight	165.81

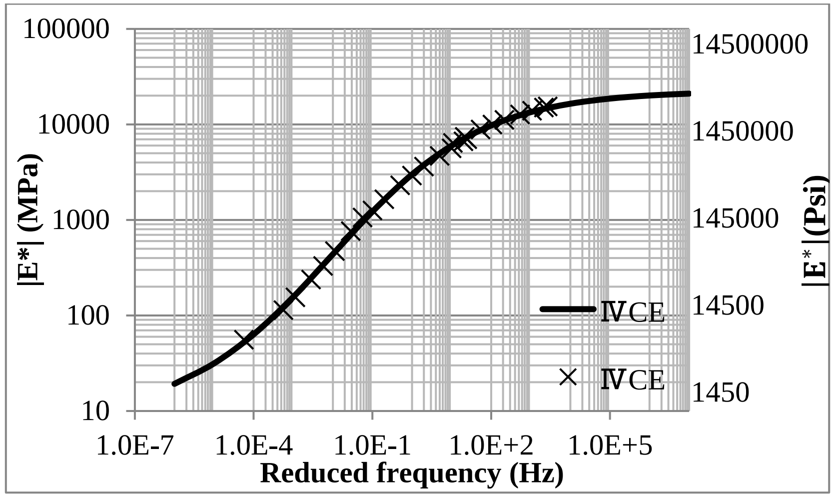

Master Dynamic Modulus Curves for Mixtures from Jefferson Surface Type C with Evotherm® and RAP

Level 2

Asphalt Mix: Aggregate Gradation	
Cumulative % Retained ¾” sieve	0
Cumulative % Retained ⅜” sieve	7
Cumulative % Retained #4 sieve	30
% Passing #200 sieve	5.09

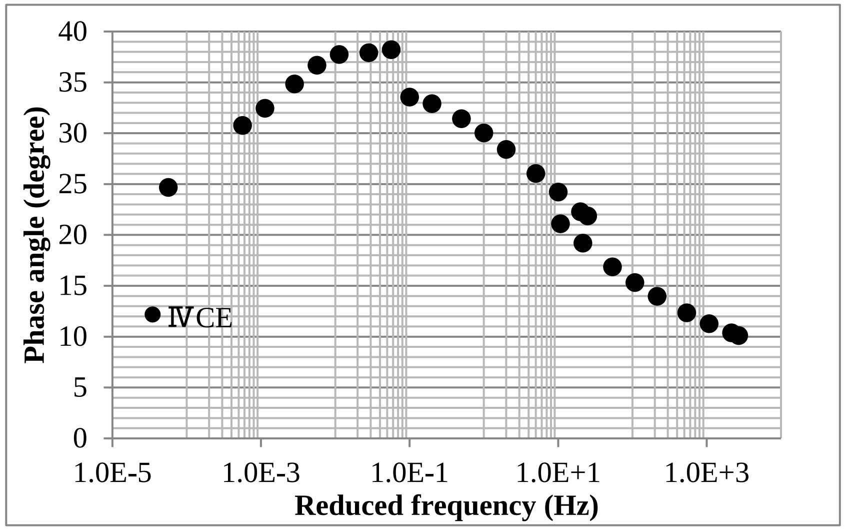

Master Phase Angle Modulus Curves for Mixtures from Jefferson Surface Type C with Evotherm® and RAP

Level 3

Asphalt Binder: Superpave Binder Grading	PG 64-22

Figure 13-41: Mixture Type: IV CF (Jefferson Surface Type C with WMA Foaming Technology and RAP)

Level 1

Asphalt Mix: Dynamic Modulus Table						
Temperature (°F)	Mixture |E*| (psi)					
	0.1 Hz	0.5 Hz	1 Hz	5 Hz	10 Hz	25 Hz
14	1517072	2011347	2197654	2552346	2671957	2802650
40	583920	1039788	1262854	1781351	1987433	2232629
70	113692	279494	394986	777094	982853	1276197
100	21804	54780	82813	209947	303274	471432
130	6760	13467	19122	47350	71506	123087

Asphalt Binder: Superpave Binder Test Data		
Temperature (°F)	Angular freq. = 10 rad/sec	
	G* (Pa)	Delta (degree)
158.0	792.60	88.98
168.8	299.28	89.22
179.6	150.21	89.46

Asphalt General: Volumetric Properties as Built	
Effective Binder (%)	12.52
Air Voids (%)	8.17
Total unit weight	165.81

Level 2

Asphalt Mix: Aggregate Gradation	
Cumulative % Retained ¾” sieve	0
Cumulative % Retained ⅜” sieve	7
Cumulative % Retained #4 sieve	30
% Passing #200 sieve	5.09

Level 3

Asphalt Binder: Superpave Binder Grading	PG 64-22

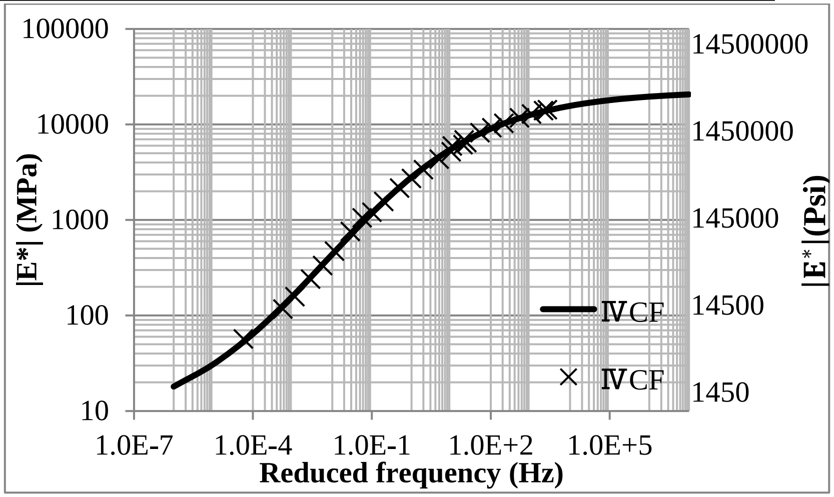

Master Dynamic Modulus Curves for Mixtures from Jefferson Surface Type C with Foaming WMA and RAP

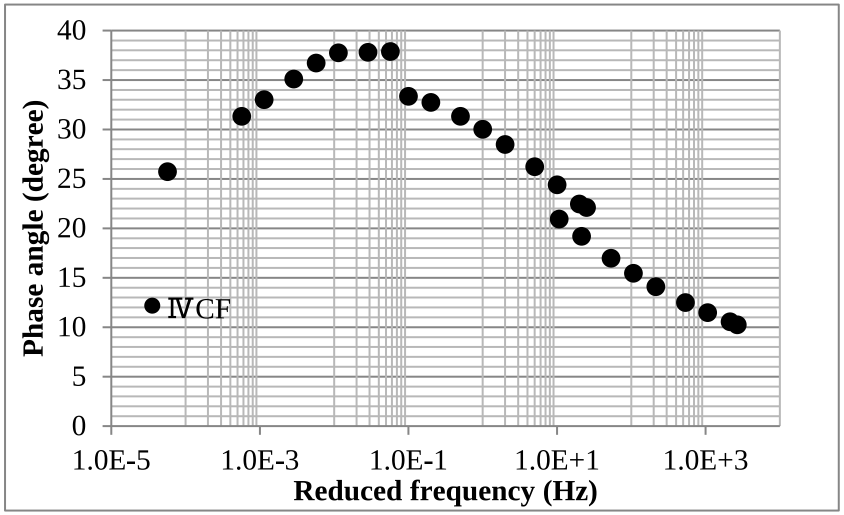

Master Phase Angle Curves for Mixtures from Jefferson Surface Type C with Foaming WMA and RAP

Figure 13-42: Mixture Type: IV CG (Jefferson Surface Type C with Long-Term Aging and RAP)

Level 1

Asphalt Mix: Dynamic Modulus Table						
Temperature (°F)	Mixture |E*| (psi)					
	0.1 Hz	0.5 Hz	1 Hz	5 Hz	10 Hz	25 Hz
14	1963546	2346450	2483273	2737193	2821809	2914300
40	1041175	1515674	1718006	2145698	2304549	2488213
70	316642	608291	773199	1220940	1427101	1696506
100	77294	170311	236841	476790	620582	845080
130	23452	47150	65546	144410	201887	308220

Asphalt Binder: Superpave Binder Test Data		
Temperature (°F)	Angular freq. = 10 rad/sec	
	G* (Pa)	Delta (degree)
158.0	792.60	88.98
168.8	299.28	89.22
179.6	150.21	89.46

Asphalt General: Volumetric Properties as Built	
Effective Binder (%)	12.52
Air Voids (%)	9.81
Total unit weight	165.81

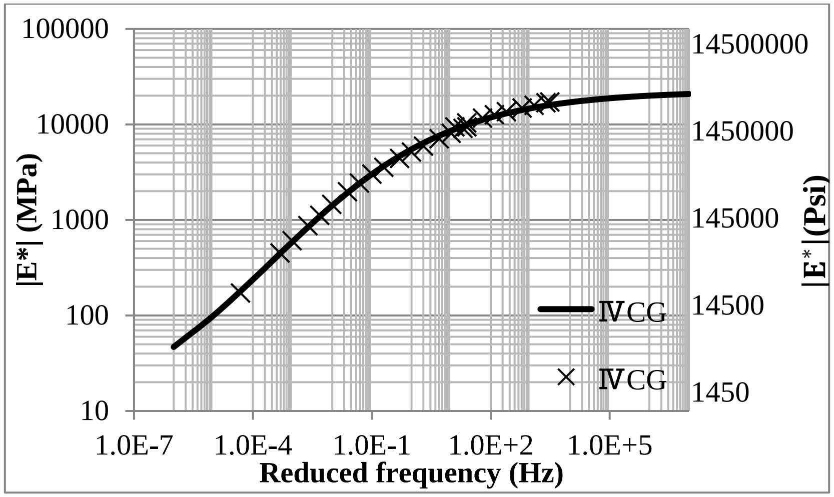

Master Dynamic Modulus Curves for Mixtures from Jefferson Surface Type C with Long-Term Aging and RAP

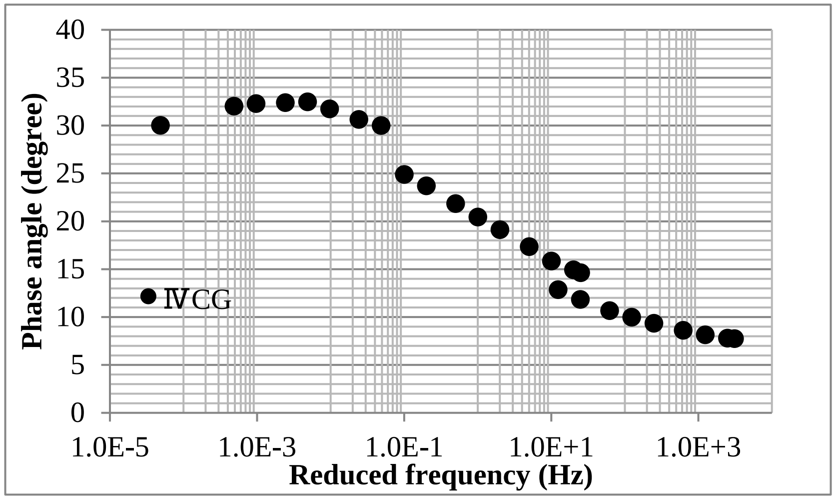

Master Phase Angle Curves for Mixtures from Jefferson Surface Type C with Long-Term Aging and RAP

Level 2

Asphalt Mix: Aggregate Gradation	
Cumulative % Retained ¾" sieve	0
Cumulative % Retained ⅜" sieve	7
Cumulative % Retained #4 sieve	30
% Passing #200 sieve	5.09

Level 3

Asphalt Binder: Superpave Binder Grading	PG 64-22

Figure 13-43: Mixture Type: IV CM (Jefferson Surface Type C with LASA 1 (Morlife®) and RAP)

Level 1

Asphalt Mix: Dynamic Modulus Table						
Temperature (°F)	Mixture |E*| (psi)					
	0.1 Hz	0.5 Hz	1 Hz	5 Hz	10 Hz	25 Hz
14	1822984	2231066	2380208	2661580	2756687	2861438
40	889692	1351380	1556440	2004588	2175889	2377128
70	242983	487098	632406	1048942	1250322	1521692
100	56848	125509	176216	368705	490263	687993
130	17870	34586	47574	104314	146896	228244

Asphalt Binder: Superpave Binder Test Data		
Temperature (°F)	Angular freq. = 10 rad/sec	
	G* (Pa)	Delta (degree)
158.0	792.60	88.98
168.8	299.28	89.22
179.6	150.21	89.46

Asphalt General: Volumetric Properties as Built	
Effective Binder (%)	12.52
Air Voids (%)	9.10
Total unit weight	165.81

Level 2

Asphalt Mix: Aggregate Gradation	
Cumulative % Retained ¾” sieve	0
Cumulative % Retained ⅜” sieve	7
Cumulative % Retained #4 sieve	30
% Passing #200 sieve	5.09

Level 3

Asphalt Binder: Superpave Binder Grading	PG 64-22

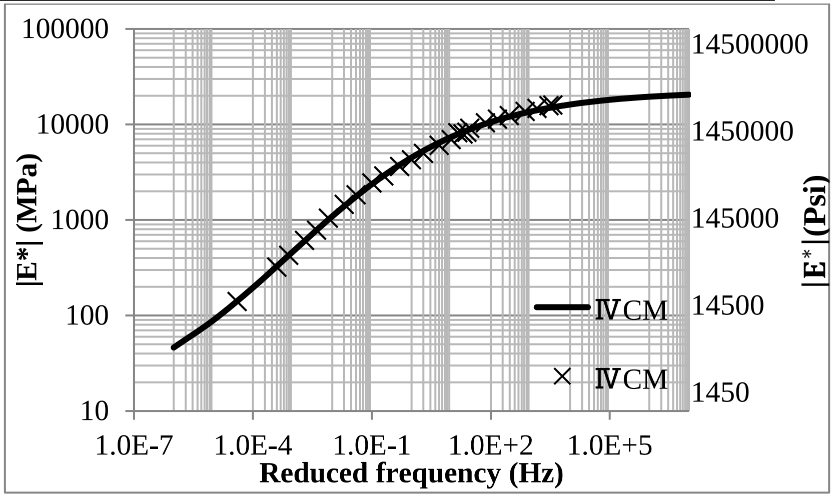

Master Dynamic Modulus Curves for Mixtures from Jefferson Surface Type C with Morlife® and RAP

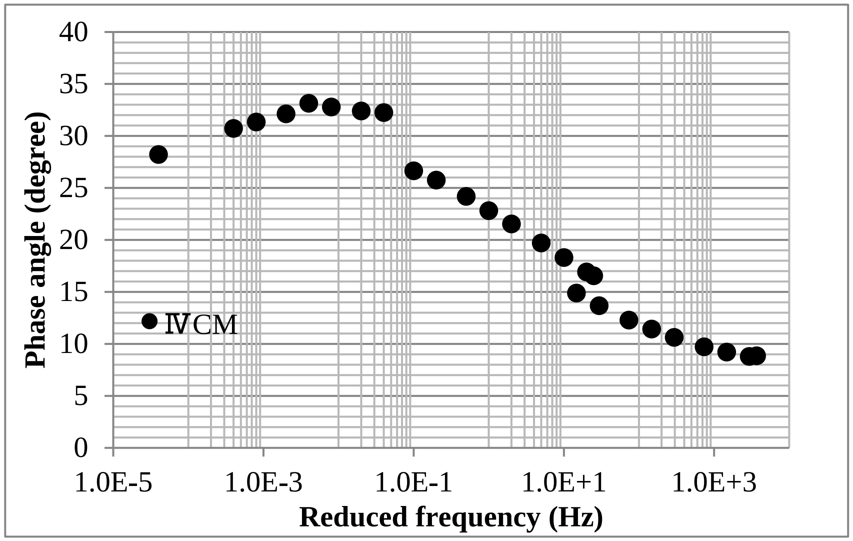

Master Phase Angle Curves for Mixtures from Jefferson Surface Type C with Morlife® and RAP

Figure 13-44: Mixture Type: IV COA (Jefferson Surface Type C with LASA 2 (Adhere®), no RAP)

Level 1

Asphalt Mix: Dynamic Modulus Table						
Temperature (°F)	Mixture |E*| (psi)					
	0.1 Hz	0.5 Hz	1 Hz	5 Hz	10 Hz	25 Hz
14	1611046	2074920	2248990	2582021	2695500	2820693
40	655385	1107504	1322778	1817059	2013018	2247090
70	133536	311163	429635	807622	1006612	1288083
100	24793	61330	91381	221965	314662	478366
130	7096	14360	20391	49646	73983	124762

Asphalt Binder: Superpave Binder Test Data		
Temperature (°F)	Angular freq. = 10 rad/sec	
	G* (Pa)	Delta (degree)
158.0	792.60	88.98
168.8	299.28	89.22
179.6	150.21	89.46

Asphalt General: Volumetric Properties as Built	
Effective Binder (%)	12.70
Air Voids (%)	8.16
Total unit weight	164.44

Level 2

Asphalt Mix: Aggregate Gradation	
Cumulative % Retained ¾" sieve	0
Cumulative % Retained ⅜" sieve	6
Cumulative % Retained #4 sieve	27
% Passing #200 sieve	5.91

Level 3

Asphalt Binder: Superpave Binder Grading	PG 64-22

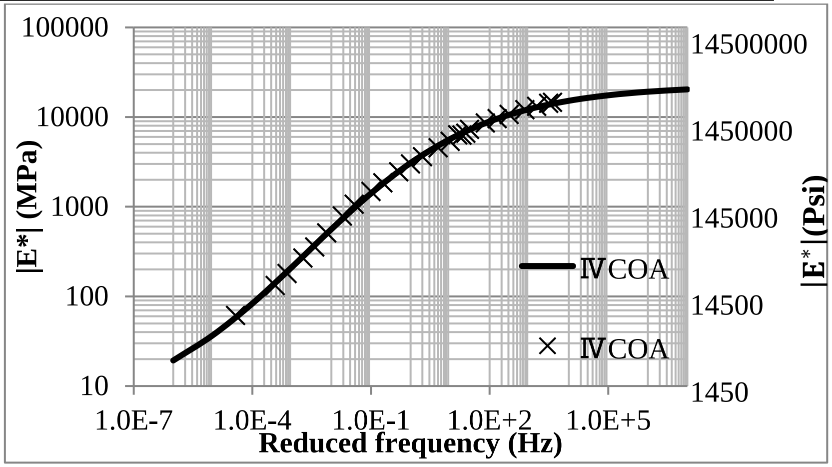

Master Dynamic Modulus Curves for Mixtures from Jefferson Surface Type C with Adhere®, no RAP

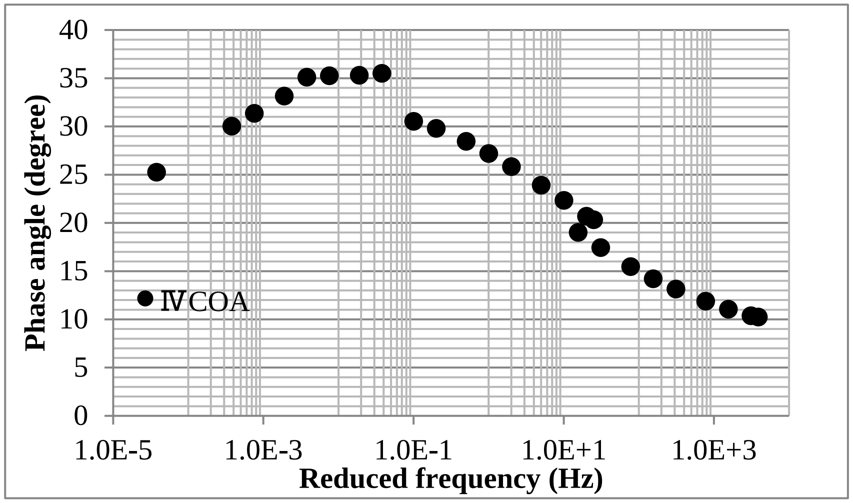

Master Phase Angle Curves for Mixtures from Jefferson Surface Type C with Adhere®, no RAP

Figure 13-45: Mixture Type: IV COE (Jefferson Surface Type C using Evotherm® WMA Chemical Additive, no RAP)

Level 1

Asphalt Mix: Dynamic Modulus Table						
Temperature (°F)	Mixture |E*| (psi)					
	0.1 Hz	0.5 Hz	1 Hz	5 Hz	10 Hz	25 Hz
14	1178282	1724487	1945350	2384281	2536725	2705106
40	364629	746115	957176	1499287	1732034	2019707
70	63301	164897	243857	543633	725644	1005979
100	14242	32760	48868	127725	191121	315236
130	5676	9849	13249	29998	44560	76810

Asphalt Binder: Superpave Binder Test Data		
Temperature (°F)	Angular freq. = 10 rad/sec	
	G* (Pa)	Delta (degree)
158.0	2995	63.7
168.8	1501	61.9
179.6	750	60.0

Asphalt General: Volumetric Properties as Built	
Effective Binder (%)	12.70
Air Voids (%)	8.16
Total unit weight	164.44

Level 2

Asphalt Mix: Aggregate Gradation	
Cumulative % Retained ¾” sieve	0
Cumulative % Retained ⅜” sieve	6
Cumulative % Retained #4 sieve	27
% Passing #200 sieve	5.91

Level 3

Asphalt Binder: Superpave Binder Grading	PG 64-22

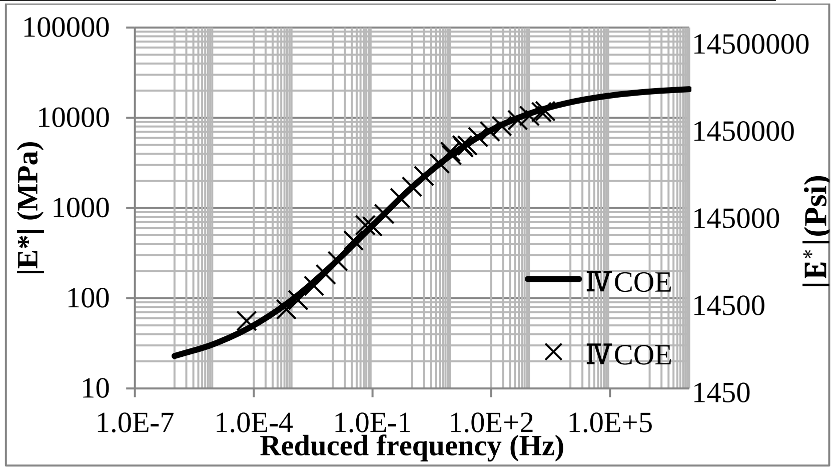

Master Dynamic Modulus Curves for Mixtures from Jefferson Surface Type C using Evotherm®, no RAP

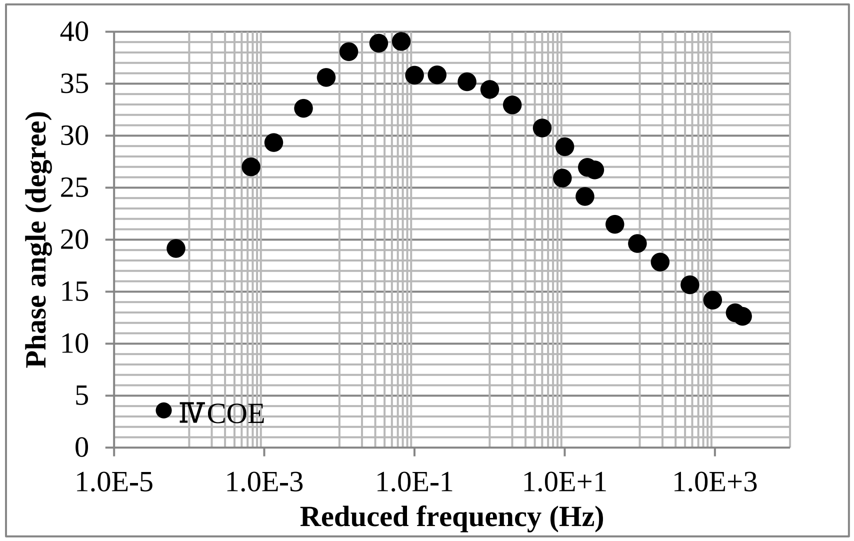

Master Phase Angle Curves for Mixtures from Jefferson Surface Type C using Evotherm®, no RAP

Figure 13-46: Mixture Type: IV COF (Jefferson Surface Type C using WMA Foaming Technology, no RAP)

Level 1

Asphalt Mix: Dynamic Modulus Table						
Temperature	Mixture |E*| (psi)					
(°F)	0.1 Hz	0.5 Hz	1 Hz	5 Hz	10 Hz	25 Hz
14	1303133	1838716	2049091	2459360	2599900	2754243
40	426610	838878	1057726	1599957	1826175	2101661
70	72782	190536	279858	606594	798182	1086264
100	14702	35573	53872	142893	213376	348909
130	5265	9631	13259	31479	47469	82912

Asphalt General: Volumetric Properties as Built	
Effective Binder (%)	12.7
Air Voids (%)	8.16
Total unit weight	164.44

Asphalt Binder: Superpave Binder Test Data		
Temperature	Angular freq. = 10 rad/sec	
(°F)	G* (Pa)	Delta (degree)
158.0	792.60	88.98
168.8	299.28	89.22
179.6	150.21	89.46

Level 2

Asphalt Mix: Aggregate Gradation	
Cumulative % Retained ¾" sieve	0
Cumulative % Retained ⅜" sieve	6
Cumulative % Retained #4 sieve	27
% Passing #200 sieve	5.91

Level 3

Asphalt Binder: Superpave Binder Grading	PG 64-22

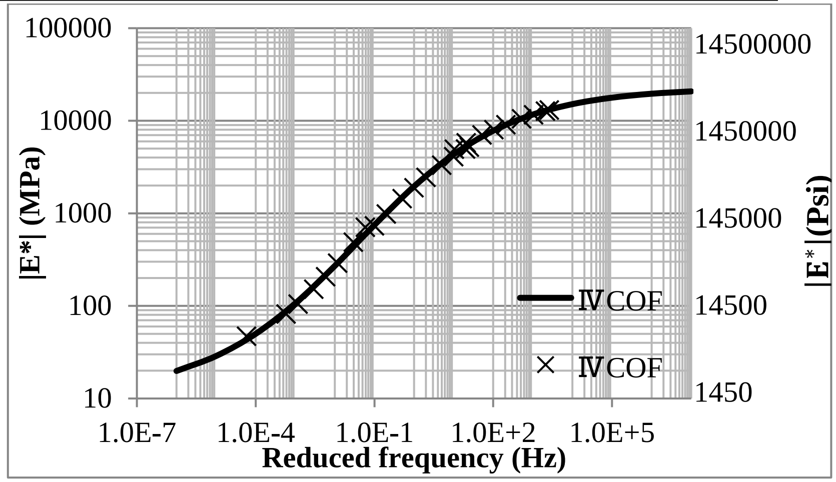

Master Dynamic Modulus Curves for Mixtures from Jefferson Surface Type C using Foaming WMA, no RAP

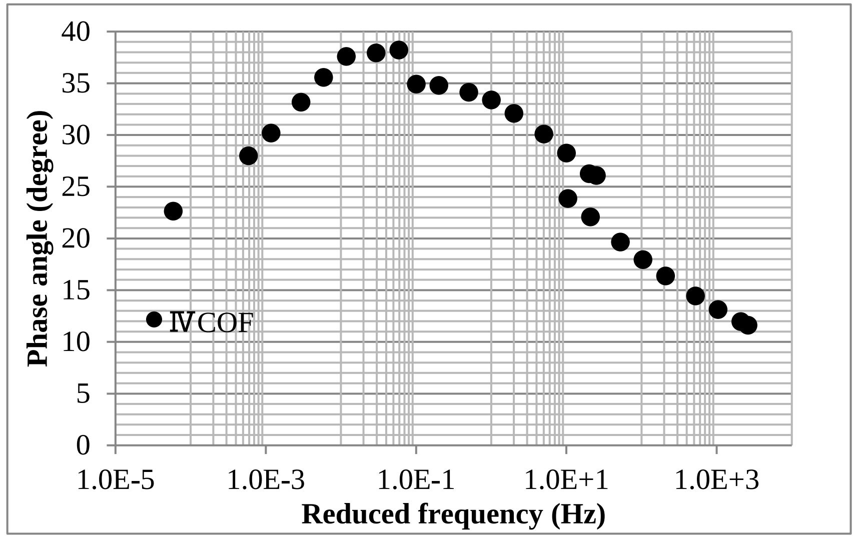

Master Phase Angle Curves for Mixtures from Jefferson Surface Type C using Foaming WMA, no RAP

Figure 13-47: Mixture Type: IV COG (Jefferson Surface Type C with Long-Term Aging, no RAP)

Level 1

Asphalt Mix: Dynamic Modulus Table						
Temperature (°F)	Mixture |E*| (psi)					
	0.1 Hz	0.5 Hz	1 Hz	5 Hz	10 Hz	25 Hz
14	1587945	1993208	2149951	2462548	2574529	2702696
40	744702	1147428	1333399	1760170	1932435	2142968
70	200471	403069	524008	877165	1052982	1296806
100	43694	101316	143612	302842	403196	567395
130	11346	24896	35651	82957	118343	185559

Asphalt Binder: Superpave Binder Test Data		
Temperature (°F)	Angular freq. = 10 rad/sec	
	G* (Pa)	Delta (degree)
158.0	792.60	88.98
168.8	299.28	89.22
179.6	150.21	89.46

Asphalt General: Volumetric Properties as Built	
Effective Binder (%)	12.7
Air Voids (%)	8.16
Total unit weight	164.44

Level 2

Asphalt Mix: Aggregate Gradation	
Cumulative % Retained ¾" sieve	0
Cumulative % Retained ⅜" sieve	6
Cumulative % Retained #4 sieve	27
% Passing #200 sieve	5.91

Level 3

Asphalt Binder: Superpave Binder Grading	PG 64-22

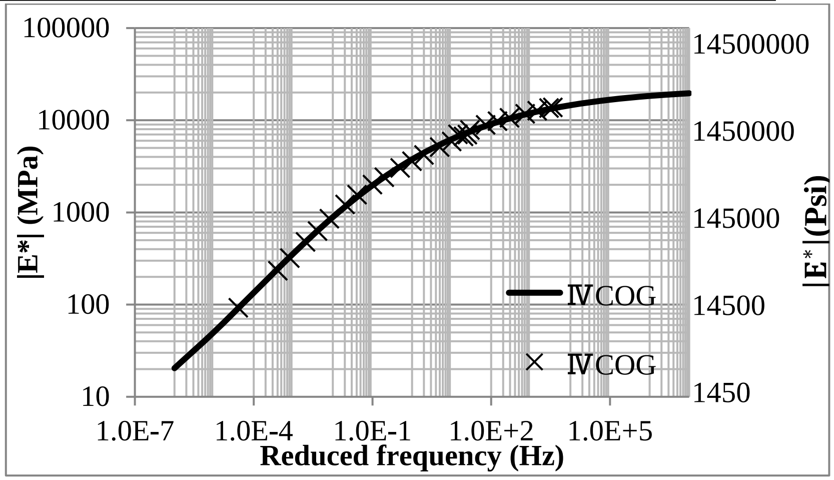

Master Dynamic Modulus Curves for Mixtures from Jefferson Surface Type C with Long-Term Aging no RAP

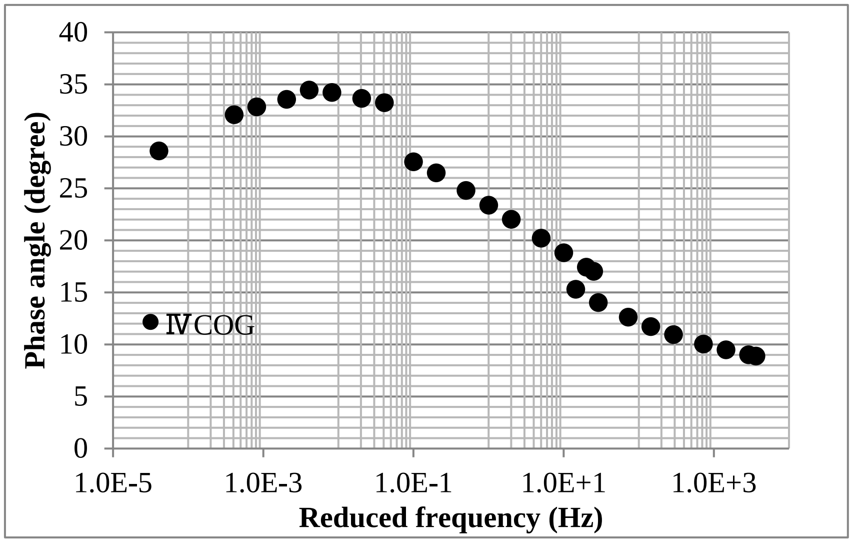

Master Phase Angle Curves for Mixtures from Jefferson Surface Type C with Long-Term Aging no RAP

Figure 13-48: Mixture Type: IV COM (Jefferson Surface Type C with LASA 1 (Morlife®), no RAP)

Level 1

Asphalt Mix: Dynamic Modulus Table						
Temperature (°F)	Mixture |E*| (psi)					
	0.1 Hz	0.5 Hz	1 Hz	5 Hz	10 Hz	25 Hz
14	1360467	1793883	1967474	2322109	2451544	2600997
40	589718	969702	1154211	1594876	1778547	2006835
70	151061	321822	429085	758392	929295	1172286
100	33761	80648	116268	256224	347801	501614
130	9345	20713	29904	71456	103351	165197

Asphalt Binder: Superpave Binder Test Data		
Temperature (°F)	Angular freq. = 10 rad/sec	
	G* (Pa)	Delta (degree)
158.0	792.60	88.98
168.8	299.28	89.22
179.6	150.21	89.46

Asphalt General: Volumetric Properties as Built	
Effective Binder (%)	12.7
Air Voids (%)	8.92
Total unit weight	164.44

Level 2

Asphalt Mix: Aggregate Gradation	
Cumulative % Retained ¾" sieve	0
Cumulative % Retained ⅜" sieve	6
Cumulative % Retained #4 sieve	27
% Passing #200 sieve	5.91

Level 3

Asphalt Binder: Superpave Binder Grading	PG 64-22

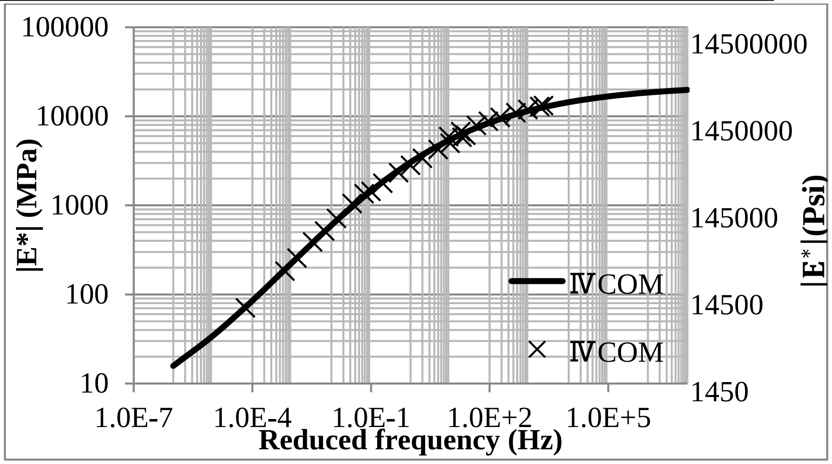

Master Dynamic Modulus Curves for Mixtures from Jefferson Surface Type C with Morlife®, no RAP

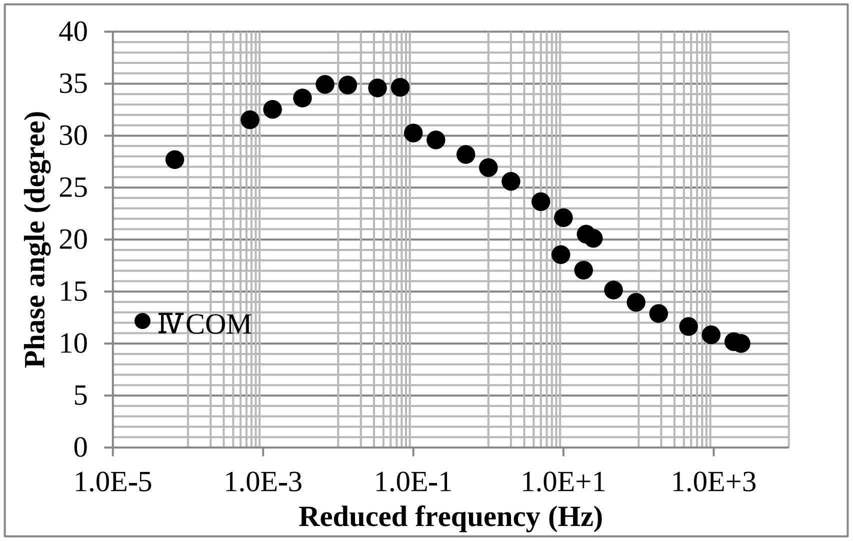

Master Phase Angle Curves for Mixtures from Jefferson Surface Type C with Morlife®, no RAP

Figure 13-49: Mixture Type: IV DO (Jefferson Surface Type D, no RAP)

Level 1

Asphalt Mix: Dynamic Modulus Table						
Temperature (°F)	Mixture |E*| (psi)					
	0.1 Hz	0.5 Hz	1 Hz	5 Hz	10 Hz	25 Hz
14	1581858	1955723	2096409	2369402	2464414	2571074
40	752222	1145952	1325146	1728421	1887543	2078681
70	205887	404128	522549	867835	1038828	1274251
100	49710	105809	146437	299175	395808	554526
130	15977	30094	40770	86076	119411	182549

Asphalt Binder: Superpave Binder Test Data		
Temperature (°F)	Angular freq. = 10 rad/sec	
	G* (Pa)	Delta (degree)
158.0	792.60	88.98
168.8	299.28	89.22
179.6	150.21	89.46

Asphalt General: Volumetric Properties as Built	
Effective Binder (%)	12.34
Air Voids (%)	9.23
Total unit weight	166.50

Level 2

Asphalt Mix: Aggregate Gradation	
Cumulative % Retained ¾" sieve	0
Cumulative % Retained ⅜" sieve	5
Cumulative % Retained #4 sieve	19
% Passing #200 sieve	5.83

Level 3

Asphalt Binder: Superpave Binder Grading	PG 64-22

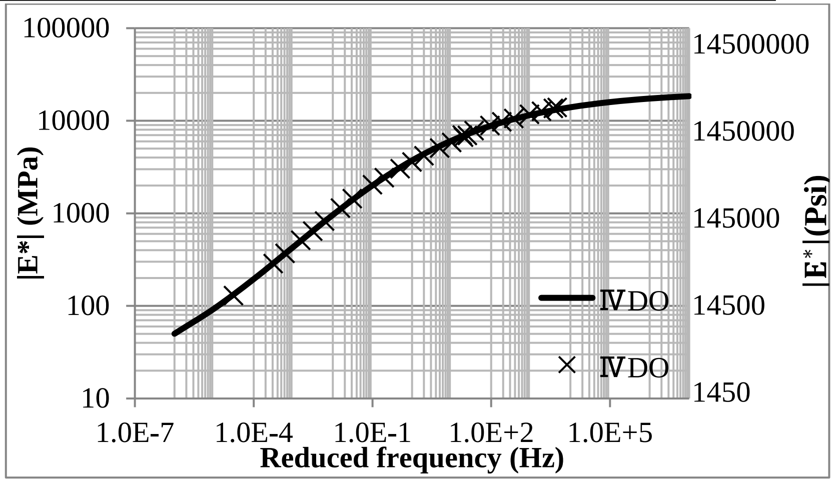

Master Dynamic Modulus Curves for Mixtures from Jefferson Surface Type D, no RAP

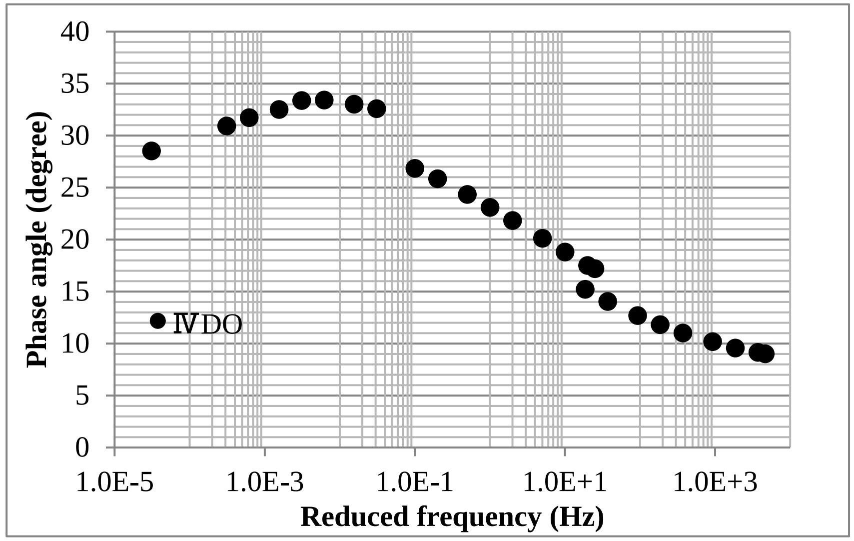

Master Phase Angle Curves for Mixtures from Jefferson Surface Type D, no RAP

Figure 13-50: Mixture Type: IV D (Jefferson Surface Type D with RAP)

Level 1

Asphalt Mix: Dynamic Modulus Table						
Temperature	Mixture |E*| (psi)					
(°F)	0.1 Hz	0.5 Hz	1 Hz	5 Hz	10 Hz	25 Hz
14	1754197	2133212	2269797	2524138	2608964	2701592
40	852628	1295575	1490828	1913269	2072898	2258870
70	224879	456081	594751	993574	1186281	1445216
100	51073	112930	159190	337611	451748	638820
130	16250	30773	42091	92055	130042	203503

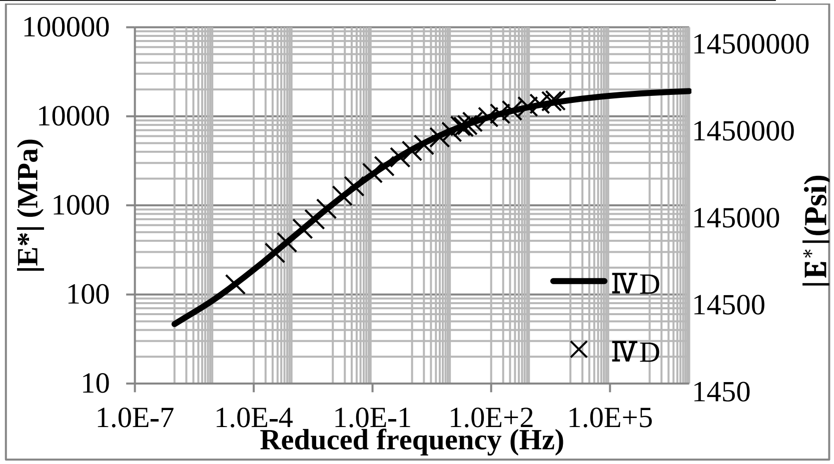

Master Dynamic Modulus Curves for Mixtures from Jefferson Surface Type D with RAP

Asphalt Binder: Superpave Binder Test Data		
Temperature	Angular freq. = 10 rad/sec	
(°F)	G* (Pa)	Delta (degree)
158.0	792.60	88.98
168.8	299.28	89.22
179.6	150.21	89.46

Asphalt General: Volumetric Properties as Built	
Effective Binder (%)	11.46
Air Voids (%)	3.30
Total unit weight	166.50

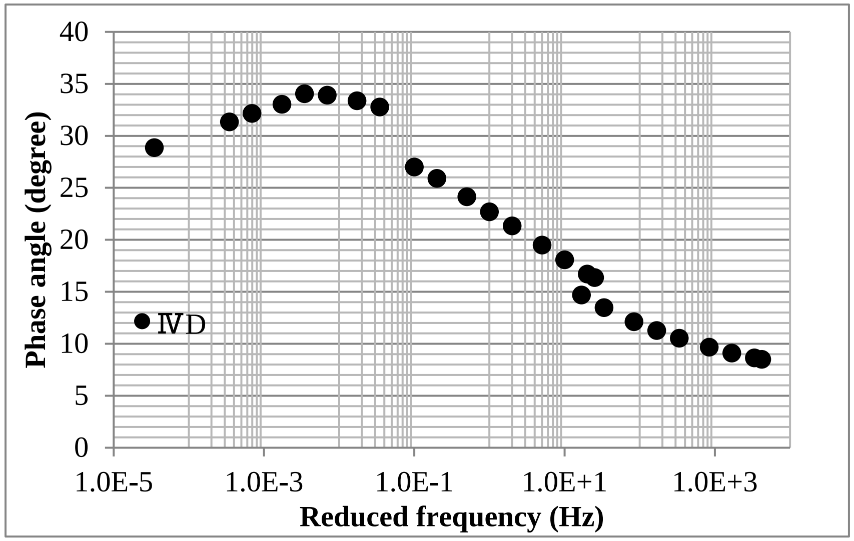

Master Phase Angle Curves for Mixtures from Jefferson Surface Type D with RAP

Level 2

Asphalt Mix: Aggregate Gradation	
Cumulative % Retained ¾" sieve	0
Cumulative % Retained ⅜" sieve	4
Cumulative % Retained #4 sieve	16
% Passing #200 sieve	5.19

Level 3

Asphalt Binder: Superpave Binder Grading	PG 64-22

Figure 13-51: Mixture Type: IV EO (Jefferson Surface Type E, no RAP)

Level 1

Asphalt Mix: Dynamic Modulus Table						
Temperature	Mixture |E*| (psi)					
(°F)	0.1 Hz	0.5 Hz	1 Hz	5 Hz	10 Hz	25 Hz
14	1414896	1801663	1951713	2250549	2357166	2478680
40	623160	991868	1165917	1571087	1736103	1938324
70	153028	319235	422437	735554	896311	1123145
100	32345	74734	106755	232662	315383	454958
130	8971	18580	26191	60225	86348	137353

Asphalt Binder: Superpave Binder Test Data		
Temperature	Angular freq. = 10 rad/sec	
(°F)	G* (Pa)	Delta (degree)
158.0	792.60	88.98
168.8	299.28	89.22
179.6	150.21	89.46

Asphalt General: Volumetric Properties as Built	
Effective Binder (%)	12.34
Air Voids (%)	9.86
Total unit weight	166.50

Level 2

Asphalt Mix: Aggregate Gradation	
Cumulative % Retained ¾” sieve	0
Cumulative % Retained ⅜” sieve	0
Cumulative % Retained #4 sieve	2
% Passing #200 sieve	7

Level 3

Asphalt Binder: Superpave Binder Grading	PG 64-22

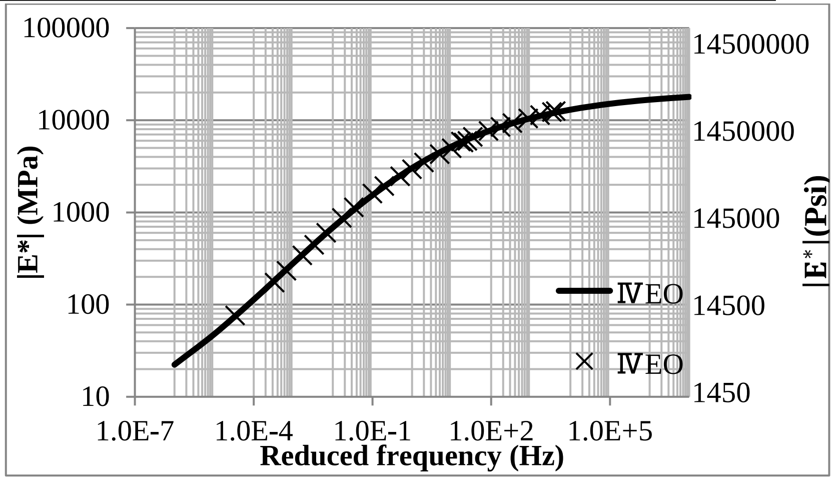

Master Dynamic Modulus Curves for Mixtures from Jefferson Surface Type E, no RAP

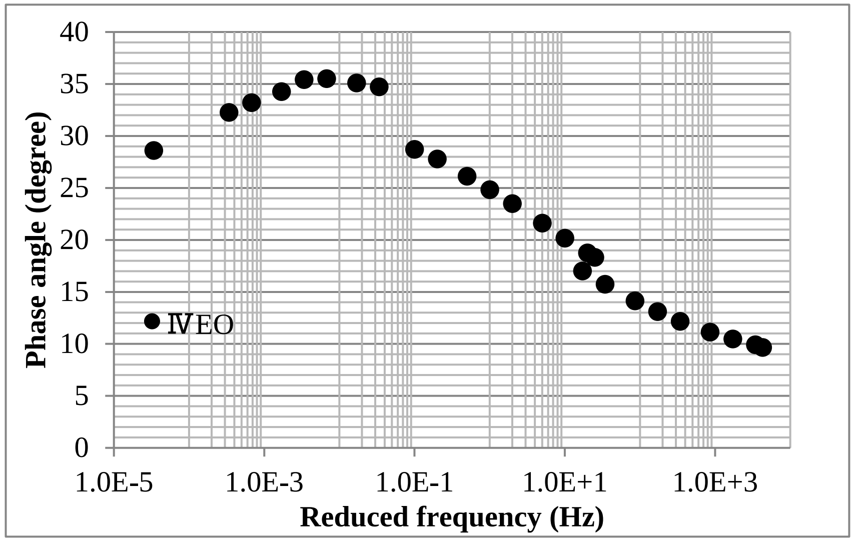

Master Phase Angle Curves for Mixtures from Jefferson Surface Type E, no RAP

Figure 13-52: Mixture Type: IV E (Jefferson Surface Type E with RAP)

Level 1

Asphalt Mix: Dynamic Modulus Table						
Temperature (°F)	Mixture |E*| (psi)					
	0.1 Hz	0.5 Hz	1 Hz	5 Hz	10 Hz	25 Hz
14	2018377	2352182	2466441	2670448	2735792	2805444
40	1100996	1566060	1758282	2150894	2291403	2449753
70	337192	629866	794871	1238973	1440521	1700075
100	89685	179618	243418	474740	614602	834235
130	33681	57211	74673	147349	199863	297524

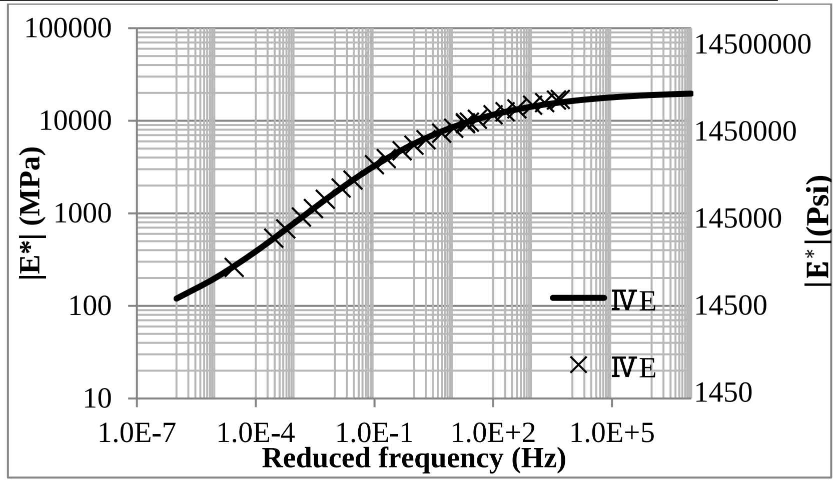

Master Dynamic Modulus Curves for Mixtures from Jefferson Surface Type E with RAP

Asphalt Binder: Superpave Binder Test Data		
Temperature (°F)	Angular freq. = 10 rad/sec	
	G* (Pa)	Delta (degree)
158.0	792.60	88.98
168.8	299.28	89.22
179.6	150.21	89.46

Asphalt General: Volumetric Properties as Built	
Effective Binder (%)	11.46
Air Voids (%)	9.73
Total unit weight	166.50

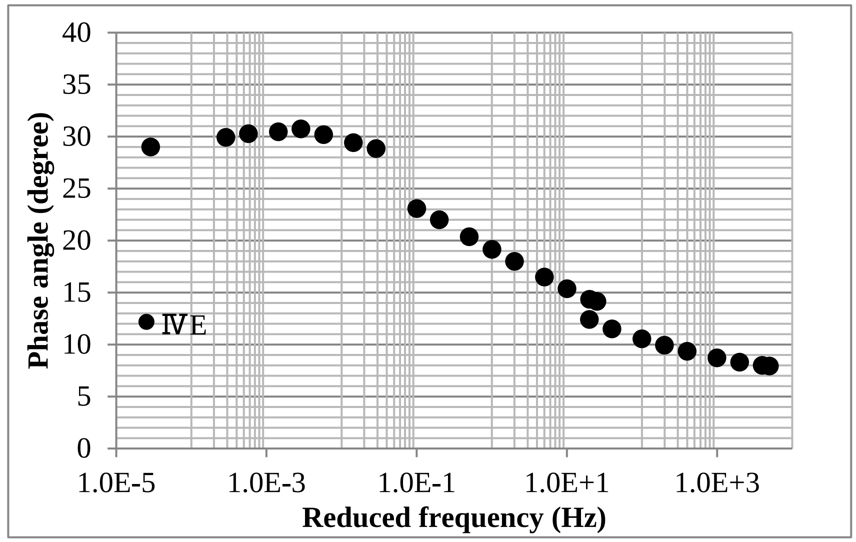

Master Phase Angle Curves for Mixtures from Jefferson Surface Type E with RAP

Level 2

Asphalt Mix: Aggregate Gradation	
Cumulative % Retained ¾" sieve	0
Cumulative % Retained ⅜" sieve	0
Cumulative % Retained #4 sieve	3
% Passing #200 sieve	8

Level 3

Asphalt Binder: Superpave Binder Grading	PG 64-22

Figure 13-53: Mixture Type: IV IAO (Jefferson Intermediate Type A, no RAP)

Level 1

Asphalt Mix: Dynamic Modulus Table						
Temperature (°F)	Mixture |E*| (psi)					
	0.1 Hz	0.5 Hz	1 Hz	5 Hz	10 Hz	25 Hz
14	1887434	2368222	2539209	2850451	2951234	3058872
40	824639	1362928	1606798	2135902	2333589	2560424
70	176107	413418	568808	1044404	1282276	1604536
100	33413	84068	126284	309400	437125	656759
130	9990	20108	28670	71145	106942	181713

Asphalt Binder: Superpave Binder Test Data		
Temperature (°F)	Angular freq. = 10 rad/sec	
	G* (Pa)	Delta (degree)
158.0	792.60	88.98
168.8	299.28	89.22
179.6	150.21	89.46

Asphalt General: Volumetric Properties as Built	
Effective Binder (%)	10.74
Air Voids (%)	6.82
Total unit weight	165.69

Level 2

Asphalt Mix: Aggregate Gradation	
Cumulative % Retained ¾" sieve	2
Cumulative % Retained ⅜" sieve	30
Cumulative % Retained #4 sieve	53
% Passing #200 sieve	3.73

Level 3

Asphalt Binder: Superpave Binder Grading	PG 64-22

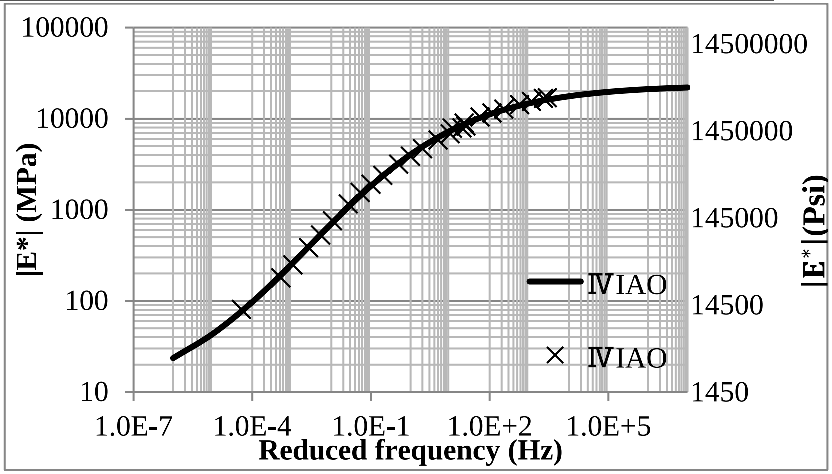

Master Dynamic Modulus Curves for Mixtures from Jefferson Intermediate Type A, no RAP

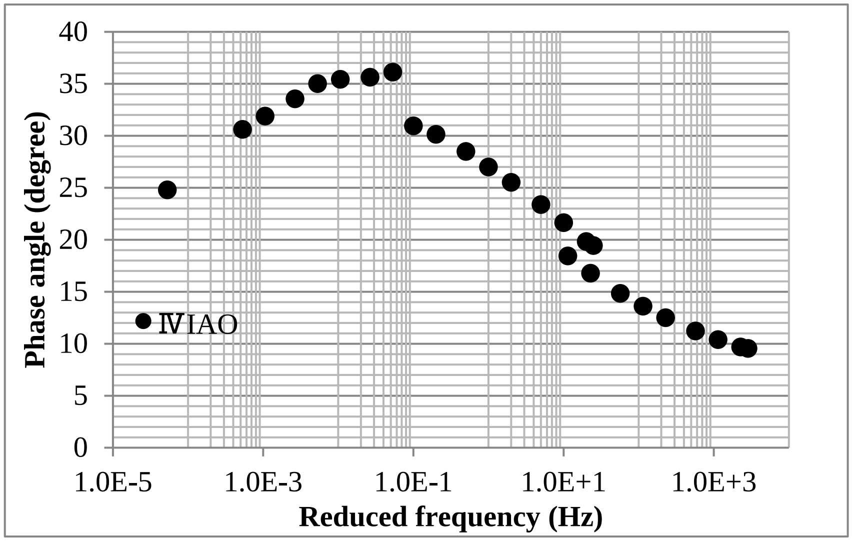

Master Phase Angle Curves for Mixtures from Jefferson Intermediate Type A, no RAP

Figure 13-54: Mixture Type: IV IA (Jefferson Intermediate Type A with RAP)

Level 1

Asphalt Mix: Dynamic Modulus Table						
Temperature (°F)	Mixture |E*| (psi)					
	0.1 Hz	0.5 Hz	1 Hz	5 Hz	10 Hz	25 Hz
14	2055469	2496207	2648749	2921477	3008521	3100840
40	998605	1553459	1791761	2287925	2467153	2669260
70	242619	537650	718406	1233768	1476190	1792581
100	47193	119254	177234	413312	567709	819936
130	13204	27939	40463	101565	151499	251983

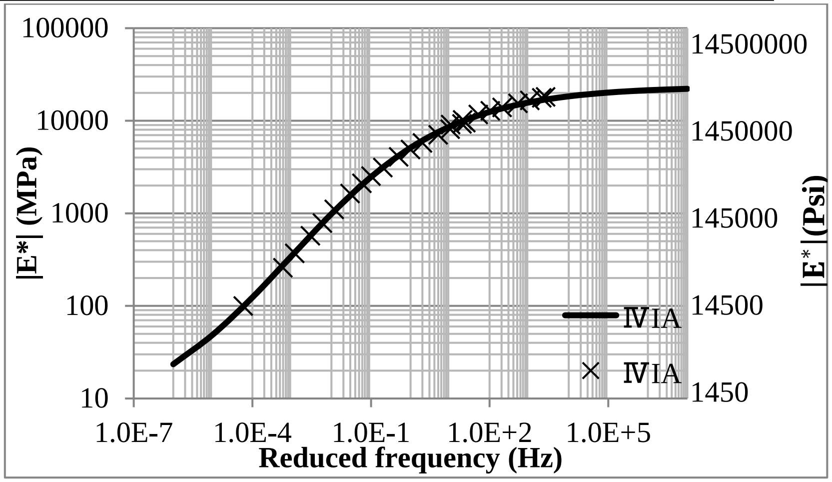

Master Dynamic Modulus Curves for Mixtures from Jefferson Intermediate Type A with RAP

Asphalt Binder: Superpave Binder Test Data		
Temperature (°F)	Angular freq. = 10 rad/sec	
	G* (Pa)	Delta (degree)
158.0	792.60	88.98
168.8	299.28	89.22
179.6	150.21	89.46

Asphalt General: Volumetric Properties as Built	
Effective Binder (%)	10.54
Air Voids (%)	6.78
Total unit weight	165.69

Level 2

Asphalt Mix: Aggregate Gradation	
Cumulative % Retained ¾" sieve	2
Cumulative % Retained ⅜" sieve	27
Cumulative % Retained #4 sieve	53
% Passing #200 sieve	3.73

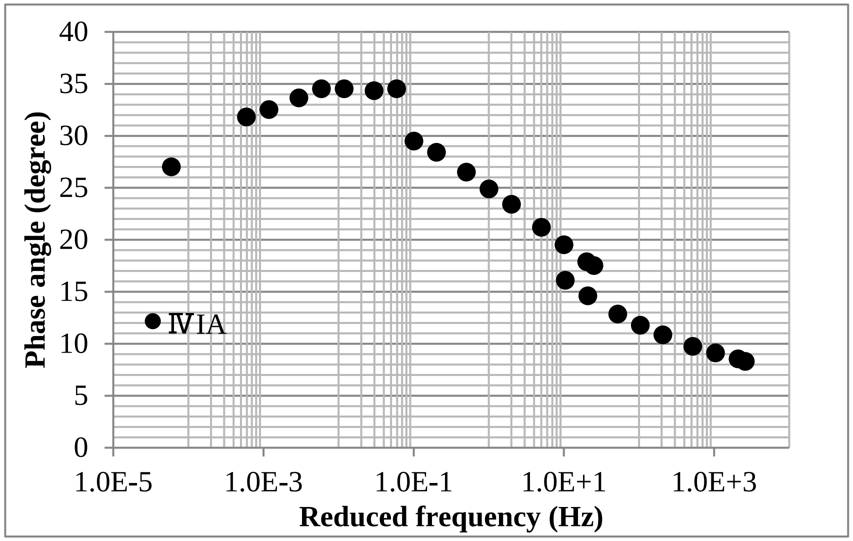

Master Phase Angle Curves for Mixtures from Jefferson Intermediate Type A with RAP

Level 3

Asphalt Binder: Superpave Binder Grading	PG 64-22

Figure 13-55: Mixture Type: IV IBO (Jefferson Intermediate Type B, no RAP)

Level 1

Asphalt Mix: Dynamic Modulus Table						
Temperature (°F)	Mixture |E*| (psi)					
	0.1 Hz	0.5 Hz	1 Hz	5 Hz	10 Hz	25 Hz
14	1737827	2248527	2431608	2764450	2871556	2985191
40	697492	1228768	1478172	2029652	2237562	2476190
70	132641	337848	480677	941533	1180558	1509701
100	23958	63145	97592	257559	375434	585410
130	7299	14791	21325	55430	85618	151325

Asphalt Binder: Superpave Binder Test Data		
Temperature (°F)	Angular freq. = 10 rad/sec	
	G* (Pa)	Delta (degree)
158.0	792.60	88.98
168.8	299.28	89.22
179.6	150.21	89.46

Asphalt General: Volumetric Properties as Built	
Effective Binder (%)	11.43
Air Voids (%)	6.64
Total unit weight	165.50

Level 2

Asphalt Mix: Aggregate Gradation	
Cumulative % Retained ¾" sieve	1
Cumulative % Retained ⅜" sieve	16
Cumulative % Retained #4 sieve	42
% Passing #200 sieve	4.57

Level 3

Asphalt Binder: Superpave Binder Grading	PG 64-22

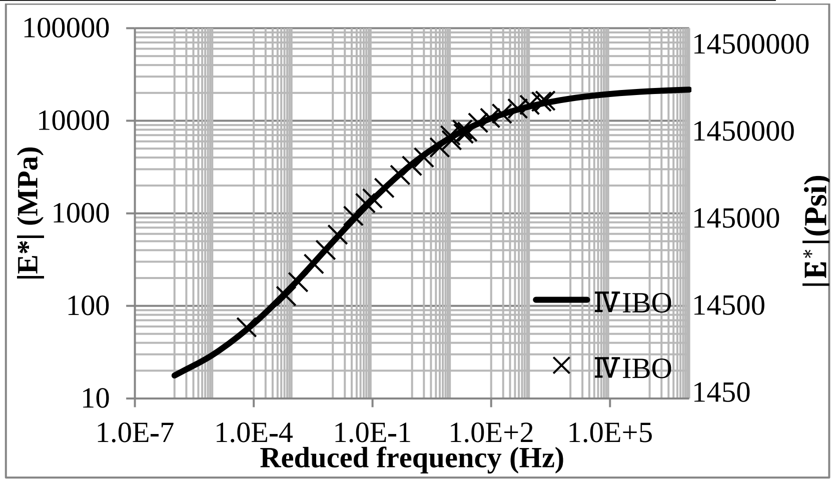

Master Dynamic Modulus Curves for Mixtures from Jefferson Intermediate Type B, no RAP

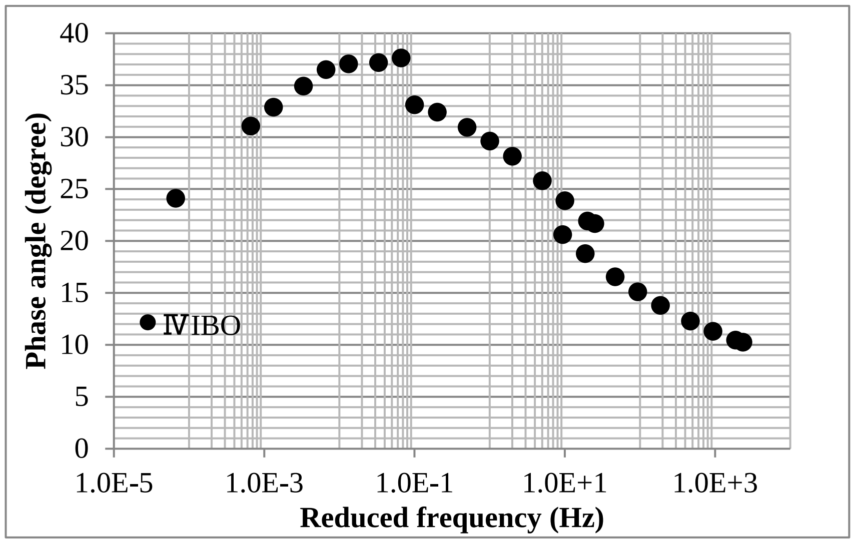

Master Phase Angle Curves for Mixtures from Jefferson Intermediate Type B, no RAP

Figure 13-56: Mixture Type: IV IB (Jefferson Intermediate Type B with RAP)

Level 1

Asphalt Mix: Dynamic Modulus Table						
Temperature (°F)	Mixture |E*| (psi)					
	0.1 Hz	0.5 Hz	1 Hz	5 Hz	10 Hz	25 Hz
14	2238597	2641514	2776257	3010767	3083725	3159962
40	1186388	1756454	1989531	2454935	2616718	2795106
70	324290	677626	882773	1435008	1681377	1992095
100	69277	166812	242257	533130	713627	996700
130	20731	42185	59990	143674	209525	337527

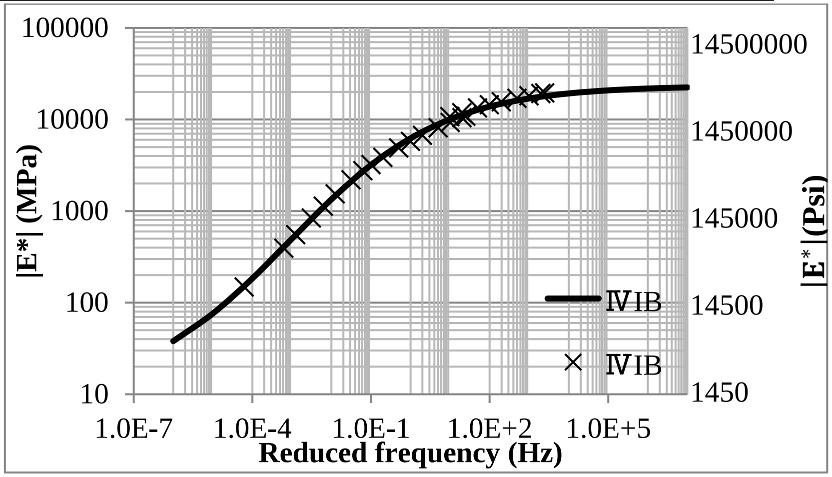

Master Dynamic Modulus Curves for Mixtures from Jefferson Intermediate Type B with RAP

Asphalt Binder: Superpave Binder Test Data		
Temperature (°F)	Angular freq. = 10 rad/sec	
	G* (Pa)	Delta (degree)
158.0	792.60	88.98
168.8	299.28	89.22
179.6	150.21	89.46

Asphalt General: Volumetric Properties as Built	
Effective Binder (%)	9.89
Air Voids (%)	7.74
Total unit weight	166.13

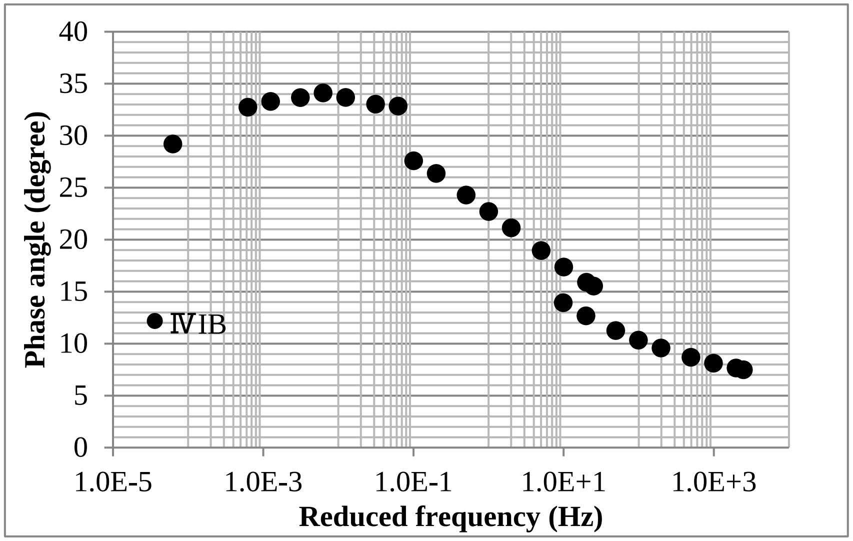

Master Phase Angle Curves for Mixtures from Jefferson Intermediate Type B with RAP

Level 2

Asphalt Mix: Aggregate Gradation	
Cumulative % Retained ¾" sieve	1
Cumulative % Retained ⅜" sieve	17
Cumulative % Retained #4 sieve	43
% Passing #200 sieve	4.8

Level 3

Asphalt Binder: Superpave Binder Grading	PG 64-22

Figure 13-57: Mixture Type: IV ICO (Jefferson Intermediate Type C, no RAP)

Level 1

Asphalt Mix: Dynamic Modulus Table						
Temperature (°F)	Mixture |E*| (psi)					
	0.1 Hz	0.5 Hz	1 Hz	5 Hz	10 Hz	25 Hz
14	1403597	1858112	2038080	2400478	2530564	2678978
40	582275	980652	1175450	1640101	1832526	2069923
70	136369	302548	410227	749300	928156	1183997
100	28634	69662	101892	234035	323646	477714
130	8031	17332	24954	60480	88677	144993

Asphalt Binder: Superpave Binder Test Data		
Temperature (°F)	Angular freq. = 10 rad/sec	
	G* (Pa)	Delta (degree)
158.0	792.60	88.98
168.8	299.28	89.22
179.6	150.21	89.46

Asphalt General: Volumetric Properties as Built	
Effective Binder (%)	12.09
Air Voids (%)	7.60
Total unit weight	165.13

Level 2

Asphalt Mix: Aggregate Gradation	
Cumulative % Retained ¾” sieve	2
Cumulative % Retained ⅜” sieve	23
Cumulative % Retained #4 sieve	45
% Passing #200 sieve	3.84

Level 3

Asphalt Binder: Superpave Binder Grading	PG 64-22

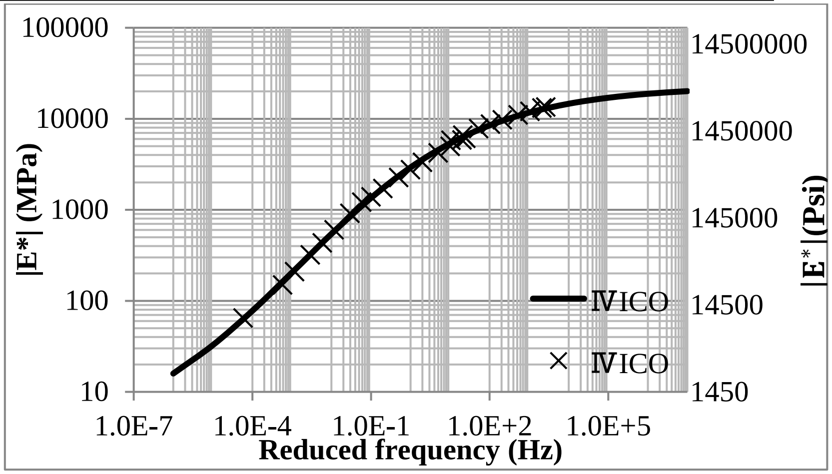

Master Dynamic Modulus Curves for Mixtures from Jefferson Intermediate Type C, no RAP

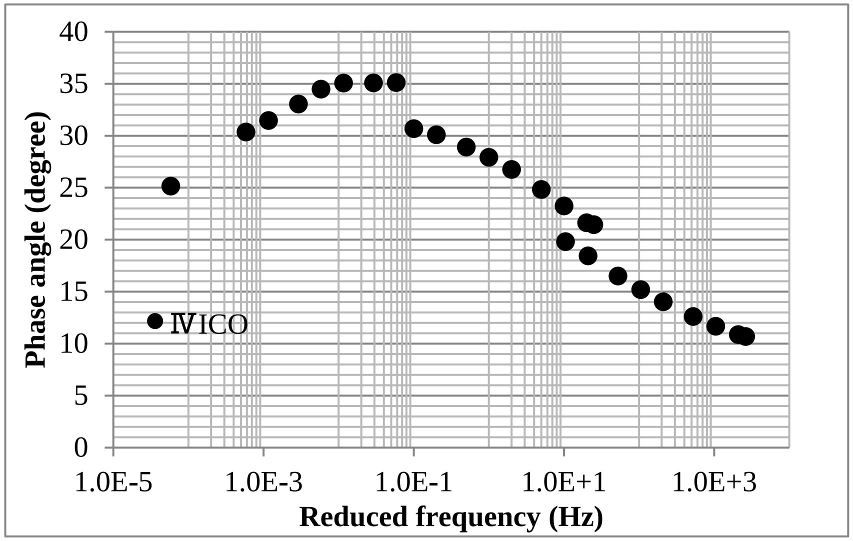

Master Phase Angle Curves for Mixtures from Jefferson Intermediate Type C, no RAP

Figure 13-58: Mixture Type: IV IC (Jefferson Intermediate Type C with RAP)

Level 1

Asphalt Mix: Dynamic Modulus Table						
Temperature (°F)	Mixture |E*| (psi)					
	0.1 Hz	0.5 Hz	1 Hz	5 Hz	10 Hz	25 Hz
14	1711266	2196608	2373090	2699918	2807442	2923326
40	703089	1206595	1441840	1965893	2166370	2399606
70	137758	340072	477175	911972	1136278	1446333
100	23887	63671	97949	252567	364009	560291
130	6571	13993	20469	53875	82961	145275

Asphalt Binder: Superpave Binder Test Data		
Temperature (°F)	Angular freq. = 10 rad/sec	
	G* (Pa)	Delta (degree)
158.0	792.60	88.98
168.8	299.28	89.22
179.6	150.21	89.46

Asphalt General: Volumetric Properties as Built	
Effective Binder (%)	11.10
Air Voids (%)	5.87
Total unit weight	166.38

Level 2

Asphalt Mix: Aggregate Gradation	
Cumulative % Retained ¾” sieve	1
Cumulative % Retained ⅜” sieve	21
Cumulative % Retained #4 sieve	44
% Passing #200 sieve	3.83

Level 3

Asphalt Binder: Superpave Binder Grading	PG 64-22

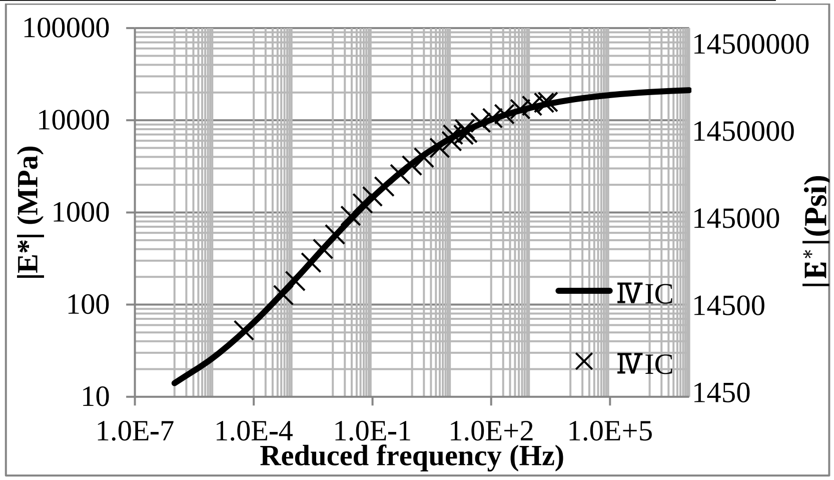

Master Dynamic Modulus Curves for Mixtures from Jefferson Intermediate Type C with RAP

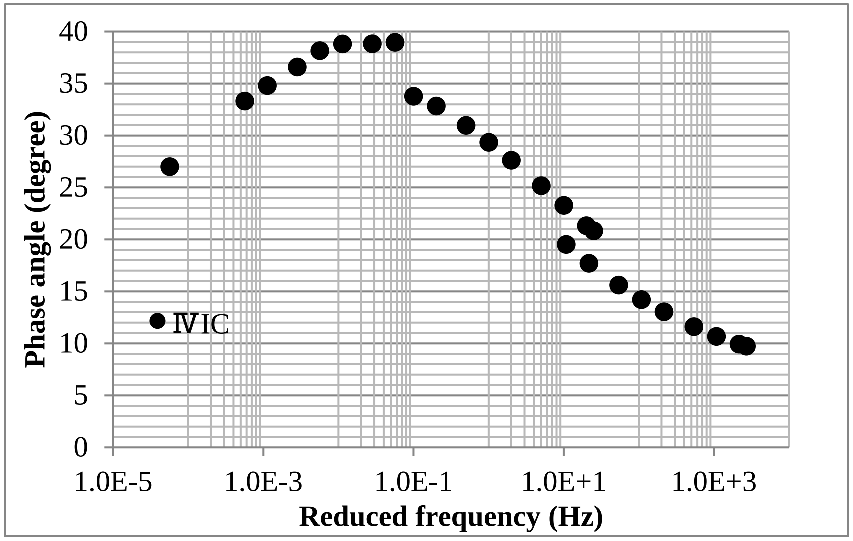

Master Phase Angle Curves for Mixtures from Jefferson Intermediate Type C with RAP

Figure 13-59: Mixture Type: IV SAO (Jefferson Base Type A, no RAP)

Level 1

Asphalt Mix: Dynamic Modulus Table						
Temperature	Mixture |E*| (psi)					
(°F)	0.1 Hz	0.5 Hz	1 Hz	5 Hz	10 Hz	25 Hz
14	1869324	2246506	2377647	2613676	2689630	2770671
40	983738	1465038	1668139	2087771	2238978	2409694
70	291988	586031	755509	1215842	1425028	1693640
100	71647	162839	230374	480921	632968	869910
130	23111	46196	64620	146541	207968	323377

Asphalt Binder: Superpave Binder Test Data		
Temperature	Angular freq. = 10 rad/sec	
(°F)	G* (Pa)	Delta (degree)
158.0	792.60	88.98
168.8	299.28	89.22
179.6	150.21	89.46

Asphalt General: Volumetric Properties as Built	
Effective Binder (%)	10.47
Air Voids (%)	5.56
Total unit weight	167.19

Level 2

Asphalt Mix: Aggregate Gradation	
Cumulative % Retained ¾” sieve	3
Cumulative % Retained ⅜” sieve	37
Cumulative % Retained #4 sieve	54
% Passing #200 sieve	4.01

Level 3

Asphalt Binder: Superpave Binder Grading	PG 64-22

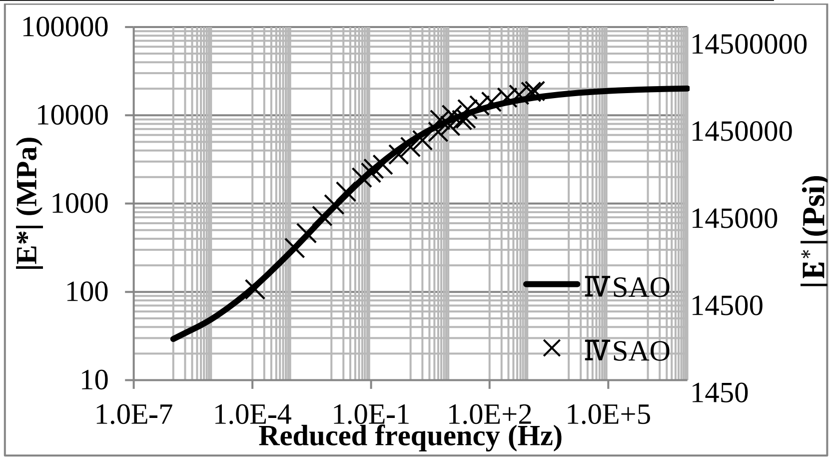

Master Dynamic Modulus Curves for Mixtures from Jefferson Base Type A, no RAP

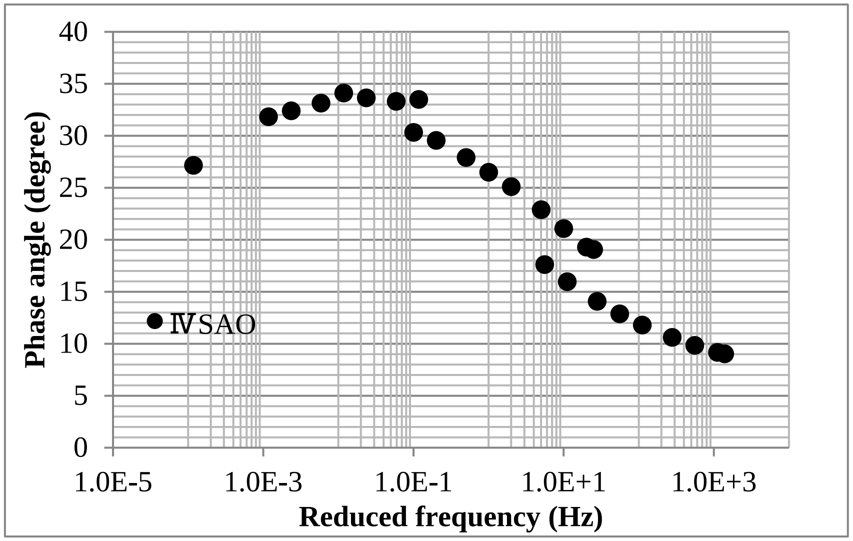

Master Phase Angle Curves for Mixtures from Jefferson Base Type A, no RAP

Figure 13-60: Mixture Type: IV SA (Jefferson Base Type A with RAP)

Level 1

Asphalt Mix: Dynamic Modulus Table						
Temperature (°F)	Mixture |E*| (psi)					
	0.1 Hz	0.5 Hz	1 Hz	5 Hz	10 Hz	25 Hz
14	2027104	2387033	2506378	2712284	2775720	2841575
40	1093015	1608994	1818342	2232560	2375058	2531034
70	313705	642839	832149	1336223	1558491	1836351
100	73255	169328	242433	519511	688901	951554
130	24139	46855	65331	150141	215596	340962

Asphalt Binder: Superpave Binder Test Data		
Temperature (°F)	Angular freq. = 10 rad/sec	
	G* (Pa)	Delta (degree)
158.0	792.60	88.98
168.8	299.28	89.22
179.6	150.21	89.46

Asphalt General: Volumetric Properties as Built	
Effective Binder (%)	11.46
Air Voids (%)	5.22
Total unit weight	165.69

Level 2

Asphalt Mix: Aggregate Gradation	
Cumulative % Retained ¾" sieve	3
Cumulative % Retained ⅜" sieve	37
Cumulative % Retained #4 sieve	50
% Passing #200 sieve	4.86

Level 3

Asphalt Binder: Superpave Binder Grading	PG 64-22

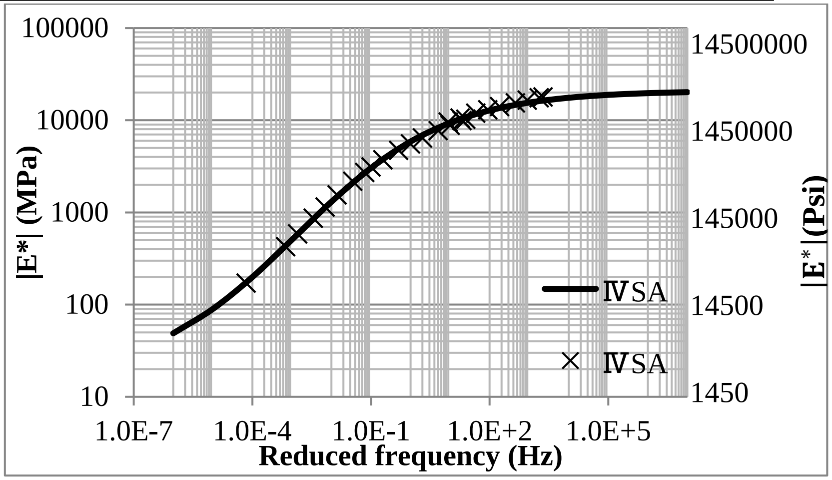

Master Dynamic Modulus Curves for Mixtures from Jefferson Base Type A with RAP

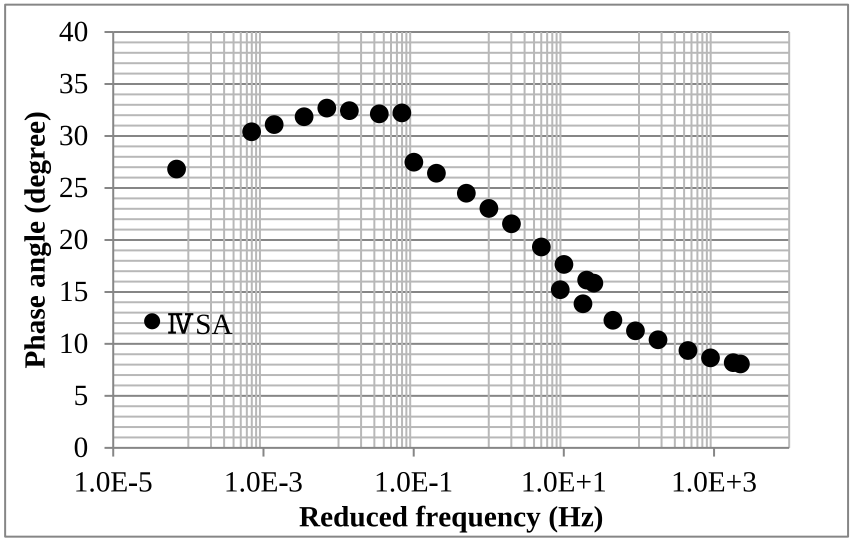

Master Phase Angle Curves for Mixtures from Jefferson Base Type A with RAP

Figure 13-61: Mixture Type: IV SBO (Jefferson Base Type B, no RAP)

Level 1

Asphalt Mix: Dynamic Modulus Table						
Temperature (°F)	Mixture |E*| (psi)					
	0.1 Hz	0.5 Hz	1 Hz	5 Hz	10 Hz	25 Hz
14	1736930	2141727	2284542	2543546	2627267	2716684
40	829787	1307609	1517550	1963577	2127674	2314679
70	210357	456737	608680	1048233	1258426	1536096
100	46224	110020	160193	361712	493055	708235
130	14628	29153	41079	97082	141624	229876

Asphalt Binder: Superpave Binder Test Data		
Temperature (°F)	Angular freq. = 10 rad/sec	
	G* (Pa)	Delta (degree)
158.0	792.60	88.98
168.8	299.28	89.22
179.6	150.21	89.46

Asphalt General: Volumetric Properties as Built	
Effective Binder (%)	12.34
Air Voids (%)	6.00
Total unit weight	165.50

Level 2

Asphalt Mix: Aggregate Gradation	
Cumulative % Retained ¾" sieve	3
Cumulative % Retained ⅜" sieve	37
Cumulative % Retained #4 sieve	56
% Passing #200 sieve	5.25

Level 3

Asphalt Binder: Superpave Binder Grading	PG 64-22

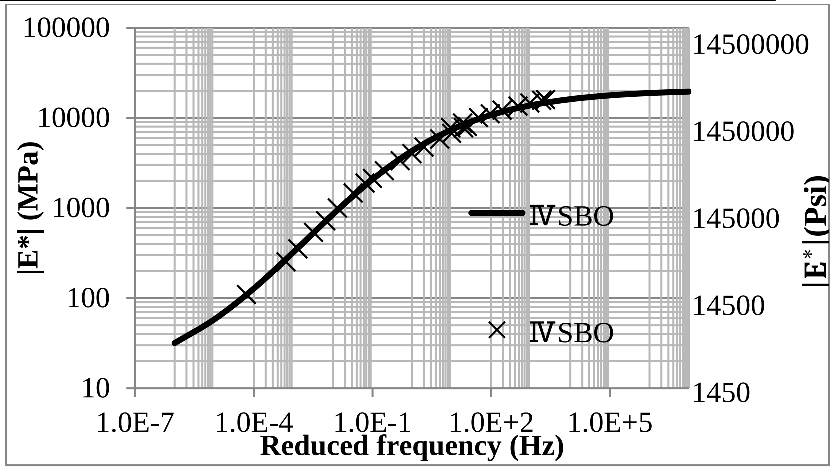

Master Dynamic Modulus Curves for Mixtures from Jefferson Base Type B, no RAP

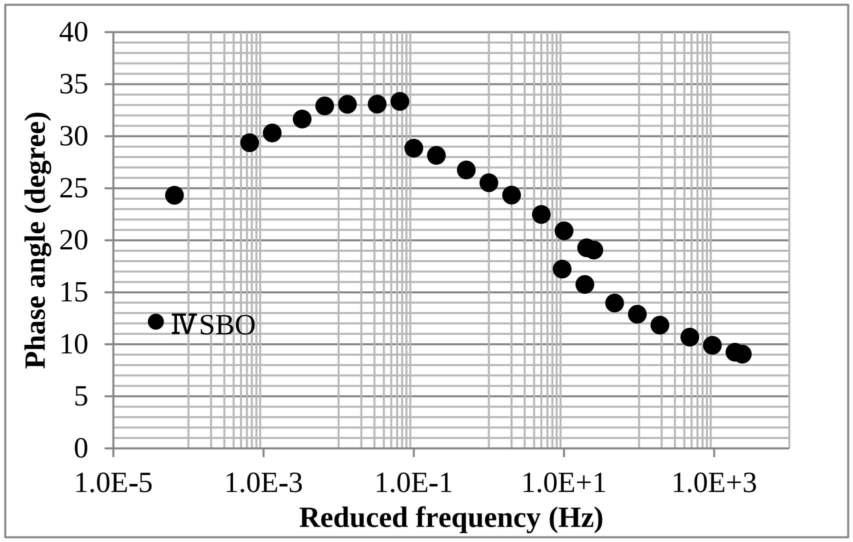

Master Phase Angle Curves for Mixtures from Jefferson Base Type B, no RAP

Figure 13-62: Mixture Type: IV SB (Jefferson Base Type B with RAP)

Level 1

Asphalt Mix: Dynamic Modulus Table						
Temperature (°F)	Mixture |E*| (psi)					
	0.1 Hz	0.5 Hz	1 Hz	5 Hz	10 Hz	25 Hz
14	1869324	2246506	2377647	2613676	2689630	2770671
40	983738	1465038	1668139	2087771	2238978	2409694
70	291988	586031	755509	1215842	1425028	1693640
100	71647	162839	230374	480921	632968	869910
130	23111	46196	64620	146541	207968	323377

Asphalt Binder: Superpave Binder Test Data		
Temperature (°F)	Angular freq. = 10 rad/sec	
	G* (Pa)	Delta (degree)
158.0	792.60	88.98
168.8	299.28	89.22
179.6	150.21	89.46

Asphalt General: Volumetric Properties as Built	
Effective Binder (%)	11.46
Air Voids (%)	6.51
Total unit weight	166.13

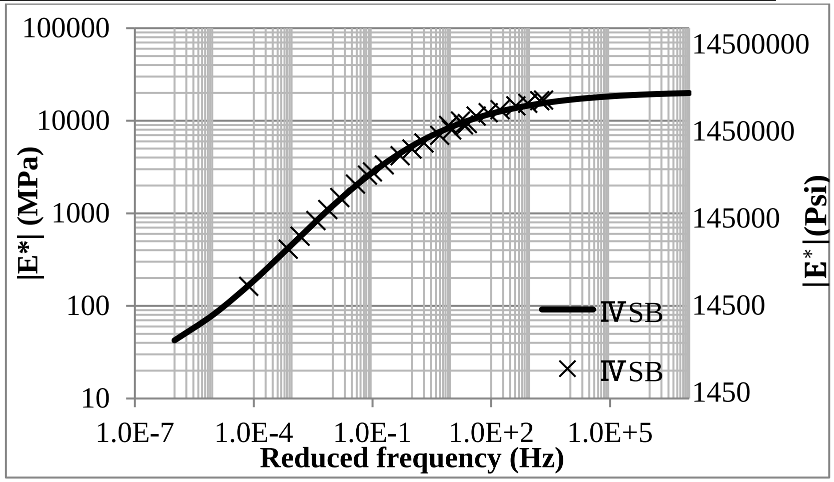

Master Dynamic Modulus Curves for Mixtures from Jefferson Base Type B with RAP

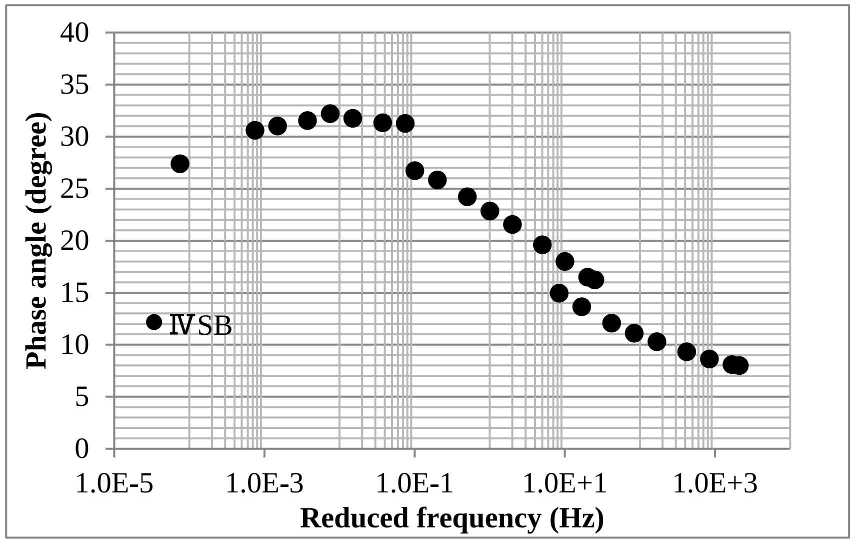

Master Phase Angle Curves for Mixtures from Jefferson Base Type B with RAP

Level 2

Asphalt Mix: Aggregate Gradation	
Cumulative % Retained ¾” sieve	3
Cumulative % Retained ⅜” sieve	37
Cumulative % Retained #4 sieve	51
% Passing #200 sieve	3.87

Level 3

Asphalt Binder: Superpave Binder Grading	PG 64-22

Figure 13-63: Mixture Type: V A (Liberty Surface Type A with RAP)

Level 1

Asphalt Mix: Dynamic Modulus Table						
Temperature (°F)	Mixture |E*| (psi)					
	0.1 Hz	0.5 Hz	1 Hz	5 Hz	10 Hz	25 Hz
14	1952642	2263926	2382891	2621653	2708671	2810042
40	1151091	1513142	1668846	2012660	2148915	2315394
70	463619	719578	850656	1190384	1345865	1553306
100	156934	270386	338227	547222	659903	828135
130	57111	97456	123630	214654	270477	362931

Asphalt Binder: Superpave Binder Test Data		
Temperature (°F)	Angular freq. = 10 rad/sec	
	G* (Pa)	Delta (degree)
158.0	2995.00	63.70
168.8	1501.00	61.90
179.6	750.50	60.00

Asphalt General: Volumetric Properties as Built	
Effective Binder (%)	11.21
Air Voids (%)	4.55
Total unit weight	167.06

Level 2

Asphalt Mix: Aggregate Gradation	
Cumulative % Retained ¾" sieve	0
Cumulative % Retained ⅜" sieve	15
Cumulative % Retained #4 sieve	54
% Passing #200 sieve	4.06

Level 3

Asphalt Binder: Superpave Binder Grading	PG 76-22

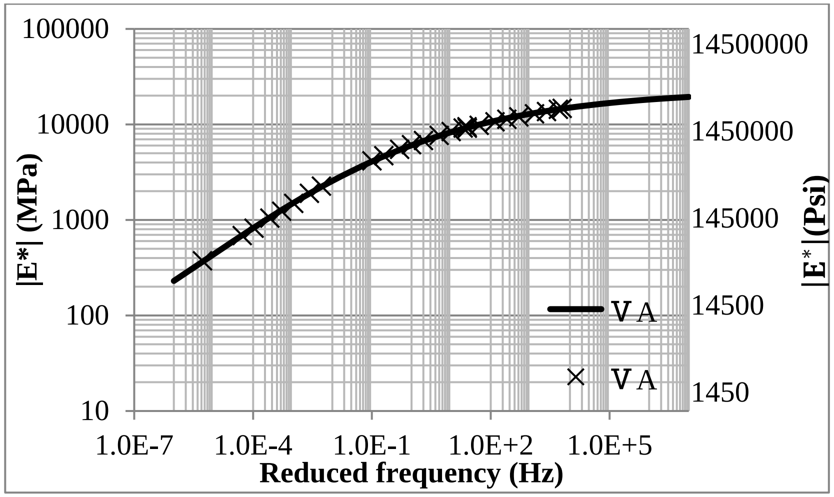

Master Dynamic Modulus Curves for Mixtures from Liberty Surface Type A with RAP

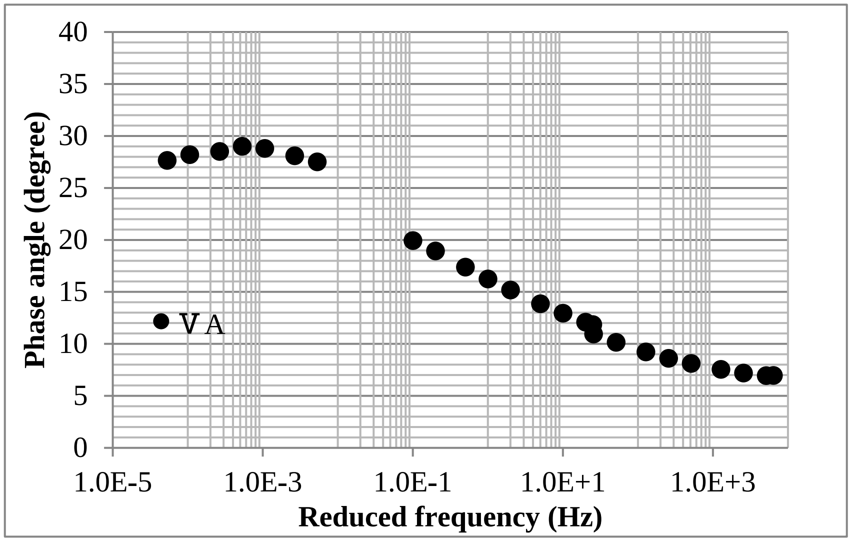

Master Phase Angle Curves for Mixtures from Liberty Surface Type A with RAP

Figure 13-64: Mixture Type: V AO (Liberty Surface Type A, no RAP)

Level 1

Asphalt Mix: Dynamic Modulus Table						
Temperature (°F)	Mixture |E*| (psi)					
	0.1 Hz	0.5 Hz	1 Hz	5 Hz	10 Hz	25 Hz
14	2443975	2749563	2850432	3025823	3080680	3138391
40	1469562	1968215	2163148	2544060	2675167	2819752
70	505494	880564	1079594	1584145	1801157	2071502
100	145602	274260	361523	661076	833250	1093870
130	58234	93586	119003	220434	290907	417926

Asphalt Binder: Superpave Binder Test Data		
Temperature (°F)	Angular freq. = 10 rad/sec	
	G* (Pa)	Delta (degree)
158.0	2995.00	63.70
168.8	1501.00	61.90
179.6	750.50	60.00

Asphalt General: Volumetric Properties as Built	
Effective Binder (%)	11.28
Air Voids (%)	5.25
Total unit weight	167.31

Level 2

Asphalt Mix: Aggregate Gradation	
Cumulative % Retained ¾” sieve	0
Cumulative % Retained ⅜” sieve	14
Cumulative % Retained #4 sieve	52
% Passing #200 sieve	3.48

Level 3

Asphalt Binder: Superpave Binder Grading	PG 76-22

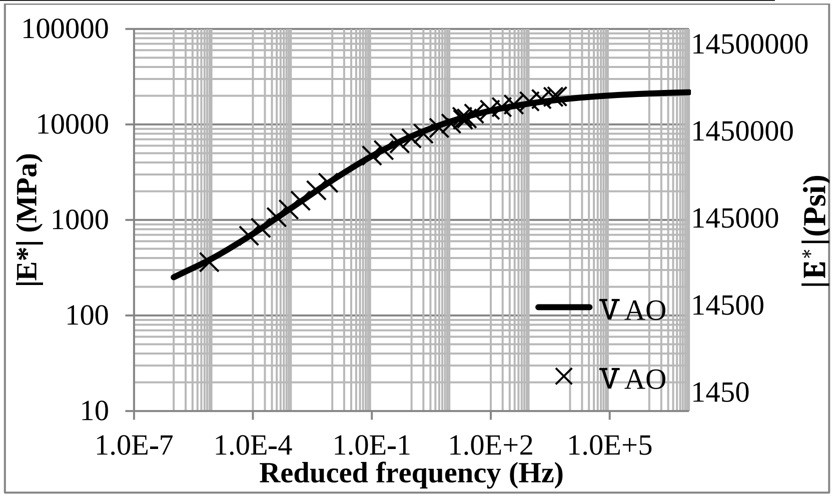

Master Dynamic Modulus Curves for Mixtures from Liberty Surface Type A, no RAP

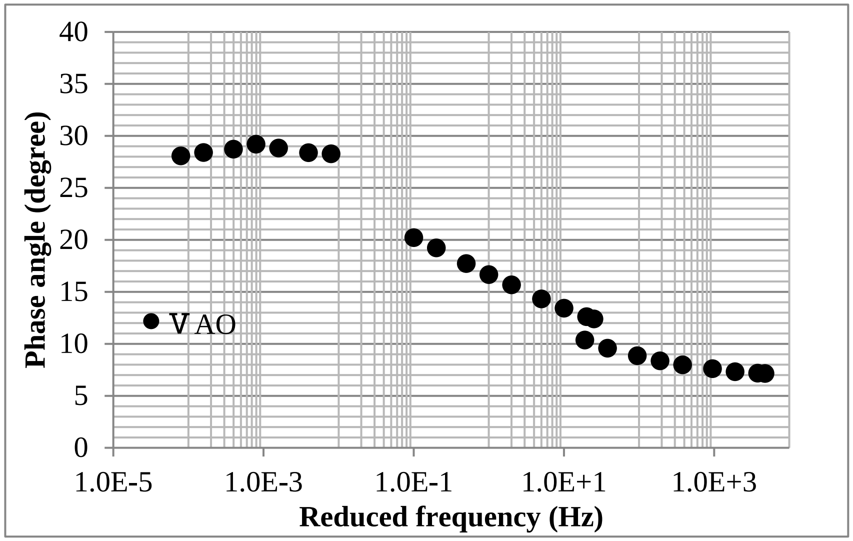

Master Phase Angle Curves for Mixtures from Liberty Surface Type A, no RAP

Figure 13-65: Mixture Type: V AG (Liberty Surface Type A with Long-Term Aging and RAP)

Level 1

Asphalt Mix: Dynamic Modulus Table						
Temperature (°F)	Mixture |E*| (psi)					
	0.1 Hz	0.5 Hz	1 Hz	5 Hz	10 Hz	25 Hz
14	2288393	2645573	2766283	2979520	3047104	3118682
40	1281333	1799724	2010512	2434638	2584236	2751328
70	404944	747735	938166	1441733	1666247	1951837
100	109909	218775	295458	570065	733762	987670
130	41828	70718	92129	180850	244554	362154

Asphalt Binder: Superpave Binder Test Data		
Temperature (°F)	Angular freq. = 10 rad/sec	
	G* (Pa)	Delta (degree)
158.0	2995.00	63.70
168.8	1501.00	61.90
179.6	750.50	60.00

Asphalt General: Volumetric Properties as Built	
Effective Binder (%)	11.21
Air Voids (%)	4.55
Total unit weight	167.06

Level 2

Asphalt Mix: Aggregate Gradation	
Cumulative % Retained ¾" sieve	0
Cumulative % Retained ⅜" sieve	15
Cumulative % Retained #4 sieve	54
% Passing #200 sieve	4.06

Level 3

Asphalt Binder: Superpave Binder Grading	PG 76-22

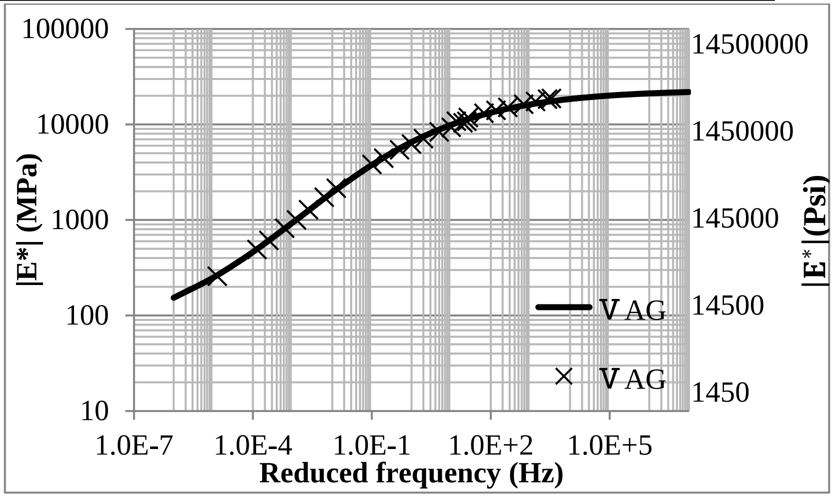

Master Dynamic Modulus Curves for Mixtures from Liberty Surface Type A with Long-Term Aging and RAP

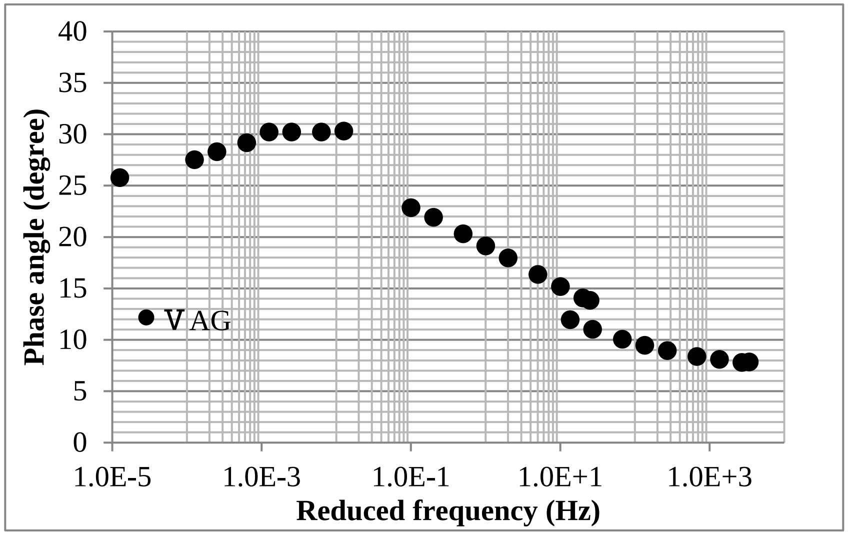

Master Phase Angle Curves for Mixtures from Liberty Surface Type A with Long-Term Aging and RAP

Figure 13-66: Mixture Type: V AN (Liberty Surface Type A with Asphalt Source 2 and RAP)

Level 1

Asphalt Mix: Dynamic Modulus Table						
Temperature (°F)	Mixture |E*| (psi)					
	0.1 Hz	0.5 Hz	1 Hz	5 Hz	10 Hz	25 Hz
14	1745403	2172679	2333478	2644573	2752309	2872730
40	816996	1258643	1461572	1920526	2101920	2319598
70	224338	439347	569427	953819	1146208	1412498
100	57897	118626	162530	328629	434696	610329
130	20743	36736	48614	98353	134760	203765

Asphalt Binder: Superpave Binder Test Data		
Temperature (°F)	Angular freq. = 10 rad/sec	
	G* (Pa)	Delta (degree)
158.0	2995.00	63.70
168.8	1501.00	61.90
179.6	750.50	60.00

Asphalt General: Volumetric Properties as Built	
Effective Binder (%)	11.28
Air Voids (%)	6.39
Total unit weight	167.06

Level 2

Asphalt Mix: Aggregate Gradation	
Cumulative % Retained ¾” sieve	0
Cumulative % Retained ⅜” sieve	14
Cumulative % Retained #4 sieve	52
% Passing #200 sieve	3.48

Level 3

Asphalt Binder: Superpave Binder Grading	PG 76-22

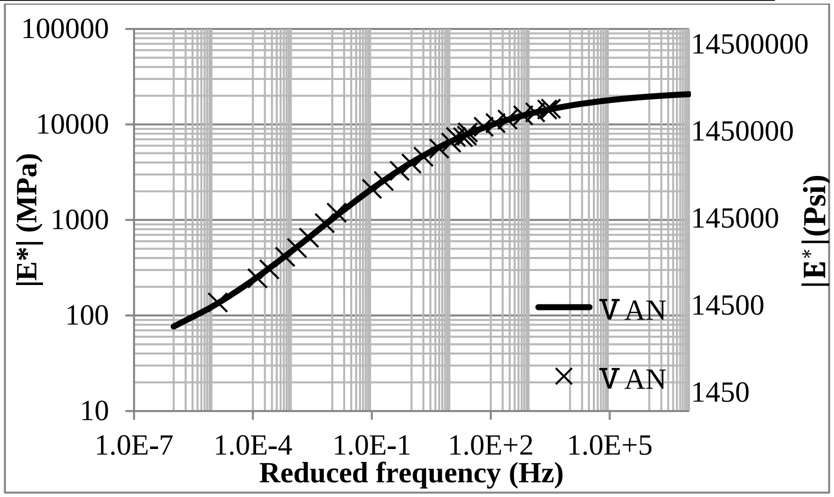

Master Dynamic Modulus Curves for Mixtures from Liberty Surface Type A with Asphalt Source 2 and RAP

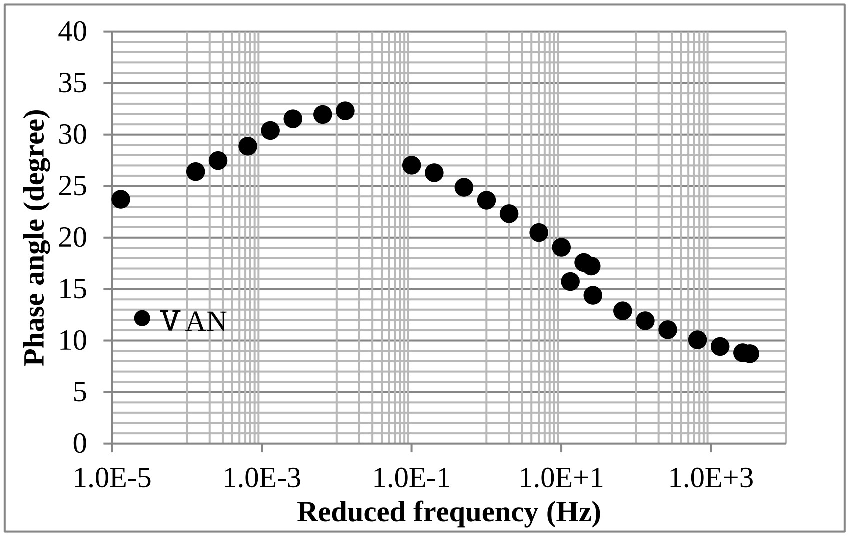

Master Phase Angle Curves for Mixtures from Liberty Surface Type A with Asphalt Source 2 and RAP

Figure 13-67: Mixture Type: V AOG (Liberty Surface Type A with Long-Term Aging, no RAP)

Level 1

Asphalt Mix: Dynamic Modulus Table						
Temperature (°F)	Mixture |E*| (psi)					
	0.1 Hz	0.5 Hz	1 Hz	5 Hz	10 Hz	25 Hz
14	2166760	2529564	2655842	2885131	2959936	3040656
40	1233106	1723353	1925370	2339781	2489407	2659431
70	422591	759798	942731	1419981	1631920	1902457
100	120863	242392	325189	609192	772307	1019661
130	43503	78637	104508	208977	281452	410906

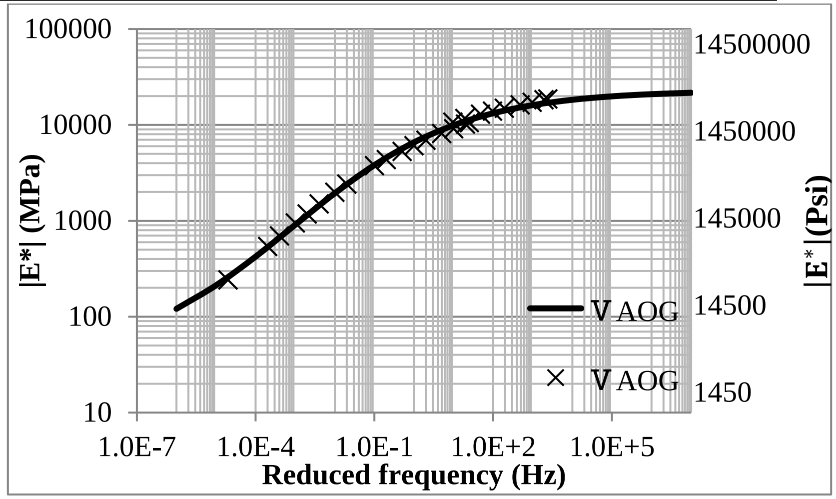

Master Dynamic Modulus Curves for Mixtures from Liberty Surface Type A with Long-Term Aging, no RAP

Asphalt Binder: Superpave Binder Test Data		
Temperature (°F)	Angular freq. = 10 rad/sec	
	G* (Pa)	Delta (degree)
158.0	2995.00	63.70
168.8	1501.00	61.90
179.6	750.50	60.00

Asphalt General: Volumetric Properties as Built	
Effective Binder (%)	11.28
Air Voids (%)	6.21
Total unit weight	167.31

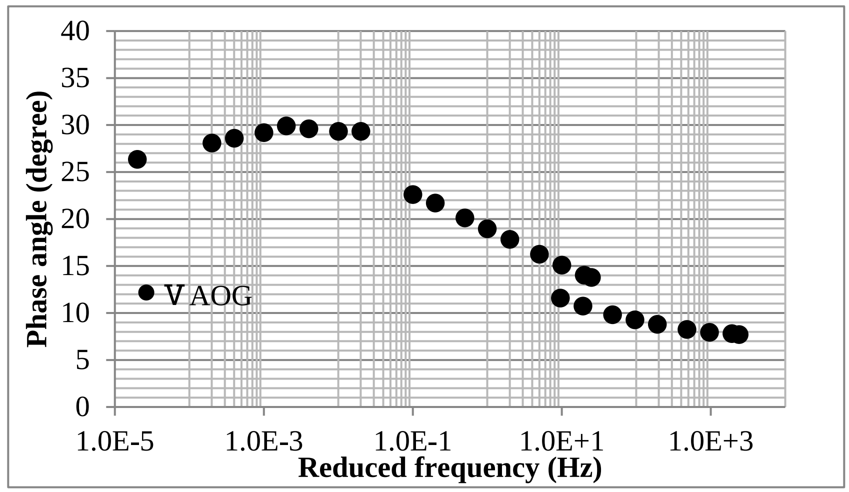

Master Phase Angle Curves for Mixtures from Liberty Surface Type A with Long-Term Aging, no RAP

Level 2

Asphalt Mix: Aggregate Gradation	
Cumulative % Retained ¾" sieve	0
Cumulative % Retained ⅜" sieve	14
Cumulative % Retained #4 sieve	52
% Passing #200 sieve	3.48

Level 3

Asphalt Binder: Superpave Binder Grading	PG 76-22

Figure 13-68: Mixture Type: V AON (Liberty Surface Type A with Asphalt Source 2, no RAP)

Level 1

Asphalt Mix: Dynamic Modulus Table						
Temperature (°F)	Mixture |E*| (psi)					
	0.1 Hz	0.5 Hz	1 Hz	5 Hz	10 Hz	25 Hz
14	1867974	2338692	2505075	2805556	2901924	3004135
40	819447	1346990	1586802	2107014	2300773	2522218
70	186008	415855	566181	1029116	1262184	1579004
100	42502	94422	136103	313074	435864	647658
130	15948	27770	37174	80921	116300	188739

Asphalt Binder: Superpave Binder Test Data		
Temperature (°F)	Angular freq. = 10 rad/sec	
	G* (Pa)	Delta (degree)
158.0	2995.00	63.70
168.8	1501.00	61.90
179.6	750.50	60.00

Asphalt General: Volumetric Properties as Built	
Effective Binder (%)	11.28
Air Voids (%)	6.21
Total unit weight	167.31

Level 2

Asphalt Mix: Aggregate Gradation	
Cumulative % Retained ¾" sieve	0
Cumulative % Retained ⅜" sieve	14
Cumulative % Retained #4 sieve	52
% Passing #200 sieve	3.48

Level 3

Asphalt Binder: Superpave Binder Grading	PG 76-22

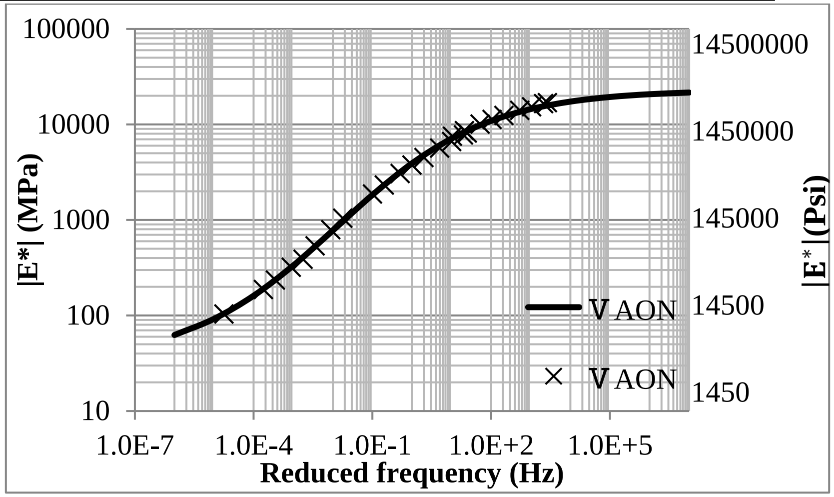

Master Dynamic Modulus Curves for Mixtures from Liberty Surface Type A with Asphalt Source 2, no RAP

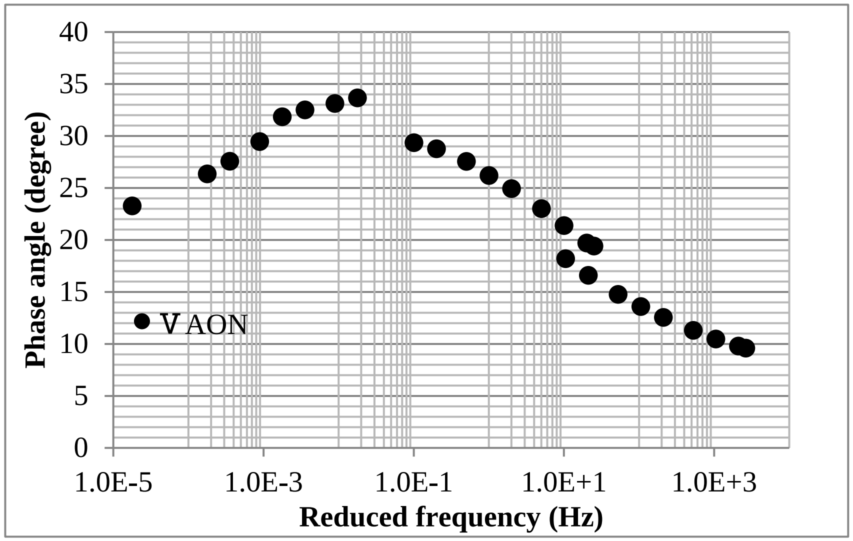

Master Phase Angle Curves for Mixtures from Liberty Surface Type A with Asphalt Source 2, no RAP

Figure 13-69: Mixture Type: V BG (Liberty Surface Type B with Long-Term Aging and RAP)

Level 1

Asphalt Mix: Dynamic Modulus Table						
Temperature (°F)	Mixture |E*| (psi)					
	0.1 Hz	0.5 Hz	1 Hz	5 Hz	10 Hz	25 Hz
14	2388388	2721503	2829898	3014876	3071404	3129890
40	1391536	1922279	2131016	2536065	2673430	2822845
70	461929	837174	1042734	1573041	1802247	2086445
100	137223	260401	346655	652836	833014	1108348
130	59406	93481	118444	220794	293721	427502

Asphalt Binder: Superpave Binder Test Data		
Temperature (°F)	Angular freq. = 10 rad/sec	
	G* (Pa)	Delta (degree)
158.0	792.60	88.98
168.8	299.28	89.22
179.6	150.21	89.46

Asphalt General: Volumetric Properties as Built	
Effective Binder (%)	11.61
Air Voids (%)	3.61
Total unit weight	167.00

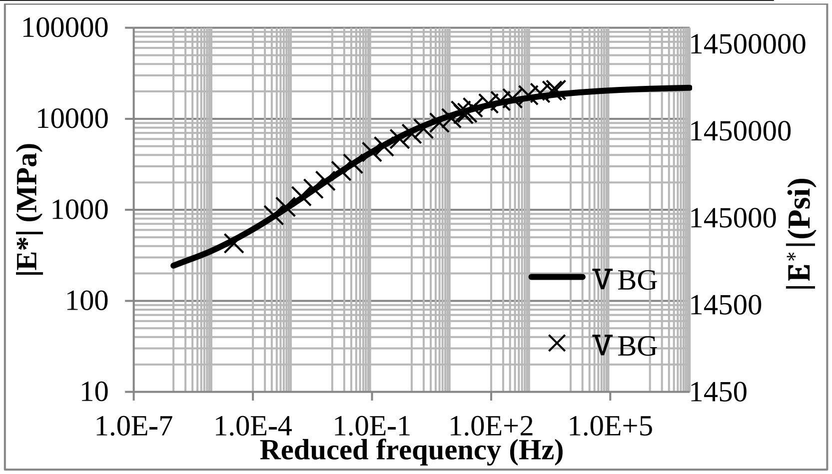

Master Dynamic Modulus Curves for Mixtures from Liberty Surface Type B with Long-Term Aging and RAP

Level 2

Asphalt Mix: Aggregate Gradation	
Cumulative % Retained ¾” sieve	0
Cumulative % Retained ⅜” sieve	7
Cumulative % Retained #4 sieve	39
% Passing #200 sieve	4.57

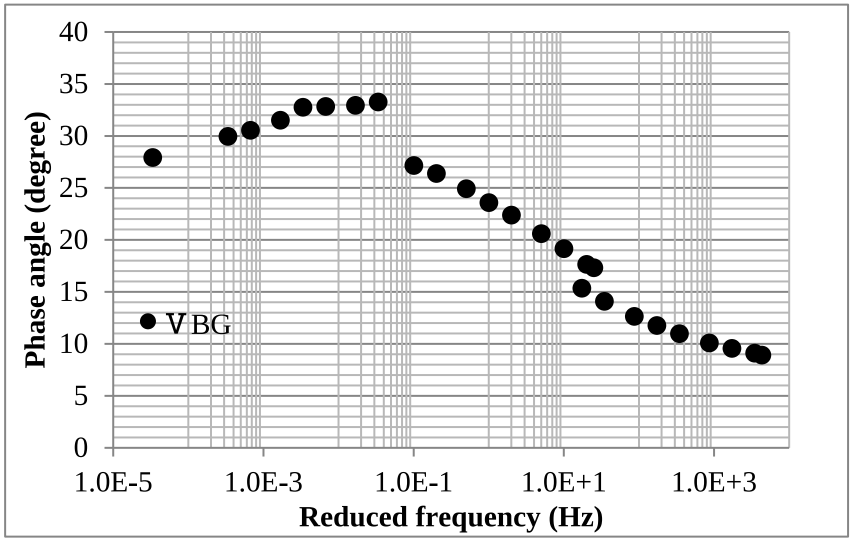

Master Phase Angle Curves for Mixtures from Liberty Surface Type B with Long-Term Aging and RAP

Level 3

Asphalt Binder: Superpave Binder Grading	PG 64-22

Figure 13-70: Mixture Type: V BO (Liberty Surface Type B, no RAP)

Level 1

Asphalt Mix: Dynamic Modulus Table						
Temperature (°F)	Mixture |E*| (psi)					
	0.1 Hz	0.5 Hz	1 Hz	5 Hz	10 Hz	25 Hz
14	1770175	2069349	2187390	2431431	2523028	2631773
40	1083647	1402353	1542336	1859262	1988288	2148964
70	511083	739034	854103	1151853	1288993	1473652
100	226628	344929	411677	607940	710427	861234
130	110402	164141	196244	298920	357717	450993

Asphalt Binder: Superpave Binder Test Data		
Temperature (°F)	Angular freq. = 10 rad/sec	
	G* (Pa)	Delta (degree)
158.070	2995	63.7
168.876	1501	61.9
179.682	750	60.0

Asphalt General: Volumetric Properties as Built	
Effective Binder (%)	11.93
Air Voids (%)	11.50
Total unit weight	167.12

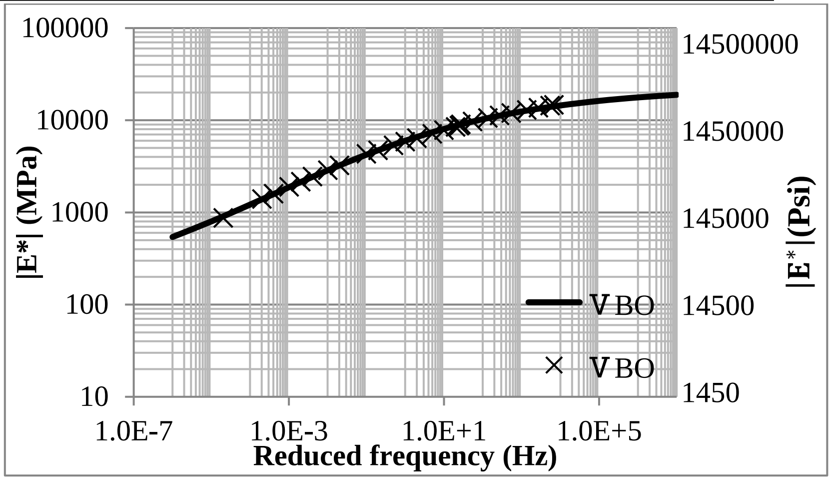

Master Dynamic Modulus Curves for Mixtures from Liberty Surface Type B, no RAP

Level 2

Asphalt Mix: Aggregate Gradation	
Cumulative % Retained ¾" sieve	0
Cumulative % Retained ⅜" sieve	6
Cumulative % Retained #4 sieve	8
% Passing #200 sieve	3.97

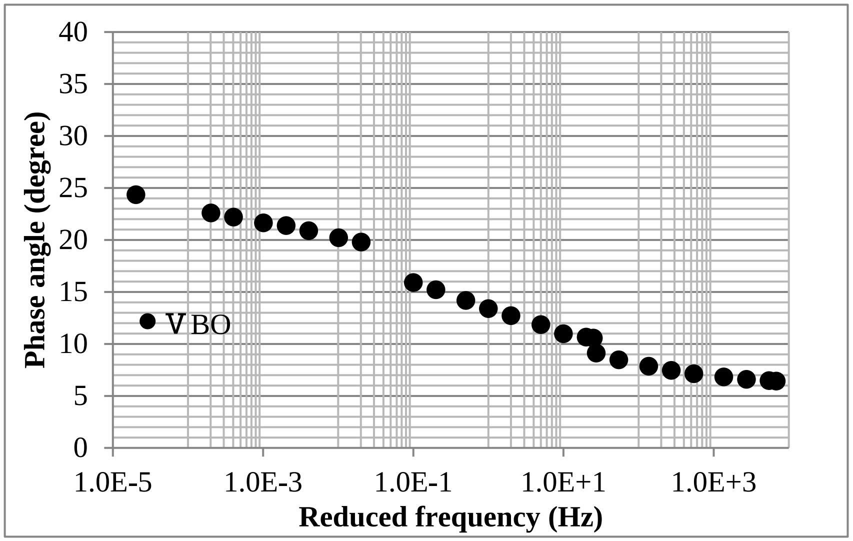

Master Phase Angle Curves for Mixtures from Liberty Surface Type B, no RAP

Level 3

Asphalt Binder: Superpave Binder Grading	PG 64-22

Figure 13-71: Mixture Type: V BN (Liberty Surface Type B with Asphalt Source 2 and RAP)

Level 1

Asphalt Mix: Dynamic Modulus Table						
Temperature (°F)	Mixture |E*| (psi)					
	0.1 Hz	0.5 Hz	1 Hz	5 Hz	10 Hz	25 Hz
14	2091271	2508227	2648455	2891937	2967161	3045225
40	1076419	1629865	1862569	2334437	2499707	2681937
70	310425	627483	816616	1342357	1583237	1891070
100	85447	177206	246214	511896	679073	945541
130	35428	59623	78321	160612	223038	342928

Asphalt Binder: Superpave Binder Test Data		
Temperature (°F)	Angular freq. = 10 rad/sec	
	G* (Pa)	Delta (degree)
158.0	792.60	88.98
168.8	299.28	89.22
179.6	150.21	89.46

Asphalt General: Volumetric Properties as Built	
Effective Binder (%)	11.93
Air Voids (%)	5.33
Total unit weight	165.63

Level 2

Asphalt Mix: Aggregate Gradation	
Cumulative % Retained ¾" sieve	0
Cumulative % Retained ⅜" sieve	6
Cumulative % Retained #4 sieve	8
% Passing #200 sieve	3.97

Level 3

Asphalt Binder: Superpave Binder Grading	PG 64-22

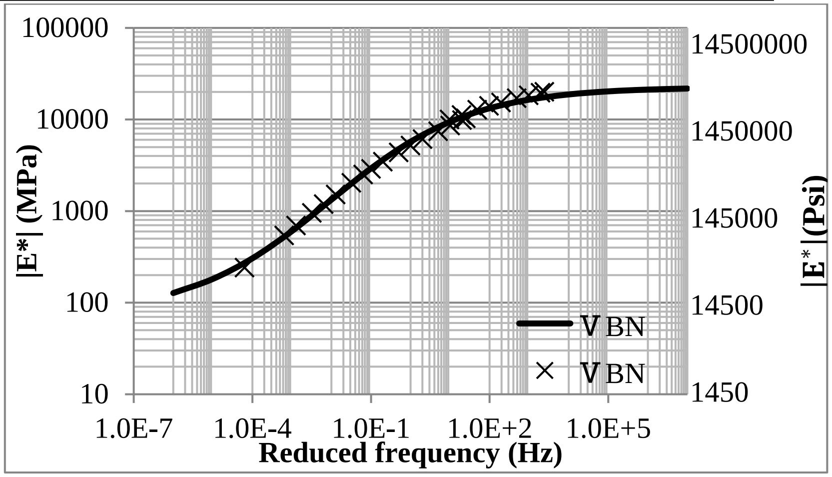

Master Dynamic Modulus Curves for Mixtures from Liberty Surface Type B with Asphalt Source 2 and RAP

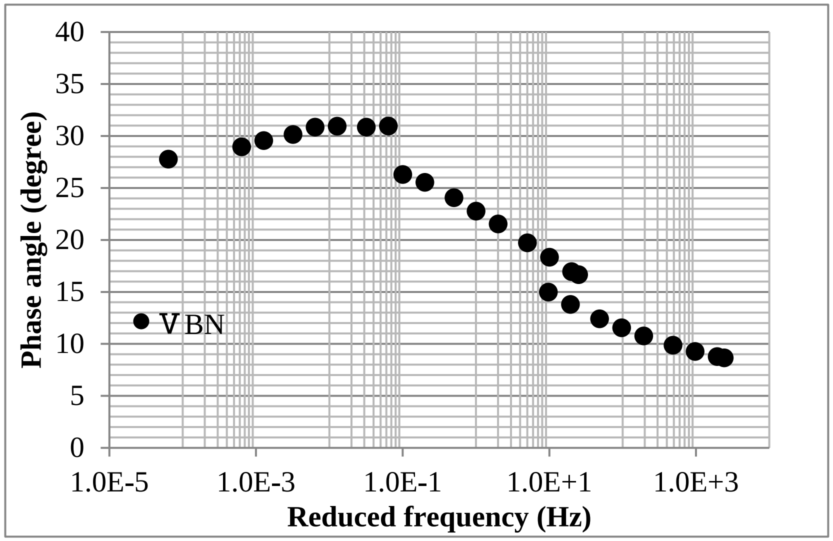

Master Phase Angle Curves for Mixtures from Liberty Surface Type B with Asphalt Source 2 and RAP

Figure 13-72: Mixture Type: V BOG (Liberty Surface Type B with Long-Term Aging, no RAP)

Level 1

Asphalt Mix: Dynamic Modulus Table						
Temperature (°F)	Mixture |E*| (psi)					
	0.1 Hz	0.5 Hz	1 Hz	5 Hz	10 Hz	25 Hz
14	1951155	2364225	2510038	2776035	2862812	2956196
40	958565	1462184	1680935	2144920	2316309	2512750
70	250684	519655	681476	1143029	1362687	1653471
100	55947	127086	181302	393082	528933	750482
130	17805	34169	47187	106087	151680	240659

Asphalt Binder: Superpave Binder Test Data		
Temperature (°F)	Angular freq. = 10 rad/sec	
	G* (Pa)	Delta (degree)
158.0	792.60	88.98
168.8	299.28	89.22
179.6	150.21	89.46

Asphalt General: Volumetric Properties as Built	
Effective Binder (%)	11.93
Air Voids (%)	6.96
Total unit weight	167.12

Level 2

Asphalt Mix: Aggregate Gradation	
Cumulative % Retained ¾" sieve	0
Cumulative % Retained ⅜" sieve	6
Cumulative % Retained #4 sieve	8
% Passing #200 sieve	3.97

Level 3

Asphalt Binder: Superpave Binder Grading	PG 64-22

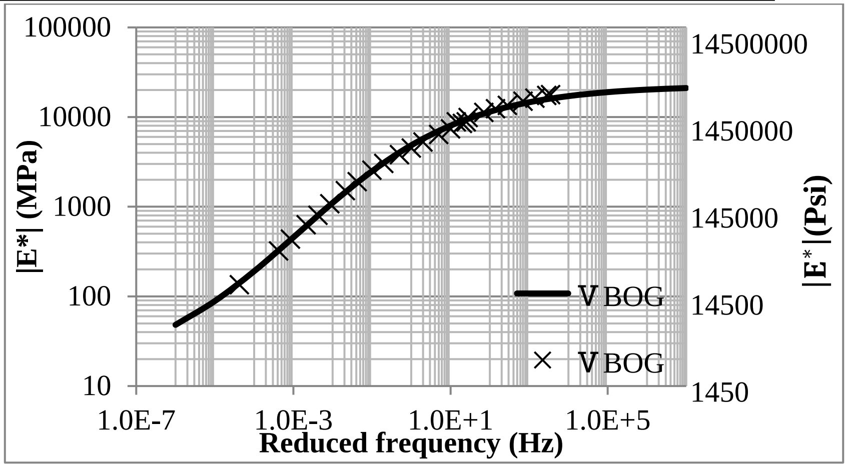

Master Dynamic Modulus Curves for Mixtures from Liberty Surface Type B with Long-Term Aging, no RAP

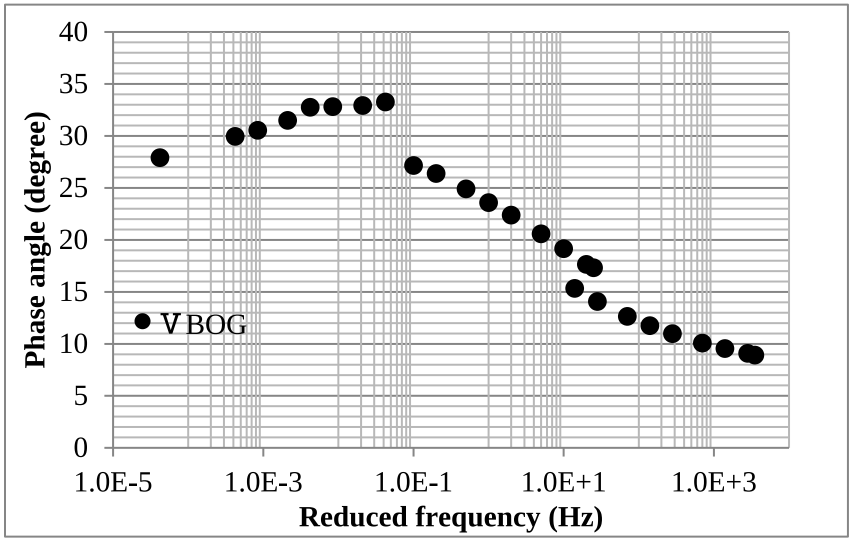

Master Phase Angle Curves for Mixtures from Liberty Surface Type B with Long-Term Aging, no RAP

Figure 13-73: Mixture Type: V BON (Liberty Surface Type B with Asphalt Source 2, no RAP)

Level 1

Asphalt Mix: Dynamic Modulus Table						
Temperature (°F)	Mixture |E*| (psi)					
	0.1 Hz	0.5 Hz	1 Hz	5 Hz	10 Hz	25 Hz
14	1667708	2169659	2352023	2686851	2795515	2911310
40	691200	1197019	1436396	1971252	2174992	2410299
70	154057	359494	498642	941981	1171211	1487439
100	35950	82559	120884	288100	406555	613469
130	13574	24463	33321	75661	110623	183140

Asphalt Binder: Superpave Binder Test Data		
Temperature (°F)	Angular freq. = 10 rad/sec	
	G* (Pa)	Delta (degree)
158.0	792.60	88.98
168.8	299.28	89.22
179.6	150.21	89.46

Asphalt General: Volumetric Properties as Built	
Effective Binder (%)	11.93
Air Voids (%)	6.96
Total unit weight	167.12

Level 2

Asphalt Mix: Aggregate Gradation	
Cumulative % Retained ¾” sieve	0
Cumulative % Retained ⅜” sieve	6
Cumulative % Retained #4 sieve	38
% Passing #200 sieve	3.97

Level 3

Asphalt Binder: Superpave Binder Grading	PG 64-22

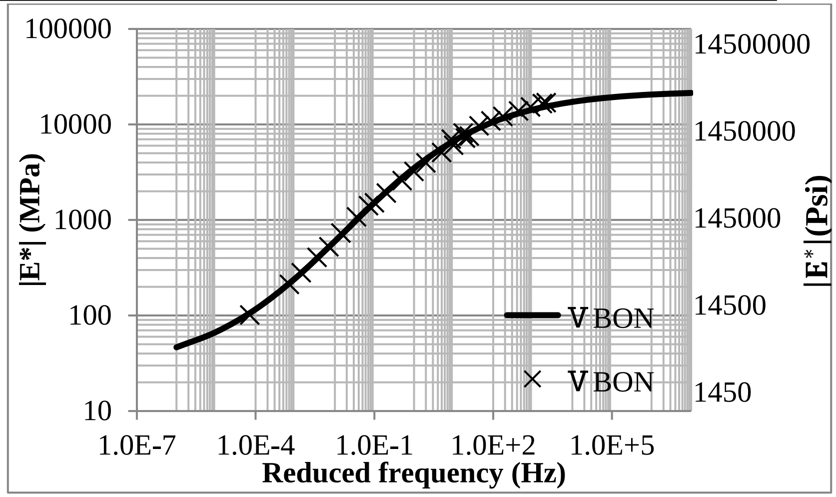

Master Dynamic Modulus Curves for Mixtures from Liberty Surface Type B with Asphalt Source 2, no RAP

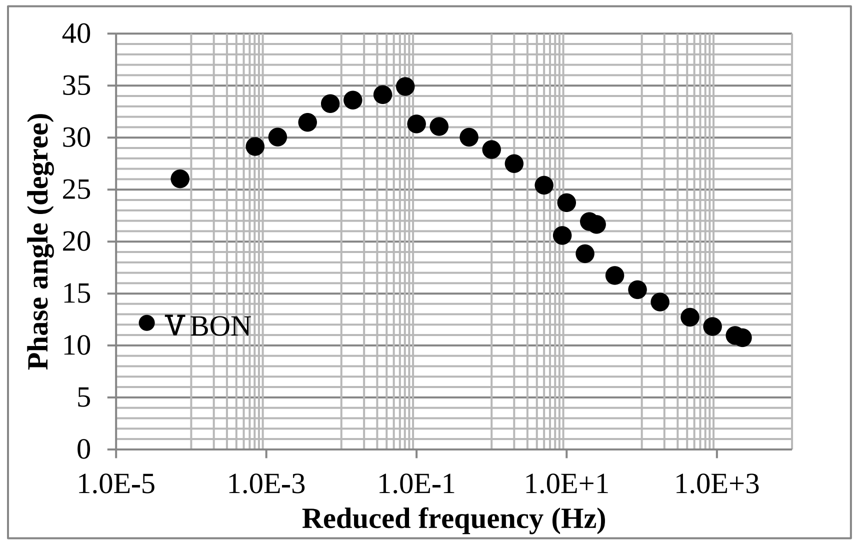

Master Phase Angle Curves for Mixtures from Liberty Surface Type B with Asphalt Source 2, no RAP

Figure 13-74: Mixture Type: V B (Liberty Surface Type B with RAP)

Level 1

Asphalt Mix: Dynamic Modulus Table						
Temperature (°F)	Mixture |E*| (psi)					
	0.1 Hz	0.5 Hz	1 Hz	5 Hz	10 Hz	25 Hz
14	2012538	2347075	2470742	2709732	2793197	2887520
40	1245205	1653244	1824203	2188234	2326422	2489843
70	548784	864563	1024016	1424756	1600869	1827824
100	208666	366122	460347	745569	894756	1110495
130	85257	148239	189723	334343	422045	564388

Asphalt Binder: Superpave Binder Test Data		
Temperature (°F)	Angular freq. = 10 rad/sec	
	G* (Pa)	Delta (degree)
158.0	792.60	88.98
168.8	299.28	89.22
179.6	150.21	89.46

Asphalt General: Volumetric Properties as Built	
Effective Binder (%)	11.61
Air Voids (%)	11.50
Total unit weight	167.00

Level 2

Asphalt Mix: Aggregate Gradation	
Cumulative % Retained ¾” sieve	0
Cumulative % Retained ⅜” sieve	7
Cumulative % Retained #4 sieve	39
% Passing #200 sieve	4.67

Level 3

Asphalt Binder: Superpave Binder Grading	PG 64-22

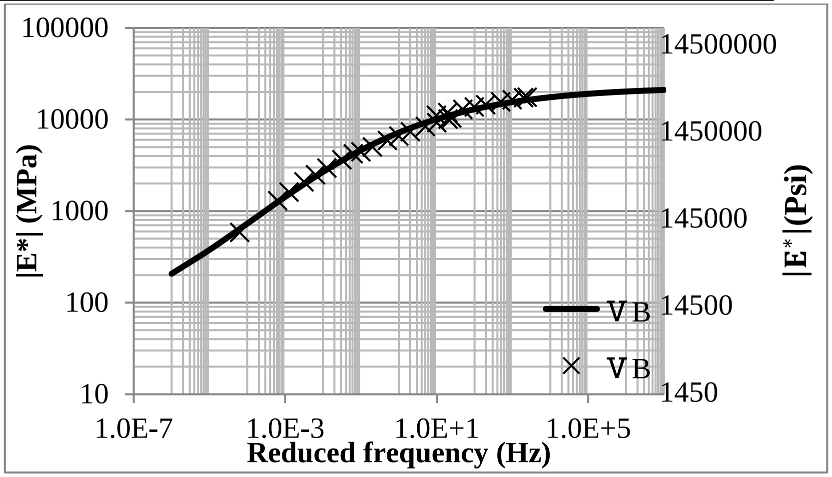

Master Dynamic Modulus Curves for Mixtures from Liberty Surface Type B with RAP

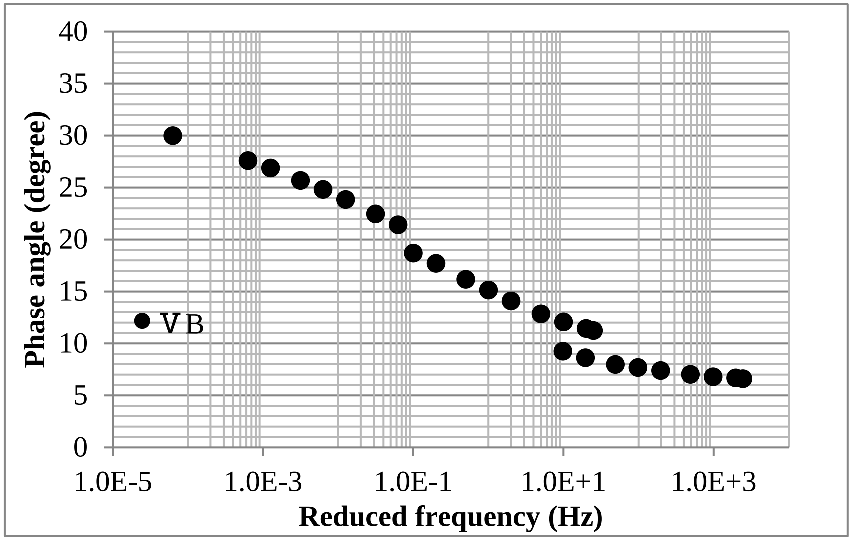

Master Phase Angle Curves for Mixtures from Liberty Surface Type B with RAP

Figure 13-75: Mixture Type: V CA (Liberty Surface Type C with LASA 2 (Adhere®) and RAP)

Level 1

Asphalt Mix: Dynamic Modulus Table						
Temperature (°F)	Mixture |E*| (psi)					
	0.1 Hz	0.5 Hz	1 Hz	5 Hz	10 Hz	25 Hz
14	1853743	2237164	2379807	2654604	2749728	2856260
40	981707	1412162	1601960	2019341	2181077	2373580
70	332793	588252	731510	1126646	1313836	1565100
100	103268	194376	255236	464999	588459	781798
130	40553	69064	89115	166727	219312	312873

Asphalt Binder: Superpave Binder Test Data		
Temperature (°F)	Angular freq. = 10 rad/sec	
	G* (Pa)	Delta (degree)
158.0	792.60	88.98
168.8	299.28	89.22
179.6	150.21	89.46

Asphalt General: Volumetric Properties as Built	
Effective Binder (%)	12.28
Air Voids (%)	5.74
Total unit weight	167.50

Level 2

Asphalt Mix: Aggregate Gradation	
Cumulative % Retained ¾” sieve	0
Cumulative % Retained ⅜” sieve	6
Cumulative % Retained #4 sieve	33
% Passing #200 sieve	5.66

Level 3

Asphalt Binder: Superpave Binder Grading	PG 64-22

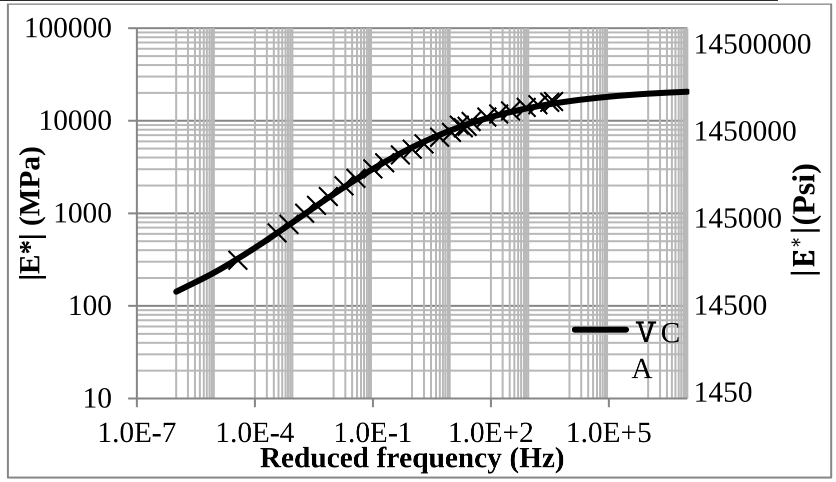

Master Dynamic Modulus Curves for Mixtures from Liberty Surface Type C with Adhere® and RAP

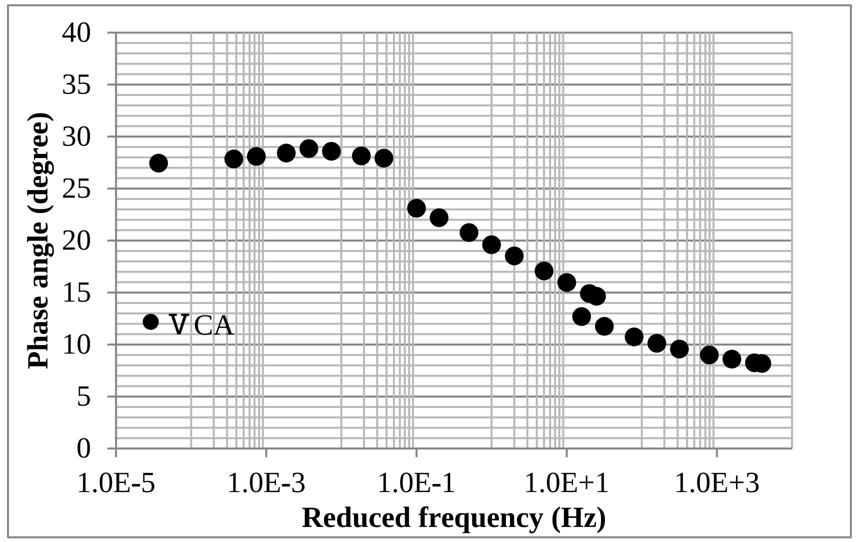

Master Phase Angle Curves for Mixtures from Liberty Surface Type C with Adhere® and RAP

Figure 13-76: Mixture Type: V CE (Liberty Surface Type C with Evotherm® WMA Chemical Additive and RAP)

Level 1

Asphalt Mix: Dynamic Modulus Table						
Temperature (°F)	Mixture |E*| (psi)					
	0.1 Hz	0.5 Hz	1 Hz	5 Hz	10 Hz	25 Hz
14	1142661	1633363	1836677	2256392	2409112	2583716
40	401421	756216	945773	1429781	1640450	1906313
70	83231	198984	281618	571066	737859	989542
100	18946	44375	65259	158323	227000	353323
130	6595	12645	17535	40705	59784	99660

Asphalt Binder: Superpave Binder Test Data		
Temperature (°F)	Angular freq. = 10 rad/sec	
	G* (Pa)	Delta (degree)
158.0	792.60	88.98
168.8	299.28	89.22
179.6	150.21	89.46

Asphalt General: Volumetric Properties as Built	
Effective Binder (%)	12.28
Air Voids (%)	5.73
Total unit weight	167.50

Level 2

Asphalt Mix: Aggregate Gradation	
Cumulative % Retained ¾” sieve	0
Cumulative % Retained ⅜” sieve	6
Cumulative % Retained #4 sieve	33
% Passing #200 sieve	5.66

Level 3

Asphalt Binder: Superpave Binder Grading	PG 64-22

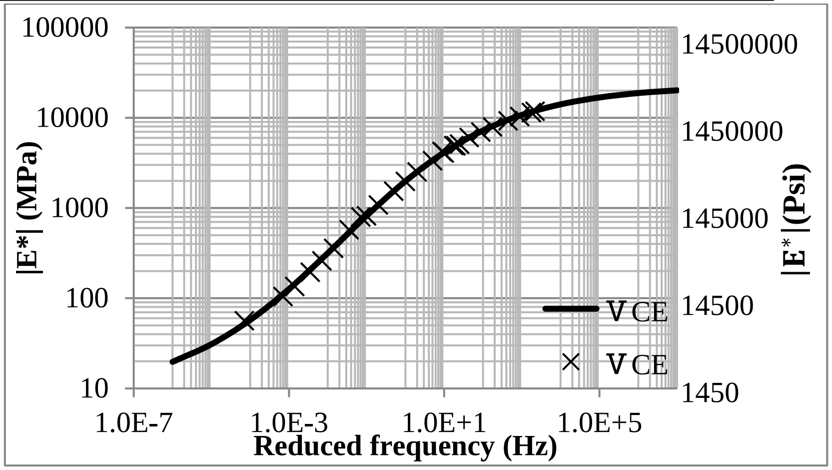

Master Dynamic Modulus Curves for Mixtures from Liberty Surface Type C with Evotherm® and RAP

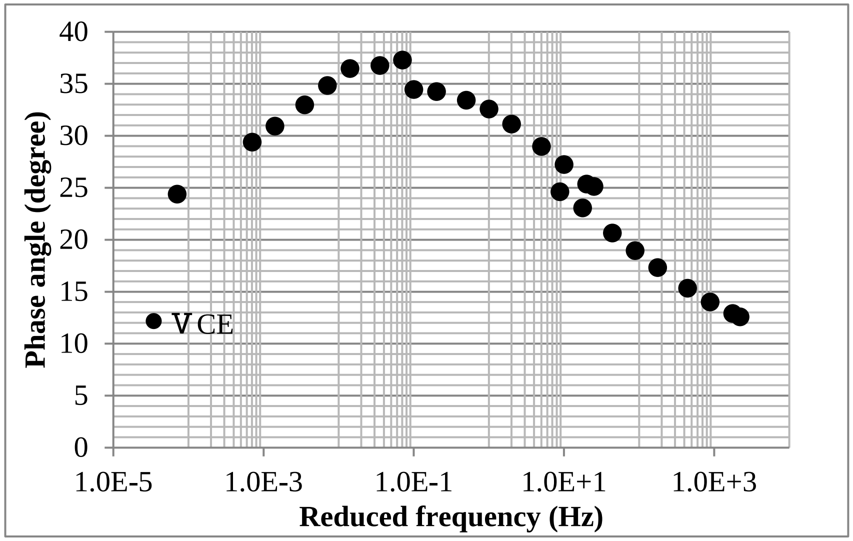

Master Phase Angle Curves for Mixtures from Liberty Surface Type C with Evotherm® and RAP

Figure 13-77: Mixture Type: V CF (Liberty Surface Type C with WMA Foaming Technology and RAP)

Level 1

Asphalt Mix: Dynamic Modulus Table						
Temperature (°F)	Mixture |E*| (psi)					
	0.1 Hz	0.5 Hz	1 Hz	5 Hz	10 Hz	25 Hz
14	1436009	1871895	2044072	2391447	2516699	2660222
40	627971	1022642	1212225	1659832	1844249	2071660
70	160088	338690	450469	791837	967929	1217004
100	35780	84145	120810	264826	359069	517315
130	10157	21801	31135	73126	105328	167846

Asphalt Binder: Superpave Binder Test Data		
Temperature (°F)	Angular freq. = 10 rad/sec	
	G* (Pa)	Delta (degree)
158.0	792.60	88.98
168.8	299.28	89.22
179.6	150.21	89.46

Asphalt General: Volumetric Properties as Built	
Effective Binder (%)	12.28
Air Voids (%)	5.73
Total unit weight	167.50

Level 2

Asphalt Mix: Aggregate Gradation	
Cumulative % Retained ¾" sieve	0
Cumulative % Retained ⅜" sieve	6
Cumulative % Retained #4 sieve	33
% Passing #200 sieve	5.66

Level 3

Asphalt Binder: Superpave Binder Grading	PG 64-22

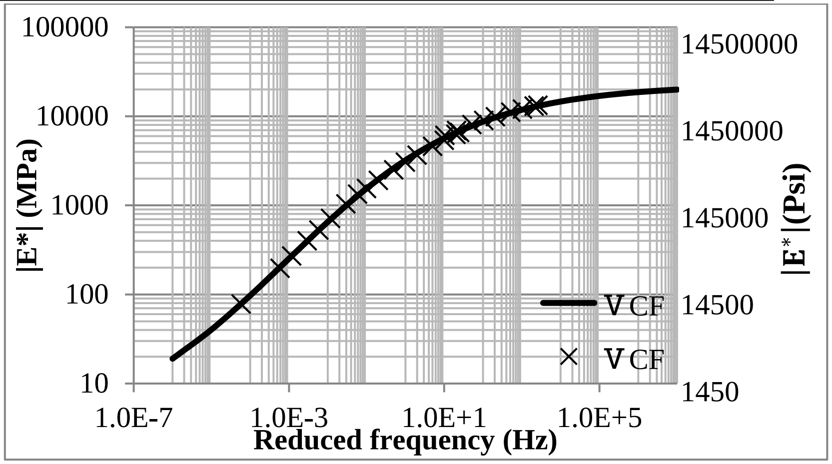

Master Dynamic Modulus Curves for Mixtures from Liberty Surface Type C with Foaming Technology and RAP

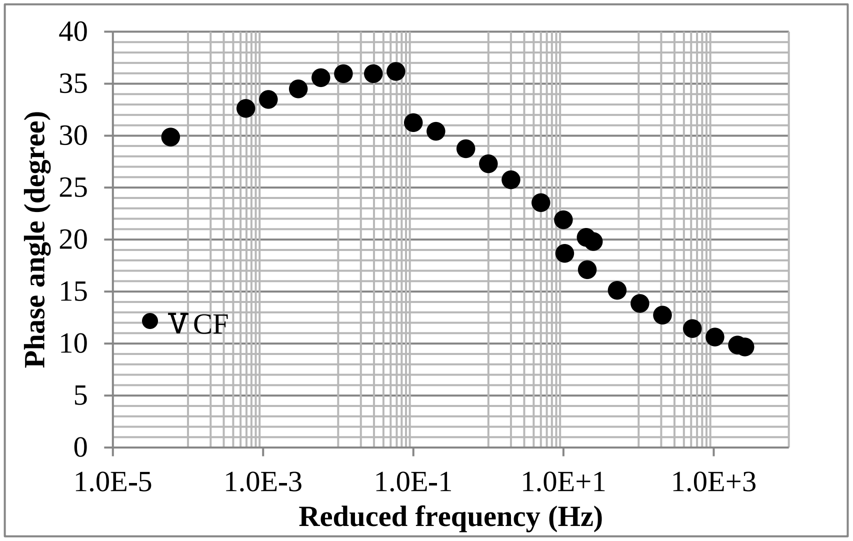

Master Phase Angle Curves for Mixtures from Liberty Surface Type C with Foaming Technology and RAP

Figure 13-78: Mixture Type: V CG (Liberty Surface Type C with Long-Term Aging and RAP)

Level 1

Asphalt Mix: Dynamic Modulus Table						
Temperature (°F)	Mixture |E*| (psi)					
	0.1 Hz	0.5 Hz	1 Hz	5 Hz	10 Hz	25 Hz
14	2199769	2525788	2640709	2852788	2923337	3000537
40	1318060	1762588	1945160	2322608	2460813	2619830
70	513967	839042	1008847	1443911	1636301	1883107
100	177336	310563	394906	667184	817677	1042534
130	75963	120914	151330	263307	335585	459227

Asphalt Binder: Superpave Binder Test Data		
Temperature (°F)	Angular freq. = 10 rad/sec	
	G* (Pa)	Delta (degree)
158.0	792.60	88.98
168.8	299.28	89.22
179.6	150.21	89.46

Asphalt General: Volumetric Properties as Built	
Effective Binder (%)	12.28
Air Voids (%)	5.68
Total unit weight	167.50

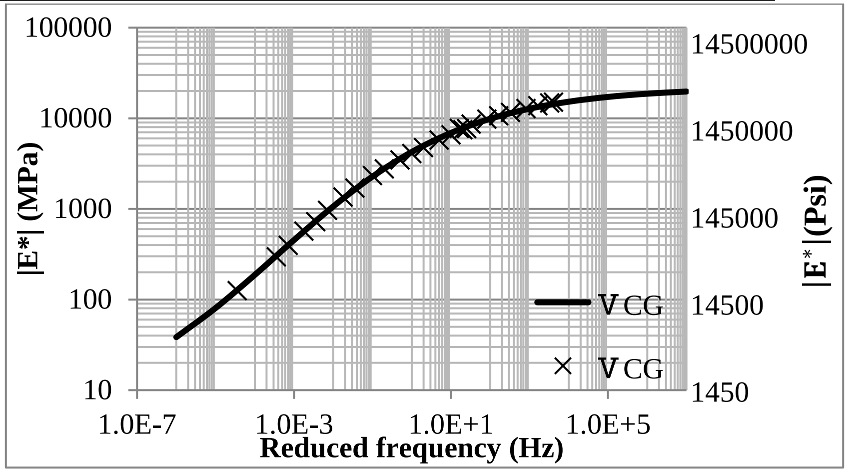

Master Dynamic Modulus Curves for Mixtures from Liberty Surface Type C with Long-Term Aging and RAP

Level 2

Asphalt Mix: Aggregate Gradation	
Cumulative % Retained ¾” sieve	0
Cumulative % Retained ⅜” sieve	6
Cumulative % Retained #4 sieve	33
% Passing #200 sieve	5.66

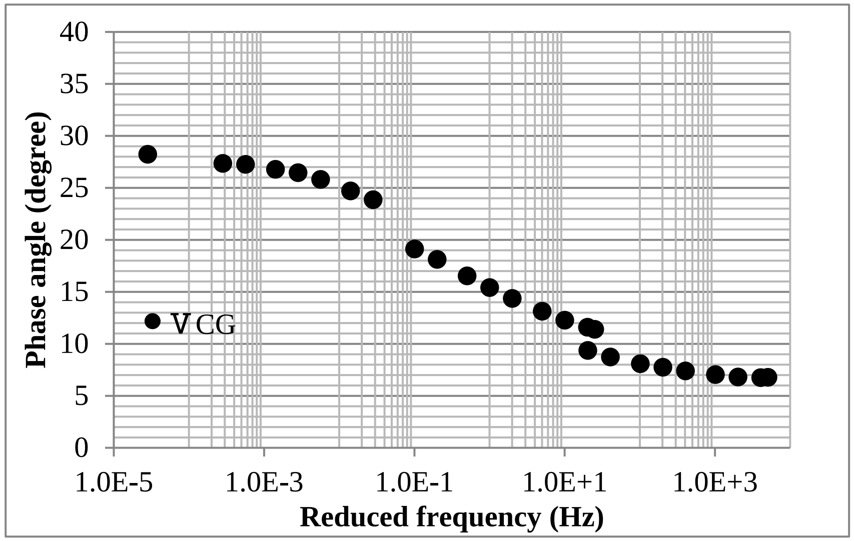

Master Phase Angle Curves for Mixtures from Liberty Surface Type C with Long-Term Aging and RAP

Level 3

Asphalt Binder: Superpave Binder Grading	PG 64-22

Figure 13-79: Mixture Type: V CM (Liberty Surface Type C with LASA 1 (Morlife®) and RAP)

Level 1

Asphalt Mix: Dynamic Modulus Table						
Temperature (°F)	Mixture |E*| (psi)					
	0.1 Hz	0.5 Hz	1 Hz	5 Hz	10 Hz	25 Hz
14	1793823	2205866	2359015	2651981	2752287	2863586
40	898259	1343668	1544068	1988715	2161318	2366103
70	281887	522576	663275	1065022	1260048	1524615
100	85092	163367	217723	413974	534193	727325
130	34570	58023	74868	142339	189698	276452

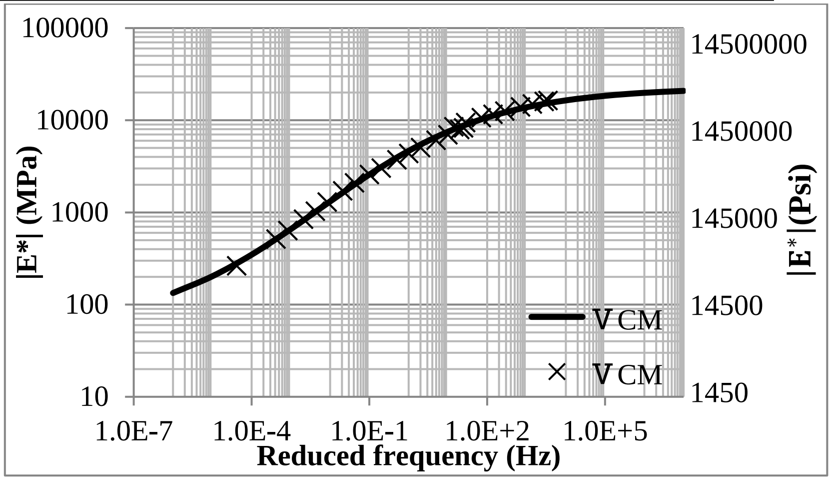

Master Dynamic Modulus Curves for Mixtures from Liberty Surface Type C with Morlife® and RAP

Asphalt Binder: Superpave Binder Test Data		
Temperature (°F)	Angular freq. = 10 rad/sec	
	G* (Pa)	Delta (degree)
158.0	792.60	88.98
168.8	299.28	89.22
179.6	150.21	89.46

Asphalt General: Volumetric Properties as Built	
Effective Binder (%)	12.28
Air Voids (%)	5.56
Total unit weight	167.50

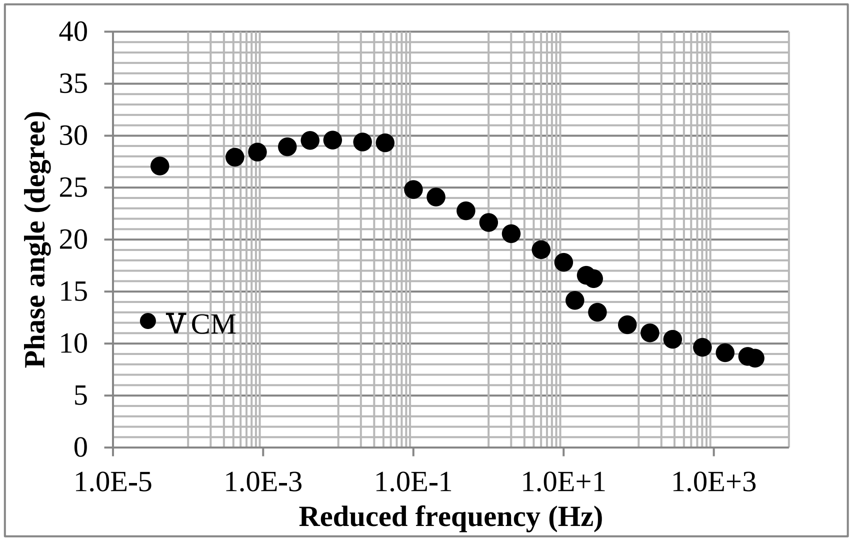

Master Phase Angle Curves for Mixtures from Liberty Surface Type C with Morlife® and RAP

Level 2

Asphalt Mix: Aggregate Gradation	
Cumulative % Retained ¾” sieve	0
Cumulative % Retained ⅜” sieve	6
Cumulative % Retained #4 sieve	33
% Passing #200 sieve	5.66

Level 3

Asphalt Binder: Superpave Binder Grading	PG 64-22

Figure 13-80: Mixture Type: V CO (Liberty Surface Type C, no RAP)

Level 1

Asphalt Mix: Dynamic Modulus Table						
Temperature (°F)	Mixture |E*| (psi)					
	0.1 Hz	0.5 Hz	1 Hz	5 Hz	10 Hz	25 Hz
14	1818384	2197922	2337453	2603107	2693937	2794836
40	925749	1360086	1551465	1969969	2130817	2320974
70	278393	522265	662727	1056900	1245393	1498950
100	73316	149338	202675	395504	513159	701202
130	25247	45777	60934	123210	167644	249682

Asphalt Binder: Superpave Binder Test Data		
Temperature (°F)	Angular freq. = 10 rad/sec	
	G* (Pa)	Delta (degree)
158.0	792.60	88.98
168.8	299.28	89.22
179.6	150.21	89.46

Asphalt General: Volumetric Properties as Built	
Effective Binder (%)	12.70
Air Voids (%)	6.29
Total unit weight	167.69

Level 2

Asphalt Mix: Aggregate Gradation	
Cumulative % Retained ¾" sieve	0
Cumulative % Retained ⅜" sieve	6
Cumulative % Retained #4 sieve	27
% Passing #200 sieve	5.91

Level 3

Asphalt Binder: Superpave Binder Grading	PG 64-22

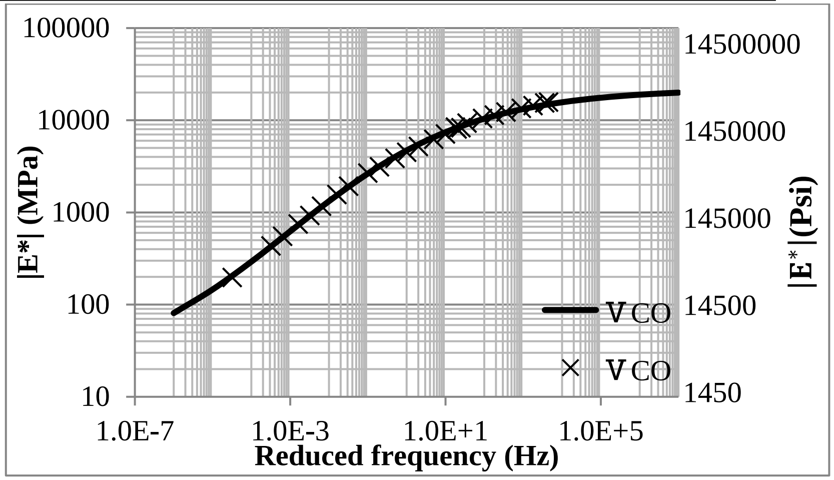

Master Dynamic Modulus Curves for Mixtures from Liberty Surface Type C, no RAP

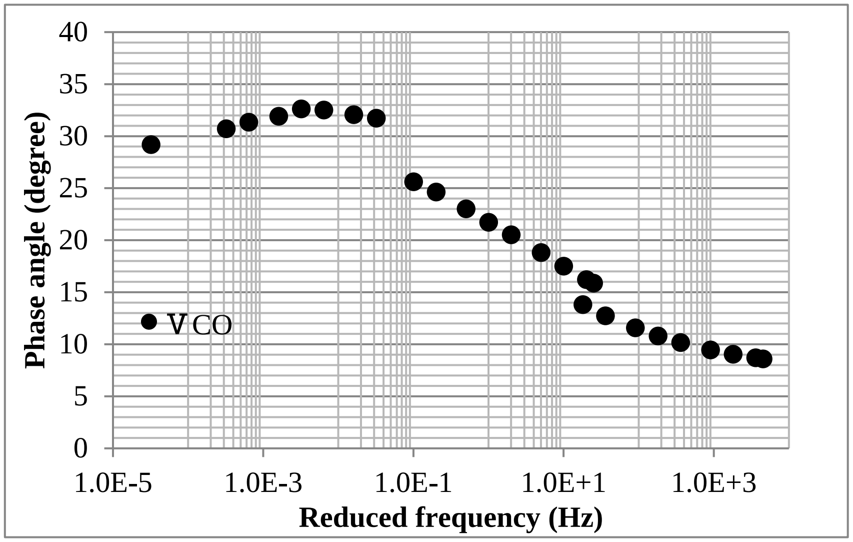

Master Phase Angle Curves for Mixtures from Liberty Surface Type C, no RAP

Figure 13-81: Mixture Type: V COA (Liberty Surface Type C with LASA 2 (Adhere®), no RAP)

Level 1

Asphalt Mix: Dynamic Modulus Table						
Temperature (°F)	Mixture |E*| (psi)					
	0.1 Hz	0.5 Hz	1 Hz	5 Hz	10 Hz	25 Hz
14	1612799	2069410	2238489	2557497	2664563	2781484
40	688772	1151128	1367555	1854906	2044203	2267155
70	154054	352478	482202	884868	1090905	1376128
100	31485	76893	113736	269824	377514	562789
130	9594	19384	27498	66484	98427	163821

Asphalt Binder: Superpave Binder Test Data		
Temperature (°F)	Angular freq. = 10 rad/sec	
	G* (Pa)	Delta (degree)
158.0	792.60	88.98
168.8	299.28	89.22
179.6	150.21	89.46

Asphalt General: Volumetric Properties as Built	
Effective Binder (%)	13.06
Air Voids (%)	6.78
Total unit weight	167.69

Level 2

Asphalt Mix: Aggregate Gradation	
Cumulative % Retained ¾” sieve	0
Cumulative % Retained ⅜” sieve	5
Cumulative % Retained #4 sieve	33
% Passing #200 sieve	5.21

Level 3

Asphalt Binder: Superpave Binder Grading	PG 64-22

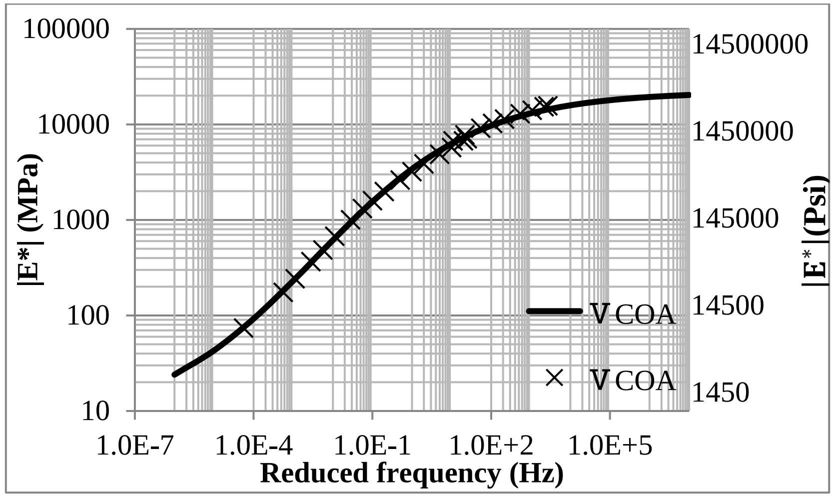

Master Dynamic Modulus Curves for Mixtures from Liberty Surface Type C with Adhere®, no RAP

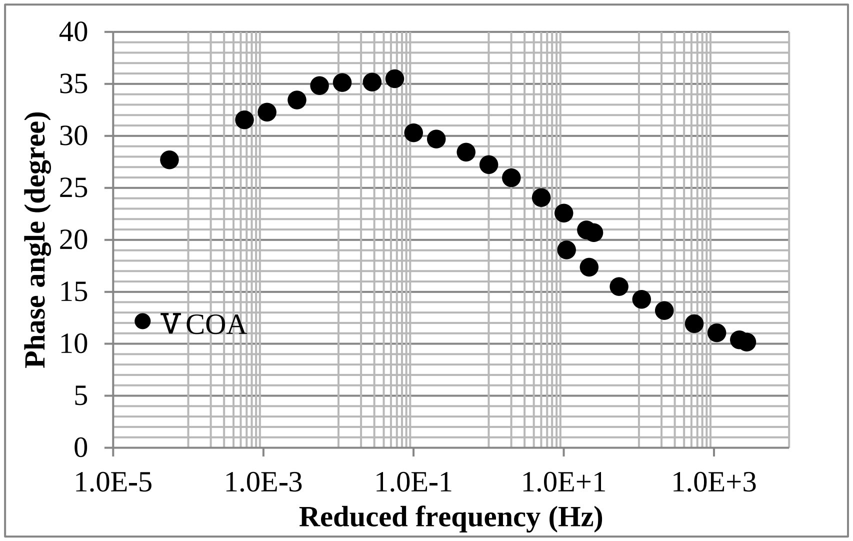

Master Phase Angle Curves for Mixtures from Liberty Surface Type C with Adhere®, no RAP

Figure 13-82: Mixture Type: V COE (Liberty Surface Type C using Evotherm® WMA Chemical Additive, no RAP)

Level 1

Asphalt Mix: Dynamic Modulus Table						
Temperature (°F)	Mixture |E*| (psi)					
	0.1 Hz	0.5 Hz	1 Hz	5 Hz	10 Hz	25 Hz
14	1430919	1871710	2043473	2384070	2504426	2640337
40	624297	1029618	1224079	1678884	1863576	2088434
70	159651	341988	457480	812026	994579	1251184
100	37448	86812	124595	274847	373997	540905
130	11701	23981	33786	78043	112198	178887

Asphalt Binder: Superpave Binder Test Data		
Temperature (°F)	Angular freq. = 10 rad/sec	
	G* (Pa)	Delta (degree)
158.0	792.60	88.98
168.8	299.28	89.22
179.6	150.21	89.46

Asphalt General: Volumetric Properties as Built	
Effective Binder (%)	13.06
Air Voids (%)	6.78
Total unit weight	167.69

Level 2

Asphalt Mix: Aggregate Gradation	
Cumulative % Retained ¾" sieve	0
Cumulative % Retained ⅜" sieve	5
Cumulative % Retained #4 sieve	33
% Passing #200 sieve	5.21

Level 3

Asphalt Binder: Superpave Binder Grading	PG 64-22

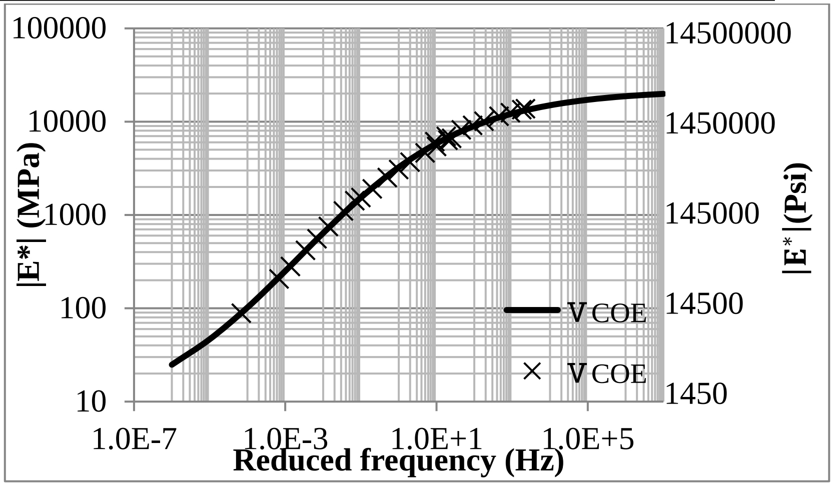

Master Dynamic Modulus Curves for Mixtures from Liberty Surface Type C using Evotherm®, no RAP

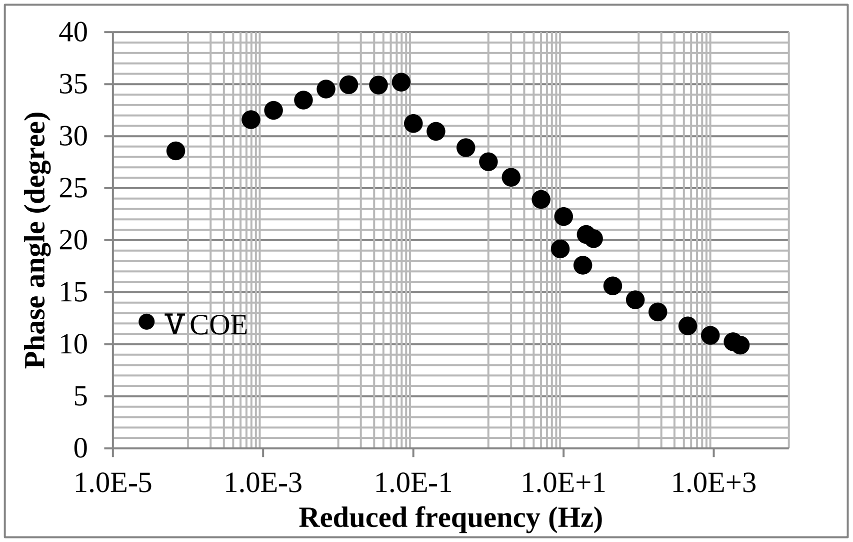

Master Phase Angle Curves for Mixtures from Liberty Surface Type C using Evotherm®, no RAP

Figure 13-83: Mixture Type: V COF (Liberty Surface Type C using WMA Foaming Technology, no RAP)

Level 1

Asphalt Mix: Dynamic Modulus Table						
Temperature (°F)	Mixture |E*| (psi)					
	0.1 Hz	0.5 Hz	1 Hz	5 Hz	10 Hz	25 Hz
14	1315991	1802527	1994266	2372850	2504849	2651863
40	476554	868123	1069773	1563965	1770408	2023725
70	97539	226792	318034	632394	810098	1073643
100	22841	50149	72281	170262	242434	375073
130	8745	15209	20279	43667	62668	102255

Asphalt Binder: Superpave Binder Test Data		
Temperature (°F)	Angular freq. = 10 rad/sec	
	G* (Pa)	Delta (degree)
158.0	792.60	88.98
168.8	299.28	89.22
179.6	150.21	89.46

Asphalt General: Volumetric Properties as Built	
Effective Binder (%)	13.06
Air Voids (%)	6.78
Total unit weight	167.69

Level 2

Asphalt Mix: Aggregate Gradation	
Cumulative % Retained ¾” sieve	0
Cumulative % Retained ⅜” sieve	5
Cumulative % Retained #4 sieve	33
% Passing #200 sieve	5.21

Level 3

Asphalt Binder: Superpave Binder Grading	PG 64-22

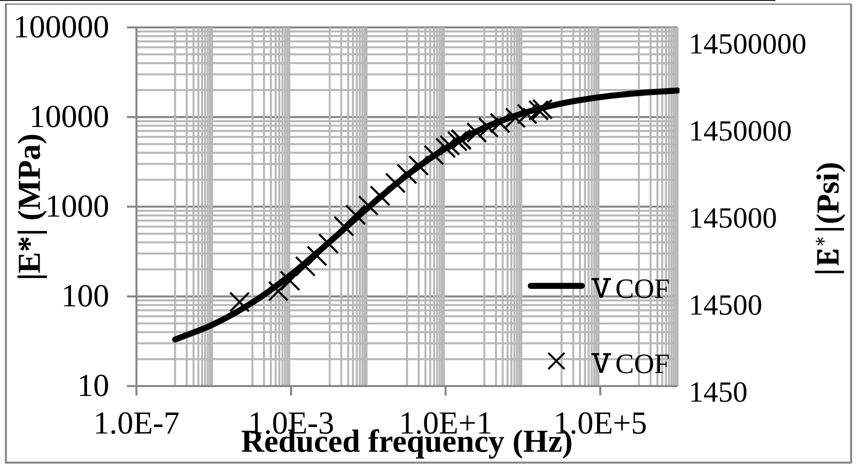

Master Dynamic Modulus Curves for Mixtures from Liberty Surface Type C using WMA Foaming Technology, no RAP

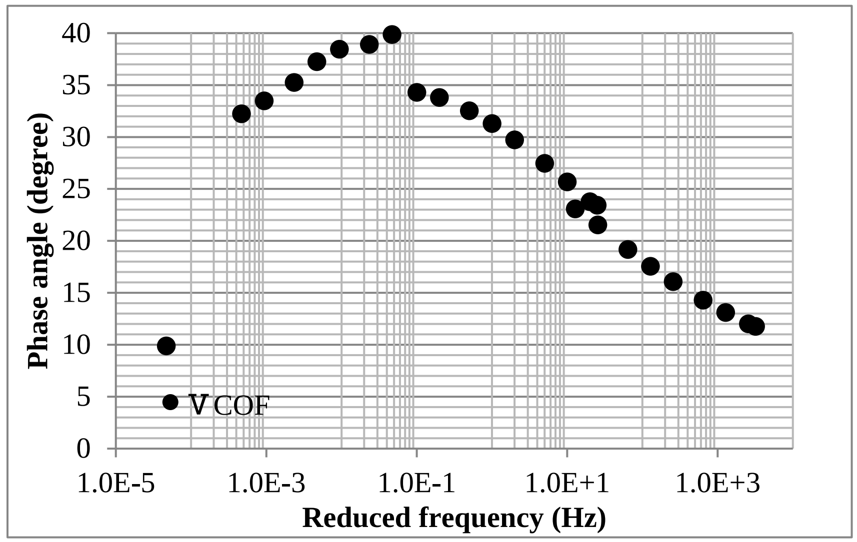

Master Phase Angle Curves for Mixtures from Liberty Surface Type C using WMA Foaming Technology, no RAP

Figure 13-84: Mixture Type: V COG (Liberty Surface Type C with Long-Term Aging, no RAP)

Level 1

Asphalt Mix: Dynamic Modulus Table						
Temperature (°F)	Mixture |E*| (psi)					
	0.1 Hz	0.5 Hz	1 Hz	5 Hz	10 Hz	25 Hz
14	1734967	2128341	2274521	2555209	2651934	2759879
40	843906	1275937	1469367	1897799	2064309	2262448
70	231442	459216	593923	980279	1168223	1423572
100	52983	117738	165103	343063	454770	636336
130	15637	31252	43380	96044	135271	209765

Asphalt Binder: Superpave Binder Test Data		
Temperature (°F)	Angular freq. = 10 rad/sec	
	G* (Pa)	Delta (degree)
158.0	792.60	88.98
168.8	299.28	89.22
179.6	150.21	89.46

Asphalt General: Volumetric Properties as Built	
Effective Binder (%)	13.06
Air Voids (%)	6.63
Total unit weight	167.69

Level 2

Asphalt Mix: Aggregate Gradation	
Cumulative % Retained ¾" sieve	0
Cumulative % Retained ⅜" sieve	5
Cumulative % Retained #4 sieve	33
% Passing #200 sieve	5.21

Level 3

Asphalt Binder: Superpave Binder Grading	PG 64-22

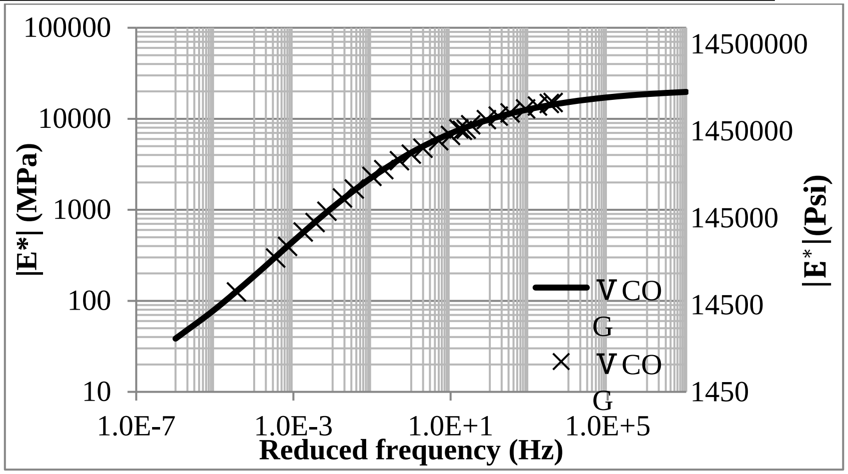

Master Dynamic Modulus Curves for Mixtures from Liberty Surface Type C with Long-Term Aging, no RAP

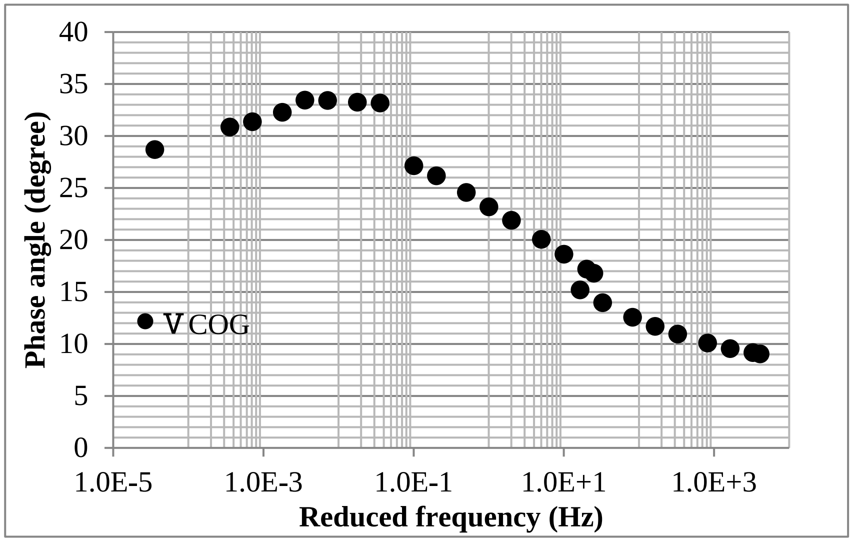

Master Phase Angle Curves for Mixtures from Liberty Surface Type C with Long-Term Aging, no RAP

Figure 13-85: Mixture Type: V COM (Liberty Surface Type C with LASA 1 (Morlife®), no RAP)

Level 1

Asphalt Mix: Dynamic Modulus Table						
Temperature (°F)	Mixture |E*| (psi)					
	0.1 Hz	0.5 Hz	1 Hz	5 Hz	10 Hz	25 Hz
14	1608812	2077259	2249872	2573087	2680538	2797053
40	645165	1110075	1331440	1834274	2030230	2260798
70	128920	306162	426884	817298	1023539	1313988
100	25276	60885	90546	222301	317574	487591
130	8159	15468	21485	50721	75263	127059

Asphalt Binder: Superpave Binder Test Data		
Temperature (°F)	Angular freq. = 10 rad/sec	
	G* (Pa)	Delta (degree)
158.0	792.60	88.98
168.8	299.28	89.22
179.6	150.21	89.46

Asphalt General: Volumetric Properties as Built	
Effective Binder (%)	13.06
Air Voids (%)	5.95
Total unit weight	169.67

Level 2

Asphalt Mix: Aggregate Gradation	
Cumulative % Retained ¾” sieve	0
Cumulative % Retained ⅜” sieve	5
Cumulative % Retained #4 sieve	33
% Passing #200 sieve	5.21

Level 3

Asphalt Binder: Superpave Binder Grading	PG 64-22

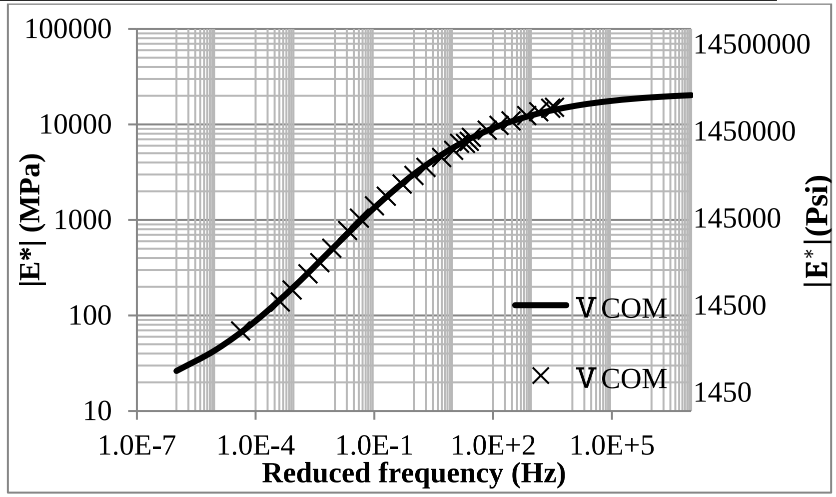

Master Dynamic Modulus Curves for Mixtures from Liberty Surface Type C with Morlife®, no RAP

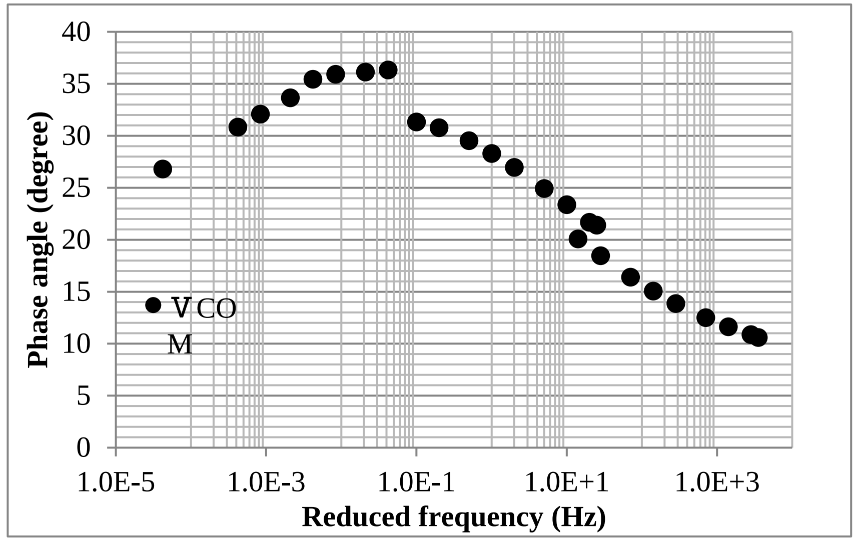

Master Phase Angle Curves for Mixtures from Liberty Surface Type C with Morlife®, no RAP

Figure 13-86: Mixture Type: V C (Liberty Surface Type C with RAP)

Level 1

Asphalt Mix: Dynamic Modulus Table						
Temperature (°F)	Mixture |E*| (psi)					
	0.1 Hz	0.5 Hz	1 Hz	5 Hz	10 Hz	25 Hz
14	1097938	1439694	1586032	1909777	2038907	2197852
40	491443	760251	892905	1225106	1372896	1567118
70	143891	269960	344507	567861	684534	854611
100	36283	76856	104643	203807	264805	364822
130	9875	21140	29467	62969	86298	128700

Asphalt Binder: Superpave Binder Test Data		
Temperature (°F)	Angular freq. = 10 rad/sec	
	G* (Pa)	Delta (degree)
158.0	792.60	88.98
168.8	299.28	89.22
179.6	150.21	89.46

Asphalt General: Volumetric Properties as Built	
Effective Binder (%)	12.28
Air Voids (%)	14.56
Total unit weight	167.50

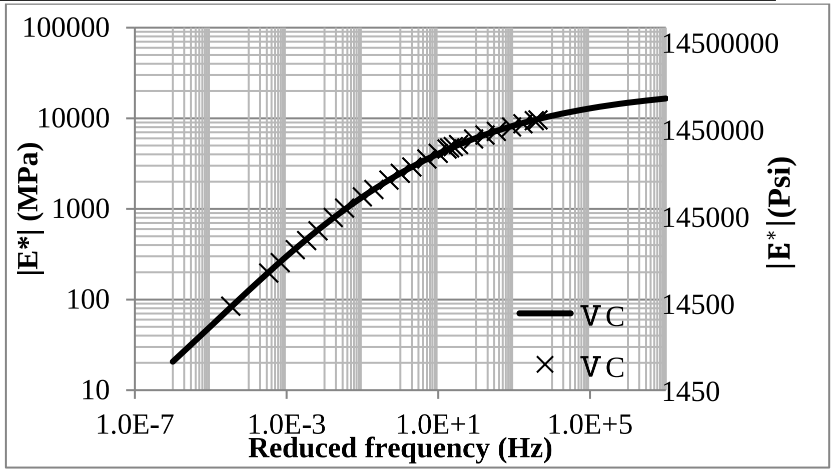

Master Dynamic Modulus Curves for Mixtures from Liberty Surface Type C with RAP

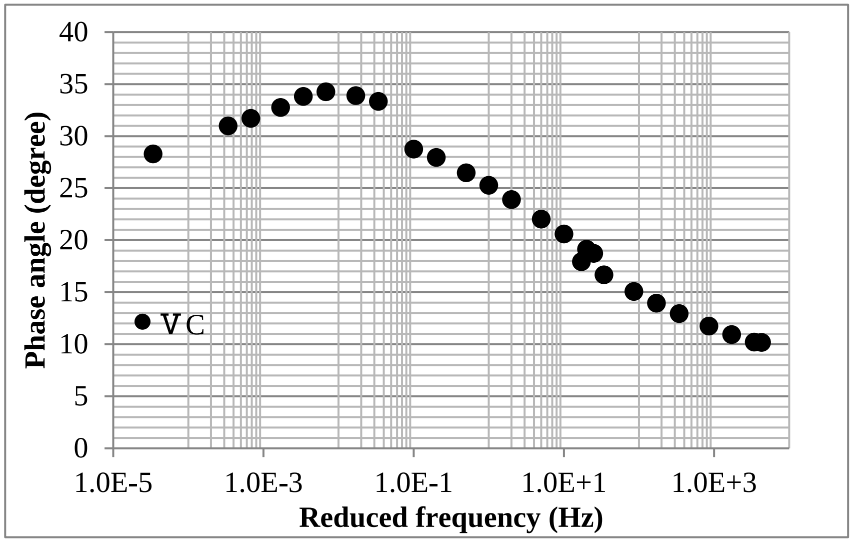

Master Phase Angle Curves for Mixtures from Liberty Surface Type C with RAP

Level 2

Asphalt Mix: Aggregate Gradation	
Cumulative % Retained ¾” sieve	0
Cumulative % Retained ⅜” sieve	6
Cumulative % Retained #4 sieve	33
% Passing #200 sieve	5.66

Level 3

Asphalt Binder: Superpave Binder Grading	PG 64-22

Figure 13-87: Mixture Type: V DO (Liberty Surface Type D, no RAP)

Level 1

Asphalt Mix: Dynamic Modulus Table						
Temperature (°F)	Mixture |E*| (psi)					
	0.1 Hz	0.5 Hz	1 Hz	5 Hz	10 Hz	25 Hz
14	1481741	1789537	1911616	2164178	2258797	2370824
40	796082	1106777	1246976	1569867	1702797	1869016
70	289060	478200	580182	858212	991433	1174558
100	90144	165434	212577	365273	451441	584274
130	30645	55673	72569	134074	173381	240493

Asphalt Binder: Superpave Binder Test Data		
Temperature (°F)	Angular freq. = 10 rad/sec	
	G* (Pa)	Delta (degree)
158.0	792.60	88.98
168.8	299.28	89.22
179.6	150.21	89.46

Asphalt General: Volumetric Properties as Built	
Effective Binder (%)	12.07
Air Voids (%)	10.73
Total unit weight	167.50

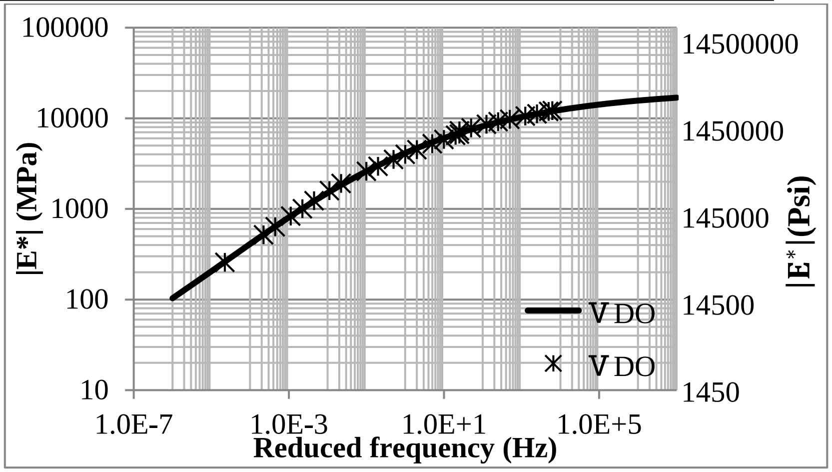

Master Dynamic Modulus Curves for Mixtures from Liberty Surface Type D, no RAP

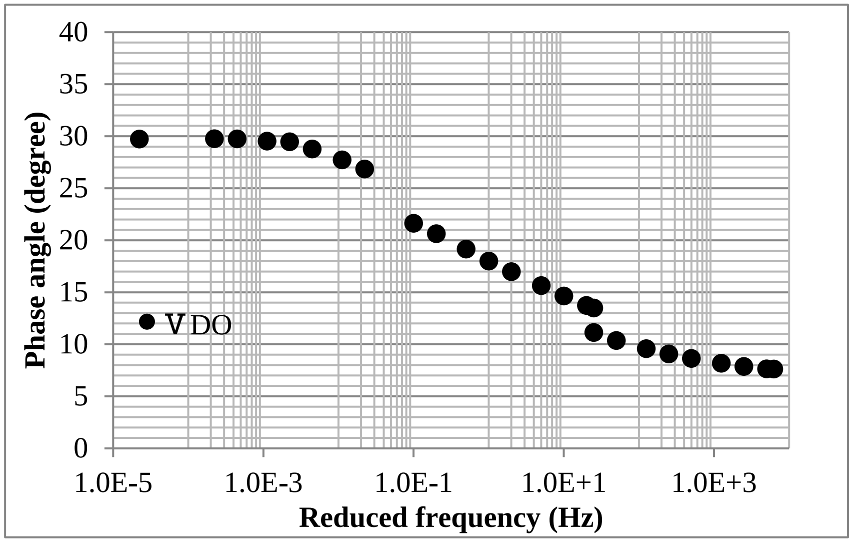

Master Phase Angle Curves for Mixtures from Liberty Surface Type D, no RAP

Level 2

Asphalt Mix: Aggregate Gradation	
Cumulative % Retained ¾” sieve	0
Cumulative % Retained ⅜” sieve	3
Cumulative % Retained #4 sieve	22
% Passing #200 sieve	5.82

Level 3

Asphalt Binder: Superpave Binder Grading	PG 64-22

Figure 13-88: Mixture Type: V D (Liberty Surface Type D with RAP)

Level 1

Asphalt Mix: Dynamic Modulus Table						
Temperature (°F)	Mixture |E*| (psi)					
	0.1 Hz	0.5 Hz	1 Hz	5 Hz	10 Hz	25 Hz
14	1633822	1969746	2099004	2357574	2450922	2558590
40	865988	1223254	1382901	1743256	1887714	2064416
70	299355	511583	628450	950023	1103943	1313863
100	91402	169812	220566	390573	488942	642421
130	33064	57903	74992	139149	181439	255343

Asphalt Binder: Superpave Binder Test Data		
Temperature (°F)	Angular freq. = 10 rad/sec	
	G* (Pa)	Delta (degree)
158.0	792.60	88.98
168.8	299.28	89.22
179.6	150.21	89.46

Asphalt General: Volumetric Properties as Built	
Effective Binder (%)	12.02
Air Voids (%)	6.73
Total unit weight	168.06

Level 2

Asphalt Mix: Aggregate Gradation	
Cumulative % Retained ¾" sieve	0
Cumulative % Retained ⅜" sieve	4
Cumulative % Retained #4 sieve	23
% Passing #200 sieve	6.7

Level 3

Asphalt Binder: Superpave Binder Grading	PG 64-22

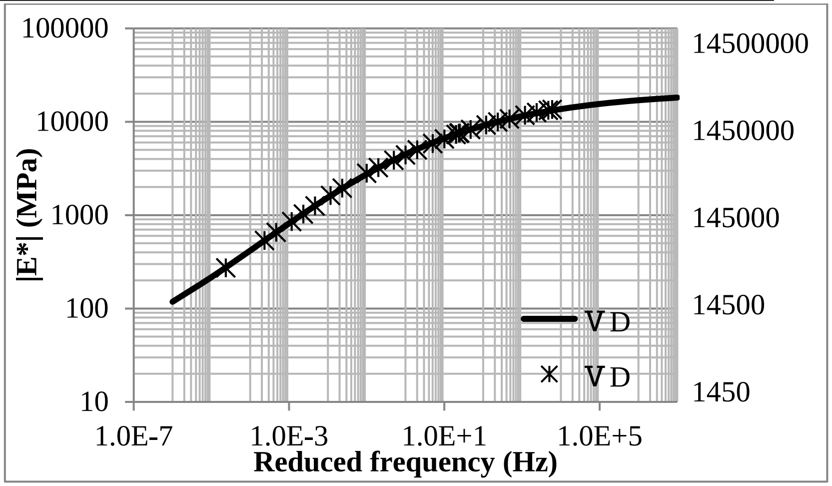

Master Dynamic Modulus Curves for Mixtures from Liberty Surface Type D with RAP

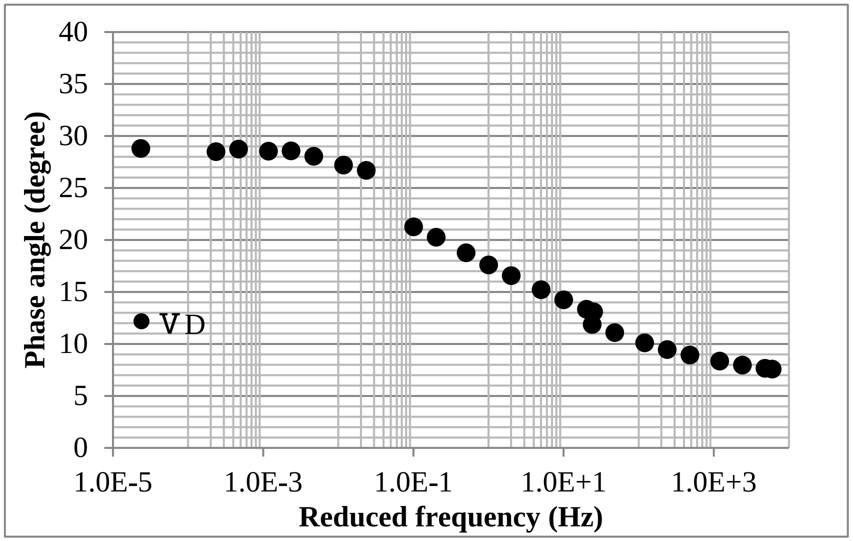

Master Phase Angle Curves for Mixtures from Liberty Surface Type D with RAP

Figure 13-89: Mixture Type: V EO (Liberty Surface Type E, no RAP)

Level 1

Asphalt Mix: Dynamic Modulus Table						
Temperature (°F)	Mixture |E*| (psi)					
	0.1 Hz	0.5 Hz	1 Hz	5 Hz	10 Hz	25 Hz
14	1295464	1572495	1686695	1933255	2030010	2148415
40	699473	958380	1077156	1358388	1478235	1632352
70	266747	425204	509157	737167	847201	1000379
100	86552	154432	195378	323618	394347	502390
130	28318	52403	68189	123429	157483	214214

Asphalt Binder: Superpave Binder Test Data		
Temperature (°F)	Angular freq. = 10 rad/sec	
	G* (Pa)	Delta (degree)
158.0	792.60	88.98
168.8	299.28	89.22
179.6	150.21	89.46

Asphalt General: Volumetric Properties as Built	
Effective Binder (%)	12.07
Air Voids (%)	15.20
Total unit weight	167.50

Level 2

Asphalt Mix: Aggregate Gradation	
Cumulative % Retained ¾” sieve	0
Cumulative % Retained ⅜” sieve	0
Cumulative % Retained #4 sieve	1
% Passing #200 sieve	7.18

Level 3

Asphalt Binder: Superpave Binder Grading	PG 64-22

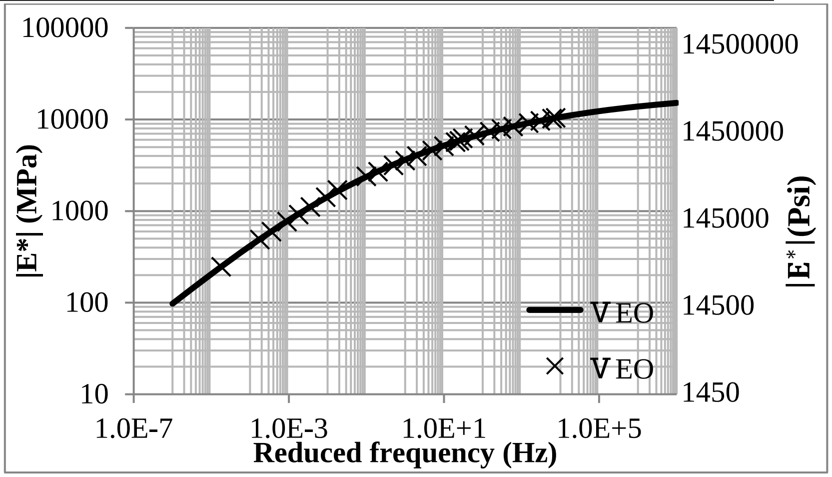

Master Dynamic Modulus Curves for Mixtures from Liberty Surface Type E, no RAP

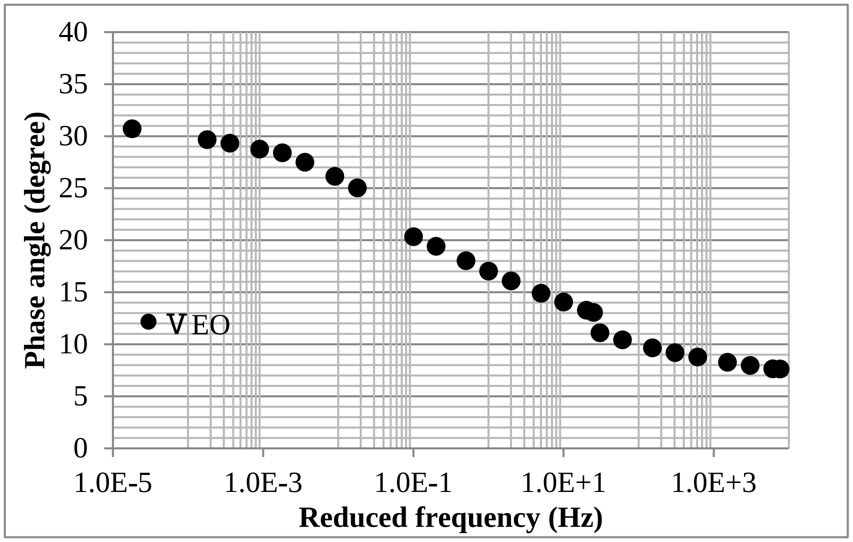

Master Phase Angle Curves for Mixtures from Liberty Surface Type E, no RAP

Figure 13-90: Mixture Type: V E (Liberty Surface Type E with RAP)

Level 1

Asphalt Mix: Dynamic Modulus Table						
Temperature (°F)	Mixture |E*| (psi)					
	0.1 Hz	0.5 Hz	1 Hz	5 Hz	10 Hz	25 Hz
14	1779466	2082672	2197997	2427427	2510070	2605443
40	1030125	1377033	1527460	1860120	1991556	2151351
70	411730	646631	769295	1092094	1241318	1441069
100	146759	248112	309567	502298	607911	767194
130	60097	97012	120878	204223	255764	341852

Asphalt Binder: Superpave Binder Test Data		
Temperature (°F)	Angular freq. = 10 rad/sec	
	G* (Pa)	Delta (degree)
158.0	792.60	88.98
168.8	299.28	89.22
179.6	150.21	89.46

Asphalt General: Volumetric Properties as Built	
Effective Binder (%)	12.02
Air Voids (%)	9.52
Total unit weight	168.06

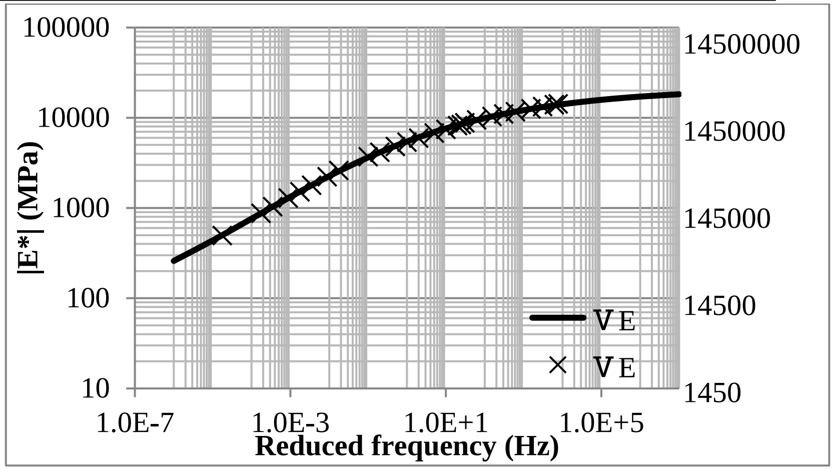

Master Dynamic Modulus Curves for Mixtures from Liberty Surface Type E with RAP

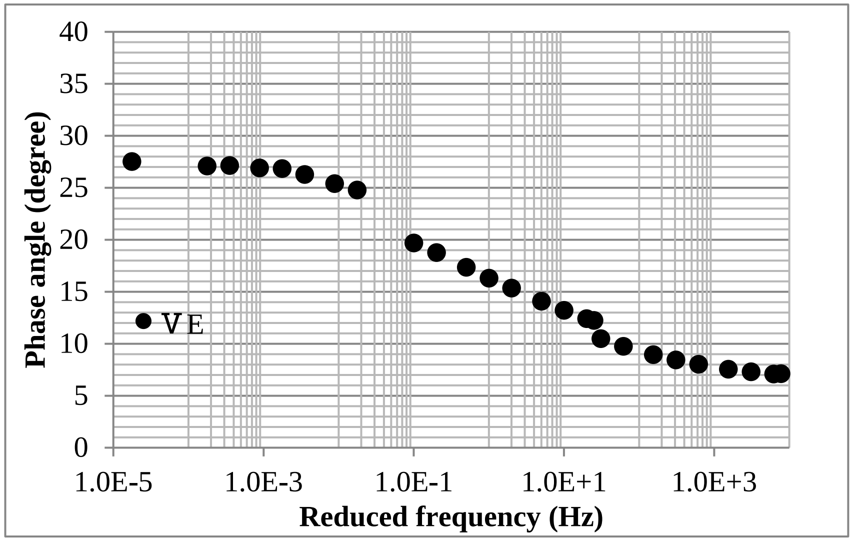

Master Phase Angle Curves for Mixtures from Liberty Surface Type E with RAP

Level 2

Asphalt Mix: Aggregate Gradation	
Cumulative % Retained ¾” sieve	0
Cumulative % Retained ⅜” sieve	0
Cumulative % Retained #4 sieve	2
% Passing #200 sieve	7.69

Level 3

Asphalt Binder: Superpave Binder Grading	PG 64-22

Figure 13-91: Mixture Type: V IAO (Liberty Intermediate Type A, no RAP)

Level 1

Asphalt Mix: Dynamic Modulus Table						
Temperature	Mixture |E*| (psi)					
(°F)	0.1 Hz	0.5 Hz	1 Hz	5 Hz	10 Hz	25 Hz
14	1836525	2290020	2455016	2763312	2866167	2978308
40	844010	1343485	1568819	2062903	2251056	2470682
70	203900	445131	595668	1041710	1261473	1559172
100	41894	101401	148285	338318	464132	674092
130	12135	25050	35684	85742	125733	205577

Asphalt Binder: Superpave Binder Test Data		
Temperature	Angular freq. = 10 rad/sec	
(°F)	G* (Pa)	Delta (degree)
158.0	792.60	88.98
168.8	299.28	89.22
179.6	150.21	89.46

Asphalt General: Volumetric Properties as Built	
Effective Binder (%)	10.47
Air Voids (%)	7.04
Total unit weight	167.19

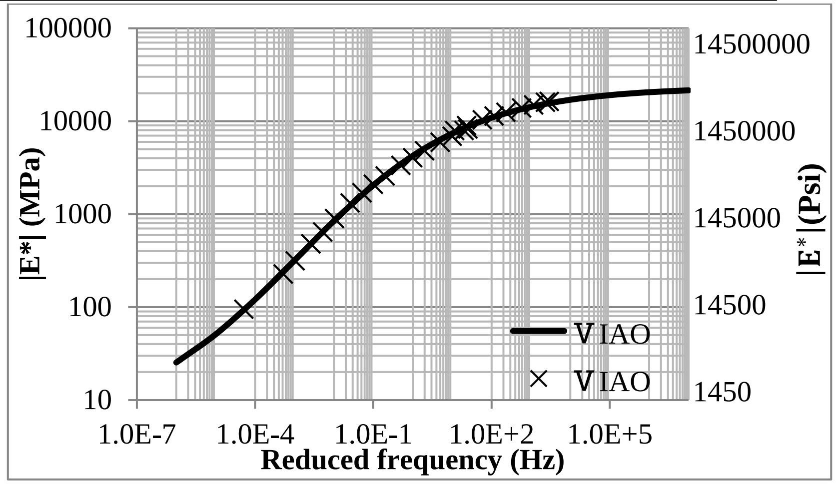

Master Dynamic Modulus Curves for Mixtures from Liberty Intermediate Type A, no RAP

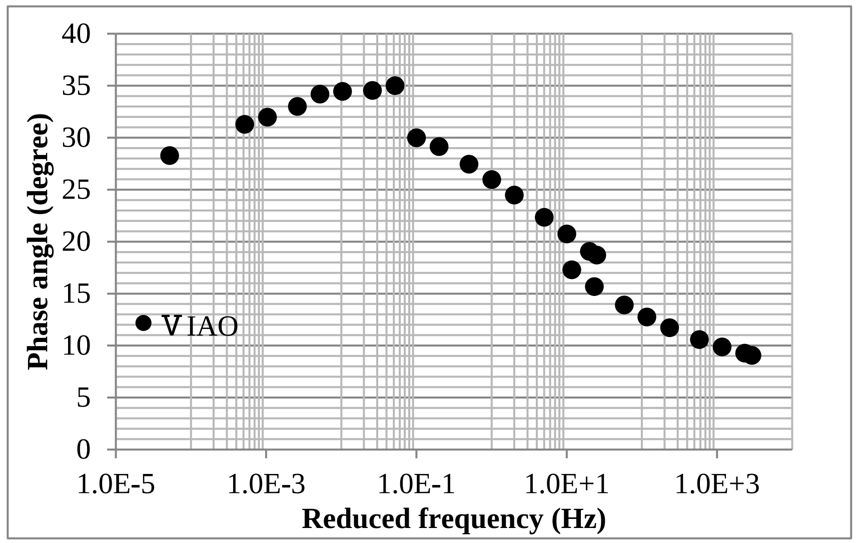

Master Phase Angle Curves for Mixtures from Liberty Intermediate Type A, no RAP

Level 2

Asphalt Mix: Aggregate Gradation	
Cumulative % Retained ¾" sieve	2
Cumulative % Retained ⅜" sieve	30
Cumulative % Retained #4 sieve	53
% Passing #200 sieve	3.73

Level 3

Asphalt Binder: Superpave Binder Grading	PG 64-22

Figure 13-92: Mixture Type: V IA (Liberty Intermediate Type A with RAP)

Level 1

Asphalt Mix: Dynamic Modulus Table						
Temperature (°F)	Mixture |E*| (psi)					
	0.1 Hz	0.5 Hz	1 Hz	5 Hz	10 Hz	25 Hz
14	1807771	2247695	2409924	2717691	2822141	2937377
40	863639	1343222	1558784	2033603	2216120	2431063
70	229828	478090	628064	1062071	1273035	1557839
100	51247	120136	172266	373695	502040	711273
130	14935	31187	44281	103539	149021	236821

Asphalt Binder: Superpave Binder Test Data		
Temperature (°F)	Angular freq. = 10 rad/sec	
	G* (Pa)	Delta (degree)
158.0	792.60	88.98
168.8	299.28	89.22
179.6	150.21	89.46

Asphalt General: Volumetric Properties as Built	
Effective Binder (%)	10.48
Air Voids (%)	7.13
Total unit weight	165.44

Level 2

Asphalt Mix: Aggregate Gradation	
Cumulative % Retained ¾" sieve	2
Cumulative % Retained ⅜" sieve	30
Cumulative % Retained #4 sieve	53
% Passing #200 sieve	3.73

Level 3

Asphalt Binder: Superpave Binder Grading	PG 64-22

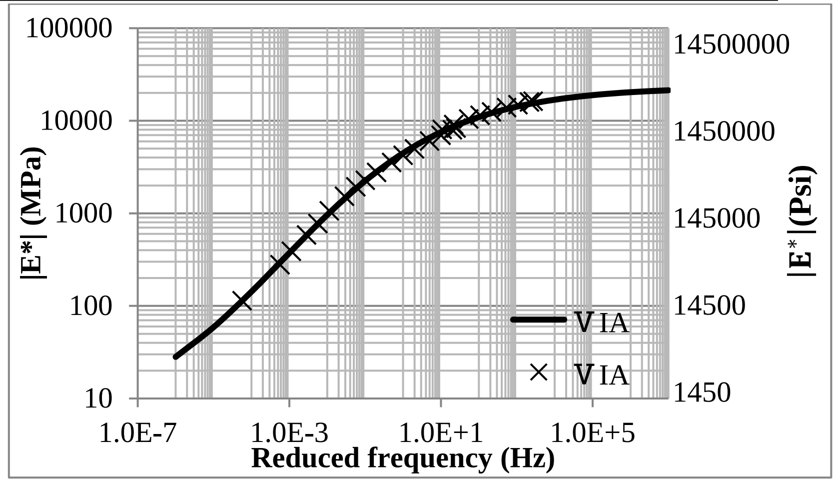

Master Dynamic Modulus Curves for Mixtures from Liberty Intermediate Type A with RAP

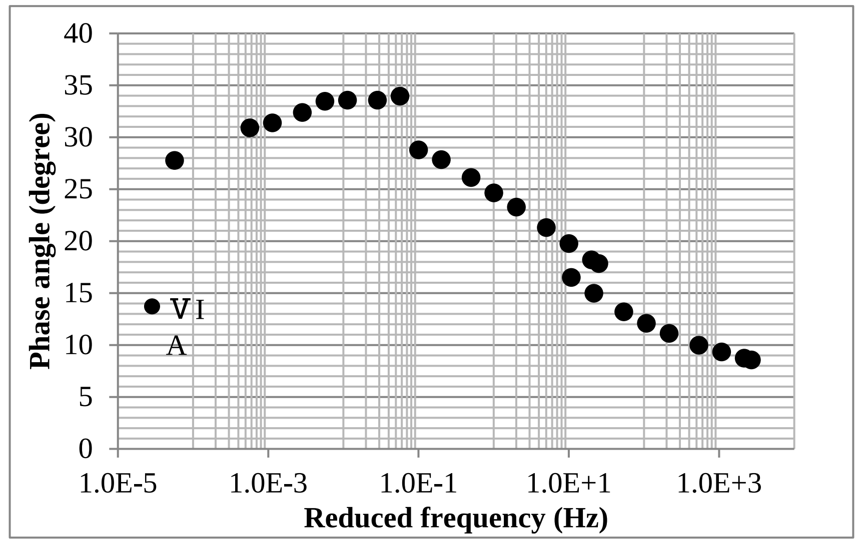

Master Phase Angle Curves for Mixtures from Liberty Intermediate Type A with RAP

Figure 13-93: Mixture Type: V IBO (Liberty Intermediate Type B, no RAP)

Level 1

Asphalt Mix: Dynamic Modulus Table						
Temperature	Mixture |E*| (psi)					
(°F)	0.1 Hz	0.5 Hz	1 Hz	5 Hz	10 Hz	25 Hz
14	1545104	1988279	2160330	2502087	2623455	2761209
40	706651	1130098	1329158	1789105	1974702	2200501
70	190410	396484	522828	898856	1087937	1350490
100	44228	103541	147987	318993	428382	608471
130	12773	27566	39410	92268	132305	208941

Asphalt Binder: Superpave Binder Test Data		
Temperature	Angular freq. = 10 rad/sec	
(°F)	G* (Pa)	Delta (degree)
158.0	792.60	88.98
168.8	299.28	89.22
179.6	150.21	89.46

Asphalt General: Volumetric Properties as Built	
Effective Binder (%)	11.43
Air Voids (%)	6.61
Total unit weight	166.94

Level 2

Asphalt Mix: Aggregate Gradation	
Cumulative % Retained ¾” sieve	0
Cumulative % Retained ⅜” sieve	20
Cumulative % Retained #4 sieve	50
% Passing #200 sieve	3.37

Level 3

Asphalt Binder: Superpave Binder Grading	PG 64-22

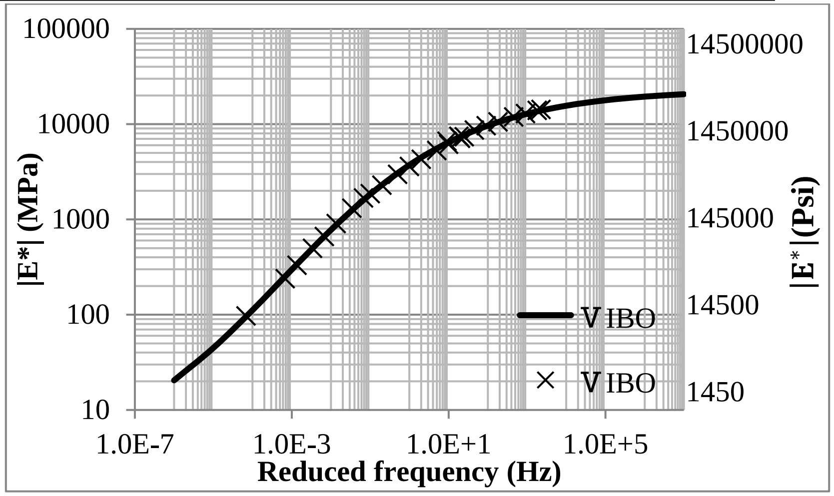

Master Dynamic Modulus Curves for Mixtures from Liberty Intermediate Type B, no RAP

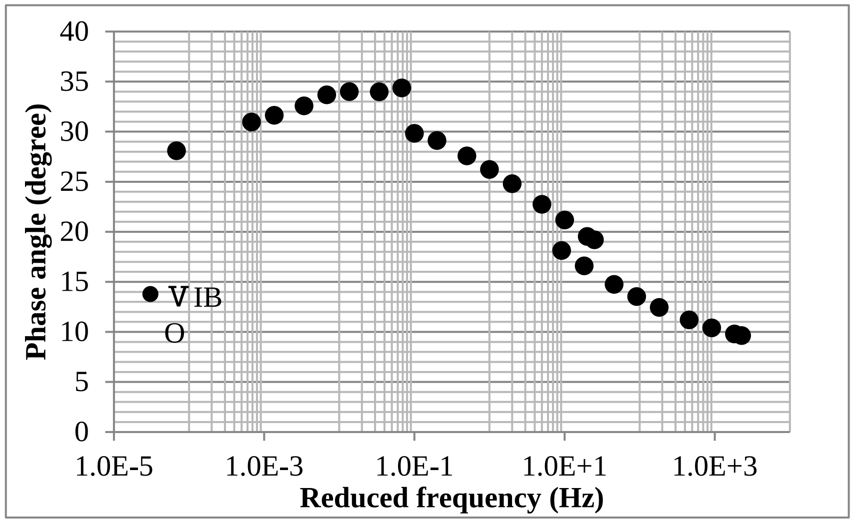

Master Phase Angle Curves for Mixtures from Liberty Intermediate Type B, no RAP

Figure 13-94: Mixture Type: V IB (Liberty Intermediate Type B with RAP)

Level 1

Asphalt Mix: Dynamic Modulus Table						
Temperature (°F)	Mixture |E*| (psi)					
	0.1 Hz	0.5 Hz	1 Hz	5 Hz	10 Hz	25 Hz
14	1821218	2258581	2419394	2723783	2826877	2940487
40	867431	1348069	1563725	2037926	2219900	2433979
70	227089	474187	623781	1057400	1268403	1553387
100	49540	116616	167602	365717	492568	700065
130	14258	29742	42248	99125	143018	228173

Asphalt Binder: Superpave Binder Test Data		
Temperature (°F)	Angular freq. = 10 rad/sec	
	G* (Pa)	Delta (degree)
158.0	792.60	88.98
168.8	299.28	89.22
179.6	150.21	89.46

Asphalt General: Volumetric Properties as Built	
Effective Binder (%)	10.85
Air Voids (%)	6.24
Total unit weight	167.00

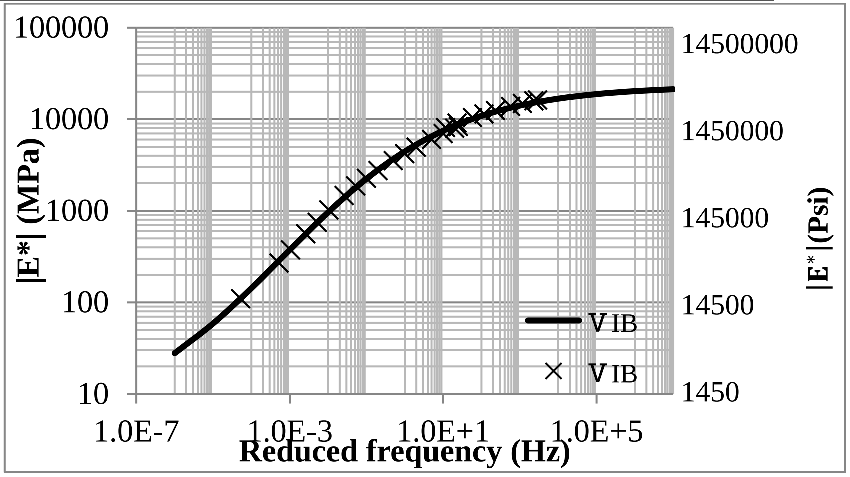

Master Dynamic Modulus Curves for Mixtures from Liberty Intermediate Type B with RAP

Level 2

Asphalt Mix: Aggregate Gradation	
Cumulative % Retained ¾" sieve	0
Cumulative % Retained ⅜" sieve	18
Cumulative % Retained #4 sieve	55
% Passing #200 sieve	3.89

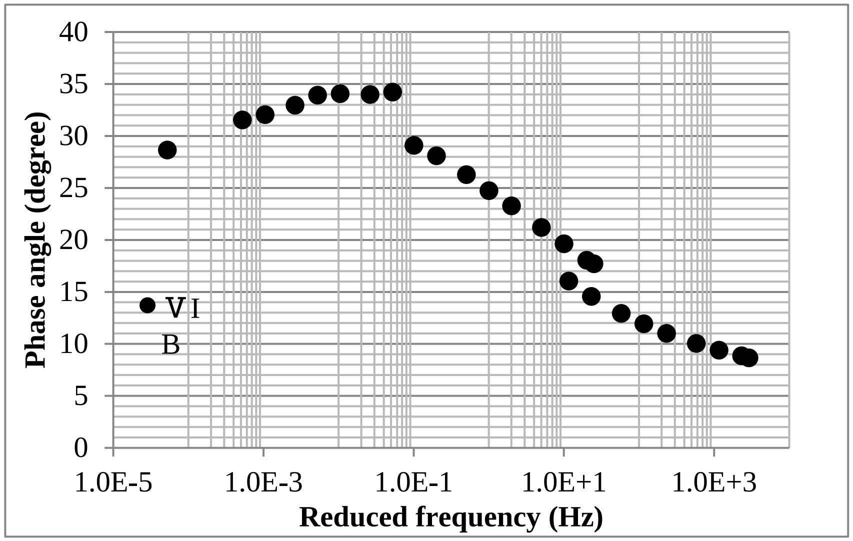

Master Phase Angle Curves for Mixtures from Liberty Intermediate Type B with RAP

Level 3

Asphalt Binder: Superpave Binder Grading	PG 64-22

Figure 13-95: Mixture Type: V ICO (Liberty Intermediate Type C, no RAP)

Level 1

Asphalt Mix: Dynamic Modulus Table						
Temperature (°F)	Mixture |E*| (psi)					
	0.1 Hz	0.5 Hz	1 Hz	5 Hz	10 Hz	25 Hz
14	1536385	1947010	2100001	2391806	2491136	2600778
40	694115	1118696	1314236	1752377	1922910	2124849
70	170840	371643	497464	874212	1062378	1320279
100	36316	87573	127628	288839	395270	573096
130	10543	22113	31601	75839	110830	180142

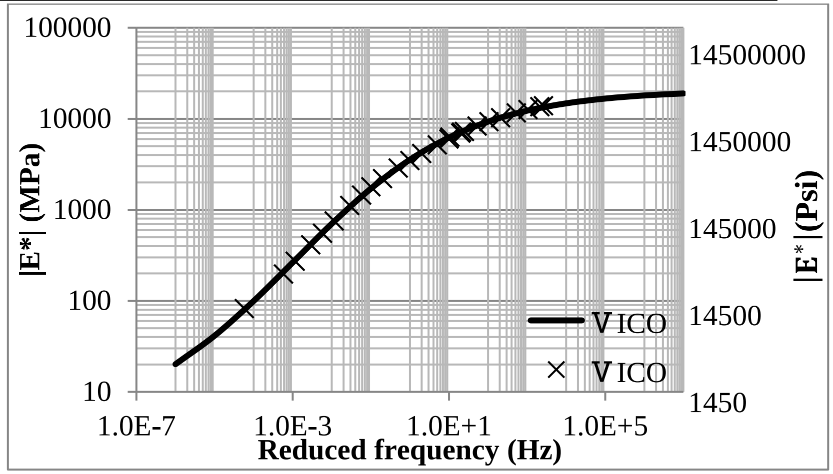

Master Dynamic Modulus Curves for Mixtures from Liberty Intermediate Type C, no RAP

Asphalt Binder: Superpave Binder Test Data		
Temperature (°F)	Angular freq. = 10 rad/sec	
	G* (Pa)	Delta (degree)
158.0	792.60	88.98
168.8	299.28	89.22
179.6	150.21	89.46

Asphalt General: Volumetric Properties as Built	
Effective Binder (%)	11.24
Air Voids (%)	6.31
Total unit weight	166.69

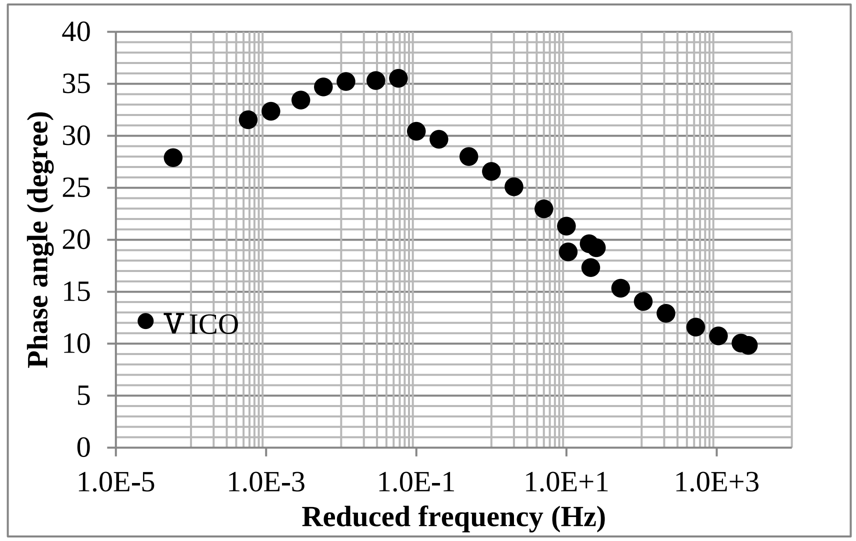

Master Phase Angle Curves for Mixtures from Liberty Intermediate Type C, no RAP

Level 2

Asphalt Mix: Aggregate Gradation	
Cumulative % Retained ¾” sieve	1
Cumulative % Retained ⅜” sieve	21
Cumulative % Retained #4 sieve	47
% Passing #200 sieve	3.97

Level 3

Asphalt Binder: Superpave Binder Grading	PG 64-22

Figure 13-96: Mixture Type: V IC (Liberty Intermediate Type C with RAP)

Level 1

Asphalt Mix: Dynamic Modulus Table						
Temperature (°F)	Mixture |E*| (psi)					
	0.1 Hz	0.5 Hz	1 Hz	5 Hz	10 Hz	25 Hz
14	1567890	1975603	2135032	2456273	2572538	2706482
40	750796	1147511	1331448	1756351	1929205	2141695
70	218392	424386	545624	896714	1070862	1312364
100	53571	117884	163628	330749	433799	600353
130	15478	32420	45409	100196	139776	213131

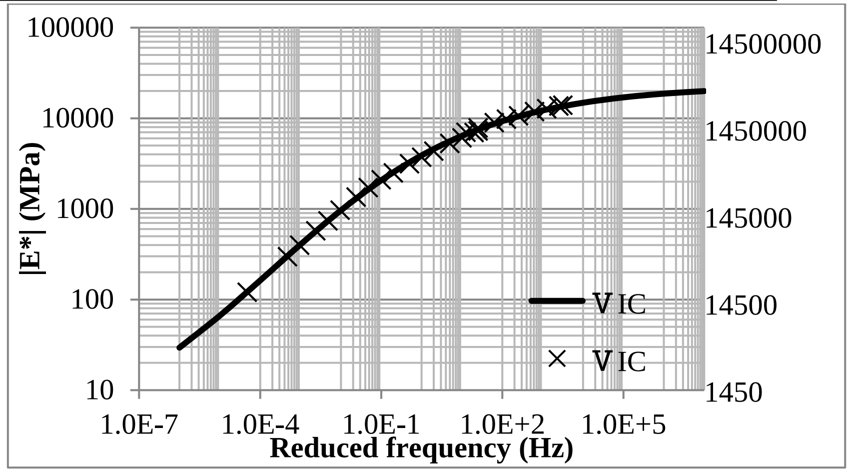

Master Dynamic Modulus Curves for Mixtures from Liberty Intermediate Type C with RAP

Asphalt Binder: Superpave Binder Test Data		
Temperature (°F)	Angular freq. = 10 rad/sec	
	G* (Pa)	Delta (degree)
158.0	792.60	88.98
168.8	299.28	89.22
179.6	150.21	89.46

Asphalt General: Volumetric Properties as Built	
Effective Binder (%)	11.24
Air Voids (%)	7.29
Total unit weight	166.69

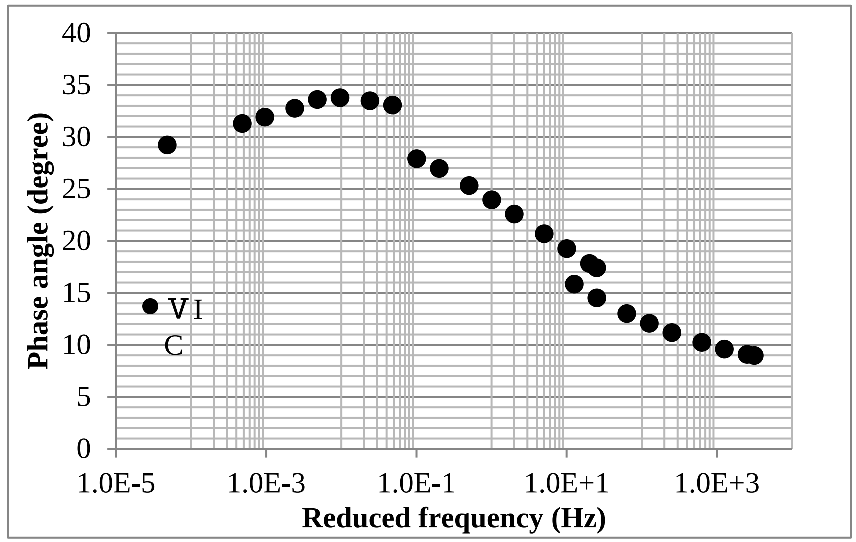

Master Phase Angle Curves for Mixtures from Liberty Intermediate Type C with RAP

Level 2

Asphalt Mix: Aggregate Gradation	
Cumulative % Retained ¾” sieve	1
Cumulative % Retained ⅜” sieve	21
Cumulative % Retained #4 sieve	47
% Passing #200 sieve	3.97

Level 3

Asphalt Binder: Superpave Binder Grading	PG 64-22

Figure 13-97: Mixture Type: V SAO (Liberty Base Type A, no RAP)

Level 1

Asphalt Mix: Dynamic Modulus Table						
Temperature	Mixture |E*| (psi)					
(°F)	0.1 Hz	0.5 Hz	1 Hz	5 Hz	10 Hz	25 Hz
14	1721171	2123334	2266206	2527247	2612333	2703722
40	830507	1301395	1508261	1949155	2112209	2298868
70	215265	463477	614981	1049892	1257014	1530497
100	47165	113462	165197	370255	502297	716917
130	14335	29517	42036	100660	146944	237838

Asphalt Binder: Superpave Binder Test Data		
Temperature	Angular freq. = 10 rad/sec	
(°F)	G* (Pa)	Delta (degree)
158.0	792.60	88.98
168.8	299.28	89.22
179.6	150.21	89.46

Asphalt General: Volumetric Properties as Built	
Effective Binder (%)	12.07
Air Voids (%)	5.52
Total unit weight	167.19

Level 2

Asphalt Mix: Aggregate Gradation	
Cumulative % Retained ¾" sieve	7
Cumulative % Retained ⅜" sieve	37
Cumulative % Retained #4 sieve	52
% Passing #200 sieve	6.01

Level 3

Asphalt Binder: Superpave Binder Grading	PG 64-22

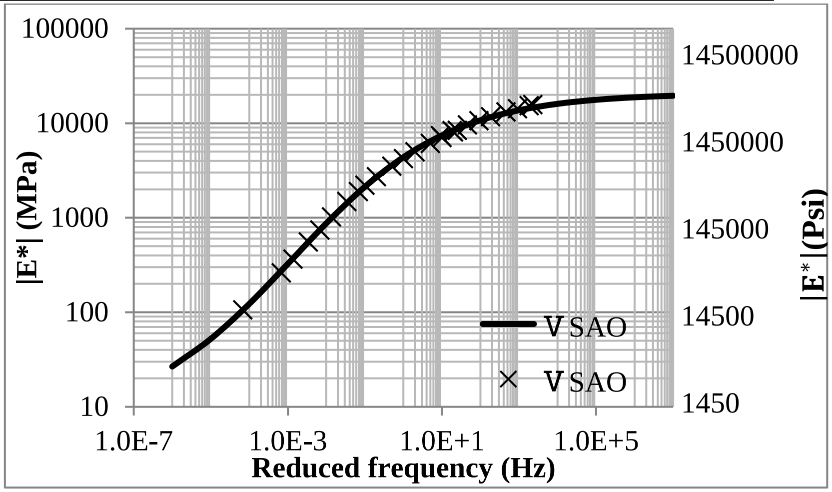

Master Dynamic Modulus Curves for Mixtures from Liberty Base Type A, no RAP

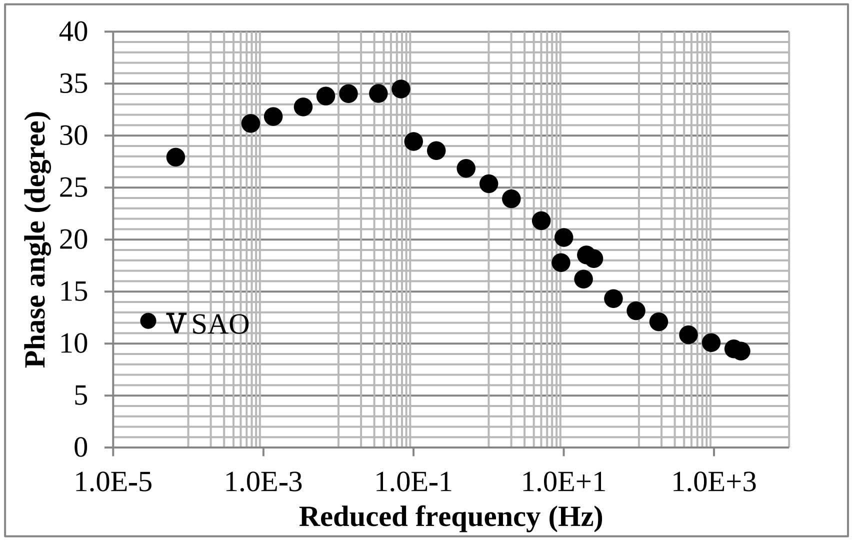

Master Phase Angle Curves for Mixtures from Liberty Base Type A, no RAP

Figure 13-98: Mixture Type: V SA (Liberty Base Type A with RAP)

Level 1

Asphalt Mix: Dynamic Modulus Table						
Temperature (°F)	Mixture |E*| (psi)					
	0.1 Hz	0.5 Hz	1 Hz	5 Hz	10 Hz	25 Hz
14	1680612	2038828	2173531	2436040	2528075	2632064
40	887712	1282794	1457416	1843494	1994238	2174827
70	296206	533605	666224	1030439	1202536	1433529
100	85084	170091	227359	424652	540212	720253
130	29114	54613	73082	146149	196164	285262

Asphalt Binder: Superpave Binder Test Data		
Temperature (°F)	Angular freq. = 10 rad/sec	
	G* (Pa)	Delta (degree)
158.0	792.60	88.98
168.8	299.28	89.22
179.6	150.21	89.46

Asphalt General: Volumetric Properties as Built	
Effective Binder (%)	12.02
Air Voids (%)	5.94
Total unit weight	166.69

Level 2

Asphalt Mix: Aggregate Gradation	
Cumulative % Retained ¾” sieve	4
Cumulative % Retained ⅜” sieve	38
Cumulative % Retained #4 sieve	52
% Passing #200 sieve	5.49

Level 3

Asphalt Binder: Superpave Binder Grading	PG 64-22

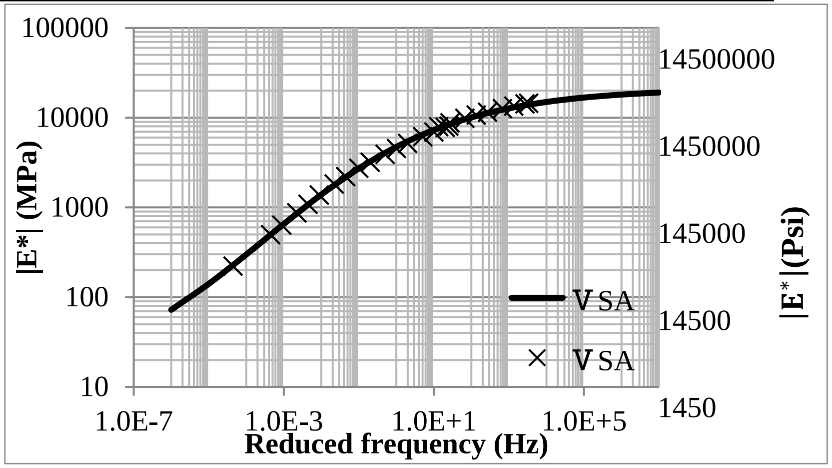

Master Dynamic Modulus Curves for Mixtures from Liberty Base Type A with RAP

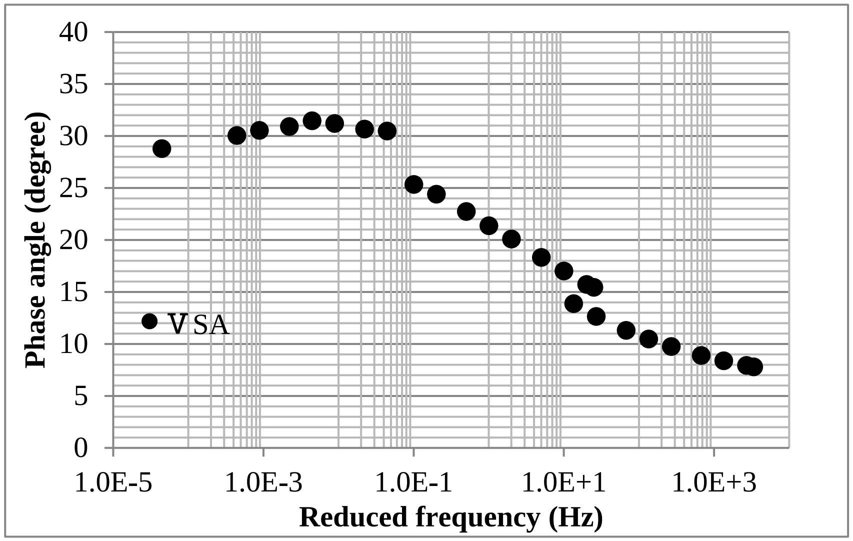

Master Phase Angle Curves for Mixtures from Liberty Base Type A with RAP

Figure 13-99: Mixture Type: V SBO (Liberty Base Type B, no RAP)

Level 1

Asphalt Mix: Dynamic Modulus Table						
Temperature (°F)	Mixture |E*| (psi)					
	0.1 Hz	0.5 Hz	1 Hz	5 Hz	10 Hz	25 Hz
14	1649769	2028097	2167681	2433263	2523793	2624031
40	832015	1252699	1439324	1847782	2004377	2188855
70	249634	486352	624153	1011553	1196094	1442887
100	64377	139507	193443	390788	511325	702854
130	20980	41200	56715	122682	170665	259715

Asphalt Binder: Superpave Binder Test Data		
Temperature (°F)	Angular freq. = 10 rad/sec	
	G* (Pa)	Delta (degree)
158.0	792.60	88.98
168.8	299.28	89.22
179.6	150.21	89.46

Asphalt General: Volumetric Properties as Built	
Effective Binder (%)	12.07
Air Voids (%)	5.18
Total unit weight	166.94

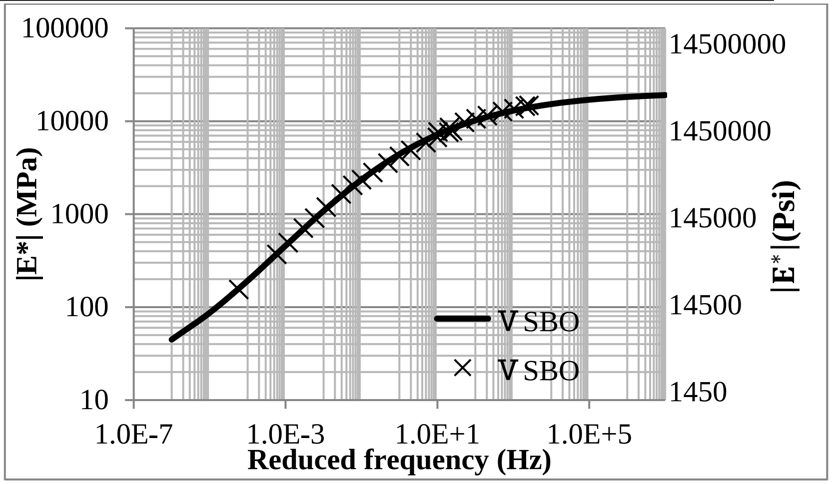

Master Dynamic Modulus Curves for Mixtures from Liberty Base Type B, no RAP

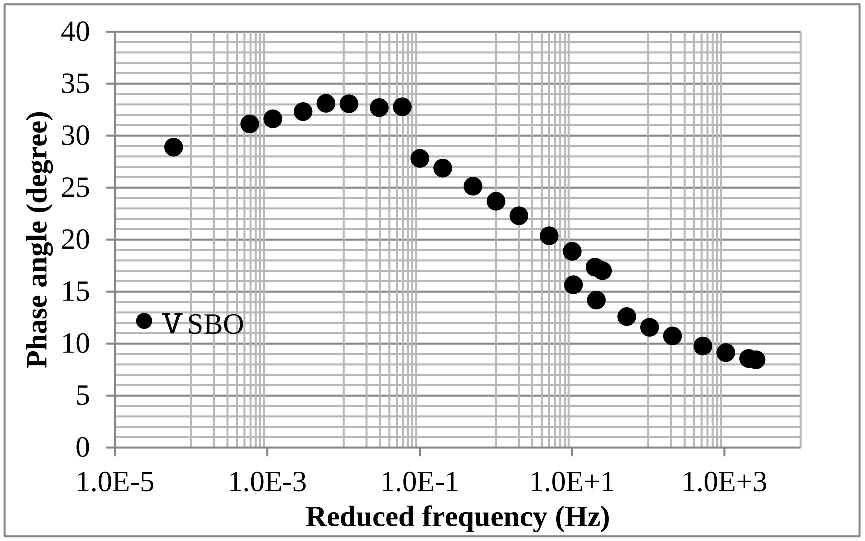

Master Phase Angle Curves for Mixtures from Liberty Base Type B, no RAP

Level 2

Asphalt Mix: Aggregate Gradation	
Cumulative % Retained ¾” sieve	4
Cumulative % Retained ⅜” sieve	37
Cumulative % Retained #4 sieve	52
% Passing #200 sieve	6.01

Level 3

Asphalt Binder: Superpave Binder Grading	PG 64-22

Figure 13-100: Mixture Type: V SB (Liberty Base Type B with RAP)

Level 1

Asphalt Mix: Dynamic Modulus Table						
Temperature (°F)	Mixture |E*| (psi)					
	0.1 Hz	0.5 Hz	1 Hz	5 Hz	10 Hz	25 Hz
14	1724646	2059361	2185480	2433041	2520768	2620776
40	969499	1350585	1515722	1877355	2018122	2187085
70	357540	612760	749021	1109251	1274698	1493763
100	108696	212787	279751	498137	620023	804041
130	35896	69592	93484	184257	243714	345791

Asphalt Binder: Superpave Binder Test Data		
Temperature (°F)	Angular freq. = 10 rad/sec	
	G* (Pa)	Delta (degree)
158.0	792.60	88.98
168.8	299.28	89.22
179.6	150.21	89.46

Asphalt General: Volumetric Properties as Built	
Effective Binder (%)	12.02
Air Voids (%)	5.48
Total unit weight	167.00

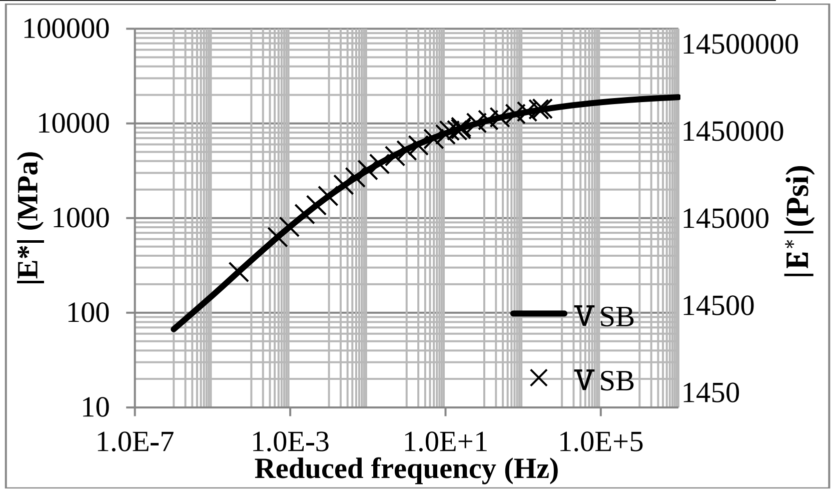

Master Dynamic Modulus Curves for Mixtures from Liberty Base Type B with RAP

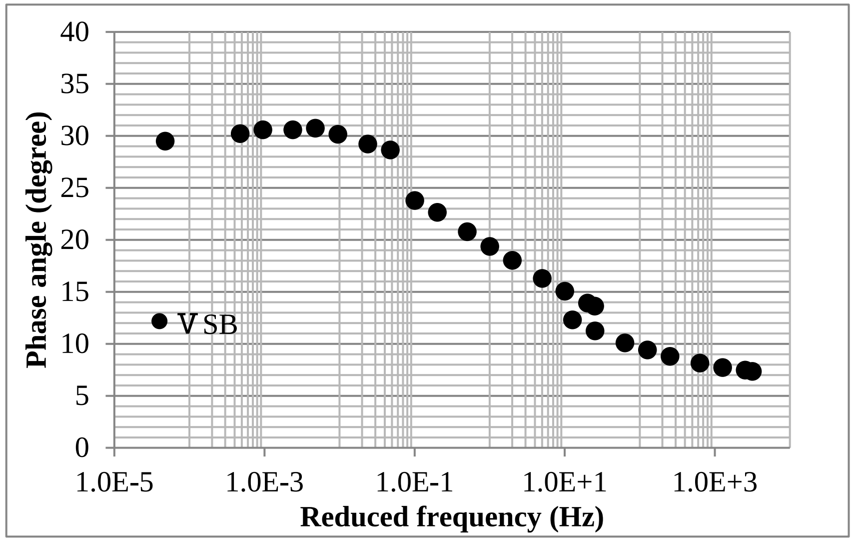

Master Phase Angle Curves for Mixtures from Liberty Base Type B with RAP

Level 2

Asphalt Mix: Aggregate Gradation	
Cumulative % Retained ¾" sieve	4
Cumulative % Retained ⅜" sieve	38
Cumulative % Retained #4 sieve	52
% Passing #200 sieve	5.49

Level 3

Asphalt Binder: Superpave Binder Grading	PG 64-22

Figure 13-101: Mixture Type: VI A (Rockingham Surface Type A with RAP)

Level 1

Asphalt Mix: Dynamic Modulus Table						
Temperature (°F)	Mixture |E*| (psi)					
	0.1 Hz	0.5 Hz	1 Hz	5 Hz	10 Hz	25 Hz
14	2263236	2636970	2764266	2990686	3062958	3139844
40	1217592	1746732	1964554	2407407	2565161	2742442
70	347116	675754	862945	1368467	1597825	1892668
100	80160	173451	241921	497203	654230	902647
130	26134	47912	64769	138375	193585	298722

Asphalt Binder: Superpave Binder Test Data		
Temperature (°F)	Angular freq. = 10 rad/sec	
	G* (Pa)	Delta (degree)
158.0	2995.00	63.70
168.8	1501.00	61.90
179.6	750.50	60.00

Asphalt General: Volumetric Properties as Built	
Effective Binder (%)	11.26
Air Voids (%)	6.44
Total unit weight	169.31

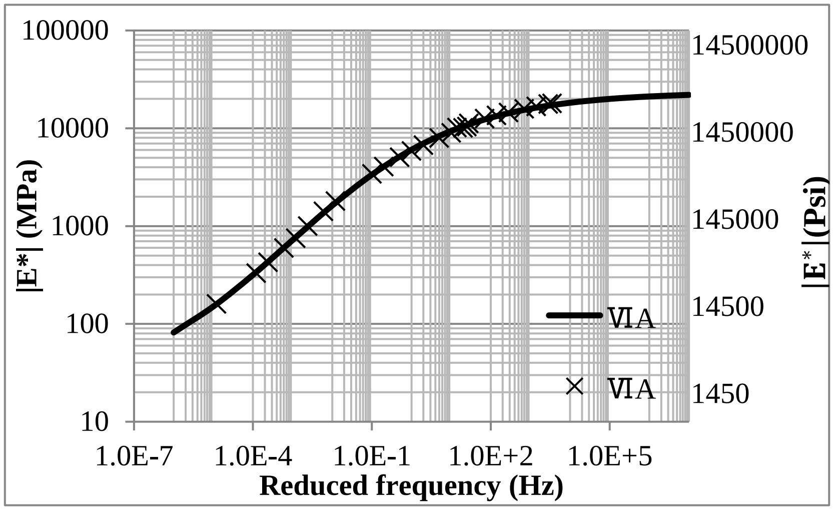

Master Dynamic Modulus Curves for Mixtures from Rockingham Surface Type A with RAP

Level 2

Asphalt Mix: Aggregate Gradation	
Cumulative % Retained ¾” sieve	0
Cumulative % Retained ⅜” sieve	17
Cumulative % Retained #4 sieve	44
% Passing #200 sieve	4.66

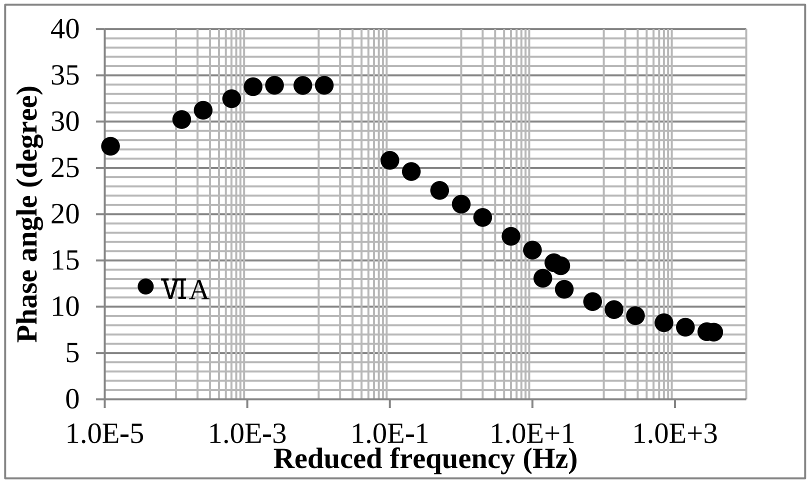

Master Phase Angle Curves for Mixtures from Rockingham Surface Type A with RAP

Level 3

Asphalt Binder: Superpave Binder Grading	PG 76-22

Figure 13-102: Mixture Type: VI AO (Rockingham Surface Type A, no RAP)

Level 1

Asphalt Mix: Dynamic Modulus Table						
Temperature (°F)	Mixture |E*| (psi)					
	0.1 Hz	0.5 Hz	1 Hz	5 Hz	10 Hz	25 Hz
14	1727195	2175261	2342965	2664355	2774298	2896038
40	791505	1250481	1462680	1941575	2129504	2353308
70	210260	427672	562035	964168	1166318	1445540
100	53186	112684	156902	328742	440459	626869
130	19063	34417	46104	96569	134461	207498

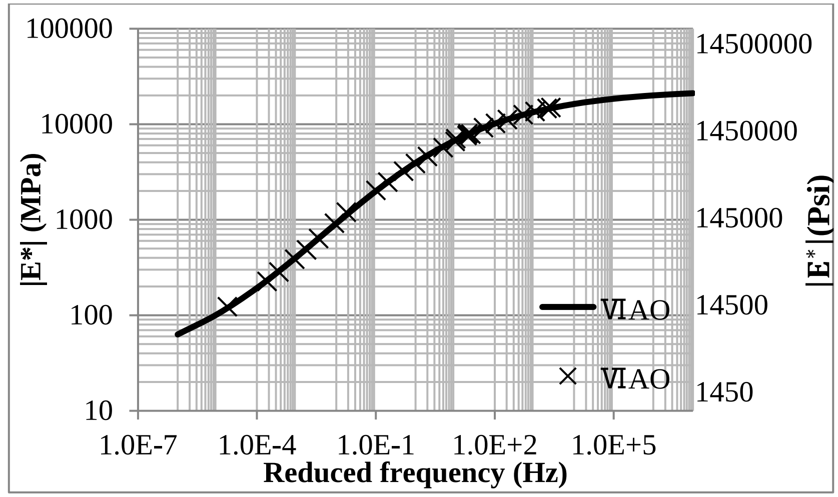

Master Dynamic Modulus Curves for Mixtures from Rockingham Surface Type A, no RAP

Asphalt Binder: Superpave Binder Test Data		
Temperature (°F)	Angular freq. = 10 rad/sec	
	G* (Pa)	Delta (degree)
158.0	2995.00	63.70
168.8	1501.00	61.90
179.6	750.50	60.00

Asphalt General: Volumetric Properties as Built	
Effective Binder (%)	11.45
Air Voids (%)	7.00
Total unit weight	169.31

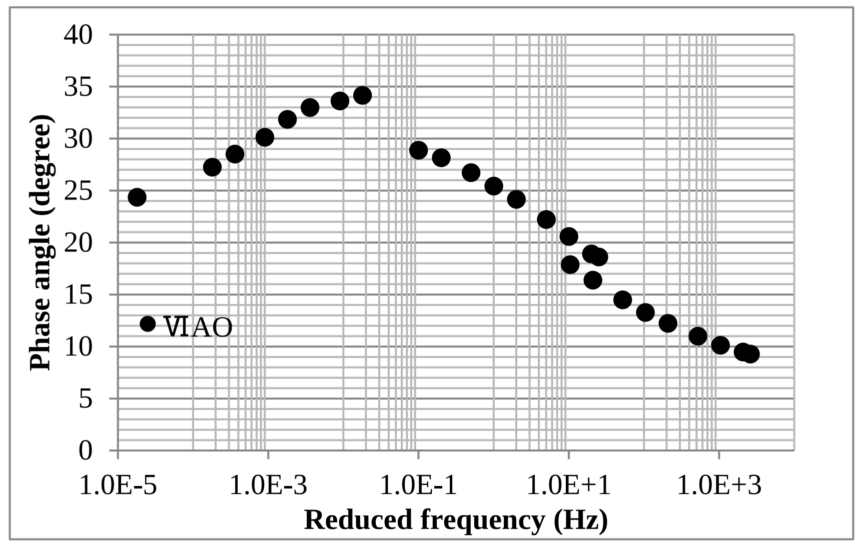

Master Phase Angle Curves for Mixtures from Rockingham Surface Type A, no RAP

Level 2

Asphalt Mix: Aggregate Gradation	
Cumulative % Retained ¾” sieve	0
Cumulative % Retained ⅜” sieve	16
Cumulative % Retained #4 sieve	42
% Passing #200 sieve	5.04

Level 3

Asphalt Binder: Superpave Binder Grading	PG 76-22

Figure 13-103: Mixture Type: VI BO (Rockingham Surface Type B, no RAP)

Level 1

Asphalt Mix: Dynamic Modulus Table						
Temperature (°F)	Mixture |E*| (psi)					
	0.1 Hz	0.5 Hz	1 Hz	5 Hz	10 Hz	25 Hz
14	1609991	2066390	2239971	2577172	2694043	2824500
40	704904	1150266	1359908	1840508	2031863	2261850
70	170814	370603	497284	884316	1081997	1357710
100	36936	87246	126365	284447	389924	568436
130	11006	22554	31886	74840	108624	175610

Asphalt Binder: Superpave Binder Test Data		
Temperature (°F)	Angular freq. = 10 rad/sec	
	G* (Pa)	Delta (degree)
158.0	792.60	88.98
168.8	299.28	89.22
179.6	150.21	89.46

Asphalt General: Volumetric Properties as Built	
Effective Binder (%)	11.76
Air Voids (%)	7.92
Total unit weight	169.31

Level 2

Asphalt Mix: Aggregate Gradation	
Cumulative % Retained ¾” sieve	0
Cumulative % Retained ⅜” sieve	6
Cumulative % Retained #4 sieve	31
% Passing #200 sieve	6.02

Level 3

Asphalt Binder: Superpave Binder Grading	PG 64-22

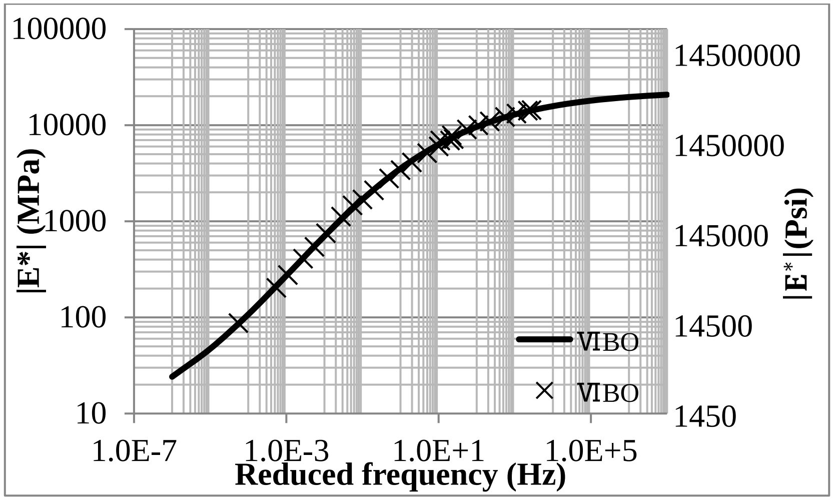

Master Dynamic Modulus Curves for Mixtures from Rockingham Surface Type B, no RAP

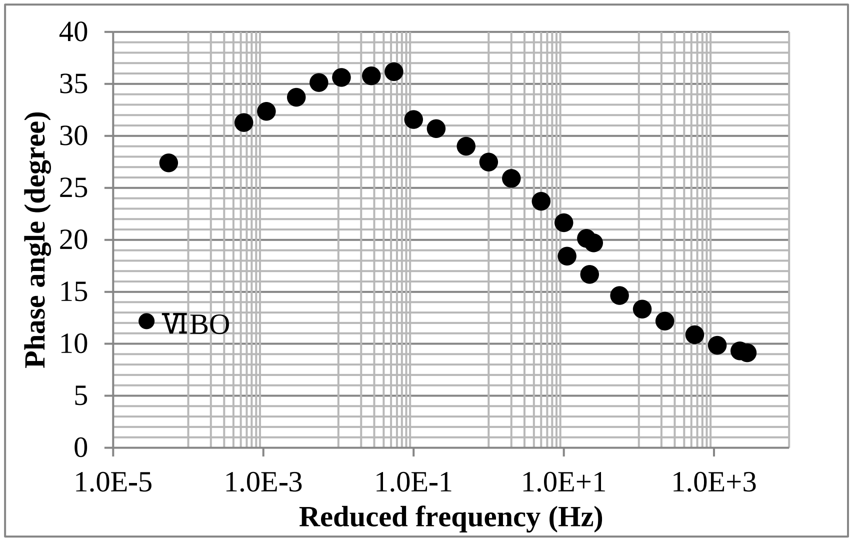

Master Phase Angle Curves for Mixtures from Rockingham Surface Type B, no RAP

Figure 13-104: Mixture Type: VI B (Rockingham Surface Type B with RAP)

Level 1

Asphalt Mix: Dynamic Modulus Table						
Temperature (°F)	Mixture |E*| (psi)					
	0.1 Hz	0.5 Hz	1 Hz	5 Hz	10 Hz	25 Hz
14	1744741	2161606	2318274	2621798	2727243	2845463
40	853126	1296245	1496293	1942938	2117849	2326973
70	245261	481987	621454	1020722	1214879	1478825
100	60171	131928	183756	375659	494637	686442
130	18569	37120	51404	112512	157318	241244

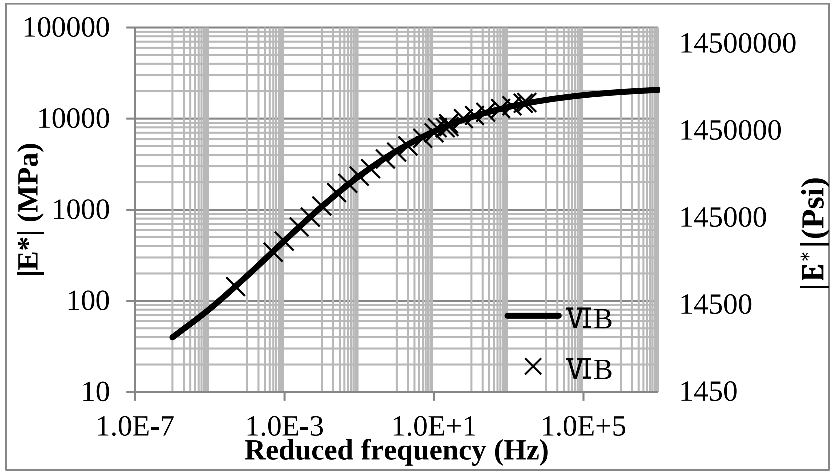

Master Dynamic Modulus Curves for Mixtures from Rockingham Surface Type B with RAP

Asphalt Binder: Superpave Binder Test Data		
Temperature (°F)	Angular freq. = 10 rad/sec	
	G* (Pa)	Delta (degree)
158.0	792.60	88.98
168.8	299.28	89.22
179.6	150.21	89.46

Asphalt General: Volumetric Properties as Built	
Effective Binder (%)	11.90
Air Voids (%)	8.33
Total unit weight	168.25

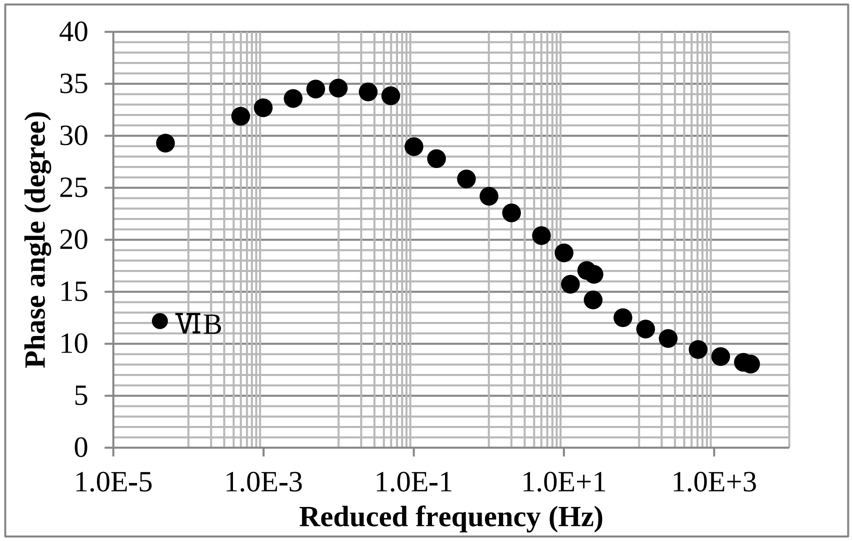

Master Phase Angle Curves for Mixtures from Rockingham Surface Type B with RAP

Level 2

Asphalt Mix: Aggregate Gradation	
Cumulative % Retained ¾" sieve	0
Cumulative % Retained ⅜" sieve	7
Cumulative % Retained #4 sieve	31
% Passing #200 sieve	5.37

Level 3

Asphalt Binder: Superpave Binder Grading	PG 64-22

Figure 13-105: Mixture Type: VI CO (Rockingham Surface Type C, no RAP)

Level 1

Asphalt Mix: Dynamic Modulus Table						
Temperature (°F)	Mixture |E*| (psi)					
	0.1 Hz	0.5 Hz	1 Hz	5 Hz	10 Hz	25 Hz
14	1395572	1861919	2043952	2403368	2529381	2670684
40	566258	977427	1179540	1658557	1854236	2092395
70	129113	294186	403886	755479	942269	1208937
100	28162	67605	99204	232393	324746	485513
130	8807	17925	25382	60521	88865	146368

Asphalt Binder: Superpave Binder Test Data		
Temperature (°F)	Angular freq. = 10 rad/sec	
	G* (Pa)	Delta (degree)
158.0	792.60	88.98
168.8	299.28	89.22
179.6	150.21	89.46

Asphalt General: Volumetric Properties as Built	
Effective Binder (%)	13.85
Air Voids (%)	6.27
Total unit weight	167.50

Level 2

Asphalt Mix: Aggregate Gradation	
Cumulative % Retained ¾” sieve	0
Cumulative % Retained ⅜” sieve	4
Cumulative % Retained #4 sieve	30
% Passing #200 sieve	4.86

Level 3

Asphalt Binder: Superpave Binder Grading	PG 64-22

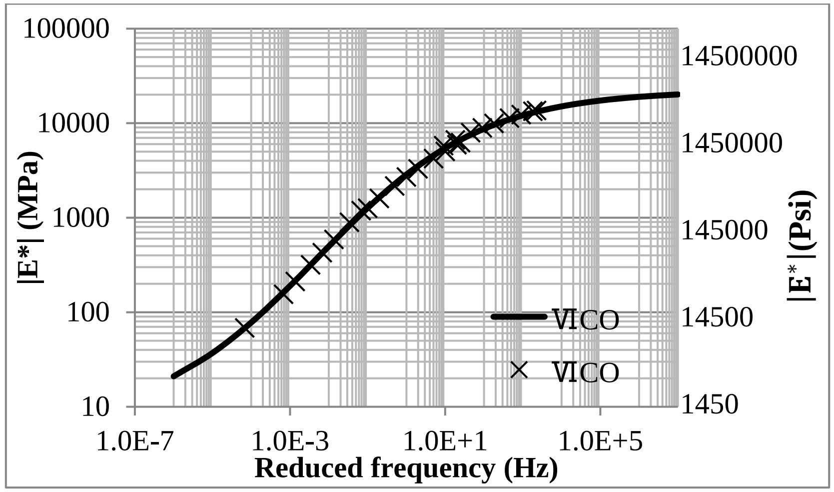

Master Dynamic Modulus Curves for Mixtures from Rockingham Surface Type C, no RAP

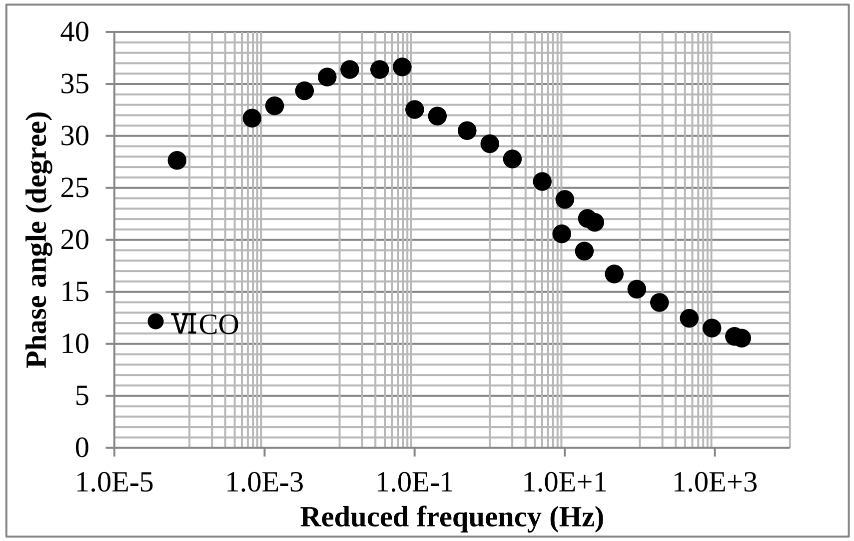

Master Phase Angle Curves for Mixtures from Rockingham Surface Type C, no RAP

Figure 13-106: Mixture Type: VI C (Rockingham Surface Type C with RAP)

Level 1

Asphalt Mix: Dynamic Modulus Table						
Temperature (°F)	Mixture |E*| (psi)					
	0.1 Hz	0.5 Hz	1 Hz	5 Hz	10 Hz	25 Hz
14	1609358	2047352	2212766	2532284	2642447	2765037
40	739470	1180432	1384803	1847263	2029324	2246709
70	196376	410264	542290	935028	1131105	1400687
100	46786	106412	151435	326928	440335	627844
130	14904	29822	41625	94265	134422	211995

Asphalt Binder: Superpave Binder Test Data		
Temperature (°F)	Angular freq. = 10 rad/sec	
	G* (Pa)	Delta (degree)
158.0	792.60	88.98
168.8	299.28	89.22
179.6	150.21	89.46

Asphalt General: Volumetric Properties as Built	
Effective Binder (%)	13.74
Air Voids (%)	5.64
Total unit weight	165.63

Level 2

Asphalt Mix: Aggregate Gradation	
Cumulative % Retained ¾” sieve	0
Cumulative % Retained ⅜” sieve	5
Cumulative % Retained #4 sieve	33
% Passing #200 sieve	5.21

Level 3

Asphalt Binder: Superpave Binder Grading	PG 64-22

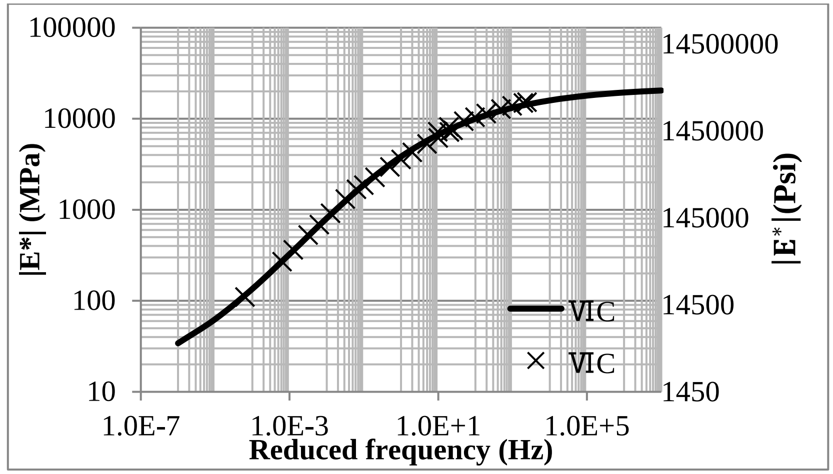

Master Dynamic Modulus Curves for Mixtures from Rockingham Surface Type C with RAP

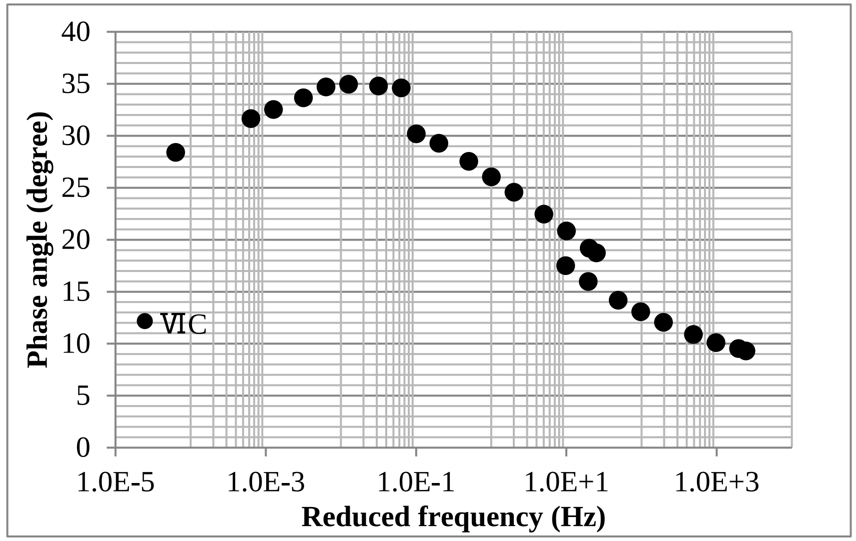

Master Phase Angle Curves for Mixtures from Rockingham Surface Type C with RAP

Figure 13-107: Mixture Type: VI D (Rockingham Surface Type D with RAP)

Level 1

Asphalt Mix: Dynamic Modulus Table						
Temperature (°F)	Mixture |E*| (psi)					
	0.1 Hz	0.5 Hz	1 Hz	5 Hz	10 Hz	25 Hz
14	1743325	2152025	2297088	2561490	2647368	2739347
40	836022	1310873	1520751	1969644	2135916	2326205
70	220729	465154	615196	1050158	1259236	1536800
100	53061	119047	169726	369917	499459	711587
130	18492	34621	47434	105484	150519	238539

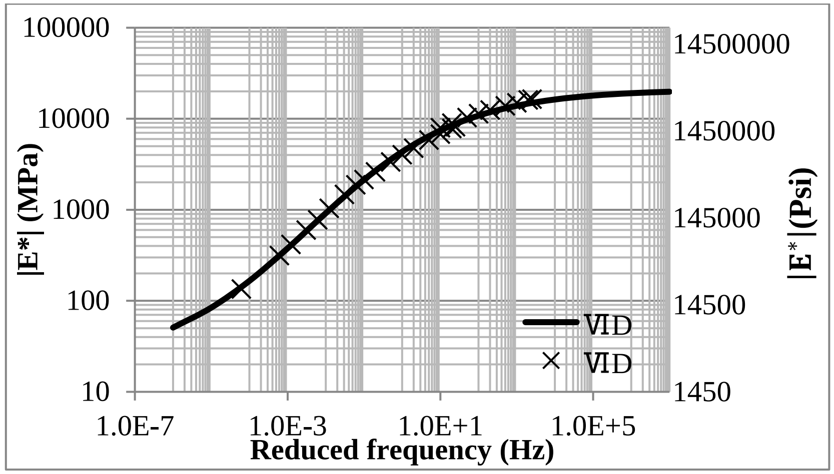

Master Dynamic Modulus Curves for Mixtures from Rockingham Surface Type D with RAP

Asphalt Binder: Superpave Binder Test Data		
Temperature (°F)	Angular freq. = 10 rad/sec	
	G* (Pa)	Delta (degree)
158.0	792.60	88.98
168.8	299.28	89.22
179.6	150.21	89.46

Asphalt General: Volumetric Properties as Built	
Effective Binder (%)	13.27
Air Voids (%)	7.37
Total unit weight	167.94

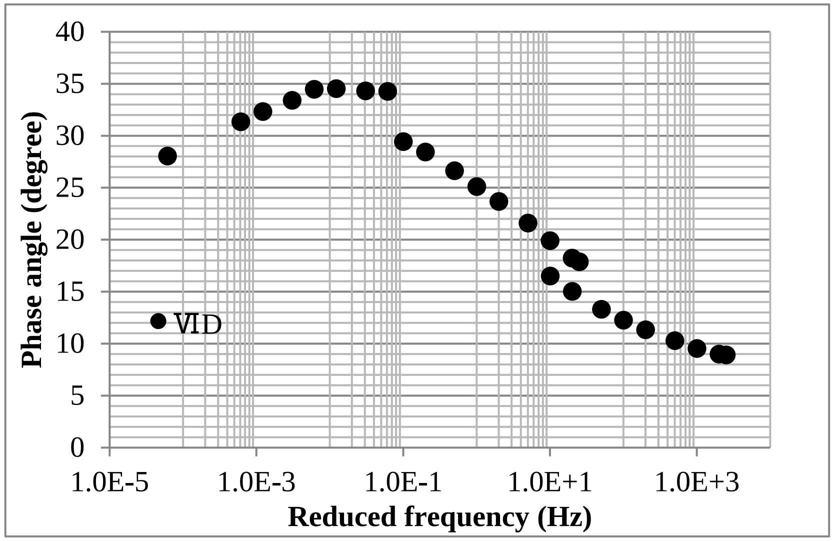

Master Phase Angle Curves for Mixtures from Rockingham Surface Type D with RAP

Level 2

Asphalt Mix: Aggregate Gradation	
Cumulative % Retained ¾” sieve	0
Cumulative % Retained ⅜” sieve	3
Cumulative % Retained #4 sieve	14
% Passing #200 sieve	7.38

Level 3

Asphalt Binder: Superpave Binder Grading	PG 64-22

Figure 13-108: Mixture Type: VII IB (Sandy Flats Intermediate B Special with RAP)

Level 1

Asphalt Mix: Dynamic Modulus Table						
Temperature (°F)	Mixture |E*| (psi)					
	0.1 Hz	0.5 Hz	1 Hz	5 Hz	10 Hz	25 Hz
14	2111234	2372891	2472532	2673633	2747782	2835147
40	1183599	1517667	1659961	1974425	2100032	2255024
70	370686	589481	702669	1000813	1140097	1329328
100	76236	144599	187579	327511	407063	530741
130	15402	29807	39836	77765	102936	147307

Asphalt Binder: Superpave Binder Test Data		
Temperature (°F)	Angular freq. = 10 rad/sec	
	G* (Pa)	Delta (degree)
158.0	792.60	88.98
168.8	299.28	89.22
179.6	150.21	89.46

Asphalt General: Volumetric Properties as Built	
Effective Binder (%)	11.11
Air Voids (%)	7.43
Total unit weight	166.94

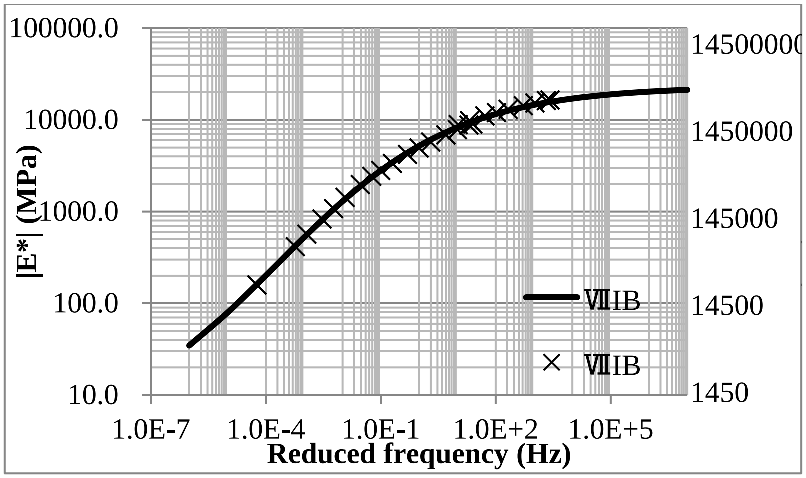

Master Dynamic Modulus Curves for Mixtures from Sandy Flats Intermediate Type B Special with RAP

Level 2

Asphalt Mix: Aggregate Gradation	
Cumulative % Retained ¾" sieve	0
Cumulative % Retained ⅜" sieve	16
Cumulative % Retained #4 sieve	50
% Passing #200 sieve	4.38

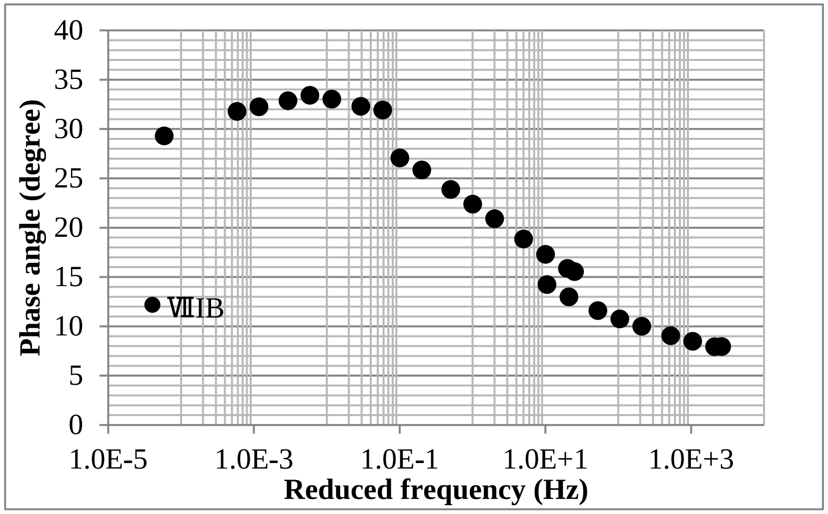

Master Phase Angle Curves for Mixtures from Sandy Flats Intermediate Type B Special with RAP

Level 3

Asphalt Binder: Superpave Binder Grading	PG 64-22